Borrower is requested to check the book and get the signatures on the torned pages, if any.

PREFACE TO THE SEVENTH EDITION

NTINUED developments in the science and art of steam turbine gineering have made the revision and enlargement of the book an solute necessity. The aims of the book and its general features, as out in the Preface to the First Edition, remain the same. New pters have been added on Vortex Flow in Steam Turbines and Experiments on Turbine Blades, while an attempt has been made bring up to date the section dealing with examples of land and rine turbines.

The author has received generous help from the following firms the British Thomson-Houston Co., Ltd., Brush Electrical Engineer- Co., Ltd., the English Electric Co., Ltd., Escher Wyss, Ltd., the neral Electric Co., Ltd., Metropolitan-Vickers Electrical Co., Ltd., A. Parsons & Co., Ltd., the Parsons and Marine Engineering rbine Research and Development Association (Pametrada), and chardsons-Westgarth (Hartlepool) Ltd. The author is also in- ted to the Council of the University of Liverpool for permission use questions from recent examination papers as examples, and the Editor of *The Engineer* for permission to reproduce, in modified rm, cross-sectional views of the 200 MW English Electric steam rbine.

W. J. K.

POOL

PREFACE TO THE FIRST EDITION

T is hardly necessary to lay stress upon the very important position f the steam turbine as a prime mover to-day. Its high commercial fficiency, its great reliability, and the ease with which it can be esigned for large powers are advantages that have placed it in a unique position. Admitting these to be the facts, there is still no excuse for another book on the subject were it not the case that many of the works that have appeared in the past few years have been over-developed along certain lines, and few have been generally useful to the engineering student. This book is written or the student, and it should prove useful to engineers and draughts- nen who are anxious to obtain a wider knowledge of the theory of the subject.

A feature of the book is the number of examples fully worked

out and also the examples set at the end of the chapters dea with the theory of steam turbines. Answers to these are prov. at the end of the book. The examples are somewhat graded it is hoped that the keen student will find these a means of tes his progress and increasing his confidence.

The various symbols used have been standardized and tabula, at the outset.

Free use has been made of the calculus, as most engineeri students nowadays have a working knowledge of the subj sufficiently extensive to enable them to integrate the simp functions and solve the differential equations commonly met wi Many points may seem to have been laboured. The justificati for this is that such points are rarely understood or are insufficien appreciated.

Much confusion exists in students' minds regarding the vari terms which are used to classify the different types of turbin It is hoped that the descriptions and diagrams of Chapter I w do much to remove this confusion. The section of the work deali with the properties of steam and with the entropy and Moiher diagrams is next introduced. In spite of the many ingenious steam diagrams which are devised from time to time, the one and only diagram, at least for impulse turbine calculations, is that of Dr. Mollier, in which total energy is plotted against entropy. Th has been used extensively to illustrate the subject. The dif subject of reheat factor or "coefficient de récupération" s explained at some length in Chapter IV.

The flow of steam through nozzles is dealt with in the usu l manner, i.e. expansion is assumed to take place in therm equilibrium. It is felt that for the student who is approachin the subject for the first time this is the simpler and easier metho In view of the theoretical importance of supersaturation, howev sufficient space has been devoted to it to explain the anom of excessive mass flow and also the supercooling effect.

The flow of steam through blades is treated along familiar lines, and in order to enhance the practical value of this section, a number of examples are worked out illustrating the usual methods of desi employed in drawing offices.

The fundamental principles underlying the design of rotors are embodied in Chapters IX and X, dealing respectively with the strength and critical speed of rotors. Here one pays a tribute to the exceptionally valuable pioneer work of Dr. de Laval, who introduced the wheel of constant strength and the flexible shaft.

For permission to publish the equations relating to the strength of hyperbolic discs, and also an account of nozzle experiments the author is indebted to Professor A. Stodola. Practical example relating to the design of discs and rotor shafts are worked out fully and should prove useful to the student and draughtsman.

In Chapter XI a few fundamental theorems relating to the determination of the principal dimensions of steam turbines are given, while the remainder of the book is devoted to illustrated descriptions of turbines and associated plant by the leading turbine builders.

In view of the importance of reduction gearing in marine work, attention is directed to Chapter XVII, in which the fundamental principles of involute gearing are set out. Every attempt has been made to bring the book up to date and a few of the recent developments are dealt with very briefly in the concluding chapter.

With respect to the preparation of the latter half of the book, the author wishes to acknowledge the cordial help he has received from the following firms, who have kindly supplied information and, in some cases, blocks: The British Ljungstrom Marine Turbine Co., Ltd., London; the British Thomson-Houston Co., Ltd., Rugby; John Brown & Co., Ltd., Clydebank; Brown Boveri & Co., London; the Brush Electrical Engineering Co., Ltd., Loughborough; the De Laval Steam Turbine Co., London (Aktiebolaget de Lavals Ångturbin); Fraser & Chalmers Engineering Works, Erith; the Metropolitan-Vickers Electrical Co., Ltd., Manchester; C. A. Parsons & Co., Ltd., Newcastle-on-Tyne; Svenska Turbinfabriks Aktiebolaget Ljungstrom, Finspong, Sweden.

The author is also indebted to the editor of *Engineering* for permission to publish a brief description of the Lunderello Natural Steam Plant and also a description of the 15,000 kW turbo-generator constructed by Messrs. C. A. Parsons & Co. for the Lots Road Power Station, London; to Messrs. J. Stevens and H. M. Hobart, the authors, and Sir Isaac Pitman & Sons, Ltd., the publishers of *Steam Turbine Engineering* for permission to use certain illustrations relating to the vertical Curtis turbine and the Rateau heat accumulator; and to the Controller of H.M. Stationery Office for permission to publish a drawing of the Brown-Curtis patented Diaphragm.

In conclusion, in spite of the large amount of arithmetical work entailed in working the examples, it is confidently hoped that errors will be "few and far between." The author will be glad, however, to receive intimations of such errors and any helpful suggestions that may come along.

W. J. KEARTON

LIVERPOOL
August, 1922

CONTENTS

CHAPTER IX

CHAPTER X

CHAPTER XI

CHAPTER XII

CHAPTER XIII

CHAPTER XIV

CHAPTER XXX

APPENDIX

INSETS

LIST OF TABLES

THE MEANING OF SYMBOLS USED THROUGHOUT THE WORK

THE number of symbols required is such that it has been necessary in some cases to employ the same symbol to represent different quantities. As this only occurs in quite different branches of the subject, no confusion should arise.

ENGLISH LETTERS

A	—	cross-sectional area of nozzle, etc.
A_m	—	mouth or outlet area of nozzle
A_t	—	throat area of nozzle
a h p	-	adiabatic horse-power of a turbine stage, based on the total internal steam flow and the stage adiabatic heat drop
B	—	axial length of journal bearing
b	=	constant in Callendar's equation of state
b	=	axial width of turbine blade
C_w	-	specific heat of water
C_p		specific heat of superheated steam at constant pressure
C_{pm}	-	mean specific heat of superheated steam at constant pressure
D	—	mean diameter of turbine blade ring, valve, etc.
E	-	internal energy (and Young's modulus of elasticity)
E_s	-	internal energy of steam
E_w	--	internal energy of water
e	=	eccentricity of journal bearing
f	—	stress
f_b	—	bending stress at root of blade
f_c	=	centrifugal stress in blade (generally at root section)
f_r	=	radial stress in disc
f_t	=	tangential stress in disc
f_{tr}	=	hoop stress in a thin ring
H	—	heat of generation of steam (and heat supplied)
H_a	=	energy available due to adiabatic expansion, i.e. the adiabatic heat drop
H_c		cumulative heat drop
H_i	-	internal work done per lb of steam
H_w		coupling work done per lb. of steam passing through the turbine
$h.p._d$		horse-power loss due to disc friction
$h.p._{bw}$		horse-power loss due to blade windage
$h.p._{wf}$		horse-power loss due to wheel friction
h	-	sensible heat
h_n	--	heat drop in nozzles
h_b	=	heat drop in blades

I = enthalpy
I_w = enthalpy of water
I_s = enthalpy of steam in any condition
I_x, I_y, etc. = second moments of area about axes XX, YY, etc.
J = Joule's mechanical equivalent of heat
K = load on turbine in kW (also the Parsons Number for a turbine)
k = ratio of relative velocity at outlet to relative velocity at inlet, in impulse turbine blades
L = latent heat of vaporization
L = circumferential length of effective bearing arc in journal bearing
l = radial height of blades
l = lift of throttle valve
m = index of v in Pv^m for expansion with friction
m = ratio of blade or nozzle height to mean diameter of turbine
N = revolutions per minute
N_c critical speed in revolutions per minute
n = index of v in Pv^n, generally for adiabatic and frictionless expansion
P = absolute pressure, lb. per square foot
P = load on journal bearing per unit width
p = absolute pressure, lb. per square inch
p = intensity of pressure in journal bearing
p_s = absolute pressure of saturated steam
p_{ss} = absolute pressure of supersaturated steam
p_{sv} = steam pressure before stop valve
p_{gv} = steam pressure before governor valve
p_o = steam pressure in first-stage nozzle box
p_e = exhaust steam pressure
p_m = mean circumferential pitch of blades
R = degree of reaction
R = radius of journal bearing
R = gas constant
R_u = universal gas constant
R = reheat factor
R_n = reheat factor for n stages
$R\infty$ = reheat factor for an infinite number of stages
r.h.p. = rim horse-power, or the power developed by the steam on the blades at the rim of the wheel
r = critical pressure ratio in nozzle flow
r radial clearance in journal bearing
S = degree of supersaturation
s.h.p. = shaft horse-power of a stage, i.e. the power transmitted by the wheel to the turbine spindle
T = absolute temperature
t = temperature in degrees Fahrenheit
U_1 = relative velocity of steam at inlet to blades
U_2 = relative velocity of steam at outlet from blades
u = mean peripheral velocity of blades

V = velocity
V_w = velocity of whirl
V_{ws} = velocity of whirl of dry steam
V_{wm} = velocity of whirl of moisture particles
v_s = specific volume of steam, cubic feet per lb.
v_w = specific volume of water, cubic feet per lb.
W = steam consumption of turbine, lb. per hour
W = work done
W_f = work done in opposing friction
w = steam flow through nozzles, etc., in pounds per second
w_i = total internal steam flow through turbine
w_n = steam flow through nozzles
w_g = steam flow through diaphragm gland
x = dryness fraction of steam
y = radial displacement of turbine wheel at any radius r
Z = coefficient of viscosity of lubricating oil

GREEK LETTERS

α = nozzle or jet angle
β_1 = blade inlet angle
β_2 = blade outlet angle
γ = absolute direction of steam leaving blades
Δ = maximum static deflection of turbine spindle, inches
ΔH = adiabatic heat drop in a stage
ϵ = eccentricity ratio of journal bearing $\left(\frac{e}{r}\right)$
η_c = thermal efficiency of cycle
η_t = thermal efficiency of turbine based on shaft work
η_r = efficiency ratio $= \left(\frac{\eta_t}{\eta_c}\right)$
η_n = nozzle efficiency
η_v = nozzle velocity coefficient
η_b = efficiency of blades
η_{gs} = gross stage efficiency
η_s = stage efficiency
η_i = internal efficiency of turbine
η_g = generator (alternator) efficiency
λ = circumferential length of nozzle arc, or in other cases, the fraction of the circumference covered by active nozzles
λ = percentage leaving loss, i.e. the ratio of the residual velocity loss to the adiabatic heat drop
μ = coefficient of friction in journal bearing
μ = coefficient of viscosity of steam
μ = number of rows of moving blades in velocity-compounded turbine

ρ = ratio of blade velocity to steam velocity
ρ_s = density of saturated steam
ρ_{ss} = density of supersaturated steam
σ = Poisson's ratio
σ = surface tension of water
ϕ = "carry-over" coefficient
ϕ = "attitude" of journal bearing
ϕ = entropy
ϕ_e = change of entropy during evaporation
ϕ_s = entropy of steam in any condition
ϕ_w = entropy of water

CHAPTER I

INTRODUCTION

1. THE steam turbine, in a crude form, is said to have been used many centuries ago, but its development as a really practical form of prime mover has only taken place during the last sixty years. To-day it stands as the most important prime mover in existence. It offers many advantages.

From a thermodynamic point of view the steam turbine occupies a favourable position, as it can translate into mechanical work a relatively large fraction of the heat energy rendered available by the expansion of the steam in the turbine. Its thermal economy is also fairly good, especially in turbines of large output and operating at fairly high pressures.

From the mechanical point of view, the turbine is ideal, because the propelling force is applied directly to the rotating element of the machine and has not, as in the reciprocating engine, to be transmitted through a system of connecting links which are necessary to transform efficiently a reciprocating motion into a rotary motion. Hence, since the steam turbine possesses for its moving parts rotating elements only, if the workmanship is good and the machine is correctly designed, it ought to be free from out-of-balance forces. In practice, a rotor weighing 20 tons or more and rotating at 1,500 revolutions per minute may be so well balanced that the motion, except for sound, is just perceptible. The significance of this statement may be appreciated when it is realized that if the same turbine rotor were out of balance to the extent of one pound at a radius of 4 ft., or in other words if the centre of gravity of the rotor were displaced only one-thousandth part of an inch from the axis of rotation, then the periodic force tending to produce vibration would be 3,070 lb. weight or 1·36 tons. When one considers that it is practically impossible to balance any reciprocating engine, the superior merits of the steam turbine in this respect are immediately apparent.

The impulses applied by the steam to the blades of a turbine come with such regularity and constancy that if the load applied to the machine is maintained constant, and therefore if the steam flow through the turbine is maintained at a steady value, the torque applied at the turbine coupling due to such impulses will be quite uniform. Therefore, if the turbine be employed to drive a machine which offers over a given period of time a sensibly constant resisting torque, the speed of the turbine and the driven machine will be very uniform.

Certain driven machines such as electric generators, centrifugal

pumps, centrifugal gas compressors, etc., when operating under steady conditions as regards output, offer a fairly constant resistance. Such machines are also essentially high-speed machines. Consequently the steam turbine is, from every point of view, eminently suitable as a prime mover for driving such machines.

The uniform turning moment and consequent uniform speed are also very desirable qualities for a prime mover required to drive certain textile machines.

A feature of considerable practical value is the entire absence of internal lubrication in steam turbines (excepting one or two small turbines). Two important advantages follow from this. In the first place, the exhaust steam is not contaminated with oil vapour and the condensed steam may be fed direct into the boilers without passing through filters. Furthermore, in certain industrial turbine plants where the whole or part of the turbine steam is used for some heating process, such steam is clean and may, in many cases, be used for direct heating. In the second place, there is a considerable saving in lubricating oil.

As the only parts of the turbine which require lubrication are the bearings supporting the rotor spindle, the governor shaft bearings and one or two gear wheels, and as there are no sliding parts, the amount of wear is negligible. The lubricating oil is circulated around the system, is cooled and filtered, and so may be used for long periods without replacement. Thus the cost of lubricating oil is negligible when compared with that for a steam engine of equal power.

The extensive use of electricity in the present age has brought into existence many large electricity generating stations. Economic considerations call for individual generating units of very large output. Similarly, the propulsion of vessels of large tonnage and at high speeds has called for machinery of such a power as would be quite beyond the possibilities of the reciprocating engine, steam or Diesel. These demands have been met with comparative ease by the steam turbine. The steam turbines of the ill-fated battle cruiser *Hood*, built in 1917, developed about 150,000 s.h.p. on 4 shafts and sent her 42,000 tons through the water at 31 knots. To-day, there are in central power stations turbines developing more than 100,000 kW, or nearly the total power of a modern battleship, on a single line of shaft.

2. Principle of Action of Steam Turbine. In the reciprocating steam engine, the pressure energy of the steam is utilized to overcome external resistances, and the dynamic action of the steam is negligibly small. Steam engines may be operated by using the full pressure without any expansion or drop of pressure in the cylinder. Such engines are said to work non-expansively. The steam turbine proper could not be operated in such a manner. The machine in which the pressure of steam is used for forcing round a rotating plate or similar device is a rotary engine and not a turbine

As a general statement, subject to the qualification that dynamic and static effects are always inter-related, it may be said that the steam turbine depends wholly upon the dynamic action of the steam. The steam is caused to fall in pressure in a passage or nozzle; due to this fall in pressure a certain amount of heat energy is converted into mechanical kinetic energy, and the steam is set moving with a greater velocity. The rapidly moving particles of steam enter the moving part of the turbine and here *suffer a change in direction of motion* which gives rise to a *change of momentum* and therefore to a *force*. This constitutes the driving force of the machine. The processes of expansion and direction-changing may occur once, or a number of times in succession, and may be carried out with differences of detail.

The passage of the steam through the moving part of the turbine, commonly called the blade, may take place in such a manner that the pressure at the outlet side of the blade is equal to that at the inlet side. Such a turbine is broadly termed an *impulse turbine*. On the other hand, the pressure of the steam at outlet from the moving blades of the turbine may be less than that at the inlet side of the blades; the drop in pressure suffered by the steam during its flow through the moving blades causes a further generation of kinetic energy within the blade and adds to the propelling force which is applied to the turbine rotor. Such a turbine is broadly termed an *impulse-reaction turbine*.

The majority of steam turbines have, therefore, two important elements, or sets of such elements. These are—

(1) *The Nozzle*, in which the steam expands from a high pressure and a state of comparative rest to a lower pressure and a state of comparatively rapid motion.

(2) *The Blade* or deflector, in which the stream of steam particles has its direction and hence its momentum changed. The blades are attached to the rotating element of the machine, or rotor; whereas, in general, the nozzles are attached to the stationary part of the turbine, which is usually termed the stator, casing or cylinder.

Although the fundamental principles on which all steam turbines operate are the same, yet the methods whereby these principles are carried into effect vary and, as a result, certain types of turbine have come into existence. We shall now attempt to classify the various types and give a very brief description of each.

3. **The Simple Impulse Steam Turbine** is shown diagrammatically in Fig. 1. The top portion of the figure shows a longitudinal section through the upper half of the turbine, the middle portion shows a development of the nozzles and blading, while the lower part of the diagram shows approximately how the absolute pressure and the absolute velocity of the steam vary from point to point during the passage of the steam through the turbine.

This type of turbine is termed a "simple" impulse turbine because the expansion of the steam takes place in one set of nozzles only. Generally the nozzle has a form similar to that shown in the sketch, Fig. 1, i.e. having a rounded entrance leading into a

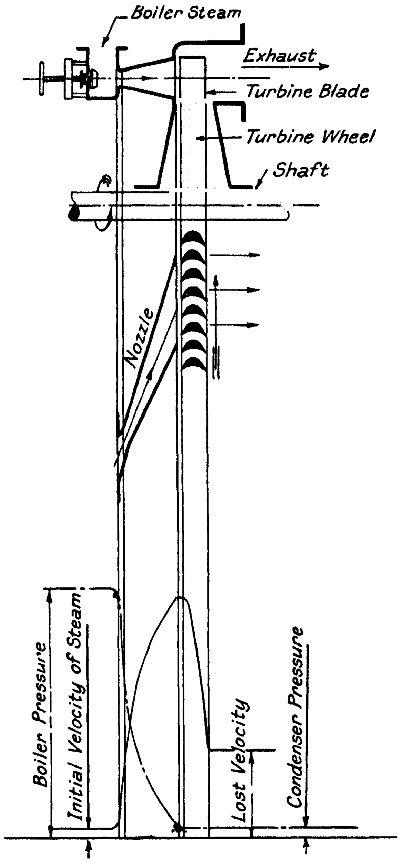


FIG. 1.—Diagrammatic Arrangement of Simple Impulse Turbine

constriction, termed the "throat," and a diverging outlet or mouth. The pressure of the steam falls from that in the steam chest to that existing in the condenser (or atmosphere, if the turbine is non-condensing), while the steam flows through the nozzle. Hence the pressure in the wheel chamber is practically equal to condenser pressure.

There is thus a relatively great ratio of expansion of the steam in the nozzles with the result that the steam issues from the nozzle

the total available energy. Consequently, the leaving loss in the pressure-compounded turbine is also only a fraction of that associated with the simple impulse turbine and is usually only about 1 or 2 per cent of the total available energy.

This type of turbine was developed by the late Professor A. Rateau, of Paris, on the one hand, and by Dr. Zoelly, of Zürich, on the other.

5. **Simple Velocity-compounded Impulse Turbine.** This type is shown diagrammatically in Fig. 3. It comprises a nozzle or set of nozzles and a wheel fitted with two or more rows of moving blades. The example shown in Fig. 3 has three rings of moving blades on the rotor and such a wheel is referred to as a "three-row wheel." There are also a number of guide blades, suitably arranged between the moving blades and set in the reverse manner. With a three-row wheel there are two rows of guide blades placed between the first and second and second and third rows of moving blades, respectively. These fixed guide blades need not necessarily extend around the full circumference of the casing. It is only necessary to arrange them roughly in front of the nozzle or nozzles but covering a somewhat larger arc of circumference than the nozzles themselves.

Steam entering the nozzle expands from the initial pressure down to the exhaust pressure. Thus, in general, the steam velocity is very high, as in the simple impulse turbine. The provision of two or more rows of moving blades, however, enables the blade velocity to be made appreciably less than would be necessary for the turbine having a single row of blades, it being assumed that the efficiency is the maximum in both cases. On passing through the first row of moving blades, the steam gives up only a part of its kinetic energy and issues from this row of blades with a fairly high velocity. It then enters the first of the two rows of guide blades and is re-directed by them into the second row of moving blades. There is a slight drop in velocity in the fixed guide blades due to friction In passing through the second row of moving blades the steam suffers a change of momentum and gives up another portion of its kinetic energy to the rotor. It is re-directed in the second row of guide blades, does work on the third row of moving blades, and finally leaves the wheel in a more or less axial direction with a certain residual velocity. This velocity is comparatively small, and hence the leaving loss is small, being about 2 per cent of the initial available energy of the steam.

For a fairly large pressure drop, say from 200 lb. per square inch absolute to 2 lb. per square inch absolute, the steam velocity is theoretically about 4,000 ft. per second. It will be shown later that with the ordinary nozzle arrangements used in practice, the most efficient speed of the blades for this type of turbine is about 0·15 of the steam speed. Thus, in this case, the blade speed would be

about 600 ft. per second, which is still fairly high. Generally speaking, owing to its low efficiency, this type of turbine having three rows of moving blades is used largely for small turbines driving auxiliary machinery. The two-row wheel is appreciably more efficient than the three-row wheel and, as will be shown later, is often incorporated in turbines of other types with advantage.

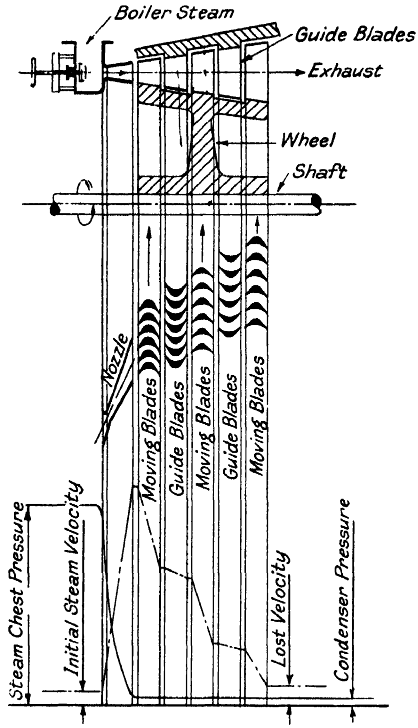


FIG. 3.—Diagrammatic Arrangement of Velocity-compounded Impulse Turbine

The turbine which has just been described and that to be described in the next paragraph were invented by the American engineer, Mr. C. G. Curtis.

6. Pressure-velocity-compounded Turbine. As has already been mentioned, the two-row wheel is more efficient than the three-row wheel. But for best economy it may be shown that the blade speed would have to be about 0·23 of the steam speed, or about 920 ft. per second. The construction of the wheel required to carry two rows of blades at this velocity would present some difficulty but is more or less possible, depending on the length of the blades. But an obvious way to reduce the blade velocity would be to split up the

available energy by having two or more simple velocity-compounded turbines in series on the same shaft. The total pressure drop is then effected in as many steps as there are wheels on the shaft, and hence the turbine is pressure-compounded as well as velocity-compounded. As in other types of impulse turbines, the steam is

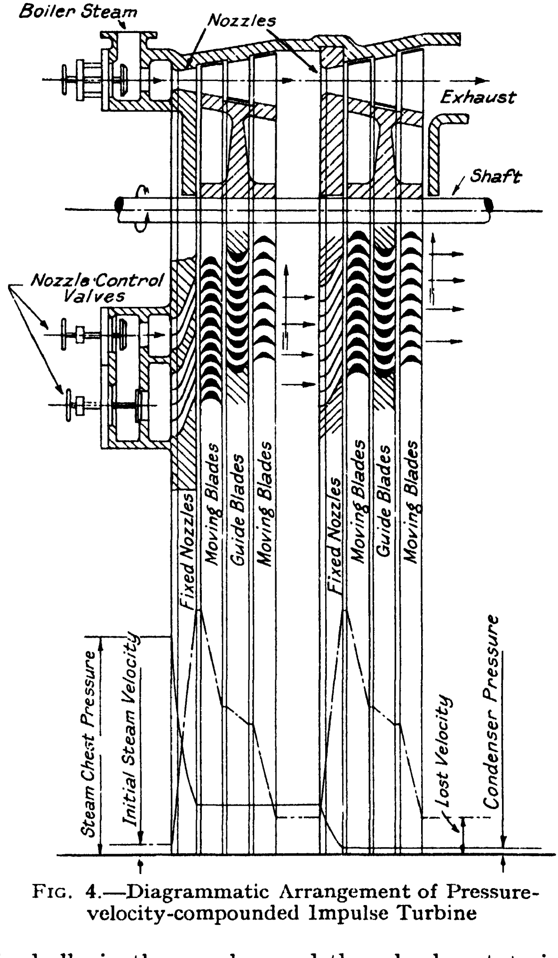


FIG. 4.—Diagrammatic Arrangement of Pressure-velocity-compounded Impulse Turbine

expanded wholly in the nozzles, and the wheels rotate in steam at constant pressure. Thus ample clearances are permissible in the radial direction, while the clearances in an axial direction should, from the point of view of efficiency, be kept as small as possible.

The middle portion of Fig. 4 is intended to show roughly how this and other types of impulse turbine may be controlled so as to give

the best efficiency under varying loads. It is well known that for high efficiency the difference between the initial pressure after the governor valve and the condenser pressure should be as great as possible. If governing is effected by throttling the steam, then at light loads the efficiency will be considerably reduced. In the diagram, Fig. 4, two sets of nozzles are shown, one set having 2 nozzles and the other 4 nozzles. Thus there are 6 nozzles in all, and for the sake of illustration we shall assume that the total power of the turbine is 60 h.p. Moreover, in order to simplify the explanation, let it be assumed that the steam delivered by each nozzle under the full pressure drop is sufficient to develop 10 h.p. Actually this assumption is not justified.

Then at full load, all 6 nozzles will be delivering steam at full pressure and the turbine will operate at maximum efficiency. Similarly, at 20 h.p. only 2 nozzles will be open, and at 40 h.p. only the set of 4 nozzles will be delivering steam, in both cases at the full pressure. Now suppose the horse-power required is only 30. The valve controlling the supply of steam to the group of 4 nozzles would have to be open, but there would have to be a certain amount of throttling of the steam, since at full pressure only 3 nozzles are required. Yet the efficiency will be higher than if the whole of the nozzles were in one group and the steam supply to that group were controlled by a single throttle valve. At 10 h.p., only the valve controlling the set of 2 nozzles would be open and there would be a certain amount of throttling.

The pressure-velocity-compounded turbine is comparatively simple in construction and is much more compact than the multi-stage pressure-compounded impulse turbine. Unfortunately, its efficiency is not so high. At one time it was widely used in power stations, but is now an obsolete type.

7. Pure Reaction Turbine. This type, which is illustrated diagrammatically in Fig. 5, comprises two or more radial tubes rotating on and communicating with another pipe or trunnion through which steam is supplied to nozzles which are screwed into the ends of the radial pipes, and arranged with their axes in the tangential direction.

Steam expands in the nozzles and issues with a certain velocity which is represented by the vector AB. If CD represents the peripheral velocity of the nozzle, then ED will represent the velocity of the steam relative to a fixed point at a given instant. Due to the change of velocity which occurs, there is a thrust or *reaction* on the rotating tube and tangential to it. This reaction constitutes the driving force, hence the name.

The pure reaction turbine is not a practical type, although efforts to develop it were made by the late Sir Charles A. Parsons.

8. Axial-flow Impulse-reaction Turbine. In this type of turbine we have a joint application of the impulse and reaction principles

of operation. There are a number of rows of moving blades attached to the rotor and an equal number of rows of fixed blades attached to the casing. The fixed blades correspond to the nozzles mentioned in connection with the impulse turbines. Steam is admitted for the whole circumference, and thus there is what is termed "all-round or complete admission." In passing through the first row of fixed blades, the steam undergoes a small drop in pressure and its velocity is somewhat increased. It then enters the first row of moving blades and, just as in the impulse turbine, it suffers a change in direction

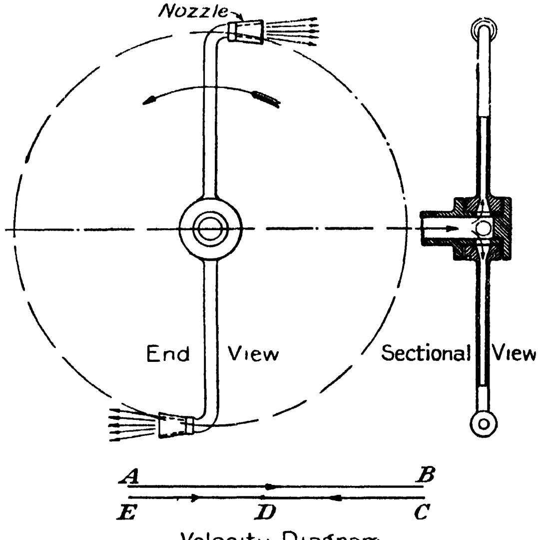


FIG. 5

and, therefore, of momentum. This gives rise to an impulse on the blades. During its passage through the moving blades, however, the steam undergoes a further small drop in pressure and, in consequence, there is a certain increase in steam velocity produced in the moving blade which gives rise to a reaction in the direction opposite to that of the added velocity. Thus the gross propelling force is the vector sum of the impulse and the reaction. This type of turbine is commonly termed a "reaction" turbine, although the term is not exact. It may here be reiterated that in the pure impulse turbine *no* expansion of the steam takes place in the moving blades.

The diagram given in Fig. 6 shows roughly how the blade heights increase as the specific volume of the steam increases with reduction in pressure; also how the pressure falls gradually as the steam passes through the groups of blades. It will be observed from the diagram

and also from the foregoing remarks that there is a pressure drop across each row of blades, fixed and moving. This is of considerable practical importance, especially at the high-pressure end of the turbine where the pressure drops are greatest, because this difference of pressure tends to force some steam through the clearance spaces

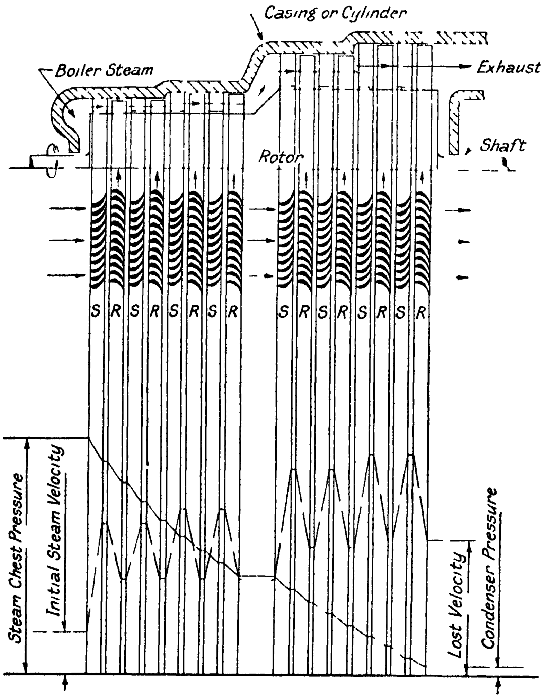


FIG. 6—Diagrammatic Arrangement of Axial flow Impulse-reaction or "Reaction" Turbine

between the moving blades and the casing and between the fixed blades and the rotor. The available energy possessed by this leaking steam is thus partly lost.

The steam velocities in this type of turbine are comparatively moderate, the maximum being, according to theory, about equal to the blade velocity. In practice, the steam velocity is commonly arranged to be greater than the blade velocity in order to reduce somewhat the total number of blade rows. The leaving loss for this type of turbine is normally about the same as for the multi-stage impulse turbine having single-row wheels. This type of turbine has been and continues to be very successful in practice. Its practical development was due to the genius and engineering skill of

the late Sir Charles A. Parsons. The turbine bears the name of its illustrious inventor.

9. **The Radial-flow Double-motion Reaction Turbine.** The turbines described hitherto, with the exception of the pure reaction turbine, have been of the axial flow type, i.e. the general direction

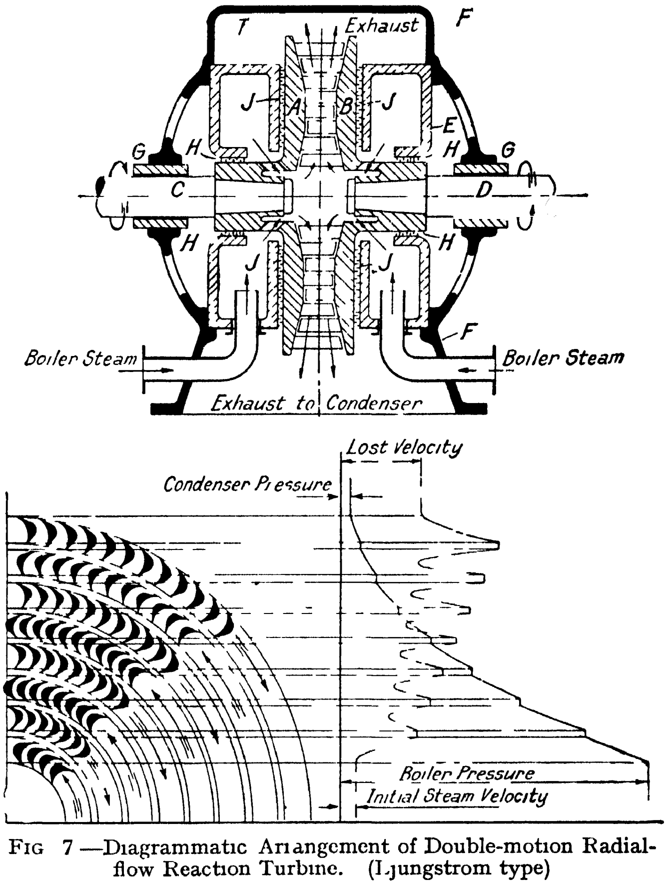


FIG 7—Diagrammatic Arrangement of Double-motion Radial-flow Reaction Turbine. (Ljungstrom type)

NOTE—In each ring of blades the blades extend round the complete circumference

of steam flow has been roughly parallel to the turbine axis. It is, however, possible to arrange the groups of blades in concentric rings and attached to the sides of separate discs. If one set of blades is stationary, then we have a single-motion radial-flow turbine. The steam may be arranged to flow from the centre outward or from the outside towards the centre. Assuming that such a turbine operates as an impulse-reaction (reaction) turbine, then the most

economical steam velocity from the blades in any stage is approximately equal to the peripheral velocity of the blades in that stage, and usually a fairly large number of stages is required.

Suppose now that the disc to which the fixed rings of blades are attached is arranged to rotate in the opposite direction to the moving blades, then the action will be generally the same as before except that the effective blade speed is doubled. Hence the steam velocity may be doubled and the turbine may, for a given size, be made more efficient. The practical construction of such a turbine presents many difficulties and is dealt with in a later chapter.

The diagram, Fig. 7, will serve to explain the main features of this type of turbine. Discs A and B are attached to the shafts C and D respectively, and these rotate in opposite directions. When this type of turbine is employed for driving electric generators, each of the shafts C and D drives a separate alternator at the same speed, the alternators running in parallel. E is the steam chest and F is the exhaust casing, from which the bearings G are suitably supported. Steam enters the steam chest E through two pipes leading from the side of the exhaust casing. The steam passes through a number of holes in the hollow shaft, as shown, and thus enters the centre space of the turbine. There is an impulse-reaction effect in every ring of blades except the first one, in which there is a reaction effect only. Special means are adopted to prevent leakage of the steam from the chest E. These means comprise an elaborate shaft packing at H to prevent leakage of steam to the atmosphere, and also concentric rings of labyrinth packing at J to prevent leakage from the steam chest into the exhaust space.

The practical representative of this type is the Ljungström turbine.

10. Combination Turbines. Any multi-stage turbine may be a combination of two or more of the types described above. Such a turbine is commonly referred to as a "combination" machine. Certain advantages which accrue to the use of two different types of turbine in the same machine will be dealt with in later sections of the book.

The most common combinations are—

(*a*) Velocity-compounded impulse wheel (or wheels) followed by several single-row impulse wheels. This is a combination of the Curtis and Rateau types.

(*b*) Velocity-compounded impulse wheel (or wheels) followed by several stages of impulse-reaction blading (Curtis-Parsons type).

(*c*) One or more single-row impulse stages followed by several stages of impulse-reaction blading (Rateau-Parsons type).

CHAPTER II

PROPERTIES OF STEAM

11. Introduction. For a study of the steam turbine from the thermodynamic point of view it is necessary to understand the various thermal properties of steam and water and also to have access to the values of those properties. Both liquid water and the dry and saturated vapour are complex substances, and their thermal properties are not related in any simple way. They can only be determined by experiment. Much painstaking experiment and research by investigators in many countries has been done in the past and the results of this work are usually embodied in carefully laid-out tables, known as Steam Tables.

Several such tables have been published from time to time. In many cases, the data given for high pressures have been obtained by a fairly extensive extrapolation of existing experimental data at normal steam pressures. In consequence, the tables differed from one another at the high-pressure end of the scale, and in making reports of tests it became necessary to specify the tables which had been used in making the calculations. Many of the tables were not thermodynamically consistent; a calculation made by using the tables in one way would not agree with another calculation having the same end in view, but utilizing the tables in a different way. The late Professor Callendar was the first to introduce a thermodynamically consistent table of properties, based on his own experimental work.

In recent years, investigators working in Great Britain, the United States, Germany, Czechoslovakia and Russia have met at five International Steam Table Conferences for the purpose of extending international agreement on the properties of steam. Such conferences have been held in London, 1929, in Berlin, 1930, in Washington, 1934, in Philadelphia, 1954, and again in London in 1956. New International Steam Tables (1)* were published in 1935.

The following steam tables have been published in recent years—

1. *The* 1939 *Callendar Steam Tables*. Compiled and edited by G. S. Callendar and A. C. Egerton, F.R.S. Published by Edward Arnold and Co., London. These tables extend to 3,200 lb. per sq. in. and 1,000° F. *The* 1939 *Heat-entropy Diagram for Steam* based on these tables and measuring 38 in. by 33 in. may be obtained from the same publishers.

2. *Abridged Callendar Steam Tables*. These are published in Centigrade or Fahrenheit units. By the late H. L. Callendar, revised by his son, Mr. G. S. Callendar. Fourth edition, published 1939 by Edward Arnold and Co.

* For literature and other references see the end of the chapter.

Unless otherwise stated, the problems set in the various parts of this book and involving the use of steam tables will be solved by using these tables.

3. *Thermodynamic Properties of Steam.* By Professor J. H. Keenan and Dr. F. G. Keyes. Published by John Wiley and Sons, Inc., New York. These tables were published in 1936 and extend to 5,500 lb. per sq. in. and 1,600° F. A large Mollier chart is included in a folder.
4. *VDI-Steam Tables.* By the late Dr. Ing. We Koch. The Fourth revised and amplified edition by Professor Ernst Schmidt was published in 1956 by Springer, Berlin, and extends to a pressure of 300 atm. and 800° C. (4,267 lb. per sq. in. and 1,472° F.).
5. *Thermodynamic Properties of Water Vapour.* By the Moscow Power Engineering Institute, in 1956. These extend to a pressure of 400 kg. per sq. cm. and 750° C. (5,689 lb. per sq. in. and 1,382° F.).
6. *Properties of Steam at High Pressures—An Interim Steam Table.* Published by the American Society of Mechanical Engineers. This interim steam table is an extension of the Keenan and Keyes steam tables into the region of 5,500 to 10,000 lb per sq. in. and 32 to 1,600° F.

12. Unit of Heat. In the centigrade system, the thermal unit is the *calorie.* If the pound is taken as the unit of mass, then the heat unit is the pound calorie; if the gramme is the unit of mass, then the corresponding heat unit is the gramme calorie, and so forth.

The calorie is then defined as the heat required to raise unit mass of pure water from a temperature t° C. to $(t + 1)$° C.

There are three such units, viz.—

(1) *The* 15° *C. gr. calorie* (t = 15° C.). This is equal to $4{\cdot}184 \times 10^7$ ergs. [1 erg = 1 dyne-cm.]

(2) *The* 20° *C. gr. calorie* (t = 20° C.). This equals $4{\cdot}180 \times 10^7$ ergs.

(3) *The mean calorie,* which is the $\frac{1}{100}$th part of the heat required to raise the temperature of 1 gr. of water from 0° C. to 100° C. According to Barnes (2), this is equal to $4{\cdot}184 \times 10^7$ ergs. Thus the mean calorie is equal to the 15° C. calorie.

Corresponding to the mean calorie, there is the *mean British Thermal Unit,* which is the $\frac{1}{180}$th part of the heat required to raise the temperature of 1 lb. of water from 32° F. to 212° F. This unit will be used throughout the book, except where otherwise stated.

Attempts have been made in recent years to express heat quantities in units which are independent of the physical properties of water. To this end the M.K.S. system, which uses the metre, kilogramme and second as the fundamental units, has been introduced. In this system the unit of force is that required to give unit mass of 1 kg. an acceleration of 1 metre per sec.^{2}; this unit is termed the Newton, and written N. Since 1 dyne gives a mass of 1 gr. an acceleration of 1 cm. per sec.^{2}, 1 N. = 10^5 dynes.

The unit of energy is the Newton-metre and is termed the joule, equivalent to 1 watt-second. In the same system of units, the

fundamental unit of pressure intensity is 1 N. per sq. metre. A more practical unit is the bar which is 10^5 N. per metre.[2] One bar is equivalent to 14·503 lb. per sq. in.

Temperatures are measured in accordance with the Kelvin

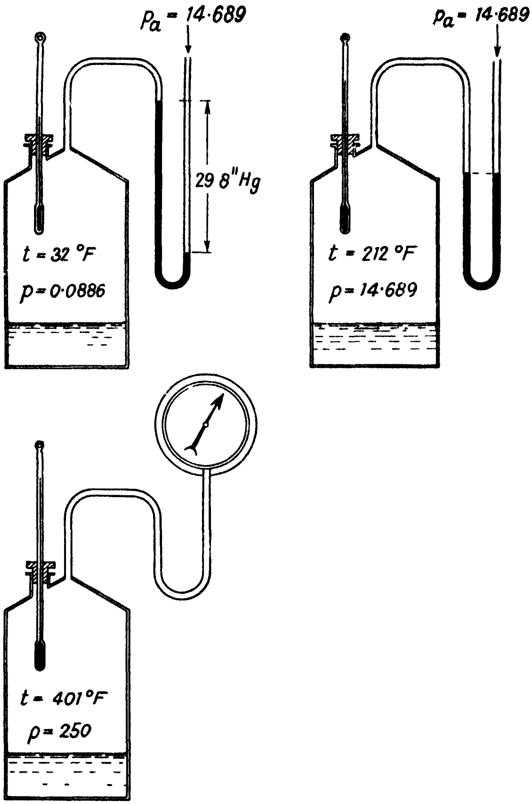


FIG. 8.—Diagram illustrating the Relationship between Temperature and Vapour Pressure

thermodynamic scale, the triple point of water being taken as 273·16° K.

Although internationally agreed steam tables might well be expressed in degrees C., bars and kilo-joules per kg., it is likely that, for many years, degrees F., lb. per sq. in. and B.Th.U. per lb. will continue to be used in this country.

The first International Steam Tables Conference formulated a heat unit to be termed *the international steam tables calorie* (written

I.T.Cal.) and defined as the $\frac{1}{860}$th part of the international kilowatt-hour. One international electrical watt = 1·0003 absolute watts. Then one mean B.Th.U. = 251·996 I.T.Cals., and one I.T.Cal. per gramme = 1·8 B.Th.U. per lb.

13. **Unit of Work.** This is the foot-pound, and is the work done in raising a mass of 1 lb. through a vertical distance of 1 ft. at sea-level in London. The acceleration of gravity, g, is there 32·19 ft. per sec. per sec.

14. **Heat and Work.** Heat may be partially converted into work and work into heat. In each case there is no loss of energy in the transformation and the rate of exchange of heat and work is such that

$$W = JH$$

where W = work done in ft.-lb.
H heat utilized or heat generated, in B.Th.U.
J = Joule's equivalent = 778·26.

15. **Relationship between Temperature and Vapour Pressure.** Consider a vessel, Fig. 8, partially filled with pure water and connected to a U-tube or a suitable pressure gauge, depending on the pressure to be measured. Assume that all gases are completely extracted from the space above the water. Then this space will be filled with water vapour which exerts a certain absolute pressure. It is found that this pressure depends on the temperature. For instance, assume first that the temperature is 32° F. and that the water is in the liquid state. Then it would be found that the pressure of the vapour would be 0·0886 lb. per sq. in. abs.

As the temperature is gradually raised, more and more of the water will be evaporated and the pressure exerted by the water vapour will gradually increase. Thus at 212° F. and at sea-level, the liquid in the manometer tube would stand at the same level in both limbs and the steam pressure would be 14·69 lb. per sq. in. abs. At 401° F., the vapour pressure would be found to be 250 lb. per sq. in. abs., the pressure indicated by a Bourdon gauge being 250 − 14·7, or 235·3 lb. per sq. in.

The relationship between temperature and vapour pressure continues up to a temperature known as the *critical temperature*, which is defined in the following manner. At all temperatures above the critical, it is impossible to liquefy water vapour by pressure, no matter how great the pressure employed. The critical temperature of water is 374·1° C. or 705·4° F. As the temperature approaches the critical, the vapour pressure also approaches a definite pressure known as the *critical pressure*. This may be defined as the vapour pressure of pure water at a temperature under but infinitely close to the critical temperature. The critical pressure of steam is about 3,206 lb. per sq. in. abs. Fig. 9 shows the variation of vapour pressure up to the critical point.

16. Sensible Heat of Water. This is defined as the amount of heat required to raise the temperature of unit mass of water to any given value. The liquid heat at the freezing point, 0° C. or 32° F., is normally taken as the arbitrary zero. Then the sensible heat at t° F. is the quantity of heat which must be added to unit mass of water to raise the temperature from 32° F. to t° F.

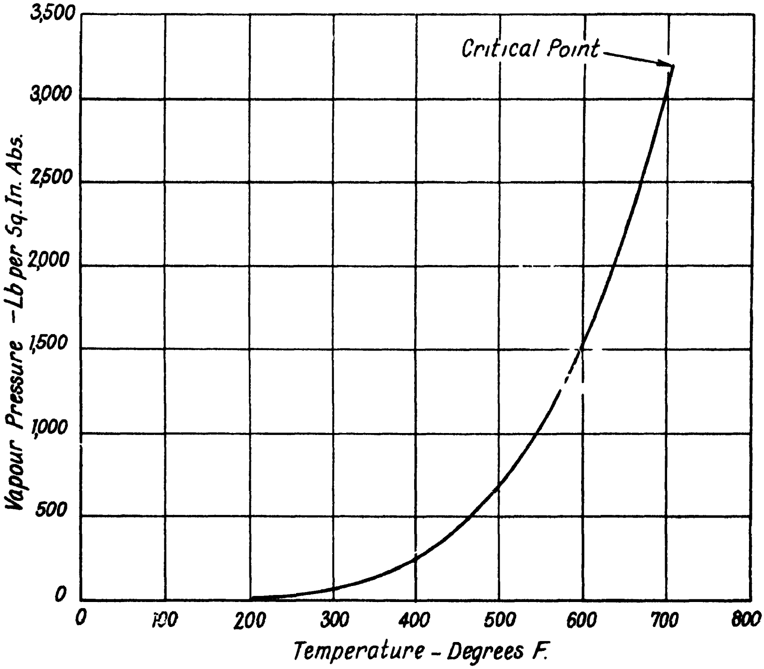


FIG. 9.—Vapour Pressure of Water

The specific heat C_w of water differs little from unity at low pressures, and for approximate calculations the sensible heat

$$h = t - 32 \text{ B.Th.U. per lb.}$$

For higher pressures, the increase in C_w with increasing temperature must be taken into account. For a small increase in temperature δt, the additional heat supplied is

$$\delta h = C_w \cdot \delta t$$

and for any range t_1 to t_2,

$$h_2 - h_1 = \sum_{t_1}^{t_2} C_w \cdot \delta t$$

Similarly, for any temperature $t°$ F., the sensible heat

$$h = \sum_{32}^{t} C_w \cdot \delta t$$

Dieterici (3) gives C_w as a function of t as follows—

$$C_w = 1{\cdot}00076 - 0{\cdot}00009855t + 0{\cdot}00000064t^2 \quad . \quad (1)$$

for temperatures between 95° F. and 572° F.

Callendar (4) gives

$$C_w = 0{\cdot}98415 + \frac{0{\cdot}9072}{t+4} + 0{\cdot}00002889t + 0{\cdot}000000278t^2 \ . \quad (2)$$

for temperatures between 32° F. and 392° F. Experimental values of C_w are shown in Fig. 10.

Actually, the heat which must be supplied to raise the temperature of unit mass of water varies, to a slight extent, according to the conditions under which the heat is supplied. This will be considered more fully in Art. 22.

17. **Latent Heat.** When, for example in a boiler, the temperature of the water has been raised to the saturation point corresponding to the pressure, the further addition of heat at constant pressure generates steam at constant temperature. The heat added during this process is termed latent heat because it is absorbed by the water without any change of temperature and so becomes "latent." More specifically, the latent heat of vaporization L is defined as the heat required to convert 1 lb. of water at the saturation temperature into 1 lb. of dry and saturated steam.

The latent heat diminishes as the saturation temperature is raised, as is shown by Fig. 11. The results arrived at by various investigators are seen to be in good agreement. At low pressures, the latent heat is given approximately by the simple linear relation—

$$L = 1{,}100 - 0{\cdot}63t \quad . \quad . \quad . \quad (3)$$

Up to a pressure of 100 lb. per sq. in. abs. the maximum deviation from the values given in the International Tables is under $\pm$ 0·5 per cent; at 250 lb. per sq. in. abs., the error reaches 2·7 per cent.

During the evaporation of water, the heat supplied is expended in two ways—

(1) In overcoming the external resistance to change of volume.

Assume that Fig. 12 (*a*) represents a cylinder fitted with a tight but frictionless piston, having an area of 1 sq. ft. The space underneath the piston is filled with 1 lb. of water at the saturation temperature corresponding to the steam pressure P lb. per sq. ft. Then the length of the cylinder occupied by the water will be v_w ft. When the water is heated and steam is being generated, the

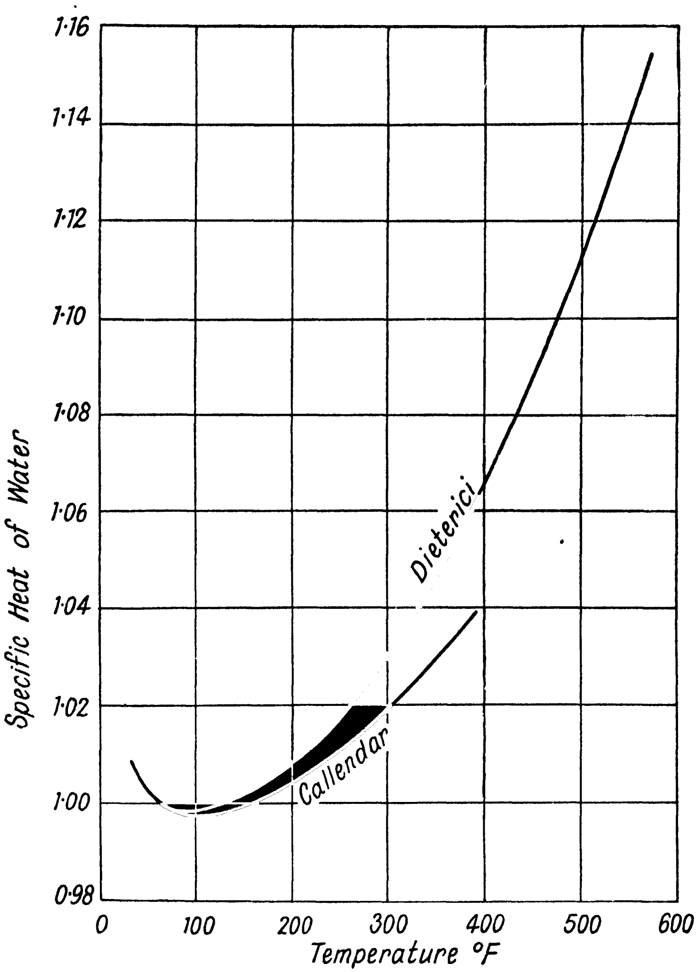


FIG. 10.—Specific Heat of Water

piston will rise; when the water has been entirely converted into dry and saturated steam, the volume occupied will be v_s. The external work done is clearly

$$P(v_s - v_w) \text{ ft.-lb. per lb.}$$

or

$$\frac{P}{J}(v_s - v_w) \text{ B.Th.U. per lb.} \quad . \quad . \quad . \quad (4)$$

(2) In overcoming the internal molecular resistance to change of state from saturated water to dry and saturated steam.

This is the change of internal energy E during evaporation, and equals $E_s - E_w$. Since, by the First Law of Thermodynamics,

$$\text{Heat supplied} = (\text{Gain of internal energy}) + (\text{External work done})$$

$$L = (E_s - E_w) + \frac{P}{J}(v_s - v_w)$$

or
$$E_s - E_w = L - \frac{P}{J}(v_s - v_w) \text{ B.Th.U. per lb.} \quad . \quad (5)$$

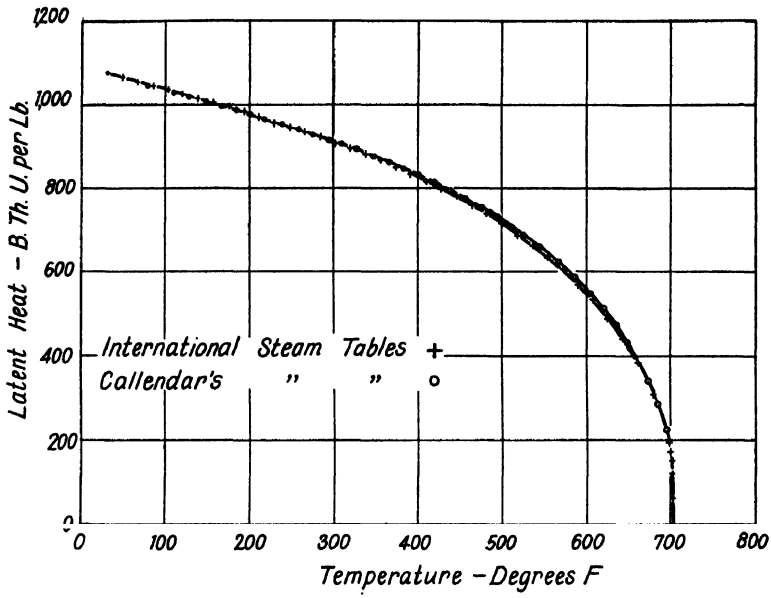


FIG. 11.—Latent Heat of Vaporization

EXAMPLE 1. Consider the generation of steam at 250 lb. per sq. in. abs. ($v_s = 1{\cdot}844$; $v_w = 0{\cdot}019$; $L = 826{\cdot}0$).

$$E_s - E_w = 826{\cdot}0 - \frac{144 \times 250}{778{\cdot}3}(1{\cdot}844 - 0{\cdot}019)$$

$$= 826{\cdot}0 - 84{\cdot}4$$

$$= 741{\cdot}6 \text{ B.Th.U. per lb.}$$

This shows that the bulk of the heat supplied is utilized in changing the internal energy of the substance.

18. Heat of Generation H. The heat required to generate unit mass of steam from unit mass of water at 32° F. may be termed the heat of generation. It is frequently called the total heat of the

steam, but as this term is sometimes (erroneously) used for another quantity which differs slightly in amount from the heat of generation, confusion is apt to arise.

$$H = \text{Sensible heat} + \text{Latent heat}$$
$$= h + L$$

19. Dryness Fraction. Steam which is taken from the steam drum of a boiler normally contains a small amount of water in the form of minute suspended drops. Then again, during the expansion of steam in the nozzles or blades of the turbine a certain amount of condensation takes place. This condensation is not due

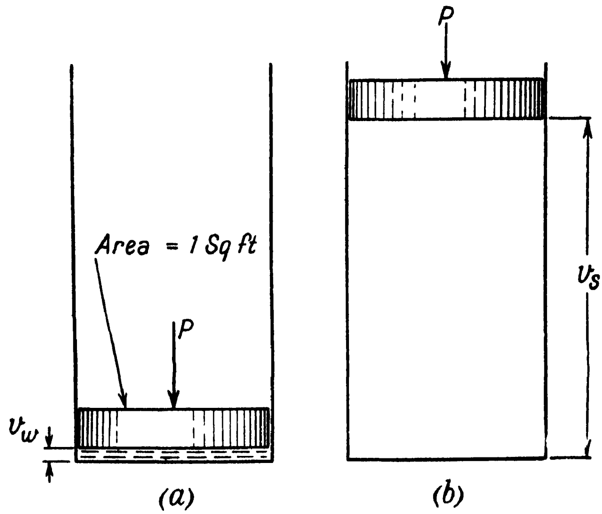


FIG. 12

to the cooling of the steam by the metal parts (since under a steady load these are at a sensibly uniform temperature) but, as will be shown later, is a natural result of the expansion. The steam condenses partially and a fine mist is formed. Such steam is said to be wet, and the mixture of dry steam and water is often referred to as "stuff." The dryness fraction x of the steam is defined as the ratio—

$$x = \frac{\text{Weight of dry steam}}{\text{Weight of stuff}}$$

The wetness fraction $1 - x$ is, similarly, the ratio of the weight of moisture to the total weight of steam and moisture.

The sensible heat of water is clearly independent of x. The heat required for the partial evaporation of 1 lb. of water is x times that required for the complete evaporation, i.e. xL.

$\therefore$ Heat of generation $= h + x\text{L}$

Initial volume of 1 lb. of water $= v_w$

Final volume of 1 lb. of stuff $= xv_s + (1 - x)v_w$

$\therefore$ Change of volume $= x(v_s - v_w)$

$\therefore$ External work done during the partial evaporation

$$= x \cdot \frac{\text{P}}{\text{J}}(v_s - v_w)$$

$$\therefore \text{E}_s - \text{E}_w = x\text{L} - \frac{\text{P}x}{\text{J}}(v_s - v_w)$$

$$= x\left\{\text{L} - \frac{\text{P}}{\text{J}}(v_s - v_w)\right\} \quad . \quad . \quad (5a)$$

20. Superheated Steam. Imagine again a cylinder, Fig. 13, having a cross-sectional area of 1 sq. ft. and containing a tight yet frictionless piston sustaining a constant load of P lb. weight and hence subjecting the water or steam to a pressure P lb. per sq. ft. The external pressure on top of the piston is assumed to be zero, so that the pressure P is absolute.

Consider case (*b*) where the steam is just dry and saturated. If a certain amount of heat equal to $(1 - x)\text{L}$ be abstracted from the steam while P is kept constant, some of the steam will condense and the volume will diminish (Fig. 13 (*c*)). If heat be again added, the suspended moisture will be evaporated at constant temperature, and once again the cylinder will contain 1 lb. of dry and saturated steam. If still more heat be added and the pressure be kept constant, the temperature of the steam will rise above the saturation temperature and the volume of the steam will increase to a value v'_s. Such steam is said to be "superheated." If the now superheated steam be gradually cooled, its temperature will fall steadily until the saturation temperature is again reached, when further cooling will cause condensation at constant temperature.

In practice, steam is superheated by heating it in a tubular superheater while the steam is actually flowing through the tubes and is not in close contact with the water in the boiler. In this case, the steam undergoes a slight pressure drop due to pipe friction, and the heating does not therefore take place at exactly constant pressure. But in many cases it is sufficiently accurate to assume that the steam is superheated at constant pressure.

The heat required to raise the temperature of 1 lb. of superheated steam by a small amount δt degrees when the steam is maintained at constant pressure is

$$\delta\text{H} = \text{C}_p \cdot \delta t$$

C_p being the instantaneous value of the specific heat of superheated steam at constant pressure for the given temperature and pressure.

The early measurements of C_p for steam at atmospheric pressure were made by Regnault (5) in 1862; he found that C_p was approximately equal to 0·48. It was many years after (1906) before the results of experiments at pressures different from atmospheric were published by Knoblauch and Jakob (6). Since then many other researches have been carried out. It is beyond the scope of this book to do other than refer to the variation of C_p with pressure and temperature. Recent measurements made at Munich by Knoblauch and Koch (7) are shown in Fig. 14. These values are for pressures ranging from 30 to 120 atmospheres (450 to 1,800 lb.

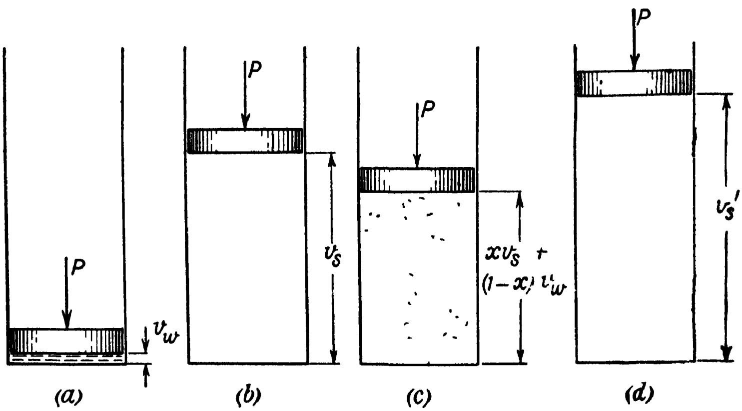


FIG. 13

per sq. in. abs.). It will be observed that the value of C_p is very high at the saturation point and falls rapidly as the temperature is increased. Similar curves based on differences between the values of the enthalpy of superheated steam published in Callendar's Revised (1939) Steam Tables are shown in Fig. 15. These values are appreciably lower than the values published by Knoblauch and Koch, and other authorities, but as the enthalpy values for dry and saturated steam published by Callendar are somewhat higher than those published by other workers, the agreement between the values of the enthalpy of superheated steam at the higher pressures is relatively good.

As C_p is variable, the total amount of heat required to superheat steam from the saturation temperature $t_{sat.}$ to some temperature t_s equals

$$H = \sum_{t_{sat}}^{t_s} C_p \,.\, \delta t$$

and is represented by the area ABCD, Fig. 14.

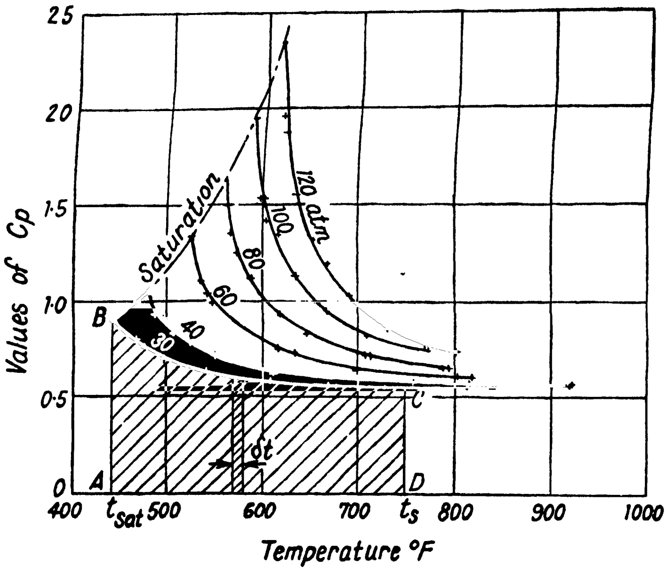


FIG 14 —Specific Heat of Superheated Steam
(*Knoblauch and Koch*)

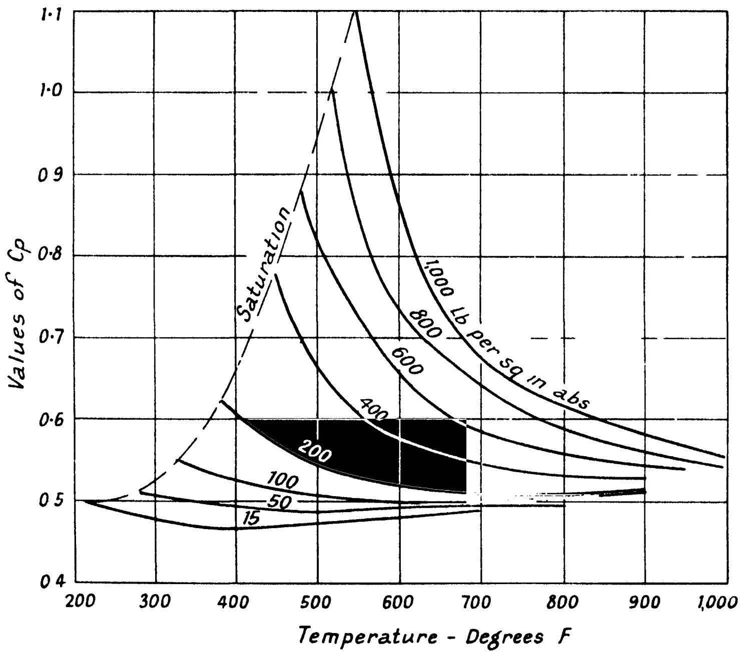


FIG 15 —Specific Heat of Superheated Steam
(*Callendar*, 1939)

The mean specific heat for the range of temperature $t_{sat.}$ to t_s is accordingly the heat supplied divided by the temperature rise, i.e.—

$$C_{pm} = \frac{\sum_{t_{sat}}^{t_s} C_p \,.\, \delta t}{t_s - t_{sat.}}$$

Values of C_{pm} calculated from Callendar's Tables are given in Fig. 16.

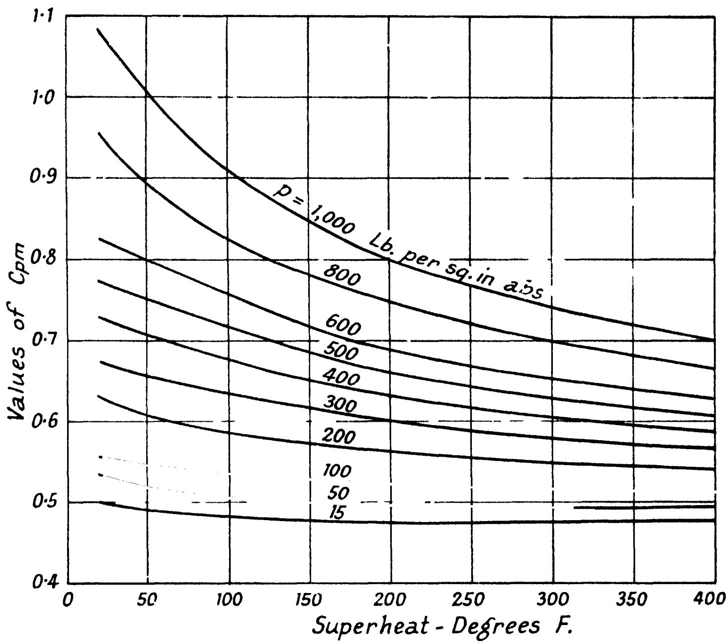


FIG. 16.—Mean Specific Heat of Superheated Steam

The external work done during superheating at constant pressure P lb. per sq. ft. is

$$\frac{P}{J}(v_s' - v_s) \text{ B.Th.U. per lb.}$$

Therefore, the change of internal energy during superheating

$$= C_{pm}(t_s - t_{sat.}) - \frac{P}{J}(v_s' - v_s)$$

21. The Enthalpy Function. The enthalpy of a substance is defined as the sum of the internal energy and the work done in forcing

unit mass of the substance into an enclosure at the constant pressure under which the substance exists.

Thus, suppose the specific volume of steam in any given condition is v_s and the pressure P. Then the enthalpy I per unit mass is

$$I = E + \frac{P \cdot v_s}{J} \quad . \quad . \quad . \quad . \quad (6)$$

As will be seen later, this is a most important quantity in steam turbine theory. The name given to this function by Mollier is "total heat," and the use of this somewhat unfortunate term has become so general in engineering work that it is doubtful whether any other term will ever be universally adopted. The term is apt to be confused with Regnault's term for the "total heat" of generation, and whilst the numerical difference between the two quantities is small at moderate pressures, there is a rather important distinction between them. The term "holotherm" has also been suggested for this function. The term "enthalpy," which was used in the first edition of this book, has been used in the recently published International Steam Tables (1). Callendar, in his work, used the term "total heat," and represents this by the symbol H for steam and h for water.

22. The Enthalpy of Water. For the purpose of tabulating values of the enthalpy of water or steam, the enthalpy of water at 32° F. is taken as the arbitrary zero.

Let v_o = volume per lb. of water at 0° C. or 32° F. ($v_o = 0{\cdot}01602$ cub. ft.).

v_w = volume per lb. of water at any pressure P lb. per sq. ft. abs.

Then
$$I_w = E_w + \frac{P \cdot v_w}{J} \quad . \quad . \quad . \quad . \quad (7)$$

At the freezing point

$$I_o = E_o + \frac{P_o v_o}{J}$$

and since I_o is arbitrarily taken to be zero, the internal energy E_o is negative and numerically equal to $\frac{P_o v_o}{J}$.

Since $P_o = 144 \times 0{\cdot}0886$, $E_o = -0{\cdot}00026$ B.Th.U. per lb. Actually, the internal energy of water at 32° F. is, of course, a large positive quantity; the apparently negative value follows from the employment of an arbitrary zero for I_w.

Further reference will now be made to the sensible heat of water. Consider the heating of unit mass of water from 32° F. to any temperature t_1° F., for which the vapour pressure is P_1. This heating may be carried out in a number of ways; only two methods will be considered.

(1) The water is first compressed (as in a feed pump) adiabatically from P_o to P_1 and is then heated at constant pressure from t_B to t_C (Figs. 17 and 18).

In any change of state, $dH = dE + \frac{P \cdot dv}{J}$.

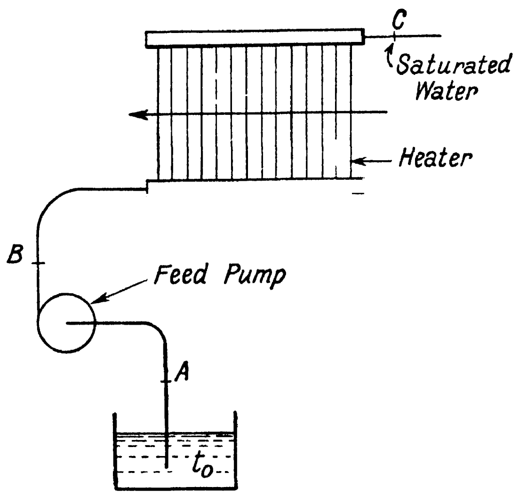


FIG. 17

Also, since
$$I = E + \frac{Pv}{J}$$
$$dI = dE + \frac{P \cdot dv}{J} + \frac{v \cdot dP}{J}$$
$$dI = dH + \frac{v \cdot dP}{J} \qquad (8)$$

From A to B, $dH = 0$, and dP is positive.

$$\therefore\ I_B - I_A = \frac{v_o}{J}(P_1 - P_o)$$

assuming that the specific volume v_o of the water remains constant during the pressure rise.

Then
$$I_B = I_A + \frac{v_o}{J}(P_1 - P_o)$$

From B to C, since $dP = 0$, $dH = dI$. Therefore the heat supplied is $I_C - I_B$, and since no heat is supplied between A and B, the whole of the sensible heat h supplied along the path ABC is

$$h_{ABC} = (I_C - I_A) - \frac{v_o}{J}(P_1 - P_o)$$

This type of heating process is the one normally used in practice. The pressure of the feed water is raised by the boiler feed pump to the boiler pressure P_1. The water is then forced into the boiler (or economizer, etc.) and heat is supplied to raise the temperature to the saturation point. It should be noted that the heat supplied

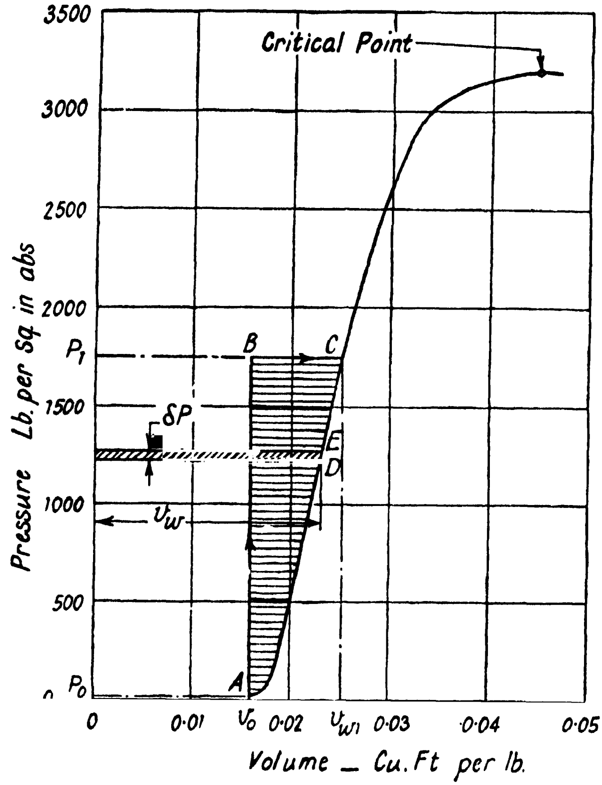


FIG. 18.—Specific Volume of Water

is less than the difference between the enthalpy values given in steam tables by the amount

$$\frac{v_o}{J}(P_1 - P_o)$$

For any exhaust pressure P_2 the values of P_2 and the corresponding specific volume v_{w2} may be substituted for P_o and v_o respectively.

(2) The water is kept in the saturated condition during the heating process. In other words, the pressure applied to the water at any instant is just equal to the vapour pressure corresponding to the

water temperature. The path of the condition point is then along the saturated liquid line ADC. This would be a difficult process to carry out.

Since for any small change of state

$$dH = dI - \frac{v\ dP}{J}$$

$$h_{ADC} = (I_C - I_A) - \frac{1}{J}\int_{P_0}^{P_1} v_w\ dP$$

Then $$h_{ABC} - h_{ADC} = \frac{1}{J}\int_{P_0}^{P_1} v_w\ dP - \frac{v_0}{J}(P_1 - P_0)$$

i e. the difference between the sensible heat along the path ABC and that along the path ADC is represented by the horizontally hatched area ABCDA. Values of $I_C - I_A$, h_{ABC} and h_{ADC} are given in the following table

p lb per sq in	$I_C - I_A$ $(I_A = 0)$	$\frac{v_0}{J}(P_1 - P_0)$	h_{ABC}	$\frac{1}{J}\int_{P_0}^{P_1} v\ dP$	h_{ADC}	$h_{ABC} - h_{ADC}$
14 7	180 1	0 0433	180 057	0 0446	180 055	0 0013
200	355 4	0 593	354 807	0 654	354 746	0 061
400	424 2	1 185	423 015	1 355	422 845	0 170
600	471 6	1 778	469 822	2 083	469 517	0 305
800	509 7	2 370	507 330	2 842	506 858	0 472
1 000	542 5	2 96	539 54	3 63	538 87	0 67
1 500	611 6	4 44	607 16	5 72	605 88	1 28
2 000	671 5	5 93	665 57	7 99	663 51	2 06
2 500	730 5	7 41	723 09	10 48	720 02	3 07
3 000	802 3	8 89	793 41	13 37	788 93	4 48
3,200	869 0	9 48	859 52	14 78	854 22	5 30

23. The Enthalpy of Steam. If the steam is dry and saturated (specific volume v_s) then the enthalpy (see eq 6)

$$I_s = E_s + \frac{P \cdot v_s}{J}$$

It has already been shown in Art 17 that

$$E_s = E_w + L - \frac{P\ v_s}{J} + \frac{P\ v_w}{J}$$

$$\therefore\ I_s = (E_w + L) + \frac{P\ v_w}{J}$$

$$= I_w + L \qquad . \qquad (9)$$

Consider the enthalpy function

$$I = E + \frac{Pv}{J}$$

Then $$\frac{dI}{dv} = \frac{dE}{dv} + \frac{P}{J} + \frac{v}{J}\cdot\frac{dP}{dv}$$

That is, for a small change of state

$$dI = dE + \frac{1}{J}(Pdv + v \cdot dP)$$

and when P is constant

$$dI = dE + \frac{P}{J} \cdot dv \quad . \quad . \quad . \quad . \quad (10)$$

But the heat supplied during a small change of state is

$$dH = dE + \frac{P}{J}dv$$

Therefore, when P is constant

$$dI = dH$$

and the gain of enthalpy is equal to the heat supplied. It follows, without further proof, that for wet steam

$$I_s = I_w + xL \quad . \quad . \quad . \quad . \quad (9a)$$

Similarly, if superheating takes place at constant pressure the enthalpy of the superheated steam is

$$I_s^1 = I_w + L + C_{pm}(t_s - t_{sat.}) \quad . \quad . \quad . \quad (11)$$

Thus, the enthalpy of steam in any condition is equal to that of water together with the heat supplied to convert 1 lb. of saturated water into steam with the given condition.

24. **Specific Volume of Steam.** If steam were a perfect gas, then the specific volume v_s, under all conditions of pressure and temperature, would be given by the well-known characteristic equation

$$v_s = \frac{RT}{P}$$

it being assumed that the steam is dry, i.e. either dry and saturated or superheated. The value of the "constant" R is given by the relation

$$R = \frac{J \cdot R_u}{m}$$

where R_u is the universal gas constant (1·985 heat units per degree) and m is the molecular weight of steam (18). Hence R for steam is 85·83 when T is expressed in degrees F. absolute.

The values of a quantity R^1 which is

$$R^1 = \frac{P \cdot v_s}{T}$$

have been calculated from Callendar's 1931 Tables for a few steam pressures and are shown in Fig. 19. This diagram shows clearly that steam behaves nearly as a perfect gas at low pressures, a fact which is borne out by the relative constancy of the specific heat at low pressures. But the curves also show clearly to what a remarkable extent the properties of steam deviate from those of a perfect gas, especially at and near the saturation point. It is apparent from Fig. 19 that the specific volume v_s is always less than the quantity $\frac{RT}{P}$ and by an amount which increases as P is increased,

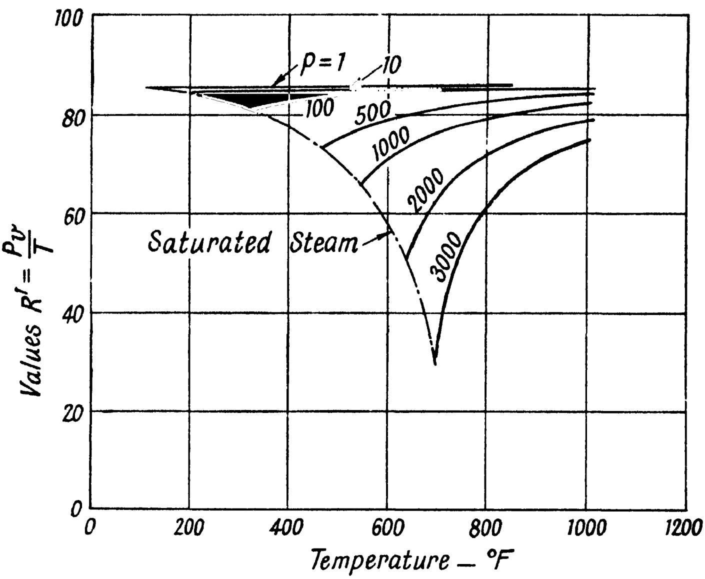


FIG 19.—Values of $\frac{Pv}{T}$ for Dry Steam

but which, at any given pressure, diminishes as T is increased. Therefore, the "equation of state" connecting P, v_s and T is likely to be of the form

$$v_s = \frac{RT}{P} - f(P, T)$$

where $f(P, T)$ represents some function of P and T. Several such equations have been proposed from time to time. As far back as 1867, Zeuner proposed the equation

$$P . v_s = 50{\cdot}93T - 192{\cdot}5 \sqrt[4]{P}$$

where P is the pressure in kg. per sq. m.
T is the temperature in degrees C. abs.
v_s is the volume in cub. m. per kg.

In British units (f.p. ° F.) this becomes

$$v_s = \frac{92{\cdot}8\text{T}}{\text{P}} - \frac{939}{\sqrt[4]{\text{P}^3}} \quad . \quad . \quad . \quad . \quad (12)$$

This equation gives results which agree fairly well with modern data at moderate pressures. It is extremely simple, but its very simplicity involves the use of an R value which is 8 per cent in excess of the theoretical value.

Professor Callendar (8) proposed the formula

$$v_s = \frac{\text{RT}}{\text{P}} - c + b \quad . \quad . \quad . \quad . \quad (13)$$

in which, with v_s in cub. ft. per lb., P in lb. per sq. ft., and T in degrees F. absolute, b is the volume of 1 lb. of water at 0° C., i.e. $b = 0{\cdot}01602$ cub. ft. The term c was called by Callendar the "co-aggregation volume" and represents the reduction in volume due to molecular association. The value of c is given as

$$c = 0{\cdot}4213\left(\frac{671{\cdot}6}{\text{T}}\right)^{\frac{10}{3}} \quad . \quad . \quad . \quad (14)$$

Hence $$v_s = \frac{85{\cdot}76\text{T}}{\text{P}} - 0{\cdot}4213\left(\frac{671{\cdot}6}{\text{T}}\right)^{\frac{10}{3}} + 0{\cdot}01602 \quad . \quad (15)$$

The specific volume of dry steam (superheated or supersaturated) is also given by the expression

$$v_s = 1{\cdot}2464\,\frac{(\text{I}_s - 835{\cdot}2)}{p} + 0{\cdot}0123$$

where I_s is the enthalpy of the dry steam, values being taken from the 1921 or 1930 Steam Tables or Diagrams.

Many years later, Professor Callendar carried out researches (9, 10, 11) on steam at pressures up to 4,000 lb. per sq. in. and at temperatures up to 950° F. He found that by slightly modifying the original equations they could be made to give the properties of steam for the full range of pressure.

The new form of the Callendar equation, used in the 1931 Callendar Steam Tables and the 1934 Abridged Callendar Steam Tables, is

$$v_s = \frac{85{\cdot}76\text{T}}{\text{P}} - \frac{c}{1 - \text{Z}^2} + b \quad . \quad . \quad . \quad . \quad (16)$$

where c has the value given in (14) above.

$$\text{Z} = 4{\cdot}0115 \,.\, \frac{c}{\text{T}} \text{ and } b = -\,0{\cdot}00280$$

Using values of I_s from the 1931 and 1934 Tables or from diagrams based thereon—

$$v_s = 1{\cdot}2464\,\frac{(I_s - 835{\cdot}2)}{p} - 0{\cdot}00212$$

In 1925, the late Dr. Mollier published his extended steam tables in which the equation of state is given as

$$v_s = \frac{85{\cdot}84T}{P} - \frac{227{\cdot}3}{\left(\frac{T}{100}\right)^{\frac{10}{3}}} - \frac{2{\cdot}72 \times 10^6}{\left(\frac{T}{100}\right)^{14}}\left(\frac{P}{100}\right)^2$$

where T is in degrees F. absolute, and P is in lb. per sq. ft.

More recent equations of state are even more complicated. For example, Koch's equation is

$$v = \frac{RT}{P} - \frac{A}{\left(\frac{T}{100}\right)^{2{\cdot}82}} - P^2\left[\frac{B}{\left(\frac{T}{100}\right)^{14}} + \frac{C}{\left(\frac{T}{100}\right)^{31{\cdot}6}}\right]$$

where A, B, and C are constants.

In most cases in practice, the specific volume will be found by direct reference to steam tables, or by interpolation from steam table data. In some cases, the required volumes may be read off the enthalpy-entropy diagram. But there are occasions when it is necessary to calculate v_s with some precision; the foregoing equations are then useful.

BIBLIOGRAPHY

(Except where otherwise stated, the figures given after each reference refer to year, volume number, and page respectively.)

1. INTERNATIONAL STEAM TABLES: *Engineering*, 1935; 140; 373. *The Engineer*, 1935; 160; 352.
2. BARNES: "The Absolute Value of the Mechanical Equivalent of Heat, in Terms of the International Electrical Units." *Proc. Royal Soc.*, 1909; 82; 390.
3. DIETERICI: "Ueber die Flussigkeitswärme des Wassers und das Mechanische Wärmeäquivalent." *Annalen der Physik und Chemie*, 1905; 16; 593.
4. CALLENDAR: "On the Variation of the Specific Heat of Water, with Experiments by a New Method." *Phil. Trans. Royal Soc.*, Series A, 1912; 212; 1.
5. REGNAULT: *Mém. de l'Inst. de France*, 1862; 26; 167.
6. KNOBLAUCH AND JAKOB: "Ueber die Abhängigkeit der spezifischen Wärme Cp des Wasserdampfes von Druck und Temperatur." *Forschungsarb., Berlin*, 1906; 35 and 36; 109.
7. KNOBLAUCH AND KOCH: "Die spezifische Wärme des überhitzten Wasserdampfes." *Zeits. des Ver. deutscher Ing.*, 1928; 72; 1733.
8. CALLENDAR: "Thermodynamical Properties of Gases and Vapours, deduced from a Modified Form of the Joule-Thomson Equation, with

special reference to the Properties of Steam." *Proc. Royal Soc.*, 1900; 67A; 266.
9. CALLENDAR: "Steam Tables and Equations, extended by Direct Experiment to 4,000 lb. per sq. in., and 400° C." *Proc. Royal Soc.*, 1928; 120; 460.
10. CALLENDAR: "Extended Steam Tables." *Proc. I. Mech. E.*, 1929; p. 507.
11. CALLENDAR: "Critical Relations between Water and Steam." *Proc. I. Mech. E.*, 1929; p. 811.
12. MOLLIER: *The Mollier Steam Tables and Diagrams.* Pitman, 1927.

EXAMPLES II

Note. In these and all other examples in this book, except where otherwise stated—

(1) Pressures are in lb. per sq. in. absolute.
(2) Specific volumes are in cub. ft. per lb.
(3) Data are taken from the 1939 edition of the *Abridged Callendar Steam Tables*.

1. Calculate the sensible heat of water at 400° F.—

(*a*) assuming the specific heat of water to be unity;

(*b*) assuming the value of C_w given by Dieterici's formula

$$C_w = 1{\cdot}00076 - 0{\cdot}00009855t + 0{\cdot}00000064t^2$$

(*c*) assuming the value of C_w given by Callendar's formula

$$C_w = 0{\cdot}98415 + \frac{0{\cdot}9072}{t + 4} + 0{\cdot}00002889t + 0{\cdot}000000278t^2$$

2. Water is heated from 32° F. ($v_w = 0{\cdot}016$) to 327·8° F. ($p = 100$, $v_w = 0{\cdot}0177$) at the constant pressure of 100 lb. per sq. in.
If the heat supplied during the process is 298·500 B.Th.U. per lb., calculate the change of internal energy.

3. Steam is generated at 100 lb. per sq. in. ($t_{sat.} = 327{\cdot}8$° F.) from water at 327·8° F. The specific volume of water at this temperature is 0·0177.
Calculate the following—

(*a*) the external work done;
(*b*) the change of internal energy.

4. 20 lb. of wet steam at $p = 250$ occupy 32 cub. ft. If the specific volume of water at 401° F. and 250 lb. per sq. in. is 0·0187, what is the dryness fraction of the steam? ($v_s = 1{\cdot}844$.)

5. The enthalpy of 1 lb. of dry and saturated steam at 500 lb. per sq. in. is 1,205·4 B.Th.U. per lb. What is the internal energy per lb. of steam and also per lb. of water? The specific volume of saturated water at $p = 500$ is 0·0197.

6. The exhaust steam from a turbine enters a surface condenser with a dryness fraction of 86 per cent. The absolute pressure in the condenser is 1 lb. per sq. in. If the final temperature of the condensate is 90° F., how much heat is rejected per lb. of steam? If the inlet temperature of the circulating water is 45° F. and the outlet temperature is 75° F., how many lb. of circulating water must be supplied per lb. of steam condensed? Assume that the specific heat of the circulating water is unity.

7. Steam is condensed in a tank containing 300 lb. of water initially at 45° F. The increase in the weight of water in a certain time is 10·8 lb. and the final temperature of the water is 80° F. Calculate the dryness fraction of the entering steam if its pressure is 200 lb. per sq. in. and if the heat loss from the tank during the period of condensation amounts to 540 B.Th.U.

8. One pound of steam, initially at 200 lb. per sq. in. and dry and saturated, is maintained at constant volume while its pressure falls to 100 lb. per sq. in. Derive the following—

(*a*) final condition of steam;
(*b*) heat rejected per lb. of steam.

The specific volume of saturated water at $p = 100$ is 0·0177 cu. ft. per lb

CHAPTER III

ENTROPY DIAGRAMS

25. The Entropy Function. Suppose that a small quantity of heat δH is added to unit mass of a substance during a small change of state. Suppose, moreover, that the said change of state is internally thermodynamically reversible. The absolute temperature T may remain constant, as, for example, during the evaporation of water at constant pressure, or the addition of the heat δH to the substance might produce a small increase in temperature δT, as, for example, during the heating of water below the saturation temperature. In the latter case, let δH be so small that δT is negligibly small compared with T. Then we may assume that T is sensibly constant. The function entropy is then defined by saying that the increase of entropy $\delta\phi$ is equal to

$$\delta\phi = \frac{\delta H}{T} \quad . \quad (17)$$

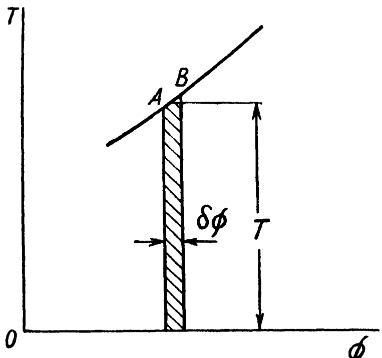


FIG. 20

If δH is positive, i.e. if heat is added, then the entropy increases; if heat is abstracted then δH and $\delta\phi$ are both negative.

The above expression shows that entropy, absolute temperature, and heat added are related in a very simple manner. Consider a diagram, Fig. 20, in which values of entropy are plotted horizontally and of the absolute temperature are plotted vertically. Let A and B be points representing two states of a substance and let the temperature difference between A and B be small, so that T is sensibly constant. Then since

$$\delta\phi = \frac{\delta H}{T}$$

$$\delta H = T \, . \, \delta\phi$$

and the area of the diagram which is cross-hatched therefore represents the heat supplied between the points A and B. It should be noted that the area under the curve AB must extend right down to the absolute zero of temperature.

Such a diagram is termed a temperature-entropy diagram, or T-ϕ chart. The T-ϕ chart for steam is a most useful instrument

for the study of problems associated with the generation and expansion of steam and will now be discussed.

26. The Temperature-entropy Diagram for Steam. Consider first the changes of entropy which take place during the heating of water. For a small rise in temperature δt or δT, the heat supplied to the water is $C_w . \delta T$, where C_w is the value of the specific heat of water at the existing temperature T.

Therefore, since $$\delta\phi = \frac{\delta H}{T}$$

$$\delta\phi_w = C_w . \frac{\delta T}{T}$$

and the total change of entropy in heating water from T_1 to T_2 would be

$$\phi_{w2} - \phi_{w1} = \sum_{T_1}^{T_2} \frac{C_w . \delta T}{T} \qquad . \quad . \quad . \quad (18)$$

It will be readily understood that the change of entropy calculated in this manner will be somewhat approximate, depending on the temperature increment δT which is chosen in making the calculation. The smaller the increments δT, the more accurate the result would be.

If the specific heat of water be assumed to be unity, as it may be for low pressures without incurring any appreciable error, then the change of entropy of water may be calculated as follows—

$$\delta\phi_w = \frac{\delta T}{T}$$

$$\therefore \phi_{w2} - \phi_{w1} = \int_{T_1}^{T_2} \frac{1}{T} . dT = \log_e \frac{T_2}{T_1} \qquad . \quad . \quad (19)$$

For the purpose of tabulating values of the entropy of water and steam in steam tables, it is customary to assume that the entropy of saturated water is zero at 32° F., i.e. when T = 492° F. abs. Accordingly, at T° F. abs.—

$$\phi_w = \log_e \frac{T}{492} \text{ (approx.)} \qquad . \quad . \quad . \quad (20)$$

If it is assumed that the specific heat of water may be represented by an equation of the form

$$C_w = a + bT + c . T^2$$

where a, b, and c are constants, then

$$\delta\phi_w = \left(\frac{a}{T} + b + cT\right)\delta T$$

and $$\phi_w = \int_{492}^{T} \left(\frac{a}{T} + b + cT\right) dT$$

$$= a \log_e \frac{T}{492} + b(T - 492) + \frac{c}{2}(T^2 - 492^2)$$

Dieterici's equation (1), Art. 16, is of this form. As already stated, it would give results which are reasonably correct up to 572° F. At still higher temperatures, the specific heat of water increases still further so that the slope of the liquid line on the T-ϕ diagram,

i.e. $$\frac{dT}{d\phi} = \frac{T}{C_w}$$

becomes smaller and smaller as the critical point is approached.

The variations of entropy during the heating of water from 32° F. to the critical point (705° F.) are shown by the curve ABC, Fig. 21. The deviation from the curve $\phi_w = \log_e \frac{T}{491 \cdot 6}$ (based on the assumption of unit specific heat) at the higher temperatures should be noted by the student.

At any absolute temperature T, the area under the curve AB represents, to some scale, the amount of sensible heat supplied to raise the water from 491·6 degrees absolute to T degrees. Thus, if 1 in. = ϕ units of entropy and 1 in. = T units of temperature, then 1 sq. in. = T × ϕ B.Th.U. per lb.

The entropy change during evaporation at constant pressure is easily calculated because the temperature T is then constant. If the evaporation is complete, the change of entropy

$$\phi_e = \frac{L}{T} \quad . \quad . \quad . \quad . \quad . \quad . \quad (21)$$

Thus, from Callendar's Tables, at 300 lb. per sq. in., t = 417·3° F. or 877·0 degrees absolute, and L = 809·8.

$$\therefore \phi_e = \frac{809 \cdot 8}{877 \cdot 0} = 0 \cdot 9233$$

If at any temperature T the entropy change BD during evaporation at T be added to the entropy of saturated water, then a point D is obtained which represents dry and saturated steam at temperature T. As the temperature is increased L diminishes and therefore ϕ_e diminishes, until at the critical point where L = 0, ϕ_e also becomes zero. The area MBDN under the line BD is clearly

$$T \times \phi_e = T \times \frac{L}{T} = L$$

and is therefore the heat supplied during evaporation. The locus of such points as D is termed the "saturation curve" or "dry steam line."

If the evaporation is partial and x is the dryness fraction, then the increase of entropy is

$$\frac{xL}{T} = x \cdot \phi_e$$

Thus the point E represents the state of steam at T and having a dryness fraction of 0·7, the point E dividing BD such that $\frac{BE}{BD} = 0{\cdot}7$. The locus of points such as E is a curve passing through the critical point C and representing a constant dryness fraction of 70 per cent.

The changes of entropy during superheating at constant pressure may be calculated in the following manner. Suppose that unit mass of steam is heated from temperature T to T + δT, and let C_p be the specific heat for the given pressure P and for the mean temperature T + $\frac{1}{2}\delta$T. Then the heat supplied is $C_p \cdot \delta T$ and the small increase in entropy

$$\delta\phi = C_p \cdot \frac{\delta T}{T}$$

The total change of entropy from the saturation temperature $T_{sat.}$ degrees absolute to any superheat temperature T_s could be found by the arithmetical integration

$$\phi_s - \phi_{sat.} = \sum_{T_{sat.}}^{T_s} C_p \cdot \frac{\delta T}{T} \quad . \quad . \quad . \quad (22)$$

By plotting the total entropy of superheated steam against the superheat temperature, the constant-pressure line DF is obtained. The vertical height from D to F is clearly the degree of superheat at F, and the shaded area NDFR represents the heat supplied during superheating.

The entropy of superheated steam should always be obtained from reliable steam tables or steam diagrams. The change of entropy during superheating may be calculated *approximately* by assuming a mean specific heat C_{pm} for the given range of temperature. Then the change of entropy is

$$\phi_s - \phi_{sat.} = C_{pm} \int_{T_{sat.}}^{T_s} \frac{1}{T} \cdot dT$$

$$= C_{pm} \cdot \log_e \frac{T_s}{T_{sat.}} \qquad (23)$$

It is assumed here that the *entropy-mean specific heat* is equal to the *temperature-mean specific heat,* which is not quite correct. The error made in such an approximation will be greater at higher pressures than at lower pressures, because of the greater variation in the specific heat at higher pressures. The error involved is not so serious as might at first be thought, as the following data show.

STEAM AT A PRESSURE OF 1,000 LB. PER SQ. IN.

Degree of superheat (° F.)	40	100	200	400
Temp.-mean specific heat, C_{pm} (Fig. 16)	1·0275	0·911	0·802	0·700
$C_{pm} \log_e \frac{T_s}{T_{sat.}}$	0·0401	0·0865	0·1456	0·2347
Entropy change derived from *Callendar's Abridged* (1939) *Steam Tables*	0·0398	0·0863	0·1465	0·2387
Error	0·0003	0·0002	0·0009	0·0040
Percentage error	0·75	0·23	0·61	1·68

If in Fig. 21 the lines GH and JK are lines of constant pressure for pressures lower than that represented by DF, and if the points F, H, and K all represent a constant degree of superheat, e.g. 150° F., then the curve FHK is known as a constant superheat line.

Curves of constant volume may be drawn on the T-ϕ diagram in the following way. Suppose, for example, it is desired to draw a constant-volume line to represent 2 cub. ft. per lb. A reference to the Callendar Tables shows that for dry and saturated steam

$$v_s = 2{\cdot}042 \text{ when } p = 225 \text{ and } T = 851{\cdot}5$$
$$v_s = 1{\cdot}999 \text{ when } p = 230 \text{ and } T = 853{\cdot}4$$

A simple linear interpolation gives

$$v_s = 2{\cdot}00 \text{ when } p = 230{\cdot}12 \text{ and } T = 853{\cdot}36$$

Then the point S on the saturation curve at T = 853·36 represents the condition of steam having a specific volume of 2·00 cub. ft. Consider a lower pressure, e.g. $p = 100$. Since the specific volume of dry and saturated steam is 4·434 cub. ft. per lb., it is clear that the steam must be wet to have a volume of only 2 cub. ft.

Then $$x \,.\, v_s + (1 - x)v_w = 2{\cdot}00$$

and since $v_w = 0{\cdot}0177$

$$4{\cdot}434x + 0{\cdot}0177 - 0{\cdot}0177x = 2{\cdot}00$$

from which $x = 0{\cdot}449$. This condition is represented by the state point T ($p = 100$, T = 787·5). Other points may be obtained in the same manner and a curve ST drawn.

If a pressure somewhat higher than 230·12 be considered, then, since the specific volume of dry and saturated steam is less than 2 cub. ft., it is clear that the steam must be mcre or less highly superheated. The precise temperature for any pressure may be

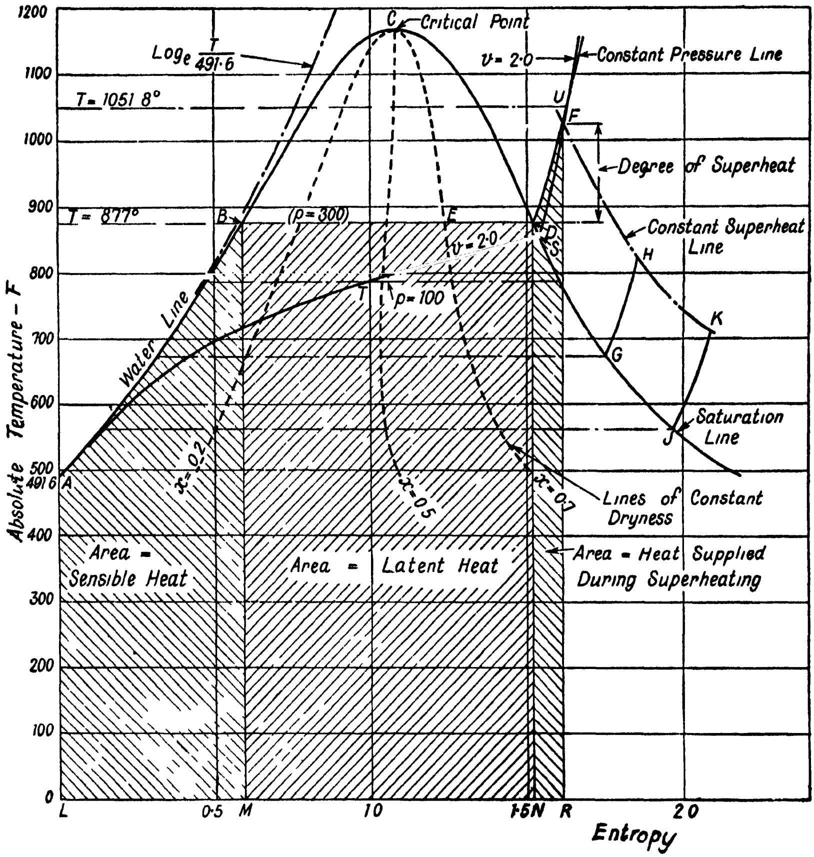


FIG. 21 —T-ϕ Diagram for Water and Steam

found by using the Callendar equation of state (15), or by interpolation from the Revised Callendar Tables. Thus, at the pressure of 300, the temperature corresponding to the volume of 2·00 cub. ft. per lb. is 592·2° F. or 1,051·8° abs. This state is represented by the point U and the complete "constant-volume" curve for $v = 2{\cdot}00$ is the discontinuous curve TSU.

27. The Enthalpy-entropy Diagram. In this diagram, proposed by the late Dr. Richard Mollier, of Dresden, and usually known as the Mollier diagram, the co-ordinates are entropy ϕ and enthalpy I.

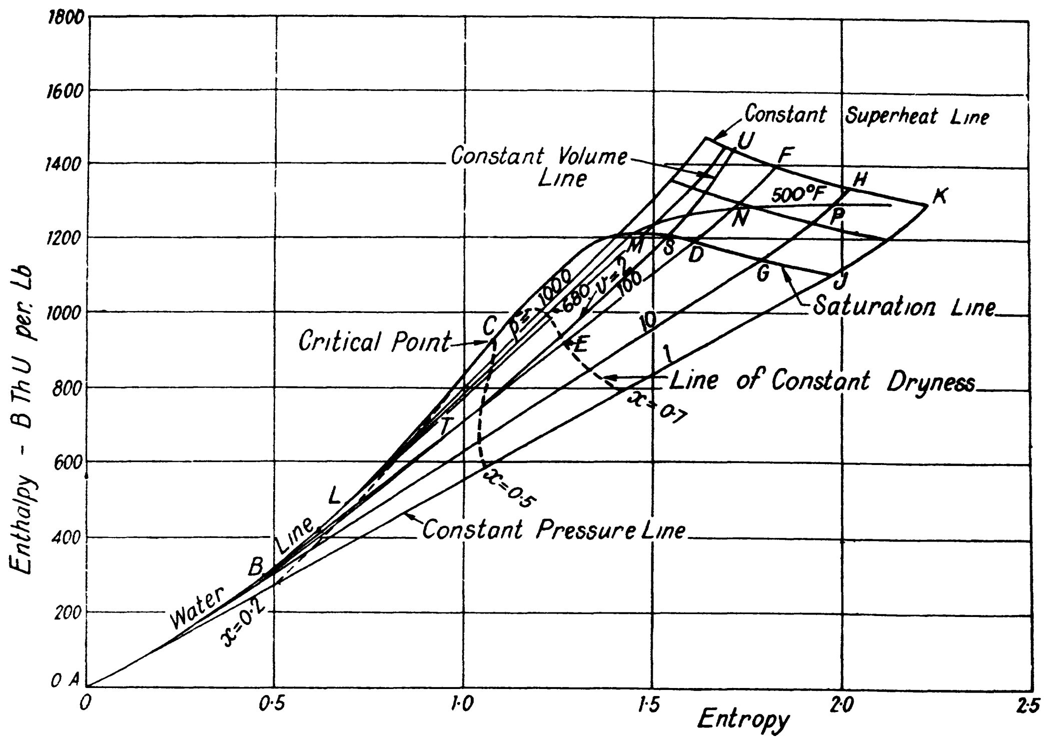


FIG. 22.—Mollier Diagram for Steam

A skeleton diagram for steam is shown in Fig. 22. The origin A represents zero entropy and zero enthalpy, corresponding to the state of water at 32° F. and under a pressure of 0·0886 lb. per sq. in. abs. Point B represents saturated water at 100 lb. per sq. in. abs. ($\phi_w = 0{\cdot}4742$; $I_w = 298{\cdot}5$). The locus of points such as B plotted up to the critical point C is the water line ABC. Point D represents dry and saturated steam at 100 lb. per sq. in. ($\phi_s = 1{\cdot}6038$; $I_s = 1188{\cdot}2$), and the locus of points such as D is the saturation line CDGJ. Since the value of I_s at the critical point is appreciably less than that at lower pressures (I_s is a maximum at about 450 lb. per sq. in., according to Callendar's Tables), the critical point is well removed from the peak of the curve, as is evident from Fig. 22.

Consider now the movement of the state point during evaporation at a pressure of 100 lb. per sq. in. abs. The initial state point is B. For any dryness fraction x, the increase in I is

$$I_s - I_w = xL$$

and the increase of entropy $\frac{xL}{T}$.

Therefore, since T is constant the increase in enthalpy is proportional to the increase in entropy, i.e. the evaporation line BD is straight. Moreover, the slope of the line is

$$\frac{I_s - I_w}{\phi_s - \phi_w} = xL \times \frac{T}{xL} = T$$

This relationship between the slope of the constant-pressure lines and temperature may be shown more generally. In Art. 23 it is shown that when P is constant

$$(dI)_p = dH = T\,.\,d\phi$$

$$\therefore \left(\frac{dI}{d\phi}\right)_p = T \qquad \text{(24)}$$

Thus all constant-pressure lines are straight in the wet region (P and T constant) and the slope of a high-pressure line is greater than that of a low-pressure line.

If lines such as BD are divided in the ratio of, say, 7 to 10, then a curve through the dividing points becomes a curve of constant dryness or quality. All such curves run to the critical point.

The constant-pressure lines may be produced into the superheat field. Since $\frac{dI}{d\phi} = T$, and T is increasing, the constant-pressure lines are now curved. If points F, H, and K be taken on different constant-pressure lines for the same degree of superheat (400° F.), then the curve drawn through such points is a curve of constant superheat.

Isothermals may be drawn in the following manner. Suppose, *for example, it is desired to draw an isothermal for 500° F. The* vapour pressure at 500° F. is 680 lb. per sq. in. abs. Therefore all points on the line LM (680 lb. per sq. in.) in the wet steam region are on the required isothermal. Consider now the pressures 100 and 10 lb. per sq. in.

Steam Pressure	Saturation Temperature	Superheat when $t = 500°$ F.
100	327·8° F.	172·2° F.
10	193·2° F.	306·8° F.

Then if points N and P be taken on the lines for $p = 100$ and $p = 10$ respectively, to represent superheats of 172·2° F. and 306·8° F. respectively, the curve MNP will be part of the required isothermal. The discontinuous line LMNP represents the complete isothermal.

Constant-volume lines, such as TSU (drawn for 2·0 cub. ft. per lb.), may be set out in the manner described in Art. 26 for the constant-volume lines on the T-ϕ chart.

The ϕ-I diagram is, without a doubt, the most useful chart ever devised for the solution of problems connected with the theory and the design of steam turbines. For practical purposes, it is usual to use the upper part of the diagram only.

28. T-ϕ and ϕ-I Diagrams for Compressed Water. In steam power plants using high-pressure steam the feed water is compressed by the boiler feed-pump to a high pressure. This compression modifies, to a slight extent, the thermodynamic properties of the water. It has been already shown in Art. 22 that the compression of the feed water to a high pressure modifies the amount of heat which must be supplied.

It is beyond the scope of this book to explain how the changes in entropy and enthalpy during isothermal compression may be calculated, but the nature of the changes may be followed from Figs. 23 and 24, based on an article (1) by the author and the Keenan and Keyes Steam Tables (2). Fig. 23 shows the T-ϕ diagram. The dotted line represents the boundary curve ABCDJ of Fig. 21. It should be noted that the curve ABC of Fig. 21 represents the relationship between the absolute temperature and the entropy of *saturated* water, i.e. water at the saturation temperature corresponding to the existing pressure. In Fig. 23, the line AB represents water at a pressure of 1,000 lb. per sq. in. abs. The point B coincides with the saturation line at an absolute temperature of 1,004·3 degrees and again near the freezing point. The deviation from the saturation line is very small and has been purposely exaggerated in the figure.

Suppose now that water enters a feed pump at a temperature of 100° F. and at the corresponding pressure $p = 0·95$. Its condition is represented by the point K. The adiabatic compression of the water to $p = 1,000$ would be represented by the vertical line

KL, and during the subsequent heating to 544·7° F., the condition point would move along the curve LB. The figure given in the last column of the table in Art. 22 is represented by the small area between KLB and the curve KB. In Fig. 23, the full line AEF represents water and steam at the critical pressure, and AGH water and steam at 4,000 lb. per sq. in. abs. The parts of the curves

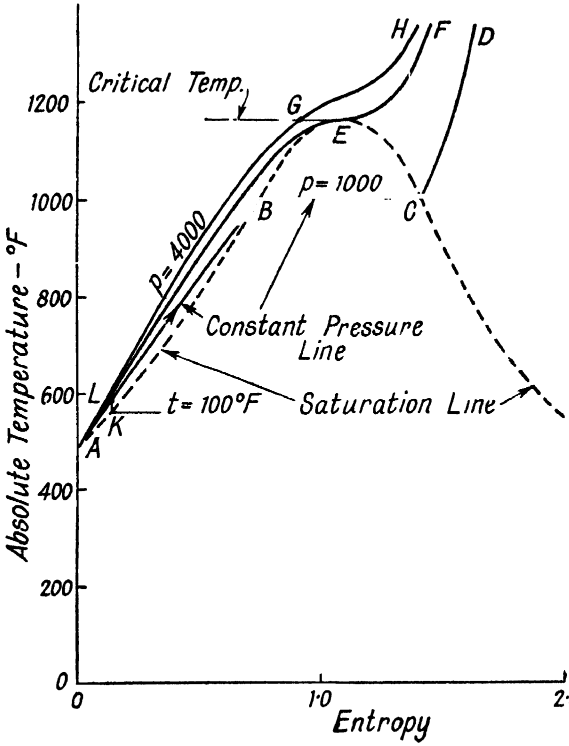


FIG 23—Sketch of T-ϕ Diagram for Compressed Water and Steam

lying below the critical temperature represent water in the liquid state, those parts above represent steam.

The ϕ-I diagram for compressed water is shown in Fig. 24. The dotted line OBE shows the relationship between I and ϕ for saturated water. Curve AB shows the same relationship for water at a pressure of 1,000, and it coincides with the saturated water line at the point $\phi = 0{\cdot}7432$ and $I = 542{\cdot}6$, but at no other point. Curve ABCD shows the complete constant-pressure line for $p = 1{,}000$. Similarly, A_1EF represents water and steam at the critical pressure, and A_2GH water and steam at $p - 4{,}000$.

Consider again the adiabatic compression of feed water from the

temperature of 100° F. to a pressure of 1,000 lb. per sq. in. The initial condition is represented by the point K on the saturation line, the compression by the adiabatic line KL, and the subsequent heating to the saturation point B by the curve LB.

It has been shown in Art. 22 that the increase in enthalpy

$$dI = dH + \frac{v \, . \, dP}{J}$$

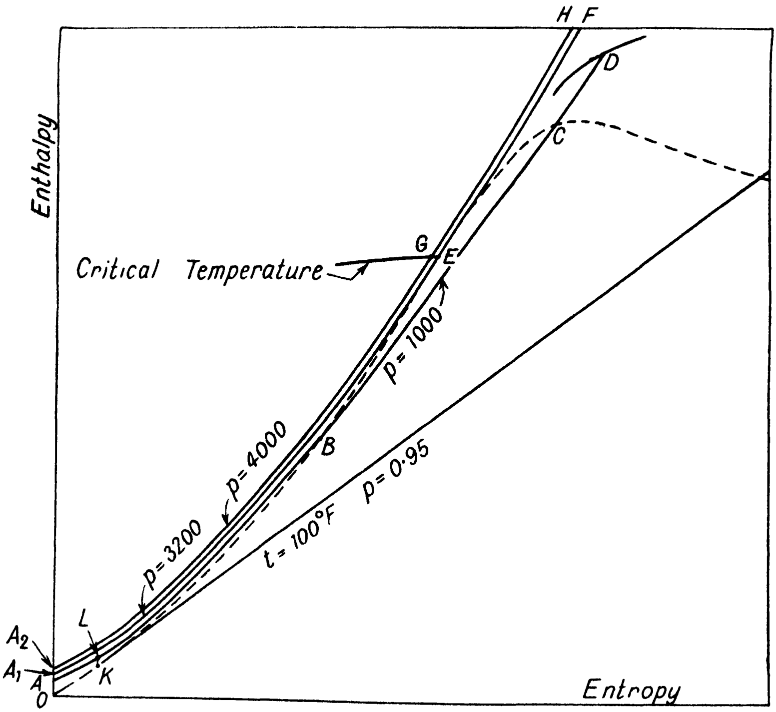


FIG. 24.—Mollier Diagram for Compressed Water

In the adiabatic compression KL, Fig. 24, $dH = 0$, and therefore

$$I_L - I_K = \int \frac{v_w}{J} \, . \, dP$$

and ignoring the extremely small change of volume during compression

$$I_L - I_K = \frac{v_w}{J} (P_L - P_K) \quad . \quad . \quad . \quad (25)$$

This simple relation would enable the change of enthalpy to be calculated for any increase of pressure at constant entropy.

Consider now the generation of steam at, say, 1,000 lb. per sq. in. from water at 100° F. and at its corresponding pressure to superheated steam at temperature t_D. During the adiabatic compression of the water to the pressure at which steam generation takes place there is, of course, no heat supplied or rejected. Since the pressure during the subsequent heating along the curve LBCD is constant, the heat supplied is exactly equal to the increase of enthalpy, i.e. to $I_D - I_L$.

$$\text{Heat supplied} = I_D - I_L$$

$$= (I_D - I_K) - \frac{v_w}{J}(P_1 - P_2) \quad . \quad . \quad . \quad (26)$$

This has already been shown in Art. 22, but is repeated here so as to make the matter clear with respect to the Mollier diagram.

29. Thermodynamic Potential. There is a further function of the state of a fluid which is defined by the equation

$$\zeta = I - T . \phi$$

This was given the name thermodynamic potential at constant pressure by Willard Gibbs (3) but is usually called Gibbs function. This is normally a negative quantity for steam or water in any state and, for practical purposes, it is more usual to write

$$G = T . \phi - I$$

where G is known as the *negative thermodynamic potential*. As will be shown in the next chapter, this function is useful in the calculation of the isentropic heat drop. Values of G are tabulated in the 1939 Abridged Callendar Steam Tables.

Consider the relation

$$G = T . \phi - I$$

Differentiating the expression, we have

$$dG = T . d\phi + \phi . dT - dI$$

$$= T . d\phi + \phi . dT - dH - \frac{v . dP}{J}$$

and, since $dH = T . d\phi$ for a reversible operation,

$$dG = \phi . dT - \frac{v . dP}{J}$$

Hence during the evaporation of water at constant pressure and temperature, $dG = 0$; i.e. the function G is the same for saturated water and for dry and saturated steam, or wet steam at the same pressure. In other words,

$$G = T . \phi_w - I_w = T . \phi_s - I_s$$

By using Clapeyron's equation

$$\left(\frac{\partial P}{\partial T}\right)_{sat.} = \frac{JL}{T(v_s - v_w)}$$

R. W. Haywood (4) has shown how to draw a curve on the T — ϕ chart which represents the Gibbs function accurately. This curve is termed the *Gibbs Line.*

From Clapeyron's equation above, it is clear that

$$v_w \cdot \frac{dP}{J} = \left(\frac{v_w}{v_s - v_w} \cdot \frac{L}{T}\right) . dT$$

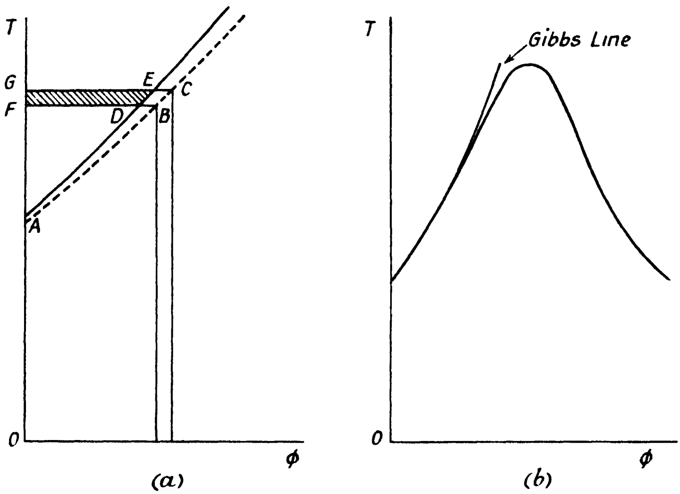


FIG. 25 Representation of Gibbs Function on Temperature-entropy Diagram

The quantity in the bracket has obviously the dimensions of entropy. Writing $\Delta\phi_w$ for this quantity, we have

$$v_w \cdot \frac{dP}{J} = \Delta\phi_w . dT$$

Let the dotted line ABC in Fig. 25 (*a*) represent the T — ϕ curve for saturated water. Then since

$$dG_w = \phi_w . dT - v_w . \frac{dP}{J}$$

$$dG_w = (\phi_w - \Delta\phi_w)dT$$

If we set off from B and C the distances BD and CE equal to

$$\Delta\phi_w = \frac{v_w}{v_s - v_w} \cdot \frac{L}{T}$$

then the cross-hatched area FDEG = dG_w. Values of $\Delta\phi_w$ are given in the following table. It will be seen that below 300° F. the values are very small and less than one per cent of the entropy of saturated

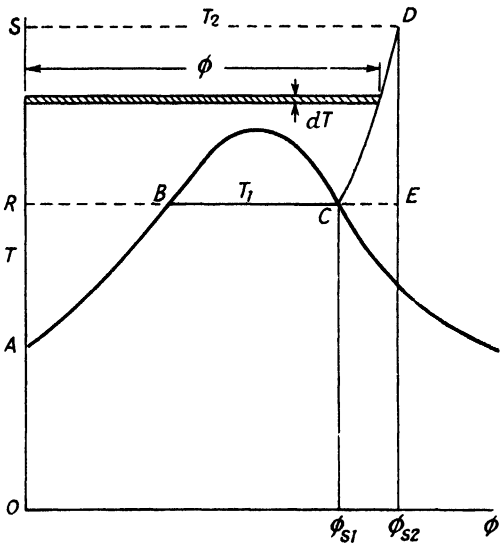


Fig. 26.—Gibbs Function for Superheated Steam

water. As the temperature is increased, however, the Gibbs Line deviates more and more from the liquid line, Fig. 25 (*b*).

Temp. F	v_w	v_s	$\frac{L}{T}$	$\Delta\phi_w$	ϕ_w
32	0·01602	3306	2·1877	0 0000106	0
100	0·01613	350·4	1·8531	0·000085	0·1295
200	0·01663	33·64	1·4824	0·00073	0·2938
300	0·01745	6·466	1·1980	0·0032	0·4369
400	0·01864	1·863	0·9608	0·0097	0·5664
500	0·0204	0·675	0·7438	0·0232	0·6887
600	0·0236	0·267	0·5176	0·0503	0·8131
700	0·0369	0·0761	0·1484	0·140	0·9905
705	0·0438	0·0589	0·0593	0·171	1·0293
705 4	0·0503	0·0503	0		1·0580

Consider now the value of G for superheated steam, and in particular the change in G during superheating at constant pressure along the line CD, Fig. 26. It has been shown that

$$dG = \phi \, . \, dT - v \, . \, \frac{dP}{J}$$

Hence along the constant-pressure line CD, $dG = \phi \, . \, dT$, and is therefore represented by the area of the cross-hatched horizontal strip in Fig. 26. The total change in G between C and D will be represented by the area RCDS.

i.e.

$$\begin{aligned} G_2 - G_1 &= \phi_{s2}(T_2 - T_1) - \text{area CDE} \\ &= \phi_{s2}(T_2 - T_1) - \{(I_{s2} - I_{s1}) - T_1(\phi_{s2} - \phi_{s1})\} \\ &= (T_2 \, . \, \phi_{s2} - I_{s2}) - (T_1 \, . \, \phi_{s1} - I_{s1}) \end{aligned}$$

which is in agreement with the definition of G. This enables the value of G_2 to be found, since the value of G_1 is given in the Abridged Steam Tables.

BIBLIOGRAPHY

1. KEARTON: "The Entropy and Enthalpy of Compressed Water At and Near the Freezing Point." *The Engineer*, 1936; 162; 662.
2. KEENAN, J. H., and KEYES, F. G.: *Thermodynamic Properties of Steam*, John Wiley & Sons, New York, 1936.
3. GIBBS: *Collected Works*, Vol. I., p. 93.
4. HAYWOOD: "The Thermodynamic Properties of Saturated Water." *Proc. I. Mech. E.*, 1952 53; 1B; 49.

EXAMPLES III

1. Show that if the specific heat of a substance be expressed by the relation $C = a + bT + cT^2$, where a, b, and c are constants and T is the absolute temperature, the change of entropy due to the heating of the substance from T_1 to T_2 is

$$\phi_2 - \phi_1 = a \, . \log_e \frac{T_2}{T_1} + b(T_2 - T_1) + \frac{c}{2}(T_2^2 - T_1^2)$$

2. Sixty units of heat are added to unit mass of a substance while its temperature is increasing from 400 to 490 degrees absolute. If the specific heat remains constant during the addition of heat, what is the change of entropy?

3. Assuming that the specific heat of water is unity and that the latent heat $L = 1{,}100 - 0{\cdot}63t$, calculate for 1 lb. of steam at $p = 100$ ($t = 327{\cdot}8°$ F.) the following quantities—

(*a*) Change of entropy during the heating of water from 32° F. to 327·8° F.

(*b*) Change of entropy during evaporation.

(*c*) Approximate change of entropy during superheating, if the degree of superheat is 200° F. ($C_{pm} = 0{\cdot}524$.)

4. Calculate the change of entropy of 1 lb. of water during the heating from 32° F. to 544·6° F. (p = 1,000), using as a basis the following modification of Dieterici's equation for the specific heat of water—

$$C_w = 1{\cdot}18124 - 0{\cdot}00068683T + 0{\cdot}00000064T^2$$

T being the absolute temperature on the Fahrenheit scale. Compare this value with that based on the assumption of unit specific heat.

5. A boiler drum has a total capacity of 1,000 cub. ft. It contains a certain amount of water and of dry and saturated steam, and the whole may be assumed to be at one temperature.

When the pressure is 200, the boiler is exactly half-full of water. Heat is then applied and the pressure is raised to 400. No steam is allowed to escape. Calculate the following—

(a) The weight of water evaporated.
(b) The total amount of heat supplied.
(c) The total change of entropy of the whole mass of water and steam.

Given the following information—

Specific volume of saturated water when p = 200, = 0·0184.
" " " " p = 400, 0·0194.

CHAPTER IV

THEORETICAL STEAM TURBINE CYCLE

30. Definition of Cycle. The object of all heat engines is to convert heat into mechanical work. In all such engines we use some substance, termed the "working substance" or "working fluid," to which we supply heat, so causing the working substance to expand, and in overcoming some external resistance to perform a certain amount of mechanical work. After the expansion process, we have some cold "body" or receiver of heat to which the working substance rejects heat before taking in a new supply of heat from the hot body or source of heat.

The working substance is said to have undergone a cycle of changes of state when, after starting from some definite initial condition, receiving a supply of heat, expanding and performing mechanical work, and finally rejecting that quantity of heat which cannot be converted into work, it is brought back to its initial state or condition.

The cycle thus defined is a *closed* cycle when it is completed within the power plant itself, as, for example, in the case of a condensing steam turbine. When the cycle is virtually completed outside the power plant, as, for example, with an engine or turbine exhausting to atmosphere, the cycle is said to be an *open* one.

31. Actual Steam Turbine Cycle. Fig. 27 shows in diagrammatic form the essential parts of a steam turbine power plant. It comprises three fundamental elements—

(1) The boiler plant, in which the working substance, water, receives heat liberated by the combustion of the fuel.

(2) The steam turbine, in which the working substance undergoes changes in pressure, temperature, and heat content, thus performing mechanical work on the shaft.

(3) The condenser, in which the working fluid gives up to the cooling water that quantity of heat which, in virtue of the Second Law of Thermodynamics, cannot be converted into work and must be rejected in order to restore the working fluid to its initial condition.

The diagram shows in outline a Babcock & Wilcox boiler with a travelling-grate mechanical stoker. After leaving the boiler proper, the products of combustion flow over the tubes of an "economizer" or feed-water preheater, and then through the air preheater. The combustion air is supplied to the top of the air preheater by the forced-draught fan, and the hot air which leaves the heater then goes direct to the internal air compartments of the mechanical stoker.

The steam is normally superheated to a relatively high temperature, and the superheater tubes must be located in the path of the products in such a way that the temperature of the products is high enough to give the required steam temperature without an excessive amount of superheater surface. In this respect, Fig. 27 is very diagrammatic.

The steam generated by the boiler is led to a vessel termed a receiver into which other boilers may deliver steam. Steam pipes connect the receiver to the individual turbines and sometimes cross-connect the receiver to another receiver. With large turbine units it is customary to employ a single receiver per turbine. The steam pipes leading from the receiver to the turbine are equipped

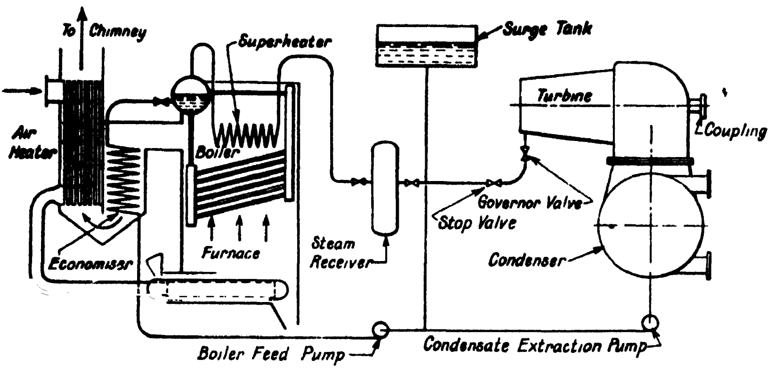


FIG. 27.—Diagrammatic Arrangement of Steam Power Plant

with suitable valves, drain valves and means for permitting expansion. There are always at least two valves, or sets of valves. One, the stop valve, is used for starting and stopping the turbine; the other, the governor valve, is automatically controlled by the speed governor and maintains the speed of rotation at a sensibly constant value in spite of variations of load.

After doing work in the turbine, the steam is condensed. In the normal surface condenser, the steam is condensed on the outer surface of a very large number of metal tubes through which the cooling or "circulating" water flows. The condensed steam or "condensate" showers down over the tubes and is extracted from the bottom of the condenser by a pump, known as the condensate extraction pump. This pump delivers the condensate to the suction side of the boiler feed-pump and the latter returns the feed water to the boiler, via the economizer. In order to allow for the varying quantity of water in the boiler at different rates of steaming, it is necessary to provide some form of storage for the condensate between the condensate extraction pump and the boiler feed-pump.

This may take the form of an open "hot-well," a sealed "surge tank," as shown in Fig. 27, or other forms.

Owing to small leakages through joints and glands which are subjected to internal pressures lower than atmospheric pressure, a certain amount of air leaks into the turbine and condenser. Unless this air is continually extracted it accumulates in the condenser and raises the exhaust pressure, with adverse effects on the turbine performance. Air pumps, usually of the steam ejector type, are provided in all cases; but their effect on the thermal quantities involved is very small.

32. **Rankine Cycle for Steam Initially Saturated.** In order to compare the performance of actual engines and turbines, certain

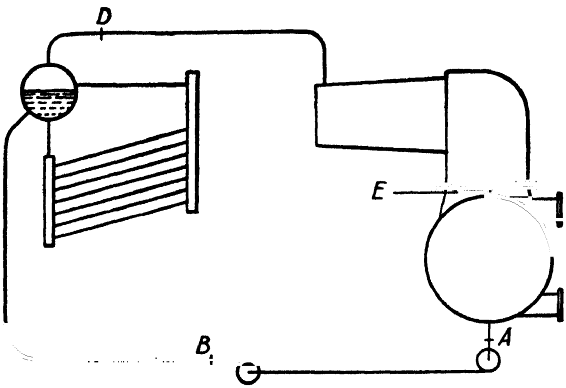


FIG. 28

theoretical or ideal cycles have been formulated. When the thermal properties of the working substance are sufficiently determined, it is possible by a study of these theoretical cycles to calculate the amount of heat which must be supplied to the working substance during one cycle, the amount of mechanical work performed by the substance under certain specified conditions, and the amount of heat which must be abstracted from the working substance in the condenser. We can thus calculate the theoretical thermal efficiency, which is the ratio of the theoretical work done to the heat supplied.

Consider, for example, a steam plant in which the steam is supplied to the turbine in the dry and saturated state. The plant is shown diagrammatically in Fig. 28, while the T-ϕ and ϕ-I diagrams for the cycle are shown in Figs. 29 and 30 respectively.

A convenient starting point in the cycle is A, at the extraction pump suction. Here we have unit mass of water in the saturated condition, at pressure p_2 and temperature T_2. This water is next raised in pressure by the combined effects of the extraction pump

and boiler feed-pump to the higher limit of pressure p_1, its condition being represented by the point B in Figs. 28, 29, and 30, which are lettered to correspond. The compression AB is adiabatic.

The water now enters the economizer and/or boiler and is first raised to the evaporation temperature T_1. During this process the state point moves along the curve BC. Moreover, as already explained (Arts. 22 and 28), the heat supplied during the process is equal to $I_C - I_B$, and is represented in Fig. 29 by the area LBCM to some scale.

The water is now completely evaporated at pressure p_1 and temperature T_1. The heat supplied is L_1 and equals $I_D - I_C$. In Fig. 29 this is represented by the area of the rectangle MCDN.

The steam is now assumed to enter the turbine, where it undergoes a drop in pressure from p_1 to p_2, usually in several stages. In the first place, the steam is assumed to pass through the turbine without any heat flowing into or out of the turbine cylinder. Furthermore, the expansion of the steam in the nozzles is assumed to take place without any surface friction losses and without the production of eddies; and the passage of steam through the rotor blades is likewise supposed to take place without friction or the dissipation of energy due to impact or eddies. If all these conditions could be satisfied then the steam would undergo the process of expansion without receiving heat in any way, either from external bodies or internally by the reception of dissipated mechanical energy in the form of heat. Such an expansion is said to be *adiabatic* and frictionless. Because the substance neither gains nor loses heat during such an expansion, the expansion takes place at constant entropy, i.e. it is *isentropic.*

An adiabatic or isentropic expansion of the swiftly moving steam in a steam turbine is utterly impossible in practice. The flow in a nozzle of good design must be attended by friction losses because of the molecular structure of, and molecular movements within, the flowing steam. Similarly, even though the rotor blades are so proportioned as to eliminate all shocks and eddies, there still remains the inevitable surface friction loss. In practice, therefore, the steam is continually receiving internally the heat equivalent of the mechanical losses incidental to the flow.

The adiabatic expansion of the steam is represented in Figs. 29 and 30 by the isentropic line DE. As soon as expansion begins, the steam (theoretically) commences to condense and at the turbine outlet has a dryness fraction x_E.

The steam is now condensed at p_2 and T_2, the working substance thus returning to its initial condition at A. The heat rejected during condensation

$$= x_E \,.\, L_2 = I_E - I_A$$

Now since all heat losses have been precluded, the work done

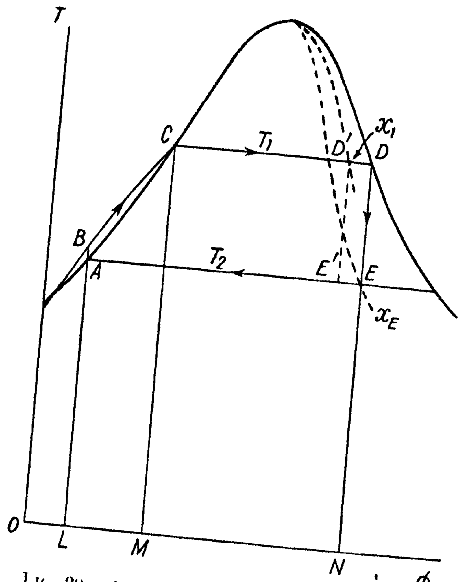


FIG. 29.—T-ϕ Diagram for the Rankine Cycle

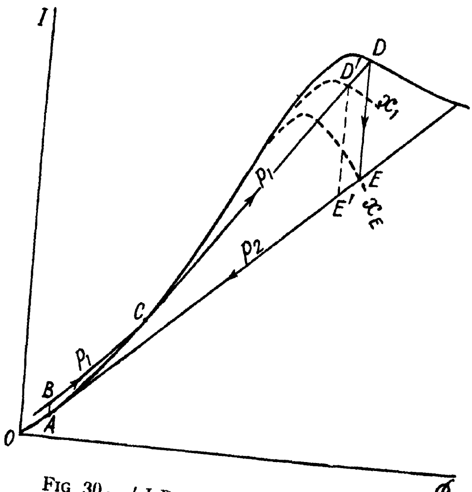


FIG. 30.—ϕ-I Diagram for the Rankine Cycle

is equal to the difference between the heat supplied and that rejected.

$$\text{Heat supplied} = (I_C - I_B) + (I_D - I_C)$$
$$= I_D - I_B$$

By eq. (26), Art. 28

$$I_B - I_A = \frac{v_{w2}}{J}(P_1 - P_2)$$

∴ Heat supplied

$$= (I_D - I_A) - \frac{v_{w2}}{J}(P_1 - P_2) \text{ B.Th.U. per lb.}$$

and heat rejected $= I_E - I_A$.

∴ Work done

$$= (I_D - I_E) - \frac{v_{w2}}{J}(P_1 - P_2) \text{ B.Th.U. per lb.} \quad . \quad . \quad (27)$$

Therefore the theoretical thermal efficiency, or cycle efficiency η_c, is

$$\eta_c = \left\{(I_D - I_E) - \frac{v_{w2}}{J}(P_1 - P_2)\right\}$$
$$\div \left\{(I_D - I_A) - \frac{v_{w2}}{J}(P_1 - P_2)\right\} \quad . \quad . \quad . \quad (28)$$

In the expression for the work done, the term $\frac{v_{w2}}{J}(P_1 - P_2)$ represents the work done by the feed-pump. Consequently, the gross work done by the turbine is given by $I_D - I_E$. Unless the pressure P_1 is relatively high the feed-pump work is small and may be neglected. The cycle efficiency is then equal to

$$\eta_c = \frac{I_D - I_E}{I_D - I_A} \quad . \quad . \quad . \quad . \quad (29)$$

The work done in an isentropic expansion may also be found by using Gibbs function G. Denoting the initial and final conditions by the subscripts 1 and 2, respectively, we may write—

$$I_1 = T_1\phi_1 - G_1$$
$$I_2 = T_2\phi_2 - G_2 \text{ (see Art. 29)}$$

Hence $I_1 - I_2 = T_1\phi_1 - T_2\phi_2 - (G_1 - G_2)$ and since $\phi_2 = \phi_1$,

$$I_1 - I_2 = (T_1 - T_2)\phi_1 - (G_1 - G_2) \text{ B.Th.U. per lb.} \quad . \quad (30)$$

If the steam has an initial dryness fraction x_1, then the adiabatic expansion is represented by the isentropic D^1E^1 and the expressions for the work done, heat supplied, etc., are as above with D^1 and E^1 substituted for D and E respectively. An explanation of the

methods of deriving the work done and the cycle efficiency will be given in the next article.

33. **Rankine Cycle for Steam Initially Superheated.** This is the cycle most frequently used in practice. The plant is shown schematically in Fig. 31 and differs from that dealt with in the previous article only in that a superheater is included.

It is unnecessary to discuss this cycle in detail and we shall proceed with an explanation of methods of deriving the values of the

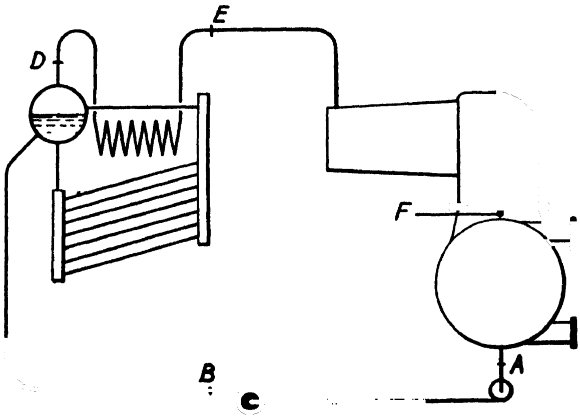


FIG. 31

heat supplied, the work done, and the thermal efficiency. Four methods will be given.

EXAMPLE 2. Steam is supplied to a turbine at a pressure of 500 lb. per sq. in. and a temperature of 800° F. It is expanded adiabatically and without friction to a pressure of 0·5 lb. per sq. in. Calculate or derive the following—

(*a*) External heat supplied per lb. of steam.
(*b*) Work done by turbine per lb. of steam.
(*c*) Net work done.
(*d*) Theoretical thermal efficiency.

Method 1. *From first principles, and assuming mean values for the specific heats of water and superheated steam.*

From Steam Tables—

Enthalpy of water

$$p = 500(t = 467{\cdot}0^\circ \text{ F.}) = 449{\cdot}6$$
$$p = 0{\cdot}5(t = 79{\cdot}6^\circ \text{ F.}) = 47{\cdot}6$$

i.e. $I_C - I_A$ (Fig. 32) $= 402{\cdot}0$.

By Art. 22, heat supplied to the saturated water (path AC)

$$= (I_C - I_A) - \frac{1}{J}\int_{P_2}^{P_1} v_w dP$$

$$= 402{\cdot}0 - 1{\cdot}7 = 400{\cdot}3 \text{ B.Th.U. per lb.}$$

Note that v_w is the specific volume of saturated water and its variation with temperature has been taken into account.

Since the temperature rise is 387·4° F., the mean specific heat of the water is 1·033.

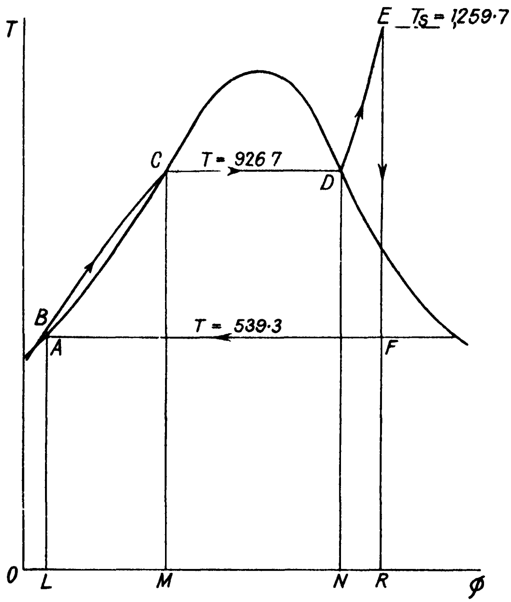


FIG. 32.—T-ϕ Diagram for Example 2

The initial superheat is 800 — 467·0, or 333·0° F., and the mean specific heat of superheated steam at 500 lb. per sq. in., according to Fig. 16, is 0·621.

Hence the total change of entropy LR, Fig. 32, is -

$$C_w \cdot \log_e \frac{T_1}{T_2} + \frac{L_1}{T_1} + C_{pm} \cdot \log_e \frac{T_s}{T_1}$$

$$= 1{\cdot}033 \log_e \frac{926{\cdot}7}{539{\cdot}3} + \frac{755{\cdot}8}{926{\cdot}7} + 0{\cdot}621 \log_e \frac{1{,}259{\cdot}7}{926{\cdot}7}$$

$$= 0{\cdot}5592 + 0{\cdot}8157 + 0{\cdot}1906 = 1{\cdot}5655$$

If it is assumed that the water is first compressed to 500 lb. per sq. in. at the temperature of 79·6° F. ($v_{w2} = 0{\cdot}01607$), the sensible heat supplied

$$= (I_C - I_A) - \frac{v_{w2}}{J}(P_1 - P_2)$$

$$= 402{\cdot}0 - \frac{0{\cdot}01607 \times 144 \times 499{\cdot}5}{778{\cdot}3}$$

$$= 402{\cdot}0 - 1{\cdot}5 = 400{\cdot}5 \text{ B.Th.U. per lb.}$$

∴ Total heat supplied externally

$$= 400{\cdot}5 + 755{\cdot}8 + (0{\cdot}621 \times 333)$$
$$= \underline{1{,}363{\cdot}0 \text{ B.Th.U. per lb.}}$$

$$\text{Heat rejected} = T_2 \times LR$$
$$= 539{\cdot}3 \times 1{\cdot}5655$$
$$= 844{\cdot}2 \text{ B.Th.U. per lb.}$$

∴ Net work done in the power plant per lb. of steam passing through the turbine, i.e. the work done by the turbine less the work done in forcing the feed water into the boiler,

$$= 1{,}363{\cdot}0 - 844{\cdot}2$$
$$= \underline{518{\cdot}8 \text{ B.Th.U.}}$$

Net thermal efficiency of cycle

$$= \frac{518{\cdot}8}{1{,}363{\cdot}0}$$

$$= \underline{38{\cdot}06 \text{ per cent.}}$$

Work done by turbine only

$$= 518{\cdot}8 + (\text{Feed pump work})$$
$$= 518{\cdot}8 + 1{\cdot}5$$
$$= \underline{520{\cdot}3 \text{ B.Th.U. per lb.}}$$

∴ Gross cycle efficiency

$$= \frac{520{\cdot}3}{1{,}363}$$

$$= \underline{38{\cdot}17 \text{ per cent.}}$$

Method 2. By the use of Steam Tables, but without the use of the Mollier diagram.

Heat supplied in cycle

$$= I_E - I_B$$

$$= (I_E - I_A) - \frac{v_{w2}}{J}(P_1 - P_2)$$

$$= (1{,}412{\cdot}2 - 47{\cdot}6) - 1{\cdot}5 = \underline{1{,}363{\cdot}1 \text{ B.Th.U. per lb.}}$$

$$\phi_F = \phi_E = 1{\cdot}6564$$

$$\therefore \ \phi_F - \phi_A = 1{\cdot}6564 - 0{\cdot}0924 = 1{\cdot}5640$$

$$\begin{aligned}\therefore \text{ Heat rejected} &= T_2(\phi_F - \phi_A)\\ &= 539{\cdot}3 \times 1{\cdot}5640\\ &= 843{\cdot}3 \text{ B.Th.U. per lb.}\end{aligned}$$

∴ Net work done per lb. of steam

$$= 1{,}363{\cdot}1 - 843{\cdot}3 = 519{\cdot}8 \text{ B.Th.U.}$$

which is practically identical with the result obtained by the previous method. The other results may be worked out by the methods given above.

Method 3. By the use of the Mollier chart.

For this purpose the large Callendar diagram was used. This is shown in skeleton form in Fig. 33, which is lettered to correspond to Fig. 32.

In using the chart, the point E is first obtained from the given initial pressure and temperature. This immediately gives the value

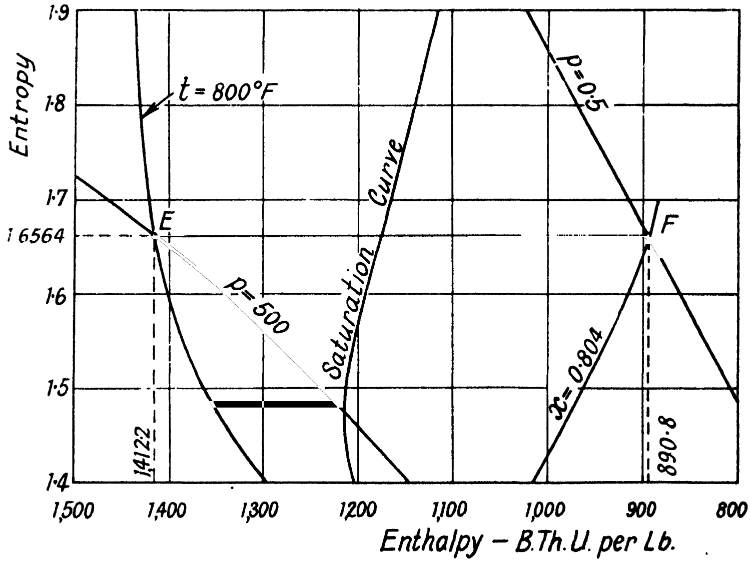


FIG. 33

of the entropy, viz. 1·6564, and of the enthalpy, viz. 1,412·2 B.Th.U. per lb. The adiabatic and frictionless expansion is represented by the constant entropy line EF, which may be drawn on a sheet of tracing paper placed over the chart. Alternatively, the point F may be simply read off the chart for the pressure of 0·5 lb. per sq. in. and the entropy 1·6564, without drawing any line at all.

The enthalpy at F is 890·8 and the dryness fraction of the steam is 0·804.

The author recommends writing down the various quantities, given and derived, in the following tabular form—

p	Condition	ϕ	I
500	$t = 800°$ F.	1·6564	1,412·2
0·5	$x = 0·804$	1·6564	890·8
			521·4

A simple subtraction then gives $I_E - I_F$, which is the work done in the turbine. This result agrees with those obtained by the two previous methods.

Method 4. *By the use of Gibbs function.*

For dry and saturated steam at 500 lb. per sq. in. $G_1 = 151·8$; $\phi_{s1} = 1·4646$; and $I_{s1} = 1,205·4$. By interpolation from data given in Callendar's Abridged Tables, we find for a pressure of 500 and a temperature of 800° F., that $I_{s2} = 1,412·2$ and $\phi_{s2} = 1·6564$.

The change in G during superheating is

$$\begin{aligned} G_2 - G_1 &= (T_2 . \phi_{s2} - I_{s2}) - (T_1 . \phi_{s1} - I_{s1}) \\ &= \{(1,259·7 \times 1·6564) - 1,412·2\} \\ &\qquad - \{(926·7 \times 1·4646) - 1,205·4\} \\ &= 674·3 - 151·8 = 522·5 \text{ B.Th.U. per lb.} \end{aligned}$$

$$\therefore \qquad G_2 = 151·8 + 522·5 = 674·3 \text{ B.Th.U. per lb.}$$

Isentropic heat drop

$$\begin{aligned} I_{s2} - I_{s0} &= (T_2\phi_{s2} - G_2) - (T_0\phi_{s2} - G_0) \\ &= \phi_{s2}(T_2 - T_0) - (G_2 - G_0) \\ &= 1,193·3 - 672·1 = \underline{521·2 \text{ B.Th.U. per lb.}} \end{aligned}$$

If the initial enthalpy is known then the isentropic heat drop is simply $I_E - I_F$, where

$$\begin{aligned} I_F &= T_F . \phi_F - G_F \\ &= (539·3 \times 1·6564) - 2·2 \\ &= 891·1 \text{ B.Th.U. per lb.} \end{aligned}$$

Hence $I_E - I_F = 1,412·2 - 891·1 = \underline{521·1 \text{ B.Th.U. per lb.}}$

Of the four methods given above, the third is the most convenient. For accurate work, however, the second method is to be preferred.

The quantity $I_E - I_F$, which is the gross amount of work done in the turbine during the adiabatic and frictionless expansion of the steam, is often referred to as the "adiabatic heat drop" or the "Rankine heat drop."

34. Superheated Steam Cycle with Superheated Exhaust. When the initial superheat is moderately high and when, as in a back-pressure turbine, the exhaust pressure is relatively high, the steam may be superheated at the end of the expansion in the turbine.

The temperature-entropy diagram for these conditions is shown in Fig. 34. The heat supplied per lb. of substance in the economizer, boiler, and superheater is equal to

$$I_E - I_B = (I_E - I_A) - \frac{v_{w2}}{J}(P_1 - P_2)$$

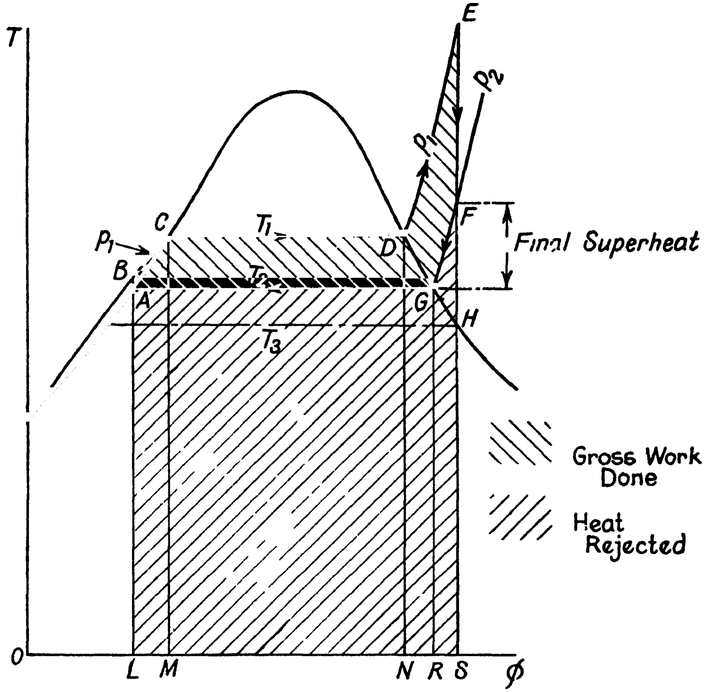


FIG 34

The steam, on adiabatic expansion, only becomes dry and saturated at the pressure p_3 corresponding to the temperature T_3, which is found by the intersection of the adiabatic and isentropic expansion line EFH with the steam saturation line. If T_3 is lower than T_2, the saturation temperature corresponding to the actual exhaust pressure, then the state point at the termination of the actual expansion will be F, the point of intersection of the isentropic EFH with the constant-pressure line GF. At the end of the adiabatic expansion the steam is superheated by the amount

$T_F - T_G$. In order to restore the steam to its initial condition as saturated water at A, it is first necessary to de-superheat it, by cooling at constant pressure p_2 to the temperature T_2 and then to condense it.

The final steam temperature T_F may be calculated as follows. The total change of entropy LS may be found either by Method 1 of the last article, or from steam tables.

Then
$$RS = C_{pm} \cdot \log_e \frac{T_F}{T_G} \text{ (approx.)}$$
$$= LS - LR$$
$$= LS - \frac{L_2}{T_2}$$
$$\text{Heat rejected} = C_{pm}(T_F - T_G) + L_2.$$

Since the heat rejection takes place at constant pressure throughout, the heat rejected also equals $I_F - I_A$. Therefore the net work done, i.e.

$$\text{Turbine work} - \text{feed-pump work}$$
$$= (I_E - I_A) - \frac{v_{w2}}{J}(P_1 - P_2) - (I_F - I_A)$$
$$= (I_E - I_F) - \frac{v_{w2}}{J}(P_1 - P_2) \text{ B.Th.U. per lb.}$$

The work done by the turbine only is $I_E - I_F$. The treatment of this case by the Mollier diagram will now be illustrated briefly by an example.

Example 3. A turbine is supplied with steam at 500 lb. per sq. in. and 800° F. The steam is expanded adiabatically to a pressure of 100 lb. per sq. in.

Derive the following—

(*a*) External heat supplied per lb. of steam.
(*b*) Condition of the steam at the end of the expansion.
(*c*) Work done by the turbine.
(*d*) Gross theoretical thermal efficiency.
(*e*) Net theoretical thermal efficiency.

(*a*) Heat supplied in cycle

$$= (I_E - I_A) - \frac{v_{w2}}{J}(P_1 - P_2) \text{ (Fig. 34)}$$
$$= (1{,}412 \cdot 2 - 298 \cdot 5) - \left(\frac{0 \cdot 0177 \times 144 \times 400}{778 \cdot 3}\right)$$
$$1{,}113 \cdot 7 - 1 \cdot 3$$
$$\underline{1{,}112 \cdot 4 \text{ B.Th.U. per lb.}}$$

(*b*) For the expansion, the following table may be drawn up with reference to the Mollier diagram, Fig. 35.

p	Condition	ϕ	I
500	$t = 800°$ F.	1·6564	1,412·2
100	$t = 408°$ F.	1·6564	1,232·0
			180·2

At F the steam has a temperature of 408° F. and a superheat = 408·0 − 327·8 = 80·2° F.

(*c*) Work done in turbine per lb. of steam = 180·2 B.Th.U.

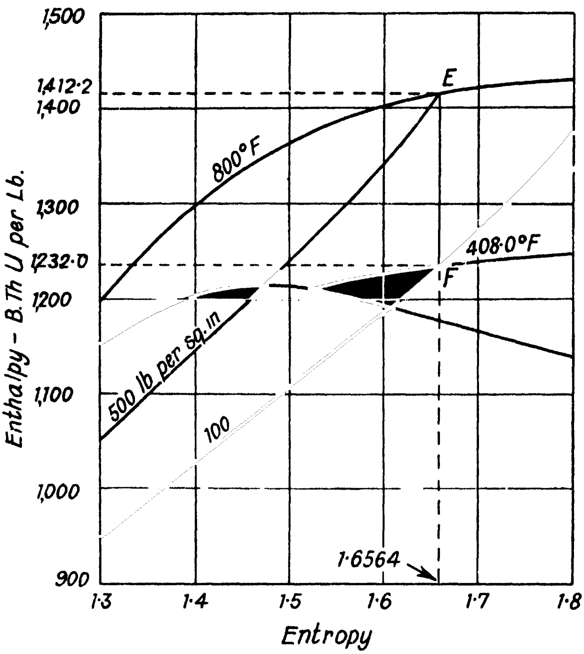


FIG. 35 — ϕ-I Diagram Illustrating Example 3

(*d*) Gross thermal efficiency $= \dfrac{180 \cdot 2}{1{,}112 \cdot 4}$

$= 16 \cdot 2$ per cent.

(*e*) Net work done = 180·2 − 1·3 = 178·9.

Net thermal efficiency $= \dfrac{178 \cdot 9}{1{,}112 \cdot 4}$

$= 16 \cdot 1$ per cent.

35. Thermal Efficiency Ratio. *In the foregoing articles we have* shown how to calculate the theoretical thermal efficiency of a steam turbine power plant. This may be conveniently referred to as the "cycle efficiency" η_c.

Then $$\eta_c = \frac{H_a}{H} \qquad . \quad . \quad . \quad . \quad (31)$$

where H_a = energy available due to adiabatic and frictionless expansion, i.e. the isentropic heat drop

and H = heat supplied in the cycle.

Owing to the various losses in the turbine, such as friction losses in the nozzles and blading, shock losses, eddy losses, disc friction and bearing friction losses, the actual work done H_w B.Th.U. per lb. of steam, at the turbine coupling, is less than H_a.

Let η_t = thermal efficiency of the turbine
= (actual coupling work per lb. of steam) ÷ (heat supplied in cycle per lb. of steam).

Then $$\eta_t = \frac{H_w}{H} \qquad . \quad . \quad . \quad . \quad (32)$$

A measure of the excellence, or otherwise, of the performance of an actual steam turbine may be obtained by comparing its thermal efficiency with that of an ideal engine operating on the Rankine cycle between the same limits of pressure and temperature as the actual machine. The ratio of the actual to the theoretical thermal efficiency is termed the *thermal efficiency ratio*, or simply, the *efficiency ratio* (η_r).

Then $$\eta_r = \frac{\eta_t}{\eta_c} = \frac{H_w}{H} \times \frac{H}{H_a}$$

$$\therefore \qquad \eta_r = \frac{H_w}{H_a} \qquad . \quad . \quad . \quad . \quad . \quad (33)$$

i.e. the efficiency ratio is equal to the ratio of the actual coupling work in B.Th.U. per lb. of steam to the adiabatic heat drop.

H_w may be calculated from test data in the following manner.

Let W = steam consumption of turbine, lb. per hour.
h.p. = horse-power developed.
kW = power developed, kilowatts.

Now 1 h.p. = 33,000 ft.-lb. per minute
= 42·43 B.Th.U. per minute
= 2,546 B.Th.U. per hour.

But 1 h.p. = 746 watts.

1 kilowatt = 1·341 h.p.
= 56·89 B.Th.U. per minute
= 3,413 B.Th.U. per hour.

Work done per lb. of steam

$$H_w = \frac{2{,}546 \times \text{h.p.}}{W} \text{ B.Th.U.}$$

$$H_w = \frac{3{,}413 \times \text{kW}}{W} \text{ B.Th.U.}$$

Efficiency ratio

$$\eta_r = \frac{2{,}546 \times \text{h.p.}}{W \,.\, H_a} \quad . \quad . \quad . \quad . \quad (34a)$$

$$\eta_r = \frac{3{,}413 \times \text{kW}}{W \,.\, H_a} \quad . \quad . \quad . \quad (34b)$$

The absolute thermal efficiency

$$\eta_t = \frac{2{,}546 \times \text{h.p.}}{W \,.\, H} \quad . \quad . \quad . \quad . \quad (35a)$$

or

$$\eta_t = \frac{3{,}413 \times \text{kW}}{W \,.\, H} \quad . \quad . \quad . \quad . \quad (35b)$$

The steam consumption expressed in lb. of steam per unit power is

$$\frac{W}{\text{h.p.}} = \frac{2{,}546}{H_w} = \frac{2{,}546}{\eta_r \,.\, H_a} = \frac{2{,}546}{\eta_t \,.\, H} \text{ lb. per h.p. hour}$$

or

$$\frac{W}{\text{kW}} = \frac{3{,}413}{H_w} = \frac{3{,}413}{\eta_r \,.\, H_a} = \frac{3{,}413}{\eta_t \,.\, H} \text{ lb. per kW hour}$$

A more detailed study of losses and of efficiencies will be given in Chapters XI and XII.

Important modifications to the steam turbine cycle due to regenerative feed-heating and reheating will be considered in Chapters XIII and XIV respectively.

EXAMPLES IV

1. Dry and saturated steam at $p = 150$ and $t_s = 358{\cdot}4°$ F. is supplied to a turbine and expanded adiabatically to $p = 1{\cdot}0$ ($t_s = 101{\cdot}7°$ F.). Calculate the following—

(*a*) Heat supplied.
(*b*) Total change of entropy.
(*c*) Heat rejected.
(*d*) Theoretical thermal efficiency.

Assume that the specific heat of water is unity and that the latent heats of vaporization at $p = 150$ and $p = 1{\cdot}0$ are 864·5 and 1,036·1 B.Th U. per lb. respectively.

2. Steam is supplied to a turbine at p = 150 (t_s = 358·4° F.) and with a dryness fraction of 80 per cent. The steam is expanded adiabatically to p = 1·0 (t_s = 101·7° F.). Calculate the following—

(*a*) Heat supplied.
(*b*) Total change of entropy.
(*c*) Heat rejected.
(*d*) Theoretical thermal efficiency.

Assume that the specific heat of water is unity and that L for p = 150 is 864·5 B.Th.U. per lb.

3. A steam turbine receives steam at p = 250 and superheated 200° F. The exhaust pressure is 1·0, and the expansion of the steam takes place adiabatically and without friction.

Using steam tables only, calculate the following—

(*a*) Heat supplied, assuming that the feed-pump supplies water to the boiler at 250 lb. per sq. in.
(*b*) Heat rejected.
(*c*) Net work done.
(*d*) Work done by the turbine.
(*e*) Thermal efficiency.
(*f*) Theoretical steam consumption.

If the actual steam consumption is 11·2 lb. per kWh, what is the efficiency ratio of the turbine? The specific volume of saturated water at p = 1·0 is 0·01614.

4. A steam turbine plant is supplied with steam at p = 250, and superheated 180° F. The exhaust pressure is 0·85. The temperature of the condensate in the hot-well is actually 90° F. (v_w = 0·0161). If the measured steam consumption is 10·9 lb. per kWh and if the boiler efficiency is 82 per cent, what is the absolute thermal efficiency of the boiler and turbine plant?

5. Two steam turbines A and B operate with the same initial pressure, namely p = 200, and the same initial superheat of 160° F. In turbine A the exhaust pressure is 1·5 (v_w = 0·01618), whereas in turbine B the exhaust pressure is 0·5 (v_w = 0·01607). Calculate the following—

(*a*) Theoretical steam consumption of turbines A and B, in lb. per kWh.
(*b*) Percentage reduction in steam consumption due to the lower exhaust pressure in turbine B.
(*c*) Theoretical thermal efficiency of turbines A and B.
(*d*) Percentage increase in thermal efficiency due to the lower exhaust pressure in turbine B.

6. Steam expands adiabatically from an initial pressure p_1 (saturation temperature = T_1 abs.) and superheated to a temperature T_s abs., to a final pressure p_2 (saturation temperature = T_2 abs.). Show that if the final pressure is lowered by an amount δp, the additional work done in the cycle per lb. of steam is approximately

$$\frac{x_2 L_2}{T_2} \cdot \frac{dT}{dp} \cdot \delta p \text{ B.Th.U.}$$

where x_2 is the dryness fraction at T_2. Assume that the water is maintained in the saturated condition during heating.

Hence calculate the increase in work done when the final pressure is changed from 0·7 to 0·6 lb. per sq. in. abs., during the adiabatic expansion of steam from p = 250 and an initial superheat of 200° F.

7 The following are the means of the observations made during a test on a steam turbine—

Duration of test	2 hr.
Power developed (turbine coupling)	4,500 kW
Total weight of steam condensed	108,000 lb.
Steam pressure at stop valve	200
Steam temperature at stop valve	600° F.
Barometric height	30·20 in. Hg.
Vacuum	28·57 in. Hg.

Calculate the thermal efficiency of the turbine and also its efficiency ratio. Assume that the condensate is returned to the boiler plant at the exhaust saturation temperature.

8. Two steam turbines operate between the same temperature limits, viz. 800° F. and 79·6° F. In turbine A the initial pressure is 200, whereas in turbine B the initial pressure is 1,000. Using either the 1939 Callendar Steam Tables or the ϕ-I Diagram, calculate the theoretical thermal efficiencies of turbines A and B and the values of the dryness fraction after adiabatic expansion.

9. Calculate the fuel cost per unit (kWh) generated in a steam power plant under the following conditions—

Steam pressure at turbine	300
Initial superheat	320° F.
Exhaust pressure	0·75
Turbine efficiency ratio	0·78
Boiler efficiency	0·82
Alternator efficiency	0·96
Calorific value of coal	12,800 B.Th.U.per lb.
Cost of coal	80s. per ton

The following assumptions may be made—

(*a*) That the feed temperature to the boiler is equal to the saturation temperature at 0·75 lb. per sq. in. abs.

(*b*) That 6 per cent of the steam generated is used to cover losses, and auxiliary power.

10. Two steam turbines A and B operate under the following conditions: initial pressure, 250; exhaust pressure, 0·7. In turbine A, the steam is initially dry and saturated, whereas in turbine B it is initially superheated by 200° F.

Using steam tables, calculate—

(*a*) Theoretical steam consumption, lb. per kWh.
(*b*) Theoretical thermal efficiency of the two turbines.
(*c*) Percentage reduction in steam consumption due to superheating.
(*d*) Percentage increase in thermal efficiency due to superheating.

11. To what temperature must steam at 500 lb. per sq. in. abs. be initially superheated so that, after adiabatic expansion to any given exhaust pressure, it may have the same condition (i.e. superheat or dryness fraction) as steam at 200 lb. per sq. in. abs. which has been initially superheated to a temperature of 520° F. and expanded adiabatically to the same exhaust pressure?

Assume that the specific heat of superheated steam at constant pressure is constant and has the values 0·58 and 0·62 at $p = 200$ and $p = 500$ respectively.

12. Steam at 200 lb. per sq. in. abs. and superheated to a temperature of 600° F. expands adiabatically to 1 lb. per sq. in. abs. Using a Mollier diagram, find the pressure at which the steam is just dry and saturated, the final dryness fraction, and the adiabatic heat drop.

13. *Assuming steam initially at a pressure of 200 and a temperature of* 600° F., and also a barometric height of 30 in. Hg., obtain from a Mollier diagram the adiabatic heat drops for the following vacua and state the percentage gain by increasing the vacuum above 25 in.: (*a*) 25; (*b*) 26; (*c*) 27; (*d*) 28; and (*e*) 29 in.

14. A steam turbine receives dry and saturated steam at $p = 200$ and exhausts at $p = 1$. Using Gibbs function find the work done in the turbine during isentropic expansion. If the actual entropy at the end of the expansion is 1·666 and there is no gain or loss of heat from the turbine cylinder, find by the use of Gibbs function the actual work done per lb. of steam and the efficiency ratio of the turbine.

CHAPTER V

THE FLOW OF STEAM THROUGH NOZZLES

36. Introduction. The object of the present chapter is to study the flow of steam as an elastic fluid flowing through passages of varying cross-sectional area. To the turbine engineer it is of the utmost importance to know what velocity will be acquired under any given conditions of expansion, and conversely what expansion conditions, such as pressure drop, must be provided in order that the steam will reach a certain velocity under any given conditions. In addition it is equally important to predict the mass flow of steam through a nozzle or similar channel of given shape under given conditions of pressure and temperature, and conversely to work out the proportions of a nozzle or blade channel to accommodate a certain rate of mass flow.

Not only is it necessary to understand the factors governing the flow under ideal conditions when the expansion is adiabatic and frictionless; it is equally important to be able to allow, at least approximately, for the effects of friction and other losses on the velocity acquired and the area required under any given conditions.

The theory is based on certain fundamental equations which will now be considered.

37. Equation of Continuity. Consider the flow of steam through a nozzle and let w be the rate of steady flow in pounds of steam per second. Consider a certain section of the nozzle where the cross-sectional area normal to the direction of steam flow is A sq. ft., and at which the volume per lb. of steam is v cub. ft. Then if the velocity across the section is uniform and equal to V ft. per sec., the volume of steam passing the given section is

$$\text{AV cub. ft. per sec.}$$

But the volume of steam flowing past the given section is also

$$wv \text{ cub. ft. per sec.}$$

Hence

$$wv = \text{AV} \quad . \quad . \quad . \quad . \quad (36)$$

This simple equation is known as the "equation of continuity" and, provided the steam fills the nozzle at every section, it must be satisfied at all points in the steam path.

38. Steady Flow Equation for Turbine, Nozzle, Blades, etc. Consider the steady flow of 1 lb. of steam through a turbine, nozzle, or a system of blades. Assume that the conditions at inlet and outlet are as represented in Fig. 36 by the suffixes 1 and 2 respectively. The turbine, nozzle, or apparatus in question is represented diagrammatically by a rectangle.

Let the steam flow towards the apparatus through a pipe of area A_1 sq. ft., and leave it through a pipe of area A_2. V_1 and V_2 are the velocities of flow through the inlet and outlet pipes respectively.

Let W = mechanical work (if any) done by the apparatus, in B.Th.U. per lb. of steam; e.g. the internal work in a steam turbine or engine. The mechanical work does not include the gain of kinetic energy in a nozzle.

H = heat supplied (if any) to the apparatus, in B.Th.U. per lb. of steam. In the case of a heat loss, H is negative.

W_f = work done in opposing the forces of friction within the apparatus.

Imagine two pistons, one in the inlet pipe and the other in the outlet pipe. If, further, we suppose that these can move without

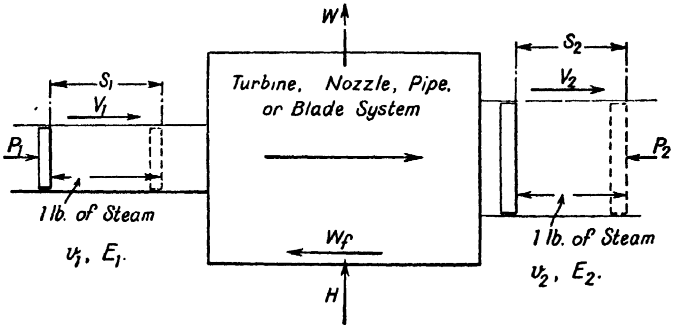


FIG. 36

friction, then they will do so with velocities equal to those of the steam in the pipes. The distance moved forward by the piston in the inlet pipe during the flow of 1 lb. of steam through the apparatus is clearly $s_1 = \frac{v_1}{A_1}$. The force on the piston is P_1A_1, and therefore the work done by the steam in forcing into the apparatus the steam which lies directly in front of it is equal to

$$\frac{P_1A_1}{J} \times s_1 = \frac{P_1v_1}{J} \text{ B.Th.U. per lb.}$$

Similarly, the work done by the steam which is leaving the apparatus in forcing out the steam which is moving immediately in front of it is

$$\frac{P_2v_2}{J} \text{ B.Th.U. per lb.}$$

The difference $\frac{1}{J}(P_1v_1 - P_2v_2)$ represents the net work done in

introducing the steam into the system and expelling it from the system, and represents a supply of energy. E_1 and E_2 represent the initial and final values of the internal energy respectively.

Then, by the Principle of the Conservation of Energy, we may write—

> (Work done by steam on inlet side of apparatus in forcing 1 lb. of steam into the apparatus) + (Initial internal energy) + (Initial kinetic energy) + (Heat supplied)
>
> = (Work done by steam in expelling 1 lb. of steam from the apparatus) + (Final internal energy) + (Final kinetic energy) + (External mechanical work performed).

i.e.
$$\frac{P_1 v_1}{J} + E_1 + \frac{V_1^2}{2gJ} + H = \frac{P_2 v_2}{J} + E_2 + \frac{V_2^2}{2gJ} + W$$

and since
$$I = \frac{Pv}{J} + E$$

$$I_1 + \frac{V_1^2}{2gJ} + H = I_2 + \frac{V_2^2}{2gJ} + W \quad . \quad (37)$$

This is the "steady flow equation" and is quite general and rigorously exact. It may be applied in many ways. Reverting for the moment to the ideal cycle considered in the previous chapter, if the initial and final kinetic energies of the steam are so small as to be negligible, and if the expansion is adiathermal ($H = 0$), then the work done

$$W = I_1 - I_2$$

this being the case whether the expansion is strictly isentropic or not.

In the special case of a nozzle, the mechanical work W is obviously zero, and the general equation for a nozzle is therefore

$$I_1 + \frac{V_1^2}{2gJ} + H = I_2 + \frac{V_2^2}{2gJ} \quad . \quad . \quad . \quad (38)$$

If the flow through the nozzle is adiathermal, then $H = 0$, and the equation becomes

$$I_1 + \frac{V_1^2}{2gJ} = I_2 + \frac{V_2^2}{2gJ}$$

Then
$$\frac{V_2^2}{2gJ} = (I_1 - I_2) + \frac{V_1^2}{2gJ}$$

or
$$V_2 = \sqrt{2gJ(I_1 - I_2) + V_1^2} \quad . \quad . \quad . \quad (39)$$

The gain in kinetic energy between any two sections of a nozzle is equal to the loss of enthalpy.

If the steam expands from a state of rest ($V_1 = 0$) then the velocity V_2 reached in the expansion is

$$V_2 = \sqrt{2gJ} \cdot \sqrt{(I_1 - I_2)} \quad . \quad . \quad . \quad (40)$$

Substituting $g = 32{\cdot}19$ ft. per sec.^{2}, and $J = 778{\cdot}3$,

$$V_2 = 223{\cdot}8\sqrt{(I_1 - I_2)} \quad . \quad . \quad . \quad (40a)$$

If the heat drop is expressed in C.H.U's per lb. of steam, then $J = 1{,}401$ and

$$V_2 = 300{\cdot}3\sqrt{(I_1 - I_2)} \quad . \quad . \quad . \quad (40b)$$

In each case, V_2 is in ft. per sec.

These expressions are quite general for adiathermal flow whether the flow is accompanied by friction losses or not. It will be observed that the term W_f does not enter into the energy equation at all, although the existence of friction naturally affects the final condition of the steam at exit from the apparatus.

In the special case of frictionless flow, the expansion is adiabatic and takes place at constant entropy. Hence the heat drop $I_1 - I_2$ is the adiabatic heat drop and may be readily obtained from a Mollier diagram, or by calculation.

39. The Momentum Equation for the Flow through a Turbine Nozzle. Consider the flow of steam through the nozzle shown in Fig. 37, and let the surfaces of constant pressure be plane surfaces transverse to the axis of the nozzle. Consider a small mass of steam enclosed between two transverse sections of the nozzle δx apart. Let the pressure on the upstream side be P and that on the downstream side $P + \delta P$, δP being negative. Moreover, let it be assumed that the steam velocity across each section is uniform. In actual fact, this is not true; the steam velocity near the walls of the nozzle varies across a relatively thin layer of fluid (the boundary layer) from zero at the surface of the wall to a value which is somewhat less than the velocity at the centre of the nozzle.

Let V = steam velocity at given section, ft. per sec.

v = specific volume of steam, cub. ft. per lb.

δF = the force of friction over the length δx which is retarding the steam.

The mass of steam enclosed between the two transverse sections is being urged forward by the resultant axial force due to steam pressure and friction. This resultant force is utilized to accelerate the mass of steam enclosed between the two sections considered. The mass enclosed is $\dfrac{A \cdot \delta x}{v}$ lb.

The forces on the enclosed mass are the following—

(1) The force on the upstream side $= P \, . \, A$.

(2) The force on the downstream side

$$= (P + \delta P)(A + \delta A) = P \, . \, A + P \, . \, \delta A + A \, . \, \delta P$$

the product $\delta P \, . \, \delta A$ being neglected.

(3) The resultant of the force exerted by the boundary walls of the nozzle. The steam exerts a pressure on the nozzle wall, and

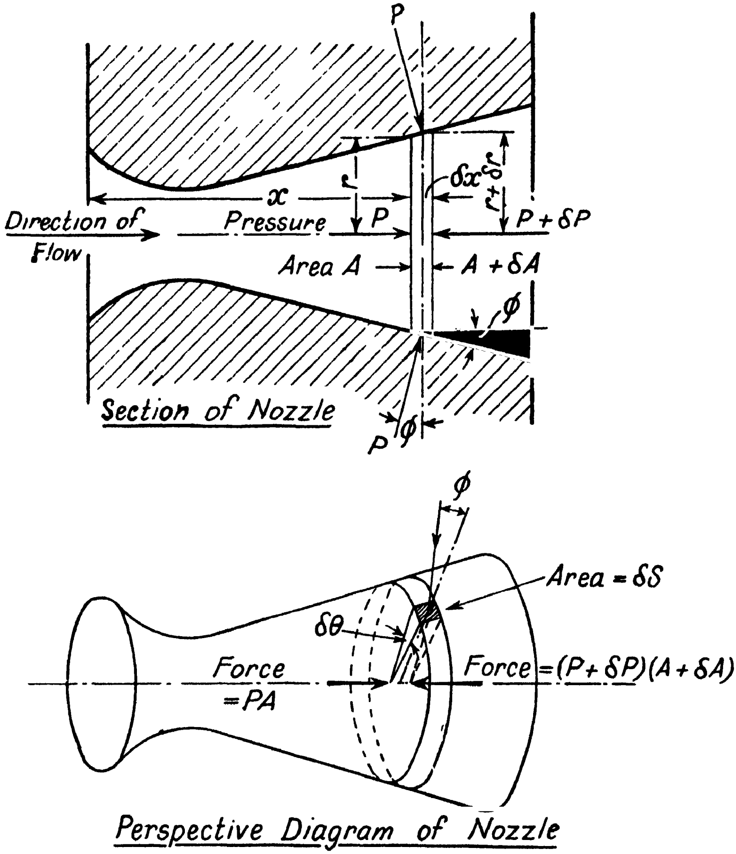


FIG. 37

equally the nozzle wall exerts a pressure on the steam. If the section of the nozzle considered lies in the diverging part of the nozzle, as shown in Fig. 37, then the force exerted by the nozzle wall on the steam is an accelerating force.

Consider the small element of area

$$\delta S = r \,.\, \delta\theta \,.\, \delta x \,.\, \sec\phi$$

The normal force on the surface is $P \,.\, r \,.\, \delta\theta \,.\, \delta x \,.\, \sec\phi$, and the axial component of this force is

$$P \,.\, r \,.\, \delta\theta \,.\, \delta x \,.\, \sec\phi \,.\, \sin\phi$$
$$= P \,.\, r \,.\, \delta\theta \,.\, \delta x \,.\, \tan\phi$$

Then the total axial force exerted by the nozzle wall on the steam is

$$2\pi \,.\, P \,.\, r \,.\, \delta x \,.\, \tan\phi$$
$$= 2\pi \,.\, P \,.\, r \,.\, \delta r$$
$$= P \,.\, \delta A$$

(4) The friction force δF lb. weight.

Therefore the resultant accelerating force

$$= P \,.\, A - P \,.\, A - P \,.\, \delta A - A \,.\, \delta P + P \,.\, \delta A - \delta F$$
$$= - A \,.\, \delta P - \delta F$$

Since mass-acceleration = accelerating force

$$\frac{A \,.\, \delta x}{v} \,.\, \frac{\delta V}{\delta t} = - g \,.\, A \,.\, \delta P - g \,.\, \delta F$$

But $$\delta t = \frac{\delta x}{V}$$

$$\therefore \quad \frac{V \,.\, \delta V}{g} = - v \,.\, \delta P - \frac{v \,.\, \delta F}{A}$$

or $$d\left(\frac{V^2}{2g}\right) = - v \,.\, \delta P - \frac{v \,.\, \delta F}{A} \quad . \quad . \quad . \quad (41)$$

The work done per second in overcoming friction over the length δx is $V \,.\, \delta F$ ft.-lb. and the mass flow per second is $\frac{AV}{v}$. Therefore, the work done per lb. of steam in overcoming friction is

$$\delta W_f = V \,.\, \delta F \times \frac{v}{A \,.\, V} = \frac{v \,.\, \delta F}{A}$$

Hence $d\left(\frac{V^2}{2g}\right) = - v \,.\, \delta P - \delta W_f$ and the gain of kinetic energy from condition 1 to condition 2 is—

$$\frac{V_2^2 - V_1^2}{2g} = - \int_{P_1}^{P_2} v \,.\, dP - \int_1^2 dW_f$$
$$= \int_{P_2}^{P_1} v \,.\, dP - W_f \quad . \quad . \quad . \quad (42)$$

where W_f is the total work done in overcoming friction between sections 1 and 2.

40. Entropy Changes with Friction. The energy equation (38) shows that in adiathermal flow (H = 0)

$$d\left(\frac{V^2}{2g}\right) = -\,J\,.\,\delta I$$

$$\therefore \qquad J\,.\,\delta I = v\,.\,\delta P + \delta W_f$$

By definition, $$I = E + \frac{Pv}{J}.$$

$$\therefore \qquad J\,.\,\delta I = J\,.\,\delta E + P\,.\,\delta v + v\,.\,\delta P$$

Because in any small change of state the sum $\delta E + \dfrac{P\,.\,\delta v}{J}$ is equal to the heat supplied, we may write—

$$\delta I = \text{Heat supplied} + \frac{v\,.\,\delta P}{J}$$

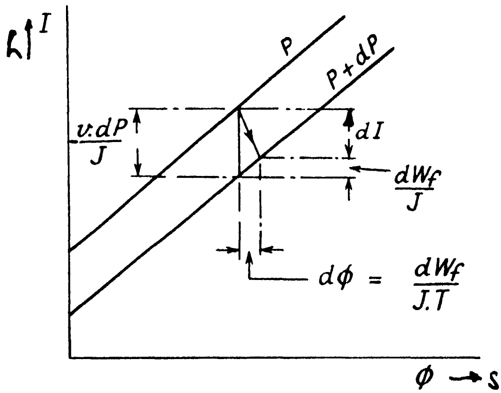


FIG. 38

We write δQ for the heat supplied in this case to distinguish it from heat supplied through the wall of the nozzle.

$$\therefore \qquad \delta Q = \delta I - \frac{v\,.\,\delta P}{J} = \frac{\delta W_f}{J} \quad . \quad . \quad . \quad (43)$$

That is, although the process is adiathermal or adiabatic, heat δQ is supplied internally equal to the friction loss $\dfrac{\delta W_f}{J}$.

For a small change of state, the change of entropy

$$\delta\phi = \frac{\delta Q}{T} = \frac{\delta W_f}{JT} \quad . \quad . \quad . \quad (44)$$

The relevant I $-$ ϕ chart for a small expansion is shown in Fig. 38. It will be seen that the slope of the constant-pressure line $P + \delta P$ is the absolute temperature T, as already proved in Art. 27.

41. Adiabatic Equation for Steam. It may be readily shown that when a perfect gas expands adiabatically the pressure p and the volume v are related by the simple expression $pv^{\gamma} = C$, where C is a constant and γ is the ratio of the specific heat at constant pressure to that at constant volume. It should be emphasized that this relation applies strictly to an ideal gas obeying the laws of Boyle and Charles and having constant specific heats. Steam, even when superheated to an appreciable extent, deviates considerably from the laws of perfect gases, and there are no real grounds for expecting that, during an adiabatic expansion of steam, the p–v relationship should be of the form

$$pv^n = \text{constant} \quad . \quad . \quad . \quad . \quad (45)$$

where n is a constant. The test is, however, easily made. Corresponding values of p and v may be obtained from a Mollier diagram and the logs. of their values plotted. Then if

$$pv^n = C$$
$$\log. p + n \log. v = \log. C$$

and we have a straight-line relationship. When the steam is assumed to be initially dry and saturated, then plots made for different initial pressures deviate very little from straight lines. Mean values of n, where

$$n = \frac{\log. p_1 - \log. p_2}{\log. v_2 - \log. v_1}$$

calculated for various ratios of $\frac{p_2}{p_1}$ and based on Callendar's Enlarged Mollier Diagram, first increase very slightly as $\frac{p_2}{p_1}$ is diminished and then diminish slightly as $\frac{p_2}{p_1}$ is further reduced. The mean value of n for the ratio $\frac{p_2}{p_1}$ is shown in Fig. 39.

Rankine (1) states that for adiabatic expansion "it has been deduced by trial that for such pressures as usually occur in the working of steam engines, $pv^{1 \cdot 11}$ = constant." Zeuner (2) gives the well-known equation $n = 1{\cdot}035 + 0{\cdot}1x_1$, where x_1 is the initial dryness fraction of the steam. This makes $n = 1{\cdot}135$ for steam initially dry and saturated. Callendar found experimentally that when steam expands in the superheated condition, the relationship between p and v is given by the expression

$$p(v - b)^{1 \cdot 3} = \text{constant} \quad . \quad . \quad . \quad . \quad (46)$$

and, since $w = 1$, $A_t = 0{\cdot}61$ sq. in. which is in fair agreement with the value 0·604 given in Fig. 47.

49. Friction in Turbine Nozzles. In the foregoing articles we have assumed that steam is a perfect inviscid fluid which flows at all velocities without "friction." In this article we shall deal very briefly with the subject of fluid friction and its application to nozzle flow.

Consider first the flow of a fluid through a straight circular tube. Osborne Reynolds showed that such a flow may take place in two quite different ways. At low velocities the flow is described as stream-line in character.

This was demonstrated by Reynolds with the simple apparatus shown in Fig. 50. Water flows from a tank through a glass tube A

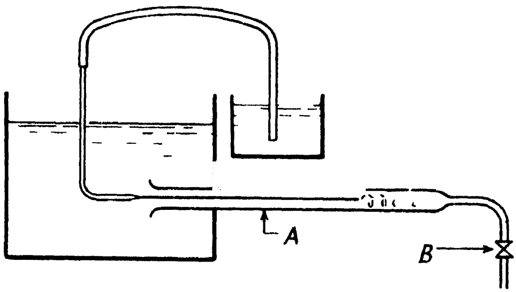


FIG 50

having a funnel-shaped inlet. The rate of flow may be controlled by means of the cock B. A thin thread of coloured liquid is allowed to flow into the centre of the tube A at about the same velocity as the water. Then at velocities under a certain value, the thread of coloured liquid will pass through the tube as a clear undisturbed thread without mixing with the surrounding water. This experiment shows that the particles of fluid are passing through the tube in directions parallel to the axis.

If the flow is increased beyond a certain rate by opening the cock B, then the thread of coloured liquid will break up owing to cross-currents in the flow. When such a flow is fully developed it is described as turbulent flow.

Reynolds also found that the pressure loss due to friction in a tube varied directly as the mean velocity with stream-line flow, but nearly as the square of the mean velocity with turbulent flow.

The distribution of velocity is also very different in the two kinds of flow. Fig. 51 shows the variation of velocity in a circular tube with viscous or stream-line flow. The velocity is nil at the tube wall and a maximum at the tube axis, the velocity curve being parabolic. It may be shown that the mean velocity is half the maximum.

With turbulent flow (Fig. 52), the velocity is again a maximum at the tube axis and nil at the tube wall. There is a thin layer of fluid adjacent to the tube wall, the laminar sub-layer, in which the flow is stream-line and across which the velocity increases rapidly. In addition there is a large central turbulent core of fluid, and between this core and the thin laminar sub-layer there is an annular transition zone.

Experiment shows that the intensity of friction R per unit of internal area of a pipe depends on the pipe diameter d, the absolute

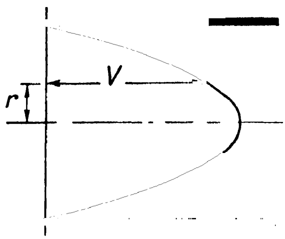


FIG. 51 Velocity Distribution in a Circular Pipe with Stream-line Flow

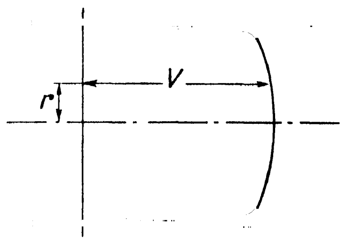


FIG. 52 Velocity Distribution in a Circular Pipe with Turbulent Flow

viscosity μ of the fluid, the density ρ of the fluid, and finally on the mean velocity V, i.e.

$$R - f(d, \mu, \rho, V)$$

Experiment also shows that, beyond a certain distance from a pipe inlet, velocity profile is constant and the flow is said to be dynamically similar. Under these conditions it may be shown by dimensional analysis that $\frac{R}{\rho V^2}$ is a function of the quantity $\frac{Vd\rho}{\mu}$. Each of the quantities $\frac{R}{\rho V^2}$ and $\frac{Vd\rho}{\mu}$ will be found to be dimensionless, i.e. its numerical value will be independent of the system of units used to express the magnitudes of the various physical quantities V, d, ρ, etc., provided a consistent system of units is employed.

The quantity $\frac{Vd\rho}{\mu}$ is known as Reynolds' number and is frequently written R_e. The quantity $\nu = \frac{\mu}{\rho}$ is termed the kinematic viscosity of the fluid. Hence $R_e = \frac{V \cdot d}{\nu}$.

The well-known experiments by Stanton and Pannell (5) on the resistance to flow through smooth brass tubes established the validity of the principle of dynamical similarity. The results are shown in Fig. 53. The left-hand part of the curve represents viscous

flow and can be predicted from theoretical considerations. When R_e reaches about 2,000 the quantity $\frac{R}{\rho V^2}$ increases rapidly, and above $R_e = 2,800$ the flow becomes wholly turbulent. These experiments were made on tubes of different diameters and with the fluids oil, air, and water. The experimental points are not shown in Fig. 53, but they covered a very narrow band which could be

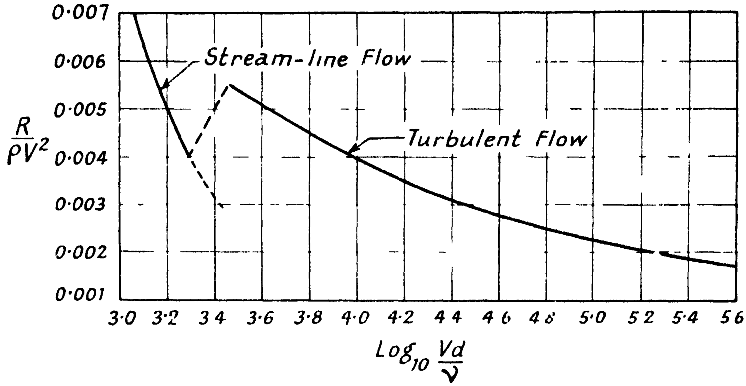


FIG. 53 Curves Based on Work of Stanton and Pannell

accepted as a unique curve. It was shown by Dr. C. H. Lees (6) that for turbulent flow,

$$\left(\frac{R}{\rho V^2} - 0{\cdot}0009\right)\left(\frac{Vd}{\nu}\right)^{0{\cdot}35} = 0{\cdot}0765 \quad . \quad . \quad (66)$$

The effect of roughness has been investigated by I. Nikuradse (7), who roughened the inside of tubes artificially by means of sand grains which were previously graded so as to obtain uniform size and shape. Experiments were made to determine the effect of different ratios r/k, where r is the radius of the tube and k the mean height of the excrescences. The results of these experiments are shown in Fig. 54. Values of $\log_{10}(100f)$ are plotted against $\log_{10} R_e$, where the friction coefficient

$$f = 2 \cdot \frac{dP}{dl} \cdot \frac{d}{\rho V^2} \quad . \quad . \quad . \quad . \quad . \quad (67)$$

Considering that the pressure drop dP over the length of pipe dl is utilized in overcoming friction, then $\frac{dP}{dl} = \frac{4R}{d}$

and $$f = \frac{8R}{\rho V^2} \quad . \quad . \quad . \quad . \quad . \quad (68)$$

This enables the results to be correlated with those shown in Fig. 53.

The surface irregularities in pipes, nozzles, etc. are not uniform and it is difficult to assess a value of the roughness factor k/r. For values of R_e greater than 10^5, Nikuradse has given the following expression for f—

$$f = \frac{1}{\left(2 \log_{10} \frac{r}{k} + 1{\cdot}74\right)^2} \quad . \quad . \quad . \quad . \quad (69)$$

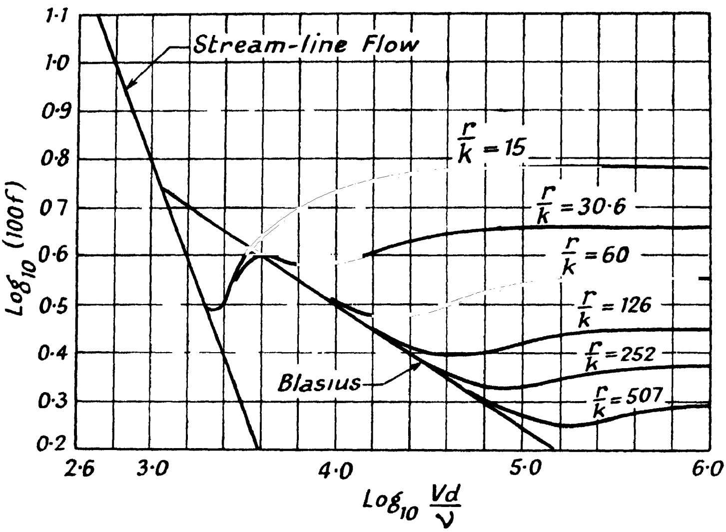


FIG. 54 – Friction Coefficient as a Function of Reynolds Number and the Surface Roughness (Nikuradse)

The straight line shown in Fig. 54 and marked Blasius (8) gives up to a Reynolds number of 80,000

$$f = \frac{0{\cdot}3164}{\sqrt[4]{R_e}} \quad . \quad . \quad . \quad . \quad . \quad (70)$$

50. Viscosity of Steam. A brief discussion of viscosity is given in Art. 243 in the Chapter on "Bearings and Lubrication." Some results obtained by H. Speyerer (9) in the ranges $p = 14$ to 142 lb. per sq. in. and $t = 212$ to 660 degrees F. may be represented very closely by the formula—

$$\mu \times 10^7 = (53{\cdot}3 + 0{\cdot}11p) + 0{\cdot}135t \quad . \quad . \quad (71)$$

where μ = absolute viscosity, $\frac{\text{lb.}}{\text{ft.-sec}}$

p = pressure, lb. per sq. in. abs.

t = steam temp. °F.

Fig. 55, reproduced by permission of the American Society of Mechanical Engineers, shows the results of experiments by Messrs.

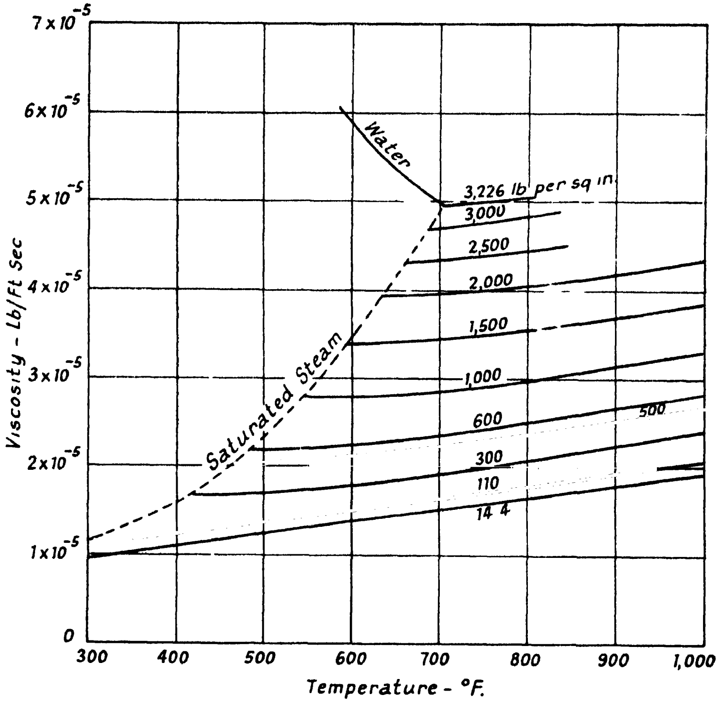


Fig. 55 – Viscosity of Water and Steam

(Reproduced by Permission of the American Society of Mechanical Engineers)

Hawkins, Solberg and Potter (10). These cover a very wide range of pressure and temperature.

51. The Meaning of Nozzle Efficiency. A steam nozzle is a device for converting energy made available by the expansion of steam (isentropic heat drop in the ideal case) into kinetic energy. Unfortunately, owing to the effects of the boundary walls of the nozzle, the steam velocity is never uniform across the outlet section, even in a simple nozzle with a straight axis. Hence, unless we have precise knowledge of the way in which the velocity varies across the nozzle,

we cannot calculate the total kinetic energy either per unit mass or per unit time.

In practical turbine calculations, however, we are driven to the assumption of uniform steam velocities at inlet to, and outlet from, nozzles.

Let V_1 = velocity at inlet to nozzle.
V_2 = velocity at outlet from nozzle.
V_{a2} = velocity at outlet from nozzle after adiabatic and isentropic expansion.
I_1 = initial enthalpy.
I_2 = final enthalpy.
I_{a2} = final enthalpy after adiabatic and isentropic expansion.

Then, assuming adiathermal expansion,

$$I_1 - I_2 = \frac{V_2^2 - V_1^2}{2gJ}$$

$$I_1 - I_{a2} = \frac{V_{a2}^2 - V_1^2}{2gJ}$$

First Definition. Nozzle efficiency is the ratio of the actual gain in kinetic energy to that due to isentropic expansion, i.e.

$$\eta_n = \frac{V_2^2 - V_1^2}{V_{a2}^2 - V_1^2} = \frac{I_1 - I_2}{I_1 - I_{a2}} \quad . \quad . \quad . \quad (72)$$

If V_1 is small compared with V_2 then the nozzle efficiency is nearly equal to

$$\eta_n = \frac{V_2^2}{V_{a2}^2} = \eta_v^2$$

where $\eta_v = \frac{V_2}{V_{a2}}$, the velocity coefficient for the nozzle.

Second Definition. The nozzle efficiency is the ratio of the final kinetic energy to the sum of the incoming kinetic energy and the isentropic heat drop. In this case,

$$\eta_n = \frac{V_2^2}{V_1^2 + 2gJ(I_1 - I_{a2})} \quad . \quad . \quad . \quad (73)$$

or

$$\frac{V_2^2}{2gJ} = \eta_n \left\{ \frac{V_1^2}{2gJ} + (I_1 - I_{a2}) \right\}$$

This assumes that, owing to shock and other entrance losses, the incoming kinetic energy is utilized with the same efficiency as the available isentropic heat drop.

Third Definition. This requires the use of two factors, (*a*) the efficiency with which the incoming kinetic energy is utilized, and (*b*) the efficiency with which the isentropic heat drop is utilized. Thus we have

$$\frac{V_2^2}{2gJ} = \eta_1 \frac{V_1^2}{2gJ} + \eta_n(I_1 - I_{a2})$$

or

$$\eta_n = \frac{V_2^2 - \eta_1 V_1^2}{2gJ(I_1 - I_{a2})} \quad . \quad . \quad . \quad . \quad . \quad (74)$$

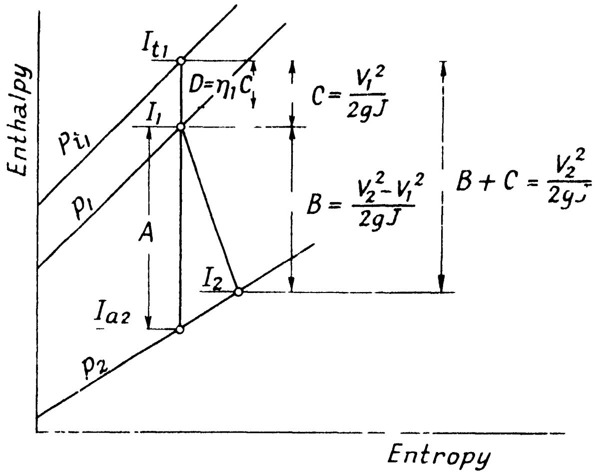


FIG. 56—Diagram Explaining Nozzle Efficiencies

This is, in effect, the method used later in connection with the flow of steam through impulse-reaction turbine blades and is identical with method 2 if $\eta_1 = \eta_n$.

The meaning of these efficiencies may be further illustrated by the $\phi - I$ diagram of Fig. 56, in which the dimension A represents the isentropic heat drop and B the actual heat drop. C is the heat equivalent of the initial kinetic energy giving the stagnation or total pressure P_{t1}. Clearly B + C represents the final kinetic energy at the nozzle outlet.

Then according to the first definition,

$$\eta_n = \frac{B}{A};$$

according to the second,

$$\eta_n = \frac{B + C}{A + C};$$

and according to the third,

$$\eta_n = \frac{B + C - \eta_1 C}{A},$$

or

$$\eta_n = \frac{B + (1 - \eta_1)C}{A}$$

EXAMPLE 6. Steam enters a nozzle with a velocity of 400 ft. per sec and issues from the nozzle at 1,230 ft. per sec., the isentropic heat drop being 29 B.Th.U. per lb. Calculate the nozzle efficiency according to the above three definitions. For the purpose of calculating the third, assume $\eta_1 = 0{\cdot}8$.

(1) $$\frac{V_1^2}{2gJ} = C = 3{\cdot}20, \quad \frac{V_2^2}{2gJ} = B + C = 30{\cdot}21.$$

Then $$\eta_n = \frac{30{\cdot}21 - 3{\cdot}20}{29{\cdot}0} = 93{\cdot}15 \text{ per cent.}$$

(2) $$\eta_n = \frac{30{\cdot}21}{29{\cdot}0 + 3{\cdot}20} = 93{\cdot}80 \text{ per cent.}$$

(3) $$\eta_n = \frac{27{\cdot}01 + (0{\cdot}2 \times 3{\cdot}20)}{29{\cdot}0} = 95{\cdot}35 \text{ per cent.}$$

52. Effect of Friction on the Critical Pressure Ratio. It is shown in Art. 123, Chapter XII, that the index of v in the expression Pv^m = constant for a small expansion in which the efficiency η is constant is also constant if the isentropic index n is constant. It is shown that

$$m = \frac{n}{\eta + n(1 - \eta)}$$

Referring to Fig 38, Art. 40, it is clear that

$$J\,dI = d\left(\frac{V^2}{2g}\right) = -\eta \, . \, v \, . \, dP$$

Then, assuming flow from rest and from a pressure P_1, at any pressure P

$$\frac{V^2}{2g} = \eta \int_{P_1}^{P} v \, . \, dP$$

If Pv^m = constant, the velocity at P

$$= V = \sqrt{\frac{2g\eta m}{m - 1} \, . \, P_1 v_1 \left\{1 - \left(\frac{P}{P_1}\right)^{\frac{m-1}{m}}\right\}} \quad . \quad . \quad (75)$$

By employing the methods of Art. 43, it may be shown that

$$\frac{w}{A} = \sqrt{\frac{2g \,.\, \eta \,.\, m}{m - 1} \frac{P_1}{v_1}\left(r^{\frac{2}{m}} - r^{\frac{m+1}{m}}\right)} \qquad . \quad . \quad . \quad (76)$$

where $r = P/P_1$. For given values of P_1, v_1, and η, w/A is a maximum when

$$r = \left(\frac{2}{m + 1}\right)^{\frac{m}{m-1}} \qquad . \quad . \quad . \quad . \quad (77)$$

Values of m and r are given in Table II. It will be seen that the effect of friction on the critical pressure ratio is small.

TABLE II

EXPONENT OF v AND THE CRITICAL PRESSURE RATIO FOR FRICTIONALLY RESISTED EXPANSION IN A NOZZLE

(*a*) Steam initially dry and saturated. n taken as 1·135.

Values of η	1·0	0·95	0·90	0·85	0·80
m	1·135	1·127	1·119	1·112	1·105
r	0·5774	0·5791	0·5807	0·5823	0·5836
K	1·0	0·971	0·942	0·912	0·882

(*b*) Steam superheated down to the critical pressure $n = 1{\cdot}3$.

Values of η	1·0	0·95	0·90	0·85	0·80
m	1·3	1·281	1·262	1·244	1·226
r	0·5457	0·5492	0·5527	0·5561	0·5594
K	1·0	0·967	0·935	0·902	0·869

According to this one-dimensional treatment, the steam velocity does not reach the local sonic velocity at the nozzle throat but at a short distance beyond it. By using the method of Art. 44, we find the velocity at the smallest section of the nozzle to be

$$V = \sqrt{\eta \,.\, g \,.\, m \,.\, Pv}$$

or

$$V = K \text{ (local sonic velocity)}$$

where

$$K = \sqrt{\frac{\eta \,.\, m}{n}}$$

Values of K are given in Table II.

At first sight it might appear that the above result, namely that the throat velocity is lower than the local sonic velocity, invalidates

the explanation of critical pressure given in Art 44 for isentropic expansion It is considered, however, that for a viscous fluid in a pipe of small diameter the compressions and rarefactions which occur in sound are no longer adiabatic and the velocity of sound will lie between Newton's isothermal value $\sqrt{gpv}$ and Laplace's adiabatic value $\sqrt{gnpv}$ Furthermore, the reduction in sonic velocity is greater the smaller the diameter of the pipe In real flows the problem is further complicated by the existence of the boundary layer

53. Critical Pressure Ratio in a Frictionally Resisted Expansion from a Given Initial Velocity. Consider an expansion from pressure P_1 lb. per sq ft and velocity V_1 ft per sec, and let P_2 be the steam pressure at the throat of the nozzle

Suppose that η is the "small stage" nozzle efficiency, i e if we assume that the actual expansion is made up of a succession of very small expansions, then the isentropic efficiency of each small expansion will be η This is not exactly identical with the nozzle efficiency (1) defined in Art 51, but the difference between the two efficiencies for an expansion down to the critical pressure is so small as to be negligible

Again, the index m of the expansion curve will be

$$m = \frac{n}{n - \eta(n-1)}$$

where n is the isentropic index

Then since

$$d\left(\frac{V^2}{2g}\right) = -\eta\, v\, dP$$

$$\frac{V_2^2 - V_1^2}{2g} = \frac{\eta m}{m-1}(P_1 v_1 - P_2 v_2)$$

and
$$V_2 = \sqrt{\frac{2g\,\eta m}{m-1} P_1 v_1 \left(1 - r^{\frac{m-1}{m}}\right) + V_1^2} \qquad (78)$$

where $r = P_2/P_1$

Also
$$\frac{w}{A_2} = \sqrt{\frac{2g\eta m}{m-1}\frac{P_1}{v_1}\left(r^{\frac{2}{m}} - r^{\frac{m+1}{m}}\right) + \frac{V_1^2 r^{\frac{2}{m}}}{v_1^2}} \qquad (79)$$

Following the methods of Art 48, we find for the maximum discharge per unit area,

$$r = \left(\frac{2}{m+1}\right)^{\frac{m}{m-1}}\left\{1 + \frac{(m-1)V_1^2}{2g\eta m P_1 v_1}\right\}^{\frac{m}{m-1}} \quad . \quad . \quad (80)$$

Since the second term in the bracket is always small compared with unity, we may write

$$r = \left(\frac{2}{m+1}\right)^{\frac{m}{m-1}}\left\{1 + \frac{V_1^2}{2g\eta P_1 v_1}\right\} \qquad . \qquad . \quad (81)$$

Note. Values of $\left(\frac{2}{m+1}\right)^{\frac{m}{m-1}}$ are given in Table II for various efficiencies.

The following examples will show the effects of friction loss on nozzle throat areas.

EXAMPLE 7. Dry and saturated steam enters a nozzle at a pressure $p = 110$ and expands from rest to the critical pressure $p = 63{\cdot}5$. Using the Mollier diagram, obtain the following—

(*a*) Outlet velocity.
(*b*) Final dryness fraction.
(*c*) Nozzle outlet area for a mass flow of 0·05 lb. per sec.
(*d*) Nozzle diameter for a round nozzle.

Assume in Case I that the flow is frictionless, and in Case II that the nozzle efficiency is 0·9.

Case I. Frictionless Expansion. The following data are obtained from the Mollier diagram—

p	x	ϕ	I
110	1·0000	1·5963	1,189·9
63·5	0·9635	1·5963	1,146·2
			43·7

Then, since $V_1 = 0$, $V_2 = 223{\cdot}8\sqrt{43{\cdot}7} = 1{,}480$ ft./sec. By interpolation from steam tables, $v_{s2} = 6{\cdot}803$.

Hence $$A_2 = (0{\cdot}05 \times 0{\cdot}9635 \times 6{\cdot}803) \div 1{,}480$$
$$= 0{\cdot}0002215 \text{ sq. ft.}$$

from which the diameter required is 0·2015 in.

Case II. Flow with Friction. Using the data given in Table II we find that, for a small stage efficiency of 0·90, the critical pressure ratio is about 0·58. Hence the critical pressure is 63·8 lb per sq. in. abs.

p	x	ϕ	I
110	1·0000	1·5963	1,189·9
63·8	0·9636	1·5963	1,146·6
			43·3
		0·9 × 43·3	39·0
63·8	0·9687	1·6018	1,150·9

Then $\quad V_2 = 223{\cdot}8\sqrt{39{\cdot}0} = 1{,}397$ ft. per sec.

Hence $\quad A_2 = (0{\cdot}05 \times 0{\cdot}9687 \times 6{\cdot}772) \div 1{,}397$

$\quad\quad = 0{\cdot}0002347$ sq. ft.

from which the diameter is 0·2074. The increase in nozzle area is 6·0 per cent; in other words, the discharge would be 6·0 per cent less than with adiabatic and frictionless flow.

EXAMPLE 8. Using the data given in Example 7, but assuming an inlet velocity of 400 ft. per sec., calculate the critical pressures, throat velocities and throat diameters for both frictionless and frictionally resisted expansions.

Case I. Isentropic Expansion. By using eq. (62), p. 96, and again assuming $n = 1{\cdot}135$, the critical pressure ratio is

$$r = 0{\cdot}577 + \frac{0{\cdot}0000621 \times 400^2}{110 \times 4{\cdot}046} = 0{\cdot}599$$

Hence the critical pressure is 65·9 lb. per sq. in. abs. From the Mollier chart

p	x	ϕ	I
110	1·0000	1·5963	1,189·9
65·9	0·9661	1·5963	1,149·1
			40·8

$$\frac{V_2^2 - V_1^2}{2gJ} = 40{\cdot}8$$

$$\frac{V_2^2}{2gJ} = 40{\cdot}8 + \frac{400^2}{2gJ} = 44{\cdot}0$$

from which $V_2 = 1{,}484$, a value almost identical with that for expansion from rest. By interpolation from steam tables, $v_{s2} = 6{\cdot}57$.

Hence $\quad A_2 = (0{\cdot}05 \times 0{\cdot}9661 \times 6{\cdot}57) \div 1{,}484$

$\quad\quad = 0{\cdot}0002189$ sq. ft.

from which the throat diameter is 0·2003 in.

Case II. Flow with Friction. The critical pressure ratio is given by eq. (80), and since $m = 1{\cdot}119$,

$$r = 0{\cdot}5807\left\{1 + \frac{0{\cdot}119 \times 400^2}{64{\cdot}4 \times 0{\cdot}9 \times 1{\cdot}119 \times 144 \times 110 \times 4{\cdot}046}\right\}^{9{\cdot}4}$$

$$= 0{\cdot}5807 \times 1{\cdot}00458^{9{\cdot}4} = 0{\cdot}6062$$

which compares with the approximate value $r = 0{\cdot}6056$ given by eq. (81).

The following figures, obtained by calculation, are set down in tabular form.

p	x	ϕ	I
110	1·0000	1·5963	1,189·9
66·66	0·9677	1·5963	1,149·8
			40·1
		$0{\cdot}9 \times 40{\cdot}1 =$	36·1
66·66	0·9709	1·6008	1,153·8

Then $$\frac{V_2^2}{2gJ} = 36{\cdot}1 + 3{\cdot}2 = 39{\cdot}3$$

and $V_2 = 1{,}403$ ft. per sec.

At $p = 66{\cdot}66$

$v_{s2} = 6{\cdot}499.$

Hence $$A_2 = (0{\cdot}05 \times 0{\cdot}9709 \times 6{\cdot}499) \div 1{,}403$$
$$= 0{\cdot}0002249 \text{ sq. ft.}$$

from which the diameter is 0·2031 in.

The following table summarizes the results obtained in the two preceding examples and shows that, owing to changes in the critical pressure due to friction and approach velocity, the required throat diameter changes very little.

V_1	η	r	V_2	Throat Dia., In.
0	1·0	0·577	1,480	0·2015
0	0·9	0·580	1,397	0·2074
400	1·0	0·599	1,484	0·2003
400	0·9	0·606	1,403	0·2031

54. **To calculate the Mass Flow through a Convergent Nozzle, given the Inlet and Outlet Areas and Pressures.** Consider a simple convergent nozzle as shown in Fig. 57. Let the inlet and outlet areas and pressures be A_1, A_2 sq. ft. and p_1, p_2 respectively. The flow lines and sections of surfaces of equal pressure are shown diagrammatically in the figure. The area A_1 should be that of the curved surface $a - a$.

Let v_1 and v_2 be the specific volumes at p_1 and p_2 respectively. The value of the index m may be calculated from the assumed nozzle efficiency and hence v_2 may be calculated from the known value of v_1. Alternatively, the conditions may be found from the Mollier chart. Similarly, V_2 may be calculated for any given value of V_1 and assumed nozzle efficiency. Again, it will be assumed that the steam velocity across any section is uniform.

The calculation is best made by successive approximations. In the first place, V_1 may be assumed to be zero, and V_2 and v_2 are calculated. Then since

$$w = \frac{A_1 V_1}{v_1} = \frac{A_2 V_2}{v_2}$$

$$V_1 = \frac{v_1}{v_2} \cdot \frac{A_2}{A_1} \cdot V_2$$

from which an approximate value of V_1 is obtained.

The value of V_2 is now re-calculated for this value of V_1. A second approximation is then made for V_1, and V_2 again re-calculated. This is usually sufficiently accurate for practical purposes.

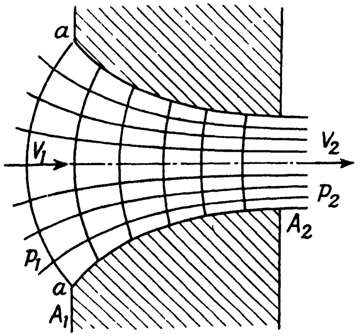


FIG. 57

EXAMPLE 9. Fig. 58 shows the developed cross-section of a turbine nozzle. The radial height is constant at 1·2 in. The pressure at inlet is 40 lb. per sq. in. abs. and the steam there is dry and saturated. Calculate the mass flow per second through the nozzle when the pressure at outlet is 26 lb. per sq. in. abs. Assume that the nozzle efficiency defined as

$$\eta_n = \frac{V_2^2}{V_1^2 + 2gJ(I_1 - I_{a2})}$$

is 92 per cent.

The inlet area of the nozzle is

$$(1{\cdot}2 \times 1{\cdot}896) \div 144 = 0{\cdot}0158 \text{ sq. ft.}$$

The width of the channel at outlet

$$= 2 \,.\, \sin 16^\circ - 0{\cdot}104 = 0{\cdot}4472 \text{ in.}$$

$$\therefore \text{ Area at outlet} = (1{\cdot}2 \times 0{\cdot}4472) \div 144$$
$$= 0{\cdot}00373 \text{ sq. ft.}$$

From the Mollier chart

p	x	ϕ	I
40	1·0000	1·6776	1,170·5
26	0·9747	1·6776	1,137·8
			32·7
		0·92 × 32·7 =	30·1
26	0·9774	1·6805	1,140·4

Hence the specific volume v_2 is $0{\cdot}9774 \times 15{\cdot}72 = 15{\cdot}37$ cu. ft. per lb. If we first assume $V_1 = 0$, then $V_2 = 223{\cdot}8\sqrt{30{\cdot}1} = 1{,}227$ ft. per sec., and since $v_1 = 10{\cdot}50$,

$$V_1 = \frac{10{\cdot}50}{15{\cdot}37} \times \frac{0{\cdot}00373}{0{\cdot}0158} \times 1{,}227$$

$$= 198 \text{ ft. per sec. (First approx.)}$$

Using this approximate value we have

$$\left(\frac{V_2}{223{\cdot}8}\right)^2 - 0{\cdot}92\left(\frac{198}{223{\cdot}8}\right)^2 + 30{\cdot}1 = 30{\cdot}82$$

from which $V_2 = 1{,}242$ ft. per sec. A recalculation gives $V_1 = 201$ ft per sec. (Second approx.) This gives $V_2 = 1{,}242$ ft.

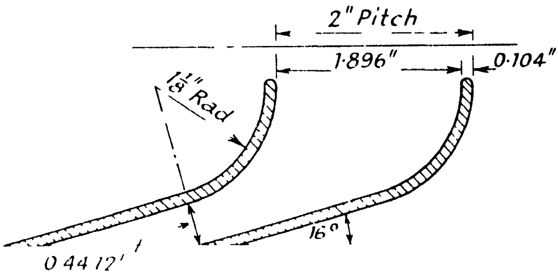


FIG. 58

per sec., the difference made by using the second approximation to V_1 being negligible.

Then the mass flow

$$w = \frac{0{\cdot}00373 \times 1{,}242}{15{\cdot}37}$$

$$= 0{\cdot}3014 \text{ lb. per sec.}$$

55. Calculation of Friction Loss in a Turbine Nozzle. The friction loss in a turbine nozzle may be estimated *approximately* on the basis of pipe friction experiments. The method may be illustrated by means of an example.

EXAMPLE 10. Fig. 59 shows the same nozzle as that of Example 9. It is required to estimate the total friction loss when the nozzle is discharging 0·3014 lb. per sec. under the same pressure conditions as those set out in Example 9. It will be assumed that the average surface roughness is 0·005 in. in height and that the nozzle efficiency is the same as in Example 9, namely, 92 per cent.

The section of the nozzle is first drawn to scale as in Fig. 59, and a number of straight lines such as A A, B B, etc. are drawn across the channel so that they are approximately equally inclined to the

walls of the nozzle. These lines are then bisected and a "centre-line" CD is drawn. A–A, etc. are assumed to be lines of constant pressure.

The line CD is now divided into a suitable number of sections and

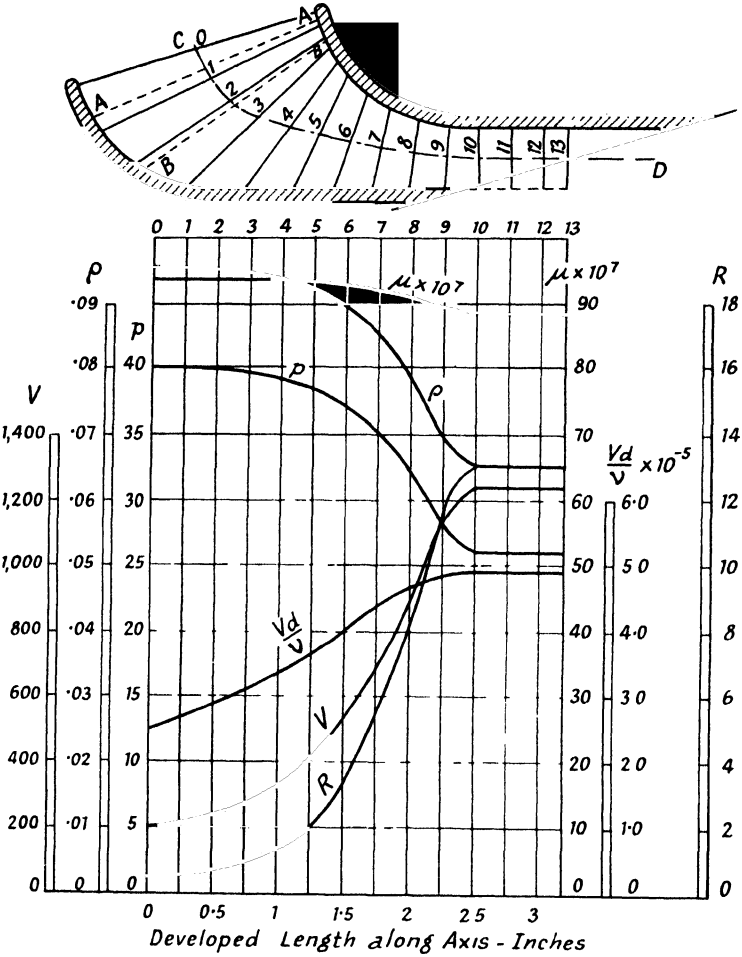


FIG 59

new radials are drawn through each of the section points 1, 2, 3, etc. The area of each section is now calculated and set out in Table III. The perimeter is then obtained and the hydraulic mean depth

$$m = \frac{\text{Area of section}}{\text{Perimeter}}$$

calculated, from which the diameter ($d = 4m$) of the equivalent round tube is obtained. It will be assumed that the work done in overcoming friction in the rectangular nozzle channel is the same as that in a round tube having the same hydraulic mean depth.

The nozzle outlet is oblique to the axis, but the surface swept by the steam is equal to that of a nozzle having an outlet face normal to the axis and terminating at section 13. This latter type of nozzle is substituted for the actual nozzle with the oblique outlet. Unfortunately, this procedure, apparently simple, involves an assumption that steam flowing through the parallel outlet suffers a loss of energy due to friction without simultaneously undergoing a drop of pressure.

The relationship between steam pressure on the one hand, and velocity, specific volume and required nozzle area on the other is derived for a flow of 0·3014 lb. per sec. The results of the calculation are shown in Fig. 59. From these curves and from the known areas at the various nozzle sections, the steam pressure, density, and velocity may be written down in Table III. The viscosity is calculated from eq. (71) and the value of Reynolds number calculated.

It will be observed that all the values of Reynolds number are greater than 10^5; consequently the value of the quantity f may be calculated from Nikuradse's equation (69). It is sufficiently accurate to assume a mean value of the equivalent radius r of the nozzle sections. This has been taken as 0·03 ft., as it applies more nearly to the sections near the outlet where the friction losses are most important.

Then
$$\frac{r}{k} = \frac{0{\cdot}03 \times 12}{0{\cdot}005} = 72$$

and
$$f = 0{\cdot}0336$$

$$\therefore \qquad \frac{R}{\rho V^2} = \frac{0{\cdot}0336}{8} = 0{\cdot}0042$$

and since R is a force in poundals,

$$R = \frac{0{\cdot}0042\rho V^2}{g} = 0{\cdot}00013\rho V^2 \, \frac{\text{lb. wt.}}{\text{ft.}^2}$$

Consider now the flow of steam over an element of length δl of the nozzle wall and let the corresponding wall surface be δS. Then the force of friction is $R \, . \, \delta S$ and the work done per second against friction is $RV\delta S$ ft.-lb.

$\therefore$ Friction loss per lb. of steam

$$= \frac{RV\delta S}{\rho AV} = \frac{R \, . \, \delta l}{\rho \, . \, m} \text{ ft.-lb.}$$

where m is the hydraulic mean depth. This expression is used for each element of the nozzle. The total friction loss is the sum of the

losses for all elements and amounts to 1,597 ft.-lb., or 2·05 B.Th.U. per lb. of steam.

Since the isentropic heat drop is 32·7 for the whole expansion and the initial kinetic energy is 0·805, the kinetic energy of the outgoing steam is

$$(32{\cdot}7 + 0{\cdot}805) - 2{\cdot}05 = 31{\cdot}455 \text{ B.Th.U. per lb.}$$

$$\therefore \qquad \text{Nozzle efficiency} = \frac{31{\cdot}455}{33{\cdot}505} = 93{\cdot}9 \text{ per cent.}$$

TABLE III

CALCULATION OF APPROXIMATE FRICTION LOSS IN A TURBINE NOZZLE

Section	Area A sq. in.	Peri-meter P in.	$m = \frac{A}{P}$ in.	Equiv Diam. d ft.	Steam Press p	Steam Density ρ	Steam Velocity V
0	2·276	6·192	0·368	0·123	40·0	0·0954	201
			0·366			0·0952	209
1	2·220	6·10	0·364	0·121	40·0		
			0·358			0·0949	232
2	2·062	5·84	0·353	0·118	39·8		
			0·343			0·0944	263
3	1·800	5·40	0·333	0·111	39·5	0·0943	280
			0·316			0·0936	304
4	1·440	4·80	0·300	0·100	39·1		
			0·282			0·0925	367
5	1·140	4·30	0·265	0·0883	38·4	0·0920	410
			0·248			0·0908	475
6	0·906	3·92	0·231	0·0770	37·1	0·0893	545
			0·216			0·0871	630
7	0·732	3·62	0·202	0·0673	35·4	0·0856	699
			0·191			0·0813	811
8	0·612	3·42	0·179	0·0597	32·1	0·0785	900
			0·173			0·0735	1,027
9	0·552	3·32	0·167	0·0555	27·9	0·0692	1,137
			0·165			0·0656	1,232
10	0·537	3·29	0·163	0·0543	26·0	0·0652	1,242
			0·163			0·0652	1,242
11	0·537	3·29	0·163	0·0543	26·0	0·0652	1,242
			0·163			0·0652	1,242
12	0·537	3·29	0·163	0·0543	26·0	0·0652	1,242
			0·163			0·0652	1,242
13	0·537	3·29	0·163	0·0543	26·0	0·0652	1,242

This is somewhat higher than the figure assumed in the calculations. The change in nozzle efficiency based on the more correct value of η_n would be very small.

The influence of surface roughness on the calculated friction loss may be gauged from the following data referring to this example—

Mean Height of Roughness k in.	Friction Loss per Lb of Steam B.Th.U.	Nozzle Efficiency Per Cent
0·002	1·56	95·3
0·005	2·05	93·9
0·01	2·60	92·2

TABLE III (*Continued*)

Section	Abs Viscosity $\mu \times 10^7$	$\frac{Vdp}{\mu} \times 10^{-5}$	$\log_{10} \frac{Vdp}{\mu}$	R lb ft^{-2}	δl in	δW_f	Time Interval δt sec.
0	93·8	2·49	5·396	0·491			
				0·563	0·25	4·0	0·000100
1							
				0·69	0·25	4·5	0·000090
2							
				0·87	0·25	6·5	0·000079
3	93·7	3·13	5·495	0·96			
				1·12	0·25	9·5	0·000068
4							
				1·56	0·25	15·0	0·000057
5	93·3	3·57	5·553	2·02			
				2·67	0·25	29·5	0·000044
6	92·9	4·04	5·606	3·44			
				4·38	0·25	58·0	0·000033
7	92·3	4·36	5·639	5·43			
				6·96	0·25	112·0	0·000026
8	91·2	4·62	5·665	8·26			
				10·27	0·25	202·5	0·000020
9	89·6	4·88	5·688	11·63			
				12·84	0·25	296·5	0·000017
10	88·9	4·94	5·694	13·04			
				13·04	0·25	307·0	0·000017
11	88·9	4·94	5·694	13·04			
				13·04	0·25	307·0	0·000017
12	88·9	4·94	5·694	13·04			
				13·04	0·2	245·0	0·000013
13	88·9	4·94	5·694	13·04			
					Totals:	1,597·0	0·000581

It may be inferred from these figures that a smooth finish to the walls of a nozzle leads to greater efficiency. At supersonic velocities in the divergent part of convergent-divergent nozzles a smooth

surface is even more important than in nozzles where the velocities are subsonic, because small surface excrescences become the source of shock waves which cause additional losses.

Over and above the surface friction losses calculated in the above example, there would be losses due to impact at the leading edge, and to secondary flows. These losses would vary in amount according to whether the design was good or bad but could never be entirely avoided.

In the last column of Table III the time interval for each element

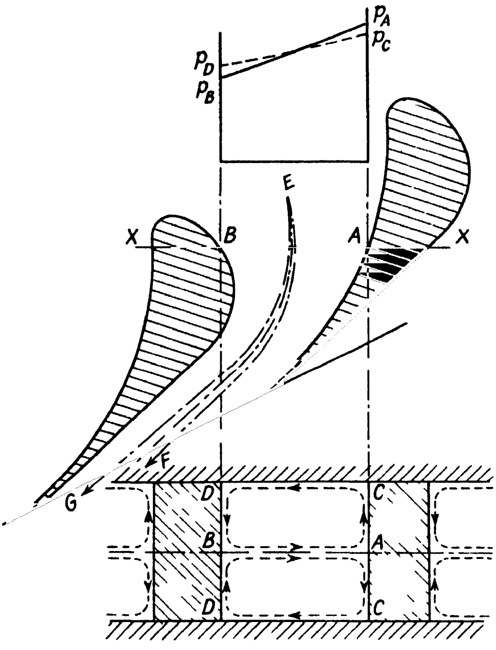


FIG. 60 Secondary Flows in Turbine Nozzles

of length δl has been calculated. The total time required for the passage of steam through the nozzle is seen to be less than $\frac{1}{1,000}$ of a second.

56. Secondary Flows in Turbine Nozzles. Certain secondary flows in turbine nozzles are produced by the combined effects of curvature and the boundary layer. Consider the curved nozzle passage shown in Fig. 60 and in particular the section X-X. Because of the curved flow path the pressures on the concave side of the passage at A will be higher than those on the convex side at B. This variation is shown diagrammatically by the full line in the auxiliary

sketch in the upper part of Fig. 60. At the upper and lower boundary walls of the passage, i.e. at the inner and outer radii, the flow velocities are lower than those in the centre or mid-height of the nozzle because of the boundary layer or friction effect. As a result, the pressure gradients across the section X–X are reduced and the pressure change at the upper and lower ends of the passage is shown by the dotted line. Thus we find $p_A > p_C$, and $p_D > p_B$, with the result that two secondary flows shown by the dotted lines are set up in the nozzle channel.

If the secondary flow is superimposed on the main flow, we find that the central part of the issuing jet will follow a path such as EF

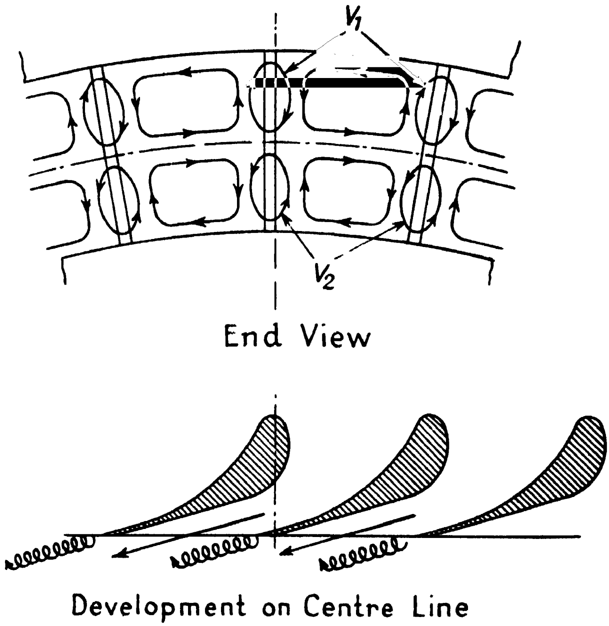


FIG. 61 Secondary Flows in Turbine Nozzles

in which the jet is underdeflected, whereas the parts of the jet near the roof and floor of the nozzle will follow a path such as EG and will tend to be overdeflected.

If, as is usual in turbine construction, a number of nozzles are arranged adjacent to each other then similar vortices will exist in the adjacent passages. Reference to the end view in Fig. 61 will show that, if such vortices persist to the nozzle outlets, then the discontinuity in velocity will set up trailing vortices V_1 and V_2 in the upper and lower halves of the stream, respectively. Such vortices will be of opposite hand and will trail from the guide vanes as shown

in the lower part of Fig. 61. They are a disturbance to the main flow and a source of loss.

57. Experimental Measurements of Steam Discharge through Nozzles. Experiments on this subject date from about 1870 and the majority have been made on nozzles of simple form, e.g. converging nozzles with rectilinear axes and outlet sections perpendicular to those axes. In most cases the mass flow has been measured directly by condensing the steam discharged by the nozzle and weighing the condensate, but in some cases indirect methods of measurement have been employed.

Experiments with Initially Dry and Saturated Steam. R. D. Napier, in a number of letters to *The Engineer* (3), discusses the subject at considerable length and gives a number of experimental results from which the following figures have been taken. These refer to tests in which the final pressure was lower than the critical. The figures given in the second column of the table below have been calculated by the author using eq. (56) and values of $f(p_1)$ taken from Fig. 39. It will be observed that the measured discharge is greater than the calculated discharge in every case, notwithstanding the fact that the experimental flow would be accompanied by losses. In some experiments made by H. Parenty (11) on the flow of initially dry and saturated steam through orifices it was also observed that

p_1 lb. per sq. in. abs.	Discharge of Steam per sq. in. of Nozzle Outlet Area per sec.		Ratio: $\frac{\text{Experimental}}{\text{Calculated}}$
	Calculated	Experimental	
30	0·445	0·451	1·013
40	0·587	0·610	1·039
45	0·659	0·682	1·035
50	0·729	0·753	1·033

the discharge was either practically equal to, or slightly greater than, the theoretical discharge.

Probably the most careful and searching experiments on the subject were made by Professor Rateau (12) in the year 1895. The nozzles used are shown in Fig. 62. A and C were convergent nozzles with a curved profile, while B was a conical convergent nozzle. The experimental results are also shown in Fig. 62, the quantity $\frac{w}{p_1 \cdot A_t}$ being plotted against p_1 plotted to a log. scale. The theoretical curve for saturated steam is based on eq. (56) and the values of $f(p_1)$ plotted in Fig. 39. Here again it is clear that, with few

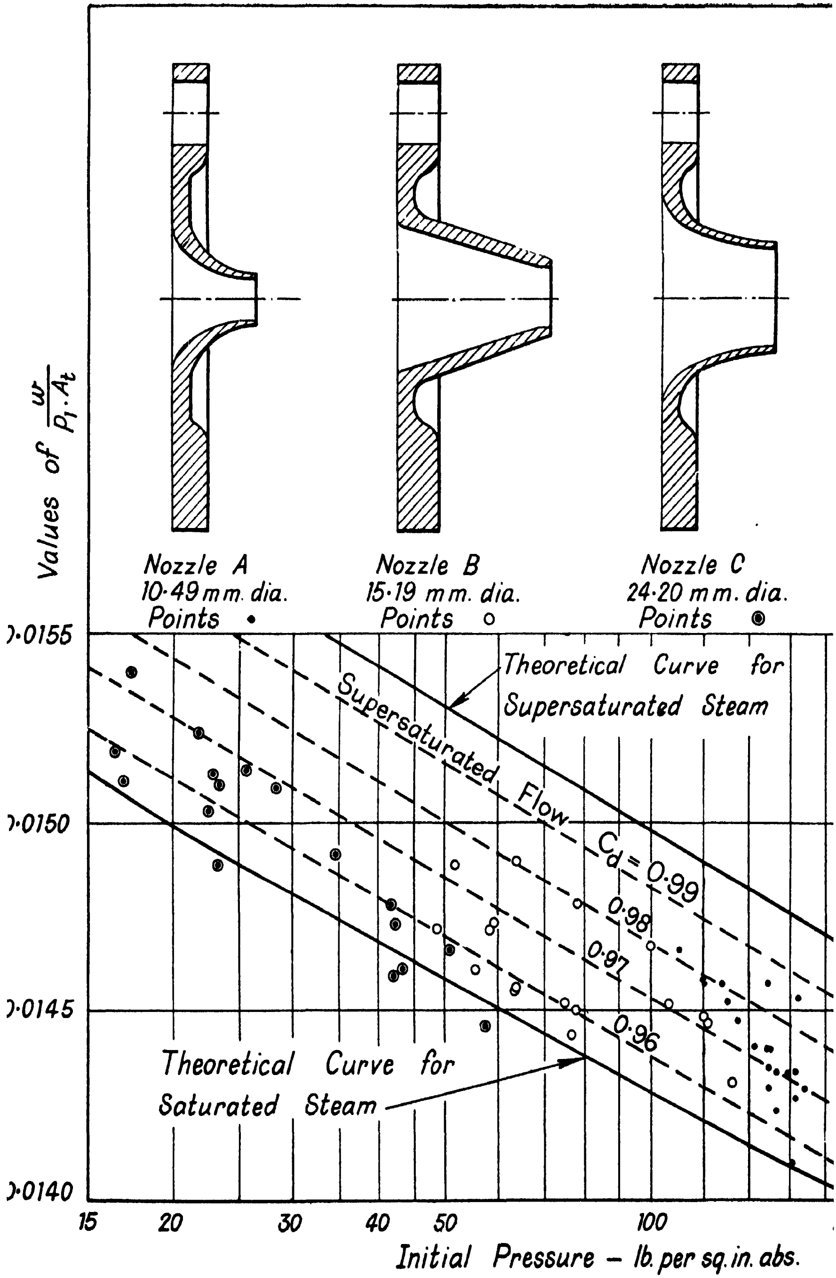


FIG. 62.—Rateau's Experiments on the Flow of Steam through Nozzles

exceptions, the experimental discharge is in excess of the theoretical. These results will be further discussed in Art. 59.

Experiments with Superheated Steam. Particulars of the mass flow with superheated steam are given in a paper by Professors Mellanby and Kerr (13). The flow through several different types of nozzles was investigated by means of a search tube and the mass flow observed by condensing the steam and weighing the condensate. We shall refer only to the results of experiments made on a simple convergent nozzle having a diameter of 0·2507 in. and an axial length of 0·25 in. Two series of tests were made on this nozzle,

p_1	t_1° F.	Initial Superheat ° F.	Ratio: $\frac{p_2}{p_1}$	C_t	C_e	Ratio: $\frac{C_e}{C_t}$
76·0	559	250·6	0·580	0·315	0·306	0·971
76·0	565	256·6	0·574	0·315	0·306	0·971
76·0	568	259·6	0·593	0·314	0·304	0·969
76·0	569	260·6	0·710	0·294	0·285	0·970
76·0	567	258·6	0·843	0·239	0·230	0·962
75·7	385	76·6	0·574	0·315	0·309	0·980
75·6	395	86·6	0·570	0·315	0·308	0·976
75·7	402	93·6	0·589	0·314	0·307	0·979
75·7	388	79·6	0·692	0·300	0·290	0·967
75·7	399	90·6	0·837	0·245	0·230	0·942

one series with a relatively high superheat and the other with a superheat which, though relatively low, is sufficiently high to maintain the steam in the superheated condition down to the critical pressure. The results are given in the table above. The coefficients C_t and C_e are, respectively, the theoretical and experimental values of the coefficient C in the expression

$$w = C \, . \, A_t \, . \sqrt{\frac{p_1}{v_1}}$$

Hence the ratio of C_e to C_t may be described as the coefficient of discharge. It will be seen that this is always lower than unity, i.e. the observed flow is always less than that calculated theoretically. In the case of the other nozzles tested, the measured flow was still lower than the theoretical flow.

58. Supersaturation in Steam Turbine Nozzles. Attention has been drawn in the preceding article to the astonishing fact that when steam, initially dry and saturated, is caused to expand in a nozzle the actual measured steam flow in lb. per sec. is in excess of that given by a theoretical analysis and expressed by eqs. (53), (55), or (56). In view of the friction losses which occur in nozzles, it would be expected that the actual discharge would be less than the theoretical value, the ratio being approximately equal to the

velocity coefficient η_v. Thus we would expect the actual mass flow to be about 3 to 5 per cent less than the theoretical, whereas experiments have shown it to be from 1 to 3 per cent greater. On the other hand, the actual discharge of superheated steam is in good agreement with the theoretical value when allowance is made for friction losses. This remarkable difference between the behaviour of dry and saturated steam and that of superheated steam is due to the fact that, during the rapid expansion of initially dry and saturated steam in a nozzle, the state or condition of the steam is not that visualized in the simple theory based on adiathermal expansion in thermal equilibrium. This theory presupposes that at every point in the expansion, condensation proceeds at the correct rate and that the heat given up by the steam due to this condensation has all been liberated. By condensation we do not mean the condensation which might take place on the walls of nozzles or blades, but true condensation within the flowing steam itself, i.e. the sudden coalescence of steam molecules to form minute droplets of water.

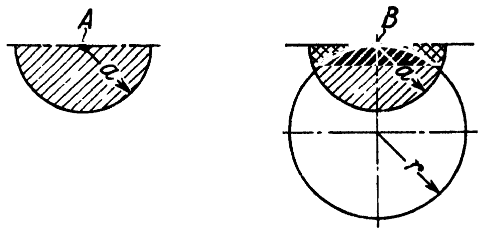


FIG. 63

Consider the vapour pressure in the neighbourhood of such a minute water droplet. The vapour pressure of water at any given temperature is that corresponding to a flat water surface. The attractive force exerted by a liquid molecule on the surrounding molecules is only effective over a very small distance, say *a*, Fig. 63. Hence a molecule A in the surface of the water is held by the attraction of the molecules lying within a hemisphere of radius *a*. Consider now a molecule B lying in the surface of a droplet of radius *r*. It will be clear that this molecule is held by a smaller force since it loses the attractive forces of the molecules lying within the sphere of action and between the outer surface of the droplet and the tangent plane at B, i.e. in the space indicated by the cross-hatching. In consequence, *at any given temperature*, the forces which tend to maintain a molecule within a liquid droplet are reduced as the droplet radius *r* is made smaller. This means that a greater number of molecules will escape into the space surrounding the droplet than would be the case with a flat liquid surface. Now the vapour pressure, being proportional to the number of vapour molecules per unit volume at the given temperature, must be greater in the space surrounding the droplet when there is equilibrium than it would be at a flat liquid surface. In consequence, the molecules of a very small water droplet will go on evaporating into a space that

*is saturated, and the space will therefore become **supersaturated*** with water vapour. This condition is commonly described by saying that the steam is supersaturated.

(It follows from the foregoing statements that during rapid expansion pure steam will not condense of itself, for if a very minute droplet were accidentally formed it would immediately evaporate. Consequently, it is quite feasible to expect that when pure steam, initially dry and saturated, is expanded rapidly it will remain dry. Under these conditions the steam expands more or less like a perfect gas and the frictionless adiabatic expansion causes its temperature to fall well below the saturation temperature corresponding to the pressure. Hence such steam is sometimes described as being ***undercooled.***)

There is, however, a limit to the expansion as a supersaturated vapour. Mr. C. T. R. Wilson (14) made experiments on the sudden expansion of air saturated with moisture. Using ordinary room air he found that a small expansion caused condensation upon the relatively large dust particles present in such air. With dust-free saturated air, rapid expansion caused a rain-like condensation when the volume ratio of expansion reached the value 1·25. In this case it was judged that condensation occurred upon ions which acted as nuclei. This occurrence was in accord with the experiments of R. von Helmholtz who observed that a jet of steam issuing from an orifice into the atmosphere was supersaturated, and that, if the jet were electrified, condensation occurred more readily.

Wilson further found that, with air freed of both dust and ions, an expansion ratio of 1·375 caused a dense cloud of mist particles to be formed. It is considered that in this case the nuclei of condensation were co-aggregations of water vapour molecules. This matter will be mentioned later. There were therefore three distinct kinds of nuclei in Wilson's experiments.

Professor Stodola (15) made some interesting experiments in which steam was caused to flow through a glass-sided nozzle of the convergent-divergent type. The pressure distribution in the nozzle was observed by means of a search tube (see Art. 65, page 146). In addition, a beam of light from an arc lamp was projected along the axis of the nozzle. The point of condensation was visible as the sudden formation of a thick mist. This occurred just beyond the nozzle throat. With an initial pressure $p = 71$, the pressure at the point of condensation was 38·5, i.e. about 0·54 times the initial pressure.

59. Equations for Supersaturated Steam. Undercooled steam behaves like superheated steam and the equation for the isentropic expansion of supersaturated vapour is

$$\frac{T_2}{T_1} = \left(\frac{p_2}{p_1}\right)^{\frac{n-1}{n}} \quad . \quad . \quad . \quad . \quad (82)$$

where p_1 and p_2 are the initial and final pressures, and T_1 and T_2 are the initial and final absolute temperatures respectively. Since $n = 1{\cdot}3$

$$\frac{T_2}{T_1} = \left(\frac{p_2}{p_1}\right)^{\frac{3}{13}} \qquad . \quad . \quad . \quad . \quad (82a)$$

In Stodola's experiment quoted above, $p_1 = 71$, $T_1 = 763{\cdot}4°$ F. abs., and $p_2 = 38{\cdot}5$. Hence $T_2 = 663{\cdot}3$, or $t_2 = 203{\cdot}7°$ F. The saturation temperature corresponding to $p = 38{\cdot}5$ is 264·9° F. Thus the steam at the point of condensation in the nozzle was undercooled by 61·2° F.

The saturation pressure p_s, corresponding to the temperature 203·7° F., is 12·4, whereas the actual pressure p_{ss} of the supersaturated steam was observed to be 38·5.

The degree of supersaturation S is defined as the ratio

$$S = \frac{p_{ss}}{p_s} \qquad . \quad . \quad . \quad . \quad (83)$$

In Stodola's experiment the degree of supersaturation reached was therefore 3·1.

More recently, Mr. J. I. Yellott, junr. (16), has carried out experiments on the flow of steam through a glass-sided nozzle. The observed degree of supersaturation varied from 3·05 to 5·64, according to the initial steam pressure.

Callendar's adiabatic equation for dry steam, which applies to supersaturated steam as well as to superheated steam, is

$$P(v - b)^{1{\cdot}3} = \text{Constant}$$

As pointed out in Art. 41, b is normally so small compared with v that it may be neglected. Hence $Pv^{1{\cdot}3} = $ constant. Then the critical pressure with adiabatic expansion of supersaturated steam is 0·5457 times the initial pressure, and the maximum discharge of steam is given by eq. (57), i.e.

$$w = 0{\cdot}3155\, A_t\sqrt{\frac{p_1}{v_1}}$$

If the steam is initially dry and saturated, we can substitute for v_1 from the equation

$$p_1 v_1^{\frac{16}{15}} = 490$$

from which

$$w = 0{\cdot}01730\, p_1^{\frac{31}{32}} . A_t \qquad . \quad . \quad . \quad (84)$$

It will be seen that the discharge given by this formula is about 5 per cent greater than that given by eq. (55); and if 3 or 4 per cent be deducted to allow for the effect of friction, the actual discharge will still be 1 or 2 per cent in excess of that based on adiabatic expansion in the saturated condition, which result agrees with those of the experimenters already mentioned.

Returning for a moment to Rateau's experiments described in Art. 57, the theoretical curve for supersaturated steam, based on eq. (84), has been drawn in Fig. 62, together with curves for varying coefficients of discharge. It will be seen that Rateau's experimental results are in agreement with the assumption of supersaturated flow and the reasonable value of C_d varying from about 0·96 to 0·97.

Consider now the adiabatic heat drop with supersaturated flow from an initial pressure P_1 to a final pressure P_2. Since by eq. (8)

$$dI = dH + \frac{v \, . \, dP}{J}$$

and

$$dH = 0. \qquad dI = \frac{v \, . \, dP}{J}$$

$$\therefore \; I_1 - I_2 = \frac{1}{J}\int_{P_2}^{P_1} v \, . \, dP$$

$$= \frac{n \, . \, P_1 v_1}{J(n-1)}\left\{1 - \left(\frac{P_2}{P_1}\right)^{\frac{n-1}{n}}\right\}$$

Since $n = 1{\cdot}3$

$$I_1 - I_2 = \frac{13}{3} \, . \, \frac{144 p_1 v_1}{J}\left\{1 - \left(\frac{p_2}{p_1}\right)^{\frac{3}{13}}\right\}$$

$$= 0{\cdot}8018 p_1 v_1 \left\{1 - \left(\frac{p_2}{p_1}\right)^{\frac{3}{13}}\right\} \text{ B.Th.U. per lb.} \qquad (85)$$

The heat drop given by this expansion is less than that due to an adiabatic expansion in thermal equilibrium.

EXAMPLE 11. Steam initially at 20 lb. per sq. in. abs. and dry and saturated expands (*a*) in the saturated condition, (*b*) in the supersaturated condition. In the latter case, condensation begins when the pressure has fallen to 10 lb. per sq. in. abs. Calculate the condition of the steam and the heat drop after expansion to 10 lb. per sq. in. in each case, assuming –

(1) isentropic expansion,

(2) expansion with a nozzle efficiency of 0·94. Assume the initial velocity to be nil.

(*a*) *Saturated Expansion.* The following data may be obtained from the Mollier diagram or by calculation—

(1)	p	x	ϕ	I
	20	1·0000	1·7327	1156·7
	10	0·9632	1·7327	1107·4
				49·3

Final dryness fraction = 0·9632.

Adiabatic heat drop = 49·3 B.Th.U. per lb.

(2) If the nozzle efficiency is 0·94, the actual heat drop = 0·94 × 49·3 = 46·34. Hence enthalpy at $p = 10$ is 1,110·36 and the dryness fraction is 0·9661.

(*b*) *Supersaturated Expansion.*

(1) $p_1 = 20;\ t_1 = 228{\cdot}0°$ F.; $T_1 = 687{\cdot}7$

By eq. (82*a*) $$\frac{T_1}{T_2} = 2^{\frac{3}{13}} = 1{\cdot}173$$

$$\therefore\ T_2 = 586{\cdot}3 \text{ and } t_2 = 126{\cdot}6° \text{ F.}$$

The actual saturation temperature corresponding to $p = 10$ is 193·2° F. Therefore the steam is undercooled 193·2 — 126·6 = 66·6° F. The saturation pressure p_s corresponding to 126·6° F. is found from the steam tables to be 2·03.

$$\therefore\ \text{Degree of supersaturation} = \frac{10}{2{\cdot}03} = 4{\cdot}93$$

$$I_1 - I_2 = 0{\cdot}8018\, p_1 v_1 \left\{1 - \left(\frac{p_2}{p_1}\right)^{\frac{3}{13}}\right\}$$

$$= 0{\cdot}8018 \times 20 \times 20{\cdot}09(1 - 0{\cdot}8521)$$

$$= \underline{47{\cdot}63 \text{ B.Th.U. per lb.}}$$

The difference between the isentropic heat drop in the stable and metastable expansions is 1·67 B.Th.U. per lb.

(2) We may, with a small error, assume that the "small stage" efficiency of the nozzle is the same as the overall efficiency, namely 0·94. Hence the index

$$m = \frac{1{\cdot}3}{1{\cdot}3 - (0{\cdot}94 \times 0{\cdot}3)} \text{ (see eq. (162), p. 295)}$$

or $$m = 1{\cdot}277$$

$$\therefore\ \frac{T_1}{T_2} = 2{\cdot}0^{\frac{m-1}{m}} = 2{\cdot}0^{0{\cdot}2169} = 1{\cdot}162$$

$$\therefore\ T_2 = 591{\cdot}7 \text{ and } t_2 = 132{\cdot}0° \text{ F.}$$

Note. This result may be obtained by assuming the low-pressure steam to be a perfect gas. Then $dI = C_p \, . \, dT$. For the isentropic case, $I_1 - I_2 = 47{\cdot}63$ and $t_1 - t_2 = 101{\cdot}4$, from which $C_p = 0{\cdot}47$. Then, if we assume C_p to be a constant, the temperature drop in this case will be

$$0{\cdot}94 \times 101{\cdot}4 = 95{\cdot}3° \text{ F.}$$

and $t_2 = 132{\cdot}7°$ F.

Taking the latter figure, we find that the steam is now undercooled by 60·5° F. and the degree of supersaturation is 10/2·388 = 4·19. The heat drop is 0·94 × 47·63 = 44·77 B.Th.U. per lb.

This expansion is shown on the ϕ - I chart, Fig. 64. AB represents the isentropic expansion in thermal equilibrium while AC shows the

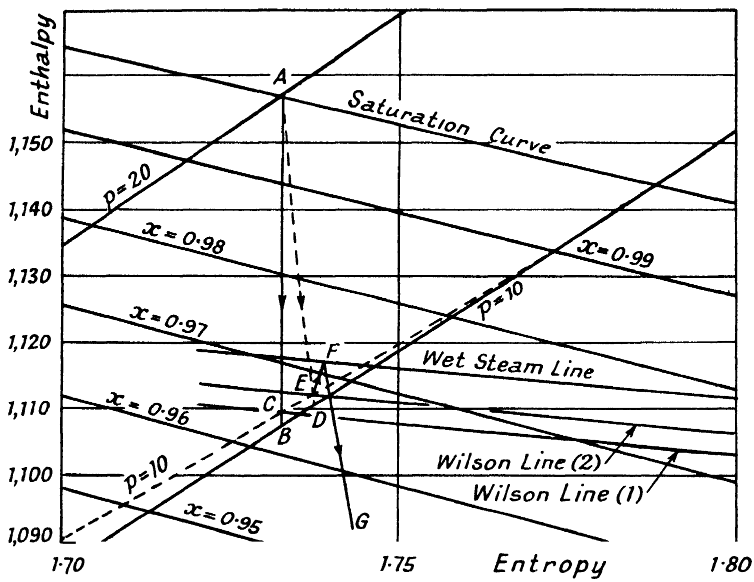


FIG. 64 ϕ-I Diagram Illustrating Example 11

expansion of the supersaturated steam. C is a point on the constant pressure line $p = 10$ (shown by the broken line) for supersaturated steam. If the expansion ended at C, the loss of energy due to delayed condensation would be 1·67 B.Th.U per lb.

Again AD and AE represent the stable and metastable expansions, respectively, when there is friction. Many years ago, H. M. Martin (17) suggested that the locus of points on the ϕ-I chart which represent the limit of supersaturated isentropic expansion should be called the Wilson Line (after Mr. C. T. R. Wilson). Martin's Wilson Line lay between the 3 per cent and 4 per cent wetness lines on the

ϕ-I chart and would pass through the point C in Fig. 64. This we shall designate Wilson line (1). Since friction losses always occur in experimental nozzles, it seems more reasonable (as suggested by Binnie and Woods) to define the Wilson line as the locus of points such as E, Wilson line (2). A difficulty is that the nozzle efficiency is not always known.

Reference will now be made to the experiments of Mr. A. M.

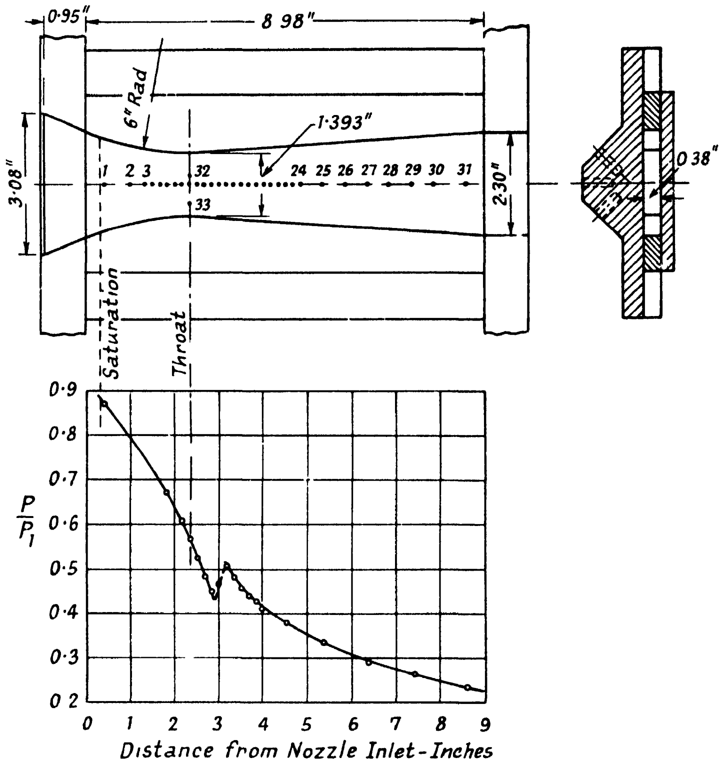


FIG 65.—Pressure Distribution in Steam Nozzle
(Binnie and Woods)
p_1 20 88 lb per sq in abs, t_1 245 7 F

Binnie and Dr. M. W. Woods (18). The object of these experiments was to measure the pressure distribution in a convergent-divergent nozzle and to study the condensation of steam during its rapid expansion in such a nozzle. The experimental nozzle, made of brass, is shown in simplified form in Fig. 65. It provides a rectangular channel 0·38 in. deep and of varying width. The pressure was measured at 31 points along the axis and at two additional points in the throat section.

Attention has already been drawn in this article to the fact that in a convergent nozzle of given throat area the mass flow with supersaturated steam is about 5 per cent greater than with saturated steam. Consequently, if during the flow of steam through a nozzle there is a sudden reversion from the supersaturated to the saturated state without a corresponding increase in nozzle area then it might be expected that a sudden pressure rise would occur at the point of condensation. This pressure rise was clearly observed in many tests. A typical pressure curve is shown in Fig. 65. If the initial superheat was raised then the pressure rise occurred later in the expansion and vice versa. The initial pressure was approximately 21 lb. per sq. in. abs. in all tests and the limiting degree of supersaturation varied from 4·1 to 5·0, allowance being made for the effects of friction.

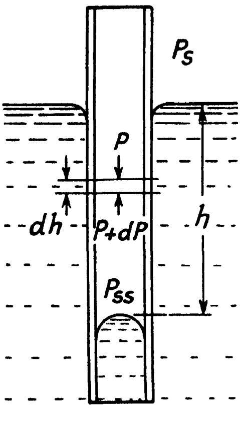


FIG. 66

The compression on reversion to the saturated state is shown in Fig. 64 by the curve EF. The locus of points such as F is known as the wet steam line. The beginning of the subsequent expansion is represented by the curve FG.

60. The Kelvin-Helmholtz Equation. The equilibrium conditions between supersaturated vapour and a curved liquid surface were first investigated by Lord Kelvin (19) and later by R. von Helmholtz (20). These conditions may be obtained as follows.

Imagine a vessel containing only water and its vapour and let a capillary tube be partly immersed in the water with its axis vertical. Suppose that the tube is made of a substance which is not wetted by water, then the liquid column in the tube will be depressed by an amount h, Fig. 66. Assume that the whole is at one absolute temperature T. Then the vapour pressure at the flat liquid surface will be the normal vapour pressure P_s corresponding to T. When equilibrium has been established there will be a column of vapour inside the capillary tube whose pressure will increase with depth. At the curved surface of the convex meniscus the vapour pressure will be P_{ss}, that of supersaturated vapour surrounding the curved surface.

Let r = radius of tube and assume that the meniscus is hemispherical.

σ = surface tension of liquid.

ρ_w = density of water.

ρ_v = density of vapour at any point in the tube.

Then the downward force on the meniscus due to the pressure P_{ss}

plus that due to surface tension will balance the force due to hydrostatic pressure, i.e.

$$\pi r^2 \,.\, P_{ss} + 2\pi r\sigma = \pi r^2(P_s + \rho_w \,.\, h)$$

$$\therefore \qquad P_{ss} - P_s = \rho_w \,.\, h - \frac{2\sigma}{r}$$

But
$$P_{ss} - P_s = \int_0^h \rho_v \,.\, dh$$

$$\therefore \qquad \int_0^h (\rho_w - \rho_v)dh = \frac{2\sigma}{r}$$

But $dP = \rho_v \,.\, dh$ or $dh = \dfrac{dP}{\rho_v}$

$$\therefore \qquad \int_{P_s}^{P_{ss}} \frac{\rho_w - \rho_v}{\rho_v} \,.\, dP = \frac{2\sigma}{r}$$

Because ρ_v is very small compared with ρ_w,

$$\int_{P_s}^{P_{ss}} \frac{\rho_w}{\rho_v} \,.\, dP = \frac{2\sigma}{r}$$

For low-pressure steam, $\rho_v = \dfrac{P}{RT}$

$$\therefore \qquad RT\rho_w \int_{P_s}^{P_{ss}} \frac{dP}{P} = \frac{2\sigma}{r}$$

i.e.
$$\log_e \frac{P_{ss}}{P_s} = \frac{2\sigma}{R \,.\, T \,.\, r \,.\, \rho_w} \qquad . \quad . \quad . \quad (86)$$

This is known as the Kelvin-Helmholtz equation. If we can assume that there is momentary equilibrium between condensation nuclei of radius r and the supersaturated steam surrounding them, then eq. (86) would enable us to calculate r if we know P_{ss}/P_s by experiment, or alternatively, we could estimate the degree of supersaturation if we knew the value of r.

Values of σ and ρ_w are given in Table IV. R for steam is 85·83 when T is expressed in degrees F. absolute.

EXAMPLE 12. Calculate the radius of the condensation nuclei in part b(2) of Example 11, page 126.

By the Kelvin-Helmholtz equation, we have

$$r = \frac{2\sigma}{R \,.\, T \,.\, \rho_w \,.\, \log_e S}$$

We have: $t = 132{\cdot}7°$ F., and $S = 4{\cdot}19$. Then $\sigma = 4{\cdot}46 \times 10^{-3}$ lb. per ft., $T = 592{\cdot}4$, and $\rho_w = 61{\cdot}50$ lb. per cu. ft.

A simple calculation shows that $r = 1{\cdot}99 \times 10^{-9}$ ft. or $6{\cdot}07 \times 10^{-8}$ cm.

The value of r given by Binnie and Woods varies from 5·7 to 6·9 × 10^{-8} cm. Similar values are obtained from Yellott's experimental results. Assuming, for example, that r = 6·07 × 10^{-8} cm., the volume of such a droplet is 9·36 × 10^{-22} cc. and its mass 9·23 × 10^{-22} gr. One gramme molecule of water vapour weighs 18 gr. and contains 6·06 × 10^{23} (Avogadro's Number) molecules. Hence the mass of the steam molecule is 2·97 × 10^{-23} gr., and the number of molecules contained in the condensation nucleus would

TABLE IV

SURFACE TENSION AND DENSITY OF WATER

The surface tension σ is for water in contact with its vapour and is expressed in lb. weight per ft. The density ρ_w is for saturated water and is expresed in lb. per cu ft.

t°F.	σ	ρ_w	t°F.	σ	ρ_w
32	5·03 × 10^{-3}	62·42	170	4·21 × 10^{-3}	60·80
40	4·99 × 10^{-3}	62·43	180	4·14 × 10^{-3}	60·58
50	4·94 × 10^{-3}	62·42	190	4·07 × 10^{-3}	60·36
60	4·88 × 10^{-3}	62·37	200	4·00 × 10^{-3}	60·12
70	4·83 × 10^{-3}	62·30	210	3·93 × 10^{-3}	59·88
80	4·78 × 10^{-3}	62·22	220	3·86 × 10^{-3}	59·63
90	4·72 × 10^{-3}	62·11	230	3·79 × 10^{-3}	59·37
100	4·66 × 10^{-3}	62·00	240	3·72 × 10^{-3}	59·11
110	4·60 × 10^{-3}	61·86	250	3·65 × 10^{-3}	58·83
120	4·54 × 10^{-3}	61·71	260	3·59 × 10^{-3}	58·55
130	4·48 × 10^{-3}	61·55	270	3·52 × 10^{-3}	58·26
140	4·41 × 10^{-3}	61·38	280	3·45 × 10^{-3}	57·96
150	4·35 × 10^{-3}	61·20	290	3·38 × 10^{-3}	57·65
160	4·28 × 10^{-3}	61·00	300	3·31 × 10^{-3}	57·33

be about 31. It is doubtful whether the Kelvin-Helmholtz equation can be applied to droplets containing such a small number of molecules.

Calculations within the temperature range for which the required physical properties are available show that the degree of supersaturation probably diminishes as the temperature of the steam is raised.

Little or nothing is known about the condition of rapidly expanding steam after condensation begins. In some of Yellott's experiments condensation appeared as a blue mist and the blue colour was maintained throughout the length of the nozzle. This indicates that there was no further growth in the size of the mist particles. If the particles had increased in size the colour of the mist would have changed towards red. Binnie and Woods made accurate measurements of the steam pressure in the nozzle after reversion, or assumed reversion. If the steam remained in thermal equilibrium during its further expansion, the measured pressures agreed quite well with those

based on the assumption of a 20 per cent loss of heat drop from the point of reversion.

The expansion of steam in a turbine takes place with such rapidity that it is doubtful whether, after condensation has actually occurred, it goes on at such a rate as to maintain thermal equilibrium at every point in the expansion.

61. Jet Deflection in Turbine Nozzles. In the preceding articles of this chapter it has been shown that there exists a certain critical pressure in nozzle flow. With steam initially dry and saturated this pressure is about 0·58 of the initial pressure, whereas with superheated steam it is about 0·55 of the initial pressure. The practical significance of the critical pressure lies in the fact that if expansion takes place in a nozzle to a pressure which is equal to or greater than the corresponding critical pressure, then the nozzle must be convergent, the mass flow being controlled by the outlet area. On

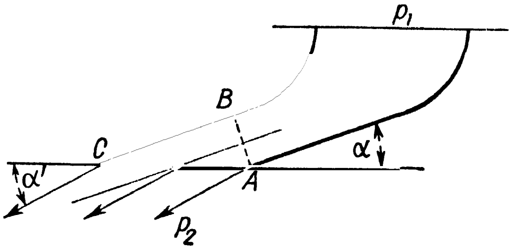


FIG. 67

the other hand, if the expansion is to extend to a pressure lower than the critical pressure, then the nozzle must be of the convergent-divergent type and, provided the pressure on the outlet side is not too high, the mass flow will be controlled by the throat area.

In view of the fact that the nozzle must be inclined to the plane of the wheel, the turbine nozzle must be provided with an oblique outlet. Fig. 67 shows diagrammatically such a nozzle of the convergent type. Provided the steam pressure p_2 on the outlet side of the nozzle is not less than the critical pressure, then the steam jet will issue at an angle equal to the vane angle α. In practice it is found that with thick guide vanes the jet angle may be less than the vane angle. If, however, the pressure p_2 is much lower than the critical pressure, then there will be an expansion in the wedge-shaped space ABC and the jet will issue at an angle α' greater than α.

The estimation of the actual jet angle α' is a matter of considerable difficulty. Two methods will be given.

(1) *Prandtl-Meyer Theory for Flow Round a Corner.* Suppose that steam or a gas flows parallel to a surface AO, Fig. 68, with a velocity V_1 which is greater than the local velocity of sound. Let

p_1 be the pressure in the space where the velocity is V_1 and suppose that the steam is flowing into a space where the pressure is p_2, lower than p_1. The flow is assumed to be adiabatic and frictionless.

No disturbance of the flow takes place until the radial OB is reached. At any point C on OB, the velocity V_1 may be resolved into two components CE and ED. It may be shown that the

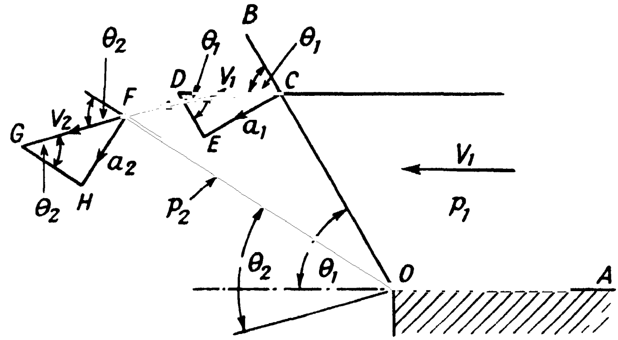


FIG. 68 – Prandtl-Meyer Flow Round a Corner

component CE perpendicular to OC is the sonic velocity a_1 corresponding to the pressure and temperature at points on OB. Hence

$$\sin \theta_1 = \frac{CE}{CD} = \frac{a_1}{V_1} = \frac{1}{M_1}$$

where M_1 is the initial Mach number. The angle θ_1 is known as the Mach angle.

Then it may be shown that any expansion which takes place must occur in the space following the radial OB, or following the plane of which OB is the trace. Moreover, the pressure p_2 will be reached at a radial OF, the velocity V_2 will be that due to isentropic expansion down to p_2 and the component FH will again be the acoustic velocity corresponding to the condition at points on OF. Radials such as OB and OF are lines of constant pressure.

Thus there is an expansion wedge COF, the stream-lines being curves such as CF. The velocity reached at p_2 will be uniform and equal to V_2 and the direction of flow will also be uniform at the angle θ_2 to OF.

Consider now the convergent turbine nozzle with a parallel outlet wall, Fig. 69. In applying the ideal Prandtl-Meyer theory we assume that the steam is flowing in parallel lines with a velocity V_1 which will be equal to the sonic velocity a_1 corresponding to the pressure and density at the throat section OA. Hence if the pressure on the

outlet side of the nozzle is lower than the critical pressure corresponding to the inlet pressure p_0, a disturbance will occur immediately after the throat section OA.

The flow is again assumed to be two-dimensional, adiabatic and frictionless. Radials through O are isobars and, if p is the pressure at all points on the radial OB, for example, then it may be shown that

$$\phi = \frac{1}{2\lambda} \cdot \cos^{-1}\left\{(n+1)\left(\frac{p}{p_0}\right)^{\frac{n-1}{n}} - 1\right\} \quad . \quad . \quad (87)$$

or

$$\frac{p}{p_0} = \left(\frac{1 + \cos 2\lambda\phi}{n+1}\right)^{\frac{n}{n-1}} \quad . \quad . \quad . \quad (87a)$$

where n = isentropic index

and

$$\lambda = \sqrt{\frac{n-1}{n+1}} \quad . \quad . \quad . \quad . \quad . \quad (88)$$

Also for any stream-line,

$$\frac{r}{r_1} = \frac{1}{(\cos \lambda\phi)^{\frac{n+1}{n-1}}} \quad . \quad . \quad . \quad . \quad (89)$$

Values of p/p_0 and r/r_1 are given in Table V while Fig. 70 shows the angle ϕ as a function of the ratio p/p_0.

TABLE V

PRESSURE RATIOS AND FLOW LINES FOR PRANDTL-MEYER EXPANSIONS

ϕ degrees	Steam Initially Dry and Saturated $n = 1{\cdot}135$		Steam Initially Superheated $n = 1{\cdot}3$	
	$\frac{p}{p_0}$	$\frac{r}{r_1}$	$\frac{p}{p_0}$	$\frac{r}{r_1}$
0	0·5769	1·000	0·5456	1·000
10	0·5680	1·015	0·5360	1·016
20	0·5424	1·063	0·5089	1·064
30	0·4980	1·145	0·4761	1·148
40	0·4451	1·277	0·4136	1·280
50	0·3827	1·471	0·3519	1·474
60	0·3194	1·746	0·2894	1·753
70	0·2578	2·133	0·2281	2·163
80	0·2004	2·703	0·1723	2·774
90	0·1500	3·551	0·1247	3·692

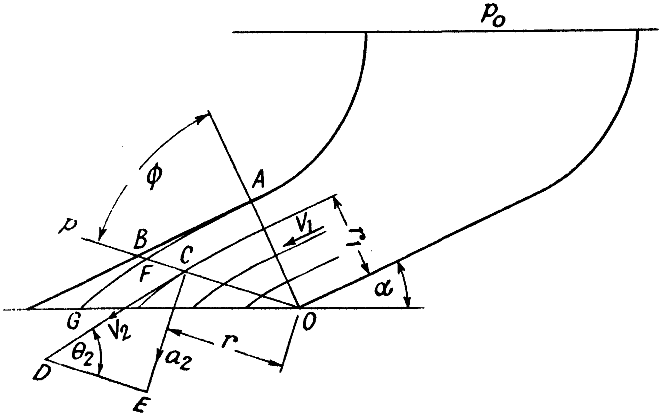


FIG. 69

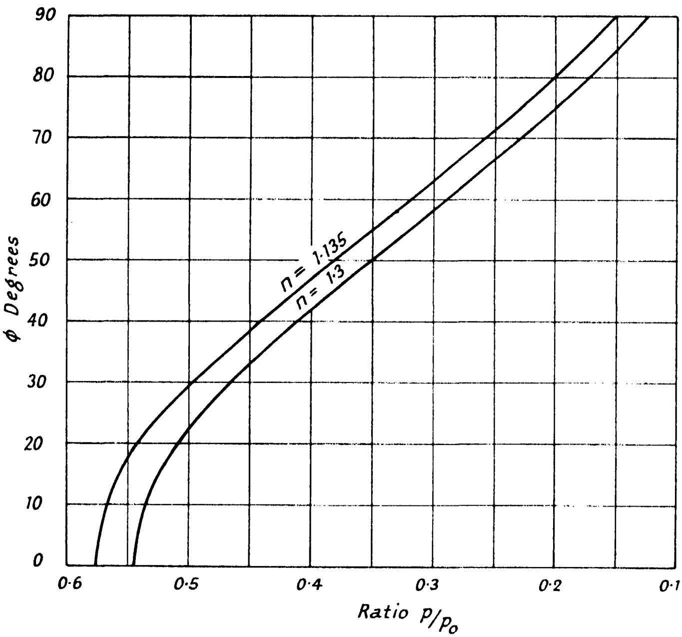


FIG. 70.—ϕ as a Function of p/p_0

It may also be shown that the angle θ_2 in the velocity triangle CDE for the point C on the radial OC is given by the relation

$$\tan \theta_2 = \lambda \cdot \cot \lambda\phi \quad . \quad . \quad . \quad (90)$$

Further, $\sin \theta_2 = \frac{a_2}{V_2}$ where a_2 is the acoustic velocity at pressure p, and V_2 is the velocity due to isentropic expansion from p_0. When the value of θ_2 is known, we may calculate the actual jet angle α', for

$$\alpha' = (\alpha + \phi + \theta_2) - 90 \text{ deg.} \quad . \quad . \quad . \quad (91)$$

There is a special value of the outlet steam pressure for which the angle ϕ is equal to the complement of the nozzle angle α. The radial isobar for the final steam pressure then coincides with the plane of the nozzle outlet and the jet deflection reaches its maximum value.

We could only expect the Prandtl-Meyer theory to give an exact result if the nozzle wall AFG, Fig. 69, were to coincide with a streamline and if the flow were truly adiabatic and frictionless. In the usual convergent nozzle with a straight wall, the jet deflection would be less than that given by the Prandtl-Meyer theory.

(2) *By the Equation of Continuity.* Suppose steam enters the nozzle at pressure p_0 and that p_1 is the throat pressure with corresponding steam velocity V_1 and specific volume v_1. Then if the pressure p_2 in the space into which the nozzle discharges is less than p_1, it may be again assumed that further expansion will take place in the wedge ABC, Fig. 71, and that the steam will issue with a velocity V_2 and specific volume v_2 reached by expansion from p_0.

Then, if w is the steam flow in lb. per sec. and if we assume uniform velocities,

$$w = \frac{A_1 V_1}{v_1} = \frac{A_2 V_2}{v_2}$$

$$\therefore \quad \frac{A_2}{A_1} = \frac{V_1}{V_2} \cdot \frac{v_2}{v_1}$$

Referring to Fig. 71, we have

$$\frac{A_2}{A_1} = \frac{CD}{AB} = \frac{CD}{AC} \cdot \frac{AC}{AB} = \frac{\sin \alpha'}{\sin \alpha}$$

$$\therefore \quad \frac{\sin \alpha'}{\sin \alpha} = \frac{V_1}{V_2} \cdot \frac{v_2}{v_1} \quad . \quad . \quad . \quad . \quad (92)$$

EXAMPLE 13. Fig. 72 shows the cross-section of a low-pressure turbine nozzle with an outlet angle of 25°. The pressure at inlet is 3·0 lb. per sq. in. abs. and the steam is initially dry and saturated. Assuming adiabatic and frictionless expansion, neglecting the initial velocity and assuming Prandtl-Meyer flow around the outlet edge

of the nozzle guide blade, find the velocity and the direction of flow at the nozzle outlet—

(*a*) if the outlet pressure is 1·2 lb. per sq. in. abs.

(*b*) if the outlet pressure is such that the angle ϕ is 65°, i.e. 90° − 25°.

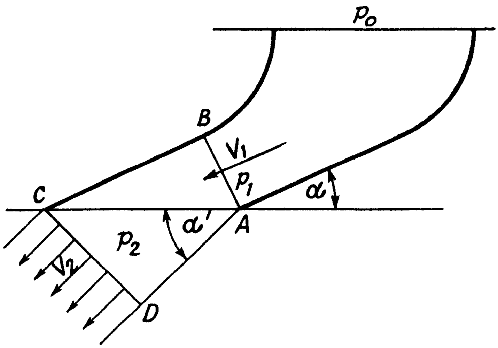


FIG. 71. Jet Deflection by Continuity

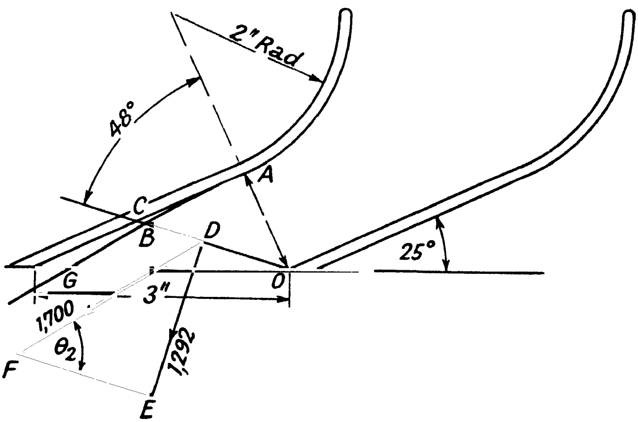


FIG. 72

In each case derive the direction of flow based on the equation of continuity.

(*a*) From Fig. 39, the isentropic index $n = 1{\cdot}119$. By substituting in eq. (87), $\phi = 48°$. Also $\dfrac{r}{r_1} = 1{\cdot}42$

$$\text{OA (Fig. 72)} = 3 \,.\, \sin 25° = 1{\cdot}2678 \text{ in.}$$

$$\therefore \qquad r = 1{\cdot}42 \times 1{\cdot}2678 = 1{\cdot}801 \text{ in.} = \text{OB}$$

$$\frac{AO}{OC} = \sin 42° = 0{\cdot}6691$$

from which OC = 1·895 in. This shows that the stream-lines deviate from the nozzle wall by a distance BC = 0·094 in.

Since $p_0 = 3{\cdot}0$, $v_0 = 118{\cdot}7$, and since $n = 1{\cdot}119$, $v_2 = 269{\cdot}2$ at $p = 1{\cdot}2$. Then the jet velocity found by the usual method is 1,700 ft. per sec.

The acoustic velocity

$$a_2 = \sqrt{gnP_2v_2}$$
$$= 1{,}292 \text{ ft. per sec.}$$

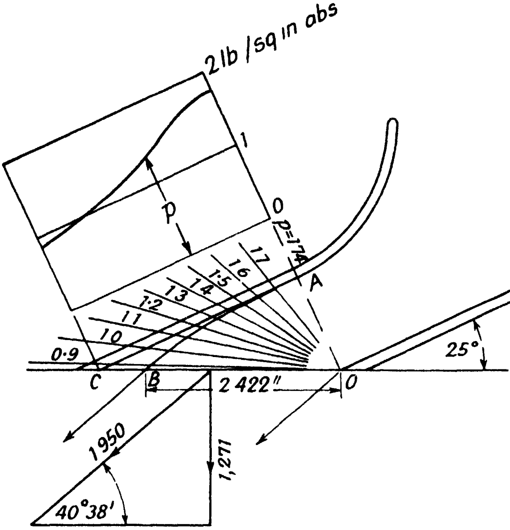


FIG. 73

Hence at any point D on the radial OB, the velocity DE normal to the radial will be 1,292 ft. per sec. and the velocity DF = 1,700.

$$\therefore \quad \sin\theta_2 = \frac{1{,}292}{1{,}700} = 0{\cdot}76 \text{ and } \theta_2 = 49° \ 30'$$

By eq. (90), $\tan\theta_2 = \lambda \,.\, \cot \lambda\phi$

$$\lambda = \sqrt{\frac{n-1}{n+1}} = 0{\cdot}237$$

$$\therefore \quad \text{Tan}\ \theta_2 = 0{\cdot}237 \cot (0{\cdot}237 \times 48°) = 1{\cdot}178$$

from which $\theta_2 = 49° \ 40'$. Then the jet angle will be—

$$\alpha' = 49° \ 40' + 25° + 48° - 90° = 32° \ 40'$$

Hence the jet deflection is 7° 40′. From the point B on the boundary of the jet, the flow will be along BG, parallel to DF. A simple calculation shows that OG = 2·54 in., i.e. the jet fills only 85 per cent of the outlet.

In using the equation of continuity, we first find the throat pressure $p_1 = 1{\cdot}74$ lb. per sq. in., $v_1 = 193{\cdot}0$, and $V_1 = 1{,}320$, by the methods already given.

$$\text{Then} \qquad \frac{\sin \alpha'}{\sin \alpha} = \frac{1{,}320}{1{,}700} \times \frac{269{\cdot}2}{193{\cdot}0} = 1{\cdot}081$$

from which $\alpha' = 27{\cdot}2$ deg. and the jet deflection is 2·2 deg.

(*b*) For $\phi = 65°$, $p_2 = 0{\cdot}295\, p_0 = 0{\cdot}885$ lb. per sq. in., and with $n = 1{\cdot}119$, $v_2 = 353{\cdot}2$. The calculated jet velocity is 1,950 ft. per sec., and the acoustic velocity 1,271 ft. per sec.

Hence in Fig. 73,

$$\sin \theta_2 = \frac{1{,}271}{1{,}950} = 0{\cdot}651$$

from which $\theta_2 = 40° \; 38'$

By eq. (90), $\tan \theta_2 = \lambda \, . \cot \lambda\phi$

$$= 0{\cdot}237 \cot (0{\cdot}237 \times 65°)$$

$$= 0{\cdot}86$$

and $\theta_2 = 40° \; 42'$, a value in fair agreement with the previous result.

Thus the calculated jet deflection in this case is 15° 42′. The ratio $r/r_1 = 1{\cdot}91$, from which $r = 1{\cdot}91 \times 1{\cdot}2678 = 2{\cdot}422$ in. Thus the jet fills only 0·807 of the nozzle outlet.

The variation of pressure along the nozzle wall AC is shown by the auxiliary diagram.

Assuming that the nozzle outlet is fully utilized and again applying the continuity equation,

$$\frac{\sin \alpha'}{\sin \alpha} = \frac{1{,}320}{1{,}950} \times \frac{353{\cdot}2}{193{\cdot}0} = 1{\cdot}238$$

$$\sin \alpha' = 0{\cdot}523 \text{ and } \alpha' = 31° \; 32'$$

i.e. the jet deflection is 6° 32′.

The problem may also be analysed by the method of Characteristics. The actual jet deflection will be affected by the flow from adjacent nozzles, if any, by the thickness of the nozzle walls when there are adjacent nozzles, and also by boundary layer growth, secondary flows and shock waves.

BIBLIOGRAPHY

1. RANKINE: *A Manual of the Steam Engine*, 1859 Edition, p. 385.
2. ZEUNER: *Technical Thermodynamics*, Vol. II, p. 83.
3. NAPIER: "The Flow of Fluids under Pressure," in letters to *The Engineer*, 1867, 23; pp 11, 80, 100, 123.

4. REYNOLDS: "On the Flow of Gases." *Phil. Mag.*, 1886; 21; 185.
5. STANTON AND PANNELL: *Roy. Soc. Phil. Trans.*, 1914; 214; 199.
6. LEES: *Proc. Roy. Soc.*, 1914; A. xci.
7. NIKURADSE: *Zeits. für angewandte Mathematik und Mechanik*, 1923; 3; 329.
8. BLASIUS: *Mitt. Forschungsarbeiten*, Vol. 131.
9. SPEYERER: *Z. V. d. I.*, 1925; 69; 747.
10. HAWKINS, SOLBERG AND POTTER: *Trans. A.S.M.E.*, 1935; 57; 395.
11. PARENTY: "Sur le débit des gaz parfaits et de la vapeur d'eau sous pression à travers les orifices." *Annales de Chimie et de Physique*, 1896; Seventh Series, Vol. 8; 5.
12. RATEAU: "The Efflux of Steam." International Engineering Congress, Glasgow, 1901, Section III. *Engineering*, 1901; 72; 444. A fuller account of Rateau's work is given in the book *Experimental Researches on the Flow of Steam through Nozzles and Orifices*, Constable, 1905.
13. MELLANBY AND KERR: "Pressure-flow Experiments on Steam Nozzles." *Trans. Inst. of Eng. and Shipbuilders in Scotland*, 1920; 64; 80.
14. WILSON: "Condensation of Water Vapour in the Presence of Dust-free Air and other Gases." *Roy. Soc. Phil. Trans.*, 1897; 189; 265.
15. STODOLA: "Die Unterkühlung beim Ausfluss gesättigten Dampfes mit Rücksicht auf die Molekularvorgänge." *Zeits. Ver. deutscher Ing.*, 1913; 57; 1776.
16. YELLOTT: "Supersaturated Steam." *Trans. Am. Soc. Mech. Eng.*, 1934; 56; 411.
17. MARTIN: "A New Theory of the Steam Turbine." *Engineering*, 1918; 106; 1 *et seq.*, "The Supersaturation Limit." *Engineering*, 1923; 115; 607.
18. BINNIE AND WOODS: "The Pressure Distribution in a Convergent-divergent Steam Nozzle." *Proc. I Mech. E.*, 1938; 138; 229.
19. KELVIN: *Proc. R.S Edin.*, 1870; 7; 63; and *Phil. Mag.*, 1871; 42; 448.
20. R. VON HELMHOLTZ: *Wied. Annalen*, 1886; 27; 509.

EXAMPLES V

1. The heat available during the adiabatic expansion of 6 lb. of steam is 240 B.Th.U. Calculate the final velocity of the steam if it was initially at rest.

2. If the efficiency of the nozzle in Question 1 is 90 per cent, calculate the exit velocity.

3. Dry and saturated steam enters a nozzle at a pressure $p = 150$ and with an initial velocity of 300 ft. per second. The outlet pressure is 90 lb. per sq. in. abs. and the outlet velocity 1,450 ft. per sec. If the heat loss from the nozzle amounts to 2 B.Th.U. per lb. of steam flowing through the nozzle, what must be the dryness fraction of the steam as it leaves the nozzle?

4. Steam expands adiabatically from an initial pressure of 200 lb. per sq. in. abs. to a pressure of 120, the relationship between pressure and volume during expansion being

$$p \,.\, v^{1\cdot135} = \text{constant}$$

If the initial specific volume of the steam is 2·29 cu. ft. per lb. and the initial velocity is 170 ft. per sec., calculate—

(*a*) Velocity at $p = 120$.

(*b*) Area required at $p = 120$ if the weight of steam discharged per sec. is 1·4 lb.

5. Steam at a pressure of 1,000 lb. per sq. in. abs. and a temperature of 1,000° F. (I = 1,503·9 B.Th.U. per lb.) expands adiabatically to a pressure of 600. Assuming that the relationship between p and T is

$$p = \text{constant} \times T^{\frac{13}{3}}$$

calculate the degree of superheat of the steam at $p = 600$, and obtain the enthalpy value by interpolation from the steam tables. Hence find the adiabatic heat drop and the velocity from rest.

6. Assuming that the ratio of the throat pressure to the initial pressure with adiabatic expansion from a state of rest is

$$r = \left(\frac{2}{n+1}\right)^{\frac{n}{n-1}}$$

where n is the exponent of v in the expression pv^n = constant, prove that the throat velocity for steam initially dry and saturated is $1{,}280 \, . \, p_1^{\frac{1}{32}}$, where p_1 is the initial pressure in lb. per sq. in. abs. Assume $n = 1{\cdot}135$ and $p \, . \, v^{\frac{16}{15}} = 490$ for dry and saturated steam.

7. Calculate the throat area of a nozzle to pass 4,200 lb. per hour, assuming that the final pressure is lower than the critical, that the steam is superheated during the whole of the expansion, and that expansion takes place without losses. Given that—

Initial pressure $p_1 = 250$.
,, superheat = 250° F.
,, specific volume = 2·56.

8. Steam expands in a nozzle under the following conditions—

Initial pressure p_1 = 240.
,, temperature = 500° F.
Final pressure p_2 = 60.
Mass flow = 1·2 lb. per sec.

Calculate the required throat and outlet areas, using the Mollier diagram—

(*a*) When the expansion is frictionless.

(*b*) When the friction loss at any pressure amounts to 10 per cent of the total heat drop down to that pressure.

9. The effective heat drop in a nozzle is 60 B.Th.U. per lb. of steam and the final pressure is 20. What is the gain of entropy during an adiathermal expansion if the nozzle efficiency is 85 per cent and the final condition of the steam is wet?

10. Steam which is initially dry and saturated expands in a nozzle from $p_1 = 200$ to $p_2 = 80$. The expansion is frictionless throughout. During the expansion from 200 to 100 lb. per sq. in., the steam remains in the dry state. What is the maximum degree of supersaturation and of undercooling?

If the steam were to revert instantaneously to the saturated state at constant enthalpy and if the further expansion takes place in thermal equilibrium, calculate the change of entropy, the loss due to undercooling, and the percentage loss.

11. The throat diameter of a nozzle is 0·25 in. If dry and saturated steam at $p = 150$ is supplied to the nozzle calculate the mass flow per second. The exhaust pressure is 20 lb per sq. in. abs. Assume frictionless adiabatic flow and that the index n is 1·135.

If 10 per cent of the isentropic heat drop is lost in friction, what should be the correct diameter at outlet for the steam to issue at the same exhaust pressure?

12. Superheated steam flows through a nozzle. At a given section of the nozzle, $p = 20$, $v = 25$ cu. ft. per lb., $V = 2{,}400$ ft. per sec. and $A = 4$ sq. in. Using eq. (59) find the approximate steam pressure at an adjacent section of the nozzle where the cross-sectional area of the nozzle is 4·2 sq. in. Assume isentropic flow.

13. Steam expands isentropically from an initial condition of rest where $p_1 = 1{,}000$, initial superheat 400° F., $I_1 = 1{,}473{\cdot}1$ B.Th.U. per lb., $v_1 = 0{\cdot}799$ cu. ft. per lb. to a pressure $p = 600$. Find the drop in pressure corresponding to a reduction in nozzle area of one per cent at the section where the steam pressure is 600 lb. per sq. in. abs. $n = 1{\cdot}3$ and the specific volume of superheated steam is given by the expression

$$v = \frac{1{\cdot}253\ (I - 835)}{p}$$

(*Liv. Un.*)

14. Steam at 150 lb. per sq. in. abs. and with an initial dryness fraction of 0·95 expands isentropically through a nozzle to a pressure of 12 lb. per sq. in. abs. Assuming that the law of the expansion is $pv^n =$ constant, find the value of n which satisfies the initial and final state points, and use this value to calculate the pressure and velocity at the throat of the nozzle. What is the required throat area of the nozzle if the mass flow is to be 0·4 lb. of steam per second?

15. Steam flows through a convergent-divergent nozzle. At a point in the convergent inlet the cross-sectional area is 0·639 sq. in., the steam pressure is 90, the degree of superheat is 140° F., and the steam velocity 400 ft. per sec. At a later section of the nozzle the cross-sectional area is 0·493 sq. in., and the steam pressure 12 lb. per sq. in. abs. If the flow is adiathermal, find the velocity and dryness fraction of the steam at the lower pressure.

It may be assumed that, for superheated steam, the specific volume is given by the expression

$$v = \frac{1{\cdot}253}{p}\ (I - 835)$$

(*Liv. Un.*)

16. Steam enters a nozzle at a pressure $p = 20$, dryness fraction 0·9 and with a velocity of 800 ft. per sec. Assuming that the adiabatic index is 1·135, find the throat pressure and the mass flow per square inch of throat area by two methods of calculation.

17. In an experiment on the expansion of steam through a nozzle, steam enters the nozzle at $p = 40$ and $t = 280°$ F. The steam expands isentropically in the dry state to a pressure $p = 18$ at which it reverts to the wet state. Calculate the radius of the condensation nuclei if at the lowest temperature reached by the expanding dry steam the surface tension of water is $4{\cdot}32 \times 10^{-3}$ lb. weight per ft. and ρ_w is 61·0 lb. per cu. ft. The universal gas constant is 1,544 ft.-lb. per mol. °F.

CHAPTER VI

STEAM NOZZLE RESEARCH

62. Introduction. The objects of steam nozzle research may be enumerated briefly as follows—

(*a*) To measure the mass flow under certain conditions of pressure and temperature and to compare it with values calculated from theory. This part of steam nozzle research has been briefly dealt with in the preceding chapter.

(*b*) To measure the velocity acquired by the steam under given conditions and compare it with the theoretical velocity.

(*c*) To determine the direction of the issuing steam jet. This has an important bearing on the design of the blades.

(*d*) To study special problems such as the distribution of pressure, effect of roughness, effect of nozzle angle, effect of entrance conditions, and so forth.

63. Reaction Method of Measuring Velocity. When a jet of fluid issues from a nozzle at a certain velocity it exerts a backward reaction on the nozzle. The simultaneous measurement of the steam flow in lb. per sec. and the force of reaction enables the velocity of efflux to be deduced.

One arrangement of apparatus is shown diagrammatically in Fig. 74. High-pressure steam passing along the pipe A enters the inside of the trunnion B and passes down the pipe C into the steam chest D to which the nozzle E is attached. The pendulum pipe C is free to swing in bearings attached to the casing F. The latter surrounds the pendulum pipe and leads to a surface condenser. The trunnion B is supported on ball bearings and packed by labyrinth packing so that there is very little friction in the apparatus. By using suitably designed packing and a suitable arrangement of leak-off connections, the errors due to steam leakage may be kept within very small limits. An arm G is attached to the trunnion so that the turning moment on the latter may be measured, e.g. by a small weighing machine. The pressure of the steam in the supply pipe may be read off the gauge H_1, while the superheat or dryness may be obtained by a thermometer or thermocouple, or by a calorimeter, respectively. A small-bore pipe K is coupled to the steam chest and led through the trunnion (not shown in diagram) to a gauge H_2, which will, therefore, give the steam pressure at the nozzle inlet. H_3 (mercury column) gives the back pressure. Suitable balance weights are added to the swinging parts so as to put them in neutral equilibrium.

A measurement of the turning moment on the trunnion enables

the reaction R to be calculated. A simultaneous reading of the mass flow w lb. per sec. must be obtained.

Then, since $$R = \frac{w \cdot V}{g} \text{ lb. weight}$$

$$V = \frac{gR}{w} \text{ ft. per sec.}$$

With reference to the testing of convergent nozzles, it may be shown that the velocity given by the above formula is strictly only the

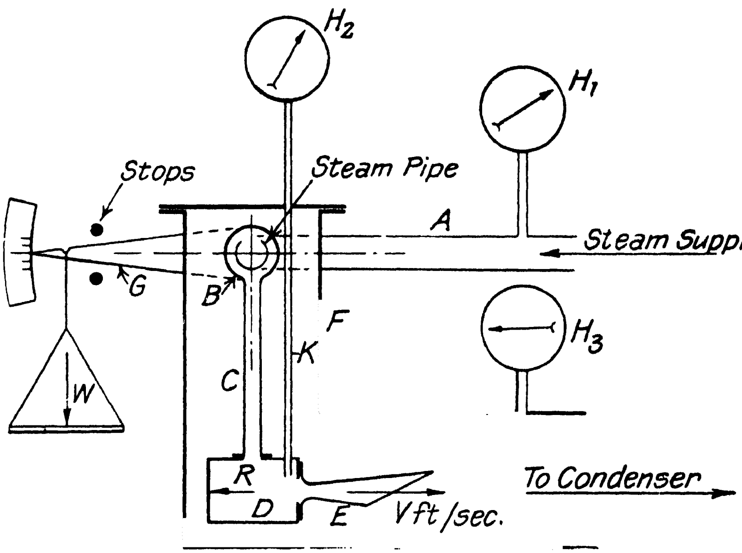


FIG. 74.—Reaction Method of Measuring Steam Velocity

velocity of efflux from the nozzle when the pressure at the nozzle outlet is equal to the pressure in the exhaust space. When steam is expanded through a convergent nozzle, the velocity of efflux increases as the external pressure is reduced until the critical pressure is reached. When the critical velocity is reached, the velocity of efflux cannot increase further, but it is found that the reaction still continues to increase owing to the fact that the steam continues to expand outside the nozzle.

64. **Impulse Method of Measuring Velocity.** In this method the steam jet, on emerging from the nozzle, is allowed to impinge on a flat plate as shown in Fig. 75. The jet spreads radially in all directions from the surface of the plate and its initial momentum is destroyed.

Let P = force on plate, lb. weight.
w = steam flow, lb. per sec.
V = jet velocity, ft. per sec.

Then
$$V = \frac{P \cdot g}{w}$$

Actually the velocity is not uniform throughout the jet; it is almost uniform over a large central area, but diminishes rapidly near the nozzle walls. If V be the velocity of a small element of steam mass δm, then the total momentum of the steam is $\Sigma V \cdot \delta m$.

Hence
$$\Sigma V \cdot \delta m = P \cdot g \quad (93)$$

If we divide the total momentum by the mass flow per second, we have
$$\frac{\Sigma V \cdot \delta m}{\Sigma \delta m} = V_1 \quad . \quad (94)$$

which is a quantity having the dimensions of a velocity and is in fact the mass-mean velocity of efflux.

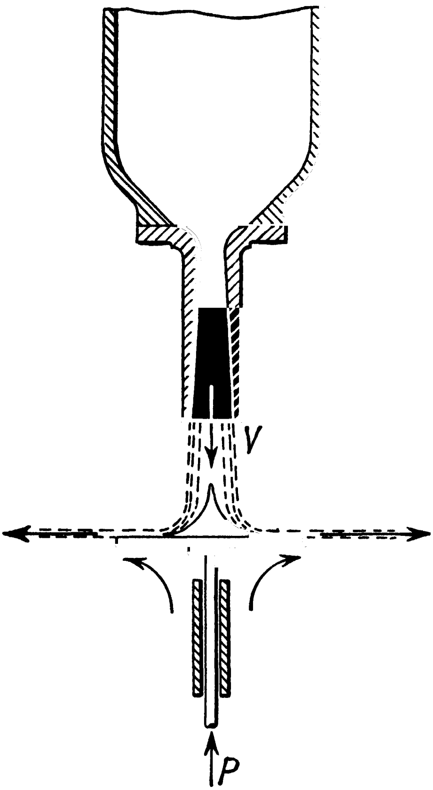


FIG. 75.—Impulse Method of Measuring Steam Velocity

The ratio $\frac{V_1}{V_t}$ (where V_t is the theoretical velocity of efflux based on the adiabatic heat drop) is the velocity coefficient η_v for the nozzle.

The simple apparatus shown in Fig. 75 is not satisfactory in use owing to the circulation currents which are set up under the plate by frictional entrainment. These appear to augment the thrust, resulting in apparent jet velocities higher than the true velocity. In the apparatus used by the Institution of Mechanical Engineers Steam Nozzles Research Committee and described in Art. 69, these objections were satisfactorily overcome.

65. Search-tube Method of Determining Pressure Distribution in a Nozzle. A small-bore tube A, Fig. 76, closed at the exhaust end and communicating with a pressure gauge B at the other end, passes

along the axis of the nozzle. Small holes are drilled in the tube in a transverse plane for the purpose of determining the pressure at the core of the stream at the particular section where the searching holes happen to be. The axial position of the searching holes can be varied by means of the micrometer wheel C. Professor Stodola (1) made some experiments in which he measured the pressures at the rim of the stream simultaneously with those at the core. He found

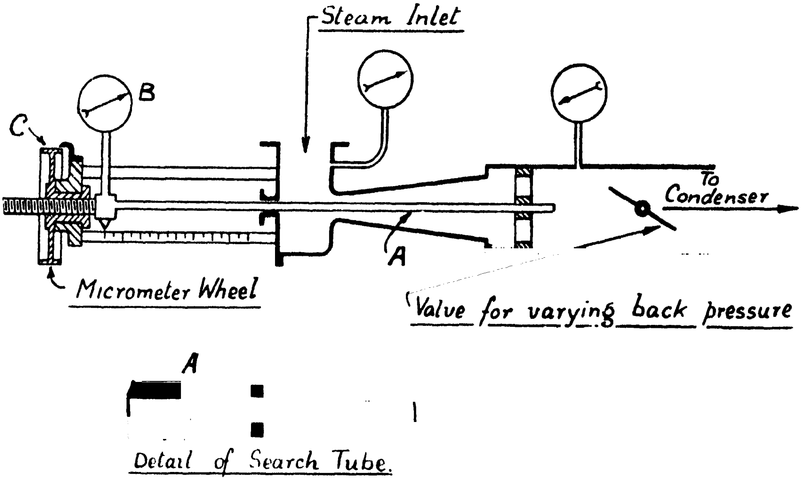


FIG. 76.—Diagrammatic Arrangement of Search-tube Apparatus

that the pressure at the axis of the stream was slightly higher than that at the rim, but the difference was very small.

Besides giving information regarding any possible disturbances in the nozzle, the results of search-tube experiments, combined with simultaneous mass-flow measurements, may be utilized for investigating the distribution of loss inside a nozzle, provided the following assumptions are made—

(*a*) That there is no heat loss by conduction through the nozzle.

(*b*) That the steam completely fills the nozzle at all sections and that the velocities of all steam particles across any section are identical.

Let I_1 = enthalpy of steam at the beginning of the expansion.
w = mass flow, lb. per sec.
V_1 = initial velocity of steam, which may be calculated from w and the initial condition of the steam.
p_2 = observed pressure at any section.
A_2 = nozzle area at any section, sq. ft.
I_2 = enthalpy at p_2.

Then by assumption (*a*)

$$\frac{V_2^2}{2gJ} + I_2 = \frac{V_1^2}{2gJ} + I_1$$

If the steam is superheated at p_2 and the specific volume is v_2, then by assumption (*b*)

$$V_2 = \frac{w \cdot v_2}{A_2}$$

Then
$$\frac{1}{2gJ}\left(\frac{w}{A_2}\right)^2 \cdot v_2^2 + I_2 = \frac{V_1^2}{2gJ} + I_1 \qquad . \quad . \quad (95)$$

The condition of the steam at p_2 to satisfy this equation may easily be found by trial and error. This enables the locus of the state point to be drawn on the Mollier chart and the loss down to any pressure to be easily determined.

If the steam is wet at p_2 and x_2 is the dryness fraction, then very nearly

$$\frac{V_2^2}{2gJ} + h_2 + x_2L_2 = \frac{V_1^2}{2gJ} + I_1$$

and since
$$w = \frac{A_2V_2}{x_2 \cdot v_{s2}}$$

$$\frac{V_2^2}{2gJ} + h_2 + \frac{A_2V_2L_2}{w \cdot v_{s2}} = \frac{V_1^2}{2gJ} + I_1 \qquad . \quad . \quad (96)$$

This equation is a quadratic in V_2, all other terms being known from the observed pressure and mass flow. When V_2 is known we can obtain the dryness fraction x_2 from the equation of continuity. By means of the Mollier chart the dryness fraction x_a, after adiabatic expansion, may be found. The energy loss in the nozzle down to the pressure p_2 will then be

$$(x_2 - x_a)L_2 \ \text{B.Th.U. per lb.}$$

66. Stodola's Search-tube Experiments. Stodola (*loc. cit.*, pp. 124 and 147) made many illuminating experiments with the aid of search tubes. Fig. 77 shows a convergent-divergent nozzle with normal inlet and outlet sections. The initial steam conditions were practically constant throughout the experiments, but the back pressure was gradually increased by the closure of a valve placed between the nozzle outlet and the condenser. Curve 1 shows the distribution of pressure in the nozzle when the outlet pressure was that for which the nozzle was designed. The other curves (2, 3, 4, etc.) show the pressure distribution as the back pressure was gradually increased.

It will be noticed that in such cases the pressure follows the correct expansion line down to a pressure which is well below the final value and then rises in sudden leaps. It appears that the

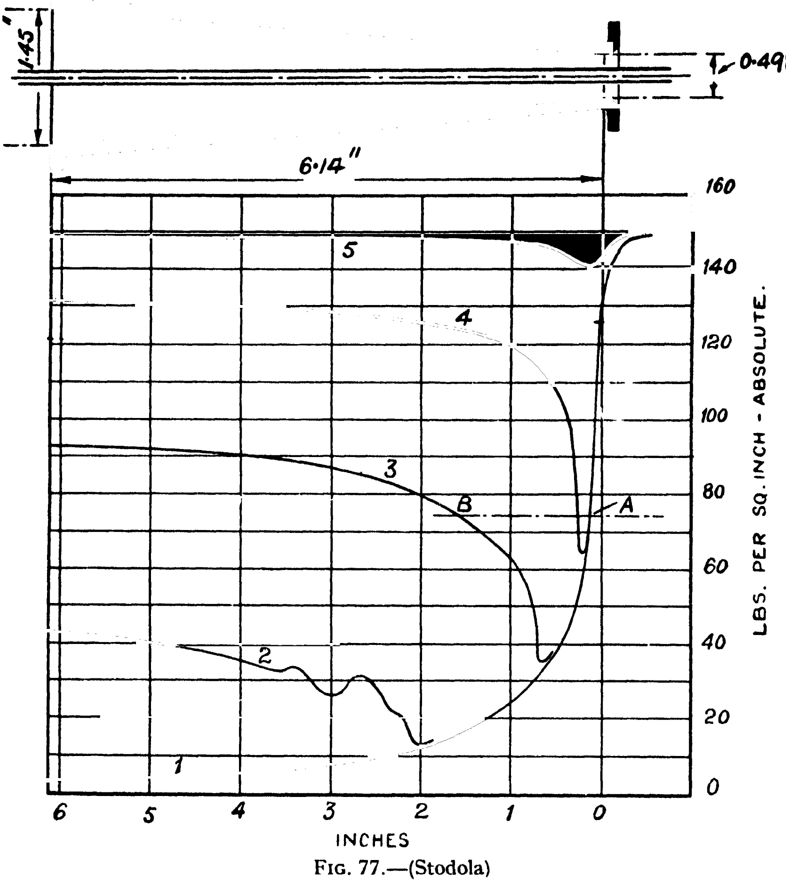


FIG. 77.—(Stodola)

steam fills the nozzle for a certain distance and expands at a rate which is controlled entirely by the area of the nozzle. Then, at a certain point, these conditions break down; the rapidly flowing steam enters a region where the steam velocity is lower, with the result that there is an impact and a sudden rise of pressure. By taking two points A and B at the intersection of a line of constant pressure AB with any one of the curves, and comparing the kinetic energy of the steam at B with that at A, it is possible

to estimate the loss of energy due to shock. Stodola points out that, except for small pressure drops, the loss of energy is great in all cases.

In some experiments with a divergent nozzle the outlet pressure was varied and the pressure before and after the nozzle outlet section was measured by means of a search tube. Some of the curves are shown in Fig. 78. When the pressure in the outlet space was lower than that corresponding to the design of the nozzle the

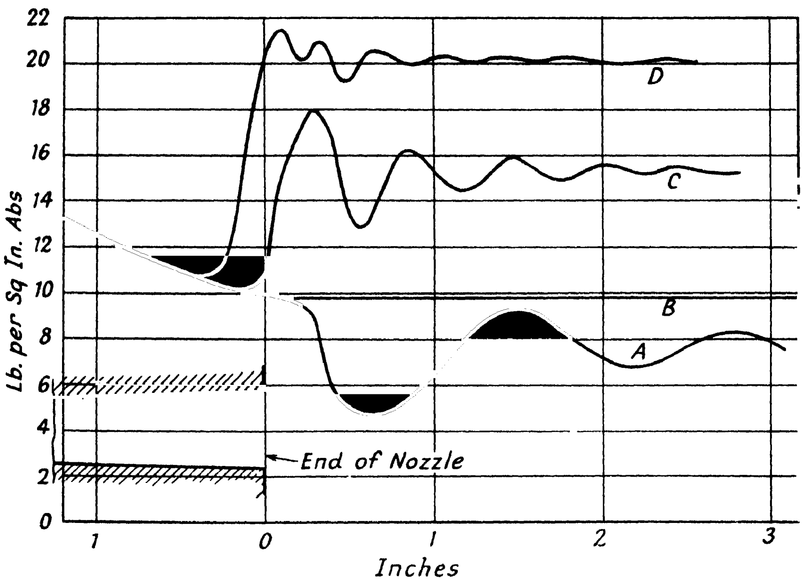


FIG. 78.—(Stodola)

pressure first dropped suddenly and then continued to oscillate, as shown by curve A. With a pressure higher than the correct back pressure there was considerable impact followed by pressure oscillations, as shown by curves C and D. In curve D, representing a pressure of 10 lb per sq. in. above the correct back pressure, the point of pressure rise extended well into the nozzle and the vibrations after the nozzle were much less intense than those of curve A. The pressures within the nozzle are not affected by the pressure changes at outlet. Curve B shows disappearance of the acoustic vibrations after adjustment of the back pressure.

Generally, the conclusions to be drawn from Stodola's experiments are that in a convergent-divergent nozzle in which the throat and mouth areas are correctly proportioned for the conditions

of working and which has a good form, the losses due to shock will be a minimum, but that if the outlet pressure is either higher or lower than that for which the nozzle is designed, considerable shock losses will occur.

67. Experimental Results obtained with Reaction Apparatus. In the year 1900 Mr. W. Rosenhain (2) published the results of some experiments made on simple forms of nozzles, including the convergent-divergent type. The velocity of efflux was determined by the reaction method.

Dr. P. Christlein (3) made experiments with apparatus similar to that shown in Fig. 74. One set of experiments was made on a single convergent-divergent turbine nozzle having a throat of circular cross-section changing to a rectangular outlet section oblique to the nozzle axis. The velocity coefficient reached its maximum value under the conditions of steam pressure and temperature, etc., for which the divergent part of the nozzle was designed, the value of η_v then being 0·946. When the conditions were allowed to deviate from the design conditions, the velocity coefficient and hence the nozzle efficiency fell away rapidly. Christlein also experimented with a group of three convergent turbine nozzles of the type in which the guide vanes are cast-in. He found that η_v increased with increasing velocity up to a theoretical steam velocity of about 1,800 ft. per sec., η_v then attaining a maximum value of about 0·93.

More recently, Messrs. Warren and Keenan (4) carried out experiments with an improved reaction apparatus. In tests on a simple convergent nozzle with a parallel outlet part the value of η_v was 0·99. In further tests on a group of four turbine nozzles having machined guide vanes the value of η_v was practically constant over a wide range of velocities and equal to 0·982. Great care was taken in these experiments to avoid errors due to circulation currents in the apparatus, but the values of the velocity coefficient appear to be rather high.

68. Institution of Mechanical Engineers Steam Nozzles Research. In the year 1914 a Committee of the Institution of Mechanical Engineers was formed in order to report upon a possible programme of research work relating to the flow of steam through nozzles. A large amount of preliminary work was undertaken, but was much interfered with by the war, and actual experimenting was not begun until September, 1921. From that time until 1930 a very considerable amount of work was done, the results being embodied in six reports (5), to which the reader is referred for fuller information. The aim of the Committee was to determine the velocity coefficient η_v for practical forms of impulse turbine nozzles, for reaction turbine blades, and also for so-called "elementary" nozzles, i.e. nozzles of simple form having the outlet plane perpendicular to the nozzle axis. Subsidiary experiments were also made to

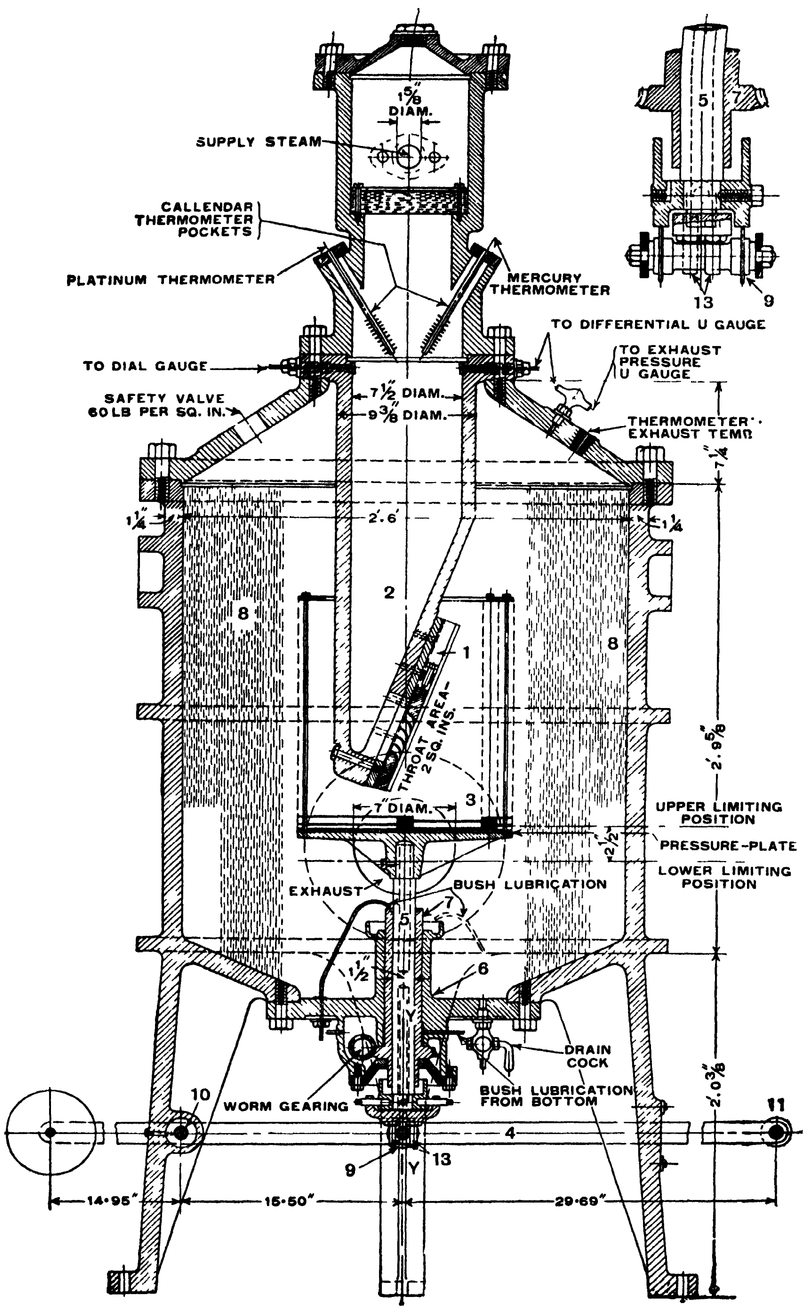


FIG. 79 — Cross sectional View of Impulse-type Nozzle Tester used by the Institution of Mechanical Engineers Steam Nozzles Research Committee

determine the effects of surface roughness in straight convergent-parallel nozzles and of curvature in impulse turbine nozzles. The impulse method (jet momentum) was adopted for measuring the jet velocities and much effort was initially expended in order

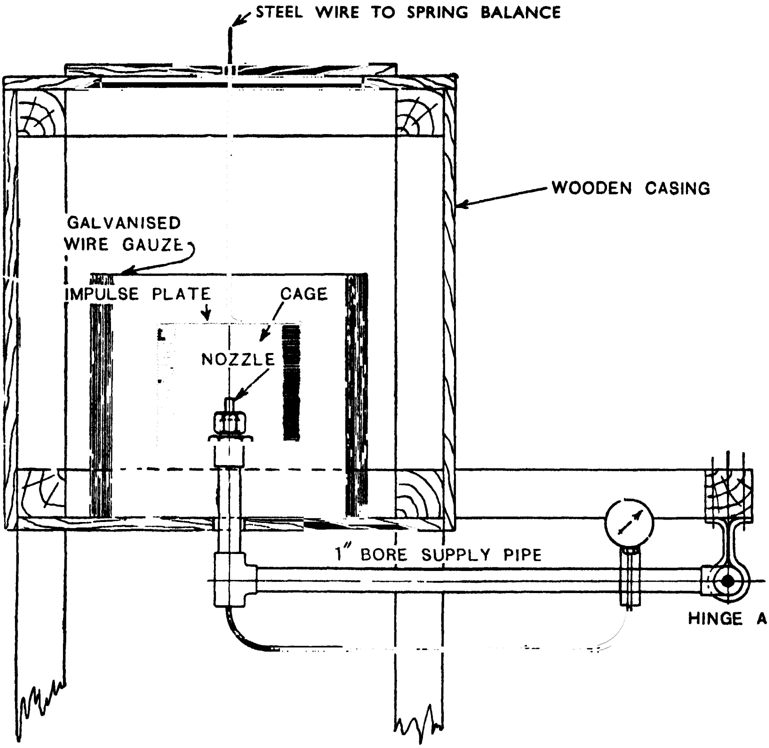


FIG. 80 —Arrangement of Apparatus for Testing Impulse Cage

to eliminate the anomalies associated with the method of measurement.

69. **Apparatus.** The apparatus used is shown in Fig. 79. The impulse plate is replaced by a cage 3, built up of thin strips of aluminium separated by thin washers, and carried on the plate proper, which is faced by layers of wire mesh and a layer of fine gauze. The object of such a design is to cause the steam to leave the cage at a low velocity and in directions entirely at right angles to the plate. The impulse is transmitted to a weighing lever 4, by means of a spindle 5, which slides in a frictionless (rotating) guide.

The nozzles to be tested are bolted to the steam chest 2. The steam exhausted from the tester is condensed in a small surface condenser and weighed.

In the preliminary experiments, the cage was tested by the method illustrated in Fig. 80. The nozzle and cage were attached rigidly together and carried by a pipe, hinged at A, supplying air under pressure. A steel wire connected the impulse plate to a sensitive spring balance. It will readily be seen that the force due to impulse opposes that due to reaction, and any difference between the two would affect the reading of the spring balance. In the early tests there was some difference between the impulse and reaction due to eddies, but when the plate was covered with felt and wire netting, the difference disappeared. For steam experiments, the felt was replaced by wire gauze.

70. **Results of Tests.** *Angle of Efflux.* In order that the nozzle might be set correctly in the tester, i.e. so that the jet would impinge normally on the plate, it was necessary to observe the exact angle of efflux of the jet. This was done by means of a balanced light metal vane placed in the steam jet. Some of the results are shown in Fig. 81. In all these cases and in all other nozzles tested, with the exception of the built-up impulse nozzle, the angle of efflux is less than the nominal angle of the nozzle. This appears to be due to the effect of the flat surface of the nozzle guide vane outlet edge in causing a suction on that part of the jet which is inclined to it at an acute angle. As the steam velocity is gradually increased it seems as though the greater momentum of the steam is more and more able to overcome this effect, and the jet efflux angle approaches nearer to the geometrical angle. In Parsons blades, where the back and front surfaces are curved and gradually approach each other at the outlet edge, the deviations of the jet from the geometrical angle are not so great.

Tests on Impulse Nozzles. Numerous tests were made on impulse turbine nozzles in which the guide vanes are cast in position. The geometrical angles of the nozzles were chosen as 12° and 20°. Some of the nozzles had thin vanes, only 0·04 in. thick, while others had vanes $\frac{3}{16}$ in. thick. A section through the latter is shown in Fig. 82. In all cases the perpendicular distance between the nozzle plates was $\frac{1}{4}$ in. The length of the parallel throat was originally $\frac{3}{4}$ in. in all cases, giving a so-called throat ratio of 3/1. In subsequent tests, the face of the whole nozzle block was machined so as to give successive throat ratios of 2/1, 1/1, and 0/1. In the last case it will be clear that the nozzle passage was entirely convergent without any parallel portion at all.

Some of the test results for the 20° nozzles are shown in Fig. 83. It will be observed that a large ratio of throat length to width is somewhat detrimental owing, probably, to the increased surface friction.

Effect of Chamfering Nozzle Plate. One important conclusion of this research work is that nozzles having thin vanes are more efficient than those having thick vanes. This is shown, for instance, by the curves in Fig. 83. The reason is probably due to the effects,

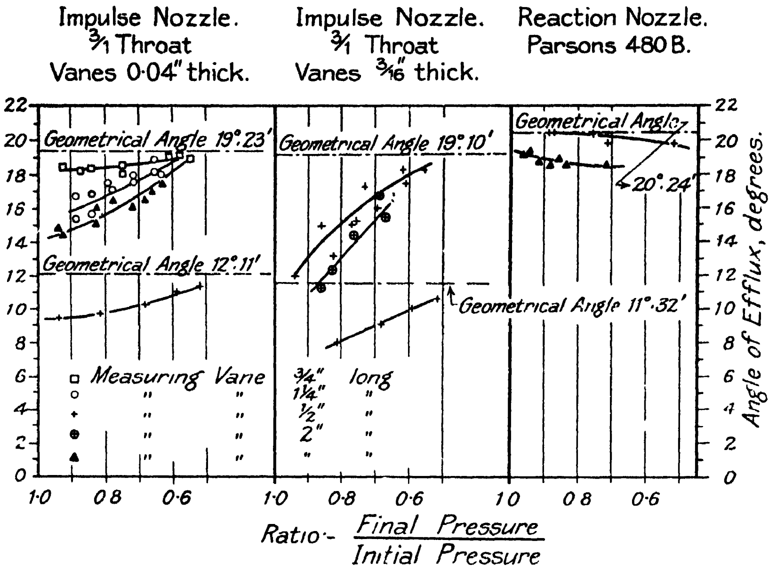


FIG. 81

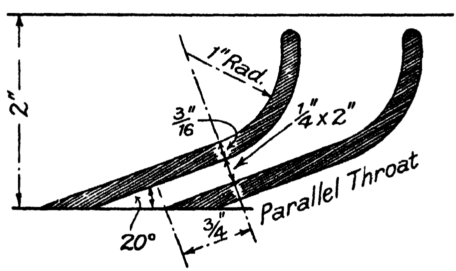


FIG. 82

already mentioned above, of the flat surface of the outlet edge of the vane, in producing deviation and instability of the jet. This flat surface may be entirely eliminated by chamfering the exit edge of the vane as shown in Fig. 84.

As thicker vanes give greater strength and rigidity to impulse turbine diaphragms, and also a greater margin of material in the event of corrosion or erosion, tests were made to determine whether the efficiency of thick-plate nozzles would be affected by chamfering

the nozzle plates in such a way as to reduce the thickness of the outlet edge to a very small dimension. Some of the results of these tests are given in the table on the next page and show that the

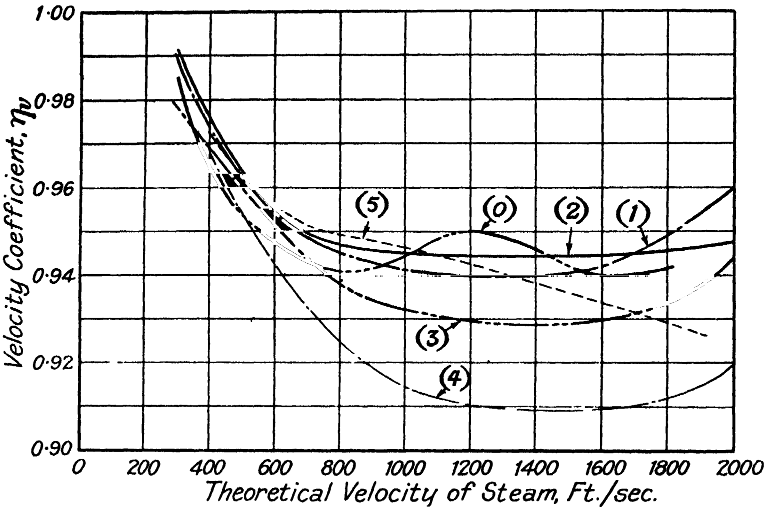


FIG. 83.—Velocity Coefficients for 20° Turbine Nozzles

Curve (0) relates to impulse nozzle with vanes 0·04 in. thick, 0/1 throat
„ (1) „ „ „ „ „ 0·04 in. „ 1/1 „
„ (2) „ „ „ „ „ 0·04 in. „ 2/1 „
„ (3) „ „ „ „ „ 0·04 in. „ 3/1 „
„ (4) „ „ „ „ „ 3/16 in. „ (Mean curve) Vane unchamfered
„ (5) relates to Parsons reaction blade 1 in wide.

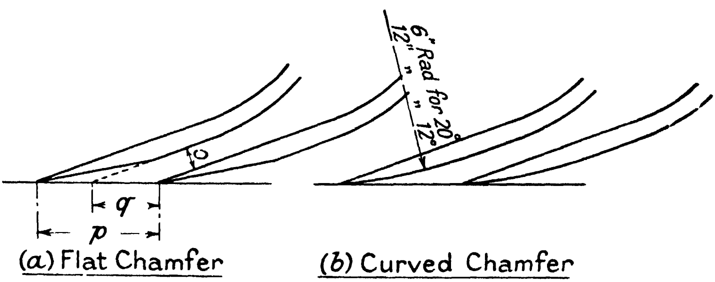


FIG 84.—Chamfering of Outlet Edges of Nozzle Plates

chamfered nozzle plate gives results practically as good as those obtained with the thin plate, irrespective of the angle of the nozzle.

As might be expected, the chamfering exerts quite an appreciable influence on the angle of efflux of the jet. The effect is to reduce the angle, and observations showed that the actual angle of efflux for pressure drops less than the critical was more nearly equal to

AVERAGE VELOCITY COEFFICIENTS FOR IMPULSE NOZZLES FOR THE VELOCITY RANGE 1,000 TO 1,700 FT. PER SEC

	20° Angle.		12° Angle.	
	3/1 Throat	0/1 Throat.	3/1 Throat	0/1 Throat
Thin plate . . .	0·932	0·946	0·905	0·944
Thick plate . . .	0·913	0·915	0·894	0·933
Thick plate, radius chamfer	0·941	0·936	0·928	0·941
Thick plate, flat chamfer .	—	0 945	—	—

the angle whose sine is o/p, Fig. 84, than the geometrical nozzle angle whose sine is o/q. With a geometrical nozzle angle of 19° 10′, the observed efflux angle of the chamfered nozzle with a throat ratio of 0/1 was about 10° 40′ at low velocities and about 12° at the critical velocity. Similarly, for a nozzle having a geometrical angle of 11° 32′, the observed angles of efflux at low velocities were about 5° 45′ for a 0/1 throat ratio and about 5° for a 3/1 throat ratio, whilst at about the critical velocity the observed angles were about 8° 20′, and 7° 30′ for the 0/1 and 3/1 throats respectively. These deviations from the nominal angle are of some importance in turbine theory and design because, as will be readily appreciated, the smaller angles lead to a greater theoretical or "diagram" efficiency and also affect the blade heights necessary to prevent the steam from blowing across the top of the blades.*

Tests of Built-up Impulse Nozzles. Some tests were made on a set of three built-up nozzles similar to those frequently used in the high-pressure stages of modern impulse turbines. A section through the test nozzle is shown in Fig. 85. The nozzle components are machined all over, so that it is possible to obtain a better surface finish than is generally obtainable with the usual "cast-in" construction, in which two of the four metal surfaces bounding the jet are rough castings. The length of parallel throat is extremely small, being only $\frac{1}{16}$ in. In making tests with this type of nozzle, the apparatus was modified so as to give the steam admission to the nozzle with less sudden changes in direction. The mean velocity coefficient for this nozzle was about 95 per cent.

Effects of Roughness. The roughness of the surface in the various nozzles tested by the Committee varied to some extent from that of well-finished machined steel, through that of drawn brass to that of a cast-iron surface. Tests undertaken to determine the effect of roughness on the velocity coefficient at various steam velocities were

* See Art. 170.

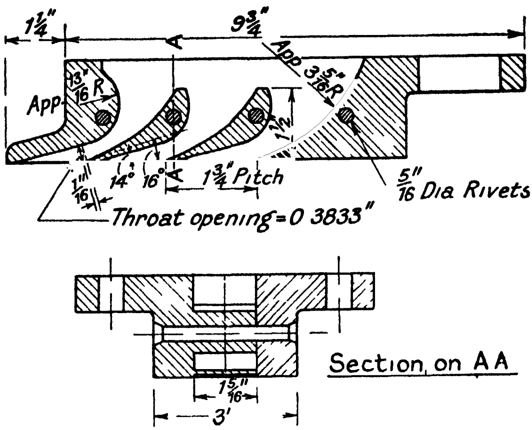


FIG 85 Built up Nozzle

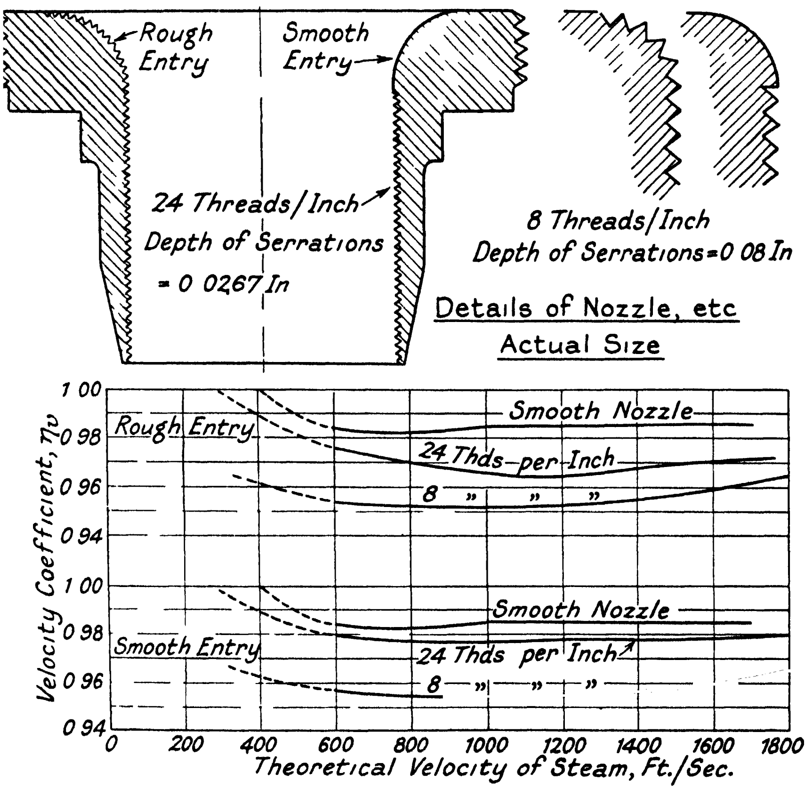


FIG 86 —Tests on Artificially Roughened Nozzles

made on straight "elementary" nozzles with a rounded inlet, the roughness being produced by means of standard Whitworth threads of 24 and 8 to the inch respectively. In one case the entry was left smooth (see Fig. 86), and in the other a number of concentric grooves corresponding to the thread in the parallel part of the nozzle were turned on the rounded inlet. The mean results are shown in Fig. 86, from which it will be seen that roughness has quite an important influence on nozzle efficiency, especially when it occurs

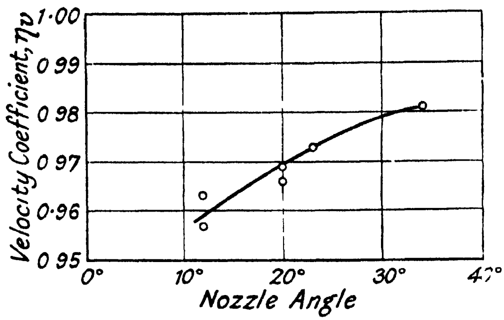


FIG 87 —Influence of Nozzle Angle on Velocity Coefficient

at the curved inlet. It is possible that the roughness which might develop on the working surfaces of actual steam turbine nozzles, due to corrosion, etc., might be so serious as to be simulated by serrations of a Whitworth thread 24 to the inch, but it is hardly likely.

Further, the roughnesses met in practical nozzles are distributed in a much more irregular fashion than those artificially produced in the experiments. Certainly the 8 threads per inch would represent a very bad case.

Effect of Nozzle Angle. The function of a turbine nozzle is not only to convert available heat energy into energy of motion, but also to direct the jet formed in a particular direction. In the actual nozzle both these operations are carried out simultaneously. It might well be imagined that the greater the angle through which the steam turns during its passage through the nozzle, the greater the inequalities in the flow and the greater the losses. In the course of its work, the committee made a number of tests on straight circular convergent nozzles with a rounded inlet and an almost parallel throat. The mean velocity coefficient for this type was about 98 per cent. In other tests with short rectangular convergent nozzles having well-rounded inlets, the mean velocity coefficient is 99 per cent. The relationship between the geometrical or nominal angle of the nozzle and the mean velocity coefficient is shown in Fig. 87, from which it will be seen that the outlet angle exerts quite an appreciable influence on nozzle efficiency. Some additional data

obtained at the works of Messrs. Metropolitan-Vickers Electrical Co., Ltd., have been used in deriving Fig. 87.

Tests to Determine the Effect of Entrance Conditions. In the final report of the Committee, an account is given of interesting tests on nozzles having various shapes of inlet. In the first place, straight nozzles of 1 in. square section and rectangular section (2 in. × ½ in.) were tested with sharp entrances, then with two edges rounded and lastly with four edges rounded. As might be expected, the sharp edges were detrimental to efficiency. Over the range of velocity from 400 to 1,200 ft. per sec., the velocity coefficient had a mean value of 0·86 to 0·87 with the sharp edges, whereas with two and four edges rounded the coefficient had mean values of about 0·96 and 0·97 respectively. With higher velocities the coefficient for the sharp-edged inlet increased steadily, and at 2,000 ft. per sec. it was almost as high as that for rounded inlet edges.

Other tests on impulse turbine nozzles, with cast-in plates having a radius of curvature of 1¾ in. as compared with ⅞ in. and 1 in. in the earlier types, were also made and showed improvements varying from 0·2 to 1·4 per cent in favour of the larger radius of curvature.

71. **Velocity Coefficients at Low Steam Velocities.** In the years following the publication of the Reports of the Steam Nozzles Research Committee attention was drawn to the unexpected result of many of the experiments, namely that below a certain steam velocity (600 to 800 ft. per sec.) the velocity coefficient increases as the steam velocity is reduced.

G. Flügel (6) carried out experiments on convergent nozzles having an axial depth of 20 mm. and a pitch of 15 mm. using a reaction tester. For all velocities lower than the acoustic the flow angle was less than the geometrical angle. The velocity coefficient increased from 0·905 at 270 ft. per sec. to 0·94 at 1,500 ft. per sec. adiabatic velocity.

Experiments were also made by E. Giffen and T. F. Crang (7) on a parallel circular nozzle $\frac{11}{32}$ in. diameter and $1\frac{1}{16}$ in. long with a slightly rounded inlet. A nozzle tester of the impulse type was used, and the results clearly showed that the velocity coefficient for the nozzle diminished steadily as the steam velocity was reduced from 1,160 to about 500 ft. per sec.

Further doubts were cast on the accuracy of the results obtained by the Steam Nozzles Research Committee, and in the light of subsequent research work Dr. H. L. Guy (8) said of an improved apparatus based on the S.N.R.C. design: "In the end we had to accept this apparatus as a comparator rather than as an absolute measuring device, and, at that, not an infallible comparator. Recognition of this limitation enhances rather than diminishes its utility, for it often tends to exaggerate or caricature the effect of differences in vane-forms." While making these criticisms Dr. Guy spoke of the very great practical importance of the researches of the S.N.R.C.

72. The Relationship between the Velocity Coefficient and the Efficiency of a Nozzle. If the velocity at outlet from a nozzle were quite uniform then the total kinetic energy of the issuing jet would be simply $\frac{V_1^2}{2g}$ ft.-lb. per pound of steam whereas the theoretical kinetic energy would be $\frac{V_t^2}{2g}$. Hence the nozzle efficiency would be $\left(\frac{V_1}{V_t}\right)^2$, i.e. η_n would equal η_v^2. This is the first kind of nozzle efficiency defined in Art. 51 and neglects the kinetic energy of the steam entering the nozzle. As pointed out in Art. 64, the velocity is not uniform throughout the jet and the ratio of the kinetic energy of the jet to the theoretical value, namely

$$\eta_n = \frac{\int V^2 \, . \, dm}{V_t^2 \int dm}$$

would not be the same as η_t^2, which is

$$\left[\frac{\int V \, . \, dm}{V_t \int dm}\right]^2$$

In an interesting paper (9) Mr. J. C. Oakden has analysed the performance of a steam turbine in which the steam flows from nozzles with a non-uniform velocity. The work done on the blading by the elements of steam moving with different velocities is then calculated from the known effect of variation of steam velocity in blades moving with a uniform peripheral velocity.

Consider a small element of steam of mass dm moving with velocity V. In Art. 78 it is shown that the blade efficiency of an impulse turbine is

$$\eta_b = 2(1 + kC)(\rho \cos \alpha - \rho^2)$$

Assuming k, C, and α to be constants,

$$\eta_b = a\rho - b\rho_1^2$$

where ρ is the ratio u/V, i.e. blade speed to steam speed, and a and b are constants.

For the element of mass dm, the work done

$$= \eta_b \cdot \frac{V^2}{2g} \, . \, dm$$

$$= \frac{V^2}{2g}\left\{a\left(\frac{u}{V}\right) - b\left(\frac{u^2}{V^2}\right)\right\} dm$$

$$= \frac{dm}{2g}(auV - bu^2)$$

Total work done by a mass of steam M

$$= \frac{au}{2g} \int V \, . \, dm - \frac{bu^2 M}{2g}$$

Let V_1 be the mass mean velocity of the steam as given by an impulse or reaction tester.

Then
$$V_1 = \frac{\int V \, . \, dm}{M}$$

$$\therefore \text{ Work done } = \frac{M}{2g} (auV_1 - bu^2)$$

$$= \frac{MV_1^2}{2g} \left\{ a \left(\frac{u}{V_1} \right) - b \left(\frac{u}{V_1} \right)^2 \right\}$$

This is identical with the work which would be done by the same mass of steam leaving the nozzles with a uniform velocity V_1. Thus with regard to the effectiveness of the steam in producing work in the blades we may assume V_1 to be the uniform outlet velocity from the nozzles. Hence η_n may be taken as equal to η_v^2. It is doubtful whether one could safely assume that the various filaments of the jet would produce effects in the blades in accordance with the usual theory without interacting with each other; nevertheless, the method gives a very simple way of assessing nozzle efficiency.

A somewhat different approach to this problem was made by Messrs. B. Hodkinson and A. E. Devey (10). Consider a small element of area δA of the outlet face of a nozzle and let ϕ be the ratio of the jet velocity over this area to the theoretical velocity due to isentropic flow. Neglect any variations of flow angle and of specific volume of the steam. Then ϕ is a measure of the velocity, $\phi \, . \, \delta A$ is a measure of the mass leaving the area δA, $\phi^2 \, . \, \delta A$ is a measure of the momentum, and finally $\phi^3 \, . \, \delta A$ is a measure of the kinetic energy leaving the area δA.

For the whole area, we may write the following expressions—

$\int \phi^3 \, . \, dA$ as a measure of the total energy leaving per unit time.

$\dfrac{\int \phi^3 \, . \, dA}{\int \phi \, . \, dA}$ is the mean energy per unit mass, i.e. the nozzle efficiency η_n.

$\dfrac{\int \phi^2 \, . \, dA}{\int \phi \, . \, dA}$ is the ratio of the total momentum to the total mass flow, i.e. the mean velocity coefficient for the nozzle η_v.

For any practicable velocity distribution which takes into account the reduction of velocity near the walls of the nozzle, η_v is always less than $\sqrt{\eta_n}$, i.e. $\sqrt{\eta_n} - \eta_v$ is always a small positive quantity. Considered in this way, the energy loss at any point, expressed as a fraction of the isentropic heat drop in the nozzle, is equal to $1 - \phi^3$. Loss contours for a nozzle are shown in Fig. 88, reproduced by permission from Messrs. Hodkinson and Devey's paper. It shows that

the losses are concentrated in the neighbourhood of the nozzle walls and are particularly high in the corners. The authors give the following as the values of the discrepancy between $\sqrt{\eta_n}$ and η_v to be expected—

Velocity Coefficient	1	0·98	0·96	0·94
Discrepancy:				
$\frac{\sqrt{\eta_n} - \eta_v}{\eta_v}$ per cent	0	0·3	0·6	0·9

73. The Use of Air for Steam Nozzle Testing. There are certain advantages to be gained if air is used in place of steam for testing

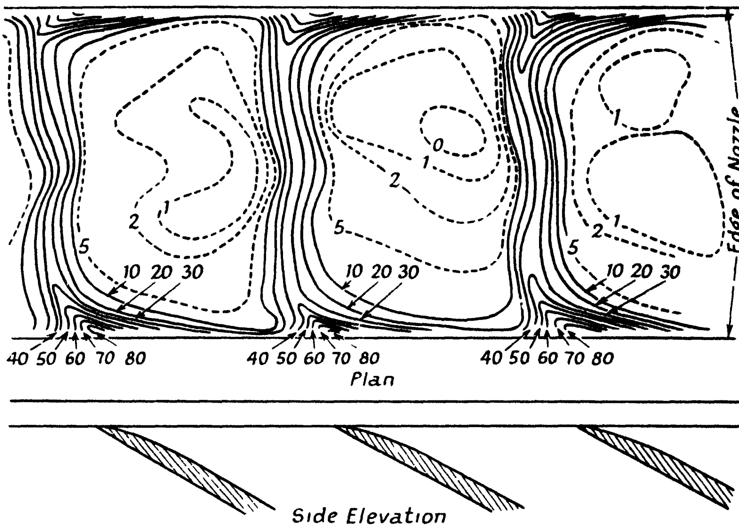


FIG. 88 Lines of Equal Energy Loss at Outlet from Nozzle

nozzles and blades. It is easier to use pitot and static pressure tubes, yaw tubes for finding the direction of flow and similar apparatus because the air may be freely discharged to the atmosphere and it is not necessary to enclose the various instruments as when steam is used. Further, in certain instances the actual mass flow of air may be measured by means of an orifice.

A difficulty which arises when steam is used is that unless the steam has a sufficiently high initial superheat there will be doubt regarding supersaturation. If the steam should be wet then it is not a homogeneous substance and the velocities of the dry steam and entrained water will not be equal.

An early worker in this field was Mr. H. Loring Wirt (11). The

basic principles of the apparatus are shown diagrammatically in Fig. 89. A group of nozzles A (usually not less than three in number) is mounted on an air receiver B which may be supplied with compressed air or with low-pressure air by a blower. A pitot or total-pressure tube C is set in the correct direction with respect to the air flow at outlet and then traversed in the direction D and at a fixed

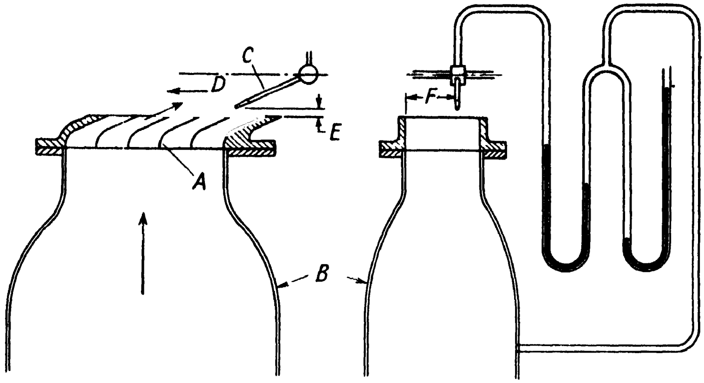


FIG. 89. Diagrammatic Arrangement of Apparatus for the Testing of Turbine Nozzles by Air

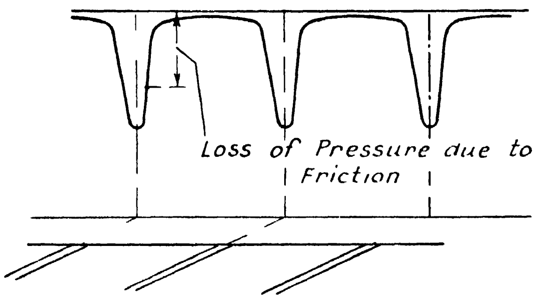


FIG. 90

distance E from the plane of the nozzle outlet and for each of a number of distances F from the side of the nozzle. The loss at each point is measured by the difference between the initial static pressure and the total pressure at outlet. The kind of record that is obtained is shown in Fig. 90 and shows that the greatest losses occur in the wakes of the guide vanes and also near the sides (roof and floor) of the nozzles. In some cases elaborate devices have been developed to integrate the curves of loss.

The use of air for testing steam turbine nozzles and blades is studied in detail in a series of articles by Dr. J. Ackeret, Dr. C.

Keller and Dr. F. Salzmann (12). It is shown that the necessary conditions for complete similarity of flow are as follows—

(*a*) Geometrical similarity of original and model.

(*b*) The fluids employed in the original and the model should have the same number of atoms and the same gamma values. If air (chiefly a mixture of two diatomic gases with $\gamma = 1{\cdot}4$) is employed in place of superheated steam (a triatomic vapour with $\gamma = 1{\cdot}3$) this condition cannot be completely satisfied.

(*c*) The Reynolds number $\frac{Vd\rho}{\mu}$ should be the same for both the original and the model flows. The results of many experiments confirm that this is probably the most important parameter necessary to ensure similarity of flow pattern. Similar values of Reynolds number enable one to construct large-scale models of nozzles or blades made of wood, metal, etc., and to employ a low-pressure air supply to provide the corresponding low velocity of flow.

The coefficient of viscosity of air may be calculated from Grindley and Gibson's equation

$$\mu = \frac{A\sqrt{T}}{1 + \frac{B}{T}} \ \frac{\text{gr.}}{\text{cm. sec.}}$$

where $A = 141{\cdot}8 \times 10^{-7}$

$B = 102{\cdot}5$

$T =$ temp. °C abs.

(*d*) The Mach number, or the ratio of the actual flow velocity to the local acoustic velocity. This parameter appears to be of small importance provided it does not exceed about 0·7.

A typical result of nozzle tests using low-pressure air and given in the paper by Ackeret, Keller and Salzmann is shown in Fig. 91. The nozzle was made of wood and given a good finish. The percentage loss is plotted against Reynolds number

$$R_e = \frac{2Vm\rho}{\mu}$$

where m is the mean hydraulic depth (area ÷ periphery) at the minimum section of the nozzle. Curves 1 and 2 show results for nozzle walls covered with sand grains 1 mm. and 0·4 mm. diameter, respectively. Curve 3 shows the losses in a plain nozzle in which the walls were sandpapered, while curve 4 shows the losses in a nozzle with lacquered walls. These tests illustrate very clearly the importance of a good surface finish. The roughness in curve 2 would correspond to excrescences in the actual nozzle about 0·02 mm. (0·0008 in.) high. The black circles show values for curve 3 obtained on a similar model of half the size.

74. Experiments on Reaction Turbine Nozzles. Some careful experiments on reaction turbine nozzles or blades were made by Mr. F. Dollin. Fig. 92 shows a diagrammatic arrangement of the apparatus used. It comprises a stationary "rotor" A which is supported at each end by members B incorporating plate springs

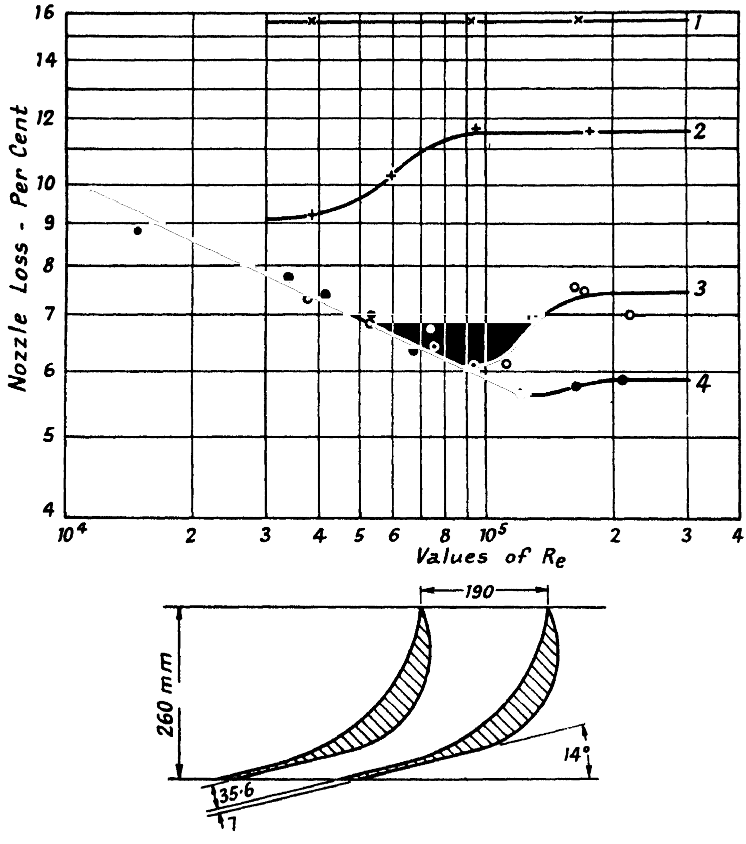


FIG. 91.– Air Tests on Model Nozzles Made of Wood

Curve 1: Nozzle walls covered with sand grains, 1 mm. diameter.
Curve 2: Nozzle walls covered with sand grains, 0·4 mm. diameter.
Curve 3: Wooden nozzle with sandpapered surfaces.
Curve 4: Wooden nozzle with lacquered surfaces.

which practically eliminate friction. Compressed air is supplied at C and enters the chamber D to the front of which the nozzle or blade group E is attached. The pipe F is surrounded by a labyrinth gland through which a small leakage of air takes place. The leakage under any given conditions of pressure is found by blanking off the nozzle plate and measuring the air flow to the apparatus. The

pressure near the nozzle inlet is measured by a tube (not shown) which is carried through the side of the inlet pipe. Since the nozzle outlet is oblique, the reaction will produce a torque on the rotor and a thrust in the direction of the arrow G. The torque is measured by

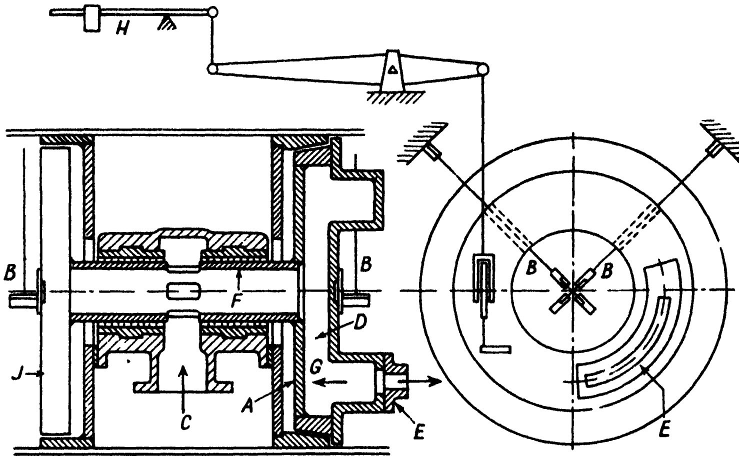


FIG. 92—Static Nozzle Tester

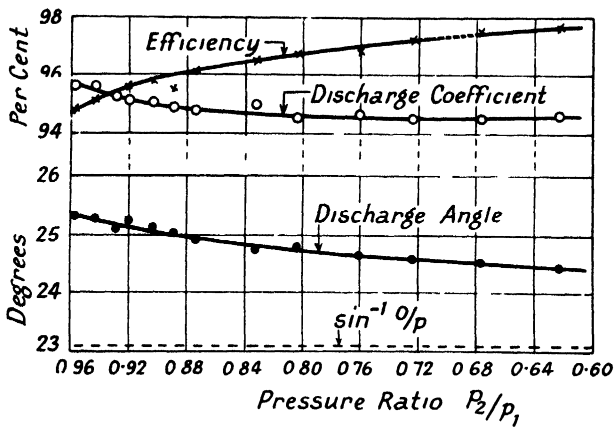


FIG. 93—Test Results on Reaction Blade

a steelyard H in which are fitted anti-friction devices, and the thrust is also measured by a similar steelyard, not shown. J is a balance weight.

Fig. 93 shows test results on a nozzle group of 10 reaction blades having an axial width of 0·75 in. and an opening coefficient of 0·39.

The discharge angle is greater than the nominal blade outlet angle.

The paper shows very clearly the influence of Reynolds number on the nozzle or blade efficiency. The Reynolds number is defined in the customary way, and Dollin has taken the hydraulic mean depth of the blade at the throat section. Thus

$$R_e = \frac{V \cdot m \cdot \rho}{\mu}$$

Fig. 94 shows the results of tests made with the static nozzle tester and with a small experimental steam turbine having 7 stages. This turbine worked in a region of Reynolds numbers much lower

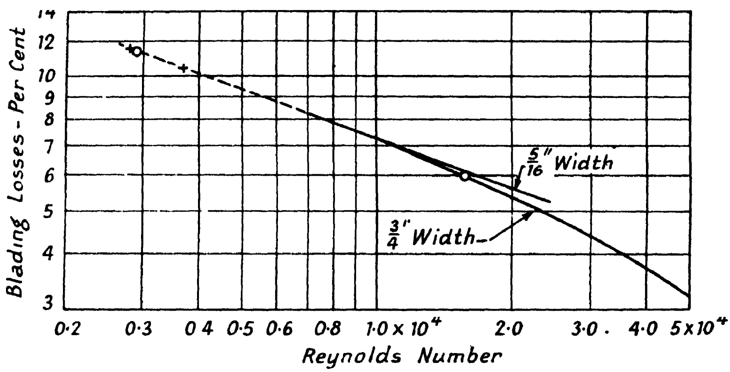


FIG. 94.—Correlation of Blading Efficiency Derived from Nozzle and Turbine Tests

Note. Crosses show turbine tests with profile C, circles show turbine tests with profile I.

than those common in commercial turbines. In Fig. 94 the loss in the nozzles is plotted against R_e, log scales being used in both cases. The results obtained for the $\frac{5}{16}$ in. wide blading are represented by the full straight line which, when produced, passes through the points representing turbine tests. The losses in the wider blades are represented by a curve falling slightly with increased Reynolds numbers.

75. **Further Steam Nozzle Tests.** Some very comprehensive tests by Professor J. H. Keenan (14) and Mr. H. Kraft (15) were made with the reaction tester mentioned in Art. 67.

Professor Keenan's tests were made on convergent-divergent nozzles of various types. The test results for one such nozzle are shown in Fig. 95. The outlet width of the nozzle is taken at the point where the axis intersects the plane of the outlet and the divergence ratio is the ratio of this width to the throat width, namely 1·38. It was found that the velocity coefficient reached its maximum value at an isentropic velocity corresponding to a divergence ratio rather less than the nominal divergence ratio of the nozzle. The important

result which emerges from this and other tests is that a convergent-divergent nozzle is efficient only when operating under conditions of pressure and velocity which approximate to those for which the nozzle is designed.

It will be noticed that for isentropic velocities lower than the sonic, the discharge coefficient is greater than unity. This is stated to be due to a diffusion process into the spaces downstream from the partition edges which causes the steam pressure in the throat to

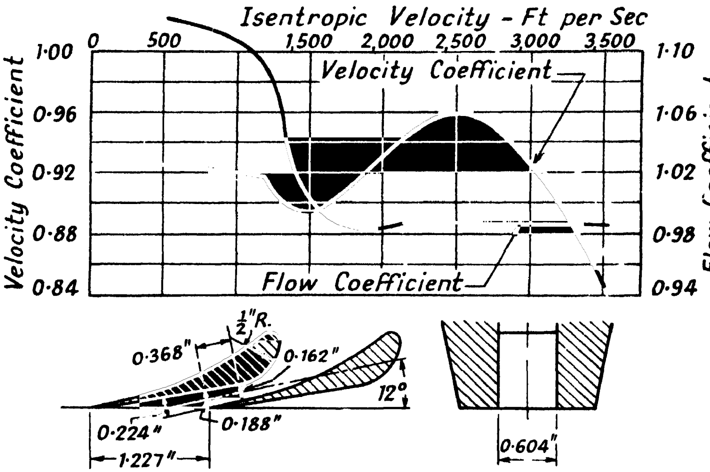


FIG. 95.- Velocity and Flow Coefficients for a Convergent-divergent Nozzle

be lower than that in the exhaust chamber, and the actual mass velocity in the throat to exceed that based on isentropic flow to the exhaust pressure.

The nozzle tests made by Kraft included the following—

(1) Tests to determine the effects of guide vane profile. For the various guide vanes tested the velocity coefficient ranged from 0·96 to 0·98 at subsonic velocities.

(2) Tests with the same guide vane set at angles 10°, 13·5°, and 17°. The 10° and 17° nozzles had the same pitch, namely 1·425 in. The 17° nozzle had a positive throat of 0·184 while the 10° nozzle had a positive throat of 0·143 in. On the other hand the angle turned through by the steam is smaller by 7°. There was little difference in the results at subsonic velocities. The 13·5° nozzle with a pitch of 1·70 in. and a negative throat of 0·10 in. gave a slightly better performance than the other two.

(3) Tests on the same guide vane at two different pitches. The outlet angle was 13·5°, and the nozzle height 2·61 in. in each case.

The nozzles with pitches of 1·425 and 1·700 in. gave velocity coefficients of about 0·97 and 0·98, respectively at subsonic velocities.

(4) Tests to find the effect of aspect ratio, i.e. ratio of nozzle height to throat width. In a nozzle with a small radial height the boundary layers on the roof and floor of the nozzle exert a proportionately greater effect than they do in a nozzle of greater radial height. Consequently, it might be expected that with other things

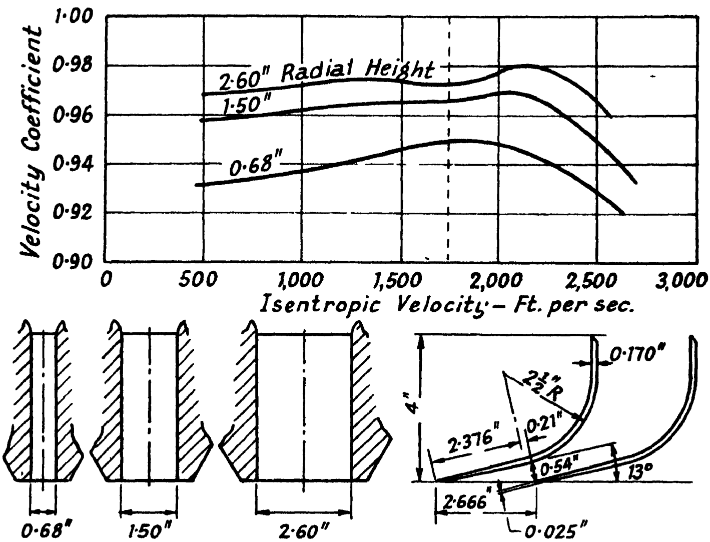


FIG. 96.—Effect of Aspect Ratio on Nozzle Velocity Coefficient

equal, a nozzle with a greater aspect ratio would show a higher efficiency. This was borne out in several tests. Fig. 96 shows the results obtained in one series of tests.

(5) Tests to determine the effect of outlet edge thickness. The results conform to those of the S.N.R.C. in that it was found that a thinner edge resulted in a rather higher velocity coefficient at subsonic velocities in a convergent nozzle.

BIBLIOGRAPHY

1. STODOLA: "Dampf- und Gas-Turbinen." 6th Ed., p. 56.
2. ROSENHAIN: "Experiments on Steam Jets." *Proc. I.C.E.*, 1900; 140; 199.
3. CHRISTLEIN: "Untersuchung über das allgemeine Verhalten des Geschwindigkeitskoeffizienten von Leitvorrichtungen des praktischen Dampfturbinenbaues." *Zeits. Ver. deutscher. Ing.*, 1911; 55; 2081.
4. WARREN AND KEENAN: "A Machine for Testing Steam-turbine Nozzles by the Reaction Method." *Mechanical Engineering*, Vol. 48, p. 227.

BIBLIOGRAPHY

1. SMITH: "A New Graphic Analysis of the Kinematics of Mechanisms." *Trans. Roy. Soc. of Edinburgh*, 1885; 32; 507. See also Dunkerley's *Mechanism*, p. 213, *et seq.*
2. ACKERET, KELLER, and SALZMANN: "Die Verwendung von Luft als Untersuchungsmittel für Probleme des Dampfturbinenbaues." *Schw. Bauzeitung*, 1934, 104.

EXAMPLES VII

1. Steam issues from the nozzles of a de Laval turbine with a velocity of 3,500 ft. per sec. The nozzle angle is 20°, the mean blade velocity is 1,200 ft. per sec., and the inlet and outlet angles of the blades are equal. The mass of steam flowing through the turbine per hour is 1,800 lb. Calculate—

   (*a*) The blade angles.
   (*b*) The relative velocity of the steam entering the blades.
   (*c*) The tangential force on the blades.
   (*d*) The horse-power developed.
   (*e*) The blade efficiency.

   Assume that $k = 0{\cdot}8$.

2. The mean diameter of the blades of an impulse turbine with a single-row wheel is 42 in. and the speed 3,000 r.p.m. The nozzle angle is 18°, the ratio of blade speed to steam speed is 0·42, and the ratio of the relative velocity at outlet from the blades to that at inlet is 0·84. The outlet angle of the blade is to be made 3° less than the inlet angle. The steam flow is 16 lb. per sec.

   Draw the velocity diagram for the blades and derive the following—

   (*a*) Resultant thrust on blades.
   (*b*) Tangential thrust on blades.
   (*c*) Axial thrust on blades.
   (*d*) Horse power developed in blades.
   (*e*) Blading efficiency.

3. In a stage of an impulse turbine provided with a single-row wheel, the mean diameter of the blade ring is 32 in. and the speed of rotation is 3,000 r.p.m. The steam issues from the nozzles with a velocity of 900 ft. per sec., and the nozzle angle is 20°. The rotor blades are equiangular and, due to friction in the blade channels, the relative velocity of the steam at outlet from the blades is 0·86 times the relative velocity of the steam entering the blades.

   What is the power developed in the blading when the axial thrust on the blades is 26·9 lb.?

4. Steam flows from the nozzles of a single-row impulse turbine with a velocity of 1,300 ft. per sec., the nozzle angle being 16°. The final absolute velocity at outlet from the blades is 308 ft. per sec. in a direction 98° 12′ with the direction of motion of the blades. If the blades are equiangular, calculate the blade horse-power when the mass flow of steam through the blading is 16·1 lb. per sec., and also calculate the friction loss per lb. of steam in the blade channels.

5. Show that in a single-stage impulse turbine with equiangular blades, provided k, the ratio of the relative velocity at outlet from the moving blades to the relative velocity at inlet, is constant, the most efficient ratio of blade velocity to steam jet velocity is independent of the value of k.

   Hence derive the optimum ratio of blade speed to steam speed and the corresponding blade inlet angle when the nozzle angle is 14°. What is the maximum blade efficiency in this case when $k = 0{\cdot}9$? Assume that the inlet and outlet angles of the blade are equal

6. The following particulars relate to a single stage of an impulse turbine—

Steam velocity at nozzle mouth	1,000 ft. per sec.
Nozzle angle	18°
Mean blade velocity	480 ft. per sec.

Draw to a suitable scale the diagram of relative velocities for the steam, assuming that the outlet angle of the blades is 3° less than the inlet angle, and that the relative velocity of the steam at outlet from the blades is 0·84 times the relative velocity of the steam entering the blades.

If the power to be developed in that stage only is to be 1,000 kW, calculate the weight of steam which must pass through the turbine per second. Neglect disc friction and leakage losses.

7. Deduce a general expression for the blade efficiency of a stage of an impulse turbine with single-row wheels, assuming equiangular blades, a nozzle angle α, and that k is the ratio of the relative velocity at outlet from the moving blades to the relative velocity at inlet. What is the maximum efficiency if $\alpha = 20°$, and $k = 0{\cdot}83$?

If the blade efficiency is to be 90 per cent of the maximum value, what are the possible ratios of blade speed to steam speed? Draw the velocity diagrams for each case and state the blade angles.

8. The nozzles in a stage of an impulse turbine are of the convergent type and are formed by "casting-in" vanes of uniform thickness. The radial height of the nozzles is 6 in., the mean diameter 46 in., the nozzle angle 18°, the vane thickness 0·116 in., and the number of nozzles in the complete ring is 72. Given that the specific volume of the steam at the nozzle outlet is 246 cub. ft. per lb., and that the velocity of the steam at the nozzle outlet is 1,200 ft. per sec., calculate the weight of steam flowing through the nozzles per second.

Calculate the power developed in the blades of the given stage, assuming that there is a single row of impulse blades having equal inlet and outlet angles, that the ratio of the relative outlet velocity to the relative inlet velocity is 0·86, and that the rotor turns at 3,000 r.p.m.

9. The adiabatic heat drop in a given stage of a multi-stage impulse turbine is 9·5 B.Th.U. per lb. of steam. The nozzle outlet angle is 16°, and the efficiency of the nozzle, defined as the ratio of the actual gain of kinetic energy in the nozzle to the adiabatic heat drop, is 92 per cent. The mean diameter of the blades is 58 in. and the revolutions per minute 1,500. Given that the "carry-over" factor ϕ is 0·88, that the blades are equiangular, and that the blade velocity coefficient is 0·87, calculate the steam velocity at outlet from the nozzles, the blade angles, and the gross stage efficiency.

10. The following particulars relate to a single-stage impulse turbine with a single row of blades—

Nozzle angle	18°
Steam velocity at nozzle outlet	800 ft. per sec.
k	0·85
Steam flow	50 lb. per sec.
Horse-power developed in blades	754

What are the possible values of the mean blade velocity, assuming that the blade outlet angle is equal to the angle made by the steam at inlet to the blades?

If the nozzle efficiency is 92 per cent and the "carry-over" coefficient ϕ is 0·9, calculate the gross stage efficiency of a multi-stage turbine operating under the same conditions with the higher blade velocity.

Work done per second

$$= \frac{w_1 \cdot V_1^2}{gJ}(2\rho \cdot \cos\alpha - \rho^2)$$

Total adiabatic heat drop per second

$$= w(h_n + h_b)$$

$$= \frac{w \cdot V_1^2}{g \cdot J \cdot \eta_n}\{1 - \phi(1 + \rho^2 - 2\rho \cdot \cos\alpha)\}$$

Since the leakage loss is practically the only loss affecting the efficiency of a reaction turbine stage—apart from blade friction and shock losses which have already been considered and whose effects are included in the above expressions—we may write –

Stage efficiency

$$\eta_s = \frac{w_1}{w} \cdot \frac{\eta_n(2\rho\cos\alpha - \rho^2)}{1 - \phi(1 + \rho^2 - 2\rho\cos\alpha)} \qquad (130)$$

If ordinary unshrouded blades are used then, since

$$\frac{w_1}{w} = 1 - \frac{3c}{l}$$

$$\eta_s = \left(1 - \frac{3c}{l}\right) \cdot \frac{\eta_n(2\rho \cdot \cos\alpha - \rho^2)}{1 - \phi(1 + \rho^2 - 2\rho \cdot \cos\alpha)} \qquad (131)$$

93. Operation of Impulse Blading with Varying Heat Drop or Variable Speed. If a turbine stage is designed for constant initial steam conditions and for a specific heat drop and blade speed, and if, moreover, the turbine stage is designed for pure impulse, then any departure from the specified conditions of operation either of stage heat drop or blade speed will cause a departure from pure impulse operation.

Let A_1 = effective area through nozzle ring, sq. ft.
A_2 = effective area through blade outlet, sq. ft.
v_1 = specific volume of steam at nozzle outlet, cu. ft. per lb.
v_2 = specific volume of steam at blade outlet, cu. ft. per lb.
w = steam flow in lb. per sec.

Under pure impulse operation v_2 is very nearly equal to v_1. For simplicity neglect the effect of guide vane thickness and blade outlet edge thickness. Then with the usual notation and referring to Fig. 128,

$$w = \frac{A_1 V_1}{v_1} = \frac{A_2 U_2}{v_2}$$

Assuming complete admission,

$$A_1 = \pi D l_1 \sin \alpha$$

$$A_2 = \pi D l_2 \sin \beta_2$$

$$\therefore \qquad U_2 \,.\, \sin \beta_2 = \frac{v_2}{v_1} \,.\, \frac{l_1}{l_2} \,.\, V_1 \sin \alpha$$

or

$$V_{a2} = \frac{v_2 l_1}{v_1 l_2} \,.\, V_{a1}$$

This equation must be satisfied in order that the equation of continuity may be satisfied simultaneously for the nozzles and blades. Its application is best illustrated by a numerical example.

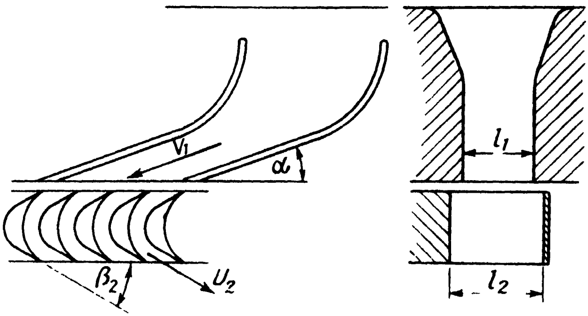


FIG. 128

EXAMPLE 18. Steam is supplied to a single-row impulse turbine at $p = 100$, dry and saturated. Under normal conditions of operation the blade velocity u is 400 ft. per sec., and the adiabatic heat drop is 21 B.Th.U. per lb. For the purposes of calculation the following may be assumed—

Nozzle angle $\alpha = 20°$; nozzle efficiency $= 0{\cdot}93$; stage efficiency $= 0{\cdot}80$; ratio $\frac{l_1}{l_2} = 0{\cdot}85$; relative velocity factor $k = 0{\cdot}9$.

Find the conditions of working—

(*a*) when the blade speed remains constant and
  (1) there is pure impulse,
  (2) adiabatic heat drop in nozzles = 32·0 B.Th.U. per lb.,
  (3) adiabatic heat drop in nozzles = 10·0 B.Th.U. per lb.;

(*b*) when the nozzle heat drop remains constant at 21·0 B.Th.U. per lb. and
  (4) u is increased to 500 ft. per sec.,
  (5) u is reduced to 300 ft. per sec.

In the first place it is necessary to find the relationship between steam pressure, adiabatic heat drop, and specific volume at the nozzle and blade outlets. This is done for the blade outlet condition by using the Mollier chart and the given efficiency of 80 per cent.

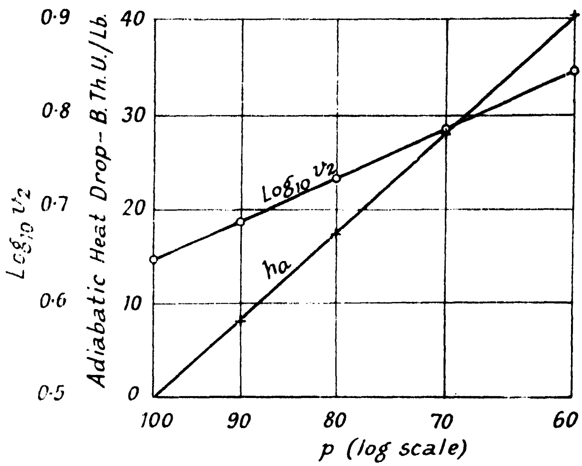


FIG. 129

The specific volume at outlet from the nozzles would be slightly less than that at the blade outlet at the same pressure, but to simplify the calculations the small difference will be neglected.

The following basic figures are then obtained—

p	I (adiabatic)	Adiabatic Heat Drop $I_0 - I$	Actual Heat Drop	Dryness Fraction x	v_s	$v = x \cdot v_s$
100	1,188·2	0	0	1·0000	4·434	4·434
90	1,180·0	8·2	6·56	0·9945	4·896	4·869
80	1,170·8	17·4	13·92	0·9898	5·472	5·413
70	1,160·2	28·0	22·40	0·9835	6·206	6·100
60	1,147·9	40·3	32·24	0·9768	7·175	7·000

For convenience in the calculations which follow, the adiabatic heat drop h_a and $\log_{10} v_2$ are plotted against $\log_{10} p$, Fig. 129.

Case 1. Pure Impulse

Heat drop in nozzles = 0·93 × 21 = 19·53 and hence $V_1 = 990$, giving $\rho = 0·404$, $p_2 = 76·38$ and $v_2 = 5·633$.

$$V_{a1} = V_1 \sin 20° = 338{\cdot}6$$

Then $$V_{a2} = 0{\cdot}85 \times 338{\cdot}6 = 287{\cdot}8$$

We find from the velocity diagram, Fig. 130, that $U_1 = 629$; $U_2 = 0{\cdot}9 \times 629 = 566{\cdot}1$; $\beta_1 = 32° 36'$; $\beta_2 = 30° 30'$.

Case 2. $h_n = 32{\cdot}0$ B.Th.U. per lb.

From Fig. 129 we find $p_2 = 66{\cdot}37$ and $v_2 = 6{\cdot}383$. Effective heat drop in nozzles $= 0{\cdot}93 \times 32 = 29{\cdot}76$.

$$V_1 = 1{,}220;\ \rho = 0{\cdot}328$$

$$V_{a1} = 1{,}220 \times 0{\cdot}342 = 417{\cdot}2$$

$$V_{a2} = 354{\cdot}6 \frac{v_2}{v_1}$$

v_2 will not now be equal to v_1 as there will be a change of pressure in the blade channels. Its value may be found by trial and error as follows.

For a first approximation we assume $v_2 = v_1$. Then $V_{a2} = 354{\cdot}6$. If there were pure impulse the relative velocity at outlet from the

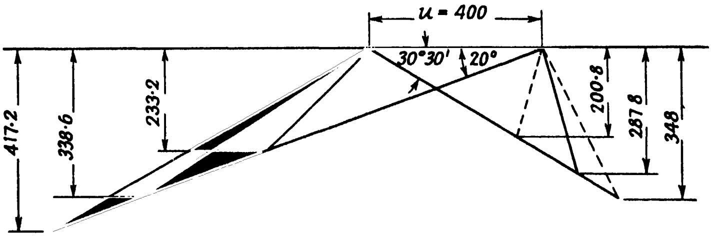


FIG. 130

blade would be $U_2{}^1 = 0{\cdot}9 \times 856 = 770$. Assuming that the steam emerges from the moving blades at the angle $\beta_2 = 30° 30'$, then, since $V_{a2} = 354{\cdot}6$, the actual relative velocity at outlet must be $354{\cdot}6 \operatorname{cosec} 30° 30' = 698$. This means that the steam velocity must be reduced from 770 to 698 ft. per sec. in the blade channels. If this reduction in velocity could be carried out without loss the change of enthalpy would be

$$\frac{770^2 - 698^2}{2gJ} = 2{\cdot}12 \text{ B.Th.U. per lb.}$$

and it would be a gain. In other words, there would be a rise in steam pressure in the moving blades, a negative heat drop and therefore a negative reaction in the blades.

If we assume a diffuser efficiency η_d of $0{\cdot}80$ (the actual value would probably be much lower) the change of enthalpy would be

$0{\cdot}8 \times 2{\cdot}12 = 1{\cdot}70$ and the stage heat drop $= 32{\cdot}0 - 1{\cdot}7 = 30{\cdot}3$ B.Th.U. per lb. Again using the same relationship between pressure and specific volume we find $v_2 = 6{\cdot}266$.

$$\therefore \qquad V_{a2} = 354{\cdot}6 \times \frac{6{\cdot}266}{6{\cdot}383} = 348 \text{ and } U_2 = 684$$

The new value of $h_b = -2{\cdot}0$ B.Th.U. per lb. and the stage heat drop $= 30{\cdot}0$. $\therefore$ $v_2 = 6{\cdot}238$ and $V_{a2} = 346$. This value is so near the previous value that further calculation is unnecessary.

It is thus clear that, if a normal impulse stage operates with fixed initial conditions but with a greater stage heat drop, then the

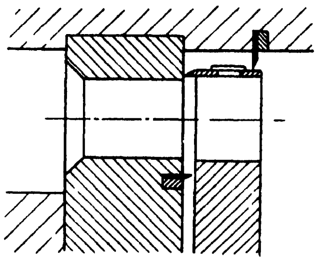


FIG 131

pressure in the clearance space between the nozzles and moving blades will be lower than that at outlet from the blades and there will be negative reaction. Such conditions are likely to lead to high losses and should be avoided. It appears from the experimental work of Faltin (see Art. 103) that even with partial admission such conditions can occur with heat drops greater than the normal.

In certain turbines, a large diameter single-row wheel is used in the first stage for governing purposes. As shown in Chapter XV the pressure in the first stage wheel chamber of such turbines will diminish as the load is reduced. In consequence, the operating conditions will deteriorate at part loads. Such deterioration can be largely avoided by the use of partial reaction. As the pressure in the clearance space is then higher than that in the wheel chamber, some form of packing should be used to reduce steam leakage, Fig. 131. When the turbine output is reduced the degree of reaction will diminish and may ultimately change from positive to negative.

Case 3. $h_n = 10{\cdot}0$ B.Th.U. per lb. Then $p_2 = 87{\cdot}9$ and $v_2 = 4{\cdot}977$.

$$\text{Effective heat drop in nozzles} = 9{\cdot}3$$

$$V_1 = 682; \ \rho = 0{\cdot}586$$

$$V_{a1} = 682 \times 0{\cdot}342 = 233{\cdot}2$$

$$V_{a2} = 198{\cdot}2 \frac{v_2}{v_1}$$

Assuming, for a first approximation, that $v_2 = v_1$ we find that for pure impulse $U_2{}^1 = 0{\cdot}9 \times 336 = 302{\cdot}4$ and $U_2 = 391$. In this case there must be an increase in relative velocity in the moving

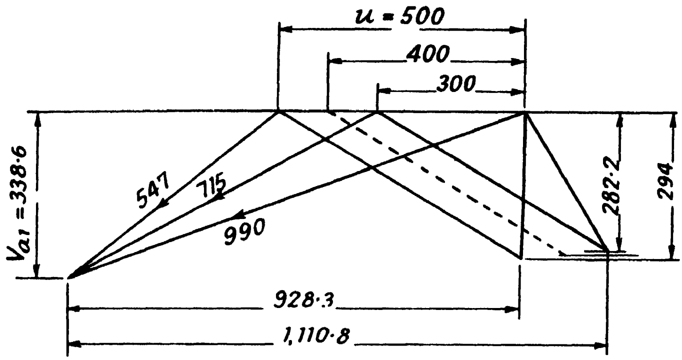


FIG. 132

	Case 4	Case 5
u	500	300
ρ	0·505	0·303
V_{a1}	338·6	338·6
1st approx ($v_2 = v_1$)		
V_{a2}	287·8	287·8
U_1	547	715
$U_2{}^1$	492·3	643·5
U_2	566·1	566·1
h_b	1·68	1·5
$h_n + h_b$	22·68	19·5
v_2	5·745	5·54
2nd approx.		
V_{a2}	293·5	283
U_2	577	557
h_b	1·94	1·66
$h_n + h_b$	22·94	19·34
v_2	5·754	5·521
V_{a2}	294	282·2

blades, i.e. a drop in pressure and positive reaction. Assuming the expansion efficiency to be 0·93, the heat drop $h_b = 1{\cdot}32$.

Then the stage heat drop $= 11{\cdot}32$, $v_2 = 5{\cdot}042$ and $V_{a2} = 200{\cdot}7$.

With the new value of V_{a2} we find $U_2 = 395$, $h_b = 1{\cdot}38$, the stage heat drop $= 11{\cdot}38$, $p_2 = 86{\cdot}3$, $v_2 = 5{\cdot}047$ and $V_{a2} = 200{\cdot}8$.

Cases 4 and 5. Consider now that the nozzle heat drop remains

constant ($V_1 = 990$) and that the blade speed is changed Then referring to Fig 132 and using the method described above the results given on page 224 are obtained

The particulars of the five cases are summarized in Table X and Fig 133 from which it will be seen that the blade speed ratio is the

TABLE X

OPERATION OF IMPULSE STAGE WITH CONSTANT INITIAL STEAM CONDITIONS AND WITH VARYING STAGE HEAT DROPS AND VARYING BLADE VELOCITIES

	1 Impulse	2	3	4	5
V_1	990	1 220	682	990	990
u	400	400	400	500	300
ρ	0 404	0 328	0 586	0 505	0 303
h_l	0	2 00	1 32	1 94	− 1 66
h_r h_b	21 0	30 0	11 32	22 94	19 34
Degree of Reaction	0	6 67	11 65	8 46	− 8 58
V_r	1 019	1 340	580 5	928 3	1 110 8
Work done B Th U per lb	16 28	21 40	9 28	18 56	13 31
Gross Stage Efficiency	77 0	71 4	81 5	80 9	68 9

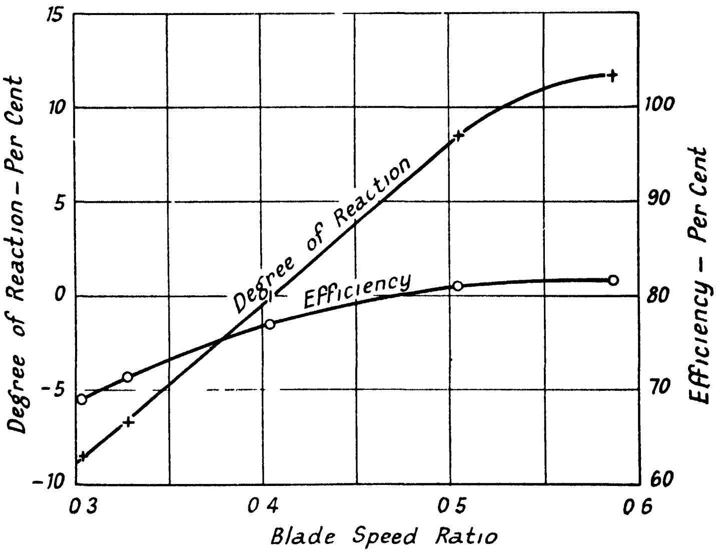


FIG 133—Calculated Performance of Impulse Stage Operating at Different Ratios of Blade Speed to Steam Speed

chief criterion of performance. The foregoing calculations must be regarded as approximate since they take no account of the effect of the varying direction of steam flow into the blades.

EXAMPLES VIII

1. The following particulars refer to a stage of a Parsons steam turbine comprising one ring of fixed blades and one ring of moving blades—

Mean diameter of blade ring	26 in.
R.p.m.	3,000
Steam velocity at exit from blades	525 ft. per sec.
Blade outlet angle	20°
Steam flow through blades	15·5 lb. per sec.

Draw the velocity diagram and derive the following—
(*a*) Blade inlet angle.
(*b*) Tangential force on ring of moving blades.
(*c*) Horse-power developed in stage.

2. In a stage of an impulse-reaction turbine operating with half-degree reaction, the fixed and moving blades are of identical section and the outlet angle is 18°. The absolute velocity of discharge from the moving blades is 130 ft. per sec. in a direction 110° to the direction of motion of the blades, and the change of velocity produced by the moving blades is parallel to that direction.

Draw the velocity diagram and derive—
(*a*) Mean velocity of the blades.
(*b*) Ratio of blade velocity to the velocity of efflux from the fixed blades.
(*c*) Work done per lb. of steam.

3. If the total tangential thrust on the blades of one ring of a Parsons turbine is 293 lb. when the blade speed is 350 ft. per sec., the weight of steam flowing through the blading per sec. is 16 lb., and the blade outlet angle is 20°, calculate the steam velocity at outlet from the blades.

If the friction losses which would occur with pure impulse are 33 per cent of the kinetic energy corresponding to the relative velocity at entry to each ring of blades, and if the expansion losses are 14 per cent of the heat drop in the blades, what would be the heat drop per ring, and the gross stage efficiency?

4. The outlet angle of the blade of a Parsons turbine is 20° and the axial velocity of flow of the steam is 0·5 times the mean blade velocity. Draw the velocity diagram for a stage consisting of one fixed and one moving row of blades, given that the mean diameter is 28 in. and that the speed of rotation is 3,000 r.p.m. State the inlet angle of the blades if the steam is to enter the blade channels without shock.

If the blade height be 2·5 in., the mean steam pressure 80, the steam dry and saturated (v = 5·466 cub. ft. per lb.), find the horse-power developed per pair of blades.

5. A blade group in a reaction turbine is of constant height. The power of the turbine is 2,000 kW, the speed of rotation 3,000 r.p.m., initial steam pressure 160 lb. per sq. in. gauge, steam initially dry and saturated, vacuum 27½ in. (30 in. barometer), and the efficiency ratio 67 per cent. The mean blade velocity in the group is to be 300 ft. per sec. and the average specific volume of the steam in the group may be taken as 10·25 cub. ft. per lb. If the ratio of the blade velocity to the steam velocity be 0·55, find the height of the blades in the group if the outlet angle is 18·5° and the effect of tip leakage be neglected.

Draw the velocity diagram for these blades and calculate the heat drop required for the group if the coefficients η_n and ϕ are 0 92 and 0 8 respectively, and there are five pairs of blades in the g oup

6 The following particulars refer to a stage of an impulse-reaction turbine—

Outlet angle of fixed blades	20°
Outlet angle of moving blades	30°
Radial height of fixed blades	4 in
Radial height of moving blades	4 in
Mean blade velocity	450 ft per sec
Ratio of blade speed to steam speed	0 625
Specific volume of steam at fixed blade outlet	20 0
Specific volume of steam at moving blade outlet	21 2

Calculate the degree of reaction the adiabatic heat drop in a pair of blade rings, and the gross stage efficiency given the following coefficients which may be assumed to be the same in both fixed and moving blades $\eta_n = 0\ 90$, $\phi = 0\ 86$

7 Steam flows into the nozzles of a turbine stage from the blades of the preceding stage with a velocity of 320 ft per sec and issues from the nozzles with a velocity of 1 000 ft per sec at an angle of 20° to the wheel plane Calculate the gross stage efficiency given the following data —

Mean blade velocity	600 ft per sec
Expansion efficiency for nozzles and blades	0 9
Carry over factor for nozzles and blades	0 9
Degree of reaction	0 26
Blade outlet angle	28

8 The following particulars refer to one stage of an impulse reaction turbine

Mean diameter	38 in
R p m	3 000
Nozzle outlet angle	20°
Nozzle height	5 in
Blade height	5 in

Specific volume of steam—

(*a*) at nozzle outlet	70 cu ft per lb
(*b*) at blade outlet	77 cu ft per lb
Steam velocity at nozzle outlet	800 ft per sec
Power developed by blades	358 h p

Calculate the heat drop in the stage the degree of reaction the outlet angle of the moving blades and the gross stage efficiency Assume that the expansion efficiency for nozzles and blades is 0 94 and that the carry over coefficient is 0 81 Neglect the effect of nozzle and blade thickness *(Liv Un)*

CHAPTER IX

VORTEX FLOW IN STEAM TURBINES

94. Introduction. The flow of steam in the nozzles and blades of a turbine has been treated as a plane flow problem hitherto in this book. In view of the fact that the actual flow in the oblique part of the nozzles is along a spiral path there must be certain inertia forces which set up a variation of steam pressure in the radial direction.

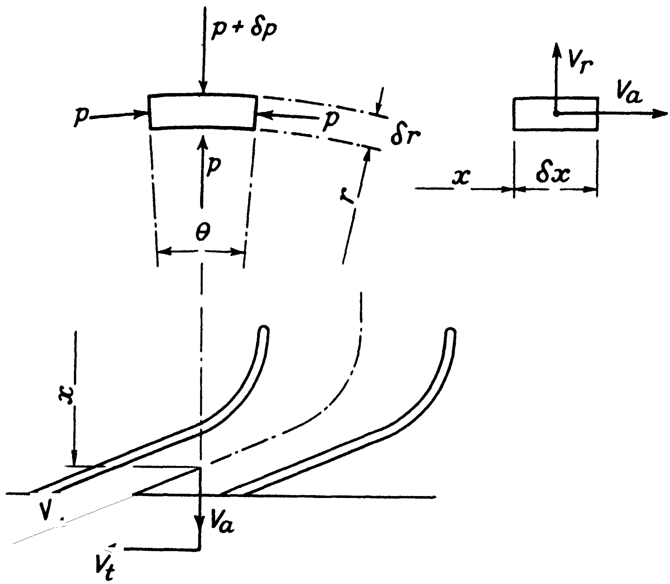


FIG. 134.—Conditions of Equilibrium in Turbine Nozzles

This radial pressure gradient may not be important in stages where the nozzle height ratio (ratio of radial height l of nozzle to mean diameter D) is small, but in those stages where the ratio is high it has a profound effect on the distribution of heat drop in the nozzles and blades, on the blade inlet and outlet angles and, therefore, on the form of the blades.

The problem seems to have been first considered by Stodola (1) in the 3rd Edition of his book as far back as 1910 but was not further pursued by him. The first use of vortex flow, as such, appears to have been made by Dr. A. A. Griffith in a single-stage turbine tested in 1929. Reference to this is made in a paper by H. Constant (2).

The basic ideas of vortex flow are set out in a paper (3) by C. R. Soderberg; sections of the new blading are also given in this paper. Mr. B. Pochobradsky introduced the modified blades into steam turbines constructed by the General Electric Co. in this country in 1935 (4).

The operation of a turbine stage in which account is taken of the effects of inertia is governed by three basic equations, namely the equations of equilibrium, continuity, and energy. These will now be considered.

95. Equation of Equilibrium. Consider an elementary volume of steam at radius r in the oblique part of the nozzle, Fig. 134. Let the tangential, axial, and radial components of velocity be V_t, V_a, and V_r, respectively. Then equating the forces and mass-accelerations in the radial direction only, we obtain the following expression –

$$(p + \delta p)(r + \delta r)\theta \,.\, \delta x + \frac{r \,.\, \delta r \,.\, \delta x \,.\, \theta}{gv} \,.\, \frac{dV_r}{dt} - p \,.\, \delta r \,.\, \delta x \,.\, \theta$$

$$= p \,.\, r \,.\, \delta x \,.\, \theta + \frac{\theta \,.\, \delta r \,.\, \delta x \,.\, V_t^2}{gv}$$

or

$$\frac{dp}{dr} = \frac{V_t^2}{gvr} - \frac{1}{gv} \,.\, \frac{dV_r}{dt} \quad . \quad . \quad . \quad (132)$$

In the following analysis, which is similar to one given in a paper (5) by the author, it will be assumed that all steam particles will move at a constant distance from the turbine axis, i.e. all spiral paths will be described on the surfaces of imaginary cylinders. It follows that $\frac{dV_r}{dt} = 0$, and that

$$\frac{dp}{dr} = \frac{V_t^2}{gvr} \quad . \quad . \quad . \quad . \quad . \quad (133)$$

96. Equation of Continuity. Fig. 135 shows in simplified form a cross-section through a turbine stage. In accordance with the conditions stipulated in the preceding article we consider an annulus of radius r and depth δr, concentric with the axis of the turbine. The conditions before the nozzles, in the clearance space between the nozzles and blades, and at the blade outlet are represented by the suffixes 1, 2, and 3, respectively. V_a is the axial velocity and δA is the effective area in the axial direction. Before the nozzles δA_1 may be taken as $2\pi r \,.\, \delta r$. At the nozzle outlet, $\delta A_2 = (2\pi r - nt \operatorname{cosec} \alpha)\delta r$, where n is the number of nozzle guide blades in the complete ring. A similar expression may be used for δA_3, or, if the thickness of the blade outlet edge is negligible, then $\delta A_3 = 2\pi r \,.\, \delta r$.

Then if δw is the rate of steam flow through any elementary annulus and if we assume uniform velocities,

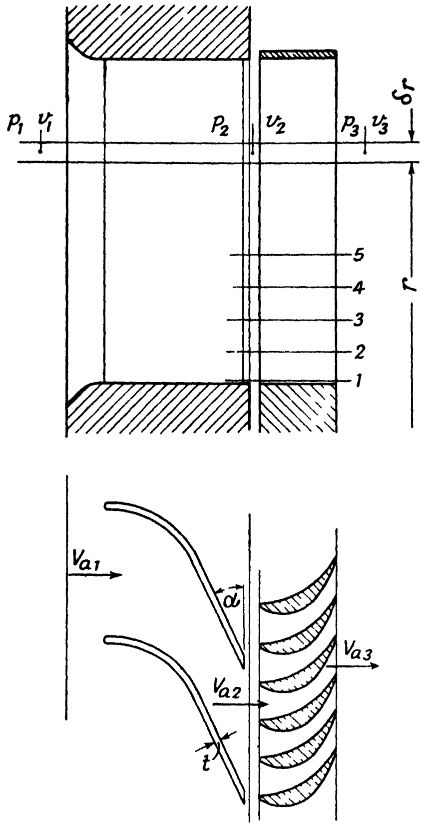


FIG. 135

$$\delta w = \frac{\delta A_1 . V_1}{v_1} = \frac{\delta A_2 . V_2}{v_2} = \frac{\delta A_3 . V_3}{v_3}$$

$$\therefore \qquad V_{a2} = V_{a1} \cdot \frac{\delta A_1}{\delta A_2} \cdot \frac{v_2}{v_1} \qquad . \quad . \quad . \quad . \quad . \quad . \quad (134)$$

and

$$V_{a3} = V_{a1} \cdot \frac{\delta A_1}{\delta A_3} \cdot \frac{v_3}{v_1} \qquad . \quad . \quad . \quad . \quad . \quad (135)$$

Since the pressures p_1 and p_3 are independent of the radius, then if the efficiency of the various elements of steam flow δw are approximately equal it follows that the specific volumes v_1 and v_3 will be

approximately uniform. Furthermore, it follows from the assumed conditions of flow that $\delta A_3 = \delta A_1$. Consequently, if we assume V_{a1} to be uniform then V_{a3} (which is the initial axial velocity into the succeeding stage, if any) will also be uniform.

97. Energy Equation. Application of equation (133) shows that the steam pressure p_2 in the clearance space increases with radius. The conditions of operation at any radius are arbitrary, but once they have been decided then the conditions at any other radii will

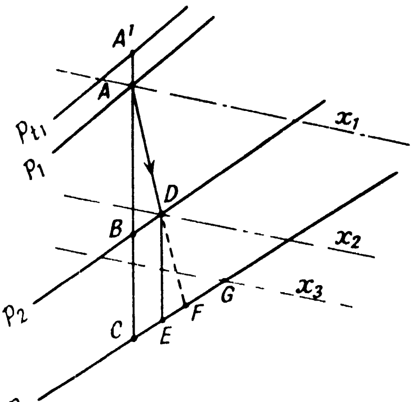


FIG. 136

also be determined, provided the equations of equilibrium, continuity, and energy are satisfied. For example, we may design for pure impulse at the innermost section 1, Fig. 135, where p_2 will be made equal to p_3. It follows therefore that for all other sections p_2 will exceed p_3, that there will be a certain proportion of the heat drop occurring in the moving blades and, therefore, partial reaction. On the other hand there could be partial reaction at the innermost section with greater degrees of reaction at other radii.

The Mollier diagram for such conditions is shown in Fig. 136. For the sake of simplicity we use the first definition of nozzle efficiency given in Art. 51. Then

$$\eta_n = \frac{I_A - I_D}{I_A - I_B}$$

and

$$V_2^2 = V_1^2 + 2gJ\eta_n(I_A - I_B)$$

DE represents the isentropic expansion of steam in the moving blades and DF the imaginary expansion with a certain "efficiency," while FG represents the other losses in the moving blades. The dryness fractions x_1, x_2, and x_3 enable us to calculate the specific volumes v_1, v_2, and v_3.

98. Constant Specific Mass Flow. The present article deals with the case mentioned in Arts. 95 and 96, in which the rate of flow (lb. per sec.) through any imaginary annulus in the nozzles and blades is constant.

The blade length is first divided into a convenient number of (say) equal parts, the conditions at each section being calculated by a trial and error method. It is preferable to begin the calculations at section 1, Fig. 135, where one of two alternatives may be adopted, namely, (1) pure impulse, or (2) partial reaction. Bearing in mind the possibility of negative reaction at part load in those stages near the exhaust end of the turbine, it is probably better to use a certain degree of reaction at the innermost section. The choice calls for judgment and experience because if too high a reaction is chosen for the innermost section of the blades then a very high degree with increased leakage losses will be experienced at the blade tips. Consideration must also be given to the steam thrust on the wheel if holes are not bored through the disc or to the steam leakage if they are. In double-flow turbines the axial thrusts due to steam pressure on the discs would balance.

The best conditions at section 1 are governed to some extent by the peripheral velocity at that section. In turbines of large output the blade speed at the root of the blade is sometimes so high that, if pure impulse conditions are assumed at the root section, and if the steam velocity V_2 is limited to the local acoustic velocity or less, then an unfavourable ratio of blade speed to steam speed may result. In such a case a moderate degree of reaction would be an advantage.

If the stage is to be designed for a given mass flow, given values of p_1 and p_3, and if the inner and outer diameters of the nozzles are fixed then the initial axial velocity V_{a1} can be calculated. Whether pure impulse or partial reaction be assumed for section 1, the pressure p_2 and volume v_2 can be found. An assumption is next made regarding the nozzle angle α and the number and thickness of the nozzle guide vanes. The area δA_2 is then calculated and hence the velocity V_{a2} from eq. (134). The nozzle angle α is then calculated from the expression $\alpha = \sin^{-1}\dfrac{V_{a2}}{V_2}$. If this does not agree with the assumed value, a recalculation is made using the latter value as a second approximation.

When the correct value of α has been found, the velocity $V_{t2} = V_2 \cdot \cos\alpha$ is calculated and used in eq. (133) to give the value $\dfrac{dp}{dr}$ at section 1. Then $(r_2 - r_1) \cdot \dfrac{dp}{dr}$ will give the rise in the pressure p_2 between r_1 and r_2, and hence the pressure p_2 at r_2 to a first approximation. This value of p_2 is then used to find V_2, the angle α, V_{a2} and V_{t2} for section 2. Using V_{t2} and v_2 the approximate value of $\dfrac{dp}{dr}$ at section 2 is obtained.

The mean of the values of $\frac{dp}{dr}$ for sections 1 and 2 will now give a more accurate value to the pressure p_2 at section 2, thus giving, finally, the values of v_2, V_2, and α. The calculations may be repeated until the difference between the results obtained is as small as desired. Once the values have been obtained for sections 1 and 2, those at section 3 may be obtained fairly rapidly by judicious extrapolation.

Referring to Fig. 136, the adiabatic heat drop in the nozzles is

$$h_n = I_A - I_B = \frac{V_2^2 - V_1^2}{2g \, . \, J \, . \, \eta_n}$$

The adiabatic heat drop in the blades is

$$h_b = I_D - I_E = I_B - I_C \text{ (very nearly)}$$

$$\therefore \qquad h_b = I_A - I_C - \frac{V_2^2 - V_1^2}{2gJ\eta_n}$$

The degree of reaction $R = 1 - \frac{V_2^2 - V_1^2}{2gJ\eta_n(I_A - I_C)}$

The performance of the blading at each section may next be analysed, Fig. 137. From the velocity V_2, the known velocity u,

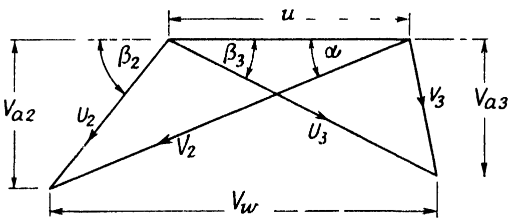


FIG. 137

and α, the relative velocity U_2 and the flow angle β_2 at inlet are found. Then using eq. (120), Art. 89, we find

$$U_3^2 = \phi \, . \, U_2^2 + 2gJ \, . \, \eta_n \, . \, h_b$$

from which U_3 is found. This combined with V_{a3} enables us to complete the velocity diagram and so calculate the blade outlet angle, work done per lb. of steam and the efficiency at the given radius.

99. Simplified Analysis for Uniform Nozzle Outlet Angle. By a suitable choice of steam velocity at section 1, the nozzle outlet angle which is calculated by the foregoing method may be made nearly constant. The following analysis yields a result which may

then be applied in a simple manner to give an approximate relationship between r and V_t.

It is again assumed that flow takes place at a constant distance from the turbine axis. Then for equilibrium,

$$v \cdot \frac{dp}{dr} = \frac{V_t^2}{gr}$$

For a small change of state,

$$J \cdot dI = J \cdot dH + v \cdot dp$$

If the flow through the nozzle is adiathermal and takes place with an efficiency η, then

$$J \cdot dH = -(1 - \eta)v \cdot dp$$

and

$$J \cdot dI = \eta \cdot v \cdot dp$$

Again, since the flow is adiathermal or adiabatic,

$$\frac{V^2}{2g} + J \cdot I = \text{constant}$$

$$\therefore \quad \frac{V_t^2}{2g} + \frac{V_a^2}{2g} + J \cdot I = \text{constant}$$

$$\frac{V_t}{g} \cdot \frac{dV_t}{dr} + \frac{V_a}{g} \cdot \frac{dV_a}{dr} + J \cdot \frac{dI}{dr} = 0$$

Now $\quad V_a = V_t \cdot \tan\alpha$, and $J\dfrac{dI}{dr} = \eta \cdot v \cdot \dfrac{dp}{dr} = \dfrac{\eta V_t^2}{gr}$

$$\therefore \quad \frac{dV_t}{V_t} + \left(\frac{\eta}{1 + \tan^2\alpha}\right)\frac{dr}{r} = 0$$

Integrating this, we have—

$$\log V_t + \eta \cdot \cos^2\alpha \cdot \log r = \log C \quad . \quad . \quad (136)$$

or

$$V_t \cdot r^{\eta \cos^2\alpha} = \text{constant} \quad . \quad . \quad . \quad (137)$$

Equation (137) may be used to find the approximate degree of reaction at any section of the blade. Since $V_t = V\cos\alpha$ and α is constant, it follows that

$$V \cdot r^{\eta \cos^2\alpha} = \text{constant}$$

Let h = stage isentropic heat drop.

h_n = nozzle isentropic heat drop at radius r.

h_{n1} = nozzle isentropic heat drop at radius r_1.

R = degree of reaction at radius r.

R_1 = degree of reaction at radius r_1.

Then assuming that η is constant and neglecting the kinetic energy of the steam entering the nozzles from the previous stage,

$$\frac{h_n}{h_{n1}} = \left(\frac{V}{V_1}\right)^2 = \left(\frac{r_1}{r}\right)^{2\eta \cdot \cos^2 \alpha}$$

$$R = 1 - \frac{h_n}{h}; \; R_1 = 1 - \frac{h_{n1}}{h}$$

$$\therefore \qquad \frac{h_n}{h} = 1 - R \text{ and } \frac{h_{n1}}{h} = 1 - R_1$$

$$\therefore \qquad R = 1 - (1 - R_1)\left(\frac{r_1}{r}\right)^{2\eta \cos^2 \alpha} \quad . \quad . \quad (138)$$

The application of this method will now be illustrated by an example

EXAMPLE 19. The following particulars refer to a low-pressure stage of a turbine—

Initial pressure	1·2 lb. per sq. in. abs.
Initial dryness fraction .	0·88.
Initial enthalpy . .	985·1 B.Th.U. per lb.
Initial entropy . .	1·7445
Pressure at stage outlet . . .	0·6 lb. per sq. in abs.
Nozzle efficiency . . .	0·94
Assumed stage efficiency . . .	0·80.
Inner radius of wheel	26 in.
Outer radius of wheel	40 in
Total steam flow	21·6 lb per sec.
Number of nozzle guide blades	56.
Thickness of nozzle guide blades .	0·176 in.
Speed	3,000 r.p.m.
Degree of reaction at inner radius	0·20.

Calculate for the inner radius and for sections with a radial increment of 2 in. the following—

(*a*) nozzle angle,
(*b*) steam pressure,
(*c*) steam velocity,
(*d*) degree of reaction.

Draw the velocity diagrams for each section of the blades assuming that $\phi = 0{\cdot}81$ and that $\eta = 0{\cdot}94$, and calculate the stage efficiency of each section.

It is first necessary to derive the relationship between steam pressure p in the range 0·6 to 1·2, steam velocity V_2, and the actual specific volume v_2 at the nozzle outlet, allowing for the initial steam velocity V_1.

Since $v_1 = 247{\cdot}4$ and the annulus area is 20·16 sq. ft.,

$$V_1 = \frac{wv_1}{A_1} = \frac{21{\cdot}6 \times 247{\cdot}4}{20{\cdot}16} = 265 \text{ ft. per sec.}$$

Hence $V_2{}^2 = V_1{}^2 + 0{\cdot}94\,(2g \,.\, J \,.\, ha)$.

The conditions at the nozzle outlet are given in Table XI for selected pressures. The values given in Table XI should be plotted

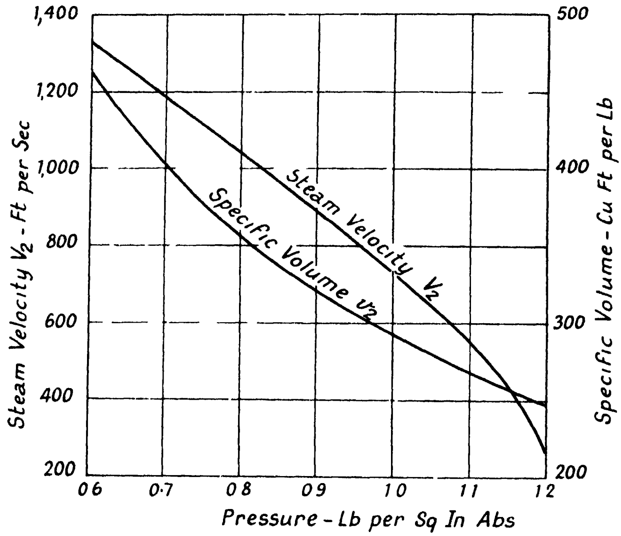


FIG. 138

to a large scale, Fig. 138, so that the values of V_2 and v_2 for any pressure p_2 may be quickly obtained.

The calculations are made by the trial and error method outlined in Art. 98, the results being set out in Tables XII and XIII. The

TABLE XI

CONDITIONS AT NOZZLE OUTLET IN EXAMPLE 19

p	h_a	V_2	v_2	p	h_a	V_2	v_2
1·2	0	265	247·4	0·80	21·5	1,041	357·0
1·1	4·9	550	267·7	0·75	24·8	1,112	378·3
1·0	9·8	730	292·0	0·70	28·3	1,183	402·6
0·95	12·6	815	305·8	0·65	32·1	1,259	431·0
0·90	15·5	895	320·9	0·60	36 3	1,335	464·0
0·85	18·5	971	337·9				

corresponding velocity diagrams are shown in Fig. 139. For the particular data chosen for this example the final absolute velocity is nearly axial and uniform at 500 ft. per sec.

Suitable blade profiles for 26 in., 33 in., and 40 in. radius are sketched in Fig. 140.

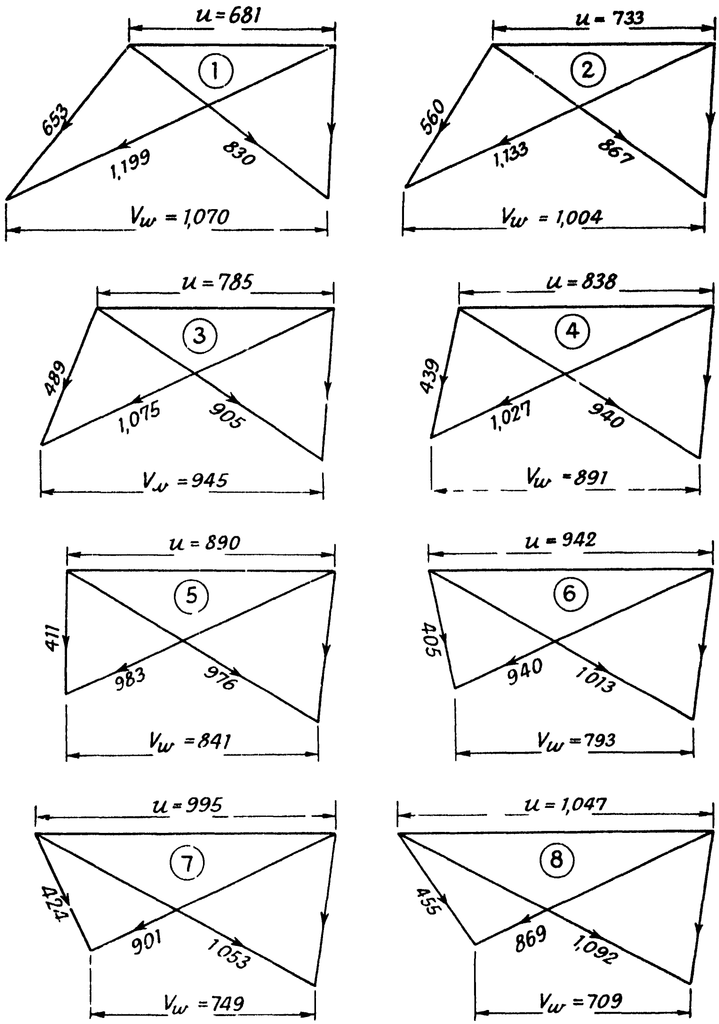


FIG. 139 – Velocity Diagrams for Various Sections of Long Blade (Example 19)

The numbers in the circles refer to the sections, see Fig. 142

TABLE XII

PRESSURES, NOZZLE ANGLES, STEAM VELOCITIES AND HEAT DROPS FOR EXAMPLE 19

Section No	r in.	Press p_2	Calculated Nozzle Outlet Angle	Steam Velocities			Isentropic Heat Drops		Degree of Reaction per cent
				V	V_a	V_t	h_n	h_b	
1	26	0 691	25° 9′	1,199	510	1,088	29·00	7·3	20·0
2	28	0·736	24° 50′	1,133	476	1,029	25·74	10·56	29·1
3	30	0·776	24° 46′	1,075	450	976	23·02	13·28	36·6
4	32	0·811	24° 39′	1,027	428	933	20·84	15·46	42·5
5	34	0·843	24° 42′	983	410	893	19·00	17·30	47·6
6	36	0·871	24° 50′	940	395	853	17·30	19 00	52·4
7	38	0 896	25° 9′	901	384	816	15·75	20·55	56·6
8	40	0·918	25° 19′	869	371	785	14·50	21·80	60·0

TABLE XIII

CALCULATED FLOW ANGLES AND STAGE EFFICIENCY FOR EXAMPLE 19

Section No.	Inlet Angle β_2	Outlet Angle β_3	Turning or Camber Angle θ	Blade Velocity u	$\rho = \frac{u}{V}$	Velocity of Whirl	Work Done B Th U. per lb.	Efficiency per cent
1	51° 24′	37° 1′	91° 35′	681	0·569	1,070	29·15	80·2
2	58 9′	35 14′	86° 37′	733	0 646	1,004	29·40	81·1
3	67° 1′	33° 32′	79° 27′	785	0·730	945	29·62	81·7
4	77° 30′	32° 4′	70° 26′	838	0·816	891	29·82	82·1
5	89° 36′	30 48′	59° 36′	890	0·905	841	29·95	82·4
6	102° 42′	29° 32′	47° 46′	942	1·002	793	29·87	82·3
7	115° 0′	28° 19′	36° 41′	995	1·105	749	29·80	82·1
8	125° 12′	27° 15′	27° 33′	1,047	1·205	709	29·62	81·7

For practical reasons a uniform nozzle angle would be used but this would not affect appreciably the results which have been worked out for the variable nozzle angle. The variation in nozzle angle required to satisfy simultaneously the equations of equilibrium, continuity, and energy can be controlled to some extent by the choice of steam velocity at the innermost section of the blades.

It is easily seen from the equation of continuity that the required nozzle angle α is such that

$$\sin \alpha = \frac{nt}{2\pi r} + \frac{V_{a1}}{V_2} \cdot \frac{v_2}{v_1} \qquad . \quad . \quad (139)$$

At the inner radius, $r = 26$ in.; $n = 56$; $t = 0{\cdot}176$ in.; $V_{a1} = 265$; $v_1 = 247{\cdot}4$. For selected velocities V_2, the steam pressure

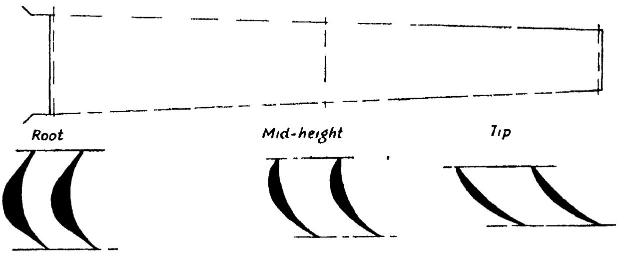


FIG. 140 Sketches of Blade Sections for Example 19

p_2 and the specific volume v_2 may be found from Fig. 138. The calculated nozzle angles are shown in Fig. 141 as a function of the steam velocity. If a steam velocity of 1,000 ft. per sec. were chosen at $r = 26$ in., then since the velocities at greater radii must diminish due to increasing pressure, the required nozzle angle must increase with radius. For the present example, the choice of 1,200 ft. per sec. at section 1 results in a slight reduction of nozzle angle with increase of radius followed by a slight increase. For a first approximation to the steam velocity at any radius, eq. (137) may be used. For instance, in the present example—

Let $\qquad V_{t1} = V_t$ at 26 in. radius,

$\qquad\qquad V_{t2} = V_t$ at 40 in. radius.

Then $\qquad \dfrac{V_{t1}}{V_{t2}} = \left(\dfrac{40}{26}\right)^{n \cdot \cos^2 \alpha}$

Assume $\alpha = 25° \; 9'$; then $\dfrac{V_{t1}}{V_{t2}} = (1{\cdot}54)^{0{\cdot}77} = 1{\cdot}395$ and since $V_{t1} = 1{,}088$, $V_{t2} = 780$.

For a first approximation, let α at 40 in. radius be 25° 9′. Then $V_2 = 860$. From Fig. 141 the corresponding angle is 25° 24′, whose cosine is 0·9033. Hence $V_2 = 864$, compared with the previously

calculated value of 868·5 ft. per sec. This close agreement shows that Fig. 141 and eq. (137) may be used together as a substitute for the trial and error method given in Art. 98.

It may be pointed out that for the above example the index n in $P \cdot v^n =$ constant is 1·1 and the sonic velocity for the pressures in the clearance space is about 1,200 ft. per sec. If the steam velocity

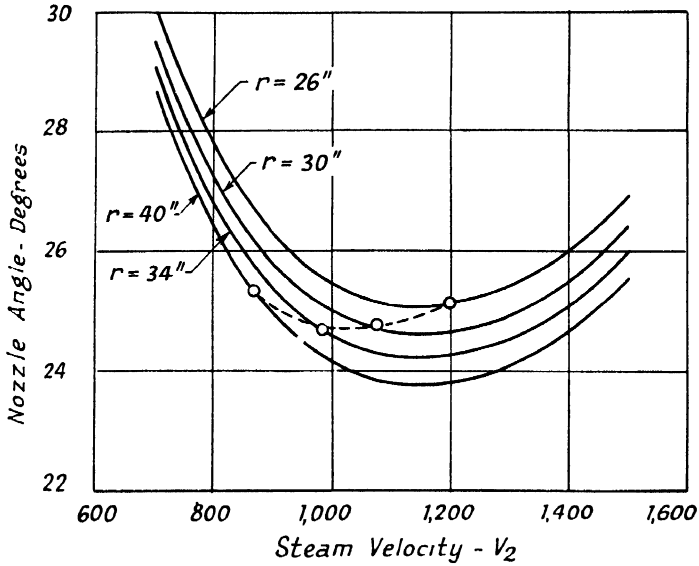


FIG. 141.—Nozzle Angle as a Function of Steam Velocity

at outlet from the nozzles exceeds this value some jet deflection will occur.

100. Vortex Flow with Constant Axial Velocity at Outlet from the Nozzles. Reference to Table XII for the preceding example shows that the axial velocity at outlet from the nozzle diminishes as the radius increases. This is to be expected since the mass flow through each elemental annulus is constant and increase of radius results in an increase of pressure and a reduction of specific volume. An alternative design may be worked out to produce a constant axial velocity at the nozzle outlet.

We have first the equation of equilibrium—

$$v \cdot \frac{dp}{dr} = \frac{V_t^2}{gr}$$

and the energy equation—

$$\frac{V_t}{g} \cdot \frac{dV_t}{dr} + \frac{V_a}{g} \cdot \frac{dV_a}{dr} + J \cdot \frac{dI}{dr} = 0$$

Since V_a is uniform and $J \, . \, dI = \eta \, . \, v \, . \, dp$

$$\frac{V_t}{g} \, . \, \frac{dV_t}{dr} + \eta \, . \, v \, . \, \frac{dp}{dr} = 0$$

$$\frac{dV_t}{V_t} + \eta \, . \, \frac{dr}{r} = 0$$

and $$V_t \, . \, r^{\eta} = \text{constant} \qquad (140)$$

If the nozzle efficiency is unity, then $V_t \, . \, r =$ constant. This is the equation of a free vortex. The application of eq. (140) to the turbine stage in Example 19 will now be given.

EXAMPLE 20. For the details given in Example 19, calculate for the inner radius and for sections with a radial increment of 2 in., the following—

(*a*) Tangential component of velocity.
(*b*) Nozzle angle.
(*c*) Steam velocity.
(*d*) Degree of reaction.
(*e*) Steam pressure.
(*f*) Efficiency.

It is first necessary to find the axial component of the velocity at outlet from the nozzles which, with the unknown variation of specific volume, will give the same total mass flow at inlet to and outlet from the nozzles, in this case 21·6 lb. per sec. This may be done by making a trial calculation similar to that which follows. This will yield the total mass flow w^1 for the assumed axial velocity $V_a{}^1$. Then, for this example, the correct axial velocity would be given very nearly by

$$V_a = \frac{21{\cdot}6}{w^1} \times V_a{}^1$$

From such a trial calculation it is found that V_a 420 ft. per sec.

The figures obtained from this assumed value of V_a are given in Tables XIV, XV, and XVI. Values of V_t are first found from eq. (140). These, combined with V_a, give the nozzle angle and the steam velocity V_2. From these the nozzle and blade heat drops h_n and h_b may be calculated, thus giving the degree of reaction. The value of

$$\frac{dp}{dr} = \frac{V_t{}^2}{gvr}$$

must be found by trial and error. This work may be done fairly simply by inferring the value of v_2 from the steam velocity V_2; in fact p_2 may be found in a similar manner.

TABLE XIV

CALCULATIONS FOR VORTEX FLOW $V_t \; r^{0 \cdot 94}$ = CONSTANT, $V_a = 420$ FT. PER SEC.

Section	Radius ft.	$r^{0\cdot94}$	V_t	$\frac{dp}{dr}$	Mean $\frac{dp}{dr}$	dp	p_2	V_2	Tan $\alpha = \frac{V_a}{V_t}$	α	Adiabatic Heat Drops h_n	Adiabatic Heat Drops h_b	Degree of Reaction per cent
1	2·167	2·068	1,123	44·5			0·691	1,199	0·3739	20° 30′	29·00	7·30	20·0
					41·25	0·0478							
2	2·333	2·218	1,047	38·0			0·7388	1,128	0·4007	21° 50′	25·40	10·90	30·0
					35·40	0·0410							
3	2·500	2·366	982	32·8			0·7798	1,069	0·4275	23° 9′	22·75	13·55	37·3
					30·55	0·0354							
4	2·667	2·514	924	28·3			0·8152	1,013	0·4553	24° 29′	20·32	15·98	44·0
					26·45	0·0306							
5	2·833	2·662	872	24·6			0·8458	969	0·4810	25° 41′	18·45	17·85	49·1
					23·05	0·0267							
6	3·000	2·808	827	21·5			0·8725	929	0·5070	26° 53′	16·80	19·50	53·7
					20·20	0·0234							
7	3·167	2·951	787	18·9			0·8959	893	0·5332	28° 4′	15·38	20·92	57·6
					17·75	0·0205							
8	3·333	3·100	749	16·6			0·9164	859	0·5604	29° 16′	14·20	22·10	60·9

TABLE XV

Calculation of Mass Flow

Section	p_2	t_2	α	cosec α	9·86 cosec α	Full Circumf.	Net Circumf.	Net Annular Area sq. ft.	δw	$\Sigma \delta w$
1	0 691	407·5	20° 30′	2·8555	28·15	163·36	135·21			0
		394·6					142·31	1·975	2·100	
2	0·7388	383·6	21 50′	2 6887	26·51	175·93	149·42			2·100
		374·1					156·42	2·174	2·440	
3	0·7798	365·0	23° 9′	2 5438	25 08	188 50	163·42			4·540
		357·8					170·35	2 365	2·780	
4	0·8152	351·1	24° 29′	2·4129	23·79	201·06	177·27			7·320
		345·1					184·07	2·558	3·116	
5	0·8458	339·6	25° 41′	2·3074	22·75	213·63	190·88			10·436
		334·1					197·63	2·742	3·446	
6	0·8725	330·0	26 53′	2 2116	21·81	226·19	204·38			13·882
		325·8					211·10	2·930	3·775	
7	0·8959	322·1	28° 4′	2·1253	20·95	238·76	217·81			17·657
		318·8					224·49	3·120	4·110	
8	0·9164	315·6	29° 16′	2·0455	20·17	251 33	231·16			21·767

TABLE XVI

CALCULATED FLOW ANGLES AND STAGE EFFICIENCY FOR EXAMPLE 20

Section No	Inlet Angle β_2	Outlet Angle β_3	Turning or Camber Angle θ	Blade Velocity u	$\rho = \frac{u}{V_2}$	Velocity of Whirl	Work Done B Th U per lb	Efficiency per cent
1	43 30	38 32	97 58	681	0 569	1,070	29 15	80 2
2	53 12	35 38	91 10	733	0 650	1 128	29 60	81 5
3	65° 58	33 37	80 25	785	0 734	948	29 75	82 0
4	78 25	31 45	69 50	838	0 825	894	29 85	82 2
5	92 24	30 16	57° 20	890	0 918	839	29 80	82 0
6	105 19	28 49	45 52	942	1 015	794	29 80	82 0
7	116 19	27 34	36 7	995	1 116	750	29 76	82 0
8	125 21	26 31′	28 8	1 047	1 217	704	29 42	81 0

Table XV gives details of the check calculation of mass flow. The total mass flow 21·767 lb. per sec. is within 0·77 per cent of the correct value. Finally, particulars of the flow angles and efficiency are given in Table XVI.

A comparison of Tables XIII and XVI shows that except for the inner sections there is no appreciable difference between blade angles, blade speed ratio, whirl velocity and efficiency for specific

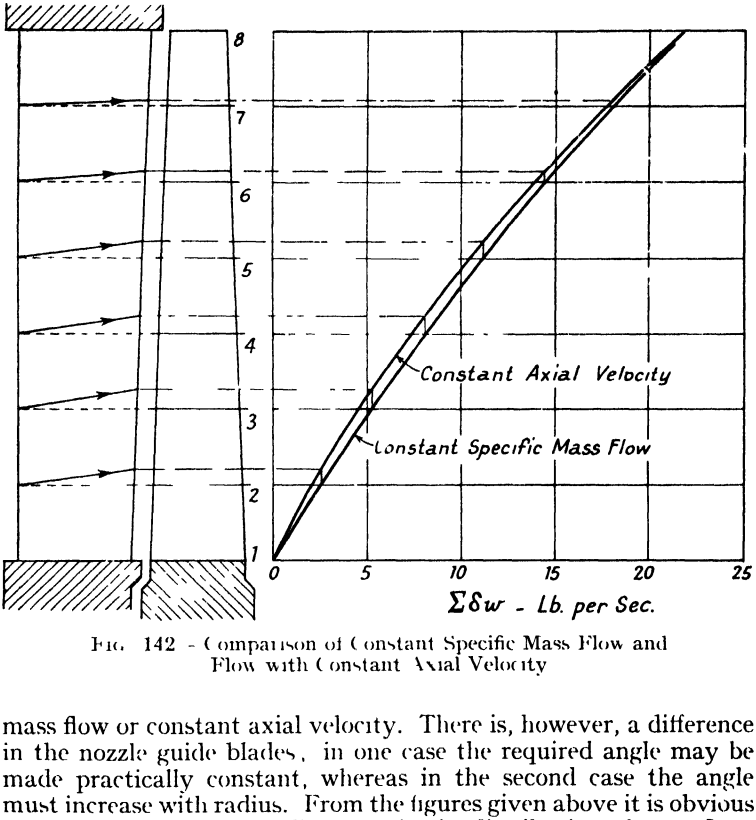


FIG. 142 - Comparison of Constant Specific Mass Flow and Flow with Constant Axial Velocity

mass flow or constant axial velocity. There is, however, a difference in the nozzle guide blades, in one case the required angle may be made practically constant, whereas in the second case the angle must increase with radius. From the figures given above it is obvious that there must be some difference in the distribution of mass flow. Fig. 142 shows the integrated mass flow $\Sigma\delta w$ plotted against radius. Since the constant specific mass flow case is worked out on the assumption of flow along cylindrical surfaces, it follows that with constant axial velocity the flow in the nozzles must be as shown by the full lines. It appears, therefore, that with constant axial velocity there must be some radial component of velocity and the original equation of equilibrium may not be satisfied.

When there is a relatively rapid change in nozzle height as in the final stages of turbines of large output, it is probable that, due to radial acceleration, the value of dp/dr in the space between the nozzles and blades will not be as great as when the flow takes place at a constant distance from the axis. This will result in a reduced rate of twist of the blades.

101. General Notes on Vortex Flow. In the past many steam turbines have been built with long blades of uniform cross-section. From some points of view it may be said that their operation has been satisfactory. The foregoing worked examples have shown, however, that when an attempt is made to establish flow through the nozzles and blades either with small radial velocity components or no radial velocity components at all, the blade angles are modified in a very considerable manner. It would appear therefore that when long blades of uniform cross-section are employed the performance of the blade is likely to be poor for two reasons—

(*a*) The blade speed increases with radius and, in consequence, the blade inlet angle should be increased so that steam may flow into the blade channel with the minimum of shock loss.

(*b*) Inertia forces will cause a rise in pressure in the clearance space which will tend to produce an increase in the degree of reaction with increase of radius. If the blade outlet angle is not reduced to satisfy the area requirements involved then there will be "negative" reaction with very considerable losses.

In a recent paper (6) on the subject by W. H. Wiebe the conditions necessary for optimum efficiency are analysed and lead to the following expression—

$$F^2 + 2F \cdot \frac{k^2}{1 - k^2} \cdot \frac{u}{V_1} \cdot \cos\alpha$$

$$= \frac{\cos^2\alpha}{\cos^2\alpha + (1 - k^2)}\left[k^2\left(\frac{u}{V_1}\right)^2 + \frac{1}{1 - k^2}\left\{1 + \nu - \left(\frac{V_{a2}}{V_1}\right)^2\right\}\right]$$

where F = reaction function = $\sqrt{1 + \nu - R}$,

k = blade velocity coefficient,

ν = carry-over fraction.

The author states that it is impracticable to solve this equation explicitly for F or to introduce the reaction R. This may be more easily accomplished in any numerical example under investigation. In actual cases the various magnitudes are set up in a table for different blade sections, for which the reaction is then calculated. This is to be used subsequently for the determination of steam velocities and blade angles, either by numerical calculations or velocity diagrams.

Applications of this relation in the paper cited show that for the best efficiencies the degree of reaction should be appreciable at the

root of the blade and then increase still more towards the tip. Whether the resultant blade would be strong enough to resist inertia and bending forces is another matter.

BIBLIOGRAPHY

1. STODOLA: *Dampf und Gas-Turbinen*, 1910, p 519.
2. CONSTANT: "The Early History of the Axial Type of Gas Turbine Engine." *Proc. I. Mech. E.*, 1945; 153; 411.
3. SODERBERG: "Recent Developments in Steam Turbines." *Mechanical Engineering* (A.S.M.E.) 1935; 57; 165.
4. POCHOBRADSKY: "Effect of Centrifugal Force in Axial-flow Turbines." *Engineering*, 1947; 163; 205.
5. KEARTON: "Effects of Inertia on Flow of Steam through Nozzles and Blading of Axial-flow Turbines." *Proc. I. Mech. E.*, 1952; 166; 429.
6. WIEBE: "Design of Warped Buckets for Optimum Efficiency." A.S.M.E. Spring Meeting, April, 1957.

CHAPTER X

EXPERIMENTS ON TURBINE BLADES

102. Early Experiments. The early experiments on turbine blades were made chiefly with the object of finding the value of the velocity coefficient k in impulse blades from which the energy changes in the blade can be calculated.

A. Rateau (1) carried out a number of experiments on stationary blades of the type shown in Fig. 108 (a). The inlet angle was 31° and the outlet angle 25°, the pitch being one-half of the width of the blades in all cases. The general results of Rateau's experiments indicate that k decreases with wider blades, the value varying from 0·65 with blades 1 in. wide to 0·83 with blades ½ in. wide. The effect of varying the relative velocity was small but the experiments showed that k increased as the steam velocity was increased. Rateau's experiments are open to criticism. The number of blades tested was small and those blades situated near the ends of the nozzle packet might have been only partially filled with steam.

N. Briling (2) carried out extensive experiments on blades of the type shown in Fig. 108 (*b*). Briling found that the blade loss is greater with narrow blades than with wide blades. He made tests on the effect of varying the blade pitch and found that the optimum pitch was given by the expression

$$p = \frac{R}{2 \sin \beta_1} \quad . \quad . \quad . \quad . \quad (141)$$

where R is the radius of the concave side of the blade. With equi-angular blades it follows that since

$$R = \frac{b}{2 \cos \beta_1}, \text{ then } p = \frac{b}{2 \sin 2\beta_1} \quad . \quad . \quad (142)$$

Although this result appears to be in agreement with later work on turbine blades, Briling's experimental methods are open to serious criticism and no further results will be quoted.

A pendulum reaction tester was adopted by P. Christlein (3). The blades under test were attached to the pendulum, steam flowing into the blades from a set of three fixed nozzles. For steam velocities ranging from 600 to 1,400 ft. per sec.,

$$k = 0{\cdot}676 + \frac{U_1}{10{,}500}$$

Little importance may be attached to these experiments because the blade pitch was less than half its optimum value and the radial height of the blades was considerably more than that of the nozzles, so that appreciable losses would be incurred due to ejector action.

103. Faltin's Experiments. All the experiments hitherto described have been made on stationary blades. A little consideration will show that the conditions when the moving blades are passing in front of stationary nozzles in an actual steam turbine are appreciably different from those which obtain in a static blade tester. Where several nozzles are used in a turbine, the impulse of the steam will vary as the blades pass in front of different sections of the nozzle and the wake of the nozzle guide blades. Furthermore, except when the nozzles extend around the complete circumference, the moving blades entering the active flow zone are successively filled with

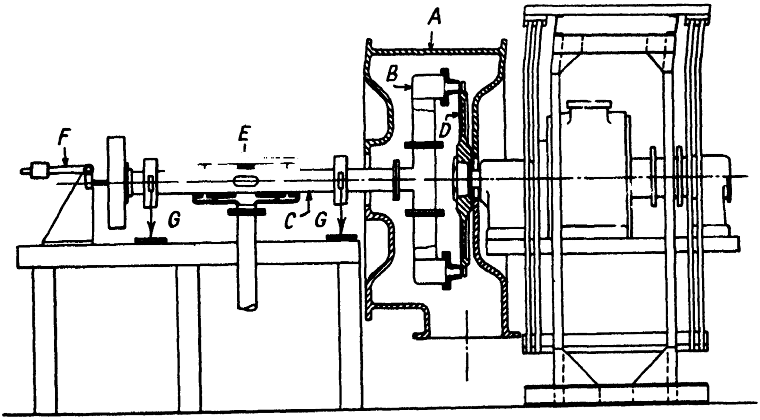


FIG. 143

steam and successively emptied as they leave the zone. In addition, centrifugal effects must play a greater or lesser part in modifying the performance of the blades.

H. Faltin (4) carried out experiments on a single-stage experimental turbine in the Technical High School, Breslau. The turbine is shown diagrammatically in Fig. 143. It comprises a housing A, a rotatably mounted steam chest B, a steam supply pipe C and a single-row wheel D. The pipe C passes through a chamber E having a gland at each end. Steam is supplied to this chamber, passes through ports in the steam pipe and so to the two radiating pipes B forming the steam chest. The opposite end of the pipe is closed. At the end of each radiating pipe there are three nozzles, Fig. 144, with cast-in vanes.

The blades on the impulse wheel had a mean diameter of 50 in. and a height of 2·756 in. As may be seen the blades are profile blades and the ratio of blade height to nozzle height, namely 1·27, is much more in keeping with practice than in the experiments of Briling and Christlein. Steam which passed through the nozzles

was condensed and weighed. The back thrust measured at F, and the reaction torque measured by the weighbridges G, combined with the steam flow gave the axial and tangential components of steam flow from the nozzles, and therefore the direction of flow and the resultant velocity. A correction was made for steam whirl in the casing. From the steam velocity V_1, the flow direction α and the blade speed u, the relative velocity U_1 could be found.

The driven dynamo was a 125 kW. machine and the whole machine was mounted on a suspended frame which served as a dynamometer.

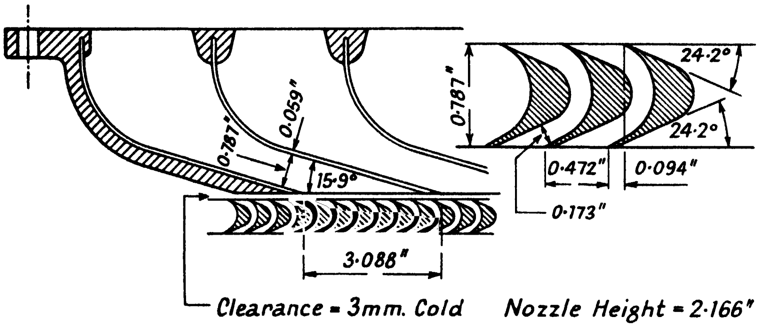


FIG. 144. – Nozzles and Blades in Faltin's Experimental Turbine

The power developed by the blades was obtained by measuring the net power developed and adding the loss due to disc friction and windage obtained from separate tests. From the blade horse-power and steam flow, the velocity of whirl V_w was calculated. Assuming flow from the blades at the correct angle β_2, the velocity U_2 could be calculated since

$$V_w = V_1 \cos \alpha - u + U_2 \cos \beta_2$$

The chief tests were made with a steam flow of 10,000 lb. per hour at 1·5 atm. abs. and about 195° F. initial superheat. Rotor speeds varied from 1,000 to 3,000 r.p.m. and u from 218 to 654 ft. per sec.

Faltin found that the pressure in the clearance space between the nozzles and blades was appreciably affected by the speed of rotation and by the heat drop. In spite of the fact that there was partial admission, it was possible to operate the turbine as a pure impulse turbine, as a turbine with partial reaction (positive) or as a turbine with negative reaction. The reasons for this are given in Art. 93.

The meaning of the velocity coefficient k as interpreted by Faltin for conditions with positive or negative reaction may be explained as follows.

Let h_b = isentropic heat drop in blades, B.Th.U. per lb.

L_b = loss in blades, B.Th.U. per lb.

Then
$$\frac{U_1^2}{2gJ} \pm h_b = \frac{U_2^2}{2gJ} + L_b$$

With frictionless flow the outlet velocity would be U_2^1, such that

$$\frac{U_1^2}{2gJ} \pm h_b = \frac{(U_2^1)^2}{2gJ}$$

Therefore the loss L_b may be expressed as

$$L_b = \{(U_2^1)^2 - U_2^2\} \div 2gJ$$

and k is then taken as the ratio U_2/U_2^1.

In cases where there is partial reaction, the value of k found by this method has not quite the same meaning as that given in Art.

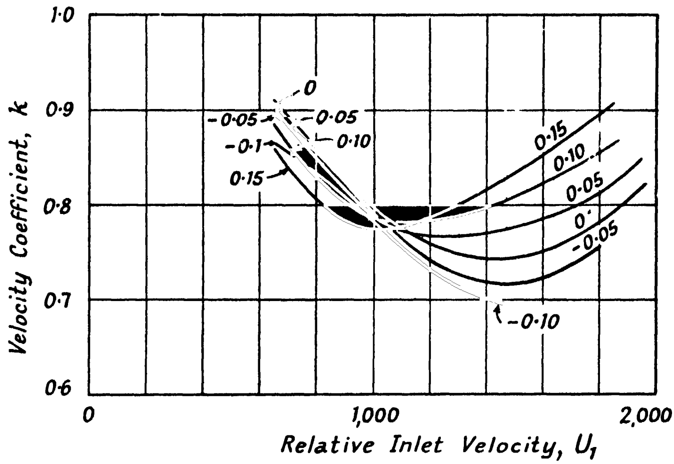


FIG. 145. - Values of k According to Faltin, for Varying Values of the Relative Inlet Velocity U_1 and for Constant Degrees of Reaction

78. Suppose we let ϕ represent the carry-over coefficient, i.e. $\phi = k^2$ for the pure impulse turbine. Then—

(*a*) For positive reaction,

$$U_2^2 = \phi U_1^2 + 2gJ \cdot \eta_n \cdot h_b$$

where η_n is the efficiency of the blades as nozzles. For ideal conditions, $\eta_n = 1$; $\phi = 1$; and $U_2 = U_2^1$.

$$(U_2^1)^2 = U_1^2 + 2gJh_b$$

and
$$k^2 = \frac{\phi U_1^2 + 2gJ\eta_n h_b}{U_1^2 + 2gJh_b}$$

In this case, k is greater than $\sqrt{\phi}$.

(*b*) For negative reaction,

$$U_2^2 = \phi U_1^2 - \frac{2g \cdot J \cdot h_b}{\eta_d}$$

where h_b is the isentropic enthalpy increase during compression and η_d is the efficiency of the blade as a diffuser. For ideal conditions, $\eta_d = 1$; $\phi = 1$; and $U_2 = U_2^1$.

$$(U_2^1)^2 = U_1^2 - 2g \cdot J \cdot h_b$$

and

$$k^2 = \frac{\phi U_1^2 - \dfrac{2g \cdot J \cdot h_b}{\eta_d}}{U_1^2 - 2g \cdot J \cdot h_b}$$

In this case, k is less than $\sqrt{\phi}$.

The values of k found by Faltin for varying degrees of reaction are given in Fig. 145. The value of k appears to reach its minimum

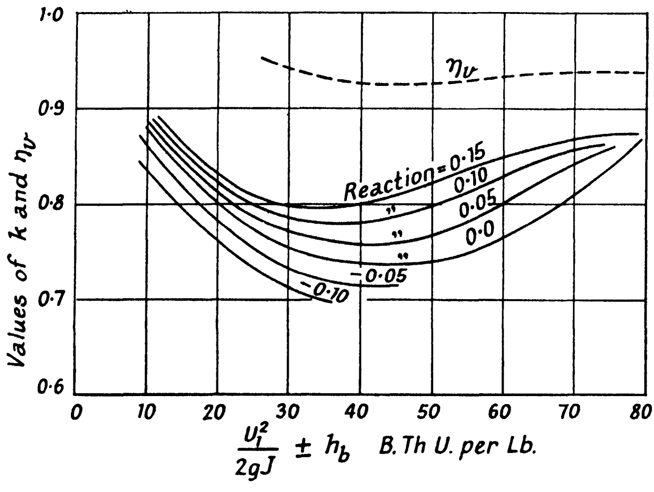


FIG. 146

value at velocities ranging from 1,000 ft. per sec. with 15 per cent reaction to 1,400 ft. per sec. with zero reaction. At a velocity of about 600 ft. per sec. the curve of k is still rising. Fig. 146 shows the results in another way together with the velocity coefficient for the nozzles. The chief point brought out by Fig. 146 is the benefit due to a moderate amount of reaction.

104. Secondary Flows in Turbine Blades. Steam flowing through turbine blades is subjected to considerable inertia forces caused by the curved path. These forces are somewhat reduced in the space near the floor and roof of the blade passage owing to the existence

there of a boundary layer. This sets up a pressure differential, in the manner explained in Art. 56 for the flow through turbine nozzles, with the result that secondary flows A and B, Fig. 147, are superimposed on the main flow. Just as in turbine nozzles such secondary flows affect the direction of flow at exit from the blade and also produce trailing vortices.

105. **Air Tests on Model Blades.** These experiments were made on stationary model impulse blades using air as the operating medium. They were carried out at the University of Liverpool by C. K.

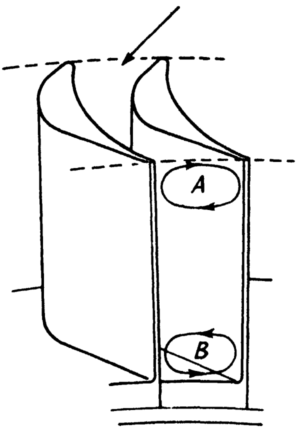


FIG. 147 Secondary Flow in Turbine Blades

Huang working under the author's direction during the period 1947–49.

In order to achieve a Reynolds number of sufficient magnitude the blades were made many times the normal size, the Reynolds number being based on the relative outlet velocity and a characteristic linear dimension equal to four times the hydraulic mean depth of the blade channel at outlet.

Details of the blades are given in Fig. 148. They were made of sheet brass 0·05 in. thick and were 8 in. wide and 12 in. high. They had inlet and outlet angles of 35 degrees. Pressure measuring holes were provided at mid-height at 9 points on the concave surface and at 11 points on the convex surface. These were connected by copper tubes $\frac{5}{64}$ in. o.d. to gauges external to the apparatus, the tubes passing through the hollow blades.

Air was supplied by a fan and delivered to the cascade through a rectangular duct A, Fig. 149. Four ducts were available, the discharge ends being tapered so that the actual flow inlet angle α_1 could be 30°, 35°, 40°, or 45°. The height h of the duct was so arranged in each case that the air passed through an integral

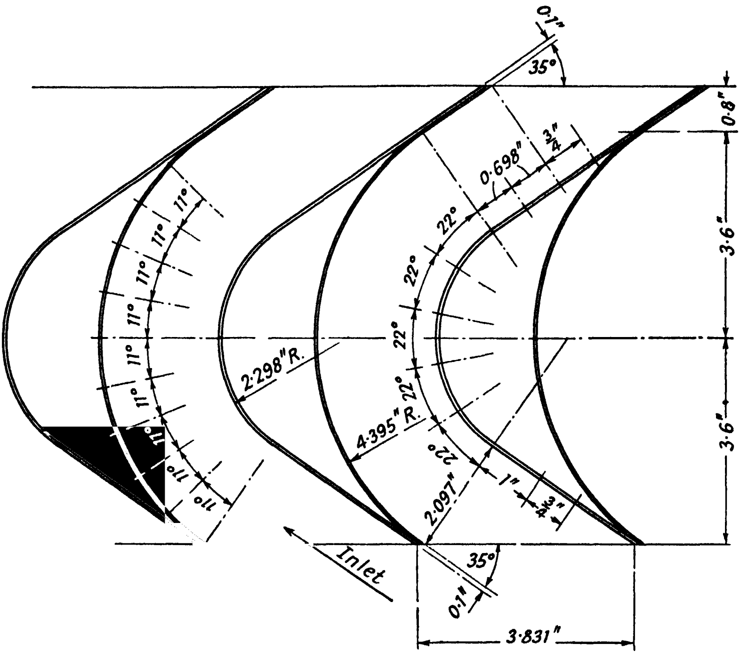


FIG. 148.—Details of Model Impulse Blades, Showing Positions of Pressure Measuring Holes

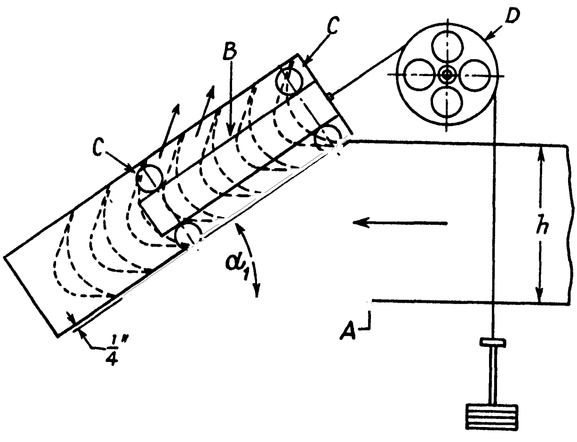


FIG. 149.—Air Tests of Model Impulse Blades

number of blade channels, i.e 6 for $\alpha_1 = 30°$ and 35°, 5 for $\alpha_1 = 40°$, and 4 for $\alpha_1 = 45°$. Preliminary experiments showed that the velocity distribution in the ducts was reasonably uniform, except near the wall of the duct.

The centre blade of the group was rigidly attached at each end to a sliding plate B guided by four pulleys C mounted on ball bearings.

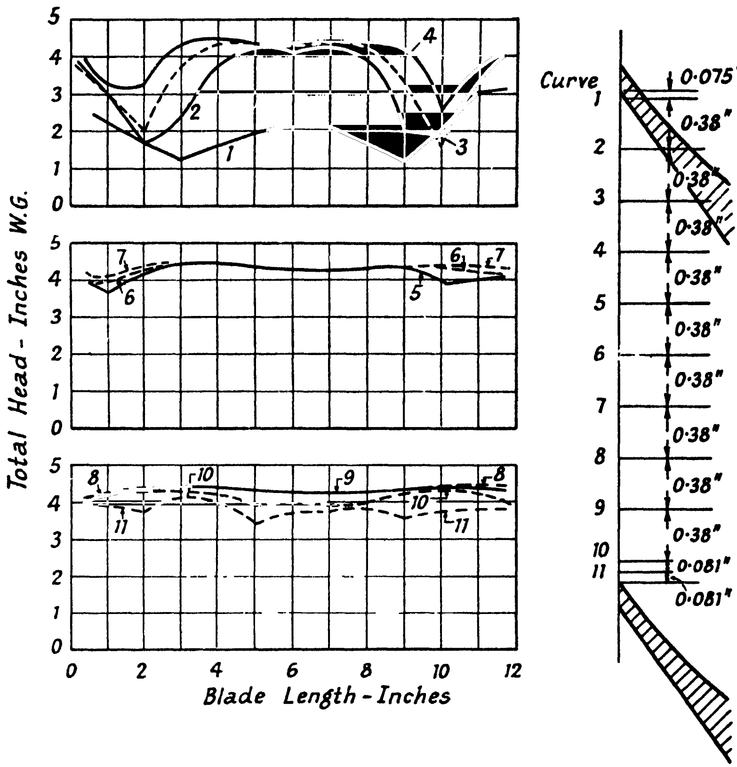


FIG. 150.—Distribution of Energy at Blade Outlet

Cords attached to the plates passed over two light pulleys D, and, by measuring the change in force, the tangential force on the blade could be found. Velocity and flow direction measurements were made at outlet from the channels adjacent to the movable blade.

The height or length of the blades was exactly equal to the width of the duct. In all cases there was a $\frac{1}{4}$ in. gap between the end of the duct and the inlet to the blades. The pressure in this gap was slightly above atmospheric, i.e. there was a certain amount of reaction.

Static head and total head were measured at the blade outlet. Fig. 150 shows the measured distribution of energy at the blade outlet for the flow inlet angle of 35 degrees. The greatest losses occur at and near the convex side of the blade. There is clear

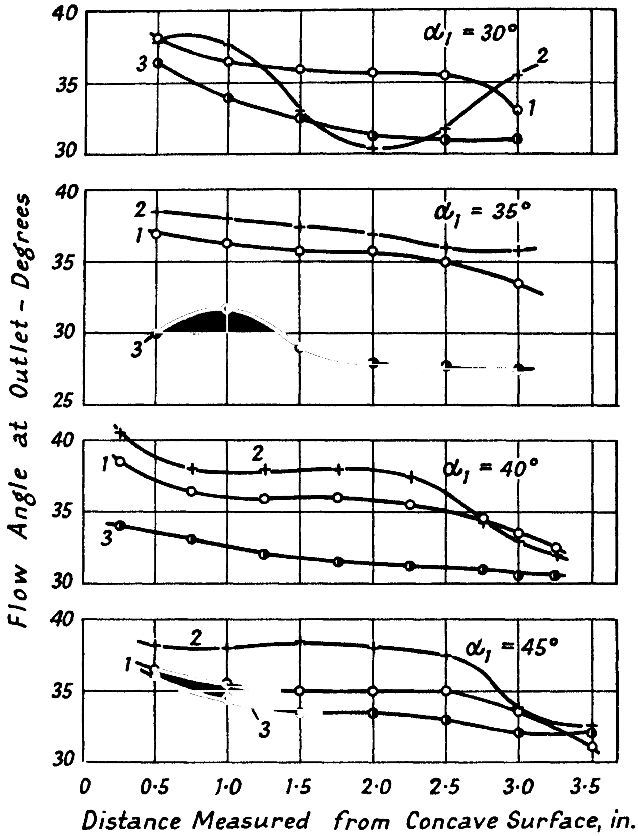


FIG 151 — Direction of Flow at Outlet from Model Impulse Turbine Blade

Curve 1 Mid height
Curves 2 and 3 Three inches and half an inch above floor of blade channel, respectively

evidence of the effect of secondary flow, especially near the convex face of the blade.

The direction of flow at the blade outlet was measured by means of a yaw tube $\frac{1}{4}$ in. o.d. and provided with three radial holes $\frac{1}{64}$ in. diameter on the same transverse plane. As the flow was fairly symmetrical about the mid-height of the blade, yaw tube traverses were made at the mid-height, at 3 in. and $\frac{1}{2}$ in. from the base of the

blade channel. The directions of flow are shown in Fig. 151 against distance x from the concave section of the blade and as a function of the various angles of incidence shown. The curves show that at mid-height the flow angle α_2 is greater than the blade outlet angle except when $i = -10°$. This corresponds to positive deviation, using normal gas turbine terminology, see arrow A, Fig. 152. Near

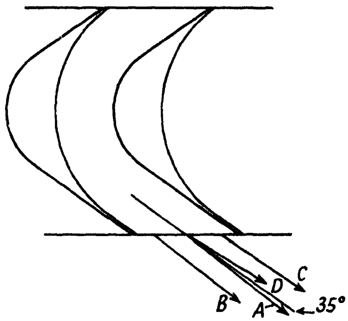


FIG. 152

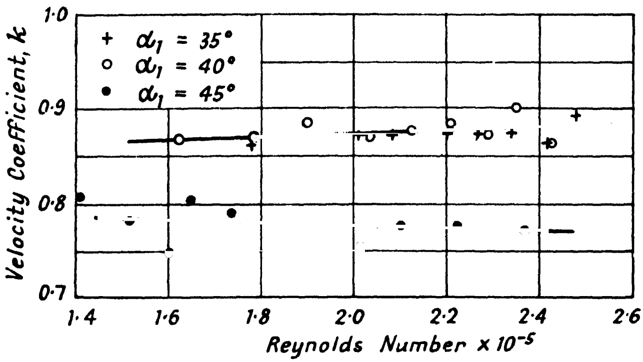


FIG. 153.- Velocity Coefficient for Model Blades Using Air

Note Reynolds number is based on a linear dimension equal to four times the hydraulic mean depth of the blade channel at outlet

the concave surface of the blade this deviation is a maximum, arrow B, whereas at the convex surface, arrow C, it is actually negative. At section 3, ½ in. from the ends of the blade channel, the deviation is negative, as shown by arrow D, in nearly all cases. This is consistent with a secondary flow.

From the measured force on the loose blade and the known air flow it was possible to calculate approximately the value of the velocity coefficient k. This is shown in Fig. 153 as a function of the

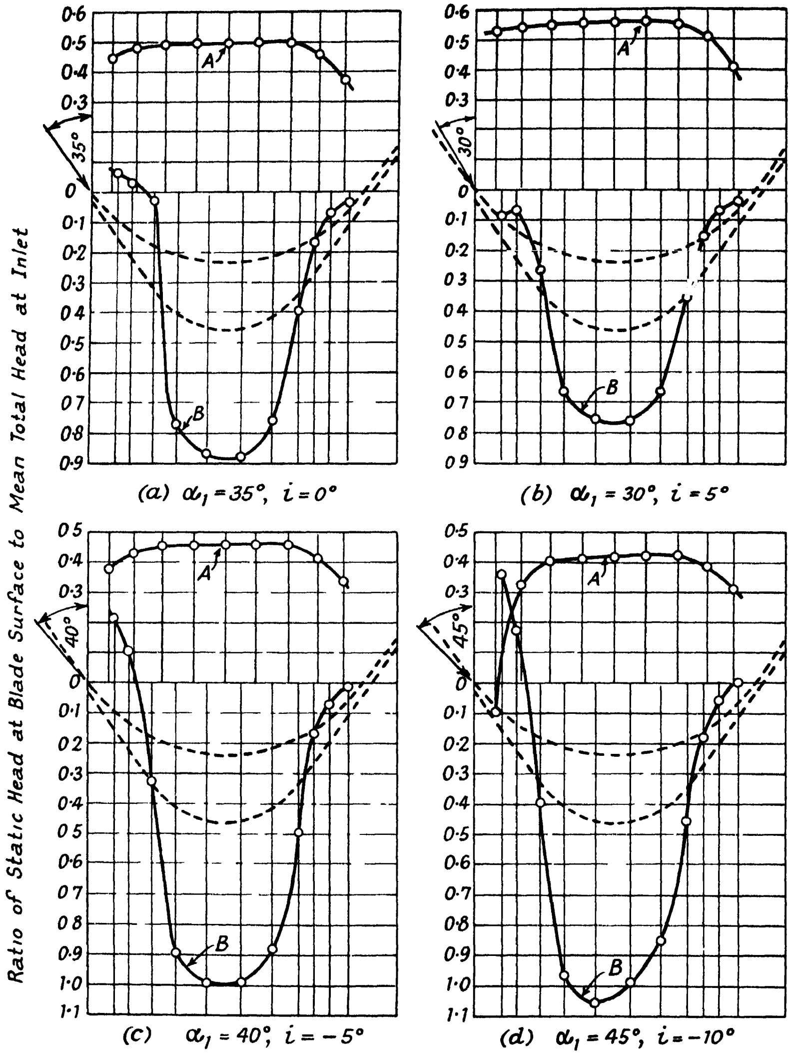


FIG. 154.- Distribution of Pressure on the Concave and Convex Sides of Model Impulse Blades

outlet Reynolds number for the blades. In calculating *k* it was assumed that the actual direction of air flow at outlet from the blades was the nominal angle of 35°; furthermore a correction was applied for the reaction effect.

The results of the pressure measurements are shown in Fig. 154 for different inflow angles. The pressure is plotted as the ratio of the static head at the blade surface to the mean total head at inlet. In all cases, A and B show the pressures on the concave and convex surfaces of the blade, respectively. The position of each pressure measuring hole is given relative to the width of the blade. When α_1 is 30° and $i = +5°$, there is an almost immediate compression on the concave side of the blade and a slight under pressure on the convex side. When the air enters at the correct angle there is a

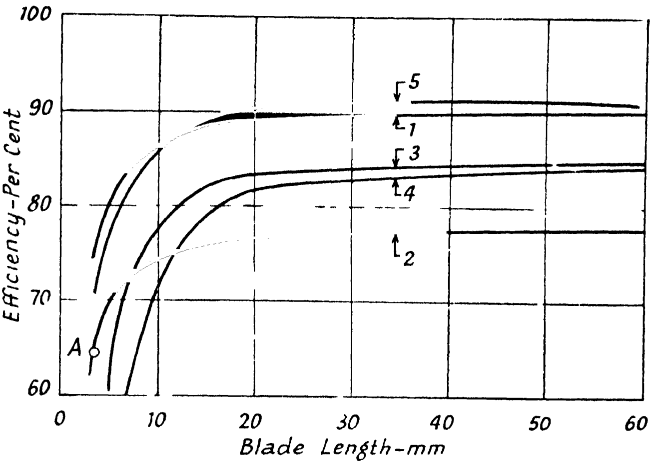


FIG. 155 Efficiency of Short Blades

Curve	Authority	$\rho - u/V_1$	α
1	F Flatt	0.6	
2	F Flatt	0.34	–
3	W Pipe	–	14°
4	I A Kraft	–	–
5	Radial flow reaction turbine with b = 10 mm	0.8	15°

slight positive pressure over the first part of the convex surface. As the inflow angle is increased the positive pressure at entry to the convex surface increases, and with $\alpha_1 = 45°$ there is a measurable under pressure on the inlet side of the concave surface. In all cases this positive pressure on the concave surface is relatively uniform, whereas the pressure on the convex side is subjected to large changes. The large under-pressure on the convex side of the blade is likely to lead to a separation of the flow from the blade surface with a consequential loss of energy.

106. Efficiency of Short Blades. Reference has already been made in Art. 82 to the loss caused by frictional entrainment of steam in the gap between the nozzles and blades of an impulse turbine. This loss is governed largely by the axial clearance and

the amount of overlap given to the blades. Some loss is therefore unavoidable, but it is clear that the loss will be relatively greater in short blades. The losses caused by secondary flows are also likely to be greater in short than in long blades.

Fig. 155, based on a diagram given by F. Flatt (5), shows turbine efficiency as a function of blade length for impulse turbines. Curves 1, 2, and 3 refer to the gross stage efficiency, whereas curve 4 gives the stage efficiency. Point A is based on tests made on blades about 0·14 in. in height and used in the first stage of a 1,000 kW. Escher Wyss turbine operating at 1,400 lb. per sq. in. gauge (see Art. 316).

107. Newer Forms of Turbine Blades. In recent years new forms of both impulse and reaction turbine blades have been introduced.

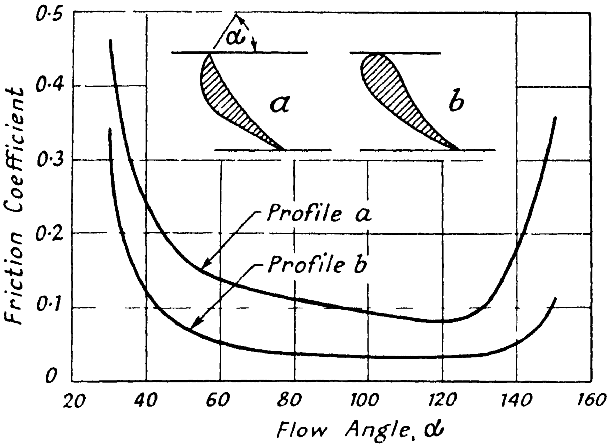


FIG. 156.—Comparison of Losses for Blades with Sharp and Well-rounded Inlet Edge

The usual form of "profile" blade shown in Fig. 109 is not suitable for stages in which, under variable load conditions, there is a change in the direction of steam flow into the blade channels. Fortunately, in constant-speed turbines, changes in direction are only met with in the first, or governing, stage and in the last one or two stages under variable load conditions (see Chapter XV). If the direction of inflow should be different from the actual inlet angle of the blade then there would be separation and severe eddy losses.

When steam is passing through a turbine blade the deflection produced by the concave surface produces a positive pressure on that surface with little or no adverse effects on the flow. The sharp changes in flow direction which occur in the blade channel, however, produce an under-pressure on the convex surface of the blade as shown in Fig. 154, followed by a rise in pressure as the channel outlet is approached. It is probable that the boundary layer will

thicken on the convex surface and that separation may occur at some point on that surface. These factors appear to have been taken into account in the design of the newer forms of blades.

It is difficult to discover where and when these modified blade forms first appeared, but experiments on two blade forms were carried out by firms of the International Ljungström Turbine Union A.-G. more than twenty years ago, (6). The forms tested are shown in Fig. 156, (*a*) showing a blade with a fairly sharp inlet edge, while (*b*) shows a modified profile with a well-rounded inlet edge. Tests were made to determine the friction loss coefficient for each type of

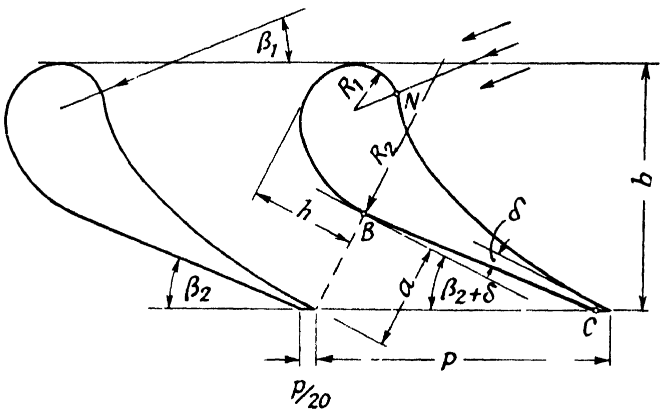


FIG. 157.—Impulse Blade Profile for Subsonic Velocities

$\beta_1 = \beta_2 = 22.5°$, $\delta = 5°$, $h = a$, $R_1 = 0.4a$, $R_2 = 2a$, $a/p \doteqdot 0.37$, $b/p \doteqdot 0.863$

blade with varying inlet angles. There is a difference of some 4·5 per cent in performance at the optimum inlet flow angle in favour of the blade with the rounded inlet.

As might be expected, the efficiency of turbine blading increases as the Reynolds number is increased. The Mach number at inlet to the blade, i.e. the ratio of the inlet velocity to the local acoustic velocity, is also an important parameter. In the majority of steam turbines the inlet Mach number is well below unity, but it may exceed unity in Curtis stages.

An attempt to standardize blade profiles for (1) subsonic, (2) near sonic, and (3) supersonic velocities has been made by Dr. G. Flugel (7). A proposed impulse blade profile for subsonic velocities is shown in Fig. 157. The profile has a well-rounded inlet edge. The convex surface may be divided into two parts, (1) the fore part from N to B, and (2) the after part from B to C. The length *h* of the fore part should naturally be made as small as possible so that, for a given blade width *b*, the blade pitch *p* can be made as large as possible. On the other hand, the fore part calls for careful design, the profile

line on the convex side running throughout without any sudden transition of curvature. In the blade shown, $h = a$ and this is stated to be the least value to obtain a flow free from separation. The nose point N is the point at which the tangent to the profile is perpendicular to the direction of inflow. The radius of curvature of the profile is the minimum at N, being equal to $0{\cdot}4a$ for the blade shown in Fig. 157. The outlet end of the blade profile is made tapered, the angle δ being about 5°; with greater velocities a smaller angle would be used.

Fig. 158 shows a reaction blade profile suitable for subsonic velocities.

In impulse blades in which the inlet velocity may approach the sonic value, local velocities may exceed the sonic velocity and compression shocks occur. This calls for careful design of the inlet

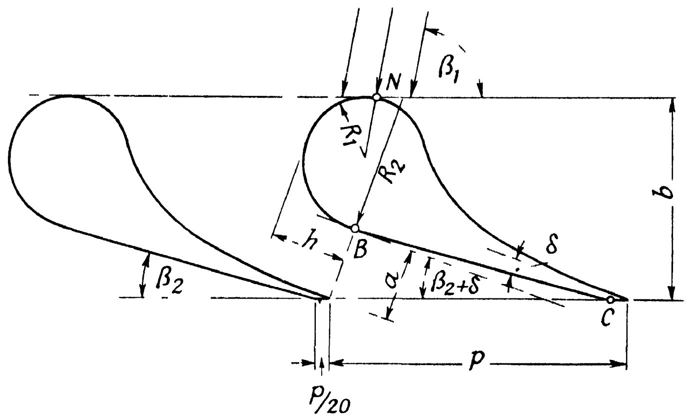


FIG 158.—Reaction Blade for Subsonic Velocities

$\beta_1 = 80°$, $\beta_2 = 15°$, $\delta = 5°$, $h = a$, $R_1 = 0{\cdot}8a$, $R_2 = 2a$, $a/p = 0{\cdot}25$, $b/p \doteqdot 0{\cdot}685$

profile with a small radius at the nose and a convex profile with as little curvature as possible. Fig. 159 shows the section of an impulse blade for near sonic velocities. The radius of the nose is made $0{\cdot}1a$. The point T is the contact point of the tangent drawn to the profile in the normal direction of inflow. The peak point S is so chosen that the tangent there is parallel to the mouth cross-section AB. It is suggested that $R_B = 2h$; $R_S = h$, and $R_T = 4h$.

Blades for impulse-reaction steam turbines may be given a section similar to that used in some gas turbines, first developed for axial-flow compressors. Here the form of the blade is defined by its centre-line, usually referred to as the camber line, the camber angle θ, the position of maximum camber a/c, the basic profile, and the maximum thickness t/c, Fig. 160.

For convenience the camber line may be either a circular arc or a

parabolic arc. For a circular arc the ratio a/c is 0·5 and the angle $\chi_2 = \chi_1$. The camber angle $\theta = \chi_1 + \chi_2$, whatever the shape of the camber line.

The basic profile may be an aerofoil such as that shown in Fig.

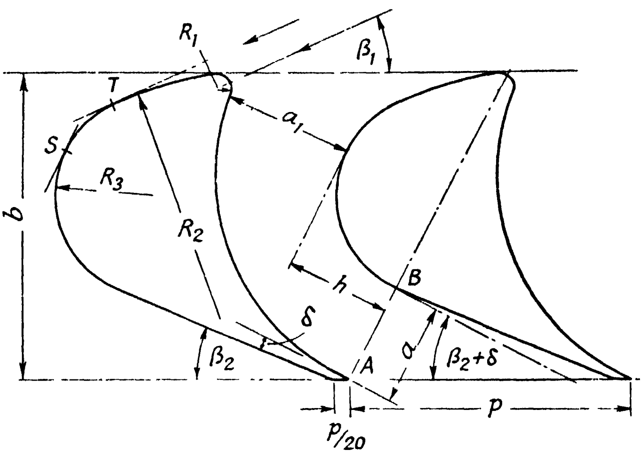


FIG. 159.—Impulse Blade Profile for Near-sonic Steam Velocities

$\beta_1 = \beta_2 = 22{\cdot}5°$; $\delta = 5°$; $h \doteqdot a$; $R_1 = 0{\cdot}1a$; $R_2 = 4a$; $R_3 = a$; $a_1 = 1{\cdot}27a$; $a/p \doteqdot 0{\cdot}37$; $b/p = 1{\cdot}1$.

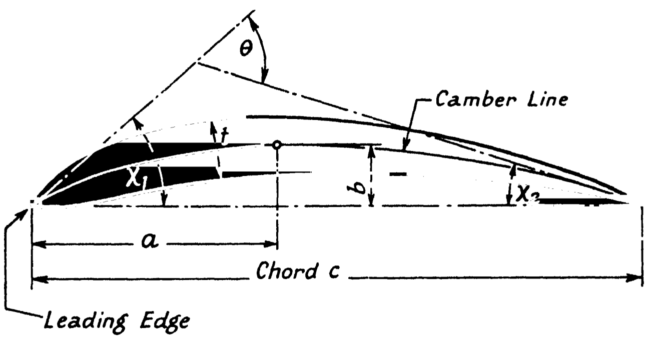


FIG. 160.—Blade of Aerofoil Section for Impulse-reaction Turbine

161, taken from a paper (8) by Mr. A. R. Howell. The thickness given in the table may be scaled up or down to give the required maximum thickness, the stations being taken along the chord line and the ordinates plotted normal to the camber line.

The setting of the blade is shown in Fig. 162, and is defined either

by the angle β_1 between the tangent to the camber line at inlet and the tangential direction or by the stagger angle γ made by the chord line and the tangential direction. It is obvious that the stagger angle $\gamma = 180° - (\chi_1 + \beta_1)$. For a circular camber line $\chi_1 = \theta/2$, and $\gamma = 180° - (\theta/2 + \beta_1)$. If α_1 is the direction of flow into the

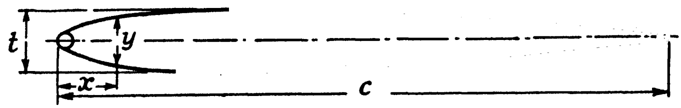


FIG. 161 —Aerofoil Profile C_4

t/c 0·10, leading edge radius – 0·12t, trailing edge radius – 0·06t
Values of semi thickness—

x/c per cent	0	1·25	2·5	5·0	7·5	10	15	20	30	40	50	60	70	80	90	95	100
$y/2c$ per cent	0	1·65	2·27	3·08	3·62	4·02	4·55	4·83	5·00	4·89	4·57	4·05	3·37	2·54	1·60	1·06	0

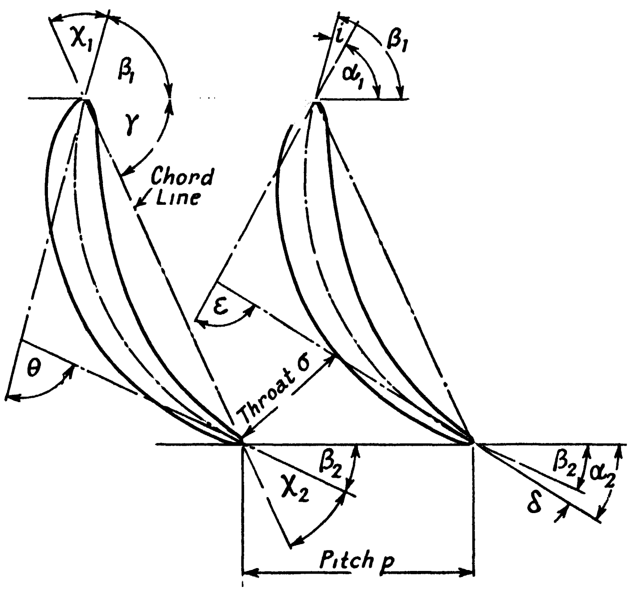


FIG 162

blade relative to the tangential direction then $i = \beta_1 - \alpha_1$ is defined as the angle of incidence. If α_1 is greater than β_1 the incidence is said to be negative. Considering the flow at outlet as a whole if α_2 is the direction, then $\delta = \alpha_2 - \beta_2$ is termed the deviation and is normally positive. The angle ε is the actual angle through

which the steam is turned and is called the deflection. It will be clear from the figure that

$$\theta = 180^\circ - (\beta_1 + \beta_2)$$
$$\varepsilon = 180^\circ - (\alpha_1 + \alpha_2)$$

or

$$\varepsilon = \theta + i - \delta$$

An important ratio is that of pitch to chord, p/c.

The channel through the blade is gradually convergent and leads to a throat of width o (opening).

The camber used in turbines is much greater than that used in

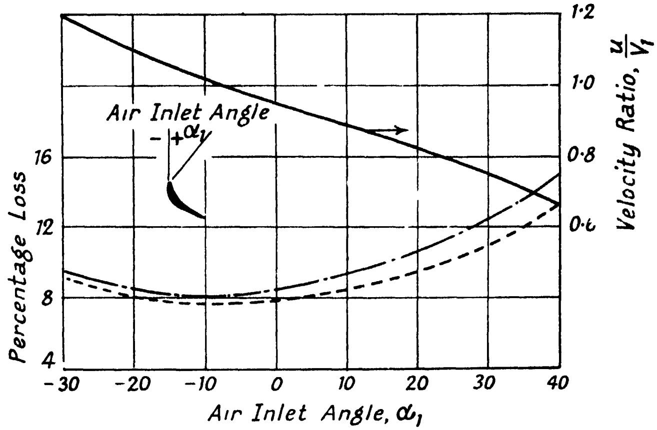


FIG 163—Comparison of Losses in Normal Reaction Blading as Determined in Turbine and Nozzle Tests

— "Alicia" turbine
- - - Nozzle tester

	Nozzle Tester	"Alicia" Turbine
Blade	640B	640B
Blade height, inch	0.875	0.875
Pressure ratio	1.10	1.01
o/p	0.37	0.35
p/c	0.592	0.598
R_e chord $\times 10^{-4}$	17.6	4.3
R_e hind 10^{-4}	1.63	0.38

axial-flow compressors. The notation used in Fig. 162 differs from that normally used in gas turbine work because the angles α and β are measured relative to the tangential and not the axial direction.

108. Tests of Impulse-reaction Blades. Reference has already been made in Art. 74 to the Parsons nozzle tester and to tests on reaction blades when functioning as stationary nozzles. In the 19th

Parsons Memorial Lecture (9) Mr. F. Dollin has given further and more recent results of tests made in the nozzle tester and in a small experimental turbine. Fig. 163, reproduced from the lecture, shows a comparison of losses in normal reaction blading ½ in. wide and 0·875 in. high as a function of the air flow inlet angle and blade speed ratio. The agreement between the results is very good, especially at the optimum flow angle. The loss is expressed as a percentage of the available energy calculated from the static pressure before and after the blades.

Some tests on a new experimental turbine are also described in

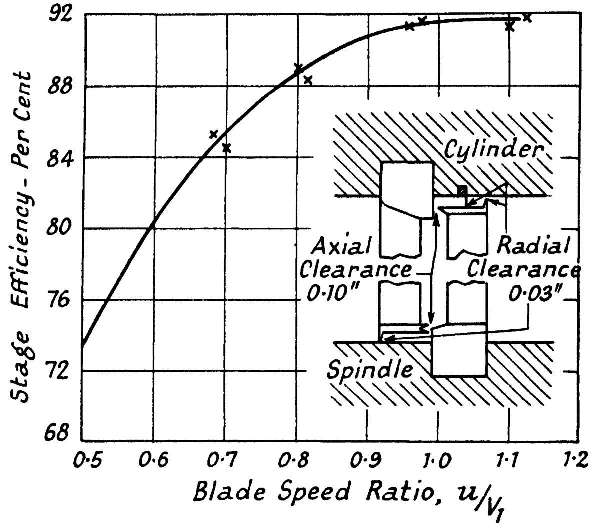


FIG. 164. - Tests on Normal Reaction Blading in a Large Experimental Parsons Turbine

Blade profile, 660B; mean blade height, 2·8 in.; R_e — chord, 13·7 × 10^4; R_e — h.m.d., 1·44 × 10^4.

this lecture. The turbine has a drum diameter of 13 in., has seven stages and its normal speed of rotation is 6,000 r.p.m. Fig. 164 shows the results of tests on normal reaction blading made in this turbine. The ordinates give the stage efficiency with clearance losses as run. Mr. Dollin states that the tests, when corrected to zero clearance, represent a blading efficiency approaching 95 per cent.

Further tests on a turbine with reaction blading are given in Art. 333. These tests were made in 1925 and it is of interest to note that Professor Stodola estimated that if the blade clearance were extrapolated to zero the blade efficiency would be 93 per cent.

Tests on a four-stage reaction turbine, having blades of a type similar to those shown in Fig. 162 and driven by air, are given in an

A.R.C. Report (10) by Messrs. Ainley, Peterson and Jeffs. The maximum total-head efficiency measured on the turbine was about 89 per cent at the highest speed tested.

BIBLIOGRAPHY

1. RATEAU: "Mode du calcul des turbines à vapeur." *Assn. Technique Maritime*, Paris, 1909.
2. BRILING: "Verluste in den Schaufeln von Freistrahldampfturbinen." *Z.V.d.I.*, 1910; 54; 265, 352, 389, and 474.
3. CHRISTLEIN: Dissertation, Oldenbourg.
4. FALTIN: "Spaltdruck und Laufradverlust." *Z.V.d.I.*, 1926; 70; 1582.
5. FLATT: "Der Einfluss der Radreibung und des Injectionsverlustes, etc;" *Stodola Festschrift*, 1929, p. 133.
6. HOFER: "Strömungsvorgänge in neuzeitlichen Dampfturbinen." *Mitt. aus den Forschungsanstalten*, G.H.H. Konzern, 1933; 7; 173.
7. FLUGEL: "Über Gestaltung und Systematik neuerer Schaufelprofile für Dampf-und Gas-Turbinen." *Forsch. Ing.-Wesens*, 1949-50; 16.
8. HOWELL: "Fluid dynamics of axial compressors." *Proc. I. Mech. E.*, 1945; 153; 441.
9. DOLLIN: "Factors influencing the continuing development of the steam turbine."
10. AINLEY, PETERSON AND JEFFS: "Overall performance characteristics of a four-stage reaction turbine." *R. & M.* No. 2416.

CHAPTER XI

INTERNAL LOSSES IN STEAM TURBINES

109. Introductory. The internal losses in steam turbines may be enumerated as follows—

(1) Nozzle losses.
(2) Blade friction losses.
(3) Disc friction losses.
(4) Partial admission losses.
(5) Gland leakage losses.
(6) Residual velocity loss.

Items (1) and (2) have already been dealt with in preceding chapters, and we now pass on to a brief consideration of the other items in turn.

110. Disc Friction. When a disc such as those used in impulse turbines is rotating in a slightly viscous fluid like steam there is a true surface friction loss due to relative motion between the disc and the steam particles. As a result, the moving disc surface exerts a drag on the steam which sets it in motion and produces a definite circulation, the character of which depends on the shape of the space enclosing the disc. Fig. 165 shows the circulation currents set up when a simple disc is rotating in an enclosure of simple shape.

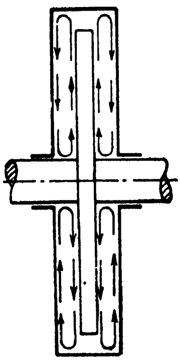


FIG. 165

It is beyond the scope of this book to consider the subject in greater detail, but brief references will be made to the more important work on the subject.

Professor Stodola (1), as the result of some experiments made on discs rotating in free air, proposed the following formula for the disc friction loss—

$$\text{h.p.}_d = \frac{C}{10^6} \cdot D^2 \cdot u^3 \cdot \rho$$

h.p._d = horse-power loss due to disc friction.
D = diameter of disc, ft.
u = peripheral velocity of disc, ft. per sec.
ρ = density of fluid in which disc is rotating, lb. per cub. ft.
C = 0·071 for *air* only.

Stodola states that the loss for an encased wheel would be less than that for a wheel rotating in free air, varying from one-quarter to one-half of that amount, according to conditions. Odell (2) also carried out experiments on discs rotating in free air. An important mathematical paper on the subject was published in 1921 by Professor von Kármán (3). In 1934, the well-known Swiss firm of

Brown Boveri & Co. published the results (4) of some experiments made on discs in a closed chamber filled with various gases.

From an analysis of these and other experimental investigations, the author has deduced the following simple relation for the power absorbed by discs and wheels that are well encased.

$$\text{h.p.}_d = C \cdot D^2\left(\frac{u}{100}\right)^3 \rho \quad . \quad . \quad . \quad (143)$$

the constant C being given by the expression

$$\log_{10} C = \bar{1}\cdot90 - 0\cdot2 \log_{10}\left(\frac{D \cdot u \cdot \rho}{\mu}\right) \quad . \quad . \quad (144)$$

D, u, and ρ have the same meanings as before and μ is the coefficient of viscosity of the steam, the unit being lb. per ft.-sec.

Between 15 and 500 lb. per sq. in., the coefficient of viscosity of dry and saturated steam, according to the work of K. Sigwart (5), is given by the following simple relation—

$$\mu = (0\cdot143t + 56\cdot0) \times 10^{-7} \frac{\text{lb.}}{\text{ft.-sec.}} \quad . \quad (145)$$

where t is the saturation temperature in degrees Fahr. Provided the steam temperature is below 700° F. the above expression may be used for superheated steam at temperature t, since the viscosity of steam is hardly affected by pressure.

EXAMPLE 21. Calculate the power absorbed in overcoming disc friction in a stage of an impulse turbine in which the disc diameter is 46 in ; r.p.m. 3,000; steam pressure 120; superheat 200° F.

From steam tables, saturation temperature = 341·3, ∴ steam temperature = 541·3° F. Substituting in eq. (145)

$$\mu = 133\cdot5 \times 10^{-7}$$

By Callendar's steam tables, $v = 4\cdot846$

$$D = \frac{46}{12} = 3\cdot833 \text{ ft.}; \; u = 602\cdot0$$

$$\therefore \quad \log_{10} C = \bar{1}\cdot90 - 0\cdot2 \log_{10}\left(\frac{3\cdot833 \times 602\cdot0 \times 10^7}{133\cdot5 \times 4\cdot846}\right)$$

$$= \bar{1}\cdot90 - 1\cdot5104 = \bar{2}\cdot3896$$

$$\therefore \; C = 0\cdot0245$$

Then

$$\text{h.p.}_d = \frac{0\cdot0245}{4\cdot846}(3\cdot833)^2 \cdot (6\cdot02)^3$$

$$= 16\cdot2$$

It is usual to drill from four to six pressure-balancing holes in turbine discs; the disturbance due to these will probably increase the disc friction loss.

111. Partial Admission Losses. Fig. 166 (*a*) shows a transverse section through a high-pressure stage of a steam turbine, in which stage, owing to the comparatively small area required for the nozzles, the latter extend over only a fraction of the circumference. For example, in Fig. 166 (*a*) the nozzles are divided into three groups, each group containing different numbers of nozzles. Allowing for the peripheral displacement due to the axial clearance between the nozzle guide blades and the blade inlet edges, the blade positions at steam inlet will be A, C, and E, and at steam outlet B, D, and F. The shaded areas in Fig. 166 (*a*) represent the active arcs, the unshaded

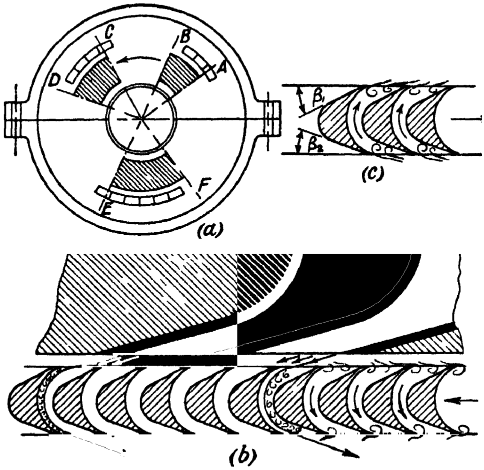


FIG. 166.—Diagrams showing Causes of Partial Admission Loss

areas represent arcs over which there is no steam flow through the blades.

Considering Fig. 166 (*b*), it will be evident that there will always be six blades which will be partially filled with steam and in which the flow will be considerably disturbed.

The movement of the blades through steam in the inactive arcs BC, DE, and FA leads to further loss. There will be certain eddies produced in the channels of the idle blades, as shown in Fig. 166 (*b*). If the blades are driven in the reverse direction, as in a marine astern turbine when the turbines are running in the ahead direction, then, due to the scooping action of the blades, the eddies produced are much more violent. Professor Stodola found that the power absorbed in driving a bladed wheel in free air in the reverse direction was five to six times that required for the normal direction. If the wheel was encased, the ratio of the loss was reduced to 1·2.

If the blade outlet angle β_2 is less than the inlet angle β_1 and if the wheel is running in the reverse direction (Fig. 166 (*c*)), then due

to the scoop action the blades act as an axial-flow fan and a flow is produced in the direction shown by the arrows. When blades having unequal angles are moving in the normal direction (Fig. 166 (*b*)), a flow is set up in the direction shown by the arrows.

The sum of the losses due to partial admission is variously described as "blade ventilation" loss, or "vane action" loss. We prefer to use the term "blade windage," which is not quite so specific.

For an unencased wheel with a single row of blades rotating in *air* in the normal (ahead) direction, Stodola gives the following expression for the blade windage loss—

$$\text{h.p.}_{bw} = 0{\cdot}458\text{D} \,.\, l^{1\cdot5}\left(\frac{u}{100}\right)^3 \,.\, \rho$$

If the nozzle arc extend over a fraction λ of the whole circumference and if this arc is continuous, then we may introduce a correction factor $(1 - \lambda)$ and so obtain the expression—

$$\text{h.p.}_{bw} = 0{\cdot}458(1-\lambda)\text{D} \,.\, l^{1\cdot5}\left(\frac{u}{100}\right)^3 \,.\, \rho \qquad (146)$$

D = mean diameter of blade ring, ft.
l = effective blade height, in.
u = mean blade velocity, ft. per sec.
ρ = steam density, lb. per cub. ft.

Professor Wm. Kerr published (6) in 1913 the results of some very careful experiments to determine the total resistance of turbine wheels. A turbine wheel was driven round in steam at different densities, the resistance being measured by noting the rate of retardation of the rotor with the power cut off. The following expression was deduced for the *total* power absorbed in wheel friction, i.e. disc friction plus blade windage—

$$\text{h.p.}_{wf} = \{\beta_1 \,.\, \text{D} + n\beta_2(1-\lambda)l^{1\cdot5}\}\left(\frac{u}{100}\right)^3 \,.\, \text{D} \,.\, \rho \qquad (147)$$

in which D, u, ρ, and λ have the same meanings as before, but l is the mean blade height in inches.

$\beta_1 = 0{\cdot}0607$; $\beta_2 = 0{\cdot}458$.
n = 1 for wheels with 1 row of blades.
= 1·23 for wheels with 2 rows of blades.
= 1·8 for wheels with 3 rows of blades.
= 2·9 for wheels with 4 rows of blades.

The first term in the bracket evidently relates to the disc friction, the second to the blade windage. This formula gives the same result as that of Stodola for single-row wheels.

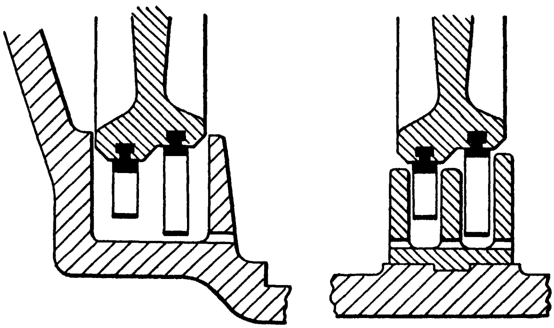
More recently, Professor Kerr has carried out further researches (7) on the subject and, by studying the action of the disc and blades separately, he has been able to evolve formulae for each loss. The formula given for the blade windage loss is

$$h.p._{bw} = \left(\frac{u}{100}\right)^3 \left(\frac{d}{10}\right)^2 \rho \left[\beta(1 - \lambda)\left\{\left(\frac{l_1}{d}\right)^{1.5} + \left(\frac{l_2}{d}\right)^{1.5}\right\}\right] \quad (148)$$

in which

d = mean diameter of blade ring in *inches*.
l_1 = blade height at inlet edge of first row, in.
l_2 = blade height at outlet edge of last row, in.
β – 9·3 for wheels with 1 row of blades.
= 12·5 for wheels with 2 rows of blades.
= 17·9 for wheels with 3 rows of blades.

The loss of power due to blade windage may be considerably reduced by enclosing the blades on both sides. Two constructions



(a) (b)

FIG. 167 —Blade Shields for Reducing Windage

for effecting this are shown in Fig. 167. In the one case, the shields are formed in the cylinder casting; in the other, separate shield rings are fitted in the cylinder.

112. Gland Leakage Losses. There is a small loss of energy in each stage of an impulse turbine owing to the leakage of steam from one wheel chamber to the next through the space between the diaphragm and the shaft, or the wheel hub, as the case may be.

There is also a certain wastage of steam at the external glands where the turbine spindle passes through the ends of the turbine cylinder, or cylinders. Broadly speaking, the glands at the high-pressure end of the turbine have to minimize the leakage of steam from the turbine cylinder to the atmosphere, whereas the function

of the low-pressure gland is to prevent the inleakage of air into the exhaust branch and condenser. For this purpose steam is supplied to the centre of the gland; some of the steam leaks into the exhaust space, but there is a slight outward flow to the atmosphere which effectively prevents the inleakage of air. The steam supplied

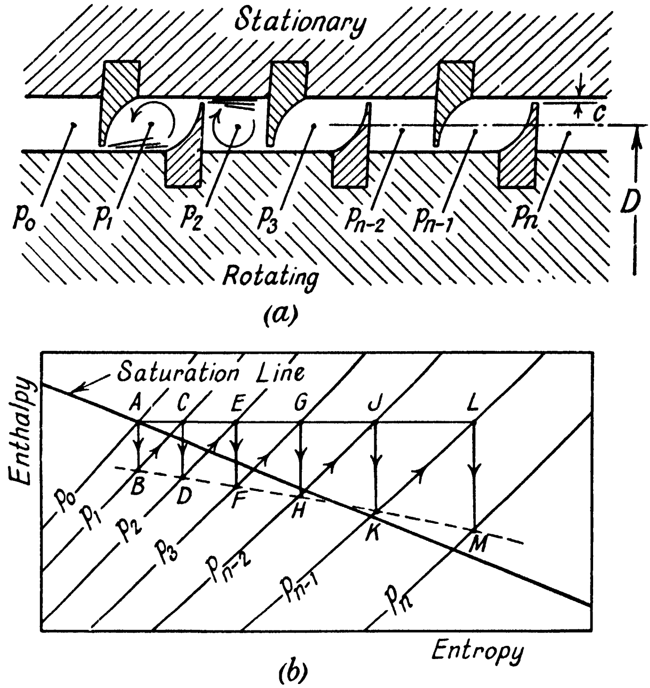


FIG. 168

to the low-pressure gland for sealing purposes may be reduced-pressure live steam or steam which has leaked through the high-pressure gland.

Under certain light-load conditions, the pressure in the first-stage wheel chamber may fall to atmospheric pressure, or below. Under these conditions it becomes necessary to supply sealing steam to the high-pressure gland to prevent an inleakage of air. It should be stated, however, that this is unnecessary when a hydraulic seal is also fitted.

Two types of gland are in general use, the carbon ring gland and the labyrinth gland. Labyrinth packing is used exclusively in diaphragm glands and in most external glands.

113. Flow of Steam through Labyrinth Packing. Fig. 168 (*a*) shows a section through a typical labyrinth packing. This comprises a

number of packing strips in the fixed housing and an equal number in the shaft or rotor. The inner ends of the fixed strips and the outer ends of the moving strips are reduced in thickness so that if there should be accidental contact, the thin edge of the packing strip will wear away without the generation of a large amount of heat which might cause distortion of the shaft, gland sleeve, or other part of the gland. There is a small radial clearance c between the strips and the housing or shaft, as the case may be. This forms a constriction through which the steam leaks. The small space between one constriction and the next is termed a "pocket" or "dwell space."

Suppose that the steam pressure on the up-stream side of the gland is p_0 and that on the down-stream side is p_n, there being n constrictions. Then, assuming that the areas through all the constrictions are the same, as soon as steady flow has been established, the pressures p_1, p_2, etc., in the dwell spaces will take up definite values. In many cases, the ratio of the pressure drop at any constriction, excepting the last, to the absolute pressure at that constriction is comparatively small. In such cases, the following approximate theory is applicable.

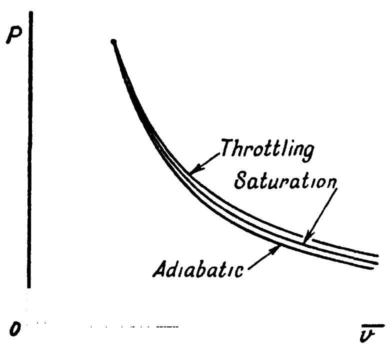


FIG. 169.—Comparison of p–v Curves from Common Initial Condition

Consider first the action in labyrinth packing. Steam expands more or less adiabatically in the first constriction from pressure p_0 to p_1. This is represented in Fig. 168 (*b*) by the isentropic line AB. On entering the dwell space, the steam sets up an eddy, but the velocity of the steam is reduced to a comparatively low value. In consequence, the kinetic energy acquired by expansion is reconverted into heat at constant pressure and the enthalpy is restored, practically, to its initial value. During this process, the state point of the steam moves along the constant-pressure line BC. The expansion in the second constriction is represented by CD, the reheating in the second dwell space by DE, and so on.

A comparison of p-v curves is made in Fig. 169. In each case the relationship between p and v is fairly well represented by an equation of the type $p \, . \, v^m =$ constant, where m has the values 1·135 and 1·0646 for the adiabatic and saturation curves respectively. For the throttling curve (I = constant) m is very nearly equal to unity. Actually, the relation between p and v for the locus BDFHKM, Fig. 168 (*b*), is a more important relation because each of these points represents the condition of the steam at outlet from

the constriction. Here, the value of m depends upon the rate of leakage, which in turn depends upon the pressure range and the number of constrictions provided. Thus m may vary between 1·02 and 1·1. Considerable simplification is achieved by assuming that m is equal to unity, and since it is rather difficult to measure the working clearance accurately it is perhaps unnecessary to attempt to calculate the leakage rate to a high degree of accuracy. The following theory must then be regarded as approximate.

Case I. Pressure Ratio for each Constriction Greater than the Critical.

Let w = mass leakage of steam, lb. per sec.
A = effective area through each constriction, sq. in.
D = mean diameter of packing strips, in.
C_c = coefficient of contraction. Owing to the one-sided contraction, this is very probably equal to about 0·8.

Then $$A = C_c \cdot \pi D \cdot c \text{ sq. in.}$$

Consider the flow at any constriction. Let p be the pressure on the up-stream side of the constriction and $p - \delta p$ the pressure on the down-stream side. Then the velocity V reached in the constriction at pressure $p - \delta p$ will be such that

$$\frac{V^2}{2g} = 144 \cdot v_m \cdot \delta p$$

where v_m is the mean specific volume of the steam. By the equation of continuity—

$$w(v + \delta v) = \frac{AV}{144}$$

or $$\frac{w}{A} = \frac{V}{144(v + \delta v)} = \frac{\sqrt{288g \cdot v_m \cdot \delta p}}{144(v + \delta v)}$$

If δp is small compared with p, then we may write

$$v \doteq v_m \doteq v + \delta v$$

$$\therefore \quad \frac{w}{A} = \frac{1}{144}\sqrt{\frac{288\,g \cdot \delta p}{v}}$$

Let $$pv = C_1, \text{ then } v = \frac{C_1}{p}$$

and $$\frac{w}{A} = \frac{1}{144}\sqrt{\frac{288g \cdot p \cdot \delta p}{C_1}}$$

It will be seen that in a gland where A is constant, the product

$p \,.\, \delta p$ is a constant, and therefore as p falls the pressure drop per constriction increases.

Squaring both sides of the expression, we have

$$\left(\frac{w}{A}\right)^2 = \frac{2g}{144C_1} \,.\, p \,.\, \delta p$$

or

$$2{\cdot}24C_1\left(\frac{w}{A}\right)^2 = p \,.\, \delta p$$

For n rings—

$$\sum_0^n 2{\cdot}24C_1\left(\frac{w}{A}\right)^2 = \int_{p_n}^{p_0} p \,.\, dp$$

or

$$2{\cdot}24n \,.\, C_1\left(\frac{w}{A}\right)^2 = \frac{1}{2}(p_0^2 - p_n^2)$$

i.e.

$$n \,.\, C\left(\frac{w}{A}\right)^2 = \tfrac{1}{2}(p_0^2 - p_n^2) \quad . \quad . \quad (149)$$

where

$$C = 2{\cdot}24C_1$$
$$= 2{\cdot}24p_0v_0$$

The rate of leakage per sq. in. of effective area, expressed in lb. per sec., is

$$\frac{w}{A} = \sqrt{\frac{p_0^2 - p_n^2}{2nC}} \quad . \quad . \quad . \quad . \quad . \quad (150)$$

C may be found for any given initial steam conditions. For dry and saturated steam, the constants have the following values—

p_0	v_0	$C_1 = p_0v_0$	C
20	20·08	401·6	900
50	8·50	425·0	952
100	4·429	442·9	992
150	3·016	452·4	1,012
200	2·293	458·6	1,027

EXAMPLE 22. Calculate the mass rate of leakage through a high-pressure turbine gland under the following conditions—

Steam pressure in first stage	160
Steam superheat in first stage	200° F.
Steam pressure in leak-off pocket . . .	40
Mean diameter of packing	8 in.
Radial clearance	0·02 in.
Number of constrictions	40

From the steam tables, when $p = 160$ and the superheat is 200° F., $I_0 = 1{,}310{\cdot}0$. By Callendar's equation—

$$v_0 = \frac{1{\cdot}2464}{160}(1{,}310{\cdot}0 - 835{\cdot}2) - 0{\cdot}002$$

$$= 3{\cdot}70$$

$$C_1 = p_0 v_0 = 160 \times 3{\cdot}70 = 592{\cdot}0$$

$$C = 2{\cdot}24 C_1 = 1{,}327$$

$$\therefore \qquad \frac{w}{A} = \sqrt{\frac{160^2 - 40^2}{2 \times 40 \times 1{,}327}} = 0{\cdot}475 \frac{\text{lb.}}{\text{in.}^2\,\text{sec.}}$$

$$A = C_c \,.\, \pi D C$$

Assuming $C_c = 0{\cdot}80$, $A = 0{\cdot}402$ sq. in.

$\therefore$ Rate of leakage $= 0{\cdot}475 \times 0{\cdot}402$

$= 0{\cdot}191$ lb. per sec.

The pressure in any dwell space may be found from eq. (149). Thus, for the last dwell space (pressure $= p_{n-1}$) we have

$$(n-1)C\left(\frac{w}{A}\right)^2 = \frac{1}{2}(p_0^2 - p_{n-1}^2)$$

Substituting values, $p_{n-1} = 46{\cdot}9$ lb. per sq. in.

Similarly $$(n-2)C\left(\frac{w}{A}\right)^2 = \frac{1}{2}(p_0^2 - p_{n-2}^2)$$

from which $p_{n-2} = 53{\cdot}1$ lb. per sq. in.

These calculations confirm what has already been stated above, namely, that the pressure drop per constriction increases as the absolute pressure falls. In the foregoing example, the pressure drops at the low-pressure end of the gland are comparatively large and the calculation would not yield a very accurate result.

The locus of the points BDFHKM in Fig. 168 (*b*) is a special curve, known as a Fanno curve, and may be derived in the following manner. It is again assumed that the steam is brought to rest after each constriction and that the whole process is adiathermal. Then if V is the velocity through any constriction, I_0 the initial enthalpy and I the enthalpy of the steam at velocity V,

$$I_0 - I = \frac{V^2}{2gJ} = \left(\frac{w}{A}\right)^2 \frac{v^2}{2gJ} = C \,.\, v^2$$

where C is a constant depending only on the value of w/A. If, therefore, a series of constant-volume lines are taken on the I-ϕ chart

and a value of w/A selected, the values of $I_0 - I$ may be set down, as shown in Fig. 170, to give points such as B on the Fanno curve.

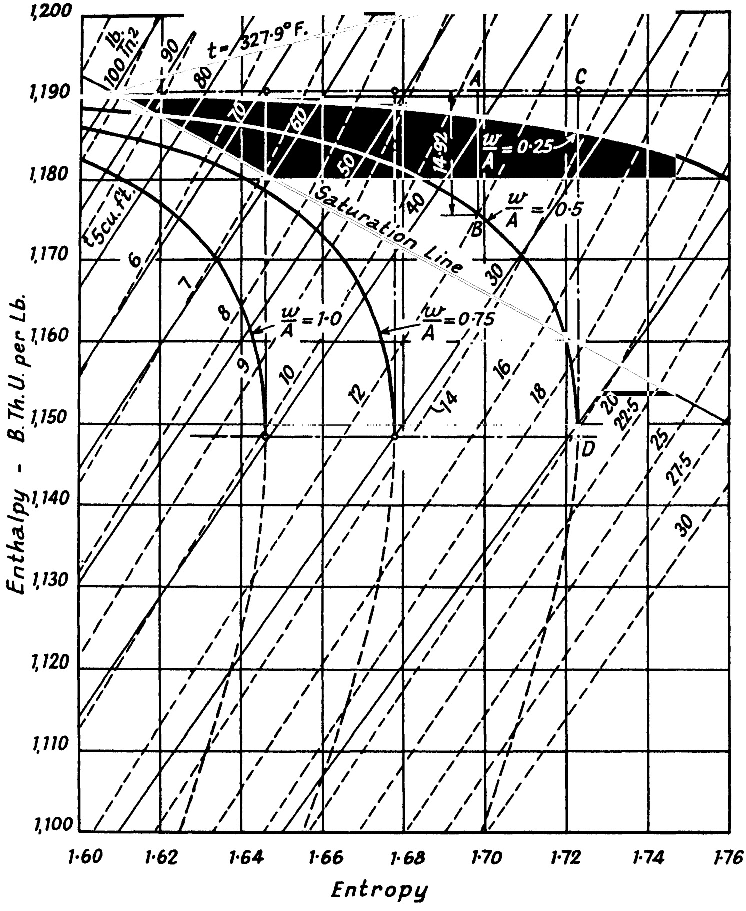


FIG. 170.—Fanno Curves on ϕ-I Chart

If w = mass flow, lb. per sec.

A = net area in sq. in.

$$I_0 - I = (0{\cdot}644\, w/A)^2 \,.\, v^2$$

Hence for $v = 12$ and $w/A = 0{\cdot}5$ (Fig. 170) $I_0 - I = 14{\cdot}92$ B.Th.U. per lb.

The complete curve may be drawn in this way. The slope (negative) gradually increases until the tangent becomes vertical at D, after which the entropy begins to diminish. This is an impossible condition in a process which is adiathermal; therefore D represents a limiting condition. It will be found that for any value of w/A the ratio p_D/p_C is the critical pressure ratio. This may be proved as follows.

In general, $dI = T \, . \, d\phi + v \, . \, \frac{dP}{J}$ and at D where $d\phi = 0$, $dI = v \, . \, \frac{dP}{J}$. By the energy equation $\frac{V \, . \, dV}{gJ} = - \, dI = - \, \frac{v \, . \, dP}{J}$.

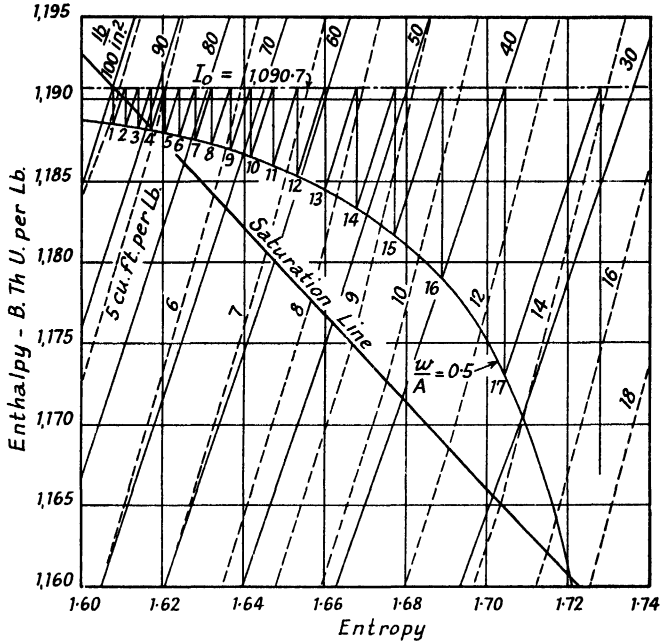


FIG. 171. Distribution of Pressure in Labyrinth Gland

Also for a constant flow area A,

$$V = \left(\frac{w}{A}\right) v \text{ and } dV = \left(\frac{w}{A}\right) dv$$

$$\therefore \qquad \left(\frac{w}{A}\right)^2 \frac{v \, . \, dv}{g} = - \, v \, . \, dP$$

$$\therefore \qquad \frac{dP}{dv} = - \frac{1}{g}\left(\frac{w}{A}\right)^2 = - \frac{1}{g}\left(\frac{V}{v}\right)^2$$

If we assume that the isentropic expansion may be represented by the equation Pv^n = constant, where n is a constant, then

$$\frac{dP}{dv} = -\frac{nP}{v}$$

$\therefore$ $V^2 = g \cdot nPv$, i.e. the velocity at the limiting point D must be the local sonic velocity. It follows that the ratio p_D/p_C is the critical.

TABLE XVII

DISTRIBUTION OF PRESSURE IN A LABYRINTH GLAND DERIVED GRAPHICALLY

Rate of flow $w/A = 0\cdot5 \dfrac{\text{lb}}{\text{in.}^2\ \text{sec.}}$ p_0 = 100 lb. per sq. in. abs. Steam initially dry and saturated.

Pocket No.	p	Pressure Ratio	Pocket No.	p	Pressure Ratio
Initial	100				0·952
		0·973	10	68·8	
1	97·3				0·947
		0·973	11	65·1	
2	94·6				0·935
		0·970	12	60·9	
3	91·7				0·930
		0·969	13	56·6	
4	88·8				0·917
		0·967	14	51·9	
5	85·7				0·894
		0·963	15	46·4	
6	82·5				0·863
		0·960	16	40·0	
7	79·2				0·805
		0·957	17	32·2	
8	75·8				
		0·954			
9	72·3				

It should be noted that the pressure on the downstream side of the final constriction may be lower than p_D.

The Fanno curve may be used for finding the pressure distribution in a labyrinth gland. Suppose, for example, that the rate of leakage is 0·5 lb. per sq. in. per sec., that the initial pressure is 100 lb. per sq. in. abs., and that the steam is initially dry and saturated. The Fanno curve, Fig. 171, is first drawn. A succession of isentropic and constant pressure lines is then drawn, as shown, giving the pressure distribution set out in Table XVII.

Under certain conditions, e.g. either a low value of the pressure p_n, or a comparatively small number of constrictions, the pressure ratio $\dfrac{p_n}{p_{n-1}}$ may be less than the critical value, i.e. 0·577 for saturated

steam, or 0·5457 for superheated steam. In that case the foregoing theory must be modified as follows.

Case II. Pressure Ratio for the Last Constriction less than the Critical Value. In this case, the rate of flow is controlled by the pressure p_{n-1} in the last pocket.

For the last constriction, we may write by eq. (52)—

$$\frac{w}{A} = C_2\sqrt{\frac{p_{n-1}}{v_{n-1}}}$$

If the steam is dry and saturated in the last pocket, i.e. at the pressure p_{n-1}, then according to eq. (53), C_2 would have the value 0·30. Reference to Fig. 168 (*b*) shows that at the beginning of the expansion in the last constriction, i.e. at point L, the steam is more or less highly superheated, and might expand down to the throat in the superheated state. Moreover, in many cases, the steam enters the gland in the superheated condition and would therefore enter the last constriction with a considerable degree of superheat. In such cases C_2 would have the value given by eq. (57), namely, 0·3155.

Assuming that $p_{n-1} \cdot v_{n-1} = C_1$

$$v_{n-1} = \frac{C_1}{p_{n-1}}$$

and

$$\frac{w}{A} = \frac{0{\cdot}3155 p_{n-1}}{\sqrt{C_1}} = \frac{p_{n-1}}{C_3}$$

where

$$C_3 = \frac{\sqrt{C_1}}{0{\cdot}3155}$$

But for $(n - 1)$ constrictions and the rate of leakage w/A, we have, by eq. (149)—

$$(n-1)C \cdot \left(\frac{w}{A}\right)^2 = \frac{1}{2}(p_0^2 - p_{n-1}^2)$$

Inserting the value $\frac{w}{A} = \frac{p_{n-1}}{C_3}$

$$(n-1)\,C\left(\frac{p_{n-1}}{C_3}\right)^2 = \frac{1}{2}(p_0^2 - p_{n-1}^2)$$

or

$$\frac{p_0}{p_{n-1}} = \sqrt{1 + 2(n-1)\frac{C}{C_3^2}} \quad . \quad . \quad (151)$$

Since $C = 2{\cdot}24C_1$ and $C_3 = \frac{\sqrt{C_1}}{0{\cdot}3155}$

$$\frac{p_0}{p_{n-1}} = \sqrt{1 + 0{\cdot}446(n-1)} \quad . \quad . \quad . \quad (152)$$

For any number n, the ratio $\frac{p_0}{p_{n-1}}$ may be calculated and thus the pressure p_{n-1} obtained. The rate of leakage may be determined from the expression

$$\frac{w}{A} = \frac{0{\cdot}3155 \, . \, p_{n-1}}{\sqrt{C_1}} = \frac{0{\cdot}3155 \, . \, p_{n-1}}{\sqrt{p_0 v_0}}$$

Values of the ratio $\frac{p_0}{p_{n-1}}$ are given in Table XVIII.

TABLE XVIII

RATIO $\frac{p_0}{p_{n-1}}$ FOR LABYRINTH GLANDS IN WHICH THE PRESSURE RATIO $\frac{p_n}{p_{n-1}}$ FOR THE LAST CONSTRICTION IS LESS THAN THE CRITICAL

Number of Constrictions	$\frac{p_0}{p_{n-1}}$ $K_1 = K_2$	$\frac{p_0}{p_{n-1}}$ $K_1 = 0{\cdot}67$, $K_2 = 0{\cdot}80$	Number of Constrictions	$\frac{p_0}{p_{n-1}}$ $K_1 = K_2$	$\frac{p_0}{p_{n-1}}$ $K_1 = 0{\cdot}67$, $K_2 = 0{\cdot}80$
2	1·202	1·278	17	2·852	3·342
3	1·376	1·507	18	2·929	3·437
4	1·529	1·705	19	3·004	3·528
5	1·668	1·882	20	3·077	3·616
6	1·797	2·044	21	3·149	3·702
7	1·917	2·194	22	3·220	3·787
8	2·030	2·334	23	3·288	3·871
9	2·137	2·467	24	3·355	3·952
10	2·239	2·593	25	3·421	4·032
11	2·336	2·712	26	3·485	4·111
12	2·430	2·827	27	3·549	4·188
13	2·520	2·938	28	3·611	4·262
14	2·607	3·044	29	3·673	4·336
15	2·691	3·145	30	3·733	4·408
16	2·773	3·249	31	3·791	4·479

The foregoing analysis is somewhat modified if the coefficient of discharge for the final constriction differs from the mean value for the preceding $n - 1$ constrictions.

Let K_1 = coefficient of discharge for constrictions in which the pressure drop is less than the critical.

K_2 = coefficient of discharge for the final constriction if the pressure drop exceeds the critical.

Then it may be shown by the methods given above that

$$\frac{p_0}{p_{n-1}} = \sqrt{1 + 0{\cdot}446(n - 1)\left(\frac{K_2}{K_1}\right)^2} \quad . \quad . \quad (152a)$$

The value of K_1 obtained by A. Egli (8) for a simplified stationary labyrinth gland with superheated steam was 0·67. In some experiments on a stationary staggered type gland with *air*, T. H. Keh and the author (9) obtained a mean value of K_1 about 0·67 and a mean value of K_2 about 0·80. Tests with single sharp-edged rings showed that the coefficient of discharge is a function of the clearance and also the pressure ratio.

EXAMPLE 23. Steam is supplied to the low-pressure gland of a steam turbine for sealing purposes. Calculate the rate of leakage into the exhaust branch, given the following data—

Shaft diameter	16 in.
Radial clearance	0·02 in.
Number of constrictions	20
Pressure of sealing steam	20
Pressure in exhaust branch	0·5
Initial superheat of sealing steam . .	60° F. ($v = 22$)

Assume (*a*) that $K_1 = K_2 = 0·8$, and (*b*) that K_1 0·67 and $K_2 = 0·8$.

(*a*) Since there are 20 constrictions, the ratio $\frac{p_0}{p_{n-1}}$ is 3·077.

$$\therefore \qquad p_{n-1} = \frac{20}{3·077} = 6·5$$

The pressure ratio for the last constriction is obviously much less than the critical. Hence the flow will be controlled by the pressure in the last dwell space.

Now $$p_0 = 20;\ v_0 = 22·0$$

$$\therefore \qquad \frac{w}{A} = \frac{0·3155 \times 6·5}{\sqrt{20 \times 22·0}}$$

$$= 0·0977 \frac{\text{lb.}}{\text{in.}^2\ \text{sec.}}$$

and since the effective leakage area is 0·804 sq. in., the approximate leakage into the exhaust branch is

$$0·0977 \times 0·804 = 0·0785 \text{ lb. per sec.}$$

(*b*) Substituting in eq. (152*a*) for n, K_1 and K_2, we find the ratio p_0 to $p_{n-1} = 3·616$. Hence $p_{n-1} = 5·53$ and $w/A = 0·0831$. Also, since the effective area is 0·804 sq. in., the rate of leakage is 0·0668 lb. per sec.

114. **Hydraulic Glands.** While we are discussing methods of preventing or minimizing leakage some attention may very properly be given to the subject of hydraulic glands, even though it has little or nothing to do with internal losses.

The hydraulic gland or water seal has been used by certain manufacturers for many years for sealing the low-pressure end of the turbine, and, in conjunction with a labyrinth gland, for sealing the high-pressure end. It consists of a "paddle wheel" (Fig. 172) keyed to the turbine shaft and rotating within a circular chamber which is in

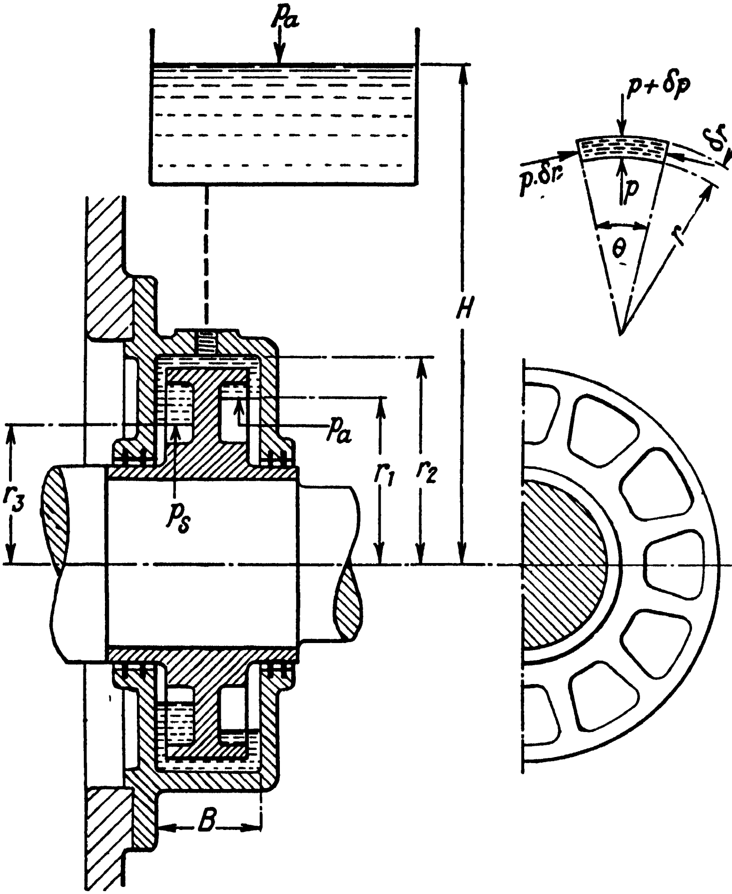


FIG. 172.—Diagrammatic Arrangement of Hydraulic Gland

halves, the upper and lower halves being bolted to the upper and lower halves of the turbine cylinder respectively. The gland chamber or box is connected to an overhead tank in which a constant level of water is maintained by a float-controlled cock. The height H is normally some 15 or 20 ft., so that in this respect the diagram is not to scale. The impeller or paddle-wheel is normally provided with radial vanes, as shown in Fig. 172, or with a number of holes bored

in the sides of the disc, but not, of course, passing right through, so that the rotation of the impeller causes a forced vortex to be set up in the chamber.

On the atmospheric side of the gland the pressure on the free surface of the water will be the atmospheric pressure p_a, whereas on the "vacuum" side that pressure will be the low steam pressure p_s. At a sufficient speed of rotation, the radii of the free surfaces on the atmospheric and vacuum sides will automatically adjust themselves to the values r_1 and r_3, the pressure at the extreme radius r_2 of the vortex balancing the pressure $p_a + \rho H$ due to the head of water in the tank.

Let ρ = density of water in lb. per cub. in. (0·0362).
g = acceleration of gravity, $32{\cdot}2 \times 12$ in. per sec.²
ω = angular velocity, radians per sec.

Considering a transverse slice of water of unit depth—

$$\text{Volume of element} = r \,.\, \theta \,.\, \delta r$$

$$\text{Centrifugal force on element} = \frac{\rho\omega^2 r^2}{g} \,.\, \theta \,.\, \delta r$$

Equating radial forces on element—

$$(p + \delta p)(r + \delta r)\theta = p \,.\, \theta \,.\, \delta r + p \,.\, r \,.\, \theta + \frac{\rho\omega^2 r^2}{g} \,.\, \theta \,.\, \delta r$$

Ignoring quantities of the second order of smallness—

$$\delta p = \frac{\rho\omega^2}{g} \,.\, r \,.\, \delta r$$

By integrating—

$$p_2 - p_1 = \frac{\rho \,.\, \omega^2}{2g}(r_2^2 - r_1^2)$$

But $$p_2 = p_a + \rho H, \text{ and } p_1 = p_a$$

$$\therefore \quad \rho H = \frac{\rho \,.\, \omega^2}{2g}(r_2^2 - r_1^2)$$

$$H = \frac{\omega^2}{2g}(r_2^2 - r_1^2)$$

i.e. $$H \text{ in.} = 14{\cdot}2\left(\frac{N}{1{,}000}\right)^2 (r_2^2 - r_1^2) \qquad (153)$$

$$p_a - p_s = \frac{\rho \,.\, \omega^2}{2g}(r_1^2 - r_3^2)$$

$$= 0{\cdot}513\left(\frac{N}{1{,}000}\right)^2 (r_1^2 - r_3^2) \text{ lb. per sq. in.} \qquad (154)$$

If a plain disc be used instead of a paddle wheel, then the mean speed of rotation of the forced vortex will probably be about one-half of the rotational speed of the shaft. An appropriate value of N will then have to be used in applying the foregoing formulae.

115. Advantages and Disadvantages of Hydraulic Glands. With ordinary labyrinth glands there is necessarily an escape of vapour into the turbine room. Under certain conditions, such vapour condenses on walls, windows and on other parts of the turbine room, and is undoubtedly a nuisance. This may be prevented absolutely by means of the hydraulic gland.

The hydraulic gland will operate automatically under all conditions of load and there is, consequently, no need to make adjustments to the gland steam supply as with certain arrangements of labyrinth glands. In turbines operating with high-temperature steam the hydraulic gland removes a considerable amount of heat from the shaft and so ameliorates conditions in the adjacent bearing.

Owing to friction losses in the gland and possibly to conduction of heat, the water in the gland is constantly being heated. Consequently, its temperature rises until it reaches the saturation temperature on the vacuum side, when a slow evaporation takes place, the vapour formed passing into the condenser. A small make-up must be constantly supplied from the overhead tank and unless a chemically pure water, such as condensate, be supplied there is a risk of scale formation in the gland.

116. Residual Velocity Loss. In a multi-stage turbine, the energy corresponding to the final absolute velocity in any stage is largely utilized in the nozzles of the succeeding stage. For a discussion of this, the reader is referred to Art. 80.

In the final stage of a turbine, however, the kinetic energy corresponding to the final absolute velocity of the steam as it leaves the wheel is either wholly or partially lost. If no attempt is made to reduce the steam velocity between the last wheel and the exhaust branch, then the kinetic energy is entirely lost. In some cases, however, guide vanes are arranged in the exhaust hood, thus providing steam passages of gradually increasing area and a certain diffuser action. When such means are effective, the final velocity of the steam may be somewhat reduced and the steam pressure at outlet from the last wheel may be slightly lower than the pressure at the exhaust branch. It is doubtful, however, whether such guide vanes do more than permit the steam to turn through a right angle with less loss than if the guide vanes were not fitted.

Let V_2 = absolute velocity of steam at outlet from last-stage wheel.

H_a = adiabatic heat drop in turbine.

Then, energy loss $= \dfrac{V_2^2}{2gJ}$ B.Th.U. per lb. and the percentage loss

due to the terminal velocity $= \frac{V_2^2}{2gJ \cdot H_a} \times 100$ per cent.

The equivalent power loss

$$= \frac{w \cdot V_2^2}{2g \times 550}$$

$$= \frac{w \cdot V_2^2}{35{,}400} \text{ horse-power}$$

where w = steam flow through turbine in lb. per sec.

In a turbine in which the steam flow in the various stages is not uniform, as for example when regenerative feed-heating is used, a somewhat different method of calculating the residual velocity (or carry-over) loss must be adopted.

Let w_0 = steam flow into turbine, lb. per sec.

w_e = total steam flow through exhaust branch or branches (if more than one exhaust is used), lb. per sec.

V_e = absolute velocity of exhaust steam.

W = total effective work done in turbine, expressed in B.Th.U. per lb. of steam entering turbine (see Chapter XIII).

Then the carry-over loss would be given by the expression

$$\frac{w_e}{w_0} \cdot \frac{V_e^2}{2g \cdot J \cdot W} \times 100 \text{ per cent}$$

This differs a little in principle from the preceding expression deduced for a constant steam flow, because here the effective work is taken as the basis instead of the isentropic heat drop. This is done for convenience.

BIBLIOGRAPHY

1. Stodola: *Dampf- und Gas-Turbinen*, 6th Ed., p. 162.
2. Odell: "Preliminary Experiments on Air Friction." *Engineering*, 1904; 77; 30.
3. Von Kármán: "Ueber laminare und turbulente Reibung." *Zeit. für angewandte Math. und Mech.*, 1921; 1; 233.
4. Ribary: "The Friction Losses of Steam Turbine Discs." *Brown Boveri Review*, 1934; 120.
5. Sigwart: *Forschungsarbeiten auf dem Gebiete des Ingenieurwesens*, 1936; 7; 109.
6. Kerr: "The Steam Friction of Turbine Wheels." *Engineering*, 1913; 96; 268.
7. Kerr: "On Turbine Disc Friction." *Jour. Roy. Tech. Coll., Glasgow*, 1924; 1; 103.
8. Egli: "The Leakage of Steam through Labyrinth Seals." *Trans. A.S.M.E.*, 1935; 57; 115.
9. Kearton and Keh: "Leakage of Air through Labyrinth Glands of Staggered Type." *Proc. I. Mech. E.* 1952; 166; 180.

EXAMPLES XI

1 Calculate the power absorbed in disc friction in a de Laval turbine having a rotor 6 5 in diameter running at 25 000 r p m —

(*a*) When the pressure in the turbine cylinder is 2 lb per sq in abs, and the steam is dry and saturated ($v_s = 173\ 5$)

(*b*) When the pressure in the turbine cylinder is 15 lb per sq in abs, and the steam is superheated 40° F ($v_s = 27\ 9$)

2 The first stage wheel of a 20 000 kW turbine is a single-row wheel having a mean diameter 84 in The speed of rotation is 1,500 r p m The condition of the steam in the first stage is as follows—

Pressure	250
Superheat	200° F
Specific volume	2 43 cub ft per lb

The blades are 1 25 in long and the active nozzles cover 40 per cent of the total circumference at full load Calculate—

(*a*) Horse power absorbed by disc friction

(*b*) Horse power absorbed by blade windage, using Kerr's 1924 formula for item (*b*)

3 The discs in the high pressure cylinder of a two cylinder steam turbine of 50 000 kW output are 36 in mean diameter the speed being 1 500 r p m Calculate the disc friction horse power in the first stage, given that the steam conditions are as follow—

Steam pressure	400
Steam superheat	320° F
Steam specific volume	1 76

4 Calculate the leakage loss through the diaphragm packing in a turbine stage under the following conditions—

Steam pressure before nozzles	200
Steam superheat before nozzles	100° F
Steam pressure after nozzles	180
Shaft diameter	10 in
Radial clearance	0 015 in
Number of constrictions	4
Coefficient of contraction	0 75

Calculate also the pressures in the dwell spaces

5 In the intermediate pressure turbine of a three cylinder marine turbine installation there is a diaphragm separating the intermediate pressure ahead turbine and the high-pressure astern turbine When the turbines are running ahead the steam pressure in the intermediate pressure exhaust is 25 lb per sq in abs the steam being dry and saturated and the high pressure astern turbine is running idly in steam at the exhaust pressure, which is 0 6 lb per sq in abs

Calculate the approximate hourly leakage of steam through the partition gland (labyrinth type) given that the shaft diameter is 9 5 in, the radial clearance of the labyrinth packing is 0 02 in, the number of constrictions 20, and the coefficient of contraction 0 8 Neglect any heat losses

6 The external shaft gland of a steam turbine consists of a section A with 24 constrictions extending between the first stage wheel chamber ($p = 400$, $v = 1\ 6$ cu ft per lb) and a pocket which communicates with a stage of the turbine where $p = 200$ together with a section B with 16 constrictions extending between the above mentioned pocket and another pocket which is connected to the exhaust branch ($p = 120$)

The shaft gland has a mean diameter of 8 in., the clearance is 0·015 in. and the discharge coefficient is 0·75. Assuming no heat loss from the gland, calculate the steam flow into the intermediate stage of the turbine per hour. (*Liv. Un.*)

7. A labyrinth gland has a mean diameter of 10 in., a clearance of 0·015 in. and 40 constrictions. Steam enters the gland at 400 lb. per sq. in. abs. and 400° F. superheat, the pressure on the downstream side of the gland being 20 lb. per sq. in. abs. If the coefficient of discharge for the first 39 constrictions is 0·67 and that for the final constriction 0·80, find the steam pressure in the last three dwell spaces and the rate of leakage through the gland.

CHAPTER XII

STATE POINT LOCUS AND REHEAT FACTOR

117. Stage Efficiency of Impulse Turbines. Consider a stage of an impulse turbine and let

w_i = total internal steam flow, lb. per sec.
w_n = steam flow through nozzles, lb. per sec.
w_g = steam flow through diaphragm gland.

Then $$w_i = w_n + w_g$$

Let h_n = adiabatic heat drop in the nozzles of a pure impulse turbine.

a.h.p. = adiabatic horse-power of the stage, i.e. the horse-power based on the total internal steam flow and the adiabatic heat drop.

s.h.p. = shaft horse-power developed in the stage, i.e. the actual power transmitted by the wheel to the rotor spindle.

Then the stage efficiency is defined as the ratio of the shaft horse-power to the adiabatic horse-power.

i.e. $$\eta_s = \frac{\text{s.h.p.}}{\text{a.h.p.}} \quad . \quad . \quad . \quad . \quad (155)$$

Now the adiabatic work done per second by w_i lb. of steam

$$= w_i \,.\, h_n \text{ B.Th.U.}$$
$$= 778{\cdot}3 w_i \,.\, h_n \text{ ft.-lb.}$$

$$\therefore \qquad \text{a.h.p.} = \frac{778.3}{550} \,.\, w_i \,.\, h_n$$

or $$\text{a.h.p.} = 1{\cdot}415 w_i \,.\, h_n \quad . \quad . \quad . \quad (156)$$

In an impulse-reaction turbine where the total adiabatic heat drop in the stage is $h_n + h_b$—

$$\text{a.h.p.} = 1{\cdot}415 \,.\, w_i(h_n + h_b) \quad . \quad . \quad (157)$$

The shaft horse-power is less than the blade or rim horse-power by the amount of power absorbed in overcoming wheel friction, i.e. the sum of the disc friction and blade windage losses. Using the symbol r.h.p. to represent the "rim" or blade horse-power—

$$\text{r.h.p.} = \text{s.h.p.} + \text{h.p.}_{d} + \text{h.p.}_{bw}$$

118. State Point Locus on ϕ-I Diagram for Single Stage of an Impulse Turbine. Consider any stage of an impulse turbine and let

A, Fig. 173, represent the initial condition of the steam on the ϕ-I diagram. Suppose that steam expands in the nozzles from p_1 to p_2. Then AB represents the adiabatic and isentropic expansion. Due to losses in the nozzles, the actual path of the state point during expansion is AC, as already explained in Art. 51.

The steam now enters the blades where the rim horse-power (r.h.p.) is developed. Basing the work done per lb. of steam on the total internal flow w_i, the work done per lb. of steam is

$$I_A - I_D = \frac{550 \times \text{r.h.p.}}{778 \cdot 3 \times w_i} \text{ B.Th.U. per lb.}$$

i.e.
$$I_A - I_D = 0 \cdot 707 \frac{\text{r.h.p.}}{w_i} \quad . \quad . \quad . \quad (158)$$

This may also be proved by the steady flow equation provided it be assumed that the absolute steam velocity at exit from the blades is identical with that of the steam entering the nozzles. The part CD of the p_2 line represents the reheating of the steam due to "blade friction" taking place, supposedly, at constant pressure. This method of showing reheating is not as accurate as it is convenient, because although the steam pressure at outlet from the blade equals that at inlet to the blade, the pressure in the blade channels is not constant.

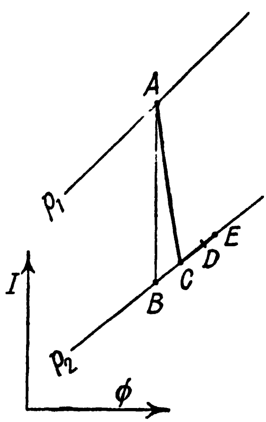


FIG. 173

Due to friction and blade windage (when it occurs) the steam is further reheated, the frictional reheat being

$$I_E - I_D = \frac{0 \cdot 707 \ . \ \text{h.p.}_{wf}}{w_i} \quad . \quad (159)$$

The point E may be obtained directly from the shaft horse-power of the stage, for, granted the conditions stated above regarding the initial and final steam velocities, then by the steady flow equation

$$I_A - I_E = 0 \cdot 707 \frac{\text{s.h.p.}}{w_i} \quad . \quad . \quad . \quad (160)$$

i.e.
$$\text{s.h.p.} = 1 \cdot 415 \ . \ w_i(I_A - I_E)$$

Also, by eq. (156), a.h.p. $= 1 \cdot 415 w_i(I_A - I_B)$

Hence
$$\eta_s = \frac{\text{s.h.p.}}{\text{a.h.p.}} = \frac{I_A - I_E}{I_A - I_B}$$

Thus, if η_s be known or assumed, the position of the end state point E for a stage may be readily obtained. The point E now becomes the initial state point for the succeeding stage of the turbine.

119. State Point Locus for Multi-stage Turbine. Suppose, for the sake of illustration, that a turbine has ten stages operating between pressure limits P_0 and P_{10}, and suppose that the stage efficiency of each stage is known and equal to η_s. Then the locus of the state point may be drawn on the ϕ-I diagram in the following manner.

Referring to Fig. 174, the initial state point A is set down according to the known initial pressure and superheat. Suppose the stage

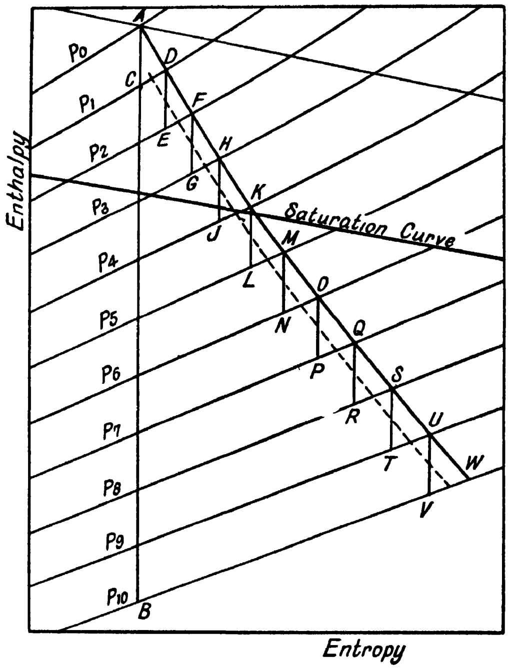


FIG. 174.—Locus of State Point on ϕ-I Diagram

pressures are P_1, P_2, . . P_{10}. AC is drawn to represent the adiabatic expansion in stage 1, and I_D is found from the relation

$$I_A - I_D = \eta_s(I_A - I_C)$$

Point D is then set down with the I_D value on the P_1 line. DE is drawn, giving $I_D - I_E$ and I_F calculated from the relation

$$I_D - I_F = \eta_s(I_D - I_E)$$

In this way the zig-zag line is drawn for the ten stages. The points D, F, H, . . . S, U, W represent the condition of the steam in the wheel chambers of the ten stages, i.e. at the blade outlets. If the nozzle efficiency is known, the condition of the steam at outlet

from the nozzles may also be obtained, giving the lower locus parallel to the curve DFH . . . UW.

Such curves are essential in the design of a steam turbine because if the efficiency of the various stages is known fairly accurately, it is possible to derive from the Mollier diagram the superheat, or dryness fraction, as the case may be, and the specific volume of the steam at the assumed pressures.

The sum of the adiabatic heat drops (AC + DE + FG + etc.) from the initial steam pressure down to any given pressure is usually termed the "cumulative" heat drop and will be represented by the symbol H_c.

120. Condition Curves. For the purpose of design the various quantities obtained from the Mollier diagram may be set out in the manner originally suggested by Professor Goudie (1). The method adopted by the author, however, is somewhat different from that given by Goudie and is shown in Fig. 175. The base of the diagram shows values of p plotted to a log. scale, the higher values being at the left-hand side since expansion proceeds from the higher pressure. Plotted values of H_c then lie on a flat curve which is easily drawn with a batten. The curves showing the degree of superheat and the wetness fraction may also be drawn in the same way. Instead of plotting values of v, the author plots $\log_{10} v$, thus obtaining (with a uniform stage efficiency) two straight lines, one for the superheat region and the other for the wet region, the two lines intersecting exactly at the pressure where the superheat vanishes.

Fig. 175 has been worked out for the following conditions—

Initial steam pressure	200 lb. per sq. in. abs.
Initial steam superheat . .	150° F.
Final steam pressure	1 lb. per sq. in. abs.
Stage efficiency	0·75
Number of stages	10

In the initial stages of the calculation, when the exact heat drop per stage is not known, the condition curve may be drawn on the Mollier diagram by a step-by-step process, the adiabatic heat drop per step being taken approximately equal to the expected stage heat drop.

Assuming that the curve H_c (Fig. 175) has been so obtained, the pressure distribution in the turbine may be worked out in the following manner. If the mean diameter of all stages is the same then, if the ratio of blade speed to steam speed is constant, it follows that the adiabatic heat drop h_n will be the same for all stages.

$$\therefore\ h_n = \frac{H_c}{10} = 38{\cdot}8 \text{ B.Th.U. per lb.}$$

Thus by subdividing H_c into ten equal parts, drawing horizontals to intersect the H_c curve and projecting vertically on to the base

line, the various stage pressures are obtained. The values of v_n, the specific volume at outlet from the nozzles, and v_b, the specific

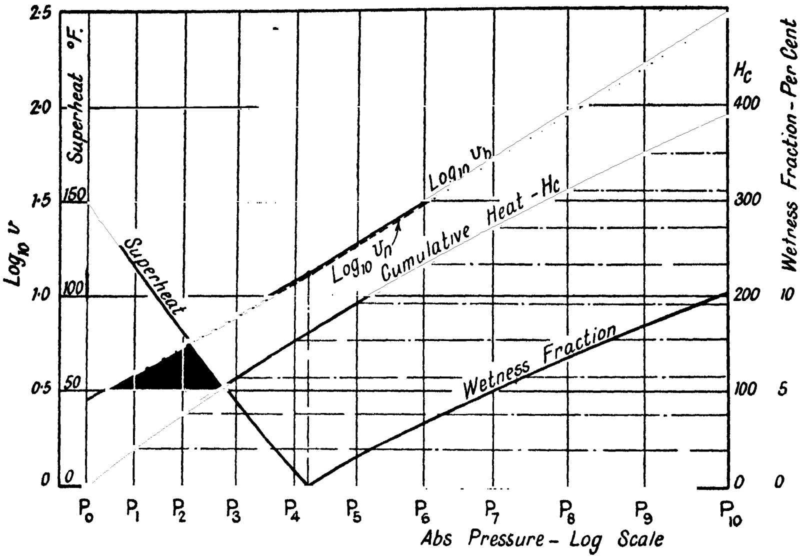


FIG. 175.—Condition Curves for Ten-stage Turbine

volume at outlet from the blades are also obtained. Such data may then be tabulated for design purposes, as shown in Table XIX.

TABLE XIX

VALUES OF STAGE PRESSURES, STEAM QUALITY, AND SPECIFIC VOLUMES FOR TEN-STAGE STEAM TURBINE

Stage No.	p	v_n	v_b	Condition of Steam at Blade Outlet
1	134·9	3·855	3·908	114·2° F. Superheat
2	89·7	5·383	5·470	78·8° F. ,,
3	57·4	7·834	7·943	42·7° F. ,,
4	35·3	11·67	11·86	7·1° F. ,,
5	21·0	18·58	18·79	1·55% Wetness
6	12·2	30·48	30·90	3·40% ,,
7	6·87	51·05	51·76	5·11% ,,
8	3·72	89·33	90·36	6·82% ,,
9	1·98	158·9	160·7	8·47% ,,
10	1·00	297·2	299·4	10·11% ,,

121. Correction for Terminal Velocity. In certain cases, e.g. the L.P. stages of turbines of large output, the final absolute velocity

at outlet from the blades in a stage is greater than the inlet velocity to the nozzles of that stage. Applying the steady flow equation, and referring to Fig. 173—

$$I_A + \frac{V_A^2}{2gJ} = I_B + \frac{V_B^2}{2gJ} + \text{Work done}$$

$$= I_B + \frac{V_B^2}{2gJ} + 0{\cdot}707\,\frac{\text{s.h.p.}}{w_i}$$

from which $$I_A - I_B = 0{\cdot}707\,\frac{\text{s.h.p.}}{w_i} + \frac{V_B^2 - V_A^2}{2gJ} \quad . \quad . \quad (161)$$

Considering the turbine as a whole, we may ignore the kinetic energy of the steam entering the first-stage nozzles. Then if V_2 represents the final absolute velocity of the steam leaving the last-stage wheel, and p_0 and p_n are the initial and final pressures, respectively, Fig. 176, then considering first the frictionless adiabatic expansion we have

$$I_A = I_B + \frac{V_2^2}{2gJ} + \text{Work done per lb.}$$

i.e. $$\text{Work done} = (I_A - I_B) - \frac{V_2^2}{2gJ}$$

This is another way of considering the residual velocity loss dealt with in Art. 116.

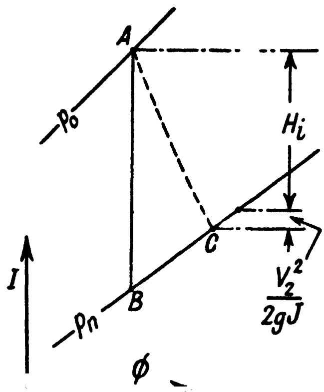


FIG. 176

Let H_i = total internal work done in turbine, B.Th.U. per lb. of steam

i.e. $$H_i = \sum_0^n 0{\cdot}707\,\frac{\text{s.h.p.}}{w_i}$$

Then $$I_A = I_C + \frac{V_2^2}{2gJ} + H_i$$

or $$I_A - I_C = H_i + \frac{V_2^2}{2gJ} \quad . \quad . \quad . \quad (162)$$

122. Reheat Factor. If a state point locus or condition curve ACDE . . UVW be drawn as shown in Fig. 174, and if the cumulative heat $H_c = \Sigma h_n$ be worked out, it will be found that H_c is somewhat greater than the adiabatic heat drop H_a = AB.

The ratio $$R = \frac{H_c}{H_a} \quad . \quad . \quad . \quad . \quad (163)$$

is known as the reheat factor. The value of R depends upon the turbine stage efficiency, the initial pressure and superheat, and on the final pressure. Since the number of stages in the turbine will depend on H_c and the Mollier diagram only gives directly the value of H_a, the reheat factor becomes an important quantity in the initial stages of design. Before giving expressions for the value of the reheat factor, we shall endeavour to explain it.

Consider first of all the expansion of initially dry and saturated steam in a turbine, and assume that expansion takes place in thermal equilibrium. Assume, for the sake of simplicity, that the turbine has only four stages. Fig. 177 shows the T-ϕ diagram

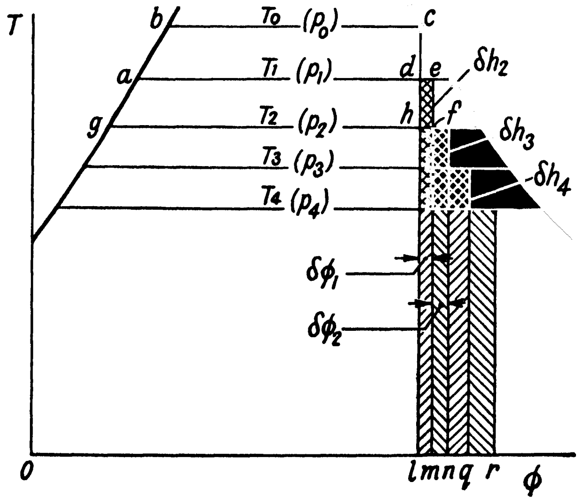


FIG. 177

and Fig. 178 the ϕ-I diagram for the expansion. These are lettered to correspond, as far as possible.

The adiabatic heat drop h_1 in the first stage of the turbine is represented by the area *abcd* in Fig. 177 and by the length *cd* in Fig. 178. This is unaffected by losses. The point *e* represents the condition of the steam at inlet to the second stage. Assuming equal initial and final velocities in each stage, then

$$I_c - I_e = \eta_s(I_c - I_d)$$

$I_e - I_d$ is termed the "frictional reheat." This is the energy dissipated in friction, shock and leakage losses and "returned" to the steam as heat. Clearly

$$I_e - I_d = (1 - \eta_s)h_1$$

and is represented by the area *ldem* in Fig. 177.

Therefore, the gain of entropy due to frictional reheating in the first stage—

$$\delta\phi_1 = (1 - \eta_s)\frac{h_1}{T_1}$$

Of the first-stage reheat, represented by the area *ldem*, the part that is available for the performance of mechanical work in the remaining stages of the turbine is the fraction $\frac{T_1 - T_4}{T_1}$, and is represented by the cross-hatched area. The increase in the adiabatic

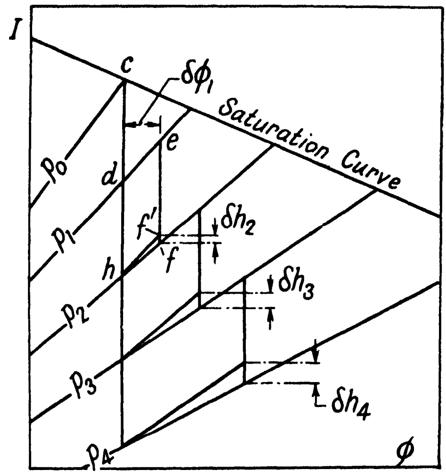


FIG. 178

heat drop in the second stage due to the friction losses in the first stage is represented by the area *defh*.

In the Mollier diagram, let *hf'* be drawn parallel to *de*. Then *def'h* is a parallelogram and *ef'* is equal to *dh*. But *ef* is the adiabatic heat drop in the second stage. Therefore, *f'f* represents the increase in the second stage adiabatic heat drop due to the friction losses in the first stage. Now the slope of a constant pressure line has been shown in Art. 27 (eq. (24)) to be equal to the absolute temperature. Thus, for *de* and *hf'*—

$$\frac{dI}{d\phi} = T_1$$

and for *hf*

$$\frac{dI}{d\phi} = T_2$$

$$\therefore\ I_f' - I_h = T_1 \,.\, \delta\phi_1$$

and

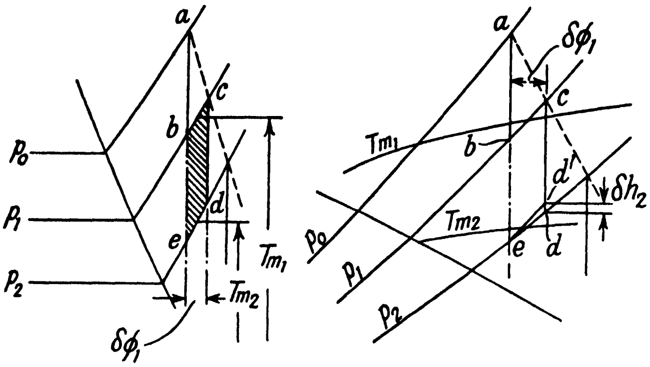
$$I_f - I_h = T_2 \,.\, \delta\phi_1$$

$$\therefore\ I_f' - I_f = \delta h_2 = (T_1 - T_2)\delta\phi_1$$

$$= \text{Area } defh \text{ (Fig. 177)}$$

A similar reheating of the steam takes place in the succeeding stages, but the availability of the reheat becomes smaller and smaller as the pressure at which reheating is effected falls. For this reason, it is preferable to have an inefficient stage, e.g. a two-row velocity wheel, at the H.P. end of the turbine rather than at the L.P. end. The total increase in the sum of the stage adiabatic heat drops is represented in Fig. 177 by the double-hatched area, and in Fig. 178 by the sum $\delta h_2 + \delta h_3 + \delta h_4$.

When the expansion in a stage takes place wholly in the superheat region, the conditions are as shown in Fig. 179 (*a*) (T-ϕ diagram) and Fig. 179 (*b*) (ϕ-I diagram). The gain in heat drop in the second



(*a*) (*b*)

FIG. 179

stage is clearly equal to the area *ebcd*, to scale, on Fig. 179 (*a*). In the ϕ-I diagram, Fig. 179 (*b*), the constant-pressure lines *bc* and *ed*, although curved, are so short that they may be considered as straight lines. As before, draw *ed'* parallel to *bc*. Let T_{m1} and T_{m2} represent the mean absolute temperatures of the steam between *b* and *c*, and between *e* and *d*, respectively.

Then $$I_{d}' - I_e = T_{m1} \cdot \delta\phi_1$$

and $$I_d - I_e = T_{m2} \cdot \delta\phi_1$$

$$\therefore\ \delta h_2 = I_{d}' - I_d = (T_{m1} - T_{m2})\delta\phi_1$$
$$= \text{Area } bcde \text{ (Fig. 179 } (a)\text{)}$$

A similar argument may be applied to other stages where expansion takes place entirely in the superheat region, or partly in the superheat and partly in the saturated region.

The reheat factor is greater, the larger the number of stages for a given pressure range and the lower the stage efficiency.

123. Reheat Factor for an Expansion with a Uniform Adiabatic Index and a Constant Stage Efficiency. Consider the frictionally

resisted expansion of steam which, when expanding adiabatically, follows the law pv^n = constant, and let η_s be the stage efficiency. Furthermore, assume that the number of stages is very large and, therefore, that the adiabatic heat drop in each stage is extremely small. In this case the condition curve, instead of being stepped, is a continuous curve, corresponding to which we have the curve BC in the p-v diagram, Fig. 180. It will be shown that given an adiabatic relation pv^n = constant, there is a corresponding equation pv^m = constant for the curve BC.

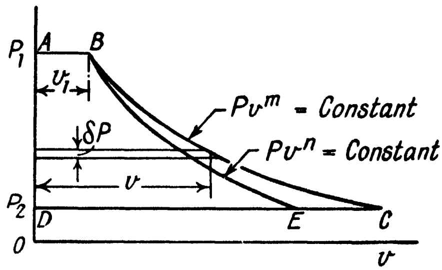


FIG. 180

In expanding from P to P + δP, the heat available is equal to $- v \,.\, \delta P$ ft.-lb., the minus sign being used because δP is negative. If the efficiency of the small expansion is η_s, the reheat is

$$\delta H = -\ (1 - \eta_s)v \,.\, \delta P \quad \text{ft.-lb.}$$

By the First Law of Thermodynamics—

Heat supplied – Work done + Gain of internal energy

or
$$\delta H = P \,.\, \delta v + \delta E$$

For an adiabatic change, since $\delta H = 0$,

$$\delta E = - P \,.\, \delta v$$

But
$$Pv^n = \text{Const.} = C$$

$\therefore$
$$\delta E = - C \,.\, v^{-n} \,.\, \delta v$$

or
$$E = - C\int v^{-n} \,.\, dv$$

$$= - C\left(\frac{v^{1-n}}{1-n}\right) + \text{Const. of integration } C_1$$

$$= - \frac{Pv}{1-n} + C_1$$

$\therefore$
$$\delta E = \frac{P \,.\, \delta v + v \,.\, \delta P}{n-1}$$

$$\therefore \qquad -(1-\eta_s)v\,.\,\delta P = P\,.\,\delta v + \frac{P\,.\,\delta v + v\,.\,\delta P}{n-1}$$

$$\therefore \qquad \{n-\eta_s(n-1)\}\frac{\delta P}{P} + n\,.\,\frac{\delta v}{v} = 0$$

Integrating—

$$\{n-\eta_s(n-1)\}\log_e P + n\log_e v = \text{Constant}$$

$$\therefore\ Pv^m = \text{Constant}$$

where
$$m = \frac{n}{n-\eta_s(n-1)} \quad . \quad . \quad . \quad (164)$$

Thus the modified expansion can be represented by the equation $Pv^m = C$, where m, the index, is a function of the adiabatic index n and the stage efficiency η_s. Provided n is constant and also that η_s is constant, m must be constant.

Referring to Fig. 180, the sum of the adiabatic heat drops in the actual turbine is represented by the area ABCD, whereas the adiabatic heat drop in the frictionless turbine is ABED.

Hence
$$R = \frac{\text{Area ABCD}}{\text{Area ABED}} = \frac{H_c}{H_a}$$

$$H_c = \frac{m\,.\,P_1v_1}{m-1}\left\{1-\left(\frac{1}{r}\right)^{\frac{m-1}{m}}\right\} \text{ ft.-lb.}$$

$$H_a = \frac{n\,.\,P_1v_1}{n-1}\left\{1-\left(\frac{1}{r}\right)^{\frac{n-1}{n}}\right\} \text{ ft.-lb.}$$

where
$$r = \frac{P_1}{P_2}$$

Hence
$$R = \frac{m(n-1)}{n(m-1)}\,.\,\frac{1-\left(\frac{1}{r}\right)^{\frac{m-1}{m}}}{1-\left(\frac{1}{r}\right)^{\frac{n-1}{n}}}$$

Substituting for m the value $\dfrac{n}{n-\eta_s(n-1)}$

$$R = \frac{1}{\eta_s}\,\frac{1-\left(\frac{1}{r}\right)^{\eta_s\left(\frac{n-1}{n}\right)}}{1-\left(\frac{1}{r}\right)^{\frac{n-1}{n}}} \quad . \quad . \quad . \quad (165)$$

124. Reheat Factors for Steam Expanding wholly in the Superheat Region. Here $n = 1{\cdot}3$ and therefore—

$$R = \frac{1}{\eta_s} \cdot \frac{1 - \left(\frac{1}{r}\right)^{0{\cdot}2308\eta_s}}{1 - \left(\frac{1}{r}\right)^{0{\cdot}2308}} \tag{166}$$

For values of η_s lying between 0·8 and unity, the reheat fraction $R - 1$ is very nearly proportional to $(1 - \eta_s)$. By plotting these values against $\log_{10} r$, the author finds that—

(1) For values of $\frac{P_1}{P_2}$ between 5 and 15—

$$R = 1 + (1 - \eta_s)\left(0{\cdot}246 \log_{10} \frac{P_1}{P_2} + 0{\cdot}003\right) \quad . \tag{167}$$

(2) For values of $\frac{P_1}{P_2}$ between 15 and 40—

$$R = 1 + (1 - \eta_s)\left(0{\cdot}205 \log_{10} \frac{P_1}{P_2} + 0{\cdot}051\right) \quad . \tag{168}$$

These formulae are theoretically correct for values of η_s between 0·8 and 1·0, and for an infinite number of stages.

125. Reheat Factors for Steam Initially Dry and Saturated and Expanding in Thermal Equilibrium. Zeuner's index $n = 1{\cdot}135$ is not the same for all initial pressures, nor is it strictly constant for the whole of any expansion. Consequently, formula (165) does not yield very reliable values of the reheat factor. The author finds that R is given sufficiently nearly for practical purposes by the equation—

$$R = 1 + (1 - \eta_s)\left(0{\cdot}09 \log_{10} \frac{P_1}{P_2} - 0{\cdot}02\right) \quad . \tag{169}$$

126. Correction for Finite Number of Stages. The expressions given above for the reheat factor apply only to a turbine having an infinite number of stages. They could be applied with little error to turbines having a relatively large number of stages. The approximate correction for a finite number of stages may be easily found provided certain simplifying assumptions are made. Figs. 181 (*a*) and 181 (*b*) show the T-ϕ diagrams for expansions in the saturated and superheat regions respectively. AB shows the adiabatic expansion and AC the actual expansion line for an infinite number of stages. In each case, let ϕ be the gain of entropy due to reheating, n the number of stages in the actual turbine, and assume that the total gain of entropy is the same for a finite as for an infinite number of stages. Let T be the temperature range AB in each case and suppose that the temperature drop in each stage is uniform.

For the purpose of the proof we shall further assume that AC is a straight line and that the constant-pressure lines in Fig. 181 (*b*) are straight. Then—

(1) Increase of adiabatic heat drop when n is infinite

$$= \text{Area ABC} = \frac{T\phi}{2}$$

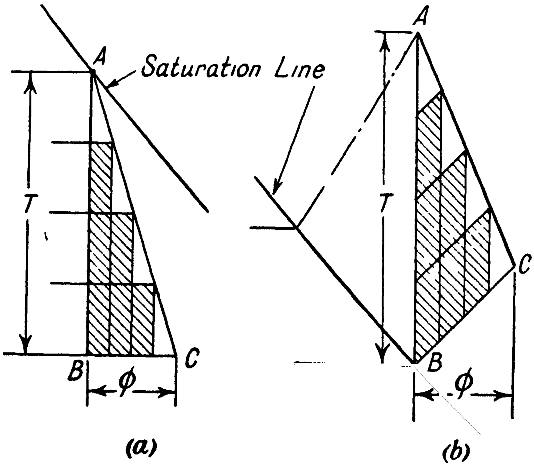


FIG. 181

(2) Increase of adiabatic heat drop when n is finite

$$= \text{Shaded area}$$

$$= \text{Area ABC} - \frac{n}{2} \cdot \frac{T}{n} \cdot \frac{\phi}{n}$$

$$= \frac{T\phi}{2}\left(1 - \frac{1}{n}\right)$$

Let R_∞ = reheat factor for infinite number of stages.

R_n = reheat factor for n stages.

Then $$R_\infty - 1 = \frac{T\phi}{2H_a}$$

and $$R_n - 1 = \frac{T\phi}{2H_a}\left(\frac{n-1}{n}\right)$$

i.e. $$\frac{R_n - 1}{R_\infty - 1} = \left(\frac{n-1}{n}\right) \quad . \quad . \quad . \quad (170)$$

127. Reheat Factors for Steam Expanding partly in the Superheated Condition and partly in the Saturated Condition. This offers a rather more complicated problem which is beyond the scope of this book. Values of R may, however, be obtained by drawing the condition curve on the Mollier chart by the step-by-step method,

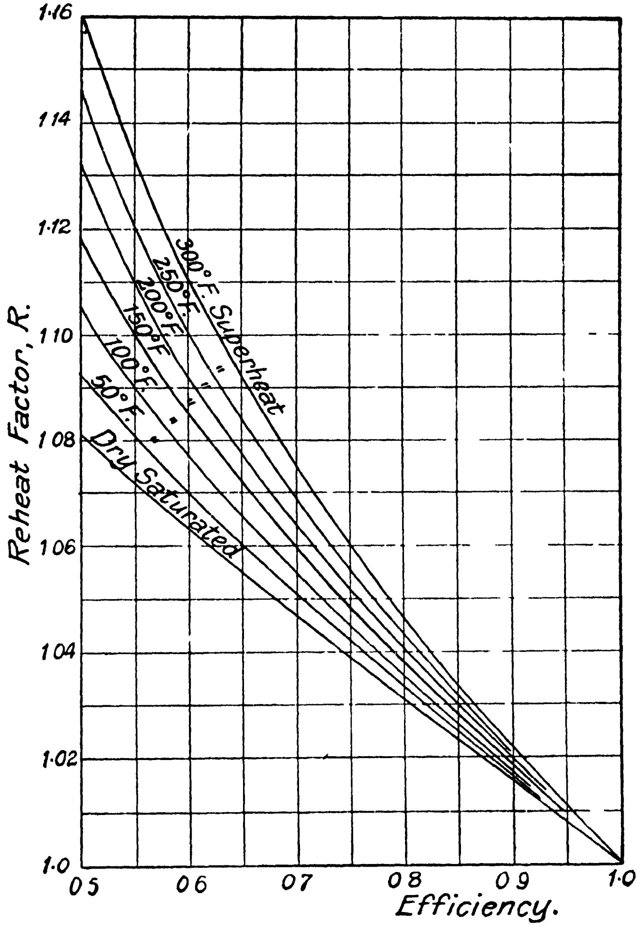


FIG. 182

using suitable heat drops. The curves given in Fig. 182 were obtained in this way for the following basic data—

Initial steam pressure . . .	200 lb. per sq. in. abs.
Exhaust steam pressure . .	1 ,, ,, ,,
Approximate stage heat drop .	40 B.Th.U. per lb.

In turbines having more than ten stages, the value of R would be slightly higher than that given by the curves.

For further work on this subject the reader is referred to articles and papers by Messrs. E. L. Robinson (2), H. G. Yates (3), R. B. Smith (4), Professor C. G. Thatcher (5), and Dr. D. M. Smith (6).

128. Internal Efficiency. The internal efficiency η_i is defined as the ratio of the internal work done in the turbine, expressed in B.Th.U. per lb. of steam, to the adiabatic heat drop,

i.e. $$\eta_i = \frac{H_i}{H_a} \qquad (171)$$

If η_s is the mean stage efficiency, then

$$\eta_s = \frac{H_i}{H_c}$$

and since $H_c = RH_a$

$$\eta_i = R \, . \, \eta_s \qquad (172)$$

BIBLIOGRAPHY

1. GOUDIE: *Steam Turbines*, Longmans, 1st Edition, 1917, p. 337.
2. ROBINSON: "Report on Reheat Factors." *Mech. Engineering*, 1928; 50; 155.
3. YATES: "Calculations of Turbine Reheat Factor from the Geometry of the Heat Chart." *The Engineer*, 1935; 160; 212.
4. SMITH, R. B.: "The Calculation of Steam Turbine Reheat Factors." *Trans. A.S.M.E.*, 1938; 60; A–156.
5. THATCHER: "Reheat Factors for Expansion of Superheated and Wet Steam." *Trans. A.S.M.E.*, 1938; 60; A–161.
6. SMITH, D. M.: "Stage Efficiency, Cumulative Heat, and Reheat Factor of Steam Turbines." *Proc. I. Mech. E.*, 1938; 140; 399.

EXAMPLES XII

1. Steam at a pressure of 100 lb. per sq. in. abs. and superheated 100° F. expands adiabatically to a pressure of 1·0 lb. per sq. in. abs. What is the difference between the initial and final enthalpy and what is the final quality of the steam? If only 60 per cent of the adiabatic heat drop is converted into mechanical work, calculate the increase in the final dryness fraction and in the final entropy value due to reheating.

2. The initial enthalpy at inlet to the nozzles of a turbine stage is 1,150 B.Th.U. per lb. and the enthalpy at outlet from the blades is 1,118 B.Th.U. per lb. If the total internal steam flow through the turbine is 24 lb. per sec., and the power absorbed in disc friction is 10 h.p., what is the work done on the blading per lb. of steam? Neglect diaphragm gland leakage.

3. The total internal steam flow through a 20,000 kW steam turbine is 54 lb. per sec. In a given stage, the diaphragm gland leakage is 0·5 lb. per sec. The mean blade speed is 550 ft. per sec. and the ratio of blade speed to steam speed is 0·5. The nozzle angle is 18°, the nozzle efficiency 0·88, the value of

k for the blades is 0·86, and the carry-over factor for the nozzles is 0·90. Given that the blade outlet angle is 36° and that the power absorbed by disc friction is 55 h.p., calculate the stage adiabatic horse-power, the shaft horse-power, and the stage efficiency.

4. The following particulars refer to a steam turbine of 25,000 kW output—

Mean diameter of last wheel	120 in.
R.p.m.	1,500
Effective height of blades on last wheel	28 in.
Exhaust pressure	0·5 lb. per sq. in. abs.
Dryness fraction of exhaust steam	0·9
Internal steam flow	8·8 lb. per kWh of turbine output

Assuming that the steam flows axially from the blades of the last wheel, calculate—

(1) Terminal velocity.
(2) Terminal velocity loss.
(3) Percentage loss, given that the adiabatic heat drop in the turbine is 474 B.Th.U. per lb.
(4) Final enthalpy value, given that the initial enthalpy value is 1,391·83 B.Th.U. per lb. and that the total internal power is 25,750 kW.

5. Steam which is initially dry and saturated at an absolute temperature T_1 expands in a turbine to an absolute temperature T_2, the stage efficiency being η_s. Assuming a very large number of stages and that the condition curve on the T–ϕ chart is a straight line, show that the reheat factor

$$R = \frac{T_1 + T_2}{2T_2 + \eta_s(T_1 - T_2)}$$

Is the actual reheat factor greater or less than this approximate value?

6. Dry and saturated steam is supplied to a four-stage steam turbine at a pressure of 200 lb. per sq. in. abs. and exhausted at a pressure of 1 lb. per sq. in. abs. If the stage efficiency is 60 per cent and the pressures in the intermediate stages are 70, 20, and 5 lb. per sq. in. respectively, derive the value of the reheat factor by using the Mollier chart.

7. Describe with reference to the T-ϕ and ϕ-I charts the effect of internal osses on the condition of the steam in a multi-stage turbine. State what is meant by "reheat factor," and state the influence of (*a*) efficiency, (*b*) the number of stages, on the value of the reheat factor

8. Steam which is initially dry and saturated is expanded in a multi-stage turbine, in each stage of which 30 per cent of the heat available is reconverted into heat. If the adiabatic index be taken as 1·135, calculate the index *m* of the expansion curve and the ratio of the sum of the stage adiabatic heat drops to the adiabatic heat drop with frictionless expansion, if the pressure-ratio of the expansion be 180.

9. Steam at a pressure of 150 lb. per sq. in. abs. and a temperature of 500° F. expands in a five-stage turbine to a pressure of 1 lb. per sq. in. abs. The steam pressures in the five stages are 70, 30, 10, 3, and 1 lb. per sq. in. respectively. The stage efficiency is 65 per cent. Tabulate the entropy and total heat data with reference to the ϕ-I chart and derive the reheat factor.

10. Given that the adiabatic index for superheated steam is 1·3, calculate the actual index for an adiathermal expansion in which the heat drops are infinitely small and the stage efficiency is 0·75. Hence calculate the theoretical reheat factor for a pressure-ratio of expansion of 20. What would be the approximate value of R for a turbine with ten stages and the same ratio of expansion?

11. Show that if a gas or dry vapour having an adiabatic index n expands with a small-stage efficiency η, the actual index of expansion is

$$m = \frac{n}{n - \eta n + \eta}$$

A multiple-stage high-pressure steam turbine is supplied with steam at 1,000 lb. per sq. in. abs. and 944·6° F. (I = 1,473·1 B.Th.U. per lb.) and exhausts at a pressure of 100 lb. per sq. in. abs., the steam being in the superheated condition during the whole of the expansion. If the small-stage efficiency is 0·82 and $n = 1{\cdot}3$, calculate the temperature and the specific volume at the end of the expansion, and the reheat factor. Given that

$$v = \frac{1{\cdot}253(I - 835)}{p}$$

for superheated steam, p being the pressure in lb. per sq. in. (*Lo*v. *Un.*)

CHAPTER XIII

REGENERATIVE FEED-HEATING

129. Introductory. In the fourth chapter of this book we have considered the simplest possible form of cycle on which a steam turbine may operate, namely, a cycle in which all the heat supplied is given externally, in which the steam is expanded adiabatically and exhausted at constant pressure. Such a cycle, termed the Rankine cycle, has formed a useful basis for comparing the performance of turbines operating under different conditions.

The object of the present chapter is to consider modifications to the usual cycle of operations which increase its thermal efficiency, and which have become standard practice in steam power plants both on land and, in the more powerful installations, at sea.

In the modified cycle steam is extracted from the turbine at one or more points in the expansion and utilized for heating the feed-water. The extracted steam gives up heat by condensing, either in a direct-contact feed heater or in a surface heater.

130. Feed-heating Systems. In order to analyse the performance of such a cycle we shall consider the systems shown diagrammatically in Fig. 183. In each case, four feed heaters are shown. In practice the number of heaters may vary from 2 to 6 (8 in one American power station), depending on conditions and on a balance between first cost and operating costs.

Fig. 183 (*a*) shows four direct-contact heaters in each of which feed-water condenses the extracted steam. The mixture of feed-water and condensed steam is extracted from each heater by a centrifugal or other type of pump which discharges into the steam space of the next high-pressure heater. In such a system the pumps serving the high-pressure heaters are operating under difficult conditions as they are dealing with saturated water at the suction side and have to deliver against high pressures. Direct-contact heaters are rarely used.

Fig. 183 (*b*) shows four surface heaters. The heater drain water, i.e. the condensed heating steam, is extracted by a drain pump and discharged into the feed pipe immediately after the heater. This system suffers from the same practical disadvantages in regard to drain pumps as that shown in Fig. 183 (*a*), except that the pumps have to deal only with condensed steam, and if one or more of them should break down the drain water could be cascaded direct to the next low-pressure heater.

A further system is shown in Fig. 183 (*c*). Surface heaters are again used but it is assumed that a part of the heating surface in each heater is arranged for drain cooling. The hot drain water is

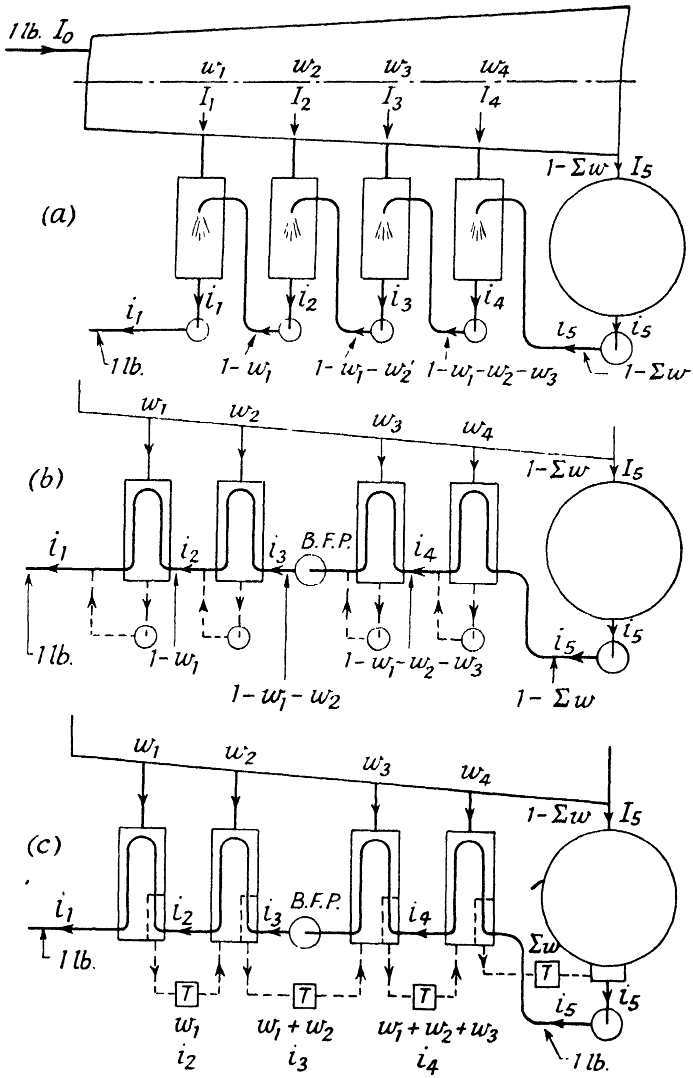


FIG. 183.—Diagrammatic Arrangements of Regenerative Feed-heating Systems

arranged to flow counter to the incoming feed-water and is assumed to be cooled to the saturation temperature existing in the next heater on the low-pressure side. Flow of drain water without the escape of steam may be controlled by steam traps T or by orifices of a certain size.

In each system it is assumed that the feed water is heated up to the steam saturation temperature in each heater. Except in those heaters where the entering steam is superheated, this assumption ignores the temperature difference required for heat transmission. It is quite easy to make allowance for this where necessary. The boiler feed pump (B.F.P.) must be arranged at a convenient point in the feed system so that there is no risk of evaporation of the feed water taking place. Its position in the system is important because the heaters that follow it must be designed for very high pressures and are accordingly costly. The effect of pressure on the enthalpy of the feed-water is neglected, but it can easily be taken into account. The enthalpies of the steam and water are represented by I and i, respectively.

It is first necessary to calculate the amount of steam bled off at each extraction point, per pound of steam entering the turbine. Considering each heater in turn and equating the heat (mass-enthalpy) entering to that leaving it, we obtain the following values—

$$w_1 = (i_1 - i_2) \div (I_1 - i_2) \quad . \quad . \quad . \quad . \quad (173a)$$

$$w_2 = (1 - w_1)(i_2 - i_3) \div (I_2 - i_3) \quad . \quad . \quad . \quad (173b)$$

$$w_3 = (1 - w_1 - w_2)(i_3 - i_4) \div (I_3 - i_4) \quad . \quad . \quad (173c)$$

$$w_4 = (1 - w_1 - w_2 - w_3)(i_4 - i_5) \div (I_4 - I_5) \quad . \quad (173d)$$

The heat supplied externally in the cycle

$$= H = I_0 - i_1 \quad . \quad . \quad . \quad . \quad (174)$$

The heat rejected $= (1 - \Sigma w)(I_5 - i_5)$

Hence the work done in the turbine per lb. of steam

$$= W = (I_0 - i_1) - (1 - \Sigma w)(I_5 - i_5) \quad . \quad . \quad (175)$$

Alternatively, the work done in the turbine may be calculated by summing up the products of the steam flows and the corresponding heat drops in the turbine stages, i.e.

$$\begin{aligned} W = (I_0 - I_1) &+ (1 - w_1)(I_1 - I_2) \\ &+ (1 - w_1 - w_2)(I_2 - I_3) \\ &+ (1 - w_1 - w_2 - w_3)(I_3 - I_4) \\ &+ (1 - w_1 - w_2 - w_3 - w_4)(I_4 - I_5) \end{aligned}$$

Thermal efficiency of cycle $\eta_{th.} = \dfrac{W}{H}$

An alternative method of dealing with the condensed heating steam is shown diagrammatically in Fig. 184. The drain water is cascaded from heater to heater through the steam traps T. The whole of the condensed bled steam is extracted from heater No. 4 by a pump and discharged into the feed main on the outlet side of heater No. 4. Again assuming no heat losses and making the same

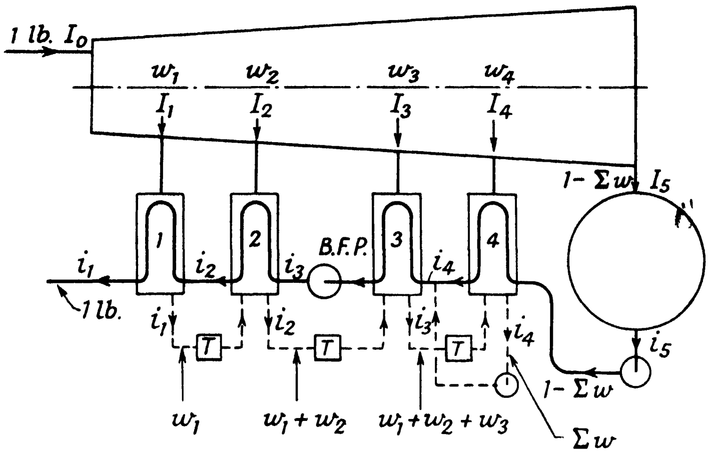


FIG. 184.—Diagrammatic Arrangement of Feed System with One Drain Pump

assumptions as before, the various amounts of steam extracted per lb. of steam entering the turbine are as follows—

$$w'_1 = (i_1 - i_2) : (I_1 - i_1) \quad . \quad . \quad . \quad . \quad . \quad . \quad (176a)$$

$$w'_2 = \{(i_2 - i_3) - w'_1(i_1 - i_2)\} : (I_2 - i_2) \quad . \quad . \quad . \quad (176b)$$

$$w'_3 = \{(i_3 - i_4) - (w'_1 + w'_2)(i_2 - i_3)\} : (I_3 - i_3) \quad . \quad . \quad (176c)$$

$$w'_4 = \{(i_4 - i_5) - (w'_1 + w'_2 + w'_3)(i_3 - i_5)\} : (I_4 - i_5) \quad . \quad (176d)$$

The thermal efficiency may be calculated as before.

A further system of dealing with the drain water is shown in Fig. 185. Here the condensed heating steam is cascaded from heaters 1 and 2 to heater No. 3 from which it is extracted by a pump and delivered to the feed pipe immediately after the heater, i.e. on the suction side of the boiler feed pump. The drains from No. 4 heater may be passed through a syphon pipe, as shown in Fig. 185, or a trap, if necessary, into the lower part of the condenser. A drain cooler may be used to transfer some of the available heat in the drain water to the feed-water if it should prove to be economical.

131. Gains due to Regenerative Feed-heating. That the systems described above will lead to a gain in thermal efficiency may be shown as follows. Consider a turbine with one stage of feed-heating, and let the amount of steam admitted to the turbine in a given interval of time be 1 + *w* lb. Furthermore, assume that *w* lb. is extracted for feed-heating and one pound is condensed. For given conditions *w* will, of course, have a definite value. In a simple non-extraction (Rankine) cycle, the amount of work done may be, for example, 40 per cent of the heat supplied, the remaining 60 per cent being carried away by the cooling water. In the extraction cycle,

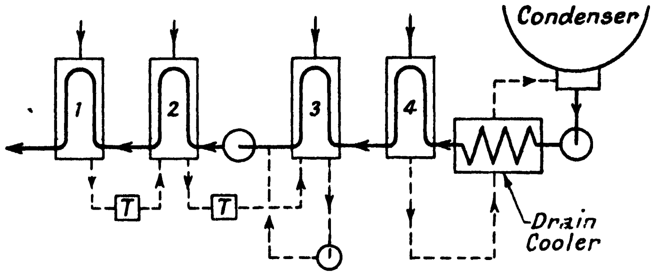


FIG. 185 Feed System with One Drain Pump and a Drain Cooler

on the other hand, the *w* lb. of steam not only does some work in the turbine by partial expansion but also gives up a certain amount of heat to the feed-water. It is thus used without waste, or almost so.

It will be clear that the bled steam must not be live steam, otherwise no work would be available; nor must it be completely expanded, otherwise it would be useless for feed-heating.

It may also be argued that in this cycle the mean temperature at which heat is supplied to the working substance is raised, hence the cycle efficiency must be higher. The process is regenerative because a part of the working fluid after partial expansion is utilized to heat itself.

The gain depends on the number of heaters used and the temperature to which the feed water is heated. Fig. 186 shows the results obtained for the following conditions and assumptions –

Initial steam pressure . . .	600 lb. per sq. in. abs.
Initial steam temperature . .	850° F.
Initial steam saturation temperature	486·3° F.
Exhaust pressure	0·505 lb. per sq. in. abs.
Exhaust saturation temperature	80° F.
Mean value of turbine stage efficiency	80 per cent.

It is assumed—

(1) That the feed outlet temperature from any heater is equal to the steam saturation temperature in that heater.

(2) That the condensed steam from each heater, together with the drains from the next high-pressure heater, is passed into the next low-pressure heater.

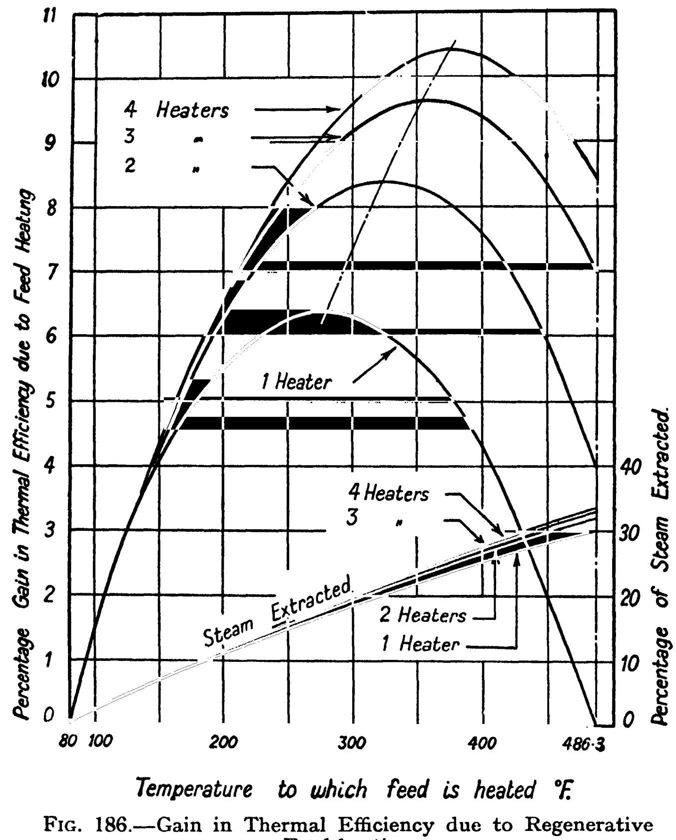


FIG. 186.—Gain in Thermal Efficiency due to Regenerative Feed-heating

(3) That the combined drains from the lowest-pressure heater are cooled in a drain cooler to 80° F.

The thermal efficiency of the turbine without feed-heating is 33·36 per cent. The percentage gain in thermal efficiency due to feed-heating in one stage reaches a maximum value of 6·45 at a temperature of 280° F., which is roughly midway between the exhaust and live steam saturation temperatures. With two or more

heaters in series, the percentage gain increases; moreover, the optimum feed temperature also increases.

Further possibilities of regenerative feed-heating may be shown by the following worked example.

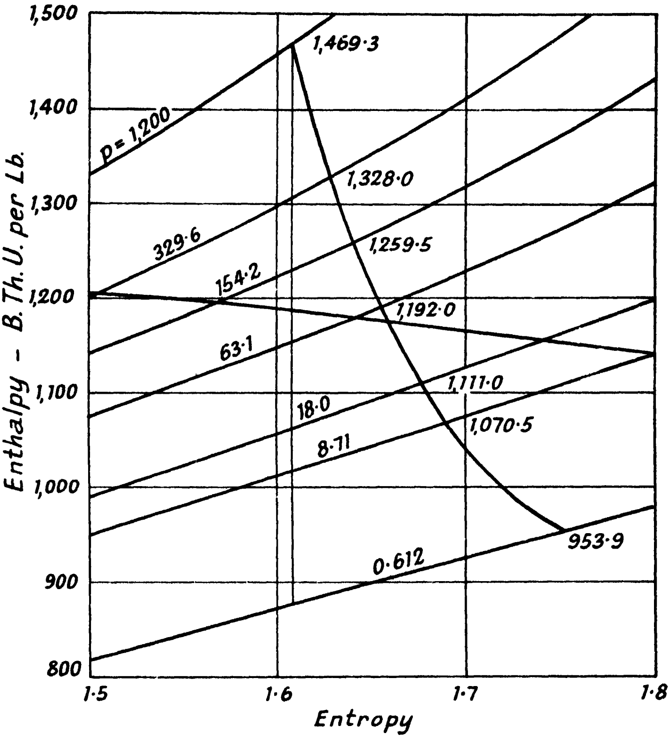


FIG. 187.—State Point Locus on ϕ-I Chart for Example 24

EXAMPLE 24. A steam turbine operates under the following conditions—

Initial steam pressure . .	1,200 lb. per sq. in. abs.
Initial steam temperature . .	950° F.
Exhaust steam pressure . .	0·612 lb. per sq. in. abs.

Turbine "dry stage" efficiency, i.e. the efficiency ratio of stages using superheated steam = 0·85. Turbine stage efficiency in stages where x is the dryness fraction = $0{\cdot}85x$.

There are 5 stages of feed-heating, the steam pressures employed (to suit the staging of the turbine) being as follows. The condition

of the steam at the given pressures was found from the condition curve, Fig. 187.

Stage No.	Pressure	Condition
1	329·6	203° F. superheat
2	154·2	114° F superheat
3	63·1	23 F. superheat
4	18·0	0·954 dry
5	8·7	0·929 dry

The condensed bled steam is to be cascaded to heater No. 5 and then extracted by a drain pump, as shown in Fig. 188. Calculations

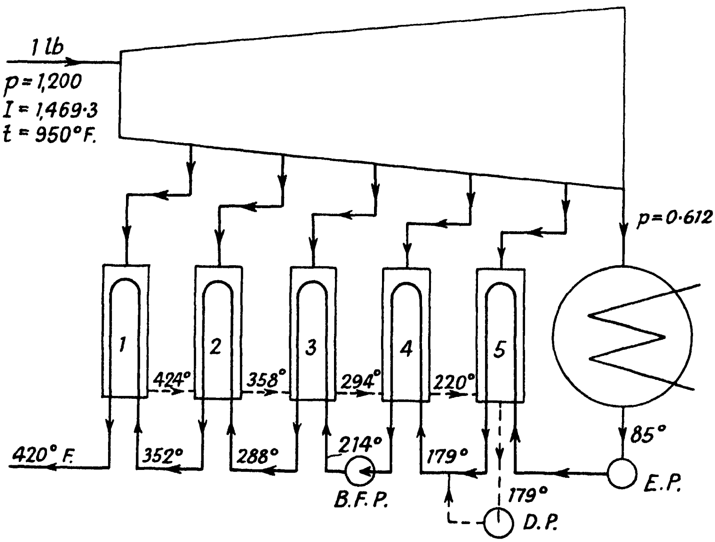


FIG. 188 Diagrammatic Arrangement of Five-stage Feed-heating System

will be made to derive the quantities of steam bled off to each heater, the work done in the turbine, the steam consumption, and thermal efficiency. Comparisons will be made between the Rankine cycle and the regenerative cycle.

(*a*) *Non Feed-heating Cycle.* The conditions for the non feed-heating cycle are first derived from the Mollier chart as follows.

p	ϕ	I
1,200	1·6077	1,469·3
0·612	1·6077	875·0

Adiabatic heat drop = 594·3 B.Th.U per lb.

By the methods derived in Chapter XII, the cumulative heat drop is found to be 624·2 B.Th.U. per lb. Hence the reheat factor is

1·054. The total work done in all the stages, allowing for the effects of wetness, is 515·4 B.Th.U. per lb.

Heat supplied = 1,469·3 − 53 = 1,416·3

∴ Turbine thermal efficiency (allowing for effects of wetness)

$$= \frac{515 \cdot 4}{1,416 \cdot 3} = 36 \cdot 39 \text{ per cent}$$

$$\text{Steam consumption} = \frac{3,413}{515 \cdot 4} = 6 \cdot 624 \text{ lb. per kW. hr.}$$

This is also the steam flow into the condenser.

(*b*) *Regenerative Cycle.* The condition of the steam, the assumed temperatures of the feed-water (making allowances for heat transmission) and the amounts of steam are given in the following table.

Heater No.	1	2	3	4	5
Steam pressure	329·6	154·2	63·1	18·0	8·7
Steam temp., °F.	628	472	320		
Saturation temp., °F.	426·2	360·6	296	222·4	187
I	1,328·0	1,259·5	1,192·0	1,111·0	1,070·5
Feed temp., heater inlet, °F.	352	288	214	179	85
Feed temp., heater outlet, °F.	420	352	288	214	179
Temp. of drain water, °F.	424	358	294	220	179
Steam extracted per lb. of steam entering turbine	0·0790	0·0658	0·0707	0·0205	0·0605
Condensed steam leaving heater	0·0790	0·1448	0·2155	0·2360	0·2965

The quantities of bled steam are calculated by using equations (176) for the assumed data.

Heat supplied = 1,469·3 − 397·0 = 1,072·3

Heat rejected = (1 − 0·2965)(953·9 − 53·0)
= 633·7

∴ Work done per lb. of steam entering turbine
= 1,072·3 − 633·7 = 438·6 B.Th.U.

Turbine system thermal efficiency

$$= \frac{438 \cdot 6}{1,072 \cdot 3} = 40 \cdot 91 \text{ per cent}$$

Percentage gain over the non feed-heating cycle
= 12·42 per cent.

Steam consumption (based on steam entering turbine)

$$= \frac{3,413}{438{\cdot}6} = 7{\cdot}782 \text{ lb. per kW. hr.}$$

This is larger than for the Rankine cycle because of the loss of work by steam extraction.

Steam flow into condenser

$$= 0{\cdot}7035 \times 7{\cdot}782 = 5{\cdot}475 \text{ lb. per kW. hr.,}$$

compared with 6·624 for the Rankine cycle, a reduction of 17·3 per cent. There would be a corresponding reduction in the cooling surface of the condenser, and a corresponding increase in the output of

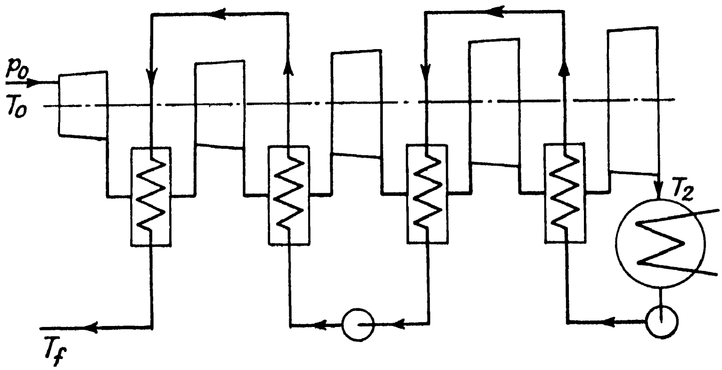


FIG. 189

the turbine for the same last-stage annulus and the same leaving velocity.

132. Ideal Feed-heating Cycle. Consider a turbine comprising, say, five cylinders arranged in series, as shown in Fig. 189. Suppose that surface heaters are arranged between the cylinders and that the feed-water passes through the heaters, as shown. It is further assumed that heat is made available for feed-heating by changing the condition of the whole of the steam passing through the turbine, i.e. by a reduction in the dryness fraction. The system thus differs from that employed in practice because in the latter a certain amount of steam is extracted from the turbine and completely condensed. It is further assumed that the feed-water is heated up to the steam saturation temperature in each stage.

The T-ϕ diagram for the cycle is shown in Fig. 190. Steam is supplied to the turbine at p_0, T_0 and I_0. The expansion in each turbine cylinder is assumed to be isentropic. The feed-water is heated to a temperature T_f degrees absolute, which is lower than the temperature at the point of intersection of the isentropic DE with the steam saturation curve; in other words, the steam entering the

first heater is saturated. This is an essential condition of the simple self-acting system shown in Fig. 189.

The heat supplied to the feed-water in the first heater is h_1, shown by the hatched area on the left-hand side of the diagram. This heat

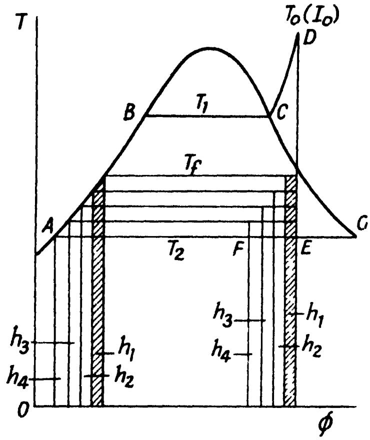


Fig. 190

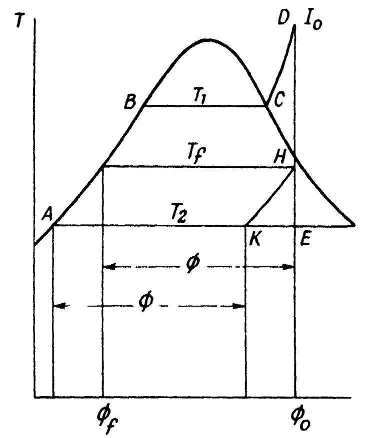


Fig. 191

is provided by a partial condensation of the working steam, the entropy change being $-h_1/T_f$. Similar changes take place in the other three heaters, giving the stepped expansion line and a final dryness fraction AF/AG.

If now the number of heaters is made infinite, then the temperature

rise in each heater becomes indefinitely small and the process becomes reversible. The expansion line HK, Fig. 191, becomes parallel to the liquid line and the constant entropy difference

$$\phi = \phi_0 - \phi_f$$

where ϕ_0 = entropy of steam at p_0, T_0

ϕ_f = entropy of water at T_f.

Let i_f = enthalpy of water at T_f

T_2 = abs. temp. of exhaust steam.

Then heat supplied = $I_0 - i_f$

and heat rejected = $T_2(\phi_0 - \phi_f)$

$$\therefore \quad \text{Thermal efficiency} = 1 - \frac{T_2(\phi_0 - \phi_f)}{I_0 - i_f} \quad . \quad . \quad (177)$$

Equation (177) appears to have been derived in the first instance by Professor F. O. Ellenwood (1) (see letters in *Engineering*, 21st January, 12th February, 27th July, 1942). It may be used as a basis for comparing the actual performance of steam turbines operating on the regenerative cycle with that of an ideal reversible cycle. As already stated, its use is limited to cases where the final feed temperature does not exceed the "intersection" temperature. This would limit the application of the formula to rather low initial steam temperatures. J. F. Field (2) has suggested that this drawback may be overcome by the provision of additional elements to compress the superheated bled steam isothermally to the corresponding saturation temperature and pressure before actually using the steam in the feed heaters. The author showed in the discussion of Field's paper that, if this process were carried out, then the state point locus with an infinite number of heaters would still be parallel to the liquid line. This extends considerably the usefulness of the Ellenwood formula.

EXAMPLE 25. Calculate the thermal efficiency of an ideal turbine plant fitted with an infinite number of feed heaters and operating with the same steam conditions as the turbine in Example 24, i.e. $p_0 = 1{,}200$; $t_0 = 950°$ F.; exhaust pressure = 0·612; feed-water temperature = 420° F.

From steam tables—

$I_0 = 1{,}469{\cdot}3$; $\phi_0 = 1{\cdot}6077$;

$i_f = 397{\cdot}0$; $\phi_f = 0{\cdot}5912$;

$T_2 = 544{\cdot}7$.

Hence theoretical thermal efficiency

$$= 1 - \frac{544{\cdot}7 \times 1{\cdot}0165}{1{,}072{\cdot}3} = 0{\cdot}4836$$

Referring to Example 24, the thermal efficiency of the ideal non-feed-heating cycle, neglecting feed-pump work, is

$$\frac{594 \cdot 3}{1{,}416 \cdot 3} = 0 \cdot 4197$$

Thus the gain due to ideal reversible feed-heating is 15·23 per cent.

The turbine thermal efficiency is 0·4091; hence the equivalent turbine cycle efficiency ratio is

$$\frac{0 \cdot 4091}{0 \cdot 4836} = 84 \cdot 6 \text{ per cent}$$

133. General Notes on Feed-heating. We have seen that the thermal efficiency of a steam turbine plant may be increased by the use of bled steam feed heaters, the percentage gain at the optimum feed temperature increasing as the number of heaters is increased. In practice the appreciable cost of the heaters, pipes, valves, and accessories puts a limit to the number of heaters employed. In large units the temperature rise of the feed-water per heater is normally about 50° to 60° F., three to five heaters being installed.

Up to the present we have only considered the influence of regenerative feed-heating so far as it affects the thermal efficiency of the turbine. It is essential, however, to remember that the turbine is only a part of an organic whole, and that if by the adoption of this method of feed-heating we render the use of an economizer unnecessary, then the flue gases will leave the boiler plant at an appreciably higher temperature, and the reduction in boiler efficiency will partly offset the increase in turbine cycle efficiency.

The solution of the problem lies in the use of air heaters wherein the flue gases are cooled by the combustion air prior to its admission to the furnace. This is, of course, but a further application of the regenerator principle. In practice, air heating possesses certain advantages and disadvantages. The mean temperature in the boiler furnace is higher when the air temperature is higher, and, in consequence, the percentage of fuel heat transmitted by direct radiation is appreciably greater. Trouble is sometimes experienced with mechanical stokers operating with preheated combustion air, and, in this respect, pulverized fuel firing would appear to be at an advantage. Some authorities state that the air temperature should not exceed about 350° F. with chain-grate stokers, but the limiting temperature depends to a large extent on the type of fuel and stoker. A somewhat recent development is to supply to the stoker itself moderately heated air at about 250° F., and to supply a quantity of secondary air above the fire at a temperature from 350° to 600° F.

Because of the fact that a certain proportion of the steam supplied to the turbine is extracted before it reaches the exhaust end,

the quantity of exhaust steam may be reduced by as much as 17 per cent per unit generated. This reduction is a considerable help to the designer who may be faced with the problem of designing a very high capacity machine. There is a reduction in the cooling surface to be provided in the main condenser, but this is actually more than offset by the necessity of providing condensing surface (of an expensive type) in the feed heaters.

BIBLIOGRAPHY

1. HIRSHFELD AND ELLENWOOD: "High-pressure, Reheating, and Regenerating for Steam Power Plants." *Trans. A.S.M.E.*, 1923; 45; 671.
2. FIELD: "A Suggested Basis of Comparison for the Efficiency of Steam Turbo-generators and Steam-electric Generating Stations." *Journal I.C.E.*, 1938; 10; 241.

EXAMPLES XIII

1. A steam turbine plant equipped with a single regenerative feed heater operates under the following conditions—

Initial steam pressure	250
Initial superheat	200° F.
Extraction pressure	30
Exhaust pressure	0·9

Compare the regenerative and non-regenerative cycles with respect to the following: (*a*) thermal efficiency, (*b*) steam consumption in lb. per kWh, and (*c*) condenser duty (steam condensed per kWh).

It may be assumed that the expansion is adiabatic, that the feed water is heated to the steam saturation temperature in the heater, and that the drain water from the heater is cooled in a drain cooler to the condenser temperature. (*Liv. Un.*)

2. Steam is supplied to a turbine at a pressure of 400 lb. per sq. in. abs. and a temperature of 712° F., and is expanded adiabatically to a pressure of 0·5 lb. per sq. in. abs. At a stage of the turbine where the pressure is 40 lb. per sq. in. abs. a connection is made to a surface feed heater in which the feed water is heated by bled steam to a temperature of 260·9° F. The condensed steam from the feed heater is cooled in a drain cooler to 79·5° F., the feed water passing through the drain cooler before entering the feed heater. The cooled drain water combines with the condensate in the well of the condenser.

Assuming no heat losses in the system, calculate the following—

(*a*) Weight of steam used for feed-heating per lb. of steam entering the turbine.

(*b*) Thermal efficiency of cycle.

3. During a test on a steam turbine equipped with a single stage of regenerative feed-heating, the following results were obtained—

Steam pressure at stop valve	300
Steam temperature at stop valve	600° F.
Steam pressure in nozzle box	250
Bled steam pressure	40
Exhaust pressure	1·0
Temperature of condensate	100° F.
Temperature of drain water leaving drain cooler .	110·7° F.
Temperature of feed water leaving feed heater .	257·6° F.
Steam entering turbine	50,000 lb. per hour

Calculate the coupling power of the turbine, assuming (1) that the drain water leaving the drain cooler enters the steam space of the condenser, (2) that the internal work done by the steam which completes its expansion is 300 B.Th.U. per lb., (3) that the condition curve on the ϕ-I diagram is a straight line, and (4) that the bearing friction and other external losses amount to 2 per cent of the internal power. (*Liv. Un.*)

4. Steam is supplied to a turbine at 450 lb. per sq. in. abs. and superheated 200° F. The turbine exhaust pressure is 1·0 lb. per sq. in. abs.

The main condensate is heated regeneratively in two stages by steam bled from the turbine at 70 lb. and 12 lb. per sq. in. abs. respectively. Calculate the weights of steam bled off at each pressure per lb. of steam entering the turbine and the theoretical thermal efficiency of the cycle.

The following assumptions are to be made—

(*a*) That the expansion of the steam in the turbine is adiabatic and frictionless.

(*b*) That the condensate is heated to the saturation temperature in each of the heaters.

(*c*) That the drain water from the H.P. heater passes through a trap without loss of heat into the steam space of the L.P. heater.

(*d*) That the combined drains from the L.P. heater are cooled in a drain cooler to the condenser temperature. (*Liv. Un.*)

5. A steam turbine operates under the following conditions—

Initial pressure	300
Initial superheat	200° F.
Final pressure	0·5

Steam is bled off from turbine stages at pressures of 70, 20, and 4 lb. per sq. in. abs. for the purpose of heating the main condensate. The expansion in the turbine is adiabatic and frictionless. It may be assumed that the condensate is heated in each heater up to the saturation temperature of the steam in that heater, and also that the drain water from each heater is cascaded through a trap into the next heater on the low-pressure side of it. The combined drains from the heater operating at 4 lb. pressure are cooled in a drain cooler to condenser temperature.

Calculate the following—

(*a*) Weight of steam extracted for each heater per lb. of steam entering the turbine.

(*b*) Thermal efficiency of cycle.

(*c*) Thermal efficiency of the Rankine cycle.

(*d*) Theoretical gain due to regenerative feed-heating.

(*e*) Steam consumption of turbine in lb. per kWh with and without regenerative feed-heating.

(*f*) Quantity of steam passing through the last-stage nozzles of a 50,000 kW turbine with and without regenerative feed-heating.

(*g*) Amount of heat carried away by the cooling water in the condenser per kWh with and without regenerative feed-heating.

6. A steam turbine plant is equipped with a single regenerative feed heater of the surface type. The condensed heating steam is withdrawn from the heater by a drain pump which delivers the hot drain water into the feed pipe immediately after the heater. Calculate the enthalpy of the feed water at outlet from the system, assuming adiabatic compression in the drain pump and no heat losses. Calculate also the weight of drain water to be pumped per hour when the steam flow into the turbine is 55,000 lb. per hr., given the following information—

Steam pressure in nozzle box	250 lb. per sq. in. abs.
Steam temperature in nozzle box . .	650° F.
Bled steam pressure	40 lb. per sq. in. abs.

Exhaust steam pressure	*0·7 lb. per sq. in. abs.*
Internal efficiency of turbine . . .	*78 per cent*
Pressure in feed pipe	120 lb. per sq. in. abs.
Condensate temperature	87·7° F.
Feed temperature at heater outlet . .	258° F.
Specific volume of water at 40 lb. per sq. in.	0·017 cub. ft. per lb.

Assume that the condition curve on the Mollier diagram is a straight line.

7. In a steam cycle operating on the theoretical regenerative feed-heating system, steam is supplied to the turbine at 600 lb. per sq. in. abs. and 850° F., and expands isentropically to 0·5 lb. per sq. in. abs. Steam is extracted at pressures of 140, 30, and 5 lb. per sq. in. abs. and condensed in surface heaters. The condition of the steam in expanding through the turbine is as follows—

Pressure	Enthalpy, B.Th.U. per lb.
600	1,435·5
140	1,263
30	1,133
5	1,013
0·5	890

Assuming that the condensed bled steam is extracted from each heater and pumped back into the feed-water main after the heater, and assuming ideal conditions throughout, calculate the quantity of steam bled off at each heater and the gain in thermal efficiency over the simple cycle. (*Liv. Un.*)

8. Calculate the thermal efficiency of an ideal regenerative cycle with an infinite number of heaters under the following conditions—

Initial steam pressure	400
Initial steam temperature	700° F.
Exhaust pressure	1·0

Assume that the feed temperature is the highest that is possible for feed-heating by saturated steam. (*Liv. Un.*)

9. A turbine operates under the following conditions, steam being bled off from two stages for feed-heating purposes

Initial steam pressure	400
Initial steam temperature	700° F.
Steam pressure in first heater	80
Steam pressure in second heater	15
Exhaust pressure	1·0
Condensate temperature	101·7 F.
Feed temperature after second heater	202° F.
Feed temperature after first heater	301° F.

The bled steam is condensed in the feed heaters and there is no cooling of the condensate. The drains from the first heater are passed through a steam trap into the second heater and the combined drains from the second heater are pumped by a drain pump into the feed pipe after the second heater.

If the internal power developed by the turbine is 12,000 kW, find the required capacity of the heater drain pump.

The efficiency ratio of the turbine is 0·8 and the condition curve on the Mollier diagram may be assumed to be a straight line. (*Liv. Un.*)

10. A steam power unit comprises four separate turbines arranged in series on the same shaft. Between each pair of turbines there is a feed-water heater of the surface type, three in all. The working steam passing from one turbine to the next passes through a feed heater and gives up heat to the feed-water

by partial condensation. The steam entering turbine No. 1 is at 600 lb. per sq. in. and 200° F. superheat, the exhaust pressure of No. 4 turbine is 1·0 lb. per sq. in. and the intermediate steam pressures are 120, 36, and 7·5 lb. per sq. in.

Assuming that the feed-water is heated up to the steam saturation temperature in each heater, that the expansion in each turbine is isentropic and that the steam flows as a homogeneous fluid, calculate the thermal efficiency of the cycle.

Calculate the thermal efficiency of the above cycle when the number of feed-heating stages is theoretically infinite. (*Liv. Un.*)

CHAPTER XIV

REHEATING AND WATER-EXTRACTION CYCLES

134. Flow of Wet Steam in Nozzles and Blades. In the foregoing chapters of this book dealing with the flow of steam through nozzles and blades it has been tacitly assumed that the steam is a homogeneous fluid and that at any point in the flow of wet steam, the steam and the suspended water particles are moving in the same direction and with identical velocities. Whilst this is a very convenient assumption, in that it simplifies the theoretical work and calculations based thereon, it is not in accord with the facts.

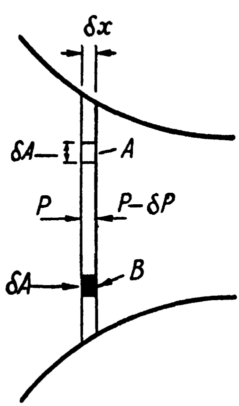


FIG 192

Consider the expansion of wet steam in a nozzle. The flowing steam will carry along with it a large number of suspended water droplets. These are of varying size. There are the exceedingly minute particles consisting of a few hundred molecules and formed by condensation an extremely short time before the instant under consideration. There will also be much larger droplets due to the joining up of smaller particles. There is, however, an upper limit to the size of such droplets.

Fig. 192 shows a section through a steam nozzle. Consider two transverse sections a distance δx apart and suppose that these sections are also sections of equal pressure P and P $- \delta$P respectively. Consider the motion of two elementary masses, one — A, of steam, and the other — B, of water, assuming for the sake of simplicity that B represents a water particle of prismatic shape instead of the natural spherical shape. It is assumed also that at the section considered the particles are, at the given instant, moving with the same velocity so that the only accelerating force is that due to the pressure drop.

Let ρ_s = density of steam, lb. per cub. ft.

ρ_w = density of water, lb. per cub. ft.

The accelerating force on the two masses is the same, namely, $g \cdot \delta P \cdot \delta A$ poundals, and since the masses are $\rho_s \cdot \delta A \cdot \delta x$ and $\rho_w \cdot \delta A \cdot \delta x$ respectively—

Acceleration of steam

$$= f_s = g \cdot \frac{\delta P}{\delta x} \cdot \frac{1}{\rho_s}$$

Acceleration of water

$$= f_w = g \cdot \frac{\delta P}{\delta x} \cdot \frac{1}{\rho_w}$$

$$\therefore \qquad \frac{f_w}{f_s} = \frac{\rho_s}{\rho_w} = \frac{v_w}{v_s}$$

At 10 lb. per sq. in.

$$\frac{f_w}{f_s} = \frac{0{\cdot}0166}{38{\cdot}37} = 0{\cdot}000434$$

At 1 lb. per sq. in.

$$\frac{f_w}{f_s} = \frac{0{\cdot}0161}{333} = 0{\cdot}0000484$$

In other words, the rate of acceleration of the steam *due to pressure difference only* is 2,300 times that of the water particle at 10 lb. per sq. in., and 20,700 times at 1 lb. per sq. in. abs.

The result is that the water particle is accelerated at a much smaller rate than the steam, and soon lags behind. Under the new conditions there is a certain relative velocity of the steam past the lagging particle which introduces a new accelerating force, for if at any point the velocity of the steam is V_s and of the moisture V_m, the relative velocity is $V_s - V_m$ and the accelerating force on the water particle *due to the relative velocity only* is

$$F = a \cdot \rho_s(V_s - V_m)^2 \cdot \delta S \text{ poundals}$$

where a = a number which is a function of the Reynolds number, but may for the purpose of this simple analysis be assumed as a constant.

δS = external surface of droplet.

Assuming a spherical droplet of diameter d, $S = \pi d^2$, and since the volume is $\frac{\pi d^3}{6}$, the mass is $\rho_w \cdot \frac{\pi d^3}{6}$.

$$\therefore \qquad \text{Acceleration } f_w = \frac{\text{Force}}{\text{Mass}}$$

$$= \frac{6a}{d}\left(\frac{\rho_s}{\rho_w}\right)(V_s - V_m)^2$$

This expression shows that the acceleration of the water particles will be least for the larger droplets and also least in the low-pressure stages where ρ_s is so very small.

The foregoing analysis of the problem is very incomplete, but it suffices to show that in the stages of a turbine where the steam is wet the water droplets do not acquire the same velocities as the expanding steam, and, moreover, that the velocity difference is

likely to be greatest for the larger particles and in the stages where the steam pressure is lowest. Theoretical calculations show that in the L.P. stages of a turbine the ratio of the moisture velocity to

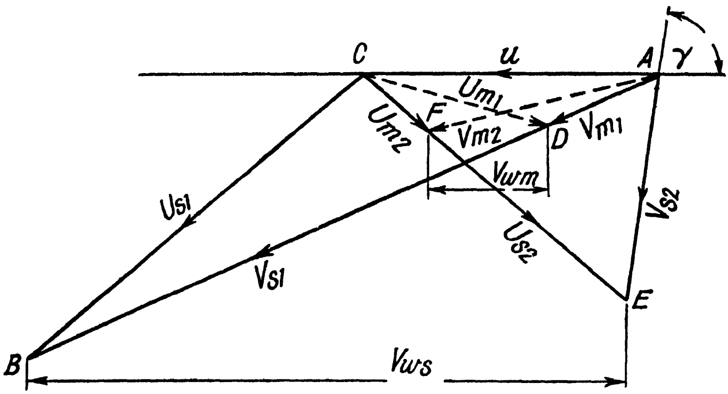


FIG. 193.—Velocity Diagram for Dry Steam and Water Particles

steam jet velocity might vary from 0·1 to 0·3, according to the jet velocity, being higher at the higher jet velocities.

Consider now the velocity diagram for an impulse turbine, Fig. 193.

Let V_{s1} = steam velocity at exit from nozzle.

V_{m1} = moisture velocity at exit from nozzle (assumed to be uniform for all particles).

$m_1 = \frac{V_{m1}}{V_{s1}}$.

U_{s1} = relative velocity of steam at inlet to blades.

U_{m1} = relative velocity of moisture at inlet to blades.

U_{s2} = relative velocity of steam at outlet from blades.

U_{m2} = relative velocity of moisture at outlet from blades.

$m_2 = \frac{U_{m2}}{U_{s2}}$.

V_{ws} = velocity of whirl for dry steam.

V_{wm} = velocity of whirl for moisture particles.

In drawing the velocity diagram it has been assumed that the entrained water issues from the nozzle in the same direction as the steam. The inlet velocity diagrams for the steam and water are ABC and ADC respectively. From the latter it is seen that the water particles entering the blades have a relative velocity U_{m1} = CD and thus strike the leading face of the blades, as shown in Fig. 194. The subsequent action in the blade channels must be

somewhat conjectural. In all probability, the spherical water droplets are flattened out and more or less broken up into smaller droplets which will be swept forward by the rapidly flowing steam with the result that the water droplets leave the blade channels with a certain relative velocity U_{m2}, which is less than U_{s2}. U_{m2} is not, by any means, uniform, but will be assumed so. It will also be assumed that the relative directions of the dry steam and entrained moisture are the same at the blade outlet.

It will be clear that the interactions of the steam and water in the blade channels will affect the velocities U_{s2} and U_{m2}. The

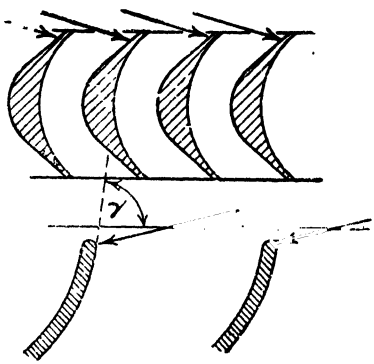


FIG. 194.—Showing Oblique Impact of Water Drops on Moving Blades and Nozzle Guide Vanes

momentum of the incoming moisture particles is practically destroyed at inlet and the available momentum is, therefore, that of the dry steam. If x is the dryness fraction of the steam, then the momentum per lb. of stuff, i.e. of steam and water mixture, is $x \,.\, U_{s1}$. With homogeneous flow, the momentum at outlet would be $k \,.\, x \,.\, U_{s1}$, where k has the usual meaning. Equating the momentum of the steam and water at outlet from the blade channel, we have

$$x \,.\, U_{s2} + (1 - x)U_{m2} = x \,.\, k \,.\, U_{s1}$$

$$U_{s2}(x + (1 - x)m_2) = x \,.\, k \,.\, U_{s1}$$

$$\therefore \quad U_{s2} = \frac{x \,.\, k \,.\, U_{s1}}{x + (1 - x)m_2} \qquad . \quad . \quad . \quad (178)$$

$$U_{m2} = \frac{m_2 \,.\, x \,.\, k \,.\, U_{s1}}{x + (1 - x)m_2} \qquad . \quad . \quad . \quad (179)$$

This enables us to complete the velocity diagram. Note that the water particles leave the wheel in the direction of AF and strike the nozzle guide vanes of the next stage obliquely, as shown in Fig. 194.

The incoming energy per lb. of stuff is

$$\frac{x \cdot V_{s1}^2}{2g} + \frac{(1 - x)V_{m1}^2}{2g} \text{ ft.-lb.}$$

The force on the blades per lb. of stuff per second is

$$\frac{1}{g}(x \cdot V_{ws} + (1 - x)V_{wm}) \text{ lb. wt.}$$

where correct account is taken of the sign of V_{wm}. Note that in Fig. 193 the component of V_{m2} in the direction of motion is greater than that of V_{m1} and that, accordingly, the sign of V_{wm} is negative.

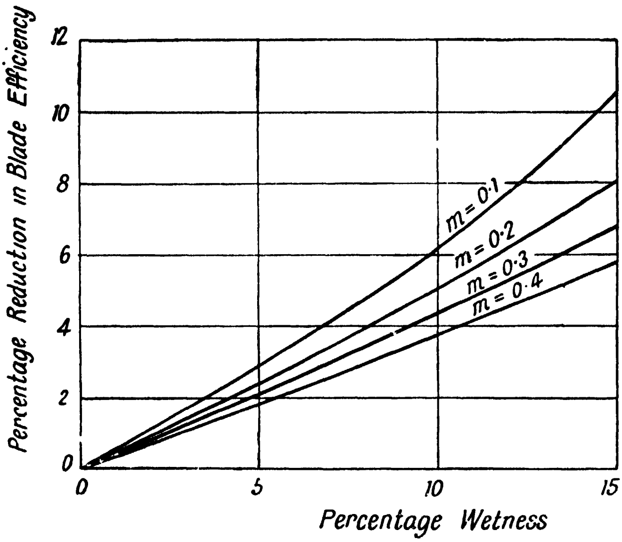


FIG. 195.—Reduction in Blade Efficiency owing to Moisture in Steam

In this way, the braking action of the water is correctly accounted for, provided the assumptions which have been stated above are reasonably correct.

Hence the work done per lb. of stuff is

$$W = \frac{u}{g}(x \cdot V_{ws} + (1 - x)V_{wm}) \text{ ft.-lb.} \quad . \quad . \quad (180)$$

and the blade efficiency is given by the expression

$$\eta_b = \frac{2u(x \cdot V_{ws} + (1 - x)V_{wm})}{V_{s1}^2(x + (1 - x)m_1^2)} \quad . \quad . \quad (181)$$

The effects of moisture based on the above tentative theory are shown in Fig. 195 for the following basic data—

Nozzle angle = 24°; $\rho = 0{\cdot}5$.

Equiangular blades, $\beta_1 = \beta_2 = 44{\cdot}6°$; $k = 0{\cdot}85$; and $m_2 = m_1$.

Taking the values at 10 per cent wetness as a basis and assuming $m = 0{\cdot}1$ only, the percentage reduction in blading efficiency is 0·62 per 1 per cent of wetness. Actually, this represents only a part of the losses in a turbine stage operating with wet steam. Owing to the interactions between the steam and suspended moisture in

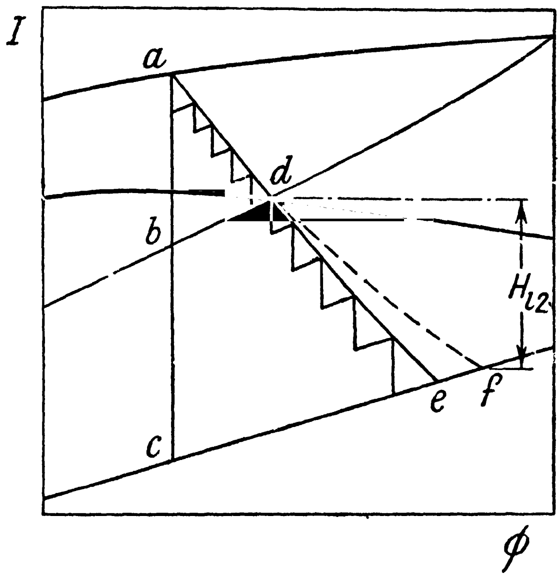


FIG 196.—Correction of Condition Curve to allow for Effects of Wetness

the nozzles, certain losses of energy occur. Moreover, after impact on the leading face of the blade, it is very probable that the water droplets resulting from the disintegration of the larger droplets will be flung outwards to a greater radius and will thus have a certain amount of kinetic energy imparted to them by the moving blades. This reduces the useful work done. It has been stated by the well-known authority, Dr. K. Baumann, (1) that the stage efficiency η_s' of a turbine stage working with wet steam is equal to the dry stage efficiency η_s multiplied by the dryness fraction,

i.e. $$\eta_s' = x \cdot \eta_s \quad . \quad . \quad . \quad . \quad (182)$$

This simple rule is apparently based on test figures and is very easily applied in practical calculations.

Considerations similar to those outlined above apply to the axial-flow impulse-reaction (Parsons) turbine. Water drops strike both fixed and moving blades obliquely.

135. Correction to Condition Curve for Wetness. If the efficiency of a stage operating with dry steam—we shall term this the dry

stage efficiency—is known, the condition curve for a constant stage efficiency may be corrected in the following manner. Referring to Fig. 196, let H_{c1} be the cumulative heat drop for the superheat part of the expansion, and H_{c2} that for the wet part.

Then $\quad I_a - I_d = \eta_s . H_{c1}$ and $I_d - I_e = \eta_s . H_{c2}$

Considering the wet stages, if h is the adiabatic heat drop in any one stage and x is the dryness fraction in that stage, then, by

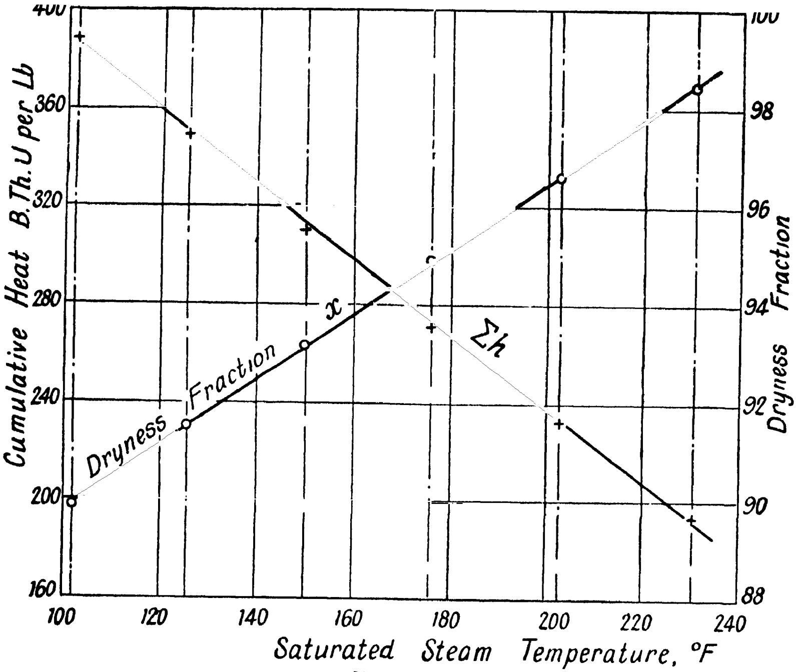


FIG. 197

eq. (182), the work done in the stage is $x . \eta_s . h$. If values of Σh and x are plotted against saturation temperature for the wet stages, it is found that the relations are linear. This is shown in Fig. 197, the data being taken from Table XIX, page 294. It is obvious, without further proof, that the internal work done in the turbine is equal to

$$H_{i1} + H_{i2} = \eta_s(H_{c1} + x_m . H_{c2})$$

where x_m is the mean dryness fraction in the wet stages.

EXAMPLE 26. Using the data given in Table XIX, page 294, and given that the stage heat drop is 38·8 B.Th.U. per lb., and that the dry stage efficiency is 75 per cent, calculate—

(*a*) Internal work done per lb. of steam, neglecting the effect of wetness.

(*b*) Internal work done per lb. of steam, taking wetness into account.

(*c*) Percentage loss due to wetness.

(*d*) Final enthalpy and dryness fraction given that the initial enthalpy is 1,288·8 B.Th.U. per lb. and the final pressure 1·0 lb. per sq. in.

From the data given in the table, it is clear that the first five stages may be assumed to operate in dry steam, and the last five in wet steam.

$$\therefore \qquad H_{c1} = H_{c2} = 5 \times 38{\cdot}8 = 194$$

(*a*) Neglecting wetness, $H_t = 0{\cdot}75 \times 388 = 291$ B.Th.U.

(*b*) Mean dryness in L.P. stages = 0·95.

$$\therefore \qquad H_{t1} + H_{t2} = 0{\cdot}75\{194 + (0{\cdot}95 \times 194)\}$$
$$= 283{\cdot}7$$

$$(c) \text{ Loss due to wetness} = \frac{7{\cdot}3}{291} \times 100 = 2{\cdot}5 \text{ per cent.}$$

(*d*) Final enthalpy = 1,288·8 − 283·7
= 1,005·1 B.Th.U. per lb.

Final dryness fraction read from Mollier chart = 0·9063. Neglecting wetness the final dryness fraction is 0·8989.

It will be clear that the modification of the condition curve will give, for a constant dry stage efficiency, slightly greater specific volumes in the L.P. stages and also a slightly higher reheat factor.

136. **Erosion of Blades.** Quite apart from causing a reduction in nozzle and blade efficiency, the presence of water in the L.P. stages sometimes brings about serious erosion of the moving blades. Reference to Figs. 193 and 194 shows that the water particles strike the leading surface of the blades with a velocity CD which, with the small ratio m_1 at present considered to obtain, is commensurate with the blade velocity. Such impact, if sufficiently heavy, produces severe local stresses in the blade material, causing the surface metal to fail and flake off.

The erosion, if any, is more likely to occur in the region where the steam is wettest, i.e. in the last one or two stages of the turbine. Moreover, as has been shown, the water droplets are concentrated in the outer parts of the flow annulus where the peripheral velocity and therefore the velocity of impact are highest. Experiments and operating experience have shown that the factors which most affect the erosion are the following—

(*a*) *The final wetness of the steam.* The consensus of opinion at the present time (1958) is that a nominal final wetness fraction exceeding about 10 per cent, combined with other factors which encourage erosion, would tend to produce severe erosion of the

blades. The final wetness obviously depends upon the initial pressure and temperature of the steam, the exhaust pressure and stage efficiency. Fig. 198 shows the final dryness fraction for various initial steam pressures and temperatures, assuming an internal stage efficiency ratio of 0·85. From these curves it is apparent that if the final wetness is to be kept below 10 per cent, then the employ-

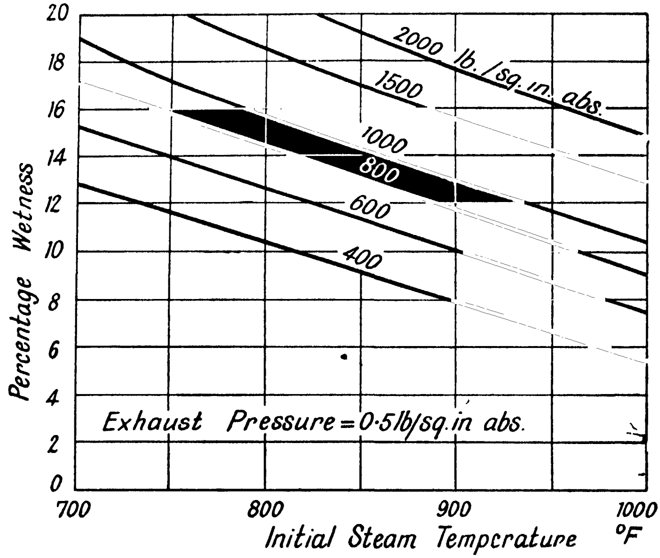


FIG. 198.—Exhaust Wetness as a Function of Initial Steam Pressure and Temperature (Internal Efficiency -- 0·85)

ment of high steam pressures and a simple non-reheating cycle must imply the use of very high initial temperatures.

(*b*) *Peripheral velocity.* In an important series of articles by Mr. F. W. Gardner (2), it is shown that the intensity of pressure produced by the impact of water drops is directly proportional to the velocity of impact, and that it does not depend on the size of the drops. It is estimated that the pressure resulting from the direct impact at 1,000 ft. per sec. amounts to about 40 tons per sq. in. When it is realized that in some cases the blade tip velocity reaches 1,500 ft. per sec., the great stresses set up by the impact of the water drops become a very serious matter. For further information on the subject of blade erosion, tests, etc., the reader is referred to the author's book, *Steam Turbine Operation.*

137. **Reheating.** Erosion difficulties due to moisture in the steam may be avoided by reheating. The whole of the steam is taken from the turbine at a suitable point and a further supply of heat is

given to it, after which the steam is readmitted to the turbine and expanded to condenser pressure.

Consider, first, the theoretical reheating cycle in which the steam is assumed to expand at constant entropy. Figs. 199 and 200 show,

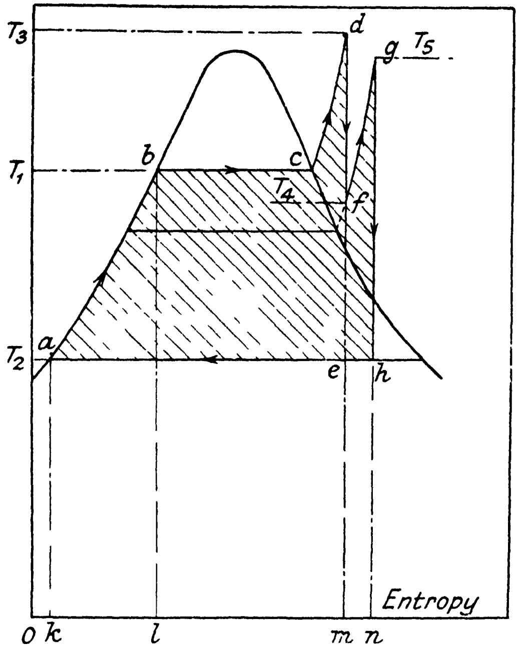


FIG. 199.—T-ϕ Chart for Simple Reheating Cycle

respectively, the T-ϕ and ϕ-I diagrams and are lettered to correspond with each other. Steam enters the turbine at p_1 and T_3 and is expanded adiabatically to a certain intermediate pressure where the state point is f and the absolute temperature T_4. Here the steam receives a further supply of heat, at constant pressure, which raises the temperature to T_5. The steam is then expanded to p_2 and T_2. This is an example of single-stage reheating.

Referring to Fig. 200—

Heat supplied $= (I_d - I_a) + (I_g - I_f)$.

Heat rejected $= I_h - I_a$.

$\therefore$ Work done $=$ Heat supplied $-$ Heat rejected

$$= (I_d - I_f) + (I_g - I_h)$$

i.e. the sum of the adiabatic heat drops df and gh.

∴ Theoretical thermal efficiency of cycle

$$\eta_c = \frac{(I_d - I_f) + (I_g - I_h)}{(I_d - I_a) + (I_g - I_f)} \quad . \quad . \quad . \quad (183)$$

Provided the last stage of the expansion terminates at the lower limit of temperature T_2, reheating generally leads to an increase in

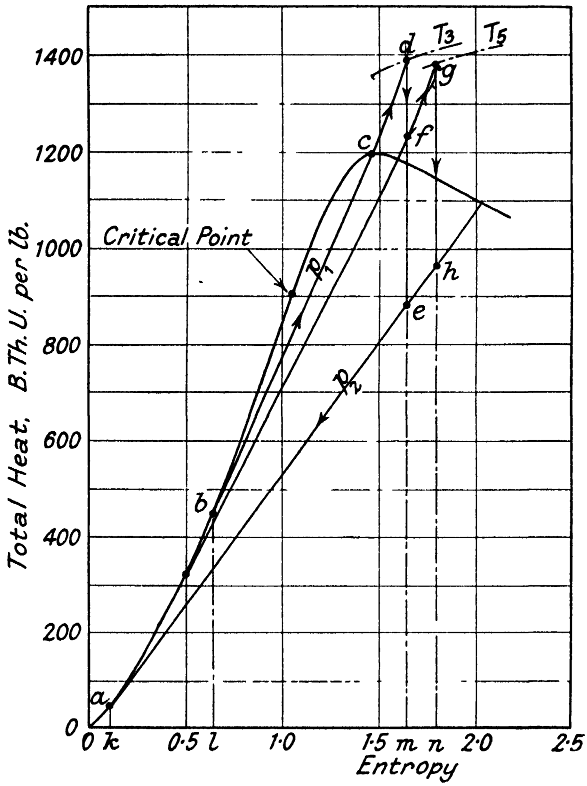


FIG. 200 —φ-I Chart for Simple Reheating Cycle

the theoretical cycle efficiency because the additional heat is supplied at a higher mean temperature. If the process is extended in its application, we may imagine a cycle such as that illustrated diagrammatically in Fig. 201 in which the steam is initially superheated to T_3 and repeatedly reheated at various pressures in such a way that the additional heat supplied to the steam is absorbed at a high mean temperature T_4, nearly equal to T_3. Such a cycle is theoretically desirable but is difficult to realize in practice. Up

to the present, practical considerations have limited the number of reheating stages to one.

Consider now the practical case of single-stage reheating. Referring to the ϕ-I chart, Fig. 202, let p_0 be the stop-valve pressure, p_1 the nozzle-box pressure, and p_3 the exhaust pressure.

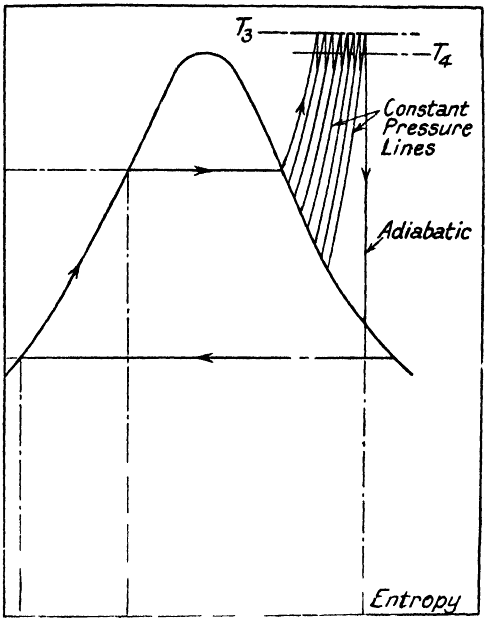


FIG. 201 —T-ϕ Chart for Multi-stage Reheating Cycle

Non-reheating Cycle. This is shown by the adiabatic and actual expansion lines *bc* and *bd*. Ignoring the effect of wetness in the L.P. stages, the internal efficiency of the turbine cycle is

$$\eta_{ci} = \frac{I_b - I_d}{I_a - I_{w3}}$$

where I_{w3} is the enthalpy of water at p_3.

Let x_3 = actual dryness fraction at p_3.

H_{c1} = cumulative heat down to saturation line.

H_{c2} = cumulative heat from saturation line down to exhaust pressure.

Then, allowing for the effects of wetness, internal work done

$$H_i = \eta_s \left\{ H_{c1} + \left(\frac{1 + x_3}{2}\right) H_{c2} \right\}$$

and

$$\eta_{ci} = \frac{H_i}{I_a - I_{w3}}$$

Reheating Cycle. Suppose that the steam is extracted at some pressure p_2 and reheated to a temperature t_2. Assume that due to resistance in the steam pipes and reheater tubes the steam re-enters the turbine at a pressure p'_2. The drop in pressure may be assumed to take place at constant enthalpy and is shown, purely for convenience in illustration, by the constant enthalpy line *ef*. *fg* shows

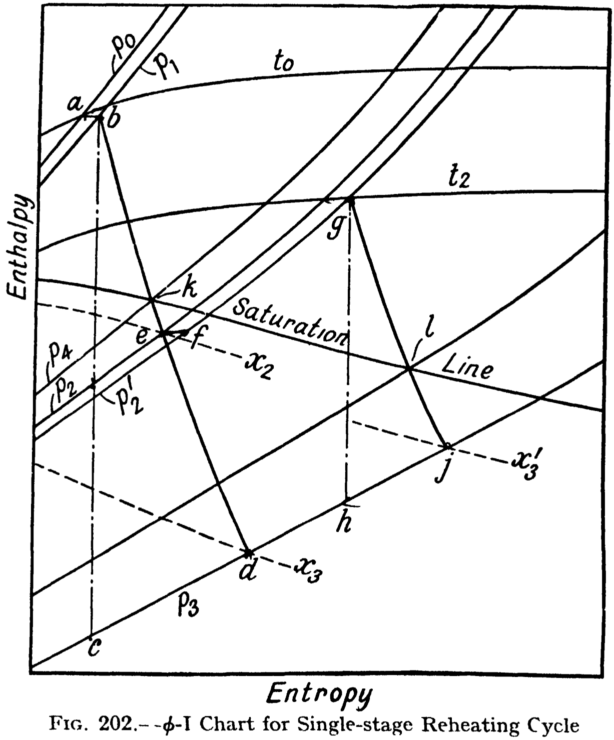


FIG. 202.—ϕ-I Chart for Single-stage Reheating Cycle

the reheating and *gj* the subsequent expansion to the exhaust pressure p_3, the new final dryness fraction being x'_3.

The heat supplied in the reheater may be deduced from the steady flow equation. Neglecting the relatively small kinetic energies of the steam at inlet and outlet, we have—

Heat supplied per lb. of steam $= I_g - I_e$.

$\therefore$ Heat supplied in cycle $= (I_a - I_{w3}) + (I_g - I_e)$.

Ignoring first the effect of wetness, the internal work done in the cycle is

$$H_i = (I_b - I_e) + (I_g - I_j)$$

$$\eta_{ci} = \frac{H_i}{(I_a - I_{w3}) + (I_g - I_e)}$$

In order to allow for the effects of wetness, suppose that—
Before reheating—

H_{c1} = cumulative heat drop down to saturation line.
H_{c2} = cumulative heat drop below saturation line.
x_2 = final dryness fraction.

After reheating—

H_{c3} = cumulative heat drop down to saturation line.
H_{c4} = cumulative heat drop below saturation line.

Suppose that the dry stage efficiency η_s is uniform for all stages. Then the total internal work

$$H_i = \eta_s\left\{H_{c1} + \left(\frac{1 + x_2}{2}\right)H_{c2} + H_{c3} + \left(\frac{1 + x'_3}{2}\right)H_{c4}\right\}$$

The heat supplied is the same as before.

EXAMPLE 27. Steam is supplied to a H.P. steam turbine at a nozzle-box pressure of 1,200 lb. per sq. in. abs., and a temperature of 800° F. The exhaust pressure is 0·5 lb. per sq. in. abs. What is the internal cycle efficiency (*a*) neglecting the effects of wetness, (*b*) allowing a standard wetness correction of 1 per cent per 1 per cent wetness? The dry stage efficiency is 80 per cent.

In an alternative cycle, steam is exhausted from the H.P. turbine at 200 lb. per sq. in. abs., reheated, and returned to the I.P. turbine at 180 lb. per sq. in. abs. and 800° F. It is then expanded to the same pressure as before and with the same dry stage efficiency. What is the internal thermal efficiency of the reheating cycle (*a*) neglecting the effects of wetness, (*b*) allowing the same wetness correction as before?

(1) *Non-reheat Cycle.* The condition curve *bd* is first drawn by a step-by-step process, Fig. 203, yielding the I values shown.

(*a*) *Neglecting effects of wetness*—

$$H_i = 1{,}382{\cdot}7 - 916{\cdot}9 = 465{\cdot}8$$

Heat supplied = 1,382·7 − 47·4 = 1,335·3

$$\therefore \qquad \eta_{ci} = \frac{465{\cdot}8}{1{,}335{\cdot}3} = 34{\cdot}88 \text{ per cent}$$

(*b*) *Allowing for wetness*—

$$H_{i1} = 1{,}382{\cdot}7 - 1{,}193{\cdot}0 = 189{\cdot}7$$

$$\text{Mean } x \text{ in lower stages} = \frac{1 + 0{\cdot}8325}{2} = 0{\cdot}9162$$

$$\therefore \qquad H_{i2} = 0{\cdot}9162\ (1{,}193{\cdot}0 - 916{\cdot}9) = 253{\cdot}0$$

$\therefore$ Internal work done = 442·7

$$\eta_{ci} = \frac{442{\cdot}7}{1{,}335{\cdot}3} = 33{\cdot}15 \text{ per cent}$$

(2) *Reheating Cycle.* The expansion line gj is first drawn by a step-by-step process and the relevant I values obtained.

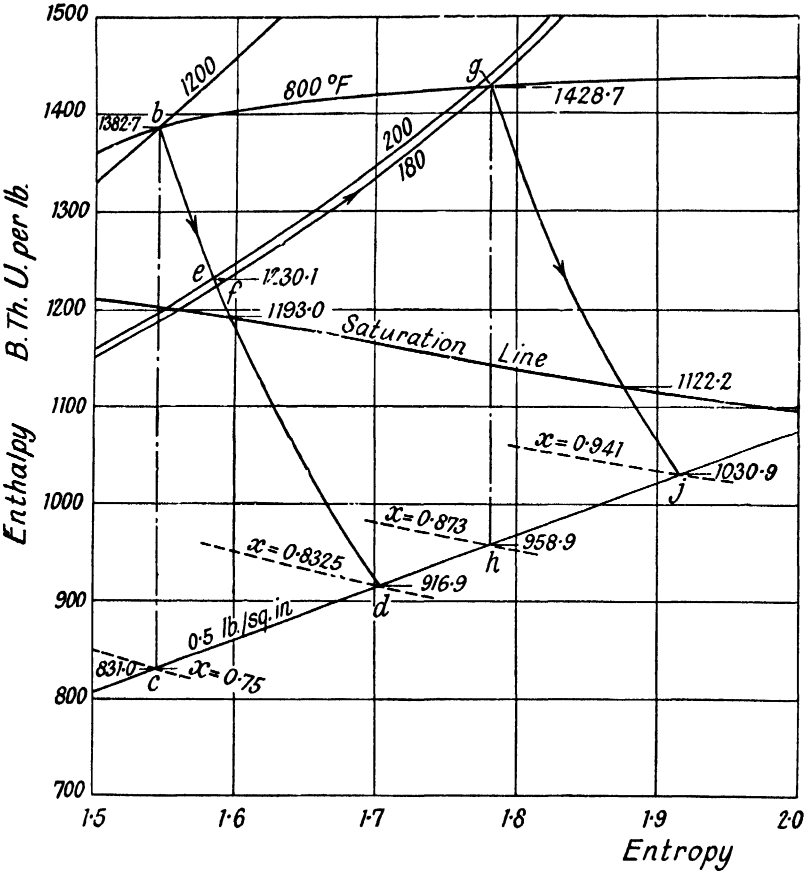


FIG. 203.—ϕ-I Chart Illustrating Example 27

(*a*) *Neglecting effects of wetness*—

For H.P. cylinder, $H_i = 1{,}382{\cdot}7 - 1{,}230{\cdot}1 = 152{\cdot}6$.

For L.P. cylinder, $H_i = 1{,}428{\cdot}7 - 1{,}030{\cdot}9 = 397{\cdot}8$.

Total internal work $= 550{\cdot}4$.

$$\text{Heat supplied} = (1{,}382{\cdot}7 - 47{\cdot}4) + (1{,}428{\cdot}7 - 1{,}230{\cdot}1) = 1{,}533{\cdot}9$$

$$\eta_{ci} = \frac{550{\cdot}4}{1{,}533{\cdot}9} = 35{\cdot}88 \text{ per cent}$$

(*b*) *Allowing for wetness*—

Mean x in L.P. stages = 0·9705.

∴ Internal work done in wet stages

$$= 0{\cdot}9705\,(1{,}122{\cdot}2 - 1{,}030{\cdot}9) = 88{\cdot}6$$

∴ Total internal work done

$$= (1{,}382{\cdot}7 - 1{,}230{\cdot}1) + (1.428{\cdot}7 - 1{,}122{\cdot}2) + 88{\cdot}6$$
$$= 547{\cdot}7$$

$$\therefore \qquad \eta_{ci} = \frac{547{\cdot}7}{1{,}533{\cdot}9} = 35{\cdot}72 \text{ per cent}$$

The percentage gain due to reheating is only 2·87 per cent if the effects of wetness are ignored, but 7·75 per cent if the effect of

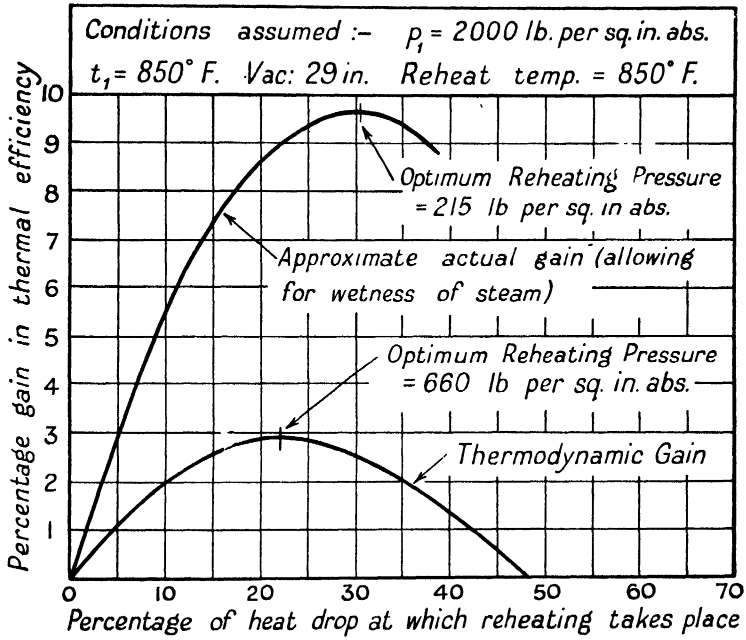


FIG. 204.—Curves Showing the Gain in Thermal Efficiency due to Single-stage Reheating at Various Pressures

wetness is taken into account. A calculation for the simple reheating cycle with isentropic expansion in both turbines and ignoring the wetness correction shows a thermal gain of a mere 1·23 per cent.

There is, for any assumed temperature conditions, as, for example, reheating of the steam to its initial temperature, a particular pressure at which it is most economical to reheat the steam. A little thought will show that if the steam is reheated early in its expansion, then the additional quantity of heat supplied will be small,

with a consequently small gain, whereas, if the reheating is done at fairly low pressures, then, although a large amount of additional heat is supplied, the steam will still have a high degree of superheat at the exhaust, with the result that a large proportion of the heat

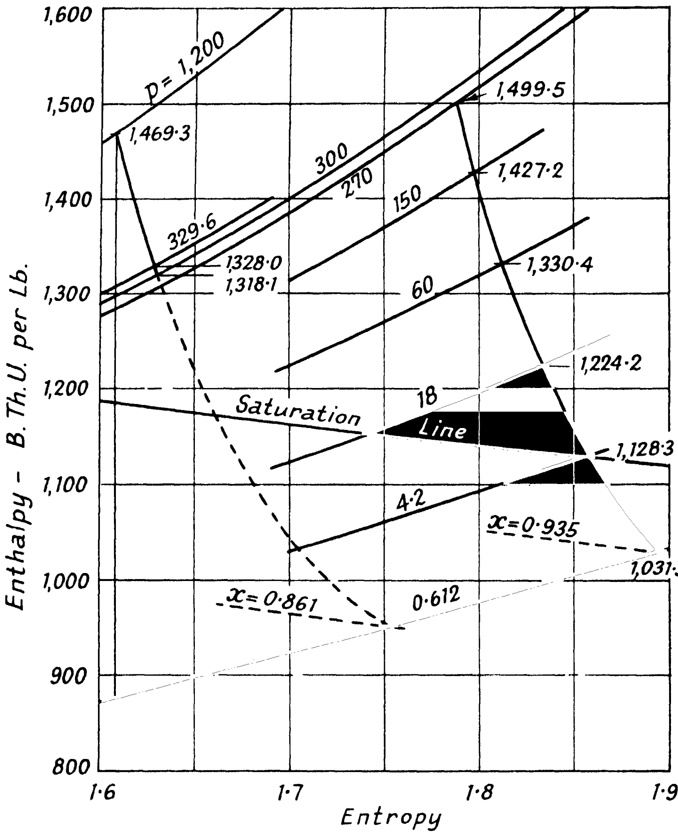


FIG. 205. —ϕ-I Diagram for Reheat Cycle

supplied in the reheating process will be thrown to waste in the condenser. This point is well shown by Fig. 204, based on calculations by the author. The following assumptions were made: (*a*) no feed-heating; (*b*) turbine stage efficiency 82 per cent for dry stages; (*c*) no allowance for pressure drop in reheater.

The thermodynamic gain shown in Fig. 204 is calculated on the assumption of isentropic expansion before and after reheating, no allowance being made for the effect of moisture. The gain is seen to be small.

The effect of regenerative feed-heating on the possible increase in thermal efficiency due to reheating and on other factors will be shown in the following example.

EXAMPLE 28. The following are the conditions of operation of a reheat turbine—

Initial steam pressure . . .	1,200 lb. per sq. in. abs.
Initial steam temperature . .	950° F.
Pressure of steam entering reheater .	300 lb. per sq. in.
Pressure of steam leaving reheater . (i.e. 10 per cent pressure drop in reheater)	270 lb. per sq. in.
Reheat temperature . . .	950° F.
Exhaust steam pressure . . .	0·612 lb. per sq. in.
"Dry" stage efficiency . . .	0·85
"Wet" stage efficiency . . .	$0{\cdot}85x$

Condition of steam extracted for feed-heating as found from the condition curve, Fig. 205—

Stage No.	Steam Pressure lb./sq. in. abs	Condition of Steam
1	329·6	Superheat = 203° F.
2	150	Superheat = 443° F.
3	60	Superheat = 303° F.
4	18	Superheat = 143° F.
5	4·2	Dry and saturated

The arrangement of the plant is shown diagrammatically in Fig. 206.

Comparisons will be made between the non-reheat and reheat cycles, with and without regenerative feed-heating.

The non-reheat cycle, with and without feed-heating, has already been dealt with in Example 24. The bled steam pressures are slightly different in the present example.

From the data given in Figs. 205 and 206 the quantities of steam bled off for feed-heating may be readily calculated as follows—

Heater No	Steam Extracted per lb of Steam Entering Turbine	Steam Flow through Turbine
		1·0000
1	0·0787	
		0·9213
2	0·0590	
		0·8623
3	0·0575	
		0·8048
4	0·0485	
		0·7563
5	0·0299	
		0·7264
	Total = 0·2736	

Considering the flow of one pound of steam into the turbine—

Heat supplied in cycle

$$= (1{,}469{\cdot}3 - 397{\cdot}0) + 0{\cdot}9213\,(1{,}499{\cdot}5 - 1{,}318{\cdot}1) = 1{,}239{\cdot}5$$

$$\text{Heat rejected} = 0{\cdot}7264\,(1{,}031{\cdot}3 - 53{\cdot}0)$$

$$= 710{\cdot}4$$

$\therefore$ Work done = 529·1 B.Th.U.

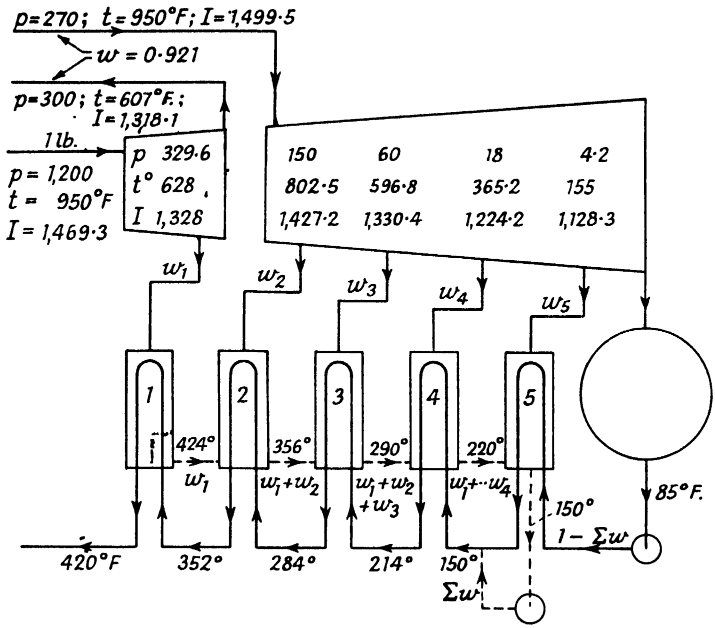


FIG 206—Diagrammatic Arrangement of Reheat Regenerative Feed-heating Cycle

It may be noted from Fig. 205 that the final wetness fraction is reduced by reheating from 13·9 to 6·5 per cent. The results of calculations are given in Table XX.

The following points may be noted from Table XX—

(1) The cumulative heat drop is increased some 17·1 per cent due to reheating.

(2) The gain in thermal efficiency is 6·55 per cent in the non-feed-heating cycle and 4·38 per cent in the feed-heating cycle. In both cases allowance is made for a 10 per cent pressure drop in the reheater.

(3) Due to the greater heat drop with reheating, the steam consumption per kW. hr. is reduced 17·1 per cent in the feed-heating cycles.

(4) The steam flow in the final stage of the turbine is reduced by 14·4 per cent in the feed-heating cycles.

TABLE XX

COMPARISON OF REHEAT AND NON-REHEAT CYCLES WITH AND WITHOUT REGENERATIVE FEED-HEATING

Note Unless otherwise stated, quantities given are for one pound of steam entering turbine.

	Non-reheat Cycle		Reheat Cycle	
	No Feed-heating	Feed-heating	No Feed-heating	Feed-heating
Cumulative heat drop .	624·2	624·2	731·0	731·0
Heat supplied . . .	1,416·3	1,072·3	1,597 7	1,239·5
Heat rejected . . .	900·9	633·7	978·3	710·4
Work done . . .	515·4	438·6	619·4	529·1
Turbine thermal efficiency per cent	36·39	40·91	38·77	42·70
Relative thermal efficiency .	1·000	- -	1·0655	—
Relative thermal efficiency .	—	1·00	—	1·0438
Steam consumption, lb /kW. hr. .	6·624	7·782	5·511	6·451
Steam flow through last stage, lb./kW. hr.	6·624	5·475	5·511	4·685
Dryness fraction of exhaust steam	0·861	0·861	0·935	0·935
Actual specific volume of exhaust steam, cu. ft /lb.	458	458	496	496
Volume of exhaust steam, cu. ft per kW. hr	3,035	2,508	2,734	2,322
Relative power output for same leaving velocity .	-	1·000		1·080

(5) In spite of the greater final specific volume, the volume flow through the last stage outlet in cu. ft. per kW. hr. is reduced by 7·4 per cent in the feed-heating cycles. Consequently, the power output may be increased by about 8 per cent for the same leaving velocity.

138. Notes on Reheating. Since the issue of the fourth edition of this book in 1944 the outlook on the subject of reheating has changed considerably. This is due, in part, to the steady increase in steam pressures and to the considerable increases in fuel costs. Besides providing an effective means of reducing the moisture content of the steam in the low-pressure stages of turbines and so improving the stage efficiencies, reheating makes it possible to achieve higher thermal efficiencies and larger power outputs for the same last wheel dimensions.

An advanced reheat-regenerative cycle for the Philo Power Station of the American Gas and Electric Service Corporation involves two-stage reheating and super-critical pressure steam. The operating conditions are as follows—

Initial steam pressure	4,500 lb. per sq. in.
Initial steam temperature	1,150° F.
First reheat pressure	1,150 lb. per sq. in.
First reheat temperature	1,050° F.
Second reheat pressure	165 lb. per sq. in.
Second reheat temperature	1,000° F.
Exhaust pressure	1·5 in. Hg.
Number of stages of feed-heating	7
Final feed temperature	515° F.
Output	125,000 kW.
Speed	3,600 r.p.m.

An overall thermal efficiency of more than 40 per cent is expected from this plant.

Owing to the fact that there is in a reheat turbine a considerable amount of steam in the turbines, reheater headers and tubes, and

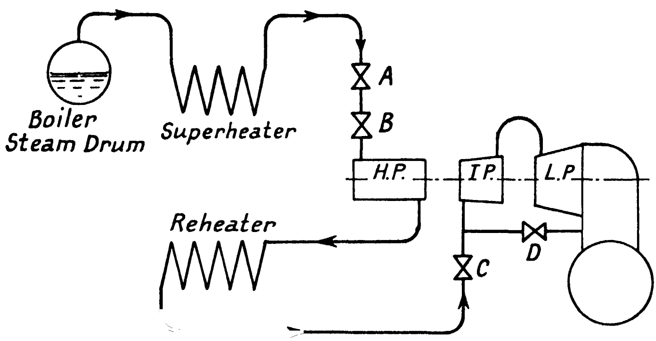


FIG. 207

steam pipes, which is beyond the control of the normal governor valve, it is necessary to provide some form of special control gear to prevent serious overspeeding of the turbine in the event of a sudden loss of load. There are many variations of this control gear but the general principle of the system often adopted nowadays is shown diagrammatically in Fig. 207. A and B are the emergency stop valve and governor valve, respectively, which are fitted to the h.p. turbine in the usual way. C is an interceptor or governor valve which controls the supply of reheated steam to the turbine in the event of a drop in load. The interceptor valve is full open at normal speed, begins to close at about 2·5 to 3 per cent above normal speed and is partially closed at speeds between 3 and 5 per cent above

normal. A dumping valve D is sometimes fitted between the interceptor valve and the turbine; it is normally shut but is opened by the action of the speed governor slightly after the intercepting valve begins to close and so enables steam to flow direct to the condenser.

139. Regenerative Water-extraction Cycle. Another method of combating the erosion problem in the L.P. stages of H.P. turbines

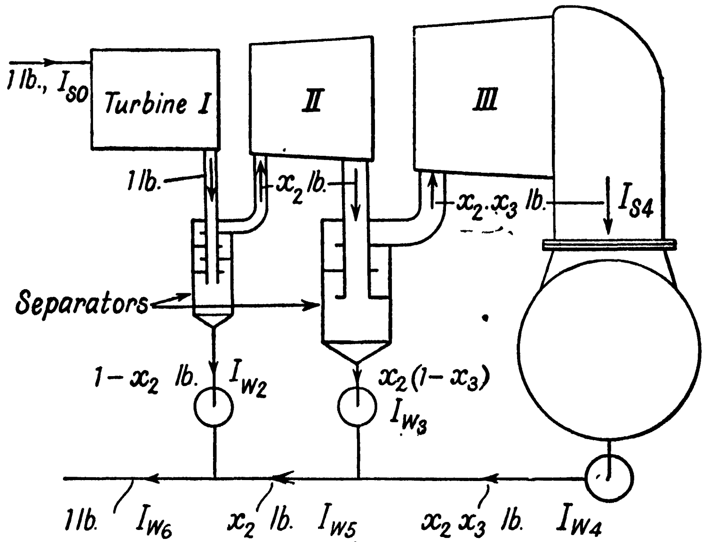


FIG. 208.—Diagrammatic Arrangement of Regenerative Water-extraction Cycle

is by the partial or complete extraction of suspended water particles from the steam during its flow through the wet stages.

As already stated in Art. 136, owing to inertia, the water droplets move radially outwards during their passage through the moving blades with the result that the larger droplets are concentrated in the outer half of the blades. The centrifugal force on a water droplet moving through a blade which has a peripheral velocity of 1,000 ft. per sec. at 1,500 r.p.m. is almost 5,000 times its own weight, but as the time of passage through the blade is exceedingly short—perhaps 0·0005 to 0·002 sec.—and as there is friction at the blade surface the actual outward movement is not so great as might be imagined. However, a certain quantity of moisture is flung off the blade, probably at the outlet side. Various water-catching devices have been installed in turbines for the purpose of trapping this water and leading it away to the condenser. Such devices are described in the author's book, *Steam Turbine Operation.*

Mr L S Robson (3) has stated that up to 40 per cent of the moisture in any given stage may be extracted by such traps This implies a reduction in the total moisture at exhaust of something like 60 per cent

In these drainage systems the water is, in some cases, drained direct to the condenser through holes drilled in the diaphragms

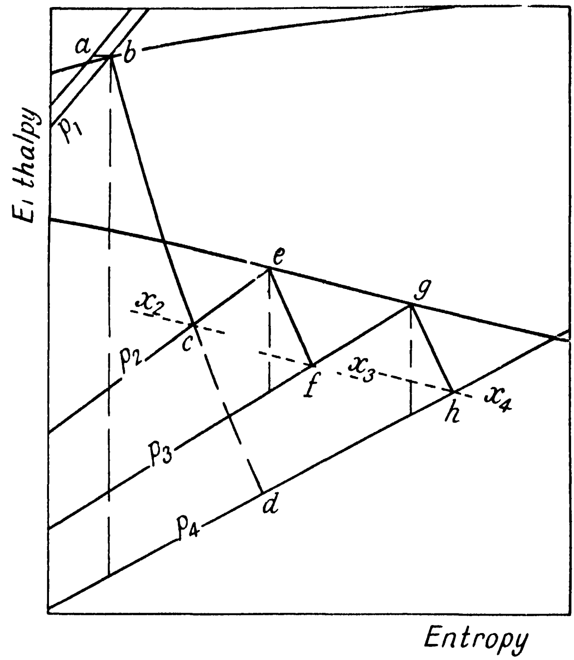


FIG. 209 ϕ-I Diagram for Water-extraction Cycle

and cylinder The sensible heat in the extracted water is thus lost In other cases, the water is cascaded from stage to stage, under these conditions there is a partial recovery of the sensible heat, for the water is partially evaporated due to the reduction of pressure

Attention has recently been directed to the possibility of effecting complete extraction of the suspended water at certain definite points in the expansion and utilizing the heat in the extracted water for feed-heating purposes Such a system with two-point extraction is shown diagrammatically in Fig 208 The extracted water is driven by pumps into the feed pipe, arrangements being made so that water only is extracted

The ϕ-I diagram for the cycle is shown in Fig 209, in which *bd* represents the condition curve for the unmodified cycle Complete extraction is assumed to take place at pressures p_2 and p_3 Suppose

that the dryness fraction at c is x_2; then the water extracted is $1 - x_2$ lb. per lb. of steam entering the turbine. Also, the weight of steam passing through turbine II is x_2 lb. This expands along ef and reaches a dryness x_3. The water extracted at the second point is $(1 - x_3)x_2$ and the steam flow through turbine III is x_2x_3. This is also the flow into the condenser.

Neglecting the extremely small increase in enthalpy due to the compression in the water extraction pumps—

$$x_2 I_{w5} = x_2 x_3 . I_{w4} + x_2(1 - x_3) I_{w3}$$

$$\therefore \quad I_{w5} = x_3 . I_{w4} + (1 - x_3) I_{w3}$$

$$\text{Also} \quad I_{w6} = x_2 . I_{w5} + (1 - x_2) I_{w2}$$

$$= I_{w2} - x_2(I_{w2} - I_{w5})$$

Heat supplied $= I_{s0} - I_{w6}$.

Internal work done

$$= (I_b - I_c) + x_2(I_e - I_f) + x_2 x_3(I_g - I_h)$$

From these expressions the internal thermal efficiency may be calculated. Similar expressions may be readily deduced for any number of extraction points. The theoretical possibilities may be gauged from the following example.

EXAMPLE 29. Steam expands in a H.P. turbine from $p_1 = 1{,}200$, $t_1 = 800°$ F. to $p = 0{\cdot}5$, the dry stage efficiency being 80 per cent. Calculate the theoretical increase in cycle efficiency with one-point and two-point regenerative water extraction over the simple non-extraction cycle. The extraction pressures should be chosen so as to give approximately equal dryness fractions at exhaust from each section of the turbine, and a uniform wetness correction of 1 per cent per 1 per cent of wetness should be used.

The data for the non-extraction cycle are the same as for Example 27, page 337. The internal thermal efficiency, allowing for wetness, is 33·15 per cent.

The extraction pressures to give approximately equal dryness fractions may be found quickly by trial and error and, together with other relevant data, are given in Table XXI. The student should verify the results given by working them out on the Mollier chart.

It would be a comparatively easy matter to dry the steam by means of a separator as it passes from one turbine cylinder to another. Unfortunately, even when there are three cylinders in series, the wetness fraction at inlet to the L.P. cylinder is comparatively small and little benefit would be obtained by extracting the moisture there. For two-point extraction, at least one of the extraction points should be located somewhere in the L.P. cylinder. Whether it will be possible to effect approximately complete extraction at such a point remains to be seen, but there is no doubt that the cycle is a promising alternative to the reheating cycle.

Readers interested in the matter should refer to a paper by Dr. Ir. W. M. Meijer (4).

TABLE XXI

Calculations for Typical Regenerative Water-Extraction Cycle

Note. The steam flows given for each turbine are per lb. of steam entering turbine I (see Fig. 208) In any turbine, x_2 is the dryness fraction at the end of expansion in that turbine, x_m is the mean dryness fraction in the wet stages, and I_1 and I_2 are the initial and final enthalpies respectively.

	One-point Extraction	Two-point Extraction
Turbine I		
Steam flow	1 lb.	1 lb.
Outlet pressure	10	26
x_2	0·9065	0·9371
x_m	0·953	0·968
I_1	1,382·7	1,382·7
I_2	1,051·2	1,102·6
Internal work done	324·85	277·2
Turbine II		
Steam flow	0·9065	0·9371
Outlet pressure	0·5	4
x_2	0·908	0·9353
x_m	0·954	0·967
I_1	1,143·0	1,162·5
I_2	995·6	1,060·6
Internal work done	127·44	92·32
Turbine III		
Steam flow	—	0·8762
Outlet pressure	—	0·5
x_2	—	0·9355
x_m	—	0·968
I_1	—	1,125·7
I_2	—	1,024·6
Internal work done	-	85·76
Enthalpies of Water		
After extraction pump	47·4	47·4
After 1st drain pump	58·0	52·16
After 2nd drain pump	—	62·13
Heat supplied in cycle	1,324·7	1,320·6
Total internal work done	452·3	455·3
Internal thermal efficiency per cent	34·14	34·47
Increase above thermal efficiency of non-extraction cycle	0·99	1·32
Percentage increase	2·98	3·98

BIBLIOGRAPHY

1. BAUMANN: "Some Recent Developments in Large Steam Turbine Practice." *Journal Inst. Elec. Eng.*, 1921; 59; 581.
2. GARDNER: "The Erosion of Steam Turbine Blades." *The Engineer*, 1932; 153; pp. 146, 174 and 202.
3. ROBSON: "The Development of Large Turbines for Land Power Installations." *Trans. Liverpool Eng. Soc.*, 1936; 57; 73.
4. MEIJER: "The Extraction of Condensate from Expanding Steam, its Effect upon the Efficiency of the Ideal Heat Cycle and its Influence upon the Selection of Initial Steam Conditions." *Trans. Inst. of Naval Architects*, 1939; 81; 36.

EXAMPLES XIV

1. The following particulars relate to a low-pressure stage of an impulse steam turbine—

Nozzle angle	24°
Dryness fraction at nozzle outlet	0·90
Steam velocity at nozzle outlet	1,400 ft per sec.
Mean velocity of water particles at nozzle outlet	200 ,, ,,
Mean blade velocity	650 ,, ,,
Ratio of relative velocity at outlet to relative velocity at inlet with homogeneous flow	0·87
Steam flow (total) lb. per sec.	140

If the blades are equiangular, calculate the horse-power developed in the blades and the blade efficiency ignoring carry-over effects—

(*a*) assuming homogeneous flow;
(*b*) assuming non-homogeneous flow.

Assume that there is no rebound at the inlet edge of the blades, that the momentum of the water particles referred to the relative velocity is reduced to zero at impact, and that the relative velocity of the water particles at outlet is 0·15 times that of the dry steam.

2. Steam is supplied to a turbine at a pressure of 500 lb. per sq. in. abs. and a temperature of 750° F. It expands at constant entropy to a pressure of 1·2 lb. per sq. in. abs. What is the dryness fraction at the end of expansion and the thermal efficiency of the cycle?

Calculate the modified exhaust condition and thermal efficiency if the steam is reheated at 80 lb. per sq. in. to a temperature of 730° F. and then expanded adiabatically to a pressure of 1·2 lb. per sq. in.

3. Steam is supplied to a turbine at a pressure of 1,000 lb. per sq. in. abs. and a temperature of 800° F., the exhaust pressure being 0·5 lb. per sq. in. abs. If the internal efficiency ratio of the turbine is 0·8, what is the internal thermal efficiency of the turbine and the final wetness fraction of the exhaust steam?

In a modified arrangement, the steam is first expanded from the initial condition given above to a pressure of 120, the internal efficiency ratio being 0·8. The steam is then reheated in a surface heater by the live steam at 1,000 lb. pressure and 800° F., to a temperature of 520° F. It is then expanded in a low-pressure turbine to 0·5 lb. per sq. in. abs., the internal efficiency ratio being 0·8. Calculate the internal thermal efficiency of the modified turbine and the final wetness fraction of the exhaust steam.

4. Steam is generated at the critical pressure ($p = 3{,}200$; $t = 706°$ F.; $I_w = I_s = 902$ B.Th.U. per lb.) and is superheated to a temperature of 806° F. The mean specific heat of the superheated steam at the critical pressure for this range is 3·48.

The steam is then throttled to a pressure of 1,000 lb. per sq in. abs., and after throttling, heat is supplied to the steam so that it becomes superheated

220° F. It is then expanded adiabatically until it is dry and saturated, when it is further heated so as to superheat it by 300° F. The steam is then further expanded adiabatically to a final pressure of 0·5 lb. per sq. in., at which pressure it is condensed.

Derive the theoretical thermal efficiency of the cycle.

5. Steam is supplied to a turbine at a pressure of 200 lb per sq. in. abs. (t = 382° F., L = 843·1) and is expanded isothermally to a pressure of 0·5 lb. per sq. in. abs. (t = 80° F., L = 1,047·0). Assuming that the specific heat of steam at 0·5 lb. pressure is 0·46, calculate the heat supplied, the heat rejected, the work done, and the thermal efficiency of the cycle.

6. Steam is supplied to a turbine at a pressure of 800 lb. per sq. in. abs. and at 840° F. It is expanded in a H.P. turbine to 80 lb. per sq. in., the internal efficiency ratio of the H.P. turbine being 0·8. The steam is reheated at constant pressure by saturated live steam and is returned to the L.P. turbine at 80 lb. pressure and 500° F. It is then expanded to 0·5 lb. per sq. in. abs. with the same internal efficiency ratio. If the mechanical efficiency of the turbine is 99 per cent and the alternator efficiency is 96 per cent, calculate the weight of steam generated by the boiler per kWh output and also the heat consumption of the turbine in B.Th.U. per kWh. Assume that the heating steam gives up heat by condensing only.

7. Calculate, using the Mollier chart, the gross and net theoretical thermal efficiencies of the following cycle—

Feed water at 80° F. (v_w = 0·016 cub. ft. per lb.) is compressed to a pressure of 1,000 lb. per sq. in. abs., and is then heated to the saturation temperature. It is evaporated at a pressure of 1,000 lb. and superheated to a total temperature of 800° F. The steam is then expanded adiabatically to a pressure of 100 lb. per sq. in. abs., at which pressure it is reheated to 700° F. It is then expanded adiabatically to 0·5 lb. per sq. in. abs., at which pressure it is condensed.

8. Steam is supplied to a turbine at a pressure of 500 lb. per sq. in. abs. and superheated 300° F. It is expanded adiabatically to 1 lb. per sq. in. abs. What is the thermal efficiency of the cycle?

In a modification of the cycle, the steam is extracted from the turbine at the point where it becomes just dry and saturated and is reheated so that its superheat is again 300° F. After further adiabatic expansion the steam is extracted at the point where it becomes just dry and saturated, and is reheated to such an extent that it becomes dry and saturated after expansion to 1 lb. per sq. in. abs. It is then exhausted and condensed.

Derive from the ϕ-I chart the reheating pressures and the final superheat of the steam as it leaves the second reheater. Calculate the thermal efficiency of the modified cycle.

9. Steam at a pressure of 400 lb. per sq. in. abs. and at a temperature of 950° F. (I_s = 1,496·2) is supplied to a steam turbine plant consisting of H.P. and L.P. turbines in tandem.

The live steam does not go direct to the H.P. turbine, but first passes through a steam reheater in which it gives up heat to reheat the steam passing from the H.P. to the L.P. turbine. The live steam enters the H.P. turbine at 400 lb. pressure and 700° F. (I_s = 1,366·2). The pressure of the steam exhausted from the H.P. turbine is 100 lb. per sq. in. abs., and the L.P. turbine exhaust pressure is 1 lb. per sq. in. abs.

What is the condition of the steam between the H.P. and L.P. turbines before and after reheating, and what is the thermal efficiency of the cycle? Assume expansion at constant entropy. (*Liv. Un.*)

10. A steam turbine plant operates between the pressures of 1,200 and 1·0 lb. per sq. in., the initial steam temperature being 800° F. Steam is extracted from the turbine at 400 lb. per sq. in. and reheated to 800° F. Due

to friction there is a drop of pressure in the reheater. Find the pressure drop in the reheater for which the gain in thermal efficiency due to reheating just vanishes. Assume isentropic expansion throughout. (*Lv. Un.*)

11. Compare the theoretical heat consumptions in B.Th.U. per kW. hr and the final wetness fraction of the exhaust steam for the following cycles in which steam is supplied to a turbine at 1,000 lb. per sq. in and exhausted at 0·5 lb per sq. in,—

(*a*) Initial steam temperature = 900° F. Overall efficiency ratio 0·82. Alternator efficiency 0·96

(*b*) Initial steam temperature 900° F. Steam reheated to 900° F. Steam pressure entering reheater 100 lb. per sq. in., steam pressure entering turbine from reheater 80 lb. per sq. in. Overall efficiency ratio of each turbine 0·82. Alternator efficiency 0·96.

Why is the performance in the second case likely to be better than that indicated by the simple theory? (*Lv. Un.*)

12. Discuss the advantages and disadvantages of reheating in steam power plants and explain why it becomes more necessary to adopt a reheat cycle with high steam pressures.

In the low-pressure turbine of a two-cylinder machine, the steam is initially dry and saturated with an enthalpy I_1. The final pressure is p_2 (liquid enthalpy i_2 and latent heat L_2). The overall efficiency ratio of the stages would be η if they were using dry steam, but with wet steam having a mean dryness fraction x_m, the efficiency ratio is $x_m \eta$. Show that the final dryness fraction of the steam at p_2 is

$$x = \frac{2(I_1 - i_2) - \eta\,\Delta H}{2L_2 + \eta\,.\,\Delta H}$$

where ΔH is the isentropic heat drop. (*Lv. Un.*)

13. A steam turbine with single-stage reheating and regenerative feed heating operates under the following conditions

Initial steam pressure	1,500.
Initial steam temp. . . .	1,000° F.
Pressure at which steam is reheated	300.
Reheat temp. at inlet to i.p. turbine . .	960° F
Feed temp. at outlet from final feed heater	420·4° F
Exhaust pressure . . .	0·8
Steam bled off before reheater .	4 per cent of steam entering turbine
Total steam bled off . .	21 per cent of steam entering turbine.
Internal efficiency of h.p. turbine . . .	0·83.
Internal efficiency of i.p. and l.p. turbines .	0·88
Efficiency of alternator	0·98.

Neglecting heat losses and pressure losses due to reheating, calculate—

(*a*) the heat rate in B.Th.U per kW. hr

(*b*) the total volume of steam passing through the exhaust in cu. ft. per sec. if the electrical output is 100,000 kW.

(*Lv. Un.*)

14. Two steam turbines operate with steam at an initial pressure of 1,500 lb. per sq. in. and an initial temperature of 1,000° F. In each turbine the steam is expanded in a high-pressure cylinder to 120 lb. per sq. in., the efficiency ratio being 80 per cent.

In turbine No. 1 the steam continues its expansion in a low-pressure turbine from 120 lb. per sq. in. to a final pressure of 0·5 lb. per sq. in., the efficiency ratio being 0·78. In turbine No. 2, the steam is reheated after its expansion

through the h.p. turbine and returned to the l.p. turbine at 100 lb. per sq. in., and 1,000° F. after which it expands to 0·5 lb. per sq. in. with an efficiency ratio 0·84.

Compare for the two power cycles—

(*a*) thermal efficiency,

(*b*) total steam consumption for a full-load output of 60,000 kW.,

(*c*) total volume of exhaust steam per second for a full-load output of 60,000 kW. (*Liv. Un.*)

CHAPTER XV

TURBINE PERFORMANCE AT VARYING LOADS

140. Methods of Governing. The object of the present chapter is to consider, in an elementary manner, the performance of steam turbines when operating at loads different from the designed or economic load. This performance will depend, to a large extent,

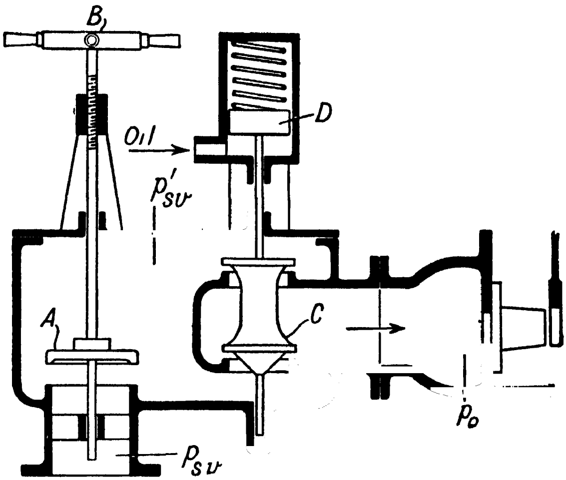


FIG. 210.—Diagrammatic Arrangement of Simple Throttle Valve

on the particular method employed for controlling the supply of steam to the turbine so that the speed of rotation will remain sensibly constant irrespective of the load. The principal methods of governing may be enumerated as follows—

(1) Throttle governing.
(2) Nozzle control governing.
(3) By-pass governing.
(4) Combinations of (1) and (2), and (1) and (3).

141. Throttle Governing. Fig. 210 shows diagrammatically the essentials of a simple throttle governing system. A is the turbine stop valve, which may be opened or closed by means of the handwheel B. The purpose of A is to start and stop the turbine; when the machine is on load the valve A is full open. The actual control of speed is effected by the governor valve or throttle C. This is usually a double-beat valve having seats of equal, or nearly equal, area and is so shaped that the forces on the valve due to static

pressure and dynamic action are balanced. Except in small turbines, the opening of the valve C is effected by an oil servo motor D which, in turn, is controlled by the centrifugal speed governor.

Suppose that $p_{s.v.}$ is the steam pressure before the stop valve. This is the pressure normally used as the datum in turbine testing. There will be a slightly lower pressure $p'_{s.v.}$ after the stop valve. In

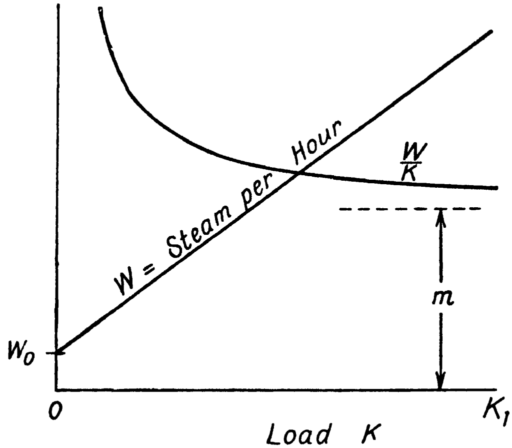


FIG 211.—Willans Line for Steam Turbine

order to effect control, the pressure p_0 in the nozzle box must be lower than $p'_{s.v.}$ The drop from $p_{s.v.}$ to p_0 appears to vary from 2 to 5 per cent of $p_{s.v.}$ at full load.

The relationship between load and steam consumption for a turbine governed by throttling is given by the well-known Willans line, Fig. 211. Numerous tests show that when a turbine is governed by throttling, the Willans line is straight.

If W_1 = steam per hour at full load.
W_0 = steam per hour at no load.
K_1 = full load (say in kW).
K = any other load.
W = steam consumption at load K.

Then
$$W = m \, . \, K + W_0 \quad . \quad . \quad . \quad . \quad (184)$$
where m is a constant.

The full-load steam consumption can be estimated fairly accurately from the heat drop and expected efficiency ratio. If the quantity W_0 could be expressed as a definite fraction of the full-load consumption, then the quantity W could be calculated for any intermediate power. For condensing turbines, the no-load steam consumption varies from about 0·10 to 0·14 times the full-load consumption.

The steam per kWh is equal to

$$\frac{W}{K} = m + \frac{W_0}{K}$$

and is shown by the curve in Fig. 211. It will be seen that the steam per kWh curve is asymptotic to the value m.

Another experimental result of considerable importance is shown in generalized form in Fig. 212. If measured steam flows W lb.

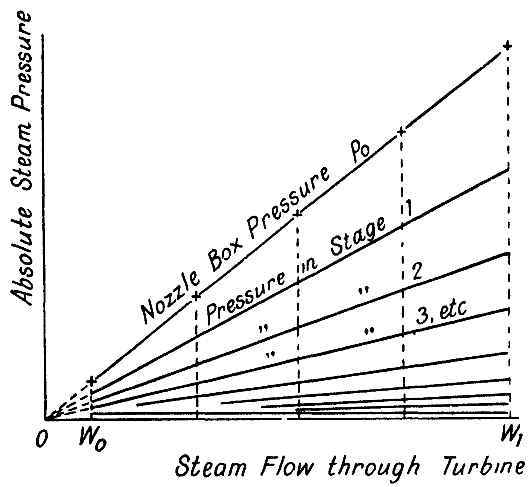


FIG 212

per hour for the range from W_0 to W_1 be plotted as abscissae and values of the nozzle-box pressure be plotted as ordinates, then the points will lie on a straight line. In many cases, the line when produced passes through the origin, showing that the steam flow is directly proportional to the nozzle-box pressure, and vice versa. In some cases, when the nozzle-box pressure is plotted against the condensate, the line when produced passes a little to the right of the origin; this is probably due to the inflow of steam supplied for sealing the low-pressure shaft gland. It is also an experimental fact that when stage pressures are plotted against steam flow, the plotted points lie on straight lines which, excepting those for the last few low-pressure stages, also pass through the origin when produced.

The two graphs may be combined, as shown in Fig. 213, to give the nozzle-box pressure at any load K. The diagram is self-explanatory and illustrates yet another experimental result, namely, that with simple throttle governing the relation between nozzle-box pressure and load is given by a straight line.

The effect of throttle governing may now be illustrated with reference to the Mollier chart, Fig. 214. It will be assumed (1) that

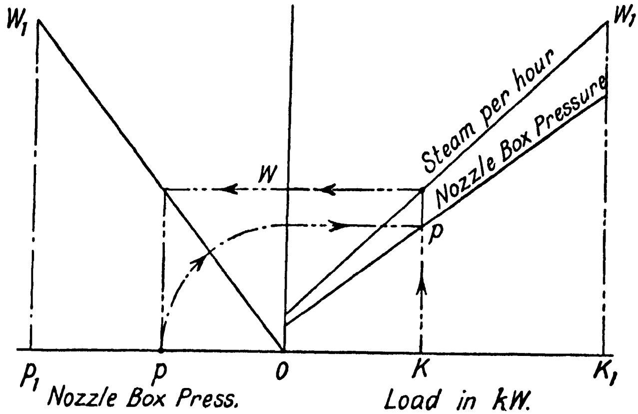


FIG. 213

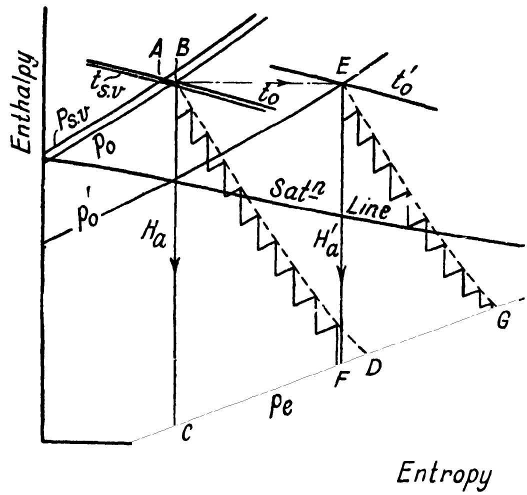


FIG. 214

the steam passes through the throttle valve with a negligible loss of heat and (2) that the vacuum in the condenser remains constant. Actually, unless the quantity of cooling water is reduced as the steam quantity entering the condenser is diminished, the steam

temperature in the condenser will fall, with a corresponding fall in the exhaust pressure.

Suppose that $p_{s.v.}$ is the steam pressure before the turbine stop valve and that p_0 is the pressure in the nozzle chest of the first stage at full load. A represents the condition before the stop valve as specified by the pressure $p_{s.v.}$ and the superheat $t_{s.v.}$ B is the condition at full load after throttling, the superheat being t_0. BC represents the adiabatic expansion to the exhaust pressure p_e, and BD the locus of actual state points.

At some fractional load where the steam flow is W′, the first-stage nozzle-box pressure will be p'_0, such that

$$p'_0 = \frac{W'}{W} \cdot p_0$$

The throttling process is conveniently represented by the line AE. As before, EF and EG show the adiabatic and actual expansion curves. It will be seen that the main effect of throttling, apart from reducing the steam flow, is to reduce the adiabatic heat drop. It will be shown later that the internal efficiency ratio η_i is not likely to be affected to any appreciable extent by the changes brought about by throttle governing. Consequently, if K_i = internal power at full load and K'_i = internal power at fractional load,

$$K_i = \frac{\eta_i \,.\, W \,.\, H_a}{3\,413}$$

and

$$K'_i = \frac{\eta_i \,.\, W' \,.\, H'_a}{3{,}413}$$

A secondary effect of throttling is to increase the initial superheat and to delay the dew point. As a result, the amount of wetness in the low-pressure stages will be reduced, with beneficial results.

142. Pressure Distribution at Varying Loads with Throttle Governing. The distribution of pressure may be found approximately by the following method. Suppose that for any given fractional load the internal steam flow derived from the Willans line is *w* lb. per second. The corresponding initial pressure is calculated and the condition curve is plotted, as shown in Fig. 214, using the method outlined in Chapter XII. The corresponding Σh and $\log_{10} v_n$ curves are drawn to a suitably large scale (Fig. 215).

Two conditions must be satisfied in each stage of the turbine. In the first place, since the nozzles are assumed to be running full, the equation of continuity must be satisfied,

i.e. $$w \,.\, v_n = A \,.\, V_1$$

where V_1 is the actual efflux velocity and A is the nozzle area. If the nozzle is convergent and the pressure drop in the nozzle is greater than the critical, then, in applying the above equation

v_n must be the specific volume at the throat, A the throat area, and V_1 the actual velocity at the throat.

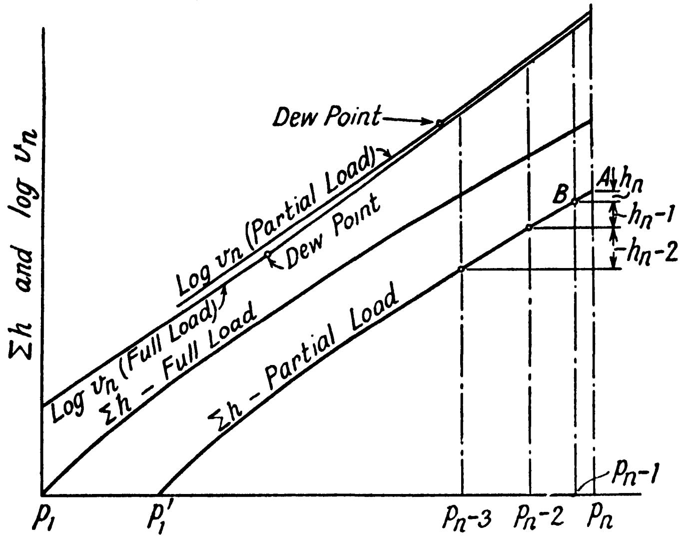


FIG. 215

In the second place, the adiabatic heat drop in a given stage equals

$$h = \left(\frac{V_t}{223{\cdot}8}\right)^2 \text{ B.Th.U./lb.}$$

and since $\quad V_t = \frac{V_1}{\eta_v}$ and $V_1 = \frac{w \cdot v_n}{A}$

$$h = \left(\frac{w \cdot v_n}{223{\cdot}8\ \eta_v A}\right)^2 \text{ B.Th.U./lb.} \quad . \quad . \quad . \quad (185)$$

Starting from the exhaust end and again assuming a constant exhaust pressure, h is calculated for the last or nth stage of the turbine, the value of v_n being taken from Fig. 215 as the exhaust specific volume and the area A being that of the nozzles in the last stage. Owing to the comparatively small value of w, the velocity V_1 is comparatively small and the heat drop h_n is smaller still. This heat drop is now set down from A and gives the point B on the Σh line. Since the Σh curve gives the sum of the adiabatic heat drops as a function of the stage pressures, it follows that if the pressure at inlet to the nozzles of the last stage is p_{n-1}, then the available adiabatic heat drop will be sufficient to generate the velocity V_1.

By projecting upwards on to the $\log_{10}v_n$ curve, the specific volume v_n at outlet from the nozzles in the preceding stage may be obtained. Using this value in eq. (185) and the appropriate nozzle area, the necessary adiabatic heat drop h_{n-1} in the penultimate stage is obtained. Setting this down as shown in Fig. 215, the pressure p_{n-2} is obtained. The calculation is thus carried out stage by stage, the information yielded being the stage pressures, specific volumes, heat drops, jet velocities, and blade speed ratios.

The above method, given in a paper by the author (1), cannot perhaps claim to be rigorously accurate, but it certainly gives results in good accord with experiment. The application of the method will now be illustrated by means of a worked example.

EXAMPLE 30. The following particulars relate to an impulse turbine of 3,000 kW, governed by simple throttling—

Initial pressure at full load . .	200 lb. per sq in. abs.
Initial superheat at full load . .	150° F.
Exhaust pressure, assumed constant.	1 lb. per sq. in. abs.
Stage efficiency	75 per cent
Number of stages	10
η_v for nozzles (assumed constant) .	0·94
Full-load steam consumption . .	10·12 lb. per sec.
No-load steam consumption . .	1·012 lb. per sec.
Mean blade velocity in each stage .	524 ft. per sec.

Nozzle angles and areas—

Stage No	Nozzle Angle	Nozzle Area Sq. Ft.
1	16°	0·0295
2	16°	0·0416
3	16°	0·0605
4	16°	0·0902
5	16°	0·1436
6	16°	0·2358
7	16°	0·395
8	16°	0·690
9	18°	1·228
10	24°	2·298

It is required to determine the steam consumption, nozzle-box pressure, stage pressures, jet velocities, and blade speed ratios at 0, $\frac{1}{4}$, $\frac{1}{2}$, and $\frac{3}{4}$ load.

The Willans line is first drawn and then, from the proportionality of steam consumption and nozzle-box pressure, the latter is calculated. These are given in Table XXII.

The expansion lines and condition curves are next drawn on the Mollier chart, as shown in Fig. 216, thus yielding data on which the curves of Fig. 217 are drawn. These curves are then used for finding the pressures and steam velocities in the various stages.

TABLE XXII

PERFORMANCE OF 3,000 kW TURBINE AT VARYING LOADS

	Load on Turbine				
	Full	¾	½	¼	0
Steam per hour	36,480	28,272	20,064	11,856	3,648
Nozzle Box Pressure	200	155	110	65	20
Nozzle Box Superheat °F	150	162·9	180	207·3	267
Heat Drop Adiabatic	369·8	354·6	333·9	302·5	229·8
Heat Drop Cumulative	388	370·1	349·9	316·8	242·4

Calculated Steam Velocities at Outlet from Nozzles

Stage No	Load on Turbine				
	Full	¾	½	¼	0
1	1,310	1,297	1,300	1,297	1,301
2	,,	1,305	1,318	1,304	1,313
3	,,	1,299	1,308	1,324	1,318
4	,,	1,320	1,326	1,340	1,350
5	,,	1,303	1,302	1,293	1,284
6	,,	1,294	1,288	1,267	1,088
7	,,	1,308	1,301	1,290	773
8	,,	1,298	1,292	1,134	475
9	,,	1,321	1,148	796	272
10	,,	1,032	745	452	146

The jet velocity at outlet from the nozzles is given in Table XXII. The calculations were made with a slide rule, and the slight irregularities of the figures are due to this and to small errors in reading from the graph.

The most important facts emerging from these calculations may be enumerated as follows—

(1) The greatest variations in steam velocity occur in the stages nearest the exhaust.

(2) Even at no-load, when the steam consumption is only one-tenth of the full-load consumption, the steam velocities in the first five stages are practically unaffected.

Consider now the flow through the blades of the last three stages. The inlet velocity triangles and the blade sections for stages 8, 9, and 10 are shown in Fig. 218. It will be seen that in stage 10 there must be serious impact losses at quarter-load and at no-load, and a rather less serious loss at half-load; in stage 9 the losses are not appreciable except at quarter-load and no load, whereas in stage 8 the impact losses are inappreciable except at no load.

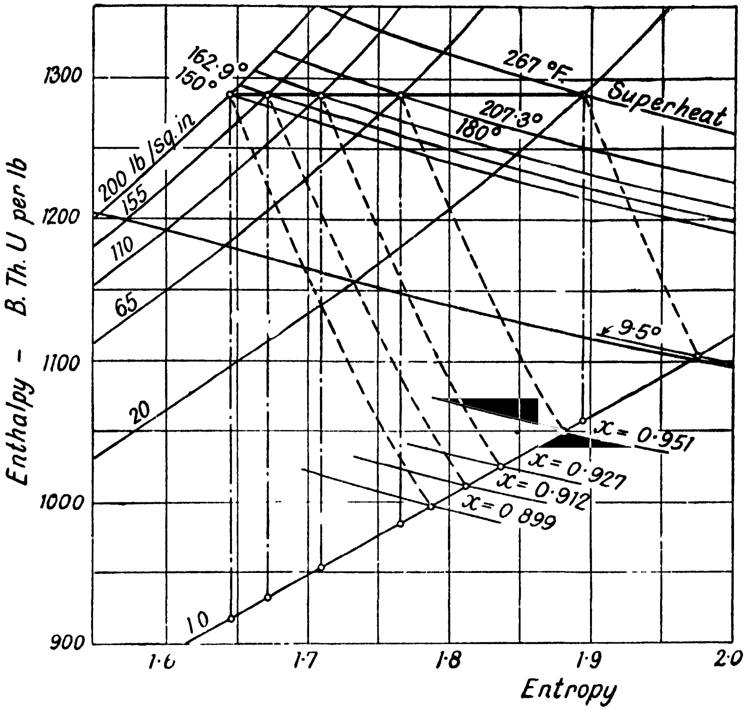


FIG. 216

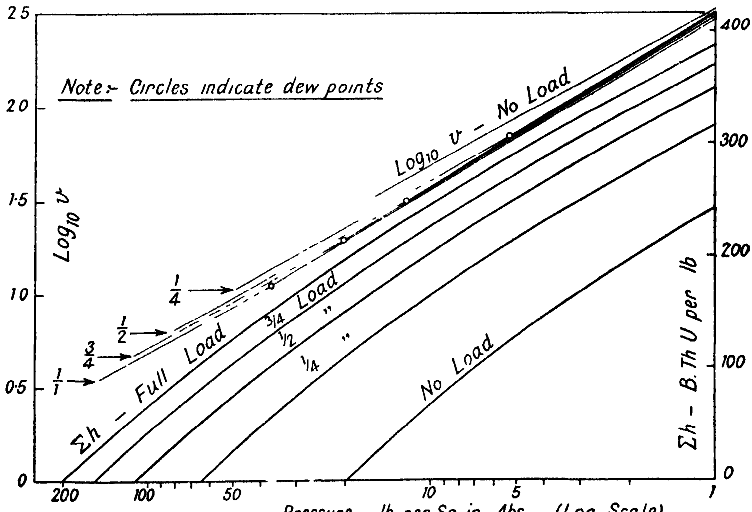


FIG. 217

In the majority of the stages, therefore, the impact losses at all loads above about quarter-load are very small. When the loss is appreciable, as in the final stage, the adiabatic heat drop in that stage is then very small and the effect on the internal efficiency of the

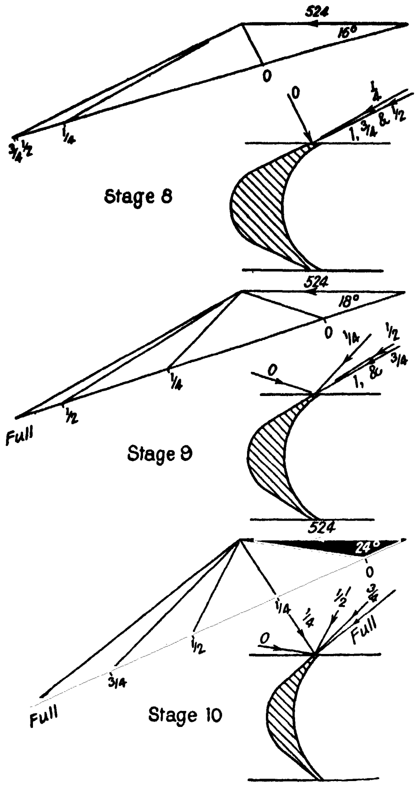


FIG 218.—Velocity Diagrams and Directions of Relative Velocities for a Steam Turbine Governed by Throttling

stages, as a whole, is inappreciable. A factor which tends to increase the stage efficiency at partial loads is the reduction in wetness in the later stages due to throttling.

If the quantity of cooling water is kept constant and, in consequence, the exhaust pressure falls as the load is reduced, the volumes of steam passing through the L.P. nozzles are not reduced to the same extent as when the exhaust pressure is kept constant. Consequently, the changes in jet velocity, etc., are not so great as those based on the assumption of a constant exhaust pressure.

143. Throttle Governing in Reaction Turbines. The methods of analysis set out in the foregoing articles are not suitable for the impulse-reaction (Parsons) turbine, owing to the large number of stages in this type. The following alternative method is especially suitable for a series of relatively small expansions such as occur in the Parsons turbine.

The two equations which must be satisfied are again the equation of continuity and the energy equation. Considering any point in the turbine, let V be the velocity at outlet from either a fixed or a moving row of blades, let p be the pressure in lb. per sq. in. abs., let P be the pressure in lb. per sq. ft. abs., let v be the specific volume of the steam in cub. ft. per lb., let A be the effective area at the outlet side of the blades, in sq. ft., and w the flow of steam *through* the blades in lb. per sec.

Then
$$w = \frac{AV}{v} = \frac{\frac{V}{v}}{\frac{1}{A}}$$

Using suffixes to represent the number of the blade rows, and assuming there are n rows of blades ($n/2$ fixed and $n/2$ moving) in the turbine—

$$w^2 = \frac{\frac{V_1^2}{v_1^2}}{\frac{1}{A_1^2}} = \frac{\frac{V_2^2}{v_2^2}}{\frac{1}{A_2^2}} = \ldots \frac{\frac{V_n^2}{v_n^2}}{\frac{1}{A_n^2}} = \frac{\sum_1^n \left(\frac{V^2}{v^2}\right)}{\sum_1^n \left(\frac{1}{A^2}\right)}$$

Suppose that the pressure drop in any given row is δP, then by the equations given in Art. 90, page 211—

$$\frac{V^2 - \phi \cdot U^2}{2g} = -\eta_n \cdot v \cdot \delta P$$

If it be assumed that the variation in blade speed ratio with variation in load is comparatively small—and judging by the performance of impulse turbines we are justified in making this assumption for all stages except the last few—then $\frac{U}{V}$ will be a constant, and assuming that ϕ is constant, we may write

$$\frac{V^2 - r \cdot V^2}{2g} = -\eta_n \cdot v \cdot \delta P$$

where $r = \frac{\phi U^2}{V^2}$, and is a constant.

$$\therefore \qquad \frac{V^2}{v^2} = -\frac{2g \cdot \eta_n}{1 - r} \cdot \frac{\delta P}{v}$$

The differential of $\frac{P}{v}$ is $d\left(\frac{P}{v}\right) = \frac{\delta P}{v} - \frac{P \cdot \delta v}{v^2}$

$$\therefore \qquad \frac{\delta P}{v} = \delta\left(\frac{P}{v}\right) + \frac{P \cdot \delta v}{v^2}$$

We shall assume, for the sake of simplicity, that for the whole expansion $Pv^m = C$, where C is a constant. The index m is given by eq. (164), page 300.

Then
$$\frac{\delta P}{P} + m \cdot \frac{\delta v}{v} = 0$$

$$\therefore \qquad \frac{P \cdot \delta v}{v^2} = -\frac{1}{m} \cdot \frac{\delta P}{v}$$

$$\therefore \qquad \frac{\delta P}{v} = \delta\left(\frac{P}{v}\right) - \frac{1}{m} \cdot \frac{\delta P}{v}$$

or
$$\frac{\delta P}{v} = \frac{m}{m+1} \cdot \delta\left(\frac{P}{v}\right)$$

$$\therefore \qquad \frac{V^2}{v^2} = -\frac{2g \cdot \eta_n}{1-r} \cdot \frac{m}{m+1} \cdot \delta\left(\frac{P}{v}\right)$$

$$\therefore \qquad w^2 = \frac{2g \cdot \eta_n}{1-r}\left(\frac{m}{m+1}\right)\frac{\frac{P_1}{v_1} - \frac{P_n}{v_n}}{\sum_1^n \left(\frac{1}{A}\right)^2} \qquad . \qquad . \qquad (186)$$

This equation is applicable to the whole, or to any group or groups of stages in the turbine. Thus, provided η_n, m, and r are constant—

$$w^2 = \text{Constant} \times \left(\frac{P_1}{v_1} - \frac{P_n}{v_n}\right)$$

or
$$w = C_1 \sqrt{\left(\frac{P_1}{v_1} - \frac{P_n}{v_n}\right)} \qquad . \qquad . \qquad . \qquad (187)$$

where
$$C_1 = \sqrt{\frac{2g \cdot \eta_n}{1-r}\left(\frac{m}{m+1}\right) \div \sum_1^n \left(\frac{1}{A}\right)^2} \qquad . \qquad . \qquad (188)$$

In a condensing turbine, the ratio $\frac{P_n}{v_n}$ is very small compared with $\frac{P_1}{v_1}$ and may be ignored. Hence we may write

$$w = C_1\sqrt{\frac{P_1}{v_1}}$$

If the turbine is governed by throttling, then the product P_1v_1 is constant, because I is constant. This follows from Callendar's equation for the specific volume of superheated steam, namely—

$$v_1 = \frac{1{\cdot}2464(I_1 - 835{\cdot}2)}{p_1} - 0{\cdot}00212$$

Neglecting the very small term, we have

$$w = C_1\sqrt{\frac{P_1p_1}{1{\cdot}2464(I_1 - 835{\cdot}2)}}$$

and since $P_1 = 144p_1$

$$w = \frac{12\,.\,C_1\,.\,p_1}{\sqrt{1{\cdot}2464(I_1 - 835{\cdot}2)}} \quad . \quad . \quad . \quad (189)$$

This expression shows that the rate of steam flow w is directly proportional to p_1, and vice versa. In the same way it may be shown that the pressure in any other row, sufficiently far removed from the exhaust end, is directly proportional to the steam flow. Consequently, in any such stage, the ratio $\frac{\delta P}{P}$ is constant.

But
$$V^2 = -\frac{2g\,.\,\eta_n}{1-r}\,.\,v\,.\,\delta P$$
$$= -\frac{2g\,.\,\eta_n}{1-r}\,.\,K\,.\,Pv$$

where K is a constant.

Since P_1v_1 is constant and Pv^m = Constant

$$Pv^m = P_1{v_1}^m$$

$$\therefore \qquad Pv - P_1v_1\left(\frac{P}{P_1}\right)^{\frac{m-1}{m}} = \text{Constant}$$

Therefore, in all stages except the last one or two, the steam velocity V is a constant, and the heat drop, blade speed ratio, etc., must also be constant. It will be seen that conditions in a Parsons turbine are affected by throttle governing in very much the same way as in an impulse turbine.

144. Nozzle Control Governing. The principle of nozzle control governing has already been outlined in Art. 6, and illustrated diagrammatically in Fig. 4. In applying the principle to land turbines,

which are almost entirely governed by automatic devices, various arrangements of valves and groups of nozzles are employed. Three arrangements are shown diagrammatically in Fig. 219. An arrangement often adopted with large steam turbines and with turbines using high-pressure steam is shown in Fig. 219 (*a*). The nozzles are divided into groups N_1, N_2, and N_3, under the control of valves V_1,

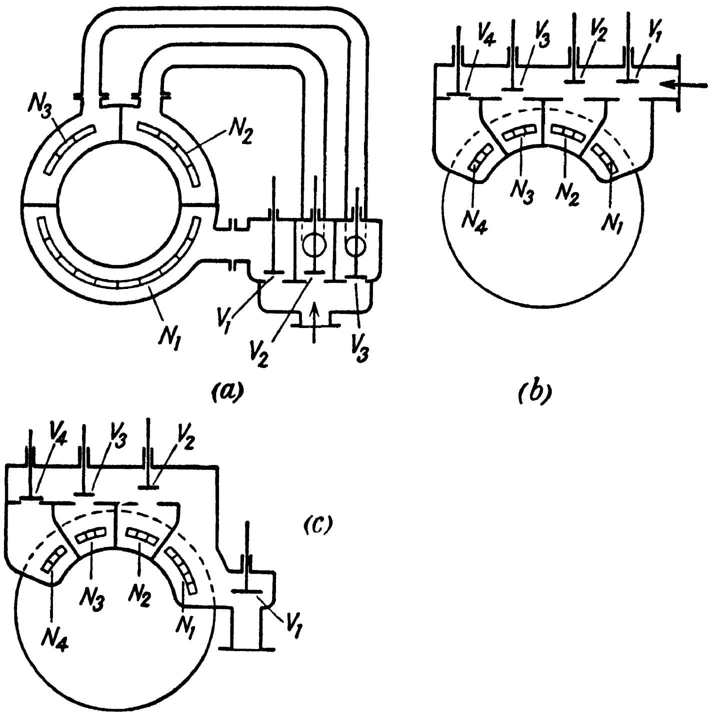


FIG. 219.—Diagrammatic Arrangements of Nozzle Control Governing

V_2, and V_3 respectively. The number of nozzle groups may vary from three to five, or more. Fig. 219 (*b*) differs from 219 (*a*) only in that the nozzle control valves are arrranged in a casting forming part of the cylinder, or bolted thereto, and containing passages leading to the individual nozzle groups. Although this arrangement is compact, the nozzles are confined to the upper half of the cylinder and the arc of admission is usually limited to 180°, or less. The number of nozzle groups varies from four to twelve. Fig. 219 (*c*) shows an arrangement sometimes employed. For the sake of illustration only four groups of nozzles are shown. The group of nozzles N_1 is under the control of the valve V_1, through which all the steam entering the turbine passes. Further admission of steam is through the

valves V_2, V_3, etc., in turn. In some instances, the nozzle group N_1 has been arranged in the lower half of the turbine and supplied with steam through a throttle V_1 up to, say, half-load. For loads greater than half-load, a further supply of steam is admitted through the valves V_2, V_3, etc.

Whatever method of construction is adopted, the nozzle control is necessarily restricted to the first stage of the turbine, the nozzle areas in the other stages remaining constant. It follows that, provided the condition of the steam at inlet to the second stage is not materially affected by the changed conditions in the first stage, the absolute pressure of the steam in front of the second-stage nozzles will be directly proportional to the rate of steam flow through the turbine.

145. Nozzle-box Pressures with Nozzle Control Governing. We shall now consider the variations in nozzle-box pressures as these affect the flow conditions in the first-stage nozzle groups. The problem will be illustrated with reference to the ten-stage impulse turbine for which the condition curve has been worked out in Art. 120 and Table XIX, page 294. Further particulars are given in Example 30 and Table XXII of the present chapter. Assume that the first-stage nozzles are divided into four groups, each group having a net area of 0·007375 sq. ft.

The pressure in the first-stage wheel chamber is represented by the straight line OA, Fig. 220, the pressure at A (full load) being 134·9 lb. per sq. in. abs. At full load, the ratio $\frac{p_2}{p_1}$ for the first-stage nozzles is 0·6745, i.e. greater than the critical pressure ratio (0·5456) for superheated steam. When steam is passing through three groups of nozzles only, the pressure in the first stage is lower than the critical. Consequently, the quantity of steam passed through each group of nozzles, i.e. 9,480 lb. per hr., is slightly greater than one-quarter of the full-load steam flow.

Consider now the operation with only one nozzle valve open. The no-load steam consumption is 3,648 lb. per hr. Consequently, valve No. 1 controls the steam supply between the limits 3,648 and 9,480 lb. per hr. Over this range the pressure in the first stage varies from 13·5 to 35, and is always lower than the critical. Consequently, with fair accuracy, we may say that the steam flow through the nozzles will be directly proportional to the absolute pressure in the nozzle box. Hence if the line OBC be drawn through the origin, then for any steam flow W_1, the pressure in the nozzle box will be p_{n1} and in the wheel chamber p_1. The valve V_1 will throttle the steam from 200 to p_{n1}.

Consider next the conditions when the load is gradually increased and valve V_2 is brought into action. At the point of opening, the steam flow through the nozzles N_2 is very small and the pressure in nozzle box 2 will be, to all intents and purposes, 35 lb. per sq. in. abs.

As the valve V_2 is opened an increasing amount, the pressure in the second nozzle box will rise from 35 to 200 lb. per sq. in. At first, the ratio $\frac{p_2}{p_1}$ for the nozzles will be close to unity and the pressure in the nozzle box will no longer be given by any straight line

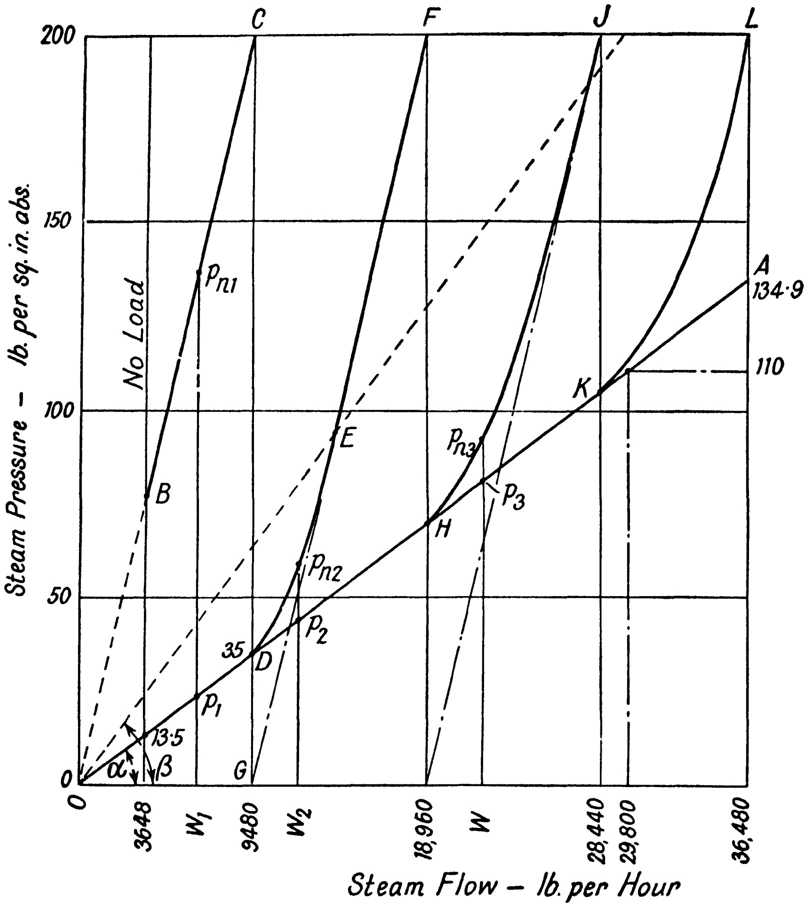


FIG. 220.—Steam Pressures in Nozzle Boxes with Nozzle Control Governing

relationship. To obtain the pressure for any given total steam flow W_2, we proceed as follows. Since the steam flow through group No. 1 is 9,480 lb. per hr., that through group No. 2 must be $W_2' = W_2 - 9{,}480$. The pressure at outlet from the nozzles

$$p_2 = W_2 \times \frac{134 \cdot 9}{36{,}480}$$

It remains to find, by trial and error, the initial pressure p_{n2} which, combined with the back pressure p_2 and the known area of the nozzles, will give a discharge W_2' lb. per hr. Such points are shown in the figure, curve DE. OE is a straight line drawn through the origin such that

$$\frac{\tan \alpha}{\tan \beta} = 0{\cdot}5457$$

the critical pressure ratio for superheated steam. Then for any steam flow, if the pressure in the nozzle box is higher than the pressure given by the line OE, the pressure drop is greater than the critical. Hence, if the points G and F are joined by a straight line, the nozzle-box pressure for a total steam flow greater than about 13,900 lb. per hr. is given by the straight line EF. The nozzle-box pressure for the full range of group 2 is given by the line DEF. Similarly, that for group 3 is given by the line HJ.

Considering next the operation when valves 1, 2, and 3 are full open, and valve 4 is partly open, up to a steam flow of 29,800 lb. per hr., the pressure drop in the first-stage nozzles is greater than the critical and the total flow through groups 1, 2, and 3 is 28,440 lb. per hr. For steam flows greater than 29,800 lb. per hr. the pressure in the first stage exceeds 110, and the discharge through the first three groups falls off slightly. This must be taken into account when calculating the nozzle-box pressure for group 4, given by the curve KL.

146. Condition Curve with Nozzle Control Governing. Consider the flow W lb. per hr., Fig. 220, and let p_{n3} be the nozzle-box pressure for group No. 3 and p_3 the pressure in the first stage. Further, let W_1, W_2, and W_3 be the steam flow through groups 1, 2, and 3 respectively. The quantity $(W_1 + W_2)$ expands from 200 down to p_3 following the locus ABC, Fig. 221. On the other hand, the quantity W_3 is throttled by the nozzle valve V_3 down to the pressure p_{n3}, and therefore its initial condition at inlet to the nozzles is given by point D. The subsequent flow in the nozzles is given by the curve DE and reheating in the blades by EF. Hence some of the steam issuing from the first-stage blades has the condition represented by the point C, whereas the small quantity has the condition F. It is improbable that these steam masses are perfectly mixed before entering the second-stage nozzles, but assuming that perfect mixing could occur, then the condition of the steam at inlet to the second-stage nozzles would be represented by point G, such that

$$(W_1 + W_2 + W_3)I_G = (W_1 + W_2)I_C + W_3 \cdot I_F$$

from which I_G may be found.

The subsequent expansion of the steam proceeds from G instead of from C. The increase in specific volume from C to G is usually fairly small, and the change in pressure distribution in the remaining

stages is so small that the previous assumption that p varies directly as W is sufficiently accurate for most purposes.

147. **Comparison of Throttle and Nozzle Control Governing.** The chief advantage claimed for nozzle control governing is the elimination of throttling losses. Actually, as we have seen, this is only partially true, because for steam flows intermediate between those corresponding to full-open positions of the consecutive nozzle control valves there is always more or less throttling at the valve which

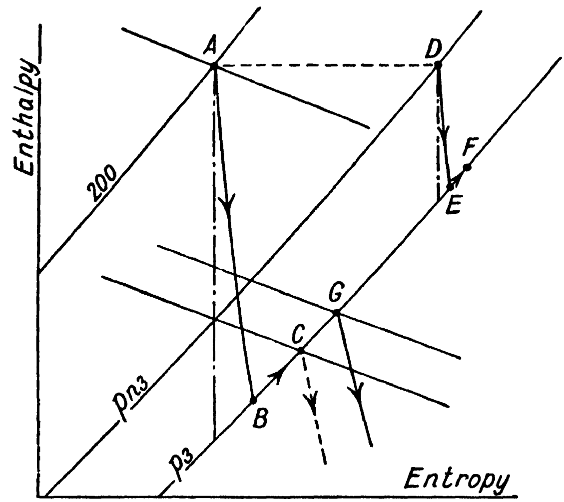


FIG. 221

is partially open. However, if the number of valves is fairly large the loss of available energy is not appreciable. The next question is the efficiency with which the extra heat drop is utilized. Since the initial steam condition at inlet to the second-stage nozzles is very nearly the same as with simple throttle governing, at light loads the distribution of pressure and of stage heat drop in the following stages is also nearly the same, i.e. the greatest changes in blade speed ratio, etc., take place in the last few stages. On the other hand, as the load is reduced the heat drop in the first stage is increased, the steam velocity V_1 is increased, and the blade speed ratio ρ is diminished. The change in ρ from full-load to no-load is quite appreciable, as shown by the figures in Table XXIII. The effect of this, however, is most marked when the designed heat drop in the first stage is comparatively small. In many cases, when nozzle control governing is used, either a large-diameter single-row wheel is used, or a two-row wheel is used in the first stage.

In addition to the great increase in jet velocity there will also be at light loads a considerable amount of jet deflection of the type

TABLE XXIII

VARIATION OF HEAT DROP IN FIRST STAGE OF 3,000 kW TURBINE GOVERNED BY NOZZLE CONTROL GOVERNING

Pressure in Nozzle Boxes Constant at 200 lb. per sq. in. abs. Initial Superheat 150° F.

Blade Velocity 524 ft. per sec. $\eta_n = 0{\cdot}9$. For other data, see Art. 145.

Steam Flow Lb. per Hour	Pressure in First Stage	Adiabatic Heat Drop	V_1	$\rho = \frac{u}{V_1}$
36,480	134·9	38·8	1,321	0·396
28,440	105·1	62·8	1,680	0·311
18,960	70·2	97·1	2,095	0·250
9,480	35·1	151·4	2,615	0·202
3,648	13·5	218·3	3,140	0·166

described in Art. 61. This will certainly lead to greater losses in the first stage.

Summing up the matter then, we may say that there is a greater heat drop available when nozzle control is employed, but that the efficiency with which the greater heat drop is utilized becomes more and more impaired as the load diminishes. Comparative tests show that when there is a fairly large heat drop in the first stage, nozzle control leads to a reduction in steam consumption.

148. **By-pass Governing.** In modern impulse turbines, and especially those operating at very high pressures, the H.P. turbine comprises a number of stages of comparatively small mean diameter. All such turbines are usually designed for a definite load, termed the economic load, at which the thermodynamic efficiency ratio of the turbine is a maximum. In the case of power station turbines, the economic load (E.L.) is made about 80 per cent of the maximum continuous rating (M.C.R.), which is the maximum output the generator is capable of giving continuously.

Owing to the very small heat drop in the first stage it is not possible, for the reasons given in the preceding article, to employ nozzle control governing efficiently. Furthermore, it is desirable to have full admission in the high-pressure stages at the economic load so as to eliminate the partial admission losses. Hence it is not possible to admit through additional nozzles in the first stage the 25 to 27 per cent extra steam necessary to generate the full output. In fact, in most cases it would be quite impossible to do so because the steam pressure in the first-stage wheel chamber would increase so much, due to the restriction at the second-stage nozzles, that it would require to be greater than the initial pressure.

These difficulties of regulation are overcome by the employment of by-pass governing, the principle of which is illustrated diagrammatically in Fig. 222. All the steam entering the turbine passes through a valve A (which is under the control of the speed governor) and enters the nozzle box or steam chest B. In certain cases, for example, this would suffice for all loads up to the economical load, the governing being effected by throttling. For loads

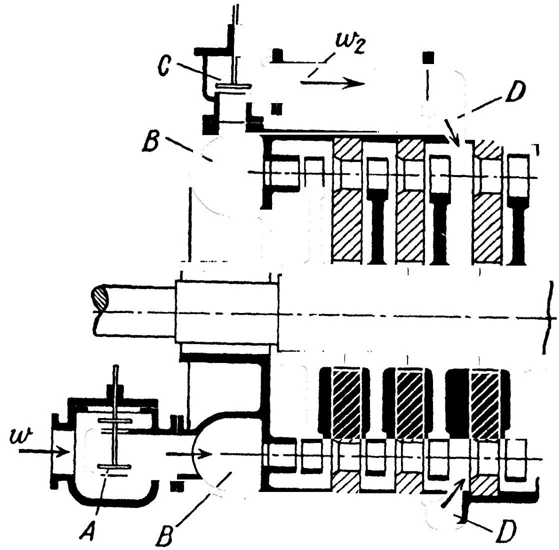


FIG. 222.—Diagrammatic Arrangement of By-pass Governing

greater than the economic load a by-pass valve C is opened, allowing steam to pass from the first-stage nozzle box into the steam belt D and so into the nozzles of the fourth stage. The valve C is not opened until the lift of the valve A exceeds a certain amount; also as the load is diminishing the valve C closes first. The by-pass valve is under the control of the speed governor for all loads within its range.

The number of by-pass valves is not always restricted to one. Fig. 223 shows the outline of the 105,000 kW steam turbine constructed by the Metropolitan-Vickers Electrical Co., Ltd., and installed in the Battersea Power Station. There are three cylinders arranged in tandem, and containing the following numbers of stages: H.P., 1-2-row wheel + 16 (single-row) stages; I.P., 18 stages; L.P., a double-flow turbine each half with 7 single-row wheels and a duplex multi-exhaust stage. For loads up to 60 per cent M.C.R., or 63,000 kW, steam is admitted before the velocity stage; for loads up to 80 per cent M.C.R., or 84,000 kW, steam is

admitted at B, after the velocity stage, while for the full output of 105,000 kW, steam is admitted at C, the first nine stages being by-passed.

149. Theory of By-pass Governing.

Let w_e = steam consumption in lb. per sec. at the economical load with no by-pass.

w = steam consumption at any load above the economical load; by-pass open.

w_1 = quantity of steam passing through the stages which are by-passed.

w_2 = quantity of steam which enters the by-pass stage.

p_n = pressure in by-pass stage at the economical load.

p_n' = pressure in by-pass stage at the higher load.

To a first approximation, i.e. neglecting the effect of by-passing

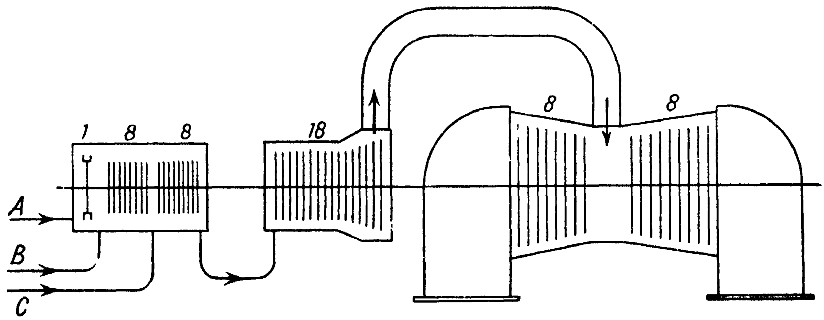


FIG. 223. Diagrammatic Arrangement of 105,000 kW Turbine showing By-pass Governing Arrangements

on the steam condition at inlet to the nozzles following the supplementary admission, we may write

$$p_n' = p_n \cdot \frac{w}{w_e}$$

The higher value of p_n' will modify the mass flow through the nozzles of the stages that are by-passed, causing it to be less than it was at the economical load. In order to find the mass flow w_1, we may proceed by a process of trial and error. Trial values of w_1 are taken, and from the known pressure p_n' and the Σh and v_n curves, the pressure distribution is calculated for the by-passed stages by the method given in Art. 142. If the trial value of w_1 is too high, the calculated nozzle-box pressure will be higher than the actual pressure, and vice versa. Having thus found the correct flow w_1, we obtain the weight of by-pass steam w_2.

Suppose now that ABCDEFG, Fig. 224, represents the course of the state point in the three by-passed stages of the turbine in Fig.

222. The steam passing through the by-pass throttle has a final state point H where, neglecting heat losses, $I_H = I_A$.

w_1 lb. of steam having the enthalpy value I_G is mixed with w_2 lb. of steam having the enthalpy I_H. The state point after mixing is J, and

$$w \cdot I_J = w_1 \cdot I_G + w_2 \cdot I_H$$

from which I_J may be found. Since I_J is greater than I_G, the condition of the steam in the succeeding stages is somewhat different from that corresponding to the economical load. A second calculation of the pressure distribution in the remaining stages will lead to a somewhat higher pressure p_n', necessitating a recalculation of w_1 and w_2. The second approximation is sufficiently accurate for all practical purposes.

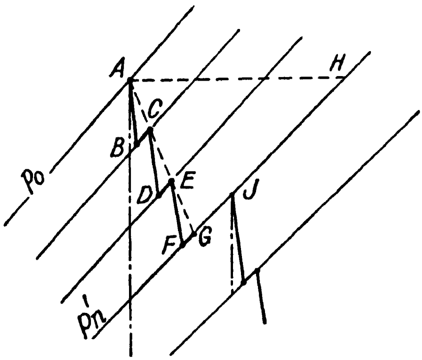


FIG. 224

150. By-pass Governing of Reaction Turbines. Owing to the pressure drop across the moving blades, it is necessary to employ full admission in reaction turbines. Consequently, it is not possible to employ any form of nozzle-control governing. The remaining alternatives are simple throttle governing and by-pass governing. The latter has been employed by Messrs. C. A. Parsons & Co., Ltd., almost from the beginning.

In the majority of Parsons turbines a single by-pass valve is employed. In the 50,000 kW two-cylinder reheat turbine for the Dunston power station, however, two such valves were fitted. Up to 30,000 kW, all the steam enters the first stage of the turbine through a throttle valve; up to 40,000 kW (the economic load) the first by-pass valve takes control; between 40,000 and 50,000 kW the control is effected by the second by-pass valve. The use of the additional by-pass valve results in a flatter steam consumption curve.

The pressures and steam flows in the by-pass stages may be found approximately by using eqs. (187) and (188) of Art. 143, page 363.

BIBLIOGRAPHY

1. KEARTON: "The Distribution of Pressure in Impulse Steam Turbines at Varying Loads." (Brit. Ass., Oxford, 1926.) *Engineering*, 1926; 122; 365.

EXAMPLES XV

1. The following data were obtained on a test of a steam turbine operating at a fractional load—

Steam pressure before governor valve .	400
Steam temperature before governor valve	700° F.
Steam pressure after governor valve .	120
Steam pressure in exhaust branch . .	1·0
Steam temperature in exhaust branch .	120° F.

What is the internal efficiency ratio of the turbine?

If the steam flow through the turbine is 4,000 lb. per hr., and the power absorbed in bearing friction and governor drive is 10 h.p., what is the approximate power at the turbine coupling?

2. The full load output of a steam turbine, measured at the coupling is 2,000 kW and the losses due to bearing friction, to the governor and oil pump drive, etc., amount to 60 kW. Steam is supplied at a pressure of 200 lb. per sq. in. abs. and superheated to 540° F. total temperature; the exhaust pressure is 1 lb. per sq. in. abs. The internal efficiency ratio at full load is 74 per cent.

What would be the coupling power of the turbine when the steam flow through the turbine is 20 per cent of that at full load, assuming (1) that the turbine is governed by throttling, (2) that the external losses are the same as at full load, (3) that the exhaust pressure remains unaffected, and (4) that the internal efficiency ratio is reduced to 68 per cent at this load?

3. A steam turbine is governed by throttling and the no-load steam consumption is found to be 12 per cent of the full-load consumption. The nozzle-, box pressure at full load is 250 lb. per sq. in. abs., the initial superheat 150° F., and the exhaust pressure 0·5 lb. per sq. in. abs. If the steam consumption at full load is 10·45 lb. per kWh, what is the efficiency ratio of the turbine at quarter, half, and three-quarter load?

4. The following particulars refer to three successive "expansions" in the I.P. section of an impulse-reaction turbine—

Group No.	Mean Diameter Inches	Blade Height Inch	Blade Outlet Angle	Total Number of Rows (fixed and moving)
1	34·125	$\frac{1}{2}$	20°	8
2	34·25	$\frac{5}{8}$	20°	8
3	34·625	1	20°	8

The blade speed ratio is 0·5, $\phi = 0{\cdot}9$, $\eta_n = 0{\cdot}9$, the index of v for adiabatic expansion is 1·135, and the stage efficiency is 0·72. Calculate the steam flow through the turbine blades when the pressure at inlet to the first group is 72 lb. per sq. in. abs. (steam dry and saturated) and the pressure at outlet from the third group is 23·5 lb. per sq. in. abs.

5. Steam is supplied to the first-stage nozzle box of a turbine at a pressure of 200 lb. per sq. in. abs. and superheated 150° F. Under maximum load conditions, the weight of steam entering the first-stage nozzles is 9·45 lb. per sec., and the by-pass steam entering the second-stage wheel chamber is 3·58 lb. per sec., the pressure in that stage being then 120 lb. per sq. in. abs.

If the enthalpy of the steam at outlet from the second-stage blades is 1,251·4 B.Th.U. per lb., calculate the enthalpy at inlet to the third-stage nozzles.

6. The following results were obtained on a full-load test of a turbo-alternator—

Output at generator terminals	10,000 kW.
Steam pressure before stop valve	450
Steam temp. before stop valve . . .	700° F.
Steam pressure in nozzle box	400
Steam pressure in exhaust branch	1·0
Steam consumption, lb. per hr.	98,600

It is estimated that the power loss due to bearing friction, governor, and oil-pump drive, etc., amounts to 110 kW. Assuming that the alternator efficiency is 95·5 per cent, what is the true internal efficiency ratio of the turbine at full load?

What is the output of the generator when the steam consumption is $\frac{1}{4}$ and $\frac{1}{2}$ of that at full load? Assume that the turbine internal efficiency ratio, the mechanical losses in kW, the exhaust pressure, and the alternator efficiency are the same as at full load, and that the turbine is governed by throttling.

(Liv. Un.)

7 Calculate the coupling power developed by a steam turbine at full load, given the following conditions—

Initial steam pressure	600
Initial steam temperature . . .	800 F.
Exhaust pressure	0·5.
Enthalpy of exhaust steam . . .	973 B.Th.U./lb.
Steam flow, lb. per hour . . .	158,000.
Mechanical losses	100 kW.

Calculate also the power developed at part load if the steam flow through the turbine is 31,600 lb. per hr., if the exhaust pressure and mechanical losses are the same as at full load, and if the internal efficiency ratio is 0·9 times that at full load. The turbine is governed by a simple throttle valve.

(Liv. Un.)

MIXED-PRESSURE TURBINES

151. Low-pressure Turbines. The exhaust steam from a non-condensing engine is normally at a temperature about 212° F., or slightly more, and is therefore well above the temperature of the

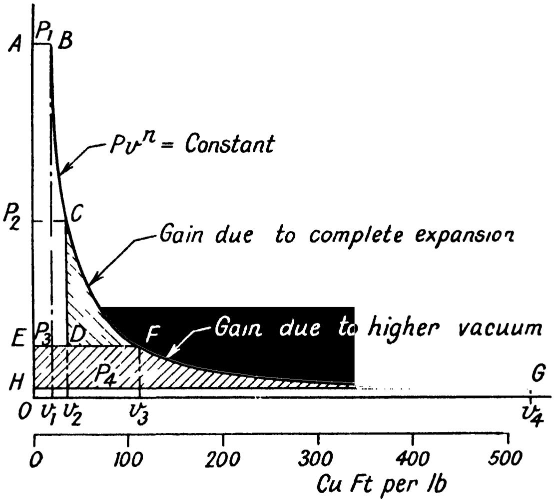


FIG. 225

available condensing water. Consequently, such steam is capable of doing work by further expansion. Owing to the complete expansion which is possible in the steam turbine it is more economical to expand the available exhaust steam in a turbine than in an engine operating with a L.P. cylinder. This may be seen from the p-v diagram, Fig. 225, which is drawn to scale for a pressure $p_1 = 20$ lb. per sq.in. abs. The hypothetical indicator diagram for a reciprocator is ABCDEA. Owing to the limitation of size of the cylinder it is necessary to release the steam at some pressure P_2 after which the steam expands in the exhaust space to the condenser pressure P_3.

Assuming that expansion in both reciprocatoı and turbine follows the law $pv^n =$ constant, and using P to represent pressures in lb. per sq. ft. abs., and v to represent specific volume, then

Work done per lb. of steam in engine

$$= P_1v_1 + \frac{P_1v_1 - P_2v_2}{n-1} - P_3\,v_2$$

This is represented by the work area ABCDEA.

In the turbine, however, the expansion is necessarily complete; the steam continues to increase in volume until the exhaust pressure P_3 is reached. The work area is ABFEA.

Work done per lb. of steam in turbine

$$= P_1v_1 + \frac{P_1v_1 - P_3v_3}{n-1} - P_3v_3$$

$$= \frac{n}{n-1}(P_1v_1 - P_3v_3)$$

$$= \frac{n \cdot P_1v_1}{n-1}\left\{1 - \left(\frac{P_3}{P_1}\right)^{\frac{n-1}{n}}\right\} \text{ ft.-lb.}$$

In considering the most economical vacuum for a reciprocating engine, we have to balance the greater amount of sensible heat to be supplied when a higher vacuum is employed, against the relatively small increase of work done. In consequence, the most economical vacuum is comparatively low, being normally about 25 in. or 26 in. Hg. In the turbine, however, there is no limit, except that imposed by the temperature of the available cooling water and those practical considerations connected with the cost of pumping, size of water pipes, etc. Consequently, the L.P. turbine has a great advantage over the L.P. reciprocator on these grounds, which are ultimately due to the limit of size of the engine cylinder.

When the reciprocator is operating continuously it is simply necessary to install a L.P. turbine and suitable condensing plant. The L.P. turbine would contain a relatively small number of stages. This represents the simplest possible arrangement of exhaust turbine.

152. The Larderello Natural Steam Power Plant. An interesting adaptation of the low-pressure steam turbine hails from Larderello in the midst of a volcanic region in the Province of Tuscany (Italy), where there is a constant emission of steam and hot water from crevices and fissures in the ground. Over a century ago, it was discovered that the hot water was highly charged with boric acid, and works have long been in existence for the extraction of boric acid on a commercial scale. Helium is another constituent of the hot water.

In order to increase the output, boreholes were put down to depths ranging from 200 to 500 ft. The pressure of the steam with no delivery was found to be as much as 45 lb. gauge, and with maximum delivery was still about 15 lb. gauge, while the temperature was about 360°F.

It was decided to put down a steam turbine plant, but the use of the natural steam in the turbine was avoided for two reasons.

In the first place, there was some doubt as to the manner in which the blades of the turbine would be affected by the gases contained in the natural steam; and, secondly, there would have been some difficulty in obtaining a sufficient vacuum in the condenser, on account of the incondensable gases in the steam. It was, therefore, decided to use the heat of the natural steam for the purpose of

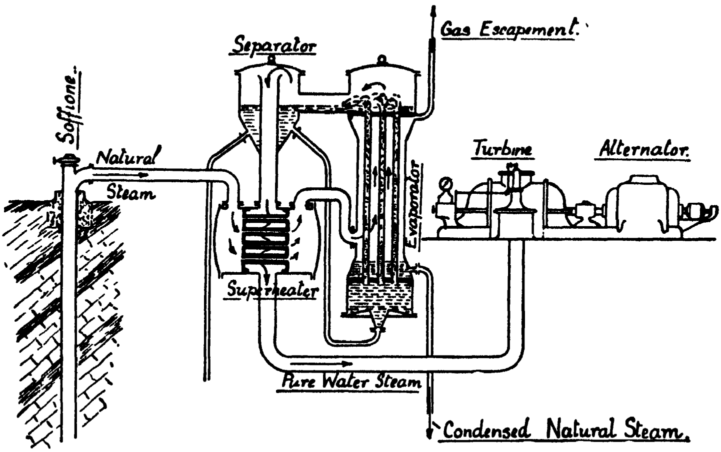


FIG. 226.—Diagrammatic Arrangement of Natural Steam Plant

evaporating pure water. The arrangement of the evaporators is illustrated diagrammatically in Fig. 226.*

The evaporators consist of a number of aluminium tubes contained in a shell of sheet iron, aluminium being used in preference to iron or steel, because the sulphuric acid contained in the natural steam would form a layer of sulphide of iron on the outside of the tubes and so lower the rate of heat transmission. The vapour passing to the turbine is superheated by the incoming natural steam. In this manner steam is generated at about 7 lb. per sq. in. gauge pressure, and supplied to the turbine governor valve at a pressure of 2·5 lb. gauge.

The first machine of 250 kW was put down in 1912, while in 1916 three units of 2,500 kW capacity were installed. The latter turbines, which were built by Franco Tosi, of Legnano, Italy, and which run at 3,000 r.p.m., are impulse-reaction (Parsons) turbines of the double-flow type. It is stated that the installation has been successful in every way.

153. **Mixed-pressure Turbine.** In many installations where a supply of exhaust steam from a non-condensing reciprocator is available, e.g. where the engine is a colliery winding engine, a

* Reproduced by kind permission from *Engineering*, 24th May, 1918, in which details of the plant are published.

haulage engine, rolling mill engine, etc., the supply of exhaust steam is intermittent. In such a case it is necessary to provide in the installation a low-pressure heat accumulator wherein the surplus exhaust steam (or its latent heat) may be stored during the time that the engine is operating, and from which the turbine may draw a supply of steam during the time that the engine is standing. Such a plant is shown diagrammatically in Fig. 227, which is self-explanatory.

In cases where the quantity of exhaust steam is not quite sufficient to produce the power required, or where it may be necessary to run

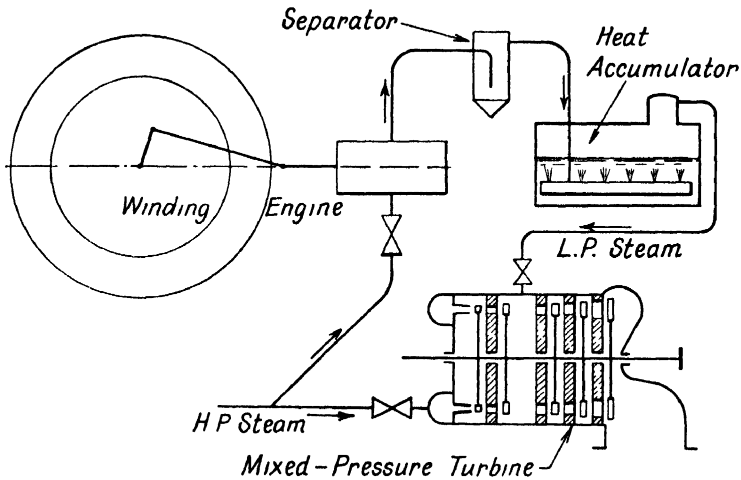


Fig. 227.—Diagrammatic Arrangement of Steam Engine, Heat Accumulator, and Mixed-pressure Turbine

the turbine during long periods when the engine is idle, the turbine is so designed that live steam may be admitted to the turbine at an earlier stage than the first L.P. stage. The turbine then consists virtually of two turbines which may be, and usually are, in the same cylinder (Fig. 227). Steam flowing from the last H P. wheel flows directly into the first nozzles of the L.P. turbine. Governor gear is provided to utilize the whole of the exhaust steam available without allowing the exhaust steam pressure to fall below a certain predetermined value, and to supply H.P. steam, as and when required, in order to maintain the turbine speed sensibly constant irrespective of load variations. There are thus three possible conditions of operation (assuming that at certain times there is sufficient L.P. steam to develop the whole of the power)—

(1) Power developed entirely by L.P. steam.
(2) Power developed entirely by H.P. steam.

(3) Power developed partly by H.P. steam and partly by L P steam.

Hence the term "mixed-pressure" turbine.

154. **Conditions of Operation of Mixed-pressure Turbine.** It is beyond the scope of this book to analyse fully the performance

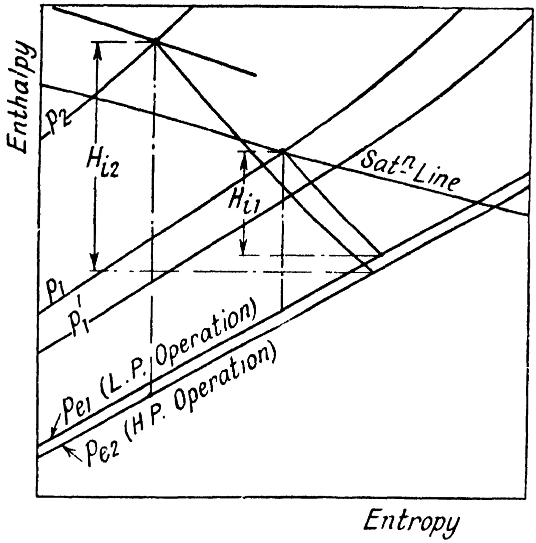


FIG. 228

of this type of turbine, but the following brief analysis may be of interest.

(1) *Power Developed Entirely by L.P. Steam.*

Let K = internal power of turbine in kW (i.e. coupling power plus mechanical losses).

p_1 = pressure of L.P. steam (assumed dry and saturated).

p_{e1} = exhaust pressure when operating with L.P. steam.

H_{i1} = internal work done per lb. of steam between the pressures p_1 and p_{e1} (Fig. 228).

W_1 = steam flow through turbine, lb. per hour.

Then
$$W_1 \times H_{i1} = 3{,}413K$$

i.e.
$$W_1 = \frac{3{,}413K}{H_{i1}}$$

Owing to the fact that H_{i1} is comparatively small, the steam consumption W_1 for a constant load K is the maximum possible, and the L.P. nozzles and blades must be made sufficiently large to pass this quantity of steam.

(2) *Power Developed Entirely by H.P. Steam.* Suppose that the

power K kW is the same as before, and that H_{t2} is the internal work done per lb. of steam under these conditions of operation (Fig. 228.) Then the hourly steam flow through the turbine is

$$W_2 = \frac{3,413 \, . \, K}{H_{t2}} \text{ lb.}$$

This will be the minimum value of W. It is to be noted that under these conditions the steam pressure at inlet to the first set of L.P.

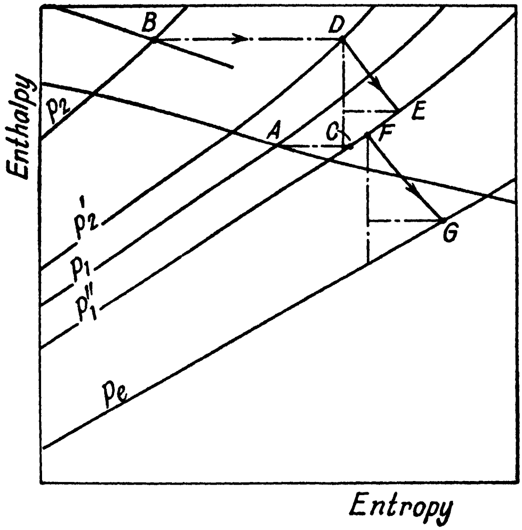


FIG. 229.—Mollier Diagram for Mixed-pressure Operation

nozzles will be no longer p_1, but will be reduced to the value p_1', such that

$$p_1' = p_1 \times \frac{W_2}{W_1}$$

The lower value of this pressure adds appreciably to the adiabatic heat drop in the H.P. stages and will, of course, affect the number of stages in the high-pressure section of the turbine.

(3) *Mixed-pressure Operation.* It will be assumed that it is required to find the steam consumption at, say, the full load when the quantity of L.P. steam available is some value W_3, less than W_1. That is, it is necessary to derive the quantity of H.P. steam W_4. This can only be found by a process of trial and error.

By an obvious method, a rough approximation to W_4 is first made. Since the total steam flow through the L.P. blading is $W_3 + W_4$, the pressure p_1'', Fig. 229, is given by

$$p_1'' = p_1\left(\frac{W_3 + W_4}{W_1}\right)$$

Assuming that the L.P. steam is again supplied dry and saturated at p_1, it is now throttled to p_1'', the final state point being C.

Suppose that the admission of H.P. steam is controlled by a throttle valve, and that in the present case the steam is throttled from p_2 to p_2'. The pressure p_2' may be obtained from a $\log_{10}p$, $-\Sigma h$, $\log_{10}v$ diagram by the method given in Art. 142, starting from the pressure p_1'' and considering the H.P stages only. This is a somewhat tedious process, for a tentative diagram would have to be drawn for an assumed value of p_2' in order to obtain a more accurate value of that pressure. Eq. (187), page 364, although derived for the reaction turbine, may be used in approximate calculations on impulse turbines. The constant C_1 may be calculated from the relation

$$W_2 = C_1\sqrt{\frac{p_2}{v_2} - \frac{p_1'}{v_1'}}$$

which applies to operation with H.P. steam only and, of course, refers only to the H.P. stages. Using this derived value of C_1 in the corresponding relation

$$W_4 = C_1\sqrt{\frac{p_2'}{v_2'} - \frac{p_1''}{v_1''}}$$

and approximating, step by step, to the values of v_1'' and v_2', the specific volumes at p_1'' and p_2' respectively, the pressure p_2' is obtained.

Having found the pressure p_2', a constant I line BD is now drawn giving the condition D in the first-stage nozzle box. The condition curve DE is drawn next.

At inlet to the L.P. stages, W_3 lb. of steam with the enthalpy value I_C are mixed with W_4 lb. having the enthalpy I_E, resulting in the enthalpy I_F where

$$I_F = \frac{W_3 \,.\, I_C + W_4 \,.\, I_E}{W_3 + W_4}$$

The condition curve FG is now drawn for the expansion of the mixed H.P. and L.P. steam in the L.P. stages.

$\therefore$ Total internal power in kW

$$= [W_4(I_D - I_E) + (W_3 + W_4)(I_F - I_G)] \div 3{,}413$$

If the calculated power is greater than K, the steam quantity W must be reduced, and vice versa.

155. Theory of Heat Accumulator. A typical steam consumption-time curve for a colliery winding engine is shown in Fig. 230. Commencing the wind at 0, steam is admitted to the cylinders at full pressure and with the link gear set to give steam for a large part of the stroke. At A the gear is linked up to cut off steam fairly early, and at B steam is shut off entirely, allowing the engine to

coast until the wind is stopped at C. The next wind is commenced at D, when the curve would be more or less repeated. It will be obvious that the area of the diagram represents the weight of steam consumed by the engine and the mean height the mean steam consumption. If the exhaust turbine is operating at a steady load and is using the whole of the steam available, then the mean height of the curve would also represent the turbine steam consumption. It will be apparent that between *a* and *b* the quantity of exhaust steam is greater than that required by the turbine, whereas between *b* and *a'* the turbine is using steam at a steady rate and there is little or none coming from the engine.

The usual L.P. heat accumulator, invented by Rateau, comprises one or more large horizontal cylindrical vessels, about 60 per cent full of water. The surplus exhaust steam is led through a pipe into the tank and allowed to pass through a large number of submerged orifices or nozzles. It is thus condensed by direct contact with the water. The latent heat is absorbed by the whole water mass as sensible heat, the temperature of the water rises, and the pressure of the steam in the space above the water also rises. This occurs from *a* to *b*, Fig. 230. As soon as the turbine begins to take more steam than is coming from the engine there is a slight reduction of pressure in the steam space of the accumulator which causes the water to evaporate. The whole water mass loses sensible heat, its temperature falls, and the steam pressure gradually falls. This regeneration period goes on from *b* to *a'* where, once again, the engine exhaust steam quantity exceeds the needs of the turbine. The quantity of steam to be condensed in the accumulator during the storage period is shown by the vertically-hatched area in Fig. 230; the quantity of steam re-evaporated is shown by the cross-hatched area, to scale. The variation of steam pressure which must be permitted depends on the variation of steam saturation temperature, and this in turn will depend on the quantity of water stored in the accumulator.

Consider the regeneration period and let

Q_1 = minimum quantity of water in accumulator, lb.
Q_2 = maximum quantity of water in accumulator, lb.
t_1 = lowest saturation temperature, ° F.
t_2 = highest saturation temperature, ° F.
L_1 = latent heat corresponding to t_1.
L_2 = latent heat corresponding to t_2.

Let Q, t, and L be values at any instant, and let the whole water mass cool by a very small amount δt, thus producing the small quantity of dry and saturated steam δQ. Then, assuming the specific heat of water to be unity

$$Q \cdot \delta t = L \cdot \delta Q$$

Writing $L = a - bt$, where a and b are positive constants

$$Q \,.\, \delta t = (a - bt)\delta Q$$

or

$$\frac{\delta Q}{Q} = \frac{\delta t}{a - bt}$$

$$\therefore \qquad \int_{Q_1}^{Q_2} \frac{1}{Q} \,.\, dQ = \int_{t_1}^{t_2} \frac{dt}{a - bt}$$

$$\therefore \qquad \log_e \frac{Q_2}{Q_1} = -\frac{1}{b} \log_e \frac{a - bt_2}{a - bt_1}$$

i.e.

$$\log_{10} \frac{Q_2}{Q_1} = \frac{1}{b} \log_{10} \frac{L_1}{L_2} \quad . \quad . \quad . \quad (190)$$

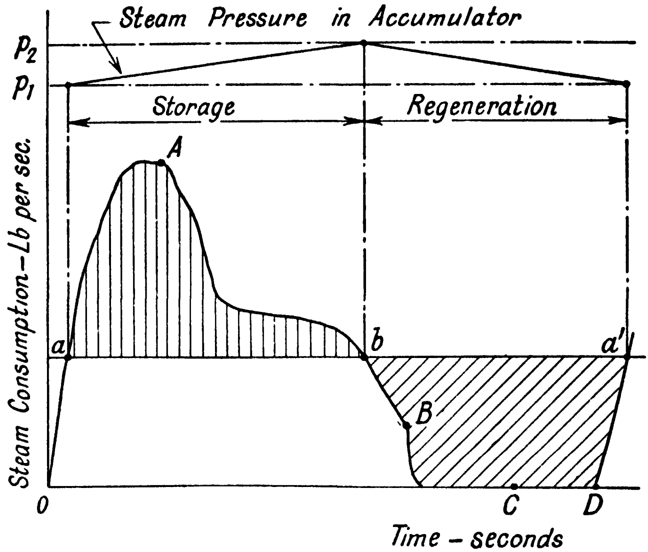


FIG. 230.—Time-Steam Consumption Diagram for Colliery Winding Engine

The weight of steam to be stored in the accumulator is $Q_2 - Q_1$. Let this be represented by W.

Then

$$\frac{Q_2}{Q_1} = 1 + \frac{Q_2 - Q_1}{Q_1} = 1 + \frac{W}{Q_1}$$

$$\therefore \qquad \log_{10}\left(1 + \frac{W}{Q_1}\right) = \frac{1}{b} \log_{10} \frac{L_1}{L_2} \quad . \quad . \quad . \quad (191)$$

W is found from the steam consumption-time curve. Hence the weight of water $Q_2 = Q_1 + W$ which the accumulator must hold

may be found for any given range of pressure and temperature in the accumulator.

EXAMPLE 31. Calculate the minimum water capacity of a low-pressure heat accumulator when the weight of steam to be stored is 1,000 lb. per cycle. The maximum and minimum steam pressures in the accumulator are 22 and 18 lb. per sq. in. abs. respectively.

When $p = 22$, $t = 233{\cdot}1°$ F.; $L = 957{\cdot}8$.

When $p = 18$, $t = 222{\cdot}4°$ F.; $L = 964{\cdot}4$.

Assuming $L = a - bt$

$$a - 222{\cdot}4b = 964{\cdot}4$$

$$a - 233{\cdot}1b = 957{\cdot}8$$

$$\therefore \quad 10{\cdot}7b = 6{\cdot}6 \text{ and } b = 0{\cdot}617$$

$$\therefore \quad \log_{10}\left(1 + \frac{1{,}000}{Q_1}\right) = \frac{1}{0{\cdot}617}\log_{10}\frac{964{\cdot}4}{957{\cdot}8}$$

$$= 0{\cdot}004833$$

$$\therefore \quad 1 + \frac{1{,}000}{Q_1} = 1{\cdot}01119$$

from which $Q_1 = 89{,}370$ lb.

$\therefore$ Least capacity $= 90{,}370$ lb.

$= 40{\cdot}4$ tons

If the circulation were imperfect and the whole of the water did not undergo the same temperature change, then a larger quantity of water would have to be stored.

EXAMPLES XVI

1. A reciprocating steam engine exhausting at 16 lb. per sq. in. abs develops 1,500 b.h.p. with a steam consumption of 23·5 lb. per b.h.p.-hr. Calculate the power available from an exhaust steam turbine utilizing all the exhaust from the above engine, assuming that the steam enters the turbine at 15 lb. per sq. in. abs., dry and saturated, that a separator in the engine exhaust pipe removes 1,300 lb. of water per hour, that the vacuum at the turbine exhaust branch is 29 in. (30 in. bar), and that the turbine thermal efficiency ratio is 70 per cent.

2. Calculate the theoretical steam consumptions in lb. per h.p.-hr. of a L.P. reciprocating engine and a L.P. turbine operating with initially dry and saturated steam at 20 lb. per sq. in. abs. when the exhaust pressure is 2·5 lb. per sq. in. abs. and the release pressure in the engine is 8 lb. per sq in. abs. Assume $n = 1{\cdot}135$ in both cases. Calculate also the steam consumption of the turbine when the exhaust pressure is reduced to 0·5 lb. per sq. in. abs.

3. A mixed-pressure turbine operates under the following conditions—

Output at turbine coupling	800 kW
Press. of L.P. steam (dry and saturated) .	18 lb. per sq. in. abs.
Press. of H.P. steam (160° F. superheat) .	180 ,, ,, ,,
Exhaust pressure	0·7 ,, ,, ,,

Assuming that the power absorbed by bearing friction, governor drive, etc., amounts to 15 kW, and that the internal efficiency ratic is 65 per cent for both H.P. and L.P. operation, calculate the steam consumptions in lb. per kW-hr. for both methods of operation. What is the steam pressure in the L.P. steam belt during operation with H.P. steam?

4. Calculate the power at the turbine coupling in Question 3 when the turbine is consuming 15,000 lb. of L.P. steam per hr., supplied at 18 lb. per sq. in. abs., dry and saturated, and 2,000 lb. of H.P. steam, supplied at 180 lb. per sq. in. abs. and 160° F. superheat. Assume—

(1) that the internal efficiency ratio of both the H.P. and L.P. sections of the turbine remains constant at 0·65;
(2) that the exhaust pressure is 0·7;
(3) that the losses due to bearing friction, etc., amount to 15 kW;
(4) that the pressure of the H.P. steam after throttling is 37 lb. per sq. in. abs.; and
(5) that the supply of H.P. and L.P. steam is controlled by throttle governing.

5. The steam consumption of a rolling-mill engine increases uniformly from zero to 13·9 lb. per sec. in the first 5 sec. of rolling, and then diminishes at a uniform rate to 4·45 lb. per sec. at the end of 30 sec. from the commencement of rolling. The engine then comes to rest. The interval between successive rolls is one minute.

The rolling engine supplies dry and saturated exhaust steam to a L.P. turbine at an average pressure of 20 lb. per sq. in. abs. The turbine exhausts at 1·0 lb. abs., and its efficiency ratio is 0·64. What is the power of the turbine?

Calculate the total weight of water to be stored in a heat accumulator to be used in conjunction with the exhaust turbine, and operating under the following conditions—

Maximum steam pressure 22 lb. abs. minimum steam pressure 18 lb. abs. Assume that the whole of the water in the accumulator is at the same temperature at any instant.

6. The steam consumption of a reciprocating steam engine varies cyclically, the rate of consumption in lb. per sec. being given by the expression

$$w = 4 + 3 \sin pt$$

where t represents time in seconds. The total time of the cycle is 120 sec. The exhaust steam is utilized in a L.P. turbine which uses all the available steam at a steady rate.

The surplus exhaust steam is stored in a heat accumulator. If the lower pressure is 15·29 lb. per sq. in. abs. ($t = 214°$ F., L = 969·1) and the higher pressure is 20·77 ($t = 230°$ F., L = 958·7), calculate the weight of steam to be stored and regenerated each cycle and the total weight of water to be stored in the accumulator.

7. A L.P. heat accumulator contains 25 tons of water at the beginning of the storage period. If the initial and final temperatures of the water are 214° F. (L = 969·6 B.Th.U. per lb.) and 228° F. (L = 961·0) respectively, calculate the weight of steam condensed in the accumulator during the storage period. The accumulator delivers steam to a L.P. turbine and the total time of regeneration is 2 min.

Assuming a mean steam supply temperature of 221° F. ($p = 17·5$ lb. abs.), that the steam is supplied dry and saturated, that the exhaust pressure is 0·75 lb. per sq. in. abs., and that the efficiency ratio of the turbine is 62 per cent, calculate the power available.

8. The time-rate of steam consumption of a colliery winding engine increases uniformly from zero to a maximum during the first 20 sec. of winding

from rest and then remains constant for a further 20 sec., when steam is shut off and the engine is allowed to coast. The total time of winding and stoppage is 2 min. and during each wind the engine consumes 600 lb. of steam. The exhaust steam from the winding engine passes to a L.P. turbine and a heat accumulator. The turbine may be assumed to utilize the whole of the exhaust steam at a steady rate.

If the maximum and minimum engine exhaust pressures are 20 lb. abs. (t = 228° F., L = 961) and 16 lb. abs. (t = 216·3° F., L = 968·1) respectively, calculate the minimum weight of water which must be stored in the heat accumulator.

9. A mixed-pressure turbine receives 15,000 lb. of live steam per hour, the pressure and temperature of the steam after the governor valve being 200 lb. per sq. in. abs. and 500° F. respectively. The turbine also receives 20,000 lb. per hour of dry and saturated steam at 20 lb. per sq. in. abs. The exhaust pressure is 0·5 lb. per sq. in. abs. If the efficiency ratios of the h.p. and l.p. stages are 0·76 and 0·70 respectively and the mechanical losses are 25 kW, calculate the output at the turbine coupling.

(*Liv. Un.*)

10. A 2,000 kW mixed-pressure turbine develops its full output when supplied with dry and saturated steam at 20 lb. per sq. in., the exhaust pressure being 1·0 lb. per sq. in., and the efficiency ratio of the turbine being 75 per cent. There is then no throttling loss.

Calculate the power output of the turbine when supplied with 15,000 lb. per hour of high-pressure steam at 200 lb. per sq. in. and 600° F. and 9,300 lb. of dry and saturated steam at 20 lb. per sq. in., the exhaust pressure remaining at 1·0 lb. per sq. in. Assume that the low-pressure steam is admitted through a throttle valve, that there is no throttling of the high-pressure steam, and that the efficiency ratios of both high-pressure and low-pressure sections of the turbine are 0·75. (*Liv. Un.*)

CHAPTER XVII

BACK-PRESSURE AND PASS-OUT TURBINES

156. Introductory. There are several industries, such as paper making, textile, chemical, dyeing, sugar refining, carpet making, brewing, and so forth, in which there is a dual demand for power and steam for heating and "process" work. It was formerly the practice to generate steam for power purposes at a moderate pressure and to generate saturated steam for process work at a pressure which gave the desired heating temperature. Such a system is obviously wasteful, for of the total quantity of heat supplied to the steam which is used for power purposes, quite 70 per cent will normally be carried away by the cooling water. Admittedly, if the engine or turbine is operated with a normal exhaust pressure, then the temperature of the exhaust steam is too low to be of any use for heating purposes; but by a suitable modification of the initial steam pressure and of the exhaust pressure, it would be possible to generate the required power and still have available for process work a large quantity of heat in the exhaust steam.

Suppose, for the sake of illustration, that in a paper mill 50,000 lb. of dry and saturated steam are required per hour at a pressure of 50 lb. gauge. Then, assuming that the condensed steam is returned to the system, the heat to be supplied for process work is 50,000 times the latent heat of dry steam at 65 lb. per sq. in abs., i.e. 45,720,000 B.Th.U. per hour. If steam is generated at 250 lb. per sq. in. gauge, then with an initial superheat of 100° F. and a turbine efficiency ratio of 70 per cent, the steam is approximately dry and saturated after expanding to 65 lb. per sq. in. abs. The useful work done per lb. of steam in expanding from 250 to 50 lb. gauge is 86·3 B.Th.U. Hence, the power available (neglecting the small mechanical losses) is

$$\frac{50{,}000 \times 86{\cdot}3}{3{,}413} = 1{,}263\,\text{kW}$$

The enthalpy of steam at 250 lb. 100° F. superheat is 1,268 B.Th.U. per lb., and that of the water returned from the plant is 267·3. Therefore the heat supplied per hour is

$$50{,}000\,(1{,}268{\cdot}0 - 267{\cdot}3) = 50{,}035{,}000 \text{ B.Th.U.}$$

This is 4,315,000 B.Th.U. more than in the simple heating system, i.e. about 9·5 per cent greater. The difference is, in fact, exactly equal to the heat equivalent of the power generated. It follows, therefore, that from the practical standpoint, provided no steam is

condensed in a separate condenser, the thermal efficiency of such a combined power and heating plant may approach unity.

Reciprocating engines and turbines are both available for use in such plants, but the latter are now almost exclusively employed, even for comparatively small outputs. An outstanding advantage of the turbine is the complete absence of internal lubrication, resulting in clean exhaust steam. Other obvious advantages are

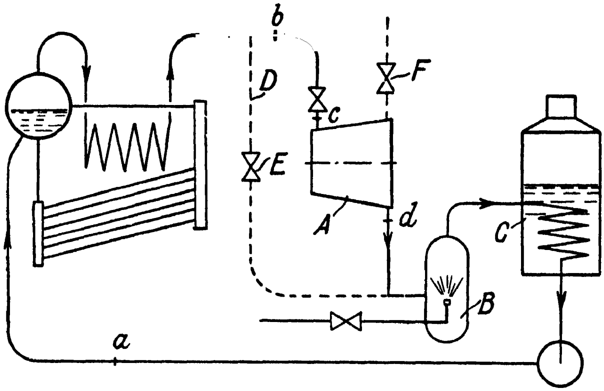


FIG. 231 —Diagrammatic Arrangement of Combined Power and Heating Plant with Back-pressure Turbine

the small space occupied, steady speed, simple control devices, and good balance.

There are two types of turbine employed in combined power and process plants, the back-pressure turbine and the steam extraction, or "pass-out," turbine.

157. **Back-pressure Turbines.** The back-pressure turbine may be employed in cases where the power which may be generated by expanding steam from an economical initial pressure down to the heating pressure is equal to, or greater than, the power requirements. The lay-out of such a plant is shown diagrammatically in Fig. 231. Steam is generated in the boiler at a suitable working pressure and admitted to the turbine A. The exhaust steam from the turbine will normally be superheated and in most cases is not suitable for process work, partly because it is impossible to control its temperature (since this will vary with the initial superheat), and partly because of the fact that the rate of heat transfer from superheated steam to the heating surfaces is lower than that of saturated steam. For these reasons, a desuperheater B is often used. A jet of water, thermostatically controlled, is sprayed into the entering steam; the steam is cooled and the spray water evaporated. The now saturated steam enters the heaters C and is entirely condensed. The condensed steam may or may not be returned to the boilers, depending on the conditions.

It is unlikely that the steam required for power generation will always be equal to that required for process work, and some means of controlling the exhaust steam pressure must be employed if variations in the pressure—and, therefore, of the steam saturation temperature—are to be avoided.

The method of control employed depends on the circumstances. If the back-pressure turbine is the only power unit, then it is fitted

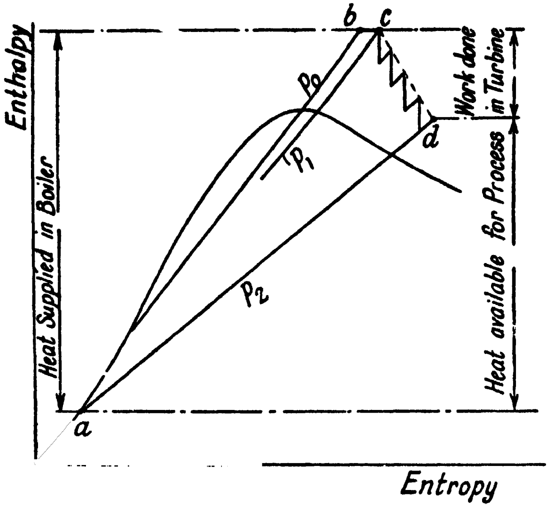


FIG. 232

with an ordinary centrifugal governor and the quantity of available exhaust steam is controlled by the load on the turbine. If the available exhaust is too small, live steam may be passed through the reducing valve E into the desuperheater. If the quantity of exhaust steam is in excess of requirements, then the excess steam may be blown to atmosphere, or into a feed tank, etc., through the valve F. Valves E and F may be operated by hand to maintain the exhaust pressure constant, or, as is more usual, by automatic control gear. If, however, the back-pressure turbine is operating in parallel with other machines, then its output is controlled entirely by the heat load. In addition to the normal speed governor, there is a pressure regulator which controls the supply of steam to the turbine so as to maintain a sensibly constant exhaust pressure.

The thermodynamics of the back-pressure turbine is extremely simple and may be explained with reference to Fig. 232, which is lettered to correspond with Fig. 231, so far as the state of the working substance is concerned. The boiler pressure is p_0, the pressure at inlet to the turbine is p_1, and the heating steam pressure is p_2. *bc* shows the throttling at the throttle valve, *cd* the expansion in

the turbine, and *da* the subsequent condensation in the heaters. This diagram shows clearly that, apart from minor heat losses, the whole of the heat supplied in the boiler is usefully employed.

Let K_i = internal power of turbine in kW.

H = heat required in heaters, B.Th.U. per hour.

W = steam flow through turbine, lb. per hour.

Then
$$W(I_d - I_a) = H$$
or
$$W = \frac{H}{I_d - I_a}$$
Also
$$3{,}413K_i = W(I_c - I_d)$$
$\therefore$
$$K_i = \frac{H}{3{,}413}\left(\frac{I_c - I_d}{I_d - I_a}\right) \quad . \quad . \quad . \quad (192)$$
Conversely
$$H = 3{,}413 \,.\, K_i\left(\frac{I_d - I_a}{I_c - I_d}\right) \quad . \quad . \quad . \quad (192a)$$

158. Pass-out Turbine. In many cases the power available from a back-pressure turbine through which the whole of the heating steam flows is appreciably less than that required in the factory. This may be due to the small heating or process requirements, to a relatively high back-pressure, or a combination of both. In such a case it would be possible to install a back-pressure turbine to provide the heating steam and a condensing turbine to generate the extra power; but it is possible, and usual, to combine the functions of both machines in a single turbine with obvious advantages and economies. Such a turbine is shown diagrammatically in Fig. 233. Live steam enters the turbine and expands through the H.P. stages before the extraction branch. Here a certain quantity of steam is continuously being extracted for heating purposes, the remainder passing through the pressure control valve into the L.P. part of the turbine.

The control gear must be designed to meet the following requirements—

(1) the speed of the turbine must be kept sensibly constant; and

(2) the pressure of the heating steam must be kept sensibly constant; both of these regardless of the variations in power and heating loads.

These requirements are adequately met by the use of (*a*) a speed governor of the normal centrifugal type which controls the admission of H.P. steam to the turbine, and (*b*) a pressure regulator, responsive to changes of pressure of the extracted heating steam and controlling the admission of steam to the L.P. stages. A change of either power load or heating load will cause both governors to operate. For example, suppose the generator load is increased; this causes a certain momentary drop of speed. In response to this

the speed governor increases the lift of the H.P. throttle valve, thus allowing more steam to enter the turbine. If no change were made in the position of the pressure control valve, the pressure in the heating steam pipe would now rise. This pressure rise actuates the oil relay in such a way as to increase the lift of the pressure control

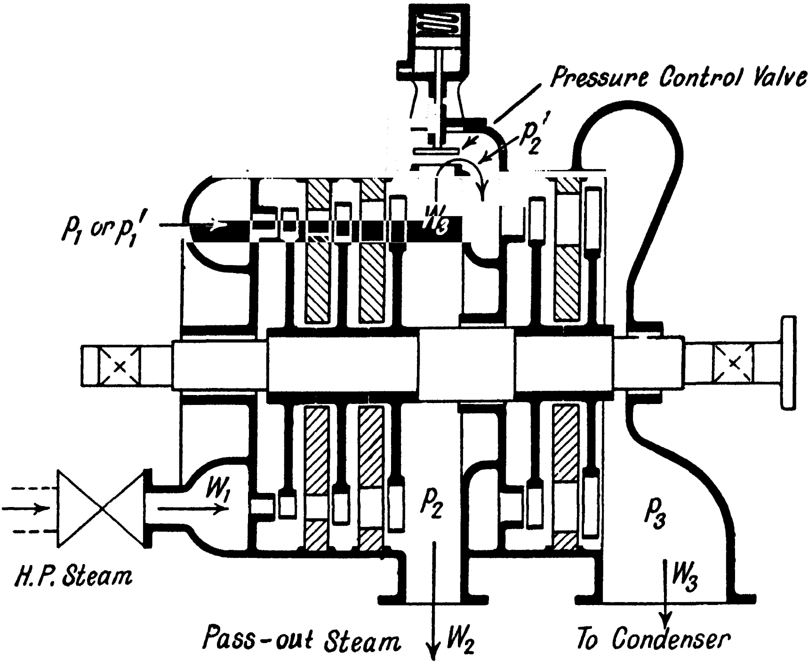


FIG. 233 —Diagrammatic Arrangement of Single-extraction Pass-out Turbine

valve and allow more steam to flow through the L.P. stages to the condenser. For a constant heat load, the weight of heating steam will remain nearly constant (it will vary slightly due to variations in its enthalpy); therefore the increase in steam flow through the L.P. stages will be practically equal to that through the H.P. stages. Thus, with a constant heat load, an increase in power load is followed by an increase in lift of the throttle and pressure control valves. Conversely, a reduction in power is followed by a reduced lift of both valves.

Suppose now that there is a sudden increase in heat load due, say, to coupling up another heater unit. The heating steam pressure will fall and so cause the lift of the pressure control valve to be reduced. This reduces the flow of steam through the L.P. stages with the

result that less power is developed in those stages, and, as the power output of the H.P. stages is as yet hardly affected, the speed of the turbine begins to fall. This causes the H.P. throttle to open, so admitting a greater quantity of steam to the turbine as a whole. It will be seen that a change in the heating load causes the lifts of the main throttle and pressure control valves to vary in opposite ways.

When the speed and pressure governors operate independently of each other it will be apparent that, provided the driven alternator is not connected electrically to any system, an increase in power

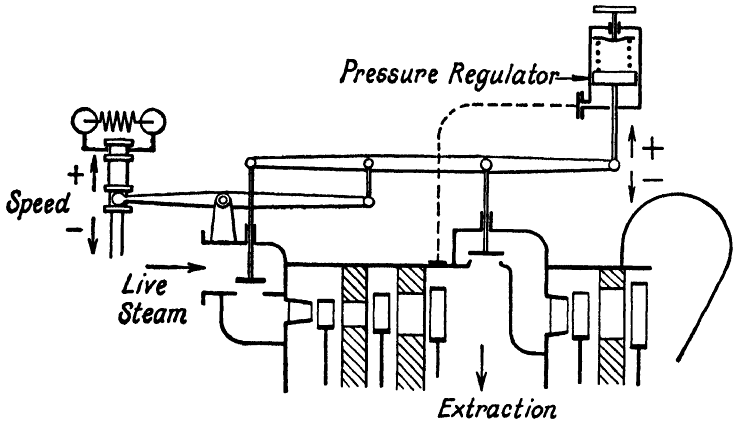


FIG. 234 —Diagrammatic Arrangement of Speed Governor and Pressure Regulator on Pass-out Turbine

load brings about an increase in pass-out steam pressure, whereas an increase in heat load causes a fall in speed. There is also a tendency to "hunting." This may be overcome by interconnecting the governor gear and the pressure regulating gear in such a way that both the throttle valve and the pressure control valve are operated simultaneously and in the correct direction. One form of such gear is shown diagrammatically in Fig. 234. In order to simplify the diagram, the oil relays have been omitted. It will be seen that a drop in speed causes both valves to lift, whereas an increase in heat load in producing a fall in heating steam pressure causes the pressure control valve partially to close and the throttle to open further.

Although both Fig. 233 and Fig. 234 show simple throttle valves controlling speed and heating steam pressure, regulation may be effected in either case, or in both cases, by some form of nozzle control gear. Moreover, steam may be extracted at two or more points.

159. Operation of Pass-out Turbine with Single Extraction. Consider the turbine shown in Fig. 233. Fig. 235 shows the Mollier

diagram when ideal nozzle-control governing is employed for both speed and pressure control, while Fig. 236 shows the Mollier diagram when throttle valves are used for both controls.

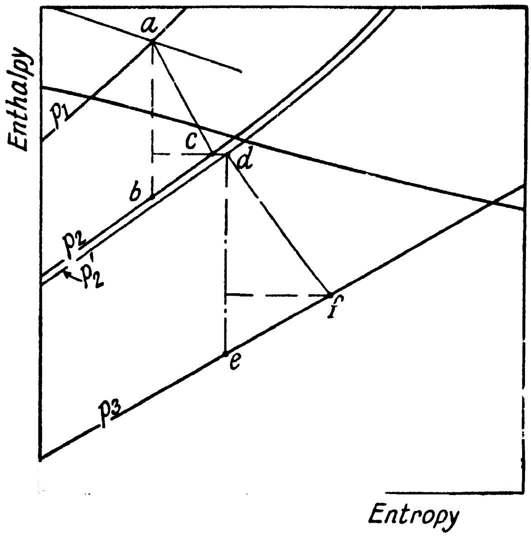


FIG 235 —Mollier Diagram for Pass-out Turbine with Ideal Nozzle-control Governing

Suppose that under any given conditions of operation—

W_1 = steam entering turbine, lb. per hour.

W_2 = steam extracted for heating, lb. per hour.

W_3 = steam entering L.P. stages, lb. per hour.

$W_{1max.}$ = maximum quantity of steam entering turbine, lb. per hour.

$W_{3max.}$ = maximum quantity of steam entering L.P. stages, lb. per hour.

$W_{1max.}$ and $W_{3max.}$ will be fixed by the specified operating conditions, i.e. power and heating ranges.

Let H = quantity of heat required, B.Th.U. per hour.

K = total internal power, kW.

K_2 = power developed by heating steam in expanding through H.P. stages.

K_3 = power developed by the remainder of the steam (W_3) in expanding through the H.P. and L.P. stages.

Then with throttle valve control

$$p_1' = \frac{W_1}{W_{1\ max.}} \cdot p_1$$

and
$$p_2' = \frac{W_3}{W_{3\ max.}} \cdot p_2$$

With nozzle control governing there will be a small pressure drop $p_2 - p_2'$ at the control valves.

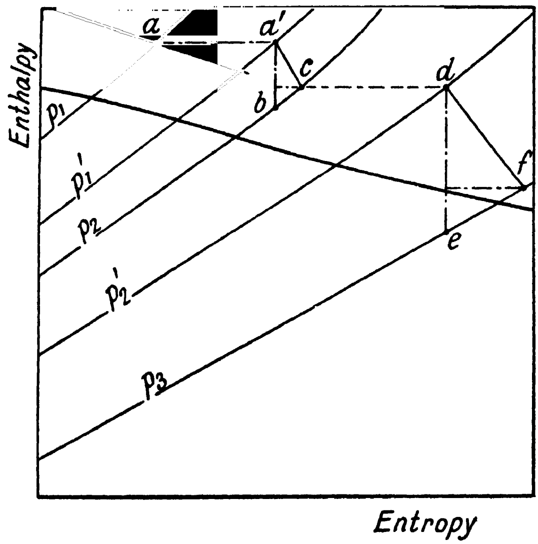


FIG. 236.—Mollier Diagram for Pass-out Turbine with Throttle Governing

The following are possible conditions of operation—

(1) *Full Extraction.* This is equivalent to back-pressure operation. Since the internal work done per lb. of steam = $I_a - I_c$,

$$W_1 = \frac{3{,}413K}{I_a - I_c}$$

Let I_{w2} = enthalpy of water at p_2.

Then heat rejected per lb. of steam = $I_c - I_{w2}$.

The total heat available is then

$$H = 3{,}413K\left(\frac{I_c - I_{w2}}{I_a - I_c}\right) \text{B.Th.U. per hour}$$

Alternatively, the power available with a heat load H is

$$K = \frac{H}{3{,}413}\left(\frac{I_a - I_c}{I_c - I_{w2}}\right) \text{kW}$$

This condition results in the largest value of the steam flow W_1. Theoretically, the pressure-control valve is closed, but in practice a small amount of steam is allowed to flow through the L.P. stages in order that the heat generated in those stages by disc friction and blade windage may be continuously removed.

(2) *No Extraction.* The turbine now operates as a normal condensing turbine, and $W_3 = W_1$. The pressure-control valve is full open and the condition curve on the Mollier diagram is practically a continuous curve. The steam consumption is

$$W_1 = \frac{3{,}413 \, . \, K}{I_a - I_f} \text{ lb. per hour}$$

This is the minimum steam consumption and is the lowest value of W_1 for any load. Consequently, with throttle governing for the H.P. section there is a considerable amount of wiredrawing at the H.P. throttle valve. Although this condition results in the minimum steam consumption for the turbine as a whole, the steam flow W_3 through the L.P. stages for any given power is greater than it is under any other conditions of operation. If the turbine is designed to develop its full output when running as a pure condensing machine, then the nozzles in the L.P. stages will be too large for most other operating conditions, and unless some form of nozzle-control governing is employed at the L.P. end there will be an appreciable amount of wiredrawing at the pressure-control valve with a corresponding loss of power. For this reason, the specified power output for no extraction should be kept as low as possible.

(3) *Partial Extraction.* (*a*) *Ideal Nozzle-control Governing.* Consider a given heat load H B.Th.U. per hour. Each lb. of steam extracted gives up an amount of heat $= I_c - I_{w2}$ (Fig. 235).

$$\therefore \qquad W_2 = \frac{H}{I_c - I_{w2}}$$

Power developed by heating steam is

$$K_2 = \frac{W_2}{3{,}413}(I_a - I_c)$$

$$= \frac{H}{3{,}413}\left(\frac{I_a - I_c}{I_c - I_{w2}}\right)$$

$$K_3 = K - K_2$$

Work done per lb. of steam expanding through H.P. and L.P. stages

$$= (I_a - I_c) + (I_d - I_f)$$

$$= I_a - I_f$$

$$\therefore \qquad K - K_2 = \frac{W_3}{3{,}413}(I_a - I_f)$$

The total steam consumption, lb. per hour, is

$$W_1 = W_2 + W_3$$

$$= \frac{H}{I_c - I_{w2}} + \frac{3{,}413\,(K - K_2)}{I_a - I_f}$$

$$= \frac{3{,}413\,.\,K}{I_a - I_f} + \frac{H}{I_c - I_{w2}}\left(\frac{I_c - I_f}{I_a - I_f}\right) \qquad . \qquad . \quad (193)$$

$$= \frac{3{,}413\,.\,K}{I_a - I_f} + W_2\left(\frac{I_c - I_f}{I_a - I_f}\right) \qquad . \qquad . \qquad . \quad (193a)$$

(*b*) *Throttle Governing.* This presents some difficulty, since the pressures p_1' and p_2' are not known until the steam flows W_1 and W_3 are known. Two alternative methods are available. In the first, the pressures p_1' and p_2' are assumed, and the values of W_1 and W_3 calculated by means of the expressions given on page 397. The assumed pressures are now corrected and a recalculation made for W_1 and W_3. These results will be approximately correct, but may be checked by a second approximation. Alternatively, a series of values of W_1 and W_3 may be taken and the corresponding heat and power output calculated. This is the more satisfactory method.

160. Steam Consumption Curves for Pass-out Turbine. These must show the relationship between three quantities, namely, the power output, quantity of pass-out steam, and the total steam consumption. The general form of the lines will be shown by means of an example.

EXAMPLE 32. Derive the steam consumption diagram for a single-extraction pass-out turbine operating under the following conditions—

Pressure of steam supplied . .	200 lb. per sq. in. abs.
Temperature of steam supplied .	440° F.
Pressure of extracted steam . .	40
Pressure of exhaust steam . .	1
Maximum load at turbine coupling .	1,000 kW.
Maximum load with no extraction .	750 kW.
Internal efficiency of H.P. and L.P. stages	0·7
Mechanical losses of turbine . .	35 kW.
Maximum steam consumption under any conditions	25,000 lb. per hour.

(Steam consumption at no load) ÷ (Steam consumption at maximum output under given condition) = 0·12 for no extraction, and 0·14 for full extraction.

Assume ideal nozzle-control governing.

From the Mollier diagram we find—

Adiabatic heat drop from 200 to 40 . .	130·5 B.Th.U./lb.
Useful heat drop from 200 to 40 . .	91·4 ,,
Adiabatic heat drop from 40 to 1 . .	230·0 ,,
Useful heat drop from 40 to 1 . .	161·0 ,,

No Extraction.

Total effective heat drop = 91·4 + 161·0 = 252·4.
Total internal power at maximum load = 750 + 35 = 785 kW.

$$\therefore \text{ Maximum steam consumption} = \frac{785 \times 3{,}413}{252 \cdot 4}$$

$$= 10{,}600 \text{ lb. per hour}$$

$\therefore$ No-load steam consumption

$$= 0 \cdot 12 \times 10{,}600 = 1{,}270 \text{ lb. per hour}$$

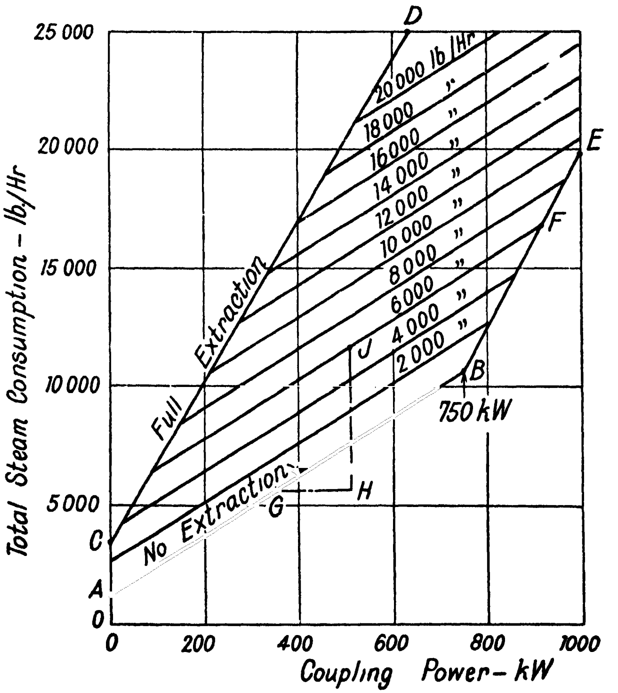


FIG 237 —Steam Consumption Diagram for Pass-out Turbine

The steam consumption line is AB, Fig. 237. Since ideal nozzle-control governing has been assumed the steam consumption line would be slightly concave upwards. For the sake of simplicity a

straight line has been drawn. A similar assumption has been made with the other lines.

Full Extraction.

$$\text{Steam consumption} = \frac{3{,}413}{91\cdot 4} = 37\cdot 3 \text{ lb. per kW-hr.}$$

$$\therefore \text{ Internal power (maximum)} = \frac{25{,}000}{37\cdot 3} = 670 \text{ kW.}$$

$$\therefore \text{ Coupling power} = 670 - 35 = 635 \text{ kW.}$$

No-load steam consumption

$$= 0\cdot 14 \times 25{,}000$$
$$= 3{,}500 \text{ lb. per hour}$$

The steam consumption line is CD.

Partial Extraction. Consider, for example, the extraction of 6,000 lb. of steam per hour. Suppose, in the first instance, that the L.P. nozzles are passing the maximum quantity of steam they are capable of passing, i.e. 10,600 lb. per hour. Then the L.P. nozzle-control valves are full open. The steam which passes right through the turbine will still develop the same internal power, i.e. 785 kW. The additional internal power developed by the extracted steam will be—

$$\frac{6{,}000 \times 91\cdot 4}{3{,}413} = 160 \text{ kW}$$

$$\therefore \text{ Total internal power} = 785 + 160 = 945 \text{ kW.}$$

$$\text{Total coupling power} = 945 - 35 = 910 \text{ kW.}$$

The total steam consumption is 10,600 + 6,000 = 16,600 lb. per hour. This condition is represented by the point F. By considering any other point G, say, on the line AB, the increment of power GH will be again 160 kW and the increment of steam consumption JH is 6,000 lb. per hour. Points such as F and J lie on a constant extraction line for 6,000 lb. of steam per hour. Such a line is obviously parallel to AB. Under the assumed conditions, the constant extraction lines are also equidistant when the increment of extraction is the same.

The straight line BE, Fig. 237, drawn through the limiting points on the constant extraction lines gives the maximum power output for a constant pass-out pressure. For all points on BE, the L.P. nozzle valves are full open, and only for steam consumptions greater than that at E are the nozzle valves partially closed.

EXAMPLES XVII

1. Steam is supplied to a back-pressure turbine at a pressure of 400 lb. per sq. in abs. and superheated 160° F. The exhaust steam from the turbine is utilized in heaters at a pressure of 40 lb. per sq. in. abs. If the amount of heat required per hour is 30 million B.Th.U., and if the efficiency ratio of the turbine is 0·75, calculate the horse-power generated and the hourly heat consumption of the plant, assuming that the condensate from the heaters is returned to the boilers at 267·2° F., and that there are no heat losses. Assume a boiler efficiency of 80 per cent.

Calculate the hourly heat consumption of a plant consisting of a condensing turbine generating the same power, supplied with steam at the same pressure and superheat, exhausting at 1·0 lb. per sq. in. abs., and having an efficiency ratio of 0·75, and separate low-pressure boilers generating dry and saturated steam at 40 lb. abs. from feed water at 267·2° F. and supplying the same quantity of heat. Assume again an efficiency of 80 per cent for the high-pressure and low-pressure boilers.

2. In a factory where L.P. steam is required for heating purposes and electrical energy is required for power purposes, it is proposed to install a back-pressure turbine to operate under the following conditions—

Initial steam pressure	250 lb. per sq. in. abs.
Initial steam temperature	600° F.
Exhaust pressure	20 lb. per sq. in abs.
Efficiency ratio of turbine	70 per cent

If the amount of heat required per hour equals 50 million B.Th.U., calculate the total power available in kW if the generator efficiency is 94 per cent. It may be assumed that the condensate drains from the heaters return to the boiler at the condensing temperature.

3. Steam is supplied to a back-pressure turbine at 200 lb. per sq. in. abs. and 500° F. It is exhausted at 20 lb. per sq. in. abs., the internal efficiency ratio of the turbine being 0·75. If the coupling power is 1,000 kW and the mechanical losses amount to 20 kW, calculate the total amount of heat available, assuming that the heater condensate temperature is 228° F.

Calculate the coupling power and the heat available when the quantity of steam is reduced to one-half of that at 1,000 kW coupling power. Assume that the turbine is governed by throttling, that the internal efficiency ratio, exhaust pressure, mechanical losses, and heater condensate temperature remain as before.

4. Calculate the maximum and minimum hourly steam consumptions of a pass-out turbine which develops 1,000 kW and which has a heat load varying from nil to 18 million B.Th.U. per hour. The operating conditions are—

Initial steam pressure	300 lb. per sq. in. abs.
Initial steam superheat	240° F.
Pass-out pressure	45 lb. per sq. in. abs.
Exhaust pressure	1·0 lb. per sq. in. abs.

The heating steam gives up heat by cooling and condensing only. The efficiency ratio of the H.P. and L.P. groups of stages may be assumed to be 0·70 under all conditions of operation, and it may be further assumed that regulation is effected by varying the number of nozzles in operation.

5. A pass-out turbine operates under the following conditions—

Initial steam pressure	300 lb. per sq. in. abs.
Initial steam temperature	700° F.
Pass-out steam pressure	40 lb. per sq. in. abs
Exhaust steam pressure	1·0 lb. per sq. in. abs.

When the turbine is developing its normal full load and giving out the

normal quantity of heating steam, the total consumption is 40,000 lb. per hour, and the weight of extracted steam is 16,000 lb. per hour.

If the total quantity of steam supplied to the turbine is 26,000 lb. per hour and the amount of heat extracted is 14 million B.Th.U. per hour, calculate the power available. The internal efficiency ratio of the H.P. and L.P. groups of stages is 0·72. The heating steam is condensed but the resulting condensate is not cooled below the saturation temperature. The admission of H.P. steam is effected by nozzle control, but the pass-out pressure is regulated by a simple throttle valve.

6. A factory has an average load of 1,000 kW and requires 15 million B.Th.U. per hour for process work. The heat is to be supplied by saturated steam which condenses in heaters at 30 lb. per sq. in. abs.

It is proposed to install a pass-out turbine to operate under the following conditions—

Initial pressure	200 lb. per sq. in abs.
Initial superheat	120° F.
Exhaust pressure	0·7 lb. per sq. in. abs.

The turbine efficiency ratio for the pressure ranges 200 to 30 and 30 to 0·7 is 0·76, and the boiler efficiency may be taken as 0·80. If the calorific value of the coal used is 12,600 B.Th.U. per lb., calculate the daily coal consumption of the factory, allowing 10 per cent for auxiliaries.

7. A factory has an average load of 1,200 kW and requires 18 million B.Th.U. per hour to be supplied by steam which condenses in heaters at 30 lb. per sq. in. abs.

Steam for power purposes is to be generated at 250 lb. per sq. in. abs. and superheated 140° F. Compare the probable fuel consumptions in the following cases—

(1) If the steam expands in the turbine to a final pressure of 0·8 lb. per sq. in. abs. and the heating steam is separately generated at 30 lb. per sq. in. abs.

(2) If the supply of heating steam is extracted from the turbine at 30 lb. per sq. in. abs., the steam not required for heating purposes being expanded to 0·8 lb. abs.

It may be assumed that the boiler efficiency is 0·76 in each case, that the turbine efficiency ratio for any range of pressure is 0·78, and that the calorific value of the coal is 12,800 B.Th.U. per lb. Both speed and pressure are regulated by nozzle control.

8. Prove that the steam flow through a multi-stage turbine is

$$w = C\sqrt{\left(\frac{p_1}{v_1} - \frac{p_2}{v_2}\right)}$$

where p_1 and p_2 are the steam pressures before the first stage nozzles and at exhaust, respectively, and v_1 and v_2 are the corresponding specific volumes.

In a back-pressure turbine the steam conditions at full load before the first stage nozzles are $p_1 = 400$, $t_1 = 700°$ F., the back pressure being 200 lb. per sq. in. abs. Under these conditions the efficiency ratio is 0·80 and the steam flow 15·3 lb. per sec. At part load the steam is throttled from the above initial condition to a pressure of 300, the back pressure remaining the same. If the efficiency ratio is 0·80 calculate the steam flow and the internal power developed. The specific volume of superheated steam may be calculated from the expression

$$v = \frac{1{\cdot}253(I - 835)}{p}$$

(*Liv. Un.*)

9. Steam is supplied to a pass-out turbine at 400 lb. per sq. in, and 520° F. The pass-out steam pressure is 60 and the exhaust pressure is constant at 1·0. The total power required is 6,000 h.p. and the heat load 50 million B.Th.U. per hour. If the efficiency ratio of the h.p. and l.p. groups of stages is 0·75, what is the total steam consumption of the turbine?

If the total steam consumption is reduced to 71,000 lb. per hour and the heat load remains the same, calculate the new power output. Assume that there is ideal nozzle-control governing at the h.p. turbine inlet, but throttle governing at inlet to the l.p. stages. *(Liv. Un.)*

10. The following results were obtained during a test of a pass-out steam turbine—

Steam pressure at turbine inlet	450.
Steam temp. at turbine inlet	700° F.
Steam pressure before 1st stage nozzles . .	350.
Pressure at which steam is extracted for heating .	70.
Pressure before l.p. first stage nozzles . .	50.
Exhaust pressure	1·0.
Temp. of condensed heating steam . . .	200° F.
Electrical power developed . . .	7,800 kW.
Discharge from surface condenser . .	60,000 lb. per hr.

Calculate the steam consumption of the turbine and the total amount of heat available, if the efficiency ratios of the h.p. and l.p. groups of stages are each 80 per cent, if the alternator efficiency is 96 per cent, and the turbine mechanical losses amount to 60 kW. *(Liv. Un.)*

CHAPTER XVIII

CONSTRUCTION OF NOZZLES AND DIAPHRAGMS

161. Introductory. The nozzle is one of the most important elements in a steam turbine, for in it takes place the conversion of pressure energy into kinetic energy. The shape and finish of the nozzle should be such that this conversion takes place with the highest possible efficiency. The basic requirements may be enumerated as follow –

(1) Sudden changes in direction of the flowing steam, especially at high velocities, should be avoided.

(2) The inlet of the nozzle should be designed to utilize the carry-over energy from the previous stage to the greatest possible extent.

(3) The wall surfaces should be as smooth as possible in order to reduce friction, especially where the steam velocity is high.

(4) The design should be such as to permit of ease of manufacture and finishing, and to enable accurate channel sections to be obtained, especially at the high-pressure end of the turbine.

There are two types of nozzle, namely, (1) the simple convergent nozzle, which is suitable for expanding steam from any given pressure to any pressure higher than the corresponding critical pressure (i.e. to a pressure greater than $0{\cdot}577\,p_1$ for saturated steam, or $0{\cdot}546\,p_1$ for superheated steam), and (2) the convergent-divergent nozzle, which is suitable for expanding steam from any given pressure to any pressure lower than the corresponding critical pressure. From the theoretical analyses given in Arts. 42 and 48, it will be clear that a given convergent-divergent nozzle will only be suitable for a definite ratio of final steam pressure to initial pressure. Suppose, for example, a convergent-divergent nozzle is designed to operate with steam at a certain initial pressure p_1 and a certain outlet pressure p_2. If the actual pressure in the space into which the nozzle discharges is higher than p_2, then as the steam in the nozzle will expand down nearly to p_2, the steam is said to be "over-expanded." If, on the other hand, the pressure on the discharge side is lower than p_2, since the nozzle is restricted in its capacity for expanding steam the steam in the nozzle is said to be "under-expanded." In both cases there are fairly serious losses involved. Consequently, every convergent-divergent nozzle requires to be carefully designed for the conditions under which it has to operate.

The convergent nozzle is not subject to the same restrictions. Provided the pressure on the outlet side does not fall below the critical pressure, the nozzle will function in a satisfactory manner in spite of variations in outlet pressure. This statement refers to efficient operation and not to mass flow.

The great majority of turbine nozzles are of the convergent type; the convergent-divergent nozzle is hardly ever used except in small turbines and in conjunction with velocity-compounded wheels.

CONSTRUCTION OF CONVERGENT NOZZLES

162. First-stage Convergent Nozzles. Fig. 238 shows a segment of nozzles suitable for the first stage of an impulse turbine of

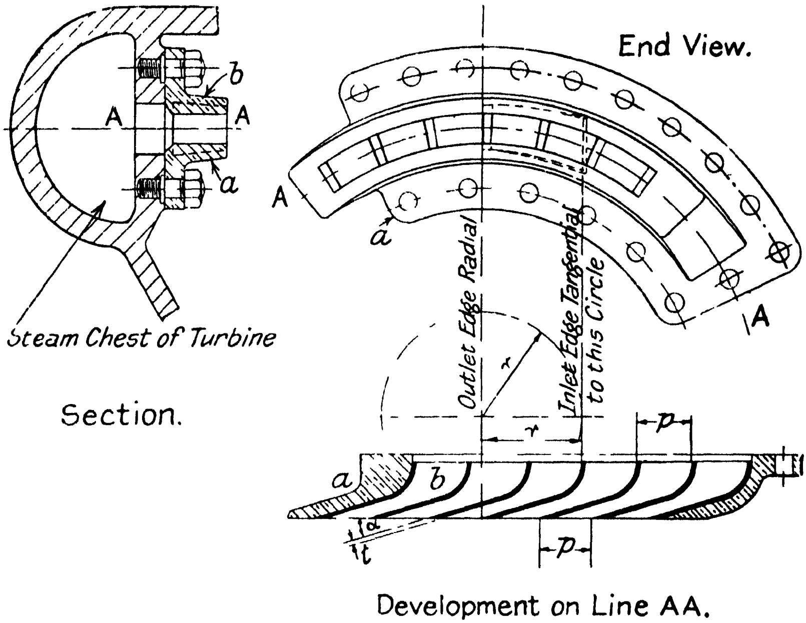


FIG 238

medium power. The segment contains six nozzles and comprises a casting *a* into which the nozzle guide vanes *b* are embedded by "casting in." The procedure adopted in the manufacture of such cast-in guide blades varies somewhat, but is generally as follows. The guide vanes are made from sheet metal of uniform thickness which is first cut to shape and then curved in a press. After certain preparation (which will be described shortly) the guide vanes, now of the correct shape and having the correct curvature at inlet, are embedded in a sand core which is to form the steam passage in the nozzles. This may be effected either by means of a core box in which the guide vanes are set, or by forming the core on a circular table, the guide vanes being set up at the correct angle and the correct distance apart. Each end of the vanes projects outward from the core as shown in Fig. 239, which shows a section through

the mould for the nozzle. When the molten metal is poured into the mould the projecting edges of the guide vanes are surrounded; on freezing of the metal the vanes become firmly held.

The circumferential pitch p of the nozzles is normally about 2 in. The outlet angle α varies from 12° to 20°. The thickness t

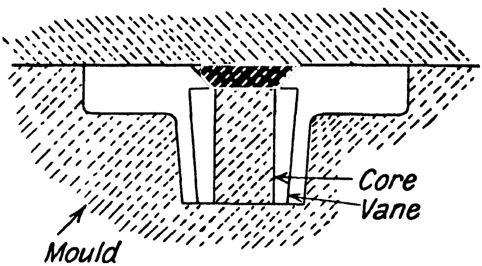


FIG. 239

of the guide vanes should be made as small as possible for the reasons given in Art. 70. It varies from 15 L.S.G. (0·072 in.) to

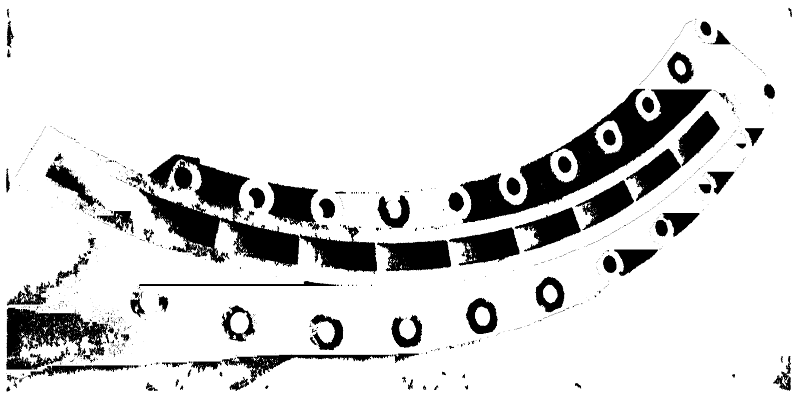


FIG. 240.—Curtis Turbine Nozzles—Exit Side

8 L.S.G. (0·160 in.). The larger thickness would only be used with long blades where strength to resist bending is required.

Fig. 240 shows a photograph of such a nozzle segment having ten nozzles.

163. Materials and Preparation of Nozzle Guide Blades. Rolled copper guide blades cast in gunmetal nozzle segments may be used for saturated steam. For superheated steam it is essential to use steel or alloy steel vanes. The metals employed include low-carbon sheet steel, 3 to 5 per cent nickel steel, stainless iron, and Hadfields' Hecla A.T.V. steel. The late Dr. O. Lasche, in his book,

Materials and Design in Turbo-Generator Plant, states that "low-carbon double-pickled steel stamping sheet, or soft tin plate made from Siemens-Martin steel of not more than 34 kg. per sq. mm. tensile (21·6 tons per sq. in.), with about 24 per cent elongation, has shown itself to be thoroughly reliable. Such material does not easily rust. Also when cast into the iron frame (diaphragm) it can take up carbon from the fluid cast iron without becoming hard or brittle."

Steel guide vanes are cleaned with acid and the ends tinned. The tinning prevents oxidation and assists in the partial alloying of the cast iron and the steel guide blade during the appreciable time that the iron is molten.

Special precautions must be taken when casting in guide blades of Hecla A.T.V. and other highly alloyed steels of this general type into brass or bronze nozzle segments or diaphragms, owing to the fact that vanes of these materials may develop cracks when quickly brought into contact with molten alloys containing zinc and tin. There is a "heat shock" effect of the hot alloy on the steel setting up strains which may cause cracking if, at the same time, an alloying action is allowed to take place between the steel and the molten metal. The measures suggested by Messrs. Hadfields, Ltd., for the lessening of the heat shock and for the minimizing or prevention of the alloying action are (1) to smoke the blades or the mould with the blades in position before closing; this may be done by means of the smoky flame of a paraffin lamp, or (2) if the above is found not to be convenient the following coatings may be used, either (*a*) graphite, or red lead, bonded with 15 per cent aqueous solution of molasses, painted evenly and dried at a temperature below 180° C., or (*b*) graphite, or red lead, mixed into a paste with palm oil rubbed evenly on the warmed blade, and then heated to 150°–180° C. The selection of the method depends upon the degree to which the brazing is desired to be carried. The use of red lead ensures a tight joint. Cracking may also be avoided by preheating the steel to a temperature of 550° C. The manufacturers also recommend a slow rate of pouring so as to lessen the heat shock. These precautions are not necessary when casting Hecla A.T.V. steel vanes in cast-iron nozzles or diaphragms owing to the absence of any alloying action.

Steel guide vanes which have been strained due to cold bending should be normalized.

164. Built-up Nozzle. An accurate nozzle segment may be obtained by the built-up construction shown in Fig. 241. This has been used in turbines constructed by Metropolitan-Vickers, Ltd., and comprises a number of vanes A, which are machined all over, placed between curved angles B, likewise machined all over. The ends of the segments are closed by pieces C of suitable shape. The guide vanes are attached to the angles by rivets D and small spigots E riveted over.

165. Diaphragm Nozzles. For high-pressure diaphragms, the built-up construction originated by the Erste Brünner Maschinenfabrik is used by many manufacturers. Details of one form of construction are shown in Fig. 242. Each diaphragm consists of a steel centre A, in halves, to which are riveted several nozzle elements B. Each of these is machined all over. The abutting edges are machined radial so that when the elements are set in the groove of the diaphragm centre they fit together and form a complete ring.

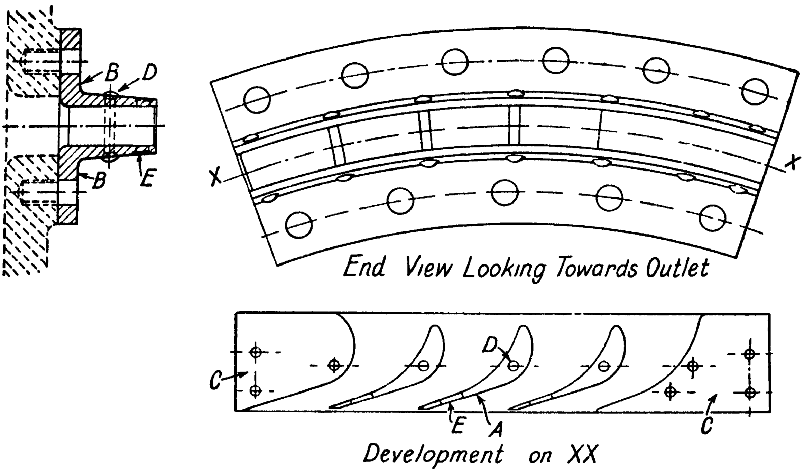


FIG. 241.—Metropolitan-Vickers Type of Built-up Nozzle

Where the admission is partial, blanks are fitted in place of guide blades. Fig. 242 (*d*) shows how the guide blades may be arranged at the horizontal joint so that a complete and uninterrupted ring of nozzles may be obtained. On the side opposite to that shown, the guide vanes would protrude from the upper half. The advantages of the construction are (1) an accurate profile of good shape is secured for the guide blade; (2) the nozzle areas are accurate; (3) where required, a nozzle may be constructed with a relatively small radial height, thus enabling full admission to be obtained and losses due to partial admission eliminated; (4) a robust construction, yet occupying a small axial length, is assured; and (5) the nozzle surfaces may be made smooth.

In turbines of medium power and in the low-pressure stages of turbines with a high output the nozzle plates in the diaphragm are frequently of the "cast-in" type already described in Art. 162. A typical construction where the ratio of nozzle height to mean diameter is relatively small is shown in Fig. 243. A method of setting out the guide vane is illustrated in Fig. 243 (*c*). The straight

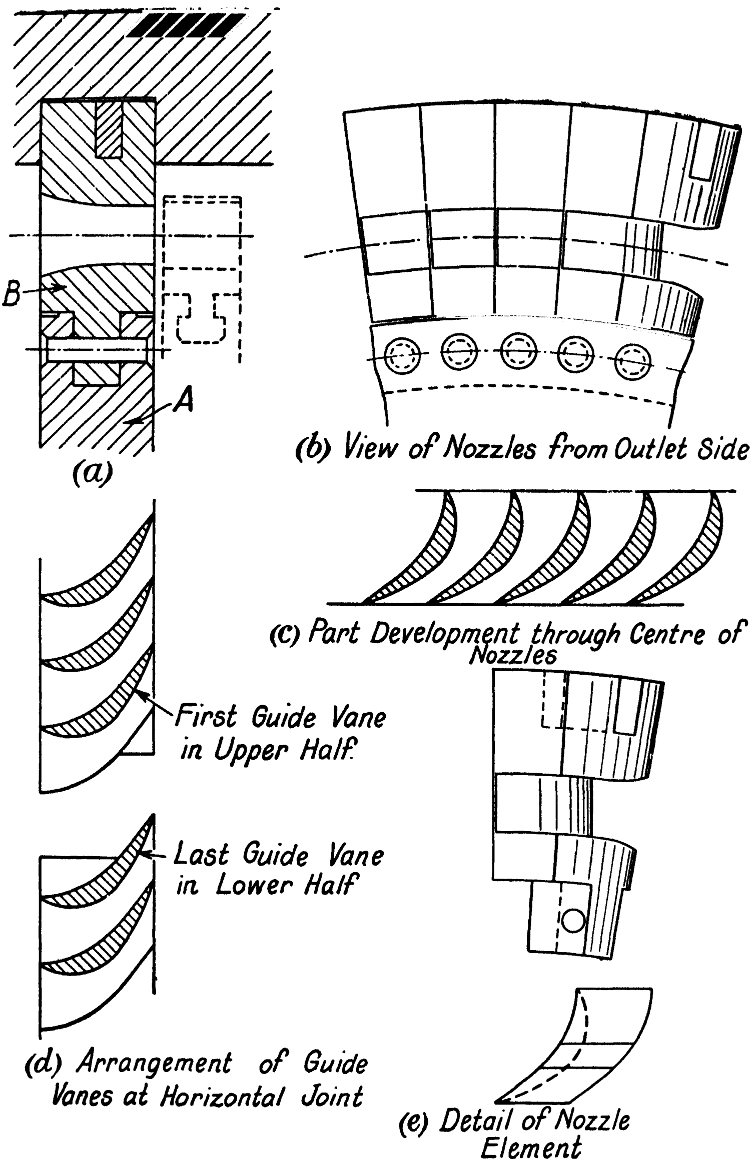


FIG. 242.—Erste Brünner Type of Built-up Nozzle

outlet parts of the vanes are first drawn at the angle α to the face of the diaphragm, and the perpendicular *bc* is drawn from *b* to the adjacent guide blade. It seems desirable to provide the nozzle

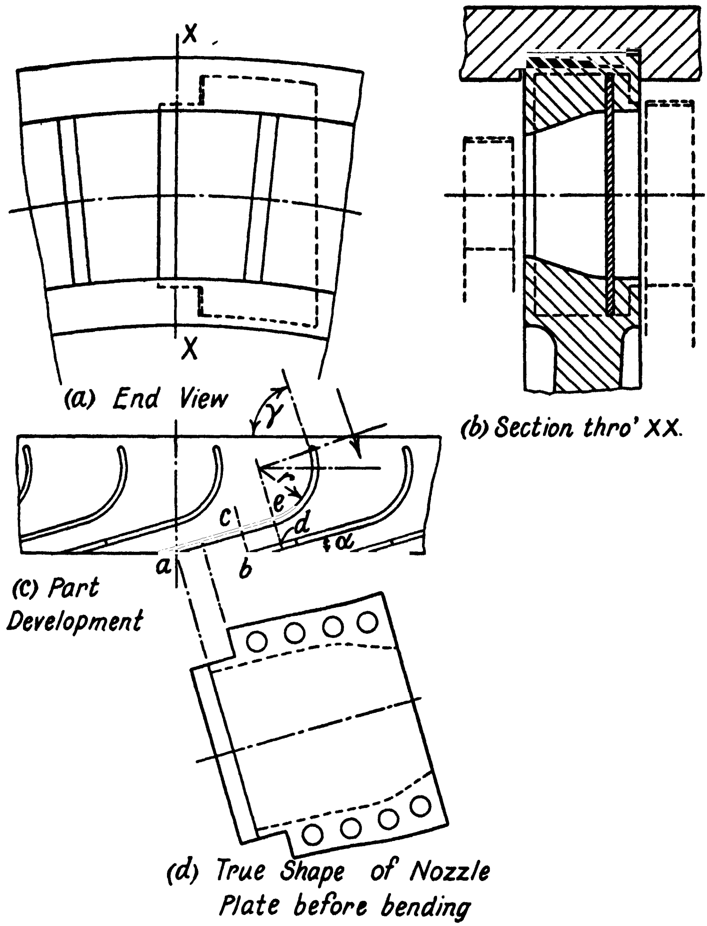


FIG. 243.—Details of Cast-in Type of Diaphragm Nozzle

with a short parallel throat to control the jet, and for this purpose *de* is drawn parallel to *bc*, the length of the parallel part being *ec*. For the effect of such a parallel throat on nozzle efficiency, the reader is referred to Art. 70. For manufacturing purposes it is desirable to shape the guide blades on a round former, and for this purpose the curved inlet portion is given a suitable radius *r*, the

centre of curvature lying on *de* produced. The inlet angle γ of the guide blade should be made to agree with the angle γ given by the velocity diagram, Fig. 99, page 175. The true shape of the nozzle plate before bending may be obtained by simple projection and development. In order to increase the union of the guide blade with the diaphragm casting the edges of the nozzle plates are either drilled, as shown, or scalloped.

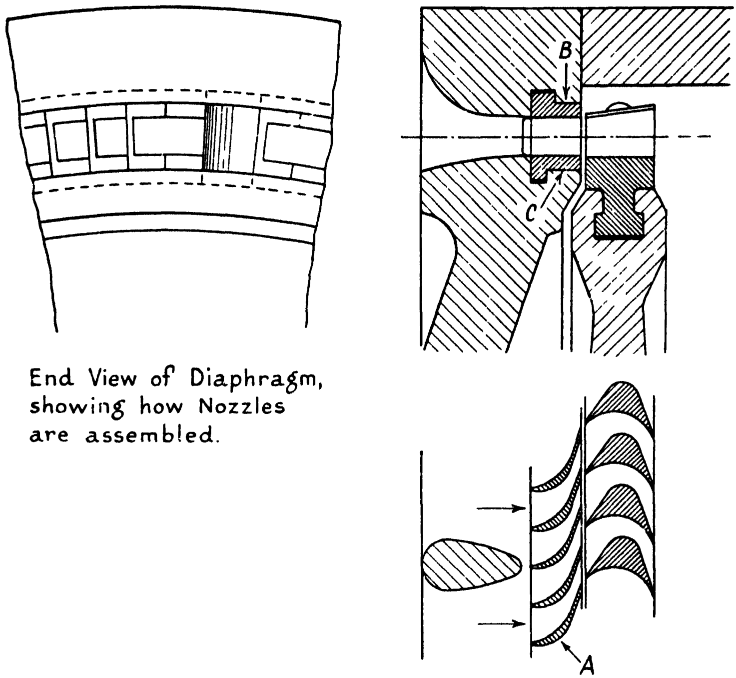


FIG. 244.—Built-up Construction of Nozzles

A form of construction used in high-pressure turbines by Escher Wyss is shown in Fig. 244. Each nozzle element comprises a guide blade A, a roof piece B and a floor piece C, machined all over and in such a way that the projections on B and C are a snug fit in grooves machined in the diaphragm casting. The construction provides nozzles with accurate smooth surfaces and a suitable ratio of pitch to nozzle height. A similar construction may be used in the first stage of the turbine. Suitable locking pieces are provided for the nozzle elements, and partial admission may be employed by substituting blanks for the nozzle elements.

CONSTRUCTION OF CONVERGENT-DIVERGENT NOZZLES

166. The de Laval Nozzle. The nozzle used in the single-stage de Laval turbine is invariably of the convergent-divergent type. The construction is shown in Fig. 245. The nozzle is of gunmetal and is provided with a rounded inlet, which forms the short convergent part of the nozzle, and a gradually diverging part. The nozzle is an easy force fit in the cylinder, the steam chest end being screwed so that the nozzle may be withdrawn when required. In a steam turbine which may sometimes run condensing and at other times

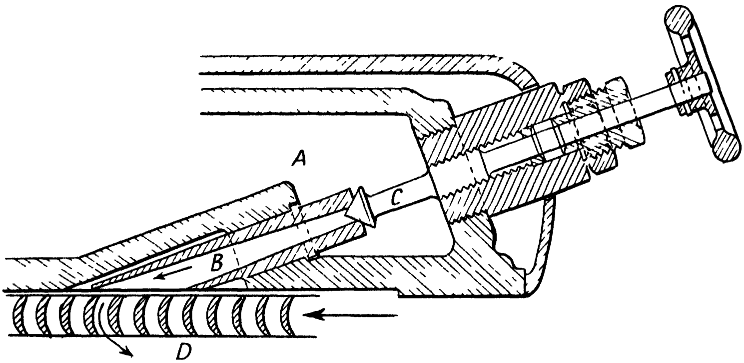


FIG 245

non-condensing, special nozzles are supplied for either condition of operation. Owing to the greater expansion ratio in the condensing nozzles and to the fact that the outlet area is the same in both types—being limited by the same blade height—the throat area of the condensing nozzles is smaller than that of the non-condensing type. Consequently, even allowing for the smaller specific steam consumption when operating condensing, the number of condensing nozzles required is about twice the number of non-condensing nozzles. The individual nozzles may be opened or closed by means of the needle-valve shown. Although the cylindrical or conical form of nozzle affords a simple construction and easy machining operations, the resulting elliptical outlet in the wheel plane cannot be ideal from an efficiency point of view, since the blade channels other than that directly in line with the nozzle axis are only partially filled with the issuing steam jet and their performance will be adversely affected by ejector action and eddy effects.

167. Machined Type of Nozzle. With the introduction, now several years ago, of velocity-compounded wheels at the high-pressure end of marine reaction turbines, the problem of constructing suitable

nozzles for the impulse stage presented itself. The pressure drop was large, often from about 180 lb. per sq. in. gauge down to about 40 lb. gauge, the number of jets was sometimes large, and the nozzles had to be so constructed as to be as efficient as possible. Moreover, there was little or no previous experience with such turbines in marine practice and the possibilities of corrosion and erosion had to be faced. One type of nozzle construction is shown in Fig. 246. The nozzle casting is of gunmetal, while the vanes are of a special metal. A number of slots are machined in the main casting or box to receive the vanes, which are machined all over, and the shape of which is indicated in Fig. 246 (*c*). That part of the vanes which is not embedded in the slots is machined to a taper, as shown in Fig. 246 (*a*), so as to give the required sectional areas at the throat and mouth of the nozzle. The chief advantages of this rather costly form of construction are—

(1) The vanes are machined all over and thus offer the minimum resistance to the flow of steam.

(2) The machining of the slots and vanes ensures correct nozzle angle and correct throat and mouth areas.

(3) The vanes may, if badly corroded or eroded, be replaced by new ones.

168. "Cast-in" Type of Convergent-divergent Nozzles. Another form of construction which has been largely adopted in marine impulse turbine stages is shown in Fig. 247. Guide blades are rolled to the section shown by the dotted lines in the upper part of the figure, are then cut to shape and cast into the nozzle segment in the usual manner. After marking-off and machining, the guide vanes are thinned down to the final section by filing.

169. Built-up Nozzle. An interesting form of nozzle construction has been used in many steam turbines constructed by the well-known Swiss firm of Brown, Boveri & Co. It consists essentially of three parts—a segmental strip *a* (Fig. 248), in which the nozzle passages are machined; a covering segment *b*, and a wedge piece *c*. These parts are bevelled as shown, and the downward pressure of the locking screws *d* on the ring *c* causes the strips *a* and *b* to be forced against the steam chest, so keeping the joints steam-tight. The set-screw *d* is covered by a cap nut *e* to prevent steam leakage. The construction has all the advantages of other built-up nozzles, namely, accurate angles, form, and areas, together with a good finish. It also facilitates examination and replacement, if necessary.

170. Loss Due to Steam Entering Blades Obliquely and Special Form of Nozzle to Minimize such Loss. Consider the form of nozzle most frequently employed in impulse turbines. This has already been described, and comprises a number of sheet metal guide vanes cast into a diaphragm or nozzle block. A longitudinal section shows a passage which is symmetrical about a straight line XX parallel to the turbine axis, Fig. 249. The outlet edge YY of the vane is,

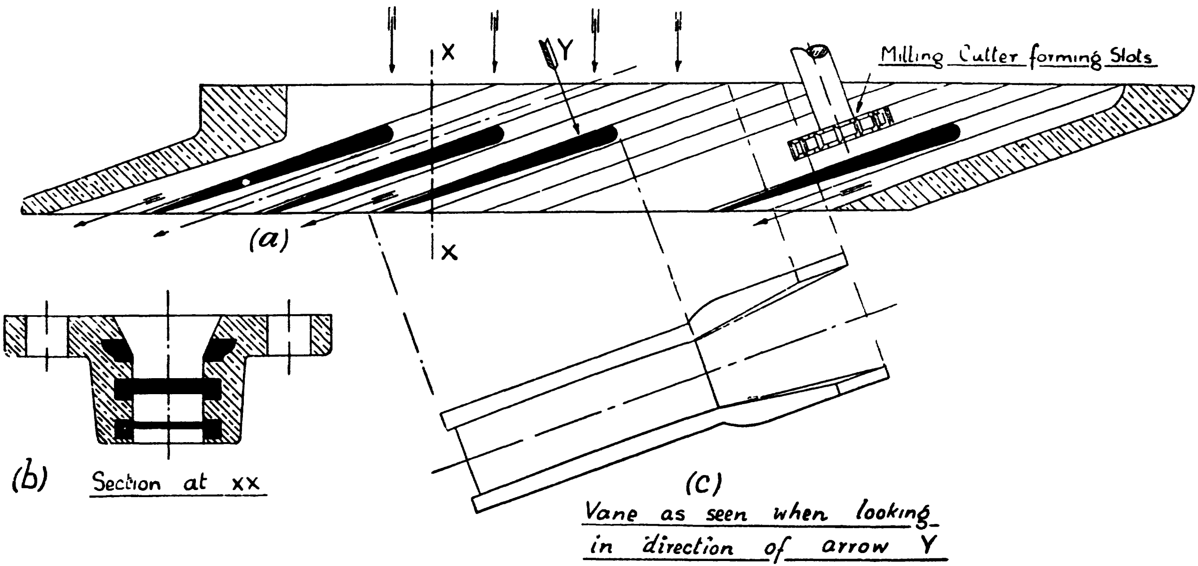

X
Y
Milling Cutter forming Slots
(a)
X
(b)
Section at XX
(c)
Vane as seen when looking in direction of arrow Y

FIG. 246

in such cases, radial, while the inlet edge Y′Y′ is tangential to a circle having the radius s. The path of a particle of steam in passing through the nozzle is a helix, but at the outlet the particle is moving along the straight line indicated by the arrows in plan and end elevation. There is always a certain clearance c between the nozzle and the inlet edge of the blading, with the result that the blade reaches the position shown before the steam enters it. The distance $x = \frac{c}{\sin \alpha}$ and is greater with small nozzle angles than with larger angles. Inspection of the figure shows—

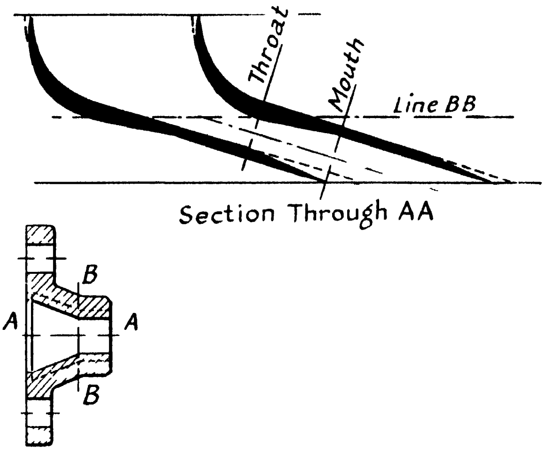


FIG. 247

(1) That the entry of the steam into the moving blade takes place at the angle ϕ to the tangent plane at the point of entry, such that

$$\tan \phi = \frac{x}{R} = \frac{c}{R \cdot \sin \alpha}$$

As a result there is a slight but somewhat indeterminate reduction in work done in the blades, together with secondary losses.

(2) If the radial height of the blade be the same as that of the nozzle, and if both are symmetrically placed about the line XX, a proportion $\frac{AB}{BC}$ of the steam flowing through the nozzles will never enter the blades at all, but will blow out into the space around the shrouding without doing any work in that row of blades. This loss may be easily avoided either by displacing the blade radially outward or, as is more usual, by making the radial height of the blades slightly greater than that of the nozzle (see also Art. 82).

The losses due to oblique entry may be minimized by laying down the nozzle section as shown in Fig. 250. For any given nozzle angle α, the blade will be in the position shown in plan when the particles of steam passing along the surface of the vane just reach

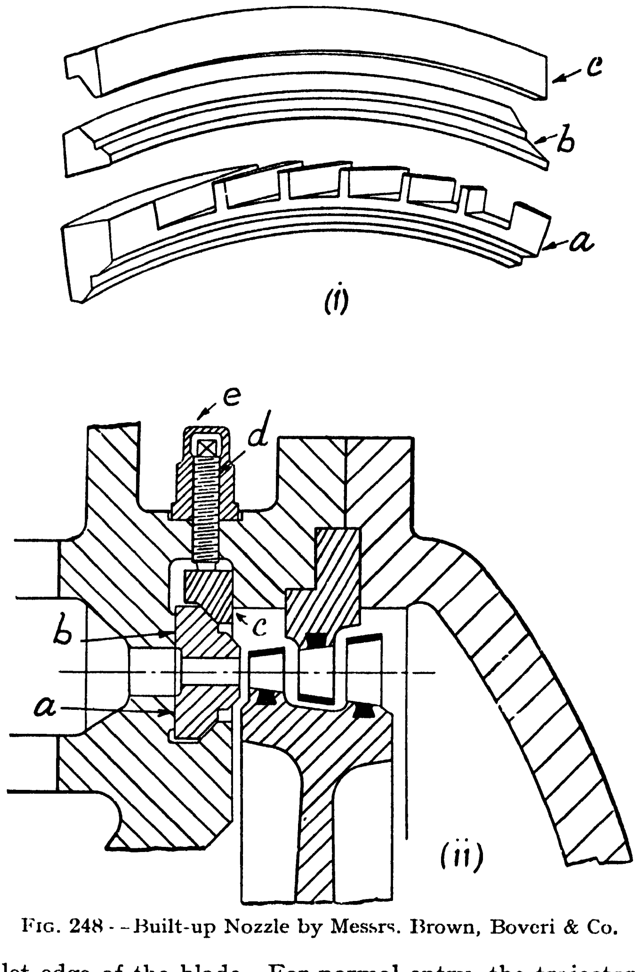


FIG. 248.—Built-up Nozzle by Messrs. Brown, Boveri & Co.

the inlet edge of the blade. For normal entry, the trajectory of a particle of steam flowing along the axis of the nozzle must be tangential to the circle of (mean) radius R at the point reached by the blade when the steam enters it, i.e. the axis of the nozzle must lie along the line DE. It is clear, then, that in a longitudinal section through the nozzle the axis will not now appear straight, but will be a curved line, curving away from the turbine axis when moving

in the direction opposite to that of steam flow. The equation to the curve may be found as follows—

Consider a transverse section distant x from the inlet edge of the moving blades. The point A lies on the axis, and the distance BA $= x \cdot \cot \alpha$.

But $\quad$ BA = ED (approximately)

$\therefore \quad$ FD $= x \cdot \cot \alpha$

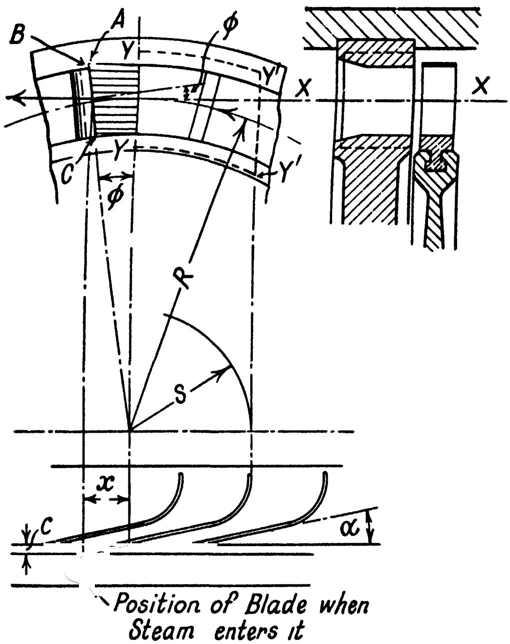


FIG 249

Let h = height of centre line above the surface of a cylinder co-axial with the turbine and having a radius equal to that of the mean blade circle.

Then
$$h = \text{EF}$$
$$= \text{OE} - \text{OF}$$
$$= \sqrt{(\text{R}^2 + x^2 \cot^2\alpha)} - \text{R}$$

Values of h have been calculated for a mean radius of 15 in., a clearance of 0·1 in., and various values of α. The results are shown in Fig. 251 (a). The axial length chosen, i.e. 2 in., is common in

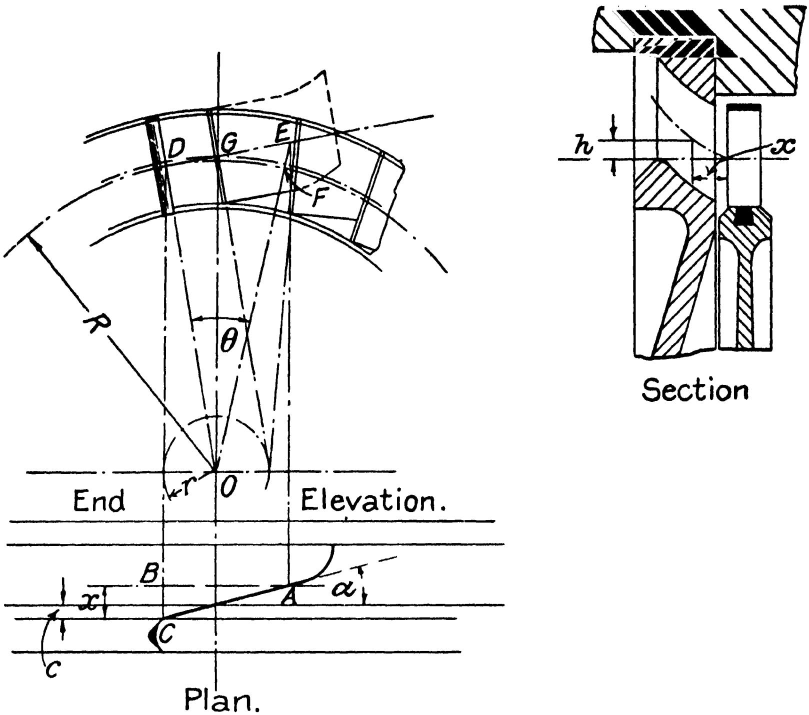


FIG. 250

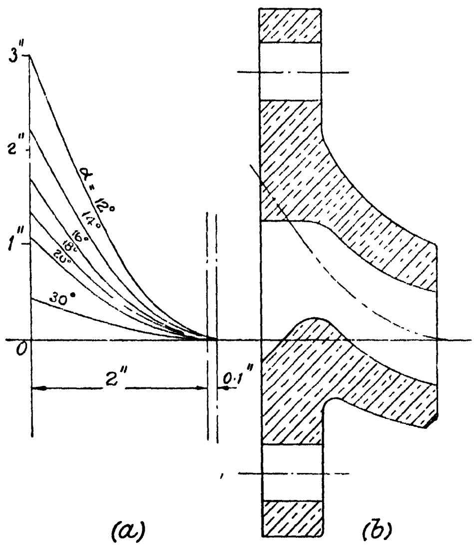


FIG. 251

practice, and the modification for the usual angles is fairly considerable. In Fig. 251 (*b*) the actual longitudinal section of a 16° nozzle with cast-in guide vanes is shown.

171. **Strength and Stiffness of Turbine Diaphragms.** In almost all steam turbines the diaphragms are in halves, being split along the horizontal diameter. This fact adds considerably to the difficulty of calculating the stresses in such diaphragms and their deflections.

Fig. 252 shows a half diaphragm of the built-up type comprising a number of nozzle elements, similar to those shown in Fig. 242,

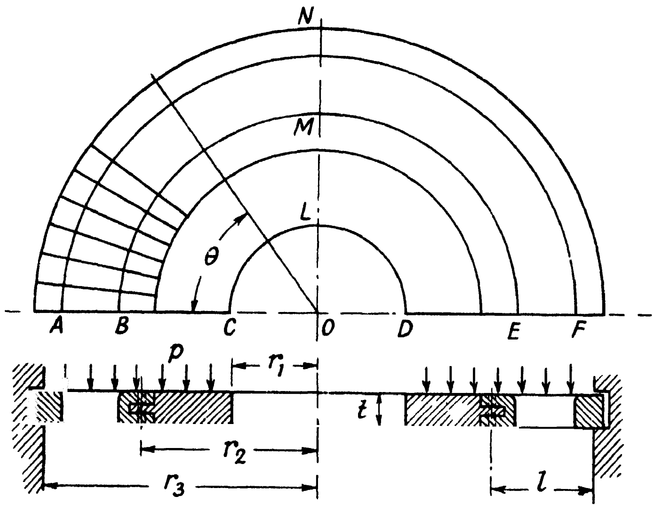


FIG. 252 Built-up Half Diaphragm

attached by rivets to a semi-circular steel centre-piece. Reference may first be made to a careful experimental investigation into the deflections and stresses in semi-circular plates with and without central holes and subjected to fluid pressure made by Dr. Huggenberger (1). The deflections were measured at several points and it was found that the greatest deflection occurred at C and D, Fig. 252, while the largest stress occurs at L on the axis of symmetry. Using a special weighing device, Huggenberger measured the reaction on the rim of the diaphragm and found that it was very high at the points A and F and fell rapidly to much lower values before rising again in the region around $\theta = 60°$ after which it fell to a second minimum at $\theta = 90°$.

The problem has been further analysed by Dr. D. M. Smith (2) who assumed the reaction per unit length of the periphery to be given by the equation

$$F = a_0 + a_1 \sin \theta$$

where a_0 and a_1 are constants (see Fig. 253). The values of a_0 and a_1 may be found by equating the total force due to rim reaction to that due to pressure and also equating the moment of the rim

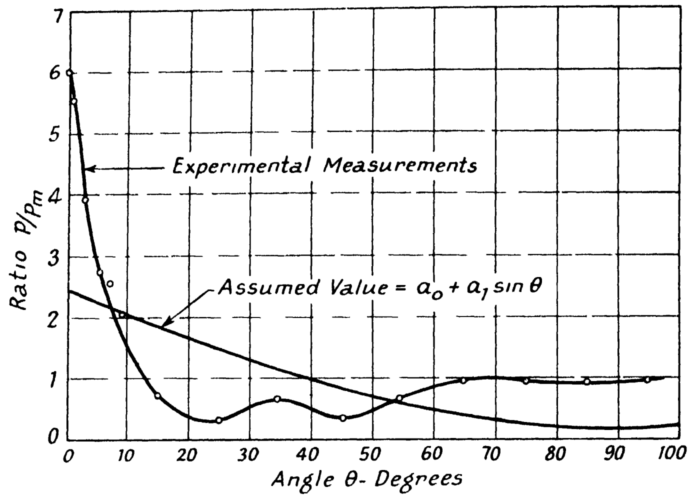


FIG 253 Distribution of Pressure Round Rim of Semi-circular Half Diaphragm

reaction about the diameter AF to the moment due to pressure difference. The constant a_1 is negative. For a narrow diaphragm (r_1/r_3 approaching unity) the reaction is nearly uniform, and for a

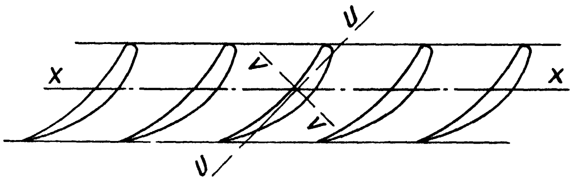


FIG 254 Section through Nozzle Guide Blades

very small central hole it may be shown that the maximum reaction per unit length is 2·42 times the mean.

It is pointed out that, since the locking strip in the periphery of the nozzles (see Fig. 242) prevents the nozzle elements from sliding over each other, the blades will not bend about the principal axes U and V but about the axis X, Fig. 254.

The deflection of the diaphragm is made up of two components (1) a deflection due to elastic distortion of the centre alone, and

(2) deflection due to the distortion of the blades alone assuming the centre rigid. The latter is stated to be about one per cent only of the former and may, therefore, be neglected. The maximum deflection due to centre distortion is given by the expression

$$\Delta_c = K_c \cdot \frac{pr_3^4}{Et^3}$$

where p = pressure difference on diaphragm
E = Young's modulus for the material.

Values of the dimensionless constant K_c are given in Fig. 255.

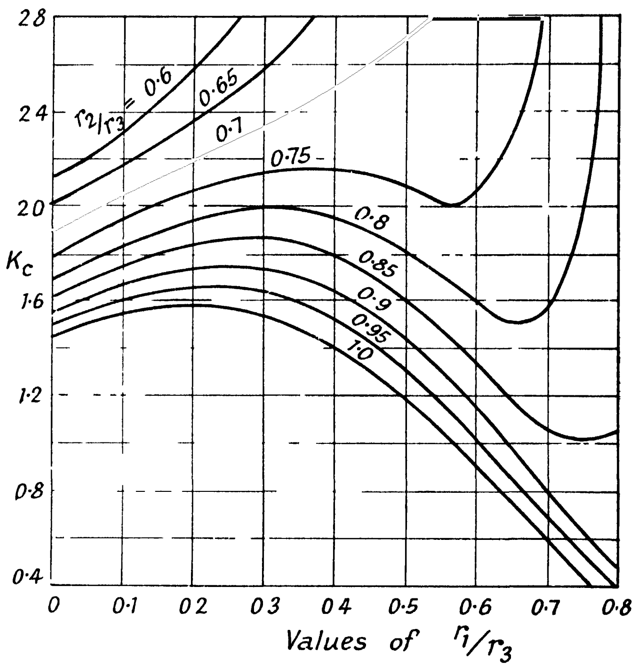


FIG. 255.—Deflection Coefficients for Centre of Built-up Diaphragm

The bending moment across a radial plane is a maximum when $\theta = 90°$, and the maximum bending stress in the centre-piece at L is given by

$$f = K_f \cdot \frac{pr_3^3}{(r_2 - r_1)t^2}$$

values of K_f being given in Fig. 256.

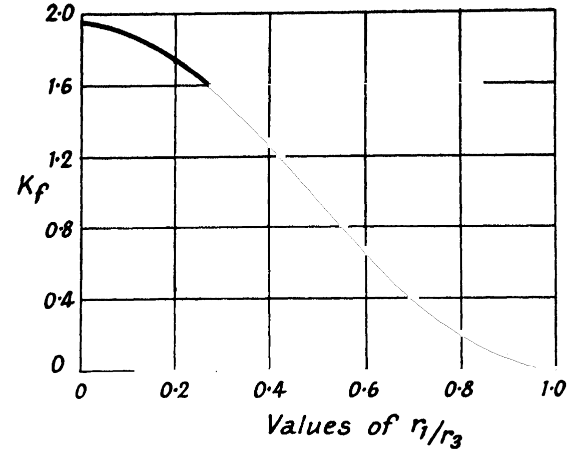


FIG. 256.—Coefficient for Maximum Stress in Diaphragm Centre

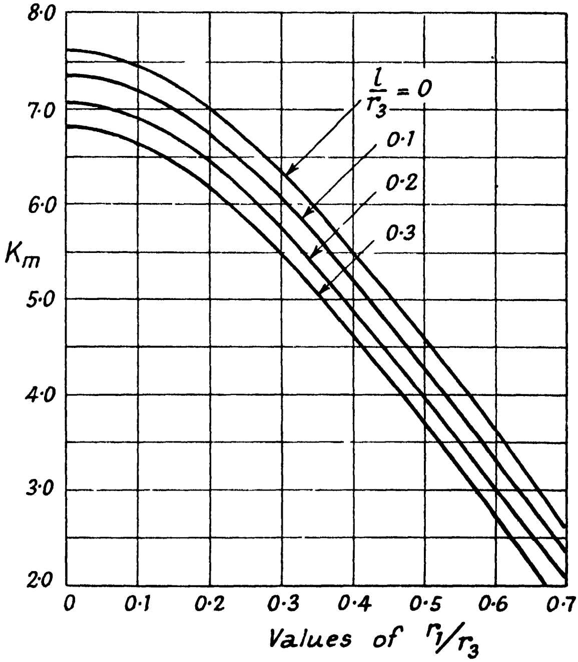


FIG. 257. Coefficients for Maximum Bending Moment in Guide Blade or Root Fastening

The bending moment in the nozzle element or blade is a maximum for the inner end of the blade adjacent to the split, i.e. at B. This maximum moment is given by the expression

$$M_b = K_m \cdot \frac{p \cdot r_3{}^2 l}{n} \text{ (see Fig. 257)}$$

where n is the number of nozzle elements in the complete circle and the value of l is as given by Fig. 252.

Valuable data on stresses and deflections of built-up and welded diaphragms are given in a paper by Mr. N. Elce (3). The half diaphragms were loaded by four hydraulic rams arranged to simulate, as far as possible, the load due to a uniform pressure difference. Experimental values are compared with those calculated from Smith's formulae given above. Expressed briefly, the test values of the maximum centre stress at L, Fig. 252, were about 0·75 times the calculated value; the maximum deflection had values 1·0 and 1·8 times the calculated value, while the maximum blade stress values, measured by strain gauges, were about 0·8 times the calculated value. The reaction distribution was also measured and is shown in Fig. 253.

Diaphragms in the high-pressure cylinders of turbines operating with high initial temperatures are subject to creep; consequently the deflection will increase with time.

BIBLIOGRAPHY

1. HUGGENBERGER: "Festigkeit halbkreisförmiger Platten und Dampfturbinen-Leiträder." *Z.V.d.I.*, 1927, 71, 949.

2. SMITH: "Deflection and Stress in Built-up Half Diaphragm." *Proc. 5th Int. Congress for Applied Mechanics*, 1938, p. 62.

3. ELCE: "Economic Basis and Character of Steam Turbine Design." *Proc. I. Mech. E.*, 1956; 170; 1022.

CONSTRUCTION OF TURBINE BLADES AND BLADE ATTACHMENTS

172. Centrifugal Stress in Turbine Blades of Uniform Cross-section. Consider a turbine blade having a constant cross-sectional area A sq. in., a mean diameter D in., a length l in., and composed of material having a density w lb. per cub. in. Let the rotational speed

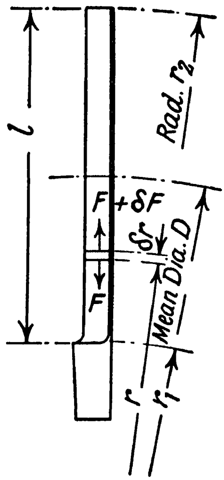


FIG. 258

be N r.p.m. and the corresponding angular velocity ω radians per sec.

Let F = internal force in blade at radius r (Fig. 258).

$F + \delta F$ = internal force in blade at radius $r + \delta r$.

Volume of blade element $= A \cdot \delta r$.

Centrifugal force on blade element $= \dfrac{wA \cdot \omega^2 \cdot r \cdot \delta r}{g}$

Then
$$F + \delta F + \frac{wA\omega^2 r \cdot \delta r}{g} = F$$

or
$$\delta F = -\frac{wA\omega^2 r \cdot \delta r}{g}$$

Then, if F_1 = internal force at root
and F_2 = internal force at tip, due to centrifugal force on shrouding—

$$F_1 - F_2 = \frac{wA\omega^2}{g} \int_{r_1}^{r_2} r \, . \, dr = \frac{wA\omega^2}{2g} (r_2^2 - r_1^2)$$

$$= \frac{wA\omega^2 Dl}{2g}$$

If the stress $f_s = \frac{F_2}{A}$ due to the shrouding be calculated separately, then the stress due to the inertia of the blade alone is

$$f_c = \frac{F_1}{A} - \frac{w \, . \, \omega^2 Dl}{2g} \text{ lb. per sq. in.}$$

Note that $g = 32{\cdot}2 \times 12$ in. per sec.²

For practical purposes, we have—

For steel blades, $w = 0{\cdot}288$ lb. per cub. in.

$$f_c = 4{\cdot}09l\left(\frac{D}{100}\right)\left(\frac{N}{100}\right)^2 \text{ lb. per sq. in.} \quad . \quad . \quad (194)$$

For brass blades, $w = 0{\cdot}31$ lb. per cub. in.

$$f_c = 4{\cdot}4l\left(\frac{D}{100}\right)\left(\frac{N}{100}\right)^2 \text{ lb. per sq. in.} \quad . \quad (194a)$$

Writing $m = \frac{l}{D}$, and u for the mean blade velocity—

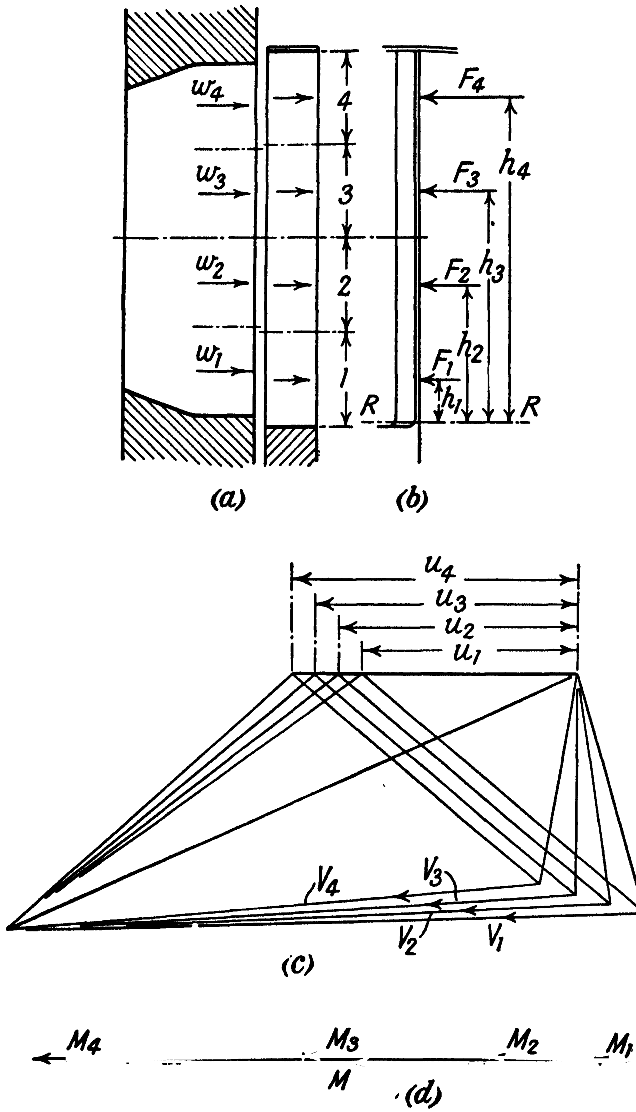
$$f_c = 0{\cdot}215\, m \, . \, u^2 \text{ for steel blades} \quad . \quad . \quad (194b)$$

$$f_c = 0{\cdot}231\, m \, . \, u^2 \text{ for brass blades} \quad . \quad . \quad (194c)$$

The resultant centrifugal stress at the root of the blade is equal to the sum of the stresses f_c and f_s, and is a uniform stress if the centroids of the blade sections lie on a radial line.

173. Bending Stresses in Symmetrical Impulse Blades of Uniform Cross-section. In addition to the centrifugal stress at the innermost blade section, there is a stress due to bending caused by the impulse. While this stress might not be large in itself, its effect on the maximum tensile stress must be considered in long blades.

It is first necessary to find the bending moment across the blade root. For this purpose, divide the nozzle and blade heights into any number, say four, equal parts, as shown in Fig. 259 (*a*) and (*b*), and calculate the steam flow through all the nozzles for each part. Let these be w_1, w_2, etc., lb. per sec. Now draw the velocity diagrams for each part of the blade, as shown in Fig. 259 (*c*), making the peripheral velocities u_1, u_2, etc., equal to that at the mid-height of the part in question. In this way, the velocity changes V_1, V_2,



w4
w3
w2
w1
4
3
2
1
F4
F3
F2
F1
h4
h3
h2
h1
R
R
(a)
(b)
u4
u3
u2
u1
V4
V3
V2
V1
(c)
M4
M3
M2
M1
M
(d)

FIG. 259

etc., are obtained. Then if n is the total number of blades on the wheel, the impulses are equal to

$$F_1 = \frac{w_1 V_1}{gn},\ F_2 = \frac{w_2 V_2}{gn},\ \text{etc.}$$

The bending moments due to impulse are

$$M_1 = F_1 h_1,\ M_2 = F_2 h_2,\ \text{etc.}$$

The resultant bending moment across R – R is then found vectorially as shown in Fig. 259 (*d*).

If the blades are profile blades constructed with unequal angles in accordance with Fig. 111, then the axis X–X, Fig. 260, is almost

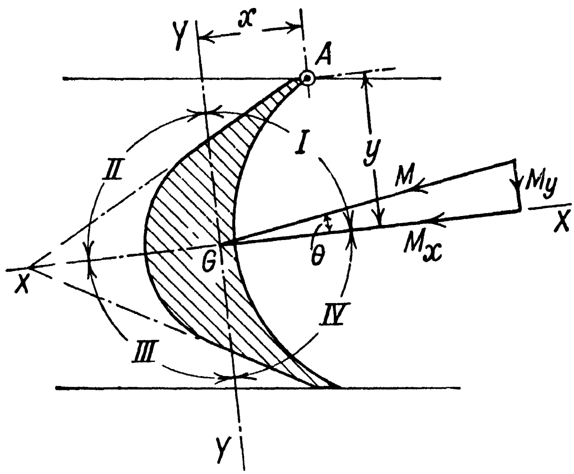


FIG 260

exactly an axis of symmetry. If G is the centroid of the blade section and YY is drawn perpendicular to XX, then XX and YY are the principal axes of the section. Suppose that the plane of M is inclined at the angle θ to XX, then M may be resolved into the two components M_x and M_y. It is obvious that M_x will produce tensile stresses in quadrants I and IV, and compressive stresses in II and III; while M_y will produce tensile stresses in I and II, and compressive stresses in III and IV. Hence, in general, the greatest tensile bending stress will occur at the point A and is equal to

$$f_b = \frac{M_x \cdot x}{I_Y} + \frac{M_y \cdot y}{I_X}$$

Therefore the maximum tensile stress will also occur at A and equals $f_s + f_c + f_b$.

174. Graphics of Blade Sections. The position of the centroid is most easily obtained by the method shown in Fig. 261. The blade section is first drawn 10 or 20 times full size. The straight line XX is drawn through the end points of the horns as shown. Then, still considering the type of profile blade shown in Fig. 111, the line XX is perpendicular to the axis of symmetry. A straight line X_1X_1 is now drawn parallel to XX and at some convenient distance a from it. The position of X_1X_1 is quite arbitrary, but is preferably taken just outside the blade section. The drawing of the blade is now

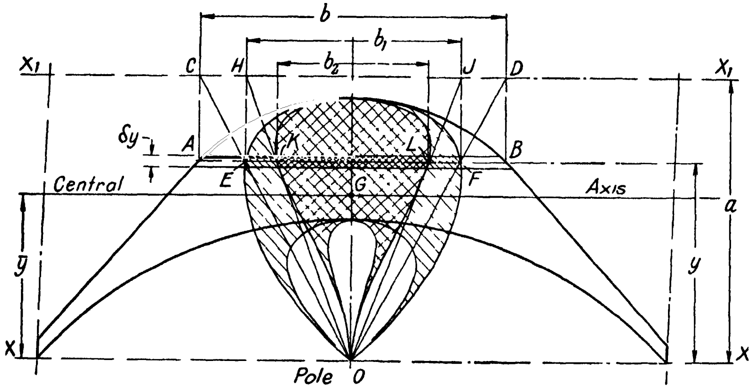


FIG. 261.—Graphical Determination of Position of Centroid and I_X

covered by a sheet of tracing paper and a number of lines such as AB are drawn parallel to XX. Perpendiculars AC and BD are drawn and OC and OD joined, intersecting AB in E and F. The locus of points such as E and F is termed the "first derived figure."

Let A $=$ area of blade section.

$A_1 =$ area of first derived figure, shown by hatching.

Then $$A_1 = \Sigma b_1 \,.\, \delta y, \text{ and since } b_1 = \frac{y}{a} \,.\, b$$

$$A_1 = \frac{1}{a}\Sigma b \,.\, \delta y \,.\, y = \frac{A \,.\, \bar{y}}{a}$$

where $\bar{y}$ is the distance of the centroid G above XX.

Hence $$\bar{y} = \frac{a \,.\, A_1}{A}$$

The second moment of area I_x about the axis XX may be found by an extension of the same method. Perpendiculars EH and FJ are drawn and OH and OJ are joined, intersecting AB in K and L.

The locus of points such as K and L is then drawn. This is termed the "second derived figure." Let A_2 be its area.

Then $$A_2 = \Sigma b_2 \,.\, \delta y$$

But $$b_2 = \frac{y}{a} \,.\, b_1 = \frac{y^2}{a^2} \,.\, b$$

$$\therefore \quad A_2 = \frac{1}{a^2} \Sigma b \,.\, \delta y \,.\, y^2 = \frac{I_X}{a^2}$$

$$\therefore \quad I_X = a^2 \,.\, A_2$$

The second moment of area about the central axis, viz. I_{CG}, may then be found by the well-known theorem—

$$I_{CG} = I_X - A \,.\, \bar{y}^2$$

This result is, however, likely to be considerably in error, because the value of $A\bar{y}^2$ is commensurate with that of I_X, and a small error in the value of I_X leads to a large error in I_{CG}.

The value of I_{CG} may be found with sufficient accuracy by drawing the first and second derived figures with reference to the central

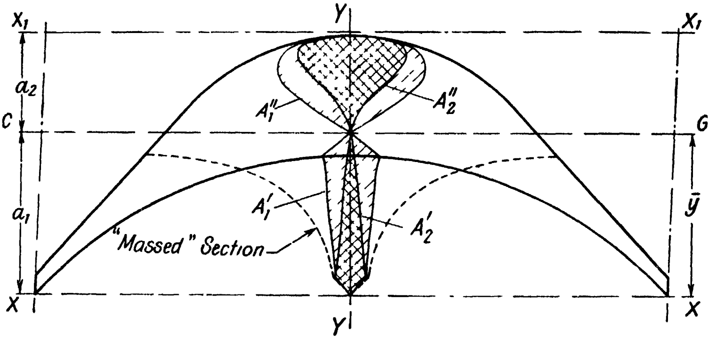


FIG. 262.—Graphical Determination of I_{CG}

axis after this has been determined. The method is illustrated by Fig. 262. Two lines XX and X_1X_1 are drawn parallel to CG at distances a_1 and a_2 from it. The original straight line XX may be conveniently used. In order to obtain a more manageable diagram, the lower part of the section is "massed" about the axis YY as shown by the dotted lines. The first and second derived figures are drawn by the method described above. Let A_2' and A_2'' be the areas of these latter.

Then $$I_{CG} = A_2' \,.\, a_1^2 + A_2'' \,.\, a_2^2$$

Where required, the second moment of area about the principal axis YY, Fig. 263, may be found by the same method. The section

is preferably massed about a line X_1X_1. In general, the component M_y of the bending moment (see Fig. 260) is so small that the stress due to it may be neglected.

When the impulse blade has no axis of symmetry, the principal axes must be found by the method given in the next article.

175. **Bending Stresses in Reaction Blades.** Owing to the fact that there is a drop in steam pressure in the channels of the rotating blades of a reaction steam turbine, there is an axial thrust on the blades due to steam pressure, in addition to the dynamic thrust due

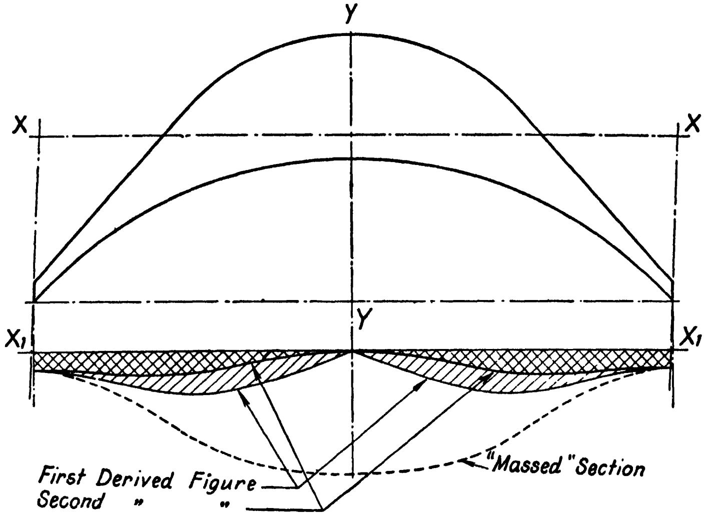


FIG. 263.—Graphical Determination of I_Y

to change of momentum. With the usual half-degree reaction, the pressure drop across the moving blades is practically equal to that across the stationary blades in any given pair. Consequently, in a group or "expansion" comprising s pairs of blades or stages, if p_1 and p_2 are the steam pressures at inlet to and outlet from the group, the pressure drop across any ring of blades is given, approximately, by the relation

$$\Delta p = \frac{p_1 - p_2}{2s} \quad . \quad . \quad . \quad . \quad (195)$$

Let n = number of blades in one ring.

θ = angle subtended by one blade (Fig. 264).

$$\theta = \frac{2\pi}{n} \text{ radian.}$$

Then area of shaded element $= r \cdot \theta \cdot \delta r$.

Axial force on shaded element $= \Delta p \,.\, r \,.\, \theta \,.\, \delta r$.

Moment of axial force about blade root

$$= \Delta p \,.\, r \,.\, \theta \,.\, \delta r(r - r_1)$$
$$= \Delta p \,.\, \theta(r^2 - r_1 r) \,.\, \delta r$$

$\therefore$ Total moment due to static pressure—

$$M_s = \theta \,.\, \Delta p \int_{r_1}^{r_2} (r^2 - r_1 r) \,.\, dr$$
$$= \theta \,.\, \Delta p \left\{\left(\frac{r_2^3 - r_1^3}{3}\right) - \frac{r_1}{2}\left(r_2^2 - r_1^2\right)\right\}$$
$$= \frac{\theta \,.\, \Delta p \,.\, l^2}{6}(2r_2 + r_1)$$

or

$$M_s = \frac{\pi \,.\, \Delta p \,.\, l^2}{3n}(2r_2 + r_1) \quad . \quad . \quad . \quad (196)$$

Note. If the dimensions are in inches and Δp is in lb. per sq. in., M_s will be a moment in lb.-in. units.

The bending moment M_d due to dynamic forces is found by the

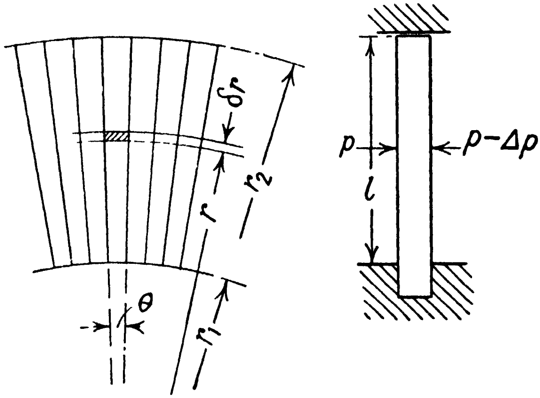


Fig. 264

method given in Art. 173 for impulse blades. The plane of this moment is nearly transverse to the turbine axis.

The moments M_s and M_d are now combined by the vector diagram, Fig. 265, to give the resultant moment M, the plane of which is perpendicular to the moment vector. It is possible that the plane of M might not pass through the centroid, in which case there will be, in addition to the bending action, a torque on the blade. It will, however, be assumed that such torque, if any, is negligibly small. Let UU and VV be the principal axes of the section. Then

M may be resolved into the components $M_u = M \cdot \cos\phi$ and $M_v = M \cdot \sin\phi$. The tensile stresses at A and B, due to bending only, are then—

$$f_b \text{ at A} = \frac{M_u \cdot u_A}{I_V} + \frac{M_v \cdot v_A}{I_U}$$

$$f_b \text{ at B} = \frac{M_u \cdot u_B}{I_V} - \frac{M_v \cdot v_B}{I_U}$$

The resultant stress is obtained by adding the centrifugal stress f_c to the bending stress f_b.

The reaction blade section has no axis of symmetry; consequently, the principal axes of the section must be found by one or

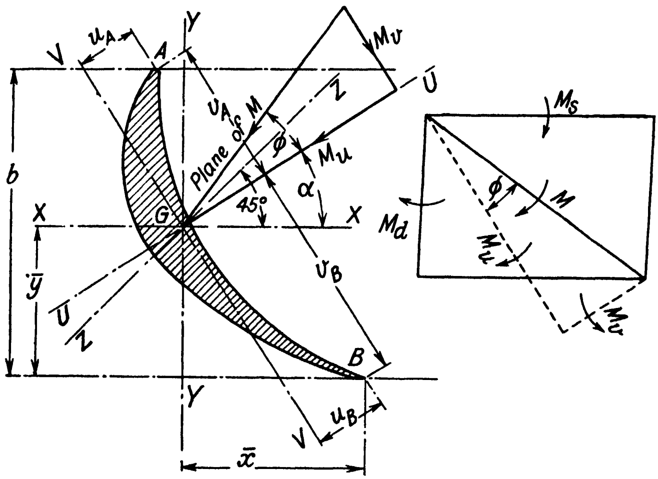


FIG. 265 —Bending Moments on a Reaction Blade

other of the methods available. As graphical integration is most easily effected the following is probably the simplest method. The centroid G is first found by the method given in Art. 174. The axes XX, YY, and ZZ are then drawn through G, XX and YY being at right angles to each other and ZZ making an angle of 45° with XX. Then if UU and VV are the principal axes of the section, UU makes an angle α with XX, such that—

$$\text{Tan } 2\alpha = \frac{2I_Z - (I_X + I_Y)}{I_X - I_Y}$$

Also $$I_U = \tfrac{1}{2}\{(I_X + I_Y) + (I_X - I_Y) \sec 2\alpha\}$$

and $$I_V = \tfrac{1}{2}\{(I_X + I_Y) - (I_X - I_Y) \sec 2\alpha\}$$

A reaction blade having the proportions given in Fig. 127, and having a width b, Fig. 265, has the following properties—

$$\bar{x} = 0{\cdot}605b;\ \bar{y} = 0{\cdot}493b;\ \alpha = 32^\circ 37';$$
$$I_U = 0{\cdot}00965b^4; \qquad I_V = 0{\cdot}00059b^4;$$
$$u_A = 0{\cdot}19b; \qquad v_A = 0{\cdot}48b;$$
$$u_B = 0{\cdot}24b; \qquad v_B = 0{\cdot}74b.$$

176. Special Form of Long Blades. It has been shown in Chapter IX that in long blades the steam pressure in the clearance space between the nozzles and blading increases as the radius increases

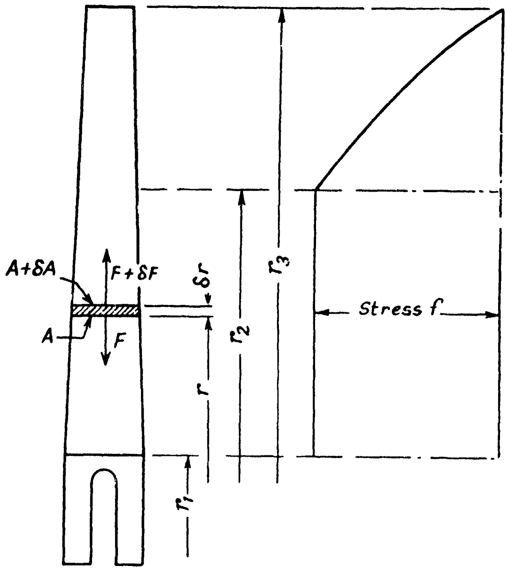


FIG. 266 Turbine Blade of Variable Cross-section

and that, if the steam flow is to take place at a constant distance from the axis of the turbine, then the degree of reaction must vary along the length of the blade, being a minimum at the inner radius and a maximum at the outer radius. This is fortunate because, as shown in Chapter IX, it leads to a blade of variable cross-section with very thin aerofoil sections at and near the blade tip and relatively heavy sections near the blade root.

Therefore, where the peripheral speed of the blade is greatest the mass per unit length of blade is the minimum, and, where the resultant centrifugal force is greatest, the blade section is the maximum. This tends to a more uniform blade stress than would be obtained in a blade of constant cross-section. In order to obtain an

even more uniform centrifugal stress, the blade is often tapered in width.

The cross-sectional area of tapered blades may be varied in such a way that the centrifugal stress is uniform over the greater part of the blade length. Using the same symbols as in Art. 172, let A be the cross-sectional area of the blade at radius r, and $A + \delta A$ the cross-sectional area at radius $r + \delta r$. Suppose that f is the uniform centrifugal stress.

The inertia force on the element is

$$\delta F = -\frac{w \,.\, A \,.\, \omega^2 \,.\, r \,.\, \delta r}{g}$$

Then since $F = fA$, and $F + \delta F = f(A + \delta A)$

$$\delta F = f \,.\, \delta A$$

$$\therefore \qquad \delta A = -\frac{w \,.\, A \,.\, \omega^2 \,.\, r}{gf} \,.\, \delta r$$

or

$$\frac{\delta A}{A} = -\frac{w \,.\, \omega^2 r}{gf} \,.\, \delta r$$

$$\therefore \qquad \int_{A_2}^{A_1} \frac{1}{A} \,.\, dA = \frac{w \,.\, \omega^2}{gf} \int_{r_1}^{r_2} r \,.\, dr$$

$$\log_e \frac{A_1}{A_2} = \frac{w\omega^2}{2gf}(r_2^2 - r_1^2)$$

i.e.

$$\log_{10} \frac{A_1}{A_2} = \frac{0{\cdot}4343 \,.\, w \,.\, \omega^2}{2gf}(r_2^2 - r_1^2) \quad . \quad . \quad (197)$$

In using this formula, one must adopt consistent units; e.g. if r_1 and r_2 are expressed in inches, then $g = 32{\cdot}2 \times 12$, w for steel $= 0{\cdot}288$ lb. per cub. in., and the stress f would be in lb. per sq. in.

The variation of stress in a blade of this kind may be as shown in Fig. 266. The outer part of the blade from radius r_2 to r_3 may be of slightly varying section in which the stress rises from zero at the tip (assuming no shrouding) to the value f at radius r_2. Between r_1 and r_2 the section is varied in such a way that f is approximately constant.

The centroids of the various cross-sections should, as far as possible, lie on a radial line so as to eliminate bending due to inertia forces. By setting the line of centroids a little forward of the radial line, the bending moment due to centrifugal force may be utilized partially to counteract the moment due to impulse. Blades of this type are usually milled in a multiple-spindle hydraulically-controlled milling machine which copies the form from a master blade.

177. General Notes on the Attachment of Turbine Blades. There is probably no detail in the construction of a steam turbine which affects the reliability of the machine more than the attachment of the blades to the rotor. The forces brought to bear on the attachment are relatively large, especially at the low-pressure end of turbines of large output. In turbines running at 3,000 r.p.m., the ratio of the centrifugal force to weight is 255*r*, where *r* is the radius

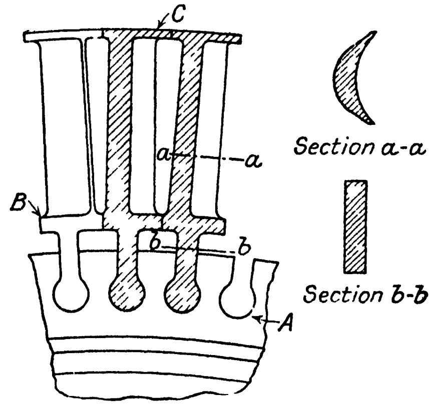


FIG. 267

in inches. Thus if the peripheral velocity is, say, 700 ft. per second, the radius is 26·75 in., and the centrifugal force on the blade is no less than 6,820 times its weight.

It is often difficult and occasionally impossible to estimate the stresses in the attachment. Approximate calculations are possible in many cases, but there is always the possibility of stress concentrations at sharp corners. In this connection, the use of a blade material having a definite yield point would seem to offer some safeguard. For these reasons the calculated stresses should be kept reasonably low.

The form of the attachment has sometimes an influence on the shape of the wheel rim and a particular design of root may involve a fairly heavy rim, thus adding to the stresses in the disc (or, alternatively, requiring a heavier disc) and possibly increasing the length of the turbine. As a general principle, the form of the attachment should be such that the centrifugal force on the blade is transmitted to the disc in the simplest and most direct manner. Furthermore, the design of the attachment should preferably be such that the security of the attachment is, so far as possible, independent of the skill of the mechanic.

178. De Laval Blade Attachment. This is illustrated in Fig. 267. A number of holes A are drilled in the rim of the wheel parallel to the axis. The slot for the blade tang is then finished by milling. The

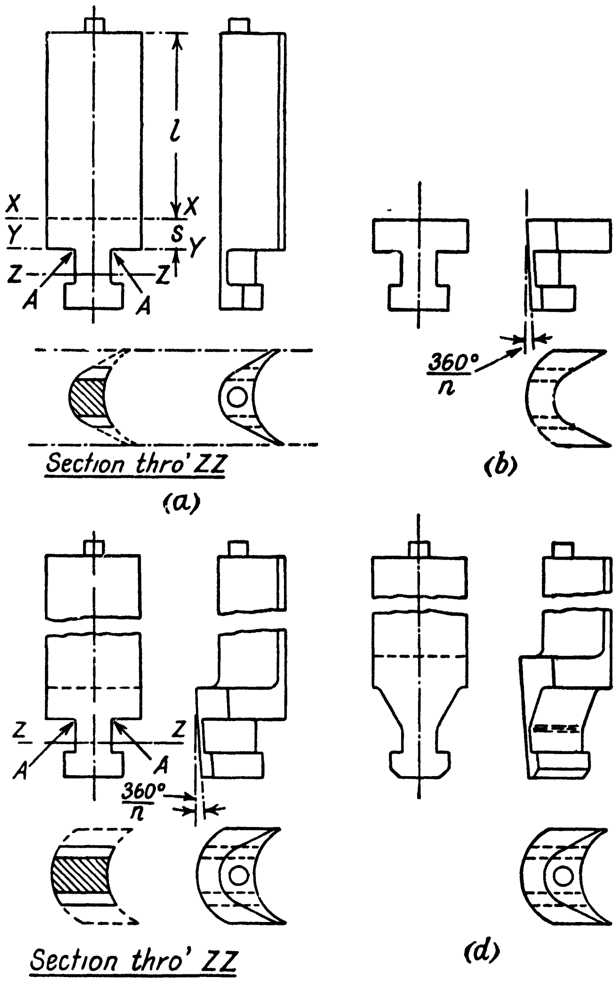
transition from the working section of the blade (section *a–a*) to the rectangular tang (section *b–b*) is obtained by the rectangular parts B, which form a continuous ring when all the blades have been inserted in the wheel. The tips of the blades are provided with integral shroudings C, which are carefully fitted so that these also form a continuous ring. The centroid of the blade section is arranged in the same radial line as that of the blade tang, so that the latter is practically free from bending stresses. The bending moment due to impulse is almost negligible. Light caulking of the wheel rim is sufficient to hold the blades in place.

179. Inverted-T Attachment. Various forms of this are shown in Fig. 268. (*a*) shows a blade with a separate spacer. This type of construction enables the blades to be cut from bars or strip of blade section formed either by rolling, drawing through dies, or by machining. The amount of machining necessary to finish the blade is small and the construction is relatively inexpensive. The spacers are shown in Fig. 268 (*b*). They are likewise cut from section bar and finished by milling. The leading edge of the spacer is given a taper, as shown, so that the blades will be set radial. The spacer stands proud of the rotor by a distance *s*. This facilitates the diaphragm construction and removes the section XX where the bending stresses are a maximum from the section YY where there is apt to be a concentration of stress at the points A.

The centroid of the section ZZ does not lie in the same radial line as the centroid of the blade section. Consequently the section is subjected to bending as well as direct tension. When the stress across section ZZ becomes excessive the blade and spacer are made from one piece, as shown in Fig. 268 (*c*). Such blades must be machined from bar of rolled "rhubarb" section, and are more costly to produce than the blades with separate spacers. In order to avoid the concentration of stress which is bound to occur at the points A, Fig. 268 (*a*) and (*c*), the blade tang is frequently tapered, as shown in Fig. 268 (*d*). The construction adds to the depth of the root, increases the cost of machining both blade and rotor, and also necessitates a somewhat heavier rim.

In long blades at moderate peripheral speeds, or blades of moderate length at high peripheral speeds, the resultant stress in the tang due to bending and direct tension is sometimes excessive when the root is constructed as shown in Fig. 268 (*c*). The bending stress may be practically eliminated by adopting the construction shown in Fig. 269. The root section is displaced circumferentially so that the resultant moment about the centroid G of the tang section due to the centrifugal force on the blade and on the part of the root above the tang is zero. Both the concave and convex parts of the root may be tapered with respect to the centre-line of the blade drawn radially through the centroid.

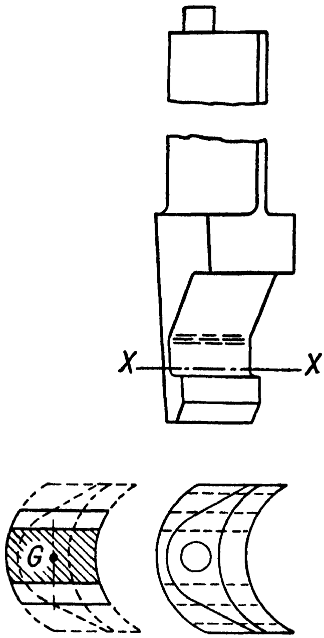
180. Stresses in Wheel Rims. The type of wheel rim commonly



l
X
X
Y
S
Y
Z
Z
A
A
Section thro' ZZ
(a)
360°/n
(b)
Z
Z
A
A
360°/n
Section thro' ZZ
(c)
(d)

FIG. 268

used with the inverted-T form of blade fastening is shown in Fig. 270 (*a*). The width of the wheel rim is an important dimension as it affects the stresses in the disc proper and, in certain cases, the



Section thro' XX

FIG 269

overall length of the turbine. It depends on the dimension d, which may be found approximately in the following manner.

Consider the section A–B on one side of the wheel rim and corresponding to one blade. This section has a circumferential width b and an axial depth d. Let G be the centroid of the section and F the total radial force on the shrouding, blade, and blade root. This force is transmitted to the rim as two equal forces $\frac{F}{2}$. By applying equal and opposite forces $\frac{F}{2}$ at the centroid G it is seen that across the section AB there are—

(1) A force $\frac{F}{2}$ producing a uniform tensile stress equal to $\frac{F}{2bd}$.

(2) A bending moment $\frac{Fa}{2}$ producing at B a tensile stress equal to $\frac{3Fa}{bd^2}$.

The resultant tensile stress at B is therefore

$$f = \frac{F}{2bd} + \frac{3Fa}{bd^2} \quad . \quad . \quad . \quad . \quad (198)$$

from which the value of d to limit the stress f to any given value may be found.

A little consideration will show that eq. 198 for the stress must err on the high side, because the strain which would accompany the

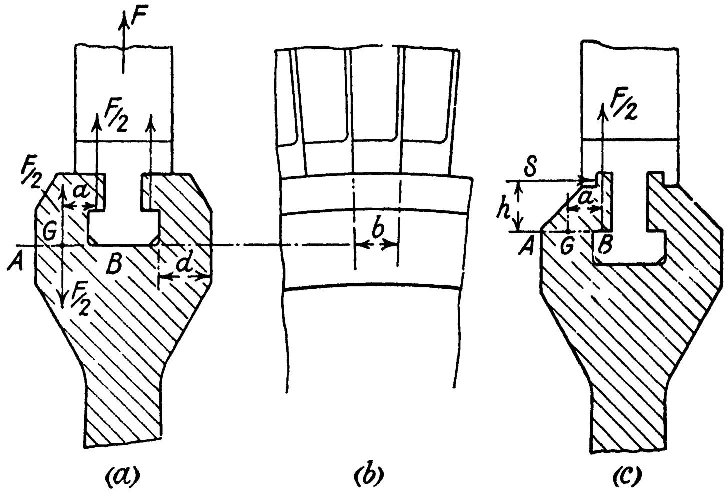


Fig. 270

bending would cause the jaws to open out slightly. But if the jaws were to open out, the circumference of the outer parts of the rim would increase and this would induce hoop stresses in the rim (over and above the usual hoop stress) which would definitely restrict the amount of bending possible.

When the width of the rim becomes excessive, the form of attachment known as the "side-grip" and shown in Fig. 270 (c) may be used. It will be clear that the tendency for the rim to open under the action of the forces $\frac{F}{2}$ will be opposed by a shearing force S across each of the snugs on the blade spacer. As a result, the bending moment across AB is reduced to some value

$$M = \frac{Fa}{2} - Sh$$

181. Serrated Blade Root. Fig. 271 shows a form of attachment suitable for fairly large centrifugal forces. The blade and spacer must be made in one piece. Serrations are machined on both sides of the root and also in the blade groove. The depth of the serrations is about $\frac{3}{32}$ times the width of the groove and the angle 45° to groove.

182. Fitting of Blades in Wheel. In all the foregoing types of fastening—with the exception of the de Laval—it is necessary to

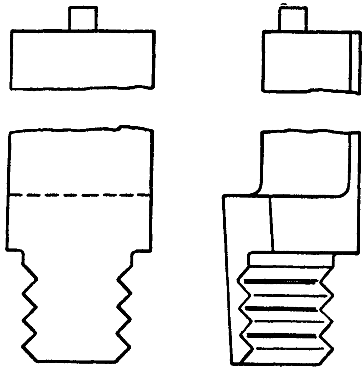
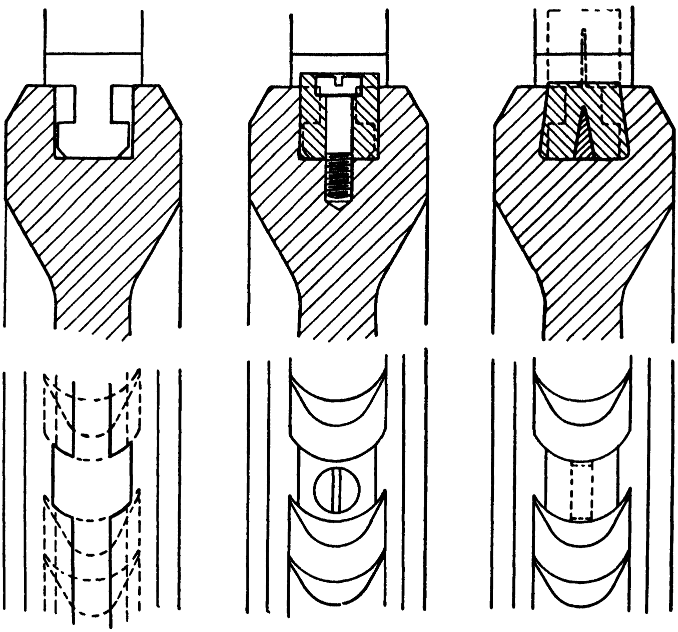


FIG. 271



(a) (b) (c)

FIG. 272

cut an opening in the wheel rim for the insertion of the blades, as shown in Figs. 272 (*a*) and 273. The blades are then inserted and driven round into place. The blades are driven hard up against a

stop inserted and wedged in the blade groove. When the blade ring is almost completed the stop is removed and a blade or two fitted in its place. The last one or two blades are carefully fitted to occupy the whole of the space except the opening. This is then filled.

Two of the several methods of filling the gap are shown in the figure. Fig. 272 (*b*) shows a filling-up piece secured by a countersunk cheese-headed screw which is prevented from slacking back

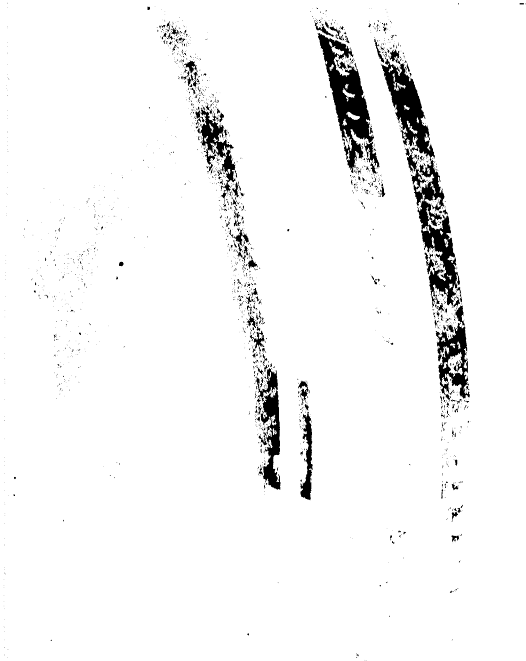


FIG 273

by bruising the head of the screw or caulking the filling-up piece. The hole for the screw weakens the rim as it breaks the continuity in the circumferential direction. In Fig. 272 (*c*) the gap is cut with a taper. A filling-up piece of soft brass, copper, or mild steel is cut to the shape shown by the dotted lines and nicked on the under side. This is then driven on to the steel wedge, which forces the filling-up piece to fill the gap completely. When either of these or similar methods is used there is, of course, a blade missing at the gap. By rather more elaborate devices it is possible to insert a special blade at the gap and so preserve a complete ring of blades.

183. Blade Attachment for High-pressure Curtis Wheel. An interesting form of construction employed on a 36,000 kW turbine built by Messrs. Brown Boveri & Co., Ltd., is described in a report of a test by Professor E. Josse (1), and illustrated in Fig. 274. The turbine operates with steam at 1,700 lb. per sq. in. and 900° F. The rotor blades on the Curtis wheel are milled out of one piece

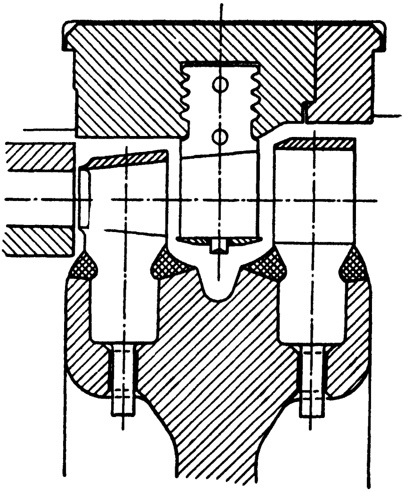


FIG. 274

along with the spacing and shrouding element, and have a very heavy profile. They are riveted into the disc and are welded together in pairs at the shrouding and are also welded to the rim of the wheel as shown. The advantages of the construction are: (1) The whole construction is very rigid; (2) it is not necessary to have a gap in the rim for the insertion of the blades; (3) the blade and wheel reach the same temperature quickly; and (4) there is no risk of the blades becoming loose in the wheel.

184. Straddle Attachment. Two forms of straddle attachment are shown in Fig. 275. For moderate speeds and short blades the type shown in Fig. 275 (*a*) is employed. The blade and spacer must be machined from one piece of metal. The blade is forked and fits tightly on to a projecting tongue on the wheel. The rivets are staggered, approximately one-half of each rivet being embedded in the blade, the effective attachment being one rivet in double shear. The rivets are slightly countersunk. When the shear stress in the rivets is excessive, as with higher speeds or longer blades, the attachment shown in Fig. 275 (*b*) is used, the rivets then being in quadruple shear. The straddle attachment enables a complete ring of blades to be employed as there is no necessity to cut any gap for

the insertion of the blades. Moreover, if the necessity should arise, one or more blades may be removed from the wheel without disturbing the remaining blades.

185. Modified Straddle Attachment. An attachment which is used in the last two or three stages of turbines of large output is shown in Fig. 276. It is really an inversion of that shown in Fig.

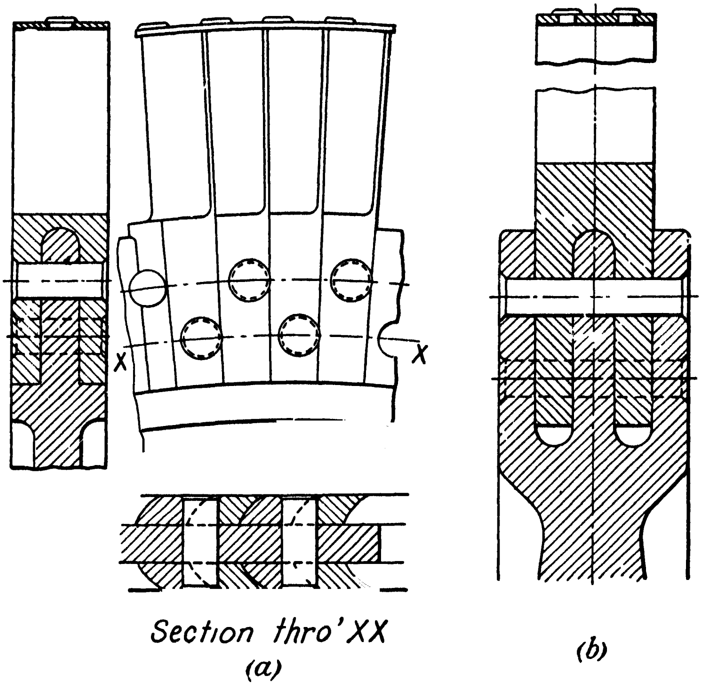


FIG. 275.—Straddle Blade Attachments

270 (*c*). The periphery of the wheel is provided with a T-shaped section. The blade root is widened, as shown, and provided with two small snugs which prevent the fork from opening out. A shearing force S will be induced in each prong and the resultant moment across the section XX will be

$$M = \frac{Fa}{2} - S . h$$

It is necessary to cut slots, shown by the dotted lines, in the T-head for the insertion of the blades, a blade being omitted at the slot. Suitable spacers, fitting tightly between the blades on either side of the slot, are fastened to the rim. By cutting two such slots at

diametrically opposite points of the wheel the balance of the wheel is not affected.

186. Side Entry Blades. These have been employed for very high peripheral speeds. The general features of the attachment are shown in Fig. 277. The rotor carries a comparatively heavy rim in which closely-spaced slots are cut, one to each blade. The slots

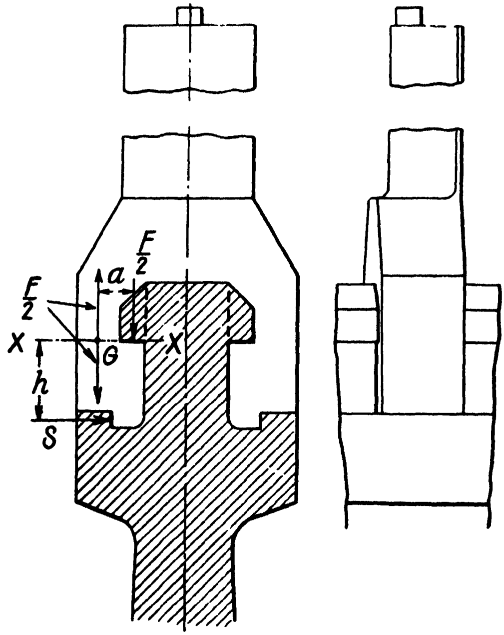


FIG. 276.—Modified Straddle Attachment

may be either parallel or skew to the axis, depending on the shape of the blade root profile. The design sometimes incorporates a principle which may be termed the principle of diminishing cross-sections. Considering the blade only, the area of the material under tension is made a maximum at section 1, where the tension in the root is the maximum. Part of the pull is taken by the outermost teeth, so that a smaller area may be employed at section 2. The teeth in line 2–2 take a further share of the pull so that the area across 3–3 may be still further reduced. On the same principle, the areas of the rim sections diminish from section 3–3 outwards. The blade root is lightly caulked to prevent it moving axially. The advantages of this form of attachment are: (1) The width of the wheel rim may be made greater than the width of the blade, so reducing the maximum stress in the fastening; (2) the bending across section 1–1 may be more or less eliminated by a suitable

positioning of the blade section with respect to section 1–1; (3) a complete ring of blades is obtained; and (4) the renewal of any blade is a relatively simple matter. The construction calls for excellent workmanship and is obviously expensive.

187. Attachment of Shrouding Strip. As the shrouding strip is attached to the blades at the extreme radius, the radial acceleration

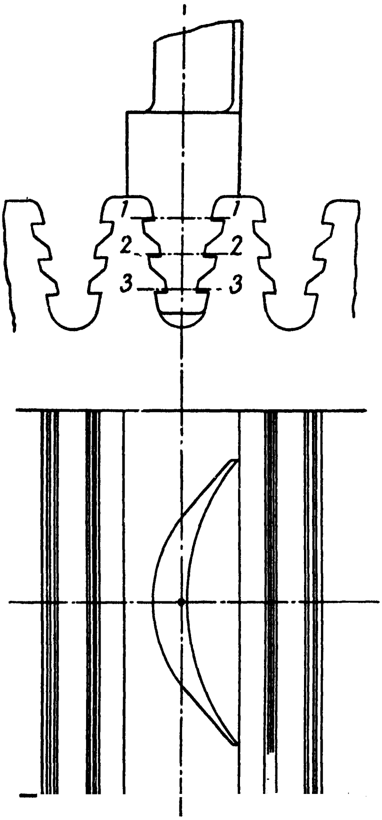


FIG 277 —Side Entry Attachment

is the maximum. Consequently, the centrifugal force is often very large and the thickness of the shrouding strip must be chosen with reference to the bending stress, the shrouding being in the condition of a continuous beam on several supports and carrying a uniformly distributed load. Typical attachments are shown in Fig. 278; (*a*) shows a round pin machined on the end of the blade, the centre being as near to the centroid as possible. In Fig. 278 (*b*) the "pip"

for the shrouding is usually formed by milling. Two types are shown. The holes in the shrouding strip are carefully punched at the correct distance apart. In the long tapered and twisted blades described in Art. 176, the outermost section of the blade is often so thin that the attachment of the shrouding is a matter of some difficulty. It

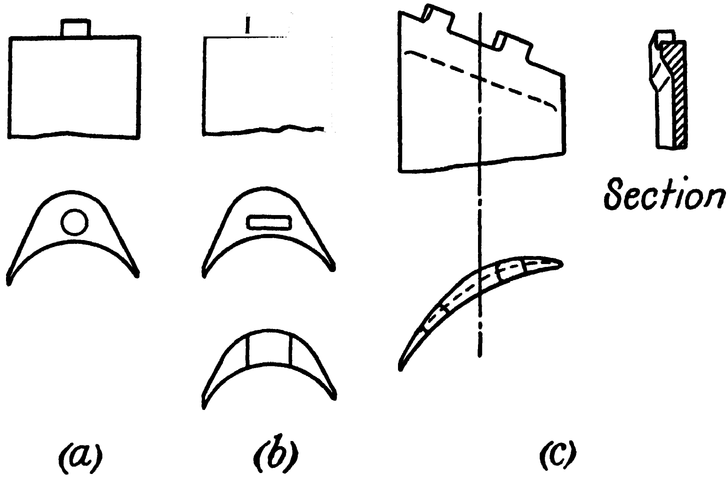


FIG 278

is necessary to use two projections and to thicken up the blade end, as shown in Fig. 278 (*c*). The section is then gradually varied so as to avoid stress concentration.

188. Attachment of Parsons Reaction Turbine Blades. The Parsons turbine has passed through an orderly evolution since its invention in 1884, and many forms of blade fastening have been used. During the period of moderate steam pressures and temperatures, the blades were usually made of drawn brass, the spacers being made of soft brass. The blades were drawn through dies of standard section and fitted into grooves of standard width.

These blades had no shrouding and a certain clearance had to be allowed between the tips of the running blades and the inside of the cylinder, and between the inside of the fixed blades and the surface of the rotor. In order to minimize the rubbing pressure and the heat generated in the event of accidental contact of the blades with the cylinder or rotor, the blade tips were thinned down.

The material used for all blading at the present time is stainless iron containing 12 to 14 per cent chromium and not more than 0·12 per cent carbon.

Unshrouded blading as described above is still used in low-pressure stages where the stress conditions permit.

189. Parsons End-tightened Blading. In the year 1912, Messrs. C. A. Parsons & Co., Ltd., introduced the so-called "end-tightened" blading, in which the clearance which governs the leakage past the blades is axial instead of radial. This form of blade is now used in all the high-pressure and intermediate-pressure stages, the thin-tipped radial-clearance blades being employed only in the low-pressure stages. The earlier form of end-tightened blading is shown in Fig. 279. Short sections of blading A are first silver-soldered at the root to the deep spacers B, after which a strip of

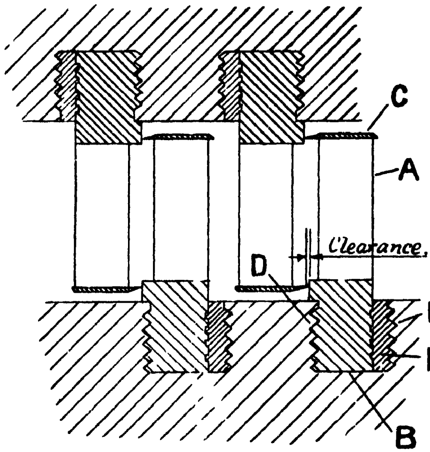


FIG 279. Details of Parsons "End-tightened" Blading

shrouding is silver-soldered to the blade tips, both operations being carried out with the blade segment assembled in a former. Serrations are then milled on one side of the roots and shallow grooves on the other, the blade segment being clamped to a radius bar during the milling operation. The rotor groove is serrated at D for the blade roots and at E for the packing pieces F. The packing pieces are inserted at the end of a blade segment and driven into position in the circumferential direction.

The shrouding strips are thinned down to a fine edge so as to reduce the rubbing surface as much as possible. It is impossible to machine the shrouding so that the axial clearance will be the same in all rows of blades. This is achieved, however, by bringing the turbine as near to its working temperature as possible and allowing the rotor to turn at a low speed. The rotor is then very gradually moved towards the steam end. In this way the proud shrouding strips are gradually worn down. When all the strips are in simultaneous contact, the rotor is moved back until there is a suitable clearance, say from 0·008 to 0·015 in., between the shrouding and the blade roots. A liner of the necessary thickness is then

fitted on the steam-end side of the Michell adjusting block so that the clearance can never be less than the prescribed amount. Another liner is fitted on the exhaust-end side of the adjusting block, a clearance of about $\frac{1}{32}$ in. being left between the block and the liner. By means of a hand-operated gear the adjusting block may be moved towards the exhaust end of the turbine a distance equal to this clearance. In this way the running clearance between the

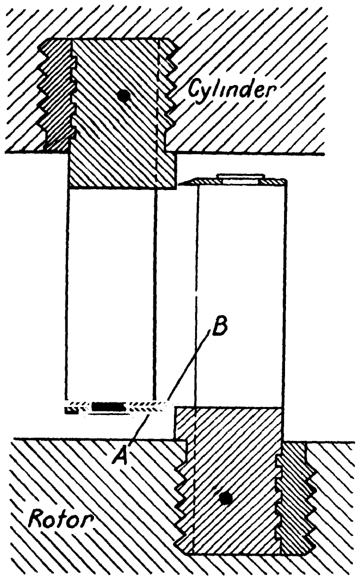


FIG 280.—Improved "End-tightened" Blading

shrouding strip and blade roots may be increased during the time that the turbine is being warmed up. When the turbine has been running for some time and all parts have reached a steady temperature, the rotor is moved forward and the clearances thus reduced to the proper amount.

From a glance at Fig. 279 it will be apparent that the flow of steam through the clearance between the fixed shrouding strip and the rotor blades will disturb the main steam flow into the moving blades. This is avoided by the device shown in Fig. 280 and first introduced by Messrs. Parsons in 1930. In addition to the ordinary shrouding strip A, attached to the stationary blades, there is a second strip B which has a tapered edge serving to deflect the leakage steam and so minimize the disturbance produced. The blades are built up in short segments consisting of about twelve blades, blades and spacers being threaded alternately on a root

wire and assembled on a former The end-tightening shrouding strip is riveted on while the blades are in the former The whole is then slowly immersed by a cam into a brazing bath, after which the blade segment is dressed up and machined In still more recent designs the root wire has been dispensed with the blades and spacers being electrically welded together while still in the former, after which they are brazed

In more recent forms of this blading, radial packing is also provided by means of a fin on the shrouding, as shown in Fig 164

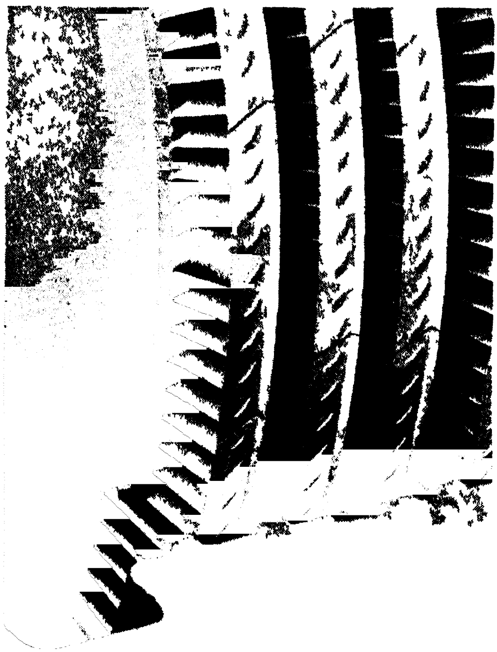


FIG. 281 —Shrouded Built up Reaction Blading

Fig 281 shows a photograph of such blading while Fig 282 shows the method of fixing segments of blading in the rotor grooves

In stages where the steam temperature is high blades with integral roots and shrouding are employed Axial seals and supplementary radial seals are provided as in the ordinary end-tightened blading For convenience in handling the blades are formed into short segments which are serrated along the root portion and secured in serrated grooves in the rotor by means of side locking strips

190. Parsons Integral Blades. In all the various attachments described above the inertia force on the blade must be transmitted through the spacers to the rotor, the bond between the blades and

spacers varying from the shearing strength of the root wire together with that of the spacer material embedded in shallow indentations to that provided by brazing and partial welding.

For long blades running at high speeds, the blade and spacer are made from one piece, as shown in Fig. 283, the root being lozenge-shaped. Such blades are rolled by a discontinuous process. Pieces



FIG 282 Method of Fixing Segments of Blading in Rotor Grooves

of rectangular bar of the correct size for the root portion are either pressed in a die or milled on the sides so as to form a T-shaped billet. The profile rolls have each a gap cut in the rim and the two rolls are so geared together that the gaps coincide and form a space which just takes the root portion of the billet. The billet is passed through the rolls a number of times until the stem is reduced to the finished blade size, the form of the root remaining unchanged. Blades manufactured in this way require no machining on the stem except cutting to length and tipping. The blade is pickled, polished, and the serrations machined on the root.

191. Blade Materials. The choice of materials for turbine blades is a somewhat difficult one and is guided by many considerations, among which are the following—

(1) *Conditions of Operation.* In the H.P. stages of certain turbines and in the I.P. stages of reheat turbines, where the temperature is high, it is essential to use a material which will be stable at high temperatures. In many cases the stresses are moderate, but if the stresses are at all appreciable then attention must be paid

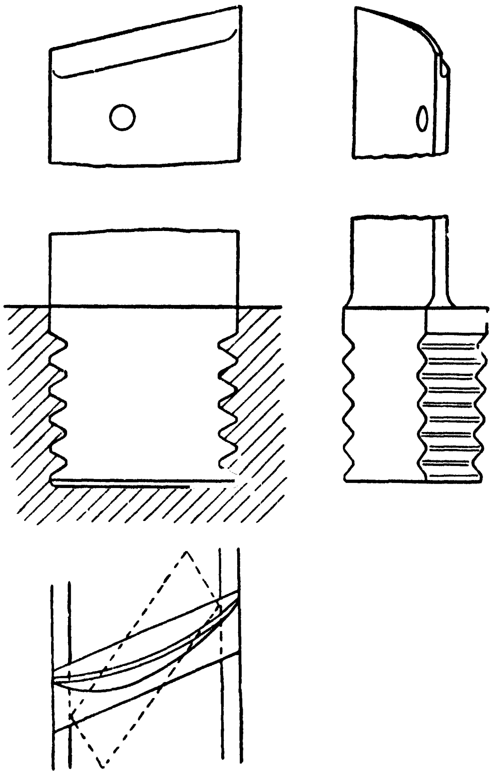


FIG 283.—Parsons Integral Blading

to the strength of the selected material at the operating temperature and, in particular, to its resistance to creep.

In the L.P. stages, where the steam is wet, and especially in the neighbourhood of the dew point, it is necessary to employ a material which resists corrosion well. In the L.P. stages of turbines of high output the stresses in the blades are very high and a material having a high tensile strength is essential. The blades in the L.P. stages should also be capable of resisting the erosive action of the water drops. Experiments have shown that this resistance is fairly well measured by the Brinell hardness number of the material. When

the peripheral velocity is very high it is not generally possible to obtain a material which, besides being hard enough, has other desirable mechanical properties such as toughness and ductility. In that case the necessary resistance to erosion is obtained by brazing special erosion shields to the blades. For further information on this side of the subject the reader is referred to the author's book, *Steam Turbine Operation.*

(2) *Methods of Manufacture.* The principal methods of manufacturing turbine blades are cold drawing, machining, drop forging, rolling, and combinations of these methods. Certain blades, such as plate and profile blades with separate spacers, and reaction blades, may be produced in strip form by cold drawing provided the material is suitable. Impulse blades with integral spacers are usually machined from bar. This is a comparatively expensive process. Drop forging is generally restricted to long blades of complicated shape, such as tapered and twisted blades. The required dies are expensive to make and costly to maintain. Rolling may be applied to impulse and reaction blades with separate spacers. The blades are passed many times through profile rolls which are gradually brought together. Smaller sections are rolled cold and frequently annealed to remove strain. The heavier blade sections are rolled hot, the strip being annealed, and pickled to remove scale. The final rolling is carried out cold between highly polished rolls which give the blade a bright and smooth surface. When brazing or hard soldering has to be done, as in the attachment of bracing wire, a material which becomes hot short at the brazing temperature should not be used.

(3) *Cost.* Certain materials have highly desirable properties, but are costly. Consequently their use is restricted to particular conditions where their properties are essential.

The following are among the better-known blading materials. The figures given for the composition are percentages.

Brass. The brass used for blading usually contains 70–72 copper and 28–30 zinc. The soft spacers are made of 63–37 alloy. Brass may be cold drawn, and it resists corrosion well. The strength falls away rapidly as the temperature is increased, and brass is unsuitable for temperatures higher than 400–450° F. It was formerly much used in reaction turbines, but is now no longer used in large turbines.

Phosphor Bronze is a copper-tin alloy to which a small amount of phosphorus is added during the melting, usually in the form of phosphor tin or phosphor copper. The phosphorus acts as a deoxidizer and its addition in small amounts improves the properties of the bronze. For a hard bronze the approximate composition is 86 copper and about 14 tin, with up to 1 phosphorus. For a softer and more ductile bronze, the composition may be 92 copper, about 8 tin, and traces of phosphorus. Phosphor bronze may be forged,

rolled, or cold drawn. It resists corrosion well and was formerly regarded as a satisfactory blading material. It is not suitable for high steam temperatures.

Manganese Copper. This is an alloy containing about 95–96 copper, 4–5 manganese, and small fractions of iron, carbon, and lead. It may be cold drawn and cold rolled. The strength falls off with increasing temperature, but not to the same extent as the copper-zinc or copper-tin alloys. It is suitable for blades under low stress up to steam temperatures of 600° F.

Nickel Brass is an alloy containing about 50 copper, 40 zinc, and 10 nickel. It may be cold drawn, giving a hard and smooth surface. The temperature limit is about 400–450° F.

Copper Nickel is an alloy containing about 80 copper, 19 nickel, and fractions of iron, manganese, etc. It may be cold rolled or drawn.

Monel Metal is produced from a Canadian ore without the separation of its chief constituent metals, nickel and copper. It contains about 67 nickel and 28 copper, together with iron, carbon, manganese, etc. Monel metal possesses very good resistance to the corrosive agents which may be present in impure steam and in addition, it retains a large proportion of its strength at high temperatures.

It is supplied by the manufacturers, Messrs. Henry Wiggin & Co., Ltd., for turbine blading in three forms: (1) As cold-rolled rectangular bar from which certain impulse sections are produced by machining; (2) in the form of cold-rolled profile strip which is now made in all the normal Parsons impulse and reaction sections, and also in the Brown Curtis impulse sections; and (3) as Monel integral root blades, somewhat similar to the Parsons integral root blades described in Art. 190. In the integral root form, the blade part is cold drawn to an accurate profile, while the root is left rough so that the turbine builder can machine it to give any wing angle desired. Monel blades have been widely used in marine work, especially in H.P. turbines.

Mild Steel is not now much used for turbines, although it has been used for the blading of certain notable turbines in the past. It is an inexpensive metal, but corrodes too easily in a damp atmosphere

Nickel Steel. Steels containing from 3 to 5 per cent nickel have been much used in steam turbines. The addition of nickel to steel increases the ultimate tensile strength and also increases the ratio of the yield point to the ultimate strength. Nickel steel is more resistant to corrosion than is mild steel. It may be forged and machined, but not welded. Steels containing 25 to 30 per cent nickel have also been tried in steam turbines, but with unsatisfactory results.

Stainless Steel is an alloy of iron, chromium, and carbon, containing 12–14 chromium and the normal percentages of carbon. Besides having valuable anti-corrosive properties, it is a very hard

material and offers a relatively great resistance to erosion. Stainless steel is air-hardening and may not be used for blades which have to be brazed during assembly. The most useful alloy of this type in turbine work is that known as *stainless iron.* This contains about 0·1 per cent of carbon. It is not an air-hardening alloy and does not, therefore, become brittle when heated. Stainless iron can be forged, rolled, easily machined, and also welded and brazed. It can be stamped and pressed and is often used for cast-in nozzle guide blades.

A.T.V. Steel. This is an alloy steel made by Messrs. Hadfield's, Ltd., of Sheffield, the brand Hecla/A.T.V. having been specially developed for steam turbine blades and nozzle guide vanes. The alloy was first developed in France about the year 1916, the letters A.T.V. being based on the words *Acier Turbines à Vapeur.* The composition of A.T.V.1 has been published (2) as: Nickel 36, chromium 12, carbon 0·25, and the rest iron. It is claimed for Hecla/A.T.V. steel that it is highly resistant to both corrosion and erosion, and that it maintains its strength well at high temperatures. It can be supplied in either the hard or soft condition according to requirements. The advantage of the harder steel is the higher ratio of yield point to ultimate stress. The mechanical properties given in Table XXIV are the minimum, test figures on samples always being higher. Hecla/A.T.V. work hardens fairly rapidly, and the shrouding pin at the blade tip should not be made larger than necessary to secure a reliable attachment.

The mechanical properties of blading materials are given in Table XXIV. The figures are not claimed to be more than a guide, as the strength of the selected materials depends so much on the actual composition and on the thermal and mechanical treatment to which the material has been subjected. The approximate working stresses at the normal speed of rotation are based on factors of safety of 3 on the yield point, 5 on the ultimate stress, and a mean value of 4 for the factors based on the yield point and the ultimate strength. The last value of the working stress is based on the suggestion of Mr. K. Baumann (3).

For notes on high-temperature blading materials see Appendix, page 837.

BIBLIOGRAPHY

1. JOSSE: Article in *Electrizitätswirtschaft,* 1935, No. 13. Extract published in *The Brown Boveri Review,* 1936; 23; 131.
2. VAN DUZER: "Pipes, Valves and Turbines for High-temperature Steam." *Metal Progress,* 1937; 31; 635.
3. BAUMANN: "Some Recent Developments in Large Steam Turbine Practice." *Journal I.E.E.,* 1921; 59; 565.

TABLE XXIV

Mechanical Properties of Turbine Blade Materials

Note. All stresses are in tons per sq in.
The following abbreviations are used: L P = Limit of Proportionality; Y.P. = Yield Point; U.S = Ultimate Stress; % El. = % Elongation, generally on 2 in.; % R.A. = % Reduction of Area; C D. = Cold Drawn, C R. = Cold Rolled; A. = Annealed; N = Normalized.

Material	Condition	L P.	Y.P.	U.S.	% El.	% R.A.	Working Stress at Normal Speed: $\frac{Y.P.}{3}$	Working Stress at Normal Speed: $\frac{U.S.}{5}$	Working Stress at Normal Speed: $\frac{Y.P. + U.S.}{8}$
Brass 63/37	C D	—	20·5	23·0	17	60	6·8	4·6	5·4
Phosphor Bronze		—	12·0	24·0	8	—	4·0	4·8	4·5
Manganese Copper	C D.	13·8	21·4	26·8	20	70	7·1	5·4	6·0
Nickel Brass		—	28·6	34·3	40	—	9·5	6·9	7·9
Copper Nickel	C R.	22·3	29·0	31·2	20	65	9·7	6·2	7·5
Monel Metal	C R. and A.	22·1	24·4	40·1	25	55	8·1	8·0	8·1
,, ,,	Profile blades C.R. or C.D., A., and finished with light C.R. or C D.	—	30·0	40·0	18	—	10·0	8·0	8·75
Mild Steel	0·13% Carbon	—	18·0	24·8	31	—	6·0	5·0	5·3
,, ,,	0·22% Carbon	—	22·8	28·7	26	—	7·6	5·7	6·4
,, ,,	0·33 C; 0·58 Mn; N.	19·5	23·5	38·2	28	61	7·8	7·6	7·7
Nickel Steel	3 Ni; 0·24 C; 0·55 Mn, N.	21·6	26·2	40·9	26	63	8·7	8·2	8·4
,, ,,	3·5 Ni; 0·32 C; 0·56 Mn	—	36·0	46·4	16	37	12·0	9·3	10·3
,, ,,	5·1 Ni; 0·2 C; 0·50 Mn	—	40·0	48·3	22	—	13·3	9·7	11·0
Stainless Iron	0·08 C	16·6	17·1	29·9	38	80	5·7	6·0	5·9
,, Steel	0·32 C	30·0	39·8	49·0	22	56	13·3	9·8	11·1
A.T.V. Steel	Hard condition	—	25·0	40·0	20	40	8·3	8·0	8·1
,, ,,	Soft condition	—	18·0	40·0	25	45	6·0	8·0	7·2

EXAMPLES XIX

1. The following particulars relate to a stage of an impulse turbine—

Mean diameter	40 in.
Nozzle height	7·4 in.
Blade height	7·9 in.
Nozzle angle	24 deg.
Number of nozzles (complete admission)	62
Thickness of nozzle guide vanes	0·104 in.
Steam velocity at nozzle outlet	1,310 ft. per sec.
Specific volume of steam at nozzle outlet	297·2 cub. ft. per lb.

Dividing the nozzle height into four equal parts, calculate the mass flow per second through each part.

2. Using the data given in Question 1 and assuming that the rotational speed is 3,000 r.p.m., divide the blade height into four equal parts and from the velocity diagrams calculate the change of velocity of the steam at the mid-height of each part. Assume $\beta_2 = 40°$, $k = 0{\cdot}85$, and that the number of blades on the wheel is 250. Hence calculate for each part the force on each blade and the bending moment about the root. Combine the bending moments graphically and find the resultant bending moment about the blade root section.

3. The impulse blade for the turbine in Questions 1 and 2 has the following proportions—

Inlet angle	44 deg.
Outlet angle	40 deg.
Blade width	1 in.
Thickness of inlet and outlet edges	0·02 in.
Radius of concave part of blade	0·673 in.
Radius of convex part of blade	0·345 in.

Draw the section of the blade enlarged to a suitable scale, and derive the following—

(*a*) Area of blade section.
(*b*) Distance of centroid from axis XX (Fig. 261).
(*c*) Value of I_Y (Fig. 260).
(*d*) Value of I_X (Fig. 260).

4. Using the notation of Fig. 260 for the turbine and blade of Questions 1, 2, and 3, find the bending moments M_x and M_y, and calculate the bending stresses at the point A. Calculate also the centrifugal stress at the innermost section of the blades, neglecting the shrouding, and hence find the maximum tensile stress in the blades. Assume that the blading material is steel.

5. The following are the particulars relating to a stage of a reaction turbine comprising one row of fixed blades and one row of moving blades—

Mean diameter of blades	72·875 in.
Height of blades	12·875 in.
Axial width of blades	1·5 in.
R.p.m.	1,800
Steam pressure before moving blades	6·0 lb. per sq. in. abs.
Steam pressure after moving blades	5·0 lb. per sq. in. abs.
Effective outlet angle of blades	20 deg.
Steam velocity at exit from guide blades	740 ft. per sec.
Steam velocity at exit from moving blades	860 ft. per sec.
Number of moving blades per row	254
Steam flow	76·1 lb. per sec.
Material of blades	Steel

Assuming that the blades have the section given in Fig. 127, and referring to Fig. 265, calculate or derive the following—

(*a*) Dynamic moment about blade root section.
(*b*) Static moment about blade root section.
(*c*) Moment component M_v.
(*d*) Moment component M_u.
(*e*) Centrifugal stress at blade root.
(*f*) Bending stress at A.
(*g*) Bending stress at B.
(*h*) Resultant stress at A.
(*i*) Resultant stress at B.

CHAPTER XX

CONSTRUCTION OF TURBINE ROTORS

192. De Laval Rotors. Two types of rotor are employed in the de Laval turbine, the type used depending on the peripheral speed which, in turn, depends chiefly on the power of the turbine.

In turbines up to about 100 h.p. the type of wheel shown in Fig. 284 is used. The hub of the wheel is bored out and a tapered steel bush is secured by a nut screwed in at one end. The enlarged end of the bush is provided with two flats which fit into a recess in the face of the hub. The spindle is provided with a short enlargement which fits tightly in the bush. A pin passing through the bush and the spindle serves to transmit the torque.

The profile of the disc is hyperbolic, and a light rim is added to carry the blades. In experiments—intentional and otherwise—in which wheels of the form used in the de Laval turbine have been run at high speeds to destruction, it has been found that the wheels break up into two or three segments, and that the centrifugal force on such parts is sufficient to do considerable damage, even after having smashed the turbine casing. To prevent any likelihood of such a disaster, a shallow groove, termed the "safety groove," is turned out at each side of the disc just under the rim. The wheel is now weakest at this section, the stresses there being some 50 per cent greater than at the most highly stressed point in the disc. Then if the turbine should be severely overspeeded, the rim parts company from the disc and usually breaks up into a number of relatively harmless fragments. In such an event the wheel will inevitably be thrown out of balance; dangerous bending of the spindle is then prevented by the casing, which is arranged to surround the hub with only a small clearance (Fig. 284).

It will be shown in Art. 208 of the next chapter that a rotating disc is very considerably weakened by drilling even a small hole at its centre. In de Laval turbines above about 100 h.p., with a mean blade velocity of about 1,130 ft. per sec., the type of disc shown in Fig. 285 is used. The disc is continuous through the centre and the thickness is so varied that the disc profile is that of the "disc of constant strength" described in Art. 213. In order to attach the lens-shaped disc to the shaft, a departure is made from the theoretical profile by providing bosses at the sides of the disc. The spindle is made in two parts, each provided with an enlarged end, recessed into the boss and secured by stud bolts.

193. Construction of Disc Rotors. A familiar form of construction employed in impulse turbines and frequently in the L.P. stages of reaction turbines comprises a number of separate discs

on a shaft. The latter may either be stepped or of uniform diameter, according to the method employed for attaching the discs.

The wheel consists of three parts: the rim which is designed to hold the blades, the hub which is attached to the shaft, and the disc proper which connects the rim and the hub. The wheel forging

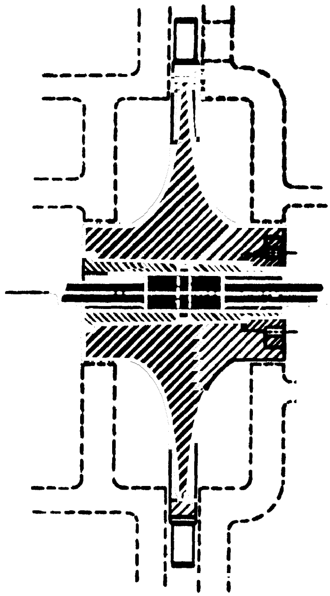


FIG. 284

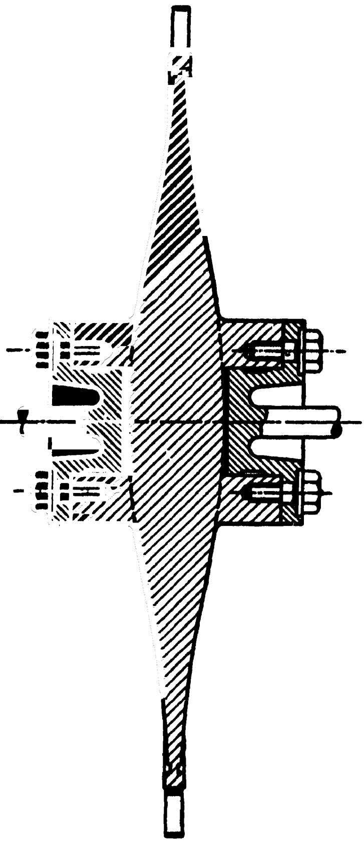


FIG 285

is prepared from a cheese of steel which is forged or pressed into disc form. The wheel is then rough machined and annealed to relieve it of internal stresses. It is afterwards carefully machined to give it the correct profile. The sides of the disc should be given a very smooth finish so as to avoid stress concentration. In the construction shown in Fig. 286, the wheels are pressed on to the shaft by means of a hydraulic press, the bore of the wheels being slightly smaller than the diameter of the shaft on which they are to be pressed.

This difference in diameter must be very carefully calculated and adhered to in the machining operations, so that even when the wheel is running at the overspeed (normally 10 per cent above normal speed) there will still be some mutual pressure between the wheel and the shaft. In starting a cold turbine, the discs will reach the

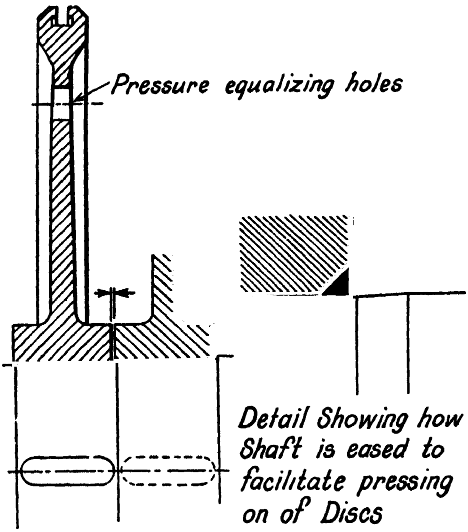


FIG. 286

working temperature sooner than the shaft. As a result, the discs expand slightly more than the shaft, and unless there is a sufficient force fit allowance they may become loose. The forcing on and removal of the discs are facilitated by heating the discs.

The torque is transmitted by sunk keys. When the torque is moderate, one key only is used for each wheel, the keys for adjacent wheels being arranged at 180° to each other. For greater torques, two keys are used. In very large units, six, and even eight, keys have been used for each wheel.

A small axial clearance is left between adjacent discs to allow for expansion due to temperature differences. The shaft is stepped so that each wheel may be easily passed over the shaft until it reaches its own seat. In order to prevent any appreciable difference of steam pressure being set up on the two sides of the disc, either at starting or during normal working (due to ejector action of the steam passing between the nozzles and blades), pressure-balancing holes are drilled in the discs. About six such holes are drilled in a part of the disc where the stresses are moderate. The edges of such holes should be well rounded off to prevent stress concentration as far as possible.

194. Mounting of Wheels on Shaft. The objections to forcing the wheels on the shaft are that the stresses in the wheel are increased due to the heavy force fit, and also that, in the event of necessity, the removal of the wheel is a matter of some difficulty. Various alternative methods have been devised and employed.

The method illustrated in Fig. 287 has been used by a number of turbine builders, chiefly on the Continent. The shaft is not stepped, and the wheel hubs are bored out slightly larger than the diameter of the shaft. Recesses are turned in each end of the wheel hubs for "supporting rings" A and B. Each ring is carefully machined to fit the shaft and the hub and is recessed to pass over

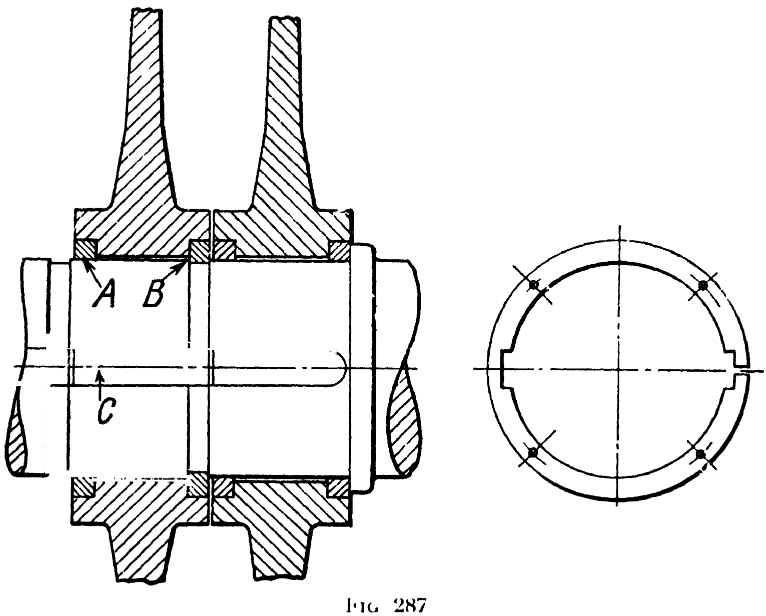


FIG. 287

the keys C. The rings are also split. A groove is turned in the spindle and the ring B is sprung into its groove just as a piston ring is. The rings B serve to locate the wheel axially. It is stated that when the wheels are rotating at their normal speed, the strains in the hub are such that the ends of the hub nip the supporting rings so that the discs are held quite tightly. Whether this is the case when the thickness of the disc at the hub approaches that of the hub itself would appear to be very doubtful. The torque is transmitted from the central part of the hub only. As there is a clearance between the shaft and the bore of the wheel and also an axial clearance between the wheels, shaft flexure does not tend to cause slackness.

A modification of the same principle is shown in Fig. 288. This method has been successfully used by Messrs. Brown Boveri & Co., Ltd. The wheels are bored out to an easy press fit on the shaft and are provided with a deep recess at each end. U-shaped chrome steel rings are forced into these recesses and are thus heavily compressed. This, while relieving the rotor of a considerable amount of stress which would be induced by the usual force fit, enables the wheel to expand slightly under stress and temperature without becoming loose or running out of centre.

The attachment shown in Fig. 289 consists of a split conical bush which is pressed into the conically-bored hub. In this way,

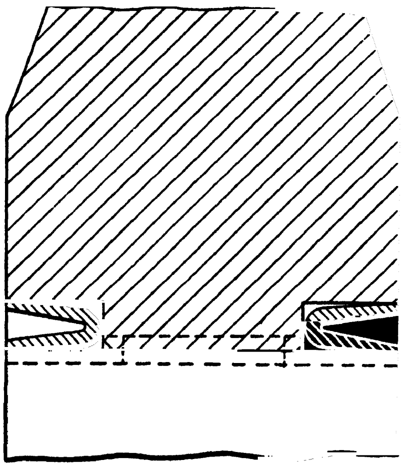


FIG. 288

the pressure between the hub and the shaft is under some control. A liner is fitted between the bush at the larger end and the adjacent disc. The bush is screwed internally at its larger end for the attachment of withdrawing gear. This mounting is used by the well-known firm of A.E.G.

Under high temperatures, steel and other alloys, when subjected to stress, undergo continually a very small but definite strain. This phenomenon is known as creep. Thus a turbine wheel rotating in high-temperature steam and thus subjected to radial and tangential stresses would gradually change in size, the diameter increasing at an extremely slow, but steady, rate. Such change of dimensions, due to creep, will obviously reduce the mutual pressure due to force fit, and the wheel will tend to become loose.

The construction shown in Fig. 290 (British Thomson-Houston Co., Ltd.) is designed to avoid this. A steel bush is pressed into the hub and a number of radial holes are drilled through the two.

Radial pins are inserted in the holes and the bush pressed on to the shaft, one or more keys serving to transmit the torque. It will be seen that even if the bore of the wheel should increase to such an extent that contact between the wheel and the lightly stressed bush should cease, the wheel will still remain concentric with the shaft.

195. **Rotors Machined from Solid Forgings.** The difficulties associated with the use of high-temperature steam and which are

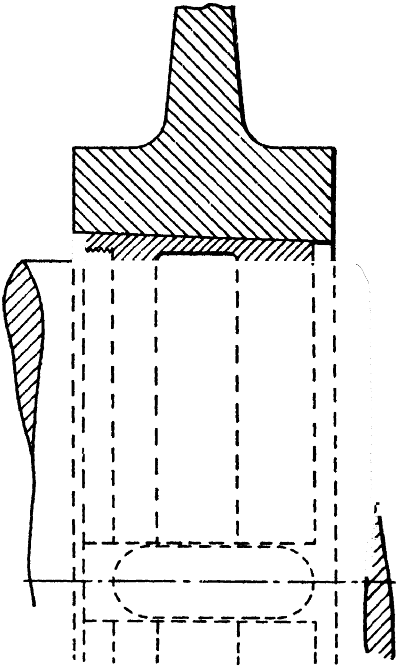


FIG. 289

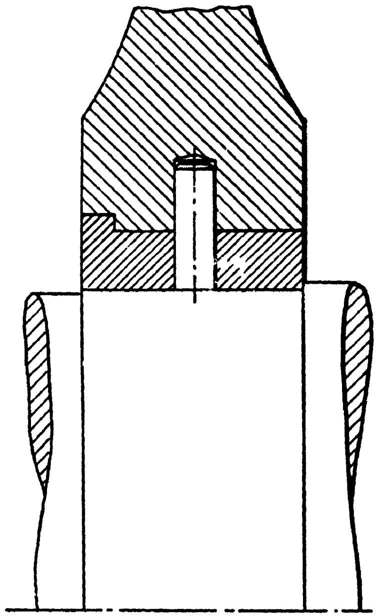


FIG. 290

briefly outlined in the preceding article led the well-known Czecho-Slovakian firm, Erste Brünner Maschinenfabrik, some years ago, to initiate the practice of machining impulse turbine rotors from solid forgings. Such a rotor is shown in Fig. 291. The high-pressure discs are frequently made of uniform thickness. Where the stresses demand it, the thickness may be slightly increased near the shaft. The blades have the same axial width as the discs, thus saving length. The advantages of the construction are obvious. Trouble due to a loose disc is impossible. Wheel hubs are avoided and thus the diameter of the diaphragm glands is the least possible and the leakage of steam is reduced. The saving in axial length is appreciable

and generally leads to a reduction in spindle diameter when compared with the normal construction.

On the other hand, it is more difficult to obtain a sound forging for such a rotor than for a single wheel of the same diameter. This limits the size of rotor for which the construction may be employed.

196. Rotors for Reaction Turbines. In the majority of reaction turbines the rotor, whatever form of construction may be employed,

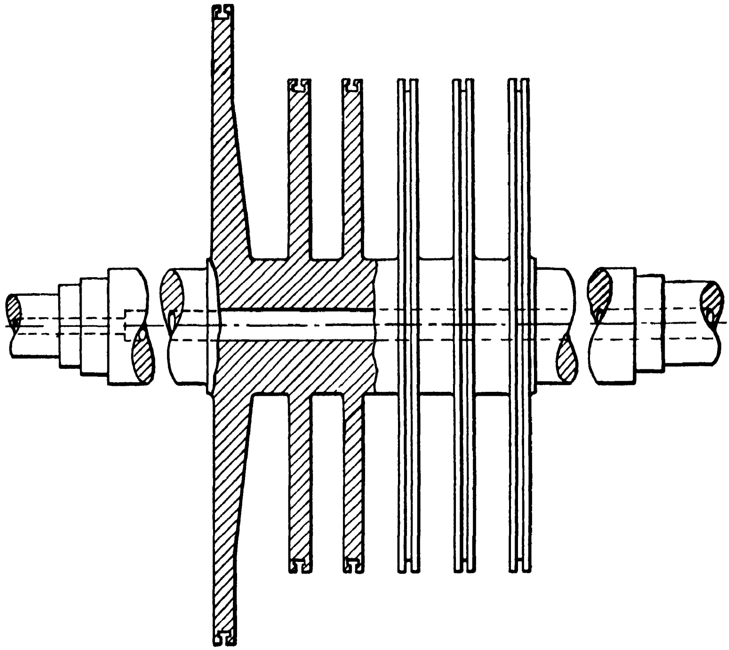


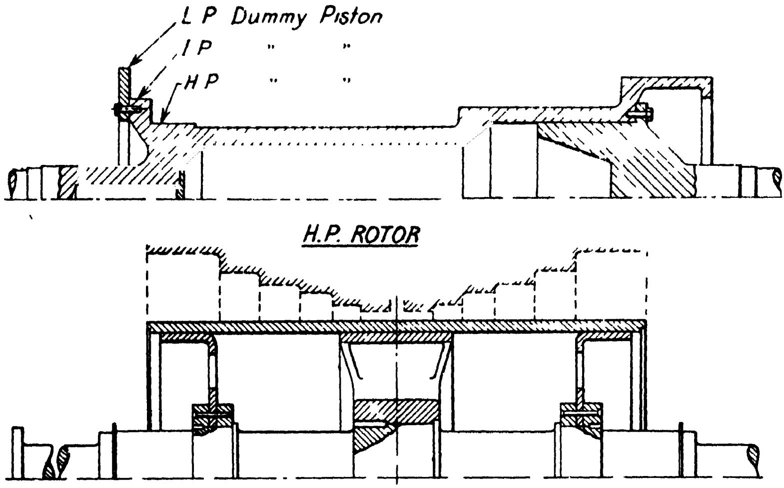
FIG. 291.—Turbine Rotor Machined from Solid Forging

is arranged to have a continuous cylindrical or conical surface. The principal exceptions to this rule are the L.P. reaction turbines constructed by Messrs. Brown Boveri & Co., Ltd.

Various forms of Parsons turbine rotor are shown in Figs. 292 to 295. Fig. 292 shows half-sections through the H.P. and L.P. rotors of a two-cylinder tandem turbine built in 1912. The H.P. rotor consists of a hollow forged steel element comprising the rotor drum and part spindle, and a spindle having an enlarged end. The former is shrunk on to the latter and further secured by screwed pins. The H.P. and I.P. dummy pistons are formed out of the rotor element, while a separate disc is used for the L.P. dummy. The mean diameter at the L.P. end is 71·5 in., the speed of rotation 750 r.p.m., and the mean peripheral speed 234 ft. per sec. The L.P. rotor

comprises a forged steel drum 86 in. external diameter and $2\frac{13}{16}$ in. thick. This is shrunk on to a cast-steel centre spider wheel which, in turn, is shrunk on to the rotor shaft. The ends of the drum are supported by mild steel discs. The mean diameter of the last blade ring is 105 in., the speed 750 r.p.m., and the mean blade velocity 344 ft. per sec.

The drum type of rotor is somewhat limited in its application owing to the stresses becoming excessive at high peripheral speeds.



DOUBLE-FLOW L.P. ROTOR

FIG. 292

The construction used in a turbine built by Messrs. C. A. Parsons & Co., Ltd., in 1916 is shown in Fig. 293. The H.P. turbine rotor is a solid forging, maximum mean blade velocity 239 ft. per sec. There are two dummy pistons, the H.P. dummy being turned from the solid forging, and the I.P. dummy being formed by two separate discs. The L.P. rotor is of the double-flow type and comprises eight heavy discs, with wide rims and hubs, shrunk on to the shaft. The mean peripheral velocity for the last row is 392 ft. per sec.

A modified form of double-flow L.P. rotor is shown in Fig. 294. The rotor is machined from a single forging. The centre part, which carries the shorter blades, is drum shaped, the outer parts, which carry the longer blades, are discs machined out of the solid. Such a construction offers great strength, especially when there is no central hole through the rotor and, of course, where the material is sound. Mean blade velocities in such a rotor appear to exceed 600 ft. per sec. In the H.P. turbine of later two-cylinder tandem

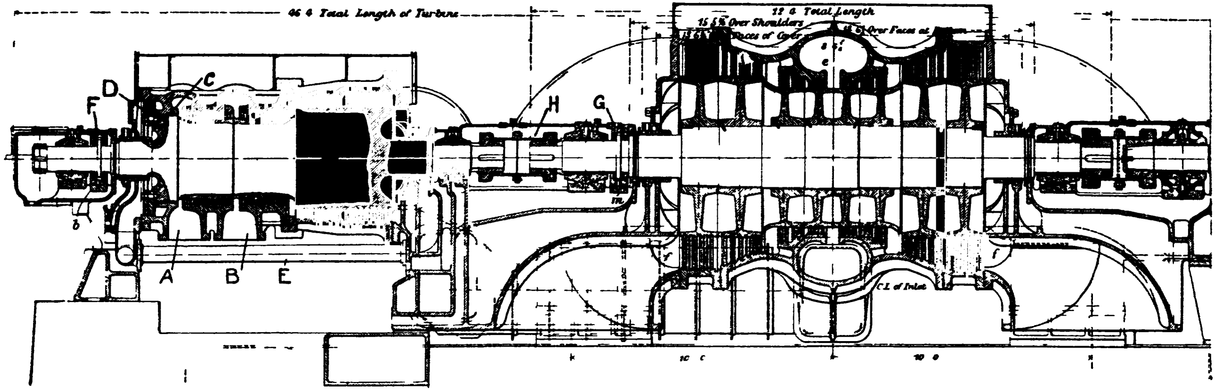


FIG 293 —15 000 kW 1,000 r p m Parsons Steam Turbine

Installed in the Lots Road Power Station of the Metropolitan District and London Electric Railway Companies

turbines, Messrs. Parsons have employed the construction shown in Fig. 295. Part of the rotor, including the dummy pistons, is turned from a solid forging. At the outlet end of the rotor, where the blades are longer and the stresses induced in the solid rotor would become excessive, a number of separate discs are shrunk on to the stepped shaft. The discs are of a relatively heavy and robust design and are

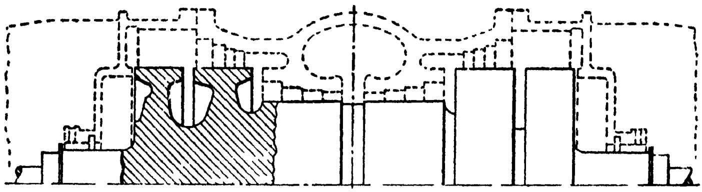


FIG. 294.—Double-flow L.P. Rotor for Parsons Turbine

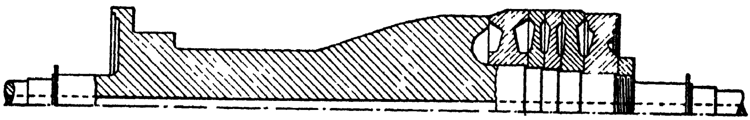


FIG. 295.—Parsons Turbine Rotor

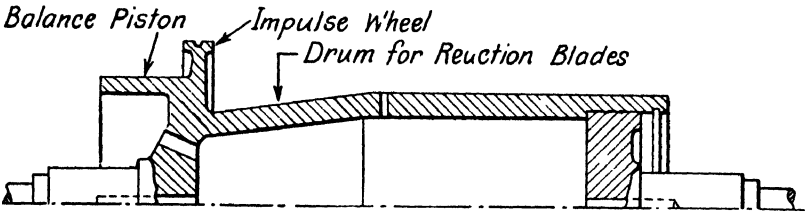


FIG. 296

butted together at the rim to eliminate any possibility of transverse vibration. A hole, not less than 2 in. diameter, is bored through the shaft from end to end. The inner surface of this hole is very carefully examined by means of an instrument comprising a mirror, lamp, and telescope, and known as a "borescope," for the purpose of detecting any minute flaws in the centre of the forging.

In recent single-cylinder turbines a similar construction has been adopted. At the L.P. end, however, discs having a diameter somewhat larger than that of the solid rotor are shrunk on.

197. **Brown-Boveri Drum Rotor.** A drum rotor for combined impulse and reaction turbines is shown in Fig. 296. This is used for powers up to about 3,000 kW and for moderate peripheral speeds. The steam end of the shaft, balance piston, Curtis wheel, and drum are made from a single forging, the exhaust end of the

shaft and its disc being likewise made from a forging. After the internal machining is completed, the drum is shrunk on to the L.P. end disc. Holes for equalizing the pressure behind the balance piston and that at an intermediate stage are bored in the drum end and through the drum itself.

198. Brown-Boveri Welded Rotor. About the year 1930, Messrs. Brown Boveri & Co. introduced a welded rotor construction, one form of which is shown in Fig. 297. The rotor comprises a number of discs and two shaft ends which are welded together at the periphery as shown in the detail view. The wheels are continuous discs,

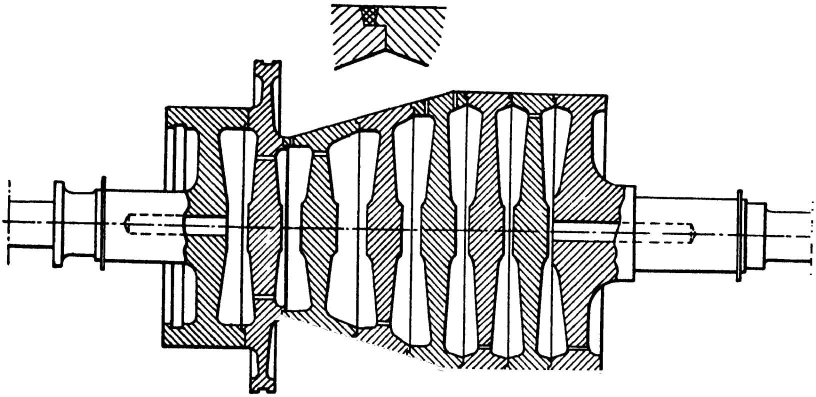


FIG. 297.—Brown-Boveri Welded Turbine Rotor

i.e. they have no central hole and are therefore much stronger than discs which have to be bored and pressed on a shaft. For an explanation of this statement, the reader is referred to Art. 208. Moreover, there are no keys, and the possibility of loose discs is entirely eliminated. The transverse rigidity of the rotor is very great and the critical speed is well above the running speed. Small holes are drilled through the discs just under the rims and also through the rims. The spaces between the discs are, therefore, filled with steam at the working temperature; this tends to prevent strains and other troubles due to differential expansion at starting and during change of load.

As shown in the inset detail of Fig. 297, the rotor discs are spigotted into one another and the remaining V filled by weld metal. The stresses in the welded seams are said to be only 700–1,500 lb. per sq. in. Owing to the large mass of the rotor, there is a considerable conduction of heat from the steel in the neighbourhood of the weld during welding, and the rate of cooling is such that the steel is hardened. In order to remove such effects the rotor is annealed at 600 to 650° C. for a prolonged period.

Before the construction was adopted as standard practice the

welded rotors were subjected to severe tests The welds were tested in tension by applying a hydraulic pressure between the discs, in shear by heating one disc and cooling the next, while the whole rotor was subjected to impact by falling weights

199. **Balancing of the Steam Thrust on the Moving Blades of Reaction Turbines.** In a pure impulse turbine the axial thrust on the blades is entirely due to the change of momentum of the steam

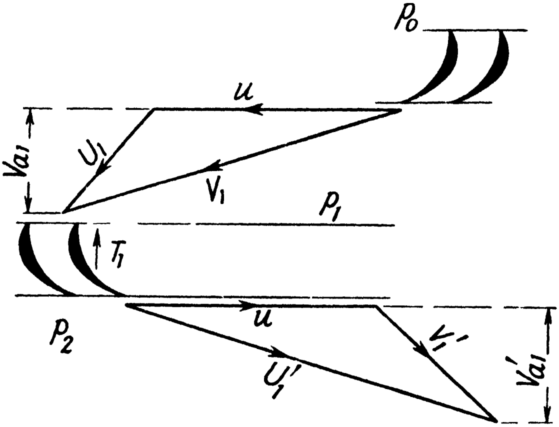


FIG 298

in the axial direction and is always a very small force In the reaction turbine, however the steam is falling in pressure during its passage through each ring of blades, fixed and moving alike, so that in addition to any force due to change of momentum there is a force due to the pressure drop across the blades The latter force may be very large and it is customary to provide some means of balancing it by steam pressure

Consider a single row of fixed or moving blades, as shown in Fig 298 The steam pressures at inlet and outlet are p_1 and p_2 respectively

Let A = annular area of blade ring, sq in

We shall indicate the quantities referring to successive rows of blades, including fixed and moving, by the suffixes 1, 2, 3, etc Then—

V_{a1} = axial component of velocity entering row No. 1
V_{a1}' = ,, ,, ,, leaving ,, ,, 1
V_{a2} = ,, ,, ,, entering ,, ,, 2
V_{a2}' = ,, ,, ,, leaving ,, ,, 2

Let T_1 = axial thrust exerted by the steam on the blades in row No 1 This is also, of course, the thrust exerted by the blades on the steam

w = mass flow of steam through blades, lb. per sec.

Then effective force on steam equals change of momentum per second.

Or $$(p_1 - p_2)A - T_1 = \frac{w}{g}(V_{a'1} - V_{a1})$$

and $$T_1 = (p_1 - p_2)A - \frac{w}{g}(V_{a'1} - V_{a1}) \quad . \quad . \quad (199)$$

This expression would give the resultant steam thrust on the first row of blades (say, fixed). Similarly, the thrust on the second row (which would be the first moving row in the group) would be—

$$T_2 = (p_2 - p_3)A - \frac{w}{g}(V_{a'2} - V_{a2})$$

In the same way we may write down the expression for the thrust on all the fixed and moving rows in the group. Signifying the last row by the suffix n and the exhaust pressure by p_e, we have—

$$T_1 = (p_1 - p_2)A - \frac{w}{g}(V_{a'1} - V_{a1})$$

$$T_2 = (p_2 - p_3)A - \frac{w}{g}(V_{a'2} - V_{a2})$$

$$T_3 = (p_3 - p_4)A - \frac{w}{g}(V_{a'3} - V_{a3})$$

$$T_n = (p_n - p_e)A - \frac{w}{g}(V_{a'n} - V_{an})$$

Reference to the velocity diagram shows that since the axial component of the steam velocity at exit from one ring of blades is the axial component at inlet to the following row, $V_{a2} = V_{a'1}$, $V_{a3} = V_{a'2}$, etc. Hence, by addition, we have—

Total thrust on all fixed and moving rows of blades

$$= \Sigma T = (p_1 - p_e)A - \frac{w}{g}(V_{a'n} - V_{a1})$$

The thrust on the rotor is that due to the moving blades and is one-half of the total thrust given above.

$$\therefore \text{ Rotor thrust } T = \tfrac{1}{2}(p_1 - p_e)A - \frac{w}{2g}(V_{a'n} - V_{a1}) . \quad . \quad (200)$$

The second term on the right-hand side of eq. (200) amounts to about 1 per cent only of the total thrust and may, therefore, be neglected.

Hence $$T = \tfrac{1}{2}(p_1 - p_e)A \quad . \quad . \quad . \quad . \quad (200a)$$

200. Proportions of Dummy Balance Pistons. Fig. 299 shows a diagrammatic section of a combination turbine consisting of an

impulse wheel followed by six expansions of reaction blades. Suppose that the axial forces due to steam pressures are balanced by a single balance piston A which rotates in the "dummy cylinder" B. The leakage of steam through the narrow annulus between the piston and cylinder is reduced to a small value by means of labyrinth packing. Suppose that the space behind the balance piston is connected to the outlet from the third expansion by the pressure-equalizing pipe C. Such connection may be made to the exhaust

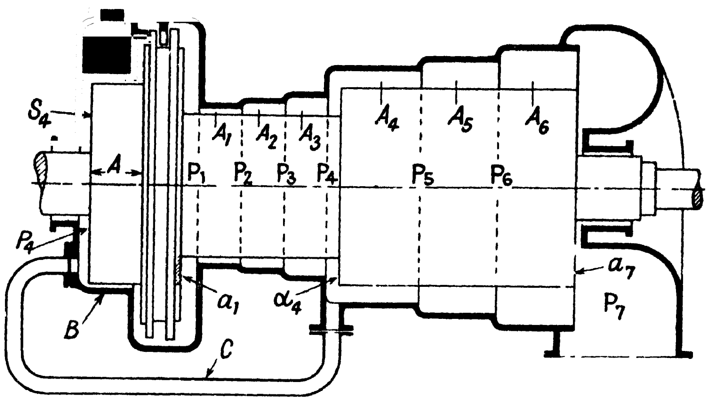


FIG. 299—Diagrammatic Arrangement of Impulse-reaction Turbine with Single Balance Piston

branch or to any L.P. stage, but the loss due to leakage will vary according to the point of connection.

Let A_1, A_2, etc., represent the annular areas of the blade rings in expansions 1, 2, etc.

Let a_1 = net annular area of the impulse wheel shoulder (in reality, of the dummy piston).

α_4 = area of rotor enlargement at outlet from third expansion.

a_7 = net area of L.P. end of rotor.

S_4 = net area of L.P. side of balance piston.

Suppose that P_1, P_2, P_3, etc., are the steam pressures at inlet to expansions 1, 2, 3, etc., at full load. The pressure on the L.P. side of the balance piston will be P_4. Then for equilibrium—

$$P_1a_1 - P_4 . S_4 = \tfrac{1}{2}\{(P_1 - P_2)A_1 + (P_2 - P_3)A_2 + (P_3 - P_4)A_3 + (P_4 - P_5)A_4 + (P_5 - P_6)A_5 + (P_6 - P_7)A_6\} + P_4\,\alpha_4 - P_7 . a_7$$

Since S_4 = (area of drum) + a_1, the above equation enables the area a_1 to be found.

Provided the governing is effected by nozzle control and no steam is by-passed beyond the first expansion, then all the steam pressures, except P_7, will vary directly as the steam flow through the turbine. Consequently, approximate balance will be obtained at all loads. The diameter of the dummy piston should be made rather less than the calculated value, so that there will be a definite thrust towards the exhaust end of the turbine. This will eliminate any tendency for the rotor to oscillate axially.

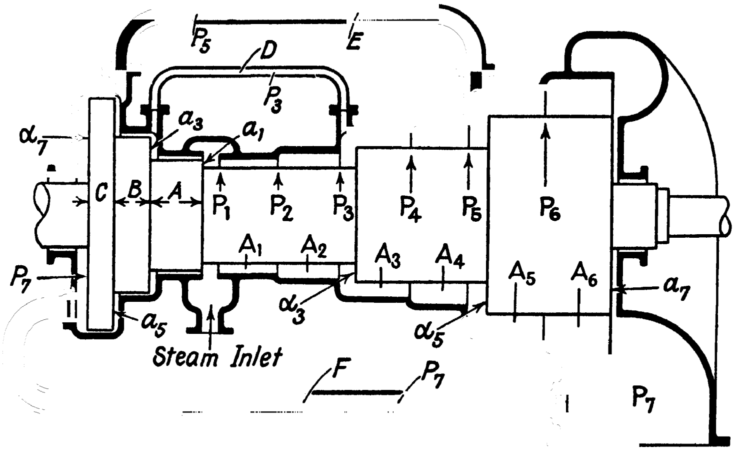


FIG. 300.—Diagrammatic Arrangement of Reaction Turbine with Three Balance Pistons

A turbine in which the rotor has three sections of different diameter is shown in Fig. 300. It will be assumed that the axial thrust is balanced by three balance pistons A, B, and C, the pressures on these being P_1, P_3, and P_5 respectively, while the pressure on the back of the L.P. dummy is the exhaust pressure P_7. D, E, and F are the pressure-equalizing pipes. Using the notation given in Fig. 300 for effective areas under pressure, then—

$$P_1a_1 = \tfrac{1}{2}\{(P_1 - P_2)A_1 + (P_2 - P_3)A_2\}$$
$$P_3(a_3 - \alpha_3) = \tfrac{1}{2}\{(P_3 - P_4)A_3 + (P_4 - P_5)A_4\}$$
$$P_5(a_5 - \alpha_5) + P_7(a_7 - \alpha_7) = \tfrac{1}{2}\{(P_5 - P_6)A_5 + (P_6 - P_7)A_6\}$$

The solution of these equations in the order given enables the areas a_1, a_3, and a_5 to be found, and hence the mean diameter of the dummy pistons.

The quantity of steam leaking past the dummy piston A is usually greater than that leaking past B. Thus the excess steam will flow through D and do work in the last four expansions of the turbine. Similarly, part of the steam which leaks through B will do useful work in the last two expansions.

The same general methods may be applied to any other arrangement of rotor and balance pistons. Packing devices for dummy pistons are described in Chapter XXIV.

EXAMPLE 33. The following particulars refer to a 2,500 h.p. reaction turbine—

Drum diameter,	H.P. section		$23\frac{5}{8}$ in.
,, ,,	L.P. ,,		$33\frac{5}{8}$,,
,, ,,	L.P. ,,		$47\frac{1}{4}$,,
H.P. Section.	1st expansion.	Blade height	$= \frac{7}{16}$ in.
,,	2nd ,,	,,	$= \frac{9}{16}$,,
,,	3rd ,,	,,	$= \frac{3}{4}$,,
I.P. Section.	1st ,,	,,	$= \frac{1}{2}$,,
,,	2nd ,,	,,	$= \frac{5}{8}$,,
,,	3rd ,,	,,	$= 1$,,
L.P. Section.	1st ,,	,,	$= 1$,,
,,	2nd ,,	,,	$= 2\frac{1}{4}$,,
,,	3rd ,,	,,	$= 3\frac{3}{4}$,,

The absolute steam pressures at entry to and exit from each expansion are set down in the diagram (Fig. 301). Calculate the diameters of the dummy pistons required in order that there may be no (appreciable) unbalanced steam thrust.

The annular areas of the blade rings are first calculated and set down as shown in Fig. 301.

Then thrust on H.P. blades $= \frac{1}{2}\{(50 \times 33{\cdot}13) + (38 \times 42{\cdot}8) + (30 \times 57{\cdot}49)\} = 2{,}504$ lb.

$$\therefore \qquad P_1 a_1 = 2{,}504$$

$$\therefore \qquad a_1 = \frac{2{,}504}{190} = 13{\cdot}2$$

Area of circle $23\frac{5}{8}$ in. diameter $= 438{\cdot}3$ sq. in.

$\therefore$ Area of H.P. dummy $= 438{\cdot}3 + 13{\cdot}2 = 451{\cdot}5$.

$\therefore$ Diameter of H.P. dummy (to nearest sixteenth of an inch) $= 24$ in.

Thrust on I.P. blades $= \frac{1}{2}\{(22 \times 53{\cdot}6) + (16 \times 67{\cdot}25) + (10{\cdot}5 \times 94{\cdot}84)\} = 1{,}625$ lb.

Thrust on shoulder between H.P. and I.P. sections of rotor $= 72 \times 449{\cdot}7 = 32{,}380$ lb.

$\therefore$ Total steam thrust in I.P. section $= 34{,}005$ lb.

$$\therefore \qquad a_2 = \frac{34{,}005}{72} = 472{\cdot}3 \text{ sq. in.}$$

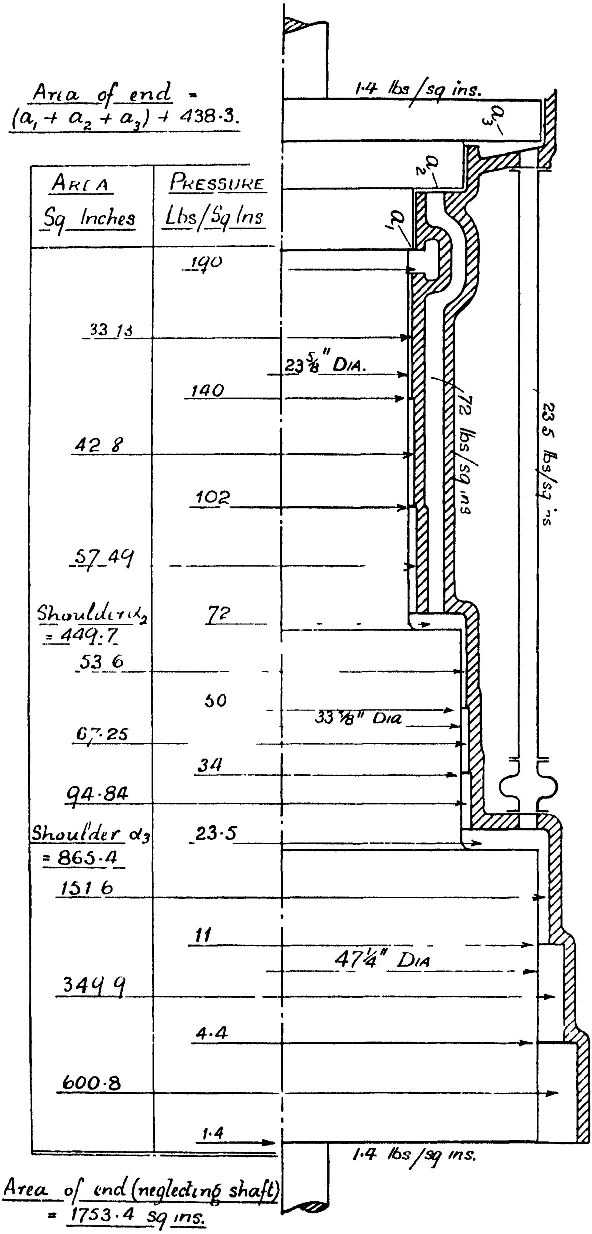


FIG. 301.—Illustrating Example on the Design of Dummy Balance Pistons

Area of circle 24 in. diameter = 452·39 sq. in.

$\therefore$ Area of I.P. dummy = 472·3 + 452·39

= 924·69 sq. in.

$\therefore$ Diameter of I.P. dummy = $34\frac{5}{16}$ in.

Thrust on L.P. blades = $\frac{1}{2}\{(12{\cdot}5 \times 151{\cdot}6) + (6{\cdot}6 \times 349{\cdot}9) + (3 \times 600{\cdot}8)\} = 3{,}003$ lb.

Thrust on shoulder between I.P. and L.P. sections of rotor

= 23·5 × 865·4 = 20,330

$\therefore$ Total steam thrust on L.P. section = 23,333 lb.

Back thrust on L.P. exhaust end of rotor

= 1·4 × 1,753·4 = 2,455 lb.

$\therefore$ Thrust to be balanced by L.P. dummy

= 23,333 – 2,455 = 20,878 lb.

Full area of L.P. dummy = 924·7 + a_3.

$\therefore$ $23{\cdot}5a_3 = 20{,}878 + 1{\cdot}4\,(924{\cdot}7 + a_3)$

or $22{\cdot}1a_3 = 22{,}173$

$\therefore$ $a_3 = 1{,}004$ sq. in.

Area of circle $34\frac{5}{16}$ in. diameter = 924·7 sq. in.

$\therefore$ Full area of L.P. dummy piston = 1,928·7 sq. in.

$\therefore$ Diameter of L.P. dummy piston = $49\frac{9}{16}$ in.

The diameters calculated above would be the mean diameters of the respective rings of labyrinth packing.

201. Couplings. Owing to the relative axial movement between a turbine spindle and the shaft of the driven machine, or between the shafts of the elements of a tandem turbine due to temperature changes, it is usually, but not always, necessary to join the shafts by means of a coupling which permits sliding in the axial direction. In some cases, there is also a change in alignment brought about either by differential expansion, slight settling of foundations, or flexibility of supports, and if the design of the coupling is such that it will permit of a small change of alignment as well, then so much the better.

A coupling suitable for turbines of small and medium power is shown in Fig. 302. The flanges are keyed to the shaft and sometimes secured by nuts as shown. The coupling bolts are screwed into one flange. Rubber bushes with metal cores are fitted over the plain ends of the bolts and have a small clearance in the holes of the other flange. This type of coupling allows for axial movement, slight lack of alignment, and also a slight torsional flexibility. Couplings of this kind have been used for the transmission of 3,000 h.p.

The well-known Parsons type of claw coupling, which has been used by practically every firm of turbine builders, is shown in Fig. 303. This comprises two claw pieces A having a number of spokes

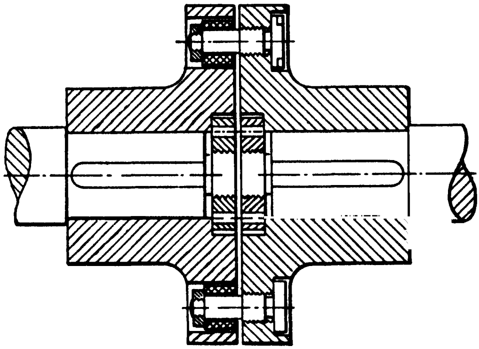


FIG. 302 — Coupling for Turbines of Small and Medium Output

with parallel sides. The sleeves B are provided with an equal number of V-shaped projections which fit between the spokes. Rings C serve to limit the axial play of the coupling. The sleeves

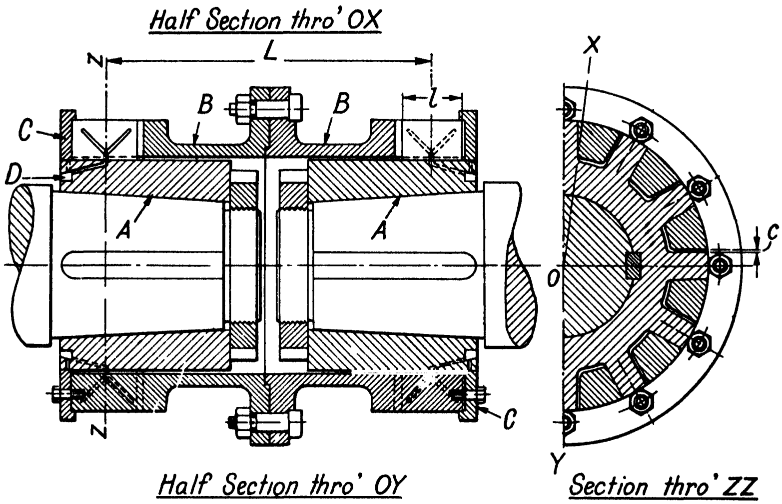


FIG 303 Parsons Type Flexible Coupling

are spigotted together and bolted. The couplings must be very accurately made so that all the teeth are in contact simultaneously.

A small clearance c is provided between the claws, as shown.

If the shaft centres remain at the same height, this clearance permits the angular misalignment between them to reach the value $\theta = \frac{2c}{l}$ radians, or $\frac{114 \cdot 6c}{l}$ deg. θ is normally 0·25 to 0·35 deg. If the shafts remain parallel, then the clearance permits a difference in height of $\frac{cL}{l}$ of the shaft centres. $\frac{L}{l}$ varies from 4 to 5.

For the purpose of lubricating the teeth on the driving side, oil is supplied—either from the adjoining bearing or by a special supply

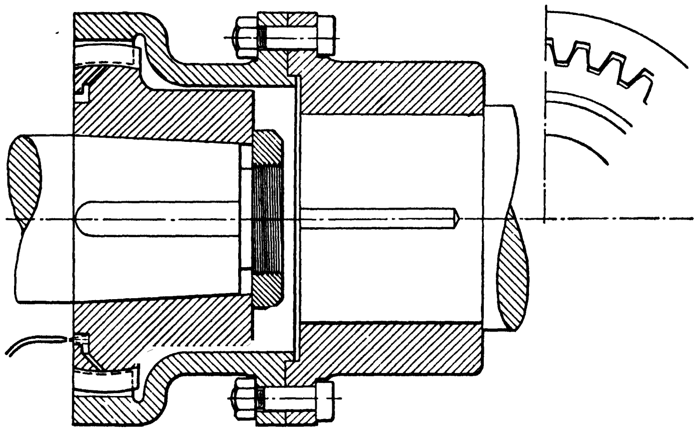


FIG. 304.—English Electric Type Flexible Coupling

pipe—to a groove D in the claw pieces. The oil passes through drilled holes to the distributing grooves on the faces of the teeth and is finally flung off by centrifugal action.

The tooth type of flexible coupling, in the form employed by the English Electric Co., Ltd., is shown in Fig. 304. A steel hub is keyed to the turbine shaft and is provided with several gear teeth at its periphery. A forged steel muff which is rigidly bolted to the driven shaft has internal teeth which gear with those on the hub. Means for lubrication are provided, as shown.

A type of coupling which has been employed successfully on some of the largest turbines built in this country is shown in Fig. 305. This is known as the Bibby coupling and is manufactured under licence from the Wellman Bibby Co., Ltd. It consists of two hubs keyed to the turbine shaft and driven shaft respectively, and provided with flanges. A number of accurately pitched grooves parallel to the axis are machined in the flanges. A tempered steel spring is bent to form a complete cylindrical grid. The segments of the spring are fitted in the grooves and the torque is transmitted from one

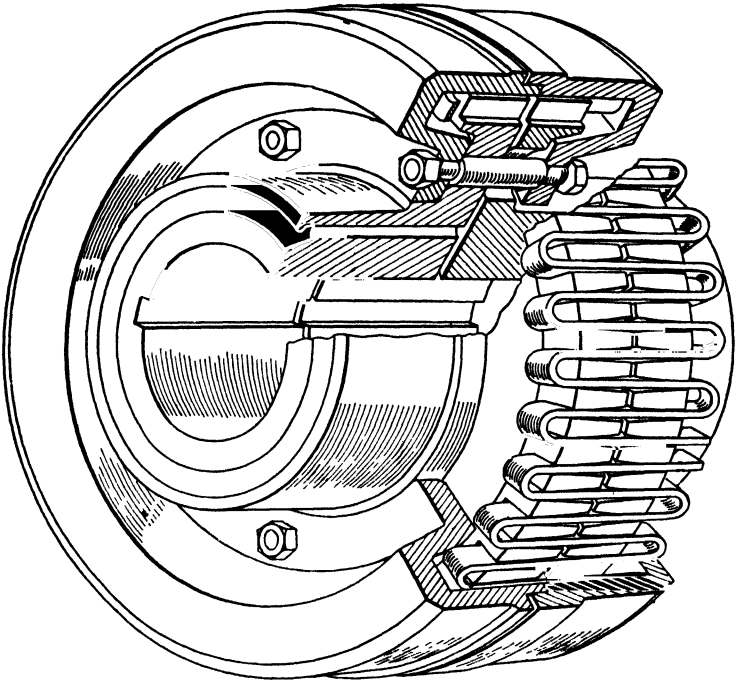


FIG. 305.—Bibby Coupling

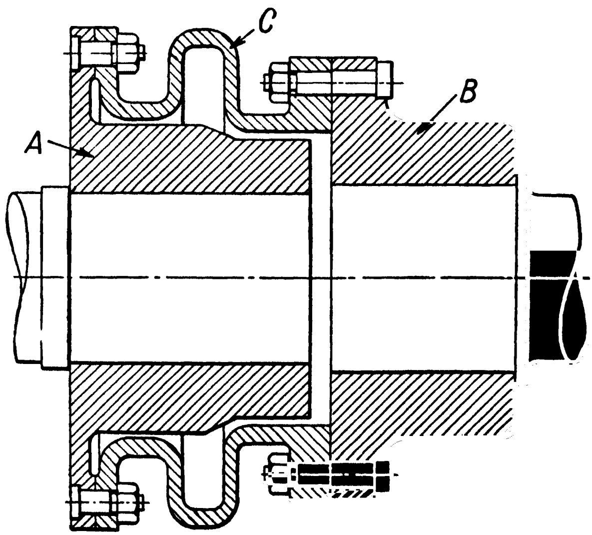


FIG. 306.—Metropolitan-Vickers Semi-flexible Coupling

flange to the other through these flexible grids. The grooves widen somewhat towards the centre so that the spring fits closely only at its outer ends. Under a normal torque the drive takes place through the relatively long unsupported stretches of the spring members, which are very flexible and resilient in this condition. An increase in torque causes the springs to deflect, thus shortening their span and increasing their rigidity. This feature, while permitting flexibility in the torsional sense, gives freedom from resonance.

A semi-flexible coupling, constructed by the Metropolitan-Vickers Electrical Co., Ltd., to couple the L.P. turbine shaft and generator in two-cylinder tandem sets, is shown in Fig. 306. Hubs A and B, keyed to the turbine shaft and alternator shaft respectively, are connected together by a forged steel muff C, which gives rigidity in torsion but a limited degree of flexibility to allow for slight misalignment.

Owing to the great increase in power output of recently developed turbines, the increased torques have resulted in such increases in the pressure between the teeth of flexible couplings that relative movement of the two parts of the coupling becomes difficult. There is a definite trend to discontinue the use of flexible couplings in such large machines and to substitute solid couplings. Experience alone will decide whether this is a step in the right direction.

CHAPTER XXI

STRESSES IN TURBINE ROTORS

202. Introductory. The stresses in turbine rotors are due primarily to the inertia of the rotor mass and depend, therefore, on the form of the rotor, i.e. on the disposition of the mass, and on the peripheral speed. In most cases, the stresses imposed are relatively

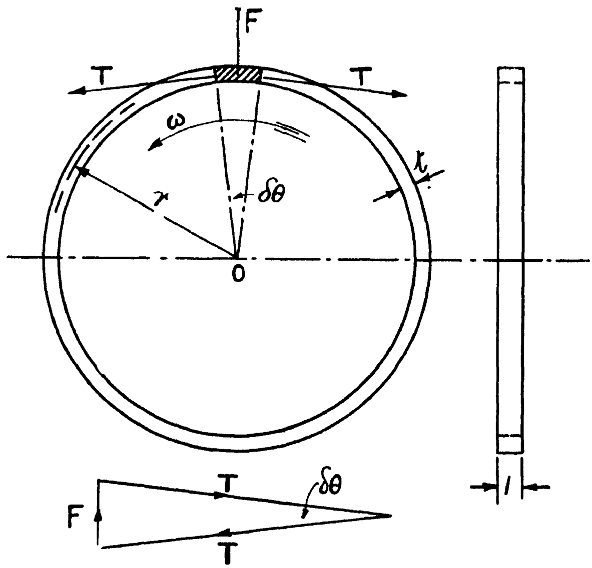


FIG. 307

high and become a very definite limiting factor in the design. Consequently, the accurate estimation of rotor stresses is a matter of great importance. For this reason, a concise outline of this branch of strength of materials is considered essential in this book, if only to pave the way to a more extended study of the subject.

203. Stress in Thin Rotating Ring. Consider a thin ring, i.e. one in which the thickness t in the radial direction is small compared with the diameter, rotating about an axis through its centre with an angular velocity ω radians per second.

Let w = density of material.

f_{tr} = stress in thin ring. This is a tangential or hoop stress.

r = mean radius of ring.

Consider a ring whose length in the axial direction is unity. The cross-sectional area is then t units and the volume of the element subtending the angle $\delta\theta$ at the centre O is $t \,.\, r \,.\, \delta\theta$.

Hence mass of element $= w \,.\, r \,.\, t \,.\, \delta\theta$.

$$\text{Centrifugal force } F = \frac{wrt\delta\theta}{g} \times \omega^2 r$$

$$= \frac{w \,.\, \omega^2 r^2 \,.\, t \,.\, \delta\theta}{g}$$

The element is in equilibrium under the action of the force F and the hoop tensions T. The angle between the two hoop tensions is $\delta\theta$ and their resultant, which is directed inwards, is $T \,.\, \delta\theta$.

$$\therefore \qquad T \,.\, \delta\theta = \frac{w \,.\, \omega^2 r^2 \,.\, t \,.\, \delta\theta}{g}$$

Since the stress f_{tr} will be equal to the force T divided by the area of the ring—

$$f_{tr} = \frac{w \,.\, \omega^2 r^2}{g} \quad . \quad . \quad . \quad . \quad . \qquad (201)$$

or if u = peripheral velocity ($u = \omega r$)

$$f_{tr} = \frac{w \,.\, u^2}{g} \quad . \quad . \quad . \quad . \quad . \qquad (201a)$$

UNITS. If w = density in lb. per cub. in.
u = peripheral velocity, ft. per sec.
g = acceleration in ft. per sec.^{2}

then $f_{tr} = \dfrac{1{,}728 \,.\, w \,.\, u^2}{144 \,.\, g}$ lb. per sq. in.

i.e. $f_{tr} = \dfrac{12w \,.\, u^2}{g}$ lb. per sq. in.

For steel, $w = 0{\cdot}283$; $f_{tr} = 0{\cdot}1055u^2$ lb. per sq. in.

204. Stresses in Turbine Rotors of the Drum Type. The stresses in a turbine rotor of the drum type are greater than those in a thin ring rotating with the same peripheral velocity owing to the additional centrifugal force imposed by the blades.

In calculating the hoop stress, the component stresses may be obtained separately, that due to the blade load being obtained as follows—

In Fig. 308, let F_b be the centrifugal force on the blades per inch of periphery over an axial length equal to the axial pitch of the blades. Let A be the net area of rotor section per axial pitch in

square inches. Then on an arc subtending an angle $\delta\theta$ at the centre O, the total force F_1 due to the blade load $= r \cdot \delta\theta \cdot F_b$.

But
$$T_1 = \frac{F_1}{\delta\theta} = r \cdot F_b$$

∴ Stress in drum due to blade load

$$= \frac{r \cdot F_b}{A} \text{ lb. per sq. in.}$$

∴ Total hoop stress $= \dfrac{12wu^2}{g} + \dfrac{r \cdot F_b}{A}$ lb. per sq. in.

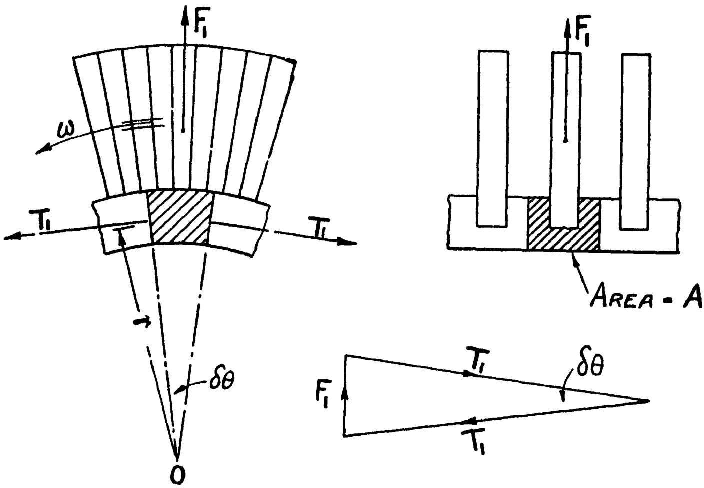


FIG 308

EXAMPLE 34. Calculate the intensity of hoop stress in a rotor of the drum type, given the following particulars—

External diameter of drum = 86 in.
Internal diameter of drum = 80¼ in.
Speed = 750 r.p.m.

Blades, 1 in. wide; 3¼ in. axial pitch; 19 in. high above rotor. Weight of blade per foot = 0·65 lb. Depth of groove, 1¼ in. Number of blades per foot of circumference, 22·2.

Mean radius of drum = 41·56 in. = 3·47 ft.

$$\therefore \quad u = \frac{3{\cdot}47 \times 2\pi \times 750}{60} = 272 \text{ ft. per sec.}$$

∴ Stress in thin ring without blading $= 0{\cdot}1055 \times (272)^2 = 7{,}800$ lb. per sq. in.

Total length of one blade = 19 + 1¼ = 20¼ in.

Total weight of one blade = 1·097 lb. (W)

Distance of centre of gravity of blade from axis of rotation = 51·875 in.

$$\omega = \frac{2\pi \times 750}{60} = 78{\cdot}5 \text{ rad. per sec.}$$

$$\therefore \text{ Centrifugal force on each blade} = \frac{W\omega^2 r}{g} = 908 \text{ lb.}$$

$$\text{Force } F_b \text{ per inch} = \frac{908 \times 22{\cdot}2}{12} = 1{,}680 \text{ lb.}$$

Net area A = (3·25 × 2·875) − 1·25 = 8·1 sq. in.

$$\therefore \text{ Stress due to blade load} = \frac{43 \times 1{,}680}{8{\cdot}1} = 8{,}925 \text{ lb. per sq. in.}$$

∴ Combined drum stress = 16,725 lb. per sq. in.

205. Stresses in Rotating Discs of Variable Thickness. Derivation of General Equations. Consider an element of a turbine wheel,

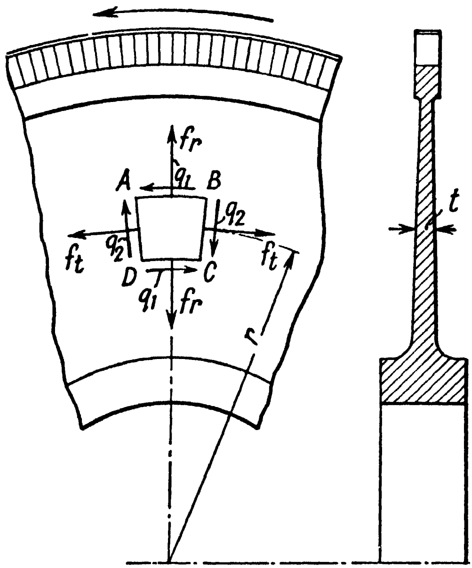


FIG. 309.—Stresses on Element of Turbine Disc

Fig. 309, bounded by radial lines AD, BC, and arcs AB, CD. The inertia forces due to the blades, the rim, and the disc itself will obviously produce direct stresses on the edges AB and CD of the element.

These are known as radial stresses. There will also be induced certain direct stresses on the radial edges AD and BC of the element in question. These are known as tangential, or hoop, stresses. Owing to the torque T applied by the blades to the rim of the wheel there will be shear stresses q_1 on the faces AB and CD (of magnitude

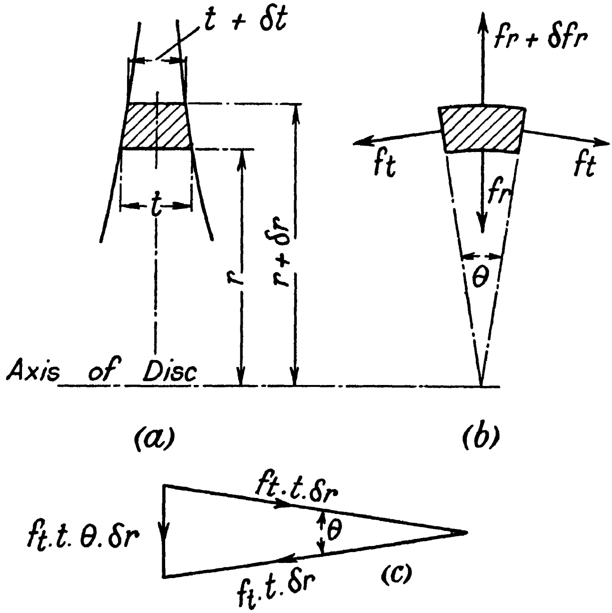


FIG. 310

$q_1 = T/2\pi r^2 t$) and complementary shear stresses $q_2 = q_1$ on the faces AD and BC. In practically all cases, the shear stresses are negligibly small when compared with the direct stresses. Consequently, in any analysis where the wheel stresses are important, the shear stresses may be ignored. The radial and hoop stresses at any point may then be regarded as principal stresses.

In the following expressions—

Let r = radius of disc at any point.

t = thickness of disc at radius r.

$\mu = \frac{w}{g}$ (inch units).

σ = Poisson's ratio = (strain at right angles to direction of stress) ÷ (strain in direction of stress).

Consider an element of a disc of variable thickness, Fig. 310. (*a*) shows a section through the axis, while (*b*) shows the stresses in side view. The element is in equilibrium under the forces due to

stress and inertia. The forces due to hoop tension are each $f_t \,.\, t \,.\, \delta r$ and their resultant, as shown in Fig. 310 (c), is $f_t \,.\, t \,.\, \delta r \,.\, \theta$, and is directed inwards.

The volume of the element is $r \,.\, t \,.\, \delta r \,.\, \theta$, and the centrifugal force on it equals $\mu\omega^2 r^2 t \,.\, \delta r \,.\, \theta$.

$$\therefore \quad (f_r + \delta f_r)(t + \delta t)(r + \delta r)\theta + \mu\omega^2 r^2 t \,.\, \delta r \,.\, \theta$$
$$= f_r \,.\, t \,.\, r \,.\, \theta + f_t \,.\, t \,.\, \delta r \,.\, \theta.$$

Working out, dividing by $\delta r \,.\, \theta$, and proceeding to the limit, we have—

$$r \,.\, t \,.\, \frac{df_r}{dr} + r \,.\, f_r \,.\, \frac{dt}{dr} + t \,.\, f_r - t \,.\, f_t = -\mu\omega^2 r^2 t$$

or

$$\frac{d}{dr}(r \,.\, t \,.\, f_r) - t \,.\, f_t = -\mu\omega^2 r^2 t. \quad . \quad . \quad (202)$$

Eq. (202) is a general equation for any rotating disc.

Suppose now that a point on the disc is at radius r when the disc is at rest (and unstressed) and that its radius is increased to $r + y$ when the disc is rotating and under stress; i.e. y is the radial displacement of a point on the disc at radius r. Then obviously the radial strain e_r will be $\frac{dy}{dr}$.

$$\text{Hoop strain } e_t = \frac{\text{Change in circumference}}{\text{Original circumference}}$$
$$= \frac{2\pi(r + y) - 2\pi r}{2\pi r} = \frac{y}{r}$$

Then

$$\mathrm{E} \,.\, \frac{dy}{dr} = f_r - \sigma \,.\, f_t$$

and

$$\mathrm{E} \,.\, \frac{y}{r} = f_t - \sigma \,.\, f_r$$

These are simultaneous equations in f_r and f_t, and give—

$$f_r = \frac{\mathrm{E}}{1 - \sigma^2}\left(\sigma \,.\, \frac{y}{r} + \frac{dy}{dr}\right) \quad . \quad . \quad (203)$$

$$f_t = \frac{\mathrm{E}}{1 - \sigma^2}\left(\frac{y}{r} + \sigma \,.\, \frac{dy}{dr}\right). \quad . \quad . \quad . \quad (204)$$

Introducing these values in eq. (202), differentiating, and multiplying throughout by $\frac{r(1 - \sigma^2)}{\mathrm{E} \,.\, t}$, we have—

$$r^2 \,.\, \frac{d^2y}{dr^2} + r\left(\frac{r}{t} \,.\, \frac{dt}{dr} + 1\right)\frac{dy}{dr} + \left(\frac{r \,.\, \sigma}{t} \,.\, \frac{dt}{dr} - 1\right)y$$
$$= -\frac{\mu\omega^2 r^3(1 - \sigma^2)}{\mathrm{E}} \quad . \quad . \quad . \quad (205)$$

This equation is quite general and is independent of the manner in which the thickness varies with radius. As will be seen, it is a homogeneous linear differential equation.

206. Disc of Constant Thickness. We shall now apply eq. (205) to find expressions for the stresses in a disc of constant thickness. Since t is a constant, $\frac{dt}{dr} = 0$, and hence—

$$r^2 \cdot \frac{d^2y}{dr^2} + r \cdot \frac{dy}{dr} - y = -\frac{\mu\omega^2 r^3 (1 - \sigma^2)}{E}$$

The solution consists of two parts, the complementary function and the particular integral. For the former, assume $y = b \cdot r^{\psi}$, where b and ψ are constants.

Then $$r^2 \cdot \frac{d^2y}{dr^2} + r \cdot \frac{dy}{dr} - y = 0$$

Since $\frac{dy}{dr} \quad b \cdot \psi \cdot r^{\psi-1}$, and $\frac{d^2y}{dr^2} = b\,(\psi^2 - \psi) \cdot r^{\psi-2}$

$$b\,(\psi^2 - \psi) r^{\psi} + b \cdot \psi \cdot r^{\psi} - b \cdot r^{\psi} = 0$$

$\therefore$ $$\psi^2 - 1 = 0$$

i.e. $$\psi = \pm 1$$

Since there are two roots, the solution is

$$y = b_1 r + \frac{b_2}{r}$$

where b_1 and b_2 are independent constants.

For the particular integral, assume $y = ar^3$, where a is a constant.

Then $$\frac{dy}{dr} = 3ar^2, \text{ and } \frac{d^2y}{dr^2} = 6ar$$

Substituting in the original equation, we have—

$$6ar^3 + 3ar^3 - ar^3 = -\frac{\mu\omega^2 r^3 (1 - \sigma^2)}{E}$$

from which $$a = -\frac{\mu\omega^2 (1 - \sigma^2)}{8E} \quad . \quad . \quad . \quad (206)$$

a is a constant which depends on the angular velocity of the disc, the density of the material, and its elastic properties.

Hence the complete solution of the equation is

$$y = ar^3 + b_1 r + \frac{b_2}{r} \quad . \quad . \quad . \quad (207)$$

Inserting now the values of $\frac{y}{r}$ and $\frac{dy}{dr}$ derived from eq. (207) in the general equations (203) and (204), we have—

$$f_r = \frac{E}{1-\sigma^2}\left\{ar^2(3+\sigma) + b_1(1+\sigma) - \frac{b_2}{r^2}(1-\sigma)\right\} . \quad (208)$$

$$f_t = \frac{E}{1-\sigma^2}\left\{ar^2(1+3\sigma) + b_1(1+\sigma) + \frac{b_2}{r^2}(1-\sigma)\right\} . \quad (209)$$

The stresses f_r and f_t cannot be calculated by means of these expressions until the two constants b_1 and b_2 have been found. These must be determined with reference to the conditions as regards stress and strain at the inner and outer boundaries of the disc. Some examples will now be given.

207. Continuous Disc of Constant Thickness. Consider first a continuous disc, i.e. a disc without a hole at the centre. Assume, further, that the disc is not subjected to any edge loading, i.e. that there are no forces imposed due to masses attached to its periphery.

Then the constants b_1 and b_2 may be found from the following conditions—

(1) The radial displacement y must be zero at the centre of the disc.

Since $$y = ar^3 + b_1 r + \frac{b_2}{r}$$

it follows that b_2 must be zero; otherwise the displacement y would be infinite at the centre.

(2) The radial stress f_r must be zero at the periphery of the disc. Then if R_2 is the outer radius, by eq. (208)—

$$b_1(1+\sigma) = -a \,.\, R_2^2(3+\sigma)$$

or $$b_1 = -a \,.\, R_2^2\left(\frac{3+\sigma}{1+\sigma}\right)$$

Therefore, for any radius r

$$f_r = \left(\frac{3+\sigma}{8}\right) . \frac{w\omega^2}{g} . (R_2^2 - r^2) \quad . \quad . \quad (210)$$

$$f_t = \frac{w\omega^2}{8g}\{(3+\sigma)R_2^2 - (1+3\sigma)r^2\} \quad . \quad . \quad (211)$$

For steel discs $w = 0{\cdot}283$ lb. per cub. in.

$\sigma = 0{\cdot}3$ approx.

Let N = r.p.m.

$$f_r = 3{\cdot}31\left(\frac{N}{1{,}000}\right)^2(R_2^2 - r^2) \quad . \quad . \quad (212)$$

$$f_t = 1{\cdot}91\left(\frac{N}{1{,}000}\right)^2(1{\cdot}74R_2^2 - r^2) \qquad . \qquad . \qquad (213)$$

If the disc had a radial stress imposed upon its periphery due to attached masses, then the constants may be found as before, except that f_r at the periphery would be made equal to the applied stress.

208. Disc of Constant Thickness with Central Hole.

Let R_1 = inner radius of disc.

R_2 = outer radius of disc.

Case 1. *Disc free from constraints.* Consider first of all a disc which is free from any applied stresses at the boundaries. Then the radial stress is zero when $r = R_1$ and also when $r = R_2$. By substituting in eq. (208) it is found that

$$b_1 = -a\left(\frac{3+\sigma}{1+\sigma}\right)(R_1^2 + R_2^2)$$

$$b_2 = -a\,.\,R_1^2R_2^2\left(\frac{3+\sigma}{1-\sigma}\right)$$

Inserting these constants in (208) and (209), we have—

$$f_r = \frac{w.\omega^2}{g}\left(\frac{3+\sigma}{8}\right)\left(R_1^2 + R_2^2 - \frac{R_1^2R_2^2}{r^2} - r^2\right) \qquad . \qquad (214)$$

$$f_t = \frac{w\,\omega^2}{8g}\left\{\left(3+\sigma\right)\left(R_1^2 + R_2^2 + \frac{R_1^2R_2^2}{r^2}\right) - (1+3\sigma)r^2\right\}. \qquad (215)$$

For steel discs —

$$f_r = 3{\cdot}31\left(\frac{N}{1{,}000}\right)^2\left(R_1^2 + R_2^2 - \frac{R_1^2R_2^2}{r^2} - r^2\right) \qquad . \qquad (216)$$

$$f_t = 1{\cdot}91\left(\frac{N}{1{,}000}\right)^2\left\{1{\cdot}74\left(R_1^2 + R_2^2 + \frac{R_1^2R_2^2}{r^2}\right) - r^2\right\} \qquad . \qquad (217)$$

In the continuous disc, the tangential and radial stresses must necessarily tend to the same value as the centre of the disc is approached. By writing $r = 0$ in eqs. (210) and (211), it is seen that

$$f_t = f_r = \left(\frac{3+\sigma}{8}\right).\frac{w\omega^2R_2^2}{g}$$

$$= \left(\frac{3+\sigma}{8}\right)f_{tr}$$

where f_{tr} is the hoop stress in a thin ring rotating with an equal peripheral velocity.

Consider now the disc with a central hole. The hoop stress given by eq. (215) is clearly the maximum when r is the least value possible, i.e. when $r = R_1$.

$$f_t\,(\text{max.}) = \frac{w\omega^2}{8g}\{(3+\sigma)(R_1^2 + 2R_2^2) - (1+3\sigma)R_1^2\}$$

When R_1 is made very small

$$f_t\,(\text{max.}) = \left(\frac{3+\sigma}{4}\right) \cdot \frac{w\,.\,\omega^2 R_2^2}{g} = \left(\frac{3+\sigma}{4}\right) \cdot f_{tr}$$

i.e. by drilling a small hole at the centre of a continuous disc free from constraints, *the maximum tangential stress is just doubled.*

The results given by eqs. (214) and (215) may be shown graphically in an interesting and instructive manner. We shall express the stress in the disc as a fraction of that in a thin ring of the same material and rotating with the same peripheral velocity.

Let $$m_0 = \frac{R_1}{R_2}, \text{ and } m = \frac{r}{R_2}$$

Since $$f_{tr} = \frac{w\omega^2 R_2^2}{g}$$

$$\frac{f_r}{f_{tr}} = \left(\frac{3+\sigma}{8}\right)\left(\frac{R_1^2}{R_2^2} + \frac{R_2^2}{R_2^2} - \frac{R_1^2 R_2^2}{r^2 R_2^2} - \frac{r^2}{R_2^2}\right)$$

$$= \left(\frac{3+\sigma}{8}\right)\left(m_0^2 + 1 - \frac{m_0^2}{m^2} - m^2\right) \quad . \quad . \quad (218)$$

$$= 0{\cdot}4125\left(m_0^2 + 1 - \frac{m_0^2}{m^2} - m^2\right) \text{ for steel}$$

$$\frac{f_t}{f_{tr}} = \left(\frac{3+\sigma}{8}\right)\left(m_0^2 + 1 + \frac{m_0^2}{m^2}\right) - \left(\frac{1+3\sigma}{8}\right)m^2 \quad . \quad (219)$$

$$= 0{\cdot}4125\left(m_0^2 + 1 + \frac{m_0^2}{m^2}\right) - 0{\cdot}2375m^2 \text{ for steel}$$

Curves showing the values of these ratios as a function of m_0 and m and for steel discs are given in Fig. 311. It will be seen that in all cases the tangential stress is a maximum at the bore and diminishes, rapidly at first, towards the periphery. The influence of the size of hole should also be noticed; as the ratio m_0 is increased the maximum and minimum hoop stresses increase until, when m_0 approaches unity, the stress is equal to that in the thin ring, while the radial stress vanishes.

Case 2. *Disc subjected to stresses at the inner and outer edges.* When the disc is subjected to radial stresses at either the bore or the periphery, or both, the radial and hoop stresses within the disc will be different from those given by the foregoing equations and the graphs of Fig. 311. There are two methods of evaluating the stresses.

Let f_1 = radial stress applied at bore (Fig. 312).

f_2 = radial stress applied at periphery (Fig. 312).

In general, it is more convenient to consider tensile stresses as positive and compressive stresses as negative. Reverting to the general

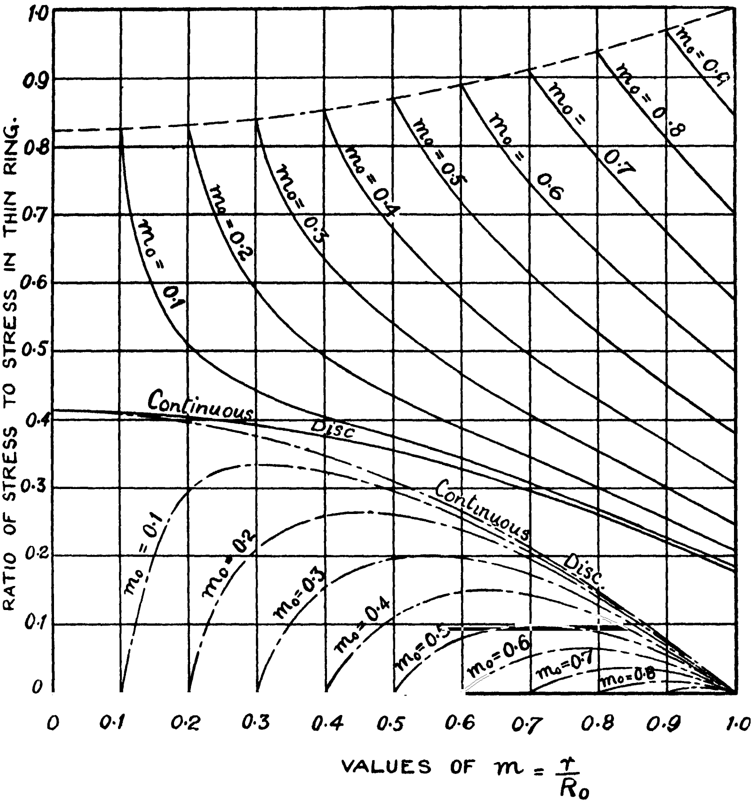


FIG. 311.—Curves Showing the Ratio of the Stress in a Disc of Uniform Thickness to the Stress in a Thin Ring with an Equal Peripheral Velocity

$$m_0 = \frac{\text{Radius of bore}}{\text{External radius of disc}}$$

eqs. (208) and (209), the constants b_1 and b_2 may be found by writing in (208) $f_r = f_1$ when $r = R_1$, and $f_r = f_2$ when $r = R_2$. This gives the necessary expressions for f_r and f_t; also, if required, the radial displacement y, by inserting the values of b_1 and b_2 in eq. (207).

In the second method the stresses due to inertia and those due to the applied radial forces are calculated separately and then

added to give the resultant stress. The stresses due to inertia are calculated by using eqs. (214) to (217). The stresses in the disc due to the applied edge stresses may be found by using Lamé's

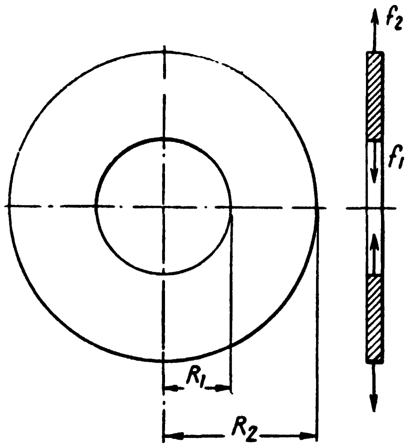


FIG. 312

equations for a thick cylinder, provided the thickness of the disc is relatively small compared with the diameter.

Then assuming that

$$f_r = A - \frac{B}{r^2}, \text{ and } f_t = A + \frac{B}{r^2}$$

where A and B are constants, and substituting $f_r = f_1$, when $r = R_1$, and $f_r = f_2$ when $r = R_2$, we have—

$$f_r = \frac{f_2 \,.\, R_2^2 - f_1 \,.\, R_1^2}{R_2^2 - R_1^2} - \left(\frac{f_2 - f_1}{R_2^2 - R_1^2}\right)\frac{R_1^2 R_2^2}{r^2} \quad . \quad (220)$$

$$f_t = \frac{f_2 R_2^2 - f_1 R_1^2}{R_2^2 - R_1^2} + \left(\frac{f_2 - f_1}{R_2^2 - R_1^2}\right)\frac{R_1^2 R_2^2}{r^2}. \quad . \quad (221)$$

EXAMPLE 35. A disc 1 in. thick, 4 in. internal diameter, and 20 in. external diameter rotates at 4,000 r.p.m. Given that the density of the material is 0·284 lb. per cub. in., and that the value of σ is 0·3, calculate the following—

(*a*) Stresses in free rotating disc.

(*b*) Stresses due to an imposed radial stress (tensile) of 6,000 lb. per sq. in. at the periphery of the stationary disc.

(*c*) Stresses due to rotation and edge load combined.

(*a*) Free Rotating Disc.

$R_1 = 2$ in.; $R_2 = 10$ in. Substituting these values in eqs. (214) and (215) we have—

$$f_r = 53{\cdot}1\left(104 - \frac{400}{r^2} - r^2\right)$$

$$f_t = 53{\cdot}1\left\{\left(104 + \frac{400}{r^2}\right) - 0{\cdot}575r^2\right\}$$

The calculated values are given in Table XXV and are shown in Fig. 313.

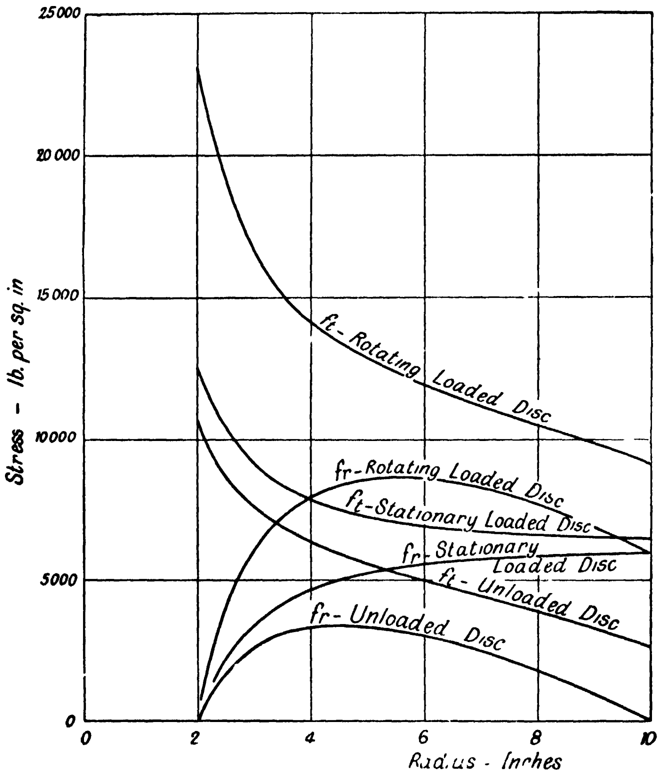


FIG. 313

(*b*) Here $f_1 = 0$; $f_2 = 6{,}000$. Substituting in eqs. (220) and (221)

$$f_r = 6{,}250 - \frac{25{,}000}{r^2}$$

$$f_t = 6{,}250 + \frac{25{,}000}{r^2}$$

The calculated values are again given in Table XXV and Fig. 313.

(c) The resultant stresses in the loaded rotating disc are found by adding the values obtained in (a) and (b) above, or by the following method.

By eq. (208)—

$$f_r = \frac{E}{1-\sigma^2}\left\{ar^2(3+\sigma) + b_1(1+\sigma) - \frac{b_2}{r^2}(1-\sigma)\right\}$$

and since
$$a = -\frac{w\omega^2(1-\sigma^2)}{8gE}$$

$$f_r = -53{\cdot}1r^2 + E\left(1{\cdot}43b_1 - 0{\cdot}77\frac{b_2}{r^2}\right)$$

When $r = 2$ in., $f_r = 0$; when $r = 10$ in., $f_r = 6{,}000$.

$$\therefore \quad b_1 = \frac{8{,}230}{E}; \; b_2 = \frac{60{,}000}{E}$$

$$\therefore \quad f_r = -53{\cdot}1r^2 + 11{,}770 - \frac{46{,}100}{r^2}$$

and
$$f_t = -30{\cdot}65r^2 + 11{,}770 + \frac{46{,}100}{r^2}$$

Apart from negligible slide-rule errors, the values given by these expressions agree with those given in Table XXV.

TABLE XXV

STRESSES IN ROTATING DISC OF CONSTANT THICKNESS SUBJECTED TO RADIAL STRESS AT PERIPHERY

(Example 35)

Radius r in.	Stresses in Unloaded Rotating Disc		Stationary Disc Considered as Thick Cylinder		Resultant Stresses in Loaded Rotating Disc	
	f_r	f_t	f_r	f_t	f_r	f_t
2	0	10,700	0	12,500	0	23,200
3	2,680	7,610	3,470	9,030	6,150	16,640
4	3,350	6,360	4,688	7,812	8,038	14,172
5	3,350	5,610	5,250	7,250	8,600	12,860
6	3,020	5,010	5,555	6,945	8,575	11,955
7	2,485	4,460	5,740	6,760	8,225	11,220
8	1,790	3,900	5,859	6,641	7,649	10,541
9	960	3,310	5,940	6,560	6,900	9,870
10	0	2,680	6,000	6,500	6,000	9,180

209. Stresses in Turbine Wheel of Constant Thickness. Fig. 314 shows a half-section through a turbine wheel forming part of a rotor turned out of a solid forging (see Fig. 291).

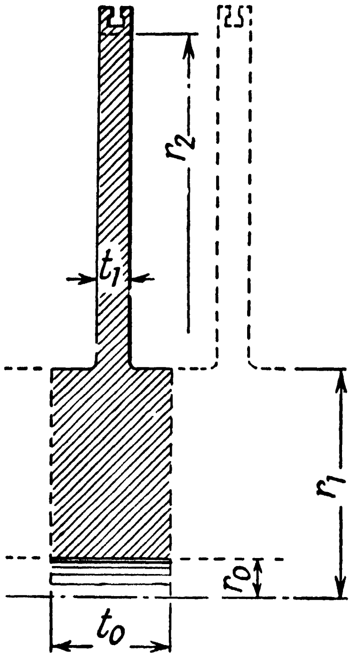


FIG 314

Let f_2 = stress due to blades, assumed to be uniformly distributed over the edge of the disc at radius r_2.

f_r = radial stress in disc proper.

f_t = hoop stress in disc proper.

f_r' = radial stress in shaft.

f_t' = hoop stress in shaft.

y = radial displacement of disc proper

y' = radial displacement of shaft.

Assume that the rotor has a hole (radius = r_0) bored through the centre, in accordance with usual practice.

We shall consider the shaft as a disc of constant thickness t_0 (equal to the axial distance between disc centres). If f_{r1} is the radial stress in the disc proper at radius r_1, then, as a rough approximation, we may regard the shaft as being subjected to a

radial stress $f_r{}'_1 = \frac{t_1 \cdot f_{r1}}{t_0}$ at its outer surface. The radial stress $f_r{}'_0$ at radius r_0 is obviously zero.

Referring to eqs. (208) and (209) for the disc of constant thickness, and using capital letters for the constants for the shaft and small letters for the disc constants, we have—

$$\frac{E}{1-\sigma^2}\left\{(3+\sigma)Ar_0^2 + B_1(1+\sigma) - \frac{B_2}{r_0^2}(1-\sigma)\right\} = f_r{}'_0 = 0$$

$$\frac{E}{1-\sigma^2}\left\{(3+\sigma)Ar_1^2 + B_1(1+\sigma) - \frac{B_2}{r_1^2}(1-\sigma)\right\} = f_r{}'_1 = \frac{t_1 \cdot f_{r1}}{t_0}$$

These are simultaneous equations in B_1 and B_2, and enable us to express B_1 and B_2 in terms of f_{r1}.

But $$f_{r1} = \frac{E}{1-\sigma^2}\left\{ar_1^2(3+\sigma) + b_1(1+\sigma) - \frac{b_2}{r_1^2}(1-\sigma)\right\}$$

Hence we can express B_1 and B_2 in terms of b_1 and b_2.

The radial displacement of the shaft at radius r_1, when under stress, must be equal to that of the disc at the same radius.

But $$y_1' = Ar_1^3 + B_1r_1 + \frac{B_2}{r_1}$$

$\therefore$ y_1' may be expressed in terms of b_1 and b_2.

But $$y_1 = ar_1^3 + b_1r_1 + \frac{b_2}{r_1}$$

Therefore, by equating y_1' and y_1 we obtain one equation connecting b_1 and b_2.

Considering now the periphery of the disc, it will be clear that—

$$\frac{E}{1-\sigma^2}\left\{ar_2^2(3+\sigma) + b_1(1+\sigma) - \frac{b_2}{r_2^2}(1-\sigma)\right\} = f_2$$

Since f_2 is known, we have a second equation connecting b_1 and b_2. The solution for b_1 and b_2 enables B_1 and B_2 to be found and the stresses in the disc and shaft to be calculated

210. Discs of Hyperbolic Section. The foregoing examples on stresses in rotating discs of uniform thickness may be summarized in a diagrammatic form in Fig. 315. In (*a*) we have a continuous disc, in which the radial and tangential stresses are equal at the centre. The radial stress is zero at the periphery and the tangential stress diminishes from the centre outwards. In (*b*) we have a disc with a central hole, while in (*c*) the conditions are the same as in (*b*) except that a radial stress of uniform intensity is applied at the periphery. In each case it will be observed that the more important stress, i.e. the tangential stress, is much greater at the inner radius than at the periphery. In many cases it is important to

reduce the weight of the rotor to a minimum, for by so doing, the critical speed of the rotor may be raised or, alternatively, the shaft diameter for a given speed may be reduced. In order to attain this end, the distribution of stress should be as uniform as possible, and the greatest stress should be as high as possible. A better distribution of hoop stress may be obtained by reducing the thickness where the stress in the disc of constant thickness is low, and

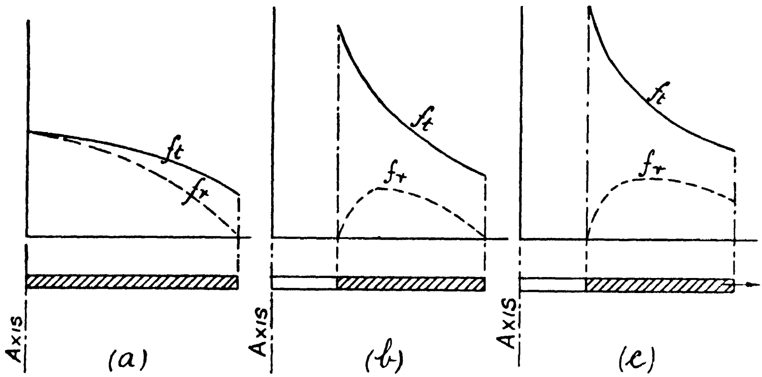


FIG 315

increasing the thickness where the stress is high; in other words, by using a disc of tapered section.

The calculation of stresses in tapered discs of conical profile presents a mathematical problem of considerable difficulty— although solutions have been found. A much simpler form to deal with mathematically is the hyperbolic profile, in which

$$t = C \cdot r^{-\alpha}$$

where C and α are positive constants (see Fig. 316). The solution for this type is due to Professor A. Stodola. (1)

Since $t = C \cdot r^{-\alpha}$, $\qquad \frac{1}{t} \cdot \frac{dt}{dr} = -\frac{\alpha}{r}$

Substituting this value in the general equation (205), Art. 205, we have—

$$r^2 \cdot \frac{d^2y}{dr^2} + r(1-\alpha)\frac{dy}{dr} - (1+\alpha\sigma)y = -\frac{\mu\omega^2 r^3(1-\sigma^2)}{E}$$

For the complementary function, write $y = b \cdot r^{\psi}$.

$$r^2 \cdot \frac{d^2y}{dr^2} + r(1-\alpha)\frac{dy}{dr} - (1+\alpha\sigma)y = 0$$

$$\therefore \quad b(\psi^2 - \psi)r^{\psi} + (1-\alpha)b \cdot \psi \cdot r^{\psi} - (1+\alpha\sigma)b \cdot r^{\psi} = 0$$

or

$$\psi^2 - \alpha\psi - (1+\alpha\sigma) = 0$$

from which $$\psi_1 = \frac{\alpha}{2} + \sqrt{\frac{\alpha^2}{4} + \alpha\sigma + 1} \quad . \quad . \quad . \quad (222)$$

$$\psi_2 = \frac{\alpha}{2} - \sqrt{\frac{\alpha^2}{4} + \alpha\sigma + 1} \quad . \quad . \quad . \quad (223)$$

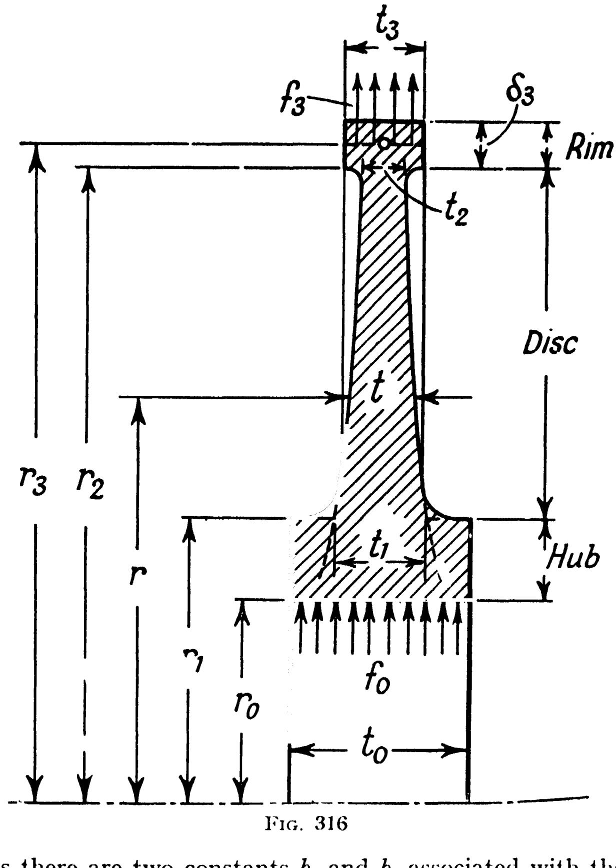


FIG. 316

Thus there are two constants b_1 and b_2 associated with the constants ψ_1 and ψ_2, and

$$y = b_1 r^{\psi_1} + b_2 r^{\psi_2}$$

For a particular integral, write $y = ar^3$.

$$\therefore \quad 6ar^3 + 3ar^3(1 - \alpha) - ar^3(1 + \alpha\sigma) = -\frac{\mu\omega^2 r^3 (1 - \sigma^2)}{\mathrm{E}}$$

from which $$a = -\frac{\mu\omega^2 (1 - \sigma^2)}{\mathrm{E}\{8 - (3 + \sigma)\alpha\}} \quad . \quad . \quad . \quad (224)$$

a is a constant depending on the speed and on the properties of the material. Then the complete solution for the radial deformation y is—

$$y = ar^3 + b_1 r^{\psi_1} + b_2 r^{\psi_2} \quad . \quad . \quad . \quad (225)$$

Inserting values of $\frac{y}{r}$ and $\frac{dy}{dr}$ in eqs. (203) and (204), we have—

$$f_r = \frac{E}{1-\sigma^2}\left\{(3+\sigma)\,ar^2 + (\psi_1+\sigma)\,b_1 r^{\psi_1-1} + (\psi_2+\sigma)\,b_2 r^{\psi_2-1}\right\} \quad (226)$$

$$f_t = \frac{E}{1-\sigma^2}\left\{(1+3\sigma)\,ar^2 + (1+\psi_1\sigma)\,b_1 r^{\psi_1-1} + (1+\psi_2\sigma)\,b_2 r^{\psi_2-1}\right\} \quad . \quad . \quad . \quad (227)$$

Here again, b_1 and b_2 are constants which must be found by reference to the conditions at the inner and outer boundaries of the disc proper.

Consider the hub first, and suppose that the mutual pressure between the shaft and the inside of the hub due to force fit is f_0 lb. per sq. in. at the running speed, or at the speed of rotation for which the stress calculations are being made. When the disc is stationary, this pressure will, of course, be much greater.

Considering the hub as a disc of constant thickness, then by eq. (208) (using capital letters for the constants to distinguish them from the disc constants) we have—

$$f_r = \frac{E}{1-\sigma^2}\left\{Ar^2(3+\sigma) + B_1(1+\sigma) - \frac{B_2}{r^2}(1-\sigma)\right\}$$

where

$$A = -\frac{\mu\omega^2(1-\sigma^2)}{8E}$$

The disc is pulling outwards on the hub over a width t_1 with a tensile radial stress f_{r1}. Then, approximately, the radial stress at the outer surface of the hub is—

$$f'_{r1} = \frac{t_1 \cdot f_{r1}}{t_0}$$

This approximation demands a sudden change in radial stress at the junction of the disc and hub which is quite impossible. We accept the approximation, however, as a rough and ready means of solving a problem of almost insuperable difficulty. Then—

$$\frac{E}{1-\sigma^2}\left\{Ar_1^2(3+\sigma) + B_1(1+\sigma) - \frac{B_2}{r_1^2}(1-\sigma)\right\} = \frac{t_1 \cdot f_{r1}}{t_0}$$

$$\frac{E}{1-\sigma^2}\left\{Ar_0^2(3+\sigma) + B_1(1+\sigma) - \frac{B_2}{r_0^2}(1-\sigma)\right\} = -f_0$$

since f_0 is compressive. These equations enable us to express B_1

and B_2 in terms of the unknown stress f_{r1}, a value of f_0 having been assumed.

Let y represent radial deformation of disc.

Let y' represent radial deformation of hub or rim.

Then y_1' for the hub at radius r_1 is—

$$y_1' = Ar_1^3 + B_1 r_1 + \frac{B_2}{r_1}$$

and may be expressed in terms of f_{r1}. But for the disc—

$$f_{r1} = \frac{E}{1-\sigma^2}\left\{(3+\sigma)\,ar_1^2 + (\psi_1+\sigma)\,b_1 r_1^{\psi_1-1} + (\psi_2+\sigma)\,b_2 r_1^{\psi_2-1}\right\}$$

Hence y_1' may be expressed in terms of the disc constants b_1 and b_2. But y_1 for the disc is $ar_1^3 + b_1 r_1^{\psi_1} + b_2 r_1^{\psi_2}$. Since the amount of radial deformation must necessarily be the same for the hub and the disc at r_1, $y_1' = y_1$. Thus we obtain one equation connecting b_1 and b_2.

In general, the rim is of comparatively small section, and we may treat it as a loaded thin rotating ring. Let r_3 be the radius to the centroid of the rim section. Due to the centrifugal force on the blades, etc., there will be a certain stress f_3 per sq. in. of periphery at radius r_3, which may be calculated. The disc is pulling inwards at radius r_2 with a stress intensity f_{r2} over the thickness t_2. Considering the forces across a diameter due, respectively, to the inertia of the rim, the stress f_3 and the stress f_{r2}, we have—

Diametral force $= 2\,(\mu\omega^2 t_3\delta_3 r_3^2 + r_3 t_3 f_3 - r_2 t_2 f_{r2})$

Let f_3' = hoop stress in rim

$$= \frac{1}{t_3\delta_3}\,(\mu\omega^2 t_3\delta_3 r_3^2 + r_3 t_3 f_3 - r_2 t_2 f_{r2})$$

Then, ignoring the radial stress, the hoop strain in the rim will be—

$$\frac{f_3'}{E} = \frac{y_2'}{r_3}, \text{ or } y_2' = \frac{r_3 \cdot f_3'}{E}$$

Thus y_2' may be expressed in terms of f_{r2}, and hence in terms of b_1 and b_2. But y_2 for the disc proper is—

$$y_2 = ar_2^3 + b_1 r_2^{\psi_1} + b_2 r_2^{\psi_2}$$

Since $y_2 = y_2'$, we obtain a second equation for b_1 and b_2, enabling these constants, and in turn B_1 and B_2, to be determined. Once these have been found, the stresses and strains in the complete rotor may be worked out.

EXAMPLE 36. Calculate the stresses in the turbine wheel shown in Fig. 317, given the following particulars—

Speed of rotation, 3,000 r.p.m.; mean radius of blades = 20 in.;

mean circumferential pitch of blades = 0·503 in.; centrifugal force on each blade, its shrouding, and the blade root = 2,210 lb.; mutual force between wheel and shaft at 3,000 r.p.m. = 500 lb. per sq. in. Assume w for steel = 0·283 lb. per cub. in.; σ for steel = 0·3.

We first find the value of α for the wheel profile. Tabulating r, t, $\log r$, and $\log t$—

Radius r	Thickness t	Log r	Log t
6·5	1·5	0·8129	0·1761
8	1·2	0·9031	0·0792
10	0·96	1·0000	$\bar{1}$·9823
13·75	0·7	1·1383	$\bar{1}$·8451

For the hyperbolic profile, $t = C \cdot r^{-\alpha}$, $\log t = \log C - \alpha \log r$,

i.e.
$$\alpha = \frac{\log \frac{t_1}{t_2}}{\log \frac{r_2}{r_1}}$$

Plotting the above values of $\log r$ and $\log t$, it will be found that $\alpha = 1·01$. For the purposes of calculation, α will be made equal to 1. Then, by eqs. (222) and (223)—

$\psi_1 = 1·744$, and $\psi_2 = -0·744$. Also, by eq. 224, $a = -\dfrac{13·99}{E}$.

In order to obtain the constants b_1 and b_2 in the stress equations (226) and (227), we consider first the hub.

Hub. $\quad f_0 = -500 \quad A = -\dfrac{\mu\omega^2(1-\sigma^2)}{8E} = -\dfrac{8·22}{E}$

Radial stress in hub—

$$f_r' = \frac{E}{1-\sigma^2}\left\{Ar^2(3+\sigma) + B_1(1+\sigma) - \frac{B_2}{r^2}(1-\sigma)\right\}$$

$$= -29·8r^2 + \frac{E}{0·91}\left(1·3B_1 - \frac{0·7B_2}{r^2}\right) \quad . \quad . \quad . \quad (a)$$

When $r = 5$ in., $f_r' = f_0 = -500$. Substituting in (a) we have—

$$B_1 - 0·0215\, B_2 = \frac{171·2}{E} \quad . \quad . \quad . \quad (b)$$

Also, when $r = 6·5$ in.—

$$f'_{r1} = \frac{1·5 f_{r1}}{3·75} = 0·4 f_{r1}$$

where f_{r1} is the stress in the *disc* at 6·5 in. radius.

Substituting in eq. (226), we have—

$$f_{r1} = -2{,}146 + 9{\cdot}06\text{E}b_1 - 0{\cdot}01864\text{E}b_2$$

$$\therefore \quad f_{r1}' = -859 + 3{\cdot}62\text{E}b_1 - 0{\cdot}00746\text{E}b_2 \quad . \quad . \quad (c)$$

By eq. (*a*) above—

$$f_{r1}' = -1{,}258 + 1{\cdot}43\text{EB}_1 - 0{\cdot}0182\text{EB}_2 \quad . \quad (d)$$

Equating (*c*) and (*d*), and simplifying—

$$\text{B}_1 - 0{\cdot}0127\text{B}_2 = \frac{279}{\text{E}} + 2{\cdot}53b_1 - 0{\cdot}00522b_2 \quad . \quad (e)$$

From (*b*) and (*e*) we obtain the values of B_1 and B_2, the hub constants.

$$\text{B}_1 = \frac{434{\cdot}7}{\text{E}} + 6{\cdot}19b_1 - 0{\cdot}0128b_2 \quad . \quad . \quad (f)$$

$$\text{B}_2 = \frac{12{,}260}{\text{E}} + 288b_1 - 0{\cdot}594b_2 \quad . \quad . \quad (g)$$

The radial deformation of the *hub* at radius r_1 is—

$$y_1' = \text{A}r_1^3 + \text{B}_1r_1 + \frac{\text{B}_2}{r_1}, \text{ and as } r_1 = 6{\cdot}5$$

$$y_1' = \frac{2{,}450}{\text{E}} + 84{\cdot}5b_1 \quad 0{\cdot}1746b_2 \quad . \quad . \quad (h)$$

But for the *disc*, $y_1 = ar_1^3 + b_1r_1^{\nu_1} + b_2r_1^{\nu_2}$.

i.e. $$y_1 = -\frac{3{,}840}{\text{E}} + 26{\cdot}18b_1 + 0{\cdot}248b_2 \quad (i)$$

Equating y_1' and y_1, we find—

$$b_1 - 0{\cdot}00726b_2 = -\frac{107{\cdot}9}{\text{E}}$$

This is one of the two expressions relating b_1 and b_2.

Considering now the rim, we have $r_3 = 14{\cdot}7$ in. The area of the rim section is $2{\cdot}84$ sq. in., and since $t_3 = 2{\cdot}125$ in., $\delta_3 = 1{\cdot}335$ in. Since the circumferential distance at $14{\cdot}7$ in. radius, corresponding to one blade pitch, is $0{\cdot}37$ in., the stress f_3 due to the centrifugal force on the blades is—

$$f_3 = \frac{2{,}210}{2{\cdot}125 \times 0{\cdot}37} = 2{,}810 \text{ lb. per sq. in.}$$

Hoop stress in rim

$$= \frac{1}{t_3\delta_3}\{\mu\omega^2t_3\delta_3r_3^2 + r_3t_3f_3 - r_2t_2f_{r2}\}$$

$$= 46{,}600 - 3{\cdot}39f_{r2}$$

Also $$y_2' = \frac{r_2 f}{E} = \frac{685{,}000}{E} - \frac{49{\cdot}9 f_{r2}}{E}$$

Substituting for $r_2 = 13{\cdot}75$ in eq. (226) for the disc—

$$f_{r2} = -9{,}590 + 15{\cdot}78Eb_1 - 0{\cdot}00503Eb_2$$

$$\therefore \quad y_2' = \frac{1{,}163{,}000}{E} - 787b_1 + 0{\cdot}2505b_2$$

Also $$y_2 = ar_2^3 + b_1 r_2^{p_1} + b_2 r_2^{p_2}$$

$$= -\frac{36{,}400}{E} + 97{\cdot}05b_1 + 0{\cdot}1423b_2$$

Since $y_2 = y_2'$, $$b_1 = \frac{1{,}380}{E}$$

and $$b_2 = \frac{205{,}200}{E}$$

Substituting in eqs. (226) and (227), we now obtain the general equations for the disc stresses—

$$f_r = -50{\cdot}75r^2 + 3{,}100r^{0{\cdot}744} - \frac{100{,}000}{r^{1{\cdot}744}}$$

$$f_t = -29{\cdot}2r^2 + 2{,}320 \,.\, r^{0{\cdot}744} + \frac{175{,}000}{r^{1{\cdot}744}}$$

The hub constants are readily found to be—

$$B_1 = \frac{6{,}348}{E}; \text{ and } B_2 = \frac{287{,}860}{E}$$

and the equations for the hub stresses—

$$f_r' = -29{\cdot}8r^2 + 9{,}070 - \frac{221{,}000}{r^2}$$

$$f_t' = -17{\cdot}2r^2 + 9{,}070 + \frac{221{,}000}{r^2}$$

The radial deformations of the disc are—

$$E \,.\, y = -13{\cdot}99r^3 + 1{,}380 \,.\, r^{1{\cdot}744} + \frac{205{,}200}{r^{0{\cdot}744}}$$

and for the hub—

$$Ey' = -8{\cdot}22r^3 + 6{,}348r + \frac{287{,}860}{r}$$

The calculated stresses and radial displacements are set out in Table XXVI and in Fig. 317. The calculations were made with an ordinary 10-in. slide rule.

It is interesting to calculate the proportion (x, say) of the mass of the rim, the centrifugal force on which is directly applied to the disc.

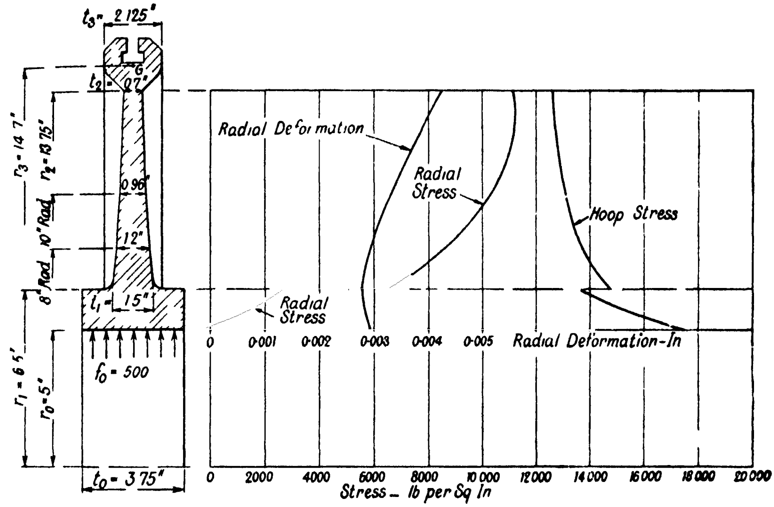


FIG. 317 Illustrating Example 36

TABLE XXVI

STRESSES AND RADIAL DEFORMATIONS IN TURBINE WHEEL OF HYPERBOLIC SECTION

Radius Inches	Stresses – Lb per sq in f_r	Stresses – Lb per sq in f_t	Radial Deformation y in
5	- 525	17,490	0 002 94
5 25	218	16,626	0 002 90
5 5	858	15,859	0 002 86
5 75	1,395	15,192	0 002 83
6	1,858	14,590	0 002 81
6 25	2,255	14,047	0 002 79
6 5	2,570	13,583	0·002 78
6 5	6,540	14,810	0 002 78
7	7,330	14,350	0 002 82
8	8 640	13,670	0 002 95
9	9,620	13,340	0 003 11
10	10,320	13,090	0 003 32
11	10,850	12,950	0 003 56
12	11,090	12,800	0·003 78
13	11,220	12,720	0·004 04
13 75	11,120	12,560	0·004 23

Consider an element of the rim corresponding to one blade. Then—

Volume of rim = $2{\cdot}84 \times 0{\cdot}37 = 1{\cdot}05$ cub. in.

Mass of rim = $0{\cdot}297$ lb.

Centrifugal force on unsupported element = 1,115 lb.

Force on blade = 2,210 lb.

$\therefore$ Total radial force = $2{,}210 + 1{,}115x$.

But this equals $0{\cdot}346t_2 . f_{r2}$, since $0{\cdot}346$ is the circumferential pitch corresponding to one blade, and as $t_2 = 0{\cdot}7$, and $f_{r2} = 11{,}120$—

$$2{,}210 + 1{,}115x = 2{,}695$$

or

$$x = 0{\cdot}435$$

This kind of information is useful in the initial stages of design, for if the permissible radial stress at the outer radius is known the thickness at the outer boundary of the disc may be readily estimated.

For analyses of the disc with sides having a straight taper, i.e. conical discs, the reader is referred to papers by Messrs. H. M. Martin (2), B. Hodkinson (3), and Dr. E. Honegger (4).

211. Stress Analysis in Rotors by Method of Superposition. If the stresses in a turbine disc are calculated for a given value of the rotational speed ω, the applied rim stress f_3 and the force-fit stress f_0, then the various constants a, A, b_1, b_2, B_1, B_2 which are found apply only to these particular conditions of speed and stress. The effects of varying the speed of rotation, the force-fit stress, etc. can only be found by repeating the calculation in which these factors are considered in combination.

It is possible, however, to calculate separately the stresses due to—

(1) the inertia of the wheel alone,

(2) the applied stress f_3 due to the blades and their attachment,

(3) the force-fit pressure f_0.

The resultant stress in the disc is then the sum of these three stresses. The stress due to the inertia of the wheel varies as the square of the speed, and the stresses due to f_3 and f_0 vary directly as the values of f_3 and f_0, respectively. This enables the effects of variations in the three factors to be calculated quickly and easily. For further particulars of the method the reader is referred to a paper (5) by the author. The method facilitates calculation of force-fit allowance, the magnitude of the force-fit pressure at any speed of rotation (and hence the speed at which a wheel will become loose) and the stresses in the stationary wheel.

212. Force-fit Allowance for Wheels Pressed or Shrunk on Shaft. If a solid shaft is subjected to a uniform stress f_0 at the surface, then it may be shown (Ref. 5) that if the axial stress in the shaft is neglected then the radial and tangential stresses are identical

throughout the shaft and equal in magnitude and sign to the applied stress f_0.

Then if the outer radius of the shaft is r_0, the change in radius y is given by the relation

$$y = \frac{r_0}{E}(f_t - \sigma f_r)$$

$$= \frac{r_0 \cdot f_0}{E}(1 - \sigma)$$

This is the radial contraction of the shaft due to the pressure intensity f_0. The change in radius of the rotor bore may be calculated by the methods given in Arts. 206, 208, and 210. This change of radius is, of course, an expansion, and the force-fit allowance on the radius is the sum of this expansion and the contraction of the shaft.

The tangential stress at the surface of a hollow shaft is

$$f_t = f_0\left(\frac{n^2 + 1}{n^2 - 1}\right)$$

where n is the ratio of the external to the internal radius of the shaft. From this and the value of f_0, the radial contraction of the shaft may be found as before.

213. The Disc of Constant Stress. If a turbine wheel can be constructed so as to be continuous through the centre, then it is possible to obtain a form which shall give a uniform stress, both radial and tangential, at all points. Such a disc is known as "the disc of constant strength."

Let $f = f_r = f_t$ be the constant stress. Substituting in eq. (202) and noting that f is a constant—

$$\frac{d}{dr}(rt) - t = -\frac{\mu\omega^2 r^2 t}{f}$$

or

$$t + r \cdot \frac{dt}{dr} - t = -\frac{\mu\omega^2 r^2 t}{f}$$

or

$$\frac{dt}{dr} = -\frac{\mu\omega^2 rt}{f}$$

$$\therefore \quad \frac{\delta t}{t} = -\frac{w\omega^2}{gf} \cdot r \cdot \delta r$$

Integrating, we have—

$$\int_{t_2}^{t_1}\frac{1}{t} \cdot dt = -\frac{w\omega^2}{gf}\int_{r_2}^{r_1} r \cdot dr$$

$$\therefore \quad \log_e \frac{t_1}{t_2} = \frac{w\omega^2}{2gf}(r_2^2 - r_1^2) \quad . \quad . \quad . \quad (228)$$

If t is the thickness at any radius r, and t_0 is the thickness at the centre, then—

$$\log_e \frac{t_0}{t} = \frac{w\omega^2 r^2}{2gf} = \frac{wu^2}{2gf} \quad . \quad . \quad . \quad (229)$$

or

$$t = t_0 \,.\, e^{-\frac{w\omega^2 r^2}{2gf}} \quad . \quad . \quad . \quad . \quad (230)$$

In employing these equations the same system of units must be used throughout.

The radial deformation y of the disc is given by the expression—

$$y = \frac{r}{E}(f_t - \sigma \,.\, f_r)$$

$$= \frac{fr}{E}(1 - \sigma)$$

and since f is a constant, y varies directly as r.

EXAMPLE 37. Calculate the thickness of a de Laval steam turbine rotor for values of the radius increasing by 1 in., given the following data: Uniform stress, 25,000 lb. per sq. in.; 10,000 r.p.m., density of steel, 0·283 lb. per cub. in.; diameter of disc just under rim, 24 in.; thickness of disc at this point, $\frac{3}{8}$ in.

$$\omega = \frac{10{,}000 \times 2\pi}{60} = 1{,}047 \text{ radians per sec.}$$

$$\therefore \quad \frac{w}{2g} \cdot \frac{\omega^2 r^2}{f} = \frac{0{\cdot}283}{64{\cdot}4 \times 12} \cdot \frac{1{,}047^2 \times r^2}{25{,}000}$$

$$= 0{\cdot}01608 r^2$$

$$\therefore \quad t = t_0 \,.\, e^{-0{\cdot}01608 r^2}$$

$$\therefore \quad \log_{10} t = \log_{10} t_0 - 0{\cdot}01608 r^2 \,.\, \log_{10} 2{\cdot}7183$$

$$= \log_{10} t_0 - 0{\cdot}00697 r^2$$

When $r = 12$ in., $t = 0{\cdot}375$ in.

Hence $t_0 = 3{\cdot}7758$.

$\therefore$ Equation for t is: $\log t = 0{\cdot}577 - 0{\cdot}00697 r^2$.

The work may be arranged as set out in Table XXVII on the opposite page.

A transverse section through one-half of the wheel is shown in Fig. 318. The method of attaching the spindle to the wheel while preserving the continuity of the disc is indicated by the dotted lines. See also Art. 192, and Fig. 285.

214. Effect of Holes in Discs. The necessity of drilling a number of pressure-equalizing holes in the wheels of impulse turbines has been pointed out in Art. 193. The influence of such holes on the maximum stresses in the disc or wheel may be approximately gauged from a consideration of the stresses at a small hole in a flat

TABLE XXVII

CALCULATIONS FOR DISC OF CONSTANT STRENGTH

r	r^2	$0{\cdot}00697r^2$	$\log_{10}t$	t
0	0	0·0	0·5770	3·7758
1	1	0·00697	0·5700	3·7156
2	4	0·02785	0·5492	3·5412
3	9	0·0626	0·5144	3·2689
4	16	0·1113	0·4657	2·9222
5	25	0·174	0·403	2·5290
6	36	0·251	0·326	2·1180
7	49	0·341	0·236	1·7220
8	64	0·445	0·132	1·3552
9	81	0·564	0·013	1·0304
10	100	0·697	$\bar{1}{\cdot}880$	0·7586
11	121	0·844	$\bar{1}{\cdot}733$	0·5407
12	144	1·003	$\bar{1}{\cdot}574$	0·3750

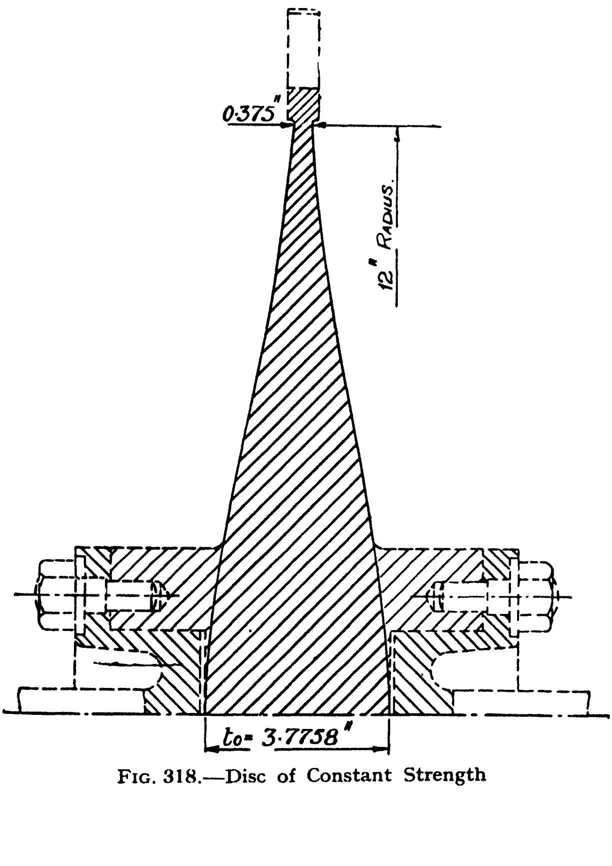


FIG. 318.—Disc of Constant Strength

plate subjected to a tension. This problem has been studied mathematically and the results checked by photo-elastic and other methods. The results may be very briefly summarized as follows. If a flat plate (Fig. 319 (*a*)) be subjected to a tensile stress which, at some distance from the hole, has a sensibly uniform value f, then the stress across the sections AB and CD varies in the manner shown by the curves, the maximum values at A and C being $3f$. The stresses at the edge of the hole are necessarily principal stresses, the radial stress (referred to hole) being zero. The tangential stress

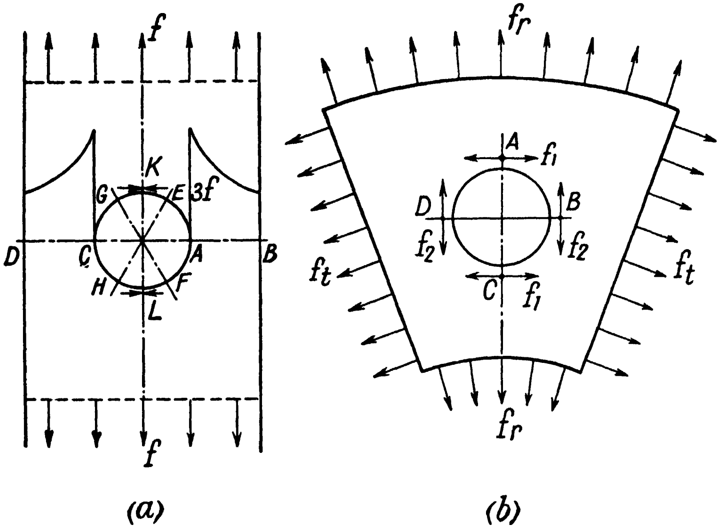


FIG. 319 Stresses at Holes

is tensile over the arcs EAF and GCH, steadily diminishing from A and C and vanishing at E, F, G, and H. Between E and G, and F and H, the tangential stress is compressive, reaching the maximum value, equal to f, at K and L.

Consider now an element of a turbine disc symmetrical about the hole ABCD, Fig. 319(*b*), and a radial line through the centre of the hole and of the disc, and suppose for the sake of illustration that at some little distance from the hole the radial and hoop stresses f_r and f_t in the disc are sensibly uniform. Then, by the principle of superposition, the stresses at A and C, acting in the direction shown by the arrows, due to the imposed disc stresses, will be approximately equal to-

$$f_1 = 3f_t - f_r$$

and the tensile stresses at B and D will be equal to—

$$f_2 = 3f_r - f_t$$

In the most favourable case, where f_r is approximately equal to f_t the concentrated stress reaches the value $f_1 = f_2 = 2f_t$ The above analysis must be regarded as approximate only, giving the order of the greatest stress rather than its absolute magnitude

The problem of stress concentration due to non-central holes in a plain disc of uniform thickness has been analysed by Dr A Quirk at the University of Liverpool, using relaxation methods and the photoelastic 'frozen stress' technique Fig 320 shows a typical

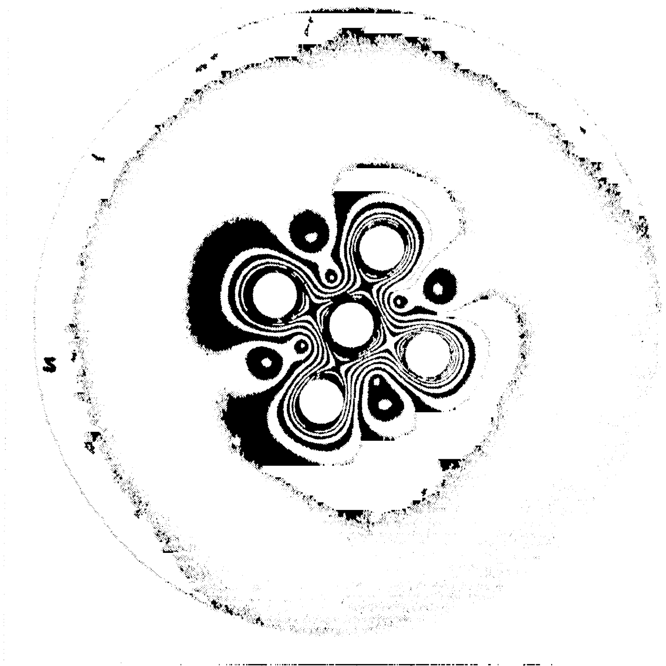


Fig 320 Photoelastic Fringe Pattern in Model Disc

fringe pattern in a disc of Dekorit U 300A 8 0 in diameter with a central hole 0 5 in diameter and having four non central holes 0 5 in diameter at a radius of 1 0 in The disc thickness is 0 189 in and the speed of rotation 2 500 r p m

Fig 321 shows the way in which the stress concentration factor K varies with the radial distance of the non central holes from the disc centre It will be seen that for the more highly stressed point B the experimental results are in fair agreement with the results obtained by the approximate method given above for the range L/R_2 0 6 – 0 75, while for point A the agreement is fairly good over the whole range of values of L/R_2

215. Pre-stressing by Overspeeding. A more favourable distribution of stress in a turbine rotor may sometimes be obtained by intentionally overspeeding the rotor and causing the elastic limit of the material to be exceeded in certain regions of the wheel. This sets up a state of stress in the stationary wheel, which, when superimposed on the stresses produced by rotation, results in a more uniform distribution of the hoop stress. The method is illustrated

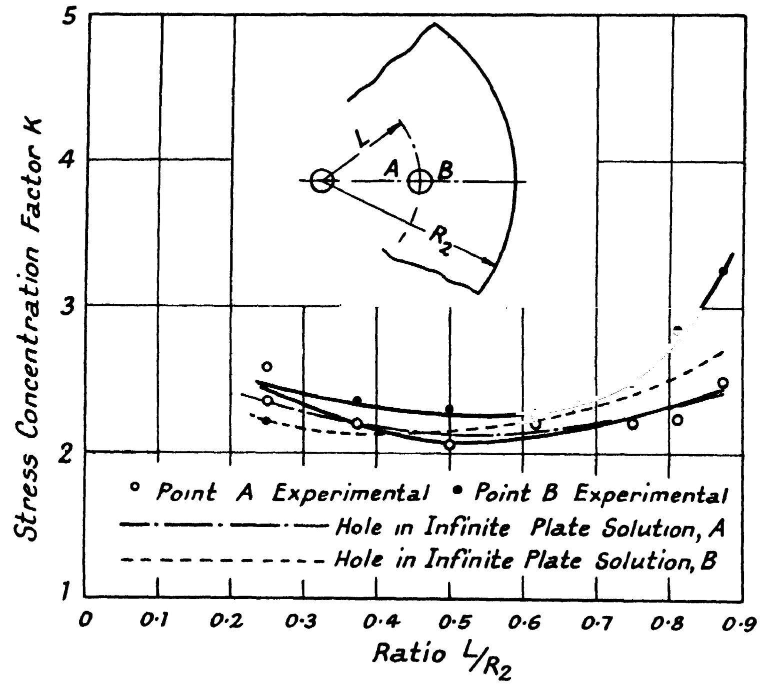


FIG. 321.—Variation of Stress Concentration Factor for Rotating Disc with Non-central Holes

by Fig. 322, which shows stress curves for a disc 40 in. diameter with a central hole 8 in. diameter. At 3,000 r.p.m. ($u = 524$ ft. per sec.) the curves of hoop stress and radial stress are A and B respectively. Suppose that the yield stress for the material is 50,000 lb. per sq. in. Then if the speed be increased to 4,320 r.p.m. the hoop stress curve is C and the radial stress curve is D. The maximum hoop stress is now just equal to the yield stress, and provided this stress is not exceeded, the disc on coming to rest will return to its former dimensions and will be quite free from stress. If now the speed is increased to, say, 5,000 r.p.m., the material near the centre of the disc will be in the plastic state and will yield at a stress equal

to, or even lower than, the yield stress. The distribution of hoop stress will then be given by a curve such as E, and of radial stress by a curve such as F. If the disc is now allowed to come to rest, the outer part of the disc contracts elastically and puts the inner part in compression. The radial stress is now entirely compressive, as shown by the curve G, while the hoop stress, curve H, is partly

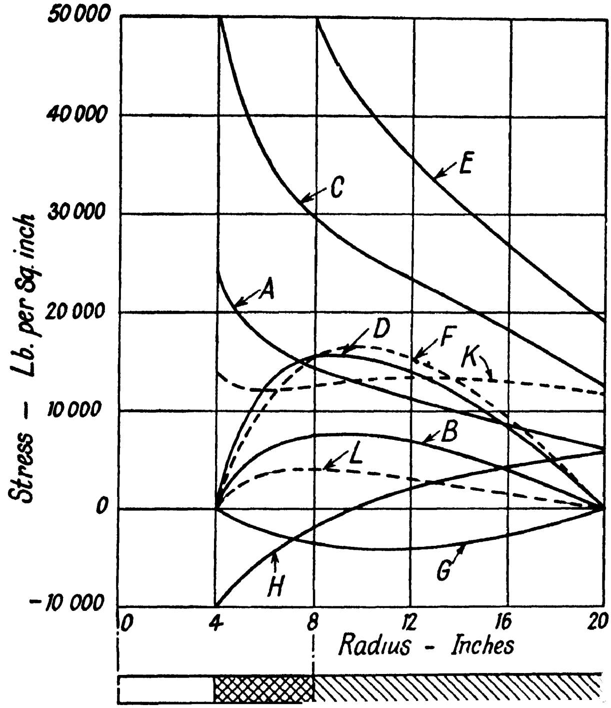


FIG. 322

compressive and partly tensile. If now these stresses are superimposed on the original stress curves A and B, we obtain the hoop and radial stress curves, K and L, respectively.

Messrs. C. A. Parsons & Co., Ltd., have used this method of overspeeding turbine rotors since the year 1905. Particulars of the method have been published in a paper (6) by Mr. C. D. (now Sir Claude) Gibb. Like most builders of large steam turbines, Messrs. Parsons have an overspeed test chamber constructed of strongly reinforced concrete 3 ft. thick, covered with earth to a depth of 15 to 18 ft. Rotors to be tested are set up in bearings in the test chamber and driven by an electric motor which is under remote control. The unbladed rough-machined shaft or disc is driven at a speed 1·5 times the normal speed. In the case of discs, the overspeed

is carried on until the eye of the disc opens out and takes a slight permanent set.

216. Materials and Working Stresses. The type of material used will depend chiefly upon the estimated stress in the rotor and on the temperature to which the discs or wheels are submitted. The subject of materials and the heat treatment thereof is so vast that it is impossible to do more than give a few scanty facts on possible working stresses.

Before touching on the subject of materials, something may be said about the term "factor of safety." This, as is well known, is taken to mean the ratio of the strength of the material, based on test bars, to the estimated maximum stress in the part under consideration. In some fields of engineering work, the ultimate strength of the material is taken as the basis; in others, it is considered that the yield point (in place of the true elastic limit, which is difficult to determine) should also be considered in estimating working stresses. While avoiding a discussion of a somewhat difficult subject, it may be said that in dealing with materials which have a well-marked yield point there seem good reasons for taking this property into account. As already stated on page 454, Mr. K. Baumann recommends that the mean of the factors of safety referred to the yield point and the ultimate strength should not be less than four when the stresses have been calculated for the normal speed.

It should be pointed out that such a factor of safety is nominal, the real factor depending on the stress conditions. According to the strain-energy theory of elastic failure (which has received a certain amount of experimental support), if a material is subjected to two principal stresses f_1 and f_2, and if the yield point of the material be f_y and Poisson's ratio be σ, then—

$$f_1^2 + f_2^2 - 2\sigma f_1 f_2 = f_y^2$$

Taking $\sigma = 0{\cdot}3$ for steel—

$$f_1^2 + f_2^2 - 0{\cdot}6 f_1 f_2 = f_y^2$$

In many turbine discs, the radial and hoop stresses are approximately equal. In such a case, a stress equal to 0·845 times the yield stress would produce elastic failure. It will be seen, therefore, that in the case we have just considered, if the apparent factor of safety based on the yield stress of the material is 3, the real factor is not 3, but 2·55, while at an overspeed of 10 per cent the real factor of safety is only a little over 2.

For rotors subjected to moderate stresses and temperatures, a plain carbon steel may be used. The properties of such a steel depend on the percentage of carbon and other elements. The following data are taken from a paper by Dr. W. H. Hatfield. Steel No. 1 had the following analysis: C 0·25; Mn 0·58; Si 0·11; Ni 0·13; while No. 2 gave: C 0·33; Mn 0·58; Si 0·21; and Ni 0·20.

The safe working stresses for steels 1 and 2 would be about 16,000 and 18,000 lb. per sq. in. respectively.

Steel No.	1		2
Heat Treatment	Normalized 890° – 900° C.	Annealed 660° C. for 48 hr.	Normalized 850° C.
Limit of proportionality	17·5 tons/sq. in.	14·7 tons/sq. in.	19·5 tons/sq. in.
Yield point	20·6 ,,	16·5 ,,	23·5 ,,
Ultimate stress	33·9 ,,	29·8 ,,	38·2 ,,
% Elongation	30·0	32·0	28·0
% Red. of area	63·6	60·0	60 7
Ratio: $\frac{\text{Y.P.}}{\text{U.S.}}$	0·61	0·55	0 62

The addition of nickel to a carbon steel increases the strength and also raises the yield point ratio. Typical properties of nickel steel are as follow—

Percentage of Nickel	3		5	
Condition	Annealed	Heat* Treated	Annealed	Heat* Treated
Yield point, tons/sq. in.	27	47	28	47
Ultimate strength, tons/sq in.	39	55	43	65
% Elongation	31	22	19	20
% Red. of area	64	57	42	60
Ratio: $\frac{\text{Y.P.}}{\text{U.S.}}$	0·69	0·85	0·65	0·72
Safe working stress, lb./sq. in.	18,500	28,500	20,000	31,000

For high temperatures and high stresses, steels containing the element molybdenum are now used. Such steels may be hardened without quenching and are thus known as air-hardening steels. A typical material of which particulars have been published is Vickers' Vibrac steel. The approximate composition of Vibrac V30 is: C 0·3; Si 0·15; Mn 0·60; P 0·03; S 0·04; Ni 2·5; Cr 0·60; and Mo 0·60. Vibrac steel, oil hardened at 840° C. and tempered at 650° C., has the following mechanical properties: Yield point, 52 tons per sq. in.; ultimate strength, 60 tons per sq. in.; per cent elongation, 21·5; per cent reduction of area, 57. The probable safe working stress for such a material is about 31,000 lb. per sq. in.

* Oil quenched at 820° C.; tempered at 650° C., and again quenched in

For a full specification regarding the heat treatment of a turbine rotor forging, the reader is referred to the paper by Mr. C. D. Gibb (6).

For notes on materials for high temperatures see Appendix, page 841.

BIBLIOGRAPHY

1. STODOLA: *Dampf- und Gasturbinen* 1924, Sixth Edition; 312–340.
2. MARTIN: "Rotating Discs of Conical Profile." *Engineering*, 1923; 115; 1.
3. HODKINSON: "Rotating Discs of Conical Profile." *Engineering*, 1923; 116; 274.
4. HONEGGER: "Festigkeitsberechnung rotierender konischen Scheiben." *Zeit. ang. Math. und Mechanik*, 1927; p. 127.
5. KEARTON: "The Calculation of the Stresses in a Turbine Wheel by the Method of Superposition." *Proc. I. Mech. E.*, 1946; 155; 73.
6. GIBB: "Post-war Land Turbine Development." *Proc. I. Mech. E.*, 1931; 120; 413.
7. HATFIELD: "Permanence of Dimensions under Stress at Elevated Temperatures." *J. Iron & Steel Inst.*, 1931, No. II, p. 215.

EXAMPLES XXI

1. Assuming that the elastic limit of nickel steel is 66,000 lb. per sq. in. and that the density is 0·283 lb. per cub. in., at what peripheral speed could a thin ring be rotated in order that the hoop stress would just equal the elastic limit? What is the alteration in diameter of a ring originally 40 in. diameter, if $E = 30 \times 10^6$ lb. per sq. in.?

2. The following particulars refer to a direct-coupled marine turbine of the reaction type—

Outside diameter of drum	113 in.
Thickness of drum	1·5 ,,
Height of blades (above drum)	10·5 ,,
Axial pitch of rotor blades	2 ,,
Circumferential pitch of blades	0·445 ,,
Depth of blade groove	0·625 ,,
Width of blade groove	0·625 ,,
Weight of blade material per ft. length	0·246 lb.
R.p.m.	320

Calculate the average hoop stress in the rim.

3. A plain continuous disc 20 in. diameter and of uniform thickness is rotating 5,000 r.p.m. Calculate the maximum intensity of stress in the disc and the increase in diameter. Assume that $w = 0{\cdot}28$ lb. per cub. in., $E = 30 \times 10^6$ lb. per sq. in., and $\sigma = 0{\cdot}3$.

4. If the disc in Question 3 is loaded with an edge load of 3,000 lb. per sq. in. of peripheral area, calculate the maximum hoop stress in the disc and the increase in diameter.

5. If a disc of 20 in. diameter of uniform thickness, rotating 5,000 r.p.m., be pierced with a hole 4 in. bore for a shaft, and subjected to an edge load at the periphery of 3,000 lb. per sq. in., calculate—

(*a*) The hoop stress at the bore.
(*b*) The hoop stress at the periphery.
(*c*) The increase in diameter at the bore.
(*d*) The increase in diameter at the periphery.

Assume that the radial stress at the bore is zero.

6 A De Laval rotor of constant strength is to be run at 16,500 r p m The disc is 10 in diameter under the rim and the thickness at that point is 0 3 in The allowable stress is 20,000 lb per sq in and the weight of the material may be assumed to be 0 283 lb per cub in Calculate the thickness of the disc (*a*) at the centre (*b*) at a radius of 3 in

7 A disc of uniform thickness has external and internal diameters of 20 and 4 in respectively, and turns at 4,000 r p m The disc carries at its periphery a ring of blades which apply to the periphery a centrifugal force of 5,000 lb per in of circumference If the maximum stress in the disc is limited to 20,000 lb per sq in , what must be the thickness of the disc? Assume $E = 30 \times 10^6$ lb per sq in , $\sigma = 0\ 3$, and $w = 0\ 283$ lb per cub in

8 A series of discs 40 in diameter and 2 in thick are arranged close together on a hollow shaft which has external and internal diameters of 10 in and 4 in respectively When the discs are turning at 2,000 r p m they are subjected to an edge load of 6 000 lb per in of circumference and an internal pressure of 1,000 lb per sq in surface due to being shrunk on the shaft What is the maximum stress in the disc?

Calculate also the amount of shrink fit on the diameter, the mutual intensity of pressure between the bore of the discs and the surface of the shaft when the rotor is at rest, and the maximum stress in the stationary disc Assume $E = 30 \times 10^6$ lb per sq in , $\sigma = 0\ 3$, and $w = 0\ 283$ lb per cub in

CHAPTER XXII

THE CRITICAL SPEED OF TURBINE ROTORS

217. Definition. Consider a symmetrical body such as a turbine rotor whose mass-centre, for one reason or another, does not quite coincide with its geometrical axis. Then as the body is rotated, there will be a certain transverse force (whose direction rotates at the same speed as the shaft) tending to deflect the shaft. It is found by experience that as the speed is increased the deflection of the shaft from its rest position also increases. As a particular speed is approached, the deflection increases very rapidly and may be so great that the shaft becomes permanently bent. If the speed be increased so rapidly that there is insufficient time for the deflection to grow, then it is found that after the above-mentioned speed is passed, the deflection begins to diminish and smoother running is obtained. The speed at which the shaft displacement tends to be very large is known as the critical speed. As the mass-centre rotates about the rest axis, the shaft behaves like a very taut skipping rope; hence the phenomenon is known as "whirling," and the critical speed is often referred to as the whirling speed. In certain cases, if the speed is increased still further a second resonant speed is encountered, then a third, and so on.

218. Balancing. Theoretically, a turbine rotor is a balanced body, but actually, errors of balance are introduced by various causes, such as—

(1) Lack of homogeneity of the material.
(2) Slight errors in machining.
(3) Differences in the pitch of the blades and also in their individual masses.

Thus it is always necessary to test the balance of a completed turbine rotor and make any adjustments necessary to ensure that the balance is as good as it is possible to make it. There are two chief methods of balancing turbine rotors, namely, the static and dynamic methods.

(1) *Static Balancing.* The simplest method of static balancing is to place the rotor with its journals on two dead level metal surfaces, which are commonly termed "knife edges," but which have a narrow flat surface. The rotor is placed in various positions and allowed to roll until it comes to rest. If rolling friction were absent the rotor would finally come to rest with its mass-centre vertically below the geometrical axis—assuming the rotor to be out-of-balance. Actually, rolling friction does not permit the mass-centre to reach this position, but if the rotor be rolled to rest in

both directions the correct direction of the mass-centre will bisect the angle between the apparent directions. Once the heavy side has been found, trial balance weights are added to the light side and varied by trial and error until the rotor will remain at rest in any position on the knife edges. The rotor may now be balanced either by attaching or removing mass from the rotor in such a way that the moment of added mass is equal to that of the trial balance weight. It is generally preferable to remove the mass by chipping and filing or by drilling holes, according to the circumstances. Some turbine builders machine special grooves in the end discs or wheels for the insertion of balancing masses which are finally secured by screws. Experiments made by the author show that the limit of accuracy possible by this method depends upon the material used for the knife edges, and may be expressed by the final displacement δ of the mass-centre from the axis of rotation.

For mild steel journals on cast-iron knife edges, $\delta = 0{\cdot}00113$ in.

For mild steel journals on hardened steel knife edges, $\delta = 0{\cdot}0004$ in.

Such a close approach of the mass-centre to the axis of rotation as 0·0004 in. may seem at first sight to be a very satisfactory result, but a simple analysis will show that the ratio of centrifugal force to the weight of the rotor is about 10 per cent at 3,000 r.p.m. and no less than 40 per cent at 6,000 r.p.m.

The following is a simple method of static balancing which gives a greater refinement than the rough method described above. Assuming that the rotor is set up on "knife edges" or rolling ways, the periphery of the wheel at one end is divided into, say, eight equal parts and these are numbered in order. To overcome rolling friction and produce an appreciable amplitude of roll, a constant mass, the "rolling weight," is attached to the rotor at each of the eight stations in turn. In each case the rolling weight is brought into the horizontal plane and the rotor then carefully released. The distance which the journal rolls along the rolling ways before coming momentarily to rest is measured for each of the eight positions. This is repeated by rolling the rotor in the opposite direction and the mean amplitude of roll obtained for each station. These values are plotted against station numbers and a curve resembling a sine curve obtained. The heavy side is indicated by the greatest amplitude. Trial masses are now added on the light side and the process repeated until the amplitudes are practically identical. By the adoption of such a method the residual displacement δ of the mass-centre should not exceed about 0·0002 in. if the balancing is done on steel knife edges.

(2) *Dynamic Balancing*. That the "static" method of balancing does not necessarily lead to good balance in the case of a complete rotor will be at once evident from Fig. 323. Let W_1 and W_2 be two out-of-balance masses in a plane containing the axis and at radii r_1

and r_2 respectively, such that W_1r_1 is equal to W_2r_2. Then, so far as it is possible to detect want of balance by "static" methods, the rotor is in perfect balance, since the moment of W_2 about the axis

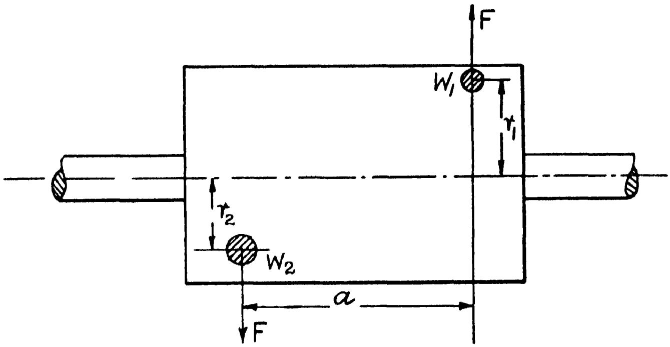


FIG. 323

will balance that of W_1 in any position. If now the rotor is made to rotate, centrifugal forces F, which are equal, act on the mass of rotor, producing a couple F*a* and causing "rough" running.

Various dynamic balancing machines have been devised and employed, but one of the most successful is the Lawaczek-Heymann

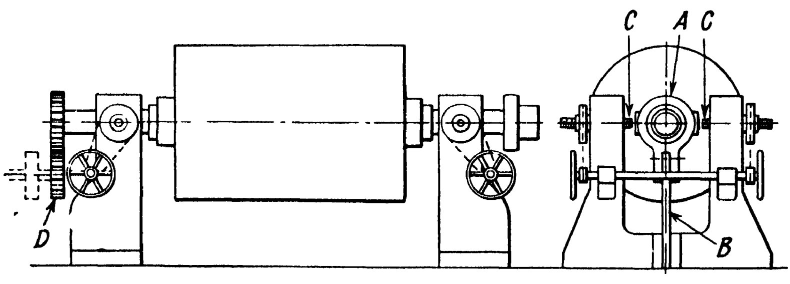


FIG 324 —Lawaczek-Heymann Balancing Machine

machine constructed by Messrs. C. Schenk, of Darmstadt. The principle of this machine is illustrated diagrammatically in Fig. 324. The rotor is carried in bearings A which are supported by a vertical spring or reed B, made of steel. This reed is rigidly fixed at its lower end in a heavy bedplate, but is free to move laterally when the screwed stops C are withdrawn. It will be clear that for any given reed and any given weight of rotor there will be a particular speed at which, if the rotor is out of balance, the inertia forces will produce resonance. The reeds are so designed that the resonant speeds vary

from 200 to 500 r.p.m. The rotor is driven by an electric motor either through a magnetic clutch or a spur gear D, which may be withdrawn. In making a balance, both ends of the rotor are locked and the rotor run up to a speed above the resonant speed. After disconnecting the driving motor, the stops are withdrawn from one of the bearings, so that it is free to oscillate, the other bearing remaining fixed. As the speed falls the oscillations increase as the resonant speed is approached. The amplitude of oscillation, magnified ten times, is recorded on a drum. Various methods are employed to detect the heavy side of the rotor. In one method a small constant mass is attached to the rotor at each of eight points equally spaced round the end wheel, and the amplitude measured. The point for which the amplitude is least shows the light side, and balance weights are added to this side until one end of the rotor appears to be balanced. The bearings at that end are now locked and the others freed. The process is repeated for the other end and a temporary balance effected. That end is next locked and a re-balance made at the end which was first balanced. This process is repeated until a correct running balance is obtained with both bearings free. The sensitivity of the Lawaczek-Heymann machine is stated to be such that the final displacement δ of the mass-centre from the axis is of the order 0·00008 to 0·0001 in. The American Westinghouse Co. have designed and constructed balancing machines operating on a similar principle. The maximum out-of-balance obtained with these machines is stated to be 1 in.-oz. per 1,000 lb. rotor weight, i.e. δ is about 0·00006 in.

However carefully a rotor may be balanced, it is essential that there should be a sufficient margin of speed between the normal speed of rotation and the critical speed. The latter must be calculated in the design stage, and the proportions of the shaft or rotor must be so chosen that the necessary margin can be guaranteed. When the critical speed is higher than the running speed, the shaft is said to be "stiff"; when it is lower than the running speed the shaft is said to be "flexible." Either type of shaft may be used for constant-speed turbines such as those driving alternators, etc., but in marine work the rotor shaft should always be stiff.

A number of special cases arise for consideration.

219. Case I. *Small-diameter Shaft Supporting a Single Wheel.* Fig. 325 shows a very light spindle freely supported in spherical bearings and supporting a single wheel of mass W lb. All deflections are much exaggerated for the sake of clearness.

Note that Δ is the *static* deflection of the shaft at the wheel centre due to the weight of the wheel only. By considering a vertical shaft we can eliminate gravity, the rest position being the straight line through the bearings.

It will be assumed that imperfections of workmanship cause a

displacement δ of the mass-centre from the geometrical centre of the wheel. At low speeds the conditions are somewhat as represented in Fig. 325 (1) and (2). There is a force due to inertia which causes an increased deflection y.

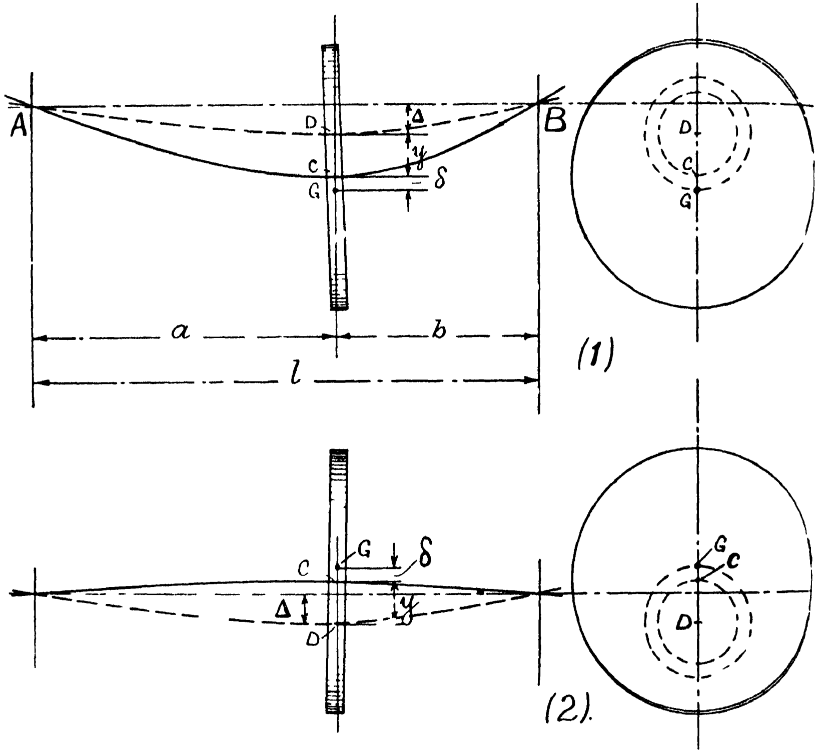


FIG. 325

In fact, the centre of gravity G rotates around the static shaft centre D in a circle whose radius is $y + \delta$, and everywhere the centrifugal force is equal to –

$$\frac{W\omega^2}{g}(y + \delta)$$

Similarly, the centre C rotates around the centre D in a circle whose radius is y; and if the stiffness of the shaft is F lb. per in. deflection at the point where the wheel is attached, i.e. if it requires F lb. to produce a deflection of unity at the point where

the wheel is attached to the spindle, then the force of restraint which just balances the centrifugal force will be—

$$Fy \text{ lb. weight.}$$

Hence
$$Fy = \frac{W\omega^2}{g}(y + \delta)$$

$\therefore$
$$y\left(F - \frac{W\omega^2}{g}\right) = \frac{W\omega^2 . \delta}{g}$$

and
$$y = \frac{\omega^2 . \delta}{\left(\frac{Fg}{W} - \omega^2\right)}$$

For any given accidental deflection δ, we may consider how y varies when ω is given different values.

(1) When ω^2 is less than $\frac{Fg}{W}$, y and δ have the same sign, and hence G is always situated from D on the other side of C. Moreover, as ω is increased, the denominator decreases and y gradually increases, until when ω^2 approaches $\frac{Fg}{W}$ the value of y approaches infinity.

(2) When ω^2 equals $\frac{Fg}{W}$, the denominator is reduced to zero and the value of y becomes infinite. This value of ω is the *critical.* It may be shown that the natural frequency of transverse vibration of the above system is—

$$\frac{1}{2\pi}\sqrt{\frac{Fg}{W}} \text{ vibrations per sec.}$$

Hence the critical speed in revs. per second is the same as the frequency of natural vibrations.

In all cases where the radii of gyration of the rotating masses are small compared with the length of the shaft, the critical speed coincides with the natural frequency of vibration. The correction required for "rotational inertia" is usually only a matter of 1 or 2 per cent, and as we usually require a figure with a margin of some 15 to 25 per cent, the effect may be neglected, and the question of critical speeds may be approached as the problem of finding the fundamental frequency of natural vibrations.

(3) When ω^2 is greater than $\frac{Fg}{W}$, i.e. when the running speed is greater than the critical, the value of the denominator increases and y is reduced. Moreover, the value of y is negative, which means that the centre of gravity G now lies between the static deflected centre D and the wheel centre C, as shown in Fig. 326, (1) and (2).

In this position the effective radius of the centre of gravity G is $y - \delta$ and, as y is further reduced, the effective radius $y - \delta$ is still further reduced. This goes on, until at a very high speed the value of $\frac{Fg}{W}$ becomes so small compared with ω^2 that y approaches the value $-\delta$ and then the wheel commences to rotate around its centre of gravity G, with great stability.

This is the principle of the *ingenious flexible shaft of Dr. de Laval.*

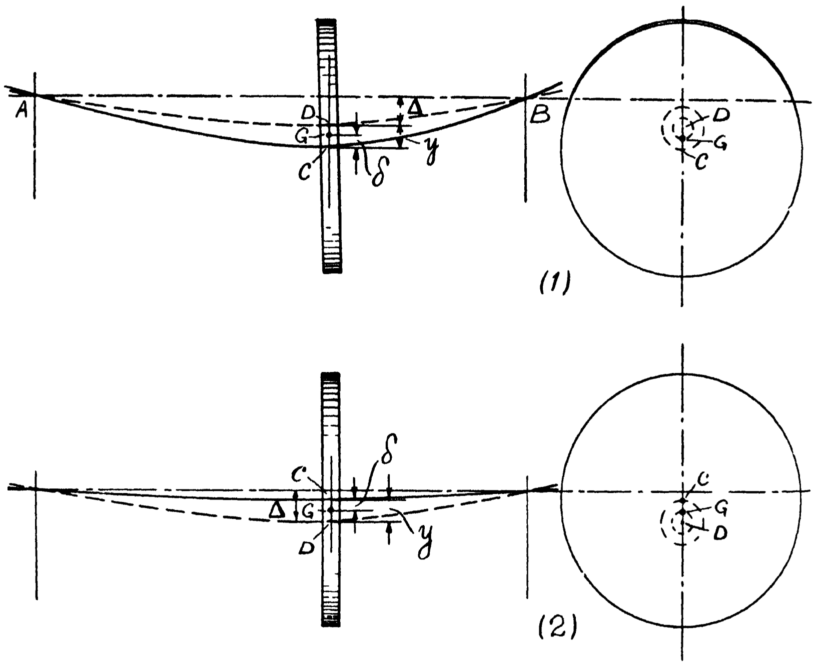


FIG. 326

In the above theory it has been shown that the whirling speed is equal to the natural frequency of transverse vibration of the same system. It has also been assumed that the centre of mass lies in the plane of bending of the shaft, i.e. y and δ are in the same straight line. At the critical speed, however, it can be shown experimentally that the centre of mass is at right angles to the plane of bending, i.e. y and δ are at right angles, while at speeds above and below the critical the truth of the previous deductions regarding the position of the mass-centre can be demonstrated.

In 1919 the late Dr. Jeffcott (1) formulated a new theory, dealing with the problem as a forced vibration. He maintained that the

shaft did not primarily rotate about its rest position, as we have assumed, but about its own centre line, i.e. that G does not rotate primarily about D at radius $y + \delta$, but about the wheel centre C, the centrifugal force being thus $\frac{W}{g}\omega^2\delta$. This force projected on to two planes at right angles introduces two similar simple harmonic forces in these planes. Two similar transverse vibrations of the same frequency ω as the disturbance and of amplitude y are thus forced, and the resultant of two such simple harmonic motions is a circular vibration of speed ω which, combined with the rotation of the shaft about its own axis, will produce rotation in a fixed bent shape. When the problem is treated in this way the same formula will be obtained as before but, in addition, all the observed phenomena can be explained.

$$\text{Hence the critical angular velocity} = \sqrt{\frac{Fg}{W}} \quad . \quad . \quad . \quad (231)$$

Let ω_c= critical angular velocity in radians per sec.

n_c= critical angular velocity in revolutions per sec.

N_c= critical angular velocity in revolutions per min.

g = acceleration of gravity (32·2 × 12 in. units).

$$\text{Since} \qquad \omega_c = \sqrt{\frac{Fg}{W}}, \; n_c = \frac{1}{2\pi}\sqrt{\frac{Fg}{W}}$$

Let l = span of bearings in inches.

I = second moment of area of shaft section (in.^{4}).

E = Young's Modulus of Elasticity.

$$\text{Then static deflection } \Delta \text{ at wheel centre} = \frac{cWl^3}{EI}$$

where c is a constant depending on the method of supporting the shaft.

$$\text{Similarly, unit deflection } 1 = \frac{cFl^3}{EI}$$

$$\therefore \qquad F = \frac{EI}{cl^3}$$

$$\text{Hence} \qquad n_c = \frac{1}{2\pi}\sqrt{\frac{EIg}{cWl^3}} = \frac{1}{2\pi}\sqrt{\frac{g}{\Delta}}$$

$$\therefore \qquad N_c = \frac{30}{\pi}\sqrt{\frac{g}{\Delta}} = \frac{187\cdot 7}{\sqrt{\Delta}} \text{ r.p.m.} \quad . \quad . \quad . \quad (232)$$

Values of c—

(1) Both ends of shaft simply supported $c = \dfrac{a^2b^2}{3l^4}$

(2) Both ends of shaft fixed $c = \dfrac{a^3b^3}{3l^6}$

(3) End A fixed, end B simply supported—

$$c = \frac{a^3b^2\,(3a + 4b)}{12l^6}$$

EXAMPLE 38. The rotor of a De Laval turbine weighs 4 lb., the shaft is $\frac{3}{8}$ in. diameter, and the span of the bearings is 14 in. The

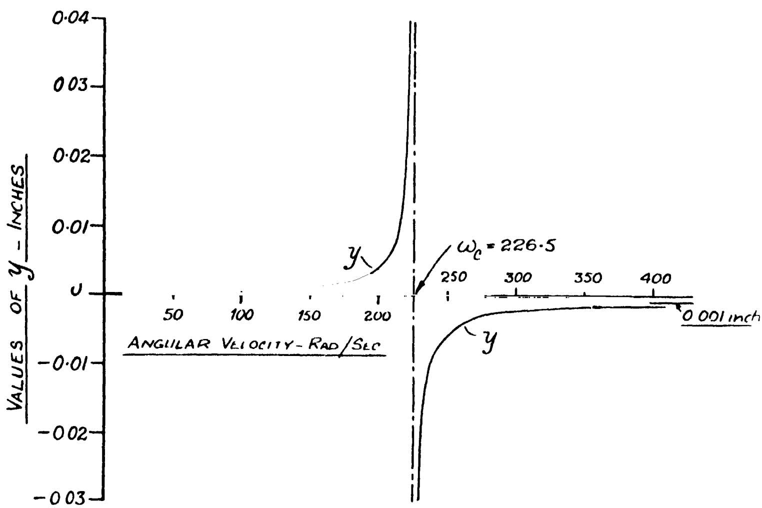


FIG. 327

wheel is 8 in. from one bearing. Calculate the critical speed, assuming both ends free and $E = 30 \times 10^6$ lb. per sq. in.

If $\delta = 0{\cdot}001$ in., calculate and plot values of y for various values of ω.

$$\text{Static deflection } \Delta = \frac{Wa^2b^2}{3EIl} \quad \left(I = \frac{\pi d^4}{64}\right)$$

$$= \frac{4 \times 8^2 \times 6^2}{3 \times 30 \times 10^6 \times 0{\cdot}0009705 \times 14}$$

$$= 0{\cdot}007539 \text{ in.}$$

$$\text{Critical speed } N_c = \frac{187{\cdot}7}{\sqrt{0{\cdot}007539}} = 2{,}162 \text{ r.p.m.}$$

Since 4 lb. produces a deflection 0·007539 in., the force to produce unit deflection must be—

$$\frac{4}{0{\cdot}007539} = \mathrm{F}$$

$$\therefore \qquad \frac{\mathrm{F}g}{\mathrm{W}} = \frac{32{\cdot}2 \times 12 \times 4}{4 \times 0{\cdot}007539} = 51{,}240$$

Hence $$y = \frac{0{\cdot}001\omega^2}{51{,}240 - \omega^2}$$

A few values of y are given below for corresponding values of ω—

ω	0	100	200	224	226	226·5	230	2,000
y	0	·00024	·00356	·0483	·365	∞	–·032	–·001013

A graph showing these results is given in Fig. 327.

220. Rayleigh's Approximate Solution for the Fundamental Frequency of a Single-span Beam or Shaft. During a free vibration the total energy of the system remains constant. Thus, considering a shaft vibrating transversely, the maximum kinetic energy as the shaft passes through its mid-position will be equal to the maximum strain energy at the end of a vibration. To evaluate these terms the displacement of every point in the shaft during vibration must be known, i.e. the shape of the vibration curve must be known.

Lord Rayleigh has shown that different assumptions regarding the shape, provided they are reasonably like the actual shape, make very little difference to the calculated frequencies, the frequency obtained always being higher than the actual, since a wrong shape means greater constraint and therefore stiffening of the shaft.

A simple assumption is to consider that the shape taken by the shaft during vibration is that of the static deflection curve when the shaft is supported horizontally, i.e. if any one point in the shaft suffers a deflection from its rest position proportional to its static deflection then the deflection of every other point is the same proportion of its static deflection. But since the amplitude does not affect the frequency, we may assume that the amplitude of vibration of any point is equal to its static deflection. This gives a very simple solution for the strain energy since the force causing this deflection is equal to the loading.

221. Case II. *Uniform Shaft with Uniformly-distributed Load, Ends Freely Supported.* (Fig. 328.)

Let l = length of shaft between bearings (inches).

w = load per in. length in lb.

I = second moment of area of shaft (inch units).

y = static deflection of shaft at a point x in. from one end.

Consider an element of the shaft δx units long. Then mass of element $= w \,.\, \delta x$.

Strain energy for element for deflection $y = \frac{w \,.\, \delta x}{2} \times y$

$\therefore$ Total strain energy for shaft $= \frac{w}{2}\int_0^l y \,.\, dx$

Let ω_c = angular velocity of shaft (critical).

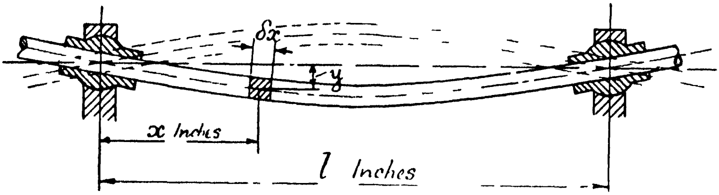


FIG. 328

Then maximum velocity of element $= \omega_c y$

and maximum kinetic energy of element $= \frac{w \,.\, \delta x \,.\, \omega_c^2 y^2}{2g}$

Hence total kinetic energy $= \frac{w\omega_c^2}{2g}\int_0^l y^2 \,.\, dx$

Equating strain energy to kinetic energy, we have—

$$\frac{w \,.\, \omega_c^2}{2g}\int_0^l y^2 \,.\, dx = \frac{w}{2}\int_0^l y \,.\, dx$$

$$\therefore \qquad \omega_c^2 = \frac{g \,.\, \int_0^l y \,.\, dx}{\int_0^l y^2 \,.\, dx}$$

It may be shown that the deflection y is given by the expression

$$y = \frac{w}{24\text{EI}}(x^4 - 2lx^3 + l^3x)$$

By substituting this value for y in the above equation and integrating, we have—

$$\omega_c^2 = \frac{97{\cdot}55\, g\text{EI}}{wl^4} \quad . \quad . \quad . \quad . \quad (233)$$

Let Δ = static deflection of shaft at the centre of its length (inches).

Then $$\Delta = \frac{5}{384}\frac{wl^4}{\text{EI}}$$

i.e. $\frac{EI}{wl^4} = \frac{5}{384\Delta}$ Hence $\omega_c^2 = \frac{97\cdot55 \times 32\cdot2 \times 12 \times 5}{384\Delta}$

$$\therefore \qquad \omega_c^2 = \frac{490}{\Delta} \quad \omega_c = \frac{22\cdot12}{\sqrt{\Delta}}$$

Hence
$$N_c = \frac{211\cdot5}{\sqrt{\Delta}} \text{ r.p.m.} \qquad . \quad . \quad . \ (234)$$

222. Other Critical Speeds. At speeds higher than the first critical speed the shaft settles down until the second critical speed is approached, when it commences to bend in the curve shown in Fig. 329 (*a*) with a nodal point at the centre of its length.

Half the length of the shaft is now under the same conditions as the whole shaft when passing through its first critical speed.

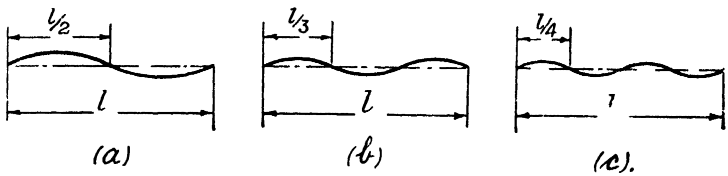


FIG. 329.—Form of Whirling Shaft at Second, Third, and Fourth Critical Speeds

Since deflection is directly proportional to (length)^4, the corresponding static deflection is now $= (\frac{1}{2})^4 = \frac{1}{16}$ of the static deflection for the fundamental critical speed. But N_c is inversely proportional to the square root of the deflection, hence N_c is 4 times the value given by the above equation. Hence the second, third, and fourth critical speeds are to the first as

$$1^2 : 2^2 : 3^2 : 4^2 \text{ or as}$$
$$1 : 4 : 9 : 16$$

Hence, in this particular case, there is a very wide range of speeds between the first and second critical speeds This is not always the case, however, as, for example, in a shaft freely supported on *three* bearings of equal span, where the second critical speed is only 1·56 times the first. In such a case, great care must be taken to ensure that, if the running speed should lie between the fundamental and second critical speeds, it is sufficiently far removed from either, being about 30 per cent in excess of the fundamental critical speed. Various factors contribute to make the practical running of flexible " three bearing " shafts a difficult proposition. The hubs of the wheels virtually increase the diameter of the shaft owing to the fact that they are forced on ; hence the probable critical speed is higher than that calculated on the bare shaft ; and

in a " three bearing " design in which the actual speed of rotation lies between the first and second critical speeds, there is some risk of the running speed being dangerously near the first critical speed.

223. Case III. *Uniform Shaft with Uniformly-distributed Load, Ends Fixed.* Let y equal the deflection of the shaft centre at any

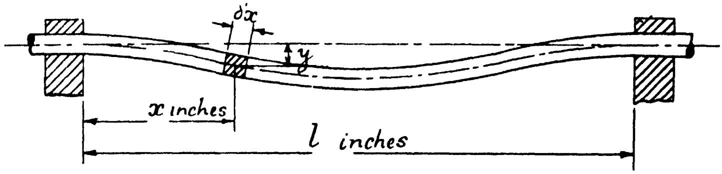


FIG. 330

distance x from the left-hand bearing. It is shown in textbooks on " Strength of Materials " that

$$y = \frac{w}{24EI}(x^2l^2 - 2lx^3 + x^4)$$

As shown in Art. 221, the critical angular velocity =

$$\omega_c^2 = \frac{g\int_0^l y \, . \, dx}{\int_0^l . y^2 . dx}$$

By substituting for y and integrating, we have—

$$\omega_c^2 = \frac{504gEI}{wl^4} \quad . \quad . \quad . \quad . \quad (235)$$

Let Δ = static deflection of shaft at the centre of its length measured in inches

$$\text{Then} \quad \Delta = \frac{wl^4}{384EI}$$

$$\text{i.e.} \quad \frac{EI}{wl^4} = \frac{1}{384\,\Delta} . \qquad \text{Hence } \omega_c^2 = \frac{504 \times 32{\cdot}2 \times 12}{384\,\Delta}$$

$$\therefore \quad \omega_c^2 = \frac{507}{\Delta} \qquad \omega_c = \frac{22{\cdot}52}{\sqrt{\Delta}}$$

$$\text{Hence} \quad N_c = \frac{215{\cdot}1}{\sqrt{\Delta}} \text{ r.p.m.} \quad . \quad . \quad . \quad (236)$$

224. Comparison of " Free " and " Fixed " Ends of Shafts. It is interesting to note the effect of fixing the ends of the shaft. When the ends are fixed, the deflection y at any point due to a given force applied at that point is much less than when the ends

are free. Hence for a constant centrifugal force $\frac{w \cdot \omega^2 y}{g}$, since y is reduced, ω^2 is increased and the critical speed is raised.

Load uniformly distributed } Thus if ω_1 = critical speed with "free" ends
,, ω_2 = ,, ,, "fixed" ,,

$$\left(\frac{\omega_2}{\omega_1}\right)^2 = \frac{504g\text{EI}}{wl^4} \times \frac{wl^4}{97 \cdot 55g\text{EI}}$$
$$= 5 \cdot 17$$
$$\therefore \qquad \omega_2 = 2 \cdot 27\omega_1$$

Whilst perfect constraint at the bearings will raise the critical speed to more than twice the value obtained with free ends, the mere fixing of the bearing brasses in the bearing block or housing could not produce such an effect unless the brasses gripped the shaft tightly. Such a condition is, of course, quite contrary to the requirements of practice. A fairly large radial clearance between the journal and the "brass" is required for lubrication purposes.

Referring to the worked example at the end of this chapter, the maximum slope at the bearings under gravity alone is 0·000127 radian; and since the bearing is 3 in. long, the total deflection of the journal at one end of the bearing, assuming the other end to act as a fulcrum, will be—

$$3 \times 0 \cdot 000127 = 0 \cdot 00038 \text{ in.}$$

when the increase of deflection due to whirling is everywhere equal to that produced by gravity. The actual oil clearance is 0·02, or

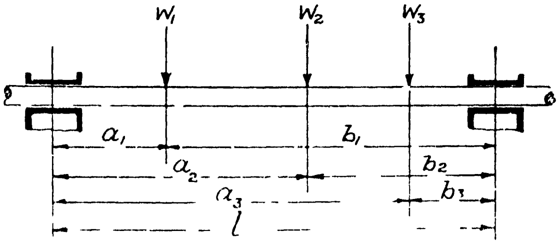


FIG. 331

50 times this amount. In other words, the brasses would not begin to exert constraint until the deflection produced at any point at the first whirling speed reached a value 50 times the normal deflection produced by gravity.

A few results for the most simple cases are summarized in Table XXVIII

TABLE XXVIII

CRITICAL SPEED OF SHAFTS IN SIMPLE CASES

$$\text{Critical speed in revs. per min.} = \frac{C}{\sqrt{\Delta}}$$

where C is a constant given in table below;
" Δ is the maximum static deflection in inches.

Conditions of Support	Type of Loading	C	Max. Deflection Δ Inches.
One end fixed	W concentrated at free end	187·7	$\frac{Wl^3}{3\,EI}$
One end fixed	*wl* uniformly distributed	235·0	$\frac{wl^4}{8\,EI}$
Two ends free	W concentrated at centre of span	187·7	$\frac{Wl^3}{48\,EI}$
Two ends free	*wl* uniformly distributed	211·5	$\frac{5\,wl^4}{384\,EI}$
Two ends fixed	W concentrated at centre of span	187·7	$\frac{Wl^3}{192\,EI}$
Two ends fixed	*wl* uniformly distributed	215·1	$\frac{wl^4}{384\,EI}$

225. Case IV. *Dunkerley's Semi-empirical Formula for the First Critical Speed of a Uniform Shaft Carrying a Number of Concentrated Loads (in the form of wheels).* The following formula is of a semi-empirical nature, and is based upon a number of valuable experiments carried out by the late Professor Dunkerley (2).

If it is assumed that the shaft is of uniform diameter or very nearly so, the formula gives results which are sufficiently accurate for most purposes.

Let N_s= critical speed of shaft alone—revs. per min.

N_1= " " when supporting W_1 only and when the influence of the shaft is neglected. (Case I.)

N_2= critical speed of shaft when supporting W_2 only.

N_3= " " " W_3 "

N_c= " of complete system.

Then $$\frac{1}{N_c^2} = \frac{1}{N_s^2} + \frac{1}{N_1^2} + \frac{1}{N_2^2} + \frac{1}{N_3^2} \quad . \quad . \quad (237)$$

EXAMPLE 39. The rotor of a De Laval turbine weighs 3·45 lb. (wheel only), and the spindle is $\frac{3}{8}$ in. diameter. The span of the bearings is 11 in., and the centre of the wheel is 6·2 in. from the centre of one of the bearings. Calculate—

(1) The static deflection of the shaft at the wheel centre.
(2) The critical speed of the rotor, assuming a weightless shaft
(3) The critical speed by Dunkerley's formula.

(1) $$I = \frac{\pi d^4}{64} = \frac{\pi \times 3^4}{64 \times 8^4} = 0{\cdot}0009705 \text{ ins.}^4$$

$$\Delta = \frac{Wa^2b^2}{3EI \,.\, l} = \frac{3{\cdot}45 \times 38{\cdot}44 \times 23{\cdot}04}{3 \times 30 \times 10^6 \times 0{\cdot}0009705 \times 11}$$

$\therefore \quad \Delta = 0{\cdot}00318$ in. **Ans.** (1)

(2) $$N_1 = \frac{187{\cdot}7}{\sqrt{\Delta}} = \frac{187{\cdot}7}{\sqrt{0{\cdot}00318}} = 3{,}329 \text{ r.p.m.} \quad \textbf{Ans. (2)}$$

(3) Deflection (maximum) of shaft due to its own weight

$$= \frac{5wl^4}{384EI} = \Delta_s$$

$w =$ (wt. per cub. inch of steel) $\times$ (Vol. of shaft per in. length)
$= 0{\cdot}283 \times 0{\cdot}7854 \times (\frac{3}{8})^2 = 0{\cdot}0312$ lb. per in.

$$\therefore \quad \Delta_s = \frac{5 \times 0{\cdot}0312 \times 11^4}{384 \times 30 \times 10^6 \times 0{\cdot}0009705} = 0{\cdot}0002044 \text{ in}$$

Hence, critical speed of shaft alone — $N_s = \dfrac{211{\cdot}5}{\sqrt{\Delta_s}}$

" " " $= \dfrac{211{\cdot}5}{\sqrt{0{\cdot}0002044}} = 14{,}760$

By Dunkerley's equation—

$$\frac{1}{N_c^2} = \frac{1}{N_s^2} + \frac{1}{N_1^2} = \frac{1}{(14{,}760)^2} + \frac{1}{(3{,}329)^2}$$

from which $N_c = 3{,}250$ r.p.m. **Ans.** (3)

Hence the correction in the above example for the mass of the shaft amounts to about 80 r.p.m. in 3,250 or about $2\frac{1}{2}$ per cent.

The number of practical examples of turbine rotors to which Dunkerley's equation can be applied is, indeed, very small. Generally, the diameter of the shaft is very variable, being much smaller at the journals than at the middle ; and the problem is

often further complicated by the fact that at the middle portion where the wheels are attached, the shaft is stepped so as to facilitate the attachment and removal of wheels.

A more exact method which is applicable to the general case of non-uniform loading and a shaft of variable cross-section is given in the following article.

226. Case V. *Critical Speed of a Shaft of Variable Cross-section and Loaded by a Number of Concentrated Loads.* Assume that the

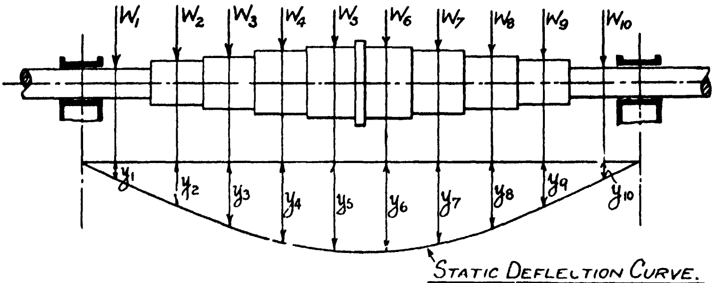


FIG. 332

non-uniform shaft in Fig. 332 is loaded with a number of concentrated loads, W_1, W_2, W_3, etc., which are arranged to include appropriate portions of the weight of the shaft. If "fixing" at the bearings is ignored, then the shaft may be treated as a beam of variable cross-section, freely supported at each end. The curve of static deflection (shown exaggerated) may then be drawn.

Let y_1, y_2, y_3, etc., represent the static deflection of the shaft at the points where the loads W_1, W_2, W_3, etc., are applied.

Then by the method of Art. 220, the total strain energy when the system is at its extreme position of vibration

$$= \frac{W_1y_1}{2} + \frac{W_2y_2}{2} + \frac{W_3y_3}{2} + \ldots$$

$$= \tfrac{1}{2}\,\Sigma Wy$$

Similarly, if ω_c = critical angular velocity, maximum kinetic energy of system

$$= \frac{\omega_c^2}{2g}\,(W_1y_1^2 + W_2y_2^2 + W_3y_3^2 + \ldots)$$

$$= \frac{\omega_c^2}{2g}\,\Sigma Wy^2$$

Hence $\omega_c^2 = \dfrac{g\Sigma Wy}{\Sigma Wy^2}$

$$\therefore \quad N_c = \frac{60}{2\pi}\sqrt{\left(\frac{g\Sigma Wy}{\Sigma Wy^2}\right)} \text{ r.p.m.} \qquad . \quad . \quad . \quad . \quad . \quad (238)$$

The derivation of the static deflection curve is a tedious process and has sometimes to be repeated two or three times during design. One method of obtaining it is to draw two funicular polygons, one giving the bending moment and the second giving the deflection. This method is described in textbooks on "Graphics" and is suitable for drawing office work.

A second method is to obtain the shearing force curve, and the bending moment, slope, and deflection curves successively, by a process of graphic integration, which may be effected largely by means of an ordinary planimeter. The latter method is illustrated by the following example—

EXAMPLE 40. To determine the critical speed of the turbine rotor shown in Fig. 333, assuming that it is freely supported by the bearings.

It is first necessary to calculate the weights which are to produce the static deflection. These include the weights of various portions of the shaft and also of the wheels. The various weights are clearly indicated in the upper portion of Fig. 333.

By taking moments of the weights about the right-hand bearing, the upward reaction at A is found to be 301 lb. The total load is 621 lb., so that the reaction at the right-hand bearing is 320 lb. With this information, the shearing force diagram (F) can be drawn.

Scale for shearing force on original 1 in. = 100 lb.
Length scale ,, 1 ,, = 4 in.

The bending moment curve may now be drawn by commencing with a zero bending moment at the extreme left hand, and integrating the shearing force diagram graphically. Thus, if any section be chosen, as at D, and A_F represents the area (positive) of the shearing force diagram from 0 to D, then since 1 sq. in. area of the shearing force diagram must represent—

$$4 \times 100 = 400 \text{ lb.-in.}$$

the bending moment M_D at D must be—

$$400\, A_F \text{ lb.-in.}$$

This may be set down to scale, giving the M curve as shown by the broken line in Fig. 333.

The scale for the M curve in the original was—

$$1 \text{ in.} = 1{,}000 \text{ lb.-in.}$$

∴ Actual height or ordinate M_D on diagram

$$= \frac{400 A_F}{1{,}000} \text{ in.}$$

It is easy to see that such work may be done by means of a planimeter and profitably set out in tabular form.

Before obtaining the slope curve, it is necessary to correct the

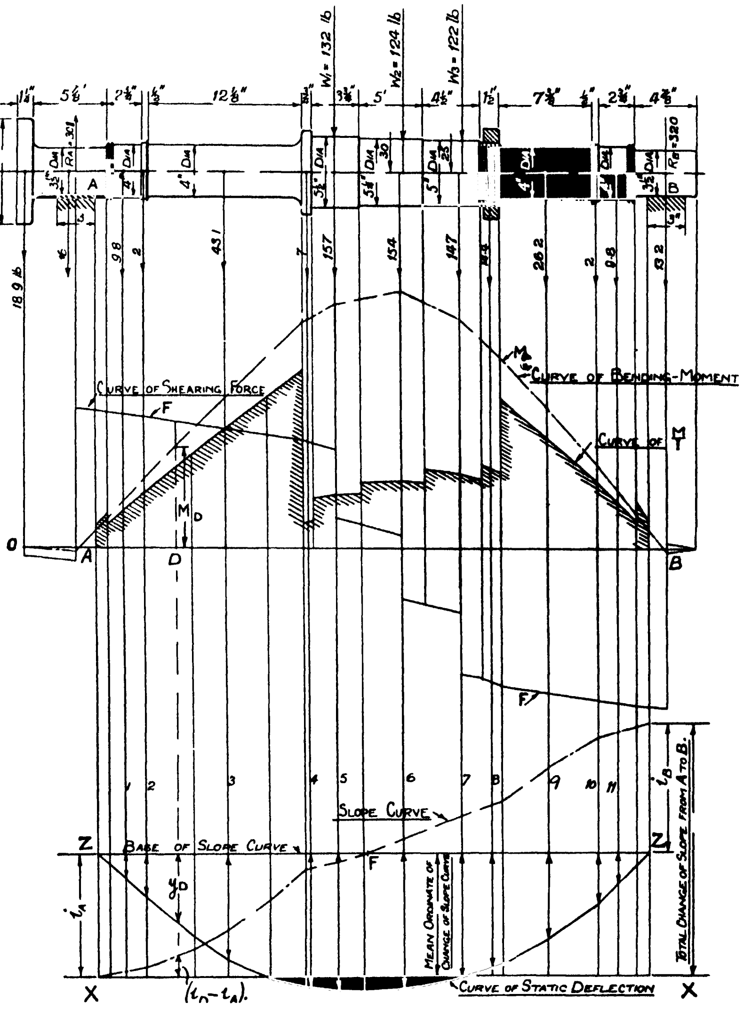


FIG. 333

Note. The original diagram was about 3·7 times this size.

bending moment curve for the varying cross-section of the shaft by dividing the values of the bending moment by the moment of inertia at each section. The derived or corrected $\frac{M}{I}$ curve is thus obtained.

Scale on original 1 in. $= 100 \frac{\text{lb.}}{(\text{inches})^3}$

It may be shown that the change of slope or inclination of a beam between any two points on it is equal to—

$$\frac{1}{E}\left(\text{Area of } \frac{M}{I} \text{ curve between those points}\right)$$

where E = Young's Modulus of Elasticity.

The $\frac{M}{I}$ curve is split up into a number of convenient sections, the areas are found, divided by E, and set up to scale on an assumed base line XX. For example, let A_M be the actual area of the $\frac{M}{I}$ curve between A and D.

$$1 \text{ sq. in. on original} = 100 \times 4 = 400 \frac{\text{lb.}}{(\text{inches})^2}$$

Then change of slope between A and D is—

$$i_D - i_A = \frac{1}{E} \times 400\, A_M. \text{ (radian)}$$

The end ordinate of this curve gives the total change of slope between A and B, which in this example works out to be 0·00024767 radian. The slope curve was set out on the original to a scale of

1 in. = 0·00005 radian

To find the true base of the slope curve, planimeter the area above XX, and divide it by the base XX, thus obtaining the mean-ordinate which in this case is also the slope or inclination of the shaft at A; setting up the mean-ordinate above XX, the true base line ZZ is obtained.

The deflection curve may now be obtained by integrating graphically the slope curve (above and below *ZZ*, *not* XX).

1 sq. in. area of slope curve = 4 × 0·00005
= 0·0002 in. deflection

Hence, if A_t = area of slope curve between A and D, deflection of D below A equals—

$$0{\cdot}0002 \times A_t \text{ in.} = y_D$$

In this way, the curve of deflection may be quickly obtained and the deflections read off at the points of application of the concentrated loads (imaginary and real). Maximum deflection in this example occurs at F (slope is zero), and equals 0·001364 in.

The information now available enables us to construct the following table—

TABLE XXIX

CALCULATION OF CRITICAL SPEED OF TURBINE ROTOR

Section	W	y	Wy	Wy^2
1 .	9·8	0·000 26	0·002 55	0·000 000 663
2 .	2·0	0·000 45	0·000 9	0·000 000 405
3 .	43·1	0·001 046	0·045 1	0·000 045 000
4 .	7·0	0·001 325	0·009 27	0·000 012 280
5 .	157·0	0·001 355	0·213	0·000 289 000
6 .	154·0	0·001 339	0·206	0·000 276 000
7 .	147·0	0·001 223	0·180	0·000 220 200
8 .	14·9	0·001 120	0·016 7	0·000 018 700
9 .	26·2	0·000 845	0·022 1	0·000 018 680
10 .	2·0	0·000 480	0·000 96	0·000 000 461
11 .	9·8	0·000 25	0·002 45	0·000 000 612
		Totals . .	0·699 03	0·000 882 001

Hence
$$\frac{g\Sigma Wy}{\Sigma Wy^2} = \frac{32{\cdot}2 \times 12 \times 0{\cdot}69903}{0{\cdot}000882001}$$
$$= 306{,}240$$

$$\therefore \qquad N_c = \frac{60}{2\pi} \cdot \sqrt{306{,}240} = 5{,}285 \text{ r.p.m.}$$

227. Relationship Between Critical Speed and Maximum Static Deflection. It will be apparent that, from the nature of the expression

$$N_c = \frac{60}{2\pi}\sqrt{\left(\frac{g \,.\, \Sigma Wy}{\Sigma Wy^2}\right)}$$

it will be generally possible to write out an expression of the form

$$N_c = \frac{C}{\sqrt{\Delta}}$$

where Δ is the maximum value of y. The exact value of C will depend on the form of the deflection curve and on the distribution of the masses. This has already been shown in connection with the simpler cases, and values of C are given in Table XXVIII. In the example worked out above—

$$C = N_c \,.\, \sqrt{\Delta}$$
$$= 5{,}285\sqrt{0{\cdot}001364}$$
$$= 195$$

This value is intermediate between the value 187·7 for a single concentrated load and 211·5 for a uniformly distributed load.

With a little judgment, the designer can guess the value of C sufficiently nearly for practical purposes, and this does away with the necessity of making the calculation of ΣWy and ΣWy^2, which, from the nature of the y values, is rather tedious.

228. Approximate Determination of Spindle Diameter. For a first approximation for calculating the critical speed, a designer is driven to a process of systematic guesswork, which may be largely assisted by drawings of a turbine similar to that proposed. The following method is suggested by the author as giving a crude formula which might be expected to give consistent results for any given type of machine.

Let N_c = critical speed of rotor in r.p.m.

N = normal " "

$r = \frac{N}{N_c}$

D = average mean diameter of discs (inches).

l = span between bearing centres (inches).

d = mean diameter of middle portion of spindle (inches)

Then intensity of load (for a given type of disc) will be approximately cD^2, where c is constant, i.e.

$$w = cD^2$$

Then for any given method of supporting the shaft—

Static deflection $\Delta = \frac{nwl^4}{EI}$, where n is constant

i.e. $$\Delta \propto \frac{D^2 l^4}{d^4}$$

$\therefore$ $$\sqrt{\Delta} \propto \frac{Dl^2}{d^2}$$

But $$N_c = \frac{C}{\sqrt{\Delta}} \text{ where C is a constant.}$$

Hence $$N_c = \frac{a_1 \cdot d^2}{Dl^2}$$

But $$N = rN_c$$

$\therefore$ $$N = \frac{r \cdot a_1 \cdot d^2}{Dl^2} = \frac{Kd^2}{Dl^2} \quad (K = ra_1)$$

or $$d = l\sqrt{\frac{ND}{K}} \qquad . \quad . \quad . \quad . \quad . \quad (239)$$

Where lightness and compactness are of importance, the value of K is large. In merchant turbines, where allowances are pretty liberal, the value of K appears to be about 3,500,000; whereas in naval impulse and reaction turbines fitted with disc wheels, the value increases to about 5,000,000. In land practice, where the disc construction is much lighter than in marine turbines and where the ratio r is larger, the value of K for the examples tested appears to exceed 6,000,000.

The method may be extended slightly by the elimination of the ratio r, i.e. by estimating the diameter d required to give a certain critical speed N_c.

Then
$$d = l\sqrt{\frac{N_c D}{K_1}} \qquad . \quad . \quad . \quad . \quad (239a)$$

For a few impulse turbines for which N_c has been calculated by the graphical method, K_1 varies from 8,000,000 to 8,500,000.

BIBLIOGRAPHY

1. JEFFCOTT. "The Lateral Vibration of Loaded Shafts in the Neighbourhood of a Whirling Speed—the Effect of Want of Balance." *Phil. Mag.*, 1919; 37; 304.
2. DUNKERLEY. "On the Whirling and Vibration of Shafts." *Phil. Trans R.S.*, 1895; 185; 279.

EXAMPLES XXII

1. The weight of a De Laval turbine wheel is 6 lb., the spindle is 0·42 in. diameter, the span of the bearings is 13 in., and the wheel centre is 7·5 in. from one end. Calculate—

(*a*) The critical speed of the rotor, assuming a weightless shaft.
(*b*) The critical speed, using Dunkerley's formula.

2. A shaft 2 in. diameter is freely supported in bearings 15 ft. apart Calculate the first and third critical speeds.

3. A shaft of uniform diameter projects a distance l through a bearing which may be assumed to fix its direction. The weight per unit length of the shaft is w lb.; and if x be any distance measured from the centre of the bearing, it may be shown that the deflection of the shaft due to gravity is—

$$y = \frac{w}{24EI}(6l^2x^2 - 4lx^3 + x^4)$$

Prove that the first critical speed is—

$$N_c = \frac{60}{2\pi}\sqrt{\frac{162\,E\,.\,I\,.\,g}{13wl^4}} \text{ (revs. per min.)}$$

4. A shaft 30 in. between bearings is to rotate at 10,000 r.p.m. If the running speed must not exceed 60 per cent of the critical speed and the bearings exert no fixing moment on the shaft, calculate the least diameter of the shaft.

5. Calculate the diameter required in Question 4 if the shaft is to run at a speed midway between the first and second critical speeds.

6. A shaft 3 in. diameter is freely supported in bearings which are 40 in. apart. The shaft supports three wheels, which are each 100 lb. weight. The centre wheel is midway between the bearings and the other two are placed 6 in. away. Calculate the critical speed of the system.

7. A shaft of variable cross-section supports a number of concentrated loads, which are arranged to take into account the weights of the various portions of the shaft. The following table gives the weights and the corresponding static deflection of the shaft at the points of application of the loads. Calculate the critical speed.

Sect.	1	2	3	4	5	6	7	8
W	20	44	130	134	138	144	44	20
y	0·0003	0·00075	0·00115	0·00138	0·0014	0·00117	0·0008	0·0003

8. The wheel of a Riedler-Stumpf turbine is 2,000 lb. weight, and is supported at the end of an overhung shaft, which is assumed to be fixed by its bearing. The distance from the edge of the bearing to the centre of gravity of the wheel is 6 in. and the speed of rotation is 3,000 r.p.m. If the critical speed is to be 30 per cent in excess of the running speed, calculate the least diameter of the shaft, neglecting the stiffening effect of flanges, etc.

CHAPTER XXIII

CONSTRUCTION OF CYLINDERS

229. Form of Cylinder. The form of the cylinder should be as simple as possible so that distortion may be avoided. In impulse turbines of all sizes, the diaphragms are usually fitted into grooves in the cylinder, provision being made in certain cases to maintain the bore of the diaphragm in correct alignment with the shaft, and yet allow for expansion. Similarly, in reaction turbines it is usually

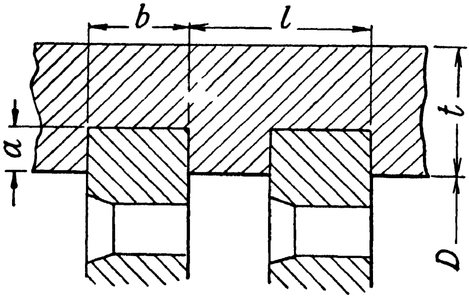


FIG. 334

the practice to fit the stationary blades direct into grooves machined in the cylinder.

Where the thickness of the cylinder is determined by its ability to withstand internal pressure, it may be calculated by the simple formula—

$$t = \frac{pD}{2f}$$

where t and D are in inches, and p is the gauge pressure and f the allowable stress in lb per sq. in. If allowance be made for the diaphragm grooves (Fig. 334), then the thickness

$$t = \frac{pD}{2f} + \frac{ab}{l}$$

For very high pressures, the thickness is preferably calculated by the formula—

$$n = \sqrt{\frac{f + p}{f - p}}$$

based on Lamé's equations for thick cylinders. Here n is the ratio of the external to the internal diameter of the cylinder.

In a single-cylinder turbine, the casting thickness can generally be reduced towards the L.P. end. At that end, the cylinder, under normal operating conditions, tends to collapse, and it is practically impossible to calculate the thickness from considerations of strength alone. Rigidity is essential, and for cylinders having diameters of

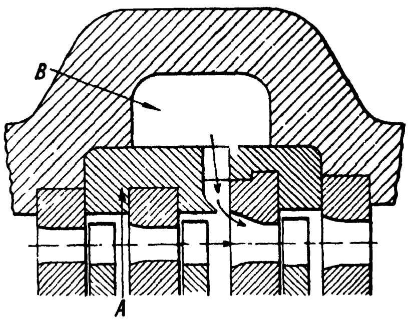


FIG. 335.—Admission of By-pass Steam in Impulse Turbine

30 in. or more, the thickness of the L.P. end may be calculated from the relation—

$$t = \frac{D}{100} + 0{\cdot}8 \text{ in.}$$

The admission of by-pass steam calls for some modification in the design of the H.P. cylinder. The by-pass steam should be admitted around the complete circumference, and in such a manner as to cause the minimum disturbance to the steam flow. Fig. 335 shows an excellent arrangement. A short inner cylinder A is fitted into a recess in the main cylinder casting, forming a steam belt B to which the by-pass steam is admitted. From this belt the steam flows through a passage and is deflected so that it enters the nozzles with the least disturbance to the steam flow from the preceding row of blades.

230. Horizontal Joint Flange. The ideal turbine cylinder would be truly circular and in one piece. The changes in temperature which occur at starting and stopping and which accompany changes of load would produce stresses in the cylinder but would not produce any distortion which might adversely affect alignment and the fine clearances which are so essential to good efficiency in high-pressure turbines.

Consider a uniform circular cylinder and suppose the inside of the cylinder is at a higher temperature than the outside. Such a condition could occur either on warming up the turbine or with an increase of load. The inner wall tends to expand more than the outer wall and this produces tensile stresses in the outer half of the cylinder wall and compressive stresses on the inner half.

For the diameter ratios experienced in high-pressure turbine cylinders, the temperature variation through the cylinder wall under steady conditions is practically linear. The maximum thermal stress (which occurs at the inner and outer surfaces of the wall) is a hoop stress and is given fairly closely by the simple formula—

$$f_t = \pm \frac{E\alpha t_1}{2(1 - \sigma)}$$

where E = Young's modulus.
α = coefficient of expansion of cylinder material.
t_1 = excess of temperature at inner wall over temperature at outer wall.
σ = Poisson's ratio for material.

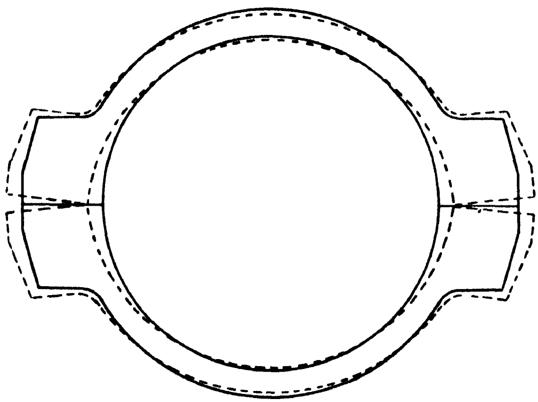


FIG. 336

The units of stress will be the same as those for E. The variation of stress across the cylinder wall is practically linear.

Thus in a cylinder 40 in. internal, and 46·4 in. external, diameter and having the inner wall 100° F. above the outer wall, the stress varies from − 9,160 at the inner surface to + 9,160 lb. per sq. in. at the outer surface. This is based on the assumption that E = 21·0 × 10^6 lb. per sq. in. at 900° F.; $\alpha = 6{\cdot}1 \times 10^{-6}$ per deg. F.; and $\sigma = 0{\cdot}3$. The stresses due to pressure must be added to the thermal stress to give the resultant hoop stress.

The ideal complete cylinder is, however, almost unattainable except for turbines with small dimensions. It is necessary to split the turbine casing horizontally to facilitate assembly and dismantling; therefore, some form of horizontal joint becomes essential. If we consider such a cylinder in halves with no very rigid attachment of the two halves at the horizontal joint, then an excess of temperature on the inside wall of the cylinder would cause expansion

on the inside and a distortion as shown, in exaggerated form, in Fig. 336. Clearly a very stiff flanged joint will be necessary to prevent such distortions and maintain a steam-tight joint, bearing in mind the possible high internal pressure.

For relatively low pressures of 150–250 lb. per sq. in., the thick-

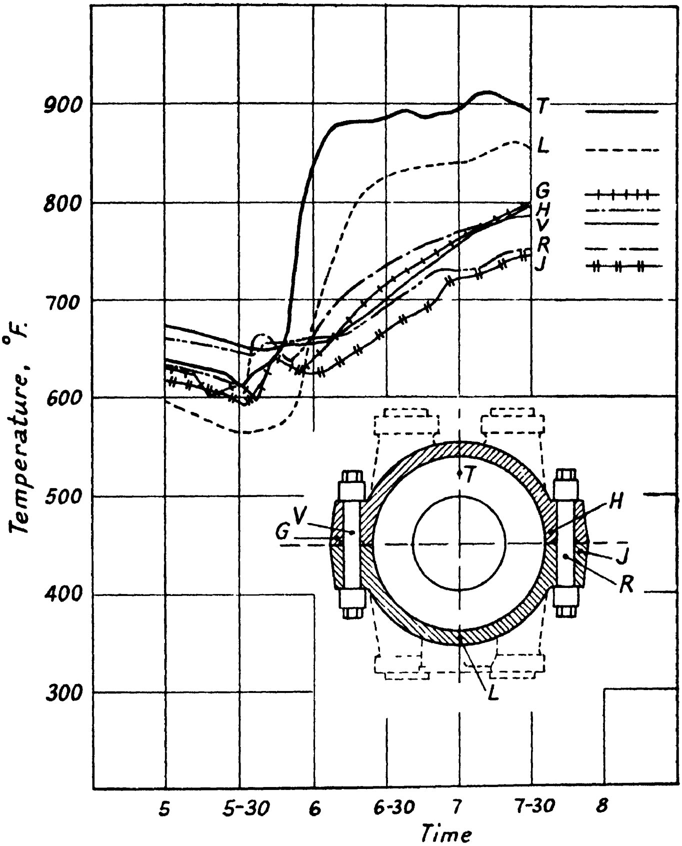


FIG. 337

ness of the flange should lie from 1·5 to 1·75 times the thickness of the cylinder. For high pressures the ratio may be 3 or more.

The flange introduces a definite lack of symmetry in the turbine cylinder, and at any given time after starting a turbine from cold, or after an increase in load, the temperature of the flange will lag behind that of the cylinder. This is well shown by Fig. 337 reproduced from a paper (1) by J. S. Hall. The wall metal is 3 in. thick and the joint bolts are $3\frac{3}{4}$ in. diameter. Curves T and L show the

temperatures of the steam and cylinder wall, respectively, from which it is seen that the rate of rise of the cylinder wall temperature is comparable with that of the steam itself. The flange temperatures are shown by the curves G and J, and for some reason one lagged behind the other. The flanges were steam heated.

When there is a considerable difference between the flange temperature and the cylinder temperature, the longitudinal expansion of the flange will be less than that of the cylinder, and this tends to produce distortion. In some cases, slots are cut from the bolt holes to the outside of the flange to relieve the stress produced by this differential expansion, Fig. 338.

The temperature of the flange may be raised more quickly by steam heating. Fig. 339 shows the cross-section of the flange of a

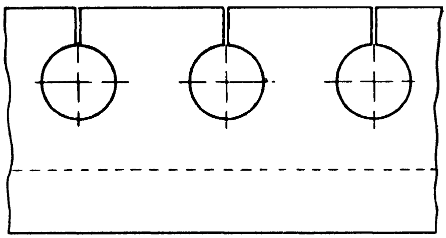


FIG. 338

high-pressure turbine by Escher Wyss and Co. showing heating passages in the outer part of the flange through which superheated steam is circulated during the warming-up period. An alternative method is shown in Fig. 340. A groove A is machined in one or both of the flanges and superheated steam circulated through the groove, connecting holes B being drilled through the side of one of the flanges. This method is widely used in this country.

231. Flange Bolts. The diameter of the bolts must be estimated from the magnitude of the bursting forces caused by internal pressure and the allowable stress at the bottom of the screw thread. The two halves of the cylinder are located accurately relative to one another by using a small number of fitted bolts, the remainder of the joint bolts having a clearance. The cylinder tends to open out at the joint when under pressure, and to counteract such a tendency the bolts should be placed as near to the metal of the cylinder as possible.

In general, and especially where alloy bolts are used, the bolts are screwed at each end as shown in Fig. 340. In way of branches, brackets, etc., and in some cases for preference, stud bolts are screwed into the lower half.

Reference has already been made to the effects of high-temperature steam when a turbine is being started or when the load is increased. The bolts for the horizontal joint are also affected by such temperature changes. In many cases the temperature of the bolts will lag

behind the flange temperature with the result that due to the expansion of the flange the bolt suffers an increase of stress over and above the normal stress due to tightening. At high temperature this will produce a small amount of creep which in the course of time will relieve the stress in the bolt and may reduce the steam-tightness of the joint. This may be avoided either by using studs (Fig. 339) or by steam heating the bolts (Fig. 340).

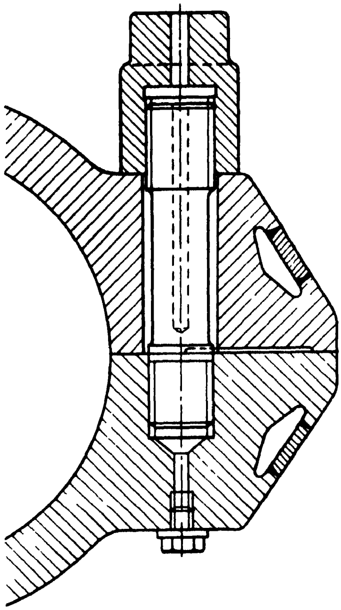


FIG. 339 Flanges of Escher Wyss H.P. Turbine, Showing Passages for Heating Steam

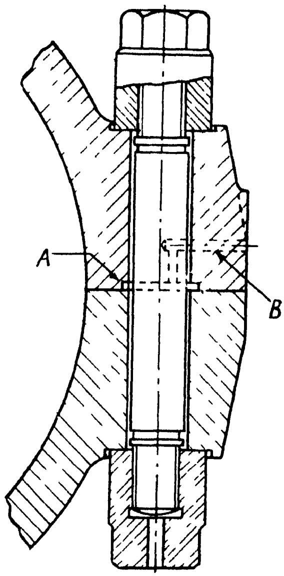


FIG. 340 – Method of Heating Flanges

The method of tightening the bolts at the horizontal joint of turbine cylinders, especially those for high steam pressures and temperatures, has undergone some modification in recent years. It was formerly the practice to hammer up the nuts with a heavy hammer. This undoubtedly puts a severe strain on the threads. In the improved method, the amount of tightening necessary to produce a certain safe stress in the bolt—and at the same time to ensure a steam-tight joint—is calculated beforehand. In closing up the cylinder, the nuts are all first tightened up by hand with the aid of a spanner. The length of the bolts is then measured by means of a special micrometer. The bolts are then heated in pairs, one on one side of the cylinder and the corresponding bolt on the other side. During the heating process the bolts expand slightly and the nuts

are gradually tightened up by hand. When the prescribed rotation of the nut has been obtained the heating of the bolt is stopped, and as the bolt cools it contracts and tightens the joint. When the bolts and flanges are completely cooled the length of the bolt is again measured by micrometer and the contraction compared with the required amount.

Two methods of heating the bolts are shown in Fig. 341. For gas

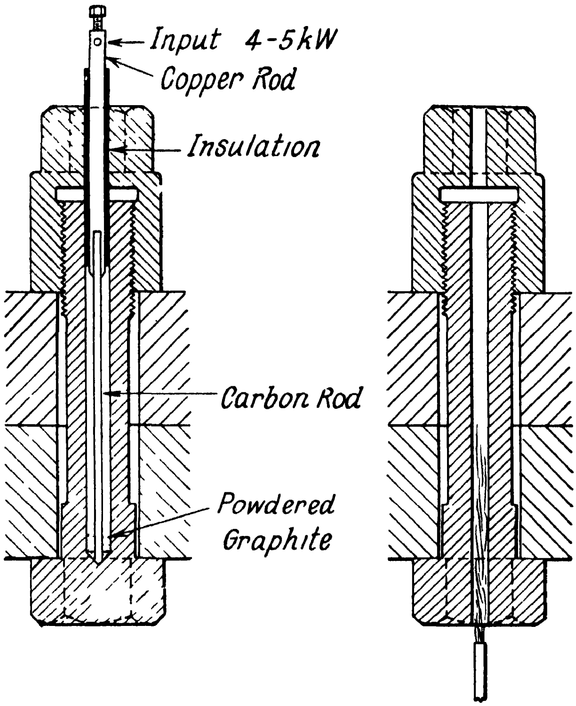


FIG 341

heating, a hole is drilled right through the bolt and cap nut. The electrical method has been developed by Messrs. C. A. Parsons & Co., Ltd. Either alternating or direct current at 100 to 200 volts is suitable. Other forms of electric heater are also used.

The amount of rotation to be given to the nut after it first becomes tight may be calculated as follows. Suppose E_1 and E_2 are Young's Moduli for the bolt and flange materials respectively, and that A_1 is the area of the bolt under a final safe tensile stress f_1, and A_2 is the area of the flange under a compressive stress f_2. Since the stress f_2 is by no means uniform, the area A_2 is somewhat difficult to estimate. With closely pitched bolts, A_2 may be taken as the product of the flange width and bolt pitch. This will err on the high

side and discretion must be used in selecting the value of A_2. Suppose that l is the combined flange thickness.

Since the bolt increases in length by the amount $\frac{f_1 l}{E_1}$ and the flange contracts by the amount $\frac{f_2 l}{E_2}$, and as $f_1 A_1 = f_2 A_2$, the total shortening of the bolt which must be produced by screwing up is—

$$x = f_1 l\left(\frac{1}{E_1} + \frac{A_1}{A_2 E_2}\right)$$

If p is the pitch of the threads, then the angle through which the nut must be turned is—

$$\frac{x}{p} \times 360 \text{ degrees}$$

When turbines have been operating for long periods at high temperatures the bolts and nuts are apt to seize when an attempt is made to unscrew the nuts. To avoid this trouble, the following practice is adopted. The bolt threads are made slightly under size and afterwards sprayed with copper or aluminium by the Schoop process. In opening up the turbine cylinder, the bolts are first heated and the nuts slacked back. If seizing should begin, a little of the sprayed metal is broken off and the nut is freed. An alternative method is to use molybdenum disulphide in petroleum jelly as a paste to be applied to the screw threads.

Plain carbon steels are used for bolts, but 3 per cent Ni steel is used in high-pressure turbines. This steel has a minimum yield point of 30 and a minimum ultimate strength of 45 tons per sq. in. For notes on bolting materials for high temperatures, see Appendix, page 837.

232. Parsons Clamped Joint Construction. Messrs. C. A. Parsons & Co. have built several three-cylinder tandem reaction turbines to operate at high steam pressures and temperatures. The conventional bolted joint is eliminated from the high-pressure cylinder and the two halves are held together by clamps which are applied or taken off by movement in the horizontal direction, Figs. 342 and 343. The flanges are made narrow and very deep, the upper face of the top flange and the lower face of the bottom flange being machined at a slope of 1 in 8 to the horizontal. The jaws of the clamps are machined to correspond. Figs. 342 and 343 show the H.P. cylinder of a 60,000 kW. turbine. The studs for the clamps are $1\frac{3}{4}$ in. diameter compared with bolts 5 in. or more in diameter for the usual bolted joint. The clamps are $4\frac{1}{4}$ in. wide and the space between them is not more than $\frac{1}{4}$ in. Consequently, the applied load is distributed almost continuously over the full length of the flange.

The method of tightening up the clamps is similar to that described

for flange bolts. Vertical holes are provided in the clamps for the insertion of carbon rods these holes are connected by horizontal

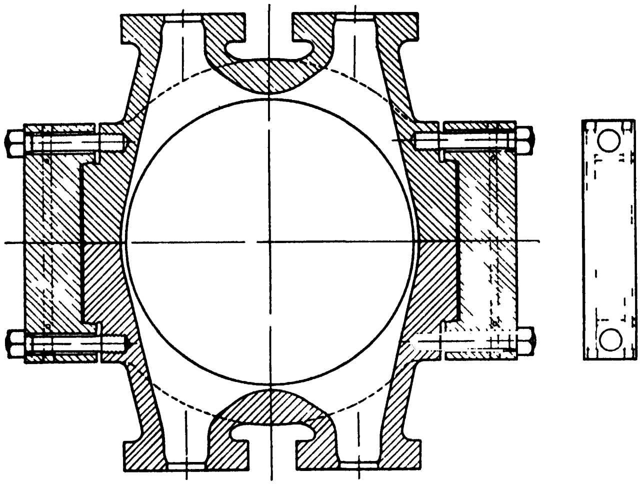


Fig. 342 Cross section through H P Cylinder with Clamp Joint

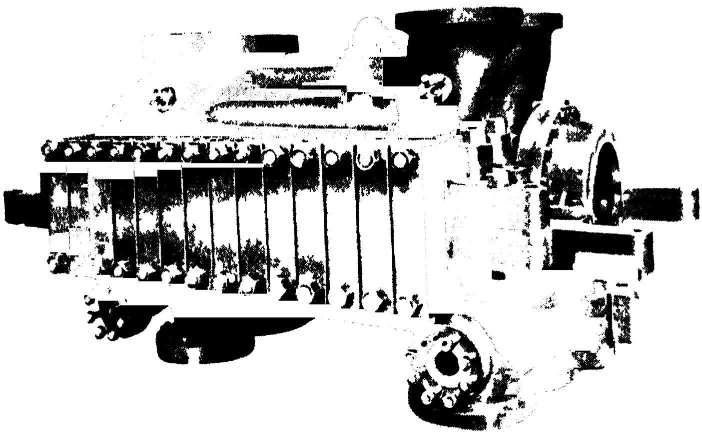


Fig. 343 H P Cylinder Showing Clamps in Position

holes, and, by suitable modification, heating steam may be circulated through the clamps when required

Fig 342 shows a cross section through the cylinder in way of the

steam inlet branches. There are four such branches and the cross-section of the steam belt narrows down to a very small area at the horizontal joint.

In way of the gland mouths at the ends of the h.p. turbine an ordinary bolted joint is used.

233. Nozzle-box Construction. A form of construction commonly used in impulse turbines is shown in Fig. 344. The nozzle boxes

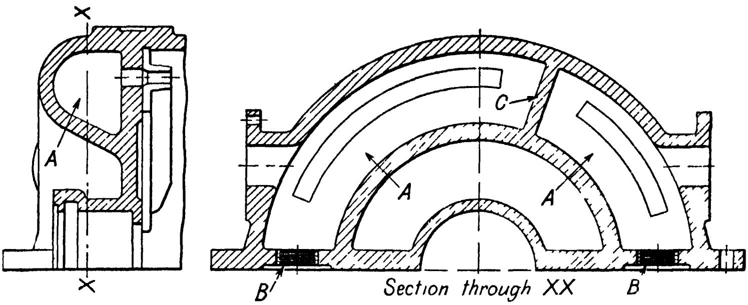


FIG. 344

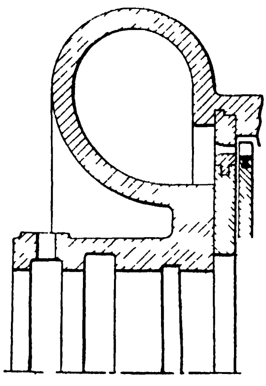


FIG. 345

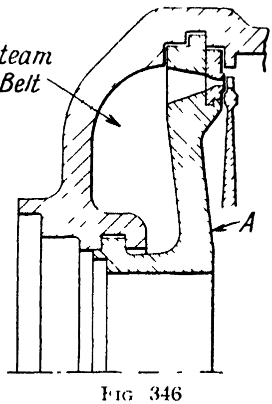


FIG. 346

or steam chests A are cored out, and may extend completely round the circumference, or only partially, as shown in Fig. 344. In the latter case the core holes at B are tapped and plugged. With nozzle-control governing (hand or automatic) the nozzle box is divided by walls C, as shown.

A simplified construction suitable for by-pass governing is shown in Fig. 345. The core for the nozzle box can be built up as part of the cylinder core. The first-stage nozzles are built up in a plate which covers the front of the nozzle box. Fig. 346 shows a similar

construction (General Electric Co., U.S.A.), the object here being to provide a steam belt of sufficiently large area. The diaphragm A is in halves.

It sometimes happens that although the live steam temperature exceeds 450° F., the limiting temperature for the employment of



FIG 347

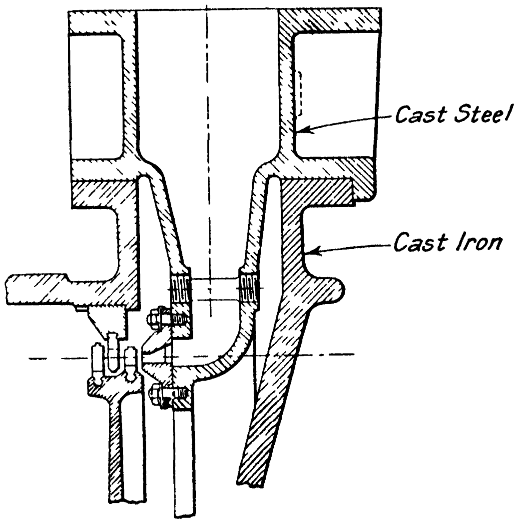


FIG 348

cast iron, the temperature of the steam after expansion through the first-stage nozzles falls below 450° F. This is especially the case when the first stage of the turbine is velocity-compounded. In such a case the cylinder may be made of cast iron and the nozzle box a steel casting inserted through an opening in the side, top, or bottom of the cylinder. Fig. 347 shows such a nozzle box as formerly used in Metropolitan-Vickers steam turbines. The part

lying within the cylinder is in the form of a curved pipe of gradually diminishing flow area. The nozzle segment is bolted to a machined face on the side. A further example, from a Brown-Curtis marine turbine, is illustrated in Fig. 348.

234. Double-cylinder Construction. For turbines of large output operating at high temperatures and high initial pressures, say in excess of 1,200 lb. per sq. in., the single casing construction presents considerable difficulties, especially in the design of flanges and the avoidance of distortion. This has led to the fairly extensive use of the double-shell construction for the high-pressure cylinder. An inner cylinder housing the nozzles, diaphragms, etc., is arranged inside an outer cylinder and maintained concentric with it. The high-pressure steam is admitted only to the inner cylinder while the space between the two cylinders is subjected either to the exhaust pressure of the high-pressure turbine or to the pressure at some intermediate stage. The inner cylinder, which is subjected to steam at the initial temperature is thus exposed to a resultant pressure difference which may be only half the initial steam pressure. Consequently, its thickness may be made smaller than that of a single-cylinder turbine.

The bolting problem is easier than in the single-cylinder machine and single-row bolts may be used for both cylinders. The inner cylinder may be made of austenitic steel to meet the high-temperature conditions. In some cases the steam between the two cylinders is used for cooling the metal of the inner cylinder and so reducing the creep strain. In certain American G.E.C. turbines with double shells an internal pipe system is provided without valves or other controls so that the inner shell bolts may be cooled by about 75° F. at high loads in order to reduce creep. At starting the bolts are steam heated in order to reduce stretching.

Examples of double-cylinder construction will be given in Chapter XXIX.

235. Construction of Exhaust End. In all condensing turbines excepting those of small output and special design, the condenser is placed underneath the turbine. This position has a number of advantages, chief among which are that the moisture formed during expansion in the turbine drains naturally into the condenser, and that the turbine may be opened up for inspection without the removal of exhaust branches. In general, the velocity of steam flow through the condenser inlet branch is less than the absolute velocity of the steam as it leaves the last wheel. The exhaust hood should be designed so that, so far as possible, the change of steam velocity will be accompanied by a small rise in pressure, but it is doubtful if such a result is ever obtained, because changes in the direction of flow, and the resulting losses, are inevitable. The shape of the upper part of the exhaust hood should be such that the flow area grows uniformly from the vertical centre-line downwards. Many

manufacturers now cast large deflector blades in the lower half, one on each side, to deflect downwards the steam from the lower half of the wheel and so prevent it from disturbing the flow of that coming from the upper half.

The exhaust-end bearing, including sometimes the generator bearing, is frequently supported from the exhaust hood, so both rigidity and strength are essential. The lower half should be stiffened by means of cast stay plates (vertical so as not to interfere with the steam flow), steel stay plates bolted to cast brackets, or by means of stay bolts, for in addition to such a load the exhaust hood has to withstand a certain collapsing pressure and an even higher test pressure.

The majority of low-pressure turbines now comprise a cast cylinder located centrally in a fabricated housing. Examples of these will be found in Chapter XXIX.

236. Cylinder Supports. Consideration must be given to the differential expansion which takes place in the turbine and its supports in order that—

(1) The turbine cylinder and rotor may remain co-axial, so maintaining the small radial clearances in the various labyrinth packings.

(2) The cylinder and rotor may expand freely without inducing heavy forces and consequent distortion.

(3) The axial clearances between the stationary and rotating parts of the turbine may not, under any conditions of operation, be reduced below certain safe limits.

Such considerations assume a special importance in turbines operating at high temperatures.

Fig. 349 shows a method commonly employed for supporting a single-cylinder condensing turbine operating at moderate pressures and temperatures. The H.P. bearing block and the L.P. end of the turbine are cast in one piece, the bearing block being supported on the bedplate at A. The L.P. end is supported by two feet or brackets B cast on the side of the cylinder and also resting on the bedplate. When the turbine has been finally lined-up, holes are drilled at C for circular keys. The cylinder is not rigidly held down at the exhaust end, but is free to slide outwards or inwards on the keys. Correct transverse alignment is maintained by a key D, fitted between a bracket on the cylinder and a recess in the bedplate, and another key at A. Thus the only fixed point is at E, which is usually arranged at the centre of the exhaust branch. All expansions must be measured from E and that at the H.P. end must be borne in mind when arranging steam connections to that end, otherwise severe strains might be thrown on the cylinder.

The temperature fall along the cylinder will be nearly linear, and if t_1 and t_2 are the temperatures at the steam and exhaust ends respectively, α the coefficient of expansion, and l the distance from

the fixed point to the H.P. end, then the movement of the cylinder towards that end will be—

$$\frac{\alpha l}{2}(t_1 + t_2)$$

For cast iron, $\alpha = 0{\cdot}0000057$ per ° F.

For forged steel, $\alpha = 0{\cdot}0000061$ per ° F.

Thus if $t_1 = 600°$ F. and $t_2 = 80°$ F., and $l = 50$ in., the expansion will be 0·097 in.

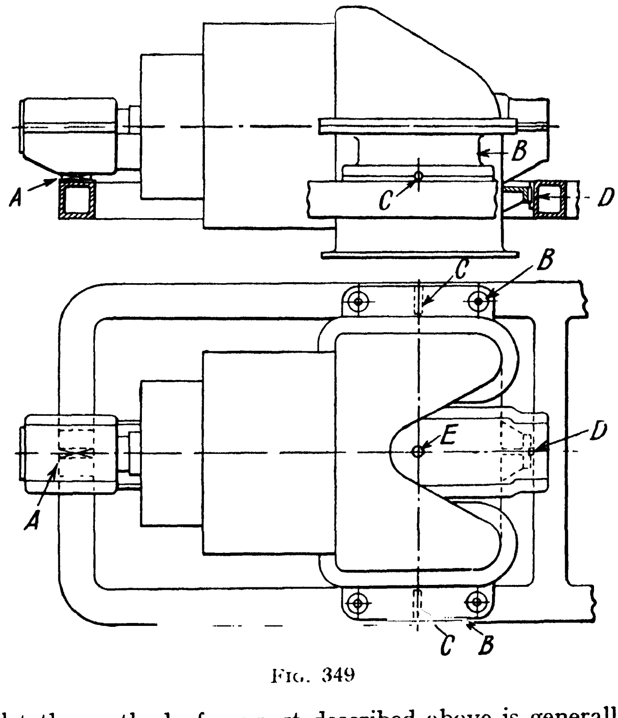


FIG. 349

Whilst the method of support described above is generally suitable for moderate pressures and temperatures, it is quite unsuitable for high temperatures. In the first place, the steam-end bearing block and the cylinder should not be cast together, otherwise a large amount of heat will be conducted to the bearing pedestal and severe strains may be brought to bear upon it. Furthermore, if the cylinder is supported from the bedplate, it is doubtful whether the cylinder and rotor will be kept truly coaxial. This is most important as the clearances in the labyrinth packings will be affected.

When the pedestal is a separate casting, the method of support shown in Fig. 350 may be employed. A half-round projecting flange A is cast on the lower half of the cylinder and is attached to the pedestal by studs or bolts in clearance holes. Keys B, C, and D are half sunk in the flange and pedestal. In spite of differential

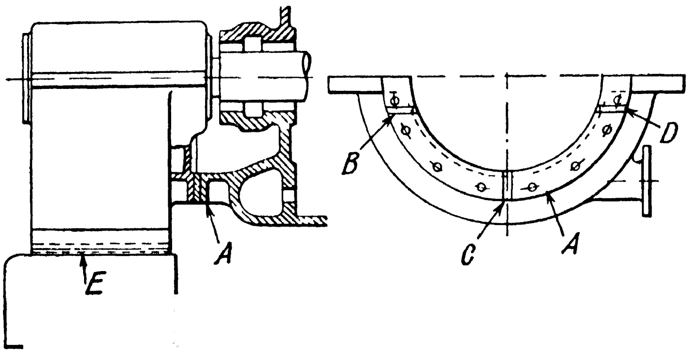


FIG. 350

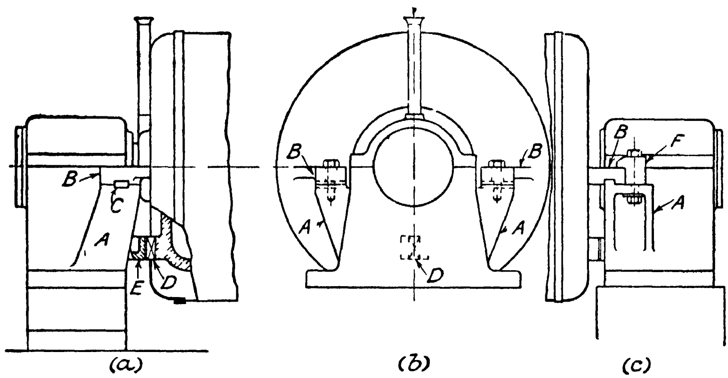


FIG. 351.—Method of Supporting High-pressure Turbine to Maintain Co-axial Alignment of Turbine Cylinder and Rotor

expansion of the cylinder and pedestal the heights of the spindle and gland centres are maintained very nearly the same by means of the keys B and D, while the transverse alignment of the cylinder and pedestal is secured by the key C. Correct alignment with axial movement is obtained by means of the key E.

A method of support which ensures good alignment is shown in Fig. 351 (*a*) and (*b*). The bearing blocks carry a support A at each side with a machined surface which lies nearly in the horizontal plane of the axis. Brackets B, cast integrally with the lower

half of the cylinder, rest on these faces and transmit to the bearing block part of the weight of the cylinder and the reaction torque. It is clear that these supports will maintain the cylinder axis at *nearly* the correct height, however the temperature of the cylinder may change. Keys C permit transverse sliding, yet keep the cylinder and pedestal in their correct relative positions. A key D, sunk partly in the bracket E and partly in a facing on the cylinder, allows for the downward expansion of the cylinder and yet maintains the transverse alignment of the cylinder axis. A slight modification of the construction is shown in Fig. 351 (*c*), in that the cylinder bracket B is held down by a wrought-steel keep F, bolted to the support A. There is, of course, a small clearance between F and B to permit sliding.

Perfection is not achieved by the method just described. If, for

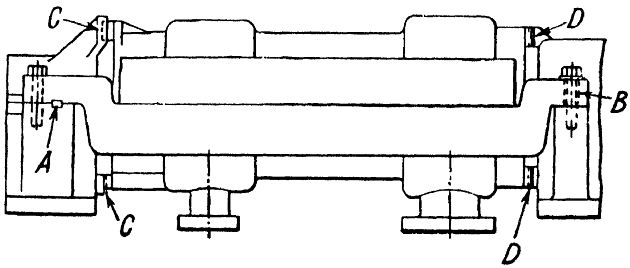


FIG. 352

example, the bracket B has a thickness of 3 in., and suppose the steam temperature is 850° F. The temperature of B, due to conducted heat, might be about 750° F. Then, assuming the bearing block to be at 100° F., the upward expansion of the cylinder relative to the rotor would be about twelve-thousandths of an inch.

An improvement is shown in Fig. 352, in which the supporting brackets for the cylinder are formed by an extension, at each end, of the flange for the lower half of the cylinder. The supporting faces are arranged exactly in the horizontal plane passing through the turbine axis. The longitudinal position of the cylinder may be fixed at either end by the keys A (which permit transverse movement), while a clearance is left in the bolt holes B at the other end. Transverse alignment is maintained by the pairs of keys C and D.

An alternative method of support employed by the British Thomson-Houston Co., Ltd., for the H.P. end of single-cylinder turbines and the H.P. casing and inlet end of the L.P. casing of two-cylinder turbines is shown diagrammatically in Fig. 353. The cylinders are supported by brackets A resting on sloping pads B forming part of the bearing housing. The planes of the pad surfaces

pass through the cylinder axis and are preferably at 45° to the horizontal, although the angle may be varied to suit individual cases. The longitudinal position of the cylinder is fixed by dowel pins C, fitted in holes which are drilled and reamed after the assembly and lining-up of the cylinders. There is a small clearance between the brackets and pads to facilitate adjustment, and actually the brackets rest on the dowel pins. The cylinders are definitely held down by bolts D, which, however, being in elongated holes, do not prevent sliding.

In Escher Wyss two-cylinder turbines in which the hot end of the

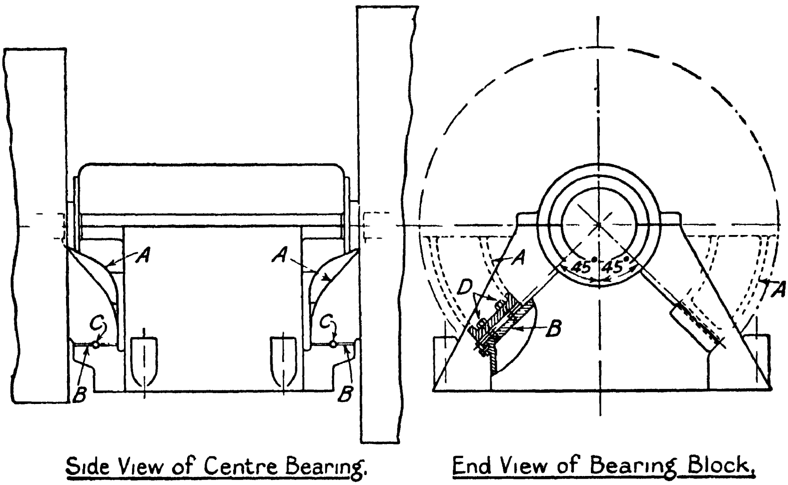


FIG. 353.—Method of Supporting Turbine Cylinders so as to Maintain Co-axial Alignment of Turbine Cylinder and Rotor

h.p. turbine adjoins the cool exhaust branch of the double-flow l.p. turbine, the bearing pedestal between the two is cooled by a constant circulation of oil. This prevents excessive thermal expansion and the resultant misalignment, as well as excessive thermal stresses in the exhaust branch.

The axial clearances between stationary and rotating parts are controlled by the relative axial movement between the cylinder or cylinders and the turbine rotor. This movement depends on the fixed points of the various cylinders, the position of the thrust bearing, or bearings, whether in multi-cylinder turbines there is one or more thrust bearings, and so on. With high steam temperatures the expansions may be considerable. Each case must be considered and the many possibilities are beyond the scope of this book.

237. Materials. The material most commonly used for cylinders

is cast iron. Owing to the phenomenon known as "growth" of cast iron, which is an increase in volume caused by a change in the internal structure of the cast iron at high temperatures, the employment of cast iron at temperatures above 450° F. is not advisable. It has been found that the tendency to growth is increased by a relatively large amount of silicon in the iron. The composition of a typical cast iron for turbine work is: C 3·3; Si 1·2; Mn 0·8; P 0·2; and S 0·1. The ultimate strength of such iron would be about 16–18 tons per sq. in., and the transverse rupture stress 24–30 tons per sq. in. The addition of small percentages of nickel (less than 2 per cent) adds to the strength of cast iron, gives it good machinability, and makes it less porous. Thus a nickel cast iron containing 3·1 C, 1·2 Si, and 1·5 Ni has a tensile strength of 17–22 tons per sq. in. and a modulus of rupture of 32–40 tons per sq. in.

For moderate steam pressures and temperatures between 450° F. and 800° F. the cylinders are made of cast steel. In single-cylinder turbines in which the initial temperature exceeds 450° F., the H.P. end of the cylinder would be made of cast steel and the L.P. end of cast iron. In two- and three-cylinder turbines, the H.P. or H.P, and I.P. cylinders would be of cast steel and the I.P. and L.P. or the L.P. cylinder only, of cast iron, according to the conditions.

For steam temperatures exceeding about 800° F. it is usual to employ an alloy steel. Such steels contain molybdenum up to 0·5–0·75 per cent and small amounts of nickel and chromium. Steel castings are cleaned, then annealed at temperatures varying between 920° and 950° F. and cooled in the furnace. After rough machining the casting may be further treated by heating it in a furnace to a temperature somewhat higher than the temperature in service.

In one or two special cases of high pressure combined with high temperature, the H.P. cylinders have been machined out of solid blocks of forged steel. Such a construction, though expensive, gives a guarantee of a sound and reliable cylinder.

See also Appendix, page 837.

BIBLIOGRAPHY

1 HALL "The Starting Rates of Steam Turbines" *The Metropolitan-Vickers Gazette*, Oct., 1954

CHAPTER XXIV

GLANDS AND PACKING DEVICES

238. Diaphragm Glands. Labyrinth glands are used almost exclusively for the purpose of minimizing the steam leakage through the diaphragm gland in impulse turbines. Various forms of diaphragm

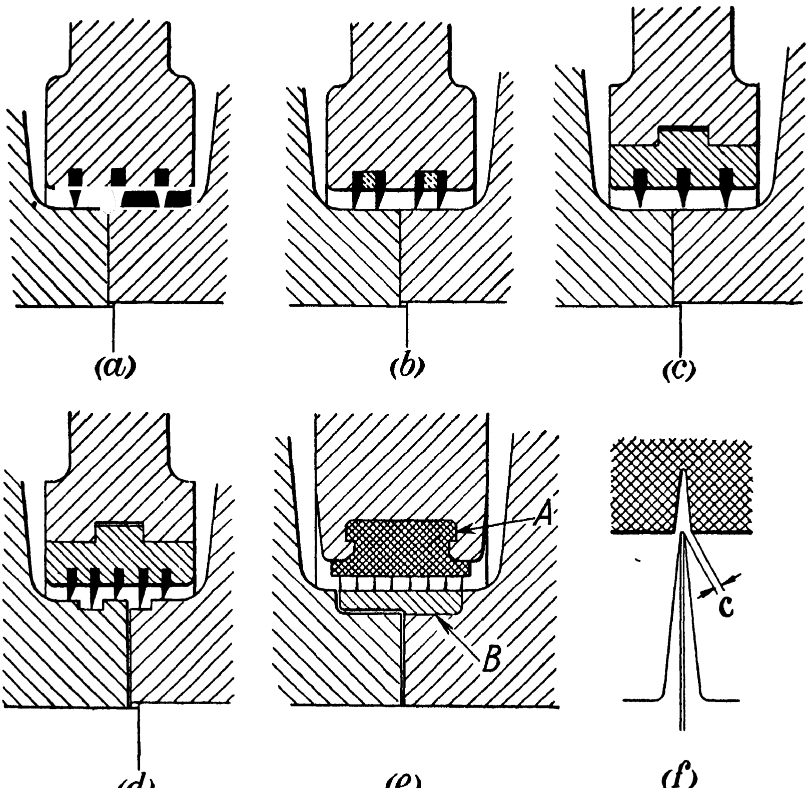


FIG. 354

gland are shown in Fig. 354. In (*a*), (*b*), (*c*), and (*d*) the packing strips are of brass or other suitable material and are caulked or rolled into the diaphragm or bush. The edge of the strip near the shaft surface is made very thin so that if rubbing should accidentally take place the thin edge of the packing strip will be quickly worn away without the generation of much local heat. Hard rubbing with the consequent heating is a possible cause of a bent shaft. Fig 354 (*a*) shows

the simplest construction; (*c*) is essentially the same except that the packing rings are carried in a separate bush. In (*a*), (*b*), and (*c*) the wheel surface is smooth and the baffling action of the rings somewhat imperfect. This is improved in Fig. 354 (*d*), grooves being turned in the wheel hub and alternate long and short packing rings used. Fig. 354 (*e*) shows a novel design of gland by Messrs. Escher Wyss Engineering Works, Ltd. A ring A of graphitic carbon is fitted in halves into the bore of the diaphragm. A steel sleeve B pressed on

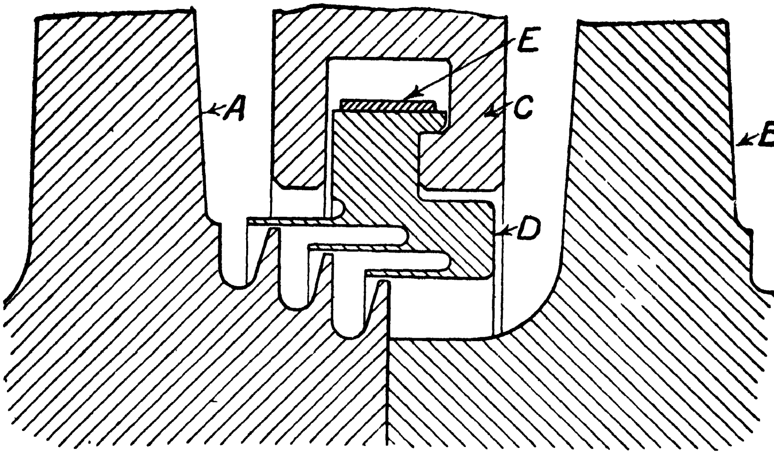


FIG. 355—Diaphragm Gland for High-pressure Steam

to one of the wheel hubs is provided with a number of sharp fins on its outer surface. The initial clearance is practically zero and normally remains very small. If the shaft should be accidentally displaced then very narrow grooves are cut in the carbon ring without damage to the fins. The clearance then controlling leakage is the small amount *c*.

An effective type of diaphragm gland employed by the Metropolitan-Vickers Electrical Co., Ltd., for turbines operating with very high steam pressures is shown in Fig. 355. A and B represent the discs of two adjacent wheels, A being on the high-pressure side of the diaphragm C. The latter has a slot bored in it which carries the packing ring D and keeps it in the central position. D is made in segments and is furnished with three thin cylindrical projecting strips. Each of the segments D is backed up by a plate spring E. Three projections are machined on the wheel hubs, and the diameters of these are such that the clearance between them and the overhanging strips is practically nil. If accidental rubbing should occur and heating take place then the rings will expand slightly and relieve the rubbing pressure. The fins on the rotor would also be heated, but here the expansion is extremely small because of the

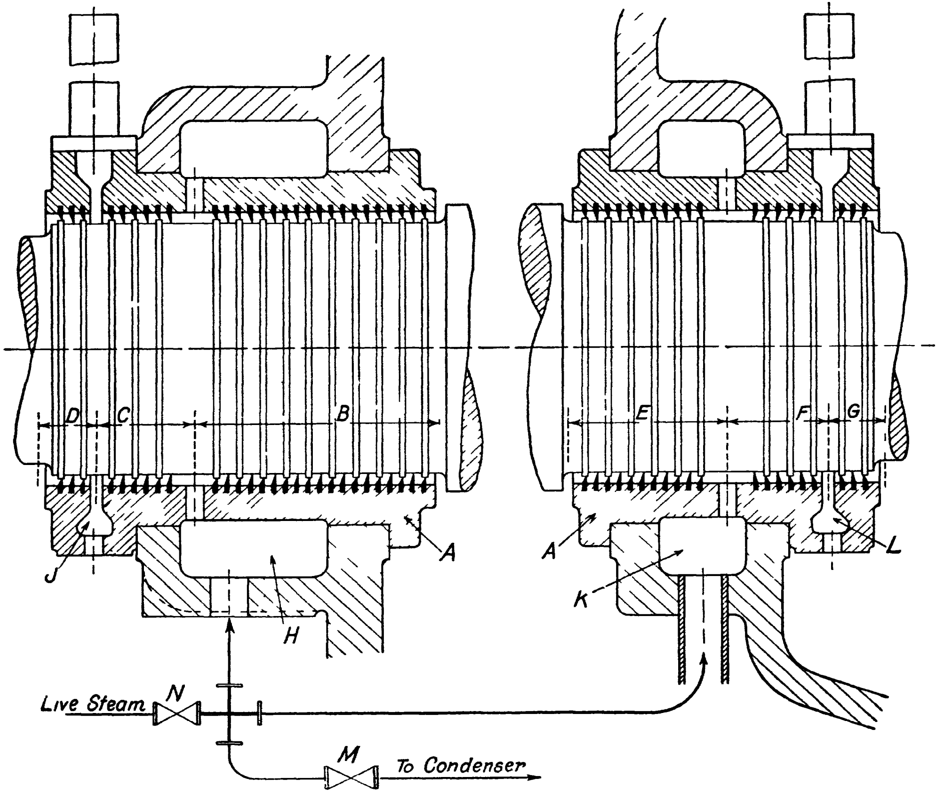


Fig. 356. Arrangement of H.P. and L.P. Glands for Condensing Turbine

restraint exerted by the more massive hub. As soon as the cause of the disturbance is removed, the fins D cool and contract and the clearance is once again restored to its original value.

239. **External Glands of the Labyrinth Type.** Fig. 356 shows in general outline the H.P. and L.P. external glands for a single-cylinder condensing turbine. Each gland comprises a bush A which is in halves, bolted together. These bushes are located by machined surfaces at each end of the cylinder and are provided with some form of labyrinth packing. In the type of gland illustrated the H.P. gland is furnished with three separate groups of packing, namely, B situated between the first-stage and the leak-off pocket H, C between H and the vapour hood J, and D between J and the atmosphere. There are three groups of packing in the L.P. gland, namely, E between the steam pocket K and the exhaust space, F between K and the vapour hood L, and G between L and the atmosphere. In general, group B contains the largest number of packing rings, while group E contains the next largest. Groups C and F are made similar, also D and G; but the number of constrictions in C and F will usually be greater than those in the outermost sections. The steam connections to such glands are shown diagrammatically in Fig. 356, and in the operation of such connections it may be said at once that the steam pressure in pocket K must be continuously maintained at a value slightly above atmospheric. There is a free connection between pockets H and K, and under normal load conditions, most of the steam which leaks past group B enters pocket K of the L.P. gland. Some of this steam flows into the turbine through group E and the rest flows outwards, so preventing an inleakage of air. If the steam pressure in the pocket H is excessive, e.g. under full load or overload conditions, then the valve M may be opened just sufficiently to maintain a slight flow of steam through the vapour pipes. At light loads the steam pressure in the first stage will fall to such an extent that there will be insufficient steam available to seal the L.P. gland. Under these conditions, live steam is admitted to both glands through the valve N.

In some cases, the H.P. gland is provided with an additional pocket on the cylinder side (Fig. 357). This is connected by an external pipe to a suitable stage of the turbine where the pressure is normally well above atmospheric. Thus a part of the leaking steam is able to do work in the L.P. stages of the turbine. It will be seen that there are now four separate groups of packing in the H.P. gland. The steam connections are shown and do not call for much explanation. Live steam is supplied continuously to the L.P. gland so that its performance is not affected by load changes. The pressure in the pocket K is then controlled by opening the valves P or Q, according as the turbine load is heavy or light.

In tandem turbines the H.P. glands are usually provided with two or even three tappings, the steam being led either to later

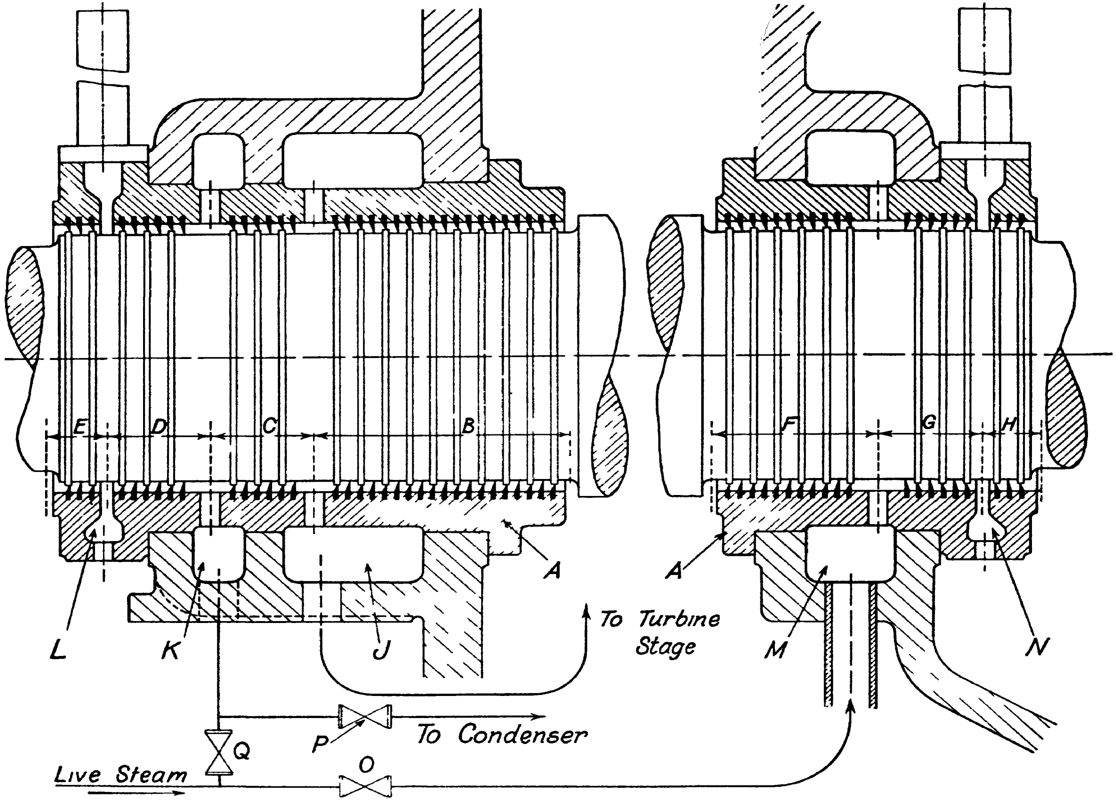


FIG. 357.—Alternative Arrangement of H.P. and L.P. Glands for Condensing Turbine

stages or to feed-water heaters, according to the conditions. Live steam connections are also fitted for steam sealing at light loads. As superheated boiler steam is used for the purpose, its temperature after wire drawing is very high indeed, and it may be advisable to desuperheat the steam before supplying it to the glands. The L.P. turbine is supplied with steam-sealed glands or hydraulic seals.

240. Forms of Labyrinth Packing. Various forms of packing are shown in Fig. 358. (*a*) shows the axial or "facial" type of packing. Shallow collars about $\frac{1}{8}$ in. wide are turned on the shaft; rings of non-ferrous metal are caulked into the gland casing. The leakage is controlled by the axial clearance c_a. In manufacture, it is impossible to machine the grooves and rings so that the clearance is uniform throughout; the rings are ground in with the rotor turning at a low speed until all are rubbing simultaneously. This type of packing is used at the end of the turbine (usually the H.P. end) adjacent to the adjusting block. The latter is then made movable in the axial direction, and on starting the turbine the rotor is first moved away from the stationary packing rings. After the turbine has been running for some time and reached its working temperature, the rotor is moved back until the clearance has the desired value. The adjusting block is then locked in this position.

Fig. 358 (*b*) shows the "radial" packing which is used at the end of the turbine remote from the adjusting block and where, owing to differential expansion, it is impossible to maintain a small axial clearance. The clearance here is a radial clearance c_r and is, apart from expansion effects, practically invariable. (*c*) shows a combined radial and axial packing giving two constrictions per ring. This, also, is used only at the end adjacent to the adjusting block where the axial clearance is under control. (*d*) is a variant of (*b*). In (*e*) a steel sleeve is fitted to the shaft and a steel bush in the cylinder end. Each is provided with a large number of closely pitched fins, turned to a knife edge and having a radial clearance. (*f*) shows a gland construction evolved by Messrs. Fraser & Chalmers Engineering Works. Both rotating and stationary parts of the gland are of steel and are provided with knife-edged fins. The pitch of one set, however, is slightly different from that of the other. Thus, if the shaft should be accidentally displaced radially, only a few rings would be damaged. Axial movement of the rotor due to expansion alters the incidence of the clearances, but the total effect of the packing remains the same. (*g*) shows an element of the new design of packing by Messrs. Escher Wyss Engineering Works. As in Fig. 354 (*e*), it comprises a ring of graphitic carbon spigoted in the gland housing and a sleeve on the spindle. The radial fins on the sleeve are initially in contact with the carbon. (*h*) shows a special design of gland for a H.P. turbine by the same firm. As will be seen, there are four constrictions for each ring.

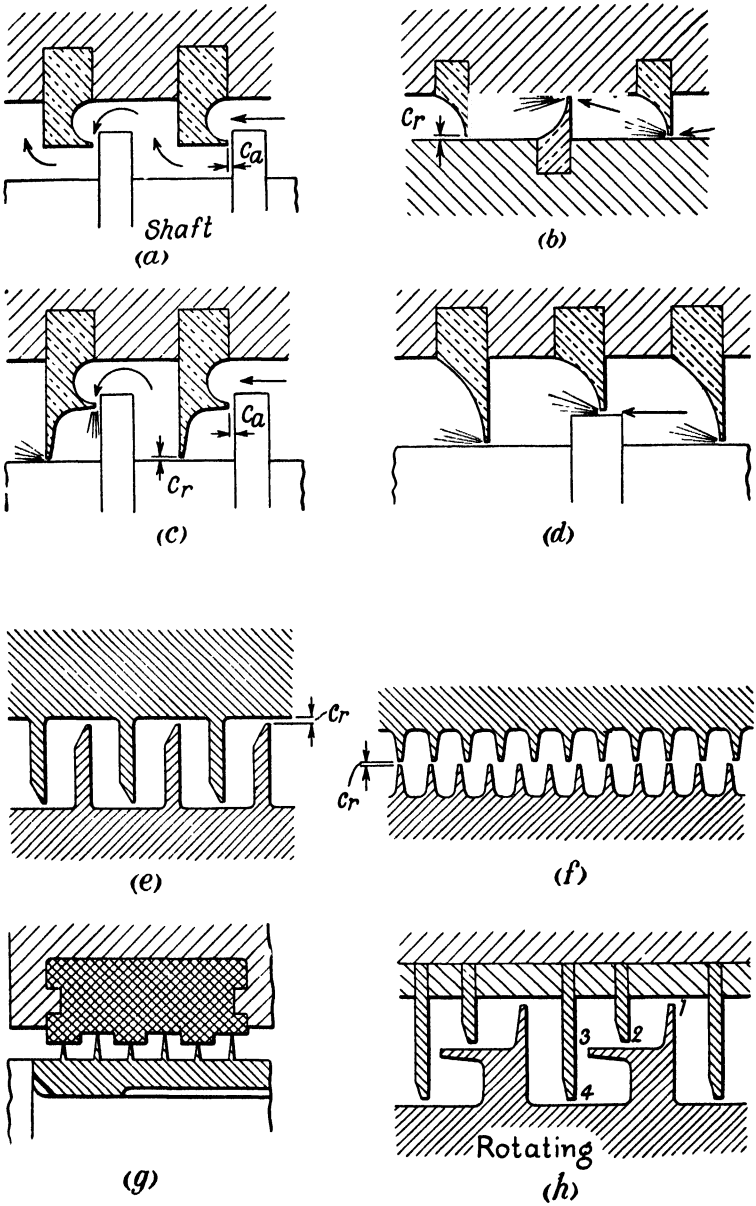


FIG. 358.—Forms of Labyrinth Packing

All the packings shown in Fig. 358 are of the rigid or non-yielding type, and therefore suffer from the disadvantage that if the shaft should be accidentally displaced, the packing strips will be permanently damaged and the leakage loss increased, to say nothing of the risk of a bent spindle. An example of yielding labyrinth packing is given in Fig. 359, showing the L.P. gland of a large

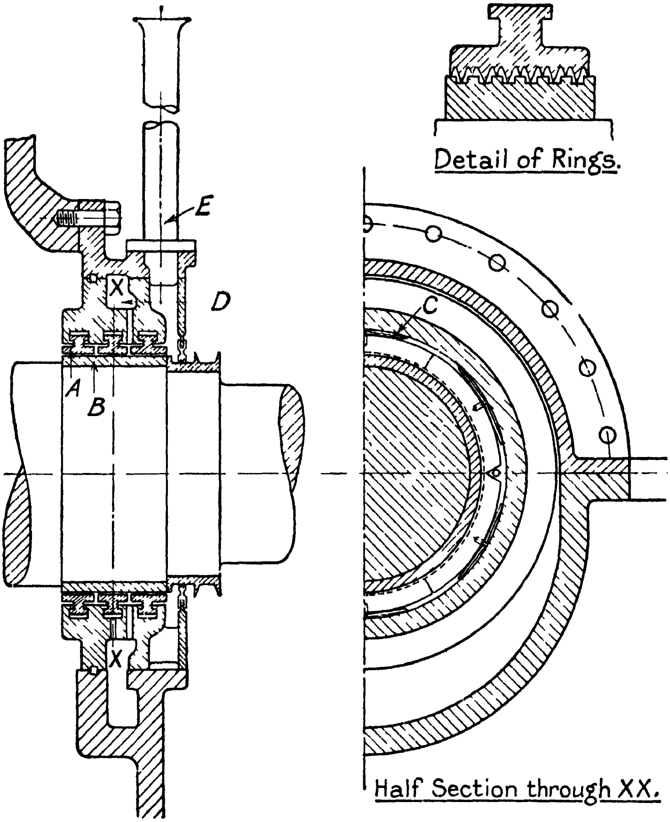


FIG. 359.—L.P. Labyrinth Gland of B.T.-H. Turbine

British Thomson-Houston turbine. A number of rings A, each formed in six segments, touch, or almost touch, the sleeve B on the shaft. The rings are held up to their work by flat plate springs C. As originally assembled, the rings are tight on the shaft, but after the turbine has been run at a low speed for a short time the fine edges of the fins ($\frac{1}{64}$ in. wide) are worn away, and the rings finally become centralized by the shoulders in the gland housing. Sealing steam is supplied to the pocket D, and leaking vapour is carried away by the pipe E.

There is another form of yielding packing in which, if rubbing between the rotating and stationary elements should take place, the stationary element is so shaped that the expansion which occurs

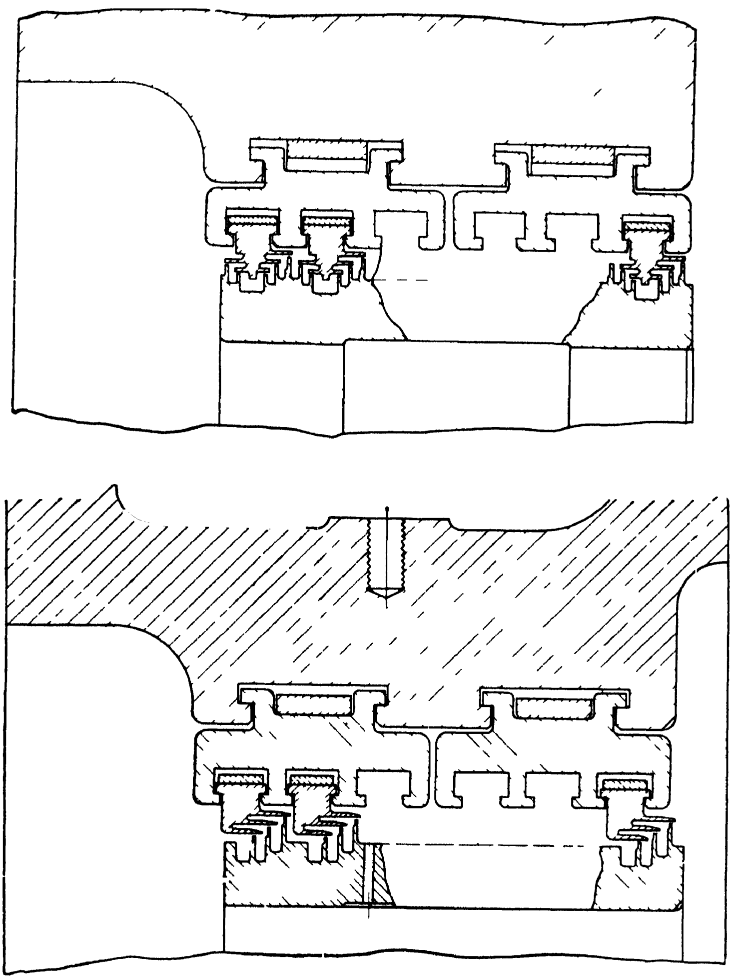


FIG. 360.—Metropolitan-Vickers Type of External Labyrinth Gland

due to heating causes that element to move outwards and so relieve the rubbing pressure. This principle appears to have been first employed in the labyrinth packings of the Ljungström turbine about the year 1912 An example of such a yielding packing has

already been given in Fig. 355. Further examples by the Metropolitan-Vickers Co. are shown in Fig. 360. Thin radial fins on the shaft sleeve mate with projecting cylindrical fins on the segmental stationary rings, which are centred by the larger rings and backed by plate springs. In the upper part of the figure, the gland has six elements providing, in all, thirty throttlings. The lower illustration shows the single type of gland which is used at the outlet end of the H.P. cylinder of tandem turbines so as to allow for the greater axial expansion at that end, the axial position of both the H.P. and L.P. turbines in such tandem sets being fixed by a thrust block fitted at the inlet end of each turbine.

The application of such glands to the high-pressure cylinder of a Metropolitan-Vickers two-cylinder turbine is shown in Fig. 361. The first section of the gland comprises 8 rings which together provide 40 throttlings. The pocket which follows is connected by a pipe to the exhaust end of the turbine. Then follow two groups of rings which provide a further 35 throttlings. Live steam may be supplied to the space between these groups for starting purposes. The outer pocket is vented and is connected to a feed-water heater.

Present practice by this firm is to discontinue the use of sleeves on the shaft as it is thought they cause non-uniform heat flow from the steam to the shaft and thus produce transient bending. The packing used is then similar to that shown in Fig. 359.

The leakage of steam into the turbine room is often a nuisance because the steam condenses on roof girders, windows, and the like. A hydraulic seal is sometimes arranged on the atmospheric side of labyrinth glands in order to stop steam leakage.

241. Carbon-ring Glands. This type of gland comprises a number of segmental rings of graphitic carbon. This material is self-lubricating. The rings are enclosed in a suitable housing. In some cases, the carbon rings are actually in contact with the spindle or sleeve thereon, but in others the lengths of the segments are such that there is a small radial clearance between the shaft and the inner surface of the rings. Such rings are said to be "arch-bound."

In all cases, the rings are held close to the shaft by a garter spring which is wrapped round the outside of the gland rings. When the rings are actually rubbing on the shaft (or sleeve) the tension of the spring should be such that the rings exert only a slight pressure on the shaft e.g. about 1½ to 2 lb. per sq. in. of ring surface.

In the arch-bound type of ring, the segments are supported, in addition, by a small coach spring (or springs) which keeps the rings centred with the shaft and yet permits freedom of movement if necessary. The radial clearance in this type should be sufficient to allow for expansion of the shaft due to temperature increase. Further, it is essential that the joints at the ends of the segments should be quite square and radial.

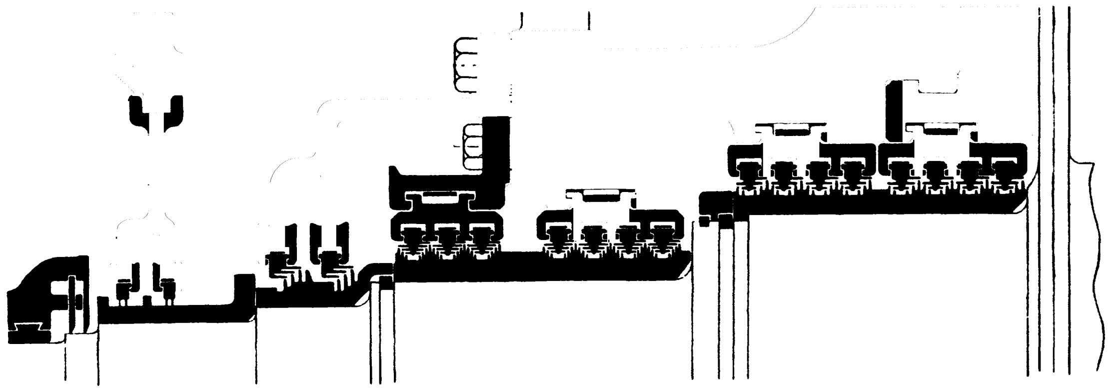


FIG. 361.—Sectional Arrangement of H.P. Inlet End Gland of Metrovick Turbine

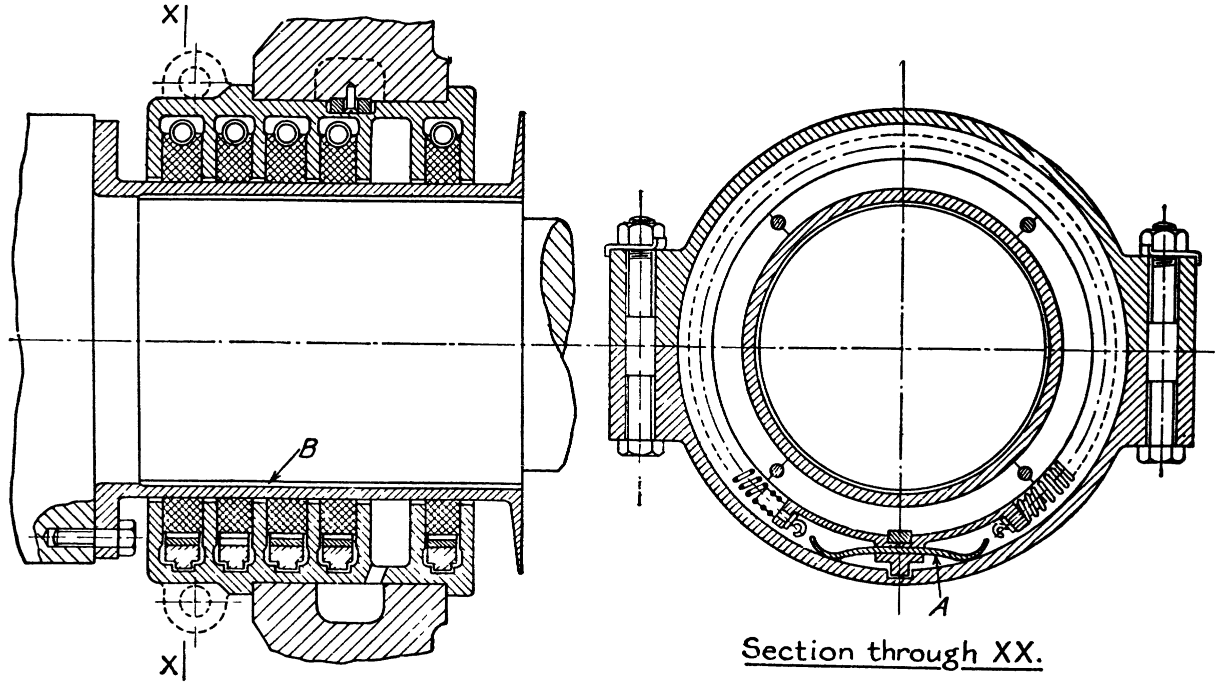


FIG 362 —Carbon-ring Gland

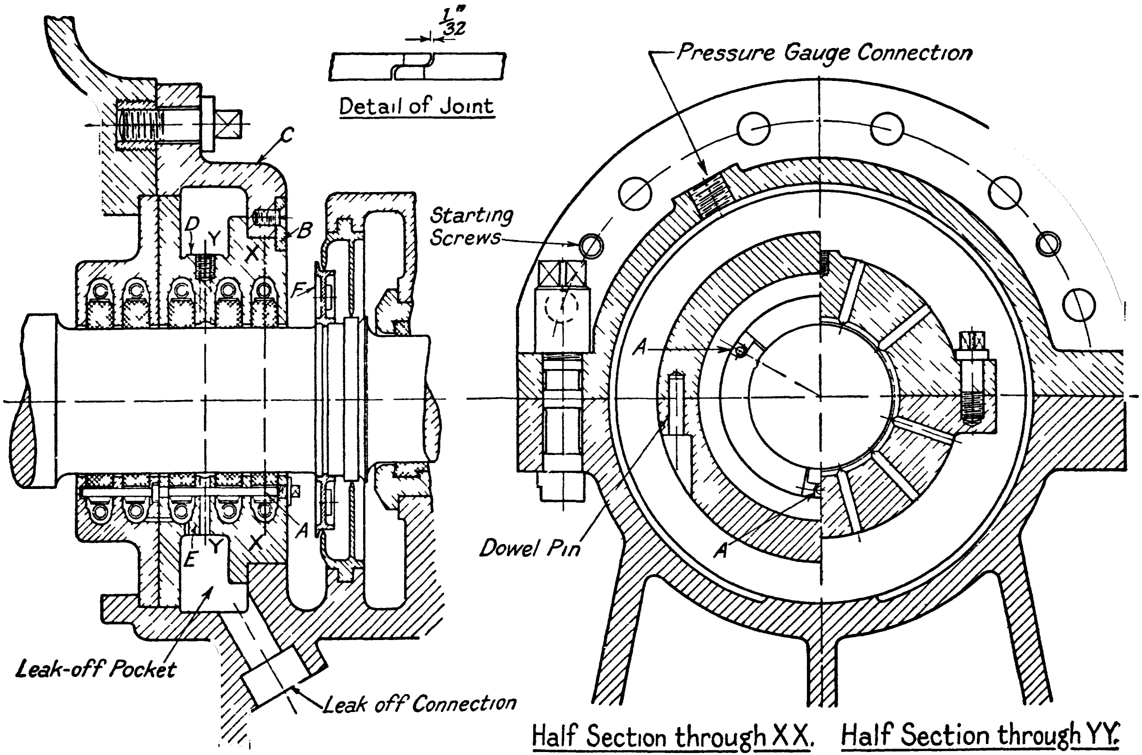


FIG 353 —Carbon packed Glands of Brown-Curtis Marine Turbine

A typical carbon-ring gland is illustrated in Fig. 362. There are four rings between the inside of the turbine and the leak-off pocket, and one between the pocket and the atmosphere. The rings are arch-bound and are supported centrally by the coach spring A. This is attached to a light casting to which the garter springs are attached. Rotation of the rings is prevented by a key sunk into the lowest segment, and by a second key in a shallow recess at the bottom of the gland housing. The outer end of the sleeve B is fin-shaped and forms a deflector which prevents steam blowing out and overheating the bearing.

The design of gland used in the well-known Brown-Curtis turbine is shown in Fig. 363. The carbon rings are arranged in three segments, each with overlapping, or scarf, joints. There is a clearance

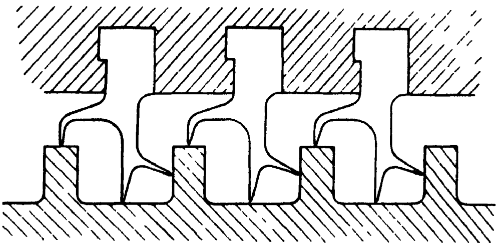


FIG. 364.—Improved Packing for Balance Pistons of Parsons Turbine

at the joint so that the rings are in contact with the shaft. Rotation of the rings is prevented by the pins A. The rings are kept in contact with the shaft by the usual garter spring, but the outer surface of the carbon is protected by a thin strip of sheet brass. The outer half of the housing is prevented from possible rotation by a sunk key plate B. A number of radial holes drilled in the housing communicate with the leak-off (or steam supply) pocket. The rotating baffle F, which is a gunmetal casting in halves, serves the dual purpose of preventing leaking steam from blowing on to the bearing, and oil from creeping along the shaft and entering the gland.

Labyrinth rings and carbon rings are sometimes combined in the same gland, the labyrinth gland being on the steam side. It is claimed that the leakage with this arrangement is lower than with an all-labyrinth gland.

242. Packing of Balance Pistons in Parsons Turbines. Labyrinth packing of some form or other is invariably used. The types shown in Fig. 358 (*a*) and (*c*) are commonly employed in land turbines, since the balance pistons are fairly close to the thrust block, and the axial clearance may be kept reasonably small (say about 0·015 to 0·02 in.). If the relative axial movement between the rotating and stationary elements is likely to be appreciable, as in

marine astern turbines for example, the radial type of packing shown in Fig. 358 (*b*) would be employed.

An improved form of dummy packing used in turbines constructed by C. A. Parsons & Co. is shown in Fig. 364. This provides three seals per ring of packing, one axial and the other two radial, thus reducing the steam leakage. A further advantage is claimed for this packing when compared with that shown in Fig. 358 (*c*). With the two-seal packing there is an appreciable difference between the diameters at which the seals operate, and, if there is wear on one or other of the packing fins, or if the axial position of the rotor changes, the effective diameter of the dummy piston will change and this will affect the residual steam thrust on the thrust bearing. With the three-seal packing, however, the mean diameter of the two radial seals is practically the same as that of the axial seal so that the effective diameter of the dummy piston is practically unaffected by relative wear or the axial position of the turbine rotor.

The clearance of the axial seal is controlled and set at the same time as the axial clearance for the end-tightened blading.

CHAPTER XXV

BEARINGS AND LUBRICATION

243. Introduction. When a lubricant such as a mineral oil is smeared over a metal surface and the surplus lubricant is wiped off it is found that there remains an exceedingly thin film on the surface. It appears that there is a bond between the molecules of the lubricant and those of the metal surface which causes the film to adhere strongly to the metal. Such a film is said to be adsorbed and is only a few molecules thick. When metal surfaces are separated by adsorbed oil films the friction is described as *boundary friction* and the lubrication as *boundary lubrication*. The force of friction with boundary lubrication is lower than the friction of dry surfaces. Owing to the imperfections of actual metal surfaces, true boundary lubrication occurs only at the "high spots" which are in contact.

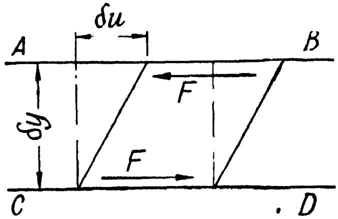


FIG. 365

If, by any means, a film of oil which is still quite thin (say 5 to 10 thousandths of an inch in thickness) but which is hundreds of thousands of molecules in thickness can be introduced and maintained between the two moving surfaces in a bearing, then the resistance to motion is due to the sliding of layers of oil over one another and is very much smaller than the resistance experienced in boundary lubrication. Moreover, the maintenance of a full and continuous film of oil between the bearing surfaces prevents any contact between the metals and thus prevents wear. Lubrication of this type is termed *film lubrication*, and the object of bearing design is to ensure complete film lubrication over the bearing surface with the minimum friction consistent with reliability and safety.

The most important property of a lubricant in film lubrication is its viscosity. Consider a fluid moving with stream line or viscous flow, i.e. with a motion free from eddies. Let AB and CD, Fig. 365, represent two imaginary parallel layers of fluid particles situated a small distance apart δy, and let δu be the velocity of AB relative to that of CD. Then the movement of AB will be opposed by a viscous drag F per unit area.

Then $$F = Z\left(\frac{\delta u}{\delta y}\right)$$

where Z is defined as the coefficient of viscosity (or simply the viscosity) of the fluid.

In the c.g.s. units, $F = \dfrac{\text{dynes}}{\text{cm.}^2}$; $\delta u = \dfrac{\text{cm.}}{\text{sec.}}$; and $\delta y = \text{cm.}$ Hence $Z = \dfrac{\text{dynes . sec.}}{\text{cm.}^2}$. This unit is known as the *poise* (after Poisieulle). The centi-poise is $\frac{1}{100}$ poise. Since 1 dyne $= \dfrac{\text{gr. cm.}}{\text{sec.}^2}$, the units of Z are also $\dfrac{\text{gr.}}{\text{cm. sec.}} \left(\dfrac{M}{LT}\right)$. To convert to British units—

$$1 \text{ Poise} = 0{\cdot}00209 \frac{\text{lb. wt. sec.}}{\text{ft.}^2}$$

$$= 0{\cdot}0000145 \frac{\text{lb. wt. sec.}}{\text{in.}^2}$$

$$= 0{\cdot}0672 \frac{\text{lb.}}{\text{ft. sec.}} \left(\frac{M}{LT}\right)$$

Typical temp.-viscosity curves for turbine lubricating oils are shown in Fig. 366, which shows clearly the influence of temperature

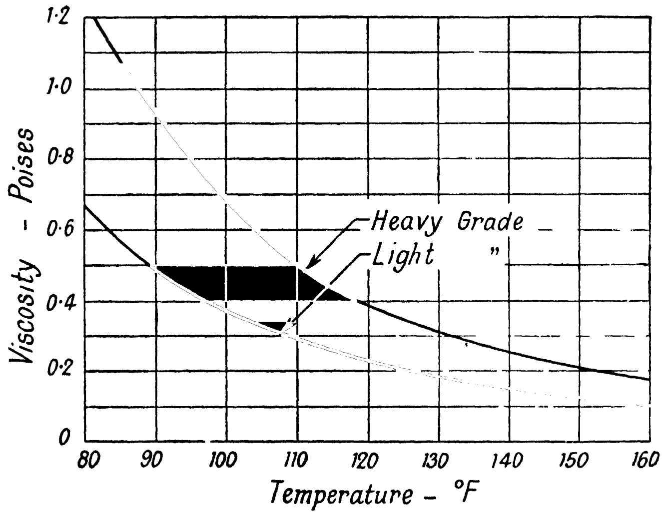


FIG. 366.—Range of Viscosity of Turbine Lubricating Oils

on viscosity. The normal range of temperature is from 110° F. to 140° F., and the tendency is to use the lighter grades of oil except where the bearing temperature is high or where the pressure intensity in the bearing is high.

244. Beauchamp Tower's Experiments. Little was known about the lubrication of journal bearings prior to the year 1883, when Beauchamp Tower published the *First Report of the Research*

Committee on Friction for the Institution of Mechanical Engineers. Subsequent reports were published in 1884, 1885, 1888, and 1891.

In most of his experiments on journal bearings, Tower used a bearing 4 in. diameter by 6 in. long, and subtending an angle of 155°. The brass rested on top of the shaft, and an oil bath was so arranged that the shaft could dip into it (see Fig. 367). Thus the oil was carried up into the brass as the shaft rotated. It was found that the brass was completely supported by an oil film. At one

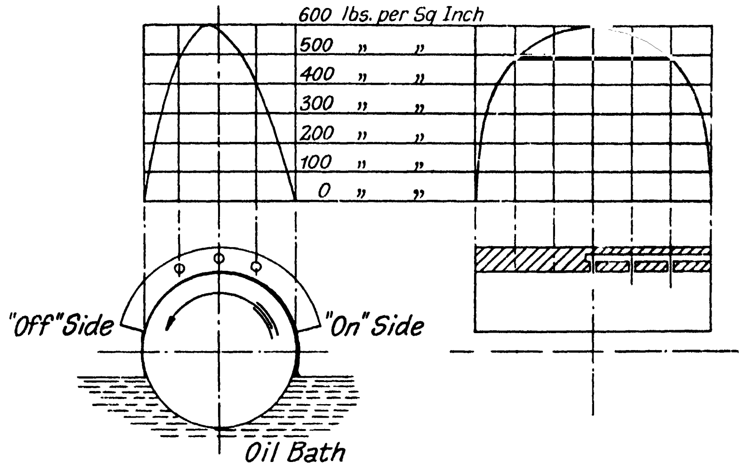


FIG 367

point in the experiments, the brass had been dismantled and a ½-in. hole was drilled in the crown for a lubricator. On running the journal without the lubricator it was found that oil was emerging from the hole. The hole was accordingly plugged with wood, but it was found that, owing to the pressure of the oil, the plug was gradually being forced out. A series of holes was now drilled in the brass at different points around its arc of contact with the oil film and along its length. By means of these holes the pressures in the bearing could be measured and curves such as those in Fig. 367 obtained. The point of maximum pressure occurs a little on the "off" side of the centre of the brass, and the brass sets itself slightly eccentric to the journal, the oil film being thicker at the "on" side than at the "off" side.

Professor Osborne Reynolds studied Tower's results and came to the conclusion that the problem could be considered from the standpoint of hydrodynamics. He deduced certain equations which have formed the basis of lubrication theory ever since. These are set out, together with analyses of Tower's results, in a classical paper (2).

245. Conditions Essential for Film Lubrication. Tower's experiments show quite clearly that in a journal bearing the pressure in the oil film is atmospheric at inlet and outlet, and that in the central plane it increases to a certain maximum and then falls away again. The same remark applies to all other transverse planes except those coinciding with the sides of the bearing, where the pressure necessarily falls to atmospheric. Certain conditions are essential for the formation of such a pressure film. These will first be considered for a bearing of infinite width, i.e. without side leakage.

Imagine that Fig. 368 represents the cross-section of two plane surfaces A and B, both of which are infinitely wide in a direction perpendicular to the plane of the paper. A is assumed to be fixed while B is moving with constant speed. Assume, in the first case, that the two surfaces are separated by a continuous film of oil, and that there is no force tending to cause one surface to move

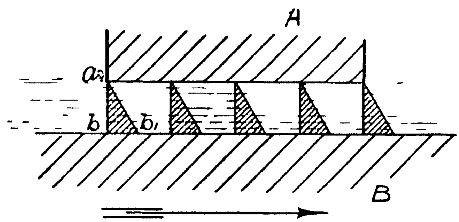


FIG. 368

towards the other. Now the oil will cling to both surfaces and hence the particles of oil adhering to A will be stationary, while those adhering to B will have the same velocity as B. The oil film is being subjected to a continuous shearing and particles lying between A and B will have a velocity proportional to their distance from A. Hence, if bb_1 represents the velocity of B, the triangles abb_1 are velocity triangles, and the area cross-hatched represents the volume of oil passing any section per unit width perpendicular to the plane of the paper. Hence the same volume of oil flows past each section, and the arrangement simply constitutes a pump operating without any pressure difference.

Assume now that both surfaces A and B are at rest, but that a force is applied which will gradually cause the two surfaces to approach each other and so squeeze out the oil film. If the dotted lines represent the initial conditions (Fig. 369) and the full lines the conditions at a later instant, it is clear that the areas a_1 and a_2 of the bulges will be equal respectively to $x_1 . \delta t$ and $x_2 . \delta t$. It will be understood that the curved lines represent successions of oil particles which were originally represented by the straight dotted lines. The existence of the bulging lines is evidence of an internal pressure in the oil, which is momentarily balancing the external forces applied to A and B.

Suppose now that the conditions assumed in the foregoing considerations exist simultaneously, i.e. that B is moving and that a force is applied to A and B tending to bring them together (Fig. 370). It is to be further assumed that the surfaces are so constrained as to remain parallel. From what has been said before, it will be

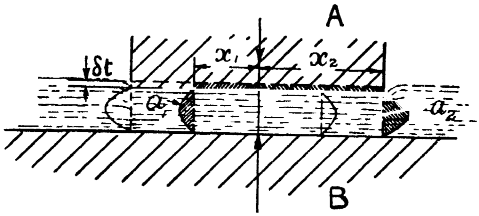


FIG 369

at once apparent that the cross-hatched areas in Fig. 370 represent the volume of oil passing any section of unit width in unit time. But these areas are not equal, and it will be seen that more oil is passing out from between A and B than is entering, and there-

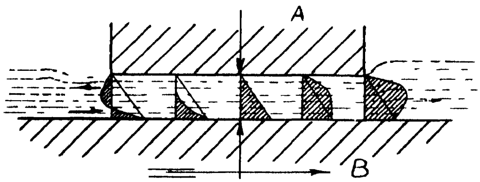


FIG. 370

fore that in a short time no oil will separate the surfaces and metallic contact will ensue.

It may be pointed out in passing that these are the conditions which exist in that type of thrust block in which one or more collars turned on the shaft abut against fixed rings or shoes. The latter are usually lined with white-metal and the oil is fed into the space between the shoe and collar at various points. In practice, the performance of this type of thrust bearing has never been satisfactory, and the maximum allowable pressure under a steady load does not exceed 30 lb. per sq. in.

Imagine now that the block A is freed from constraint (Fig. 371) and allowed to tilt relative to the surface B. Then if the tilt be such that the effective cross-hatched areas are equal at all points, a constant quantity of oil will pass between the two spaces. Moreover, the oil film is capable of sustaining and, therefore, of generating a certain pressure. This simple analysis shows that the essential condition for a pressure film is that the space between the two surfaces should be tapered or wedge-shaped.

This requirement may be shown more convincingly as follows. Let A and B, Fig. 372, be two parts of a journal bearing or Michell thrust block separated by a film of oil. Suppose that A is stationary and that B moves with a velocity u_1. The oil particles in contact with A will be at rest, while those in contact with B will be

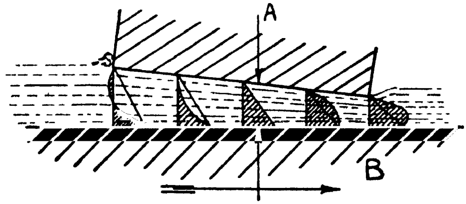


FIG. 371
The actual inclination of A to B is about 1 in 3,000

moving with a velocity u_1. The linear velocity of fluid particles in the film will vary in a definite manner across the depth of the film.

It is assumed that the depth of the bearing perpendicular to the paper is infinite, and that fluid particles move only in planes parallel

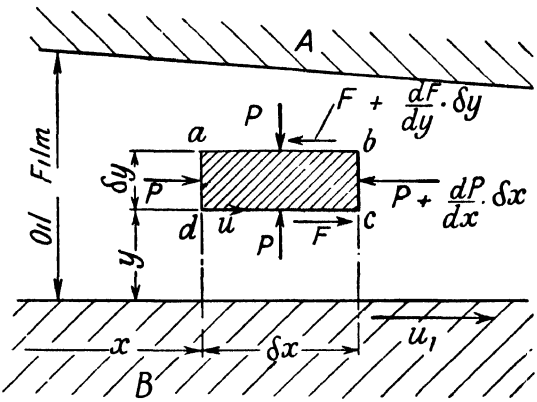


FIG. 372

to the plane of the paper. Consider a small prismatic element of fluid *abcd* of length δx, height δy, and unit depth. It will be assumed that for any value of x, the pressure intensity at any point in the film is P, i.e. P is independent of y. When x increases to $x + \delta x$, P increases to $P + \frac{dP}{dx} . \delta x$. Let the velocity of the fluid particles at a height y above B be u, and suppose that this velocity does not vary in the z direction. If the velocity gradient in the y

direction is $\frac{du}{dy}$, then the shearing stress in the oil film is

$$F = -Z\left(\frac{du}{dy}\right), \text{ because } \frac{du}{dy} \text{ is negative.}$$

Now, if $\frac{du}{dy}$ is constant, i.e. if the change of velocity is uniform across the depth of the film, then F is constant. If $\frac{du}{dy}$ varies, then F will also vary, and

$$\frac{dF}{dy} = -Z\left(\frac{d^2u}{dy^2}\right)$$

Considering the forces acting on the fluid element in the direction of motion (others balance), we have—

$$\frac{dP}{dx} \cdot \delta x \cdot \delta y = -\frac{dF}{dy} \cdot \delta y \cdot \delta x$$

$$\therefore \quad \frac{dP}{dx} = -\frac{dF}{dy} = Z\left(\frac{d^2u}{dy^2}\right)$$

Consider the journal bearing used in Tower's experiments. Suppose that the two surfaces are developed so that one of them, e.g.

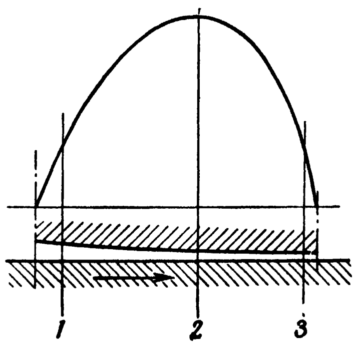


FIG. 373

the moving surface, is plane (Fig. 373). Then at the "on" side, section 1, $\frac{dP}{dx}$ is positive; at section 2, where P is a maximum, $\frac{dP}{dx} = 0$; while at the "off" side, section 3, $\frac{dP}{dx}$ is negative. In order to satisfy these requirements, the variation of velocity across the oil film at the points considered must be such that $\frac{d^2u}{dy^2}$ is positive, zero, and negative at sections 1, 2, and 3 respectively. The

necessary variations are shown in Fig. 374. It will be seen that these are the same as shown in Fig. 371.

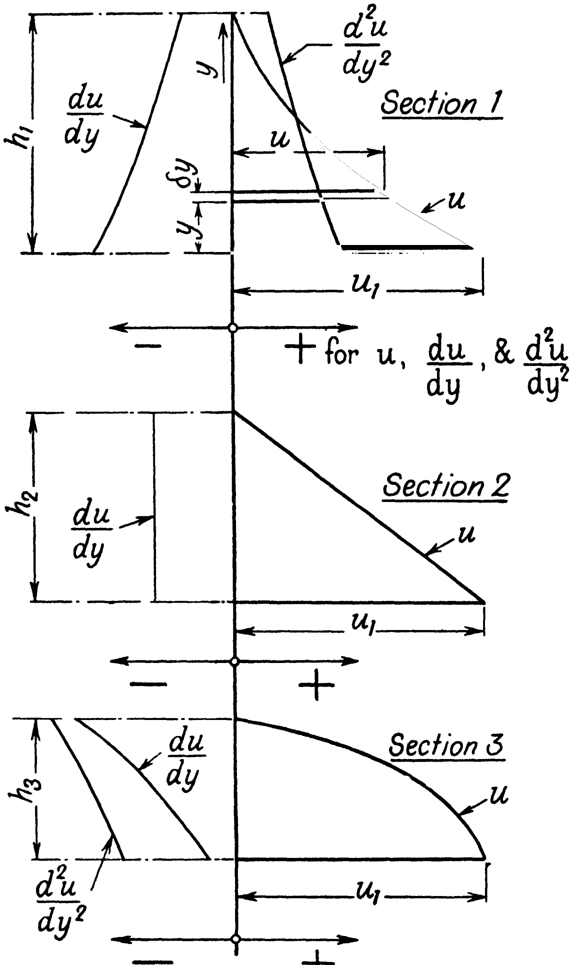


FIG. 374.—Variation of Velocity in Oil Film at Different Sections of Fig. 373

Consider now the quantity of fluid flowing past any section per unit depth perpendicular to the paper. This is obviously

$$Q = \int_0^h u \, . \, dy = h \, . \, u_m$$

where h is the thickness of the oil film measured perpendicular to the moving element, and u_m is the mean velocity of the fluid film. Since there is no side leakage, the volume of oil passing all three sections must be the same. Then since $u_{m1} < u_{m2} < u_{m3}$, $h_1 > h_2 > h_3$. That is to say, the oil film must converge in the direction of motion of the moving element.

If, as in actual bearings, there is side leakage, then the quantity of oil moving forward is continually being diminished, and an even greater convergence of the oil film becomes necessary.

246. The Journal Bearing. The essential parts of a journal bearing are shown in Figs. 375 and 376, the clearances being greatly

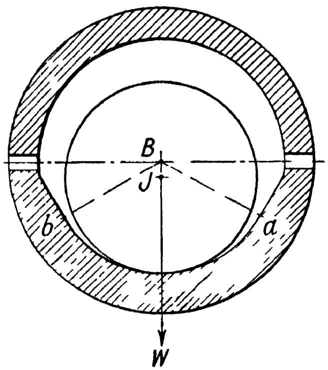


Fig. 375

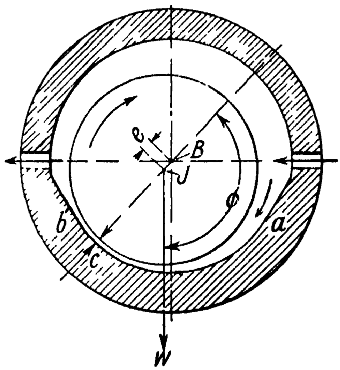


Fig. 376

exaggerated for the sake of clearness. It was formerly the practice to "bed" the journal into the "brass" by scraping the white-metal lining until the radius of the lower part of the brass was equal to that of the journal. In such a case, any possible movement of the journal which takes place when the journal begins to rotate does not lead to the formation of a satisfactory wedge-shaped film of oil, and it is difficult, if not impossible, for true film lubrication of such a bearing to take place.

In most cases, the lower part of the bearing is now bored out to a radius which is slightly larger than that of the journal itself. In some cases the clearance in the upper part of the bearing is made still larger, except at the ends of the bearing where a smaller clearance is employed in order to prevent excessive side leakage of oil. The arc *ab* represents the true bearing surface. Above *a* and *b*, the white-metal is scraped away to provide a large clearance. J and B represent the centres of the journal and bearing respectively.

Fig. 375 represents the bearing with the journal at rest. The journal is lying in the bottom of the brass, contact being along a comparatively narrow strip of bearing surface with a high intensity of pressure. Assuming clockwise rotation of the journal, it would

appear that at the first instant of movement the journal would tend to roll slightly to the right and upwards. But slipping would soon take place and there would be appreciable relative motion between the journal and the brass. During this stage the lubrication would be of the boundary type, although if the journal were kept rotating slowly it is quite likely that metallic contact and wear would ultimately take place. If, however, the speed be gradually raised and if oil be supplied at the "on" side, then oil will

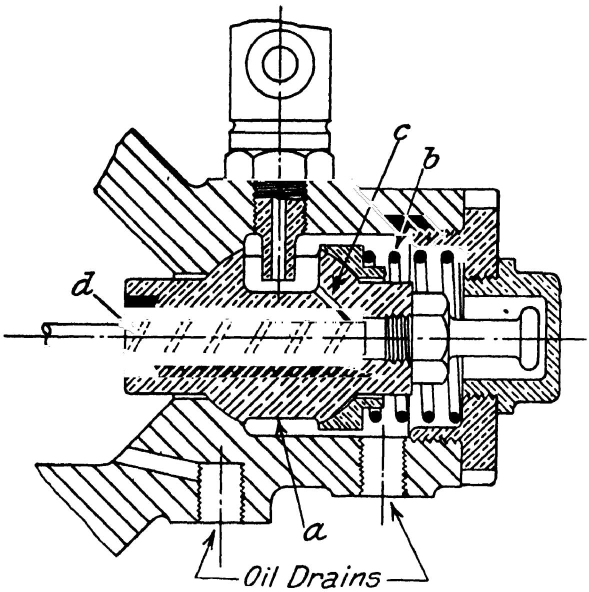


FIG. 377.—Bearing for De Laval Turbine

be dragged into the clearance space to a greater and greater extent. If the conditions are favourable, a continuous film of oil will form from a to b. It will be seen from Fig. 376 that for the formation of the necessary converging film of oil, the journal must move upwards and to the left. The final position of the journal is such that the resultant force due to the oil pressures generated in the oil film just balances the load on the journal. The distance JB is termed the "eccentricity" of the bearing, and the angle ϕ between the line of centres and the load line is termed the "attitude."

It will be clear that the oil film has its least thickness at c, Fig. 376, where the line of centres crosses the film. This minimum thickness equals $r - e$, where r is the radial clearance in the lower half and e is the eccentricity JB in the running position. From c to b the film is divergent, and in this part the pressure might fall below atmospheric so that air is drawn in. In such a case the film might

break down and metallic contact ensue. For this reason, the arc *ab* should not subtend too great an angle at the bearing centre. An angle of 110 to 120° is commonly used in turbine work. Professor Goodman, experimenting in 1885, showed that by reducing the arc of contact from 180° to 30°, other things remaining equal, the frictional resistance was progressively reduced.

247. Construction of Journal Bearings. In very small turbines drip feed lubrication may be employed. Fig. 377 shows a bearing for a small de Laval turbine. The bearing shown supports the

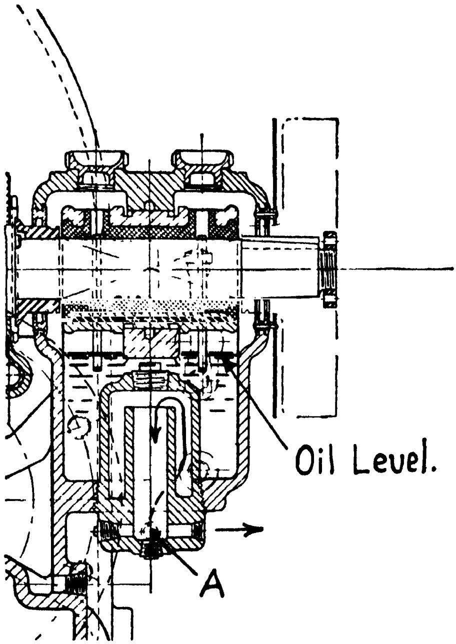


FIG. 378.—Water-cooled Ring oiled Bearing on Terry Steam Turbine

turbine spindle at the end remote from the gearing, and consists of a bronze bush *a*, in one piece, and lined with white-metal. The bush is ball seated and, having little more than its own weight to support, is held in position by the compression of a light spring *b*. The oil dropping in from the sight feed enters the bearing at one end by the hole *c*. To distribute the oil satisfactorily, a shallow helical groove *d* is cut in the bush, the oil being carried to the other end of the bearing by the drag of the shaft.

A ring-oiled bearing for a Terry steam turbine is shown in Fig. 378. The bearing comprises a bush lined with white-metal and is provided with two rings dipping into an oil bath. Rotation of the

shaft causes the rings to rotate and oil to be lifted into the bearing. A simple method of cooling the oil is shown. Cooling water is supplied at A, rises in the annular space between the core and the outer chamber, and flows downwards through the central core to the outlet pipe.

Considering the larger forced-lubricated bearings, it may be stated that practice differs chiefly in respect of the following—

(*a*) Methods of boring out the white-metal.
(*b*) Methods of supporting the bearing.
(*c*) Methods of introducing the oil into the bearing.

Three methods of boring out the white-metal lining are indicated in Fig. 379. In (*a*) the brass is simply bored out truly circular with a diametral clearance of about 0·002 in. per inch of journal

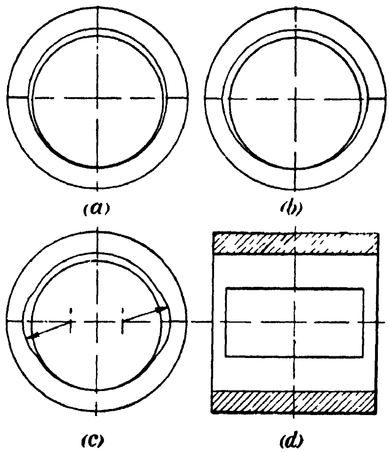


FIG. 379

diameter. With small bearings, the clearance would be larger—from 0·003 to 0·005 in. In (*b*) the brass is bored out circular, but with temporary liners between the two halves. When the liners are removed and the bearing is assembled the horizontal clearance is greater than the vertical. In (*c*) the bearing is first bored out cylindrical with the clearances stated above, and then the sides are eased as shown, except at the ends of the bearing (see (*d*)).

Methods of supporting the brass and of introducing the oil will be considered together. The rigid type of support is well exemplified by the marine turbine bearing shown in Fig. 380. The bearing consists of bronze shells *a* lined with white-metal and bedded into the bearing block and keep. Lubricating oil is supplied through a hole in the side of the bearing block to the annular passage *b*, from whence it passes through the rectangular opening *c* into the space

between the journal and the brass. The curved dotted line *d* indicates the boundary of that part of the white-metal on either side of the horizontal joint which is eased off to facilitate entry of the oil. The dimension E is made about $\frac{D}{6}$.

Instead of fitting a pressure gauge (which might soon get out of order) to indicate the presence, or otherwise, of a plentiful supply

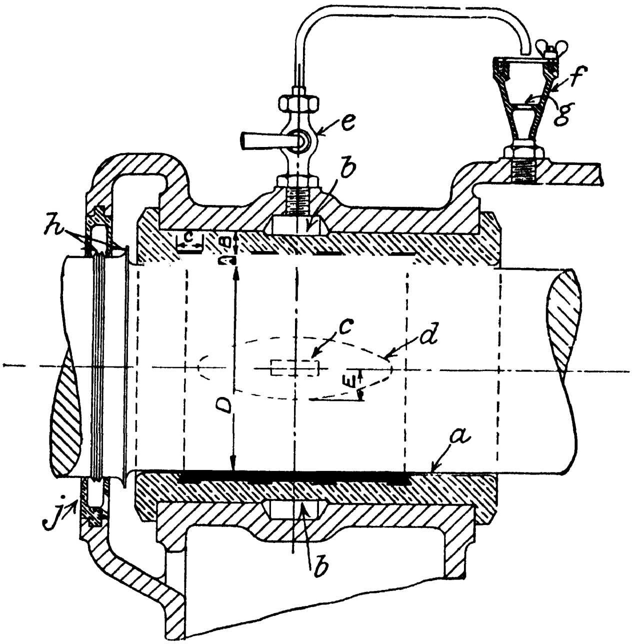


FIG. 380—Bearing for Marine Turbine

of oil, a test cock *e*, which may be opened occasionally, is fitted. This cock is in communication with the oil supply passage *b*, and discharges into a funnel *f* fitted into the side of the bearing keep. The oil thus returned to the oil well is strained through a strip of wire gauze *g*. The oil leaking from the side of the bearing is prevented from creeping along the shaft into the turbine glands by the centrifugal throwers *h*, while the light baffle *j* serves the dual purpose of preventing oil and oil vapour from leaking out of the bearing housing and of minimizing the heating of the bearing by leakage of steam from the gland.

It will be noticed that the bronze portion of the bearing extends somewhat on either side of the white-metal, forming what is termed

a "safety strip." Should the white-metal flow, owing to overheating of the bearing, the rotor drops through a small distance on to the safety strip and may be so supported until steam is shut off. This would prevent a dangerous stripping of the blades, and would for a short time, provided the supply of oil is maintained,

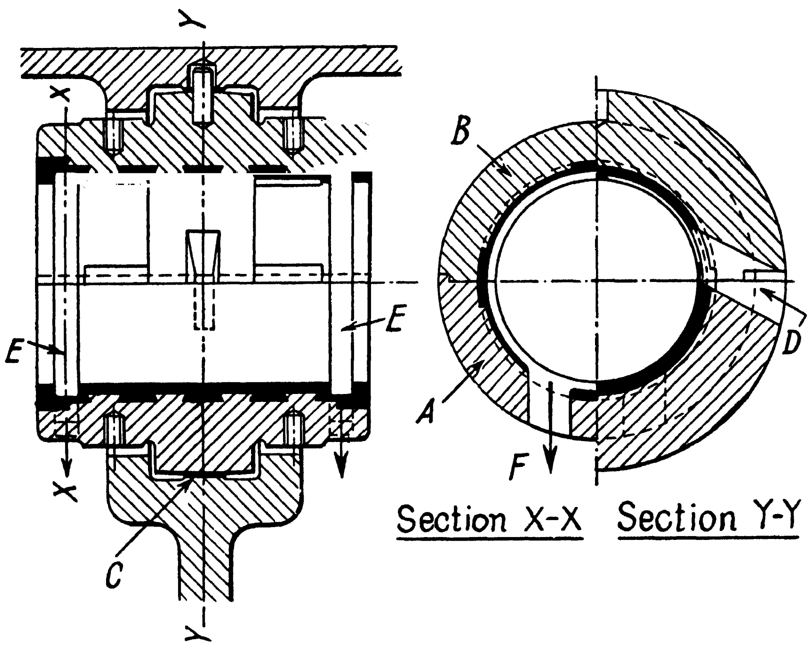


FIG. 381

prevent serious damage to the shaft. The safety strip is usually about 0·015 in. below the white-metal all round.

The minimum thickness of the white metal $= A = \frac{D}{50} + \frac{3}{16}$ in.; $B = \frac{D}{10}$ for journals 4 in. dia. and over; $C = \frac{D}{13} + \frac{1}{2}$ in.

Fig. 381 shows a turbine bearing by Messrs. Brown Boveri & Co., Ltd. The bearing consists of two halves A and B spigoted together and supported at C over a short length, so that the bearing can tilt slightly and thus yield to change in slope of the shaft. Oil enters at D at the "on" side. Oil leaking from the sides of the bearing flows into the grooves E and issues from the openings F. This device, widely used on turbine bearings, prevents oil from

creeping along the shaft in quantity and considerably lightens the duty of the oil throwers.

A bearing construction of considerable interest is shown in Fig.

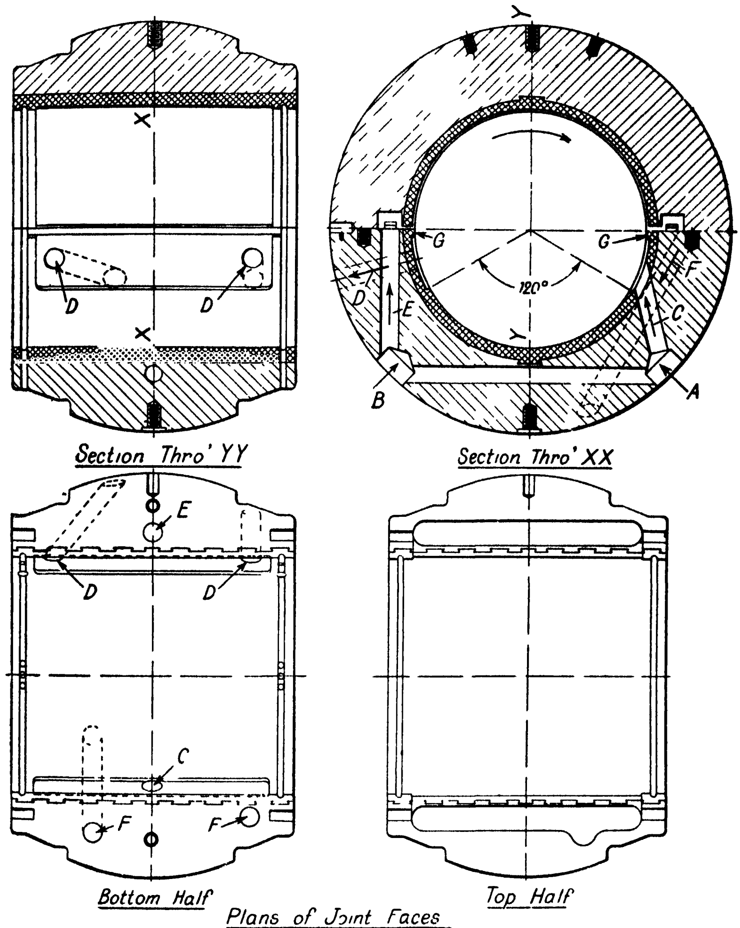


FIG 382 - Spherically-seated Journal Bearing

382. It is designed to support a journal 20 in diameter on a British Thomson-Houston steam turbine The bearing is supported in a spherical seating in the pedestal. There are two definite supplies of oil, one for lubrication purposes and the other for cooling. The oil is supplied through ports in the seating and enters the lower half of the bearing at A and B. The lubricating oil proper enters

the bearing through the hole C and, after passing round the lower part, escapes through holes D. The cooling oil passes in through the hole E and, after passing through a narrow slit, enters the top half. It is dragged round by the journal surface and escapes through a long slit and finally by way of the holes F. At each side of the bearing the white-metal is carried out at G to within 0·003 in. of the shaft to form a wiper or scraper. This wiper prevents either the lubricating oil or the cooling oil from being circulated round

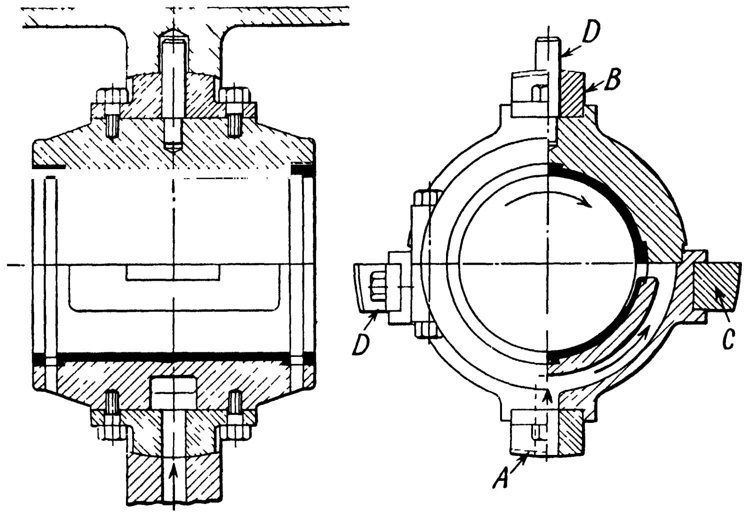


FIG 383.—Sphericallv-seated Bearing with Detachable Pads

the bearing, and has been found to effect a considerable reduction in power loss.

A form of bearing which is widely used in steam turbines is shown in Fig. 383. The bearing is again supported in a spherical seating which allows freedom of alignment, but the steel pads A, B, C, and D are detachable. Between the pads and the bearing shell are a few thin liners which differ in thickness by small amounts. By changing these liners, the centre of the bearing may be adjusted for vertical or horizontal position. Lubricating oil is supplied through a hole in the pedestal and passes through a cored passage in the lower half of the bearing. A stop-pin D prevents the bearing from rotating.

248. Materials. The material most commonly used for the bearing shell is cast iron. Where greater strength or rigidity is desired, cast steel is employed, while in naval work bronze is mostly used. In all cases, the bearings are lined with white-metal. Longitudinal and circumferential dovetail grooves secure the lining in

the shell. In addition a bond is obtained by tinning the inside of the bearing shells before the white-metal is poured in.

Typical analyses of white-metal, given in a paper by Drs. H. L. Guy and D. M. Smith (3), are as follow—

	For Ordinary Conditions	For High Temp Conditions
Tin	78	86
Antimony	13	8·5
Copper	6	5·5
Lead	3	

249. Design of Journal Bearings. The basic data for design are the total load W and the speed of rotation. The quantities which have to be determined include the radius of the journal, the axial width of the bearing, the angle which the effective bearing surface subtends at the centre of the bearing, the radial clearance, and the quantity of oil to be supplied per unit time.

The design of turbine bearings has been largely based on experience. Before film lubrication was understood and long after it had been explained by Osborne Reynolds, it was thought that, as in dry friction, the coefficient of friction would be constant and, in consequence, the heating effect in a bearing would be proportional to the product pu, where p is the pressure in lb. per sq. in. of projected area and u is the velocity of the journal surface. In accordance with this idea, the value of this product was kept within certain limits. This led, in many cases, to turbine bearings in which the ratio of width to radius was sometimes greater than 6. It is now realized that the pu product has little or no significance and, as a result, shorter bearings are used, the ratio of width to radius being from 1 to 1·5, and occasionally as low as 0·5. The pressure per sq. in. of projected area varies from 30 to 200 lb., the normal values ranging from 80 to 120. Owing to the increase in output of high-speed turbines, the journal surface speed has steadily increased and now often reaches 150 to 160 ft. per sec. As already stated, the effective bearing angle is normally 110° to 120°. The radial clearance ranges from 0·001 to 0·0015 in. per inch diameter.

There are many factors which tend to make the design and operation of turbine bearings a matter of trial and error. In the first place, the variation in the viscosity of the oil due to the rise in temperature which takes place during its passage through the bearing makes any theoretical treatment of the subject difficult. The radial expansion of the journal due to temperature rise is often

commensurate with the radial clearance allowed and should be specially considered in the case of turbines operating with high temperature steam. In this connection a water seal provides a valuable cooling agent between the gland and the bearing. Then finally the distortion of the bearing under heavy loads may produce appreciable changes in curvature and clearance.

A method of design, based on hydrodynamic principles, has, nevertheless, been put forward by Professor H. W. Swift (4). This method is based partly on a theoretical paper (5) by himself, and partly on a paper by Dr. Albert Kingsbury (6). The following brief summary of the method is set out for 120° bearings only, since this is the type approaching nearest those used in steam turbines. For the more complete application of the method the reader is referred to the original paper.

Let W = total load on bearing, lb.
R = radius of journal, in.
B = axial width of bearing, in.
L = circumferential length of effective bearing arc, in.
r = radial clearance, in.
ω = angular velocity of journal.
P = load per unit width $= \dfrac{W}{B}$.
Z = viscosity of oil, lb. wt. in. sec. units
u = surface speed of journal, in. per sec.
ε = eccentricity $= \dfrac{e}{r}$ (see Fig. 376).

Then it may be shown for an infinitely wide bearing without side leakage that $\left(\dfrac{P}{Zu}\right)\left(\dfrac{r^2}{R^2}\right)$ is a function of the eccentricity ε for a given bearing angle. $\left(\dfrac{P}{Zu}\right)\left(\dfrac{r^2}{R^2}\right)$ is a dimensionless quantity which is termed the load criterion. Writing Δ for this, the calculated relationship between Δ and ε is shown in Fig. 384. It will be observed from this that greater values of the load criterion Δ are associated with greater values of ε and, therefore, with thinner oil films.

It may also be shown mathematically that $\dfrac{\mu R}{r}$ is a function of ε, the relationship for a bearing without side leakage is shown in Fig. 384, the curve being a rough interpolation between curves for bearing angles of 90° and 180°.

The design of the bearing should be such that—

(1) The thickness of the oil film at the point of closest approach should be as great as possible. This leads to maximum reliability.

(2) The coefficient of friction μ should be as small as possible.

The minimum thickness of the oil film is $t = r(1 - \varepsilon)$. For any value of ε, the corresponding value of Δ may be obtained from

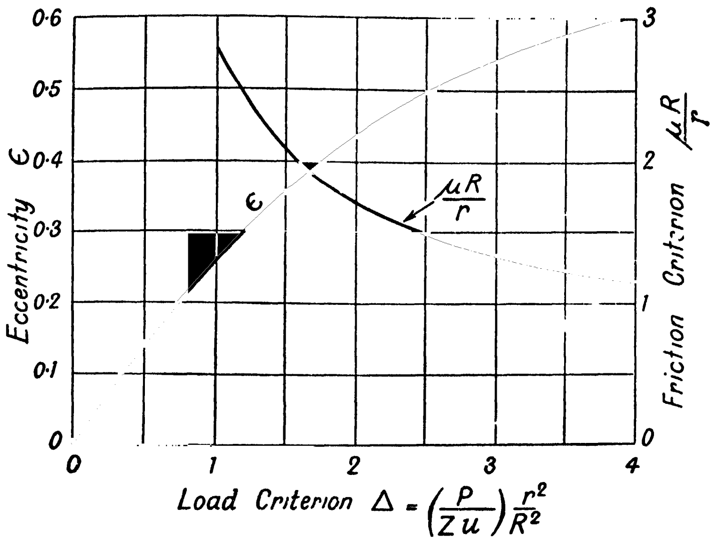


FIG. 384 —120° Journal Bearings of Infinite Width

Fig. 384. From this we may calculate $\frac{r}{R}\sqrt{\frac{P}{Zu}}$ and hence $\frac{t}{R}\sqrt{\frac{P}{Zu}}$, termed the film thickness characteristic of the bearing. Values of this are plotted in Fig. 385.

Similarly, since for any given value of ε we have corresponding values of $\frac{r}{R}\sqrt{\frac{P}{Zu}}$ and $\frac{\mu R}{r}$, it follows we have also values of $\mu\sqrt{\frac{P}{Zu}}$, the friction characteristic of the bearing, Fig. 385. Inspection of Fig. 385 shows that the thickness characteristic is a maximum and the friction characteristic a minimum when ε is about 0·5 for the infinitely wide 120° bearing, and

$$\left[\frac{t}{R}\sqrt{\frac{P}{Zu}}\right]_{B=\infty} = 0{\cdot}794 \quad . \quad . \quad . \quad (240)$$

$$\left[\mu\sqrt{\frac{P}{Zu}}\right]_{B=\infty} = 2{\cdot}34 \quad . \quad . \quad . \quad (241)$$

The effect of side leakage of oil in a bearing of finite width is to reduce the load-carrying capacity and to increase the coefficient of

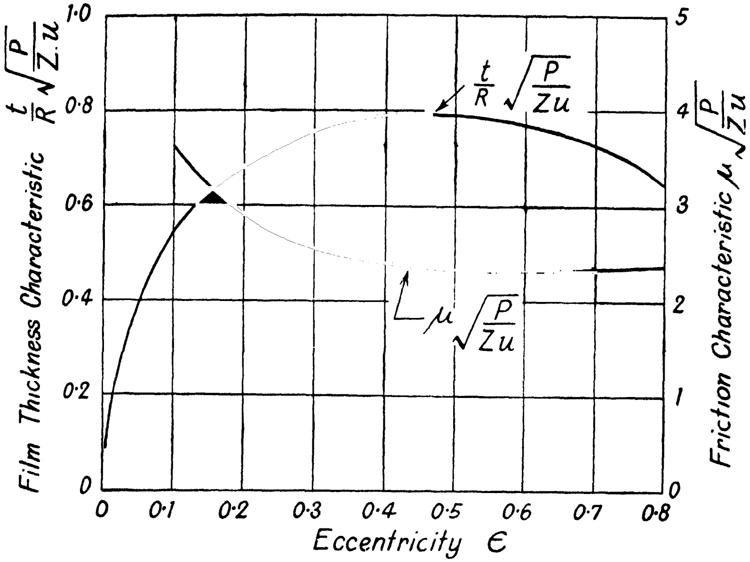


FIG. 385.—120° Journal Bearings of Infinite Width

friction. Kingsbury, employing an electrical analogy, has obtained the relationship between p_0, p, μ_0 and μ, where—

p_0 = pressure intensity in bearing of infinite width
p = pressure intensity in bearing of finite width
μ_0 = coefficient of friction in bearing of infinite width
μ = coefficient of friction in bearing of finite width.

These ratios are plotted in Fig. 386 for various values of L/B.

Now $$\frac{t}{R}\sqrt{\frac{P}{Zu}} = \frac{t}{R^2}\sqrt{\frac{R}{B}}\sqrt{\frac{W}{\omega Z}}$$

$$\therefore \quad \frac{t}{R^2}\sqrt{\frac{W}{\omega Z}} = \frac{t}{R}\sqrt{\frac{B}{R}}\sqrt{\frac{P}{Zu}}$$

$$= \sqrt{\frac{p}{p_0}\cdot\frac{B}{R}}\left[\frac{t}{R}\sqrt{\frac{P}{Zu}}\right]_{B=\infty}$$

$$= 0{\cdot}794\sqrt{\frac{p}{p_0}\cdot\frac{B}{R}} \quad . \quad . \quad . \quad . \quad (242)$$

Also $$\mu\sqrt{\frac{P}{Zu}} = \frac{\mu}{R}\sqrt{\frac{R}{B}}\sqrt{\frac{W}{\omega Z}}$$

$$\therefore \quad \frac{\mu}{R}\sqrt{\frac{W}{\omega Z}} = \sqrt{\left(\frac{\mu}{\mu_0}\right)^2\left(\frac{p}{p_0}\right)\frac{B}{R}}\left[\mu\sqrt{\frac{P}{Zu}}\right]_{B=\infty}$$

$$= 2{\cdot}34\sqrt{\left(\frac{\mu}{\mu_0}\right)^2\left(\frac{p}{p_0}\right)\frac{B}{R}} \quad . \quad . \quad . \quad (243)$$

If varying values of $\frac{B}{R}$ be taken it will be found that the friction is least when $\frac{B}{R}$ equals 2. It increases rapidly for lower values but only slowly for higher values.

Although such methods might give reliable results for partial bearings, the power losses worked out on the coefficient of friction

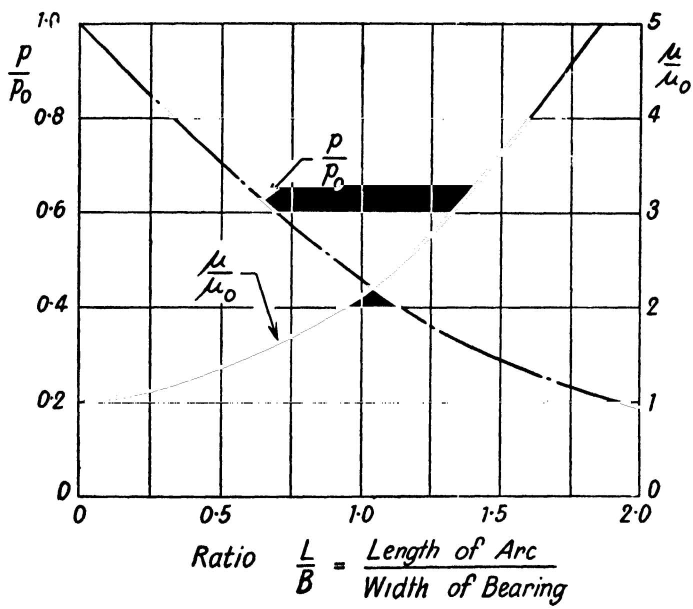


FIG. 386.—Correction Curves for Bearings of Finite Width

derived by their use are generally less than those measured experimentally on actual turbine bearings, the ratio of the actual to the theoretical value being from 1·5 to 2·0. This is probably due to the fact that the actual bearing, although sometimes provided with a fairly large clearance at the top, does embrace the journal for 360 degrees. Moreover, oil is circulating around the complete bearing. Tests on a given type of bearing have shown quite definitely that the power absorbed is increased when a greater quantity of oil is supplied to the bearing.

EXAMPLE 41. The load on a journal bearing is 12,000 lb., and the speed 3,000 r.p.m. Calculate suitable proportions for the bearing, assuming a pressure of 120 lb. per sq. in. of true projected area. Calculate also the least thickness of the oil film, the radial clearance, the coefficient of friction and the theoretical power loss due to friction. Assume that the mean viscosity of the lubricating oil is 0·2 poise.

We shall assume a bearing angle of 120° and a "square" bearing, i.e. B = 2R.

$$\text{Then the projected area} = 2BR\cos 30^\circ$$
$$= 4R^2 \cos 30^\circ = 3{\cdot}464R^2$$
$$\therefore \quad 3{\cdot}464R^2 = 12{,}000 \div 120 = 100 \text{ sq. in.}$$
$$R = 5{\cdot}375 \text{ in.}$$
$$\therefore \quad \text{Dia. of journal} = 10\tfrac{3}{4} \text{ in.}$$
$$\text{Length of bearing} = 10\tfrac{3}{4} \text{ in.}$$

Assuming these dimensions are acceptable we would proceed as follows, basing the calculations on the assumption that $\varepsilon = 0{\cdot}5$.

$$\omega = 314{\cdot}2 \text{ radians per sec.}$$

$$Z = 0{\cdot}2 \text{ poise} = 0{\cdot}0000029 \frac{\text{lb. wt. sec.}}{\text{in.}^2}$$

$$\text{Length of bearing arc } L = 11{\cdot}26 \text{ in.}$$

$$\therefore \quad \frac{L}{B} = \frac{11{\cdot}26}{10{\cdot}75} = 1{\cdot}05$$

Then by Fig. 386, we have $\frac{p}{p_0} = 0{\cdot}43$, and $\frac{\mu}{\mu_0} = 2{\cdot}27$.

$$\text{Then} \quad \frac{t}{R^2}\sqrt{\frac{W}{\omega Z}} = 0{\cdot}794\sqrt{0{\cdot}43 \times 2} = 0{\cdot}736$$

$$\therefore \quad t = 0{\cdot}736R^2\sqrt{\frac{\omega Z}{W}} = 0{\cdot}00586 \text{ in.}$$

This is the least thickness of the oil film, i.e. about 6 thousandths of an inch. Since $\varepsilon = 0{\cdot}5$, the radial clearance must be $2 \times 0{\cdot}00586 = 0{\cdot}0117$, say 0·012 in. This is 0·0011 in. per in. diameter, which is in line with current practice.

$$\frac{\mu}{R}\sqrt{\frac{W}{\omega Z}} = 2{\cdot}34\sqrt{\left(\frac{\mu}{\mu_0}\right)^2\left(\frac{p}{p_0}\right)\frac{B}{R}} = 4{\cdot}92$$

$$\therefore \quad \mu = 4{\cdot}92R\sqrt{\frac{\omega Z}{W}} = 0{\cdot}00727$$

$$\therefore \text{ Frictional force} = 0{\cdot}00727 \times 12{,}000 = 87{\cdot}2 \text{ lb.}$$

Since the surface speed of the journal is 141 ft. per sec.—

$$\text{Theoretical power loss} = \frac{87{\cdot}2 \times 141}{550}$$

$$= 22{\cdot}3 \text{ h.p. or } 16{\cdot}7 \text{ kW}$$

250. The Journal Centre Locus. The path in which the journal centre J moves when the load on the bearing is constant and the speed of rotation or the viscosity of the oil are changed is termed the journal centre locus. Let the quadrant of the circle in Fig. 387 be drawn with centre B corresponding to the centre B of the lower part of the bearing, Figs. 375 and 376, and with radius BJ equal to the radial clearance r. Then J represents the lowest and rest position of the journal. Although Reynolds published his classical equations in 1886, it was not until 1904 that Professor Sommerfeld, in a masterly study (7) of the 180° journal bearing, worked out the locus of the journal centre. BCDE shows the calculated locus for clockwise rotation. It may be shown that the actual position taken up by the journal centre depends on the dimensionless quantity $\frac{Zu}{P}$. If Z and P are assumed to be constant then the position of the journal centre depends only on the surface speed u, i.e. on the speed of rotation. As the speed is increased the journal centre moves in the direction EDCB, and vice versa. This means that if the speed is falling the journal centre moves in the direction of E and ultimately the journal would seize at the *side*. In a later analysis, Professor Gümbel arrived at the conclusion that the locus was approximately the semi-circle BFJ, which gave J as the seizing point—a more rational result. Swift (5) has more recently analysed the same problem and shown that for stability the locus for the 180° bearing should be the curve BCGJ, which coincides with part of Sommerfeld's curve. For the 120° bearing the theoretical locus is the curve BHJ. With an eccentricity ε equal to 0·5, the running position of the journal centre is H and the attitude $\phi = 144°$.

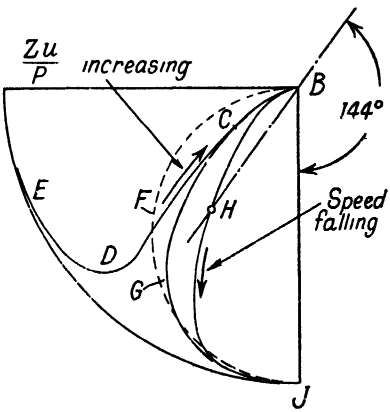


FIG. 387.—Journal Centre Loci

251. Conditions during Stopping and Starting. Consider a turbine which is being shut down. As the speed falls, the load criterion $\left(\frac{P}{Zu}\right)\left(\frac{r^2}{R^2}\right)$ increases, and as the curve of Fig. 384 shows, the

eccentricity ε increases. Thus the journal centre gradually moves from H towards J, Fig. 387, the oil film becoming thinner and thinner. When the speed has fallen to a certain critical value the oil film becomes exceedingly thin and breaks down. The lubrication

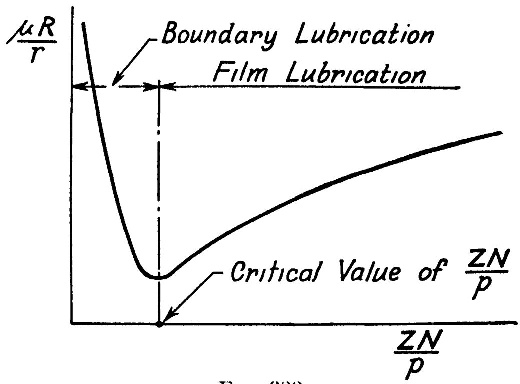


FIG. 388

changes from film lubrication to the boundary type and the coefficient of friction increases as the speed falls. The relationship between $\frac{\mu R}{r}$ and $\frac{ZN}{p}$ is shown by Fig. 388.

Messrs. S. A. and T. R. McKee (8) carried out experiments on a bearing in which $B/R = 2$; $r/R = 0{\cdot}002$ approx.; and $p = 192$ lb. per sq. in. Two mineral oils were used having widely different viscosities. From results obtained, the author has calculated that the critical values of $\frac{ZN}{p}$ at which the type of lubrication changes is about $0{\cdot}605 \times 10^{-6}$ for bronze bearings and $0{\cdot}208 \times 10^{-6}$ for babbitt bearings.

In a paper (9) on journal bearings, Mr. Francis Hodgkinson describes experiments made on a large steam turbine with the object of finding the lowest speed at which the oil films could be maintained. The turbine was allowed to come to rest under its own momentum. Accurate speed measurements were made and from these the retardation was carefully calculated. It was found that with oil temperatures of 115° F. and 95° F. the retardation suddenly increased when the speed had fallen to 19 r.p.m. and 16 r.p.m. respectively. From the data given in the paper, the critical values of $\frac{ZN}{p}$ work out at $0{\cdot}38 \times 10^{-6}$ and $0{\cdot}53 \times 10^{-6}$ respectively. These values are necessarily approximate, since all four bearings would hardly reach the critical state at the same speed.

It appears, therefore, that for bearings lined with white-metal

and lubricated with mineral oils, the critical value of $\frac{ZN}{p}$ is in the neighbourhood of $0{\cdot}5 \times 10^{-6}$.

In starting a turbine, the conditions are somewhat different. As already explained in Art. 246, the first tendency is for the journal to roll on to the "on" side; slipping then takes place and the lubrication is of the boundary type. In general, however, the acceleration will be relatively high and film lubrication will soon be initiated. There is no doubt, however, that the most arduous conditions as regards wear occur at starting and stopping.

252. Turning Gear. If a turbine is shut down and the rotor allowed to rest in one position for an appreciable time, then due to unequal heating the spindle bends. If the turbine is a large one, considerable vibration may occur when the turbine is started again and it may be some hours before the machine can be safely run at its full speed. For this reason, most large steam turbines are provided with motor-driven turning gear to keep the rotor turning slowly while the machine is off load. If the speed of turning is too low for film lubrication to be effective (see preceding article), a special lubricating oil pump is installed. This is a reciprocating pump, sometimes having a separate plunger to each bearing and supplying oil at a pressure of 1,000–1,500 lb. per sq. in. This provides a film of oil under each journal and, while preventing metallic contact, reduces the power required for turning. The Parsons 50,000 kW turbines at Dunston are turned at 13 r.p.m. when off load.

253. Thrust Bearings. In impulse turbines there is a certain force in the axial direction due to the change of momentum of the steam in that direction, as explained in Art. 77. This force tends to push the rotor towards the exhaust end of the turbine, but the total force is usually quite small. In many large so-called impulse turbines, however, the last few stages operate with partial reaction, and the axial forces on the rotor are considerably increased. In Parsons turbines, the axial forces on the moving blades are very large, but these are largely balanced by the steam pressures on the balance pistons. There is, however, a certain moderate residual thrust.

In all cases, a thrust bearing is provided, not only to support the axial force on the rotor but also to fix accurately the axial position of the rotor relative to the casing. The types of thrust bearing which are used in turbine work may be enumerated as follows—

(1) Plain collar type; (2) Bevelled collar type; (3) Kingsbury or Michell type; and (4) Plain collar with fixed inclined thrust pads.

254. Plain and Bevelled Collar Bearings. The plain collar type of bearing comprises a number of collars turned on the shaft working in a fixed housing which must of course, be in halves. The housing

is lined with white-metal. Oil is supplied through a number of radial holes to the inner edges of the collars and taken off through a number of radial holes at the outer side of the recesses (Fig. 389 (*a*)). It has already been shown in Art. 245 that the plain collar type of bearing is fundamentally unsound. Improved performance may

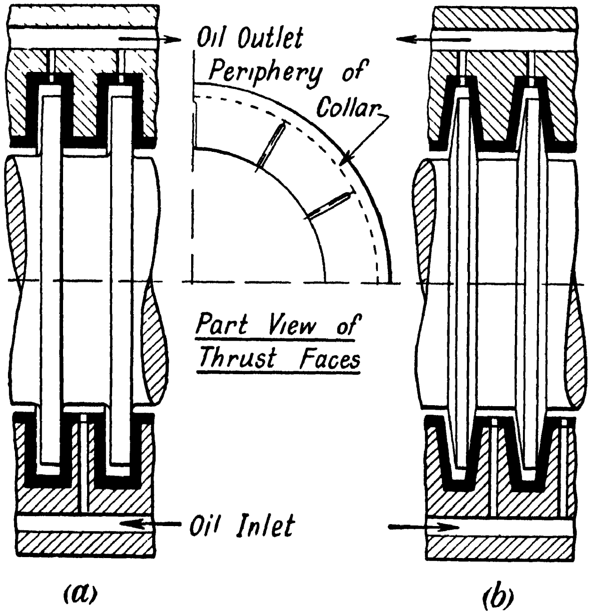


FIG. 389.—Multi-collar Thrust Bearings

be obtained by dividing up the bearing surfaces into sectors and providing radial grooves to distribute the oil to the leading edges of such sectors, as shown in the figure. The sides of such grooves should be well rounded. Fig. 389 (*b*) illustrates the principle of the bevelled collar thrust bearing. It is said to be capable of carrying heavier loads than the plain collar bearing. A tapered film may be obtained with this type of bearing by displacing the axis of the housing with respect to that of the shaft. The allowable pressures in collar bearings is about 20 lb. per sq. in. for the plain collar and 60 lb. per sq. in. for the bevelled collar.

255. Tilting Pad Thrust Bearings. The first tilting pad thrust bearing was made by the American engineer, Albert Kingsbury, in the year 1899. It was independently developed by the Australian engineer, Mr. A. G. M. Michell, who published a mathematical study of the subject in 1905. While the priority of Kingsbury's invention is fully acknowledged, the name of Michell is usually

associated with the tilting pad bearing in this country. Accordingly, it will be described, for the sake of brevity, as the Michell bearing.

The essential feature of the Michell thrust bearing, i.e. the tilting pad, is shown diagrammatically in Fig. 390. The pad rests against a fixed abutment, being supported on a canting ridge parallel to

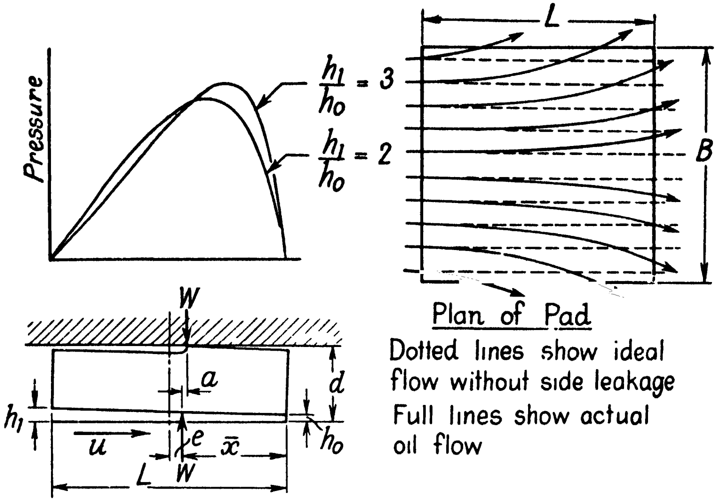


FIG. 390

the outlet edge of the pad. It is thus enabled to tilt at a slight angle to the moving surface of the thrust collar and so permit the formation of a wedge-shaped oil film. The principle has already been explained in Art. 245 and illustrated by Figs. 371 and 374. The theory is fully set out in Dr. R. O. Boswall's book (10).

Consider first the comparatively simple case of a pad of infinite width (B $= \infty$), and assuming that the viscosity Z remains constant. The moving surface is also assumed to be infinitely wide and to move with a uniform velocity u. h_1 and h_0 are the thicknesses of the oil film in inches at the inlet and outlet edges respectively.

Let L = length of pad in direction of motion, in.

u = surface velocity, in. per sec.

W_1 = load per in width, lb.

$\bar{x}$ = distance from outlet edge to centre of pressure, in.

e = eccentricity of load, in.

Then it may be shown that $W_1 = C_1\left(\frac{Z \cdot u \cdot L^2}{h_0^2}\right)$

and that $$\mu = C_2\left(\frac{Z \cdot u}{W_1}\right)^{\frac{1}{2}}$$

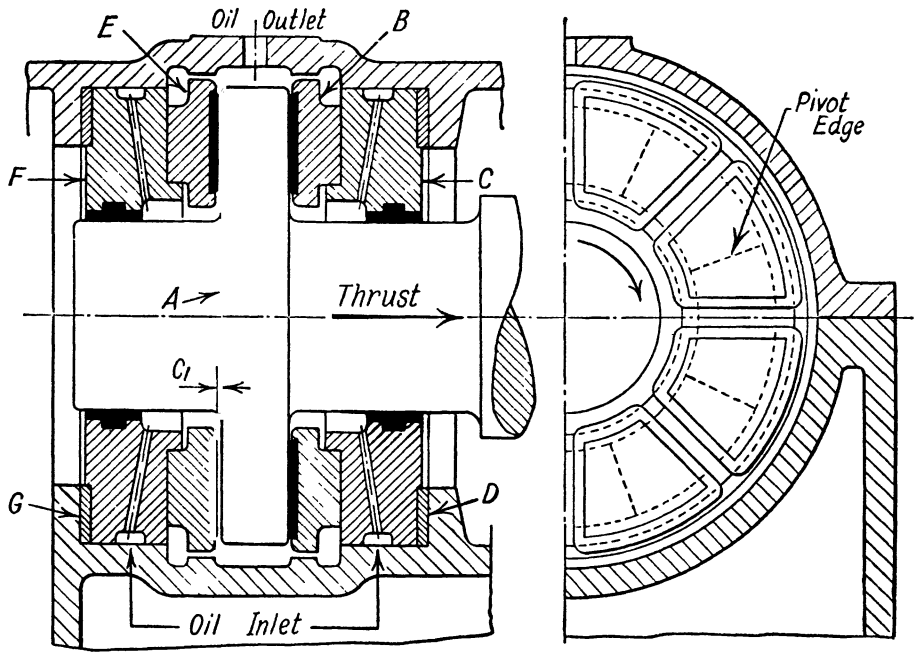


Fig. 391.—Michell Thrust Block

The following values are obtained for different values of the film thickness ratio $\frac{h_1}{h_0}$—

$\frac{h_1}{h_0}$	C_1	$\frac{\bar{x}}{L}$	$\frac{e}{L}$	C_2
1	0	0·5	0	—
2	0·1590	0·432	0·068	1·94
3	0 1476	0·392	0·108	1·82

The curves in Fig. 390 show the calculated distribution of pressure for different film thickness ratios. It will be seen that the loading is definitely eccentric, the centre of pressure being on the outlet side of the centre-line of the pad.

For equilibrium, the supporting edge must be displaced by a small amount a from the centre of pressure. Taking moments about the tilting edge—

$$W . a = \mu W . d$$

or

$$a = \mu d$$

Since d is normally about 0·3L and as μ is not usually more than 0·01, a = 0·003L, an amount which may be neglected.

In actual thrust blocks, the pads are of finite width and oil leaks from the sides. The load-carrying capacity is lower than that of infinitely wide pads, while the coefficient of friction is greater. If we assume that the pads are square and that the velocity u is again uniform, then the correction for load-carrying capacity may be obtained from Kingsbury's curve, Fig. 386. The corrected ratios and constants for the *square* pad are as follow —

$\frac{h_1}{h_0}$	C_1	$\frac{\bar{x}}{L}$	$\frac{e}{L}$	C_2
2	0·0690	0 419	0 081	2·76
3	0·0678	0·374	0 126	2·38

Note.—In using the value of C_2 for finding μ, the actual value of W_1 for the square pad must be inserted in the formula

For a full analysis of the problem and of the more practical case of the sector-shaped pads the reader is recommended to study Boswall's book.

EXAMPLE 42. The thrust block of a steam turbine contains 16 pads, each equivalent to a square of 1·75 in. side. The mean diameter of the pads is 12·5 in. and the speed 3,000 r.p.m. Assuming

that the mean viscosity of the lubricating oil is 0·2 poise, that the minimum thickness of the oil film is 0·0015 in., and that the thickness ratio is 2, calculate the total load which the thrust block can support. What is the theoretical power lost in overcoming friction, and what is the required eccentricity of the pads?

Area of each pad = 3·06 sq. in.

$$u = 1{,}962 \text{ in. per sec.}$$

$$Z = 0{\cdot}2 \text{ poise} = 0{\cdot}0000029 \frac{\text{lb. wt. sec.}}{\text{in.}^2}$$

$$h_0 = 0{\cdot}0015 \text{ in.} \qquad L = 1{\cdot}75 \text{ in.} \qquad C_1 = 0{\cdot}069$$

Load per in. width $W_1 = C_1\left(\frac{ZuL^2}{h_0^2}\right) = 535$ lb.

∴ Load on each pad = 535 × 1·75 = 936 lb.

∴ Mean pressure on pads = 305 lb. per sq. in.

Total load on thrust block = 16 × 936 = 15,000 lb.

$$\mu = C_2\left(\frac{Zu}{W_1}\right)^{\frac{1}{2}}$$

$$\frac{Zu}{W_1} = \frac{0{\cdot}0000029 \times 1{,}962}{535} = 0{\cdot}00001065$$

$$\left(\frac{Zu}{W_1}\right)^{\frac{1}{2}} = 0{\cdot}00326. \quad C_2 = 2{\cdot}76$$

∴ $\mu = 0{\cdot}00326 \times 2{\cdot}76 = 0{\cdot}009$

Total friction force = 0·009 × 15,000 = 135 lb.

∴ Theoretical power loss $= \frac{135 \times 1{,}962}{12 \times 550} = 40{\cdot}2$ h.p. or 30 kW.

The actual power loss would be appreciably in excess of this, because of the pumping action of the collar and other hydraulic losses.

Eccentricity $e = 0{\cdot}081 \times 1{\cdot}75 = 0{\cdot}142$ in.

256. Construction of Michell Thrust Bearings. Fig. 391 shows a section through a Michell bearing for a steam turbine. A single collar A is turned on the shaft and abuts against a number of thrust pads B. These are supported by a ring C. A similar set of pads E on the non-working side of the block abut against a ring F. The rings C and F are divided by a horizontal joint. The pads E are provided to take any accidental thrust in the direction opposite to that of the normal thrust.

The axial position of the rotor is adjusted during erection by machining the liner D to a definite thickness. A small clearance c_1,

known as the "oil clearance," must be provided between the collar and the surging pads E when the collar is hard up against the working pads in order to allow ample space for the formation of satisfactory oil films between the collar and pads. This clearance varies from about 0·010 to 0·015 in. according to the size of the thrust block, and is fixed by giving the liner G a suitable thickness. Lubricating oil is supplied to the centre of the block under a slight pressure, and after passing through the bearing it escapes through an

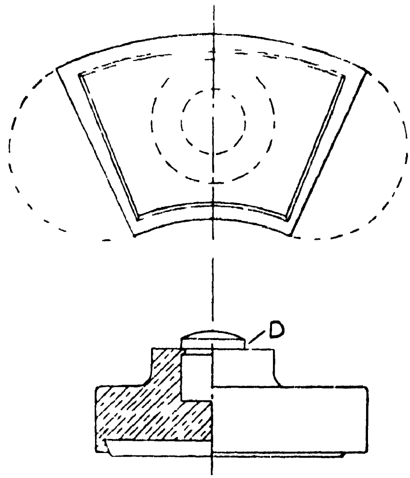


FIG. 392.—Michell Bearing Pad

outlet at the top. This ensures that the bearing is flooded with oil at all times. The rate of oil flow is controlled by a restriction orifice in the outlet pipe.

In marine turbines, where the rotor must be able to turn in both directions, it is usual to support the thrust pads on a hardened steel pin D, Fig. 392, which abuts against a hardened steel plate in the supporting ring. According to theory, this would result in an oil film of uniform thickness ($h_1 = h_0$) and thus incapable of supporting any load. In practice such pads operate quite satisfactorily provided the inlet edge is slightly rounded off. A contributory factor to this satisfactory operation is probably the drop in viscosity caused by the rise in temperature as the oil flows under the pad. This causes a reduction in oil pressure towards the "off" side with a consequent shift of the centre of pressure towards the centre of the pad. Some of the earlier thrust pads were made kidney-shaped, as shown by the dotted lines, Fig. 392. Owing to the effects of side leakage, however, pads of such shape are apt to run dry at the

"off" sides. Pads approximately square give a much better performance.

In land turbines, construction takes a variety of forms. Thus the thrust bearing may be arranged (*a*) quite separate from the journal bearing, (*b*) in the same housing as the journal bearing, but to one side of it, and (*c*) in the centre of the journal bearing. In all cases the lubricating oil is supplied to the inner side of the pads. Fig. 393 shows part sections of a separate thrust bearing. The

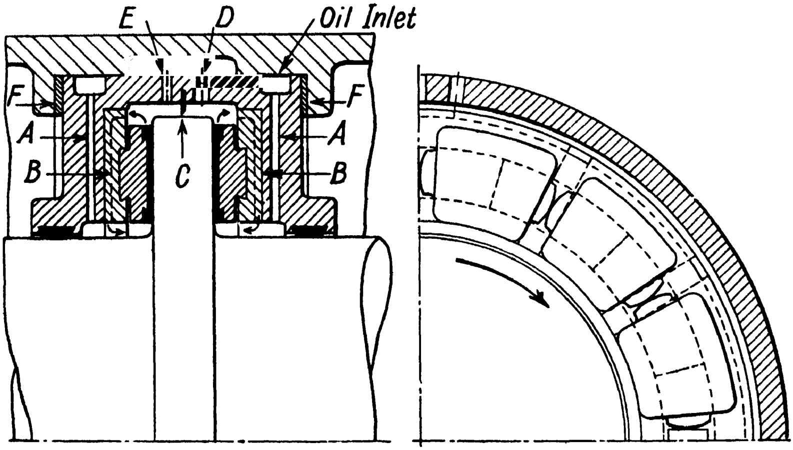


Fig. 393

pads are located in a dovetail groove in a supporting ring, and are supported eccentrically on a canting ridge. They are made in a complete ring which is white-metalled and machined before being cut up into separate pads. The pads are then scraped up individually to fit a gauge. Oil is led to the centre of the housing by a number of radial holes A. The rotation of the collar produces a certain pumping action. Channels B, cut in the seating ring between the pads, enable the oil to flow back to the centre and so re-circulate through the pads.

In some cases, a baffle plate C is placed around the periphery of the thrust collar so that restriction orifices D and E of different areas may be used with the object of allowing a greater circulation of oil on the loaded side. The axial position of the rotor may be fixed by means of liners F.

In many turbines, and especially in reaction turbines with end-tightened blading, provision is made for adjusting the axial position of the rotor while the turbine is running. The two halves of the thrust block are bolted and keyed together and move as one. The axial movement is effected by screws operated through worm gear and is limited by liners.

Some manufacturers make special provision for equalizing the loads on the pads. Fig. 394 (*a*) shows the method employed by the American Westinghouse Co., Ltd., and is self-explanatory. Messrs. Brown Boveri & Co., Ltd., use the construction shown in Fig. 394 (*b*). Hardened steel discs are recessed in the ends of the pads and rest against steel balls. The latter are borne by the fixed abutment and are maintained in position by a light metal cage.

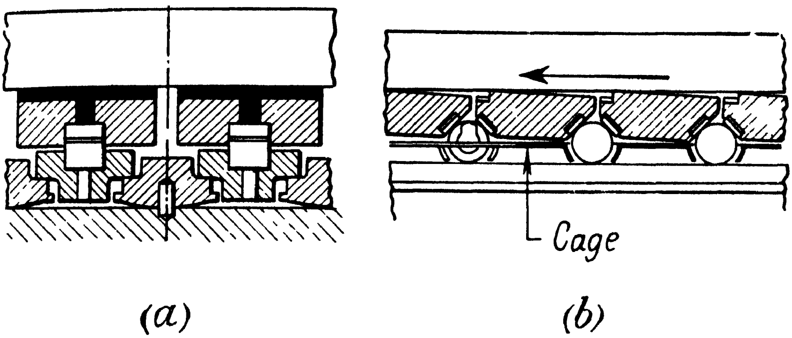


FIG. 394 Methods of Equalizing Loads on Thrust Pads

By suitably locating the discs in the pads, the necessary eccentric loading may be achieved.

257. **Plain Collar Thrust Bearing with Fixed Inclined Thrust Surfaces.** In this type of bearing one or more thrust collars are employed. The bearing surfaces are divided up into a number of sectors, as shown in Fig. 395, each sector being tapered so that the oil film diminishes in thickness in the direction of motion of the collar. It is found that a better performance is obtained if the bearing surface is also tapered so that the oil film diminishes in thickness from the centre outwards at the inlet edge. The actual bearing surfaces are of white metal and oil is supplied to them by the radial grooves shown. When the taper is accurately and uniformly machined, such bearings are capable of supporting mean pressures up to a maximum of 450 lb. per sq. in. With such high pressures the total thrust may generally be taken on a single collar.

258. **Forced Lubrication Systems.** Fig. 396 shows the essential features of a forced lubrication system as used on land turbines. The pump, which is normally of the positive action gear type (see Fig. 397) usually delivers the whole of the oil required for lubrication and governing at the pressure required for the governor gear oil relays, i.e. about 50 to 80 lb. per sq. in. As the oil for operating the relays is only required intermittently the surplus is allowed to pass through a relief valve set to lift at the relay pressure. The oil used in the governor relays is not usually cooled. Oil for lubrication is passed through a reducing valve which is so adjusted that the oil

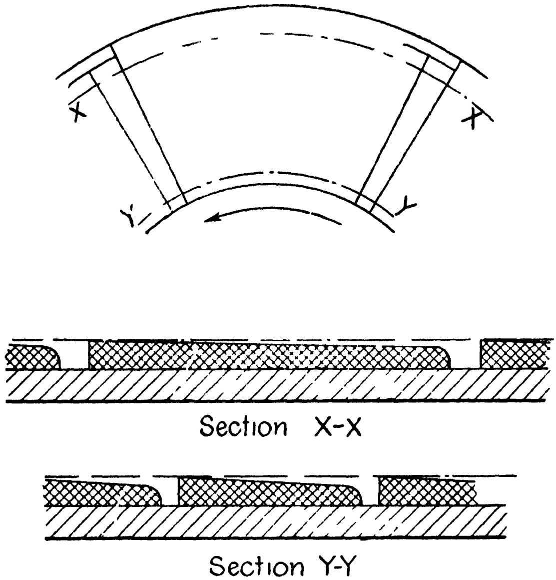


FIG. 395.—Thrust Bearing with Fixed Inclined Surfaces

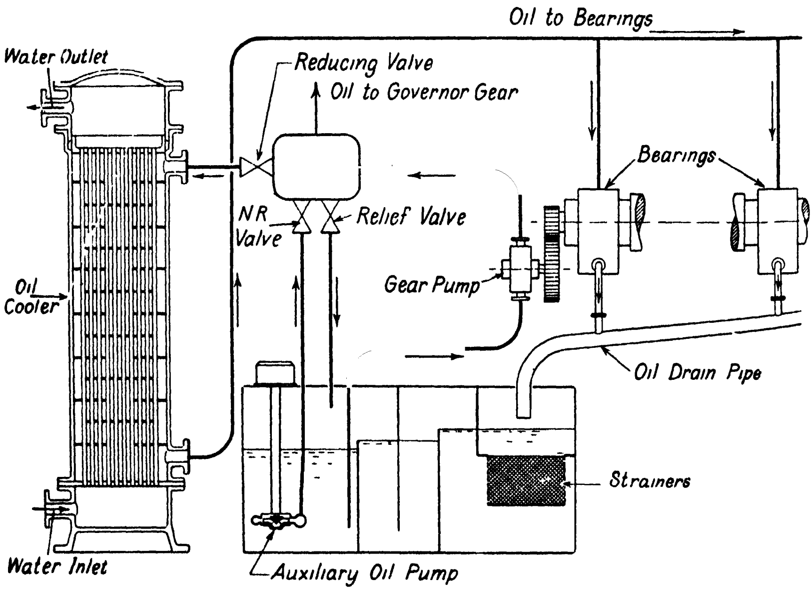


FIG. 396.—Diagrammatic Arrangement of Forced Lubrication System

supply pressure at the bearings is about 5 to 10 lb. per sq. in. It is passed through the oil cooler at the reduced pressure. A bus pipe supplies oil to all the bearings. Similarly, a large bus pipe



FIG. 397 Gear Pump

collects the oil from all the bearings and leads it to the oil drain tank. This pipe must be large enough to carry the oil with the pipe only partly filled so that air bubbles have a chance to break. In the arrangement shown in Fig. 396 the oil strainers are placed

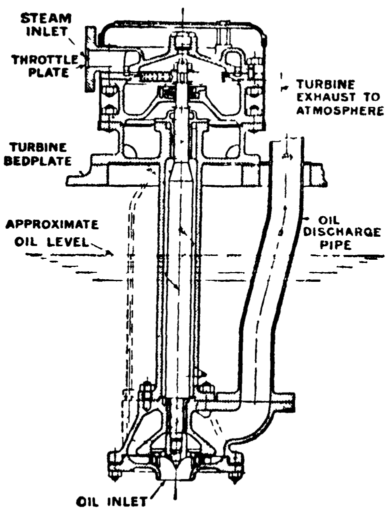
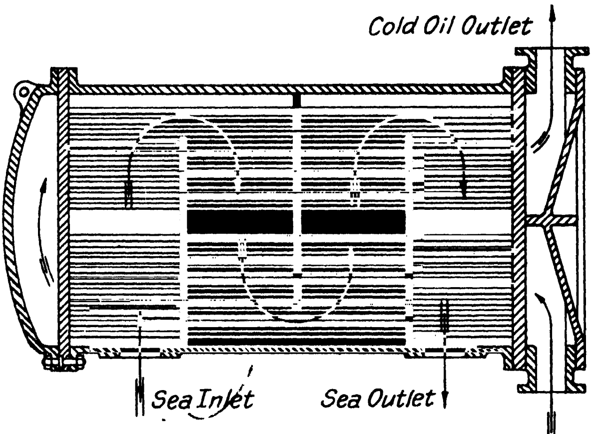


FIG. 398—Turbine-driven Auxiliary Oil Pump

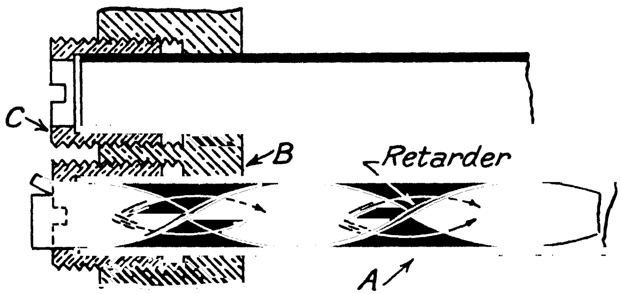
on the oil inlet side of the tank. In other cases the strainers are arranged at the pump suctions.

The auxiliary oil pump comes into operation at starting and stopping when the oil pressure falls below a certain value. It is also an emergency stand-by pump and is capable of supplying the

same quantity as the main oil pump. The type most commonly used is the turbine-driven centrifugal pump, Fig. 398. In the particular example shown, there is a single impulse wheel with blades formed by semicircular channels milled in the periphery. In other



(a) MARINE OIL COOLER.



(b) TUBE PLATE DETAILS.

FIG. 399

cases a two-row Curtis wheel is employed. The turbine is usually placed on the cover of the oil drain tank with the impeller immersed in oil. The steam supply to the turbine is controlled automatically by the oil pressure in the system.

In the oil cooler shown in Fig. 396, the cooling water passes through the tubes, the oil flow around the tubes being made as sinuous as possible by means of several baffle plates. In marine practice, it is usual to arrange the oil flow through the tubes, the sea water flowing across them (Fig. 399).

The oil tanks should be large enough to allow a considerable time to elapse between the oil draining back into the tank and re-entering the pump. This assists in breaking up the froth and is said to retard the deterioration of the oil. In modern turbine plants the tank normally contains 6 to 10 minutes' supply.

BIBLIOGRAPHY

1 TOWER, B. "First Report of Friction Experiments." *Proc.I.Mech.E.*, 1883, p. 632; 1884, p. 29: 1885, p. 58.
2 REYNOLDS, O. "On the Theory of Lubrication and its Application to Mr. Beauchamp Tower's Experiments." (*a*) *Phil. Trans. R.S*, 1886; 177; 157. (*b*) *Collected Papers*, Vol. 2, 228.
3. GUY, H L., and SMITH, D.M. "Steam Turbine Journal Bearings." *I.Mech.E.* General Discussion on Lubrication and Lubricants, 1937, p. 109.
4. SWIFT, H. W. "Hydrodynamic Principles of Journal Bearing Design." *Proc.I.Mech.E.*, 1935; 129, 399.
5. SWIFT, H. W. "The Stability of Lubricating Films in Journal Bearings." *Proc.I.C.E.*, 1932; 233, 267.
6. KINGSBURY, A. "On Problems in the Theory of Fluid Film Lubrication with an Experimental Method of Solution." *Trans. A.S.M.E.*, 1931; PME 53-5; 59.
7. SOMMERFELD, A. "Zur hydrodynamischen Theorie der Schmiermittelreibung." *Zeits. Math. Phys*, 1904; 50; 97.
8. McKEE, S. A., and McKEE, T. R. "Journal Bearing Friction in the Region of Thin Film Lubrication." *J.S.A.E.*, 1932; 31, 371.
9 HODGKINSON, F. "Journal Bearing Practice" *Proc I Mech E.*, 1929, p 843
10. BOSWALL, R. O. *The Theory of Film Lubrication*. Longmans, 1928.

CHAPTER XXVI

GOVERNORS AND GOVERNOR GEARS

259. Introduction. In the operation of a steam turbine there are, or may be, a certain number of variables, such as the initial steam pressure, the exhaust or back pressure, the steam flow through the turbine per unit time, the total energy output, the speed of rotation, or, in a pass-out turbine, the quantity and pressure of the pass-out steam. The purpose of the governor gear may be broadly defined as maintaining one or more of these variables sensibly constant while others vary.

In a normal condensing turbine driving an alternator or a d.c. generator, the energy output will vary in accordance with the load, and the function of the governor gear is to regulate the supply of steam to the turbine so that the speed of rotation shall remain almost constant. As has already been stated in Chapter XV, this may be done by throttling the entering steam, by changing the area through the first stage nozzles, or by admitting steam to a later stage of the turbine.

In a back-pressure turbine supplying exhaust steam for heating purposes, the supply of steam to the turbine may be controlled in such a way that the back pressure is kept sensibly constant. On the other hand, in a pass-out turbine, the governor must control the flow of steam in such a way that the turbine speed and the pressure of the pass-out steam are reasonably constant. This involves a regulation of the total amount of steam admitted to the high-pressure stages of the turbine and of the steam supplied to the low-pressure stages following the pass-out branch.

In general, therefore, governors fall within two classes, (1) those which are responsive to a change of speed, and (2) those which are responsive to a change of steam pressure.

In normal condensing turbines subject to load variation, a speed governor only is employed. In back-pressure turbines and also in pass-out turbines, both speed and pressure governors are used. In marine turbines, provided the propeller is sufficiently immersed, the turbine will be loaded in accordance with the quantity of steam supplied to it. The power output varies in a regular way as the speed is altered because, if the speed is reduced the power required to drive the propeller will fall off, and vice versa. Consequently, both speed and power may be controlled simply by regulating the supply of steam to the turbine. This is done by hand. Only in case of the propeller coming out of the water, a broken propeller shaft, or some such contingency which suddenly unloads the turbine is the latter likely to accelerate dangerously. To meet this possibility, it is usual to fit an overspeed governor.

The majority of speed governors are of the fly-ball type, but fluid-pressure governors, usually in the form of a centrifugal pump impeller on the turbine spindle, may also be used for speed control. The fly-ball type of governor will now be considered.

260. The Governor. Fig. 400 shows the essential parts of the type of governor mostly used in steam turbines. It comprises a yoke A mounted on a shaft B and supporting two weights C. The

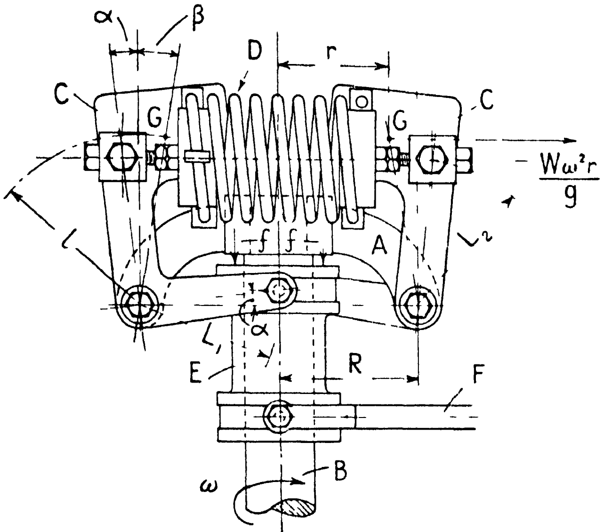


FIG. 400.—Turbine Governor with Weights Connected Directly by Side Springs

centrifugal force on the weights is balanced by the tension in the side springs D. The movement of the governor weights is transmitted through bell-crank levers to a sleeve E and thus through the lever F to the governor valve or relay gear, as the case may be. This type of governor is nearly frictionless and is therefore relatively sensitive. Owing to the fact that the centrifugal force on the weights is more or less directly opposed by the tension in the springs, the only force to be transmitted through the fulcrum pins is that necessary to move the sleeve. In many cases the fulcrum pins are supported by ball bearings.

Consider the mechanics of such a governor.

Let W = mass of each weight (centroid G).

ω = angular velocity in radians per sec.

$2f$ = total force due to friction in the governor mechanism transferred to the sleeve and acting in the direction

opposite to that of sleeve motion. Note: It is a single force, but the two is taken for convenience.

Let P = force due to springs.

Then, considering a vertical governor in the position shown in Fig. 400, and taking moments about either of the fulcrum pins,

$$\frac{W}{g}\omega^2 r\, l\,.\cos\beta \pm f L_1 \cos\alpha = PL_2\cos\alpha + Wl\,.\sin\beta$$

$$\therefore \qquad \frac{W}{g}\,.\,\omega^2 r \pm \frac{fL_1}{l}\,.\,\frac{\cos\alpha}{\cos\beta} = \frac{PL_2}{l}\,.\,\frac{\cos\alpha}{\cos\beta} + W\tan\beta$$

If friction be neglected,

$$\frac{W}{g}\omega^2 r = \frac{PL_2}{l}\,.\,\frac{\cos\alpha}{\cos\beta} + W\tan\beta$$

The force $\frac{W}{g}\omega^2 r$ is termed the "disturbing force" and the force $\frac{PL_2}{l}\,.\,\frac{\cos\alpha}{\cos\beta} + W\tan\beta$ is termed the "controlling force." In a horizontal governor the effect of gravity on one weight just counterbalances that on the other, and the term W tan β vanishes. In any case it is small compared with the other term and may generally be neglected. As the cosines of the small angles α and β are sensibly equal to unity, the controlling force is given very nearly by $\frac{PL_2}{l}$.

It is clear that for a constant speed ω, the disturbing force is simply proportional to the radius r, and that the disturbing force at various speeds will be represented by straight lines through the origin (Fig. 401). If N_0 is the normal speed of the turbine, and r_1 and r_2 are the extreme radii of the governor weights, then the disturbing forces at these radii are F_1 and F_2, respectively.

If the governor is to be *isochronous*, i.e. if the disturbing force at the constant speed N_0 is to be equal to the controlling force for all positions of the governor weights, then it is clear that the line AB represents the force to be exerted by the spring.

Such a governor would be useless in practice, because any slight changes in speed due to change of load would cause the weights to move to either extreme position, and so cause hunting.

Since the radius of the governor weights naturally tends to increase when the speed increases, the controlling force exerted by the springs must increase at a greater rate than the disturbing force for constant speed if the governor is to be stable. In other words, the rotational speed at which there is equilibrium must increase with increase of radius, and vice versa. Under these conditions, the controlling force would be represented by a straight line such as CD. N_1 would be the lowest speed corresponding to the radius

r_1 of the governor weights and N_2 would likewise be the highest speed corresponding to the radius r_2.

If the effects of friction and gravity be ignored then

$$\frac{W\omega^2 r}{g} = mP, \text{ where } m = \frac{L_2}{l} \text{ very nearly.}$$

The force P exerted by the two springs may be written $P = a + br$, where a and b are constants. Hence ma is the negative intercept

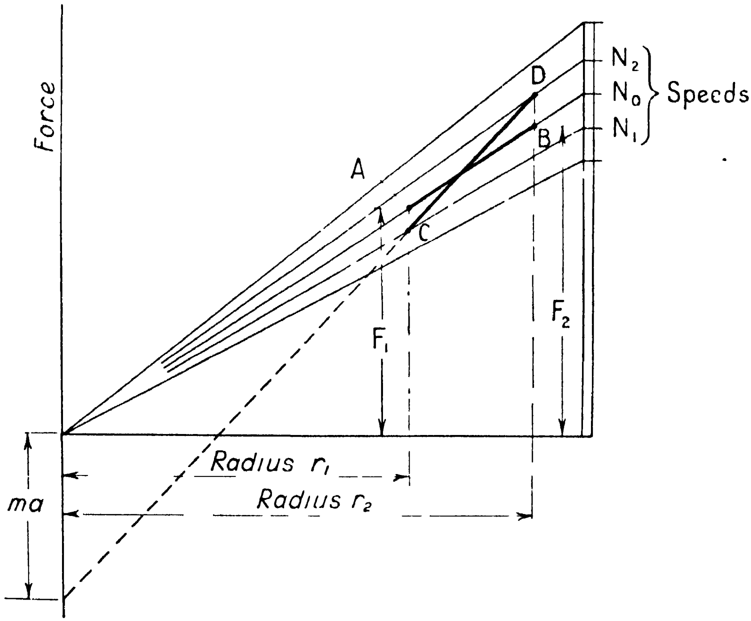


FIG. 401—Force Diagram for Governor, Neglecting Friction

on the force axis (Fig. 401) and mb is the positive slope of the straight line CD.

Thus $$\frac{W\omega^2 r}{g} = m(a + br) \text{ (very nearly)}$$

and $$\omega^2 = \frac{mg}{W}\left(\frac{a}{r} + b\right)$$

This expression enables the relationship between speed and radius, and hence between speed and sleeve travel, to be found in any given case. Such a relationship is shown in Fig. 402. The curve is very flat and is nearly a straight line.

If the weights of a stable frictionless governor are displaced from their equilibrium position and then suddenly released they

will oscillate about the position of equilibrium. The period of oscillation will depend on the restoring force and on the mass of the governor weights. In general, a high-speed governor with small masses will have a shorter period than a low-speed governor with large masses. Moreover, other things being equal, the greater the regulation of the governor, i.e. the greater the percentage change in speed corresponding to the full movement of the governor weights,

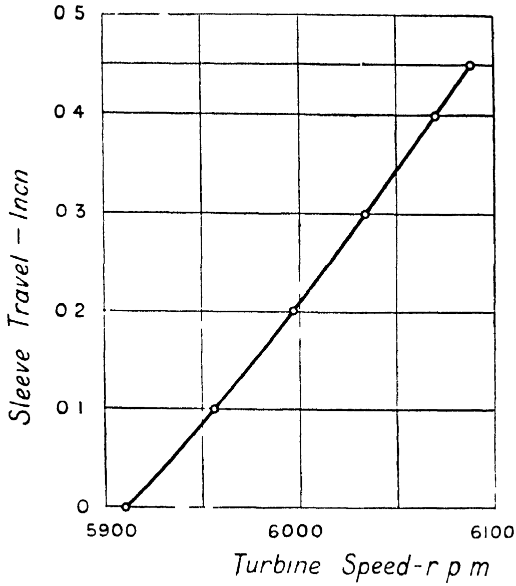


Fig 402

the greater the restoring force and hence the shorter the period of oscillation. Considerable damping forces are always present due to friction.

A short period governor is generally desirable so that the response of the turbine to these oscillations will be small. A further advantage of the small-mass high-speed governor is that in view of its low inertia it responds more quickly to change of speed.

261. Simple Governor without Relay. In turbines of small power in which the valves are light and the forces on them due to steam flow are inappreciable, the governor may be arranged to actuate the throttle valve directly. Fig. 403 shows a Terry turbine having a simple and robust governor of this type. The governor is mounted directly on the end of the turbine spindle and is of the Hartnell type in which the centrifugal force on the weights is balanced by the compression of the spring. In order to reduce friction, the governor weights are fulcrumed on hardened steel knife edges and

No. 1 the regulation is 3 per cent, the change of frequency for an increase of output of 10,000 kW is 1·5 per cent and the frequency would be 49·25. This condition, load being 22,000 kW, is represented by the point C. Since there is assumed to be straight-line regulation, the relationship between frequency and load will be given by the straight line AC.

Similarly, an increase of 10,000 kW on turbine No. 2 reduces the

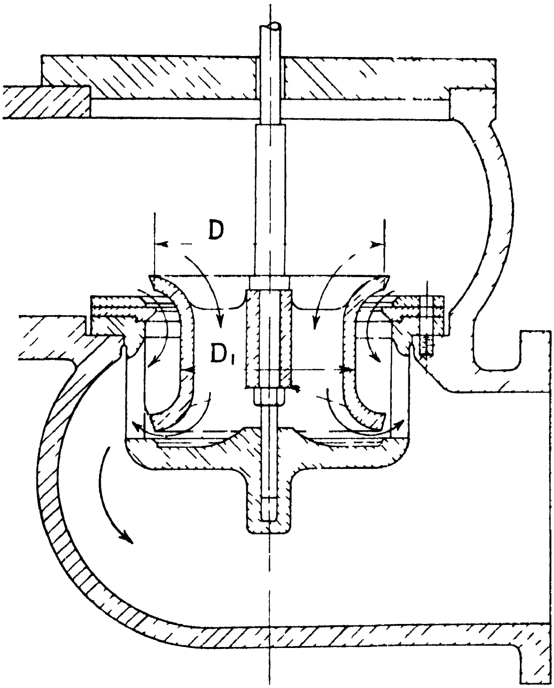


FIG. 407 —Simple Double-seated Throttle Valve

frequency from 50 to 49·6, point D. The total power line is found by adding the powers of turbines 1 and 2. Taking point E on this line for 55 megawatts and drawing a horizontal straight line, the outputs of turbines 1 and 2 are given (points F and G) as 19 and 36 megawatts, respectively, and the frequency as 49·48.

265. The Throttle Valve. Various forms of throttle valve are used to control the admission of steam to a steam turbine. The commonest form is the double-seated equilibrium valve in which the forces due to steam pressure are either completely or partially balanced. There are, however, certain dynamic forces on the valve caused by the flow of steam through it.

Fig. 407 shows a simple double-beat throttle valve in which the

steam flows through the valve seat in a direction perpendicular to the axis of the valve. The outer portion of the valve is attached to the central boss by ribs or wings, the number of such ribs being about three or four. The steam which passes through the lower seat flows through the inner part of the valve.

In another form of valve, shown in Fig. 408, the part of the

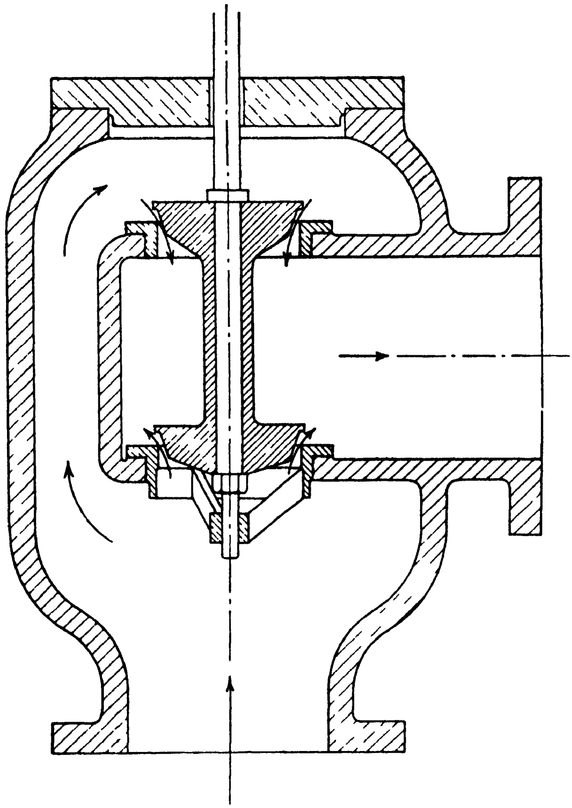


FIG. 408.—Throttle Valve with Shaped Profile

valve which controls the actual throttling of the steam is given a special shape. The direction of steam flow in passing through the valve is more or less parallel to the valve axis. With a valve body of the type shown in Fig. 408 the valve may be made solid, but in certain cases the valve body is modified in form and part of the steam passes through the hollow valve to the upper or lower seat, as the case may be.

In the simple type of throttle valve the seat diameter is sometimes made equal to the diameter of the pipe. The larger the

diameter of the valve, the smaller the required lift at full load and the less sensitive the governor gear as a whole. Consequently, a somewhat smaller valve and a larger lift would appear to provide more stable governing. On the other hand, too small a valve leads to higher steam velocities through the centre of the valve and through the passages close to the valve seat. In shaped valves

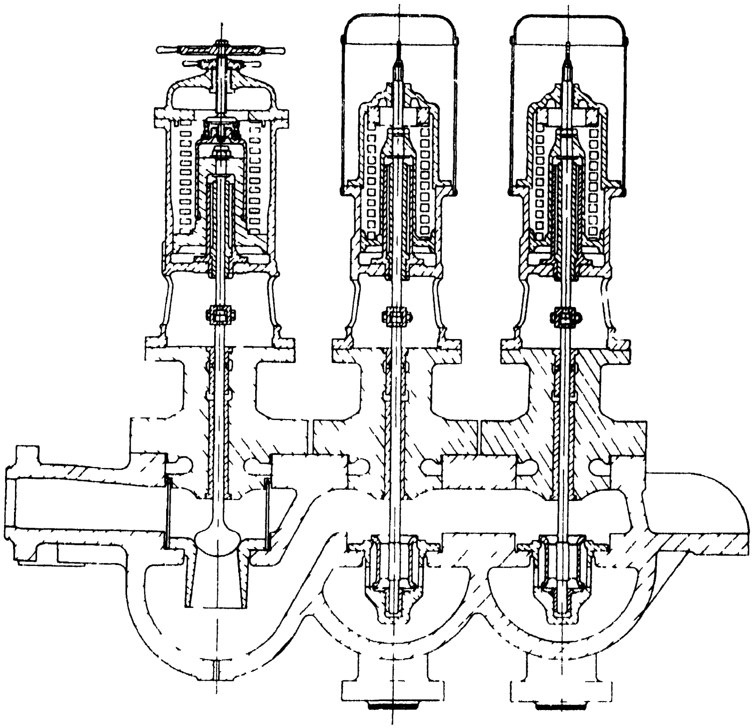


FIG. 409.—Section through High-pressure Steam Chest

of the second type, the seat diameter is normally about 0·7 times the pipe diameter.

Fig. 409 shows the section through the high-pressure steam chest for a Parsons turbine of fairly large output. The valve on the left is the emergency stop valve. For large units operating at high pressures and temperatures this valve is a single-seated mushroom valve with a hemispherical head. This type of valve is used because of the difficulty in keeping double-beat valves tight under high steam conditions. The mushroom valve is relatively small and the steam velocity through it is accordingly high. In order to reduce the loss due to this high velocity, a diffuser is arranged directly after the

valve seat. The two governor valves are double-beat valves, the seats being formed in separate forged steel cages.

For high-pressure turbines of large output, two such steam chests are used, one being arranged on each side of the turbine in a symmetrical manner. The outlets from the throttle valves are connected to the inlet branches on the high-pressure turbine by "U" and "S" pipes in such a way that all thrusts on the cylinder are balanced.

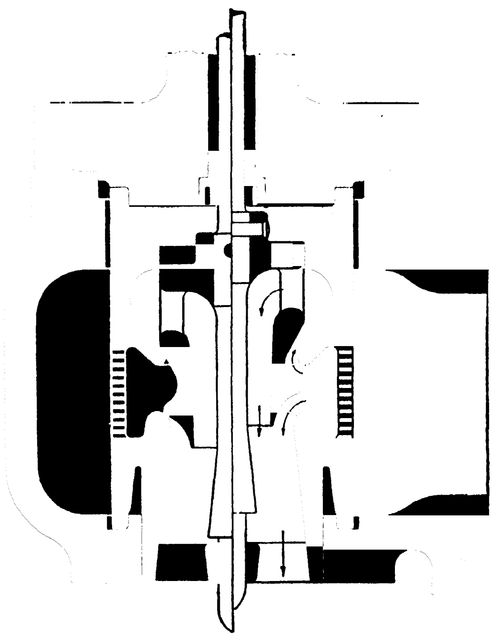


FIG. 410. Combined Section of Double-beat Governor Valve. Left Hand Closed, Right Hand Open

A steam strainer surrounds the emergency stop valve. For very high steam pressures and temperatures the throttle valves are also of the mushroom type and the steam chest is a forging instead of a casting.

For high steam conditions, the type of governor valve illustrated in Fig. 410 is employed by the Metropolitan-Vickers Electrical Co., Ltd. The left-hand half of the section shows the valve closed and the right-hand half shows it in the normal open position. It will be seen that when the valve is in the open position, curved passages with gradual changes of area are provided, thus enabling the use of high steam velocities, reduced valve diameter, and less likelihood of valve seat leakage when the valve is closed. The

symmetrical formation of the valve and its seatings ensure that the seal at the valve seats will not be affected by thermal expansion.

266. Flow of Superheated Steam Through Throttle Valves. In practically all cases, the steam passing through a throttle valve is in the superheated condition. Assume that the steam pressure before the valve is P_1 and after the valve P_2 lb. per sq. ft., and that the efficiency of the valve, considered as a nozzle, is η. Then assuming that the velocity of the steam before expansion through the valve is negligibly small the velocity V_2 through the valve is given by the expression

$$\frac{V_2^2}{2g} = \eta \int_{P_2}^{P_1} v \, . \, dP$$

Let n be the adiabatic index (1·30) for superheated steam and let m be the actual index for the frictionally resisted expansion. Then, as shown in Art. 123,

$$m = \frac{n}{n - \eta (n - 1)}$$

Then
$$\frac{V_2^2}{2g} = \eta_n \cdot \frac{m}{m-1} \left\{ P_1 v_1 - P_2 v_2 \right\}$$

$$= P_1 v_1 \left[\frac{\eta_n \, . \, m}{m - 1} \left\{ 1 - r^{\frac{m-1}{m}} \right\} \right]$$

where
$$r = \frac{P_2}{P_1} .$$

from which
$$V_2 = \sqrt{P_1 v_1 \left[\frac{2g \, . \, \eta_n \, m}{m - 1} \left\{ 1 - r^{\frac{m-1}{m}} \right\} \right]} \quad . \qquad (244)$$

Let w = steam flow through valve in lb. per second.

A_1 = total effective area required, sq. ft.

A = ,, ,, ,, ,, sq. in.

Then
$$\frac{w}{A_1} = \frac{V_2}{v_2}$$

$$= \sqrt{\frac{P_1}{v_1} \left[\frac{2g \, . \, \eta_n m}{m - 1} \left\{ r^{\frac{2}{m}} - r^{\frac{m+1}{m}} \right\} \right]}$$

$$= C_1 \sqrt{\frac{P_1}{v_1}} \quad . \quad . \qquad (245)$$

where
$$C_1 = \sqrt{\frac{2g \, . \, \eta_n \, . \, m}{m - 1} \left\{ r^{\frac{2}{m}} - r^{\frac{m+1}{m}} \right\}} \quad . \quad . \quad . \qquad (246)$$

If p_1 = initial pressure in lb. per sq. in. abs.

Then
$$\frac{w}{A} = C\sqrt{\frac{p_1}{v_1}} \qquad . \quad . \quad . \quad (247)$$

where
$$C = \frac{C_1}{12}.$$

Values of C are given in Table XXX and in Fig. 411.

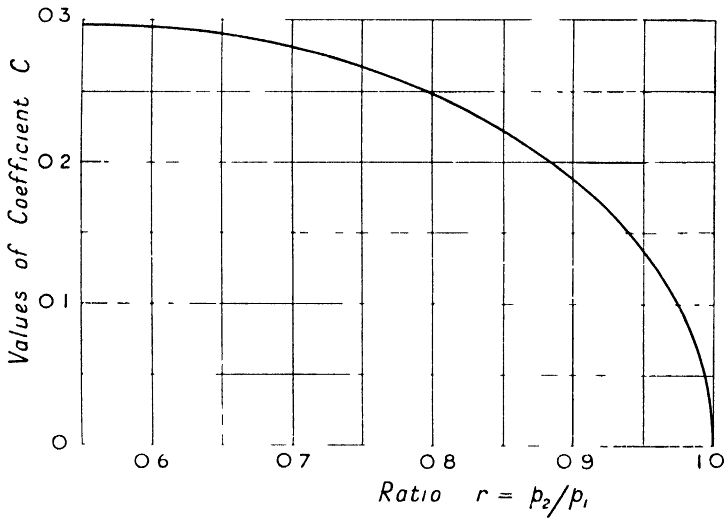


FIG. 411.—Coefficient for Discharge of Superheated Steam through Throttle Valve

TABLE XXX

VALUES OF FACTOR C

Assumed efficiency η_n = 0 9.

,, adiabatic index n = 1·3

Actual index m = 1·262

r	C	r	C
0·55	0·2963	0·93	0·1613
0 60	0·2947	0·94	0·1502
0·65	0·2901	0 95	0·1382
0·70	0·2806	0·96	0·1241
0·75	0·2674	0·97	0·1082
0·80	0·2479	0·98	0·0891
0·85	0·2236	0·99	0·0650
0·90	0·1894	0·995	0·0451
0·91	0·1799	1·000	0·0
0·92	0·1712		

267. Design of Simple Throttle Valve. We shall now consider the characteristics of the type of throttle valve shown in Fig. 407. This is best done by taking a specific example.

EXAMPLE 44. Calculate the throttle valve areas necessary for the 3,000 kW turbine of example 30, page 359, at different loads. Hence, having selected a suitable diameter for the valve, calculate the variation of lift with turbine output and hence the variation of turbine speed with varying outputs.

The pressure in the nozzle box is 200 lb. per sq. in. abs. The area through the valve at full load will depend entirely on the steam pressure before the valve, i.e. the steam pressure after the stop valve. The greater the pressure difference across the throttle valve the greater the steam velocity through the valve and the smaller the required lift. In this case we shall assume that the steam pressure just before the throttle valve is 204 lb. per sq. in. abs., i.e. that the pressure drop across the valve is 4 lb. per sq. in., or 2 per cent of the initial pressure.

As the enthalpy after throttling, corresponding to $p = 200$ lb. per sq. in. and 150° F. superheat, is 1,288·8 and as the pressure before throttling is 204 lb. per sq. in. abs. then using the original Callendar equation, we obtain the specific volume

$$v = \frac{1{\cdot}2464\,(1{,}288{\cdot}8 - 835{\cdot}2)}{204} = 2{\cdot}765 \text{ cu. ft./lb.}$$

Assume a mean steam velocity through the main steam inlet pipe = 100 ft. per second; then since the steam flow per second at full load = 10·12 lb. per second, the pipe area

$$A = \frac{10{\cdot}12 \times 2{\cdot}765}{100} \times 144 = 40{\cdot}4 \text{ sq. in.}$$

Thus the required pipe diameter = 7·17 in., say 7 in.

Consider the area through the valve at full load.

Let w = total steam flow through the valve, lb. per sec.

A = effective area through valve, sq. in.

D = valve diameter, in inches.

l = valve lift, inches.

Then, since the valve is double-beat, the effective area is $2\pi D \, . \, C_c \, . \, l$, where C_c is the coefficient of contraction. The latter quantity can be determined only by experiment and its value is very uncertain. It would depend on the shape of the valve and its seat. For the purpose of this example, we shall assume that C_c = 0·8.

Then $$A = 5{\cdot}03\, Dl.$$

Then, by eq. (247) of Art. 266,

$$A = \frac{w}{C\sqrt{\frac{204}{2 \cdot 765}}} = \frac{w}{8 \cdot 59\,C} \text{ sq. in.}$$

Let p_0 = nozzle box pressure

p_{sv} = stop valve pressure.

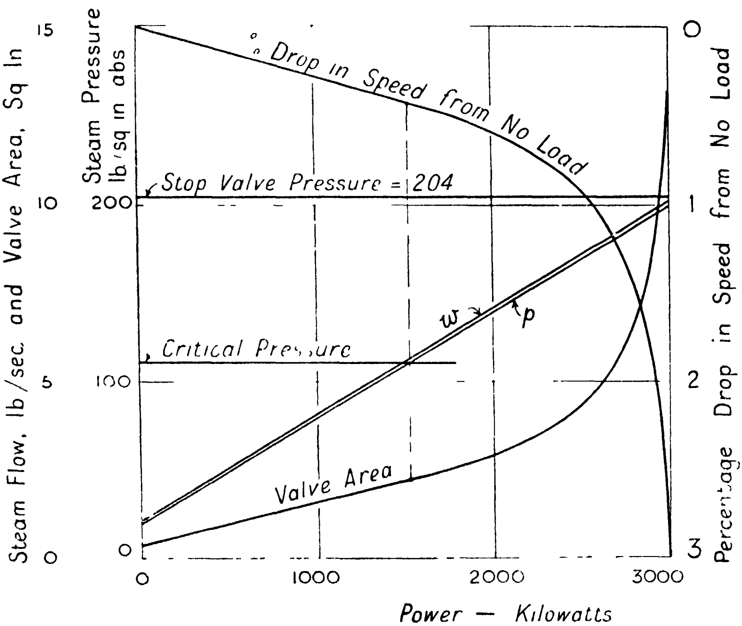


FIG. 412

Then at full load $\frac{p_0}{p_{sv}} = \frac{200}{204} = 0 \cdot 980$, for which $C = 0 \cdot 089$.

Hence $A = \frac{10 \cdot 12}{8 \cdot 59 \times 0 \cdot 089} = 13 \cdot 25$ sq. in.

i.e. $5 \cdot 03\, Dl = 13 \cdot 25$

or $Dl = 2 \cdot 64$.

Thus the valve diameter depends on the selected ratio of lift to diameter. The permissible value of this ratio depends upon the ratio of the diameters D_1 to D, Fig. 407. In order to limit the velocity of the steam through the centre of the valve, this ratio is usually made about 0·76 to 0·80. Hence if the control of steam flow is to take place at the valve seat, the lift of the valve should not

exceed about 0·1 of the diameter. Hence, making $l = 0 \cdot 1$ D, the valve diameter D = 5·14, say 5 in.

Hence area through valve $= 2\pi \times 5 \times 0{\cdot}8\, l$

$= 25{\cdot}1\, l$ sq. in.

The calculation of areas is given in Table XXXI for different loads. The values of the nozzle box pressure p_0 are taken from Fig. 412 and thus values of the ratio $\frac{p_0}{p_{sv}}$ calculated. The corresponding values of the coefficient C are then taken from Fig. 411. In the next column, values of the steam flow w are set down from Fig. 412. The required effective area is then calculated by eq. (247) and from this the valve lift is calculated. In the next column of the table, the valve lift from the no-load position is set down by deducting the lift at no-load from all values of the lift. In a simple linkage between the governor sleeve and the throttle valve spindle, such as that shown in Fig. 404, the travel of the governor sleeve is directly proportional to the valve lift, and if the relationship between sleeve travel and governor speed is taken to be linear, then the percentage drop in speed from the no-load speed in the given case is—

$$\frac{l_1}{0{\cdot}512} \text{ Governor Regulation,}$$

l_1 being the valve lift from the no-load position. Assuming the governor regulation to be 3 per cent in this case, we obtain the speed changes given in the last column of the table.

TABLE XXXI

CALCULATION OF THROTTLE VALVE LIFTS AND TURBINE SPEED CHANGES WITH VARIATION OF LOAD IN A 3,000 kW STEAM TURBINE

Load kW	p_0	$\frac{p_0}{p_{sv}}$	C	w	Effective Area A sq. in.	Valve Lift l inches	Lift of Valve from No-load Position	% Drop in Speed
0	20	0·098	0·2963	1·012	0·398	0·016	0	0
500	50	0·245	,,	2·532	0·995	0·040	0·024	0·140
1,000	80	0·392	,,	4·052	1·592	0·063	0·047	0·275
1,500	110	0·540	,,	5·562	2·182	0·087	0·071	0·415
1,600	116	0·569	0·296	5·872	2·306	0·092	0·076	0·445
1,800	128	0·628	0·292	6·479	2·58	0·103	0·087	0·509
2,000	140	0·686	0·283	7·086	2·92	0·116	0·100	0·585
2,200	152	0·745	0·269	7·693	3·33	0·133	0·117	0·684
2,400	164	0·805	0·246	8·305	3·93	0·157	0·141	0·825
2,600	176	0·863	0·215	8·907	4·82	0·192	0·176	1·030
2,800	188	0·922	0·170	9·513	6·51	0·260	0·244	1·430
2,900	194	0·951	0·137	9·816	8·35	0·333	0·317	1·850
3,000	200	0·980	0·089	10·12	13·25	0·528	0·512	3·000

On examining Table XXXI and Fig. 412 it will be seen that up to about half load, the drop in pressure across the throttle valve exceeds the critical, and the required area through the valve is directly proportional to the steam flow. Moreover, the percentage drop in speed is uniform. At loads greater than half load, however, the pressure drop across the valve is less than the critical and, as full load is approached, the velocity of flow through the valve falls to such an extent that the required valve area,

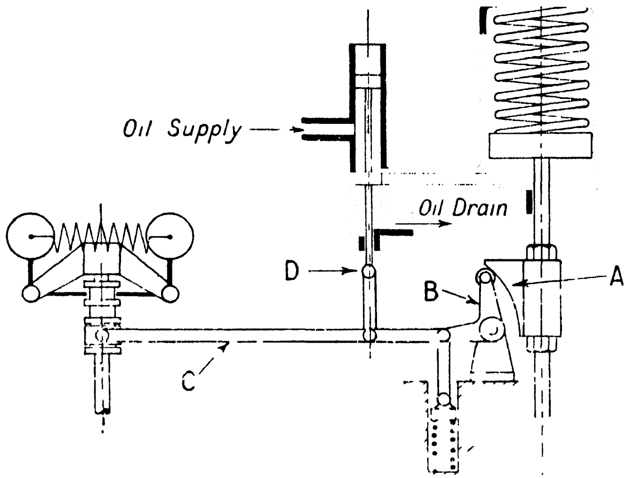


FIG. 413. Diagrammatic Arrangement of Relay Gear Modified to give Approximately Straight-line Regulation

and hence the valve lift, increases rapidly. In association with this, the speed changes quite rapidly as full load is approached, unless some adjustments are made by means of the speeder gear.

268. Modified Linkages to give a Closer Approach to Straight-line Regulation. In order to obtain a more uniform change of speed with change of load, the linkage between the governor and the throttle valve spindle is sometimes modified. Such a modification is shown in Fig. 413. Here a plate cam A is fixed to the throttle valve spindle; this actuates a bell crank lever B to which the floating lever C is attached. The curvature of the cam is greatest at the top and least at the bottom. Bearing in mind that, for a steady condition, the point D must be fixed, it will be clear that as the lift of the throttle valve is increased towards the full-load lift, the

$$\frac{\text{Governor sleeve travel}}{\text{Throttle valve lift}}$$

ratio diminishes, thus reducing the change of speed which would otherwise take place above half load.

Another form of gear, described in a paper by Mr. C. D. (now Sir Claude) Gibb, is shown in Fig. 414. Here a toggle joint A causes the upper end of the link B to move in a slot machined in the floating lever C. The increased lift of the throttle valve above half load

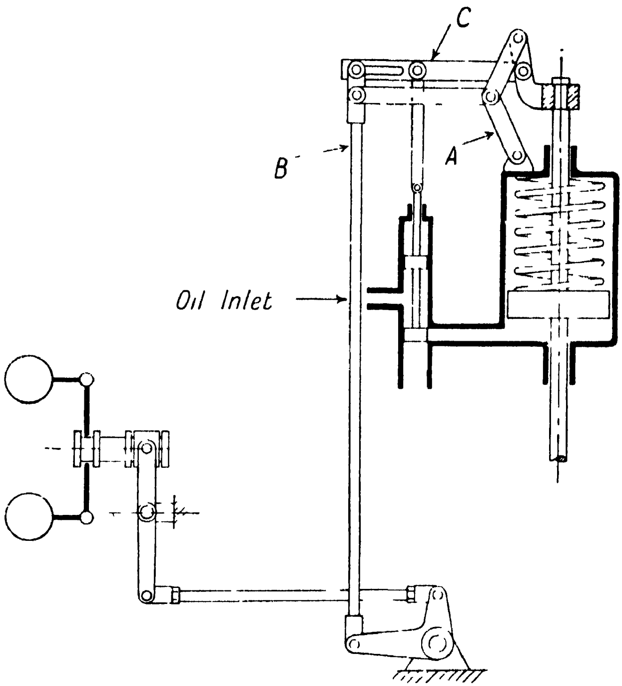


FIG. 414.—Diagram of Relay Gear with Toggle Joint Mechanism to give Closer Approximation to Straight-line Regulation

again causes the ratio of governor sleeve travel to throttle valve lift to fall off as the full-load lift is approached.

The satisfactory operation of such gears would appear to be dependent on the maintenance of a steady steam pressure at the stop valve; for if, at full load, the stop valve pressure is higher than the normal value, the greater pressure drop across the throttle will enable the necessary steam flow to be maintained with a smaller lift than normal and hence with a smaller variation of speed from the no-load value.

269. Design of Shaped Throttle Valve. The area through the valve shown in Fig. 408, corresponding to any value of the lift, depends on the shape of the tapered part of the valve. By selecting

a suitable shape, an arbitrary relationship between load and turbine speed may, to a certain extent, be obtained. But there are limits imposed by the conditions of operation as will be shown by means of an example.

The diameter of the valve is generally made from 0·7 to 0·75 times the diameter of the steam pipe, but the ratio is, of course, quite arbitrary. The lift is also arbitrary but may be made from 0·12 to 0·2 times the diameter of the valve. The coefficient of contraction is probably not the same for the two seats owing to the different conditions of approach.

EXAMPLE 45. Derive the shape of a throttle valve suitable for the 3,000 kW turbine of example 30, page 359.

The pipe diameter will be made the same as in the previous example, viz. 7 in. Taking the valve diameter as 0·7 times the pipe diameter, we have a diameter of 4·9 in., say, 5 in. We shall assume that the lift of the valve from the no-load position is equal to 0·2D, i.e. 1 in.

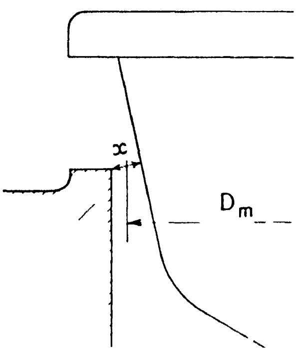


FIG. 415

We shall first attempt to design the valve so as to obtain straight-line regulation, i.e. the change in speed, plotted against load, is represented by a straight line. Since the relationship between governor travel and speed is very nearly linear, we may assume with very small error, that the relationship between valve lift and load is also linear. On this basis the data in Table XXXII were obtained for two values of the stop-valve pressure, viz. 205 and 210 lb. per sq. in. absolute. The method of calculating the effective area is the same as that used in the preceding example and need not be given in detail. In calculating the "opening" x of the valve, Fig. 415, it is assumed that the coefficient of contraction is 0·8 for the upper seat and 0·9 for the lower seat. Hence the total effective area—

$$A = \pi D_m \,.\, x\,(0{\cdot}8 + 0{\cdot}9)$$
$$= 5{\cdot}34\, D_m \,.\, x.$$

x is calculated by successive approximations.

In obtaining the shape of the valve, the lift is set down to an enlarged scale, as shown in Fig. 416, as though the valve remained stationary and the valve seat moved downwards as the valve opened. The various "openings" are then set out as arcs of circles and a curve drawn tangential to them. It will be seen that this method is successful up to a lift of 0·825 when $p_{sv} = 205$, and 0·875 when $p_{sv} = 210$. Above these lifts, the openings increase so rapidly that there is interference. It will be seen that the interference is smaller

at the higher pressure, and it is quite possible to obtain a valve shape which will result in straight-line regulation provided the pressure drop across the throttle valve is made sufficiently high. The resulting change in the upper part of the valve is relatively small.

We shall now set out a practical shape of valve for the second case, i.e. when the pressure before the throttle is 210 lb. per sq. in. absolute. First set down the full lift of one inch from the no-load position, Fig. 417. To the same scale draw an arc of radius 0·344 in.

TABLE XXXII

CALCULATION OF "OPENING" OF THROTTLE VALVE REQUIRED TO GIVE STRAIGHT-LINE REGULATION

Lift of Valve above No-load Position (Inches)	Load kW	p_{sv} = 205		p_{sv} = 210	
		Effective Area sq. in.	"Opening" x Inch	Effective Area sq. in.	"Opening" x Inch
0	0	0·396	0·0149	0·386	0·0145
0·1	300	0·751	0·0283	0·733	0·0276
0·2	600	1·107	0·0418	1·080	0·0408
0·3	900	1·460	0·0554	1·426	0·0541
0·4	1,200	1·820	0·0692	1·774	0·0675
0·5	1,500	2·175	0·0829	2·122	0·0810
0·6	1,800	2·560	0·0980	2·480	0·0950
0·7	2,100	3·075	0·118	2·962	0·113
0·8	2,400	3·87	0·149	3·66	0·141
0·825	2,475	4·16	0·161	3·91	0·151
0·85	2,550	4·48	0·174	4·18	0·162
0·875	2,625	4·88	0·190	4·49	0·174
0·9	2,700	5·40	0·211	4·90	0·191
0·925	2,775	6·06	0·238	5·40	0·212
0·95	2,850	6·99	0·277	6·04	0·237
0·975	2,925	8·68	0·350	6·97	0·276
1·0	3,000	11·98	0·500	8·55	0·344

as shown. Reference to Table XXXII will show that the "opening" for straight-line regulation varies uniformly from no-load up to a load of about 1,800 kW when the lift is 0·6 in. and the opening 0·095 in.

Draw arcs of circles from centres A and B with radii of 0·0145 in. and 0·095 in., respectively for lifts of 0 and 0·6 in. from the no-load position. Draw a straight line CD tangential to these arcs, and draw BD perpendicular to CD. The required profile of the valve below point D may be any curve to which CD is a tangent and which touches the circle of 0·344 in. radius. Assume that the curve is a circular arc. The centre of this lies on BD produced and the radius,

found by trial, is 0·15 in. By tapering the valve uniformly up to the seat, a lift of 0·075 in. is obtained at no-load for a radial clearance of 0·005 in.

By setting off the various openings required for different loads we obtain the corresponding valve lifts. For example, setting off the distance 0·237 in. for 2,850 kW we obtain the lift 0·871 in. Assuming the change in speed to be approximately proportional to the movement of the governor sleeve the speed at any load may

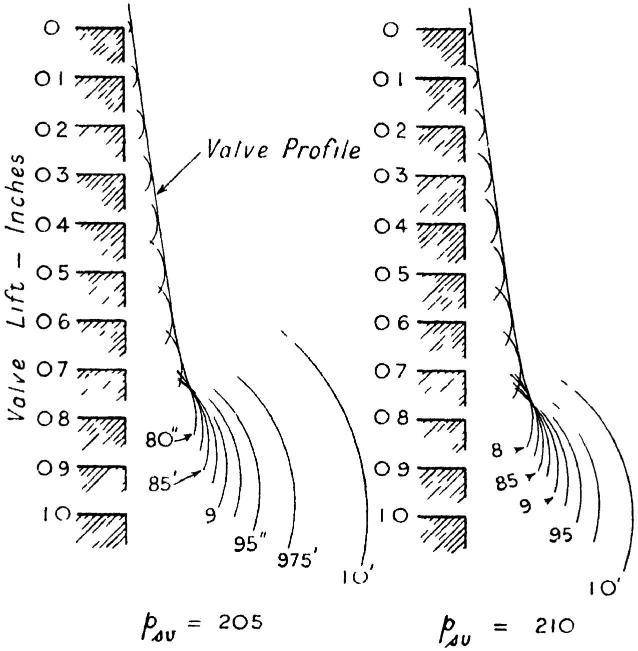


FIG 416 —Derivation of Valve Profile

be calculated. These figures are given in Table XXXIII and Fig. 418. It will be seen that this valve profile gives a close approximation to straight-line regulation.

270. Nozzle Control Governor Gear. Automatic control of a number of separate nozzle valves may be effected in several ways. Each valve may have its own relay cylinder and pilot valve, the linkage being arranged so that with increasing load the valves are opened in a certain order, and with a diminishing load they close one after another in the reverse order. Alternatively, the valves may be opened mechanically by a single relay cylinder and a system of levers and links in which there is a certain amount of lost motion. In another method, the nozzle valves are arranged in a row, e.g. on top of the turbine, and opened, in order, by levers actuated by cams.

Fig. 419 shows a B.T-H. turbine employing this form of governor gear, Fig. 420 shows a diagrammatic arrangement, while Fig. 421 gives a section through a nozzle valve.

Each cam is positive in its action and consists of a pair of discs carrying a roller in the space between them. This engages with a horse-shoe shaped lever which, as the cam rotates, either opens or closes a nozzle valve. The cam shaft is rotated by a servo motor

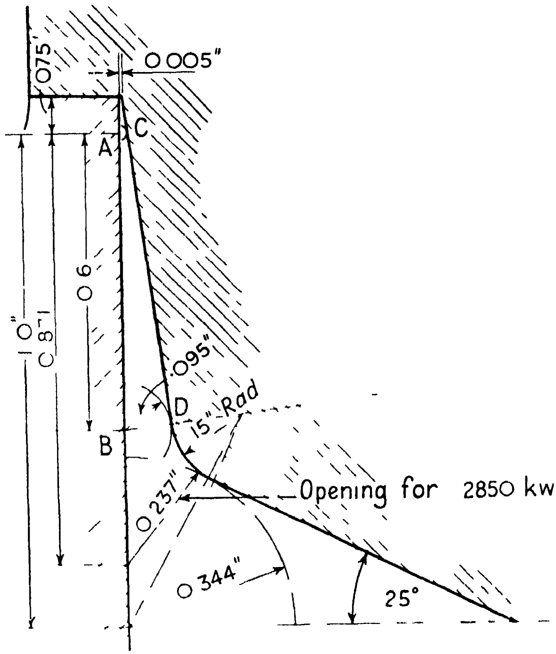


FIG. 417

of the moving blade type, the operating fluid being lubricating oil under a pressure of about 50 lb. per sq. in. A small pinion on the end of the cam shaft engages with a rack which is connected to one end of the floating lever and moves the pilot valve back to its mid-position when any rotation of the cam shaft has taken place. Oil exhausted by the servo motor and also oil passing through the high-pressure by-pass valve is supplied to the bearings at a pressure of 5 to 10 lb. per sq. in.

The action of the governor may now be briefly described. If, owing to an increase of load on the turbine, the speed should fall slightly, the governor sleeve will move downwards, so raising the pilot valve above its central position, in which position it covers both ports. A certain amount of high-pressure oil is thus admitted

to one side of the moving blade of the servo motor and an equal amount is expelled from the other side. The rotation of the cam shaft will either open another valve or increase the lift of the one

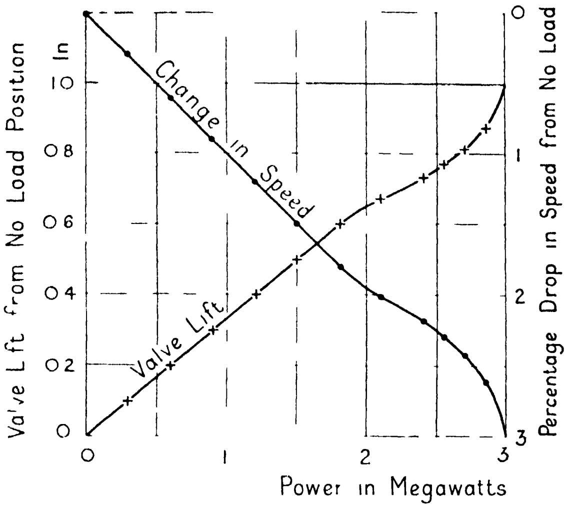


FIG. 418 Characteristics of Throttle valve Shown in Fig 417

TABLE XXXIII

THROTTLE VALVE LIFT AND SPEED CHANGES FOR A 3,000 kW STEAM TURBINE

Note Governor Regulation assumed to be 3 per cent

Load kW	Valve Lift from No-load Position Inches	% Drop in speed from No load	Load kW	Valve Lift from No load Position Inches	% Drop in speed from No-load
0	0	0	2,100	0.671	2.013
300	0.100	0.3	2,400	0.730	2.190
600	0.200	0.6	2,550	0.767	2.301
900	0.300	0.9	2,700	0.807	2.421
1,200	0.400	1.2	2,850	0.871	2.613
1,500	0.500	1.5	3,000	1.000	3.000
1,800	0.600	1.8			

last opened. As the cam shaft rotates, the pinion and rack tend to move the pilot valve back to its central position. Equilibrium of the gear is only possible when the pilot valve is in its central position, and thus in order to meet the steam demand due to an increase in

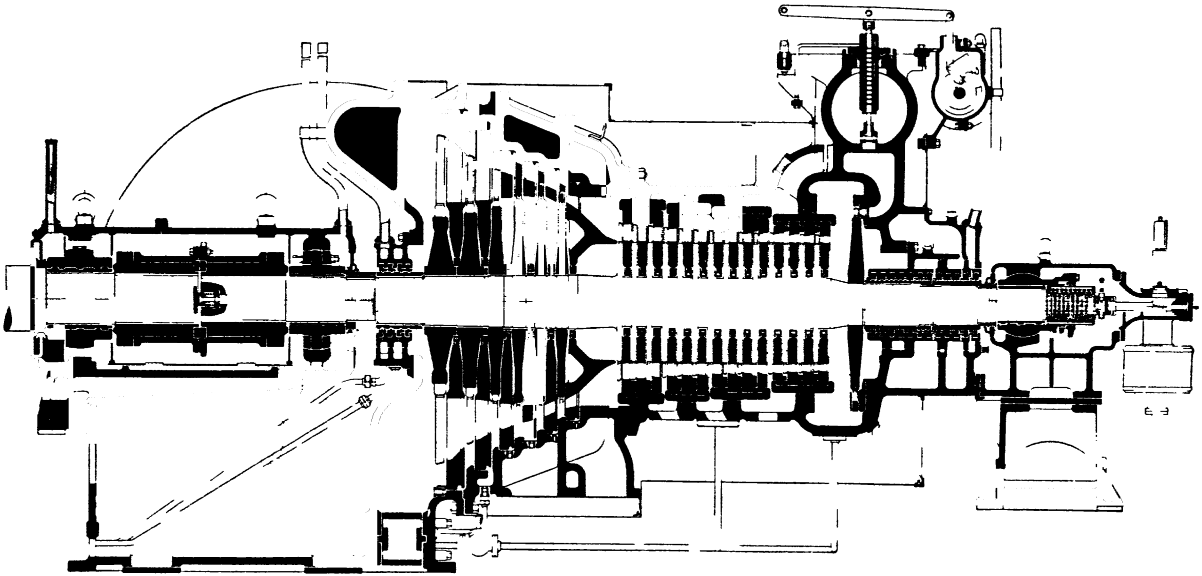


FIG. 419.—Sectional Elevation of B.T.H. Turbine with Nozzle Control Governor Gear

load there will be a definite reduction in turbine speed, and vice versa.

271. Oil Pressure Governing without Linkage. A relatively simple and easily adaptable form of governor gear is shown diagrammatically in Fig. 422. The governor actuates a small piston valve, A balanced by a similar piston B. Oil under pressure is supplied to

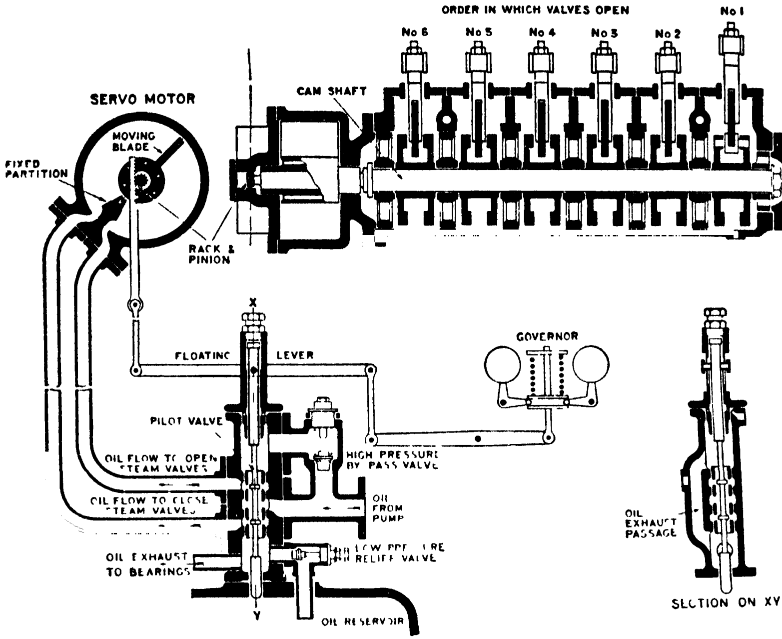


FIG. 420.—Diagrammatic Arrangement of Nozzle Control Governor Gear for B.T.-H. Turbine

the pipe C, and through the port D to the space between A and B. A further port E, when uncovered by the valve A, permits oil to escape. The pipe C is also coupled to the underside of the relay cylinder, the relay piston being spring-loaded on its upper side.

The volume of oil delivered by the oil pump will be nearly constant at all loads, and the pressure of the oil in the pipe C will depend on the port opening *l*; the larger the opening the lower the pressure, and vice versa. But the oil pressure also depends on the lift of the throttle valve, for if this be increased the compression of the spring above the relay piston is greater and the oil pressure under the piston must also be greater. Consequently, there is a correspondence between the lift of the throttle valve and the position of the piston valve A, which, in turn, depends on the speed of the turbine.

It will be seen from a study of Fig. 422 that, just as in the ordinary type of relay with links, an increase of load is accompanied by a reduction in speed, and vice versa. A form of speeder gear is shown in Fig. 422. The sleeve in which the ports are cut may be moved inwards or outwards by means of the handwheel F, rotation of the sleeve being prevented by the feather G. To raise the speed, the sleeve is moved inwards. This reduces the opening l, raises the oil pressure, and increases the lift of the throttle valve. Conversely, the speed is lowered by moving the sleeve outwards.

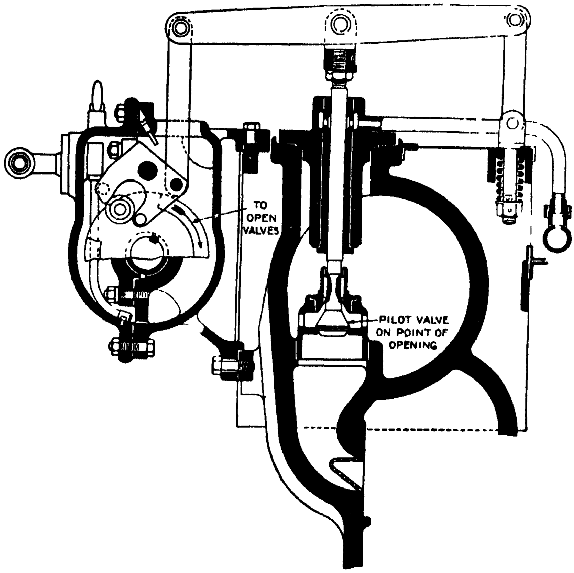
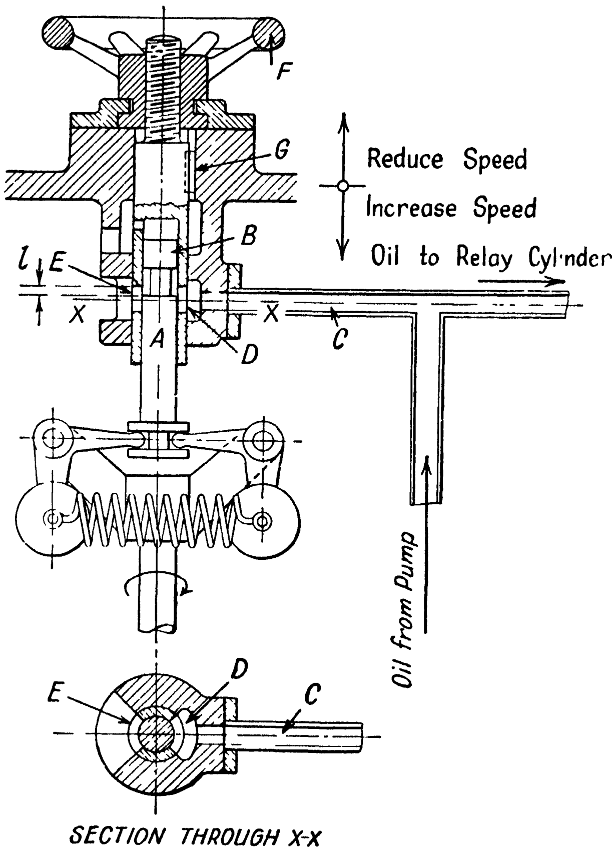


FIG. 421.—Sectional View of Nozzle Control Valve with Cam-operated Gear

The same type of gear may be used with nozzle-control valves. Here each valve has its relay piston, but the spring loads are made progressively greater so that as the oil pressure is increased, due to a drop in speed, the valves open in turn.

272. Compound Oil Relay. In turbines with large throttle valves, or those operating with high-pressure steam, the dynamic forces on the throttle valve may be appreciable, and are sometimes sufficiently large to interfere with the satisfactory operation of the relay gear described in the previous article. A compound relay is sometimes employed in such cases. One type is shown in Fig. 423. There are two oil systems operating at different pressures. The first, operating at a variable pressure, is controlled by the governor and is coupled to A, Fig. 423. The second, which is kept at a constant and relatively high pressure, is connected to B. Thus the

governor regulates the oil pressure under the spring-loaded piston C, and hence controls the position of the pilot valve D. The duty of the governor is, therefore, light and the sensitivity of the gear is not affected by dynamic forces on the throttle valve. The valve



SECTION THROUGH X-X

FIG. 422.—Diagrammatic Arrangement of Oil Relay Gear without Links

D works in the hollow piston rod of the main relay piston E, and oil admitted at B has free access to the space under D. If, due to an increase of load, the speed falls, the increase of oil pressure under C raises D and admits high-pressure oil to the underside of E This is forced upwards until the pilot valve D again covers its port Similarly, a drop in load causes an increase in speed, the oil pressure under C is reduced, C and D move downwards, and some of the oil

under E is allowed to escape into the space above E. The throttle is thus partially closed until there is equilibrium. Provision is made for continuously draining the spaces above the pistons C and E.

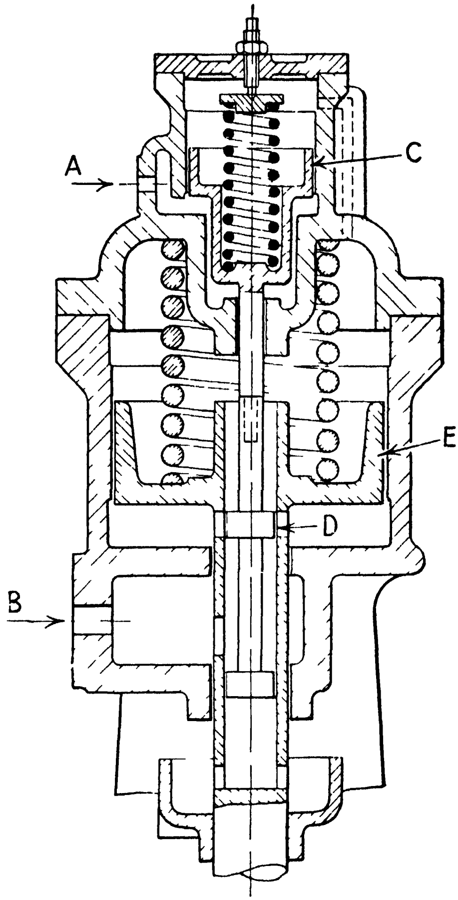


FIG. 423 Compound Relay Gear

An alternative form of relay operating on a similar principle and employed on turbines constructed by Messrs. C. A. Parsons & Co., Ltd., is shown diagrammatically in Fig. 424.

At the high-pressure end of the turbine there is a cross shaft driven by worm gearing from the turbine spindle and carrying at one end the speed governor and at the other end two oil pumps. One of these is a low-pressure pump supplying lubricating oil and

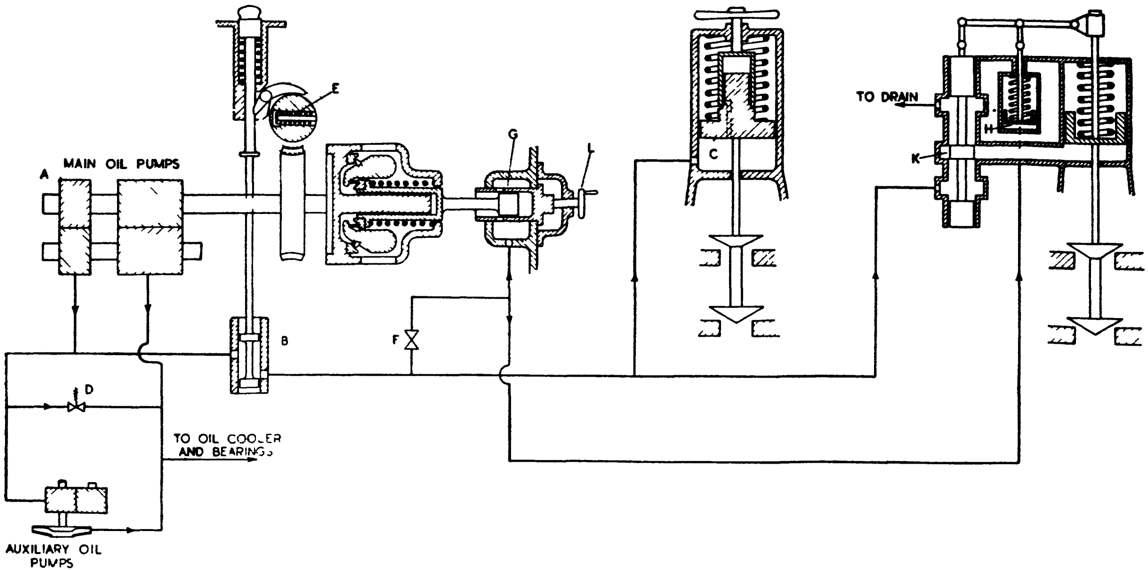


FIG 424 —Governing System for Parsons Turbine

the other a high-pressure pump A supplying oil for governing. The pressure of the oil supplied for governing is kept sensibly constant by a relief valve D which discharges to the lubricating oil supply system.

The governing oil passes through the trip gear B to the piston C of the combined emergency stop valve. A branch from the pressure oil pipe passes through the control valve F to a space surrounding the ported governor bush G. A piston valve sliding in G and operated by the speed governor regulates the opening of the port, the rate of oil leakage, and hence the oil pressure in the pipe after the control valve F. The oil pressure, thus controlled by the speed governor, does not act direct on the main relay piston, but on an auxiliary piston H which actuates the pilot valve K. It will be seen that for equilibrium, since the pilot valve must occupy its central position covering the oil port, the throttle valve will follow the movement of the piston H, the ratio of their displacements depending only on the dimensions of the linkage.

It will be clear that a small displacement of H, producing a displacement of the pilot valve K will admit the high-pressure relay oil to the relay piston and so provide a large restoring force. The control valve F acts as a choke and prevents the flow of oil, through the ports in the sleeve G and to the cylinder H, from affecting the oil pressure in the relay pipe.

If the turbine speed should rise due to a reduction of load, the governor will move the piston in G to the right, thus increasing the area of the open port, reducing the pressure of the oil under the piston H and partially closing the throttle valve. A fall in turbine speed will cause the reverse effects. The speed of the turbine may be changed by rotating the wheel L which moves the sleeve G inwards or outwards according to whether the speed is to be reduced or increased.

If the emergency governor E should come into operation, it trips the vertical plunger and lifts the piston valve in B. This releases the oil pressure from under C and H, and causes the emergency valve and main throttle to close.

The combined emergency stop valve is illustrated in greater detail in Fig. 425. The upper part of the valve spindle carries a piston D, to the underside of which oil from the power supply is admitted. The piston is held down against the pressure of this oil by a hand-controlled sleeve, the end of which abuts against a shoulder on the piston. In order to open the valve, the handwheel must be screwed down so that the ports J in the piston D are closed, thus allowing the oil pressure to build up under the piston. The sleeve is then raised by turning the handwheel when the piston will rise under the action of the oil pressure, the shoulder on the piston D being kept all the time in contact with the end of the sleeve.

Should the oil pressure fail at any time, due to the operation of the trip gear or for any other reason, the valve will at once shut automatically. The piston will be forced downwards by the strong spring above it, returning the valve rapidly to its seating. As soon as the piston begins to move, the sleeve H will lose contact with the piston D, so that any oil remaining under the piston will be free to escape through the ports J in the piston which are normally

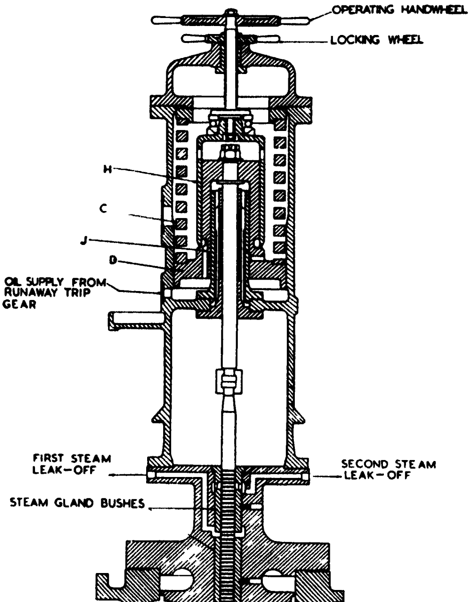


FIG. 425 — Relay for Emergency Stop Valve

kept closed by the end of the sleeve. To limit the flow of oil when the ports are uncovered, a diaphragm, pierced only by a small hole, is fitted in the oil supply pipe.

273. Governor Gear for Mixed-pressure Turbine. The function and operation of mixed-pressure turbines has already been explained in Chapter XVI. A typical governor gear for such a turbine is shown diagrammatically in Fig. 426. The gear is designed to maintain a sensibly constant speed of rotation and to utilize only low pressure steam so long as a supply of such steam is available. It will be clear that if the supply of low-pressure steam should fail then its pressure would rapidly fall. Thus the governor gear comprises two

main elements, a speed-responsive element, i.e. the ordinary centrifugal governor A, and a pressure-responsive element, or "pressure governor" B.

The speed governor controls the relay piston C in the usual manner and this, in turn, controls the position of the point D on the

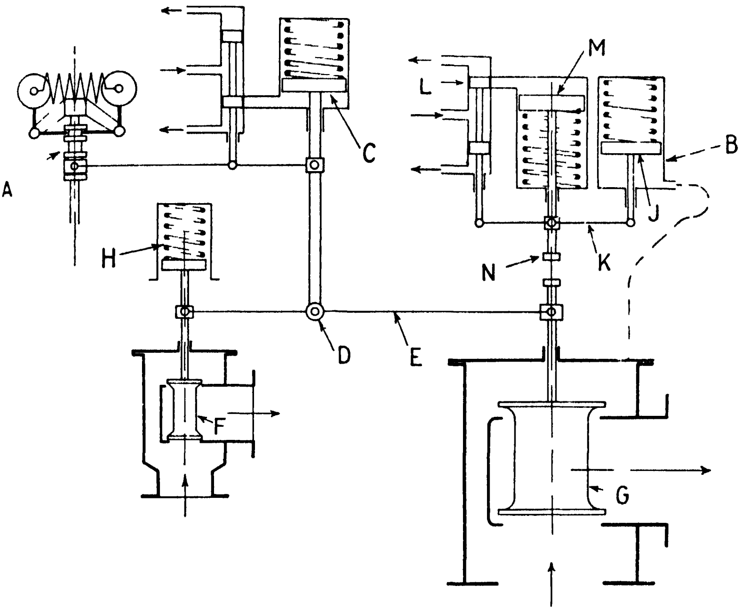


FIG. 426 Diagrammatic Arrangement of Governor Gear for Mixed-pressure Turbine

link E, which is connected at one end to the high-pressure throttle valve F and at the other end to the low-pressure throttle valve G. A spring H is compressed to such an extent that, taking into account the weight of the valves F and G and of their spindles, etc., the moment of the forces on the left of D is greater than that of the forces on the right of D. Consequently, provided the valve G is free to lift, any upward movement of the point D will cause the l.p. throttle valve to open to a greater extent, whereas any downward movement of D would partially close the valve. Meanwhile the h.p. throttle valve is held shut. Under these conditions, the governor gear operates in the same manner as any normal relay gear, a fall in turbine speed due to increase of load causing the lift of the l.p. throttle valve to increase, and vice versa. Moreover, only l.p. steam is being used.

The pressure governor B comprises a spring-loaded piston J

subjected on its underside to the pressure of the available l.p. steam. The piston rod is connected through the floating lever K to the pilot valve L which controls the supply of oil to the relay piston M. The piston rod N is not fastened in any way to the spindle of the throttle valve G, but downward movement of M and N may cause the valve G to be entirely or partially closed. It will be clear

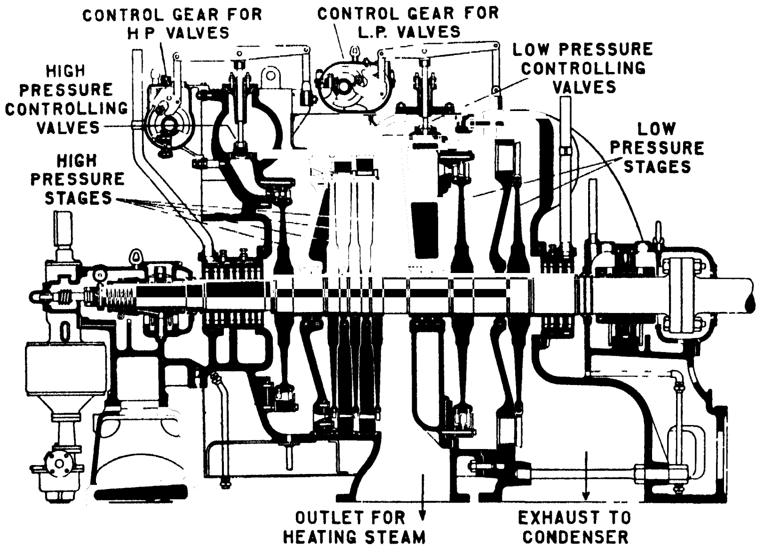


FIG. 427.—Sectional Elevation of B.T.-H. Pass-out Turbine with Cam-operated H.P. and L.P. Valve Gear

without further explanation that as the pressure of the l.p. steam falls, the relay piston M moves downwards, partially closing the valve G. Any such closure of the valve G causes the h.p. throttle valve F to open, thus supplying live steam to the h.p. stages of the turbine. These are mixed-pressure conditions of operation. If the supply of l.p. steam fails completely, then the valve G is forcibly closed and the turbine runs as a high-pressure unit.

274. Governor Gear for Pass-out Turbine. The general principles of the pass-out turbine and its governor gear have been outlined in Chapter XVII. A sectional elevation of a British Thomson-Houston pass-out turbine is given in Fig. 427. There are four impulse stages in the high-pressure section and two in the low-pressure section. A two-row velocity wheel forms the first stage in each section. Nozzle control governing similar to that described in Art. 270 is employed for both the h.p. and l.p. controlling valves, the valves being cam-operated in each case.

The advantages of interconnecting the speed governor and pressure regulator have already been explained in Art. 158. The governors for the B.T.-H. turbine, shown diagrammatically in Fig. 428, are interconnected in the same way. A point on the h.p. rack forms a fulcrum for the floating lever which is connected to each of the pilot valves.

If the action of the mechanism is traced out, it will be seen that if the power load should be reduced while the heating load remains

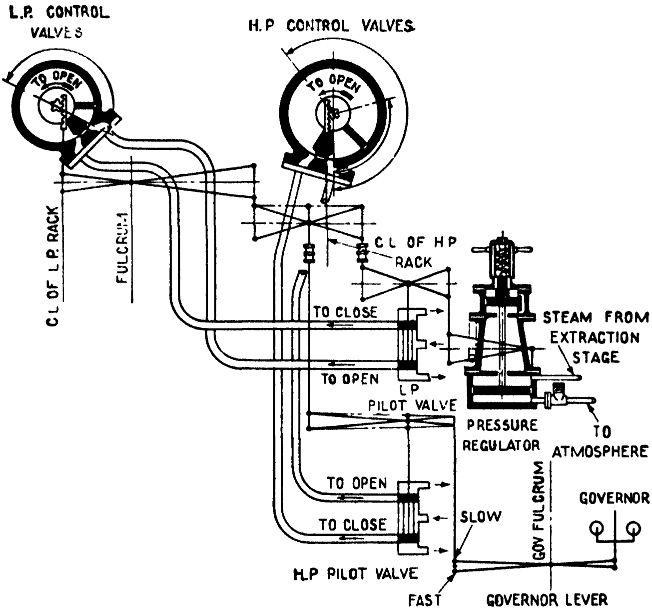


FIG. 428.—Diagram showing the Action of Cam-operated H.P. and L.P. Valve Gear for B.T.-H. Pass-out Turbine

constant, the increase of speed causes the h.p. pilot valve to be lowered, thus partially closing the h.p. control valves. The consequent upward movement of the h.p. rack tends to restore the h.p. pilot valve to its mid-position and simultaneously raises the l.p. pilot valve, thus admitting oil to the l.p. servo-motor and partially closing the l.p. control valves. The clockwise movement of the l p. servo-motor lowers the l.p. rack and tends to restore the l.p. pilot valve to its central position. It will be seen, therefore, that this corresponds to the action of the governor gear shown in Fig. 234.

Suppose now that the heating load is reduced while the power load remains constant. Then the heating steam pressure will rise and cause the l.p. pilot valve to be lowered. This first increases the

opening of the l.p. control valves, but as soon as the servo-motor begins to move, the upward movement of the l.p. rack causes the h.p. pilot valve to move downwards as well as moving the l.p. pilot valve towards its central position. Thus the h.p. control valves are partially closed.

It will be seen, therefore, that a change in turbine speed due to a change in load causes both h.p. and l.p. control valves to move the same way, i.e. both to close or both to open, whereas a change in heating load causes these valves to move in opposite directions. This, also, is in agreement with Fig. 234.

The heating steam pressure may be regulated, within limits, by varying the tension in the spring in the pressure regulator.

In certain cases, the low-pressure control valves are replaced by a circular grid-iron valve covering the inlet to the first stage of the l.p. section of the turbine. The partial rotation of the grid-iron valve causes a change in the area through the nozzles and is effected by an external hydraulic cylinder.

275. Fluid-pressure Governors. As already mentioned in Art. 259, fluid-pressure governors are sometimes used to control the speed of steam turbines in place of the more conventional fly-ball type. An impeller of some form is attached to the turbine shaft or is driven from it through gearing. The operating medium may be either air or oil. The fluid pressure produced by the rotation of the impeller is caused to act either directly on a piston operating the throttle valve or, more usually, on a relay actuating such a piston. The fluid pressure generated varies as the square of the speed and the change of pressure produced by a change of speed is utilized to operate the throttle valve.

276. Early Parsons Air Governor. The fluid-pressure governor was first used on Parsons' turbine and is shown in Fig. 429. A collar A is provided on the shaft and has a series of communicating radial and axial holes which make it, in effect, a small centrifugal impeller. On the side having the axial holes, the impeller runs in close proximity to the bearing housing B, the upper part of which has a cast pipe C which makes the air pressure behind the bellows D and in the chamber E above the oil reservoir equal to that in the space F. The diaphragm D is connected by a rod to a lever actuating the steam throttle valve.

When the impeller is rotating at speed, since the air pressure at the periphery is atmospheric, a sub-atmospheric pressure is produced in the space behind the diaphragm D. This tends to pull the diaphragm inwards against the tension of a spring and so partially close the throttle valve. This part of the governor gear by itself would keep the turbine speed sensibly constant.

These turbines were, however, used to drive direct-current generators in which there was a considerable voltage drop with increase of load. This was corrected by an auxiliary electrical

governor which, as the current in the field winding decreased, caused air to enter the governor at G and so open the throttle and raise the speed sufficiently to bring back the voltage to the normal value.

The partial vacuum produced by the impeller was also used for priming the lubricating system. When the turbine was brought up

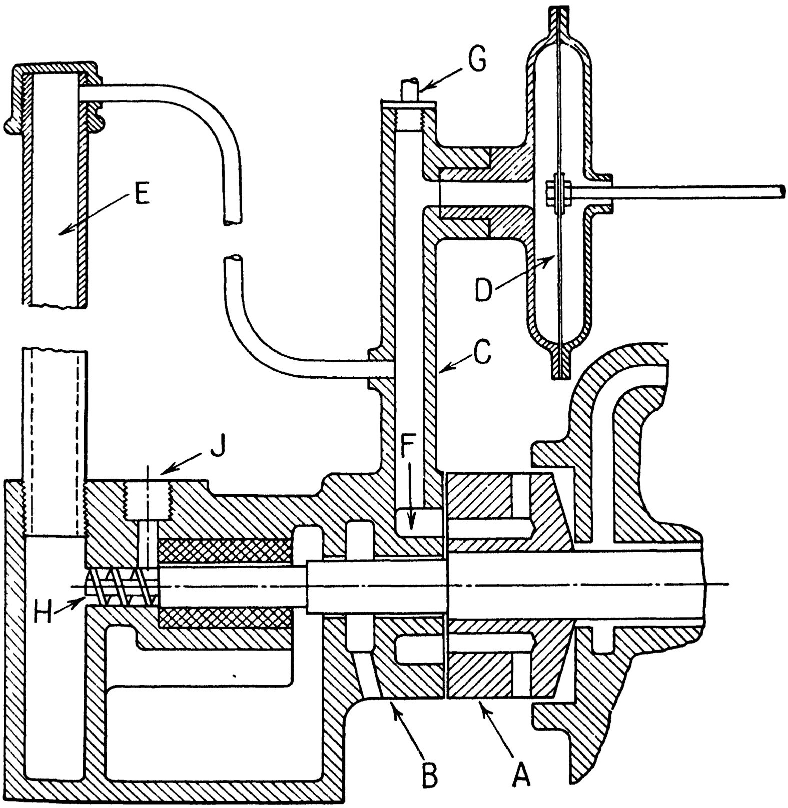


FIG. 429.—Air Governor on Early Parsons Turbine

to speed, the partial vacuum maintained in the chamber above the oil reservoir caused the oil to be forced into this chamber by atmospheric pressure. The end of the turbine spindle was provided with a worm H running in a closely fitting housing opening into the passage between the air chamber and the oil reservoir, so that as the oil rose in the passage it flowed into the worm pump which delivered it to the turbine bearings via the outlet J.

There have been many other applications of the fluid-pressure governor. Particular mention may be made of that developed by Sulzer Brothers about 1911.

277. Westinghouse Fluid-pressure Governor. The Westinghouse Electric and Manufacturing Company, Philadelphia, now use fluid-pressure governors on steam turbines of all sizes.

Fig. 430 shows a cross-section through a 2,500 kW Westinghouse impulse-reaction turbine, designed for an operating speed of 3,600 r.p.m., in which the construction of the type of oil governor employed on the smaller turbines can be seen. The governor oil impeller A on the end of the spindle supplies oil to the sensitive control piston B, an enlarged detail of which is shown in Fig. 431. The control piston B works within the operating or relay piston C, which has ports D and E communicating with the spaces above and below the piston, respectively. The pressure oil is admitted to the inside of the control piston, and so has access to the recess F. The unrecessed portion G of the control piston covers the ports D with a very small amount of lap when the gear is in the neutral position, and controls the admission and release of the pressure oil to and from the upper side of the relay piston. The space beneath the operating piston is connected by a drain pipe to the oil tank. As may be seen from Fig. 430, the spring H is connected at its lower end to the sliding block J. The normal operating oil pressure is 60 lb. per sq. in.

An increase in turbine speed brings about an increase of oil pressure which, acting on the control piston against the tension of the spring, causes it to move upwards, and so uncover the ports G. Oil under pressure is thus allowed to escape from the upper side of the relay piston, and the latter thus moves upward slightly and partially closes the throttle valve. These movements are brought about by the compression in the spring which tends to close the throttle valve.

Stability is obtained in the following manner. The levers K and L are so arranged that as the relay or operating piston is moving upwards, the sliding block J moves upwards at a slower rate, and the tension of the spring gradually increases. Thus, for every turbine speed and, consequently, every oil pressure, there is a definite position of the operating piston with respect to its cylinder and, hence, a definite throttle opening and corresponding power. This differential follow-up motion is not absolutely essential, but without its use, the design of a satisfactory spring is a matter of some difficulty.

Governors of this type are ordinarily given a speed variation of from 4 to 6 per cent. For large central station turbines, the speed variation is usually set at 4 per cent. The speed changer is the hand- or motor-operated screw M, which actuates the fulcrum link N, and so varies the tension in the spring H.

The oil from the main tank is forced up to the impeller suction

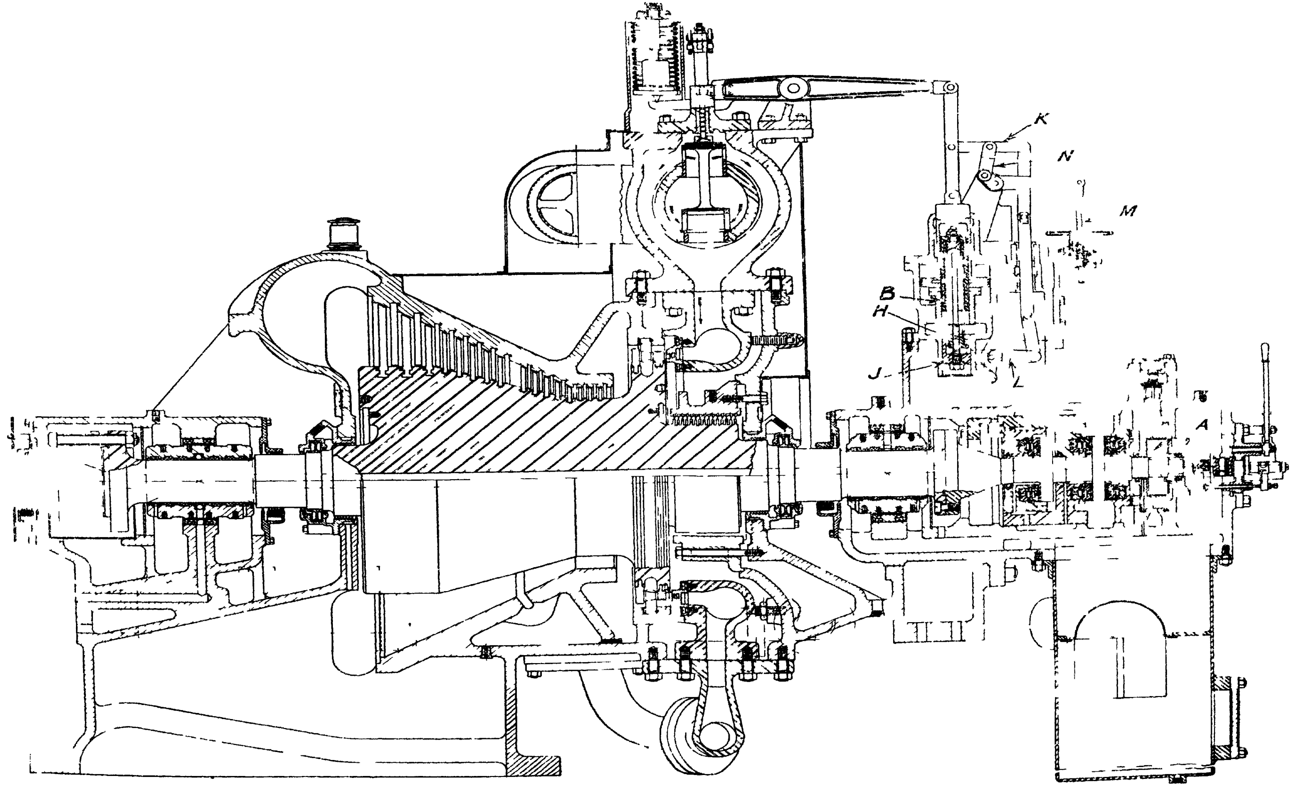


Fig. 130 2 500 kW Westinghouse Turbine with Oil Governor

by a hydraulic ejector. The ejector is, in turn, supplied with high-pressure oil from the discharge of the governing impeller. The cycle is started by the usual steam-driven auxiliary pump.

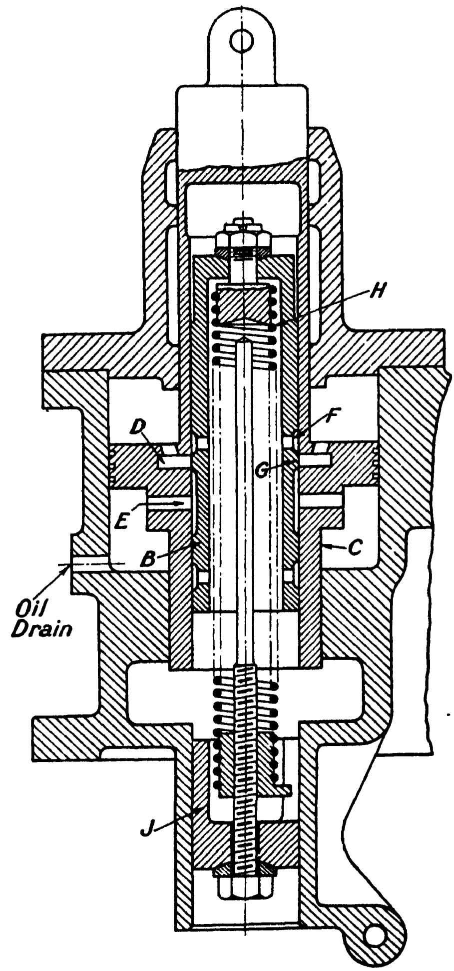


FIG. 431.—Details of Control Piston

A diagrammatic arrangement of the oil governor mechanism for a 40,000 kW turbine is shown in Fig. 432, which is largely self-explanatory. The oil pump impeller is formed on an extension of the turbine shaft, and delivers oil at a pressure of 80 lb. per sq. in. to the relay. It will be seen that the relay is in equilibrium under

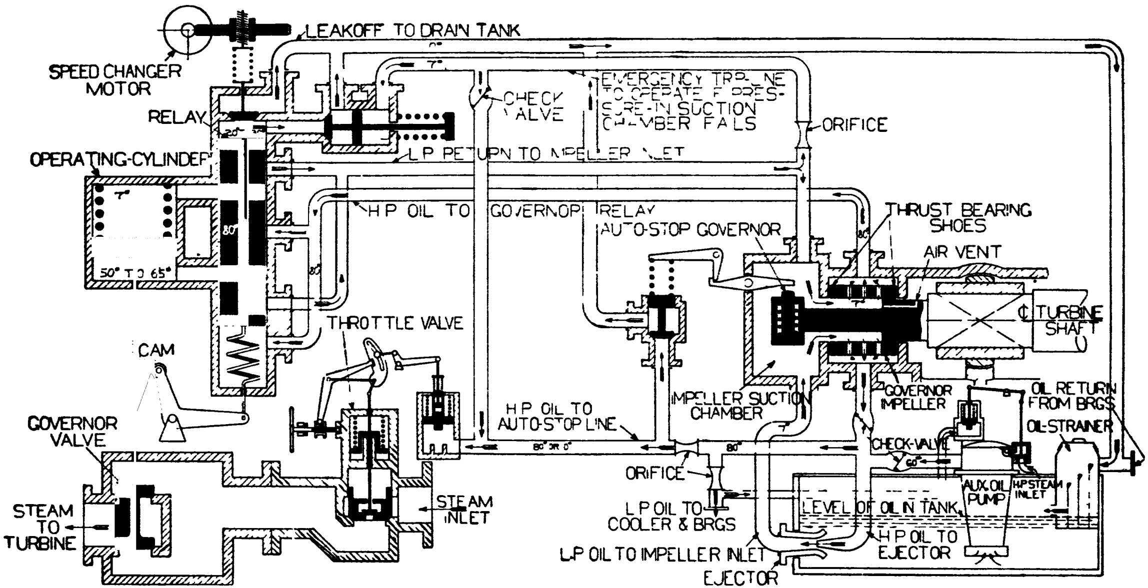


Fig. 432.—Diagrammatic Arrangement of Oil Pressure Governor for 40,000 kW Westinghouse Turbine

the action of forces produced by the full oil pressure, a spring, and a variable oil pressure. The force exerted by the spring balances the difference between the forces produced by the operating oil pressure and the leak-off oil pressure. Stability is secured by a cam-operated bell crank which restores the relay to its neutral position after a change in speed has taken place, by altering the spring tension to balance the changed oil pressure.

Speed change, for paralleling, etc., is effected by varying the back pressure on the upper side of the sensitive piston, there being a small flow through the relief valve at all times, by way of the orifice shown.

While the oil ejectors are extremely reliable for the purpose of supplying oil to the impeller suction, a low-pressure closing device has been provided, so that in the event of the supply of suction oil to the main impeller being lost, the low-pressure closing device will operate and shut the main valve.

Details of the actual governor mechanism are shown in Fig. 433.

Section BB is a section through the speed changer leak-off valve and low-pressure closing device. Note the leak-off passage to the right, shown diagrammatically in Fig. 432 by a central hole in the relay valve. Section AA is through the main throttle and relay valves, and relay gear. Section KK is through the drip collector, taking leakage oil from above the valve spindle guide.

The impellers for a 60,000 kW, 1,800 r.p.m. turbine are shown in Fig. 434. In order to give a flat characteristic curve, radial vanes are used. The impeller does not resemble a centrifugal pump of the ordinary type, as the overhanging rim that forms the pumping part of the impeller is simply a part of the forged steel shaft end, with radial holes drilled for the flow of oil. Actually, the collar on the shaft functions, in addition, as the Michell thrust bearing. The adjusting gear for the latter is clearly shown in the illustration. The Westinghouse Company have attempted in this design to obtain an impeller which would hold a large volume of oil, passing through the impeller at a low velocity, thus permitting the air to be separated and forced to the centre of the impeller, from which it passes out through an air vent drilled in the shaft. The smaller impeller, which is of higher capacity, furnishes the oil for the bearings.

A number of points arise for consideration in connection with oil pressure governors. It might be thought that the constant churning of the oil would cause oxidation and sludging. Actual experience has shown that such is not the case, probably owing to the continual de-aeration of the oil. The reduction in density of the oil as its temperature rises causes a reduction in the pressure generated at any given speed, and thus tends to bring about a change of speed. This is compensated in two ways. Firstly, by immersing the governing springs in the hot oil, which, it will be noted, is done in every

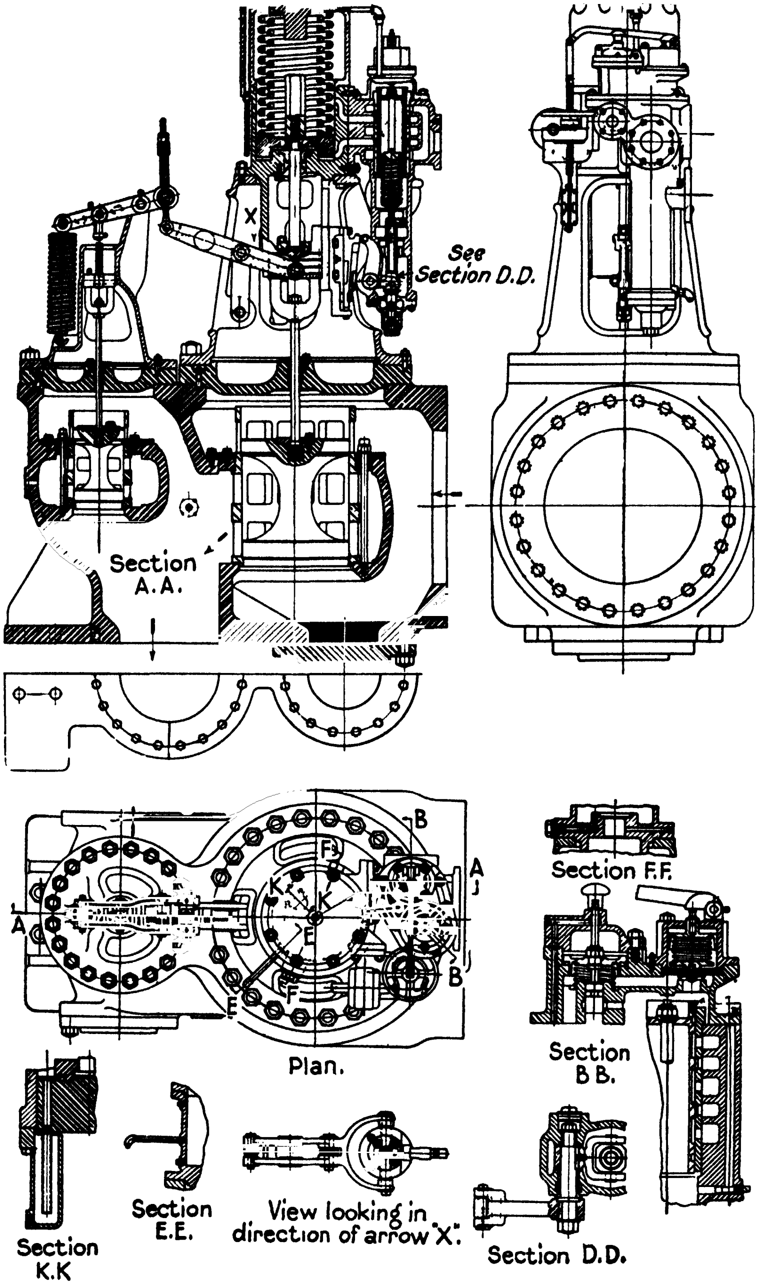


Fig. 433.—Details of Throttle Valves and Governor Gear for 40,000 kW Westinghouse Turbine

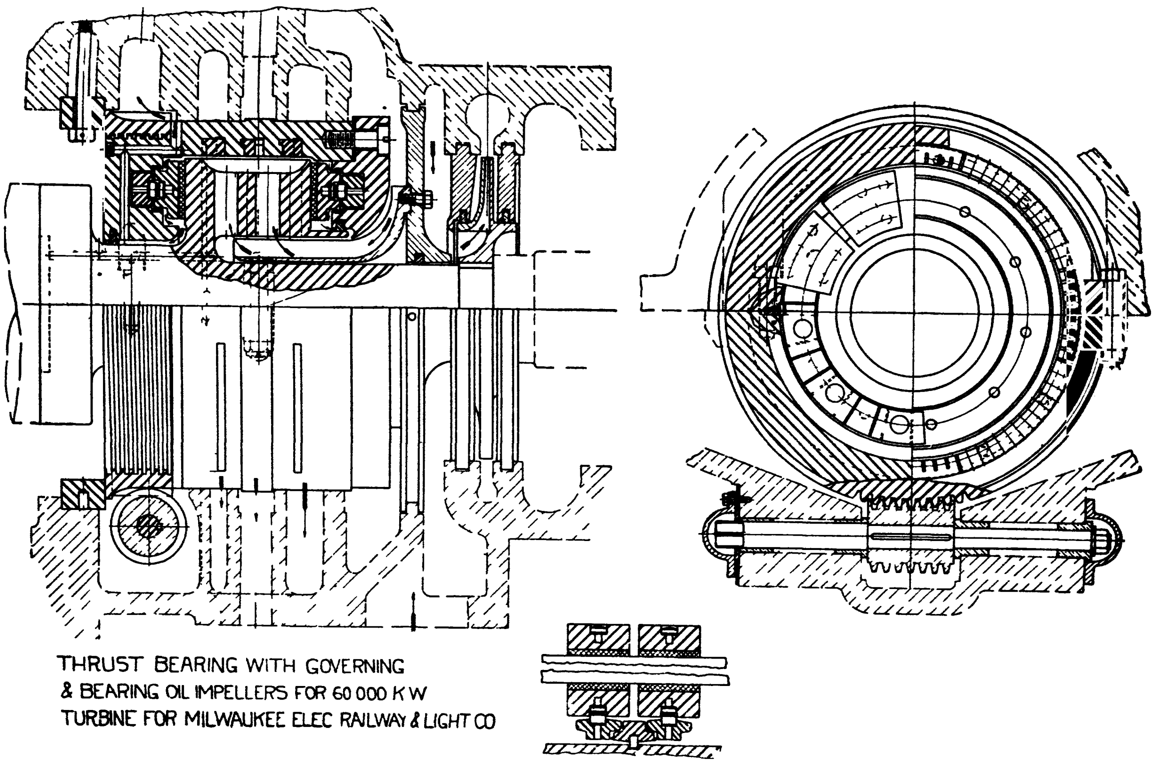


FIG 434 —Impellers for 60,000 kW Turbine

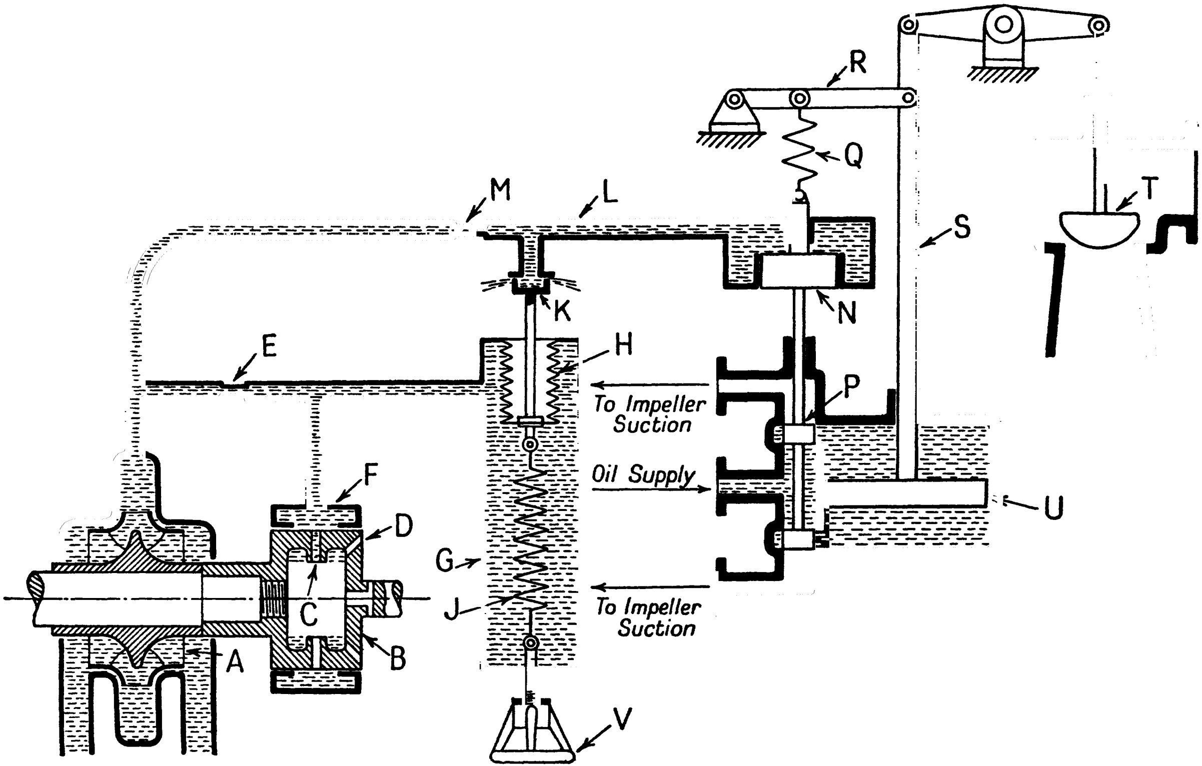


Fig. 435.—Diagrammatic Arrangement of Fluid Pressure Governor Gear on Westinghouse Steam Turbine

case. There is thus a partial compensation for the reduction in density, as the lowering of the elastic modulus gives a corresponding reduction in load due to the spring. The remainder of the compensation comes about by reason of the fact that with hotter and less viscous oil, the air separation in the impeller is more complete.

278. Westinghouse Fluid-pressure Governor with Governor Transformer. A more recent form of the Westinghouse governor is illustrated in diagrammatic form in Fig. 435. This type of governor is used on central station machines and the modifications which have been made in the earlier types have for their object to make the governor gear more sensitive to small changes of speed.

The impellers A and B are mounted on the turbine shaft. A is the main oil pump and supplies all the oil required while the turbine is operating at normal speed. It is a centrifugal pump and discharges at a pressure of about 120 to 150 lb. per sq. in. gauge at the normal operating speed with 10 to 30 lb. per sq. in. g. suction pressure. During the starting period oil is supplied to the impeller suction by the auxiliary oil pump, as the impeller is not self-priming. Under normal operating conditions the suction is supplied by an ejector which utilizes a part of the high-pressure oil from the impeller discharge as the operating medium.

The ejector is designed to handle all the oil required for lubrication and for normal leakage. The relay piston discharges directly into the impeller suction line and therefore does not add load to the ejector.

The governor impeller B is made integrally with the overspeed trip body and consists of a hollow cylindrical body with a series of radial tubes C. It is also connected to the drain chamber of the bearing pedestal by a number of holes D. An air vent is provided at the centre and communicates with two radial holes in the overspeed trip body.

Oil from the main pump A is admitted through a variable orifice E into the annular chamber F and maintains a small flow through the impeller holes into the drain chamber. With the impeller B rotating the centrifugal force of the oil in the radial tubes opposes the flow of oil through the holes and maintains in the chamber F a pressure which varies as the square of the turbine speed, being about 30 lb. per sq. in. g. at 3,600 r.p.m. The variable orifice E must be so adjusted that the oil supply to the impeller is slightly in excess of the normal leakage around the governor impeller B. This ensures that the impeller tubes will be full of oil and will thus function correctly.

The space F is connected to a chamber G which forms part of the governor transformer and contains a flexible metal bellows H and a load spring J. Connected to the bellows is a small "cup" valve K which controls the flow of oil from a space L which is supplied with high-pressure oil through a choke M. The pressure of the oil in the

chamber L will depend on the opening of the cup valve. Furthermore, the force on the cup valve depends on the pressure of this oil, and under all conditions the cup valve is in equilibrium under the action of the forces due to (1) the oil pressure on the bellows H, (2) the tension of the spring J, and (3) the pressure of the oil in L. It will be apparent, therefore, that an increase in oil pressure in G caused by an increase of turbine speed will be followed by an increase in the secondary control oil pressure in the chamber L. Such pressure increase is transmitted to the upper side of the relay piston N which is, in effect, coupled to the relay piston valve P. A tension spring Q connects the upper end of N to the follow-up lever R which is attached to the relay piston rod S. As shown in the diagram, the relay piston controls the opening of the steam valve T.

The piston N is held in equilibrium by the oil pressure above it and the tension of the spring Q and this latter depends on the position of the main relay piston U. We have seen that the pressures in G and in L depend on the turbine speed and, therefore, for every turbine speed there is a corresponding equilibrium position of the throttle valve T.

The combination of the chamber G with its bellows H, the cup valve K and the piston N operating the pilot valve P is termed the governor transformer and its purpose is to magnify the relatively small pressure changes delivered by the governing impeller into larger pressure changes which are utilized to actuate the pilot valve of the servomotor. Assuming that the mechanism is in operation, the following describes a complete cycle of control.

If the load increases, the turbine speed decreases and the governing oil pressure below the transformer bellows H decreases, thus allowing the tension spring J to move the transformer cup valve K downwards. Downward movement of this valve passes more oil to the drain chamber, thus decreasing the pressure of the governing secondary control oil in L. With the reduction of pressure in L, the existing force of the oil pressure below the bellows H again balances the pressure above the cup valve.

The decreased governing secondary control pressure thus established by the transformer cup valve has at the same time decreased the downward force on the piston N. This causes an upward movement of the pilot valve P with the result that high-pressure oil is admitted above the main operating piston U and the space beneath U is connected to the impeller suction. The main relay piston U is therefore moved downward thus increasing the opening of the steam throttle valve. The downward movement of the main relay piston decreases the tension in the spring Q until the diminished spring tension balances the decreased secondary control pressure and thus returns the relay to its neutral position.

If the load decreases, the turbine speed increases and generally things happen in the reverse order to that described above.

279. Speeder Gear. If the turbine is running alone and is controlling frequency then the speed of rotation may be changed by changing the tension of the spring J. This may be effected by turning the handwheel V, usually by remote control. If the spring tension is increased, then since the turbine speed is, for the time being, constant, the oil pressure under the bellows H remains unchanged and the opening of the cup valve K will increase, with a consequent reduction of oil pressure in L. This causes the piston N and the pilot valve P to be displaced upwards with the result that the main relay piston U is lowered and the opening of the throttle valve T increased. As already explained above, downward movement of U reduces the tension in the spring Q which balances the reduced pressure in L. The increased opening of the throttle T will raise the turbine speed and the oil pressure in G. This increase in oil pressure will partially balance the increased tension in the spring J. The oil pressure in L will still be lower than its former value and will correspond to the reduced tension in the spring Q. Thus, for every setting of the speeder gear there will be a corresponding equilibrium speed at a given load.

A reduction of the tension in J would likewise cause the oil pressure in L to rise, with the result that the pilot valve P would be lowered, the piston U raised, and the throttle valve T partially closed.

If the turbine is driving an alternator which is electrically connected to other sets and is, therefore, running at a more or less fixed speed, then the speeder gear may be used for increasing or reducing load on the turbine in question. For example, if the tension in the spring J is reduced, the pressure in L will be increased, and the resultant downwards movement of N and P will cause the throttle valve T to close partially. Equilibrium will be restored by the increased tension in Q, and the amount of movement of T will depend entirely on the amount by which the tension in J is reduced. Similarly, load may be added to the turbo-alternator, within the limits of the set, by increasing the tension in the speed changer spring.

280. Governor Anticipatory Gear. In many steam turbines operating with steam at high pressures and temperatures, the steam chests and valves are placed near the high-pressure turbine, connection being made to the inlet branches of that turbine by pipes which are made as flexible as possible. In consequence, the steam contained in these pipes, in the turbine cylinders and in the pipes connecting one cylinder to another, is beyond the control of the governor valves.

Moreover, due to the use of a rotational speed of 3,000 r.p.m., even in the largest units, the rotor diameters and hence their inertias are relatively small. If the turbine should be unloaded suddenly then the "locked up" steam will continue to expand to condenser pressure and so accelerate the turbine. The normal governor gear is responsive only to a change of speed and cannot

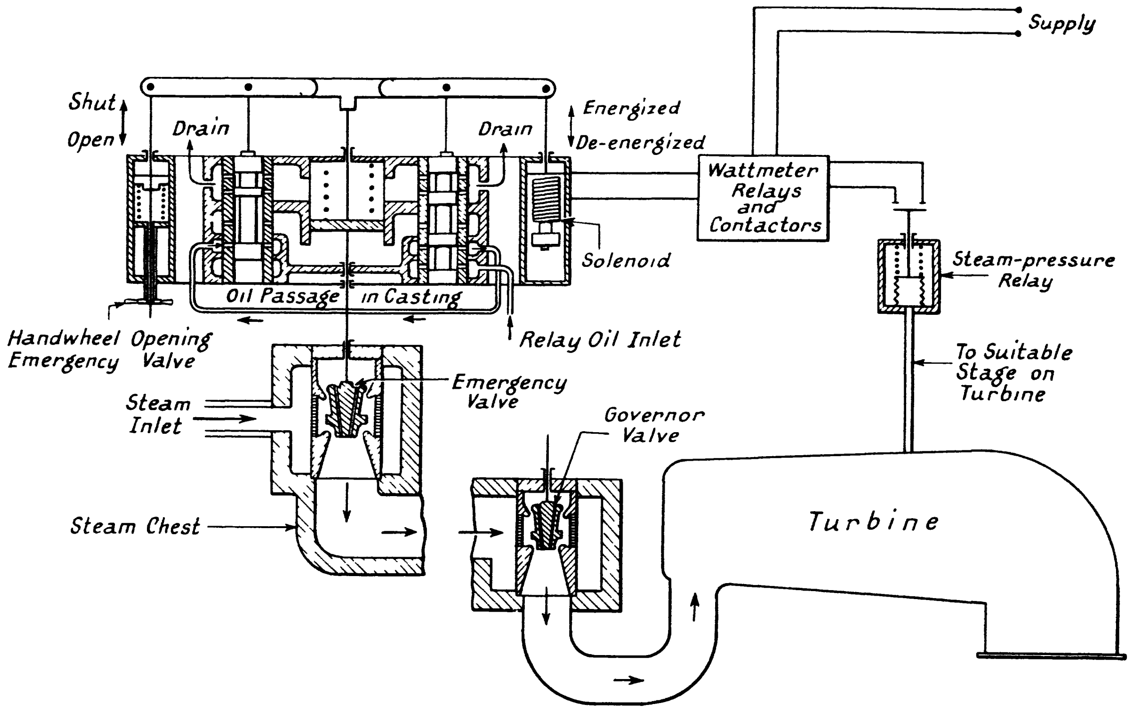


FIG 436 —Diagrammatic Arrangement of Metropolitan-Vickers Governor Anticipatory Gear

close the throttle valves instantaneously. The total increase of speed which would occur on the sudden release of load is made up of three amounts, viz. (1) the permanent increase due to change of load, (2) the increase of speed due to the time lag in closing the throttle valves, and (3) the increase due to expansion of the steam contained in the system. Under certain conditions the speed rise would cause the emergency governor to operate.

Most large steam turbines are now fitted with additional gear, the purpose of which is to anticipate the normal speed governor and close either the throttle valves or the emergency valve, and prevent a large increase of speed when a sudden drop in load occurs.

Below a certain power, the pressure and density of the contained steam will be insufficient to accelerate the rotor sufficiently to cause the emergency governor to act. Accordingly, the anticipatory gear is arranged to operate only if the initial load on the machine exceeds a certain fraction of the full load. Under normal conditions with gradual load changes the gear is inoperative.

Fig. 436 shows in diagrammatic outline the control gear as fitted to turbines constructed by the Metropolitan-Vickers Electrical Co., Ltd. Important elements of the control gear are a wattmeter relay, a steam-pressure relay and a solenoid which becomes energized when the coil circuit is closed. This circuit may be closed (*a*) by the wattmeter relay when the load falls below a certain amount, e.g. 10 per cent of full load, and (*b*) by the steam-pressure relay when the pressure exceeds that corresponding to a certain proportion, e.g. 50 per cent of the full load. If the steam pressure is lower than this value or if the load on the generator exceeds the present limit, the gear will not operate.

It will be seen from Fig. 436 that, when the solenoid is energized, the upward movement of the pilot valve on the right will release to drain oil from the underside of the central relay piston, at the same time cutting off pressure-oil supply to the pilot valve on the left. This action rapidly closes the emergency valve and so prevents overspeeding. If the solenoid is de-energized, say by the resumption of load or fall in steam pressure, the pilot valve on the right is lowered; this closes the escape to drain and admits pressure-oil to the pilot valve on the left, which causes the emergency valve to re-open.

The gear is also used for opening and closing emergency valve.

In reheat turbines the interceptor valves between the reheater and the i.p. or l.p. turbine inlet belt are operated in the same manner as the emergency valve.

281. Vacuum Unloading and Trip Gear. Loss of vacuum is usually caused through failure in the supply of cooling water. Most large steam turbines are provided with special governor gear which is superimposed on the normal speed governor and comes into action when the vacuum falls below a certain value, say 25 in. Hg.

The gear comprises a metal bellows connected to the exhaust branch and operating an oil-pressure release valve or a relay, as the case may be, which partially closes the throttle valve and so unloads the turbine. If the vacuum should continue to fall, the steam supply will be gradually reduced and reach zero at a vacuum of about 17 to 20 in. Hg. If the interruption is temporary then the restoration of the normal vacuum will allow the speed governor to take control of the steam supply to the turbine. If, however, the vacuum falls to a certain limiting value, say 17 in. Hg., it actuates a trip mechanism which closes the emergency valve. When this occurs the generator should be disconnected from the busbars in order to prevent over-heating of the turbine blades due to motoring.

CHAPTER XXVII

SPEED AND OUTPUT OF STEAM TURBINES

282. Relationship between Cumulative Heat Drop, Mean Diameter, Speed of Rotation, and Number of Stages in Impulse Turbines. It has been shown in Art. 80, Chapter VII, that the efficiency of a multi-stage impulse turbine equipped with single-row wheels depends on ρ, the ratio of blade speed to steam jet speed.

Consider first of all a turbine in which the cumulative heat drop is H_c, and assume for the sake of simplicity that the mean diameter D (and hence the mean blade velocity u) is uniform throughout the turbine. Assume, further, that the nozzle angle is the same for all stages. The increase in this angle which usually occurs in the last few stages will affect the result only slightly and can be ignored.

By eq. (105), Art. 80, the required adiabatic heat drop per stage is ΔH, where

$$\Delta H = V_1^2\{1 - \phi[k^2 + \rho^2(1 - k^2) - 2(\rho \cos \alpha - \rho^2)(k^2 + kC)]\} \div 2gJ \cdot \eta_n$$

i.e.

$$\Delta H = \frac{V_1^2 \cdot F_1}{2gJ}$$

where F_1 is a function of ρ, k, ϕ, C, α, and η_n. If k, ϕ, and C be assumed to have constant values and if values of η_n appropriate to selected values of α are taken, then F_1 is simply a function of ρ.

If n is the number of stages, then $\Delta H = \frac{H_c}{n}$, since the heat drop per stage is uniform.

$$\therefore \qquad \frac{V_1^2 \cdot F_1}{2gJ} = \frac{H_c}{n}$$

and

$$V_1^2 = \frac{2gJ \cdot H_c}{n \cdot F_1}$$

Now

$$u = \frac{\pi D}{12} \times \frac{N}{60} = \frac{DN}{229}$$

where D = mean dia. of blades, in.

N = r.p.m.

$$\therefore \qquad \rho = \frac{u}{V_1} = \frac{DN}{229}\sqrt{\frac{n \cdot F_1}{2gJ \cdot H_c}}$$

$$= \frac{1}{229 \times 223{\cdot}8}\sqrt{\frac{n \cdot D^2N^2}{H_c}} \cdot \sqrt{F_1}$$

or $$\rho = \frac{1}{51\cdot2}\sqrt{F_1}\sqrt{\frac{K}{H_c}} \quad . \quad . \quad . \quad (248)$$

where $$K = n\left(\frac{D}{10}\right)^2\left(\frac{N}{100}\right)^2$$

Also $$\frac{K}{H_c} = \frac{2{,}620\,\rho^2}{F_1} \quad . \quad . \quad . \quad (249)$$

K is known as the Parsons number for the turbine. Since the efficiency of a turbine depends chiefly on the value of ρ, it will be clear

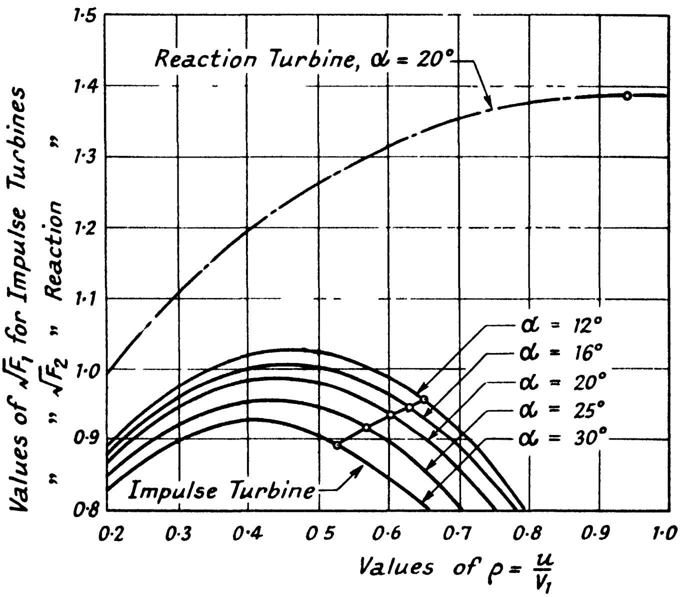


FIG 437

that for a given turbine operating under given steam conditions, the performance will depend on the value of $\frac{K}{H_c}$, which may be termed the efficiency factor. This quantity is often termed the "quality factor" of the turbine.

When the diameter is variable, the value of K is the sum of the products $\left(\frac{D}{10}\right)^2\left(\frac{N}{100}\right)^2$.

i.e. $$K = \sum_0^n\left(\frac{D}{10}\right)^2\left(\frac{N}{100}\right)^2$$

Since $$u = \frac{DN}{229}, \ K = 0{\cdot}0525\Sigma u^2$$

If u_1 is the mean blade velocity in metres per sec., then $K = 0{\cdot}5653\Sigma u_1^2$.

Values of $\sqrt{F_1}$ are shown in Fig. 437. These are based on the same data as Fig. 107, namely: $k = 0{\cdot}90$; $C = 1$; $\phi = 0{\cdot}95$,

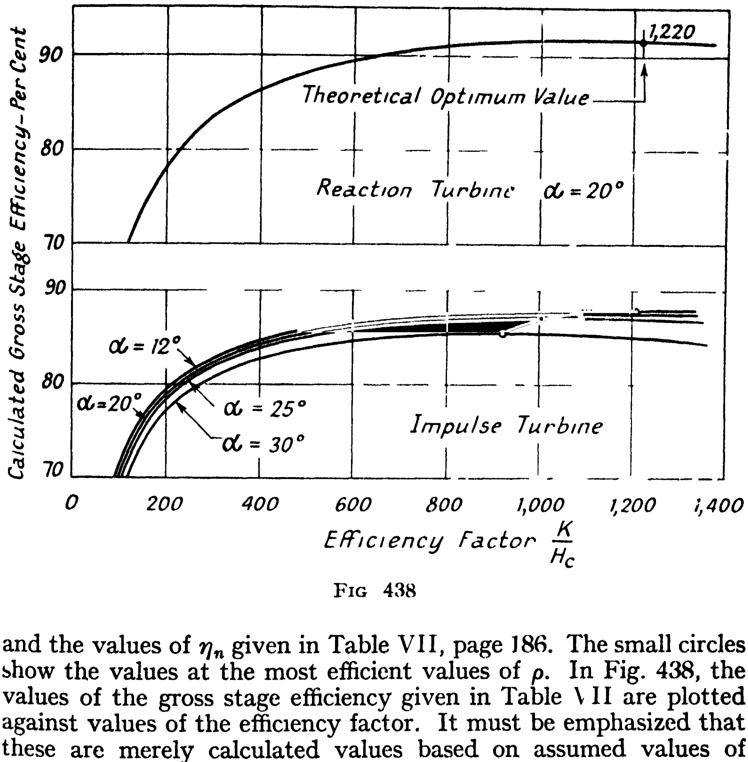


FIG 438

and the values of η_n given in Table VII, page 186. The small circles show the values at the most efficient values of ρ. In Fig. 438, the values of the gross stage efficiency given in Table VII are plotted against values of the efficiency factor. It must be emphasized that these are merely calculated values based on assumed values of the coefficients. Nevertheless, they show in a qualitative manner the influence of the efficiency factor on the expected efficiency of a multi-stage impulse turbine. Taking 20° as a representative nozzle angle it will be seen that the most economical value of the efficiency factor is about 1,080. In practice, no advantage would be gained by exceeding this number and for obvious reasons a smaller value would generally be employed.

283. Relationship between Cumulative Heat Drop, Mean Diameter, Speed of Rotation, and Number of Stages in Reaction Turbines. Suppose there are n stages in the turbine, each stage comprising

one fixed and one moving row of blades. Then by eq. (125), Art. 90, the heat drop per stage is—

$$\Delta H = \frac{V_1^2}{2gJ} \cdot F_2$$

where $$F_2 = 2\{1 - \phi(1 + \rho^2 - 2\rho \cos \alpha)\} \div \eta_n$$

$\therefore$ $$V_1^2 = \frac{2gJ \cdot H_c}{n \cdot F_2}$$

and $$\rho = \frac{u}{V_1} = \frac{1}{51{\cdot}2} \sqrt{F_2} \sqrt{\frac{K}{H_c}}$$

or $$\frac{K}{H_c} = \frac{2{,}620\rho^2}{F_2}$$

Values of $\sqrt{F_2}$ are shown in Fig. 437, and values of the gross stage efficiency plotted against those of the efficiency factor in Fig. 438. The most economical value of the latter is 1,220 for the selected data, which are the same as those in Art. 90.

It will be seen from Fig. 438 that—

(1) the efficiency curves are very flat for both types of turbine; an appreciable reduction in the efficiency factor below the optimum value produces a relatively small change in efficiency ratio;

(2) there is not a very great difference between the optimum values of $\frac{K}{H_c}$ for both types of turbine.

An important conclusion of the above analysis is that, *irrespective of the power of a steam turbine*, for a given heat drop the K value must be the same if the same theoretical efficiency ratio is to be realized. Suppose, for example, two impulse turbines, one of 2,000 kW and another of 10,000 kW, are to be constructed to operate with steam at 250 lb. per sq. in. and 700° F. and, say, an exhaust pressure of 1 in. Hg. absolute. Suppose that the speed of the two turbines is to be the same, say 3,000 r.p.m. Then the sum Σu^2 must be the same for both turbines and if the same number of stages is employed the mean diameter of the two turbines must be the same. It is true that the nozzle and blade areas of the 10,000 kW turbine will be about five times as large as those of the 2,000 kW turbine, but as regards the leading dimensions, i.e. diameters of wheels, diaphragms, and of the cylinder, length of cylinder, size of spindle, etc., the 2,000 kW turbine will be almost identical with the 10,000 kW turbine. The difference in the total cost will not be appreciable, and hence the cost per kW capacity will be much less for the greater output. This limitation may be overcome in certain cases by the use of reduction gearing between the turbine and the driven machine, thus enabling a smaller turbine running at a higher speed to be employed.

Since, for a given set of conditions, the value nD^2N^2 must be a constant, a smaller value of the quantity nD^2 is obtained by adopting a higher speed of rotation. In other words, by increasing the speed N to the highest possible value, a smaller and consequently cheaper turbine will result. As shown in Art. 285, this procedure is limited by considerations of output.

The efficiency factor is not the sole criterion of efficiency. The actual efficiency ratio of a turbine will also depend on—

(1) the excellence, or otherwise, of the design in so far as losses due to partial admission, windage, eddies, etc., are kept within small limits;

(2) the finish of the nozzle and blade surfaces; and

(3) the characteristics of the cycle in so far as losses due to moisture in the L.P. stages are concerned.

284. Comparison of Pressure-compounded and Velocity-compounded Turbines. Consider a turbine consisting of a number of pressure-compounded single-row wheels and another containing a certain number of velocity-compounded wheels.

Let n_p, N_p, D_p, etc., refer to pressure-compounded turbine.

n_v, N_v, D_v, etc., refer to velocity-compounded turbine.

μ = number of rows of moving blades in each stage of the velocity-compounded turbine.

It has been shown in Art. 85 that for the simple case of frictionless flow and no carry-over, the condition for maximum efficiency is that—

$$\rho_v = \frac{\rho_p}{\mu}$$

Hence
$$\sqrt{\frac{K_v}{H_c}} = \frac{1}{\mu}\sqrt{\frac{K_p}{H_c}}$$

Hence, for the same cumulative heat drop—

$$K_p = \mu^2 . K_v$$

i.e.
$$n_p(D_p . N_p)^2 = \mu^2 . n_v(D_v . N_v)^2 \quad . \quad . \quad . \quad (250)$$

Thus for the same value of DN (i.e. for the same blade velocity) and for equal relative efficiency—

$$n_p = \mu^2 . n_v$$

that is to say—

One two-row velocity wheel will replace 4 single wheels.
One three-row velocity wheel will replace 9 single wheels.
One four-row velocity wheel will replace 16 single wheels.

In calculating the value of the efficiency factor $\frac{K}{H_c}$ for velocity-compounded or combination turbines, it is preferable, for the

purposes of direct comparison, to modify the value of n and express it as an equivalent number of pressure-compounded stages.

EXAMPLE 46. Compare the relative rotative speeds of a de Laval steam turbine 8 in. mean diameter and a three-row velocity-compounded two-stage turbine having a wheel 40 in. mean diameter, both turbines having the same heat drop.

$$n_p(D_p \cdot N_p)^2 = \mu^2 \cdot n_v(D_v \cdot N_v)^2$$

In this example, $n_p = 1$, $n_v = 2$, $\mu = 3$ rows.

Hence
$$\frac{N_p}{N_v} = \mu \cdot \frac{D_v}{D_p} \cdot \sqrt{\frac{n_v}{n_p}}$$
$$= 3 \cdot \frac{40}{8}\sqrt{\frac{2}{1}} = 21{\cdot}2$$

285. Relationship between Output, Speed, and Blade Velocity in Impulse Turbines. The power output of a steam turbine depends upon (1) the mass of steam which passes through the turbine per unit time, (2) the adiabatic heat drop, and (3) the efficiency ratio.

Let HP = power output at turbine coupling, h.p.
kW = power output at turbine coupling, kW.
H_a = adiabatic heat drop, B.Th.U. per lb.
η_r = efficiency ratio of turbine.
w = weight of steam passing through turbine per second.
x_e = dryness fraction of steam at exhaust.
v_e = specific volume of dry and saturated steam at the exhaust pressure.
V_1 = steam velocity at exit from nozzles in last stage.
u = mean blade velocity in last stage.
α = nozzle angle in last stage.
l = nozzle height in last stage.

Then
$$w = \frac{2{,}546\ \text{HP}}{3{,}600\eta_r \cdot H_a} = \frac{3{,}413\ \text{kW}}{3{,}600\eta_r \cdot H_a}$$

∴ Volume of steam passing through last-stage nozzles
$$= w \cdot x_e \cdot v_e \text{ cub. ft. per sec.}$$

The area available through the nozzles may be set down with reference to Fig. 439. As already explained in Chapter XVIII, the L.P. nozzles are formed by casting-in sheet metal guide vanes in the diaphragm. The effective area of the channel in each nozzle is

$$l(p_m \cdot \sin\alpha - t) = c \cdot l \cdot p_m \sin\alpha$$

where
$$c = \frac{p_m \cdot \sin\alpha - t}{p_m \cdot \sin\alpha}$$

The factor c may be termed the "thickness coefficient" for the nozzle, since it takes into account the partial obstruction of the

nozzle passages due to the finite thickness of the guide vanes. Values of c are given in Fig. 440 for a standard mean pitch of 2 in. and different vane thicknesses.

If, as is usual, the nozzles extend round the full circumference, the number of nozzles is obviously $\frac{\pi D}{p_m}$.

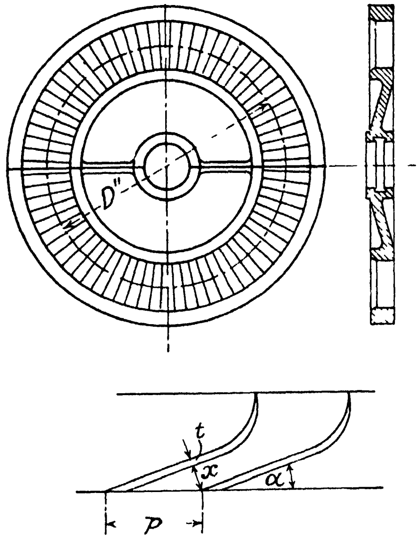


FIG 439

$$\therefore \qquad \text{Total area} = A = \frac{\pi D l \,.\, c \,.\, \sin\alpha}{144} \text{ sq. ft.}$$

Writing
$$m = \frac{l}{D}$$

$$A = \frac{\pi m D^2 c \,.\, \sin\alpha}{144}$$

$\therefore$ Volume of steam flowing per second

$$= AV_1 = \frac{\pi m D^2 c \,.\, V_1 \,.\, \sin\alpha}{144}$$

Since
$$D = \frac{229u}{N}, \text{ and } V_1 = \frac{u}{\rho}$$

Vol. per sec.
$$= \frac{\pi \times (229)^2}{144} \times \frac{mcu^3 \,.\, \sin\alpha}{N^2 \,.\, \rho}$$

Equating this to the volume based on the steam flow and transposing, we have—

$$\left(\frac{u}{100}\right)^3 . \sin\alpha = 0{\cdot}617\left(\frac{\mathrm{HP}}{1{,}000}\right)\left(\frac{\mathrm{N}}{1{,}000}\right)^2 . \frac{x_e v_e . \rho}{mc\eta_r \mathrm{H}_a} \quad . \quad (251)$$

$$\left(\frac{u}{100}\right)^3 . \sin\alpha = 0{\cdot}827\left(\frac{\mathrm{kW}}{1{,}000}\right)\left(\frac{\mathrm{N}}{1\ 000}\right)^2 . \frac{x_e v_e \rho}{mc\eta_r \mathrm{H}_a} \quad . \quad (252)$$

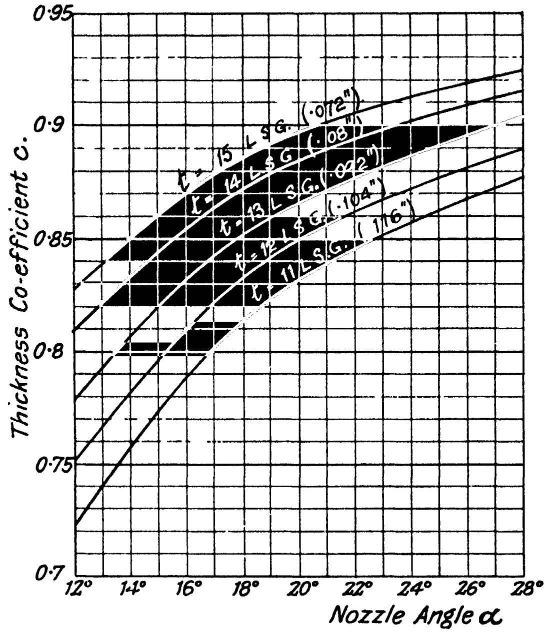


FIG. 440.—Thickness Coefficients for Turbine Nozzles

Alternatively—

$$\mathrm{HP} = 1{,}620\,\frac{u^3}{\mathrm{N}^2} . \frac{mc . \sin\alpha . \eta_r \mathrm{H}_a}{x_e v_e \rho} \quad . \quad . \quad (253)$$

$$\mathrm{kW} = 1{,}208\,\frac{u^3}{\mathrm{N}^2} . \frac{mc . \sin\alpha . \eta_r \mathrm{H}_a}{x_e v_e \rho} \quad . \quad . \quad (254)$$

These expressions are correct only for a non-extraction turbine with a single exhaust. For two similar exhausts, the constants in eqs. (251) and (252) are halved, while those in eqs. (253) and (254) are doubled, and so on. Moreover, the expressions are only applicable to pure impulse turbines.

Considering in turn the factors involved—

(1) x_e is found direct from the Mollier chart.

(2) v_e depends on the exhaust pressure, i.e. the vacuum. The higher the vacuum, the greater v_e and the smaller the limiting output of the turbine, other things being equal.

(3) ρ depends on the efficiency required but is arbitrary. If u is high in the last stage and ρ is given the same value as in preceding stages it is possible that the jet velocity will exceed the critical, in which case unless convergent-divergent nozzles are employed a certain amount of jet deflection will take place (see Art. 61). In such cases partial reaction might be employed; in fact a moderate amount of reaction is often used in so-called impulse turbines.

(4) The value of m is arbitrary, but in a turbine in which the output is relatively high for the speed of rotation the value of m must be made as great as possible, otherwise a large nozzle angle will have to be used. But it would appear that for good design and satisfactory efficiency there is a limit to the value of m for constant nozzle angle, pure impulse operation, and a blade of uniform cross-section. For example, in an impulse turbine in which the pressure gradient in the clearance space between the nozzles and blades is ignored, in which the nozzle outlet angle is 25° and the blade speed ratio 0·5, the direction of flow into the moving blades differs from the direction at the mean (design) radius by the angles i_1 and i_2 at the innermost and outermost radii, respectively,

Value of $m = \frac{l}{D}$	i_1 degrees	i_2 degrees
0·1	− 3·32	+ 3·75
0·2	− 6·28	+ 7·95
0·3	− 8·92	+ 12·67

A more serious feature, as explained in Art. 93, is the negative reaction that would occur at radii less than the mean radius, the most unfavourable conditions occurring near the blade root. Even with partial reaction at the mean radius these effects might still occur.

For the last few stages in turbines of large output, some form of vortex flow would be adopted. In the turbines constructed by one well-known manufacturer, vortex blading is used in all stages in which the ratio of the outer to the inner radius of the blade exceeds 1·15.

(5) The value of c depends on the nozzle angle α and the thickness of the guide blades. Since α may be the unknown, the calculation may have to be made by trial and error.

(6) η_r and H_a are known or assumed.

If N is known, then the product $u^3 \sin \alpha$ is derived, and in general u will be fixed by the size of the nozzle angle. If, however, N is arbitrary, as, for example, in the case of small geared sets, α and u may be chosen arbitrarily and the required value of N calculated.

If this proves unsuitable, then either u or α, or both, may be modified. It will be clear that, given the output and steam conditions, the number of solutions is very large indeed.

EXAMPLE 47. An impulse turbine is required to develop 3,000 kW at 3,000 r.p.m., with the following steam conditions—

Initial pressure	300 lb. per sq. in. abs.
Initial temperature . . .	700° F.
Vacuum	29 in. Hg.

Calculate the required mean blade velocity in the last stage and the mean diameter of the blade ring in that stage for the following nozzle angles: 20, 22, 24, 26, 28, and 30 degrees. Make the following assumptions—

Efficiency ratio = 0·75; $m = 0{\cdot}18$; $\rho = 0{\cdot}55$; mean pitch of nozzles = 2 in.; guide vane thickness = 0·104 in.

From the ϕ–I chart we find the adiabatic heat drop to be 467·6, and the dryness fraction of the exhaust steam, after allowing for losses, to be 0·932. On substituting in eq. (252), we obtain the following expression—

$$\left(\frac{u}{100}\right)^3 = \frac{118{\cdot}7}{c\,.\sin\alpha}$$

The remainder of the calculation is best arranged in tabular form as follows—

α	$\sin\alpha$	c	u ft. per sec.	D in.
20	0·3420	0·850	742	56·6
22	0·3746	0·862	717	54·8
24	0·4067	0·872	695	53·0
26	0·4384	0·881	675	51·5
28	0·4695	0·890	657	50·1
30	0·5000	0·896	642	49·0

EXAMPLE 48. Calculate suitable speeds of rotation and corresponding mean diameters (of last stage) for a geared turbine of 800 h.p. under the following conditions—

Initial steam pressure . . .	200 lb. per sq. in. abs.
Initial steam temperature . .	600° F.
Vacuum	28 in. Hg.
Efficiency ratio	0·72
Mean blade velocity . . .	500 ft. per sec.

Make calculations for the following nozzle angles in the last stage: 20, 22, 24, 26, 28, and 30 degrees, and assume: Admission = Complete; $m = 0{\cdot}15$; $\rho = 0{\cdot}5$; $p_m = 2$ in.; $t = 0{\cdot}104$ in.

From the Mollier diagram we find that the adiabatic heat drop is 386·3 and the actual exhaust dryness fraction is 0·947.

Substituting values in eq. (253), it will be found that—

$$\left(\frac{\text{N}}{1{,}000}\right)^2 = 65\cdot8\, c \,.\, \sin \alpha$$

Since $$u = \frac{\text{DN}}{229},\ \text{D} = \frac{229 \times 500}{\text{N}} = \frac{114{,}500}{\text{N}}$$

The following results are then obtained—

α	$\sin \alpha$	c	N r.p.m.	D in.
20	0·3420	0·850	4,370	26·2
22	0·3746	0·862	4,605	24·9
24	0·4067	0·872	4,830	23·7
26	0·4384	0·881	5,095	22·5
28	0·4695	0·890	5,245	21·8
30	0·5000	0·896	5,425	21·1

This example shows that by the use of reduction gearing, turbines of relatively small output may be constructed in the form of high-speed machines of small dimensions.

286. Relationship between Output, Speed, and Blade Velocity in Reaction Turbines. In Art. 91 it is shown that for an impulse-reaction turbine—

$$\text{D}^2 l = \frac{10{,}510 w_1 \,.\, v_s \,.\, \rho}{\text{N} \,.\, \sin \alpha}$$

In the symbols of the previous article, v_s is equal to $x_e v_e$. w_1 is the "working steam" in lb. per sec. In the last stage of the turbine, the tip clearance loss will generally be so small that w_1 is practically equal to w, the quantity of steam supplied to the turbine per second.

Writing $l = m\text{D}$, $\text{D} = \frac{229u}{\text{N}}$, and substituting $\frac{2{,}546\text{HP}}{3{,}600\eta_r \text{H}_a}$ for w_1—

$$\left(\frac{u}{100}\right)^3 . \sin \alpha = 0\cdot617 \left(\frac{\text{HP}}{1{,}000}\right)\left(\frac{\text{N}}{1{,}000}\right)^2 \frac{x_e v_e \rho}{m \,.\, \eta_r \,.\, \text{H}_a} \quad . \quad (255)$$

Similarly—

$$\left(\frac{u}{100}\right)^3 . \sin \alpha = 0\cdot827 \left(\frac{\text{kW}}{1{,}000}\right)\left(\frac{\text{N}}{1{,}000}\right)^2 \frac{x_e \,.\, v_e \rho}{m \,.\, \eta_r \,.\, \text{H}_a} \quad . \quad (256)$$

As the value of ρ must be greater for the reaction turbine than for the impulse turbine in order to realize the same relative efficiency, the product $u^3 \,.\, \sin \alpha$ must be greater for the same output. In other words, the limiting output of the reaction turbine is smaller than that of an impulse turbine operating under otherwise identical conditions. This limit to the output of reaction turbines is obviated in a manner similar to that employed to increase the output of

impulse turbines, namely, by gradually increasing the blade (equivalent nozzle) angles in the final stages. The last few groups of blading are made of the same height, but the blade outlet angle is progressively increased by the use of quarter-wing, semi-wing, three-quarter-wing, and full-wing blades (Fig. 441). It is difficult, if not impossible, to state the outlet angle of a reaction blade because the tangents to the back and front curved surfaces give two different values α_1 and α_2, as shown in Fig. 441 (*a*). The values given under

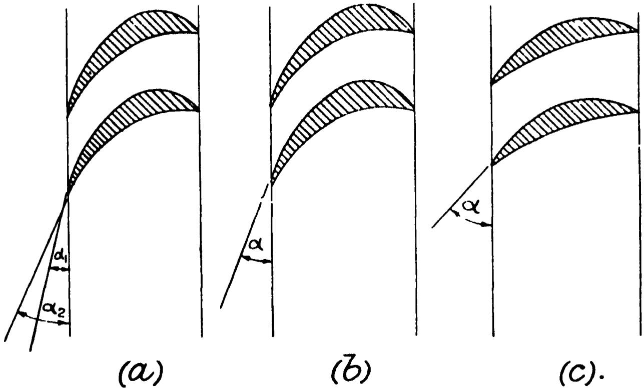


FIG. 441

(*a*) Section through "normal" reaction turbine blade. Mean outlet angle 18°-20°.
(*b*) "Semi-wing" blade. Outlet angle about 30°.
(*c*) "Full-wing" blade. Outlet angle about 45°.

Fig. 441 are mean values, but in any case they are varied to suit requirements. Instead of stating the outlet angle of the blade, the ratio of the effective area through the blade outlet to the full area of the annulus is sometimes given. This is termed the "opening." Interesting particulars are given in Mr. R. H. Parsons' book, *The Development of the Parsons Steam Turbine*, of an 8,500 kW steam turbine installed in Sheffield power station. The last four pairs of blades were made 9 in. high on a rotor 60 in. diameter.

	Opening 0	$\sin^{-1} 0$
1st pair, fixed and moving	0·35	20·5 deg.
2nd pair, fixed and moving	0·50	30·0 ,,
3rd pair, fixed and moving	0·61	37·6 ,,
4th pair, fixed	0·71	45·3 ,,
4th pair, moving	0·83	56·1 ,,

As in impulse turbines, the employment of long blades (large values of *m*) involves variations in steam pressure within the blade due to inertia, with the result that the degree of reaction is variable along the length of the blade. The expressions given in this article are, therefore, only applicable to moderate values of *m*.

In large power station turbines of the Parsons type the last few stages have individual wheels whose mean diameter increases progressively towards the exhaust end. The blades are long and are designed for vortex flow.

287. Turbine Output and Stress in Last Row of Blades. It has been shown in Art. 172 that the centrifugal stress in turbine blades of uniform cross-section is given by the expression—

$$f_c = 0{\cdot}231 m_1 u^2 \text{ for brass blades}$$

$$f_c = 0{\cdot}215 m_1 u^2 \text{ for steel blades}$$

where m_1 is the ratio of the blade length to the mean diameter of the blade ring. Eq. (254) may be written

$$\text{kW} = \frac{1{,}208u}{\text{N}^2} \cdot \frac{c \,.\, \sin\alpha \,.\, \eta_r \,.\, \text{H}_a}{x_e v_e \,.\, \rho} \,.\, mu^2$$

Considering steel blades only (as brass is unsuitable for high stresses), we have

$$m_1 u^2 = 4{\cdot}65 f_c$$

Assuming, for simplicity, that the length of the blade is equal to the height of the nozzle (in many turbines of large output there is little difference), then $m_1 = m$.

$$\therefore \qquad \text{kW} = \frac{5{,}610u \,.\, f_c}{\text{N}^2}\left(\frac{c \,.\, \sin\alpha \,.\, \eta_r \,.\, \text{H}_a}{x_e v_e \rho}\right) \qquad . \qquad . \quad (257)$$

Thus for fixed values of the quantities within the bracket, the limiting output of the turbine varies—

(1) directly as the maximum centrifugal stress in the blades;
(2) directly as the mean blade velocity;
(3) inversely as the square of the speed of rotation.

$$\text{Alternatively } f_c = \frac{\text{N}^2 \,.\, \text{kW}}{5{,}610u}\left(\frac{x_e \,.\, v_e \,.\, \rho}{c \,.\, \sin\alpha \,.\, \eta_r \text{H}_a}\right) \qquad . \qquad . \quad (258)$$

The output may be considerably increased for the same value of the maximum stress if the cross-sectional area of the blade is gradually increased from tip to root (see Art. 176).

288. Carry-over Loss. Reference to the velocity diagram for an impulse wheel shows that the absolute velocity of the steam at exit from a wheel is approximately axial. In estimating the carry-over loss (see Art. 116) it is sufficiently accurate to assume that the steam flows into the exhaust belt in the axial direction. This statement also applies to the reaction turbine when the ratio of blade velocity to steam velocity is reasonably near to the optimum value.

(*a*) *Single-flow Turbine.* The volume of steam flowing into the exhaust belt of a turbine without steam extraction in any form and having only one exhaust branch is

$$\frac{2{,}546 \text{ HP}}{3{,}600} \frac{x_e v_e}{\eta_r \text{H}_a} \text{ cub. ft. per sec.}$$

The area available for flow (see Fig. 442)

$$= \frac{\pi D l}{144} = \frac{\pi m_1 D^2}{144} \text{ sq. ft.}$$

$$\therefore \qquad \text{Velocity at exit} = \frac{32{\cdot}42 \text{ HP } x_e v_e}{m_1 D^2 \eta_r H_a}$$

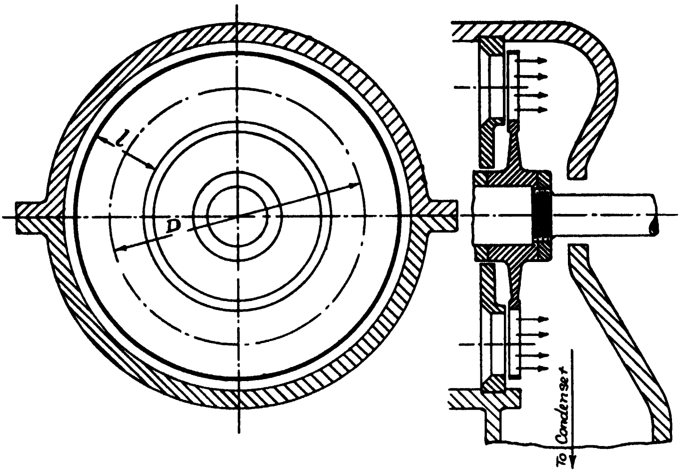


FIG. 442

The heat equivalent of the kinetic energy in B.Th.U. per lb.

$$= \left\{\frac{32{\cdot}42 \text{ HP } x_e v_e}{223{\cdot}8\, m_1 D^2 \eta_r H_a}\right\}^2$$

Hence we may express the residual velocity loss as a percentage λ of the adiabatic heat drop, from which

$$\text{D inches} = \frac{1}{\sqrt[4]{\lambda}}\sqrt{\frac{1{\cdot}45 \text{ HP } x_e v_e}{m_1 \,.\, \eta_r \; H_a^{1{\cdot}5}}}$$

$$= \frac{1}{\sqrt[4]{\lambda}}\sqrt{\frac{1{\cdot}94 \text{ kW } x_e v_e}{m_1 \,.\, \eta_r \,.\, H_a^{1{\cdot}5}}} \quad . \quad . \quad . \quad (259)$$

Consider now the case of turbines from which steam is extracted for feed-water heating. Suppose that for each pound of steam entering the turbine—

W = work done, B.Th.U.

Σw = total extraction, lb. of steam.

Then defining the percentage carry-over loss λ as the ratio of the

kinetic energy of the steam leaving the final row of moving blades to the work done in the turbine,

$$\text{D inches} = \frac{1}{\sqrt[4]{\lambda}}\sqrt{\frac{1{\cdot}45\ \text{HP}\ (1 - \Sigma w)\ x_e v_e}{m_1 \text{W}^{1\cdot5}}}$$

$$= \frac{1}{\sqrt[4]{\lambda}}\sqrt{\frac{1{\cdot}94\ \text{kW}\ (1 - \Sigma w)\ x_e v_e}{m_1 \text{W}^{1\cdot5}}} \quad . \quad (260)$$

(*b*) *Multi-exhaust Turbines.* As will be seen in Art. 291, the limiting output of steam turbines is frequently increased by the use of two or more similar exhausts, the steam flow being divided at a certain point in the expansion and the subsequent expansion of the steam taking place in two or more L.P. blade systems working in parallel. Then since the area varies as D^2—

if D_1 = calculated diameter of single-flow turbine

,, D_2 = calculated diameter of double-flow turbine

,, D_3 = calculated diameter of triple-flow turbine, etc.,

then $D_2 = \frac{D_1}{\sqrt{2}}$; $D_3 = \frac{D_1}{\sqrt{3}}$; $D_4 = \frac{D_1}{2}$, etc.

289. Conditions in Turbines with Vortex Flow. Referring to Fig. 135 and considering the conditions at inlet to a stage and at outlet from the moving blades of the same stage, then it follows from continuity that the axial component of velocity at outlet from the blades is

$$V_{a3} - V_{a1} \cdot \frac{A_1 v_3}{A_3 v_1}$$

Due to friction on the roof and floors of nozzle and blade passages, the axial velocity is generally a maximum about mid-height and falls off somewhat towards the inner and outer diameters. If, however, it is assumed that V_{a1} is uniform, then since the specific volumes v_1 and v_3 will be sensibly uniform and independent of radius, the axial velocity V_{a3} may be assumed to be sensibly constant.

If D is the mean diameter of the blades,

$$w = \frac{\pi m_1 D^2}{144} \cdot \frac{V_{a3}}{v_3}$$

from which either w, D, or V_{a3} may be found if the other quantities are known.

Reference to Fig. 139 will show that at the innermost section of the blade with vortex flow where the degree of reaction is small, the steam velocity from the fixed nozzles is high. In turbines of large power this velocity may reach and exceed the sonic velocity. At the outermost blade section where the degree of reaction may be

relatively high the steam velocity is greatest at outlet from the moving blade and may well reach or exceed the sonic velocity. If the outlet velocity should exceed the local acoustic velocity then there would be shock losses accompanied by a certain amount of jet deflection.

If V_3 represents the velocity relative to the moving blade at outlet and α_3 is the flow angle, then

$$V_{a3} = V_3 \cdot \sin \alpha_3$$

If, for example, V_3 is limited to the acoustic velocity then V_{a3} can be increased only by increasing α_3, with some loss of efficiency.

In stages with wet steam the acoustic velocity is an uncertain quantity but for present purposes may be calculated from the expression

$$a = \sqrt{gnPv}$$

where v is the specific volume of dry vapour and n is the corresponding isentropic index, about 1·11.

Then $$a = 71{\cdot}7\sqrt{pv}$$

290. Methods of Increasing the Limiting Output of Steam Turbines. The increasing use of electrical energy for domestic and industrial purposes has led to a continuous increase in the size of generating stations. In the replacement of obsolete plant, or the design of new extensions, the engineer is faced with the problem of selecting a size for the generating units. Choice is influenced by a number of factors such as reliability, space available, necessity of providing a standby machine, first cost, and thermal efficiency Turbines of larger size are not, in general, so reliable as smaller machines. They require more time for warming-up, and load must not be applied too quickly, otherwise dangerous heat stresses and also vibrations may be set up. On the other hand, the first cost of turbine plant per unit capacity diminishes as the size is increased, and, further, the overall thermal efficiency of large units is generally higher than that of smaller machines. The tendency has been, and still is, to install larger and still larger machines. The high-powered turbine presents an interesting and sometimes difficult problem in design, chiefly on account of the enormous volume of steam which must pass through the final stages of the turbine.

For current (1956) practice in which all large steam turbines are equipped with five to eight stages of regenerative feed-heating and in some cases with one stage of reheating, and in which the final stage blading operates with variable reaction, the output of the turbine is limited mainly by—

(1) the annulus area per exhaust

$$\frac{\pi m_1 D^2}{144} \text{ sq. ft.}$$

(2) the allowable axial velocity V_a across the annulus.

Using the same symbols as in Art. 288 it is easy to show that the available output per exhaust, for a mean blade velocity u ft. per sec., is—

$$\text{kW kilowatts} = \frac{1{,}208\ Wm_1V_au^2}{(1 - \Sigma w)x_e v_e N^2} \qquad (261)$$

The expression shows that the maximum output varies directly as W. This is increased by raising the initial steam pressure and also

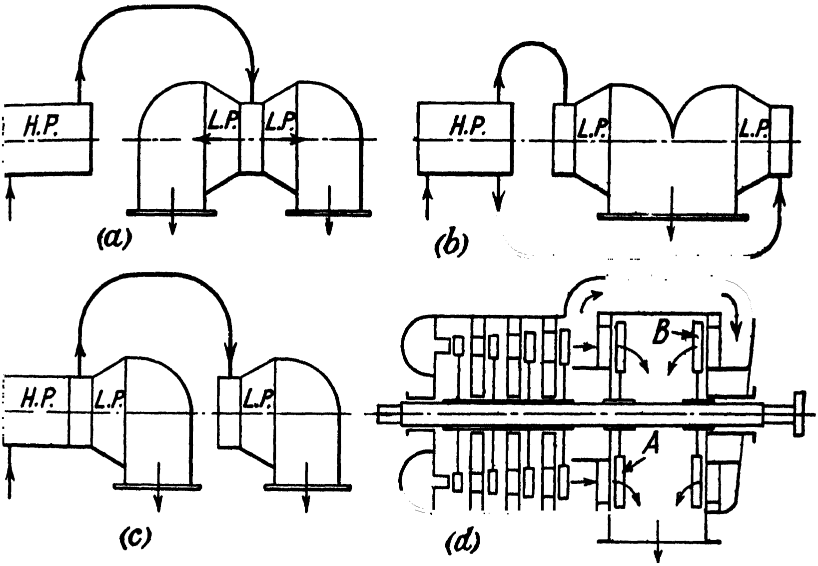


FIG. 443 — Turbines with Two Exhausts

by reheating. The ratio m_1 is limited by the mean blade speed and the allowable stresses in the blade and its attachment to the rotor. The paramount importance of blade velocity is evident but it is obviously affected by the ratio m_1 and the mechanical properties of the available materials. Σw depends on the economical feed temperature; with higher pressures the value of Σw is increased. The final dryness fraction x_e depends mainly on the initial steam pressure and whether reheating is adopted. The final specific volume v_e depends mainly on the condenser pressure; it is inversely proportional to this pressure for normal conditions. The influence of rotational speed is very great, and output may be greatly increased by using lower rotational speeds. In spite of this, current practice is to use a speed of 3,000 r.p.m. in this country and 3,600 r.p.m. in America for the largest outputs up-to-date (1956).

291. Multi-exhaust Turbines. The 3,000 r.p.m. turbine is an attractive machine owing to the small sizes and masses of its parts, and the limitations to the output of a single-flow machine may be readily overcome by carrying out part of the expansion in a normal single-flow turbine and the subsequent part in two or more similar low-pressure turbines operating in parallel.

Various arrangements of two-exhaust turbines are shown diagrammatically in Fig. 443. In (*a*) there is a H.P. turbine with a double-flow L.P. turbine necessitating the use of two condensers,

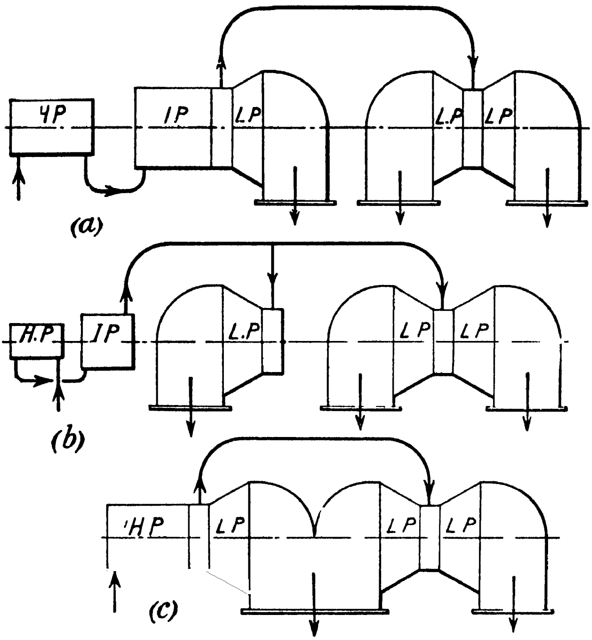


FIG. 444.—Turbines with Three Exhausts

(*b*) shows a H.P. turbine having two receiver connections leading steam to the opposite ends of a double-flow L.P. turbine with a single exhaust branch and a single condenser. In (*c*) the H.P. and one section of the L.P. turbine are arranged in the same cylinder the other half of the steam being led to a second L.P. turbine identical with the other. Fig. 443 (*d*) shows a turbine with a divided flow, in which half the steam flows direct through the wheel A into the exhaust branch, the other half passing through wheel B. In calculating the K value of multi-exhaust turbines the sum

$$\sum\left(\frac{D}{10}\right)^2\left(\frac{N}{100}\right)^2$$

is calculated for only one of the L.P. stage groups and added to that for the H.P. stages down to the point where the flow is divided.

Various arrangements of turbines with three exhausts are shown in Fig. 444. Each diagram shows an arrangement which has actually been used in practice and is self-explanatory. Turbines are under construction on the lines shown in Fig. 444(*a*) for an output of

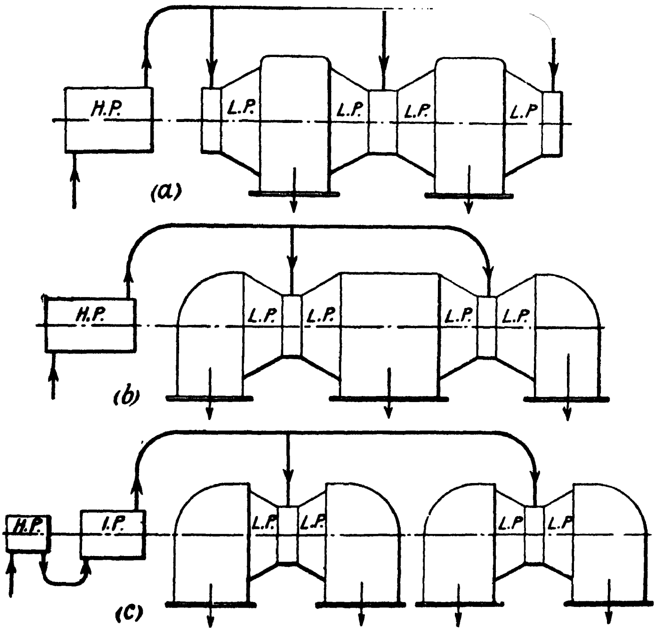


FIG. 445.—Turbines with Four Exhausts

200 MW. at 3,000 r.p.m. Fig. 445 shows turbines operating with four exhausts.

Data relating to turbines of large output are given in Tables XXXIVA and XXXIVB. These have been collected from various sources, but for much of the information given the author is indebted to two well-known papers (1 and 2) by Mr. K. Baumann. The data are arranged in chronological order. In order to show the increase which has taken place in the output per exhaust, this has been reduced to a standard exhaust pressure of 1 in. Hg. and a standard speed of 3,000 r.p.m. in accordance with the following simple formula, based on eq. (254) and on the assumption that $p_e v_e$ is approximately constant for small changes of exhaust pressure—

$$kW_1 = kW\left(\frac{1}{p}\right)\left(\frac{H_{a1}}{H_a}\right)\left(\frac{N}{3{,}000}\right)^2 \quad . \quad . \quad (262)$$

TABLE XXXIVa

Particulars of Turbines of Large Power

Meanings of Abbreviations: M.C.R. = Max. continuous rating, i.e. the maximum output which the generator is capable of giving continuously. E.R. = Economic rating, i.e. the power at which the turbine operates most economically. Where this has not been stated by the manufacturer, it has been taken as 80 per cent of the M.C.R. p_s = stop valve pressure, lb. per sq. in. abs. t_s = steam temp. at stop valve, °F. Firms: A.E.G. = Allgemeine Elektrizitäts-Gesellschaft, Berlin; Al. = Alsthom; B.T.H. = British Thomson-Houston Co., Ltd.; E.E. = English Electric Co., Ltd.; F. & C. = Messrs. Fraser & Chalmers Eng. Works; G.E. = General Electric Co., U.S.A.; M.A.N. = Maschinenfabrik Augsburg-Nürnberg A.G.; M.V. = Metropolitan-Vickers Electrical Co., Ltd.; A.C.O. = Ateliers de Construction Oerlikon; C.A.P. = Messrs. C. A. Parsons & Co., Ltd.; W.E. = Westinghouse Electric & Manufacturing Co., U.S.A.

Ref. No.	Firm	Power Station	Year	Output kW		Speed r.p.m.	Operating Conditions			No. of Shafts	No. of Cyls.	No. of Exhs.	kW per Exhaust (E.R.)	
				M.C.R.	E.R.		p_s	t_s	Vac. at E.R. in. Hg. Abs.				Actual	Reduced to 1 in. Hg. and 3,000 r.p.m.
1	C.A.P.	Commonwealth, Fisk Street, Chicago	1912	25,000	20,000	750	215	588	1·0	1	2	2	10,000	625
2	C.A.P.	Lots Road, London	1915	18,000	15,000	1,000	215	600	1·0	1	2	2	7,500	833
3	W.E.	Commonwealth, N.W., Chicago	1917	30,000	25,000	1,200	—	—	1·0	1	2	2	12,500	2,000
4	G.E.	Detroit Edison, Connor's Creek	1918	45,000	35,000	1,200	—	—	1·0	1	1	1	35,000	5,600
5	G.E.	Commonwealth, N.W., Chicago	1918	35,000	25,000	1,500	—	—	1·0	1	1	1	25,000	6,250
6	G.E.	Commonwealth, Fisk Street, Chicago	1918	30,000	22,500	1,800	—	—	1·0	1	1	1	22,500	8,100
7	A.E.G.	Rheinische Westfälische Kraftwerke, Cologne	1919	50,000	40,000	1,000	—	—	2·0	1	1	1	40,000	—
8	C.A.P.	Mersey Power Co.	1921	12,500	10,000	3,000	265	650	1·0	1	2	2	5,000	5,000
9	C.A.P.	Lots Road, London	1924	18,000	15,000	2,000	290	650	1·0	1	1	1	15,000	6,670
10	C.A.P.	Brimsdown B., London	1926	25,000	20,000	3,000	305	700	1·0	1	2	3	6,670	6,670
11	M.A.N.	Hamburg	1928	36,000	27,000	3,000	512	770	1·14	1	3	3	9,000	8,000
12	A.E.G.	Zschornewitz	1929	85,000	70,000	1,500	207	680	1·8	1	2	2	35,000	5,200
13	Al.	Comines	1929	30,000	24,000	3,000	270	725	1·17	1	3	2	12,000	10,400
14	G.E.	Philo, Ohio Power Co.	1929	165,000	132,000	1,800	615	725	1·0	3	3	2	66,000	—
15	C.A.P.	Dunston	1930	50,000	40,000	1,500	615	800	1·0	1	2	1	40,000	10,000
16	M.V.	Victoria Falls, South Africa	1930	32,500	30,000	3,000	215	625	1·8	1	2	2·5	—	—
17	F. & C.	Battersea, London	1930	30,000	24,000	3,000	315	750	1·0	1	2	2	12,000	12,000
18	A.C.O.	St. Denis, Paris	1931	50,000	40,000	3,000	995	932	0·926	1	4	4	10,000	10,700
19	Al.	St. Denis, Paris	1931	50,000	40,000	3,000	797	842	0·926	1	3	3	13,333	14,300
20	C.A.P.	Hackney, London	1931	30,000	24,000	3,000	365	750	1·3	1	2	2	12,000	9,500
21	B.T.H.	Barking, London	1931	75,000	60,000	1,500	615	800	1·0	1	3	2	30,000	7,500
22	M.V.	Battersea A., London	1936	105,000	84,000	1,500	615	850	0·9	1	3	2	42,000	11,570
23	E.E.	Ferrybridge, Yorks	1938	40,000	32,000	3,000	615	850	1·2	1	2	2	16,000	13,600

TABLE XXXIVB

PARTICULARS OF FINAL STAGE OF TURBINES OF LARGE POWER

Note. The stress in a parallel blade has been calculated for steel blades by means of the formula: $f_c = 0{\cdot}215\ mu^2$ lb. per sq. in. The real stress in many cases is appreciably less than the value given, due to the use of tapered blades.

Ref. No. Table XXXIVA	Diameter, inches		Useful Blade Length in	$m = \frac{l}{D}$	u ft. per sec.		Leaving Area per Exhaust sq. ft.	f_c Parallel Blade tons per sq. in.
	Mean	Tip			Mean	Tip		
1	105	124	19	0·181	344	406	43·6	2·05
2	89·5	104	14·5	0·162	391	455	28·3	2·38
3	98	116	18	0·184	514	608	38·4	4·65
4	140	174	34	0·243	734	912	104	12·53
5	120	148	28	0·234	787	970	73·3	13·90
6	100	124	24	0·24	787	975	52·3	14·25
7	134	154	20	0·149	585	674	58·5	4·89
8	47·5	57	9·5	0·2	622	747	9·85	7·43
9	80	100	20	0·25	698	873	34·9	11·67
10	54·27	68·54	14·27	0·263	711	899	16·85	12·73
11	66·93	80·95	14·02	0·210	875	1,060	20·45	15·40
12	114·2	137·82	23·62	0·207	748	900	58·9	11·10
13	61	75·82	14·82	0·243	798	992	19·7	14·82
14	110	145	35	0·318	865	1,140	84·0	22·80
16	47·125	61·25	14·125	0·300	617	800	14·5	10·97
17	60	76·5	16·5	0·275	735	1,000	21·6	16·25
18	61·5	75·5	14·0	0·228	805	990	18·8	14·18
19	64·96	79·51	14·55	0·224	852	1,040	20·6	15·60
20	59·25	73·5	14·25	0·241	775	960	18·4	13·87

where kW_1 = reduced output per exhaust
kW = actual output per exhaust
p = exhaust pressure, in. Hg. abs.
H_{a1} = adiabatic heat drop to 1 in. Hg.
H_a = adiabatic heat drop to actual exhaust pressure
N = actual speed, r.p.m.

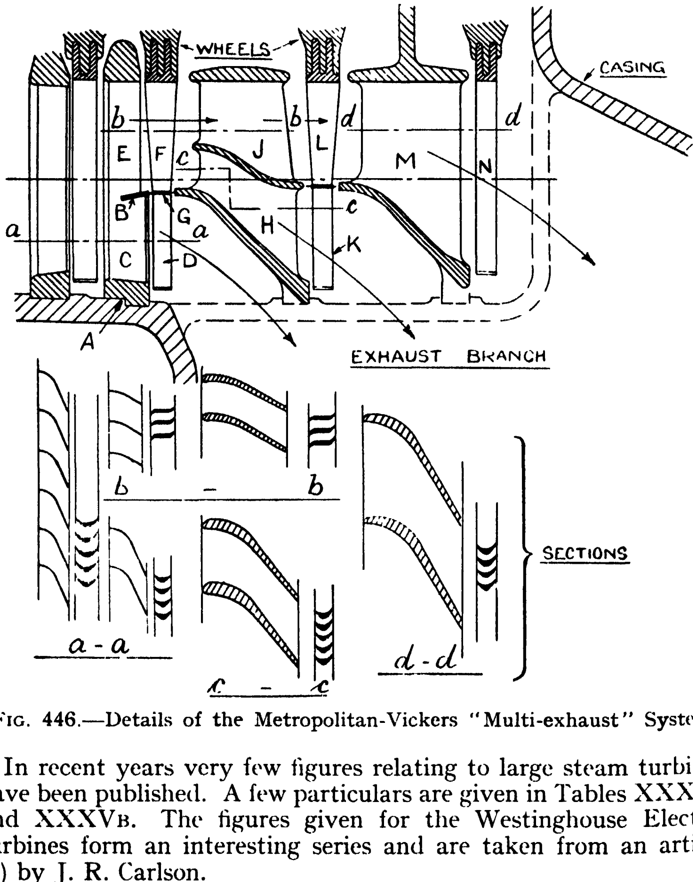


FIG. 446.—Details of the Metropolitan-Vickers "Multi-exhaust" System

In recent years very few figures relating to large steam turbines have been published. A few particulars are given in Tables XXXVA and XXXVB. The figures given for the Westinghouse Electric turbines form an interesting series and are taken from an article (3) by J. R. Carlson.

292. The Baumann Multi-exhaust Turbine. A very ingenious method of providing a greater area at the exhaust end of steam turbines was devised some years ago by Mr. K. Baumann of the Metropolitan-Vickers Electrical Co., Ltd. The principle of the system will be explained with reference to Fig. 446, showing a part section of the last few wheels at the exhaust end of the turbine.

TABLE XXXVA

PARTICULARS OF SOME RECENT LARGE STEAM TURBINES

Note. When two steam temperatures are given, the second temperature is the reheat temperature.

Ref. No.	Firm	Year	Output MW.	Speed r p m.	Operating Conditions			No. of Exhausts	MW. per Exhaust
					p_s	t_s	Vacuum In. Hg.		
1	Westinghouse Electric Corporation, U S A	1925	7·5	3,600	300	600		1	7·5
2	,, ,,	1928	12·5	3,600	400	750		1	12·5
3	,, ,,	1935	33	3,600	850	900		1	33·0
4	,, ,,	1940	80	3,600	1,250	950		2	40·0
5	,, ,,	1945	110	3,600	1,450	1,000		2	55·0
6	,, ,,	1950	150	3,600	1,800	1,000 / 1,000		3	50·0
7	,,	1951	200	3,600	2,400	1,100 / 1,050		3	67·0
8	General Electric Co. of England	—	60	3,000	900	900	28·7	2	30·0
9	,, ,, ,,	—	200	3,000	2,365	1,050 / 1,000	28·7	3	66·7
10	Metropolitan-Vickers	1954	60	3,000	900	900	28·9	2	30·0
11	Richardsons Westgarth Brown Boveri	1954	60	3,000	1,350	950	29·1	4	15·0

TABLE XXXVB

PARTICULARS OF FINAL STAGE OF TURBINES OF LARGE POWER

See note at head of Table XXXIVB

Ref No Table XXXVA	Diameter, in		Useful Blade Length	$m = \frac{l}{D}$	Blade Velocity, ft /sec.		Leaving Area per Exhaust	kW per sq ft	f_c Parallel Blade
	Mean	Tip	in		Mean	Tip	sq ft		tons per sq in.
1	46	58	12	0 261	723	911	12·1	620	13·1
2	56	73	17	0 304	880	1,147	20·8	600	22·5
3	60	80	20	0 333	943	1,258	26·2	1,260	28·4
4	60	80	20	0 333	943	1,258	26·2	1,526	28·4
5	65	88	23	0·353	1,021	1,382	32·6	1,690	35·5
6	65	88	23	0·353	1,021	1,382	32·6	1,536	35·5
7	75	100	25	0 333	1,179	1,571	40·9	1,640	44·4
8	75	95	20	0·267	983	1,245	32·7	917	24·7
9	90	120	30	0 333	1,180	1,570	59·0	1,130	44·5
10	75	96·5	21 5	0·287	983	1,264	35·2	1,130	26·6
11	63·05	78·80	15·75	0·25	826	1,031	21 7	691	16·3

Steam expands in passing through the earlier stages of the turbine until it reaches the special diaphragm A, where a circular division ring B splits up the steam into two portions. The vanes C of the diaphragm A are normal in shape, forming convergent nozzles which expand the steam down to condenser pressure. The portion of the steam flowing through C passes through the outer parts of the blades

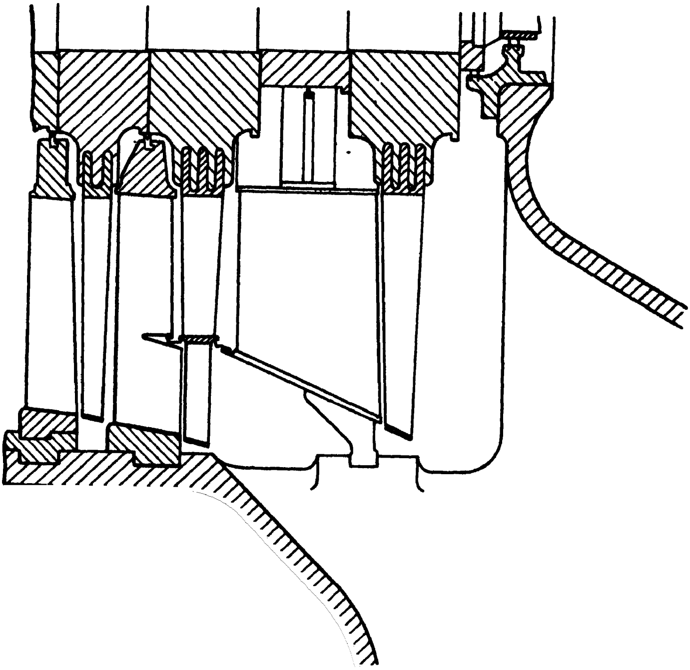


FIG. 447. Metropolitan-Vickers Multi-exhaust Blading

(which are shaped as ordinary impulse blades) and then flows into the condenser.

The vanes E of the diaphragm A have a large outlet angle and allow the steam to flow through with only a small drop of pressure and a relatively small increase in velocity. The part F of the blade, lying between the dividing ring G and the disc, is designed for a small amount of reaction, the steam undergoing a certain drop in pressure and an increase in velocity. The steam issuing from the blades F is now divided in the succeeding diaphragm in the same way. One part is expanded to condenser pressure in H and does work on the blades K. The other part passes through J and L into the diaphragm M with only a small drop in pressure and, in doing so, does a small amount of work on the inner part L of the blades. On

reaching the diaphragm M, this steam is expanded down to condenser pressure and does work on the impulse blades N.

The leaving area may be increased by the following amounts by this construction—

No. of Additional Rows of Exhaust Blades	Percentage Increase in Leaving Area
1	60
2	120
3	170

Owing to the special shape of the blade root, the power increase is greater than the increase in leaving area, and it is claimed that with three additional rows of blades the power may be increased four times for the same speed and factor of safety. In recent years the application of the Baumann multi-exhaust system appears to have been restricted to the use of one extra row of blades, which, when employed in a double-flow turbine, gives about three times the leaving area of a single-flow turbine of normal design. Fig. 447 shows a part section of a low-pressure steam turbine with the multi-exhaust system as at present employed. The action may be followed from the foregoing description.

BIBLIOGRAPHY

1. BAUMANN, K. "Some Recent Developments in Large Steam Turbine Practice." *Journal I.E.E.*, 1921; 59; 565.
2. BAUMANN, K. "Neuere grosse Dampfturbinen." Paper read at World Power Conference. *Z.V.d.I.*, 1930; 74; 805.
3. CARLSON, J. R. "Another Step in Turbine Blade Evolution." *Westinghouse Engineer*, May 1952, p. 96.

EXAMPLES XXVII

1. Calculate the required K value for a multi-stage impulse turbine under the following conditions: Cumulative heat drop = 465 B.Th.U. per lb.; nozzle angle = 18°; $\rho = 0{\cdot}5$; $C = 1$; $\eta_n = 0{\cdot}92$; $\phi = 0{\cdot}9$; and $k = 0{\cdot}85$.

If the speed of rotation is 3,000 r.p.m. and the mean blade velocity is to be 600 ft. per sec., calculate the number of single-row stages required if the mean diameter is uniform throughout the turbine.

2. The leading dimensions of a 30,000 kW steam turbine are as follows—

Stage No.	Mean Dia. in.	Stage No.	Mean Dia. in.
1	66·5	8	81·5
2	62·0	9	86·0
3	64·0	10	90·0
4	66·5	11	95·0
5	70·0	12	102·0
6	74·0	13	109·0
7	77·5	14	118·0

The first stage is a two-row wheel, the remainder single-row wheels.

Calculate the K value and the efficiency factor, given the following data—

Initial steam pressure	200 lb. per sq. in. abs.
Initial steam temperature	640° F.
Exhaust pressure	0·7 lb. per sq. in. abs.
Reheat factor	1·05
R.p.m.	1,500

Hence calculate the ratio of blade speed to steam speed in the single-row stages, assuming that it is uniform in those stages and has one-half of this value in the two-row stage. Assume that F_1 is unity.

3. Compare the relative rotative speeds of the following steam turbines when using steam having the same initial and final pressures. The speed of the de Laval turbine may be taken as 25,000 r.p.m.

(*a*) De Laval turbine, 6 in. mean diameter.

(*b*) Velocity-compounded turbine having four two-row wheels, 42 in. mean diameter.

(*c*) Pressure-compounded impulse turbine having 25 wheels, 30 in. mean diameter.

Neglect the effects of carry-over energy from stage to stage.

4. A set of turbines is to be designed for a net s.h.p. of 3,130. The final specific volume of the steam is 239 cub. ft. per lb., the adiabatic heat drop is 325 B.Th.U. per lb., the efficiency ratio is 0·7, the blade velocity 400 ft. per sec., and the blade speed ratio 0·4. Assume that the vane angle in the last-stage diaphragm is 28°, a thickness coefficient of 0·89, and a nozzle height 17 per cent of the mean diameter. Calculate—

(*a*) The mean diameter of the last-stage nozzles.

(*b*) The revolutions per minute.

5. A marine steam turbine is required to develop 3,600 s.h.p. with steam at 200 lb. per sq. in. abs. and 600° F. and an exhaust pressure of 1·0 lb. per sq. in. abs. The efficiency ratio of the turbine is 73 per cent and the carry-over loss is to be limited to 1·5 per cent of the adiabatic heat drop. The length of the blades in the last stage is limited to 0·2 of the mean diameter in that stage. Calculate the required mean diameter of the final L.P. stage and the speed of the L.P. turbine if the mean blade velocity is limited to 450 ft. per sec.

6. A steam turbine is to operate with steam at 400 lb. per sq. in. abs. and at 700° F., and with an exhaust pressure of 0·5 lb. per sq. in. abs. The actual enthalpy of the exhaust steam is estimated to be 981 B.Th.U. per lb., after allowing for internal losses. Steam is bled off at 40 lb. per sq. in. abs., and from the dimensions of the feed heater it is estimated that the feed temperature at outlet from the heater will be 260° F. and that the temperature of the condensed heating steam (which enters the steam space of the condenser) will be 90° F. The main condensate temperature may be taken as 79·5° F.

Calculate the required height of the last-stage nozzles if the output of the turbine is to be 3,000 kW at 3,000 r.p.m. Assume that $u = 600$ ft. per sec., $\rho = 0{\cdot}48$, $\alpha = 28°$ $(c = 0{\cdot}877)$, and that the condition curve on the $\phi - I$ diagram may be taken as a straight line.

7. Steam is supplied to an impulse turbine at 600 lb. per sq. in. abs. and at 800° F. It is first expanded to 100 lb. per sq. in., the internal efficiency ratio being 82 per cent. It is then reheated at this pressure to 600° F., after which it is expanded to 0·5 lb. per sq. in. abs., the internal efficiency ratio during the latter expansion also being 82 per cent. If $m = 0{\cdot}18$, $\alpha = 30°$ $(c = 0{\cdot}884)$,

$\rho = 0{\cdot}48$, and N = 3,000 r.p.m., show that the maximum output cannot exceed

$$\text{kW} = 17{\cdot}7\left(\frac{u}{100}\right)^3$$

where u is the mean peripheral velocity in the last stage. What is the limiting output of a turbine operating under such conditions when there are three exhausts and u = 700 ft. per sec.?

8. A number of steam turbines have to be built to operate with steam at 400 lb. per sq. in. abs. and at 700° F., the exhaust pressure being 1·0 lb. per sq. in. abs. The energy loss due to the residual velocity of flow into the exhaust belt is not to exceed 2 per cent of the adiabatic heat drop, and the length of the last row of blades is not to exceed 20 per cent of the mean diameter of the blades. If the efficiency ratio of the turbines is 78 per cent, show that the mean diameter of the last ring of blades must not be less than

$$\text{D (inches)} = 0{\cdot}461\sqrt{\text{HP}}$$

where HP represents the horse-power of any turbine in question. Assume that the internal efficiency ratio is equal to the efficiency ratio.

9. Using the data given in Question 8, show that the maximum power HP that can be developed for a given centrifugal stress f_c at the root of the blade in the last stage, at a speed N r.p.m., is—

$$\text{HP} = \frac{5{,}740{,}000\, f_c}{\text{N}^2}$$

Assume that the blades have a uniform section and are of steel.

Hence find the limit in power for a speed of 3,000 r.p.m. and a stress of 16,000 lb. per sq. in.

10. The following particulars relate to a steam turbine which is required to develop 104,000 kW. internal power. actual internal work done per lb. of steam entering turbine = 440 B.Th.U.; total steam extracted for feed-heating = 0·28 lb. per lb. of steam entering turbine; number of similar exhausts = 3; speed = 3,000 r.p.m.; exhaust pressure = 0·55 lb. per sq. in abs.; dryness fraction of exhaust steam = 0·88; allowable carry-over loss = 2·5 per cent; ratio m_1 = 0·32 for last stage.

Calculate the following—

(*a*) Steam flow through each exhaust, lb. per sec
(*b*) Axial steam velocity at outlet from last stage.
(*c*) Required mean diameter of last stage wheels.
(*d*) Blade length in last stage.
(*e*) Tip speed of last stage blades.

CHAPTER XXVIII

THE LJUNGSTRÖM TURBINE

293. Theory of the Ljungström Turbine. The elementary features of the Ljungström turbine have already been outlined in Chapter I. It is essentially an outward-radial-flow turbine in which there are two rotors turning in opposite directions. It operates on the impulse-reaction (so-called "reaction") principle, with half-degree

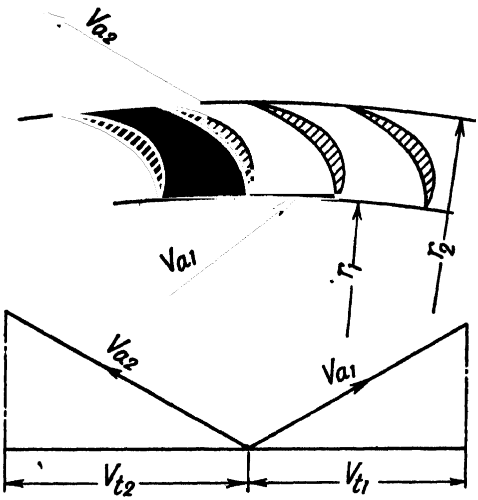


FIG 448

reaction. In turbines of large output, the required outlet area at the low-pressure end is obtained by the use of one or two axial-flow stages. Details of this and other constructional features will be given later in this chapter.

We shall first derive an expression for the work done in a radial-flow turbine. Suppose that the peripheral velocities at the inlet and outlet of a single ring of blades (see Fig. 448) are u_1 and u_2, and that the absolute steam velocities are V_{a1} and V_{a2}. Let V_{t1} and V_{t2} be the tangential components of these velocities, and assume that the steam flow through the blade ring is w lb. per sec. Then since the torque is equal to the change of moment of momentum per second—

$$\text{Torque T} = \frac{w}{g}\,(\text{V}_{t2}\,.\,r_2 - \text{V}_{t1}\,.\,r_1)$$

where correct account is taken of the signs of V_{t1} and V_{t2}. For instance, in Fig. 448, if V_{t2} is taken as positive, V_{t1} must be taken as negative.

$$\text{Work done per sec.} = \omega T$$

$$= \frac{w}{g}(u_2 . V_{t2} - u_1 V_{t1})$$

and the work done per lb. of steam

$$W = \frac{1}{g}(u_2 V_{t2} - u_1 V_{t1}) \text{ ft.-lb.}$$

$$W = \frac{1}{gJ}(u_2 V_{t2} - u_1 V_{t1}) \text{ B.Th.U.} \quad . \quad . \quad (263)$$

The upper part of Fig. 449 shows a part longitudinal section and a part transverse section through four rows of blades. It will be assumed in the following analysis that—

(1) All the blades, except those in the innermost ring, have the same cross-section and that they are all set similarly in the rotors. They have, therefore, all the same outlet angle.

(2) In all rings of blades, the ratio of the relative steam velocity at outlet to the peripheral velocity at the outlet edge of the blade ring is constant, i.e. that $\rho = \frac{u}{V}$ is a constant.

Giving all dimensions in foot units—

Let r_0 = inner radius of first ring.
r_1, r_2, r_3, etc., be the outer radii of rings 1, 2, 3, etc., respectively
u_1, u_2, u_3, etc., be the peripheral velocities at the *outer* edge of the rings 1, 2, 3, etc., respectively.

Consider first of all the flow of steam through the first ring of blades. Steam will flow into that ring with a velocity V_0 (AB) which may be assumed to be radial and to be given by the expression

$$V_0 = \frac{w . v_0}{2\pi r_0 . l_0}$$

where l_0 = axial length of blades at r_0
v_0 = specific volume of steam at blade inlet.

This is combined with the peripheral velocity u_0 (AC), giving the relative velocity U_0 (CB) and the inlet angle BCA of the first ring of blades. The steam issues from the first ring of blades with a velocity V_1 (DE) relative to the blades, the absolute velocity being AE. The tangential component of the absolute velocity at outlet is

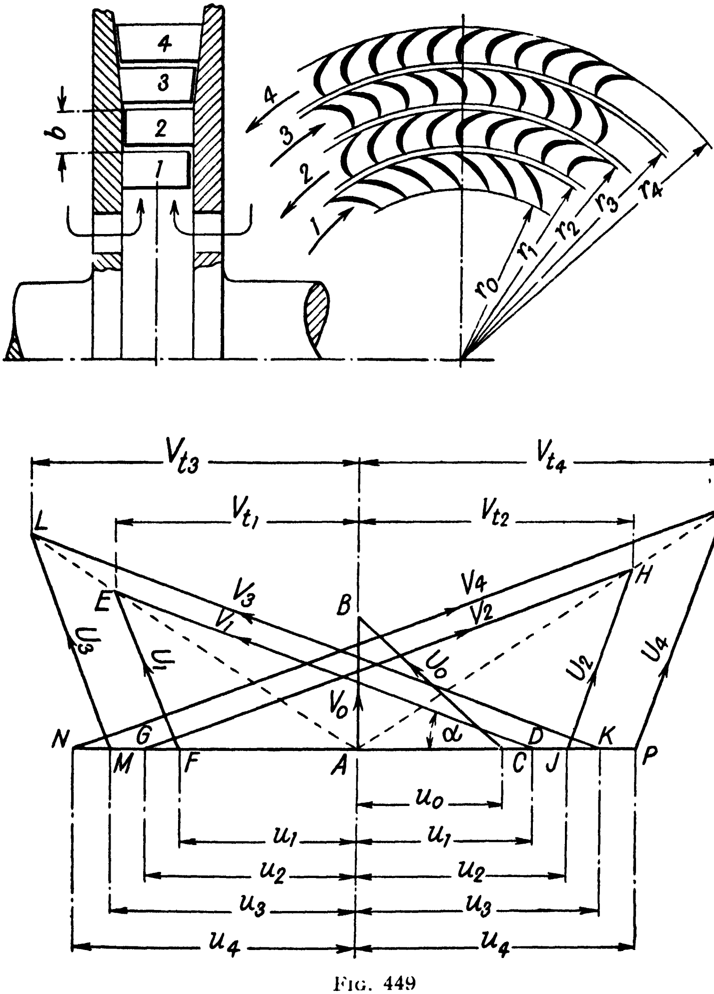

4
3
2
1
b
r_0
r_1
r_2
r_3
r_4
V_{t3}
V_{t4}
V_{t1}
V_{t2}
L
O
E
H
B
V_3
V_1
V_4
V_2
U_3
U_1
U_0
U_2
U_4
V_0
α
N
G
M
F
A
C
D
J
K
P
u_0
u_1
u_2
u_3
u_4

FIG. 449

V_{t1}, and since the initial absolute velocity is radial, the work done in the innermost blade ring per lb. of steam is

$$W_1 = \frac{u_1 V_{t1}}{gJ} \text{ B.Th.U.}$$
$$= \frac{1}{gJ}(u_1 V_1 \cos\alpha - u_1^2)$$

By the steady-flow equation (37), and assuming no loss of heat from the stage—

$$\text{Work done} = \text{Initial kinetic energy} + (I_0 - I_1) - \text{Final kinetic energy}$$
$$= \frac{V_0^2}{2gJ} + (I_0 - I_1) - \frac{AE^2}{2gJ}$$
$$= \frac{V_0^2}{2gJ} - \frac{V_1^2 + u_1^2 - 2u_1V_1\cos\alpha}{2gJ} + I_0 - I_1$$

Equating these two expressions for the work done, we have

$$I_0 - I_1 = \frac{1}{2gJ}(V_1^2 - V_0^2 - u_1^2)$$
$$= \frac{1}{2gJ}\{V_1^2 - U_0^2 - (u_1^2 - u_0^2)\} \quad . \quad . \quad (264)$$

If the flow is frictionless, then $I_0 - I_1$ is the required adiabatic heat drop. If not, then the adiabatic heat drop

$$h_1 = \frac{1}{2gJ \cdot \eta_n}\{V_1^2 - k^2U_0^2 - (u_1^2 - u_0^2)\} \quad . \quad (265)$$

where η_n is the efficiency of the blades considered as nozzles (see Art. 89) and k has the same meaning as the blade velocity coefficient in impulse turbines.

Consider now the expansion of steam in the second ring of blades. The relative velocity at inlet is U_1 (FE) at r_1, and at outlet is V_2 (GH). The tangential components of the absolute velocities at inlet and outlet are, respectively, V_{t1} and V_{t2}. Hence the work done per lb. of steam is numerically equal to

$$\frac{1}{gJ}(u_2V_{t2} + u_1V_{t1})$$

since V_{t1} and V_{t2} are of opposite sign.

$$\therefore \quad \text{Work done} = \frac{1}{gJ}(u_2V_2\cos\alpha - u_2^2 + u_1V_1\cos\alpha - u_1^2)$$

Then, by the steady-flow equation—

I_1 + (Initial kinetic energy referred to absolute velocity) = (Work done) + I_2 + (Final kinetic energy referred to absolute velocity).

$$\therefore \qquad I_1 - I_2 = (\text{Work done}) + \frac{(AH)^2}{2gJ} - \frac{(AE)^2}{2gJ}$$

$$I_1 - I_2 = \frac{1}{gJ}(u_2V_2 \cos\alpha - u_2^2 + u_1V_1\cos\alpha - u_1^2)$$

$$+ \frac{1}{2gJ}(V_2^2 + u_2^2 - 2u_2V_2\cos\alpha)$$

$$- \frac{1}{2gJ}(V_1^2 + u_1^2 - 2u_1V_1\cos\alpha)$$

$$I_1 - I_2 = \frac{1}{2gJ}(4u_1V_1\cos\alpha - u_2^2 - 3u_1^2 + V_2^2 - V_1^2)$$

But
$$V_1^2 = U_1^2 - 4u_1^2 + 4u_1V_1\cos\alpha$$

$$\therefore \qquad I_1 - I_2 = \frac{1}{2gJ}\{V_2^2 - U_1^2 - (u_2^2 - u_1^2)\}. \qquad . \quad (266)$$

If the flow is frictionless, then $I_1 - I_2$ represents the *adiabatic* heat drop in the blades of the second row. If the flow is not frictionless, then the adiabatic heat drop is

$$h_2 = \frac{1}{2gJ\eta_n}\{V_2^2 - k^2U_1^2 - (u_2^2 - u_1^2)\}. \qquad . \quad (267)$$

The term $\frac{u_2^2 - u_1^2}{2gJ}$ in the above equation represents a reduction in the value of $I_1 - I_2$ due to the forced vortex action in the blade ring.

Writing down the adiabatic heat drops in the several rings of blades, we have

$$h_1 = \frac{1}{2gJ\eta_n}\{V_1^2 - k^2U_0^2 - (u_1^2 - u_0^2)\}$$

$$h_2 = \frac{1}{2gJ\eta_n}\{V_2^2 - k^2U_1^2 - (u_2^2 - u_1^2)\}$$

$$h_3 = \frac{1}{2gJ\eta_n}\{V_3^2 - k^2U_2^2 - (u_3^2 - u_2^2)\}$$

$$h_{n-1} = \frac{1}{2gJ\eta_n}\{V^2_{n-1} - k^2U^2_{n-2} - (u^2_{n-1} - u^2_{n-2})\}$$

$$h_n = \frac{1}{2gJ\eta_n}\{V_n^2 - k^2U^2_{n-1} - (u^2_n - u^2_{n-1})\}$$

If it be assumed that the velocity coefficient k and the efficiency η_n remain constant throughout, then the sum of the adiabatic heat drops for all the stages considered is

$$\Sigma h = \frac{1}{2gJ\eta_n}\{(V_1^2 + V_2^2 + \ldots V_n^2) - k^2(U_0^2 + U_1^2 + \ldots U^2_{n-1}) - (u^2_n - u_0^2)\}$$

Considering the velocities U_1, U_2, U_3, etc., we may write—

$$U_1^2 = V_1^2 + 4u_1^2 - 4u_1V_1 \cos \alpha$$
$$U_2^2 = V_2^2 + 4u_2^2 - 4u_2V_2 \cos \alpha, \text{ etc.}$$

Furthermore, with negligible error, we may write for the numerical value of U_0^2—

$$U_0^2 = V_0'^2 + 4u_0^2 - 4u_0V_0' \cos \alpha$$

where V_0' is a fictitious velocity, such that

$$\frac{u_0}{V_0'} = \rho$$

Substituting the above values of U_0^2, U_1^2, etc., in the above expression for Σh, we have

$$\Sigma h = \frac{1}{2gJ\eta_n}\{(V_1^2 + V_2^2 + \ldots V_n^2) - k^2(1 + 4\rho^2 - 4\rho \cos \alpha)(V_0'^2 + V_1^2 + \ldots V^2_{n-1}) - \rho^2(V_n^2 - V_0'^2)\}$$

But

$$V_0' = \frac{u_0}{\rho} = \frac{\omega r_0}{\rho}$$

$$V_1 = \frac{u_1}{\rho} = \frac{\omega r_1}{\rho}$$

$$V_n = \frac{u_n}{\rho} = \frac{\omega r_n}{\rho}$$

$$\therefore \quad \Sigma h = \frac{\omega^2}{2gJ\eta_n\rho^2}\{(r_1^2 + r_2^2 + \ldots r_n^2) - k^2(1 + 4\rho^2 - 4\rho \cos \alpha)(r_0^2 + r_1^2 + \ldots r^2_{n-1}) - \rho^2(r_n^2 - r_0^2)\}$$

Suppose that in any group of blade rings to which these relations may be applied, the radial depth of the blades, plus the small radial clearance between adjacent blade rings, is a constant dimension b

Then $r_1 = r_0 + b$; $r_2 = r_0 + 2b$; $\ldots r_{n-1} = r_0 + (n-1)b$, and $r_n = r_0 + nb$

$r_1^2 = r_0^2 + 2br_0 + b^2$; . . . $r^2_{n-1} = r_0^2 + 2(n-1)b \cdot r_0 + (n-1)^2b^2$; and $r_n^2 = r_0^2 + 2nbr_0 + n^2b^2$.

The sum of the series $r_1^2 + r_2^2 + \ldots r_n^2$ is

$$nr_0^2 + n(n+1)br_0 + n(n+1)(2n+1)\frac{b^2}{6}$$

and of the series $r_0^2 + r_1^2 + \ldots r^2_{n-1}$ is—

$$nr_0^2 + n(n-1)br_0 + n(n-1)(2n-1)\frac{b^2}{6}$$

$$\therefore \qquad \Sigma h = \frac{\omega^2}{2gJ \cdot \eta_n \cdot \rho^2}\left\{\left[nr_0^2 + n(n+1)b \cdot r_0 + \frac{n(n+1)(2n+1)b^2}{6}\right] - k^2(1 + 4\rho^2 - 4\rho\cos\alpha)\left[nr_0^2 + n(n-1)br_0 + \frac{n(n-1)(2n-1)b^2}{6}\right] - \rho^2(2nbr_0 + n^2b^2)\right\} \quad . \quad . \quad . \quad (268)$$

This expression will give the sum of the adiabatic heat drops in a group of n rings in which the innermost radius is r_0 ft. and the outermost radius r_n ft. The dimensions b must also be given in foot units. If inch units are preferred, then the whole expression must be divided by 144.

294. Optimum Ratio of Blade Speed to Steam Speed. In order to determine this, consider the adiabatic heat drop in any given blade ring, e.g. ring 3, Fig. 449. Then—

$$h_3 = \frac{1}{2gJ\eta_n}\{V_3^2 - k^2U_2^2 - (u_3^2 - u_2^2)\}$$

In general, the ratio $\frac{b}{r}$ is about 0·03 to 0·04; hence the difference between u_3 and u_2 is small compared with either of them and we may, allowing a small error for the sake of simplicity, neglect the term $u_3^2 - u_2^2$ in the above expression.

$$\therefore \qquad h_3 \doteqdot \frac{1}{2gJ\eta_n}\{V_3^2 - k^2(V_2^2 + 4u_2^2 - 4u_2V_2\cos\alpha)\}$$

By the same approximation, V_3 may be written as V_2. Then—

$$h_3 = \frac{V_2^2}{2gJ\eta_n}\{1 - k^2(1 + 4\rho^2 - 4\rho\cos\alpha)\}$$

The work done per lb. of steam in the third ring of blades is

$$W_3 = \frac{1}{gJ}(u_3V_{t3} - u_2V_{t2})$$

$$= \frac{u_2}{gJ}(V_{t3} - V_{t2}) \text{ approximately}$$

$$= \frac{2u_2}{gJ}(V_2 \cos \alpha - u_2)$$

$$= \frac{2V_2^2}{gJ}(\rho \cos \alpha - \rho^2)$$

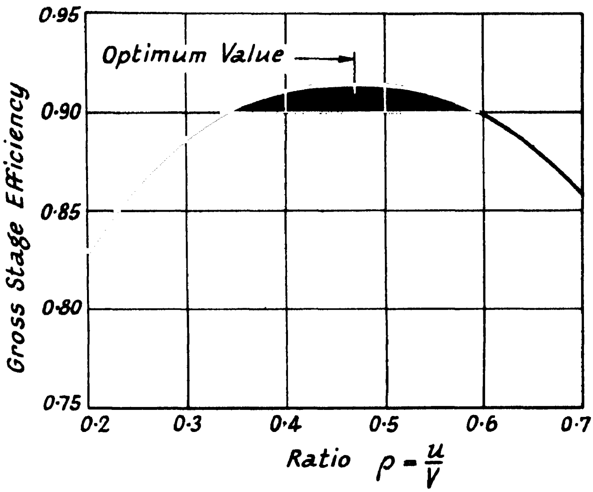


FIG 450—Calculated Stage Efficiency of Ljungstrom Type of Steam Turbine

The gross stage efficiency (neglecting leakage and any rotation losses) is equal to

$$\eta_{gs} = \frac{W_3}{L}$$

$$\eta_{gs} = \frac{4\eta_n(\rho \cos \alpha - \rho^2)}{1 - k^2(1 + 4\rho^2 - 4\rho \cos \alpha)} \quad . \quad . \quad (269)$$

If we assume constant values for the coefficients $\eta_n = 0{\cdot}938$ and $k = 0{\cdot}9$, which, it must be stated, are merely assumptions guided by nozzle and blade experiments, then for a uniform blade outlet angle of 20°, the estimated values of the gross stage efficiency are given in Table XXXVI and Fig. 450. Inspection of eq. (269) and of Fig. 450 shows that the gross stage efficiency is a maximum when

$\rho = \frac{\cos \alpha}{2} = 0{\cdot}47$ for 20° blades. It should be noted that if the blade speed ratio is taken to mean the ratio of the *relative* blade velocity to the steam velocity at exit from the blades, then since the relative velocity of the blades is twice the blade velocity in each ring, the most economical ratio of blade speed to steam speed is $\cos \alpha$, or about 0·94 for 20° blades, just as in the Parsons turbine.

TABLE XXXVI

ESTIMATED GROSS STAGE EFFICIENCIES AND VALUES OF THE EFFICIENCY FACTOR FOR LJUNGSTRÖM DOUBLE-MOTION TURBINE

Basic Data: Blade outlet angle = 20°; $\eta_n = 0{\cdot}938$; $k = 0{\cdot}9$.

ρ	Gross Stage Efficiency	Values of $f_3(\rho)$			$\frac{K}{H_e}$ when $\frac{b}{r} = 0{\cdot}04$
		$\frac{b}{r} = 0{\cdot}03$	$\frac{b}{r} = 0{\cdot}04$	$\frac{b}{r} = 0{\cdot}05$	
0·1	0·682	0·526	0·537	0·547	48
0·2	0·829	0 732	0·738	0·744	142
0·25	0·864	0·810	0·814	0·818	201
0·3	0·887	0·872	0·874	0·876	270
0·35	0·902	0·917	0·917	0·917	350
0·4	0·911	0·945	0·944	0·943	444
0·45	0·915	0 957	0·955	0·953	556
0·5	0·914	0·952	0·949	0·946	690
0·55	0·909	0·931	0·927	0·923	855
0·6	0·899	0·893	0·889	0·886	1,061
0·65	0·883	0·839	0·834	0·830	1,327
0·7	0·858	0 768	0·763	0·759	1,682

EXAMPLE 49. The following particulars refer to the inner group of blading in a Ljungström turbine—

Inner diameter of first blade ring	4 in.
Dimension b (Fig. 449)	$\frac{1}{4}$ in.
Number of rings of blades on each rotor . . .	10
Blade outlet angle	20°
R.p.m. of each rotor	3,000

Assuming that $\rho = 0{\cdot}4$, $\eta_n = 0{\cdot}9$, and that $k = 0{\cdot}87$, calculate the total adiabatic heat drop in the group of blades.

$$\omega = \frac{3{,}000 \times 2\pi}{60} = 100\pi. \quad n = 20$$

$$r_0 = 2 \text{ in.} = \tfrac{1}{6} \text{ ft.} \quad b = \tfrac{1}{4} \text{ in.} = \tfrac{1}{48} \text{ ft.}$$

Substituting the given data in eq. (268)—

$$\Sigma h = 13{\cdot}68\,(3{\cdot}261 - 0{\cdot}312 - 0{\cdot}050)$$
$$= 39{\cdot}7 \text{ B.Th.U per lb. of steam}$$

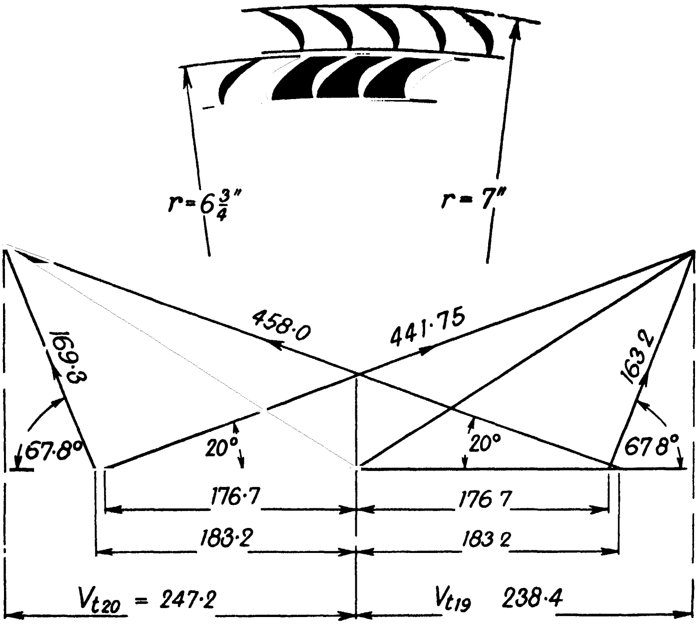


FIG 451 —Illustrating Example 50

EXAMPLE 50. Calculate for the outermost ring in the blade group mentioned in Example 49 the following—

(*a*) Blade inlet angle,
(*b*) Velocities of whirl;
(*c*) Torque applied by blades to the disc;
(*d*) Work done per lb. of steam,
(*e*) Adiabatic heat drop in ring,
(*f*) Gross stage efficiency,
(*g*) Power developed in blade ring.

The steam flow per second is 20 lb

A simple calculation shows that the external radius of the 19th ring is 6¾ in. and of the 20th ring 7 in.

$\therefore$ Peripheral velocity of 19th ring = 176·7 ft./sec.

" 20th " = 183·2 "

$$V_{19} = \frac{176{\cdot}7}{0{\cdot}4} = 441{\cdot}75; \quad V_{20} = \frac{183{\cdot}2}{0{\cdot}4} = 458{\cdot}0$$

The velocity diagrams for the 19th and 20th blade rings are shown in Fig. 451 and require no explanation. The blade inlet angle is 67·8°. The velocities of whirl are respectively 238·4 and 247·2 ft. per sec.

$$\text{Torque} = \frac{w}{g}(V_{t20} \cdot r_{20} - V_{t19} \cdot r_{19})$$

$$= \frac{20}{32{\cdot}2}\left\{\left(247{\cdot}2 \times \frac{7}{12}\right) + \left(238{\cdot}4 \times \frac{6{\cdot}75}{12}\right)\right\}$$

$$= 172{\cdot}8 \text{ lb.-ft.}$$

$$\text{Work done per sec.} = \omega \times \text{Torque}$$

$$= 100\pi \times 172{\cdot}8 = 54{,}290 \text{ ft.-lb}$$

$\therefore$ Work done per lb. of steam = 2,714·5 ft.-lb.

= 3·49 B.Th.U.

Adiabatic heat drop in blade ring

$$= \frac{1}{2gJ \cdot \eta_n}\{V_{20}^2 - k^2 \cdot U_{19}^2 - (u_{20}^2 - u_{19}^2)\}$$

$$= \{458^2 - (0{\cdot}87 \times 163{\cdot}2)^2 - (183{\cdot}2^2 - 176{\cdot}7^2)\}$$

$$\div (64{\cdot}4 \times 777{\cdot}8 \times 0{\cdot}9) = 4{\cdot}156 \text{ B.Th.U. per lb.}$$

$$\therefore \quad \text{Gross stage efficiency} = \frac{3{\cdot}49}{4{\cdot}156} = 84 \text{ per cent}$$

$$\text{Power developed} = \frac{54{,}290}{550} = 99{\cdot}8 \text{ h.p.}$$

$$= 73{\cdot}6 \text{ kW}$$

295. **Calculation of Blade Lengths.** Suppose that the blade rings have been set down provisionally, i.e. that the blade rings have been divided into groups of a certain radial depth b (Fig. 449) and the inner and outer radii and the number of rings in each group determined. Then the adiabatic heat drop in each group (or part of a group) may be estimated by using eq. (268). If a condition curve similar to Fig. 175 has been drawn in accordance with the specified steam conditions, then, knowing the distribution of adiabatic heat drop, the steam pressures and specific volumes may be obtained at inlet to, and outlet from, each group.

Suppose that at outlet from a particular blade ring v is the specific volume of the steam, V is the relative velocity, l is the axial length of the blades (measured in foot units), and x the "opening" per blade, Fig. 452. Then if there are m blades in the ring—

$$m \,.\, x \,.\, l = \frac{w \,.\, v}{V}$$

or

$$l = \frac{w \quad v}{m \,.\, x \,.\, V}$$

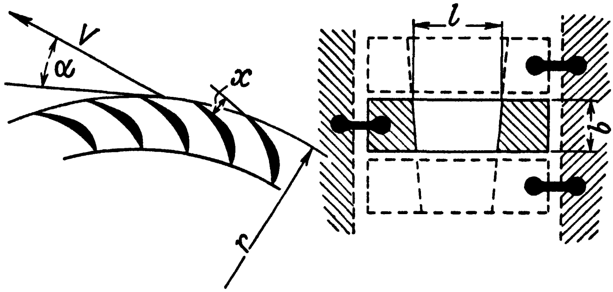


FIG. 452 —Diagram Illustrating Calculation of Blade Lengths

If the thickness of the blade outlet edge be t, then

$$x = \frac{2\pi r \,.\, \sin \alpha}{m} - t$$

from which

$$l = \frac{wv}{V(2\pi r \,.\, \sin \alpha - mt)} \quad . \quad . \quad . \quad (270)$$

If the thickness t be neglected—

$$l = \frac{wv}{2\pi \,.\, r \,.\, V \,.\, \sin \alpha} \quad . \quad . \quad . \quad (270a)$$

Owing to inertia forces, each blade is in the condition of a beam subjected to a uniformly distributed force and more or less rigidly fixed at the ends in the relatively stiff supporting rings. This produces a bending action, to which must be added the bending due to impulse and reaction. Consequently, if the ratio l/b exceeds a certain value, which will depend mainly on the peripheral velocity of the ring in question, the bending stresses will become excessive and the effective steam-carrying part of the blade must be divided into two or more parts, each suitably strengthened by the supporting rings. Examples of this are given later in this chapter.

296. Relationship between Cumulative Heat Drop, Speed of Rotation, Number of Blade Rings, and Diameter of Blade Rings in the Ljungström Turbine. It has been shown that the adiabatic heat drop in the nth blade ring is

$$\Delta H_n = \frac{1}{2gJ \cdot \eta_n} \{V_n{}^2 - k^2 \cdot U^2{}_{n-1} - (u_n{}^2 - u^2{}_{n-1})\}$$

But $\quad U^2{}_{n-1} = V^2{}_{n-1} + 4u^2{}_{n-1} - 4u_{n-1} \cdot V_{n-1} \cdot \cos\alpha$

$$\therefore \ \Delta H_n = \frac{1}{2gJ \cdot \eta_n} \{V_n{}^2 - k^2(V^2{}_{n-1} + 4u^2{}_{n-1} - 4u_{n-1}V_{n-1} \cdot \cos\alpha) - (u_n{}^2 - u^2{}_{n-1})\}$$

Writing $\chi = 1 - \frac{b}{r}$ (see Fig. 449) and assuming that ρ is uniform throughout the turbine, then—

$$u_{n-1} = \chi \cdot u_n; \ u_n = \rho \cdot V_n; \ u_{n-1} = \rho \cdot V_{n-1}; \quad \therefore \ V_{n-1} = \chi \cdot V_n.$$

$$\therefore \qquad \Delta H_n = \frac{V_n{}^2}{2gJ\eta_n} \{1 - k^2\chi^2(1 + 4\rho^2 - 4\rho\cos\alpha) - \rho^2(1 - \chi^2)\}$$

i.e.

$$\Delta H_n = \frac{V_n{}^2}{2gJ} \cdot f_3(\rho) \qquad . \quad . \quad (271)$$

where

$$f_3(\rho) = \frac{1}{\eta_n} \{1 - k^2\chi^2(1 + 4\rho^2 - 4\rho\cos\alpha) - \rho^2(1 - \chi^2)\} \quad . \quad . \quad . \quad . \quad (272)$$

$f_3(\rho)$ is a function of η_n, k, χ, α, and ρ. If η_n, k, χ, and α are given constant values, then $f_3(\rho)$ is a function of ρ only.

It follows that if D is the diameter of the nth ring in inches, and N is the speed of each rotor—

$$\rho = \frac{u_n}{V_n} = \frac{DN}{229} \sqrt{\frac{f_3(\rho)}{2g \cdot J}} \sqrt{\frac{1}{\Delta H_n}}$$

Therefore, for the whole turbine—

$$\rho = \frac{1}{51 \cdot 2} \sqrt{f_3(\rho)} \sqrt{\frac{K}{H_c}} \qquad . \qquad . \quad (273)$$

where K is the Parsons coefficient for the turbine and equals

$$\sum_0^n \left(\frac{D}{10}\right)^2 \left(\frac{N}{100}\right)^2$$

where n is now the total number of rings (both wheels).

Values of $f_3(\rho)$ are given in Table XXXVI for various values of b/r. In the same table are given values of $\frac{K}{H_c}$ for values of ρ, based on a value of $b/r = 0{\cdot}04$, which is about the mean value of this ratio in actual Ljungström turbines. Fig. 453 shows the calculated values of the gross stage efficiency plotted against values of the efficiency factor.

297. General Description. The Ljungström turbine was invented and designed by two Swedish brother engineers, Dr. Birger and Mr Fredrik Ljungström, about the year 1912. The new machine was a

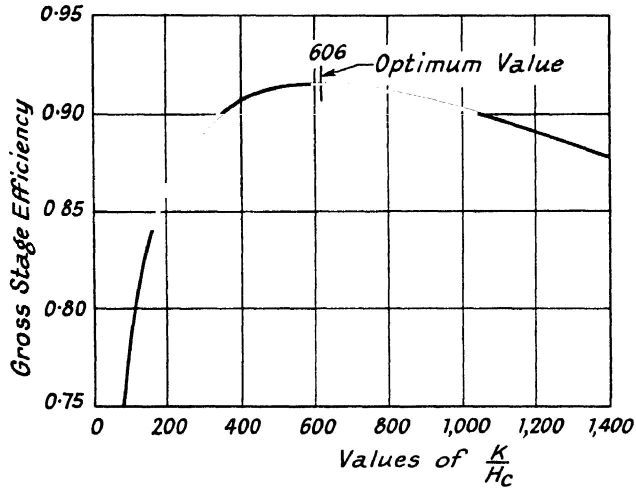


FIG. 453 —Calculated Stage Efficiency of Radial-flow Double-motion Turbine against Efficiency Factor

radical departure from the then existing ideas of steam turbine construction, and embodied several ingenious devices to reduce steam leakage and damage due to differential expansion, and also to minimize heat losses by conduction and radiation. So well conceived was the original design that to-day, after over forty years' experience, it stands almost unaltered except to meet the needs imposed by its application to larger powers. It is constructed in Sweden by the parent company, the Svenska Turbinfabriks Aktiebolaget Ljungström, and in England by the Brush Electrical Engineering Co., Ltd., of Loughborough.

The reader who is unfamiliar with the general features of the Ljungström turbine is asked to read Art. 9 and study Fig. 7 before reading the following description.

The construction adopted depends, to some extent, on the output of the turbine. Fig. 454 shows a section through the upper half of

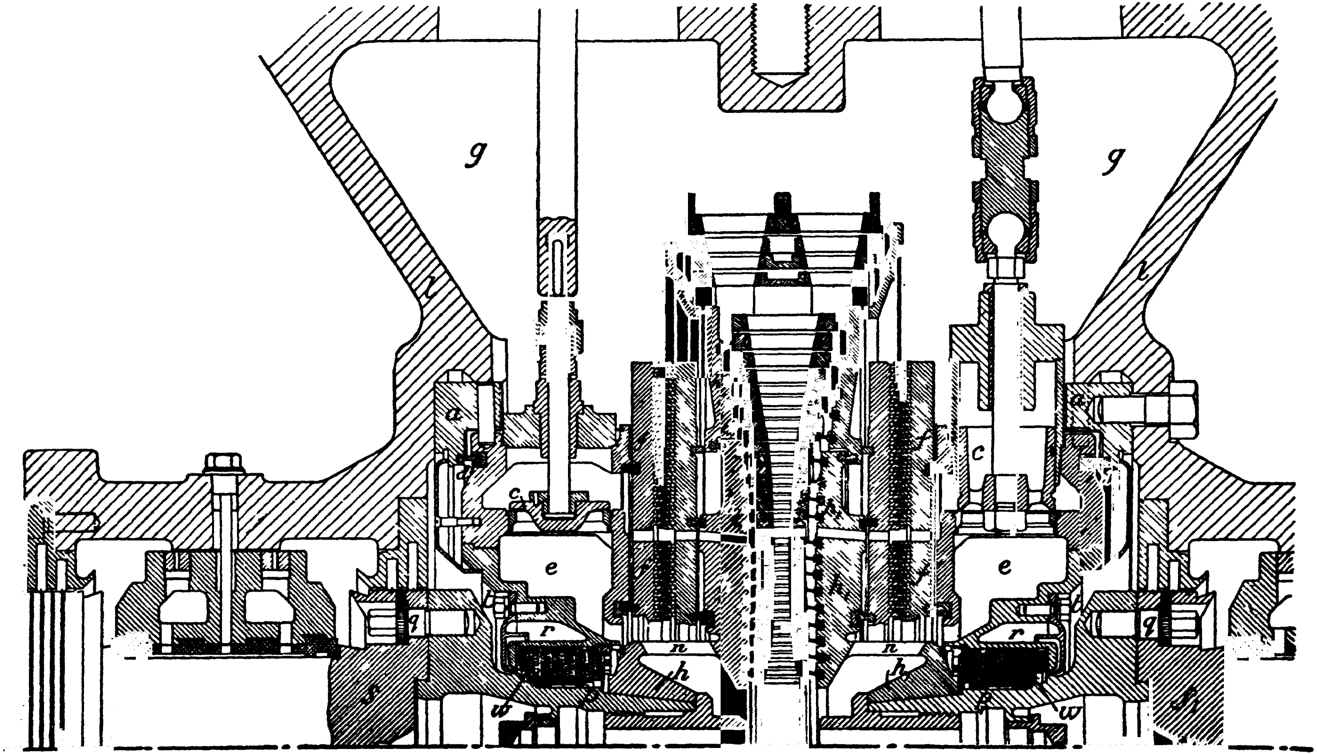


FIG 454

the blade system of a 1,875 kW turbine. The steam chests *e* (right and left) are flexibly mounted in the flanges *a* by the dumb-bell joint rings *d*, symmetrical expansion of the steam chests being further ensured by radial locating pins. The fixed balance discs *f*, with their labyrinth packing, are secured to the steam chests by expansion rings.

Very short turbine spindles *p* are spigoted into the alternator rotor shafts *s* and s_1 and carry the turbine rotors *h* and h_1. As will be seen from the figure, the alternate blade rings are carried on each rotor, the blade rings also being attached to the rotor discs by means of dumb-bell expansion rings. The rotating balance discs are connected to the rotor discs by the same method.

Steam enters the turbine through the side of the exhaust branch, Fig. 455, and passes through branch pipes into the lower part of the steam chests. Under normal load conditions the steam flows into the inner part *e* of the steam chests, through ports *n* cut in the hub of the rotors and so to the centre of the blade system. The steam, under the difference of pressure between the steam chest and the surrounding exhaust space *g*, then flows radially outwards through the blade system.

The variation in blade length may be noted. At first, the growth of area due to the increasing diameter is greater than that required due to the increasing volume of steam, bearing in mind that the steam velocity also increases as the diameter increases. In the later stages, however, the rapid increase in steam volume calls for longer blades. As a result the blade length diminishes up to about the eighteenth stage, thereafter it increases. It may be said that the variation in blade length is not directly related to the shape of a convergent-divergent nozzle because, whereas in the nozzle the steam velocity is a continuous function of the pressure, in the turbine it is not.

At the thirty-sixth blade ring the safe limit of blade length has been reached, bearing in mind the stresses due to bending, and in the remaining four stages the blades are each subdivided into two parts of equal length.

For loads above the economical load, either the right-hand overload valve *c* is automatically opened by the governor or the hand-operated left-hand overload valve *c* is opened. In either case, steam is admitted, in amount depending on the overload, through openings in the balance discs and rotor discs to the space after the eighteenth blade ring.

Leakage of steam from the steam chest to the atmosphere is reduced to a very small amount by the labyrinth packing *w*. Details of this will be given in Art. 301.

The employment of two or more blades in parallel in the low pressure part of the blade system has already been mentioned Fig. 456 shows a somewhat old design of a 5,000 kW turbine by the

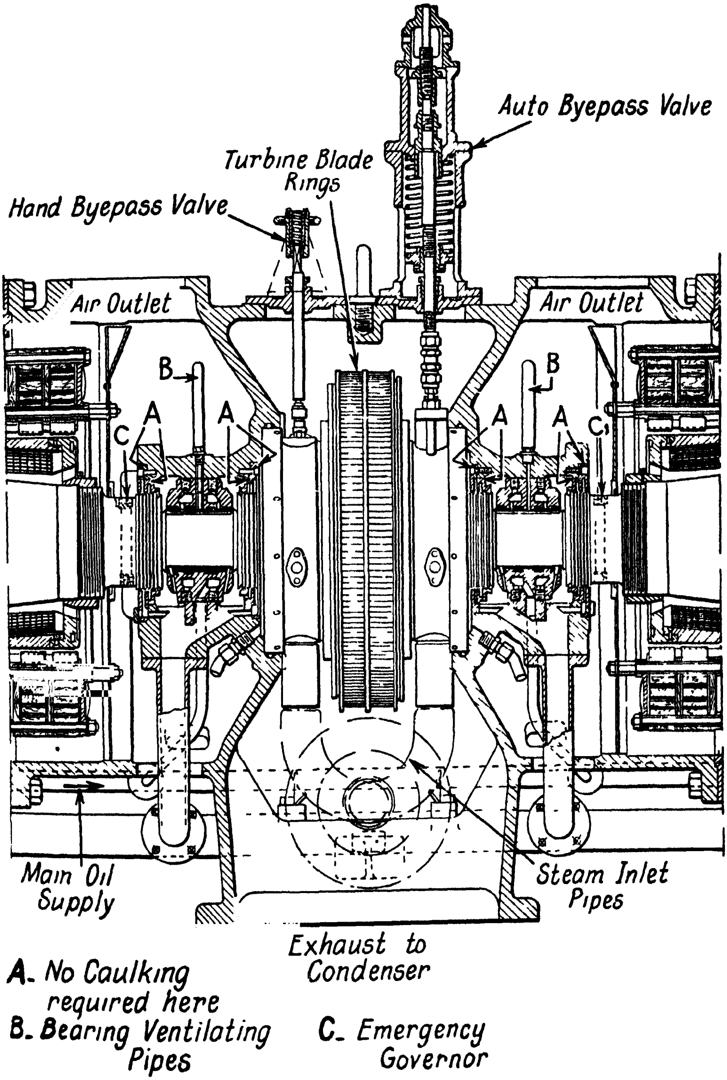


FIG 455 —Part Section of 1,875 kW Brush Ljungstrom Turbine

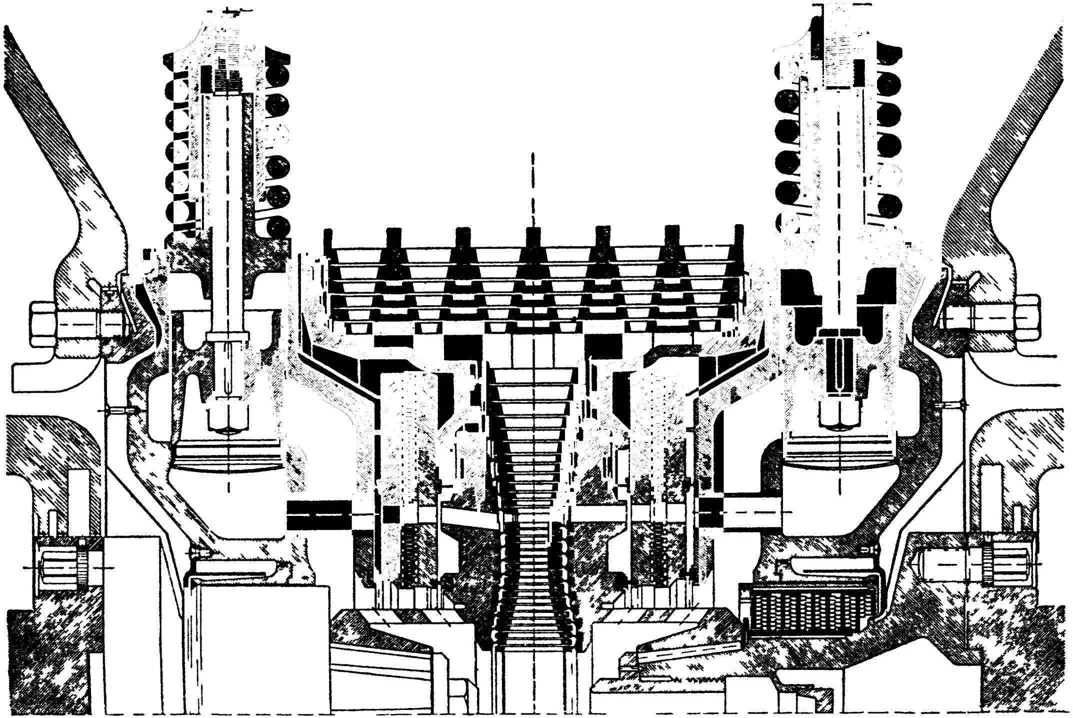


Fig. 456 — Section through the Upper Half of a 5 000 kW Ljungstrom Turbine

Svenska Turbinfabriks Aktiebolaget Ljungström of Finspong, Sweden, in which the blades of the last six stages are subdivided into six sections. The inertia forces on the blades are borne by the intermediate supporting rings to which the blades are attached These are, of course, continuous rings. It will be observed that in the outer rings where the axial length of the supporting rings is reduced, owing to the greater length of the working blades, the necessary area of the ring is obtained by increasing its depth.

There is obviously a limit to the extent to which the L.P. blades may be subdivided, and in the more recent designs the necessary area through the L.P. blades is obtained by the use of one or two stages of axial-flow blading. Fig. 457 shows a cross-section through a Brush Ljungström turbine of 7,000 kW capacity in which a disc carrying one ring of axial-flow impulse-reaction blading is attached to each rotor by a number of taper pins. The final stage is thus a double-flow reaction turbine.

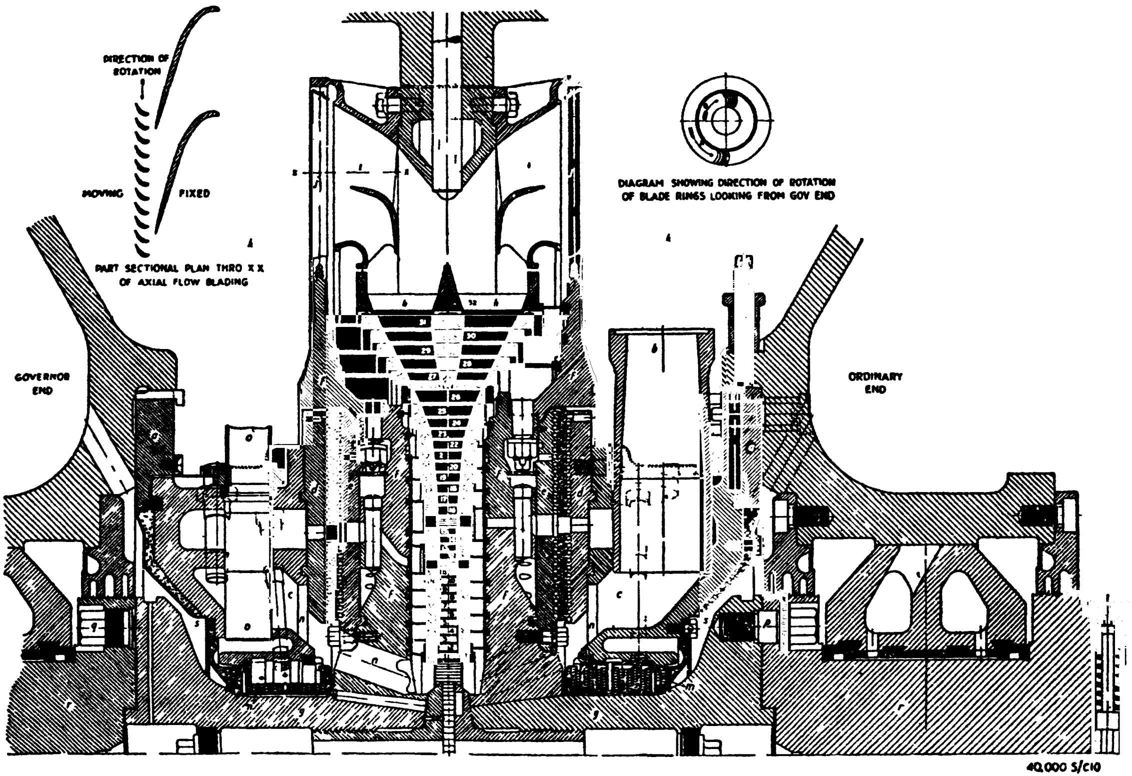
The general arrangement of the turbine is shown in Fig. 458. The turbine proper is supported on the exhaust flange of the condenser, the only foundations required being those for the condenser. Each turbine rotor is coupled direct to an alternator rotor. The alternator frames are overhung, but the overhung weight is taken by four steel struts which transmit the load to heavy brackets on the condenser. The two alternators operate in parallel. An exciter is arranged at one end of the set, the governor being located at the other.

A further application of the same principle is illustrated in Fig. 459, which shows a section through the upper half of a 15,000 kW 3,000 r.p.m. Brush Ljungström turbine. A low-pressure cylinder A, surrounding the radial-flow blading system, is fitted with two sets of nozzle vanes or fixed blades B and D, whilst each rotor carries a ring of blades C and E mounted on the stiff discs F and G respectively. Sections through the blading and nozzles are shown in Fig. 459.

Steam is tapped off for regenerative feed-heating at three points, namely, H (high-pressure steam), I (intermediate-pressure steam), and from L for low-pressure steam.

Designs have been produced for Ljungström turbines to develop 30,000 kW at 3,000 r.p.m. and 60,000 kW at 1,500 r.p.m.

298. Blade Construction. Two methods of constructing the blades and their supporting rings are employed. That used for turbines up to 4,000 kW is illustrated in Figs. 460 to 463. The blades themselves are milled out of round nickel steel bar, ground up in the direction of steam flow and afterwards cut off to the required length, a tongue of metal being left at each end, as shown by 17, Fig. 460. The blades are fitted into slots punched in discs (15) which have previously been turned to the channel section shown in the same illustration. The blades are held at the correct angle and distance apart by means



DIRECTION OF ROTATION
MOVING
FIXED
PART SECTIONAL PLAN THRO X X OF AXIAL FLOW BLADING
DIAGRAM SHOWING DIRECTION OF ROTATION OF BLADE RINGS LOOKING FROM GOV END
GOVERNOR END
ORDINARY END
40,000 S/C10

FIG 457

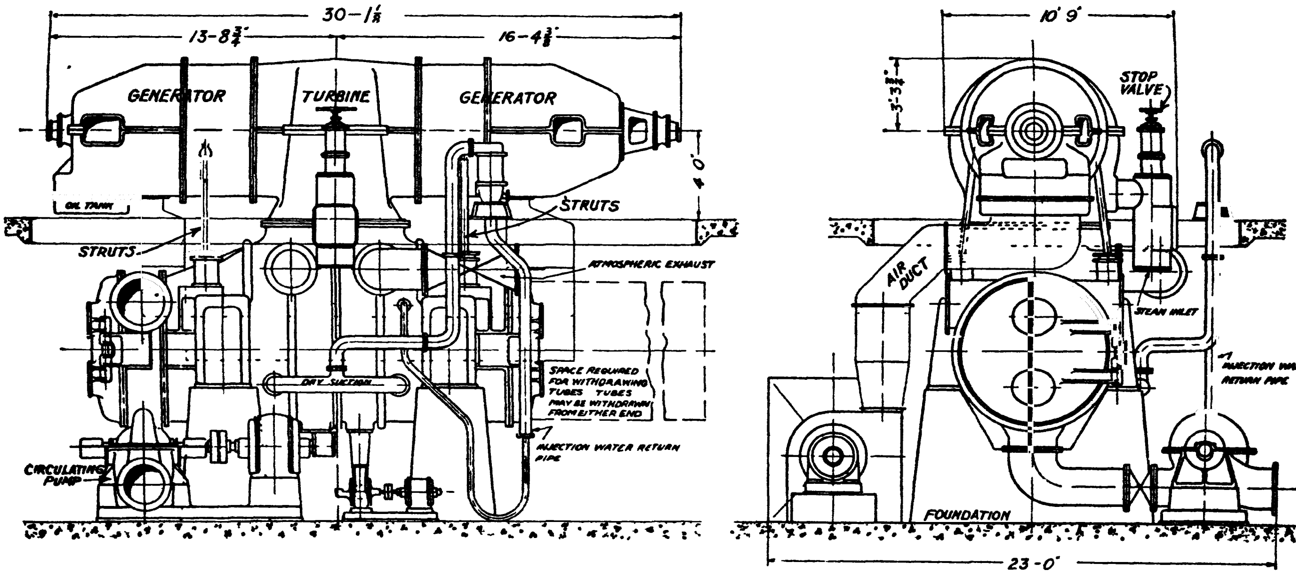


FIG 458 —General Arrangement of 7,000 kW Ljungström Turbine

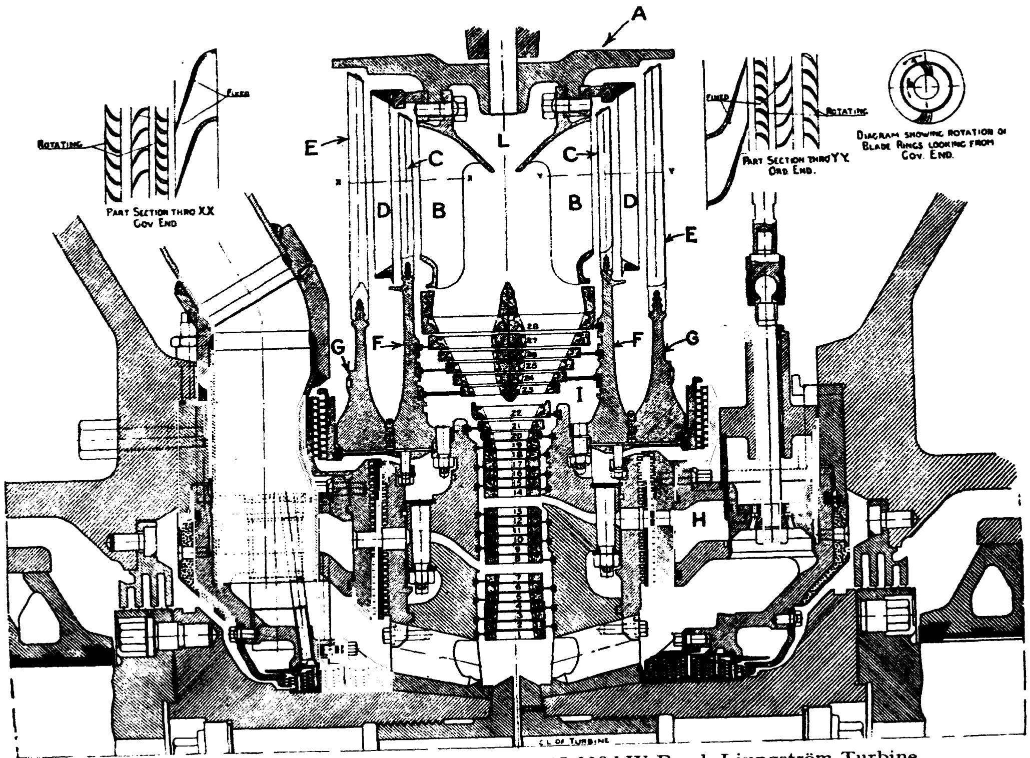


FIG. 459.—Section through Blade System of 15,000 kW Brush Ljungström Turbine

of thin sheet iron strips (20) and then welded into the discs. After the sheet iron strips have been removed, the welding discs are turned off so as to produce the dovetail profile indicated in Fig. 461. This

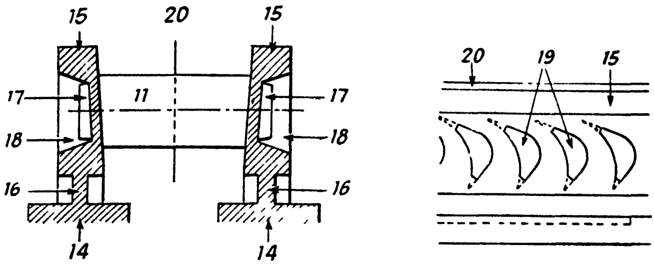


FIG. 460

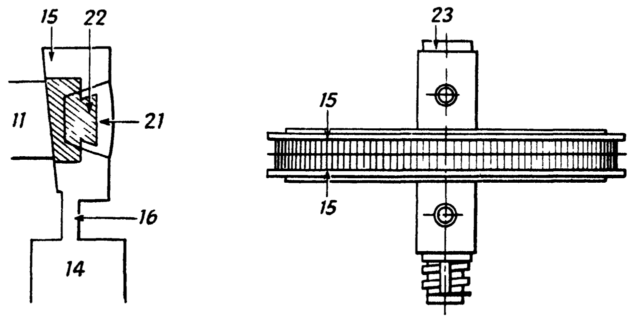


FIG. 461

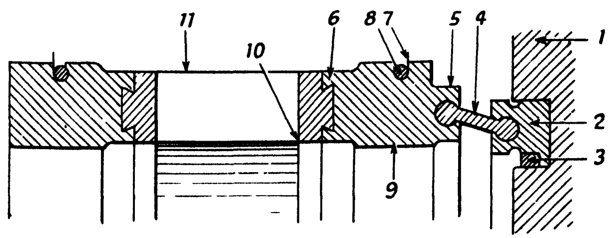


FIG. 462.- Section of Finished Blade Ring

dovetail consists partly of blade metal, welding ring, and partly of weld metal, and has insufficient strength to resist the inertia forces. In the completed blade ring, Fig. 462, the inertia forces are taken by the supporting rings 9. The complete blade ring is attached to the

rotor disc by the dumb-bell ring 4, one end of the latter being gripped by the supporting ring 9, the other end by the ring 2, which is secured by the caulking strips 3. A section of the supporting ring before rolling is shown in Fig. 463. The projecting edges *a* and *b* are rolled over to grip the dovetail of the blades; the edges *c* and *d* being likewise rolled over to grip the expansion ring.

Steam leakage from one ring to the next is reduced to the minimum by the packing strips 7, Fig. 462, of nickel or steel, which are held in grooves by the caulking strips 8.

The dumb-bell expansion ring, which is such a feature of the Ljungström turbine, enables contiguous parts of the turbine to adjust their positions relative to one another when their dimensions are changed due to the effects of temperature and stress and yet

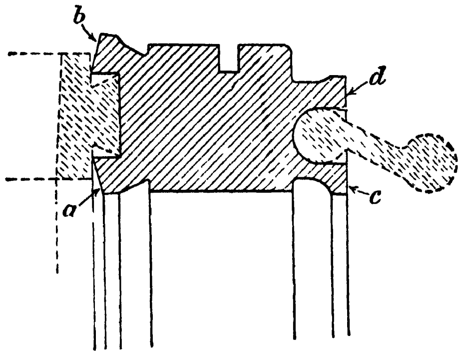


FIG. 463.—Section of Strengthening Ring before Rolling

maintain perfect alignment. Moreover, the small cross-section of the ring reduces the heat conduction to small limits.

The type of blade construction which has just been described is used for small machines and for the inner rings of large turbines. For the larger turbines the blades shown in Fig. 464 are used. They are machined frcm very strong alloy steel bar, usually chrome nickel molybdenum steel. At each end of the blade there is a radial dovetail root which fits into a corresponding taper dovetail slot milled out of the inner face of each strengthening ring, Fig. 465. Before assembly, every blade root is carefully fitted by hand in the corresponding ring slot, first at one end of the blade and then at the other. Only when all blades have thus been bedded is assembly of the ring started. The final operation in driving the blades home is effected by running the ring at a certain overspeed, when all blades move outwards the last few thousandths of an inch to their final positions in the taper grooves under the action of centrifugal force.



Fig 464

Examples of more recent Brush-Ljungstrom turbines employing the newer form of blading are given in Figs. 466 and 467. Fig. 466 shows a half-section through the blade system of a 20 MW. 3,000 r.p.m. condensing turbine. There are 28 radial-flow stages of which the six outer stages are fitted with the newer blade construction In addition, there are two low-pressure axial-flow stages in parallel

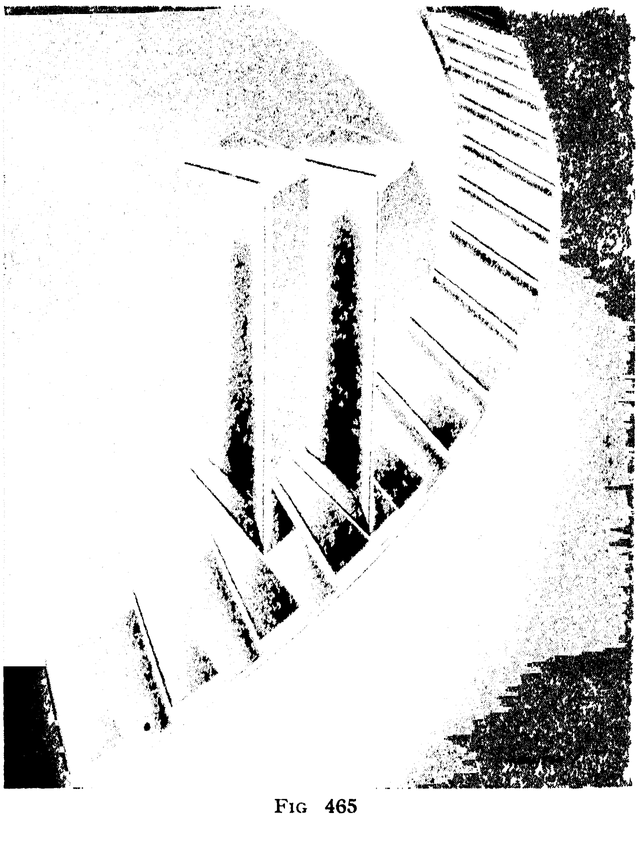


FIG 465

The cylinder for these is split at the horizontal joint for dismantling purposes, its alignment is maintained by radial pins. Steam is extracted at three points for feed-heating.

In the low-pressure cylinder a groove is machined on each side and in the plane of the first l p axial-flow moving blades. A continuous ring which is fitted into the groove carrying the fixed row of blades forms a channel, so that water droplets in the steam thrown

off by centrifugal force may be caught and run off to the bottom of the groove from whence they drop into the condenser.

Fig. 467 shows a 60 MW. 1,500 r.p.m. condensing turbine. There are 45 radial-flow stages of which the last 7 are furnished with the newer type of blade construction. It will be seen that in neither the 20 MW. nor 60 MW. turbine has it been necessary to use the divided blade which was a feature of the earlier turbines. Steam is bled off for 4-stage feed-heating.

299. Disc Construction. Reference to the foregoing cross-sections

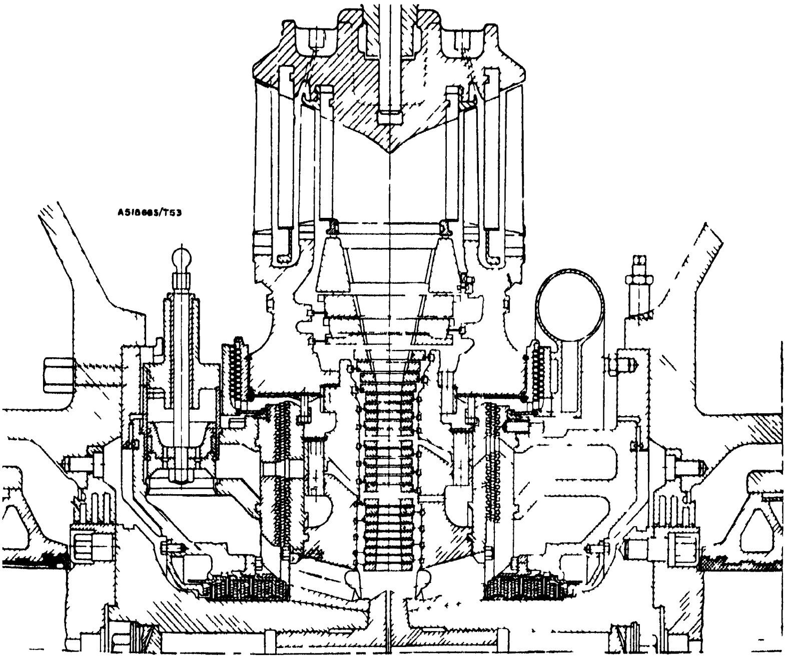


FIG. 466

of Ljungström turbines will show that in all cases the rotor discs are built-up from two or three concentric parts, the individual parts being attached to each other in such a way that each part may expand or contract radially without putting any appreciable strain on the adjacent part. This prevents excessive thermal stresses due to the temperature gradient along the steam path.

In the smaller turbines, Figs. 454 and 456, the disc elements are attached to each other by dumb-bell rings, whereas in the larger machines the attachment is made by radial bolts. The discs and spindles are made from chrome-molybdenum alloy steel.

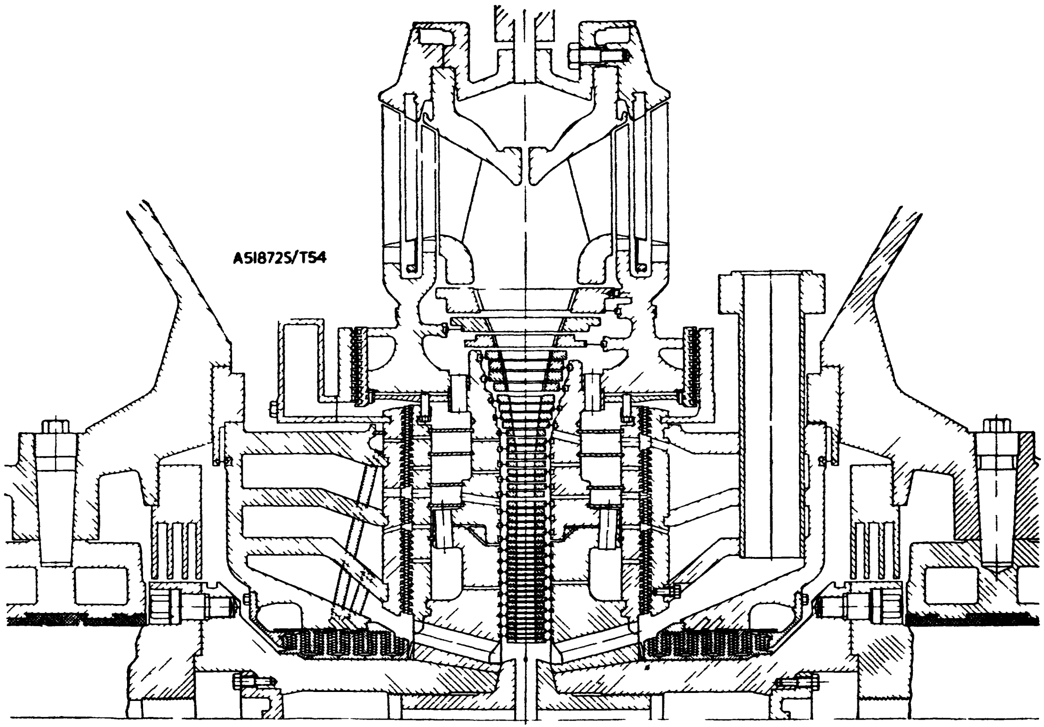


Fig 467

300. Balancing Arrangements. Reference has already been made in Art. 9 to the balancing discs attached to the steam chests and rotors. The labyrinth packing for these discs is shown in detail in Fig. 468 A number of grooves are turned in the fixed and moving discs and a projecting ring between each pair of grooves fits into a groove on the opposite disc. Such projecting rings are furnished with a groove into which is fitted a thin strip of nickel having a fine clearance. The total number of constrictions is obviously twice the number of grooves. The temperature conditions are practically the same for the fixed and moving dummy discs, and hence the clearances will hardly vary and may, therefore, be made very small.

301. Shaft Glands. The shaft glands have to be packed against

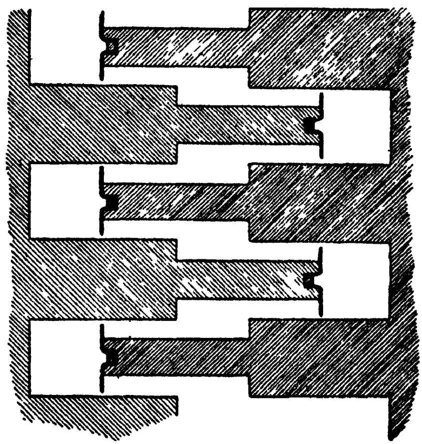


FIG 468 —Labyrinth Packing for Ljungstrom Turbine Balancing Discs

the full steam pressure and are one of the most ingenious features of the turbine. Each gland comprises a number of fixed and rotating elements as shown in Fig. 469. Each element is machined out of the solid in such a way that a number of thin cylindrical rings project from the central web, the outer end of each ring being turned over at 45 degrees. A small running clearance is allowed. The gland shown in Fig. 469 provides 72 throttlings.

In the glands for the 60 MW. turbine shown in Fig. 467, there are two leak-off connections from the gland to stages 18 and 33, respectively.

The steam escaping from the final constriction is arranged to blow through a diffuser into a special pocket. The escaping steam, leaving the last constriction of the packing with a high velocity, produces an ejector action and so draws air into the said pocket

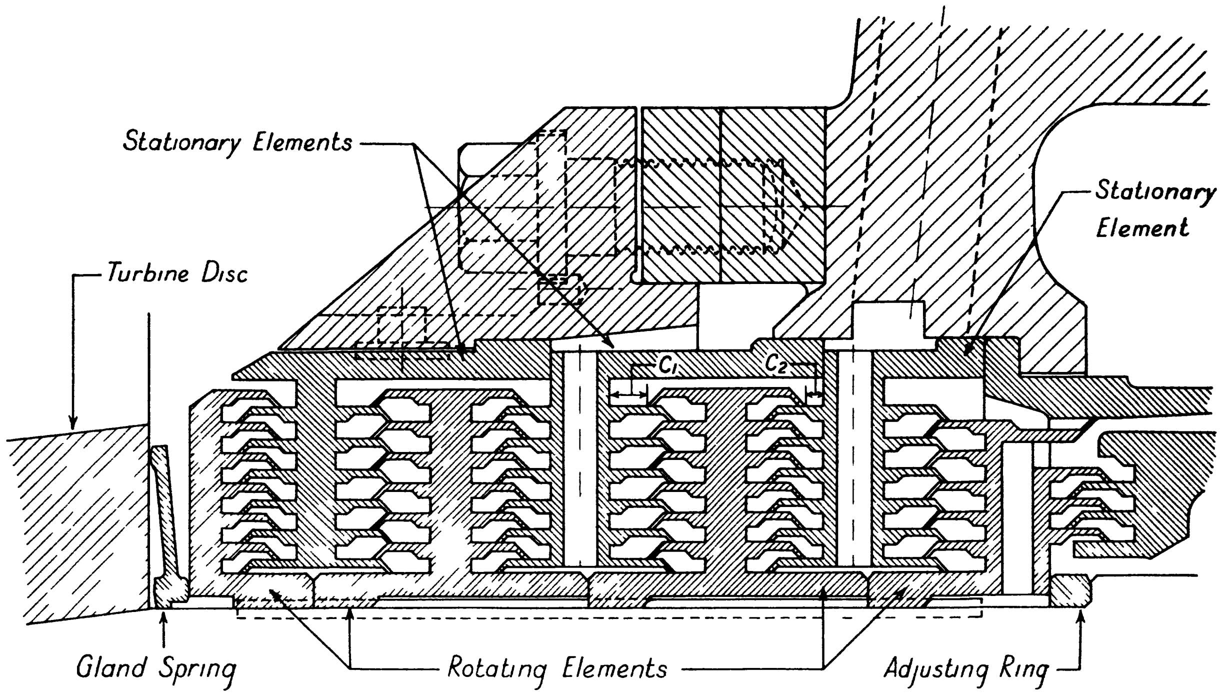


Fig. 469 Section of Shaft Gland Showing Axial Clearances

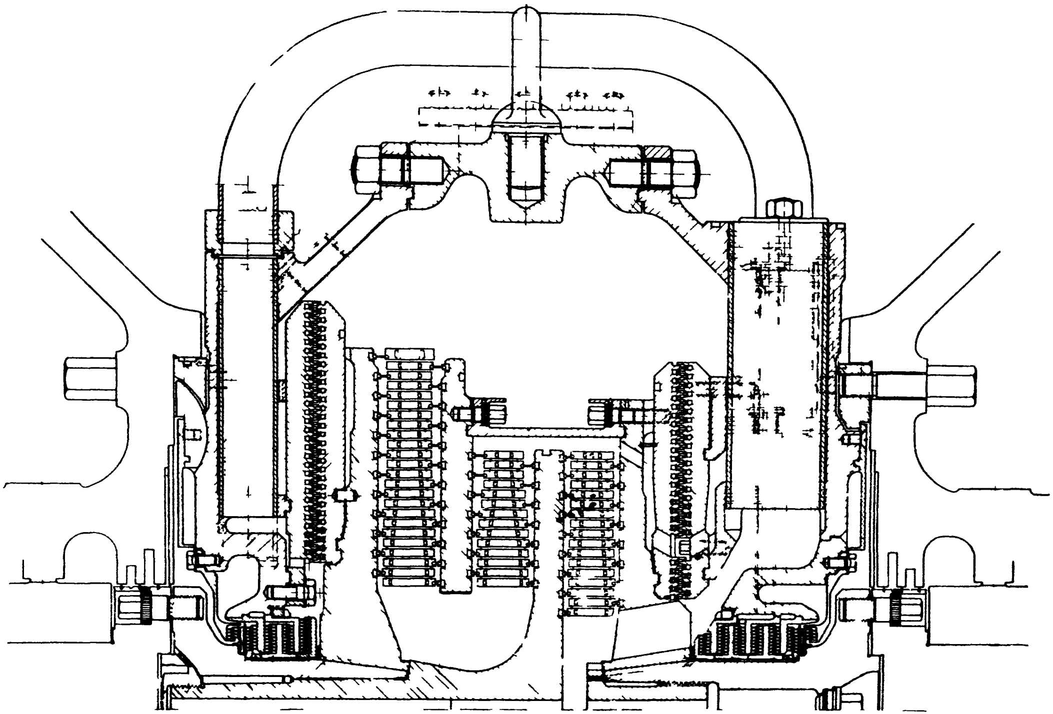


FIG 470 —Section of Ljungstrom Turbine with Moller System of Blades

through the five constrictions seen at the right of Fig. 469. The mixture of air and steam is led away to a separate condenser. The object of this arrangement is to prevent the escaping steam from leaking into the restricted space between the gland and the main bearing.

302. Multiple Radial-flow Turbine. Reference has been made in Art. 295 to the limit set by the radial-flow blades to the maximum steam flow through the turbine. There is also a certain economic limit to the minimum steam flow at entrance to the high-pressure blading, because in small units the losses due to leakage between the blade rings tends to become excessive. Further, in small units of normal design, a large number of stages can only be used if the radial depth of the rings is made very small. This difficulty is overcome in a design due to Mr. Möller of the STAL works in Finspong, Sweden.

Fig. 470, taken from the lecture (1) by Dr. Fredrik Ljungström, shows a section through a turbine with the Möller system of blades. Here the turbine is provided with four discs and three sets of blading arranged with series flow. It will be seen that half the blade rings are attached to two discs on the right-hand shaft while the other half are attached to two discs on the left-hand shaft. Thus 27 pairs of blade rings are provided in a relatively small radial space. Steam enters at the right-hand side and leaves the blade system at the left-hand side.

303. General Notes. The Ljungström turbine has been constructed in units up to 40 MW. with a speed of 3,000 r.p.m. for each rotor and in units up to 65 MW. at 1,500 r.p.m.

In the radial-flow blading all parts of the blades are subjected to almost identical conditions as regards steam velocities, flow angles, etc. Owing to the small diameters of the first few stages of the turbine, reasonable blade lengths may be used.

The steam chests are machined from forgings and are solids of revolution without any longitudinal joint. All parts of the turbine are free to expand or contract radially under stress and temperature changes. The blade rings are of comparatively small mass and will quickly respond to changes in steam temperature. Moreover, the difference in diameter between adjacent rings is small, so that the relative movements due to temperature and stress are very small indeed. As a result the turbine may be started and put on load without any preliminary heating. The 7,000 kW. turbine has been run up in less than five minutes from cold, and the 12,500 kW. turbine has been started from cold and been ready for load in about twelve minutes. Consequently, the Ljungström turbine is particularly suitable for a peak-load and reserve power station. There are such stations at Västeras and Malmö in Sweden, and, by special design of the auxiliaries to facilitate quick starting, it is possible to start either of the 65,000 kW. turbines at Västeras and have it on

full load in less than ten minutes. It is unnecessary to turn the turbines or to supply heat to them when they are inoperative.

A few results of tests on Ljungström turbines will be found in Chapter XXX.

BIBLIOGRAPHY

1. LJUNGSTRÖM. "The Development of the Ljungström Steam Turbine and Air Preheater." *Proc. I. Mech. E.*, 1949; 160; 211.

CHAPTER XXIX

EXAMPLES OF CONSTRUCTION

304. Turbines for Electricity Generating Stations. The continuous increase in the use of electrical energy has made necessary the construction of several additional generating stations in various parts of the country. The use of a nation-wide grid has made it possible to increase the output of individual power stations. Generally speaking, provided reliability can be assured, increased economy in first cost and operating costs may be achieved by installing in such generating stations the largest units practicable. A certain amount of standardization has been attempted by the Central Electricity Authority, the following being brief particulars—

Power MW.	Steam Pressure p.s.i.g.	Steam Temp °F.	Reheat Temp. °F.	Approx. Final Feed Temp °F.
30	600	850	—	340
60	900	900	—	385
100	1,500	1,050		400
120	1,500	1,000	1,000	435
200	2,350	1,050	1,000	460

All turbines operate at 3,000 r.p.m. The final feed temperatures quoted will doubtless be economic values and lie between 0·7 and 0·73 times the initial steam saturation temperatures.

In current British practice for large power station turbines the following features are fairly general—

(*a*) The steam chests are usually placed alongside the high-pressure turbine and connected to the cylinder by a symmetrical arrangement of fairly flexible steam pipes.

(*b*) Velocity wheels are frequently used in the first stage of the high-pressure turbine in order to reduce the pressure and temperature of the steam to which the h.p. turbine cylinder is exposed.

(*c*) Some form of barring or turning gear is provided at the coupling between the l.p. turbine and the generator so that the turbine may be kept in slow rotation during the warming-up process and also after the turbine has come to rest and is cooling down. This is done to prevent bending of the rotor shaft.

(*d*) Provision is usually made in the last two or three stages of the l.p. turbine for the drainage of water flung off the blades by centrifugal action.

(*e*) In all cases, the cylinders are supported in such a way that there is freedom for expansion and contraction due to temperature changes without disturbing the vertical or transverse alignment. That is, the cylinder and rotor remain concentric. In double-shell turbines, the inner shell is so supported within the outer casing that they remain co-axial and hence concentric with the rotor. When there is a radial steam pipe passing through the outer casing into the inner cylinder, the latter is fixed longitudinally in the plane of the two inlets.

(*f*) Where wheels are shrunk on to the rotor spindle, the running speed of the rotor may be above the first transverse critical speed. Where a gashed rotor is used, the running speed is usually kept well below the first critical.

The 200 MW. turbine has three flows in the low-pressure stages. With four flows and other things equal the output could be increased to 267 MW. Due to improvements in efficiency resulting from the greater total steam flow per second and from various improvements in design it is estimated that this power could be increased to 275 MW. Still further advantages may be obtained by using a cross-compound unit with a four-flow l.p. turbine on each shaft. Turbines of this type, to develop 550,000 kW., are now being considered in this country. An arrangement with distinct possibilities is shown in diagrammatic plan view in Fig. 471.

High-pressure steam is supplied to a double-flow high-pressure turbine A. Owing to the large mass flow of steam it is possible to adopt the double-flow construction and yet have blades which are long enough to yield a good efficiency. Furthermore, by supplying steam to the centre of the turbine instead of admitting it to one end of a single-flow turbine, it is possible to eliminate the loss due to a shaft gland subjected to either the full inlet steam pressure or to the steam pressure in the first stage. Exhaust steam from A enters the double-flow intermediate-pressure turbine B on the other shaft. This possesses the advantages mentioned above for the h.p. turbine. Exhaust steam from B then passes to the reheater.

Steam returning from the reheater enters four second-i.p. single-flow turbines C which are mounted at each end of a low-pressure turbine housing D. After expansion through the second-i.p. turbines the total steam flow is divided, as shown, into eight equal parts, four parts passing directly through the four single-flow l.p. turbines E, and the other four parts passing through the two double-flow l.p. turbines F, with wheels similar to those in E.

In the arrangement of the steam connections to the various turbine cylinders, the aim would be perfect symmetry in order to minimize the risk of distortion.

Generally, the high-pressure section of large turbines is made relatively small in diameter with the following advantages—

(1) The thickness of the cylinder for a given initial steam pressure

may be made smaller, whether a single-shell or double-shell construction is employed.

(2) Complete admission is generally possible without the use of very short blades.

(3) The total power loss due to disc friction and windage is reduced.

In the following articles the current practice of leading firms is illustrated by selected examples.

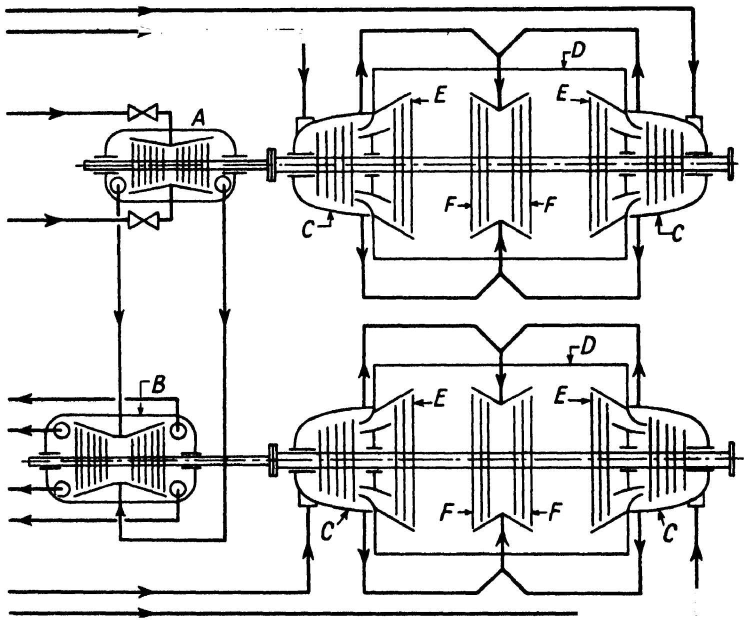


FIG. 471.—Diagrammatic Arrangement of Two-shaft 550 MW. Steam Turbine

305. 60 MW. English Electric Turbine. Fig. 472 shows a longitudinal section through a three-cylinder tandem turbine which is installed in the Drakelow "A" Power Station of the C.E.A. East Midlands Division. The turbine develops 60 MW with the following steam conditions—

Initial steam pressure	1,500 p.s.i.g.
Initial steam temperature	1,050° F.
Number of stages of feed heating . .	6
Final feed temperature at maximum load	430° F.
Vacuum	28·75 in. Hg.

The h.p. and i.p. turbines are of the impulse type with 11 and 19 stages, respectively. Boiler steam is supplied to two forged

alloy steel chests, one on each side of the h.p. turbine, containing the combined stop and emergency valve together with a governing valve. Each steam chest is connected to the turbine by two pipes, one entering the upper half and the other entering the lower half of the nozzle box. Governing is effected by throttling only.

The first stage of the h.p. turbine is a two-row velocity stage which brings about an appreciable drop in steam pressure and temperature. The h.p. and i.p. rotors are machined out of solid forgings, the h.p. rotor being of molybdenum-vanadium steel and the i.p. rotor of carbon steel. The first-stage h.p. nozzle gives full admission and is made in four quadrants. Each is machined from the solid in high-tensile stainless iron.

The double-flow l.p. turbine has an impulse wheel in the first stage enabling a considerable heat drop to be utilized with a minimum leakage loss. The remaining seven stages operate on the reaction principle. The spindle of the l.p. turbine is of carbon steel with discs of nickel steel shrunk on.

There are six main bearings and three flexible couplings. Each turbine is provided with its own thrust block and the h.p. and i.p. turbines are provided with hand gear for giving axial movement to the thrust blocks while the turbine is operating, controlling the effects of differential expansion during starting and change of load. Provision is also made for h.p. cylinder flange steam heating.

The main oil pump is situated in the i.p. pedestal and driven from the steam end of the i.p. rotor through helical gearing.

306. 200 MW. English Electric Turbine. This is a three-cylinder tandem turbine operating at a speed of 3,000 r.p.m. with the following steam conditions --

Inlet steam pressure . .	2,350 p.s.i.g.
Inlet steam temperature .	1,050° F.
Reheat temperature . .	1,000° F.
Number of stages of feed-heating	6
Final feed temperature . .	460° F.
Vacuum	28·7 in. Hg.

Fig. 473 shows a section through the high-pressure turbine, part of which is of double-shell construction. Steam enters the nozzle box through four radial pipes A, which are provided with piston-ring packing. After partial expansion through eight stages of impulse blading accommodated in the inner shell, the pressure of the steam is 837 p.s.i.a. and the temperature 793° F. This steam now flows in the reverse direction in the space between the inner and outer shells to enter the last four impulse stages in which it expands to a pressure of 490 p.s.i.a. and a temperature of 677° F. before passing to the reheater.

Steam returning from the reheater at 441 p.s.i.a. and 1,000° F.

enters the i.p. turbine nozzle box B of a short inner cylinder C by way of four radial steam pipes, Fig. 474. This inner cylinder contains the first three stages of impulse blading and, like the inner cylinder of the h.p. turbine, is located by pads and keys so that, while being free to expand and contract under temperature changes it remains concentric with the outer cylinder and with the rotor.

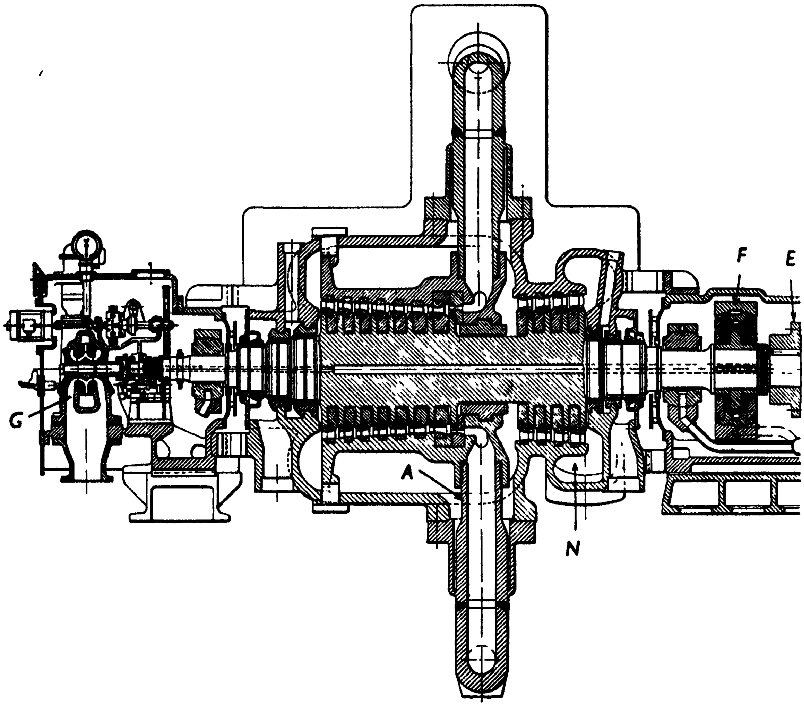


FIG. 473.*—Section of H.P. Turbine of English Electric 200 MW. Turbine

The axial position is fixed in the plane of the steam inlet pipes, freedom for axial movement being allowed at other points.

There follow five more impulse stages in which the steam expands to 52 p.s.i.a. and 515° F. At this point the steam flow divides; about one-third passes through a single-flow l.p. turbine arranged in the same casing as the i.p. stages, while about two-thirds of the steam passes through two connecting pipes D into the centre of the double-flow l.p. turbine, Fig. 475. All three l.p. expansions exhaust into a common exhaust chamber and single-shell condenser.

* *Note*: Figs. 473, 474 and 475 are adapted from drawings published in *The Engineer*, by kind permissio· of the Editor.

Steam is bled from the double-flow l.p. cylinder for feed-heating, but not from the corresponding stages in the i.p. turbine casing.

The h.p. and i.p. rotors are machined from solid forgings; the l.p. turbines have discs shrunk on and keyed to the shafts. The first stage of each l.p. turbine has impulse blading and the remainder

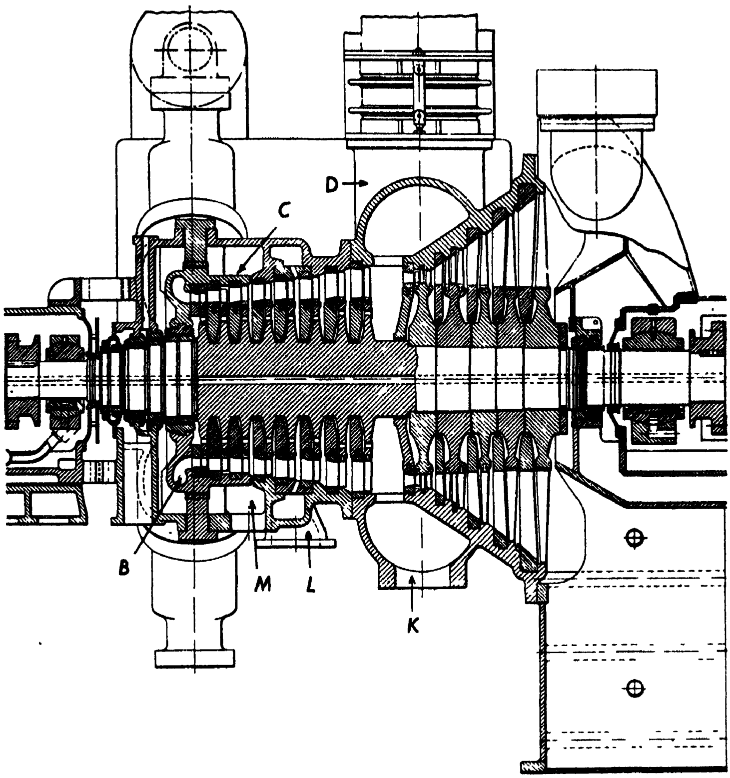


FIG. 474.—Section of I.P. Turbine of English Electric 200 MW Turbine

of the l.p. stages have vortex blading. The active length of the blades in the last stage is 27 in.

The three rotors are coupled together by "solid" couplings E, for the reasons given in Art. 201. There is only one thrust block F, arranged between the h.p. and i.p. cylinders so as to minimize the differential expansion between rotating and stationary elements in those turbines. By adopting solid couplings and reducing the number of thrust blocks to one as compared with three in the 60 MW. turbine shown in Fig. 472, it is possible to reduce the overall length

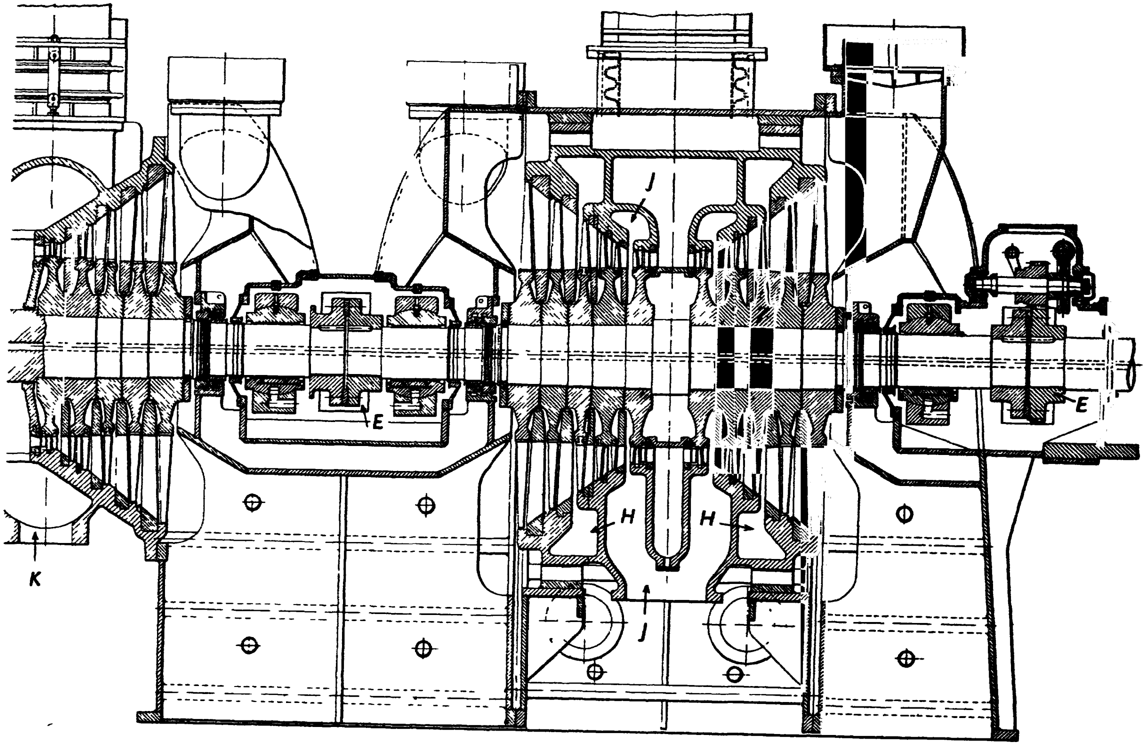


Fig. 475 — Section of L P Turbine of English Electric 200 MW Turbine

of the 200 MW. turbine until it is only 6 ft. greater than the length (about 50 ft.) of the 60 MW. turbine.

There is full admission to all stages of the h.p. turbine at all times. This is done to avoid vibration which might occur in the moving blades if partial admission were adopted. The outer casing of the double-flow l.p. turbine and the exhaust end of the single-flow l.p. turbine are fabricated. Due to their large size they have to be made in a number of sections for transport purposes and seal-welded in the power station. The inner casings carrying the diaphragms and fixed blades are steel castings.

The main oil pump is a double-inlet centrifugal pump G driven direct from the turbine spindle.

The bleed points are H and J in the l.p. cylinder; K, L, and M in the i.p. cylinder, and N in the h.p. turbine exhaust before the reheater.

307. 30 MW. General Electric Co. Steam Turbine. This turbine, constructed by the General Electric Co., Ltd., of England, is illustrated in Fig. 476. It is a 3,000 r.p.m. machine with the following steam conditions—

Initial pressure . . .	600 p.s.i.g.
Initial steam temperature .	850° F.
Stages of feed-heating . .	4
Final feed temperature . .	340° F.
Vacuum	28·7 in. Hg.

There are 8 stages in the h.p. section, the first being a two-row wheel, 3 stages in the i.p. section, and 6 stages in the l.p. section. Vortex flow is employed in the longer blades. In some of the l.p. stages a small degree of reaction is introduced at the inner diameter in order to ensure subsonic speed of approach of the steam relative to the moving blades.

The rotor comprises a stout shaft with separate discs. Each disc after blading is statically balanced and, after the assembly of the wheels on the spindle, the whole rotor is dynamically balanced. The blades are attached to the wheels by a straddle, or modified straddle, fastening and if a blade is accidentally damaged it may be removed and replaced without disturbing the other blades on the wheel.

Due to the use of partial reaction in certain stages, there is a steam thrust towards the exhaust end. This is largely balanced by the steam pressures on the dummy balance piston A, adjacent to the two-row wheel. This piston is packed with the vernier packing illustrated in Fig. 358(*f*). The space behind the dummy piston is connected to the bleeder connection for No. 3 heater, i.e. after the eleventh stage. The residual thrust, always acting in one direction, is taken up by the Michell thrust block B.

For smaller machines the main oil pump is of the gear type. For

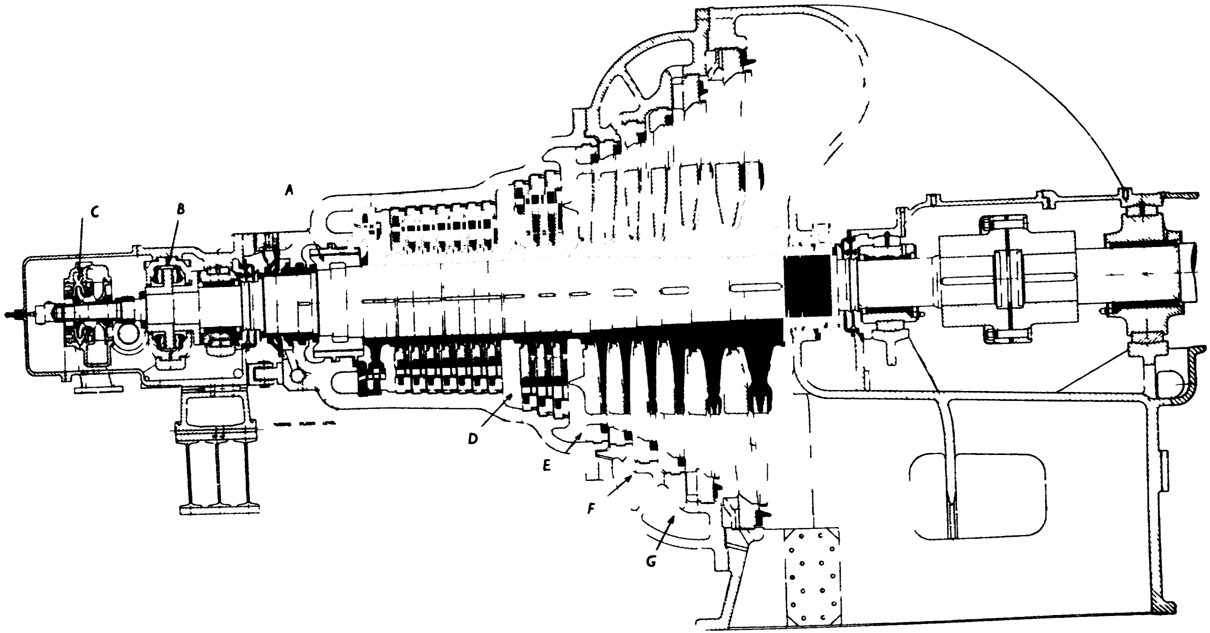


FIG 476—G E C 30 MW Turbine

the larger turbines, as shown in Fig 476 a centrifugal pump C, mounted direct on the rotor spindle, may be used This eliminates the gear drive from the turbine spindle An auxiliary ejector supplies

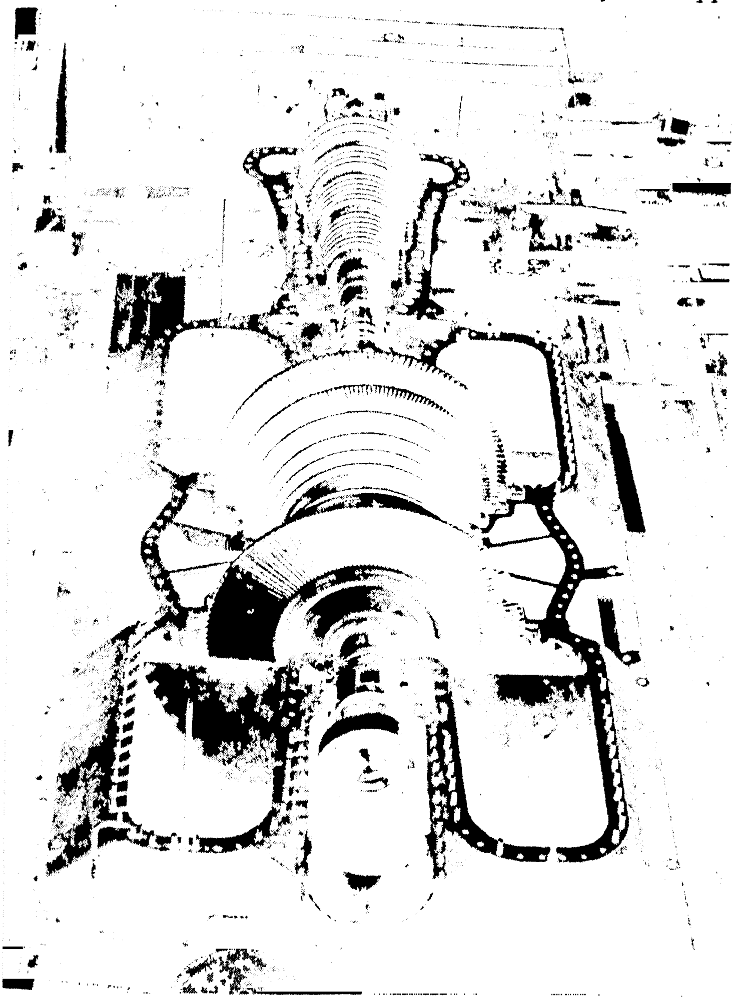


FIG 477 60 MW General Electric Steam Turbine during Erection in the Erith Works

oil at a pressure slightly above atmospheric to the pump suction Part of the discharge from the pump is used in the ejector to draw oil from the oil tank through a non return valve and deliver it to the main pump suction The rest of the oil discharged from the

pump is available for governing and, at a lower pressure, for lubrication.

The cylinder consists of three separate castings, the middle section having two cored belts for steam extraction. The bleed points are D, E, F, and G. The mean diameter of the last stage wheel is about 75 in. and the blade length approximately 20 in.

Fig. 477 shows a two-cylinder 60 MW. General Electric turbine during erection in the works at Erith. There are 20 stages in the h.p. and 6 stages in the l.p. turbine.

308. 120 MW. General Electric Steam Turbine. This is a three-cylinder reheat turbine designed to operate at 3,000 r.p.m. under the following full-load steam conditions—

Initial steam pressure . .	1,500 p.s.i.g.
Initial steam temperature . .	1,000° F.
Reheat steam temperature . .	1,000° F.
Stages of feed-heating . .	6
Final feed temperature . .	435° F.
Vacuum	28·9 in. Hg.

Fig. 478 shows a part sectional drawing of the whole unit, while Figs. 479, 480 and 481 show sections through the h.p., i.p., and l.p. turbines to different scales. The three cylinders contain 9, 13, and 4 stages, respectively.

The high-pressure turbine has a double-shell, both shells being of relatively simple shape. Steam enters the cylinder at A, there being in all four radial pipes arranged symmetrically and provided with piston-ring packing. Steam leaves the h.p. turbine by the branches B and returns to the reheater.

Steam returning from the reheater enters the i.p. cylinder by branches C after passing through the interceptor valves and the reheat emergency valves. The main body of the i.p. cylinder is of very simple shape and is provided with four liners to support eleven of the diaphragms and provide belts for bled steam. Steam leaves the i.p. turbine by way of two side branches D connected to the inlet branches E on the l.p. turbine.

Steam flows in opposite directions through the h.p. and i.p. turbines, and placing the thrust block F between the two turbines ensures the minimum relative axial movement between the rotors and stationary elements of the two turbines at their steam inlet ends.

The method of supporting and locating the casings is similar to that described in the next article for the 200 MW. turbine.

The rotors of both the h.p. and i.p. turbines are machined from solid forgings. The blades are attached by rivets, the drilling of the rivet holes in the rotor being done by a drilling head of special design. Vortex blading is used in all turbines and the resultant steam thrust on the blades is partially balanced by the dummy piston G on the i.p. rotor.

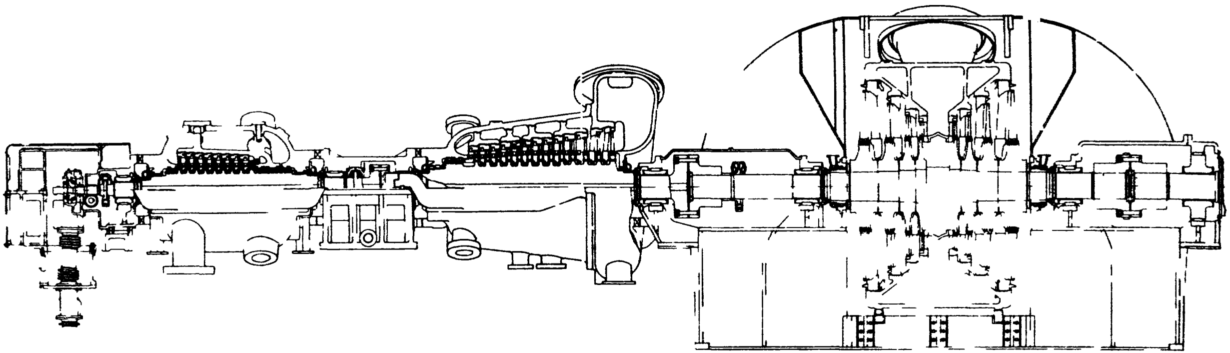


FIG 478 —General Arrangement of G E C 120 MW Turbine

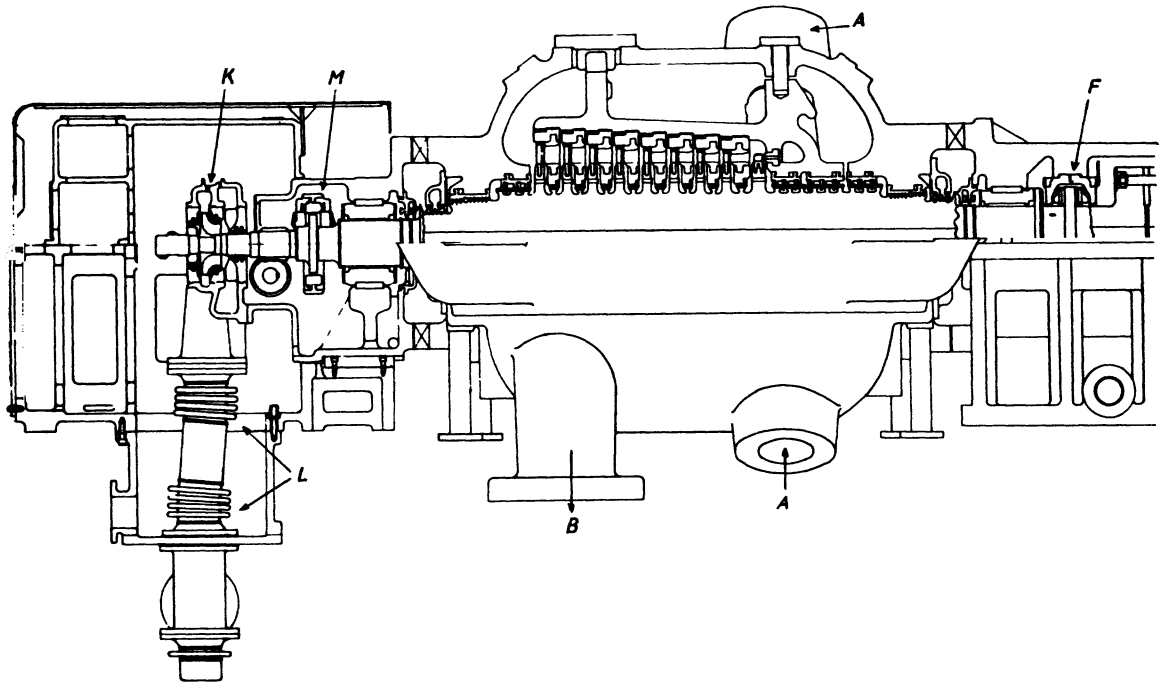


Fig 479 – Section of H P Cylinder of 120 MW G E C Turbine

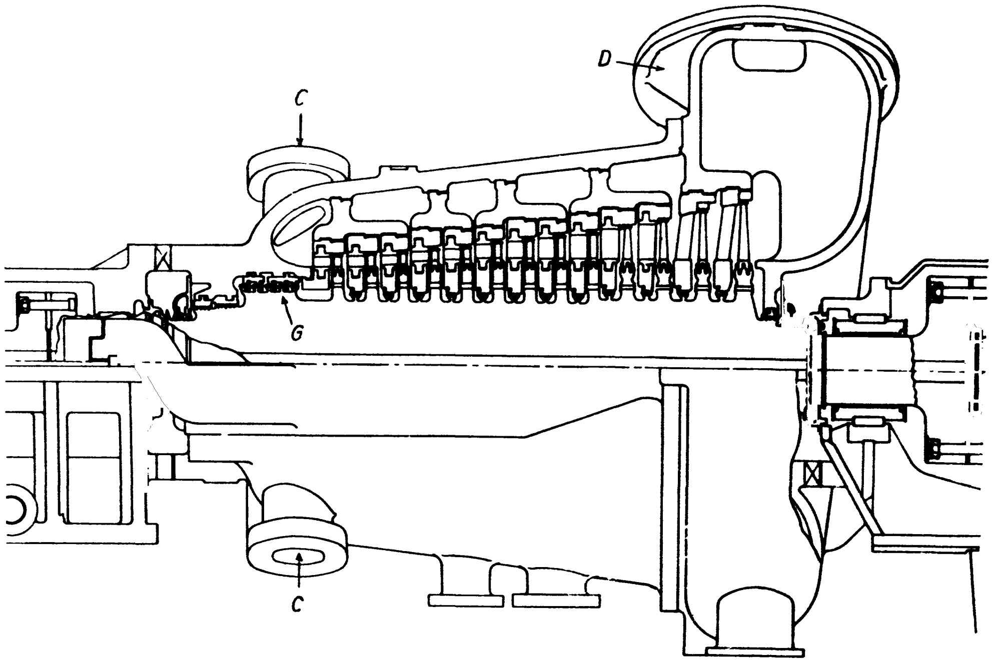


FIG. 480 —Section of I P Cylinder of 120 MW. G.E.C. Turbine

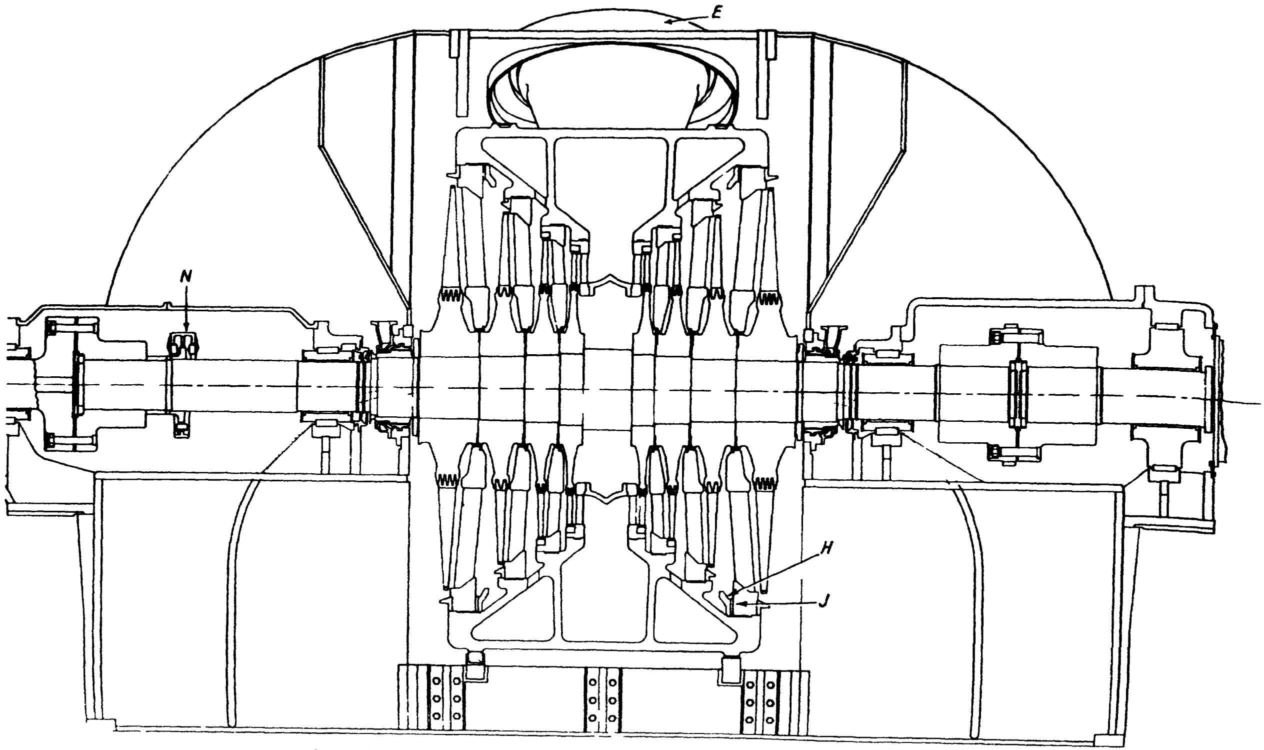


Fig. 481. Section of L.P. Cylinder of 120 MW G.E.C. Turbine

Reference will now be made to the interstage packing and the shaft glands. A section through the former is shown in Fig. 482. The fins are the standard G.E.C. vernier-labyrinth type, one half being carried on the stationary ring A, the other half being turned on a ring B projecting from the surface of the rotor. In the event of accidental rubbing the heat generated in the rotating element is largely confined to the ring B and will not cause bending of the rotor. The undercutting of the ring B not only assists in localizing

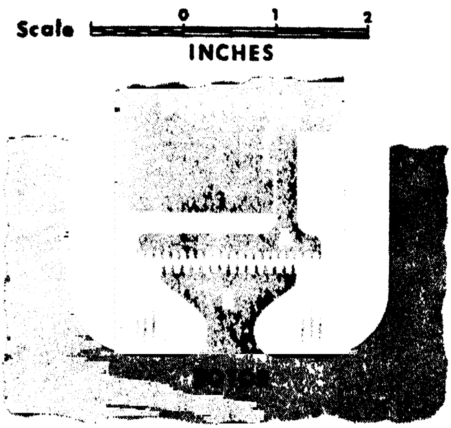


FIG 482.—Diaphragm Packing for Stages with Integral Discs

the heating, but permits the use of a large fillet at the junction of the discs and the shaft. Enough metal is left on B to permit re-turning of the fins in case of damage.

The same general principles are employed in the packing for the shaft glands and balance pistons, as shown in Fig. 483. Each fixed element, except the first, is provided with a baffle which prevents steam which is escaping from each element of packing from impinging on the following element. Experience has shown that, unless the baffle is provided, this action results in unpleasant noise.

The outer casing of the l.p. turbine, Fig. 481, is fabricated from steel plates and is provided with a single exhaust branch on the under side. The inner casing is of cast-iron. In the penultimate stage a ring H is fitted for the purpose of trapping water flung from the blades by inertia. Such water is drained through a series of holes J and ultimately runs into the condenser.

The oil pump K is of the centrifugal type with the impeller mounted direct on the rotor spindle. Steel bellows L in the inlet and outlet pipes allow for forward movement of the pump due to expansion of the h.p. and i.p. turbines. Two indicators M and N

arranged at the exhaust ends of the h.p. and i.p. turbines, respectively, give the differential axial movement between the rotors and pedestals at these points and form part of the supervisory equipment.

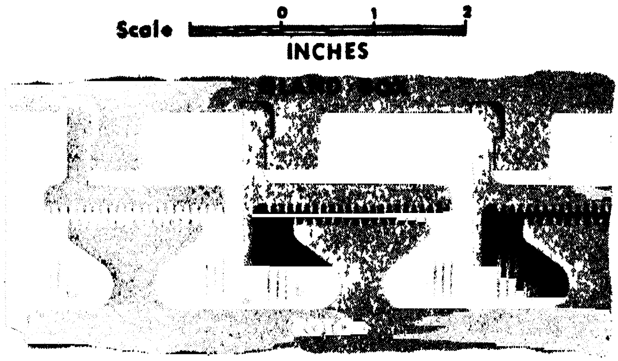


FIG 483. Shaft Glands and Balance Piston in High-temperature Regions

309. General Electric 200 MW. Turbine. This is virtually a four-cylinder turbine operating at 3,000 r.p.m. under the following steam conditions at full load—

Pressure at inlet to h.p. valve chests	2,365 p.s.i.a.
Temperature at inlet to h.p. valve chests	1,050° F.
H.p. turbine exhaust pressure to reheater	490 p.s.i.a.
Pressure at inlet to i.p. casing	441 p.s.i.a.
Temperature at inlet to i.p. casing	1,000° F.
I.p. turbine exhaust pressure to second i.p. turbine	41·2 p.s.i.a.
Pressure at point where flow divides	12·0 p.s.i.a.
Exhaust pressure	28·7 in. Hg.
Stages of feed-heating	6
Final feed temperature	460° F.

Fig. 484 shows the arrangement of the turbine as a whole. On the left is the h.p. turbine, then the i.p. turbine, next a casing containing the two-stage second i.p. turbine and one flow of the l.p turbine, then finally the double-flow l.p. turbine.

The axial location of the whole system of turbine casings is determined by a pair of transverse keys on the feet of the l.p. outer casing adjacent to the end of the single exhaust flange nearest to the i.p. turbine. The bearing pedestal between the l.p. and i.p. casings is rigidly bolted to a fabricated steel framework (shown in Fig. 488) attached to the l.p. exhaust casing containing the first three l.p



FIG 484 —General Arrangement of G E C 200 MW Turbine

stages. The supporting feet at the inlet end of this casing and those at the exhaust end of the i.p. casing rest on the bearing pedestal, level with the centre-line of the machine, but are free to slide both axially and transversely. The i.p. casing is coupled axially to the adjacent l.p. casing.

The intermediate bearing pedestal A, Fig. 485, between h.p. and i.p. casings and the governor bearing pedestal at the exhaust end of the h.p. turbine are rigidly bolted to steel support plates embedded in the foundations. Thermal expansion of the turbine casings is

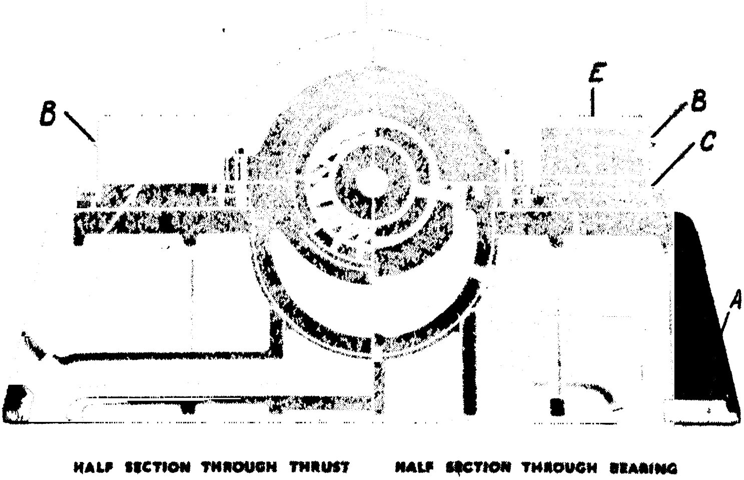


FIG. 485 Intermediate Bearing Pedestal on 200 MW Reheat Turbine

accommodated by resting the casing feet B on inner housings C which carry the bearings and rest on the stationary main pedestals A, just below the turbine centre-line. Thus the sliding surfaces of all casings are in line and this results in smoothness of sliding and minimum risk of misalignment due to axial thrust.

The under surfaces D of the supporting feet at the ends of the h.p. and i.p. casings are brought up level with the centre-line of the turbine. In this way the centre-line of the casings is maintained coincident with the shaft centre over the whole range of casing temperatures. The casings are free to expand laterally on their supporting surfaces and are coupled axially to the inner sliding bearing housings by means of transverse keys E in the supporting feet. Lateral location of the casings is maintained by vertical keys on their central planes.

A single Michell thrust bearing is fitted between the h.p. and i.p

turbine casings and moves axially with the inner casing of the bearing pedestal.

All turbine rotors are coupled together by rigid couplings and their critical speeds are well above the running speed. Apart from the velocity stage in the h.p. turbine, all blading is of vortex design.

The casing of the h.p. turbine, Fig. 486, is of double-shell construction, the steam pressure between the two casings being 490 p.s.i.a. at full load. Steam is led through four radial pipes having piston-ring joints into the nozzle beit of the inner casing. This belt extends around the whole periphery except at the horizontal joint where it is blanked off to relieve the pressure on the inner casing bolting. The blanking walls are faired off against the inlet edges of two diametrically opposite nozzle guide vanes so that a full ring of nozzles is utilized. Full admission must, of course, be employed at all loads.

The complete h.p. rotor is machined from a solid forging. There are 8 stages, the first being a two-row velocity wheel with each row of moving blades on its own disc. The packings used throughout the turbine are similar to those described for the 120 MW. General Electric turbine.

The i.p. turbine, Fig. 487, has 11 stages. The rotor is again machined from a single forging and is provided with a balance piston at the steam inlet end. The cylinder is a cast-steel single shell of simple shape. There are four liners which support the diaphragms. Steam from the reheater enters the casing through four branches.

Fig. 488 gives a section through the second i.p. turbine and the l.p. turbines. Steam from the first i.p. turbine flows into the second through two U-shaped underfloor pipes. After expansion through two stages, the steam flow is divided ; about one-third passes through the three stages on the same rotor and about two-thirds passes through two connecting pipes to the centre of the double-flow l.p. turbine.

A solid forged rotor is used in order to avoid the high stresses which would occur in separate discs already highly stressed due to centrifugal loading and being keyed to shafts transmitting a high torque. The couplings are also forged solid with the shaft.

The l.p. turbine outer casing is fabricated from steel plate and is supported at the ends on feet resting on cast-iron blocks which in turn rest on solid concrete. The side walls of the lower half of the casing are stiffened by rigid girders having a depth equal to the vertical distance between the centre-line of the cylinder and the exhaust flange. The inner casing carrying the diaphragms is of cast-iron.

The blading of the last stages in each of the three exhaust flows has a working length of 30 in. on a base diameter of 60 in. The leaving velocity is 680 ft. per sec. at full load. Fig. 489 shows one of the blades. The blade is 6 in. wide at the root and is attached to

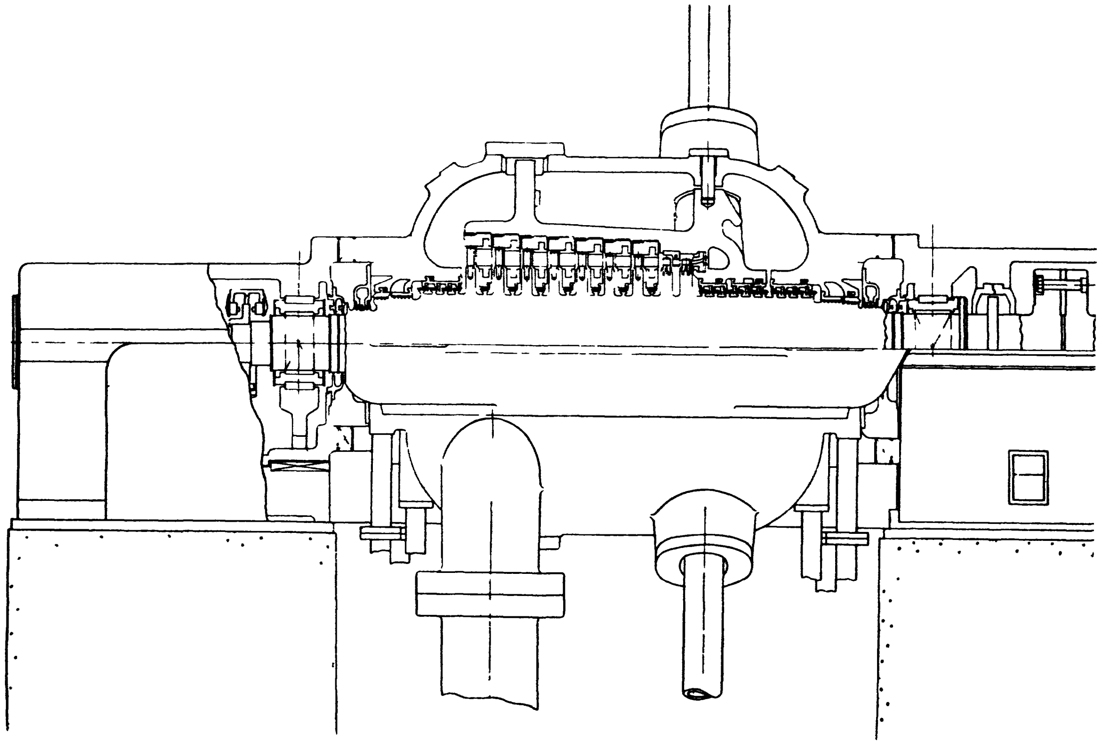


FIG. 486 Section of H.P. Cylinder of G.E.C. 200 MW Turbine

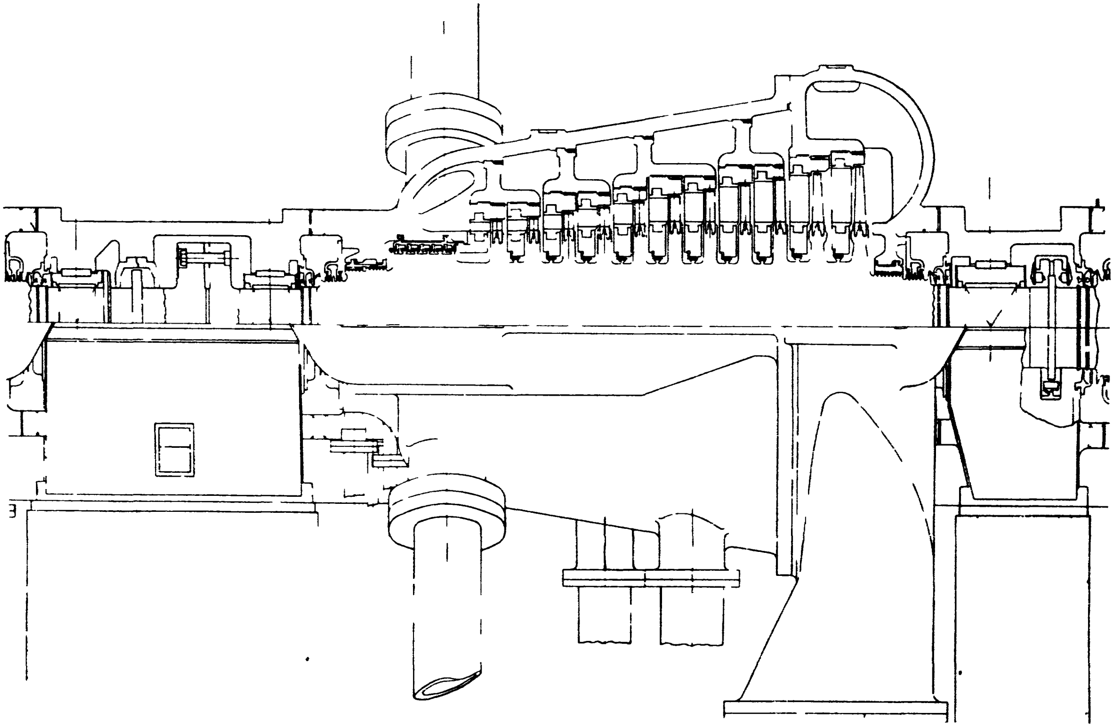


FIG. 487 Section of I P Cylinder of G E C 200 MW Turbine

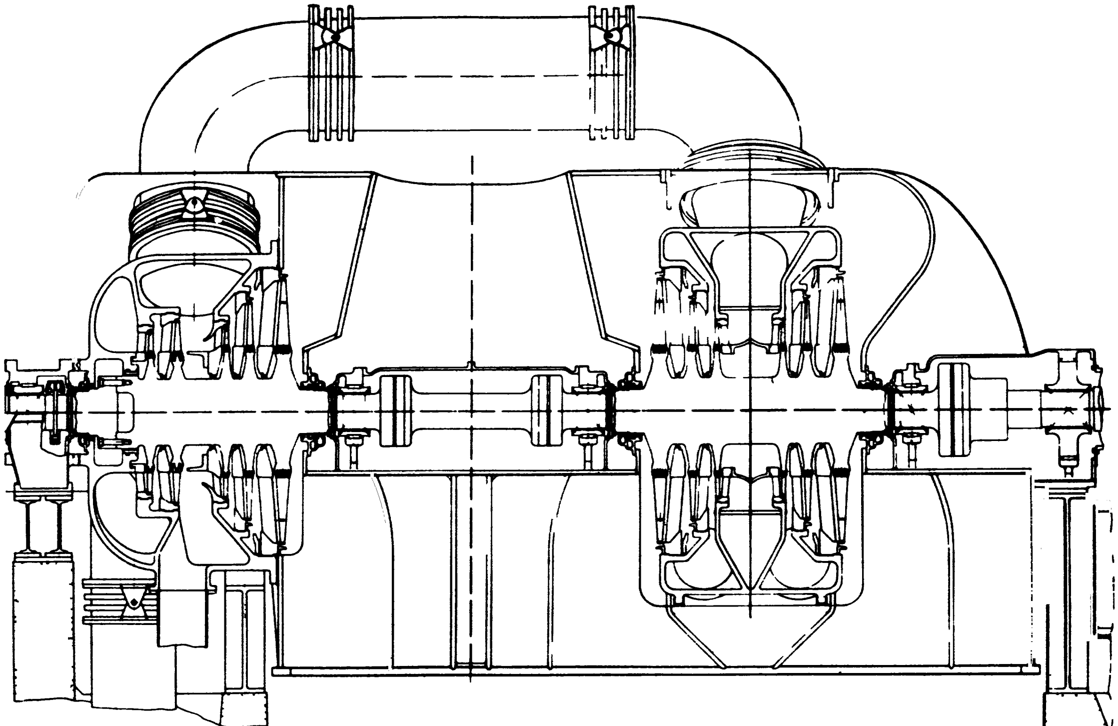


FIG. 488. Section of Second I.P. and L.P. Turbine of G.E.C. 200 MW Turbine

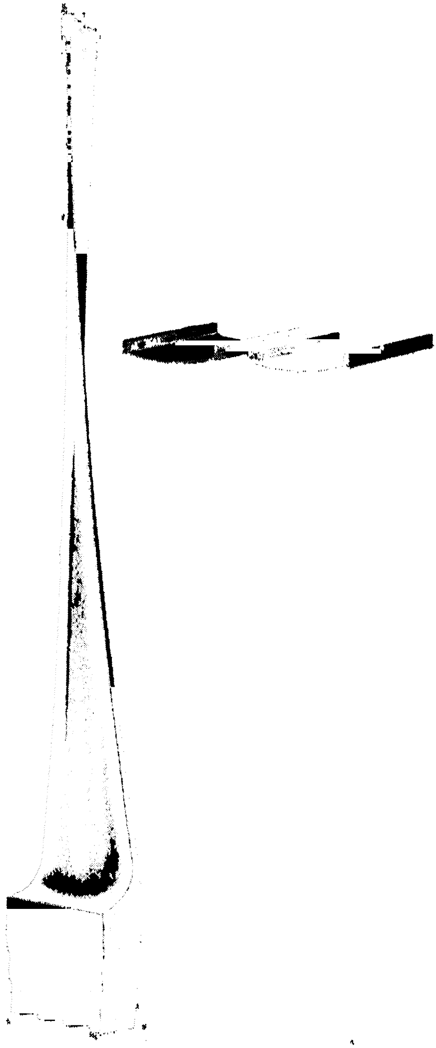


FIG. 489.—Last-stage Blade and Inverted Arch Cover Band, G.E.C. 200 MW Turbine

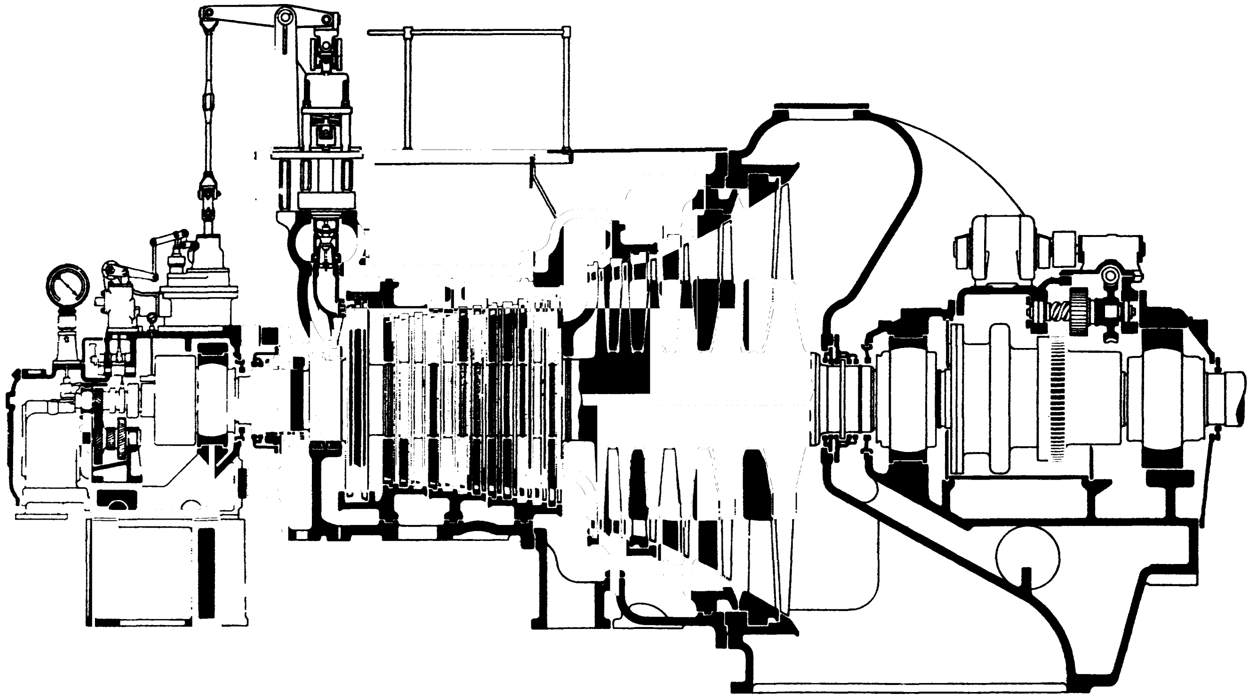


Fig. 490 Metrovick 30 MW Steam Turbine

the rim of the wheel by a multiple-prong riveted type of fastening. The tips of adjacent blades are fastened together by an inverted-arch type of cover band which is secured to the blades by six rivets. There is an increase in the radius of the blade tips due to the increase in the wheel diameter caused by stress, the increase in the blade length due to centrifugal stress, and with vortex flow an increase due to thermal effects. Thus the circumferential distance between adjacent blades must increase. The elasticity of the cover band provides for this, the inertia forces on the arch causing the arch to

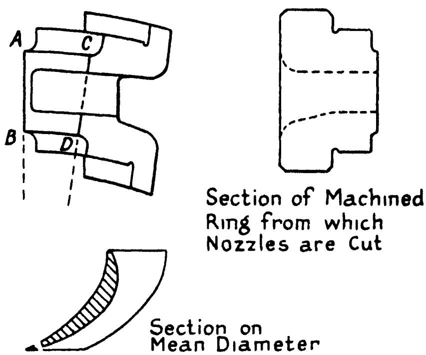


FIG. 491. -Metrovick Slip-in Nozzles

deflect outwards and so increase the distance between the side flanges. The same type of construction is employed for the single row of lacing and avoids the use of brazing or welding.

310. 30 MW. Metrovick Steam Turbine. This turbine constructed by the Metropolitan-Vickers Electrical Co., Ltd. is shown in Fig. 490. It is a single-cylinder machine designed for the following steam conditions—

Stop-valve pressure	900 p.s.i.g.
Stop-valve temperature	900° F.
Vacuum	29 in. Hg.
Number of feed-heaters	4.
Final feed temperature	385° F.

There are 19 stages in all, the first stage being a two-row velocity wheel. The whole rotor is machined from a single forging. The blades for the two-row wheel are carried on a simple disc of uniform thickness, also machined from the rotor forging. The discs for the following twelve stages are of relatively light construction but the wheels for the last six stages become increasingly heavy as the length of the blades increases.

The steam chest is formed integral with the upper half of the h.p. end casing. Steam passing through the throttle valves enters the inserted nozzle box. This is fitted with slip-in nozzles of the type shown in Fig. 491. A ring is machined to the section shown and the nozzles are then cut from this in such a way that the edges AB and CD are radial. The nozzle elements are fitted into a groove in the nozzle box, the ends of the nozzle group being sealed off.

Internal liners are used to support all diaphragms except that for the last stage. This not only simplifies the outer casing but provides steam belts from which steam may be bled for feed-heating. Provision is made for the extraction of suspended moisture flung off the blades in the last few stages.

311. 100 MW. Metrovick Steam Turbine. This is a two-cylinder turbine of the "close-coupled" type, a longitudinal section of which is given in Fig. 492. The steam conditions are as follows—

Stop-valve pressure	1,500 p.s.i.g.
Stop-valve temperature	1,050° F.
Vacuum	28·9 in. Hg.
Number of feed-heaters	6.
Final feed temperature	400° F.

The speed is 3,000 r.p.m. An important feature of this turbine is the fact that there are only three bearings in the turbine proper. The h.p. turbine rotor is supported on two journal bearings A and B, and is coupled rigidly to one end of the l.p. rotor, the coupling C being inside the l.p. cylinder. The remaining bearing is at D. By this construction the overall length of the turbine is considerably reduced. During erection of the turbine it is, of course, necessary to couple the flange at the exhaust end of the h.p. rotor to the facing on the l.p. rotor and then lift the rotor as a whole.

There are 17 stages in the h.p. turbine, the first being a two-row wheel. The double-flow l.p. turbine contains four normal stages and one two-wheel multi-exhaust stage. Both rotors are machined from solid forgings. A low-pressure unbladed rotor of similar design but for a 60 MW. Metrovick turbine is shown in Fig. 493.

Because of the high initial steam pressure the h.p. turbine cylinder is of double-shell construction, the space around the inner shell being subjected to the steam pressure in the ninth stage. Steam which has passed the governor valves enters the inner cylinder through four radial steam pipes. One of these is shown in detail in Fig. 494. The steam pipe A is screwed into and welded to an element B carrying a flange ring C. The whole is designed to provide flexibility between the flange ring and the joint face and accommodate differential expansions. A flange ring D is screwed on to the extension pipe E which enters a boss F on the inner shell. Piston rings allow for relative movement while minimizing steam leakage. Screws G are provided for withdrawing the pipe E from the inner shell.

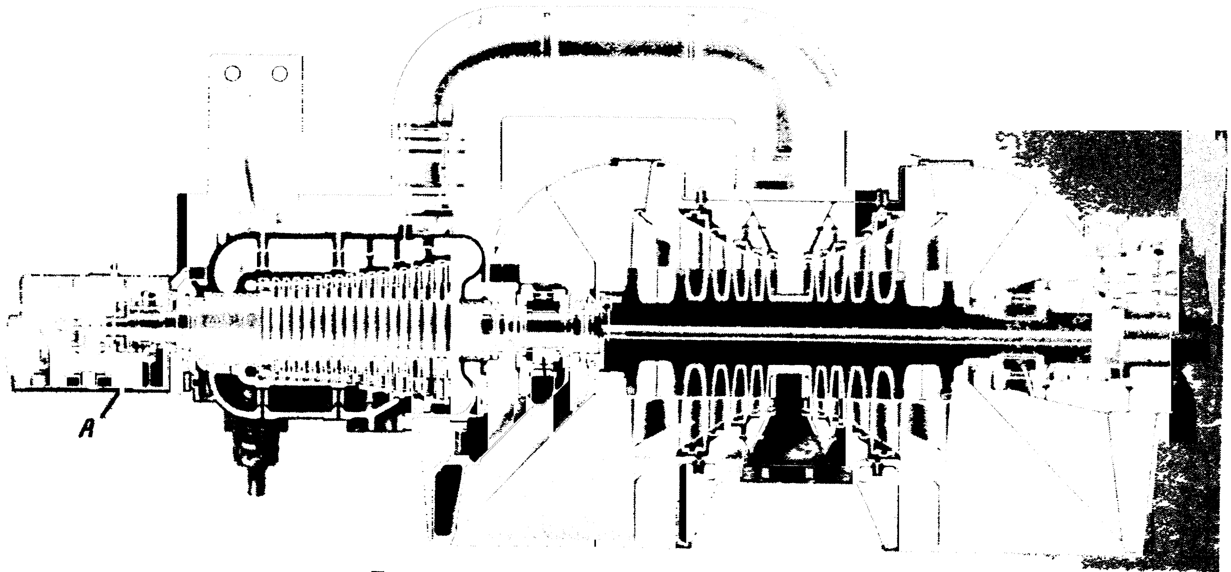


FIG 492 Metrovick 100 MW Steam Turbine

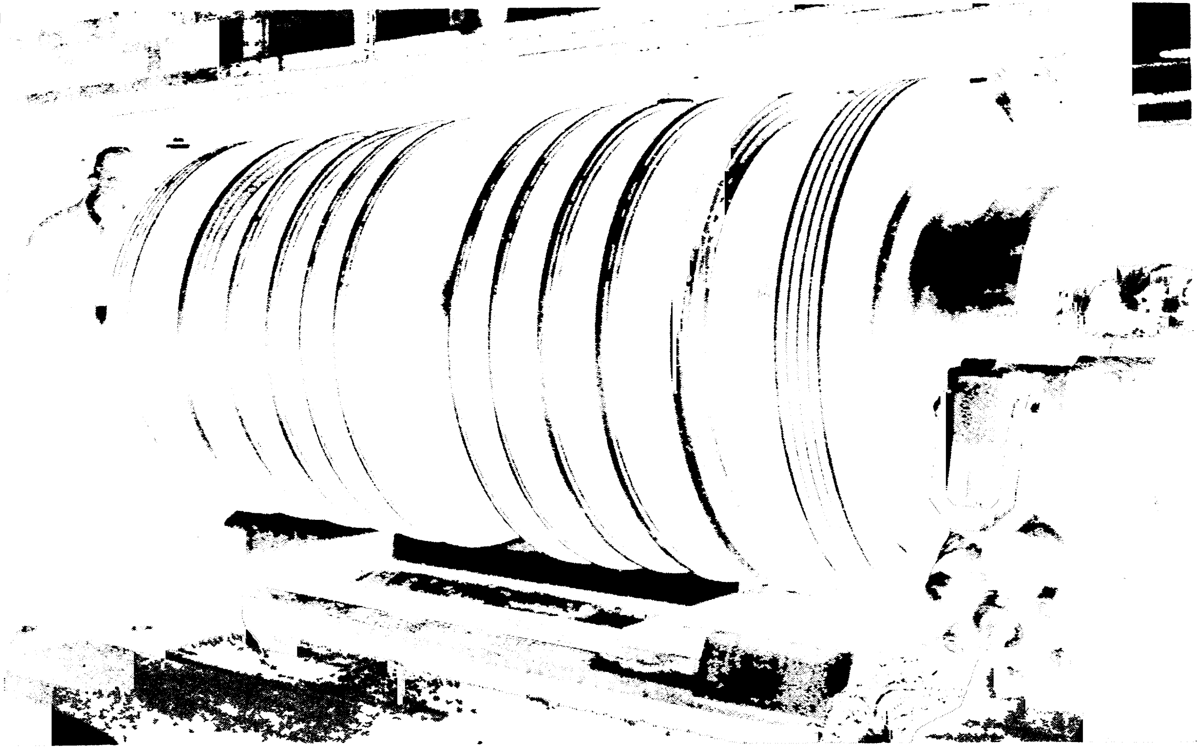


Fig. 493. Unbladed Rotor for Double-flow I.P. Turbine of 60 MW Output

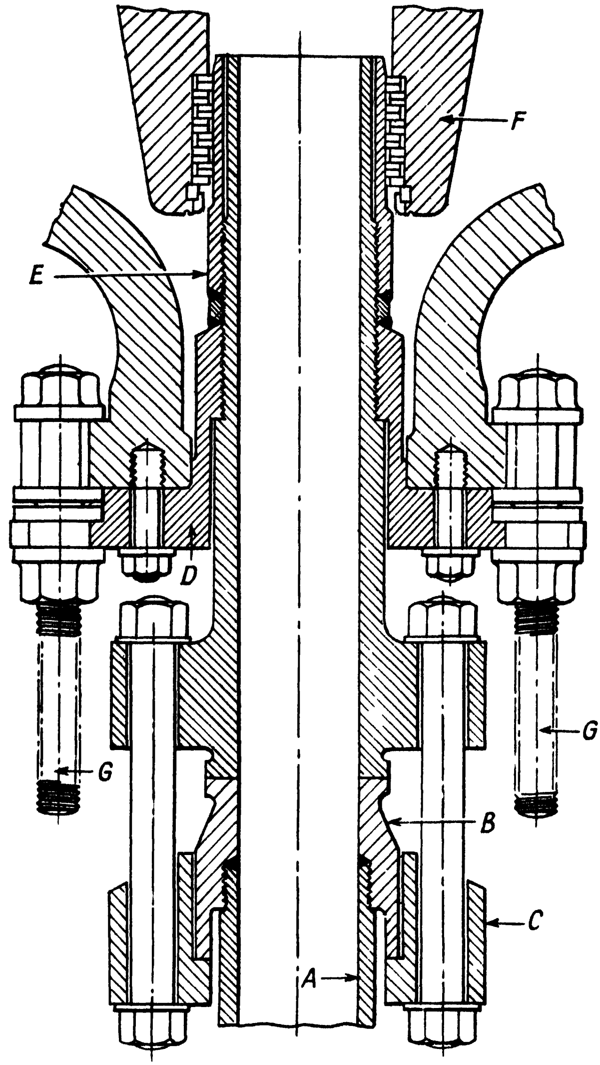


FIG. 494 Radial Steam Pipes for H P Cylinder

The high-pressure cylinders are of cast alloy steel; the low-pressure cylinder is mainly fabricated, the only cast parts being the liners for carrying the diaphragms.

At the inlet end of the h.p. turbine there is a long labyrinth gland providing in all about 200 throttlings, while at the l.p. end there is a similar gland with about 54 constrictions. Water seals at each end

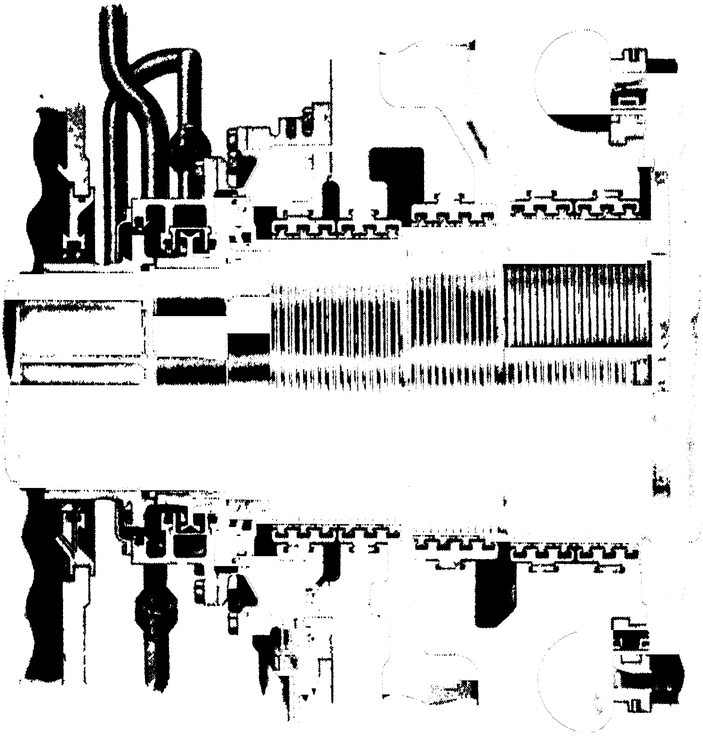


FIG. 495 Shaft Gland for 60 MW H P Metrovick Turbine

of the h.p. turbine prevent leakage of steam into the turbine room Similar hydraulic seals are used at each end of the l p. turbine.

A somewhat similar high-pressure shaft gland, in this case for a 60 MW. turbine, is shown in Fig. 495. There are three groups of packing with three leak-off connections. Baffle rings are turned on the rotor spindle and the gland elements, of the spring-back type provide in all 144 constrictions. On the bearing side of the gland may be seen the runner and casing for the hydraulic seal.

312. Parsons 60 MW. Turbine. A compact two-cylinder Parsons turbine to develop 60 MW. at 3,000 r.p.m. is illustrated in Figs. 496

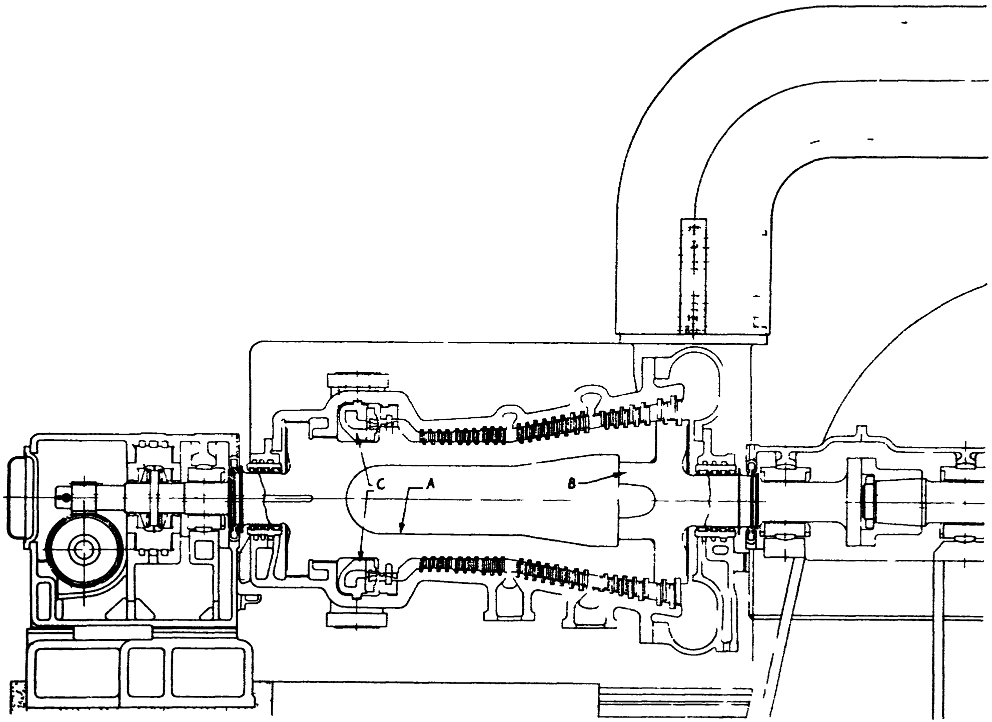


FIG 496 —Parsons 60 MW Turbine Section through H P Turbine

and 497. The high-pressure turbine comprises a two-row velocity wheel in the first stage followed by 25 stages of reaction blading, the first 18 of these being end-tightened. The low-pressure turbine has 9 stages in each flow.

The h.p. rotor consists of a hollow forging A integral with the shaft at the high-pressure end and a forging B integral with the shaft at the low-pressure end and spigoted and shrunk into A. It is further secured by bolts and, in addition, driving dowels are fitted. Two dummy balance pistons are provided. The l.p. rotor consists of a shaft on to which two sets of six heavy-section wheels are shrunk.

The h.p. cylinder is an alloy steel casting. Steam at the initial pressure and temperature is confined to separate cast alloy steel nozzle boxes C, arranged symmetrically in the upper and lower halves of the cylinder. The inlet pipes of the nozzle boxes are welded to the inlet branches on the cylinder castings. The central part of the l.p. cylinder is a casting while the two exhaust ends are fabricated. Chambers D and E are formed for the collection of bled steam. Grooves F are provided in the penultimate stage for the collection of water drops thrown off the blades.

The axial position of the rotors is governed by a single Michell thrust bearing at the steam end of the h.p. turbine. The rotors are coupled by rigid couplings.

313. 125 MW. Parsons Steam Turbine. Figs. 498, 499 and 500 show longitudinal sections through a three-cylinder Parsons turbine designed to develop a maximum and economic power of 125 MW at 3,000 r.p.m. The steam conditions at full load are as follows—

Initial steam pressure	1,425 p.s.i.g.
Initial steam temperature	1000° F.
H.p. turbine exhaust pressure	400 p.s.i.g.
I.p. turbine inlet pressure	360 p.s.i.g.
I.p. turbine inlet temperature	1000° F.

The high-pressure turbine cylinder is of the double-shell type, transverse sections being given in Figs. 501 and 502. The inner cylinder is maintained concentric with the outer cylinder by means of radial pins and keys. Steam is admitted through four pipes A, Fig. 501, bolted to the outer casing by means of a flange B which is welded to a petticoat which, in turn, is welded to the pipe. The pipe extends radially inwards and passes through a gland in the inner casting to the nozzle box C. There are no nozzle control valves and the impulse stage operates with the maximum arc of admission. Following the two-row wheel there are 11 stages of end-tightened reaction blading. Steam exhausted from the h.p. turbine passes through two branches D in the lower half of the casing on its way to the reheater.

Steam from the reheater enters the i.p. cylinder through two branches E in the lower half, and two similar branches F in the upper

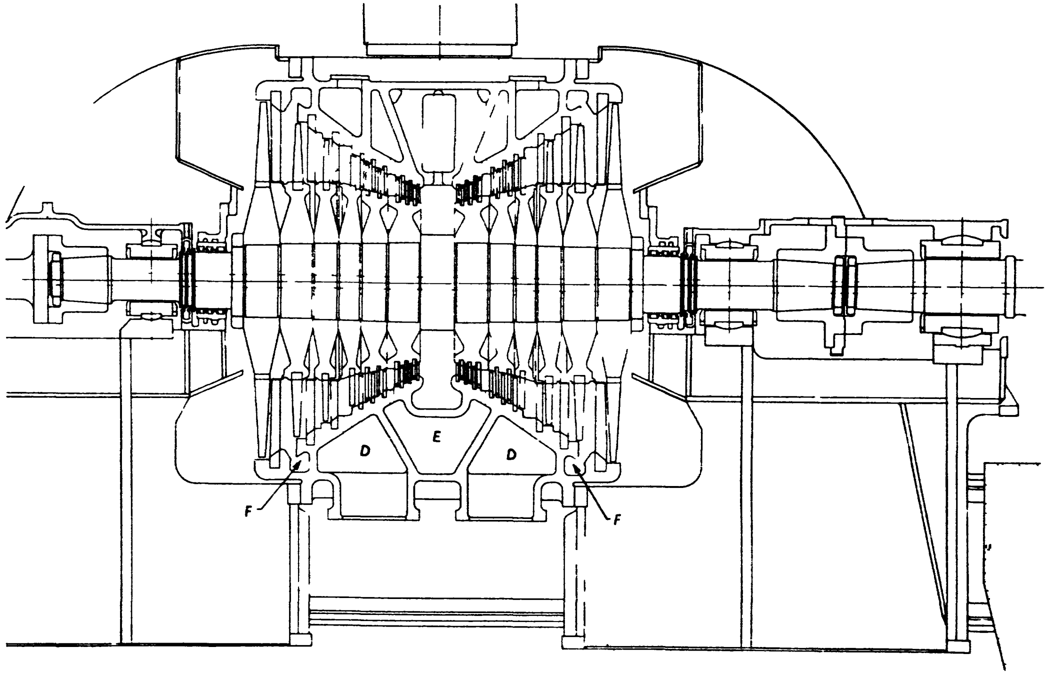


FIG 497 —Parsons 60 MW Turbine Section through L P Turbine

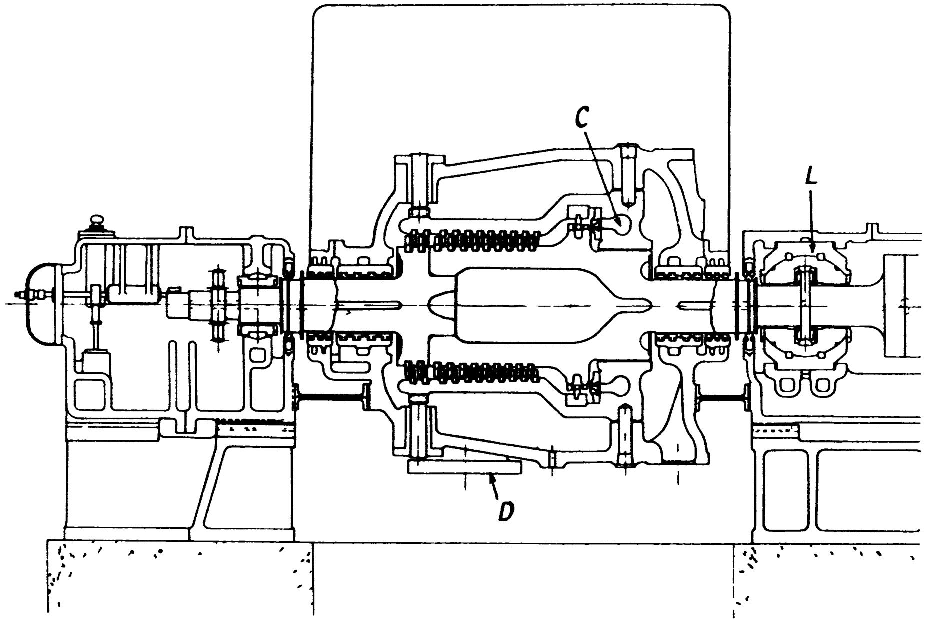


Fig 498 —Parsons 125 MW Turbine Section through H P Turbine

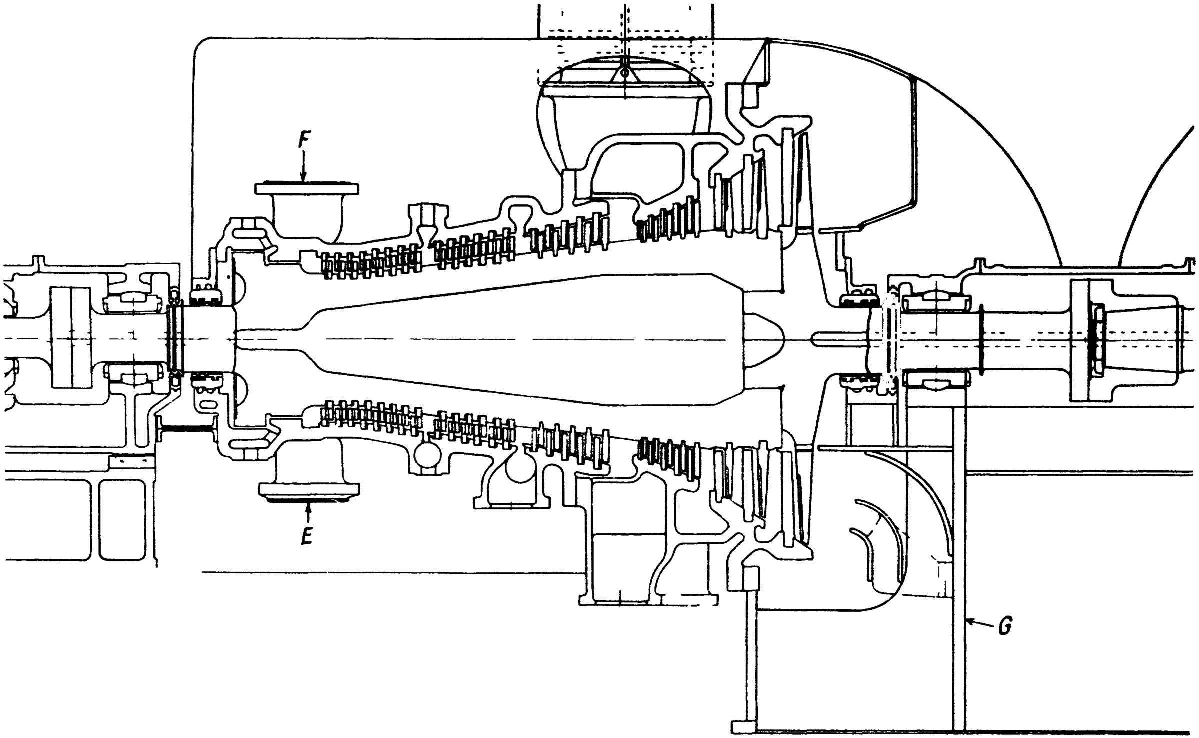
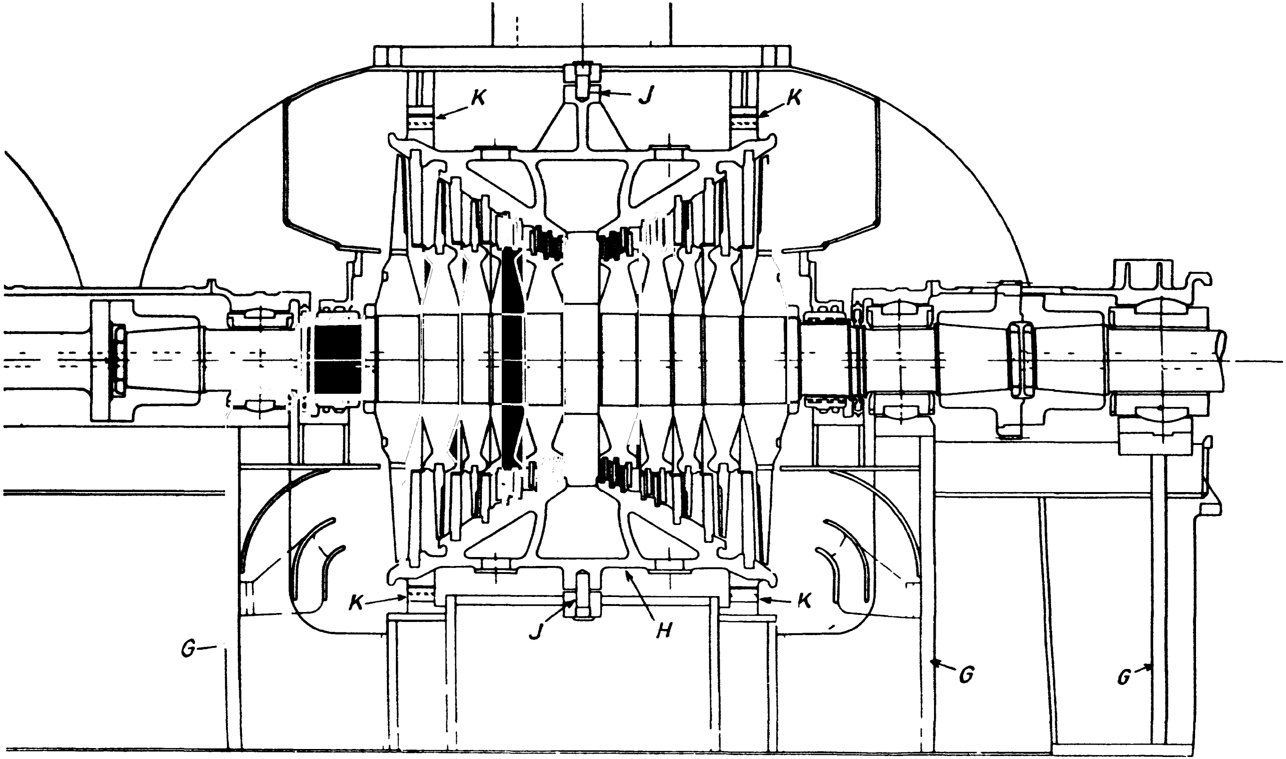


Fig 499.—Parsons 125 MW Turbine: Section through I P. Turbine



Fi 500 I 125 MW Unit Section through L P Turbin

half of the cylinder. There are 19 stages of reaction blading in the i.p. turbine proper, the first 14 stages being end-tightened.

At full load, the steam pressure at outlet from the 19th stage is about 20 p.s.i.g. and at this point the flow is divided, one part passing through low-pressure blading on the i.p. rotor, the remainder

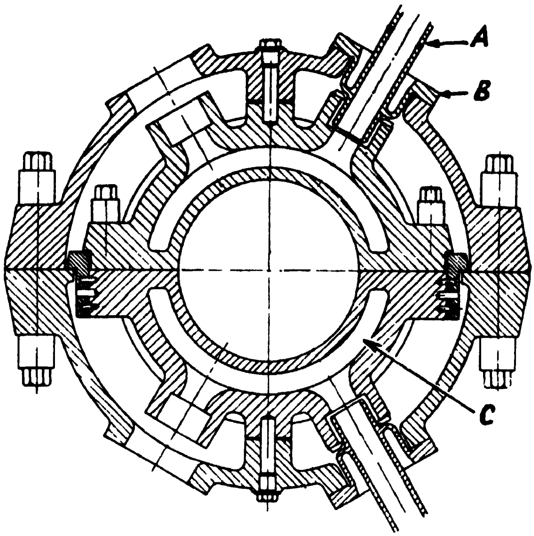


FIG. 501 — Transverse Section through Nozzle Box of H.P. Parsons Turbine

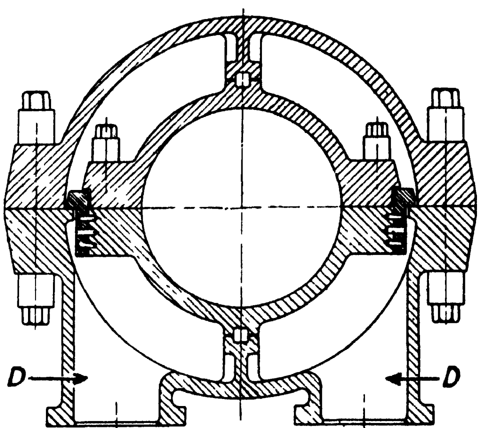


FIG. 502.—Transverse Section through Outlet End of Parsons Double-shell H.P. Turbine

passing through two connecting pipes to the centre of the double-flow l.p. turbine.

The exhaust hood at the end of the i.p. cylinder and the outer casing of the l.p. turbine form one large fabricated housing with a single exhaust outlet. The lower half of this housing forms a strong structure which supports the weight of the l.p. turbine. Strong transverse members G support the bearings. A cast centre H in the l.p. turbine which carries all the fixed blades is located centrally by means of radial pins J and keys K.

Hollow forged rotors are employed in the h.p. and i.p. turbines and rigid couplings are used throughout. The steam ends of the h.p. and i.p. turbines are adjacent to each other and the combined journal and thrust bearing L is arranged between them, so that axial differential expansion between rotating and stationary elements in the two turbines will be a minimum. One dummy balance piston is arranged in the h.p. turbine and two in the i.p. turbine. Provision is made for the drainage of moisture flung off the blades in the penultimate stage of the l.p. turbine and erosion shields are provided on the blades of the last three stages.

314. 60 MW. Richardsons Westgarth-Brown Boveri Steam Turbine. The following description refers to the second of three Richardsons Westgarth-Brown Boveri turbines installed in Portobello power station, Midlothian. This is a cross-compound steam turbine of somewhat unusual design. The output is 60 MW. at 3,000 r.p.m. under the following steam conditions.

	Steam pressure lb./sq. in. abs.	Steam temperature °F.
Stop valve . .	1,360	950
First stage . .	1,095	906
H.p. turbine exhaust	512	708
I.p. turbine inlet .	498	706
I.p. turbine exhaust .	124	410
L.p. turbine inlet .	122	400
Vacuum . . .	29·1 in. Hg.	

There are six stages of feed-heating, the condition of the steam at the heater inlets being as follows—

Heater No.	Steam pressure lb./sq. in. abs.	Steam temperature °F.
1	398	657
2	210	514
3	124	410
4	49·8	280
5	17·1	220
6	3·98	153

There is no reheating.

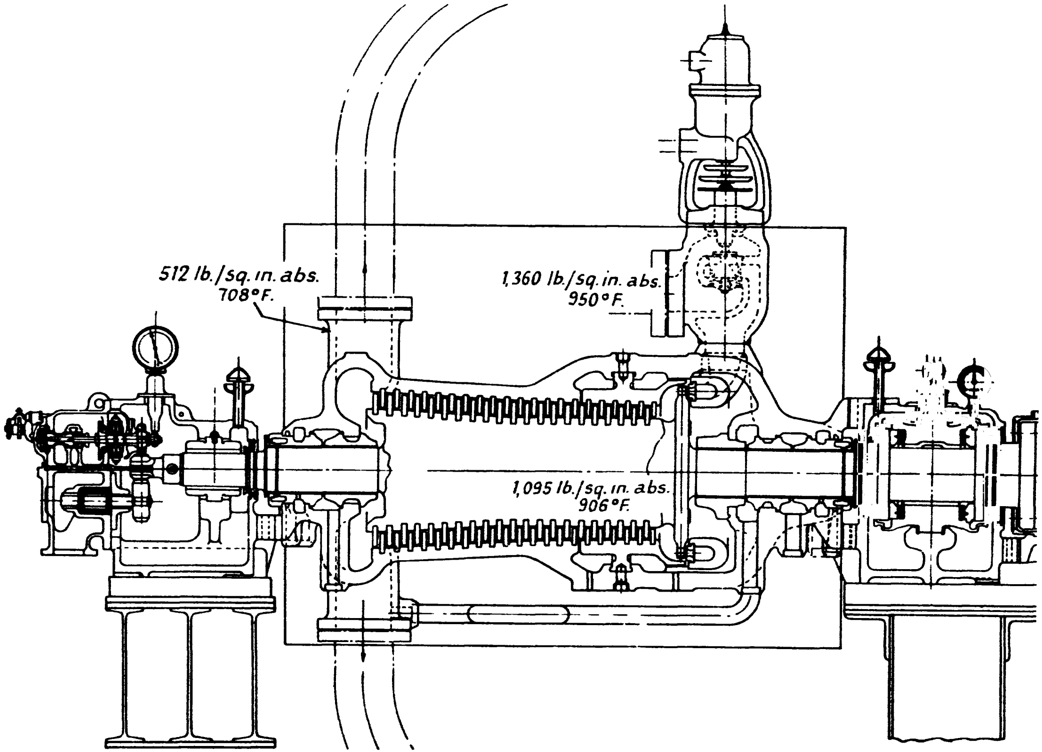


FIG. 503.—Richardsons Westgarth 60 MW. Turbine: Section through H.P. Turbine

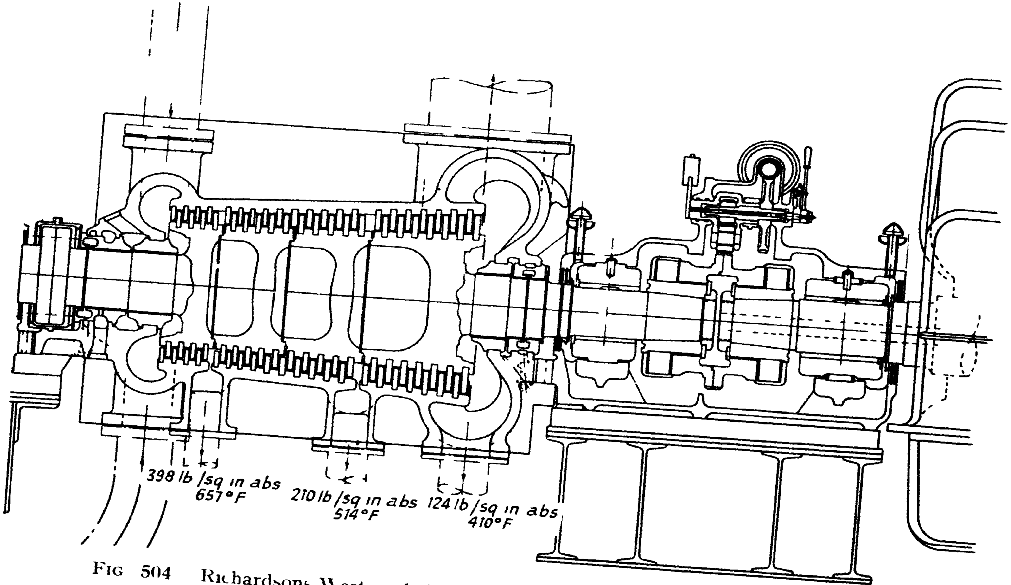


Fig. 504. Richardsons Westgarth 60 MW Turbine. Section through I.P. Turbine

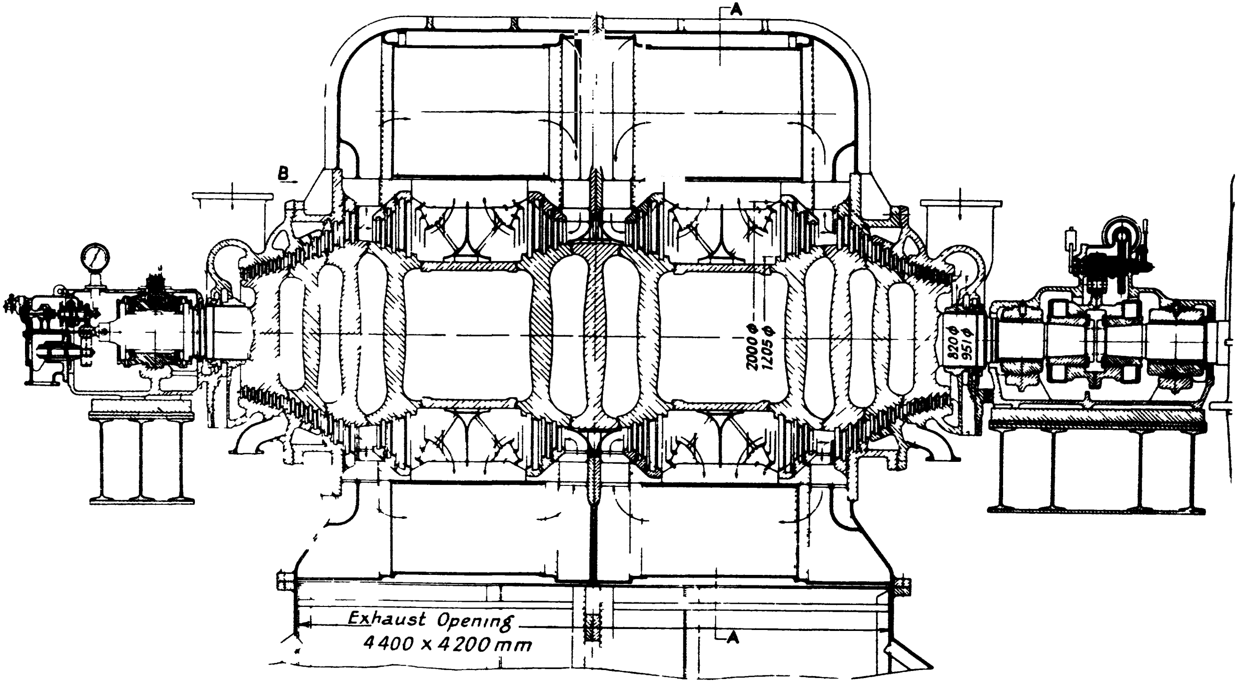


FIG. 505. Richardsons Westgarth 60 MW Turbine. Section through I. P. Turbine

The cross-compound arrangement was used because of space considerations in the power station. The h.p. and i.p. turbines are on one line and the l.p. turbine on the other.

Figs. 503 and 504 show sections through the h.p. and i.p. turbines respectively. There is an impulse wheel 30 in. diameter in the first stage of the h.p. turbine. All the rest of the blading operates on the reaction principle. Steam flows in the h.p. and i.p. turbines are

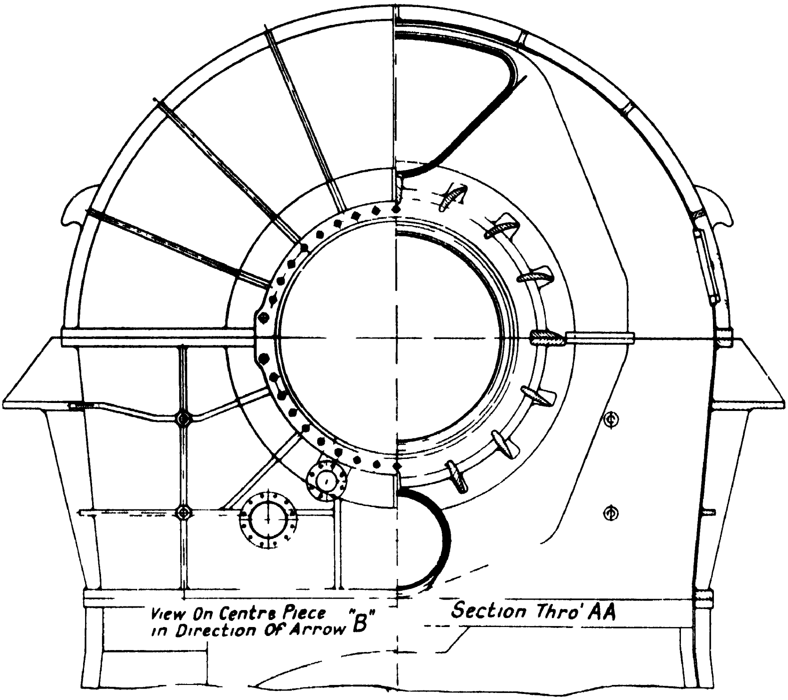


FIG. 506.—Richardsons Westgarth 60 MW Turbine. Half End View and Half Section through L.P. Turbine

opposite in direction and the steam thrusts on the two rotors and blading are practically balanced. A Michell thrust bearing with two collars is combined with the centre journal bearing and serves to locate the axial position of the rotor. By placing the thrust bearing between the steam ends of the two turbines the relative axial movement between the stationary and moving elements under change of load conditions is reduced to a minimum.

The high-pressure turbine rotor is a solid ferritic forging of low carbon vanadium steel. The impulse blades are welded to the rotor. The i.p. turbine rotor consists of a number of nickel steel forgings

which are spigoted together and welded (see Art. 198). Both rotors have 21 reaction stages and the two turbines together develop approximately 30 MW.

The l.p. turbine is shown in longitudinal section in Fig. 505, while Fig. 506 gives two transverse sections through the turbine. The whole machine comprises two single-flow turbines with 13 stages at each end with steam flows in opposite directions and in

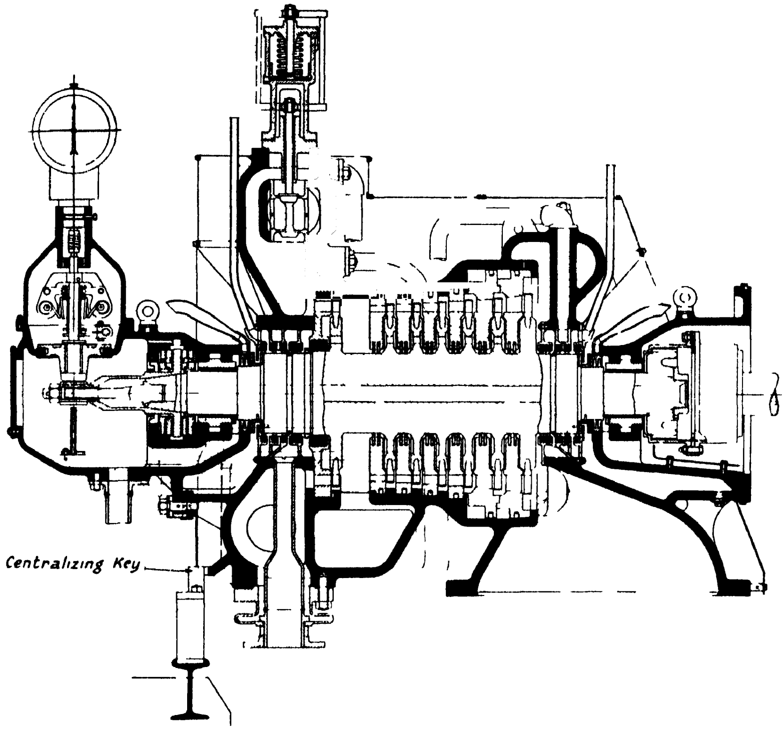


FIG. 507 Back-pressure Turbine Constructed by the Brush Electrical Engineering Company, Ltd

which steam is expanded at full load from 122 to 3·98 lb. per sq in. absolute, and four single-flow turbines, each with three reaction stages in which steam is expanded from 3·98 to 0·44 lb. per sq. in. absolute. In other words, the first 13 stages are arranged as a double-flow turbine and the last 3 as a quadruple-flow turbine. The ducts for conveying one-eighth of the total steam to the innermost stages are shown in Figs. 505 and 506.

The outer casing of the centre part of the l.p. turbine is fabricated, while the end cylinders and the inner parts of the centre section which carry the fixed blades are of cast-iron.

Particulars of the last-stage blading of this turbine are given in Tables XXXVA and XXXVB. Tests were made on the first of these turbines in November, 1953. During that month the electricity sent out amounted to 41·88 million kWh. and the coal consumption was 18,023 tons, or 0·964 lb. per kWhr. As the calorific value of the coal was 11,054 B.Th.U. per lb., the overall thermal efficiency was 32·0 per cent.

315. Brush Back-pressure Turbine. The purpose of back-pressure turbines has already been outlined in Chapter XVII and it will suffice to give a few examples of construction.

A back-pressure turbine constructed by the Brush Electrical Engineering Co., Ltd., is shown in Fig. 507. This is supplied for powers up to 3,500 kW. and is designed for a speed of 10,000 r.p.m. reduced by gearing to a speed suitable for the driven machine. There are seven stages with blades designed for vortex flow. The blades are of stainless material and are provided with serrated integral roots.

Up to about 80 per cent of the maximum continuous rating, steam is admitted to the turbine through a number of nozzle control valves controlled by the speed governor through the customary oil relay. For loads in excess of this, an automatic by-pass admits steam to the second stage nozzles.

316. Escher Wyss Back-pressure Turbines. Reference will first be made to an interesting turbine constructed in 1925 by Escher Wyss and Co., Zürich, for the Siemens-Schuckertwerke, Berlin, to operate in conjunction with an experimental Benson boiler. The following particulars relate to the operating conditions, etc.—

Output (D.C. machine)	1,000 kW.
Initial steam pressure	1,415 lb./sq. in. (abs.)
Initial steam temperature	750° F.
Exhaust pressure	200 lb./sq. in. (abs.)
Turbine speed	10,000 r.p.m.
Generator speed	3,000 r.p.m.
Mean diameter of 1st stage	6·7 in. (u = 293 ft./sec.)
Mean diameter of 9th stage	10·6 in. (u = 464 ft./sec.)
Nozzle height, 1st stage	0·12 in.
Nozzle height, 9th stage	0·27 in.

There are many interesting features about this turbine. The casing is made in two parts; the main part is one piece of forged steel without any horizontal joint; the exhaust end is also a single piece steel casting. Such a cylinder construction eliminates the difficulty of sealing the horizontal joint and also gives a symmetrical casing which is not likely to give trouble due to distortion. To insert the turbine rotor and diaphragms, the casing is set up with its axis vertical and these parts are inserted into the open end.

The small height of the nozzles called for very careful machining

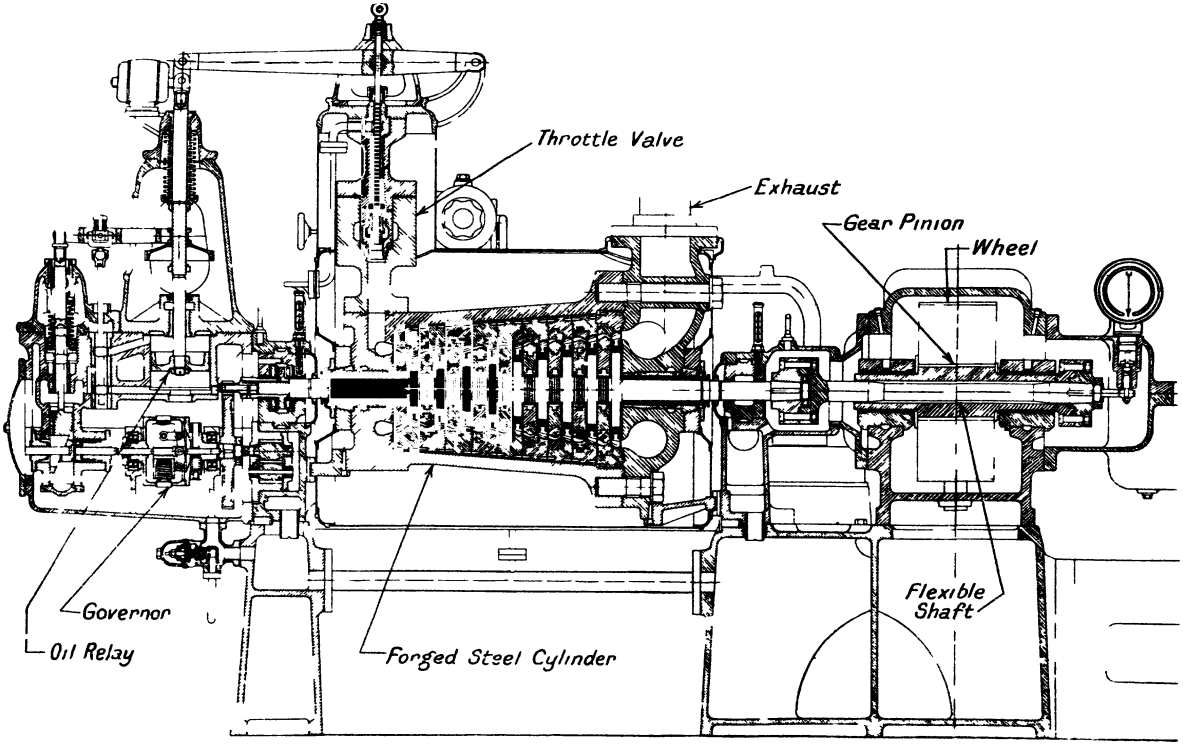


FIG 508 —Sectional Elevation of Escher Wyss H P Primary Turbine
Initial pressure = 1 415 lb per sq in abs Exhaust pressure 220 lb per sq in abs 1 000 kW

The nozzles are made in single pieces, machined on all surfaces and held together by means of rings. To avoid leakage, the joints between the individual pieces are welded. The diaphragms are provided at their periphery with resilient supports in order to permit of their expansion in the cold casing when the turbine is being warmed up. The supports may be seen in Figs. 509 and 510.

Attention is drawn to the curved shape of the longitudinal section of the nozzles (see Fig. 509). This shape has been adopted to ensure

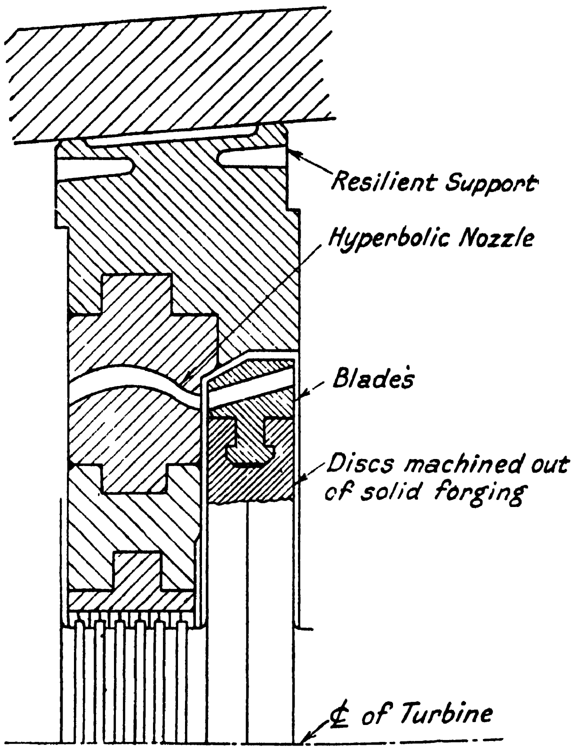


FIG. 509.—Half Section through One Stage of Escher Wyss Primary Turbine

that the steam issuing from the nozzles will fill the blade channel at inlet and flow in at right angles to the inlet edge of the blade. The theory underlying this construction is already given in Art. 170

The h.p. gland has to pack against the exceptionally high pressure of 1,220 lb. per sq. in., and the gland loss on test proved to be 925 lb. per hour. In order to limit the gland leakage losses to a reasonably small value, the shaft diameter had to be kept as small as possible, and to this end a flexible shaft is used having a critical speed of

2,800 r.p.m. The operating speed is therefore 3·57 times the first critical speed. To give the shaft the adequate support necessary for satisfactory running, each bearing is provided with two short bearing surfaces. This is used in preference to a long bearing which might cause excessive heating of the oil. At the high-pressure end of the turbine, the Michell adjusting block is conveniently arranged

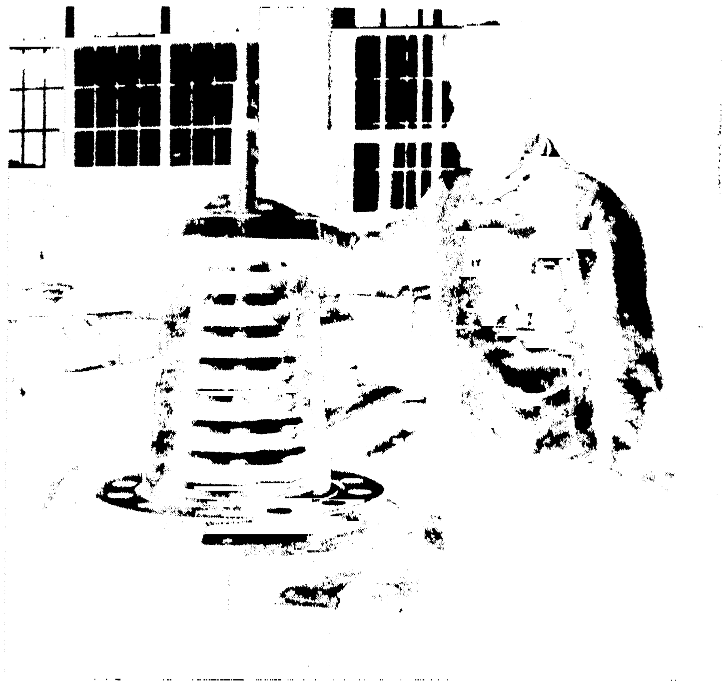


FIG 510—View of Partially Assembled Escher Wyss Primary Turbine

between the two halves of the journal bearing. It is said that the transition through the first critical speed is hardly discernible.

Very comprehensive tests were carried out on this experimental turbine, the efficiency ratio being determined both by measuring the turbine output and by deducing the actual heat drop from observations of the steam admission and exhaust pressures and temperatures. An internal efficiency ratio of 64 per cent was recorded, and deducting 7 per cent for gearing and gland losses, the overall efficiency ratio of about 57 per cent was obtained, which, in view of the extremely small nozzle and blade heights and the high pressure, must be regarded as a satisfactory result. Some idea of the small dimensions of the turbine may be obtained from Fig. 510.

The turbine now to be described is also a back-pressure unit

constructed by Escher Wyss and Co. for the Spulen and Hülsenfabrik Emil Adolff in Reutlingen and put into operation in 1953. When compared with the 1,000 kW. turbine just described and put into operation in 1925, it serves to show the considerable progress made in the use of high-temperature steam. The operating conditions are as follows—

Output	3,000 kW.
Initial steam pressure . .	100 atm.
Initial steam temperature . .	600° C. (1,112° F.)
Exhaust pressure . . .	11 atm.
Turbine speed	10,000 r.p.m.
Steam flow	25 tons per hour.

A section through the turbine is shown in Fig. 511. There are nine impulse stages. Because of the small steam flow the speed of rotation was made 10,000 r.p.m. In spite of the resulting small diameter of the wheels, the blade heights are still very small. All stages have full admission, except the first.

The rotor is an austenitic steel forging and the cylinder an austenitic steel casting. The cylinder has a flanged joint with austenitic bolts. Provision is made for heating the flanges externally by a system of pipes forming a screen at the side of each flange, steam being circulated through the pipes during the heating period.

In order to avoid unsymmetrical heating of the cylinder when starting, the turbine was made as symmetrical as possible, steam being supplied through two pairs of control valves, one pair on the top and the other pair on the bottom of the cylinder. Furthermore, steam is exhausted through two similar pipes, one on each half of the cylinder.

In order to protect the spindles of the control valves from the steam at 1,112° F., steam is supplied at A from a stage of the superheater where the steam temperature is 450° C. (842° F.). The cooling steam escapes from B. The spindle and glands are cooled by steam which is extracted from the turbine after the first stage through the pipe C, from whence it passes through a heat exchanger placed in the exhaust steam pipe before entering the pipe D leading to the interior of the shaft gland.

In order to avoid expansion difficulties the diaphragms and glands are also made of austenitic steel.

317. Marine Turbines. The marine steam turbine power plant presents many special problems in design, and in the following brief notes only a few outstanding matters will be mentioned.

The most efficient speed of rotation of the screw propeller depends on a number of factors but is always very low compared with the customary rotational speeds of steam turbines. In consequence it is advantageous to couple the turbine and propeller shafts through

reduction gearing. In general, current practice is to employ double-reduction gearing of the double-helical type.

The turbine may have one, two or three cylinders in series, the arrangement adopted depending on the total power, the initial

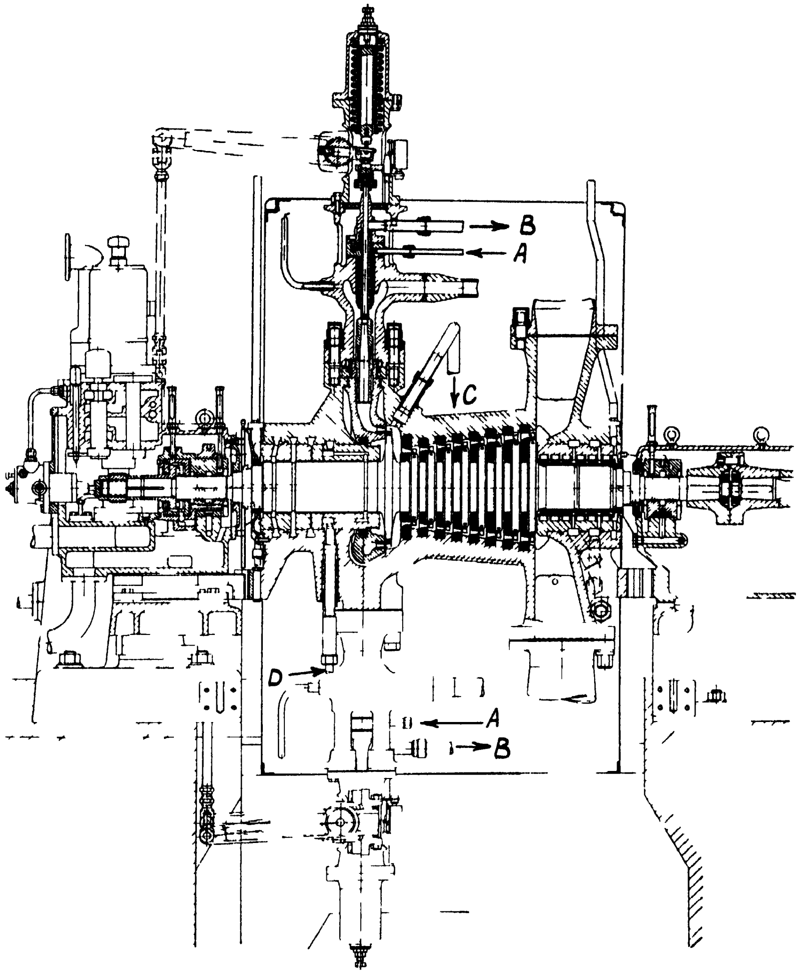


FIG. 511. Escher Wyss Back-pressure Turbine for Steam at 100 atm and 1,112° F.

steam pressure and temperature and, to some extent, on the loading of the gear teeth. As in land practice, higher steam conditions would be employed with higher powers, but as reliability is of such paramount importance in marine work it is probable that at any stage

of development steam pressures and temperatures used in marine turbines will be lower than those used in land installations of similar power.

When two or three turbines are used in series, different ratios of speed reduction are both possible and advisable. Thus, it is generally advantageous to use a high speed of rotation for the high-pressure turbine; this leads to a reduction in the mean diameter of the blade rings and yields a blade length which is not too small in relation to the rotor diameter. On the other hand, the requirements of steam flow through the last stage of the low-pressure turbine lead to a larger mean diameter and a lower speed of rotation.

It is, of course, necessary to provide an astern turbine or turbines. For economic reasons the astern turbine cannot be made as efficient as the ahead; the astern stages are much fewer in number and, in consequence, the "K" value is much smaller than the ahead figure. The nozzles of the astern turbine are usually designed to pass the same total quantity of steam as the ahead nozzles and, depending on the K value, the astern power available may vary from 50 to 70 per cent of the full ahead power.

318. Pametrada Marine Turbines. In 1944 the leading British marine engineering firms engaged in the manufacture of turbines co-operated to set up a research organization for the purpose of improving and developing steam and gas turbine propulsion machinery. Other objects were to advise member firms on all matters associated with the design and layout of marine turbines and gearing. This organization was called the Parsons and Marine Engineering Turbine Research and Development Association, a title usually abbreviated to PAMETRADA.

Fig. 512 shows a single-cylinder turbine which was developed for the propulsion of cross-channel steamers on a short sea route. As the time of crossing is short the boilers and turbines do not reach steady conditions of operation for more than a small fraction of the total time. Consequently the loss of efficiency which follows the adoption of a relatively simple turbine is less serious than it would be in a power plant which is operating continuously.

Fig. 513 shows a view of the turbine and gearing during erection in the shop. It will be seen that the turbine power is transmitted to two first-reduction wheels and then through two pinions to the main gear wheel. The primary wheels are connected to the secondary pinions by quill shafts passing through the hollow pinions.

Referring to Fig. 512, it will be seen that the ahead turbine, to the left, has one two-row wheel followed by ten single-row impulse wheels, while the astern turbine comprises a two-row wheel and a single-row impulse stage. A and B are the ahead and astern nozzle boxes, respectively. In each case steam is supplied from a branch at the side of the outer casing, provision being made for differential expansion. The ahead and astern sections are separated by two

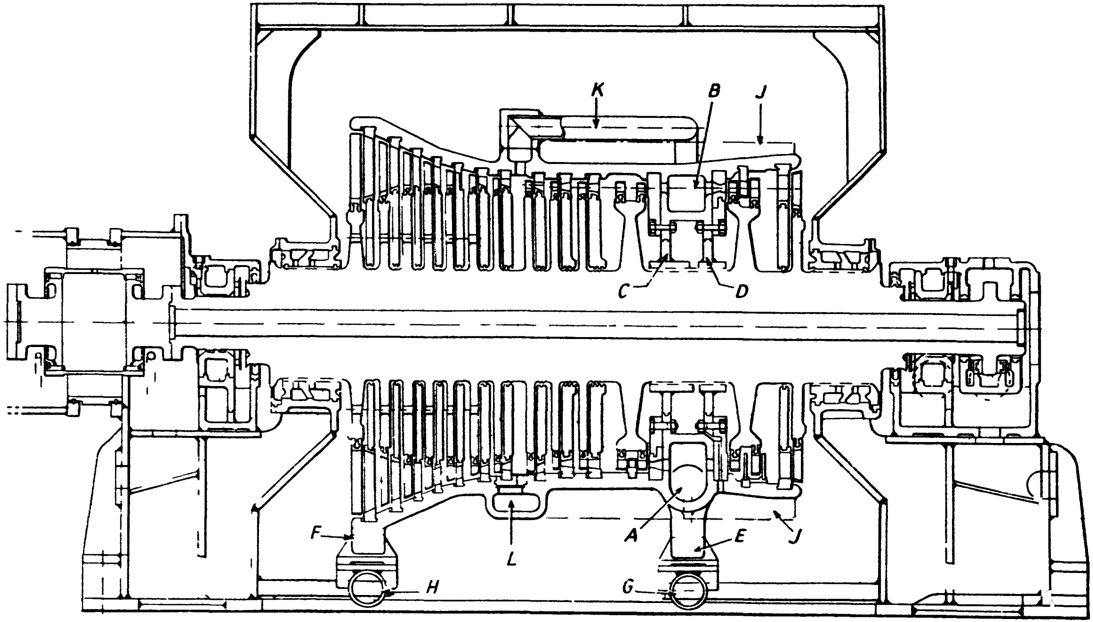


FIG 512 —Single-cylinder Marine Turbine of Pametrada Design

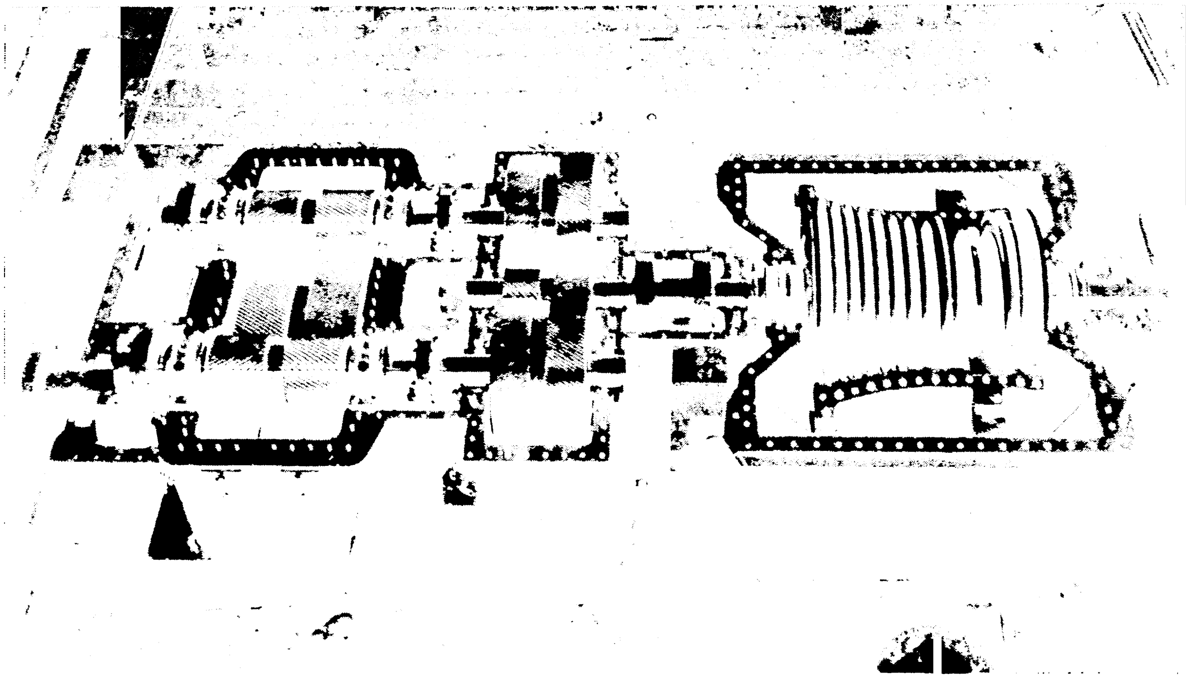


FIG 513 —View of Single-cylinder Marine Turbine and Double-reduction Gearing

diaphragms C and D supported centrally from the nozzle boxes and provided with labyrinth glands.

The rotor is machined from a single forging and is supported on bearings with steel shells and a thin lining of white metal. The cylinder consists of an inner barrel of cast-steel and an outer casing which is fabricated. Both are split at the horizontal centre-line. The lower part of the outer casing forms a strong beam which supports the whole turbine. The inner cylinder is supported by two

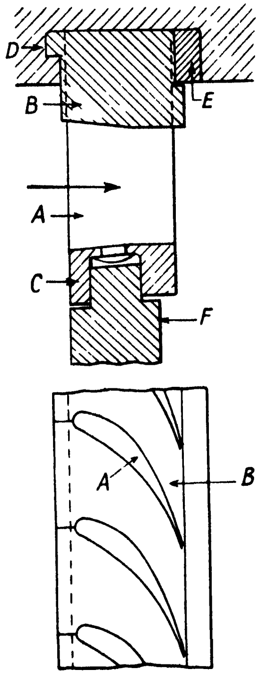


FIG. 514.— Pametrada Built-up Diaphragm

pairs of palms on the outer casing at the level of the horizontal centre-line (see Fig. 513); these maintain vertical alignment. Fore-and-aft location is fixed by the forward pair of palms which are in the same transverse plane as the nozzle belt. Transverse alignment is secured by keys E and F which are located by guides attached to the rigid stays G and H in the lower half of the casing. Heat loss from the inner to the outer casing is minimized by the use of a radiation shield J in the upper and lower halves of the turbine.

Steam leaking from the gland in the diaphragm between the ahead and astern turbines enters the ahead turbine after the fourth stage

by way of the pipe K. Steam is bled from the same stage by a short belt L in the lower half.

It is claimed for the design that, as the centre part of the turbine is hot when the ship is running ahead, the walls of the astern nozzle box would be at a temperature above the figure at which condensation would be produced by the admission of astern steam.

The diaphragms used in this and other marine turbines of Pametrada design are built up in the manner shown in Fig. 514. The nozzle guide vanes A are cut to length from rolled strip of the required cross-section and spaced by packers B which are also of

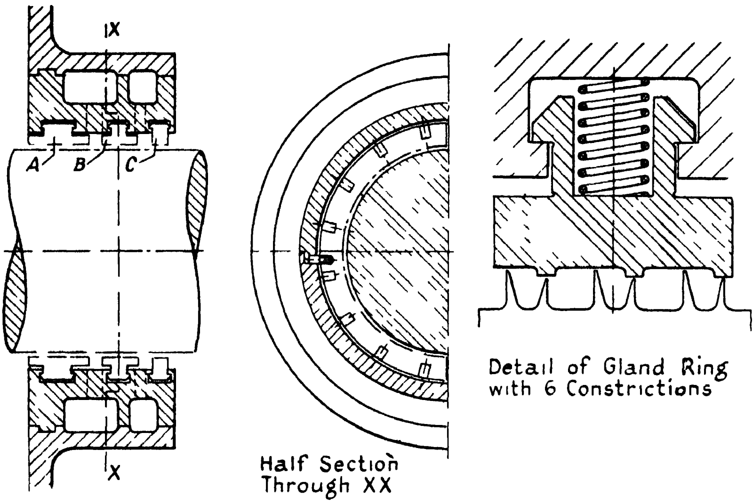


Fig 515 Spring-back Type of Pametrada Shaft Gland

rolled section. In manufacture, blades and packers are assembled into groups of convenient length, usually composed of about six blades, and brazed together to form a complete segment. The inner ends of the guide blades are provided with tenons which fit into holes in the channel-section shrouding strip C. The tenons are afterwards riveted over and brazed. The packers are provided with a projecting ring D which fits into a groove in the cylinder. The segments are finally secured in the cylinder grooves by the locking strips E which are inserted peripherally. The diaphragm centre consists of a steel plate F, in halves, which is spigoted into the channel C. The load due to steam pressure difference is carried by the outer segments which are encastered in the cylinder. Supporting keys keep the steel centre coaxial with the outer segments and with the rotor.

The type of labyrinth gland recently introduced in marine turbines of Pametrada design is shown in Fig. 515. This represents a typical

shaft gland and comprises three "spring-back" gland rings A, B, and C, giving respectively, 6, 4, and 2 throttlings. In this case the rings are in four segments, as shown in the half end view, and each segment is held against the locating surface in the housing by four helical springs of special material. The segments are prevented from rotating by check plates at the horizontal joint. The packing fins are machined on the surface of the rotor spindle.

The diaphragm glands are also of the spring-back type. Fig. 516 shows the construction for a gland with one strip, i.e. two throttlings per ring. An increased number of throttlings may be provided by using wider rings.

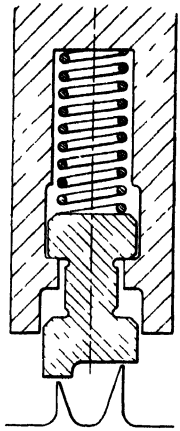


FIG. 516.—Pametrada Diaphragm Glands

A two-cylinder marine turbine of Pametrada design is shown in Figs. 517 and 518, while Fig. 519 shows the lower half of the high-pressure cylinder and the rotor.

The cylinder is of double-shell construction, the inner cylinder being a casting of suitable alloy steel and the outer casing being fabricated from steel plate. As may be clearly seen from Fig. 519, the inner cylinder is supported on brackets on the inner side of the outer casing, provision being made for differential expansion and for maintaining concentricity of cylinder and rotor. The side members of the outer casing are extended fore and aft to form a girder which supports the h.p. astern turbine at the forward end. Cross girders between the side members support the bearings.

There are 16 single-row impulse wheels in the h.p. ahead turbine. High-pressure steam is admitted to the branch A and flows in the forward direction. The exhaust steam leaves by way of the branch B on the top half of the casing. As the steam pressure in the outer casing is not usually more than 30–40 lb. per sq. in. g. a box-shaped casing may be used for the lower half without much difficulty. The top half of the casing is semi-cylindrical in shape. The inner casing is not lagged but heat loss is reduced by a thin sheet steel radiation shield C.

The h.p. astern turbine is a two-row wheel D housed in a separate cylinder of cast alloy steel. The latter is supported so as to maintain concentricity of casing and rotor. Steam is supplied to the branch E and exhausted at F. The turbine develops about one-third of the astern power and the design has proved very satisfactory in operation.

A section through the l.p. ahead and astern turbine for the same installation is given in Fig. 518. This is also of double-shell construction comprising cast-steel inner cylinders supported and located by the fabricated steel outer cylinder.

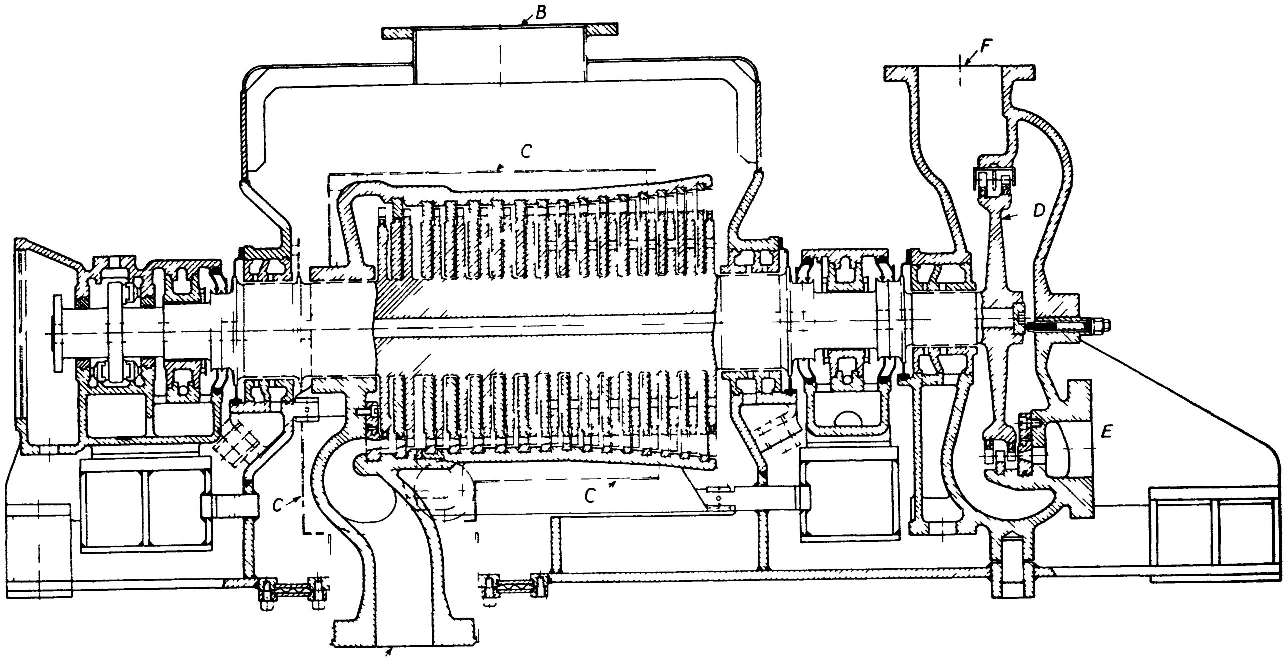


Fig. 517 High pressure Ahead and Astern Turbine of Pametrada Design

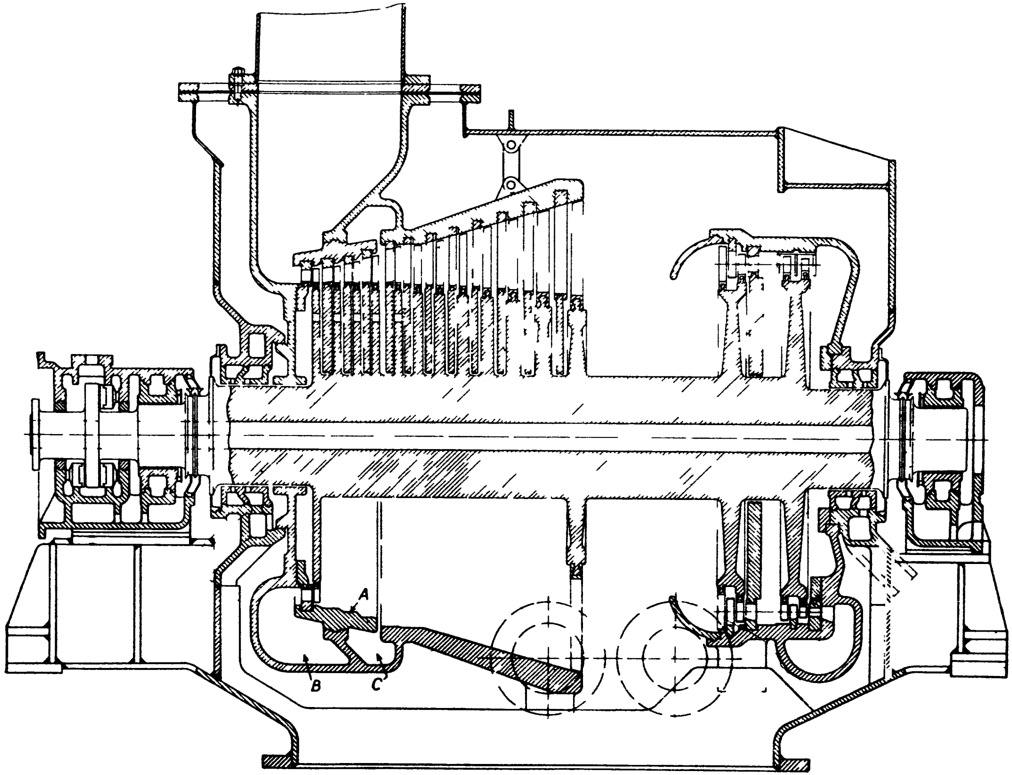


FIG 518—Low-pressure Ahead and Astern Turbine of Pametrada Design

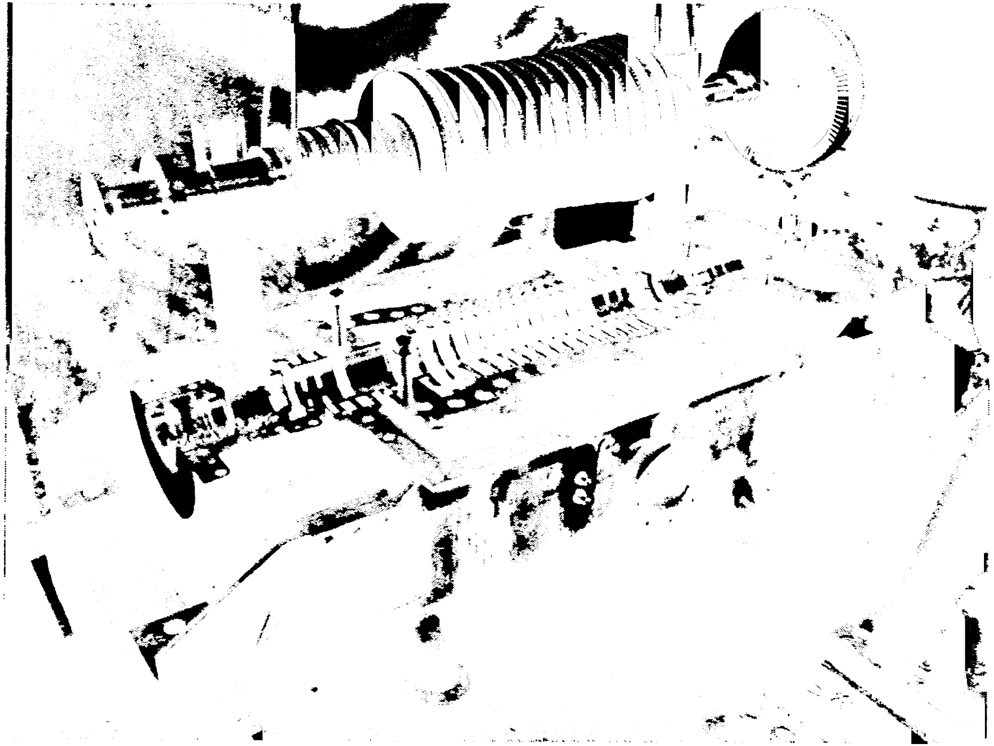


Fig. 519. High-pressure Ahead and Astern Turbine of Pametrada Design

The ahead turbine has five impulse stages followed by seven reaction stages. The rotor is machined from a single forging. A cylinder liner A is provided to carry the fixed nozzles for four stages and at the same time provide a steam belt B and a further belt C for bled steam. This construction simplifies both moulding and fettling. The l.p. astern turbine has two velocity stages and is quite independent of the l.p. ahead turbine.

319. **Metropolitan-Vickers Marine Turbines.** Three sets of turbines were constructed for the Blue Funnel cargo liners "Nestor," "Neleus" and "Theseus," completed in 1952, 1953, and 1954, respectively. These ships carry about 9,500 tons d.w. and have a speed of 16 knots. The turbines are designed for the following conditions—

Maximum power	8,000 s.h.p.
Maximum propeller speed . . .	112 r.p.m.
Economic power	7,250 s.h.p.
Economic propeller speed . . .	108 r.p.m.
Initial steam pressure	600 p.s.i.g.
Initial steam temperature (ahead) . .	950° F.
Initial steam temperature (astern) .	750° F.
Vacuum	28·5 in. Hg.
Speed of h.p. turbine (max. rating) .	6,000 r.p.m.
Speed of i.p. turbine (max. rating) .	4,500 r.p.m.
Speed of l.p. turbine (max. rating) .	3,000 r.p.m.

Sections through the three turbines are given in Figs. 520, 521, and 522. The high-pressure turbine contains a two-row wheel and eight single-row impulse stages. The rotor is machined from a single forging of molybdenum steel and is furnished with stainless steel blades. The diaphragms are of molybdenum steel plate to which fully machined nozzles of one-half per cent molybdenum steel are riveted.

The upper half of the cylinder is of cast molybdenum-vanadium steel, while the lower half which is not subjected to such arduous steam conditions is of cast molybdenum steel. There are three groups of nozzles fitted into inserted nozzle boxes. The steam supply to each group is controlled by a valve, the three valves being opened in sequence by means of a handwheel.

The intermediate-pressure turbine accommodates thirteen stages. The cylinder is of cast-steel but the diaphragms are of molybdenum steel plate with fully machined nozzles of the same material.

The low-pressure turbine has eight ahead stages and three astern stages, the first of these being a two-row wheel. The rotor has separate discs shrunk on and keyed to the shaft. The blades are of stainless steel attached to the rotor by the straddle method. The cast-iron diaphragms have cast-in guide vanes of rustless steel plate. As may be seen from Fig. 522, the cylinder is a composite

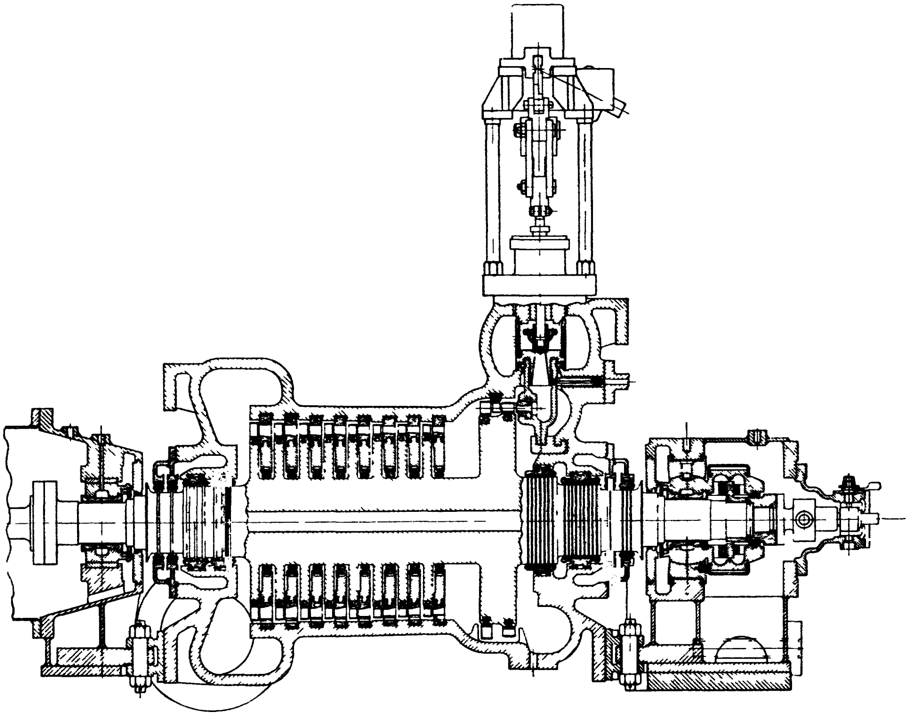


FIG 520 Metrovick Marine Turbine for s s Nestor H P Turbine

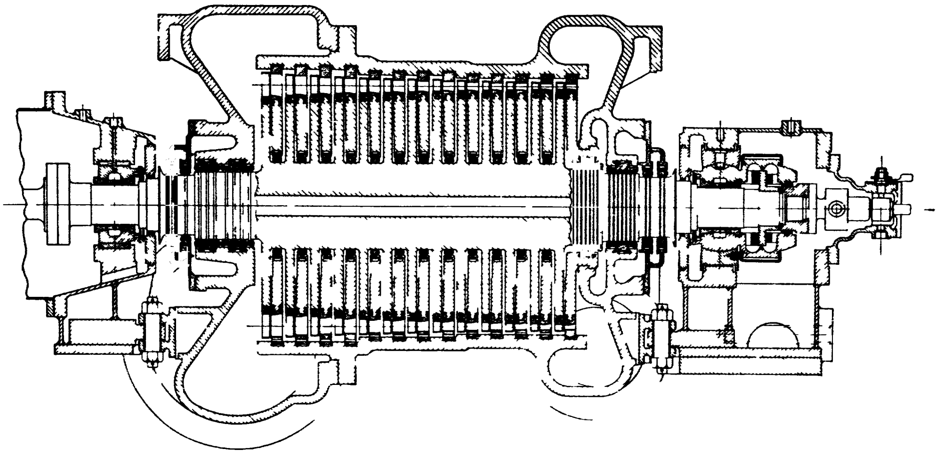


Fig 521 Metrovick Marine Turbine for s s "Nestor" I P Turbine

structure partly cast and partly fabricated. The lower half of the cylinder and the condenser shell form one structure.

Motor-driven turning gear coupled to one end of the l.p. pinion is provided to turn the turbines while warming up or after a stop, in

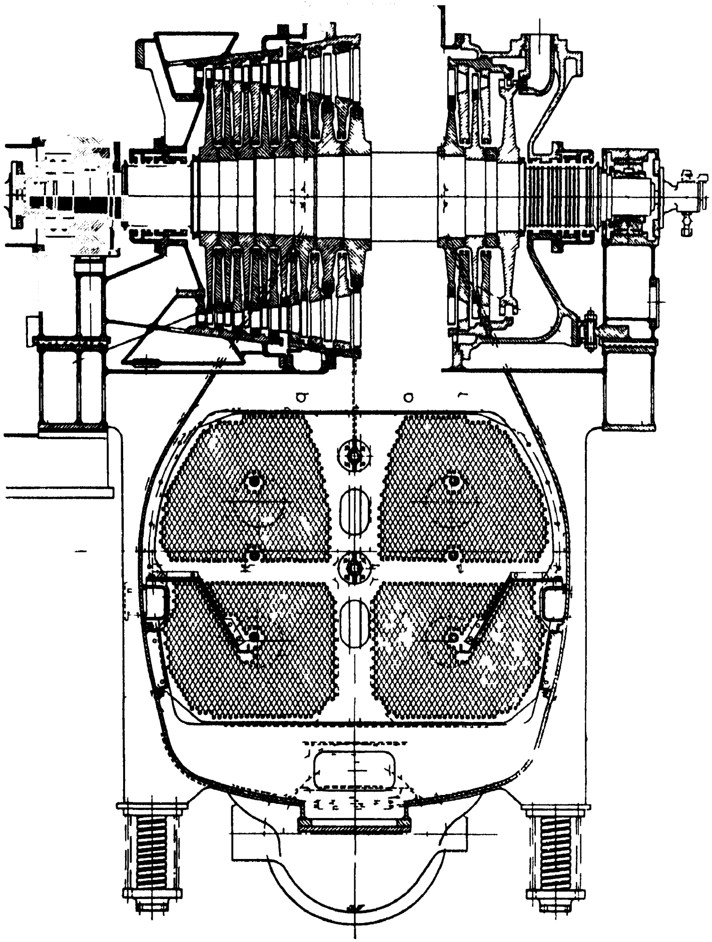


FIG. 522.—Metrovick Marine Turbine for s.s. Nestor. L.P. and Astern Turbine and Condenser.

order to avoid thermal distortion. This gear gives the propeller shaft one revolution every 10 minutes. The motor is remote controlled and an interlock prevents engagement of the clutch while the turbines are rotating; it also prevents the admission of steam to either ahead or astern turbines while the turning gear is engaged.

320. English Electric Marine Turbines for "Daring" Class Destroyers. This machinery comprises two sets of turbines, one on each side of the ship, each set consisting of a high-pressure and a low-pressure ahead turbine and two astern turbines housed in the same casing as the l.p. ahead turbine.

The turbines are all impulse and are designed for the following conditions—

Power per set		27,000 S.H.P. plus 10 per cent
Maximum speed:	h.p. turbine .	8,250 r.p.m.
	l.p. turbine .	6,380 r.p.m.
Steam conditions at turbine stop valves—		
Pressure		550–650 p.s.i.g.
Temperature		825° F.
Vacuum at full power . .		27·5 in. Hg.

The high-pressure turbine, Fig. 523, has nine stages with a velocity-compounded wheel in the first stage. Since naval vessels spend a large proportion of their steaming-time at low power, in order to improve the efficiency under these conditions the power is regulated as far as possible by varying the number of nozzles in action. Steam admission to the turbine is controlled by a single handwheel which operates four valves in sequence. The first three valves control individually the three separate nozzle groups shown in Fig. 524. The fourth valve admits additional steam to an overload belt, this steam entering at *B*, thus by-passing the first three stages to give maximum power. In order to simplify the cylinder casting in way of the overload belt, a liner *C*, carrying three diaphragms, is fitted.

The Michell thrust bearing is arranged in the pedestal at the steam end of the turbine. This pedestal is fixed to the engine seating; while the pedestal at the aft end is arranged to slide on horizontal liners (not shown) which are just below the turbine centre-line. Transverse alignment is maintained in the usual manner by vertical keys *D* and *E*.

At the steam end of the turbine there are three labyrinth shaft glands, *F*, *G*, and *H*, with glands *J* and *K* at the exhaust end, respectively similar to *G* and *H*. The leak-off pocket between *F* and *G* is connected to the branch *L* at the exhaust end. The steam escaping from the middle of glands *H* and *K* is led to a gland steam condenser.

Fig. 525 shows a section through the low-pressure turbine, while Fig. 526 shows a transverse section through the centre-line *A*–*A*.

The l.p. ahead turbine is a double-flow machine with six stages. The cylinder is centrally supported in a strong fabricated outer casing. Referring to Fig. 526, the cylinder rests on liners *B* and may expand in the lateral direction. The fore-and-aft position is

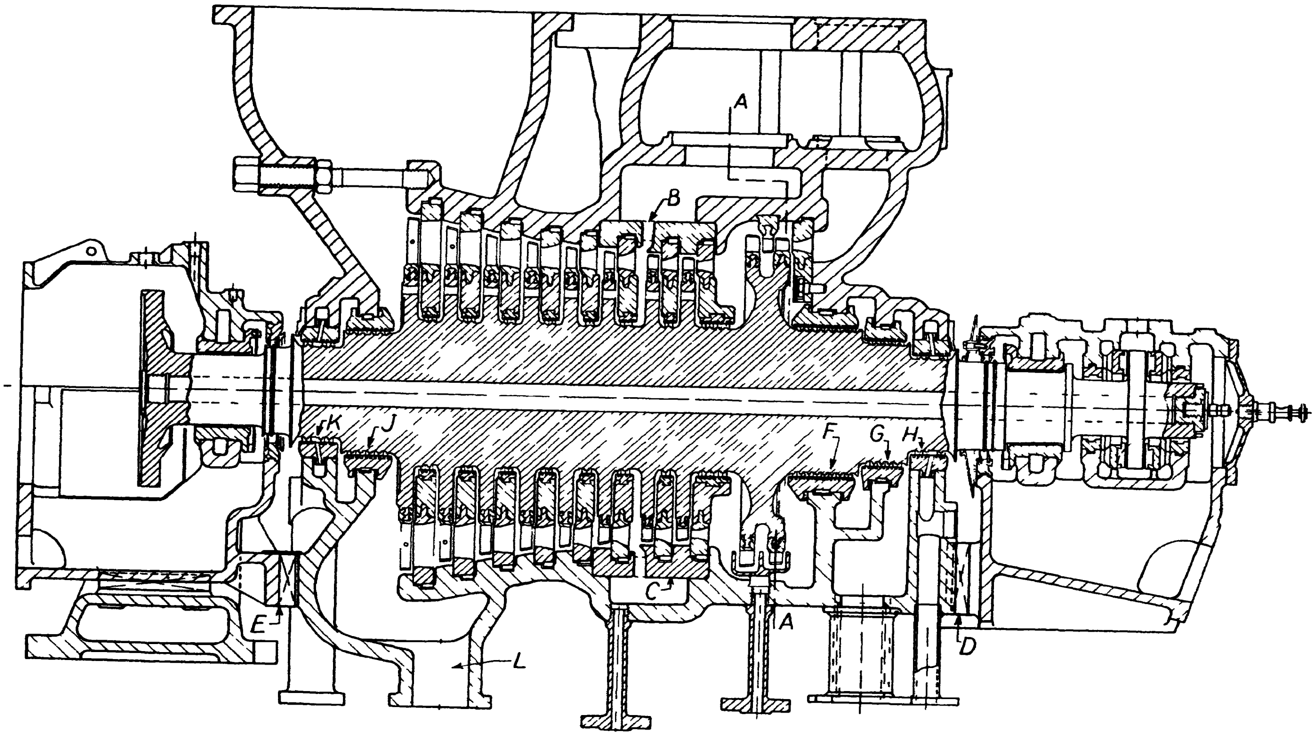


Fig 523 High pressure Turbine for Daring Class Destroyers

centralized by a block *C*, while the transverse alignment is maintained by a long fore-and-aft key *D*. Heat loss to the condenser is minimized by the lagging *E* supported by a light casing.

The astern turbine consists of two velocity-compounded wheels, one wheel at each end of the casing. The nozzle box castings *F* are

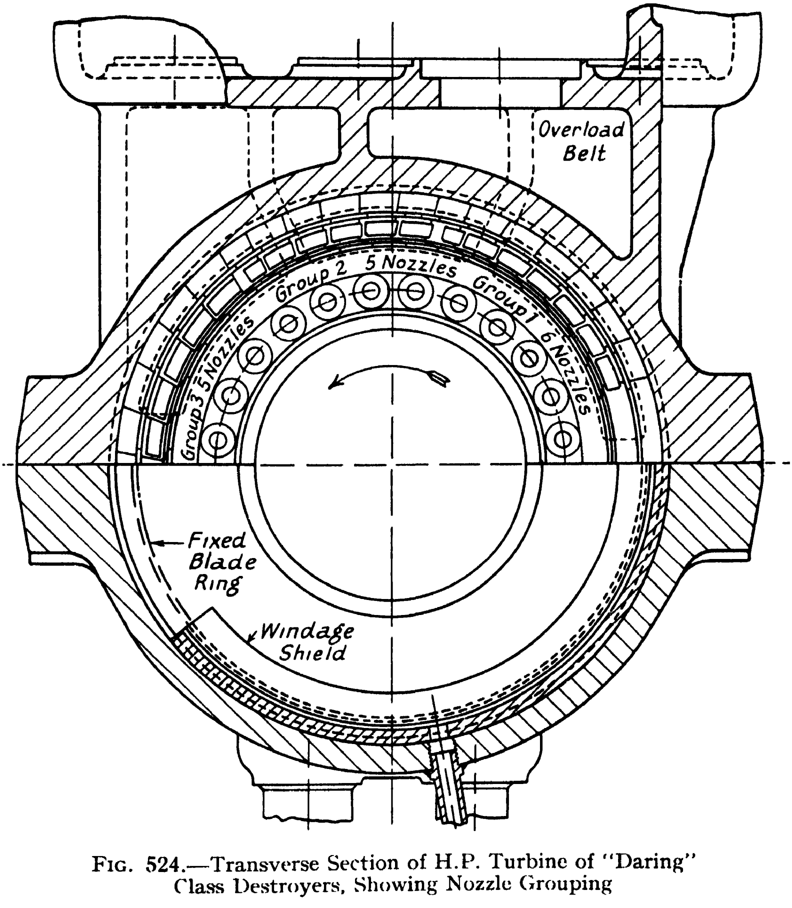


FIG. 524.—Transverse Section of H.P. Turbine of "Daring" Class Destroyers, Showing Nozzle Grouping

made in halves with a horizontal joint and support the fixed blades and a deflector *G*. Alignment of the nozzle boxes with the cylinder end casting is maintained by an ample number of radial dowels *H*. Astern steam is supplied to the two inlet branches *J*, relative movement between the inner end of the astern steam pipes and the inlet branch on the nozzle boxes being catered for by a piston-ring joint.

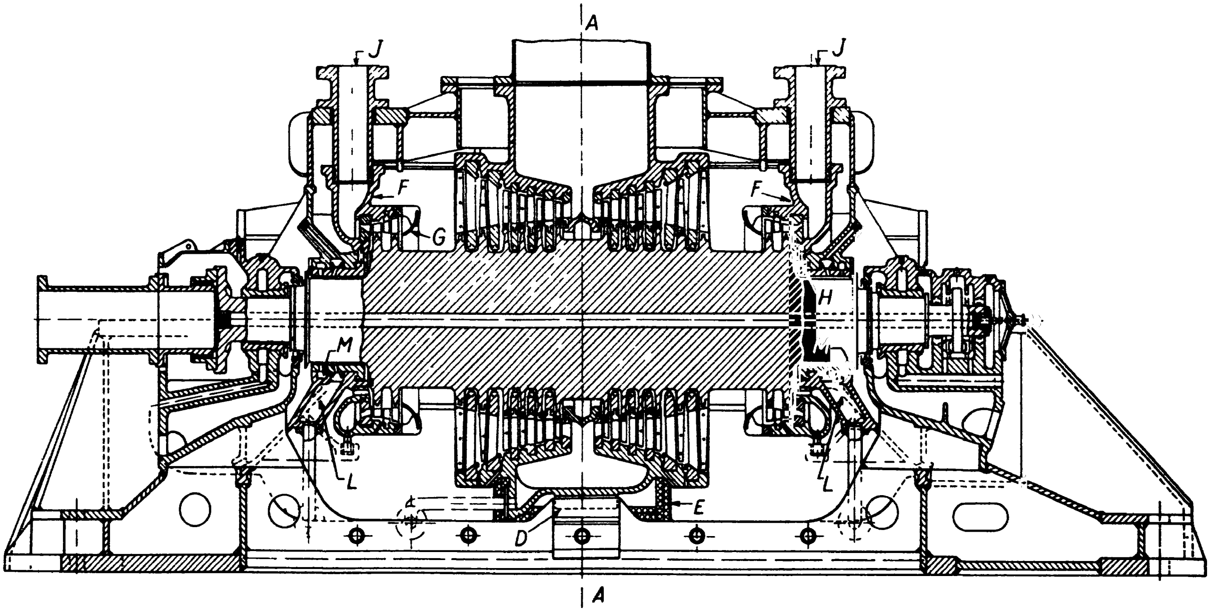


FIG 525 —Low-pressure and Astern Turbines for "Daring" Class Destroyers

Rectangular-shaped doors *K* extending nearly the full length of the outer casing give access to the bolting at the horizontal joints of the l.p. ahead internal cylinder and the astern nozzle boxes.

For gland sealing, steam is supplied to the pockets *L*, while the leakage from the pocket *M* is piped to a gland condenser. Water catchers are arranged in the fourth and fifth l.p. ahead stages with drains direct to the condenser.

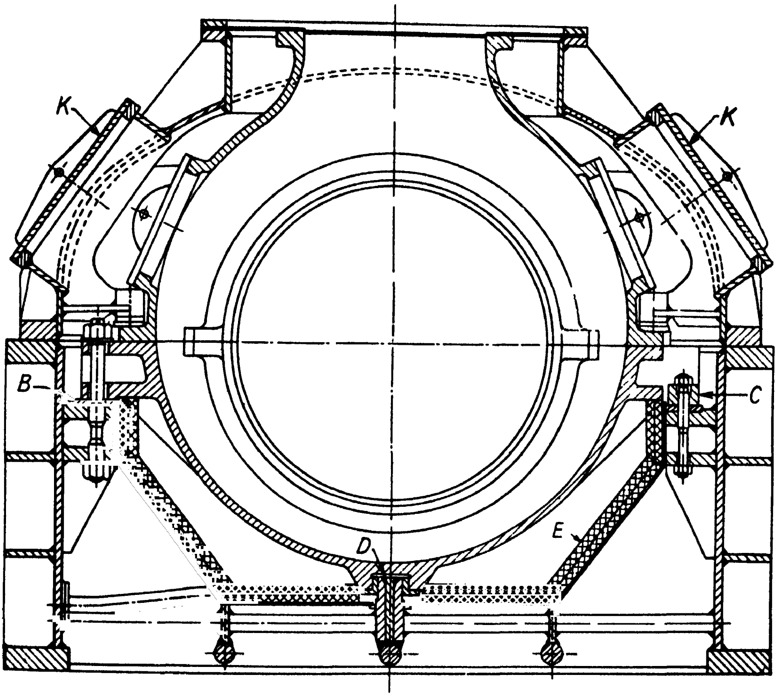


FIG. 526.—Transverse Section on line A-A, Fig. 525

321. English Electric Marine Turbines for H.M. Frigates of the "Blackwood" Class. The frigates of the "Blackwood" Class are propelled by two sets of turbines, each set giving a maximum power of 15,000 h.p. when supplied with steam at 583-490 p.s.i.a. and 827° F. The vacuum is 23·0 in. Hg. at full power with sea water at 80° F.

Each set of machinery comprises a cruising turbine on the outboard side and a main turbine. The cruising turbine is installed in order to improve the economy at low powers and is coupled to a primary pinion through a clutch which is disengaged when the power reaches one-third of full power. Above this power, all load is taken by the main turbine. On declutching the cruising turbine, a small

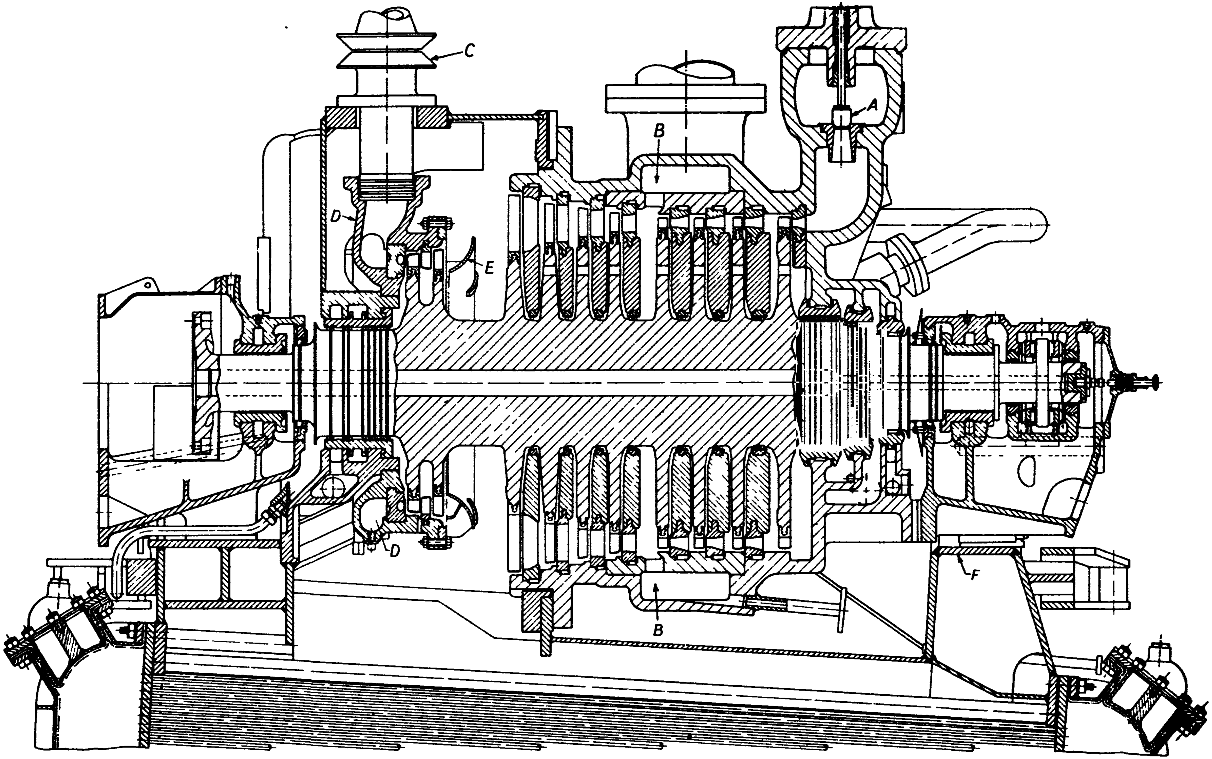


FIG. 527 Main Ahead and Astern Turbine of "Blackwood" Class of Frigates

amount of steam is supplied to it to keep it turning at about 400 r.p.m. in order to prevent the rotor hogging. The maximum speed of the main turbine is 5750 r.p.m.

Fig. 527, published by permission of the Admiralty, shows the cross-section through the main turbine. The ahead turbine has eight impulse stages of approximately uniform mean diameter. The rotor, including coupling and thrust collar, is machined from a single forging. The nozzles of the first seven stages are of the built-up type; in stage 8 the nozzle blades are cast-in. Four nozzle-control valves *A* regulate the admission of steam to the first stage and ensure considerable economies in steam consumption at reduced powers down to about 5,000 h.p. Below this power the cruising turbine comes into action and exhausts into the belt *B*.

The astern turbine is a two-row velocity wheel and develops 5,000 s.h.p. Astern steam is supplied at *C* and passes through a pipe to the cast-steel nozzle box *D*, the inlet pipe being provided with a piston-ring joint. A deflector *E* prevents the steam discharging from the astern blading from blowing direct on to the moving blades of the last ahead stage.

The forward bearing pedestal is supported on a fabricated platform *F* which is welded to the condenser shell, while at the aft end the fabricated turbine cylinder is extended downwards and becomes part of the condenser.

322. Steam Turbines for Nuclear Power Stations. The purpose of this section is to consider the special features, if any, which are likely to be met in steam turbines for nuclear power stations.

There are several possible types of thermal reactor but it appears likely that for some years to come the graphite-moderated gas-cooled reactor using natural uranium as the fuel will be the only one used in this country for outputs exceeding 60 MW. This is the type of reactor employed at Calder Hall power station and is to be used in the power stations recently authorized by the Central Electricity Authority.

Analysis has shown that for such a reactor the thermal efficiency is greater if a dual-pressure cycle is adopted. A diagrammatic arrangement of the reactor and a single heat exchanger of the Calder Hall plant is shown in Fig. 528. There are four heat exchangers or boilers arranged symmetrically around each of the two reactors. The fuel used is natural uranium, and carbon-dioxide is the gas employed to convey heat from the reactor to the heat exchanger. For good thermal efficiency the temperature of the gas entering the heat exchanger should be as high as possible. This temperature is limited by the properties of the canning materials employed in the reactor and in the Calder Hall plant has been selected as about 640° F. The temperature of the CO_2 returning to the reactor is about 275° F. The gas is circulated through the reactor by a blower. Referring to Fig. 528, one sees that the hot gases entering the heat

exchanger pass successively over the h.p. steam superheater A, the h.p. evaporating tubes B, the h.p. secondary economizer C, the l.p. steam superheater D, the l.p. evaporating tubes E, and the combined l.p. and h.p. primary economizer F. Forced circulation is used for both h.p. and l.p. boilers.

In each of the eight heat exchangers for the two reactors the steam generated by the h.p. boiler is 99,000 lb. per hour (77 per cent of the

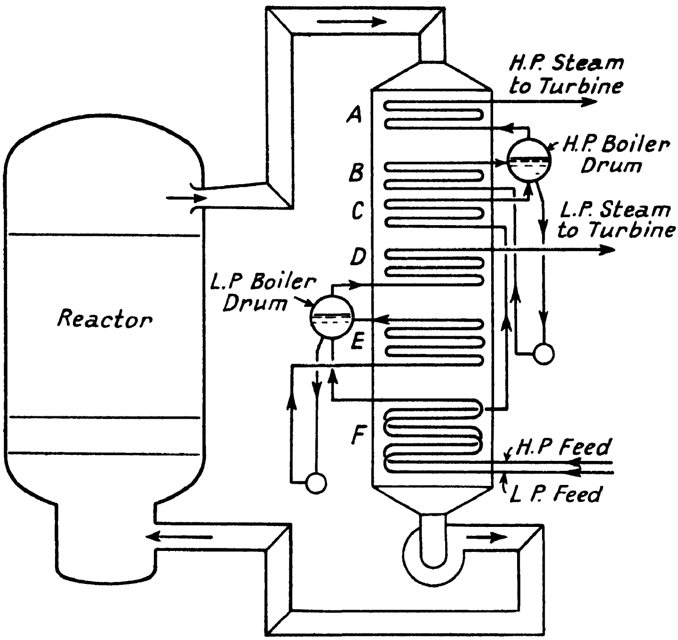


FIG 528—Diagrammatic Arrangement of Nuclear Reactor and Heat Exchanger

total) and by the l.p. boilers 29,650 lb. per hour, under the following conditions—

H.p. steam pressure	210 p.s.i.a.
H.p. steam temperature	595° F.
L.p. steam pressure	62·7 p.s.i.a.
L.p. steam temperature	350° F.
Feed temp. at economizer inlet . . .	100° F.
Heat taken up by water and steam . .	46·15 MW.

The turbine room at Calder Hall contains four Parsons turbo-alternators, each having a normal rating of 21 MW. The plant, however, is provided with a design margin sufficient to enable it with certain modifications to give an output of 23 MW.

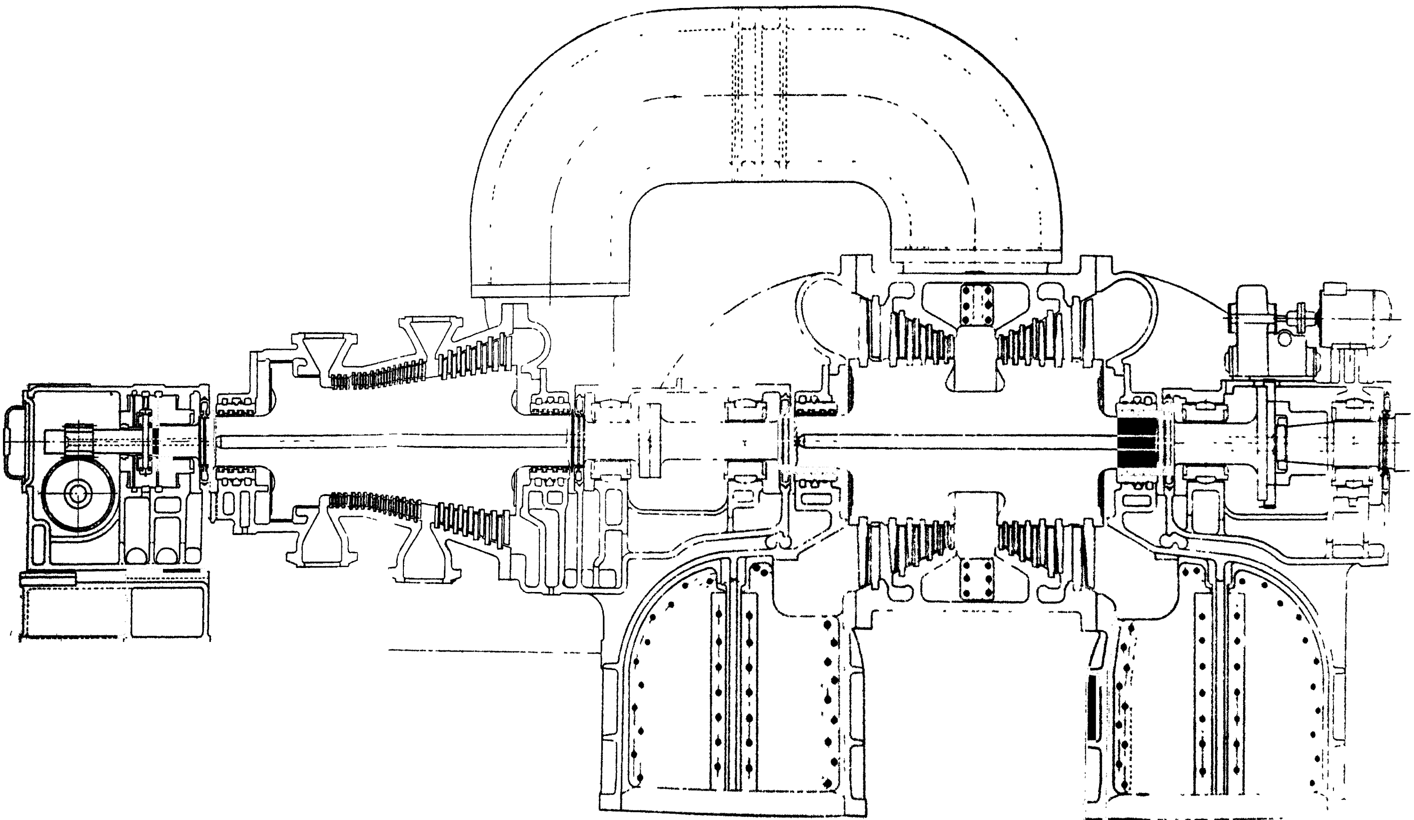


FIG. 529 - Parsons 21,000 kW. Turbine for Calder Hall Power Station

A cross-sectional drawing of the turbine is given in Fig. 529, facing this page. The h.p. section of the high-pressure turbine contains 15 stages with end-tightened blading. "Low-pressure" steam is admitted through upper and lower branches on the cylinder and mixes with the high-pressure steam to expand through 7 stages before being transferred to the 6-stage double-flow l.p. turbine.

The steam conditions at the turbine are—

H.p. steam pressure	200 p.s.i.a.
H.p. steam temperature	595° F.
L.p. steam pressure	52·7 p.s.i.a.
L.p. steam temperature	340° F.
Vacuum (30 in. Bar.)	28·25 in. Hg.

The turbines are, of course, mixed-pressure machines, the theory of which is given in Art. 154. Calculations show, however, that at full load the condition of the h.p. steam after expansion to the point where l.p. steam is admitted is almost the same as that of the l.p. steam, so that little or no change of state will occur on mixing. The wetness of the exhaust steam is estimated to be about 11 per cent.

The condensate is delivered to full capacity series deaerators before it is returned to the boilers at 100° F. To ensure that this temperature remains constant irrespective of variations in climatic conditions, heat exchangers supplied with raw water are provided in the feed line.

323. Control Gear for Calder Hall Turbines. Each turbine is provided with steam chests at each inlet containing a runaway stop valve and governor valve. In addition, an overriding control is provided to open or close the h.p. governor valve so as to maintain the pressure in the steam main at 185 p.s.i.g.

A diagrammatic arrangement of the control gear is given in Fig. 530. The plant may be operated at any power down to 10 per cent full load. As far as possible the gas temperatures at inlet to and outlet from the reactor are kept constant, and are controlled partly by varying the speed of the blowers.

Referring to Fig. 530, A and B are the gear pumps driven by the turbine and supplying, respectively, lubricating oil and power oil, the latter at 70 lb. per sq. in., the pressure being controlled by a valve C which when open allows the surplus oil to pass to the lubricating oil system. D is the emergency trip valve. E is a valve controlling the flow of power oil to the governor relay system. The plunger F is operated by the speed governor and controls the oil pressure under the auxiliary pistons G and H which, in turn, control the opening of the h.p. and l.p. throttle valves through the customary oil relays.

The h.p. transformer is provided with a bellows regulator actuated by the pressure of the h.p. steam. If the latter should fall then the piston will move downwards and raise the pilot valve thus allowing

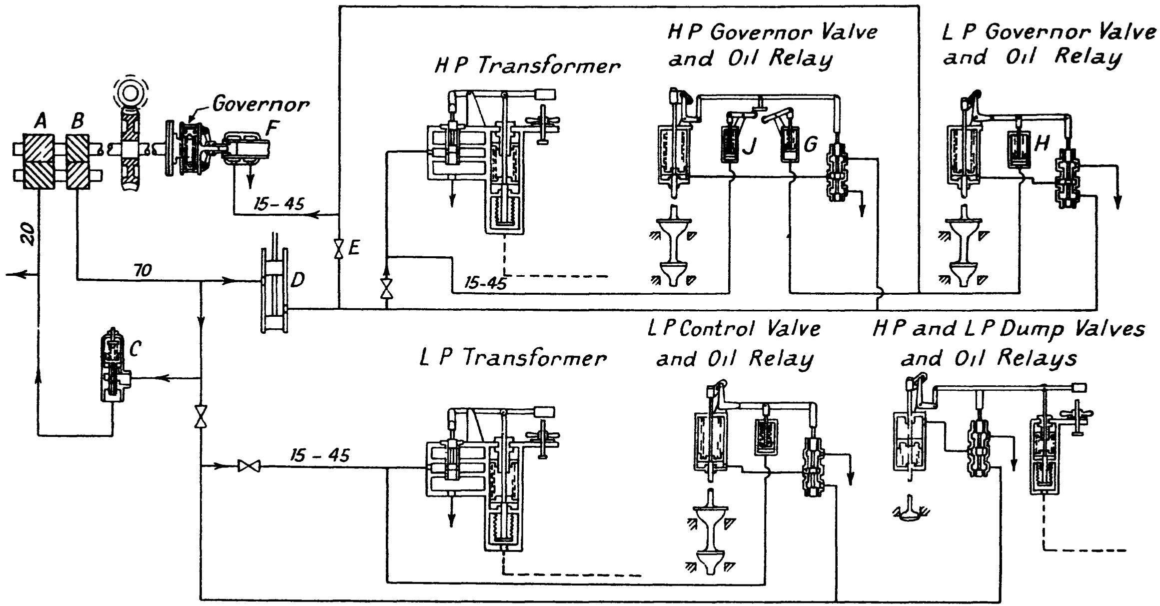


FIG 530 —Diagrammatic Arrangement of Control Gear for Calder Hall Turbines

Oil pipe lines are shown by full lines the figures giving the operating pressures in lb per sq in gauge The dotted lines repersent steam pressure connections *Note* Auxiliary lubricating and power oil pumps are not shown

oil to leak away from under the auxiliary piston J. This reduces the opening of the h.p. throttle valve and maintains the h.p. steam pressure near to its correct value.

At part load, excessive cooling of the CO_2 in passing through the heat exchanger is avoided by raising the pressure of the l.p. steam. Between full load and 10 per cent load the l.p. steam pressure is raised from 38 to 120 p.s.i.g. This is done by remote control of the l.p. transformer which operates in the same manner as the h.p. transformer and will regulate the steam pressure in the l.p. boiler at any desired value within the range.

To allow for the possibility of the station being suddenly disconnected from the grid when on load, two dump condensers are provided each capable of taking the whole of the steam diverted from two turbo-alternators. A sudden loss of load would cause an instantaneous rise in turbine speed and closing of the governor valves. This in turn would raise the pressure in both steam mains and cause the dump valves to open, allowing the steam to pass to the atmosphere through weight-loaded atmospheric valves. Steam is prevented from entering the dump condensers by isolating valves which are interlocked with the circulating water system so that they cannot be opened until circulating water is passing through the dump condensers. On sudden loss of load, therefore, it is necessary for the attendants to start the circulating water pumps and then open the isolating valves, upon which the steam will enter the dump condensers. These condensers are protected from the action of high-temperature steam by the installation of spray desuperheaters in the steam mains and condensers.

324. Turbines for the Nuclear Power Station in Ayrshire. This power station is to be built by the G.E.C.-Simon Carves Atomic Energy Group for the South of Scotland Electricity Board and will have an installed capacity of 360 MW. and a net output of 320 MW. There are to be two graphite-moderated reactors cooled by carbon-dioxide gas.

There are eight steam raising units associated with each reactor. These are generally similar to the heat exchangers for Calder Hall power plant shown diagrammatically in Fig. 528, but the various elements of the heat exchanger are arranged in a rather different way. The hot CO_2 flowing downwards through the steam raising unit passes over the following sections in succession, (1) h.p. superheater, (2) l.p. superheater, (3) h.p. evaporator, upper bank, (4) h.p. evaporator, lower bank, (5) l.p. evaporator, and (6) h.p. and l.p. combined economizer. This arrangement results in a higher steam temperature for the l.p. steam entering the turbine.

The gas temperatures at inlet to and outlet from the steam raising units are 745° F. and 392° F., respectively. In each of the sixteen heat exchangers, the steam generated by the h.p. boiler is 142,200 lb. per hour (67·3 per cent of the total) and by the l.p. boiler

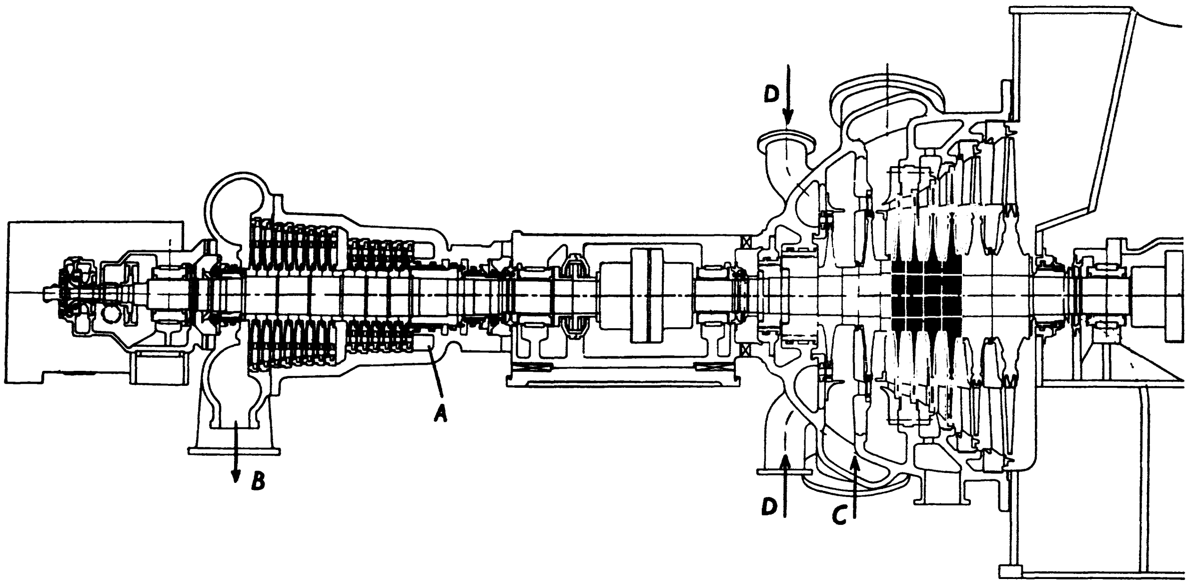


FIG 531 —Section through G E C High-pressure, Intermediate-pressure and one-third of Triple-flow Low-pressure Turbines for Ayrshire Nuclear Power Station

69,100 lb. per hour (32·7 per cent of the total) under the following conditions—

H.p. steam press. at superheater outlet	600 p.s.i.a.
H.p. steam temp. at superheater outlet	700° F.
L.p. steam press. at superheater outlet	170 p.s.i.a.
L.p. steam temp. at superheater outlet	670° F.
Feed temp. (h.p. and l.p.)	296° F.

There are six turbo-generators in the station, each with a continuous maximum rating of 60 MW. at 3,000 r.p.m. The steam conditions at the turbines are as follows—

Steam press. at h.p. stop valves	575 p.s.i.a.
Steam temp. at h.p. stop valves	690° F.
Steam press. at l.p. stop valves	155 p.s.i.a.
Steam temp. at l.p. stop valves	660° F.
Exhaust pressure, abs.	1·15 in. Hg.

Sections through the turbines are shown in Figs. 531 and 532. Each set comprises a high-pressure turbine, a two-stage intermediate pressure turbine, and a triple-flow low-pressure turbine. High-pressure steam enters the steam belt A and leaves the h.p. turbine at B, passing to the branch C on the i.p. turbine and so entering the nozzles of the second stage of that turbine. Low-pressure steam is supplied to the branches D and thus passes through the first stage of the i.p. turbine before mixing with the partially-expanded h.p. steam. At outlet from the second stage of the i.p. turbine, the steam flow is divided into three parts.

The decision to use a triple-flow l.p. turbine is the result of the following considerations—

(1) Due to the relatively low steam conditions, the steam flow through the l.p. turbine is considerably greater than in a conventional turbine of the same power.

(2) It is estimated that the wetness fraction of the exhaust steam will be about 13 per cent. In order to reduce possible blade erosion, a moderate blade speed has been employed.

(3) It was desired to reduce the leaving loss.

Solid couplings and shrunk-on wheels are used throughout. Both h.p. and i.p. turbines are provided with balance pistons. Steam is bled from the turbines to raise the feed temperature to 296° F.

The turbines are pressure governed, the steam pressures in the system being controlled by the turbine steam regulating valves. The presence of the first-stage nozzles in the i.p. turbine stabilizes the operation of the l.p. steam regulating valve. The steam regulating valves are controlled to maintain nearly constant pressure in the steam main, the control having a slightly rising pressure/load characteristic, so that stable operation may be obtained when the

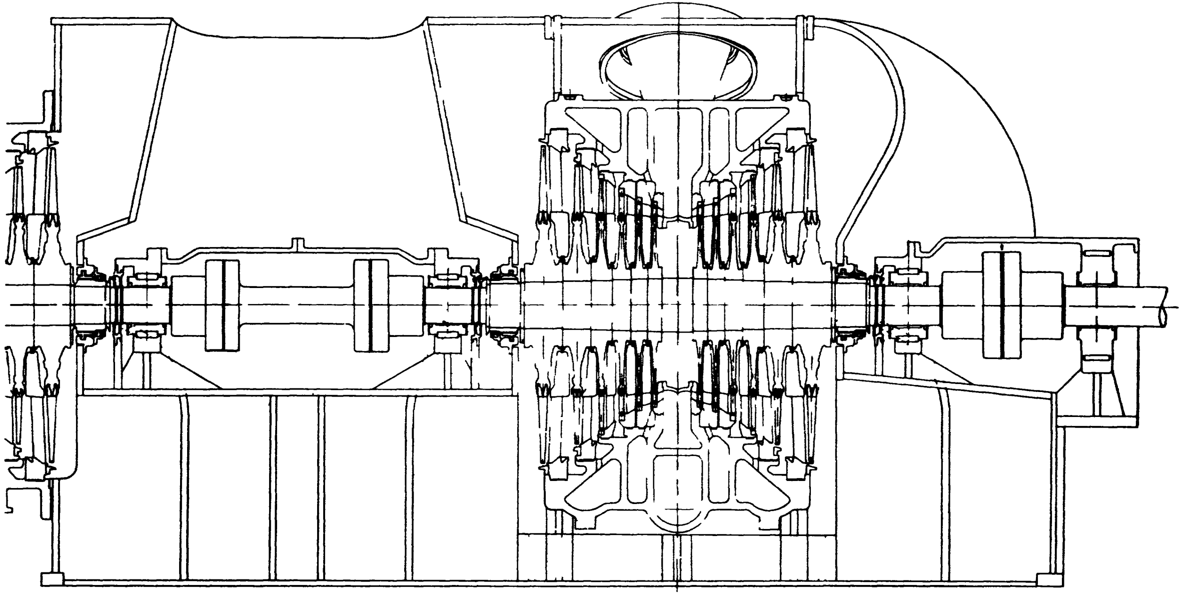


FIG 532 —Section through G E C Double flow Low pressure Turbine for Ayrshire Nuclear Power Station

machines are running in parallel. The distribution of load among the sets is adjusted by manual control of the pressure setting of the valves.

The turbines are also fitted with normal speed control gear for starting purposes and for the prevention of overspeeding.

Two dump condensers, operating at atmospheric pressure with spray desuperheaters, are provided. Steam is released to the dump condensers through automatic pressure-controlled valves.

CHAPTER XXX

TEST RESULTS

325. Objects of Testing. When, after the customary negotiations between the purchaser and manufacturer, a firm of turbine builders finally undertake to construct a steam turbine, they usually give certain guarantees regarding the performance of the completed machine. In the case of a turbo-alternator a certain steam pressure and temperature (to be measured before the stop valve) are specified, together with a certain vacuum at the turbine exhaust flange. With these stipulated steam conditions, the turbine builder will guarantee that at the maximum load, and at certain percentages of that load, the steam consumption per kWh output will not exceed a certain specified amount.

A typical set of guarantee figures for a 20,000 kW turbo-generator runs as follows—

Steam pressure at stop valve	250 lb. per sq. in. gauge
Steam temperature at stop valve . .	650° F.
Vacuum (30 in. barometer)	29·0 in. Hg.

Guaranteed steam consumption—

Load	% Max. Load	Lb. per kWh
20,000	100	10·32
16,000	80	10·32
12,000	60	10·92

Sometimes the guarantee is given in the form of a heat consumption per kWh. This is really equivalent to guaranteeing a certain overall thermal efficiency. For example, the following is the guaranteed performance of a 20,000 kW steam turbine equipped with regenerative feed heaters—

Steam pressure at stop valve	400 lb. per sq. in. gauge
Steam temperature at stop valve . .	725° F.
Vacuum	28·8 in

Heat consumption at stop valve per kWh at the generator terminals—

Load	% Max. Load	B.Th.U. per lb.	Corresponding Thermal Efficiency
20,000	100	11,185	30·5 per cent
16,000	80	10,986	31·1 ,,

The primary object of commercial testing is to determine whether or not the guaranteed performance is actually achieved. Practically all such tests must be carried out on site, as it is not generally possible either to provide sufficient load or sufficient steam to carry out a test in the maker's works, except in the case of relatively small units.

In the course of such acceptance tests, additional information is often obtained which is useful to the designer in enabling him to

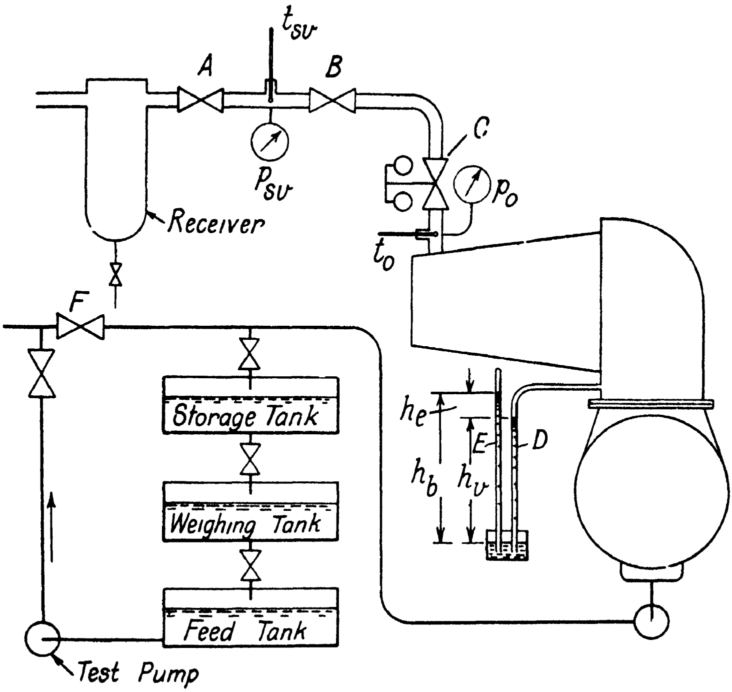


FIG 533 — Diagrammatic Arrangement of Test Apparatus

check the internal performance of the machine or examine the performance of some section of the turbine. Such analyses will be given in detail in later paragraphs.

326. Test Apparatus. The layout for a typical turbine test is shown in Fig. 533. The valves in the steam pipe are (1) the isolating valve A, (2) the stop valve B, and (3) the governor, or throttle valve C. The pressure and temperature of the steam are measured before the stop valve, and when the information is desired, after the throttle valve, i.e. at inlet to the nozzle box of the first stage in an impulse turbine or the steam belt in a reaction turbine. The vacuum gauge is shown diagrammatically and, of course, is not to

scale. A glass tube D, which must be at least 30 in. long, is connected at the top to a point on the exhaust branch or, alternatively, to a perforated pipe inserted through the exhaust branch and extending across it. The lower end of D dips into a vessel containing mercury, the surface of which is exposed to the atmosphere. E is a barometric tube which also dips into the same vessel. The height h_v is the so-called "vacuum" and may be expressed in inches or cm. of mercury. The height h_b is, of course, the barometric height. As the pressure on the surface of the mercury in the barometer is the negligibly small vapour pressure of mercury at the air temperature (0·0000142 lb. per sq. in. abs. at 60° F.), the difference of pressure h_e is, to all intents and purposes, the absolute pressure of the exhaust steam, expressed in inches or cm. of mercury. The corresponding pressure p_e in lb. per sq. in. abs. is

$$p_e = 0{\cdot}491 \times (h_e \text{ in. Hg.})$$

$$p_e = 0{\cdot}1934 \times (h_e \text{ cm. Hg.})$$

The steam consumption of the turbine may be measured by any one of several methods. The most accurate is by weighing the quantity of condensate in a given time. One method is indicated in Fig. 533. Three tanks are arranged as shown. The valve F in the feed pipe is closed, or a blank flange is inserted. The condensate is first allowed to flow into a storage tank. At approximately regular intervals of time a certain quantity of water is weighed in the weighing tank and then allowed to pass into the feed tank, from whence it is withdrawn by a special test pump. Other methods of measuring condensate by weighing tanks, calibrated tanks, and venturi meters are described in the author's book *Steam Turbine Operation*. Notes on steam meters are given in the same book. Various tests should be made to determine the condenser leakage, if any, and any other water leakage into the turbine. It is outside the scope of this book to deal with these methods. Full particulars will be found in the British Standard Test Code for Acceptance Tests for Steam Turbines No. 752—1940.

If the turbine is coupled to a D.C. or A.C. generator, the generator output is determined by established methods. In the case of a marine turbine, the power is calculated from a measurement of the torque in the propeller shaft by means of a torsionmeter together with a measurement of the rotational speed obtained by means of an integrating revolution counter.

327. Correction Factors. It is almost impossible to regulate the operating conditions during a test so that the steam pressure and temperature before the stop valve and the vacuum in the exhaust branch have the precise values specified in the guarantee. This is especially true of the initial steam temperature. Consequently, it becomes necessary to apply certain corrections

to the measured steam or heat consumption to allow for these deviations. A discussion of these correction factors will be found in the author's *Steam Turbine Operation*.

TEST RESULTS

The object of the present chapter is not to explain the technique of turbine testing but to present to the reader a few selected reports of tests. The object is to show to what stage of perfection the modern steam turbine has attained. So far as possible, the tests reported have been carried out by independent authorities of repute. For obvious reasons, the heat drop data and the resulting efficiencies are given exactly as in the original reports; as these have been based on different Steam Tables they are not strictly comparable, but the differences are probably small. In some cases the author has had regretfully to convert Continental units to British units in order to preserve similarity in presentation.

Before giving test results for turbines of moderate and large output a few results for the single-wheel de Laval turbine will be given.

328. Tests on Single-wheel de Laval Turbines. Some test results for de Laval turbines of the original single-wheel design are given in Table XXXVII. Test No. 1 gives results of a test carried out on a small de Laval turbine by the author, while the remainder are given by the De Laval Steam Turbine Co., whose figures are given in columns 1–7; while column 8, giving the efficiency ratio, has been calculated from the data supplied. The losses due to bearing friction, disc friction, and blade windage are comparatively small, and the principal reason for the differences in the efficiency ratio is the fact that, for economic reasons, the ratio of blade velocity to steam velocity is further removed from the theoretical optimum value in the smaller turbines than in the larger ones. From approximate data regarding the dimensions of the turbines in question, the ratio of blade speed to steam speed is given in column 12. Tests show that the multi-stage de Laval turbines reach much higher efficiency ratios than those given in Table XXXVII.

329. Tests on 15,000 kW Impulse Turbine. Table XXXVIII gives results (1) obtained during tests made on February 12, 1924, on a 15,000 kW impulse turbine, operating at 1,500 r.p.m., constructed by the B.T.-H. Company, Ltd., and installed in the Grove Road Power Station, London, of the Central Electric Supply Company. Great care was exercised in carrying out the tests and in making all measurements. The steam consumption was determined by weighing the condensate in special water-weighing tanks placed on weighbridges. The conditions were kept as near guarantee conditions as possible so that very small corrections had to be applied to the observed steam consumptions, as may be seen from

TABLE XXXVII

Test Results for de Laval Steam Turbines

1	2	3	4	5	6	7	8	9	10	11	12
Ref. No.	Rated B H P	Steam Pressure lb per sq in abs	Initial Super heat ° F	Vacuum per cent	Back Pressure lb. per sq in abs	Steam Cons lbs per B H P hour	Effy Ratio per cent	Adiabatic Heat Drop B Th U per lb	Theo Steam Velocity V	Approx. Blade Velocity u	Approx. $\rho = \frac{u}{V}$
1	18·19*	105·6	51·5	87·8	1·79	25·7	36·1	275·2	3,720	627	0·169
2	50	141·7	—	84	2·35	23·1	40·6	271·5	3,690	860	0·233
3	100	167	40	83	2·5	18·0	49·5	286	3,790	1,135	0·300
4	150	126·6	148	84	2·35	16·82	52·3	290	3,820	1,135	0·297
5	150	115·7	207	94·4	0·82	15·2	47·8	351	4,200	1,135	0·27
6	250	132	—	93	1·03	14·1	58·7	308	3,930	1,280	0·326
7	300	208	69	88	1·765	13·94	56·3	325	4,040	1,375	0·341
8	300	137·2	26	90	1·47	15·68	54·7	297	3,860	1,375	0·357
9	330	153	204	94	0·88	12·65	55·0	367	4,300	1,375	0·32
10	500	104	—	93·5	0·955	15·2	56·5				
11	500	200	118	88	1·765	13·35	57·5				

* Actual test B.H P

TABLE XXXVIII

TESTS ON 15,000 kW IMPULSE TURBINE

No. of Test	1	2	3	4	5
Duration . . . min.	60	60	30	60	60
Load	Full	¾	½	Full	1¼
p_{sv} lb. per sq. in. gauge	193·1	194·1	193·7	195·3	191·0
t_{sv} . . . ° F.	634·9	628·4	635·1	620·3	623·3
Superheat . . ° F.	249·8	242·9	249·8	234·3	239·0
Vacuum at exhaust flange in. Hg. (30 in. Bar.) .	27·93	28·22	28·46	27·92	27·62
Net condensate lb. per hr.	165,030	125,555	85,110	167,280	207,025
Net output . . kW	15,189	11,509	7,623	15,279	18,855
Steam consumption at test conditions lb. per kWh	10·87	10·91	11·17	10·95	10·98
Corrected steam consumption	10·80	10·82	11·12	10·76	10·76
Overall efficiency ratio of turbine and alternator under test conditions per cent	79·06	77·50	74·04	79·14	80·46
Estimated efficiency of alternator . per cent	96·50	—	—	96·50	97·0
Efficiency ratio of turbine alone under test conditions . . per cent	81·93	—	—	82·02	82·95

Table XXXVIII. The tests were carried out under the supervision of the consulting engineers, Messrs. Kennedy and Donkin.

The tests were worked out on the basis of Callendar's Steam Tables. Bearing in mind that the efficiency ratio is based on the steam conditions before the stop valve, the result is very satisfactory.

330. **Tests on 35,000 kW Impulse Turbine.** The following particulars relate to tests on one of three 35,000 kW turbo-generators constructed by the Metropolitan-Vickers Electrical Co., Ltd., and installed in the Deptford West Power Station, London.

The economic load is 28,000 kW, i.e. 80 per cent of the maximum continuous load. The turbines are designed to operate with steam at 350 lb. per sq. in. gauge and at 750° F. with the following vacua—

At	100	per cent	full	load	28·75	in. Hg.
,,	80	,,	,,	,,	29·00	,,
,,	60	,,	,,	,,	29·12	,,
,,	40	,,	,,	,,	29·18	,,

The turbine has two cylinders in tandem, the particulars being as follows—

Cylinder	No. of Stages	Mean Dia. in.	Mean Blade Velocity
H.P.	24	42	275
L.P.	15	62¾–84	411–550

Speed: 1,500 r.p.m.
Total K value: 273,250

Steam is bled from the L.P. turbine at three points for feed-heating, the final feed temperature being 250° F. Evaporators are incorporated in the feed-heating system of each turbine. The test results (2) are given in Table XXXIX.

TABLE XXXIX

TEST RESULTS FOR 35,000 kW IMPULSE TURBINE

Test No.	1	2	3	4
Nominal load: . . . per cent	40	60	80	100
Turbine Readings—				
p_{sv} . . . lb. per sq. in. gauge	346·8	341·7	342·9	350·4
t_{sv} . . . . ° F.	759·6	749·8	761·4	784·9
Superheat at stop valve . . ,,	324·7	316·3	327·6	349·1
Vacuum at exhaust . . in. Hg.	29·114	28·950	28·873	28·581
Final feed temperature . . ° F.	211·7	220·3	239·6	257·8
Electrical Readings—				
Net load . . . . . kW	14,346	21,011	28,382	35,701
Power factor	0·94	0·94	0·95	0·945
Water Measurements—				
Total water weighed . lb. per hr.	145,545	208,335	271,170	346,420
Ejector steam ,,	1,500	1,500	1,500	1,500
Raw water evaporated ,,	5,609	8,318	10,913	14,050
Net steam consumption ,,	138,436	198,517	258,757	330,870
Raw water evaporated in per cent of net steam consumed . . .	4·05	4·18	4·23	4·25
Test consumption (including feed heaters and evaporators) lb. per kWh	9·650	9·448	9·117	9·268
Heat Consumption and Thermal Efficiency—				
Enthalpy at stop valve B.Th.U. per lb.	1,400·0	1,395·1	1,401·1	1,413·0
Enthalpy of feed leaving last feed heater . . B.Th.U. per lb.	179·7	188·3	207·9	226·3
Net heat supplied ,, ,,	1,220·3	1,206·8	1,193·2	1,186·7
Test heat consumption at generator terminals (feed-heating and evaporation) B.Th.U. per kWh	11,776	11,402	10,878	10,998
Test thermal efficiency at generator terminals . . per cent	28·97	29·92	31·36	31·02
Generator efficiency . ,,	94·57	96·00	96·75	97·08
Test thermal efficiency at turbine coupling (feed-heating and evaporation) . . . per cent	—	31·17	32·41	31·95

331. Tests on 11,000 kW Impulse Turbine. The calculation of thermal efficiency, efficiency ratio, etc., from test data will now be illustrated by data obtained by Professor Stodola during a test (3) on an 11,000 kW turbine constructed by the Escher Wyss Engineering Works, of Zürich. The leading particulars of the turbine are given in Table XL. The following are additional particulars—

$$K = 270,500$$

BEARINGS:

Steam End. Diameter: 180 mm. = 7·09 in.
Length: 360 mm. = 14·17 in.
Projected area = 100·2 sq. in.

Exhaust End. Diameter: 200 mm. = 7·87 in.
Length: 400 mm. = 15·75 in.
Projected area = 124 sq. in.

Glands. Packed with carbon rings. Shaft diameter at glands = 220 mm. = 8·66 in. Radial clearance = 0·4 mm. = 0·016 in. Leakage through both glands estimated to be 265 lb. per hour.

TABLE XL

PARTICULARS OF 11,000 kW STEAM TURBINE

Speed: 3,000 r.p.m.

Stage No.	Mean Diameter in.	Mean Blade Velocity ft./sec.	Nozzle Angle		Blade Angle	
			Inlet	Outlet	Inlet	Outlet
1	47·2	618	90	14	30	20
2	48·0	629	120	14	30	20
3	49·0	641	115	14	30	20
4	51·2	670	120	14	30	20
5	53·1	696	120	12	30	20
6	55·5	727	120	11	28	20
7	57·5	753	125	10	28	20
8	59·8	783	125	10	28	20
9	61·4	804	130	12·5	28	20
10	63·0	825	120	18	33	35

The test results are given in Table XLI. Tests 1 and 2 were preliminary tests, while 3 and 4 were the principal tests.

Detailed Analysis of Full Load Test. Fig. 534 shows the performance of the turbine at full load, Test No. 4, set down on the $\phi - I$ chart, while the full working out of the test data is given in Table XLII.

The adiabatic heat drops are the values given by Professor Stodola, converted into British units. Point A, Fig. 534, represents the steam condition on the boiler side of the stop valve, while D

TABLE XLI

Test Results for 11,000 kW Impulse Turbine

Notes.—p_{gv} and p_0 are the steam pressures before the governor valve and before the first-stage nozzles respectively.

t_{gv} and t_0 are the steam temperatures before the governor valve and first-stage nozzles respectively

p_c = pressure in condenser.
p_e = pressure behind the last wheel.

All pressures in lb. per sq. in. abs.
All temperatures in deg. F.

Test No.	1	2	3	4
Duration . . . . . min.	51	109	45	120
Bar. height . . . in. Hg.	29·20	29·07	29·80	29·80
p_{sv}	212·1	210·4	192·0	197·6
t_{sv}	616·6	636·9	663·4	662·9
p_{gv}	206·3	209·0	191·4	195·1
t_{gv}	614·0	634·0	661·2	659·7
p_0	14·28	93·28	131·6	178·6
t_0	586·4	617·3	653·5	657·2
p_c	0·646	0·343	0·427	0·606
p_e	0·653	0·395	0·484	0·664
Steam rate . . . lb. per hr.	10,380	61,550	83,870	113,000
Gland loss (estimated) . ,,	265	265	265	265
Total steam rate . . ,,	10,645	61,815	84,135	113,265
R.p.m.	3,045	3,040	3,041	3,041
Power at switchboard . . kW	0	5,477	7,966	10,975
Total loss of alternator . . ,,	300	479	543	596
Power at turbine coupling . ,,	300	5,956	8,509	11,571
Efficiency of alternator . per cent	—	92·0	93·6	94·9
Steam consumption, referred to power at turbine coupling lb. per kWh	35·46	10·38	9·888	9·788

shows the condition in the nozzle box at inlet to the first-stage nozzles. At full load, the pressure at the outlet side of the last wheel had a mean value 0·664, while the pressure in the condenser was 0·606 lb. per sq. in. abs. The various adiabatic heat drops may be readily obtained from a good ϕ — I chart, or by calculation. These are set down in Table XLII, the reference letters on Fig. 534 being given a more general interpretation.

Since the power at the turbine coupling is 11,571 kW, and the

total steam rate is 113,265 lb. per hour, the work done at the coupling is

$$\frac{11{,}571 \times 3{,}413}{113{,}265} = 348{\cdot}5 \text{ B.Th.U. per lb. of steam}$$

As the heat drop AC at full load is 427·1, the efficiency ratio of the turbine based on the coupling power, the steam conditions before the stop valve, and the pressure in the condenser is

$$\eta_r = \frac{348{\cdot}5}{427{\cdot}1} \times 100 = 81{\cdot}59 \text{ per cent}$$

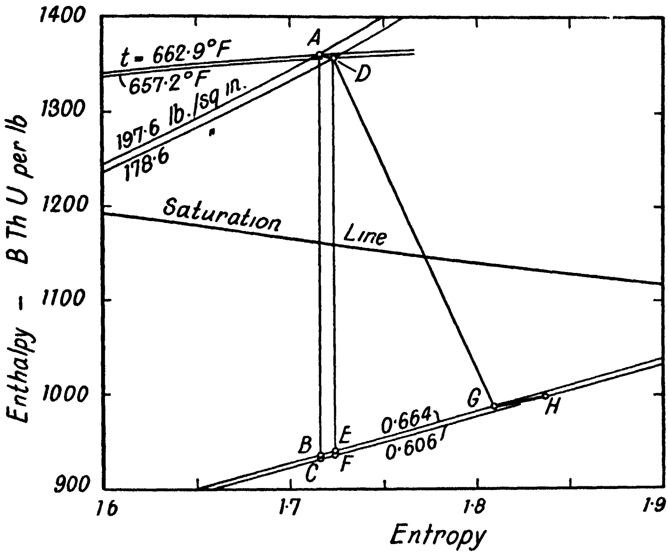


FIG. 534.—Mollier Diagram for Full-load Test of 11,000 kW Turbine

Similarly, the efficiency ratio based on the coupling power, the steam conditions in the nozzle box, and the steam pressure at outlet from the last stage wheel is

$$\frac{348{\cdot}5}{414{\cdot}7} \times 100 = 84{\cdot}03 \text{ per cent}$$

From the experience of the builders and from special tests, the mechanical losses were estimated to be made up as follows—

High-pressure bearing	34·9 kW
Low-pressure bearing	49·5 ,,
Adjusting block, oil pumps, and governor drive	30·6 ,,
Total external loss . . .	115·0 ,,

This was assumed to be the same in all tests, and, added to the coupling power, gives the internal (shaft) output of the turbine. The heat drop corresponding to the internal power is found as above, together with the corresponding efficiency ratios. Deducting the

TABLE XLII

DEDUCTIONS FROM DATA OBTAINED DURING TEST OF 11,000 kW STEAM TURBINE

Note.—All heat drops are in B.Th.U. per lb. of steam. All efficiencies are expressed as percentages.

Test No.	1	2	3	4
Adiabatic heat drop AC (Fig. 534) .	—	449·7	442·1	427·1
,, ,, ,, DE ,, .	252·5	395·7	413·3	414·7
,, ,, ,, DF ,, .	253·3	402·5	417·8	419·3
Heat drop corresponding to power at coupling	—	328·7	345·0	348·5
Efficiency ratio based on coupling power, steam condition before stop valve, and pressure in condenser .	—	73·11	78·05	81·59
Efficiency ratio based on coupling power, steam condition in nozzle box, and pressure at outlet from last wheel	—	83·08	83·49	84·03
Internal power . . . kW	415	6,071	8,624	11,686
Heat drop corresponding to internal power	—	335·1	349·7	351·9
Internal thermal efficiency ratio based on the steam condition in the nozzle box and the steam pressure at outlet from the last wheel	—	84·68	84·61	84·85
Internal thermal efficiency ratio based on the steam condition in the nozzle box and the pressure in the condenser	—	83·25	83·68	83·93
Reheat referred to adiabatic heat drop based on steam condition in nozzle box and the pressure at outlet from the last wheel . . per cent	—	3·85	3·79	3·69
Final velocity of steam at outlet from the last wheel . ft. per sec.	—	565	627	670
Corresponding loss . B.Th.U. per lb.	-	6·37	7·85	8·97
Terminal velocity loss referred to adiabatic heat drop DE . per cent	—	1·61	1·90	2·16

heat drop corresponding to the internal power from the enthalpy at D, we obtain the enthalpy at G, the point G representing the condition of the steam at outlet from the last wheel.

From the velocity diagrams for the last stage of the turbine, Professor Stodola was able to calculate the final velocity of the steam from that stage. These values are given in Table XLII, together with the outlet velocity loss.

Suppose that H, Fig. 534, represents the condition of the steam entering the condenser, and—

Let W_i = internal work, B.Th.U. per lb. of steam

V_c = velocity of steam entering condenser

V_0 = outlet velocity from last wheel.

Then, by the steady-flow equation and assuming that the steam velocity in the nozzle box is small—

$$I_D = I_G + W_i + \frac{V_0^2}{2gJ}$$

and

$$I_D = I_H + W_i + \frac{V_c^2}{2gJ}$$

$$\therefore \quad I_H - I_G = \frac{V_0^2 - V_c^2}{2gJ}$$

This enables the point H to be obtained.

The steam consumption curve is given in Fig. 535. With simple throttle governing, this curve is a straight line and corresponds to the well-known Willans line for steam engines. The steam consumption at zero coupling power is 8,000 lb. per hour, which is about 7 per cent of the full-load consumption. Another important relation, which has already been discussed in Art. 141, is shown by Fig. 536. To all intents and purposes, the test points lie on a straight line which passes through the origin, or more accurately, slightly above it, owing to the effect of gland leakage.

From an analysis of the test data, Professor Stodola estimated that the efficiency of the stage working under the best conditions (stage 6, with blades about 2·4 in. long), excluding wheel friction and leakage, and without deducting the loss due to ejector action, would be about 90 per cent.

332. Tests on 10,000 kW Impulse Turbine Operating with Steam at 1,000° F. The following brief account is of tests made on a steam turbine supplied to the Detroit Edison Company in the year 1931 by the British Thomson-Houston Co., Ltd., of Rugby. The plant comprises a two-cylinder tandem turbine, a 12,500 kVA generator, and three regenerative feed heaters. The turbine was designed for a pressure of 380 lb. per sq. in. abs., a steam temperature of 1,000° F. at the throttle, and an exhaust pressure of 1 in. Hg. abs. It operates at 3,600 r.p.m. and is of the impulse type with

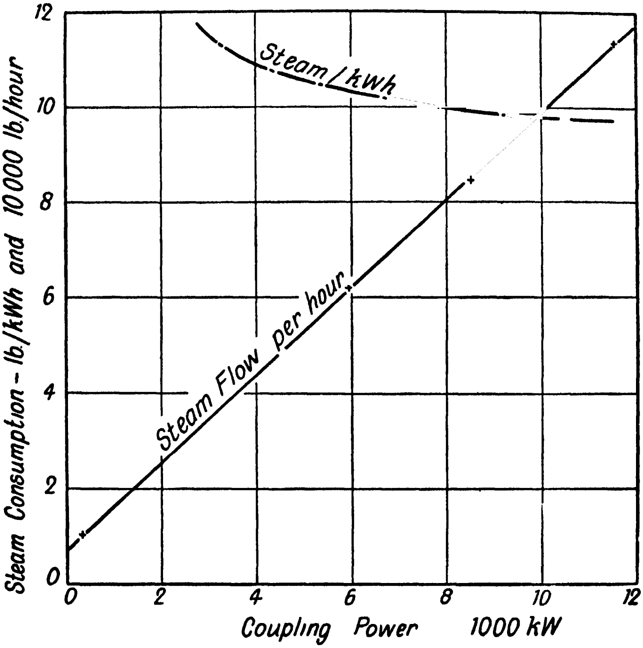


FIG 535.—Steam Consumption Curves for 11,000 kW Turbine

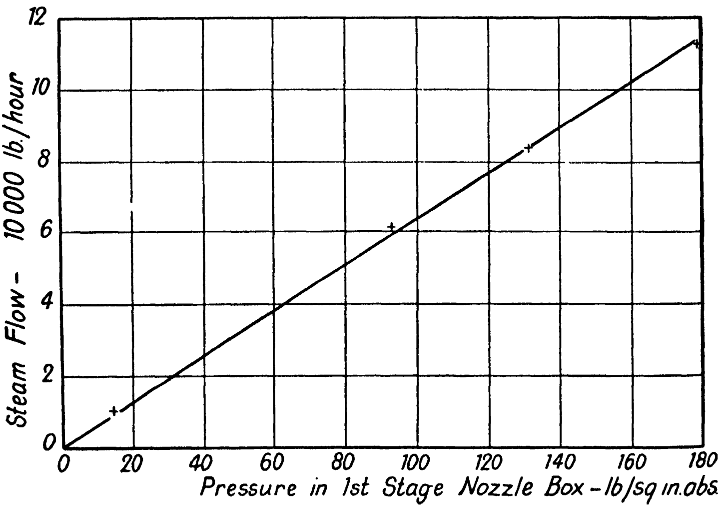


FIG. 536

9 stages in the H.P. cylinder and 11 in the L.P. cylinder. The mean diameter of stages 1, 2, 9, 10, and 20 are 32·5, 23, 23·5, 32, and 50 in. respectively.

The three feed heaters are of the horizontal 4-pass type with the following heating surfaces—

Heater	Connected to Turbine Stage No	Heating Surface sq ft
H P.	9	284
I P	14	303
L P.	17	463

The arrangement of the heater drains is shown in Fig. 537. It will be seen that the drain water from the H P. heater is cascaded into the

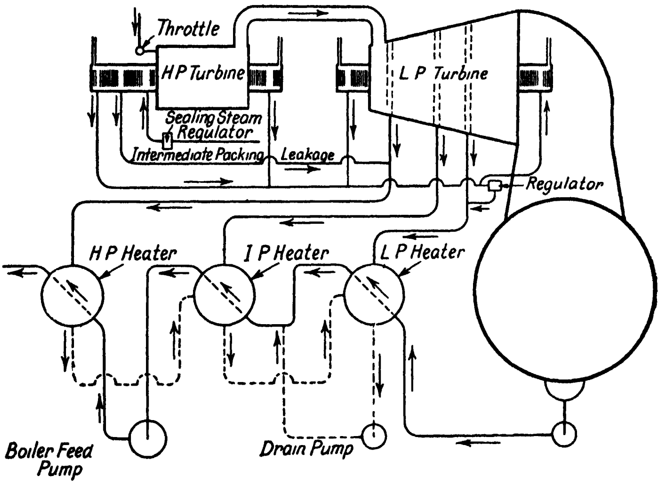


FIG 537 —Diagrammatic Arrangement of 10,000 kW B T -H Turbine

I.P. heater; the combined drains from the latter are then cascaded into the L.P. heater, while the combined drains from the three heaters are extracted by a drain pump from the L.P. heater and delivered to the feed pipe after that heater.

Special attention was paid to the steam-end glands of the H.P. turbine, because leakage of the high-temperature steam through the gland might cause serious heating of the shaft and bearing. The axial length of the H.P. gland is greater than that taken up by the

wheels in the H.P. cylinder. The steam leaving the first-stage wheel has a temperature of about 930° F., and is prevented from passing through the gland by using saturated steam of slightly higher pressure as sealing steam. When the sealing steam regulator is set to give a pressure at inlet to the packing 0·5 lb. per sq. in. above that in the first-stage wheel chamber, the leakage of saturated steam past the inner packing into this chamber amounts to about 10 per cent of the total sealing steam, or about 0·6 per cent of the total flow to

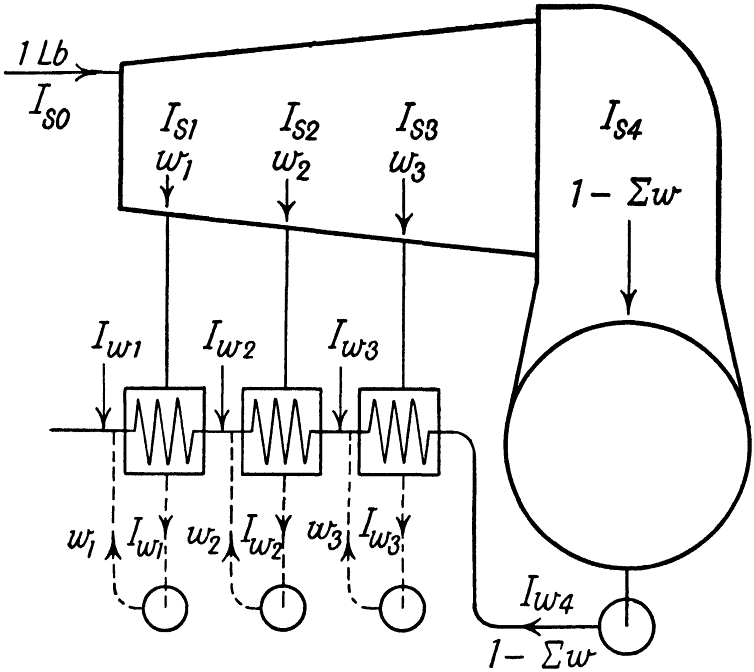


FIG. 538

the turbine for a load of 10,000 kW. As shown in Fig. 537, part of the sealing steam from the intermediate H.P. packing passes into the H.P. feed heater, while the remainder passes on to the outer packing. Part of the leakage through the outer packing seals the gland at the exhaust end of the L.P. turbine while the remainder passes through a pressure regulator into the L.P. feed heater.

Live steam for the turbine was taken from the boilers at 700° F. and further superheated in an oil-fired superheater. Thus steam at any temperature between 700° F. and 1,000 ° F. could be supplied to the throttle by controlling the fuel supply to the secondary superheater. A summary of the tests (4) at 1,000° F. is given in Table XLIII.

In calculating the thermal efficiency of the ideal "unit" (the term "unit" being used to represent the combination of turbine and feed heaters) which corresponds to the actual unit, it is assumed that the steam expands isentropically and that the number of feed-heating stages is the same as in the actual unit, the temperature reached by the feed water in each stage being assumed equal to the saturation temperature of the steam extracted from the turbine at the stage in question. Then following the method of Art. 130 (and neglecting the slight effect of the drain pumps on the water enthalpies) and referring to Fig. 538, the following relations may be obtained—

$$w_1 = \frac{I_{w1} - I_{w2}}{I_{s1} - I_{w2}}$$

$$w_2 = \frac{(1 - w_1)(I_{w2} - I_{w3})}{I_{s2} - I_{w3}}$$

$$w_3 = \frac{(1 - w_1 - w_2)(I_{w3} - I_{w4})}{I_{s3} - I_{w4}}$$

The available energy due to the expansion of the steam through the turbine, expressed in B.Th.U. per lb.

$$= I_{s0} - I_{s4} - w_1(I_{s1} - I_{s4}) - w_2(I_{s2} - I_{s4}) - w_3(I_{s3} - I_{s4}) = \Sigma h$$

Since the heat supplied in the cycle $= I_{s0} - I_{w1}$, the thermal efficiency of the ideal unit is

$$\eta_c = \frac{\Sigma h}{I_{s0} - I_{w1}}$$

Normally, a steam turbine has only one supply of steam, i.e. the amount coming through the throttle valve, but in this case the turbine has two sources of supply. The chief supply is, of course, that through the throttle valve; the secondary supply is the steam supplied to the regulator for the purpose of sealing the high-pressure glands. As already stated, the sealing steam is saturated. In determining the equivalent steam conditions for the corresponding ideal cycle, the following method was adopted.

Let W_a = actual flow of throttle steam, lb. per hour

W_b = actual flow of sealing steam, lb. per hour

$W_1 = W_a + W_b$ = actual total flow

I_a = enthalpy of steam at entrance to throttle

I_b = enthalpy of sealing steam at entrance to regulator

I_{s0} = enthalpy of steam entering the corresponding ideal unit at state 0.

Then
$$I_{s0} = \frac{W_a \cdot I_a + W_b \cdot I_b}{W_1}$$

TABLE XLIII

SUMMARY OF TESTS ON 10,000 kW TURBINE WITH STEAM AT 1,000° F.

1. Net load at generator terminals, kW	10,068	8,034	5,986	4,042
2 Temperature, ° F.—				
(*a*) Steam entering throttle	1,003	1,006	1,004	1,005
(*b*) Sealing steam entering regulator	445	448	450	452
(*c*) Feed water leaving 9th-stage heater	337	322	304	282
3. Abs. pressure, lb. per sq. in.—				
(*a*) Steam entering throttle	392	390	393	387
(*b*) Sealing steam entering regulator	391	405	415	420
(*c*) Steam at 9th-stage bleeder nozzle	128	103	78	55
(*d*) Steam at 14th-stage bleeder nozzle	40·5	32·5	24·3	17·4
(*e*) Steam at 17th-stage bleeder nozzle	10·5	8·4	6·3	4·5
(*f*) Steam entering condenser	0·50	0·49	0·46	0·52
4. Steam rate, lb. per kWh—				
(*a*) To throttle	8·388	8·403	8·519	8·965
(*b*) To sealing-steam regulator	0·541	0·530	0·523	0·559
5. Generator efficiency (including bearings, ventilation, and excitation), per cent	95·58	95·07	94·11	91·90
6. Energy consumption rate, B.Th.U. per kWh—				
(*a*) Complete unit (turbo-generator and heaters)	10,731	10,890	11,186	11,995
(*b*) Turbine and heaters	10,257	10,353	10,527	11,023
7. Thermal efficiency, per cent—				
(*a*) Complete unit	31·81	31·34	30·51	28·45
(*b*) Turbine and heaters	33·28	32·97	32·42	30·96
(*c*) Corresponding ideal unit	41·86	42·00	42·28	41·59
8. Engine efficiency, per cent—				
(*a*) Complete unit	75·99	74·62	72·16	68·41
(*b*) Turbine and heaters	79·50	78·49	76·68	74·44

I_{s1}, I_{s2}, I_{s3}, and I_{s4} are the enthalpies after isentropic expansion, and I_{w1}, I_{w2}, I_{w3}, and I_{w4} are the enthalpies of saturated water at the bleed pressures p_1, p_2, p_3, and p_4 respectively.

The heat consumption of the plant is

$$H = \frac{W_1(I_{s0} - I_f)}{K} \text{ B.Th.U. per kWh}$$

where I_f is the enthalpy of water at the actual feed temperature on test.

Then the thermal efficiency of the actual unit is

$$\eta_{th} = \frac{3,413}{H}$$

The ratio η_{th}/η_c is described as the engine efficiency of the complete unit (turbine-generator and heaters).

If η_g = efficiency of generator, then—

$$\frac{\eta_{th}}{\eta_c \times \eta_g} = \text{engine efficiency of the turbine and heaters only.}$$

The test data were worked out on the basis of Keenan's Steam Tables.

Tests were also made at steam temperatures of 700°, 800°, and 900° F. The heat consumption under these conditions and at varying

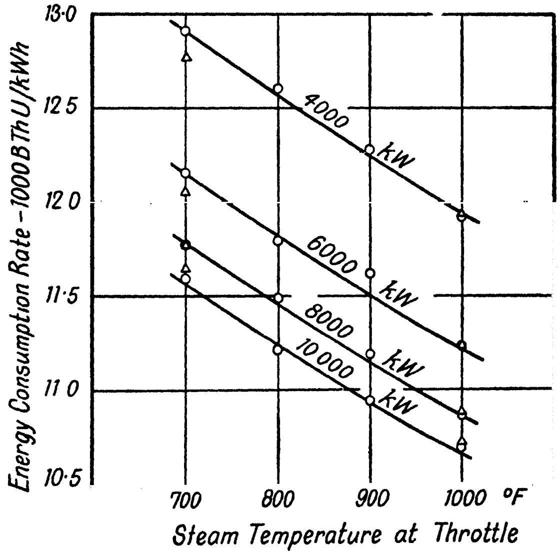


FIG. 539.—Energy Consumption Rate of 10,000 kW B.T.-H. Turbo-generator and Three Heaters.

Note.—Triangles show test points when exhaust pressure was regulated to approximately 1 in. Hg. abs. Circles show results of tests with unregulated exhaust pressure.

loads is shown in Fig. 539. The curves show that the heat consumption rate for the unit was decreased by 7 per cent by raising the initial temperature from 700° F. to 1,000° F.

The heat losses by radiation and convection from the turbine, heaters, bled-steam pipes, and feed pipes were all estimated from the test data. Radiation accounts for some 65 per cent of the total

loss, which amounted to 224,900 B.Th.U. per hour. Table XLIV gives the energy balance for the unit for a generator load of 10,068 kW and a steam temperature of 1,000° F. The loss due to radiation and convection is seen to amount to 0·2 per cent of the heat energy supplied, or 0·6 per cent of the turbine output.

TABLE XLIV

ENERGY BALANCE FOR 10,000 kW TURBINE

Energy Distribution	B.Th.U. per lb. of Total Flow to Turbine	Per cent
Energy delivered by turbine shaft . .	400·0	33·3
Energy lost by radiation and convection .	2·5	0·2
Energy rejected to condenser (by balance)	798·5	66·5
Total energy supplied . .	1,201·0	100·0

333. Tests on 1,000 kW Back-pressure Combination Turbine. The following tests (5) were made in May, 1925, by Professor Stodola on a Brown-Boveri back-pressure turbine, and are of special interest because of the care taken to determine the performance of the reaction blading. The turbine had a single-row impulse wheel in the first stage (mean diameter not stated) and 28 reaction stages on a drum 460 mm. diameter. The reaction blade height varied from 30 mm. in the first stage to 60 mm. in the last. Thus the mean diameter increased from 490 mm. (19·3 in.) to 520 mm. (20·5 in.) and at a speed of 3,000 r.p.m. the mean blade velocity from 253 to 268 ft. per second. The mean tip clearance was 0·73 mm. (0·029 in.) or 1·62 per cent of the mean blade height.

The test results for the complete turbine at generator outputs of 788 kW and 950 kW are given in Table XLVA.

The steam leaking through the balance piston labyrinth packing was condensed and weighed. By deducting this from the main condensate the weight of steam passing through the turbine blades could be determined.

The losses due to bearing friction, oil pump, and governor drive were determined in the following manner. The uncoupled turbine was driven at speed in a rarefied atmosphere by artificial means. At first the vacuum was the highest possible; then more and more air was allowed to leak into the casing. During these experiments the steam pipe was still coupled to the turbine but the valve was shut and a drain pipe on the main steam pipe was kept open so as to ensure that no steam leaked into the turbine. By partial closure of valves leading to the condenser the vacuum was diminished, and so the amount of work absorbed for different densities could be determined. The turbine could be quite filled with air whose density

TABLE XLVA

TEST RESULTS FOR COMPLETE 1,000 kW BACK-PRESSURE COMBINATION TURBINE

	Test No.	6	7
Item No.	Duration . . . . . . min.	60	60
	Barometric height . . . in. Hg.	28·78	28·78
	Steam pressures, lb. per sq. in. abs.—		
1	Before nozzles	139·9	154·2
2	After impulse wheel	108·6	119·1
3	Exhaust belt	39·75	39·46
	Steam temperatures, ° F.—		
4	Before nozzles	534·1	545·9
5	After impulse wheel	491·0	500·0
6	Exhaust belt	308·2	302·5
	Steam flow, lb. per hour—		
7	Through reaction blading	29,990	32,990
8	Through dummy piston	1,000	1,150
9	Total	30,990	34,140
10	R.p.m.	3,000	3,000
	Output, kW—		
11	At alternator switchboard	788·0	950·0
12	Total loss in alternator	53·5	60·8
13	Turbine coupling power	841·5	1,010·8
14	Efficiency of alternator . . per cent	93·6	94·0
15	Total steam consumption in lb per kWh at coupling	36·84	33·78
16	Bearing friction, oil pump, and governor power . . . kW	22·8	22·8
17	Disc friction and blade windage of impulse wheel . . . kW	12·65	13·75
18	Internal power of turbine (13) + (16) ,,	864·30	1,033·60
19	Blade power of turbine (17) + (18) ,,	876·95	1,047·35

could be determined by the pressure and temperature. The plotting of the test points against density with constant speed yielded a straight line. The intercept on the power axis is the power required to overcome bearing friction and the governor and oil-pump drive. The bearings were brought to the same temperature and the oil pump delivery at the same pressure and quantity as during the power tests.

The heat balance and internal efficiency ratios are worked out in Table XLVB, which does not call for any further explanation.

In order to test the reaction blading separately and so avoid roundabout calculations of its efficiency, the impulse wheel was stripped of blades and the nozzles were built out so that the steam could pass over the impulse wheel to the reaction blading with only a slight drop in pressure. The results of these tests are set out in Table XLVIA, while the heat balance, given in Table XLVIB,

TABLE XLVB

HEAT BALANCE FOR COMPLETE 1,000 kW BACK-PRESSURE COMBINATION TURBINE

Note.—Item Nos. are continued from Table XLVA

Item No.	Test No.	6	7
20	Adiabatic heat drop for impulse wheel B.Th.U. per lb.	26·273	27·016
21	Internal heat drop for impulse wheel B.Th.U. per lb.	18·788	20·021
22	Theoretical power of impulse wheel, based on total steam flow . . . . . kW	239	270
23	Internal power of impulse wheel, based on total steam flow and on condition of steam kW	171	200
23*a*	Blade power of impulse wheel (17) + (23) ,,	183·65	213·75
24	Adiabatic heat drop for reaction blading B.Th.U. per lb.	91·316	99·993
25	Internal heat drop for reaction blading B.Th.U. per lb.	80·435	86·578
26	Theoretical power in reaction section, based on working steam only . . . . kW	803·3	967·3
27	Internal power in reaction section, based on working steam only and on condition of steam . . . . kW	707·6	837·6
28	Total theoretical power of working steam (22) + (26) . . . . . . kW	1,042·3	1,237·3
29	Total internal power of working steam (23) + (27) . . . . . . kW	878·6	1,037·6
30	Efficiency ratio $= \frac{\text{Coupling power}}{\text{Theo. power of working steam}} = \frac{(13)}{(28)}$ . . . . per cent	80·7	81·7
31	Internal efficiency of turbine calculated from press. and temp. of working steam $= \frac{(29)}{(28)}$ . . . . per cent	84·3	83·9
32	Internal efficiency of turbine calculated from measured power of working steam per cent	82·9	83·5
32*a*	Turbine efficiency $\frac{\text{Blade power}}{\text{Theo. power of working steam}} = \frac{(19)}{(28)}$ . . . . per cent	84·1	84·6
33	Internal efficiency of impulse stage, based on steam condition . . . . per cent	71·5	74·1
33*a*	Impulse wheel efficiency $= \frac{\text{Blade power}}{\text{Theo. power of total steam}} = \frac{(23a)}{(22)}$ . . . per cent	77·0	79·2
34	Internal efficiency of reaction blading based on steam condition . . . per cent	87·9	86·6
35	Total adiabatic heat drop . B.Th.U. per lb.	116·627	125·588
36	Theoretical power based on total steam flow and on steam condition at nozzle inlet and in exhaust branch . . . . kW	1,058	1,257
37	Efficiency based on the total steam flow, on the coupling power, and on the steam condition at inlet to the nozzles and in the exhaust belt . . . . per cent	79·5	80·4

leads to an analysis of the internal efficiency of the reaction blading. This was determined in two ways: firstly, by the ratio of the actual heat drop (determined from the initial and final condition of the steam) to the adiabatic heat drop, and secondly, by the ratio of the actual work done to that which would be available in a perfect turbine. In estimating the internal work done by the reaction blading, an allowance was made for the disc friction of the impulse wheel. The results of these tests are shown in Fig. 540, efficiency being

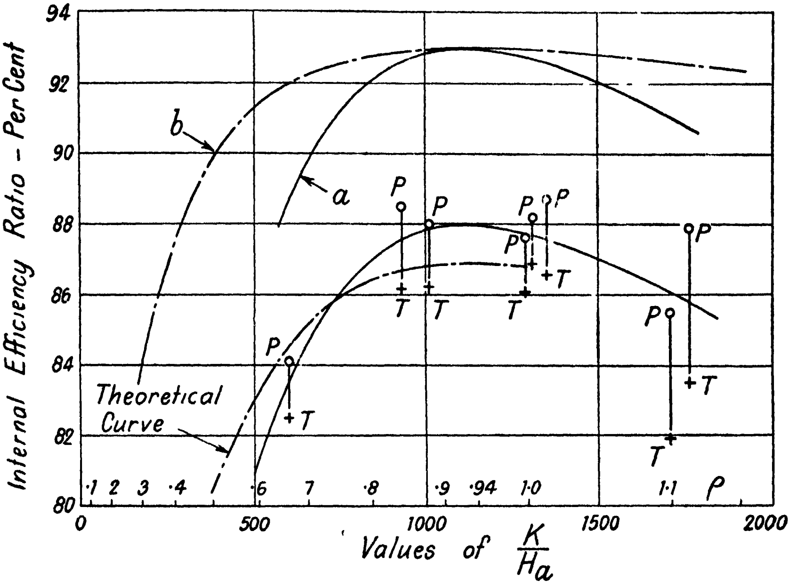


FIG 540 —Results of Tests on 10,000 kW Back-pressure Turbine

plotted against values of $\frac{K}{H_a}$. Points marked P are based on the estimated internal power; those marked T are based on the condition (temperature) of the steam. The author's theoretical curve, taken from Fig. 303,* is shown for comparison. It must be remembered that the theoretical curve is drawn on the assumption of constant coefficients, which implies that for each value of $\frac{K}{H_a}$ a different blade angle would be used. If, as in the actual turbine, a deviation from the optimum value of $\frac{K}{H_a}$ involved shock losses due to incorrect blade angle, then the two curves would be in better agreement.

It should be noted that the internal efficiency reaches the relatively

* Sixth Edition.

TABLE XLVIa

Test of Reaction Blading of 1,000 kW Back-pressure Combination Turbine

Item No.	Test No.		1	2	3	4	5	1*a*	2*a*
	Duration	min.	60	45	45	45	40	90	85
	Bar. height	in. Hg.	28·73	28·73	28·73	28·73	28·73	28·47	28·47
	Steam pressures, lb. per sq. in. abs.—								
1	Before reaction blading		92·51	90·20	111·5	96·20	75·65	94·19	93·22
2	Back pressure		39·46	28·13	48·01	39·88	39·53	39·21	39·30
	Steam temperatures, ° F.—								
3	Before reaction blading		452·0	450·4	453·5	441·2	433·5	449·9	431·9
4	In exhaust space		302·6	254·2	305·9	293·7	325·2	296·7	285·1
5	Steam condensed in main condenser	lb. per hr.	26,140	26,590	31,180	27,340	19,750	26,420	26,170
6	Steam leakage through dummy piston	,,	917	922	1,107	955	721	946	988
7	Total steam consumption	,,	27,057	27,512	32,287	28,295	20,471	27,366	27,158
8	R.p.m.		3,000	3,000	3,000	*3,500*	3,000	3,000	*2,500*
9	Power at alternator switchboard	kW	436·8	608·0	526·3	443·1	217·4	455·5	448·5
10	Total loss in alternator	,,	41·8	47·3	44·3	53·2	41·1	42·5	34·5
11	Power at turbine coupling	,,	478·6	655·3	570·6	496·3	258·5	498·0	483·0
12	Alternator efficiency	per cent	91·3	92·7	92·3	89·3	84·1	91·5	92·9
	Steam consumptions, lb. per kWh								
13	Steam used in turbine / Coupling power		54·63	40·58	54·64	55·08	76·40	53·06	54·18
14	Total steam consumption / Coupling power		56·54	41·99	56·58	57·01	79·18	54·95	56·23
15	Power for bearing friction, etc.	kW	27·8	27·7	28·7	41·94	27·8	27·9	18·4
16	Internal power = (11) + (15)	,,	506·4	683·0	599·3	538·24	286·3	525·9	501·4

TABLE XLVIB

HEAT BALANCE FOR TESTS ON REACTION BLADING OF 1,000 kW BACK-PRESSURE COMBINATION TURBINE

Note.—Items Nos. are continued from Table XLVIA

Item No.	Test No.		1	2	3	4	5	1a	2a
17	Adiabatic heat drop	B Th U. per lb	75·497	99·562	73·897	76·414	57·836	76·979	73·831
18	Internal heat drop	,, ,,	65·018	85·858	64·049	63·765	47·322	66·879	63·671
19	Theoretical power of working steam $= \frac{(5) \times (17)}{3,413}$	kW	578·3	776·4	675·5	612·2	335·0	596·5	566·5
20	Theoretical power of total steam $= \frac{(7) \times (17)}{3,413}$	,,	598·5	803·0	699·5	633·8	347·4	617 5	587·7
21	Efficiency ratio $= \frac{(11)}{(20)}$	per cent	80·0	81 6	81·6	78·3	74·4	80·6	82·2
22	Efficiency ratio $= \frac{(11)}{(19)}$	,,	82·8	84·4	84·5	81·1	77·2	83·5	85·3
23	Internal efficiency of the working steam based on the steam conditions at inlet and outlet	per cent	86·1	86·24	86·6	83·5	81·9	86·9	86·2
24	Internal efficiency of the working steam based on the internal power relative to the state of the steam at inlet and outlet	per cent	87 6	88·0	88·7	87·9	85·5	88·2	88·5

high value of 88 per cent. Professor Stodola estimated that by extrapolating the blade clearance to zero, the blade efficiency (corresponding to our gross stage efficiency) would reach the very high value of 93 per cent. The estimated gross stage efficiency is shown by the curve *a*. Taking η_{gs} as 0·93 when $\rho = 0·9$, and assuming $\alpha = 20$ degrees and $\eta_n = 0·944$ (based on the Institution of Mechanical Engineers Steam Nozzle Research Committee's work), the author estimates that the value of the carry-over coefficient ϕ in eq. 124 is 0·888. The corresponding gross stage efficiency is then given by the curve *b*.

334. **Tests on 36,000 kW Steam Turbine Operating with Steam at 1,700 lb. per sq. in. abs. and with Live Steam Reheating.** The following report is an abridgment of an article published (6) in the *Brown Boveri Review* describing tests made by Professor E. Josse. The tests are of interest because of the high initial steam pressure and because of the comparative data with and without reheating by live steam.

The turbine, constructed by Messrs. Brown Boveri & Co., Ltd., is of the three-cylinder type, the L.P. cylinder being of the double-flow type. It is designed for steam at 1,700 lb. per sq. in. abs. and at 896° F. at the inlet nozzles, for intermediate superheating up to 680° F. at inlet to the I.P. cylinder, and with two extraction branches for feed-heating, of which, usually, only the low-pressure extraction branch is used in service. The speed of the turbine is 3,000 r.p.m. Particulars of the wheels and blading are given in Table XLVII.

TABLE XLVII

PARTICULARS OF WHEELS AND BLADING OF 36,000 kW TURBINE

D = mean dia. of blades in inches; u = mean blade velocity, ft. per sec., l = blade heights, inches.

Turbine	No. of Stages	D	u	l	$\sum\left(\frac{D}{10}\right)^2$
H.P.	1 Curtis (2-row wheel)	39·37	515	1st row—1·10 2nd row—1·38	31·0
	32 Reaction	21·26	279	1·61—3·38	144·8
I.P.	18 Reaction	40·16	525·5	2·16—8·47	290·4
L.P.	6 Reaction	56·5	739	3·46—14·36	191·8

$$\text{Total} \sum\left(\frac{D}{10}\right)^2 = 658·0$$

Hence
$$K = 658\left(\frac{3,000}{100}\right)^2 = 591,000$$

and
$$\frac{K}{H_c} = \frac{591,000}{640·6} = 922$$

If, in Art. 282, the effect of carry-over from one stage to the next be neglected, and if the nozzle efficiency be taken as unity, then the quantity F_1 becomes unity. Consequently, by eq. (248)—

$$\rho = \sqrt{\frac{K_p}{2{,}620H_c}}$$

in which we write K_p to represent the Parsons number of a pressure-compounded impulse turbine with single-row wheels. Even when carry-over and nozzle losses are taken into account the value of F_1 is nearly unity at the optimum ρ and for the usual nozzle angles.

Considering next the corresponding expression for the reaction turbine deduced in Art. 283, the value of the quantity F_2 is practically equal to 2 at the most economical value of ρ, and we may write

$$\rho = \sqrt{\frac{K_r}{1{,}310 . H_c}}$$

where K_r represents the Parsons number for a reaction turbine. Thus, for comparative values, $K_p = 2K_r$. It is shown in Art. 284 that $K_p = \mu^2 . K_v$. Hence for a two-row Curtis wheel, $K_p = 4 . K_v$ and $K_r = 2K_v$. This simple relation has been used in calculating the K value of the whole turbine. It will be seen from Fig. 438 that the value of $\frac{K}{H_c}$ is relatively high for this turbine.

Owing to circumstances, it was impossible to test the turbine at its most economical load of 30,000 kW. Tests were made at 25,000 kW and 19,000 kW. The tests at 25,000 kW are alone reported here. Three tests were carried out, the turbine being operated –

(*a*) With reheating and single-stage feed-heating.
(*b*) With reheating but without feed-heating.
(*c*) Without reheating and without feed-heating.

The arrangement of the plant, showing the test points, is shown in Fig. 541. The principal test results are given in Table XLVIII. It will be seen that the gain due to reheating alone is 0·52 per cent on 32·65 per cent, i.e. 1·6 per cent. The gain due to feed-heating alone is 1·55 per cent on 33·17 per cent, i.e. 4·7 per cent.

Calculation of Efficiency Ratio. The results of the tests without feed-heating, and with and without reheating, are given in Table XLIX. The H.P. turbine uses about 37 per cent of the total heat drop, and of this about half is used in the Curtis stage. From temperature measurements, the efficiency of the Curtis stage was estimated to be from 60 to 62 per cent. The efficiency ratio of the H.P. turbine as a whole is about 73 per cent; thus the efficiency ratio of the reaction stages is about 80 per cent. The internal efficiency ratio of the I.P. cylinder is 88 per cent.

The internal efficiency ratio of the L.P. turbine could not be

determined from the condition of the steam at exhaust because the steam was wet. The output of the H.P. and I.P. turbines was calculated and deducted from the estimated total internal power of the turbine; this then gave the internal power of the L.P. turbine. In Test No. 3 without reheating, no separate estimate of power for the I.P. and L.P. cylinders is made because the steam at outlet from the I.P. turbine is saturated and, therefore, its enthalpy cannot be

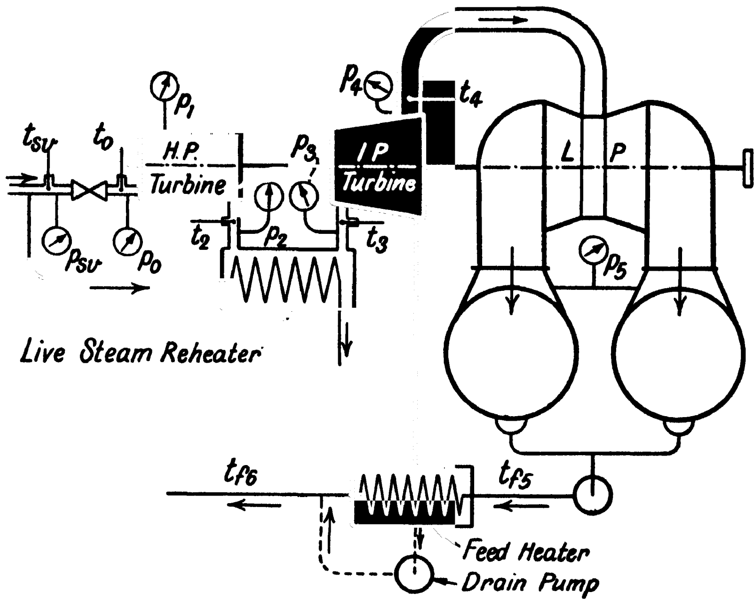


FIG. 541.—Diagrammatic Arrangement of 36,000 kW Steam Turbine with Live Steam Reheating

evaluated. The separate calculation has been omitted from Table XLIX for both tests. It should be observed that the live steam reheating reduces the wetness of the exhaust steam from 12·8 to 5·9 per cent and raises the combined efficiency ratio of the I.P. and L.P. turbines from 77·9 to 80·7 per cent.

It should be stated that in estimating the efficiency ratio of the whole turbine, the adiabatic heat drop is the sum of the three partial drops in the three turbines, and this is appreciably greater than the straight adiabatic heat drop from the initial condition Usually, the overall efficiency ratio of a condensing turbine is referred to the straight adiabatic heat drop, but this is not possible in the present case because of the intermediate reheating. If the heat regained in the H.P. turbine owing to the non-isentropic expansion is taken into account, and if the I.P. and L.P. turbines be taken

TABLE XLVIII

TEST MEASUREMENTS OBTAINED DURING TESTS ON 36,000 kW TURBINE WITH REHEATING BY LIVE STEAM

Test No.	1	2	3
Conditions	Reheating and Feed-heating	Reheating No Feed-heating	No Reheating No Feed-heating
Output at generator terminals . kW	24,940	25,411	22,656
Output at turbine coupling . . ,,	26,050	26,522	23,822
Total steam consumption lb. per hr.	184,900	184,800	183,100
Specific steam consumption, lb. per kWh			
(a) referred to generator output	7·416	7·271	8·083
(b) referred to turbine output	7·101	6 968	7·688
Steam Pressures lb. per sq. in. abs.			
Before stop valve . . . p_{sv}	1,716	1,722	1,730
After governor valve 1 and in nozzle box 1 . . . . . p_0	1,696	1,701	1,701
H.P. 1st-stage wheel chamber . p_1	573	572	559
H.P. cylinder exhaust . . p_2	162	157·3	122·2
I.P. cylinder inlet . . . p_3	135	135	117
I.P. cylinder exhaust . . p_4	11·2	12·5	11·5
Exhaust branch (mean) . . p_5	0·768	0·768	0·740
Steam Temperatures ° F.			
Before stop valve . . . t_{sv}	891·0	889·7	886·5
In nozzle box 1 after throttling at constant enthalpy . . . t_0	888·8	888·1	884·7
H.P. cylinder exhaust . . t_2	441·5	441·9	399·2
I.P. cylinder inlet . . . t_3	662·0	662·7	399·2
I.P. cylinder outlet . . . t_4	218·3	235·9	199·4
Condensate Temperatures ° F.			
Inlet to feed heater . . . t_{f5}	92·7	92·7	90·5
Outlet from feed heater . . t_{f6}	187·2	—	—
Enthalpy of Steam B.Th.U. per lb. (Knoblauch, 2nd Edition)			
Before stop valve	1,422·2	1,421·1	1,418·4
H.P. cylinder exhaust . . .	1,240·6	1,241·3	1,223·6
I.P. cylinder inlet	1,357·5	1,357·9	1,223·6
I.P. cylinder exhaust . . .	1,154·3	1,162·3	—
Specific heat consumption of turbine referred to coupling power B.Th.U. per kWh	9,828	10,290	10,460
Thermal efficiency of turbine referred to coupling power . . per cent	34·72	33·17	32·65

TABLE XLIX

Results of Tests on 36,000 kW Turbine without Feed-heating, and with and without Reheating

Test No.	2	3
Conditions	With Reheating	Without Reheating
Internal output of turbine . . . . . kW	26,952	24,252
Heat drop utilized in turbine corresponding to internal power . . . . . B.Th.U. per lb.	497·7	451·8
Heat drop utilized in H.P. turbine ,,	179·8	194·8
Heat drop utilized in I.P. and L.P. turbines B.Th.U. per lb.	317·9	257·0
Enthalpy of steam in exhaust branch corresponding to heat drop utilized	1,040·0	966·6
Wetness of exhaust steam . . . . per cent	5·9	12·8
H.P. Cylinder		
Adiabatic heat drop referred to conditions in nozzle box No. 1 . . . . . B.Th.U. per lb.	246·6	266·6
Efficiency ratio based on pressure and temperature of steam . . . . . . per cent	72·9	73·0
I.P. and L.P. Cylinders		
Adiabatic heat drop . . B.Th.U. per lb.	394·0	329·9
Efficiency ratio . . . . . per cent	80·7	77·9
Total adiabatic heat drop . . B.Th.U. per lb.	640·6	596·5
Steam consumption with adiabatic expansion lb. per kWh	5·327	5·722
Efficiency ratio of turbine referred to coupling power per cent	76·5	74·4

as one, an overall efficiency ratio of the turbine of 80 per cent is reached. Moreover, the turbine ran on partial load. One nozzle valve was completely closed and another throttled. It may be presumed that better results would have been obtained if the tests had been made at higher turbine loads.

The ϕ — I diagram for Test No. 2 (with reheating) is shown in Fig. 542.

335. **Tests on a 40,000 kW Parsons Turbine with Flue-gas Reheating.** In contrast to the results given in the previous article the following results obtained during tests on a turbine in which the steam is reheated by flue-gases are of considerable interest. The turbine in question was constructed by Messrs. C. A. Parsons & Co., Ltd., and installed in the Barking Power Station of the County of London Electric Supply Co. The turbine is a cross-compound machine, consisting of a H.P. and one L.P. turbine on one line and the I.P. and the other L.P. turbine on the other line. Each L.P.

turbine is a double-flow machine. Each line generates 20,000 kW at 3,000 r.p.m. The steam is reheated after the H.P turbine to the initial temperature of 700° F. Three-stage regenerative feed-heating is employed. The results given in Table L were published in *The Engineer* (7).

Without feed-heating and assuming frictionless and adiabatic expansion, the heat consumptions without and with reheating are

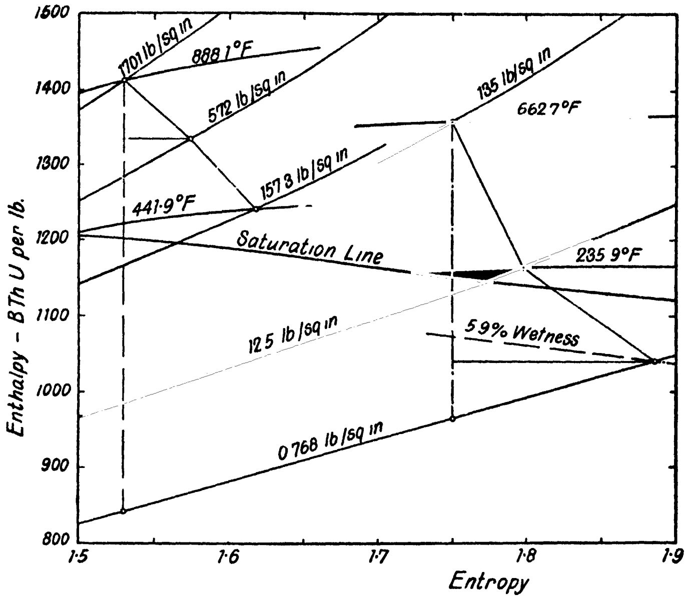


FIG 542 —ϕ – I Diagram for Test No 2, with Live Steam Reheating

9,445 and 9,223 B.Th.U. per kWh respectively. Thus the theoretical saving due to reheating is only 2·35 per cent. The difference between this and the actual saving of 7·53 per cent is undoubtedly due to the reduction of the effects of moisture in the intermediate and low-pressure cylinders which is brought about by reheating. The smaller saving under feed-heating conditions is due, of course, to the smaller steam flow in the I.P. and L.P. cylinders, especially in the low-pressure stages of the latter.

336. Test Results for Ljungström Turbines. A few test results for Ljungström turbines are given in Table LI. The first two were published in a paper (8) by Mr. O. Wiberg. The third group of figures refers to a turbine in the reserve power station at Västerås, Sweden. It should be pointed out that the turbine efficiency ratio given in the Table is referred to the condition of the steam

after the steam inlet valve and the net steam consumption of the turbine, i.e. excluding the steam consumption of the ejectors.

The Brighton turbine was constructed by the Brush Electrical

TABLE L

SUMMARY OF RESULTS OF TESTS ON PARSONS 40,000 KW TURBINE WITH FLUE-GAS REHEATING

Note. The following tests were made at the economical load.

	Specified Conditions with Reheating and Feed-heating	As Run			
		No Feed-heating		Feed-heating	
		No Reheat	Reheat	No Reheat	Reheat
Load . . . kW	35,000	31,230	37,978	30,172	35,930
Steam Pressures lb. per sq. in. g.					
Before stop valve . .	350	353·6	356·6	354·5	357·7
H.P. exhaust . .	—	37·1	49·3	34·4	47·1
I.P. inlet . . .	40	36	45·2	33·7	42·2
Vacuum . in. Hg.	1	1·39	1·40	1·15	1·19
Steam Temperatures ° F.					
Before stop valve . .	700	697	708	700	693
H.P. exhaust . .	360	334	373	327	353·5
I.P. Inlet . . .	700	352	700	318	698
Feed Temperature ° F.					
Entering drain cooler .	85	—	—	92·16	93·4
Leaving H.P. heater .	250	—	—	251·5	258
Steam Consumption lb. per kWh					
As run	—	9·81	8·01	10·25	8·54
Corrected . . .	—	9·70	7·97	10·22	8·44
Heat Consumption B.Th.U. per kWh					
As run	—	12,857	11,857	11,878	11,239
Corrected . . .	—	12,826	11,859	11,828	11,179
Saving due to reheating per cent	—	—	7·53	—	5·48

Engineering Co., Ltd. The test (9) was made at the economic load of 30,000 kW. The steam conditions in this case were taken before the turbine stop valve. Four-stage bled-steam feed-heating raised the feed temperature to 333·9° F. The heat consumption of the

turbine on test was 9,759 B.Th.U. per kW.hr., giving a turbine thermal efficiency of 35 per cent.

337. **Tests on 100,000 kW Non-reheat Turbo-generator.** These tests were made on a two-cylinder tandem turbine constructed by the General Electric Co., of America, and installed in the Essex Generating Station of the Public Service Electric and Gas Co., New Jersey.

TABLE LI

TESTS ON LJUNGSTROM TURBINES

Power Station	Year	Max Output kW	Test Output kW	Press after Stop Valve lb/sq. in abs	Temp after Stop Valve °F	Vacuum in Hg (30in. Bar.)	Steam Consumption lb/kWh	Turbine Efficiency Ratio per cent
Homburg	1928	14,000	8,450	156·4	635	29·10	9·81	85·6
			11,931	210·0	675	28·78	9·44	85·8
			14,436	213·2	653	28·47	9·95	85·1
Stuttgart	1929	15,600	6,072	204·7	738	29·02	9·42	82·9
			9,307	301·5	738	28·84	9·02	83·5
			12,362	374·0	739	28·58	8·91	84·0
			15,015	443·5	748	28·61	8·73	82·8
			15,575	460·5	748	28·23	9·00	82·1
Vasterås	1931	50,000	14,826	118·9	788	28·47	9·83	89·0
			14,890	117·3	693	28·83	10·12	89·3
			15,015	111·6	783	29·37	9·06	88·0
			15,193	109·9	685	29·61	9·35	85·7
			29,958	214·6	797	28·05	8·88	90·3
			31,232	210·4	797	29·12	8·40	87·4
Brighton	1938	37,500	30,254	656	814	28·96	8·632	—

The set was placed in service in December, 1947 and the tests made in February, 1948 (10).

The steam conditions are as follows—

Initial steam pressure	. 1,250 lb. per sq. in. g.
Initial steam temperature	. 1,000° F.
Mean cooling water temp.	. 60·6° F.
Mean condenser vacuum	. 28·64 in. Hg.
8-stage feed-heating to 477°	at full load.

The drain water from the heaters is cascaded and then passed through a drain cooler into the condenser. Most of the losses were used for feed-heating.

The high-pressure turbine has 19 stages in all. Fig. 543 shows diagrammatically the arrangement of nozzle control and by-pass valves for this turbine. There are eight nozzle control valves A, arranged symmetrically, four in the upper, and four in the lower

half of the cylinder. These regulate the supply of steam to the first-stage wheel. There are also four by-pass valves B which by-pass stages two and three. These are also divided equally between the upper and lower halves of the cylinder. With load being added, seven of the primary valves open consecutively; then for the eighth admission four by-pass valves are opened; and finally for the ninth admission the eighth primary valve is opened. As will be seen from

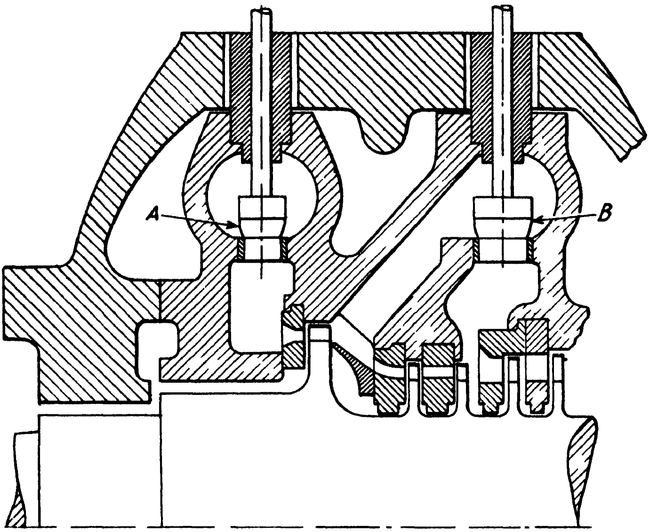


FIG. 543.—Diagrammatic Arrangement of Nozzle Control and By-pass Valves on American G.E.C. 100 MW Turbine
(Reproduced by permission of the American Society of Mechanical Engineers)

the test results, this arrangement gives a very flat heat consumption curve.

The low-pressure turbine is a double-flow machine with 5 stages. The speed is 3,600 r.p.m.

During the tests the total drain flow was calculated from heat balances for each individual heater and the drain cooler. This was found to be greater than the calculated extraction flows to the eight heaters. The difference was assumed to be moisture flung off the blades and carried into the extraction pipes. The amount was about 10,000 to 12,000 lb. of water per hour and was almost independent of the load. The two last stages in the l.p. turbine were fitted with moisture catchers that drained into the condenser hotwell. This drainage was not measured.

Heat consumption results are given in Fig. 544. The heat consumption of the turbine-generator is defined as that quantity of heat supplied by the boiler necessary to produce one net kWhr. of electricity. The net kilowatt output is defined as the output at the

terminals of the two generators less the electrical inputs to the generator fields.

The test results were corrected to the stated initial steam conditions, exhaust pressures of 1·0, 1·5, 2·5, and 3·5 in. Hg. absolute, and feed-heater terminal temperature differences as given in the turbine specification. Each test point corresponds to a condition in which a definite number of control valves were full open. The curves between the test points are based on tests on other turbines, the

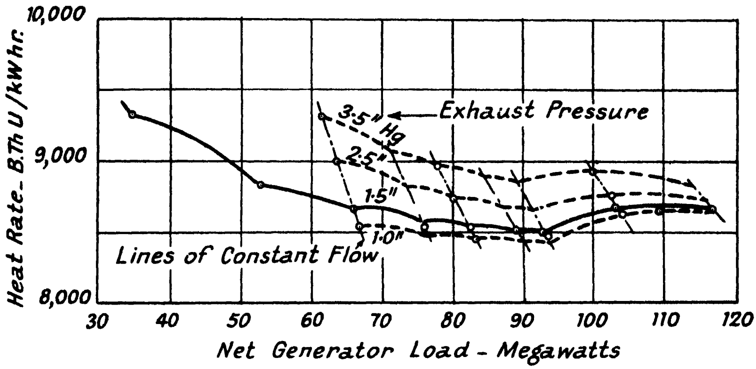


FIG. 544 —Test Results for Essex No 1 Turbo-generator
(Reproduced by permission of the American Society of Mechanical Engineers)

rise in heat consumption after passing a test point being due to the throttling of the steam at the control valve which is just opening.

The amount of steam extracted for feed-heating is about 22 per cent at 35 MW. and 32 per cent at 117 MW. At the most efficient load of 93 MW. and an exhaust pressure of 1·5 in. Hg. absolute the heat consumption of the set was 8,498 B.Th.U. per kWhr. giving a thermal efficiency of 40·16 per cent. The overall heat consumption of the boiler, turbine, feed heaters and auxiliaries at the most economical point during the winter months was 10,100 B.ThU. per kWhr., giving a thermal efficiency of 33·79 per cent.

338. Tests of British 30 MW and 60 MW. Turbo-generators. Some authoritative data on the performance of recent British steam turbo-generators is given in a paper (11) by Mr. H. S. Horsman. The following notes are extracted from his paper.

The terminal conditions for the 30 MW. turbines are as follows—

Steam pressure . . .	600 lb. per sq. in. g.
Steam temperature . .	850° F.
Vacuum at 24 MW. . .	28·8 in. Hg.
Final feed temperature at 24 MW.	330° F.
Stages of feed-heating . .	4.

The following average results were obtained during 33 official tests at the economic rating of 24 MW.—

Heat consumption (corrected)	10,139 B.Th.U. per kWhr.
Standard deviation . .	270 B.Th.U. per kWhr.

Thirty official tests on 60 MW. turbo-generators were analysed. The results given refer to the economic rating which, for these machines, is usually the continuous maximum rating but is occasionally only 80 per cent of that.

The following are the standard conditions and the corrected performance figures for the 60 MW. turbo-generators—

Steam pressure . . .	900 lb. per sq. in. g.
Steam temperature . .	900° F.
Vacuum	28·8 in. Hg.
Final feed temperature .	385° F.
Stages of feed-heating . .	5.
Average heat consumption .	9,307 B.Th.U. per kWhr.
Standard deviation . .	155 B.Th.U. per kWhr.

BIBLIOGRAPHY

1. "Steam Turbine Efficiencies." *Engineering*, 1924; 118; 704. Letter to the Editor from Mr. F. Samuelson.
2. "35,000 kW. Turbo-Generator at Deptford West Power Station." *Engineering*, 1932; 133; 302.
3. STODOLA, A.: "Leistungsversuche an einer 11,000 kW.-Zoelly-Dampfturbine." *Zeits des Vereines deutscher Ingenieure*, 1927; 71; 747.
4. CARTER, W. A., and ELLENWOOD, F. O.: "The Thermal Performance of the Detroit Turbine Using Steam at 1,000° F." *Trans. Am. Soc. Mech. Eng.*, 1934; 56; 477.
5. STODOLA, A.: "Leistungsversuche an einer Gegendruck-Dampfturbine." *Zeits. des Vereines deutscher Ingenieure*, 1925; 69; 1177.
6. "Results of Tests Carried Out on a 36,000 kW. Steam Turbine, 120 kg./cm.², 480° C., with intermediate Superheating and Extraction, delivered to the Witkowitzer Bergbau-und Eisenhüttengewerkschaft." Extract of an article published in the *Elektrizitätswirtschaft*, 1935, No 13, and published in the *Brown Boveri Review*, 1936, 23, 131.
7. "The Development of the Parsons Steam Turbine." *The Engineer*, 1934; 157; 448.
8. WIBERG, O.: "Recent Development of Radial-flow Turbines for Large Outputs." World Power Conference Sectional Meeting, Tokyo, 1929.
9. "Ljungström Turbo-Generator Sets at Brighton." *The Engineer*, 1939, 167; 615.
10. RENTON, V. S., and NEAL, S.: "Heat Rate Test Results of the 100,000 kW. Essex Turbine Generator." *Trans. A.S.M.E.*, 1950; 72; 285.
11. HORSMAN, H. S.: "Testing of Boilers and Turbo-Alternators in Power Stations of the Central Electricity Authority." *Proc. I. Mech. E.*, 1956 170; 545.

MATERIALS FOR STEAM TURBINES

THE purpose of this appendix is to discuss very briefly some of the factors which affect the choice of materials for the various parts of steam turbines. No attempt will be made to consider the very complex subject of alloy steels.

We have seen that, since the lowest temperature in the steam cycle is fixed mainly by the temperature of the available condenser cooling water, the thermal efficiency can only be increased by using

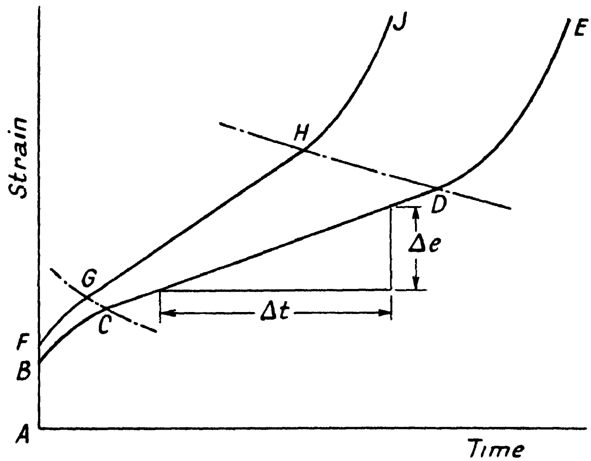


FIG. 545.— Strain-Time Curve, Showing Creep

steam at the highest permissible temperature and at a high initial pressure. The highest permissible steam temperature is limited mainly by the mechanical properties of the available materials when exposed to high-temperature steam. The association of a high working pressure with a high temperature raises the stresses to which pressure parts are subjected and so aggravates the problem.

Creep of Metals. At high temperatures, steels and certain alloys, when subjected to stress, undergo a gradual change of dimensions which is known as *creep*. Fig. 545 shows an idealized strain-time diagram for such a material. The material is assumed to be under a constant single stress, usually a tension, and at a constant temperature. AB represents the strain due to the initial imposition of the stress. From B to C the strain increases but at a rapidly diminishing rate; this is known as primary creep. From C to D the strain

increases at an approximately steady rate; this stage is known as secondary creep. In the third or tertiary stage from D to E the strain increases more and more rapidly and fracture of the test piece occurs at E.

From a practical point of view, the secondary creep is of greatest importance, and the applied stress should always be such that at the operating temperature the life of the part should be appreciably less than the time reached at the end of the secondary creep.

Considering a time interval Δt hours during the secondary creep

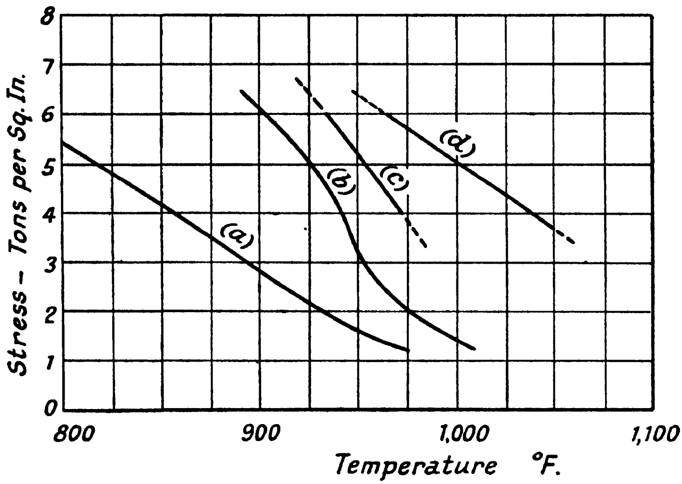


FIG. 546.—Stress-Temperature Curves for Various Steels giving 0·1 per cent Creep in 100,000 hours

(*a*) Plain carbon steel.
(*b*) 0·5 per cent molybdenum steel.
(*c*) Molybdenum-vanadium steel, normalized.
(*d*) Molybdenum-vanadium steel, normalized and tempered.

period, let the increment of strain be Δe. Then the ratio $\frac{\Delta e}{\Delta t}$ is defined as the creep rate. Since e is the ratio of extension to original gauge length, the dimension of creep rate is $\frac{1}{\text{Time}}$. It is obvious that for parts of steam turbines in which clearances and dimensions must be maintained closely during the life of the machine, only very small creep rates are permissible. The "life" is often taken to be 100,000 hours or 11½ years, and for many parts of the turbine the maximum strain during that period is limited to 0·1 per cent. If the strain during primary creep be ignored, this implies a creep rate of 10^{-8}, or one hundred-millionth per hour.

For any given temperature the creep rate is greater the higher the

applied stress, and vice versa. This is shown in Fig. 545 in which the curve FGHJ shows the strain for a stress which is higher than that giving the strain curve BCDE. Conversely, for a constant stress the creep rate is higher for a higher temperature and vice versa.

The influence of temperature on the permissible stress for a few materials is shown in Fig. 546, taken from a paper (1) by D. W. Crancher and based on the work of H. J. Tapsell and R. W. Ridley. This is based on a creep of 0·1 per cent in 100,000 hours. It will be seen that, in the range 850 to 950° F., the use of 0·5 per cent molybdenum steel allows a stress to be carried approximately twice that permissible with a plain carbon steel.

Somewhat greater stresses may be used if a greater rate of creep is allowed, but, where the creep must be limited, the severe limitations of these alloys will be at once apparent. For steam temperatures above 1,050° F. it is probable that austenitic steels having a

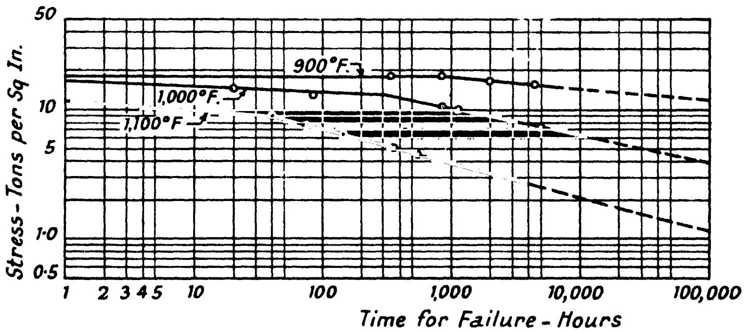


FIG 547 —Stress-Time for Failure Curves for C-Mo Steel

Circles indicate intergranular fracture

percentage composition: 18 Cr; 12 Ni and 1 Cb (Columbium or Niobium) will have to be used. These steels possess certain disadvantages such as high cost, a high coefficient of expansion and a low thermal conductivity, the combination of the two last properties tending to produce high thermal stresses. There is also some doubt whether their use will permit a higher temperature to be used than is possible with ferritic steels if the total creep is to be limited to a similar amount for the long period of 100,000 hours. This uncertainty arises because of the absence of data for very long test periods and because of the doubt as to how the extrapolation of existing data should be made.

There are three interdependent variables in creep, namely, creep rate, temperature and stress. Moreover, the creep properties of an alloy steel are considerably influenced by the alloying elements and their amounts, and by the heat treatment given to the steel. No

attempt will be made, therefore, to give any further data on the subject. A very brief bibliography is given at the end of this Appendix.

Stress to Rupture. In another form of test for materials required for high-temperature operation, tests are made at constant temperature on a series of test pieces of a given alloy which have had the same heat treatment. Each test piece is subjected to a constant stress, but the stresses applied to the several test pieces are varied so that the time to fracture varies from a few hundred hours up to some thousands of hours. The log of the stress is plotted against the log of the time to fracture, as shown in Fig. 547 (adapted from Fig. 3 of paper "Some Effects of Composition and Heat Treatment on the High-Temperature Rupture Properties of Ferrous Alloys," by R. H. Thielemann, *Proc. A.S.T.M.*, 1940; 40; 788). If the alloy remains structurally stable and free from surface deterioration then the log-log plot results in a single straight line. If, however, there should occur either a change of structure or surface then the log-log plot yields two straight lines with different slopes.

In either case if the line is produced to a certain specified rupture time, e.g. 10,000 hours or 100,000 hours, then the corresponding stress at this time is termed the stress to rupture. The values obtained in the test, i.e. the nominal applied stress and the time to fracture, are both known with certainty and it is believed that extrapolation up to 100,000 hours is possible. To obtain the working stress, a factor of safety of about 2 is sometimes used, based on the rupture stress for 100,000 hours.

Resistance to Scaling. Another factor of importance at high temperatures, say above 1,000° F., is the scaling or oxidation of steel in the presence of steam. The presence of oxygen in the steam may be due to oxygen dissolved in the feed water or to oxygen set free by dissociation. In either case the amount of oxygen would be very small. The addition of chromium improves the oxidation resistance of steel.

Turbine Cylinders. Plain carbon steel is satisfactory for cast cylinders and steam chests up to 800° F. By the addition of 0·5 per cent molybdenum, steel may be used for steam up to about 850° F. For temperatures in the range 850° to 1,000° F., a steel containing 1·0 per cent chromium and 0·5 per cent molybdenum is used for steam pipes, steam chests and cylinders. Owing to the reduction in the creep properties of this alloy as the temperature is increased, use is sometimes made of the element vanadium in an alloy containing 0·5 Mo, 0·3 Va and 0·12 carbon.

For the h.p. and i.p. outer casings of the English Electric 200 MW. turbine shown in Figs. 473 and 474, the steel has the following percentage composition—

C 0·15 max.; Si 0·2 to 0·5; Mn 0·4 to 0·7; Ni 0·3 max.; Cr 0·5 max.; Mo 0·5 to 0·7; S 0·05 max.; P 0·05 max.; Va 0·20 min.,

while the steel for the h.p. and i.p. inner casings which are subjected to the highest temperature steam has the following composition—

C 0·16 max.; Si 0·4 max.; Mn 0·4 to 0·6; Ni 0·5 max.; Cr 2·75 to 3·25; Mo 0·5 to 0·7; S 0·05 max; P 0·05 max.; Va 0·7 to 0·9; W 0·4 to 0·6.

These figures are given in an article by Mr. John Caldwell (2).

Turbine Rotors. The high-pressure rotors, and the intermediate-pressure rotors in reheat turbines, are exposed to high-temperature steam and require material with good creep properties. On the other hand, the low-pressure rotors of turbines of large output are usually subjected to heavy blade loads and require high strength at moderate temperatures. Roughly speaking, the composition of the alloy steels used for rotors is similar to that of the cast steels used for cylinders subjected to the same range of temperature.

For example, in the article by Mr. Caldwell quoted in the preceding section, the following composition and mechanical properties are given for the rotors of the English Electric 200 MW. turbine.

H.p. and I.p. Shafts: C 0·25 max., Si 0·35 max.; Mn 0·4 to 0·7; S 0·04 max.; P 0·04 max.; Mo 0·5 to 0·85; Va 0·25 to 0·4; Ni 0·5 max.; Cr 0·6 max. Ultimate tensile strength 40 tons per sq. in. minimum. Yield point 25 tons per sq. in. minimum. Creep stress for 0·1 per cent strain in 100,000 hr. at 1,000° F. = 4 tons per sq. in.

L.p. Shaft: C 0·35 to 0·40; Si 0·2 to 0·25; Mn 0·6 to 0·9; S 0·04 max.; P 0·04 max.; Ni 0·3 max.; U.T.S. 38 tons per sq. in. Y.P. 20 tons per sq. in.

L.p. Discs: C 0·3 to 0·4; Si 0·35 max.; Mn 0·6 to 0·9; S 0·04 max.; P 0·04 max.; Mo 0·5 to 0·7 max., Ni 0·5 max.; Cr 3·0 to 3·5 max. U.T.S. 55 tons per sq. in. minimum. Y.P. 45 tons per sq. in. minimum.

Brief reference will now be made to a problem which has arisen in connection with certain turbine rotors of carbon-molybdenum steel. Occasionally these rotors are found to bend slightly when heated and to straighten again when allowed to cool. On further heating deflection again occurs and on cooling the rotor spindle again becomes straight. Although the deflection produced may not be more than about 0·01 in., the resultant roughness of running is unacceptable (see Art. 218).

The problem has been investigated by Mr. A. Barker and Dr. F. W. Jones (3), who examined two rotors which exhibited this thermal instability. It was found that the deflection was caused by a difference in the coefficient of expansion of the steel on opposite sides of the rotor due to non-uniformity of heat treatment. It was also shown that by a suitable heat treatment in which the rotor was rotated at a very slow speed the difference in the coefficient of expansion could be removed.

It is now customary to check the thermal stability of rotors, which will be exposed to high-temperature steam during operation,

in a test which is sometimes called "a heat indication test." This check is made before the rotor is bladed. The rotor is placed in an electrically-heated oven and supported on bearings external to the oven. It is driven at a low speed (about 2 r.p.m.) by an electric motor. The rotor is heated up slowly to a temperature above the operating temperature and during the test the deflection of the rotor is measured at certain points along its length. The test is usually extended for some hours at a steady temperature. In certain cases where two parts of a rotor are to be exposed to steam at radically different temperatures, a special design of oven is employed so that operating conditions may be simulated as nearly as possible.

BIBLIOGRAPHY

1. CRANCHER: "Steam Pipe Materials for Advanced Steam Conditions." *Trans. Inst. Marine Eng.*, 1952; 64.
2. CALDWELL. "Large High-Pressure High-Temperature Steam Turbines." *The Engineer*, 1956; 201; 662.
3. BARKER and JONES. "The Reversible Bending of Turbine Shafts with Temperature." *Proc. I. Mech. E.*, 1955; 169; 853.

The following publications deal with creep and creep data.

Books

1. *High-Temperature Alloys*, C. L. CLARK. Sir Isaac Pitman & Sons, Ltd., 1953.
2. *Metallic Creep and Creep Resistant Alloys*, A. H. SULLY. Butterworth's Scientific Publications, 1949.
3. *Creep of Metals*, H. J. TAPSELL. Oxford University Press, 1931.

Papers and Reports

1. "Testing of Materials for Service in High-Temperature Steam Plant." By R. W. BAILEY and A. M. ROBERTS. *Proc. I. Mech. E.*, 1932; 122, 209.
2. "Utilization of Creep Test Data in Engineering Design." By R. W. BAILEY *Proc. I. Mech. E.*, 1935; 131; 131.
3. "Creep Properties of Steels Utilized in High-Pressure and High-Temperature Superheater and Steam Pipe Practice."
   Part 1: "Carbon steels" by H. J. TAPSELL. *Proc. I. Mech. E.*, 1944, 151; 54.
   Part 2: "0·5 per cent molybdenum steels" by H. J. TAPSELL and R. W RIDLEY. *Proc. I. Mech. E.*, 1945; 153; 181.
4. "Creep under Complex Stress Systems at Elevated Temperatures." By A. E. JOHNSON. *Proc. I. Mech. E.*, 1951; 164; 432.
5. Report on "The Elevated-temperature Properties of Chromium-Molybdenum Steels." *A.S.T.M.*, 1953.
6. "Creep and Fracture of Metals at High Temperatures." Proceedings of a Symposium held at the N.P.L., 1954. H.M.S.O., 1956.

ANSWERS TO EXAMPLES

II (page 36)

1. (*a*) 368; (*b*) 374·096; (*c*) 372·511 B.Th.U. per lb.
2. 298·469 B.Th.U. per lb.
3. (*a*) 81·70; (*b*) 808·0 B.Th.U. per lb.
4. 0·8664.
5. 1,119·6; 447·8 B.Th.U. per lb.
6. 902·9 B.Th.U., 30·1 lb.
7. 0·847.
8. (*a*) 0·5145 dry; (*b*) 400·94 B.Th.U. per lb.

III (page 52)

2. 0·1353.
3. (*a*) 0·4714, (*b*) 1·1346; (*c*) 0·1185.
4. 0·73713; 0·7144.
5. (*a*) 190 lb.; (*b*) 2,029,600 B.Th.U.; (*c*) 2,289 units of entropy.

IV (page 69)

1. (*a*) 1121·2 B.Th.U. per lb.; (*b*) 1·4336; (*c*) 804·7 B.Th.U. per lb.; (*d*) 28·2 per cent.
2. (*a*) 948·3 B.Th.U. per lb., (*b*) 1·2222; (*c*) 686·0 B.Th.U. per lb.; (*d*) 27·66 per cent.
3. (*a*) 1248·1; (*b*) 850·0; (*c*) 398·1; (*d*) 398·8 B.Th.U. per lb.; (*e*) 31·95 per cent, (*f*) 8·558 lb. per kW-hr.; 76·4 per cent.
4. 20·56 per cent.

		Turbine A	Turbine B
5.	(*a*)	9·72	8·40
	(*b*)		13·60
	(*c*)	0·290	0·3267
	(*d*)		12·65

6. 7·38 B.Th.U. per lb.
7. 22·60 per cent; 71·45 per cent.
8. Turbine A: 34·56 per cent; 0·860. Turbine B: 40·82 per cent; 0·758.
9. 0·574 penny.

		Turbine A	Turbine B
10.	(*a*)	9·338	8·214
	(*b*)	31·97 per cent	32·98 per cent
	(*c*)		12·0 per cent
	(*d*)		3·16 per cent

11. Initial superheat = 292·8° F.
12. 41·1 lb. per sq. in. abs.; 0·8355; 386·3 B.Th.U. per lb.
13. (*a*) 338·0; (*b*) 350·3; (*c*) 365·7; (*d*) 386·9; (*e*) 421·7 B.Th.U. per lb. (*a*) 0; (*b*) 3·6; (*c*) 8·2; (*d*) 14·4; (*e*) 24·8 per cent.
14. 335·9; 268·9 B.Th.U. per lb., 80·0 per cent.

V (page 141)

1. 1,416 ft. per sec.
2. 1,343 ft. per sec.

3. 0 963
4. (*a*) 1 467 ft per sec (*b*) 0 494 sq in
5. 351 1° F 1,428 5 B Th U per lb 75 4 B Th U per lb
1,943 ft per sec
7. 0 374 sq in
8. (*a*) 0 366 0 487 sq in (*b*) 0 388 0 521 sq in
9. 0 0154
10. 2 955 70 5° F 0 0029 2 215 B Th U per lb 3 01 per cent
11 0 104 0 365 in
12. 17 28 lb per sq in abs
13. 35 5 lb per sq in
14. 1 13 87 lb per sq in abs 1,460 ft per sec , 0 182 sq in
15. 2 760 ft per sec 0 97
16. 13 96 lb per sq in abs 0 381 lb per sec
17. 1 86 × 10 ⁹ ft or 5 66 10 ⁸ cm

VII (page 205)

1. (*a*) 29° 48′, (*b*) 2,405 ft per sec , (*c*) 58 4 lb , (*d*) 127 2, (*e*) 73 8 per cer
2. (*a*) 642, (*b*) 640, (*c*) 47 5 lb (*d*) 640, (*e*) 82 8 per cent
3. 375 h p.
4. 646 8, 2,660 ft -lb per lb
5. 0 4851, 26 5°, 89 4 per cent
6. 56 3 lb
7. 80 8 per cent, (1) 0 3208, $\beta_1 = 29°$, (2) 0 6188, $\beta_1 = 47°$
8. 7 4 lb , 252 h p
9. 690 ft per sec , 34°, 84 8 per cent
10. 408 and 353 ft per sec , 82 9 per cent

		First Moving Row	Second Moving Row
11.	(*a*)	2,678	663
	(*b*)	441	109
	(*c*)	20 3	11 5
	(*d*)	305 h p	75 5 h p
	70 3 per cent		

		First Row	Fixed Row	Second Row
12.	(*a*)	19 9°	25°	38°
	(*b*)	605 h p	—	171 h p
	(*c*) 74 per cent			

VIII (page 226)

1. (*a*) 49° 32′, (*b*) 311 lb , (*c*) 192
2. (*a*) 331 5 ft per sec , (*b*) 0 84, (*c*) 4 330 ft -lb
3. 500 ft per sec , 10 23 B Th U per lb , 80 5 per cent
4. 53° 4′, 683
5. 1 06 in , 51 1 B Th U per lb
6. 27 8 per cent, 14 14 B Th U per lb , 86 1 per cent
7. 86 3 per cent
8. 17 7 B Th U per lb 31 4 per cent 29 6°, 88 3 per cent

XI (page 288)

1. (*a*) 0 039 h p , (*b*) 0·174 h p
2. (*a*) 65 4 h p , (*b*) 49 0 h p
3. 1 77 h p
4. 0 316 lb per sec , 195·2, 190 3, 185 2 lb per sq in abs

5. 218 lb.
6. 586 lb. per hour.
7. 79, 101, 118.3 p.s.i.a., 1230 lb. per hour.

XII (page 304)

1. 310.1 B.Th.U. per lb., 0.832 dry, 11.97 per cent, 0.2209.
2. 25,100 ft.-lb.
3. 1,925, 1,465, 76.2 per cent.
4. (1) 482 ft. per sec., (2) 4.64 B.Th.U. per lb., (3) 0.98 per cent, (4) 987.60 B.Th.U. per lb.
6. 1.056.
8. m = 1.091, 1.086.
9. 1.055.
10. m = 1.209, 1.0805, 1.0725.
11. 449° F., 5.19 cu. ft. per lb., 1.0438.

XIII (page 320)

	Rankine Cycle	Regenerative Cycle
1. (*a*)	32.1	33.90 per cent
(*b*)	8.46	9.14 lb. per kWh.
(*c*)	8.46	7.82 lb. per kWh.

2. 0.166 lb., 38.8 per cent.
3. 5,300 h.p.
4. 0.116 lb. at 70 lb., 0.0797 lb. at 12 lb. pressure, 37.5 per cent.
5. (*a*) w_1 = 0.0838, w_2 = 0.0772, w_3 = 0.0525 lb., (*b*) 37.7 per cent, (*c*) 34.75 per cent, (*d*) 8.5 per cent, (*e*) 8.60 and 7.70 lb., (*f*) 338,000 and 385,000 lb. per hour, (*g*) 5,630 and 6,405 B.Th.U.
6. 228.44 B.Th.U. per lb., 8,140 lb.
7. w_1 = 0.1012, w_2 = 0.0794, w_3 = 0.0700 lb., 9.67 per cent.
8. 38.2 per cent.
9. 22,500 lb. per hour.
10. 39.6, 40.7 per cent.

XIV (page 349)

1. (*a*) 6,040 h.p., 77.87 per cent, (*b*) 5,196 h.p., 74.57 per cent.
2. 0.819, 35.4 per cent, 0.933, 36.2 per cent.
3. 32.6 per cent, 0.14, 33.4 per cent, 0.104.
4. 41.0 per cent.
5. 1732.1, 1186.0, 546.1 B.Th.U. per lb., 31.5 per cent.
6. 8.18 lb., 10,850.
7. 41.0, 40.8 per cent.
8. 36.0 per cent, 62.2 and 8.0 lb. per sq. in. abs., 280° F., 35.8 per cent.
9. Superheat before reheating = 54° F., and after reheating = 316° F., 35.3 per cent.
10. 92 lb. per sq. in.
11. (*a*) 10,415, 0.12, (*b*) 10,040, Steam superheated 26° F.
13. 8,980, 60,480.
14. Turbine No. 1—35.5 per cent, 399,000 lb. per hour, 63,000 cu. ft.
Turbine No. 2—37.9 per cent, 315,300 lb. per hour, 60,870 cu. ft.

XV (page 375)

1. 66.2 per cent, 380 h.p.
2. 219 kW.
3. 57.4, 69.5, 75.0 per cent.
4. 8.26 lb. per sec.

5. 1,261 B.Th.U. per lb.
6. 82·1 per cent; 1,940; 4,480 kW.
7. 20,020; 2,880 kW.

XVI (page 386)

1. 1,935 h.p.
2. 23·15; 18·37; 11·41 lb. per h.p. hr.
3. 26·9; 13·99 lb. per kWh; 9·38 lb. per sq. in. abs.
4. 950 kW.
5. 755 h.p.; 12,300 lb.
6. 114·6 lb.; 6,950 lb.
7. 820 lb.; 1,160 h.p.
8. 33,700 lb.
9. 2,195 kW.
10. 1,598 kW.

XVII (page 401)

1. 1,930 h.p.; 43,700,000 B.Th.U. per hour. 61,600,000 B.Th.U. per hour.
2. 2,190 kW.
3. 23,000,000 B.Th.U. per hour. 351 kW., 11,970,000 B.Th.U. per hour.
4. 22,020; 11,210 lb. per hour.
5. 1,600 kW.
6. 26·8 tons per day of 24 hours.
7. 3,530; 2,685 lb. per hour.
8. 9·79 lb. per sec.; 388 kW.
9. 85,200 lb. per hour; 4,140 h.p.
10. 117,000 lb. per hour; 60,500,000 B.Th.U. per hour.

XIX (page 456)

1. 2·126; 2·392; 2·660; 2·920 lb. per sec.
2. 1,346; 1,276; 1,202; 1,133 ft. per sec.
0·366; 0·379; 0·398; 0·411 lb.
0·361; 1·121; 1·962; 2·840 lb. in.
6·28 lb. in. inclined at 4 degrees to wheel plane.
3. (*a*) 0·121 sq. in.; (*b*) 0·26 in.; (*c*) 0·000842 in.^{4}; (*d*) 0·0059 in.^{4}
4. M_x = 6·276 lb. in. M_y = 0·219 lb. in.
Due to M_x 1,940 lb. per sq. in.
Due to M_y 20 lb. per sq. in.
11,610 lb. per sq. in.
13,570 lb. per sq. in.
5. (*a*) 55·8; (*b*) 79·3; (*c*) 34·6; (*d*) 88·4 lb. in.; (*e*) 12,400; (*f*) 8,950; (*g*) 9,840; (*h*) 21 350; (*i*) 22,240 lb. per sq. in.

XXI (page 514)

1. 790 ft. per sec.; 0·088 in.
2. 4,520 lb. per sq. in.
3. 8,200 lb. per sq. in; 0·00232 in.
4. 11,200 lb. per sq. in; 0·00372 in.
5. (*a*) 22,790; (*b*) 7,386 lb. per sq. in; (*c*) 0·00304; (*d*) 0·00432 in.
6. (*a*) 1·174; (*b*) 0·7188 in.
7. 1·116 in.
8. 18,275 lb. per sq. in; 0·00647 in.; 7,720; 8,750 lb. per sq. in.

XXII (page 538)

1. (*a*) 2,480 r.p.m.; (*b*) 2,428 r.p.m.
2. 294·4; 2,649 r.p.m.

4. 3·145 in.
5. 0·755 in.
6. 3,215 r.p.m.
7. 5,360 r.p.m.
8. 2·55 in.

XXVII (page 688)

1. K = 302,000; 16.
2. K = 256,000; 590; 0·475.
3. (*a*) 22,500; (*b*) 893; (*c*) 1,000.
4. (*a*) 38·8 in.; (*b*) 2,360 r.p.m.
5. 34·8 in.; 2,960 r.p.m.
6. 7·7 in.
7. 18,200 kW.
9. 10,200 h.p.
10. 53·8; 742 ft. per sec.; 73·2 in.; 23·4 in.; 1,266 ft. per sec.

NAME INDEX

SUBJECT INDEX